Particle Physics

Yury Holubeu *

November 19, 2025

This note is not intended for distribution.

Particle physics is discussed in detail. Links below show contents of solved problems, summary of special topics. I used the following literature.

Contents

Preface and main motivation **9**

I —— Typical Particle Physics in a Nutshell —— 10

1 Main Information About Particles (???) 10
1.1 Overview of main properties and reactions . . . 10
1.1.1 Main Parameters of the Particles . . . 11
1.1.2 Typical Motion in Colliders (!!!) . . . 15
1.1.3 The Standard Model: Main Formulas (????) . . . 16
1.1.4 Standard Model: Main Details (????) . . . 16
1.1.5 Types of plots for experimental results . . . 16
1.1.6 Main Experimental Predictions of Hypothetical Theories . . . 16
1.2 General overview of Standard model . . . 16
1.2.1 First Look at Quantum Fields by Tong . . . 16
1.2.2 On problems of Standard model (???) . . . 16
1.3 The Strong Force by Tong . . . 16
1.4 The Weak Force by Tong . . . 17
1.5 What We Dont Know by Tong . . . 17
1.6 Strong Force in a Nutshell . . . 17
1.7 Weak Force in a Nutshell . . . 17
1.7.1 $C-, P-, CP$ symmetries for particles (???) . . . 17
1.8 Some Other Topics . . . 18
1.8.1 H5: Electron-Proton Elastic Scattering . . . 18
1.8.2 H6: Deep Inelastic Scattering . . . 32
1.8.3 H7: Symmetries and the Quark Model . . . 48
1.8.4 H8: Quantum Chromodynamics . . . 68
1.8.5 H9: The Weak Interaction and V-A . . . 95
1.8.6 H10: Leptonic Weak Interactions and Neutrino Deep Inelastic Scattering . . . 107
1.9 Properties of Typical Particles . . . 122
1.9.1 p, n, α-Particle . . . 122
1.9.2 Other Typical Mesons . . . 123
1.9.3 Photons, Z and W-bosons . . . 126
1.9.4 Neutrinos . . . 128
1.9.5 The Higgs Boson . . . 128
1.10 Mathematics and physics for particle physics . . . 128
1.10.1 Algebras for particles (???) . . . 128
1.11 Some Important Experiments . . . 128
1.12 Derivation of Some Typical Properties of Some Particles . . . 129
1.12.1 Muon's anomalous magnetic moment . . . 129

II Particle Physics Fundamentals and Standard Model 130

*https://yuriholubeu.github.io/, yuri.holubev@gmail.com

2 General Understanding of Particles and Their Interactions **130**
2.1 QFT Templates for Particle Physics (!??!??) . . . 130
2.2 Description of Decays and Scatterings . . . 130
2.3 α-decay . . . 130
2.4 β-decay . . . 130
2.5 Weak Interactions . . . 142

3 Physics of Hadrons **146**

4 Particles by Tong **146**
4.1 1 Introduction . . . 147
4.1.1 1.1 Quantum Fields . . . 152
4.1.2 1.2 Natural Units . . . 155
4.1.3 A Interlude: The Road to Discovery . . . 159
4.2 2 A First Look at Quantum Fields . . . 166
4.2.1 2.1 Matter Fields and Force Fields . . . 166
4.2.2 2.2 Quantum Electrodynamics . . . 172
4.2.3 2.3 Renormalisation . . . 180
4.2.4 B Interlude: Looking to the Sky . . . 185
4.3 3 The Strong Force . . . 193
4.3.1 3.1 Yang-Mills Theory . . . 194
4.3.2 3.2 Quarks . . . 199
4.3.3 3.3 Baryons . . . 203
4.3.4 3.4 Mesons . . . 208
4.4 4 The Weak Force . . . 227
4.4.1 4.1 The Structure of the Standard Model . . . 228
4.4.2 4.2 The Higgs Field . . . 234
4.4.3 4.3 Flavours of Fermions . . . 246
4.4.4 4.4 Neutrinos . . . 258
4.4.5 D Interlude: Big Science for Weak Things . . . 267
4.5 5 What We Don't Know . . . 281
4.5.1 5.1 Beyond the Standard Model . . . 283
4.5.2 5.2 Gravity . . . 296
4.5.3 5.3 Cosmology . . . 301

5 Leptons and Quarks by Okun **313**
5.1 1 Introduction . . . 313
5.1.1 1.1. Quark currents . . . 315
5.1.2 1.2. On the color of weak currents . . . 316
5.1.3 1.3. Currents and processes . . . 317
5.1.4 1.4. About the outline of this book . . . 319
5.2 2 Structure of weak currents . . . 320
5.2.1 2.1. Left-handed charged currents . . . 320
5.2.2 2.2. Breaking of $\boldsymbol{P}$ - and $\boldsymbol{C}$-invariance . . . 322
5.2.3 2.3. Universality of the charged current . . . 322
5.2.4 2.4. The neutral current . . . 323
5.3 3 Muon decay . . . 324
5.3.1 3.1. Decay amplitude . . . 324
5.3.2 3.2. Decay probability . . . 325
5.3.3 3.3. Decay of polarized muon . . . 327
5.3.4 3.4. Qualitative discussion . . . 329
5.4 4 Strangeness-conserving leptonic decays of hadrons. Properties of the ud current . . . 329
5.4.1 4.1. Isotopic properties of the ud current . . . 330

5.4.2 4.2. Relationship between the vector current ud and the isovector electromagnetic current . . . 330
5.4.3 4.3. Weak charge . . . 331
5.4.4 4.4. Chiral invariance . . . 332
5.5 5 Leptonic decays of pions and nucleons . . . 333
5.5.1 5.1. $\pi \to \ell\nu$ decays . . . 333
5.5.2 5.2. $\pi^+ \to \pi^0 e^+ \nu$ decay . . . 334
5.5.3 5.3. β-decay of the neutron . . . 335
5.5.4 5.4. Vector form factors . . . 335
5.5.5 5.5. Axial form factors . . . 337
5.5.6 5.6 The probability of $\boldsymbol{\beta}$-decay. Angular correlations . . . 339
5.5.7 5.7. $\Sigma^\pm \to \Lambda e^\pm \nu$ decays . . . 340
5.6 6 Leptonic decays of K-mesons and hyperons . . . 340
5.6.1 6.2. SU(3) and SU(2) properties of the us current . . . 341
5.6.2 6.3. $K_{\ell 2}$ decays . . . 342
5.6.3 6.4. K_{t3} decays . . . 343
5.6.4 $65 K_{\mu 3}$ decays . . . 344
5.6.5 6.6. K_{e4} decays . . . 345
5.6.6 6.7. Leptonic decays of hyperons . . . 345
5.7 7 Strangeness-changing non-leptonic interactions . . . 348
5.7.1 7.1. Properties of the bare non-leptonic lagrangian . . . 348
5.7.2 7.2. The inclusion of hard gluons . . . 349
5.7.3 7.3. The gluonic monopole . . . 351
5.7.4 7.4. Effective non-leptonic lagrangian . . . 354
5.8 8 Phenomenology of non-leptonic decays of hyperons . . . 355
5.8.1 8.1. Relativistically invariant amplitude . . . 355
5.8.2 8.2. Non-relativistic form of the amplitude . . . 356
5.8.3 8.3. Spin correlations in hyperon decays . . . 356
5.8.4 8.4. Isotopic amplitudes and the $\boldsymbol{\Delta T = \frac{1}{2}}$ rule . . . 357
5.8.5 8.5 Phases of the S - and P -wave amplitudes . . . 359
5.8.6 8.6. SU(3) relation between amplitudes of hyperon decays . . . 361
5.9 9 Dynamics of non-leptonic decays of hyperons . . . 362
5.9.1 9.1. Quark graphs . . . 362
5.9.2 9.2. Factorization of external diagrams for the decay $\boldsymbol{\Lambda^0 \to p\pi^-}$ . . . 364
5.9.3 9.3. Enhancement of the contribution of right-handed quarks . . . 366
5.9.4 9.4. $\Lambda^0 \to \mathbf{n}\boldsymbol{\pi}^0$ decay . . . 367
5.9.5 9.5. Ω-hyperon decays . . . 368
5.10 10 Non-leptonic decays of K-mesons . . . 369
5.10.1 10.1. K_1^0 and K_2^0 mesons . . . 369
5.10.2 10.2. Isotopic relations for $K \to 2\boldsymbol{\pi}$ decays . . . 371
5.10.3 10.3. Quark graphs for $K^\pm \to \pi^\pm \pi^0$ decays . . . 372
5.10.4 10.4. $K \to 3\pi$ decays . . . 374
5.11 11 Neutral K-mesons in vacuum and in matter . . . 376
5.11.1 11.1. $\boldsymbol{K^0 \leftrightarrow \bar{K}^0}$ transitions and the $\boldsymbol{K_1^0 - K_2^0}$ mass difference . . . 376
5.11.2 11.2. Glashow-Iliopoulos-Maiani mechanism . . . 378
5.11.3 11.3. Oscillations of strangeness . . . 379
5.11.4 11.4. Regeneration . . . 380
5.12 12 Violation of $\boldsymbol{CP}$ invariance . . . 383
5.12.1 12.1. $K_L^0 \to \pi^+\pi^-$ decay . . . 383
5.12.2 12.2. Other observed $\boldsymbol{CP}$ violating effects . . . 384
5.12.3 12.3. Superweak mixing . . . 385
5.12.4 12.4. On decays of the K_S^0 meson . . . 386
5.12.5 12.5. Violation of time-reversal invariance and the neutron dipole moment . . . 387

5.12.6 12.6. Gedanken experiments . . . 388
5.13 13 Decays of the $\boldsymbol{\tau}$-lepton . . . 389
5.13.1 13.1. ν_τ neutrino . . . 389
5.13.2 13.2. Decays $\tau^- \to \mu^- \bar{\nu}_\mu \nu_\tau$ and $\tau^- \to \mathbf{e}^- \bar{\nu}_\mathbf{e} \nu_\tau$ . . . 390
5.13.3 13.3. Semi-hadronic decays. General remarks . . . 390
5.13.4 13.4. Decay $\tau \to \pi \nu_\tau$ . . . 391
5.13.5 13.5. Decay $\tau \to \rho \nu_\tau$ . . . 392
5.13.6 13.6. Decays $\tau \to \nu_\tau + 2n\pi$ . . . 394
5.13.7 13.7. Decays $\tau \to \nu_\tau + (2n+1)\pi$ . . . 398
5.13.8 13.8. Decays $\tau \to \nu_\tau + \mathbf{K} + n\pi$ . . . 399
5.13.9 13.9. Summary of results . . . 399
5.14 14 Decays of charmed particles . . . 399
5.14.1 14.1. Leptonic and non-leptonic decays . . . 400
5.14.2 14.2. The role of virtual gluons . . . 401
5.14.3 14.3. Selection rules for $T-, U-$, and $V-$ spin . . . 402
5.15 15 Weak decays of b- and t-quarks . . . 403
5.15.1 15.1. Unitary $n \times n$ matrix . . . 404
5.15.2 15.2. Angles $\boldsymbol{\theta}_1, \boldsymbol{\theta}_2, \boldsymbol{\theta}_3$ and phase $\boldsymbol{\delta}$ . . . 405
5.15.3 15.3. Metastability of the b-quark . . . 406
5.15.4 15.4. Contribution of t-quarks to $\mathbf{K^0} \leftrightarrow \overline{\mathbf{K}}^{\mathbf{0}}$ transitions . . . 407
5.15.5 15.5. Cascade decays of **b** - and **t**-hadrons . . . 409
5.16 16 Neutrino-electron interactions . . . 409
5.16.1 16.1. Kinematics of $\boldsymbol{\nu} + \mathbf{e} \to \boldsymbol{\nu} + \ell$ reactions . . . 409
5.16.2 16.2. Cross section of the $\nu_\mu \mathrm{e}^- \to \nu_\mathrm{e} \mu^-$reaction . . . 412
5.16.3 16.3. Cross section of the $\bar{\nu}_\mathrm{e} \mathbf{e}^- \to \bar{\nu}_\mu \boldsymbol{\mu}^-$reaction . . . 413
5.16.4 16.4. Elastic νe and $\bar{\nu}$ e scattering induced by the charged current . . . 414
5.16.5 16.5. Cross sections for the νe and $\bar{\nu}$ e scattering: general formulas . . . 416
5.16.6 16.6. Other effects of the νe interaction . . . 417
5.16.7 16.7. Creation of muon pairs by neutrinos in the Coulomb field of the nucleus . . . 418
5.17 17 Neutrino-nucleon interactions . . . 420
5.17.1 17.1. Kinematics . . . 420
5.17.2 17.2. Quasi-elastic scattering . . . 421
5.17.3 17.3. Partons . . . 423
5.17.4 17.4. Kinematics of lepton-parton collisions . . . 424
5.17.5 17.5. Lepton-parton collision cross sections . . . 424
5.17.6 17.6. Parton distributions . . . 426
5.17.7 17.7. Cross sections of deep-inelastic processes . . . 428
5.17.8 17.8. Production of strange and charmed particles . . . 428
5.17.9 17.9. Phenomenology of deep-inelastic processes . . . 429
5.17.10 17.10. The parton model and quantum chromodynamics . . . 430
5.18 18 Renormalizability . . . 431
5.18.1 18.1. Why do we need renormalizability? . . . 431
5.18.2 18.2. Unitarity limit . . . 432
5.18.3 18.3. Intermediate bosons . . . 432
5.18.4 18.4. Wave function of the vector boson . . . 434
5.18.5 18.5. Digression on the photon mass . . . 435
5.18.6 18.6. Vector boson propagator . . . 436
5.19 19 Gauge invariance . . . 437
5.19.1 19.1. Global abelian symmetry $\mathbf{U(1)}$ . . . 437
5.19.2 19.2. Global non-abelian symmetry SU(2) . . . 437
5.19.3 19.3. Local abelian symmetry . . . 437
5.19.4 19.4 Digression on baryonic and leptonic photons . . . 438
5.19.5 19.5. Local SU(2) symmetry . . . 439

5.19.6 19.6. Panegyric to Yang-Mills theory . . . 441
5.19.7 19.7. How to take masses into account? . . . 442
5.20 20 Spontaneous symmetry breaking . . . 443
5.20.1 20.1. Spontaneous breaking of discrete symmetry . . . 443
5.20.2 20.2. Spontaneous breaking of global $U(1)$ symmetry . . . 446
5.20.3 20.3. Spontaneous breaking of global SU(2) symmetry . . . 448
5.20.4 20.4. Spontaneous breaking of abelian gauge symmetry . . . 448
5.20.5 20.5. On the conservation of electric charge . . . 449
5.20.6 20.6. Spontaneous breaking of local SU(2) symmetry . . . 450
5.21 21 Standard model of the electroweak interaction . . . 451
5.21.1 21.1. Main features of the model . . . 452
5.21.2 21.2. Nine terms of the lagrangian . . . 453
5.21.3 21.3. Masses of **W** - and **Z**-bosons . . . 454
5.21.4 21.4. Relation between electric charge and the constants g and g' . . . 456
5.21.5 21.5. Relation between the vacuum-expectation value η and the Fermi constant G 457
5.21.6 21.6. More about the masses of the W - and Z -bosons . . . 458
5.21.7 21.7. Electron mass . . . 458
5.21.8 21.8. Introduction of other leptons and quarks . . . 459
5.22 22 Neutral currents . . . 461
5.22.1 22.1. Scattering of ν_e and $\overline{\nu}_e$ on the electron . . . 462
5.22.2 22.2. Scattering of ν_μ and $\overline{\nu}_\mu$ on the electron . . . 464
5.22.3 22.3. Annihilation $e^+e^- \to \mu^+\mu^-$ . . . 465
5.22.4 22.4. Neutral currents and neutrino-nucleon interaction . . . 468
5.22.5 22.5. Isotopic properties of the neutral current . . . 470
5.22.6 22.6. Parity non-conservation in scattering of electrons by nucleons . . . 471
5.22.7 22.7. Parity non-conservation in atoms . . . 473
5.22.8 22.8. P-odd nuclear forces . . . 474
5.23 23 Properties of intermediate bosons . . . 474
5.23.1 23.1. Decays of W-bosons . . . 475
5.23.2 23.2. Decays of Z -bosons . . . 476
5.23.3 23.3. Production of Z -bosons . . . 476
5.23.4 23.4. Production of W-bosons . . . 477
5.23.5 23.5. Colliding beam projects . . . 479
5.23.6 23.6. DUMAND . . . 480
5.24 24 Properties of Higgs bosons . . . 481
5.24.1 24.1. On the H-boson mass . . . 481
5.24.2 24.2. The role of **H**-bosons at high energies . . . 482
5.24.3 24.3. Coupling of **H**-bosons to heavy quarks . . . 484
5.24.4 24.4. Coupling of **H**-bosons to gluons . . . 485
5.24.5 24.5. "Higgs charge" of nucleons . . . 486
5.24.6 24.6. Digression on the trace of the energy-momentum operator . . . 487
5.24.7 24.7. Coupling of **H**-bosons to **W** - and **Z**-bosons . . . 488
5.24.8 24.8. Coupling of **H**-bosons to photons . . . 489
5.24.9 24.9. General remarks on Higgs bosons . . . 490
5.25 25 Grand unification . . . 491
5.25.1 25.1. Three generations of fermions . . . 491
5.25.2 25.2. Quintet and decuplet in SU(5) . . . 492
5.25.3 25.3. 24 vector bosons . . . 493
5.25.4 25.4. Running coupling constants . . . 493
5.25.5 25.5. Unstable proton . . . 496
5.25.6 25.6. Grand Higgs bosons . . . 498
5.25.7 25.7. The **SO(10)** group and other orthogonal groups . . . 500
5.25.8 25.8. The exceptional groups . . . 501

5.26 26 Superunification . . . 502
5.26.1 26.1. Supersymmetry . . . 502
5.26.2 26.2. Sub-quarks? . . . 503
5.27 27 Particles and the universe . . . 504
5.27.1 27.1. Hot universe . . . 504
5.27.2 27.2. Upper bound on the neutrino mass . . . 507
5.27.3 27.3. Ont the number of possible types of neutrinos . . . 507
5.27.4 27.4. Concentration of relic quarks . . . 508
5.27.5 27.5. On baryonic asymmetry of the universe . . . 509
5.28 28. Bibliography . . . 510
5.28.1 28.1. Monographs. Proceedings of conferences . . . 511
5.28.2 28.2. Decays of leptons and hadrons . . . 513
5.28.3 28.3. Neutrino reactions . . . 519
5.28.4 28.4. Weak interactions at high energies . . . 522
5.28.5 28.5. Models of grand and super unification . . . 526
5.28.6 28.6. Particles and the universe . . . 527
5.28.7 28.7. Supplementary bibliography (autumn 1980) . . . 531
5.29 29 Appendix (Some useful formulas) . . . 537
5.29.1 29.1. Pseudoeuclidean metric . . . 538
5.29.2 29.2. Groups . . . 538
5.29.3 29.3. Properties of Dirac matrices . . . 546
5.29.4 29.4. Rules for the calculation of probabilities . . . 551
5.30 30 Tables of experimental data* . . . 554
5.30.1 30.1. Physical and numerical constants and parameters . . . 555
5.30.2 30.2. Tables of particle properties . . . 558
5.30.3 30.3. Weak decays and $\Delta I = \frac{1}{2}$ rule* . . . 568
5.30.4 30.4. CP and CPT invariances* . . . 574
5.30.5 30.5. Conservation of leptonic numbers . . . 576
5.30.6 30.6. Selection rules for the weak current* . . . 577

6 Standard Model by Zhou **579**
6.1 Introduction . . . 579
6.1.1 Particle and Interactions . . . 579
6.1.2 Symmetries and Conservation Laws . . . 582
6.1.3 Bound States . . . 586
6.1.4 Quantum Chromodynamics . . . 591
6.2 Symmetries . . . 595
6.2.1 Chiral and Gauge Symmetries . . . 595
6.2.2 Discrete Symmetries . . . 598
6.2.3 Parity . . . 601
6.2.4 Charge Conjugation . . . 604
6.2.5 Time Reversal . . . 609
6.3 Spontaneous Symmetry Breaking . . . 611
6.3.1 Classical Fields . . . 611
6.3.2 Quantum Fields . . . 613
6.3.3 Gauge Theories . . . 616
6.3.4 Quantization . . . 620
6.4 Electroweak Theory . . . 622
6.4.1 Gauge Theory . . . 622
6.4.2 Coupling to Matter . . . 624
6.4.3 Symmetries of the Standard Model . . . 630
6.4.4 Electroweak Decays . . . 635
6.4.5 CP Violation . . . 640
6.5 Neutrinos . . . 642

6.5.1 Historical Review . . . 642
6.5.2 Neutrino Oscillations . . . 644
6.5.3 Neutrino Masses . . . 649
6.6 Quantum Chromodynamics . . . 651
6.6.1 Hadron Production . . . 651
6.6.2 Deep Inelastic Scattering . . . 656
6.6.3 Chiral Symmetry . . . 659
6.6.4 Chiral Perturbation Theory . . . 662
6.6.5 The Strong CP Problem . . . 664

III Reactions and Decays of Particles 667

7 Other reactions 667
7.1 Rare Weak Decays of the Omega Baryon by Mommers . . . 667
7.1.1 Introduction . . . 667
7.1.2 Theoretical preliminaries . . . 670
7.1.3 Chiral perturbation theory . . . 683
7.1.4 The heavy-baryon formalism . . . 693
7.1.5 Nonleptonic three-body Omega decays . . . 701
7.1.6 Semileptonic and radiative Omega decays . . . 724

IV Problems 732

8 Typical Problems (???) 732

V —— Special Particle Physics in a Nutshell —— 733

9 Other Statements 733
9.1 Other Phenomena . . . 733
9.2 Particles in Cosmology . . . 733
9.3 Hypothetical Properties of Particles and Theories in a Nutshell . . . 733

VI Experimental particle physics 734

10 Phenomena that are Used for Measurements 734
10.0.1 Motion in Collider . . . 734

11 Registration of Particles 734

12 Some Experimental Setups 734
12.0.1 COMPASS . . . 734

VII Other Topics 735

13 Lists and Tables of Properties of Particles 735
13.0.1 Electron . . . 735
13.0.2 Positron . . . 739
13.0.3 Photon . . . 740
13.1 Hypothetical Particles from Cosmology . . . 743

14 Exotic Particles **743**
14.1 Particles in Riemannian Surface . . . 743
14.1.1 General Questions about Particles in Riemannian Surface . . . 743

15 Other Phenomena **743**
15.1 Passing Through Matter . . . 743
15.2 Air shower (???) . . . 743

16 Grand Unified Theories **743**
16.1 GUE . . . 743

17 Theories about Which It is Hard to Think Seriously **743**
17.0.1 Phoenix theory (???) . . . 743
17.1 Ancient Theories (???) . . . 743

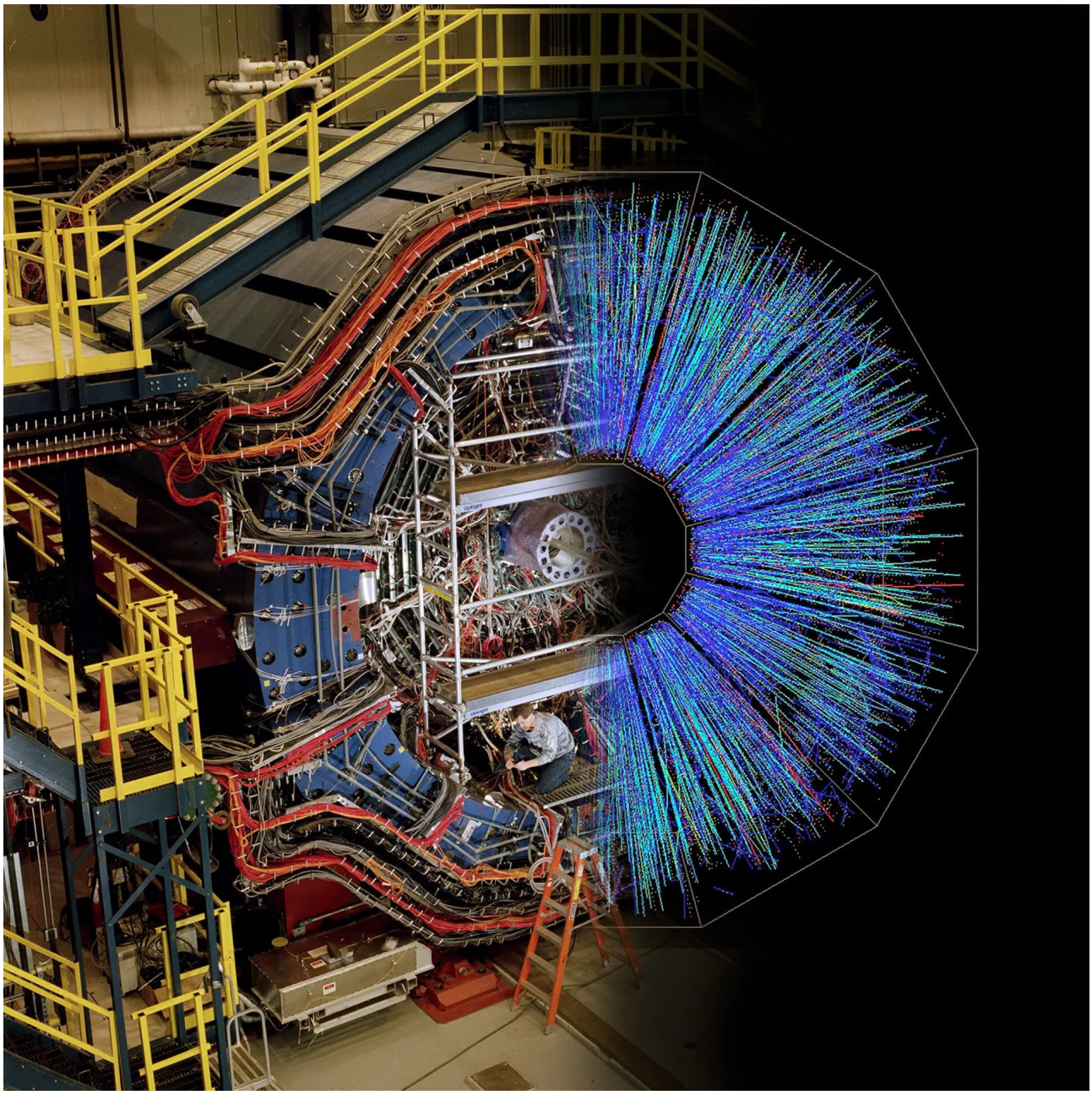
VIII Appendix **744**

A Introduction **744**
A.1 Extra Motivation . . . 744
A.2 Approach to Particle Physics . . . 746
A.3 Literature on Particle Physics . . . 746
A.3.1 Main Literature . . . 746
A.3.2 Special Theoretical Literature . . . 747
A.3.3 Special Experimental Literature . . . 748
A.3.4 Other Literature . . . 748
A.4 History in a Nutshell . . . 749
A.5 Popular Introduction . . . 749
A.6 Definitions . . . 750
A.7 Puzzles for Different Cases . . . 750
A.7.1 Typical Fundamental Questions . . . 750
A.7.2 Fun General Questions . . . 752
A.7.3 Fun Hypothetical Questions . . . 752
A.7.4 Very Hard, Unanswered General Questions . . . 752

B Special Mathematics and Physics **752**
B.1 Algebra for Particle Physics . . . 752
B.2 Physics for Particle Physics . . . 752
B.2.1 Symmetries . . . 752
B.2.2 Spinors . . . 753

C Bibliography **754**

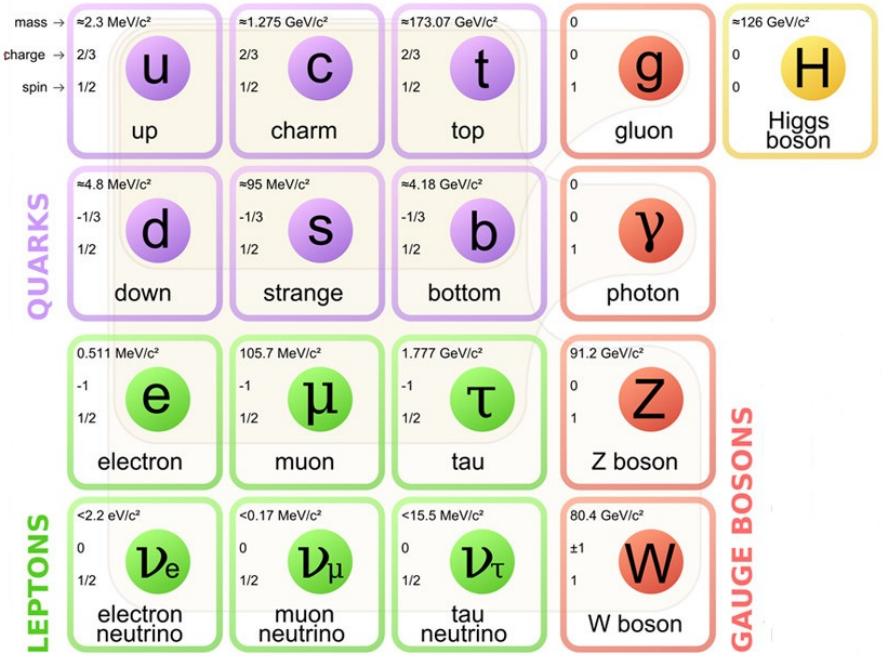
Preface and main motivation



Part I
Typical Particle Physics in a Nutshell

1 Main Information About Particles (???)

1.1 Overview of main properties and reactions



type		mass	spin	g
quarks	$t, \bar{t}$	173 GeV	$\frac{1}{2}$	$2 \cdot 2 \cdot 3 = 12$
	$b, \bar{b}$	4 GeV		
	$c, \bar{c}$	1 GeV		
	$s, \bar{s}$	100 MeV		
	$d, \bar{s}$	5 MeV		
	$u, \bar{u}$	2 MeV		
gluons	g_i	0	1	$8 \cdot 2 = 16$
leptons	$\tau^{\pm}$	1777 MeV	$\frac{1}{2}$	$2 \cdot 2 = 4$
	$\mu^{\pm}$	106 MeV		
	$e^{\pm}$	511 keV		
	$\nu_\tau, \bar{\nu}_\tau$	< 0.6 eV	$\frac{1}{2}$	$2 \cdot 1 = 2$
	$\nu_\mu, \bar{\nu}_\mu$	< 0.6 eV		
	$\nu_e, \bar{\nu}_e$	< 0.6 eV		
gauge bosons	W^+	80 GeV	1	3
	W^-	80 GeV		
	Z^0	91 GeV		
	γ	0		2
Higgs boson	H^0	125 GeV	0	1

Overview of properties

Масса нейтрона: $m_n = 939.565379 \pm 0.000021$MB,

масса протона: $m_p = 938.272046 \pm 0.000021$M B;

выделяемая при бета-распаде нейтрона энергия, которая делится между протоном, электроном и нейтрино: $m_n - m_p = 1.2933322 \pm 0.0000004$ МэВ.

Время жизни нейтрона: 880.0 ± 0.9 сек. или 14.667 ± 0.015 мин.

Масса электрона: $m_e = 0.510998928 \pm 0.000000011M_\ni$B;

масса мюона: $m_\mu = 105.6583715 \pm 0.0000035M_\ni$B

высвобождаемая при распаде мюона максимально возможная энергия которую мог бы получить электрон: $m_\mu - m_e = 105.15$M$_\ni$B,

время жизни мюона: $(2.1969811 \pm 0.0000022) \cdot 10^{-6}$ сек.

Масса тау-лептона: $m_\tau = 1776.82 \pm 0.16$ МэВ

время жизни тау-лептона: $(290.6 \pm 1.0) \cdot 10^{-15}$ сек.

Particle $^{\text{charge}}$	Quark content	Mass [MeV]	Spin $^{\text{parity}}$	Mean lifetime [s]
π^+	$u\bar{d}$	139.57039 ± 0.00018	0^-	$(2.6033 \pm 0.0005) \times 10^{-8}$
π^-	$d\bar{u}$	139.57039 ± 0.00018	0^-	$(2.6033 \pm 0.0005) \times 10^{-8}$
π^0	$\frac{1}{\sqrt{2}}(u\bar{u} - d\bar{d})$	134.9768 ± 0.0005	0^-	$(8.43 \pm 0.13) \times 10^{-17}$
Ξ^-	dss	1321.71 ± 0.07	$\frac{1}{2}^+$	$(1.639 \pm 0.015) \times 10^{-10}$
Ξ^0	uss	1314.86 ± 0.20	$\frac{1}{2}^+$	$(2.90 \pm 0.09) \times 10^{-10}$
Ξ^{*-}	dss	1535.0 ± 0.6	$\frac{3}{2}^+$	$(6.7 \pm 1.3) \times 10^{-23}$
Ξ^{*0}	uss	1531.80 ± 0.32	$\frac{3}{2}^+$	$(7.2 \pm 0.4) \times 10^{-23}$
Ω^-	sss	1672.45 ± 0.29	$\frac{3}{2}^+$	$(0.821 \pm 0.011) \times 10^{-10}$

Таблица 2.1: Свойства фундаментальных взаимодействий.

Тип взаимодействия	Сильное	Электро-магнитное	Слабое	Гравита-ционное
Сила взаимодействия	1	1/137	10^{-6}	10^{-38}
Переносчик взаимодействия	глюон	фотон	W^+, W^- Z^0-бозоны	гравитон(?)
Масса переносчика	0	0	$W^\pm$ 80 ГэВ, Z^0 91 ГэВ	0
Спин переносчика	1	1	1	2(?)
Радиус взаимодействия	10^{-15} м	∞	10^{-18} м	∞
Участники взаимодействия	адроны	заряженные частицы	все частицы	все частицы

Overview of reactions

1.1.1 Main Parameters of the Particles

(пока что без структуры)

изоспин

углы смешивания

очень тоже известная тема.

античастицы

крч как встречусь с ними снова - впишу про это. очень много деталей.

Покая ч знаю, что..

свойства античастиц

Они отличаются только изоспином и магнитным моментом

аннигиляция античастиц

хз

резонансы

(пока что вне структур)

брейт-вигнеровские частицы

Арганд-плот

описание его и зачем он нужен.

да хз, зачем на самом деле, изучу, потом напишу.

магнитный момент

аномальный магнитный момент

Как мы видели, значение фактора Ланде $g = 2$ есть прямое следствие калибровочной инвариантности взаимодействия с безмассовым векторным полем и рецепта минималъной связи заряда с полем: длинная ковариантная производная или обобщенный импульс.

Однако при наличии спина существует также возможность введения калибровочньх взаимодействий посредством связи инвариантного тензора напряженности $F_{\mu\nu}$ с тензором спина $\hat{\sigma}^{\mu\nu}$, так как каждый из них антисимметричен.

Дополнительный вклад в действие для спинора Дирака запишем в виде

$$S_{\text{anomal}} = -\int \mathrm{d}^4 x a \frac{e\hbar}{4mc^2} F_{\mu\nu} \bar{\psi} \hat{\sigma}^{\mu\nu} \psi$$

$$\hat{\sigma}^{0\alpha} = \mathrm{i}\gamma_5 \sigma^\alpha = \mathrm{i} \begin{pmatrix} 0 & \sigma^\alpha \\ \sigma^\alpha & 0 \end{pmatrix}, \quad \hat{\sigma}^{\alpha\beta} = \varepsilon_{\alpha\beta\gamma}\sigma^\gamma = \varepsilon_{\alpha\beta\gamma} \begin{pmatrix} \sigma^\gamma & 0 \\ 0 & \sigma^\gamma \end{pmatrix} \text{(предст. Дирака)}$$

В нерелятивистском приближении $p \to 0$ биспинор Дирака сводится к нерелятивистскому спинору $\psi \approx (\varphi, 0)$.

Поэтому в аномальном взаимодействии 11.42) ненулевой вклад дает только диагональный член с $\hat{\sigma}^{\alpha\beta}$

$$S_{\text{anomal}} \approx -\int \mathrm{d}^4 x a \frac{e\hbar}{4mc^2} F_{\alpha\beta} \varepsilon_{\alpha\beta\gamma} \varphi^\dagger \sigma^\gamma \varphi$$

так что стандартная связь компонент тензора напряженности с магнитным полем $F_{\alpha\beta}\varepsilon_{\alpha\beta\gamma} = -2\mathcal{H}^\gamma$ приводит к

$$S_{\text{anomal}} \approx +\int \mathrm{d}t \int \mathrm{d}^3 r \varphi^\dagger (\sigma \cdot \mathcal{H}) a \frac{e\hbar}{2mc}$$

т. е. к аномальному магнитному моменту частицы со спином $1/2$:

$$\mu = (1+a)\frac{e\hbar}{mc}(s\cdot\mathcal{H})$$

Таким образом, вообще говоря, магнитный момент за счет аномального вклада мог бы принимать произвольные значения.

Однако в квантовой теории поля, учитывающей петлевые поправки в теории возмущений, прямое включение члена с аномальным магнитным моментом недопустимо, так как он приводит к так называемым неперенормируемым поправкам: петлевые по- правки могут принимать конечные значения только при введении бесконечно счетного числа новых членов взаимодействий с соответствующими новыми константами.

Чтобы избежать подобного логического тупика, сводящего пред- сказательную силу теории к нулю, необходимо положить исходный или, как говорят, затравочный аномальный магнитный момент равным нулю. Тогда учет петлевых поправок становится однозначным (теория перенормируема), и эти поправки в теории возмущений приводят к малому по константе взаимодействия α_{em} аномальному магнитному моменту частицы со спином $1/2$, так что согласно Швингеру

что согласуется с экспериментом. Поскольку отклонения аномального магнитного момента от расчетного свидетельствовало бы о наличии неизвестного типа взаимодействий, изме- рения аномального магнитного момента с высочайшей точностью находятся на переднем фронте современных экспериментальных исследований: точность для мюона достигла двенадцати порядков значащих цифр. В настоящее время данные согласуются с расчетами на основе калибровочных теорий электромагнитных, слабых и сильных взаимодействий.

вычисление магнитных моментов барионов

научимся их считать

Задача

Вычислить магнитные моменты барионов в составной модели конституэнтных (составных) $u-, d$ - и s -кварков:

протона $p=(uud)$, нейтрона $n=(ddu)$ и заряженных сигма-гиперонов $\Sigma^+=(uus), \Sigma^-=(dds)$.

Считать, что барионы являются антисимметричными состояниями кварков трех цветов: квантовое число $\alpha=\{1,2,3\}\equiv\{$ синий, красный, желтый $\}$, так что, например, цветовое состояние протона $\mid \text{color} \rangle = \frac{1}{\sqrt{6}}\varepsilon_{\alpha\beta\gamma}u^\alpha u^\beta d^\gamma$.

Заряды кварков положить равными $Q_u=2/3$ $Q_d=Q_s=-1/3$ в единицах заряда протона e, в то время как массам кварков сопоставить реалистические значения $m_u=m_d=330\text{МВ}, m_s=480\text{МВ}$. Массу нуклона считать равной $m_N=940$ МэВ.

Выразить результат в единицах ядерного магнетона $\mu_N=\frac{e\hbar}{2m_Nc}$. Сравнить с экспериментальными данными: $\mu_p=2,79\mu_N, \mu_n=-1,91\mu_N$ $\mu_{\Sigma^+}=2,46\mu_N, \mu_{\Sigma^-}=-1,16\mu_N$. Какой вывод можно сделать о значениях g -факторов конституэнтных кварков в барионах?

Решение.

Барионы, рассматриваемые в задаче, являются основными состояниями для каждой из заданных кварковых систем, т. е. кварки находятся в s -волновых конфигурациях с нулевым орбитальным моментом.

Более того, модель конституэнтных кварков предполагает, что движением кварков в барионах можно пренебречь: кварки покоятся в системе покоя бариона, так что энергия связи мала, и масса бариона приближенно дается суммой масс конституэнтных кварков, $M_B\approx\sum\limits_q m_q$ Поэтому в задаче о магнитных моментах пространственная часть волновой функции кварков несущественна (она симметрична по перестановкам тождественных кварков),

и вектор состояния бариона по сути сводится к произведению состояний, факторизованных по цвету и спину:

$$|\text{baryon}\ \rangle = |\text{color}\ \rangle|\ \text{spin}\rangle.$$

Цветовое состояние определено условием задачи. Оно является нормированным на единицу. Важно, что это состояние является антисимметричным по перестановке кварков, так как в каждом из рассматриваемых барионов есть по паре тождественных кварков, которые являются фермионами.

Состояние тождественных фермионов, согласно принципу Паули, должно быть антисимметрично по перестановке частиц. Отсюда с учетом антисимметрии цветовой части состояния следует, что спиновая часть волновой функции должна быть симметричной относительно перестановки тождественных кварков. Поэтому спиновое состояние, скажем, пары u - кварков имеет спин $S = 1$, т. е. является векторным, а состояние с нулевым спином, скалярное состояние, запрещено. Полный спин исследуемых барионов равен $1/2$. Его можно представить как сумму спина двух тождественных кварков и третьего кварка, т. е. как результат сложения спина 1 и спина $1/2$. Например, для состояния протона $|j, m\rangle$

$$|1/2, +1/2\rangle_p = \sqrt{\frac{2}{3}}|1, +1\rangle|-\rangle_d - \sqrt{\frac{1}{3}}|1, 0\rangle|+\rangle_d$$

где $|\pm\rangle_d$ - спиновое состояние d -кварка, а спиновые состояния пары u -кварков задаются стандартным образом:

$$\begin{gathered}|1, +1\rangle = |+\rangle_{u_1}|+\rangle_{u_2} \\ |1, 0\rangle = \tfrac{1}{\sqrt{2}}\left(|+\rangle_{u_1}|-\rangle_{u_2} + |-\rangle_{u_1}|+\rangle_{u_2}\right)\end{gathered}$$

Найдем магнитный момент бариона как среднее значение суммы проекций магнитных моментов кварков на ось z в заданном нами состоянии:

$$\mu_B = \left\langle \sum_q g_q \frac{e\hbar}{2m_q c} Q_q s_z^q \right\rangle = \frac{e\hbar}{2m_N c}\left\langle \sum_q \frac{m_N}{m_q} Q_q g_q s_z^q \right\rangle = \mu_N \left\langle \sum_q \frac{m_N}{m_q} Q_q g_q s_z^q \right\rangle$$

где $g \approx 2$ для дираковской частицы. Для протона, очевидно, действие операторов спина кварков с соответствующими факторами дает

$$\sum_{q=u_1,u_2} \frac{m_N}{m_u} Q_u g_u s_z^q |1, +1\rangle = g_u \frac{m_N}{m_u} Q_u |1, +1\rangle$$

$$\sum_{q=u_1,u_2} \frac{m_N}{m_u} Q_u g_u s_z^q |1, 0\rangle = 0$$

$$\frac{m_N}{m_d} Q_d g_d s_z^d |\pm\rangle = \pm \frac{g_d}{2}\frac{m_N}{m_d} Q_d |\pm\rangle$$

В итоге магнитный момент протона равен

$$\mu_p = \mu_N \left\{ \frac{2}{3}\left(g_u \frac{m_N}{m_u} Q_u - g_d \frac{m_N}{2m_d} Q_d \right) + \frac{1}{3} g_d \frac{m_N}{2m_d} Q_d \right\} = \mu_N \left\{ g_u \frac{4}{9}\frac{m_N}{m_u} + g_d \frac{1}{18}\frac{m_N}{m_d} \right\}$$

Совершенно аналогично для нейтрона [1] $n = (ddu)$

$$\mu_n = \mu_N \left\{ g_d \frac{2}{3}\frac{m_N}{m_d} Q_d - g_u \frac{1}{6}\frac{m_N}{m_u} Q_u \right\} = \mu_N \left\{ -g_d \frac{2}{9}\frac{m_N}{m_d} - g_u \frac{1}{9}\frac{m_N}{m_u} \right\}$$

для гиперона $\Sigma^+ = (uus)$

$$\mu_{\Sigma^+} = \mu_N \left\{ g_u \frac{2}{3} \frac{m_N}{m_u} Q_u - g_s \frac{1}{6} \frac{m_N}{m_s} Q_s \right\} = \mu_N \left\{ g_u \frac{4}{9} \frac{m_N}{m_u} + g_s \frac{1}{18} \frac{m_N}{m_s} \right\}$$

для гиперона $\Sigma^- = (dds)$

$$\mu_{\Sigma^-} = \mu_N \left\{ g_d \frac{2}{3} \frac{m_N}{m_d} Q_d - g_s \frac{1}{6} \frac{m_N}{m_s} Q_s \right\} = \mu_N \left\{ -g_d \frac{2}{9} \frac{m_N}{m_d} + g_s \frac{1}{18} \frac{m_N}{m_s} \right\}$$

В ведущем приближении положим g -факторы для всех кварков равными 2. Тогда в сравнении с экспериментом получим - ведущее приближение:

$$\mu_p = 2,85\mu_N, \quad \mu_n = -1,90\mu_N, \quad \mu_{\Sigma^+} = 2,75\mu_N, \quad \mu_{\Sigma^-} = -1,05\mu_N$$

- эксперимент:

$$\mu_p = 2,79\mu_N, \quad \mu_n = -1,91\mu_N, \quad \mu_{\Sigma^+} = 2,46\mu_N, \quad \mu_{\Sigma^-} = -1,16\mu_N$$

Это сравнение указывает на то, что g -факторы близки к теоретико-полевому значению, которое не учитывает квантовые эффекты. Оценим величину этих эффектов. Для этого составим следующие правила сумм, которые позволяют получить значения g -факторов из экспериментальных данных путем разрешения выражений для магнитных моментов как уравнений для g -факторов. В самом деле, например,

$$\frac{1}{\mu_N} (4\mu_p + \mu_n) = \frac{5}{3} g_u \frac{m_N}{m_u}$$

Отсюда получаем, что с экспериментом согласуется значение

$$g_u \approx 1,97$$

Аналогично, для d -кварка находим

$$\frac{1}{\mu_N} (\mu_p + 4\mu_n) = -\frac{5}{6} g_d \frac{m_N}{m_d} \Rightarrow g_d \approx 2,04$$

Однако эти поправки лишь слегка уменьшают разногласие в значениях магнитных моментов для гиперонов. Конечно, согласие применяемой модели с экспериментом можно улучшить, учитывая, например, энергию связи кварков: эффективные массы кварков будут несколько больше для более тяжелых по сравнению с нуклонами гиперонов, - - и вводя другие поправки [2]

Тем не менее, можно считать, что упрощенная картина представления сложных барионных систем в виде трех покоящихся конституэнтных кварков дает правильные качественные результаты с точностью лучше 10% для магнитнь̈х моментов g -факторами кварков, близкими к 2.

а какие выводы мы делаем?

1.1.2 Typical Motion in Colliders (!!!)

классика теорпола и очень полезная тема

(проработаю заготовку эту!!)

1.1.3 The Standard Model: Main Formulas (????)

(????)

1.1.4 Standard Model: Main Details (????)

1.1.5 Types of plots for experimental results

типы графиков

какие есть?

типичные графики

просто списком их приведем, что самое основное, в какие графики смотрят чаще всего люди?

я пока что хз.

1.1.6 Main Experimental Predictions of Hypothetical Theories

(??? I'll collect them here later, it will be very useful)

1.2 General overview of Standard model

1.2.1 First Look at Quantum Fields by Tong

2.1 Matter Fields and Force Fields 30 2.1.1 Spin 31 2.1.2 The Dirac Equation 32 2.1.3 Anti-Matter 33 2.1.4 Massless Particles 37 2.2 Quantum Electrodynamics 38 2.2.1 Feynman Diagrams 41 2.2.2 What is a Feynman Diagram Really? 44 2.2.3 New Particles From Old 47 2.3 Renormalisation 48 2.3.1 The Long, Confusing History of Renormalisation 51 B Interlude: Looking to the Sky 55 B.1 The Positron 56 B.2 Expecting a Meson 59 B.3 The Muon and the Pion 60 B.4 The Beginning of the Deluge 63

1.2.2 On problems of Standard model (???)

(про это рассуждения)

1.3 The Strong Force by Tong

3.1 Yang-Mills Theory 65 3.1.1 Gluons and Asymptotic Freedom 67 3.1.2 The Mass Gap 71
3.2 Quarks 72 3.2.1 Colour 7 3.2.2 A First Look at Mesons and Baryons 75
3.3 Baryons 77 3.3.1 Protons and Neutrons 77 3.3.2 Delta Baryons 79 3.3.3 Strangeness 80
3.3.4 The Eightfold Way 82
3.4 Mesons 84 3.4.1 Pions 84 3.4.2 The Eightfold Way Again 86
C Interlude: The Rise of the Machine 90
C.1 The Cyclotron 90
C.2 The Synchrotron 96
C.3 Quarks 101

1.4 The Weak Force by Tong

4.1 The Structure of the Standard Model 112
4.1.1 Parity Violation 112 4.1.2 A Weak Left-Hander 114 4.1.3 A Perfect Jigsaw 118
4.2 The Higgs Field 121 4.2.1 The Higgs Potential 122 4.2.2 W and Z Bosons 127 4.2.3 Weak Decays 129
4.3 Flavours of Fermions 136 4.3.1 Yukawa Interactions 136 4.3.2 Symmetry Breaking 138 4.3.3 Quark Mixing 141 4.3.4 CP Violation and Time Reversal 146 4.3.5 Conservation Laws 149
4.4 Neutrinos 154 4.4.1 Neutrino Masses 155 4.4.2 Neutrino Oscillations 161
D Interlude: Big Science for Weak Things 167
D.1 The Neutrino 168
D.2 Not P and Not CP Either 172
D.3 The Bosons of the Weak Force 176
D.4 Neutrino Oscillations 182

1.5 What We Dont Know by Tong

5.1 Beyond the Standard Model 190 5.1.1 Unification 191 5.1.2 The Higgs Potential 197 5.1.3 A Bit of Flavour and Strong CP 205
5.2 Gravity 209 5.2.1 Quantum Gravity 212
5.3 Cosmology 217 5.3.1 The Cosmological Constant 218 5.3.2 Dark Matter 223 5.3.3 Baryogenesis 227 5.3.4 Primordial Fluctuations

1.6 Strong Force in a Nutshell

1.7 Weak Force in a Nutshell

(потом додумаю)

1.7.1 $C-, P-, CP$ symmetries for particles (???)

(??? вопросы про это еще есть, вроде как тема важная, на вики написано, что нобелевскую премию за нее дали.)

P симметрия

почему P симметрии не хватает

(перепишу подробно и конкретно позже!)

В 1954г обнаружены распады K^+ в 2π и 3π, которые имеют различные четности, таким образом, P четность не сохранялась.

Также изучался β-распад поляризованных ядер ^{69}Co

тут что-то тоже такое было.

решение было в рассмотрении CP симметрии

почему CP симметрии не хватает

О теории Печчеи — Квинн (!??!??????)

(вики см. например)

Теория Печчéи — Квинн в физике элементарных частиц — самое известное решение сильной CP-проблемы, то есть экспериментально наблюдаемого отсутствия нарушений CP-инвариантности в квантовой хромодинамике (КХД).

T симметрия и распространение назад во времени и память о прошлом

Vertasium раздул, а мне сказать нечего.

CPT теорема

и как это доказать?

1.8 Some Other Topics

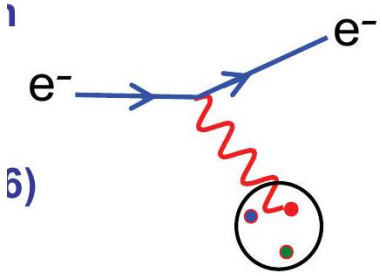
1.8.1 H5: Electron-Proton Elastic Scattering

Electron-Proton Scattering

In this handout aiming towards a study of electron-proton scattering as a probe of the structure of the proton

- Two main topics:
- $e^- p \to e^- p$ elastic scattering (this handout)

But first consider scattering from a point-like

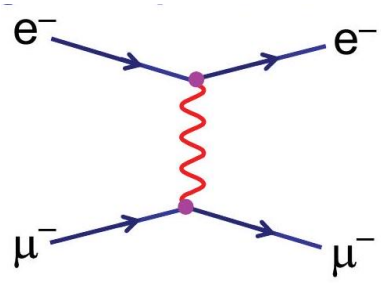


particle e.g.

$$e^- \mu^- \to e^- \mu^-$$

i.e. the QED part of $(e^- q \to e^- q)$

- Two ways to proceed:



- perform QED calculation from scratch (Q10 on examples sheet)

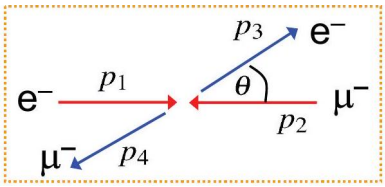
$$\left\langle |M_{fi}|^2 \right\rangle = \frac{8e^4}{(p_1 - p_3)^4} \left[(p_1 \cdot p_2)(p_3 \cdot p_4) + (p_1 \cdot p_4)(p_2 \cdot p_3) \right] \tag{1}$$

- take results from $e^+e^- \to \mu^+\mu^-$and use "Crossing Symmetry" to obtain the matrix element for $e^-\mu^- \to e^-\mu^-$(Appendix I)

$$\left\langle |M_{fi}|^2 \right\rangle = 2e^4 \frac{(p_1 \cdot p_4)^2 + (p_1 \cdot p_2)^2}{(p_1 \cdot p_3)^2} \qquad (2) \qquad = 2e^4 \left(\frac{s^2 + u^2}{t^2} \right)$$

- Work in the C.o.M:

$$p_1 = (E, 0, 0, E) \quad p_2 = (E, 0, 0, -E)$$
$$p_3 = (E, E\sin\theta, 0, E\cos\theta)$$
$$p_4 = (E, -E\sin\theta, 0, -E\cos\theta)$$

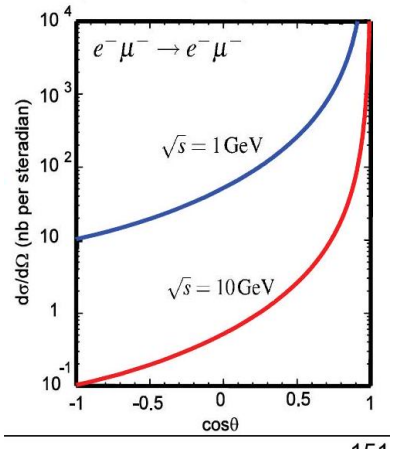


giving $p_1 \cdot p_2 = 2E^2$; $\quad p_1 \cdot p_3 = E^2(1 - \cos\theta)$; $\quad p_1 \cdot p_4 = E^2(1 + \cos\theta)$

$$\Rightarrow \left\langle |M_{fi}|^2 \right\rangle = 2e^4 \frac{E^4(1+\cos\theta)^2 + 4E^4}{E^4(1-\cos\theta)^2}$$

$$\frac{\mathrm{d}\sigma}{\mathrm{d}\Omega} = \frac{1}{64\pi^2 s} \left\langle |M_{fi}|^2 \right\rangle = \frac{e^4}{8\pi^2 s} \frac{\left[1 + \frac{1}{4}(1+\cos\theta)^2\right]}{(1-\cos\theta)^2}$$

-The denominator arises from the propagator $-ig_{\mu\nu}/q^2$ here $q^2 = (p_1 - p_3)^2 = E^2(1 - \cos\theta)$ as $q^2 \to 0$ the cross section tends to infinity.

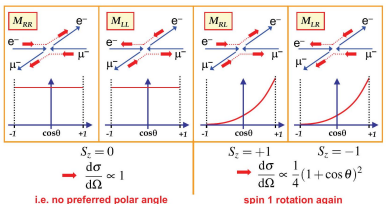


- What about the angular dependence of the numerator?

$$\frac{\mathrm{d}\sigma}{\mathrm{d}\Omega} = \frac{e^4}{8\pi^2 s} \frac{\left[1 + \frac{1}{4}(1+\cos\theta)^2\right]}{(1-\cos\theta)^2}$$

-The factor $1 + \frac{1}{4}(1 + \cos\theta)^2$ reflects helicity (really chiral) structure of QED

- Of the 16 possible helicity combinations only 4 are non-zero:



i.e. no preferred polar angle

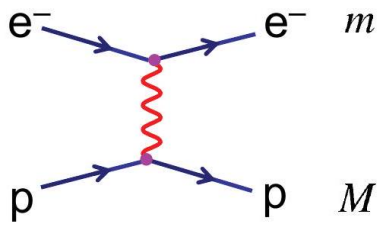
- The cross section calculated above is appropriate for the scattering of two spin half Dirac (i.e. point-like) particles in the ultra-relativistic limit (where both electron and muon masses can be neglected). In this case

$$\left\langle |M_{fi}|^2 \right\rangle = 2e^4 \frac{(p_1 \cdot p_4)^2 + (p_1 \cdot p_2)^2}{(p_1 \cdot p_3)^2}$$

-We will use this again in the discussion of "Deep Inelastic Scattering" of electrons from the quarks within a proton (handout 6).

- Before doing so we will consider the scattering of electrons from the composite proton - i.e. how do we know the proton isn't fundamental "point-like" particle?

- In this discussion we will not be able to use the relativistic limit and require the general expression for the matrix element (derived in the optional part of Q10 in the examples sheet):



$$\left\langle |M_{fi}|^2 \right\rangle = \frac{8e^4}{(p_1 - p_3)^4} \left[(p_1 \cdot p_2)(p_3 \cdot p_4) + (p_1 \cdot p_4)(p_2 \cdot p_3) - (p_1 \cdot p_3) M^2 - (p_1 \cdot p_4) m^2 + 2m^2 M^2 \right]$$

Probing the Structure of the Proton

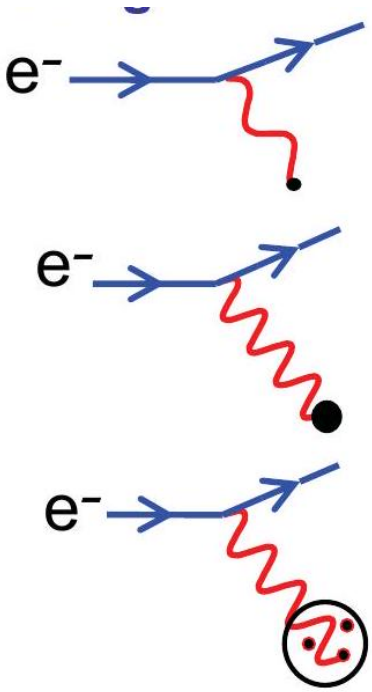
$\star$ In $e^- p \to e^- p$ scattering the nature of the interaction of the virtual photon with the proton depends strongly on wavelength

- At very low electron energies $\lambda \gg r_p$: the scattering is equivalent to that from a "point-like" spin-less object

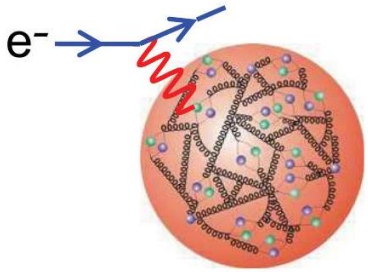
- At low electron energies $\lambda \sim r_p$: the scattering is equivalent to that from a extended charged object

- At high electron energies $\lambda < r_p$: the wavelength is sufficiently short to resolve sub-structure. Scattering from constituent quarks

- At very high electron energies $\lambda \ll r_p$: the proton appears to be a sea of



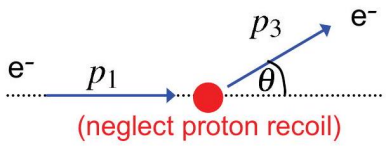
quarks and gluons.



Rutherford Scattering Revisited

⋆ Rutherford scattering is the low energy limit where the recoil of the proton can be neglected and the electron is non-relativistic

- Start from RH and LH Helicity particle spinors



$$u_\uparrow = N\begin{pmatrix} c \\ e^{i\phi}s \\ \frac{|\vec{p}|}{E+m}c \\ \frac{|\vec{p}|}{E+m}e^{i\phi}s \end{pmatrix} \quad u_\downarrow = N\begin{pmatrix} -s \\ e^{i\phi}c \\ \frac{|\vec{p}|}{E+m}s \\ -\frac{|\vec{p}|}{E+m}e^{i\phi}c \end{pmatrix} \quad \begin{array}{rcl} N & = & \sqrt{E+m}; \\ s & = & \sin(\theta/2); \quad c = \cos(\theta/2) \end{array}$$

- Now write in terms of: $\alpha = \frac{|\vec{p}|}{E+m_e}$ Non-relativistic limit: $\alpha \to 0$ Ultra-relativistic limit: $\alpha \to 1$

$$\implies \quad u_\uparrow = N\begin{pmatrix} c \\ e^{i\phi}s \\ \alpha c \\ \alpha e^{i\phi}S \end{pmatrix} \quad u_\downarrow = N\begin{pmatrix} -s \\ e^{i\phi}c \\ \alpha s \\ -\alpha e^{i\phi}c \end{pmatrix}$$

and the possible initial and final state electron spinors are:

$$u_\uparrow(p_1) = N_e \begin{pmatrix} 1 \\ 0 \\ \alpha \\ 0 \end{pmatrix} \quad u_\downarrow(p_1) = N_e \begin{pmatrix} 0 \\ 1 \\ 0 \\ -\alpha \end{pmatrix} \quad u_\uparrow(p_3) = N_e \begin{pmatrix} c \\ S \\ \alpha c \\ \alpha S \end{pmatrix} \quad u_\downarrow(p_3) = N_e \begin{pmatrix} -s \\ c \\ \alpha S \\ -\alpha c \end{pmatrix}$$

- Consider all four possible electron currents, i.e. Helicities $R \to R, L \to L, L \to R, R \to L$

$$\mathrm{e}^- \to \tag{4}$$
$$\mathrm{e}^- \smile \mathrm{e}^- \bar{u}_\downarrow(p_3)\,\gamma^\mu u_\downarrow(p_1) = (E+m_e)\left[\left(\alpha^2+1\right)c, 2\alpha s, -2i\alpha s, 2\alpha c\right] \tag{5}$$
$$\mathrm{e}^- \smile \mathrm{e}^- \bar{u}_\uparrow(p_3)\,\gamma^\mu u_\downarrow(p_1) = (E+m_e)\left[\left(1-\alpha^2\right)s, 0, 0, 0\right] \tag{6}$$
$$\mathrm{e}^- \Rightarrow \tag{7}$$

- In the relativistic limit ($\alpha = 1$), i.e. $E \gg m$

(6) and (7) are identically zero; only $R \to R$ and $L \to L$ combinations non-zero - In the non-relativistic limit, $|\vec{p}| \ll E$ we have $\alpha = 0$

$$\bar{u}_\uparrow(p_3)\,\gamma^\mu u_\uparrow(p_1) = \bar{u}_\downarrow(p_3)\,\gamma^\mu u_\downarrow(p_1) = (2m_e)\,[c,0,0,0]$$
$$\bar{u}_\uparrow(p_3)\,\gamma^\mu u_\downarrow(p_1) = -\bar{u}_\downarrow(p_3)\,\gamma^\mu u_\uparrow(p_1) = (2m_e)\,[s,0,0,0]$$

i.e. Helicity eigenstates $\neq$ Chirality eigenstates
-The initial and final state proton spinors (assuming no recoil) are:

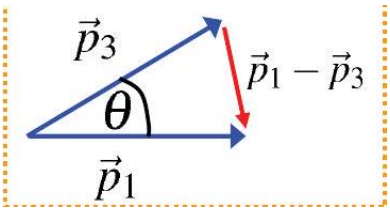
$$u_\uparrow(0) = \sqrt{2M_p} \begin{pmatrix} 1 \\ 0 \\ 0 \\ 0 \end{pmatrix} \quad u_\downarrow(0) = \sqrt{2M_p} \begin{pmatrix} 0 \\ 1 \\ 0 \\ 0 \end{pmatrix}$$

Solutions of Dirac equation for a particle at rest
giving the proton currents:

$$j_{p\uparrow\uparrow} = j_{p\downarrow\downarrow} = 2M_p(1,0,0,0)$$
$$j_{p\uparrow\downarrow} = j_{p\downarrow\uparrow} = 0$$

-The spin-averaged ME summing over the 8 allowed helicity states

$$\left\langle \left| M_{fi}^2 \right| \right\rangle = \frac{1}{4}\frac{e^4}{q^4}\left(16M_p^2 m_e^2\right)\left(4c^2+4s^2\right) = \frac{16M_p^2 m_e^2 e^4}{q^4}$$



where

$$q^2 = (p_1 - p_3)^2 = (0, \vec{p}_1 - \vec{p}_3)^2 = -4|\vec{p}|^2 \sin^2(\theta/2)$$

$$\left\langle \left| M_{fi}^2 \right| \right\rangle = \frac{M_p^2 m_e^2 e^4}{|\vec{p}|^4 \sin^4(\theta/2)}$$

Note: in this limit all angular dependence is in the propagator

- The formula for the differential cross-section in the lab. frame was derived in handout 1:

$$\frac{\mathrm{d}\sigma}{\mathrm{d}\Omega} = \frac{1}{64\pi^2}\left(\frac{1}{M + E_1 - E_1\cos\theta}\right)^2 |M_{fi}|^2 \tag{8}$$

- Here the electron is non-relativistic so $E \sim m_e \ll M_p$ and we can neglect E_1 in the denominator of equation (8)

$$\Rightarrow \frac{\mathrm{d}\sigma}{\mathrm{d}\Omega} = \frac{1}{64\pi^2 M_p^2}|M_{fi}|^2 = \frac{m_e^2 e^4}{64\pi^2 |\vec{p}|^4 \sin^4(\theta/2)}$$

- Writing $e^2 = 4\pi\alpha$ and the kinetic energy of the electron as $E_K = p^2/2m_e$

$$\left(\frac{\mathrm{d}\sigma}{\mathrm{d}\Omega}\right)_{\text{Rutherford}} = \frac{\alpha^2}{16E_K^2 \sin^4\theta/2} \tag{9}$$

⋆ This is the normal expression for the Rutherford cross section. It could have been derived by considering the scattering of a non-relativistic particle in the static Coulomb potential of the proton $V(\vec{r})$, without any consideration of the interaction due to the intrinsic magnetic moments of the electron or proton. From this we can conclude, that in this non-relativistic limit only the interaction between the electric charges of the particles matters.

The Mott Scattering Cross Section

- For Rutherford scattering we are in the limit where the target recoil is neglected and the scattered particle is non-relativistic $E_K \ll m_e$
- The limit where the target recoil is neglected and the scattered particle is relativistic (i.e. just neglect the electron mass) is called Mott Scattering
- In this limit the electron currents, equations (4) and (6), become:
- It is then straightforward to obtain the result:

$$\longrightarrow \left(\frac{\mathrm{d}\sigma}{\mathrm{d}\Omega}\right)_{\text{Mott}} = \underbrace{\frac{\alpha^2}{4E^2\sin^4\theta/2}}_{\substack{\text{Rutherford formula} \\ \text{with } E_K = E\ (E \gg m_e)}} \underbrace{\cos^2\frac{\theta}{2}}_{\substack{\text{Overlap between initial/final} \\ \text{state electron wave-functions.} \\ \text{Just QM of spin 1/2}}} \tag{10}$$

Rutherford formula with $E_K = E\ \ (E \gg m_e)$

⋆ NOTE: we could have derived this expression from scattering of electrons in a static potential from a fixed point in space $V(\vec{r})$.

The interaction is ELECTRIC rather than magnetic (spin-spin) in nature.

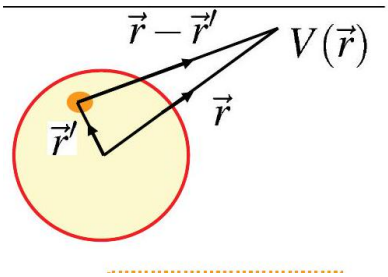
⋆ Still haven't taken into account the charge distribution of the proton.....

Form Factors

- Consider the scattering of an electron in the static potential due to an extended charge distribution.

-The potential at $\vec{r}$ from the centre is given by:

$$V(\vec{r}) = \int \frac{Q\rho\left(\vec{r}'\right)}{4\pi\left|\vec{r}-\vec{r}'\right|} d^3\vec{r}' \quad \text{with} \quad \int \rho(\vec{r})\mathrm{d}^3\vec{r} = 1$$



-In first order perturbation theory the matrix element is given by:

$$M_{fi} = \langle\psi_f|V(\vec{r})|\psi_i\rangle = \int e^{-i\vec{p}_3\cdot\vec{r}} V(\vec{r}) e^{i\vec{p}_1\cdot\vec{r}}\ \mathrm{d}^3\vec{r}$$
$$= \iint e^{i\vec{q}\cdot\vec{r}} \frac{Q\rho\left(\vec{r}'\right)}{4\pi\left|\vec{r}-\vec{r}'\right|} \mathrm{d}^3\vec{r}'\mathrm{d}^3\vec{r} = \iint e^{i\vec{q}\cdot(\vec{r}-\vec{r}')} e^{i\vec{q}\cdot\vec{r}'} \frac{\vec{p}_1}{4\pi\left|\vec{r}-\vec{r}'\right|} \mathrm{d}^3\vec{r}'\mathrm{d}^3\vec{r}$$

- Fix $\vec{r}'$ and integrate over $\mathrm{d}^3\vec{r}$ with substitution $\vec{R} = \vec{r} - \vec{r}'$

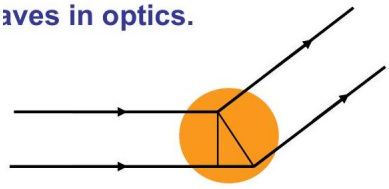
$$M_{fi} = \int e^{i\vec{q}\cdot\vec{R}} \frac{Q}{4\pi|\vec{R}|} \mathrm{d}^3\vec{R} \int \rho\left(\vec{r}'\right) e^{i\vec{q}\cdot\vec{r}'} \mathrm{d}^3\vec{r}' = \left(M_{fi}\right)_{\text{point}}\ F\left(\vec{q}^2\right)$$

⋆ The resulting matrix element is equivalent to the matrix element for scattering from a point source multiplied by the form factor

$$F\left(\vec{q}^2\right) = \int \rho(\vec{r}) e^{i\vec{q}\cdot\vec{r}}\ \mathrm{d}^3\vec{r}$$

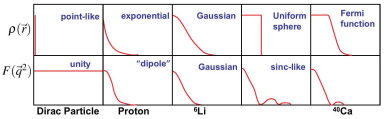
$$\left(\frac{\mathrm{d}\sigma}{\mathrm{d}\Omega}\right)_{\text{Mott}} \rightarrow \frac{\alpha^2}{4E^2\sin^4\theta/2} \cos^2\frac{\theta}{2} \left|F\left(\vec{q}^2\right)\right|^2$$

-There is nothing mysterious about form factors - similar to diffraction of plane waves in optics.



-The finite size of the scattering centre introduces a phase difference between plane waves "scattered from different points in space". If wavelength is long compared to size all waves in phase and $F\left(\vec{q}^2\right) = 1$

For example:

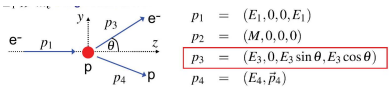


- NOTE that for a point charge the form factor is unity.

Point-like Electron-Proton Elastic Scattering

- So far have only considered the case we the proton does not recoil...

For $E_1 \gg m_e$ the general case is



- From Eqn. (2) with $m = m_e = 0$ the matrix element for this process is:

$$\left\langle |M_{fi}|^2 \right\rangle = \frac{8e^4}{(p_1 - p_3)^4} \left[(p_1 \cdot p_2)(p_3 \cdot p_4) + (p_1 \cdot p_4)(p_2 \cdot p_3) - (p_1 \cdot p_3) M^2 \right] \tag{11}$$

- Experimentally observe scattered electron so eliminate p_4
- The scalar products not involving p_4 are:

$$p_1 \cdot p_2 = E_1 M \quad p_1 \cdot p_3 = E_1 E_3 (1 - \cos\theta) \quad p_2 \cdot p_3 = E_3 M$$

- From momentum conservation can eliminate $p_4 : p_4 = p_1 + p_2 - p_3$

$$\begin{aligned} p_3 \cdot p_4 &= p_3 \cdot p_1 + p_3 \cdot p_2 - p_3 \cdot p_3 = E_1 E_3 (1 - \cos\theta) + E_3 M \\ p_1 \cdot p_4 &= p_1 \cdot p_1 + p_1 \cdot p_2 - p_1 \cdot p_3 = E_1 M - E_1 E_3 (1 - \cos\theta) \\ p_1 \cdot p_1 &= E_1^2 - |\vec{p}_1|^2 = m_e^2 \approx 0 \quad \text{i.e. neglect } m_e \end{aligned}$$

- Substituting these scalar products in Eqn. (11) gives

$$\begin{aligned} \left\langle |M_{fi}|^2 \right\rangle &= \frac{8e^4}{(p_1 - p_3)^4} M E_1 E_3 \left[(E_1 - E_3)(1 - \cos\theta) + M(1 + \cos\theta) \right] \\ &= \frac{8e^4}{(p_1 - p_3)^4} 2 M E_1 E_3 \left[(E_1 - E_3) \sin^2(\theta/2) + M \cos^2(\theta/2) \right] \end{aligned} \tag{12}$$

- Now obtain expressions for $q^4 = (p_1 - p_3)^4$ and $(E_1 - E_3)$

$$\begin{aligned} q^2 = (p_1 - p_3)^2 &= p_1^2 + p_3^2 - 2 p_1 \cdot p_3 = -2 E_1 E_3 (1 - \cos\theta) && (13) \\ &= -4 E_1 E_3 \sin^2\theta/2 && (14) \end{aligned}$$

NOTE: $q^2 < 0$ **Space-like**

- For $(E_1 - E_3)$ start from

$$q \cdot p_2 = (p_1 - p_3) \cdot p_2 = M\,(E_1 - E_3)$$

and use $(q + p_2)^2 = p_4^2 \quad q = (p_1 - p_3) = (p_4 - p_2)$

$$\begin{aligned} q^2 + p_2^2 + 2q \cdot p_2 &= p_4^2 \\ q^2 + M^2 + 2q \cdot p_2 &= M^2 \\ \longrightarrow q \cdot p_2 &= -q^2/2 \end{aligned}$$

- Hence the energy transferred to the proton:

$$E_1 - E_3 = -\frac{q^2}{2M} \tag{15}$$

Because q^2 is always negative $E_1 - E_3 > 0$ and the scattered electron is always lower in energy than the incoming electron

- Combining equations (11), (13) and (14):

$$\begin{aligned} \left\langle |M_{fi}|^2 \right\rangle &= \frac{8e^4}{16E_1^2 E_3^2 \sin^4\theta/2} 2ME_1E_3 \left[M\cos^2\theta/2 - \frac{q^2}{2M}\sin^2\theta/2 \right] \\ &= \frac{M^2 e^4}{E_1 E_3 \sin^4\theta/2} \left[\cos^2\theta/2 - \frac{q^2}{2M^2}\sin^2\theta/2 \right] \end{aligned}$$

- For $E \gg m_e$ we have (see handout 1)

$$\begin{aligned} \frac{\mathrm{d}\sigma}{\mathrm{d}\Omega} &= \frac{1}{64\pi^2}\left(\frac{E_3}{ME_1}\right)^2 |M_{fi}|^2 \\ \frac{\mathrm{d}\sigma}{\mathrm{d}\Omega} &= \frac{\alpha^2}{4E_1^2 \sin^4\theta/2}\frac{E_3}{E_1}\left(\cos^2\theta/2 - \frac{q^2}{2M^2}\sin^2\theta/2\right) \end{aligned} \tag{16}$$

$$\alpha = \frac{e^2}{4\pi} \approx \frac{1}{137}$$

Interpretation

So far have derived the differential cross-section for $e^-p \to e^-p$ elastic scattering assuming point-like Dirac spin 1/2 particles. How should we interpret the equation?

$$\frac{\mathrm{d}\sigma}{\mathrm{d}\Omega} = \frac{\alpha^2}{4E_1^2 \sin^4\theta/2}\frac{E_3}{E_1}\left(\cos^2\theta/2 - \frac{q^2}{2M^2}\sin^2\theta/2\right)$$

- Compare with

$$\left(\frac{\mathrm{d}\sigma}{\mathrm{d}\Omega}\right)_{\text{Mott}} = \frac{\alpha^2}{4E^2 \sin^4\theta/2}\cos^2\frac{\theta}{2}$$

the important thing to note about the Mott cross-section is that it is equivalent to scattering of spin 1/2 electrons in a fixed electro-static potential. Here the term E_3/E_1 is due to the proton recoil.

$$\frac{\mathrm{d}\sigma}{\mathrm{d}\Omega} = \frac{\alpha^2}{4E_1^2 \sin^4\theta/2}\frac{E_3}{E_1}(\cos^2\theta/2 - \underbrace{\frac{q^2}{2M^2}\sin^2\theta/2}) $$

-the new term: $\propto \sin^2\frac{\theta}{2} \longleftrightarrow$ Magnetic interaction: due to the spin-spin interaction

- The above differential cross-section depends on a single parameter. For an electron scattering angle θ, both q^2 and the energy, E_3, are fixed by kinematics

- Equating (13) and (15)

$$-2M\,(E_1 - E_3) = -2E_1E_3(1-\cos\theta)$$
$$\frac{E_3}{E_1} = \frac{M}{M + E_1(1-\cos\theta)}$$

- Substituting back into (13):

$$\Rightarrow q^2 = -\frac{2ME_1^2(1-\cos\theta)}{M + E_1(1-\cos\theta)}$$

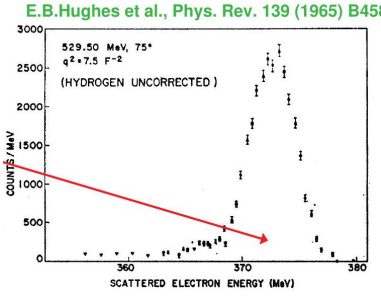
e.g. $\mathrm{e^-p} \to \mathrm{e^-p}$ at $E_{\text{beam}} = \mathbf{529.5MeV}$, look at scattered electrons at $\theta = 75°$
For elastic scattering expect:

$$E_3 = \frac{ME_1}{M + E_1(1-\cos\theta)}$$
$$E_3 = \frac{938 \times 529}{938 + 529\,(1-\cos 75°)} = 373\text{MeV}$$

The energy identifies the scatter as elastic.
Also know squared four-momentum transfer

$$|q^2| = \frac{2 \times 938 \times 529^2\,(1-\cos 75°)}{938 + 529\,(1-\cos 75°)} = 294\text{MeV}^2$$

E.B.Hughes et al., Phys. Rev. 139 (1965) B458



Elastic Scattering from a Finite Size Proton

⋆ In general the finite size of the proton can be accounted for by introducing two structure functions. One related to the charge distribution in the proton, $G_E\left(q^2\right)$ and the other related to the distribution of the magnetic moment of the proton, $G_M\left(q^2\right)$

- It can be shown that equation (16) generalizes to the ROSENBLUTH FORMULA.

$$\frac{\mathrm{d}\sigma}{\mathrm{d}\Omega} = \frac{\alpha^2}{4E_1^2 \sin^4\theta/2}\frac{E_3}{E_1}\left(\frac{G_E^2 + \tau G_M^2}{(1+\tau)}\cos^2\frac{\theta}{2} + 2\tau G_M^2 \sin^2\frac{\theta}{2}\right)$$

with the Lorentz Invariant quantity:

$$\tau = -\frac{q^2}{4M^2} > 0$$

- Unlike our previous discussion of form factors, here the form factors are a function of q^2 rather than $\vec{q}^2$ and cannot simply be considered in terms of the FT of the charge and magnetic moment distributions.

But $q^2 = \left(E_1 - E_3\right)^2 - \vec{q}^2$ and from eq (15) obtain

$$\Rightarrow \quad -\vec{q}^2 = q^2\left[1 - \left(\frac{q}{2M}\right)^2\right]$$

So for $\frac{q^2}{4M^2} \ll 1$ we have $q^2 \approx -\vec{q}^2$ and $G\left(q^2\right) \approx G\left(\vec{q}^2\right)$

- Hence in the limit $q^2/4M^2 \ll 1$ we can interpret the structure functions in terms of the Fourier transforms of the charge and magnetic moment distributions

$$G_E\left(q^2\right) \approx G_E\left(\vec{q}^2\right) = \int e^{i\vec{q}\cdot\vec{r}}\rho(\vec{r})\mathrm{d}^3\vec{r}$$
$$G_M\left(q^2\right) \approx G_M\left(\vec{q}^2\right) = \int e^{i\vec{q}\cdot\vec{r}}\mu(\vec{r})\mathrm{d}^3\vec{r}$$

- Note in deriving the Rosenbluth formula we assumed that the proton was a spin-half Dirac particle, i.e.

$$\vec{\mu} = \frac{e}{M}\vec{S}$$

- However, the experimentally measured value of the proton magnetic moment is larger than expected for a point-like Dirac particle:

$$\vec{\mu} = 2.79\frac{e}{M}\vec{S}$$

So for the proton expect

$$G_E(0) = \int \rho(\vec{r})\mathrm{d}^3\vec{r} = 1 \quad G_M(0) = \int \mu(\vec{r})\mathrm{d}^3\vec{r} = \mu_p = +2.79$$

- Of course the anomalous magnetic moment of the proton is already evidence that it is not point-like!

Measuring $G_E(q^2)$ and $G_M(q^2)$

- Express the Rosenbluth formula as:

$$\frac{\mathrm{d}\sigma}{\mathrm{d}\Omega} = \left(\frac{\mathrm{d}\sigma}{\mathrm{d}\Omega}\right)_0 \left(\frac{G_E^2 + \tau G_M^2}{(1+\tau)} + 2\tau G_M^2 \tan^2\frac{\theta}{2}\right)$$

where

$$\left(\frac{\mathrm{d}\sigma}{\mathrm{d}\Omega}\right)_0 = \frac{\alpha^2}{4E_1^2 \sin^4\theta/2}\frac{E_3}{E_1}\cos^2\frac{\theta}{2}$$

i.e. the Mott cross-section including the proton recoil. It corresponds to scattering from a spin-0 proton.

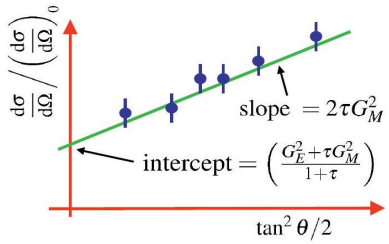
- At very low $q^2 : \tau = -q^2/4M^2 \approx 0$

$$\frac{\mathrm{d}\sigma}{\mathrm{d}\Omega} \Big/ \left(\frac{\mathrm{d}\sigma}{\mathrm{d}\Omega}\right)_0 \approx G_E^2(q^2)$$

- At high $q^2 : \tau \gg 1$

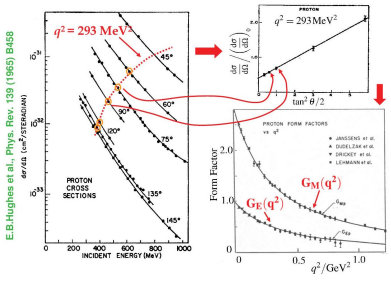
$$\frac{\mathrm{d}\sigma}{\mathrm{d}\Omega} \Big/ \left(\frac{\mathrm{d}\sigma}{\mathrm{d}\Omega}\right)_0 \approx \left(1 + 2\tau\tan^2\frac{\theta}{2}\right) G_M^2(q^2)$$

- In general we are sensitive to both structure functions! These can be resolved from the angular dependence of the cross section at FIXED q^2



EXAMPLE: $e^- p \to e^- p$ at $E_{\text{beam}} = 529.5\text{MeV}$

- Electron beam energies chosen to give certain values of q^2
- Cross sections measured to 2-3 %



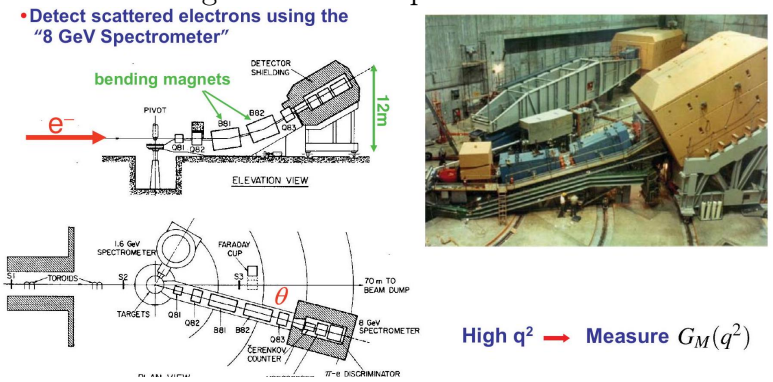
NOTE

Experimentally find $G_M(q^2) = 2.79 G_E(q^2)$ i.e. the electric and and magnetic form factors have same distribution

Higher Energy Electron-Proton Scattering

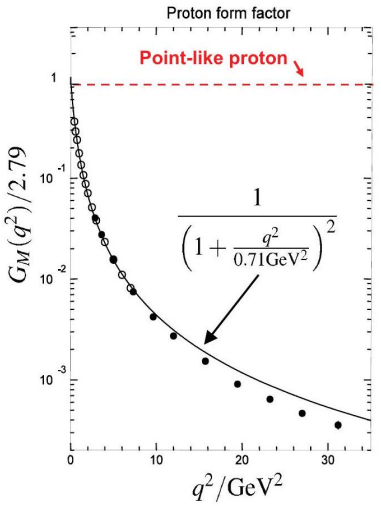
⋆ Use electron beam from SLAC LINAC: $5 < E_{\text{beam}} < 20\text{GeV}$

- Detect scattered electrons using the "8 GeV Spectrometer"



High q^2 → Measure $G_M\left(q^2\right)$
PLAN VIEW
HODOSCOPES π-e DISCRIMINATOR
P.N.Kirk et al., Phys Rev D8 (1973) 63

High q^2 Results



R.C.Walker et al., Phys. Rev. D49 (1994) 5671 A.F.Sill et al., Phys. Rev. D48 (1993) 29 ⋆ Form factor falls rapidly with q^2
-Proton is not point-like

- Good fit to the data with "dipole form":

$$G_E^p\left(q^2\right) \approx \frac{G_M^p}{2.79} \approx \frac{1}{\left(1+q^2/0.71\text{GeV}^2\right)^2}$$

⋆ Taking FT find spatial charge and magnetic moment distribution

$$\rho(r) \approx \rho_0 e^{-r/a}$$
$$a \approx 0.24\text{fm}$$

with

- Corresponds to a rms charge radius

$$r_{rms} \approx 0.8\text{fm}$$

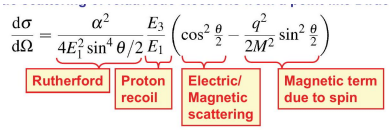
⋆ Although suggestive, does not imply proton is composite!

- Note: so far have only considered ELASTIC scattering; Inelastic scattering is the subject of next handout

)Try Question 11)

Summary: Elastic Scattering

⋆ For elastic scattering of relativistic electrons from a point-like Dirac proton:



⋆ For elastic scattering of relativistic electrons from an extended proton:

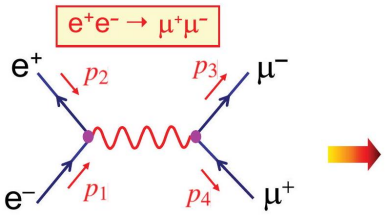
$$\frac{\mathrm{d}\sigma}{\mathrm{d}\Omega} = \frac{\alpha^2}{4E_1^2 \sin^4\theta/2}\frac{E_3}{E_1}\left(\frac{G_E^2 + \tau G_M^2}{(1+\tau)}\cos^2\frac{\theta}{2} + 2\tau G_M^2 \sin^2\frac{\theta}{2}\right)$$

Rosenbluth Formula

⋆ Electron elastic scattering from protons demonstrates that the proton is an extended object with rms charge radius of ~ 0.8fm

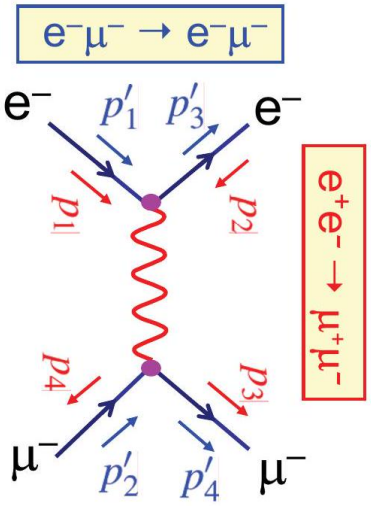
Appendix I: Crossing Symmetry

⋆ Having derived the Lorentz invariant matrix element for $e^+e^- \to \mu^+\mu^-$ "rotate" the diagram to correspond to $e^-\mu^- \to e^-\mu^-$and apply the principle of crossing symmetry to write down the matrix element!



⋆ The transformation:

$$p_1 \to p_1'; p_2 \to -p_3'; p_3 \to p_4'; p_4 \to -p_2'$$



Changes the spin averaged matrix element for

$e^- e^+ \to \mu^- \mu^+$
$p_1 p_2 \quad p_3 p_4$

$e^- \mu^- \to e^- \mu^-$
$p_1' p_2' \quad p_3' p_4'$

-Take ME for $e^+e^- \to \mu^+\mu^-$(page 143) and apply crossing symmetry:

$$\left\langle |M_{fi}|^2 \right\rangle = 2e^4 \frac{(p_1 \cdot p_3)^2 + (p_1 \cdot p_4)^2}{(p_1 \cdot p_2)^2} \Rightarrow \left\langle |M_{fi}|^2 \right\rangle = 2e^4 \frac{(p_1' \cdot p_4')^2 + (p_1' \cdot p_2')^2}{(p_1' \cdot p_3')^2} \tag{1}$$

1.8.2 H6: Deep Inelastic Scattering

e^-p Elastic Scattering at Very High q^2

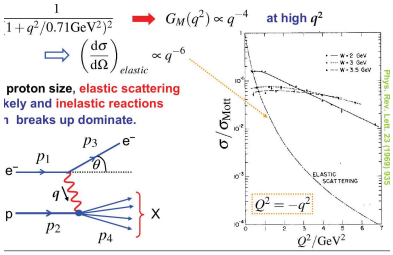
⋆ At high q^2 the Rosenbluth expression for elastic scattering becomes

$$\left(\frac{d\sigma}{d\Omega}\right)_{\text{elastic}} = \frac{\alpha^2}{4E_1^2 \sin^4 \theta/2} \frac{E_3}{E_1} \left(\frac{q^2}{2M^2} G_M^2 \sin^2 \frac{\theta}{2}\right) \quad \tau = -\frac{q^2}{4M^2} \gg 1$$

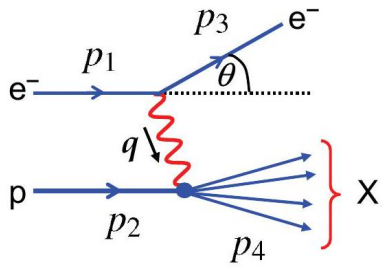
- From e^-p elastic scattering, the proton magnetic form factor is

$$G_M\left(q^2\right) \approx \frac{1}{\left(1 + q^2/0.71\text{GeV}^2\right)^2} G_M$$
$$\longmapsto \left(\frac{d\sigma}{d\Omega}\right)_{\text{elastic}} \propto q^{-6}$$

- Due to the finite proton size, elastic scattering at high q^2 is unlikely and inelastic reactions where the proton breaks up dominate.



Kinematics of Inelastic Scattering



- For inelastic scattering introduce four new kinematic variables:

x, y, v, Q^2
Define:

$$x \equiv \frac{Q^2}{2p_2 \cdot q}$$

Bjorken **x**
(Lorentz Invariant)
where

$$Q^2 \equiv -q^2$$

$$Q^2 > 0$$

- Here $M_X^2 = p_4^2 = (q + p_2)^2 = -Q^2 + 2p_2 \cdot q + M^2$

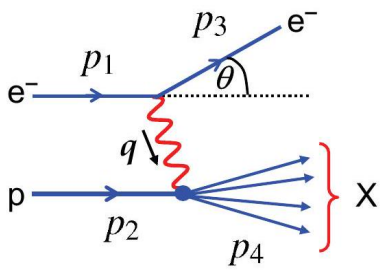
$$\Rightarrow \quad Q^2 = 2p_2.q + M^2 - M_X^2 \quad \Rightarrow \quad Q^2 \leq 2p_2.q$$

Note: in many text books W is often used in place of M_X
Proton intact
$M_X = M$
Define:

$$y \equiv \frac{p_2 \cdot q}{p_2 \cdot p_1}$$

(Lorentz Invariant)
-In the Lab. Frame:

$$p_1 = (E_1, 0, 0, E_1) \quad p_2 = (M, 0, 0, 0)$$
$$q = (E_1 - E_3, \vec{p_1} - \vec{p_3})$$
$$\Rightarrow \quad y = \frac{M\,(E_1 - E_3)}{M E_1} = 1 - \frac{E_3}{E_1}$$



So y is the fractional energy loss of the incoming particle

$$0 < y < 1$$

-In the C.o.M. Frame (neglecting the electron and proton masses):

$$p_1 = (E, 0, 0, E); \quad p_2 = (E, 0, 0, -E); p_3 = (E, E\sin\theta^*, 0, E\cos\theta^*)$$
$$\rightarrow \quad y = \frac{1}{2}(1 - \cos\theta^*) \qquad \text{for } E \gg M$$
$$v \equiv \left.\frac{p_2 \cdot q}{M}\right| \quad \text{(Lorentz Invariant)}$$

$\star$ Finally Define:

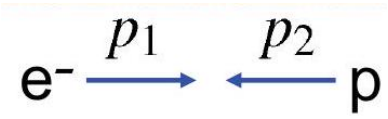
- In the Lab. Frame: $\quad v = E_1 - E_3$

v is the energy lost by the incoming particle

Relationships between Kinematic Variables

- Can rewrite the new kinematic variables in terms of the squared centre-of-mass energy, s, for the electron-proton collision

$$s = (p_1 + p_2)^2 = p_1^2 + p_2^2 + 2p_1 \cdot p_2 = 2p_1 \cdot p_2 + M^2 + \nu\Big)^2_{e^4}$$
$$2p_1 \cdot p_2 = s - M^2$$



- For a fixed centre-of-mass energy, it can then be shown that the four kinematic variables

$$Q^2 \equiv -q^2 \quad x \equiv \frac{Q^2}{2p_2 \cdot q} \quad y \equiv \frac{p_2 \cdot q}{p_2 \cdot p_1} \quad v \equiv \frac{p_2 \cdot q}{M}$$

are not independent.

- i.e. the scaling variables x and y can be expressed as

$$x = \frac{Q^2}{2Mv} \qquad y = \frac{2M}{s - M^2}v$$
$$xy = \frac{Q^2}{s - M^2} \quad \Rightarrow Q^2 = \left(s - M^2\right)xy$$

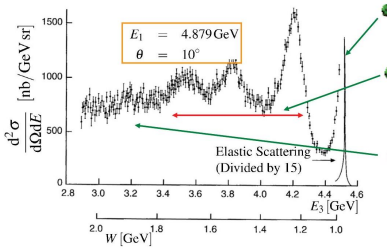
- For a fixed centre of mass energy, the interaction kinematics are completely defined by any two of the above kinematic variables (except y and v)

- For elastic scattering ($x = 1$) there is only one independent variable. As we saw previously if you measure electron scattering angle know everything else.

Inelastic Scattering

Example: Scattering of 4.879 GeV electrons from protons at rest

- Place detector at 10° to beam and measure the energies of scattered e^-
- Kinematics fully determined from the electron energy and angle !
- e.g. for this energy and angle: the invariant mass of the final state hadronic system $W^2 = M_X^2 = 10.06 - 2.03E_3$ (try and show this)



Elastic Scattering

proton remains intact

$$W = M$$

Inelastic Scattering produce "excited states"
of proton e.g. $\Delta^+(1232)$

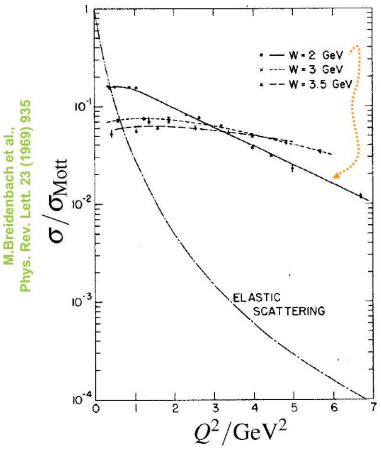
$$W = M_\Delta$$

Deep Inelastic Scattering
proton breaks up resulting in a many particle final state

$$\text{DIS} = \text{large } W$$

Inelastic Cross Sections

- Repeat experiments at different angles/beam energies and determine q^2 dependence of elastic and inelastic cross-sections



Elastic → Inelastic Scattering

*** Recall: Elastic scattering (Handout 5)**

- Only one independent variable. In Lab. frame express differential cross section in terms of the electron scattering angle (Rosenbluth formula)

$$\frac{\mathrm{d}\sigma}{\mathrm{d}\Omega} = \frac{\alpha^2}{4E_1^2 \sin^4 \theta/2} \frac{E_3}{E_1} \left(\frac{G_E^2 + \tau G_M^2}{(1+\tau)} \cos^2 \frac{\theta}{2} + 2\tau G_M^2 \sin^2 \frac{\theta}{2} \right) \quad \tau = \frac{Q^2}{4M^2}$$

Note: here the energy of the scattered electron is determined by the angle.

- In terms of the Lorentz invariant kinematic variables can express this differential cross section in terms of Q^2

(Q13 on examples sheet)

$$\frac{\mathrm{d}\sigma}{\mathrm{d}Q^2} = \frac{4\pi\alpha^2}{Q^4} \left[\frac{G_E^2 + \tau G_M^2}{(1+\tau)} \left(1 - y - \frac{M^2 y^2}{Q^2} \right) + \frac{1}{2} y^2 G_M^2 \right]$$

which can be written as:

$$\frac{\mathrm{d}\sigma}{\mathrm{d}Q^2} = \frac{4\pi\alpha^2}{Q^4} \left[f_2\left(Q^2\right) \left(1 - y - \frac{M^2 y^2}{Q^2} \right) + \frac{1}{2} y^2 f_1\left(Q^2\right) \right]$$

⋆ Inelastic scattering

- For Deep Inelastic Scattering have two independent variables. Therefore need a double differential cross section

Deep Inelastic Scattering

- It can be shown that the most general Lorentz Invariant expression for $e^- p \to e^- X$ inelastic scattering (via a single exchanged photon is):

$$\frac{\mathrm{d}^2\sigma}{\mathrm{d}x\ \mathrm{d}Q^2} = \frac{4\pi\alpha^2}{Q^4} \left[\left(1 - y - \frac{M^2 y^2}{Q^2} \right) \frac{F_2\left(x, Q^2\right)}{x} + y^2 F_1\left(x, Q^2\right) \right] \tag{1}$$

INELASTIC SCATTERING
ELASTIC SCATTERING
c.f. $\frac{\mathrm{d}\sigma}{\mathrm{d}Q^2} = \frac{4\pi\alpha^2}{Q^4} \left[\left(1 - y - \frac{M^2 y^2}{Q^2} \right) f_2\left(Q^2\right) + \frac{1}{2} y^2 f_1\left(Q^2\right) \right]$
We will soon see how this connects to the quark model of the proton

- NOTE: The form factors have been replaced by the STRUCTURE FUNCTIONS

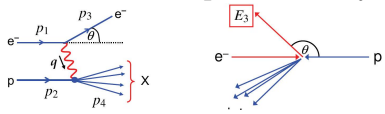
$$F_1\left(x, Q^2\right) \quad \text{and} \quad F_2\left(x, Q^2\right)$$

which are a function of x and Q^2: can not be interpreted as the Fourier transforms of the charge and magnetic moment distributions. We shall soon see that they describe the momentum distribution of the quarks within the proton

⋆ In the limit of high energy (or more correctly $Q^2 \gg M^2 y^2$) eqn. (1) becomes:

$$\frac{\mathrm{d}^2\sigma}{\mathrm{d}x\ \mathrm{d}Q^2} = \frac{4\pi\alpha^2}{Q^4} \left[(1-y) \frac{F_2\left(x, Q^2\right)}{x} + y^2 F_1\left(x, Q^2\right) \right] \tag{2}$$

- In the Lab. frame it is convenient to express the cross section in terms of the angle, θ, and energy, E_3, of the scattered electron - experimentally well measured.

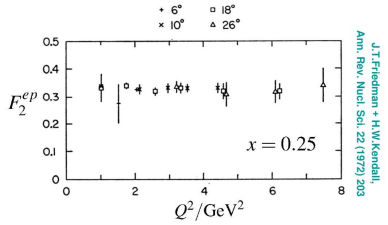


$$Q^2 = 4E_1E_3\sin^2\theta/2; \quad x = \frac{Q^2}{2M\left(E_1 - E_3\right)}; \quad y = 1 - \frac{E_3}{E_1}; \quad v = E_1 - E_3$$

-In the Lab. frame, Equation (2) becomes: (see examples sheet Q13)
$\frac{\mathrm{d}^2\sigma}{\mathrm{d}E_3\ \mathrm{d}\Omega} = \frac{\alpha^2}{4E_1^2\sin^4\theta/2}\left[\frac{1}{v}F_2\left(x,Q^2\right)\cos^2\frac{\theta}{2} + \frac{2}{M}F_1\left(x,Q^2\right)\sin^2\frac{\theta}{2}\right]$
Electromagnetic Structure Function
Pure Magnetic Structure Function

⋆ To determine $F_1\left(x,Q^2\right)$ and $F_2\left(x,Q^2\right)$ for a given x and Q^2 need measurements of the differential cross section at several different scattering angles and incoming electron beam energies (see Q13 on examples sheet)

Example: electron-proton scattering F_2 vs. Q^2 at fixed x



- Experimentally it is observed that both F_1 and F_2 are (almost) independent of Q^2

Bjorken Scaling and the Callan-Gross Relation

⋆ The near (see later) independence of the structure functions on Q^2 is known as Bjorken Scaling, i.e.

$$F_1\left(x,Q^2\right) \to F_1(x) \quad F_2\left(x,Q^2\right) \to F_2(x)$$

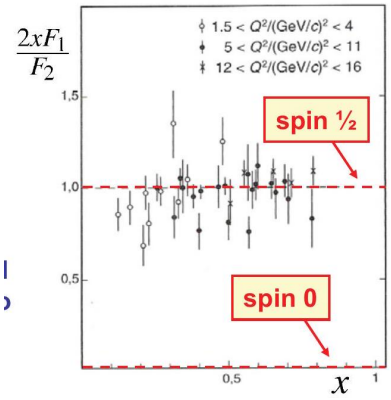
-It is strongly suggestive of scattering from point-like constituents within the proton

⋆ It is also observed that $F_1(x)$ and $F_2(x)$ are not independent but satisfy the Callan-Gross relation

$$F_2(x) = 2xF_1(x)$$

- As we shall soon see this is exactly what is expected for scattering from spin-half quarks.
- Note if quarks were spin zero particles we would expect the purely magnetic structure function to be zero, i.e.

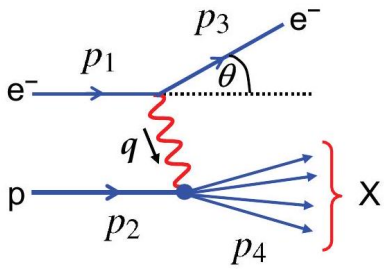
$$F_1(x) = 0$$



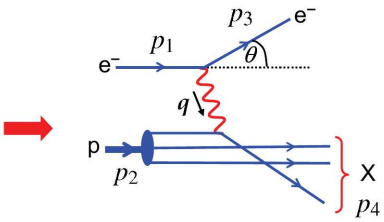
The Quark-Parton Model

- Before quarks and gluons were generally accepted Feynman proposed that the proton was made up of point-like constituents "partons"

- Both Bjorken Scaling and the Callan-Gross relationship can be explained by assuming that Deep Inelastic Scattering is dominated by the scattering of a single virtual photon from point-like spin-half constituents of the proton.



Scattering from a proton with structure functions



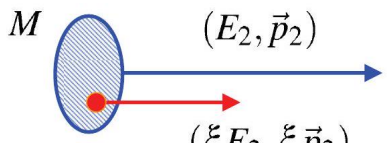
Scattering from a point-like quark within the proton
⋆ How do these two pictures of the interaction relate to each other?

- In the parton model the basic interaction is ELASTIC scattering from a "quasi-free" spin-1/2 quark in the proton, i.e. treat the quark as a free particle!

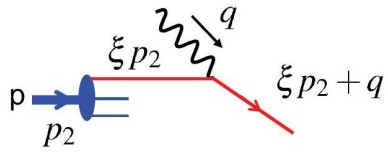
-The parton model is most easily formulated in a frame where the proton has very high energy, often referred to as the "infinite momentum frame", where we can neglect the proton mass and $p_2 = (E_2, 0, 0, E_2)$

- In this frame can also neglect the mass of the quark and any momentum transverse to the direction of the proton.

- Let the quark carry a fraction ξ of the proton's four-momentum.



$(\xi E_2, \xi \vec{p}_2)$



- After the interaction the struck quark's four-momentum is $\xi p_2 + q$

$$(\xi p_2 + q)^2 = m_q^2 \approx 0 \quad \Rightarrow \quad \xi^2 p_2^2 + q^2 + 2\xi p_2 \cdot q = 0 \quad \left(\xi^2 p_2^2 = m_q^2 \approx 0\right)$$

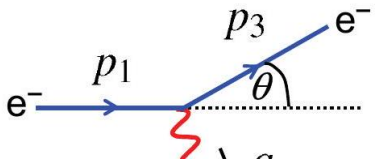
$$\rightarrow \xi = \frac{Q^2}{2p_2 \cdot q} = x$$

Bjorken x can be identified as the fraction of the proton momentum carried by the struck quark (in a frame where the proton has very high energy)

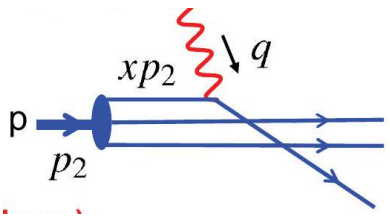
- In terms of the proton momentum

$$s = (p_1 + p_2)^2 \simeq 2p_1 \cdot p_2 \quad y = \frac{p_2 \cdot q}{p_2 \cdot p_1} \quad x = \frac{Q^2}{2p_2 \cdot q}$$

- But for the underlying quark interaction



$$s^q = (p_1 + xp_2)^2 = 2xp_1 \cdot p_2 = xs$$
$$y_q = \frac{p_q \cdot q}{p_q \cdot p_1} = \frac{xp_2 \cdot q}{xp_2 \cdot p_1} = y$$



$$x_q = 1 \quad \text{(elastic, i.e. assume quark does not break up)}$$

-Previously derived the Lorentz Invariant cross section for $e^-\mu^- \rightarrow e^-\mu^-$ elastic scattering in the ultra-relativistic limit (handout 4 + Q10 on examples sheet). Now apply this to $e^-q \rightarrow e^-q$

$$\frac{d\sigma}{dq^2} = \frac{2\pi\alpha^2 e_q^2}{q^4}\left[1 + \left(1 + \frac{q^2}{s_q}\right)^2\right]$$

- Using

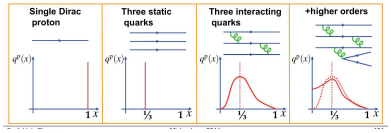
$$
\begin{aligned}
-q^2 = Q^2 &= \left(s_q - m^2\right) x_q y_q \\
\frac{\mathrm{d}\sigma}{\mathrm{d}Q^2} &= \frac{2\pi\alpha^2 e_q^2}{Q^4}\left[1 + (1-y)^2\right] \\
\frac{\mathrm{d}\sigma}{\mathrm{d}Q^2} &= \frac{4\pi\alpha^2 e_q^2}{Q^4}\left[(1-y) + \frac{y^2}{2}\right] \qquad (3)
\end{aligned}
$$

⋆ This is the expression for the differential cross-section for elastic $\mathrm{e}^{-}\mathrm{q}$ scattering from a quark carrying a fraction x of the proton momentum.

- Now need to account for distribution of quark momenta within proton

⋆ Introduce parton distribution functions such that $q^{\mathrm{p}}(x)\mathrm{d}x$ is the number of quarks of type q within a proton with momenta between $x \to x + \mathrm{d}x$

- Expected form of the parton distribution function?



⋆ The cross section for scattering from a particular quark type within the proton which in the range $x \to x + \mathrm{d}x$ is

$$
\frac{\mathrm{d}^2\sigma}{\mathrm{d}Q^2} = \frac{4\pi\alpha^2}{Q^4}\left[(1-y) + \frac{y^2}{2}\right] \times e_q^2 q^{\mathrm{p}}(x)\mathrm{d}x
$$

⋆ Summing over all types of quark within the proton gives the expression for the electron-proton scattering cross section

$$
\frac{\mathrm{d}^2\sigma^{\mathrm{ep}}}{\mathrm{d}x\ \mathrm{d}Q^2} = \frac{4\pi\alpha^2}{Q^4}\left[(1-y) + \frac{y^2}{2}\right]\sum_q e_q^2 q^{\mathrm{p}}(x) \qquad (5)
$$

⋆ Compare with the electron-proton scattering cross section in terms of structure functions (equation (2)):

$$
\frac{\mathrm{d}^2\sigma}{\mathrm{d}x\ \mathrm{d}Q^2} = \frac{4\pi\alpha^2}{Q^4}\left[(1-y)\frac{F_2\left(x, Q^2\right)}{x} + y^2 F_1\left(x, Q^2\right)\right] \qquad (6)
$$

By comparing (5) and (6) obtain the parton model prediction for the structure functions in the general L.I. form for the differential cross section

$$
F_2^{\mathrm{p}}\left(x, Q^2\right) = 2xF_1^{\mathrm{p}}\left(x, Q^2\right) = x\sum_q e_q^2 q^{\mathrm{p}}(x) \Rightarrow
$$

Can relate measured structure functions to the underlying quark distributions

The parton model predicts:

- Bjorken Scaling $F_1(x, Q^2) \to F_1(x) \quad F_2(x, Q^2) \to F_2(x)$
- Due to scattering from point-like particles within the proton
- Callan-Gross Relation $F_2(x) = 2xF_1(x)$
- Due to scattering from spin half Dirac particles where the magnetic moment is directly related to the charge; hence the "electro-magnetic" and "pure magnetic" terms are fixed with respect to each other.

⋆ At present parton distributions cannot be calculated from QCD

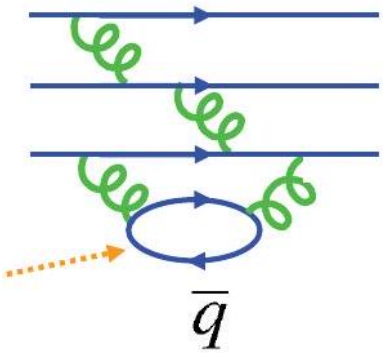
- Can't use perturbation theory due to large coupling constant

⋆ Measurements of the structure functions enable us to determine the parton distribution functions!

⋆ For electron-proton scattering we have:

$$F_2^{\mathrm{p}}(x) = x \sum_q e_q^2 q^{\mathrm{p}}(x)$$

- Due to higher orders, the proton contains not only up and down quarks but also anti-up and anti-down quarks



(will neglect the small contributions from heavier quarks)

- For electron-proton scattering have:

$$F_2^{\mathrm{ep}}(x) = x \sum_q e_q^2 q^{\mathrm{p}}(x) = x\left(\frac{4}{9}u^{\mathrm{p}}(x) + \frac{1}{9}d^{\mathrm{p}}(x) + \frac{4}{9}\bar{u}^{\mathrm{p}}(x) + \frac{1}{9}\bar{d}^{\mathrm{p}}(x)\right)$$

- For electron-neutron scattering have:

$$F_2^{\mathrm{en}}(x) = x \sum_q e_q^2 q^{\mathrm{n}}(x) = x\left(\frac{4}{9}u^{\mathrm{n}}(x) + \frac{1}{9}d^{\mathrm{n}}(x) + \frac{4}{9}\bar{u}^{\mathrm{n}}(x) + \frac{1}{9}\bar{d}^{\mathrm{n}}(x)\right)$$

- Now assume "isospin symmetry", i.e. that the neutron (ddu) is the same as a proton (uud) with up and down quarks interchanged, i.e.

$$d^{\mathrm{n}}(x) = u^{\mathrm{p}}(x); \quad u^{\mathrm{n}}(x) = d^{\mathrm{p}}(x)$$

and define the neutron distributions functions in terms of those of the proton

$$u(x) \equiv u^{\mathrm{p}}(x) = d^{\mathrm{n}}(x); \quad d(x) \equiv d^{\mathrm{p}}(x) = u^{\mathrm{n}}(x)$$
$$\bar{u}(x) \equiv \bar{u}^{\mathrm{p}}(x) = \bar{d}^{\mathrm{n}}(x); \quad \bar{d}(x) \equiv \bar{d}^{\mathrm{p}}(x) = \bar{u}^{\mathrm{n}}(x)$$

giving:

$$F_2^{\mathrm{ep}}(x) = 2xF_1^{\mathrm{ep}}(x) = x\left(\frac{4}{9}u(x) + \frac{1}{9}d(x) + \frac{4}{9}\bar{u}(x) + \frac{1}{9}\bar{d}(x)\right) \tag{7}$$

$$F_2^{\mathrm{en}}(x) = 2xF_1^{\mathrm{en}}(x) = x\left(\frac{4}{9}d(x) + \frac{1}{9}u(x) + \frac{4}{9}\bar{d}(x) + \frac{1}{9}\bar{u}(x)\right) \tag{8}$$

- Integrating (7) and (8):

$$\int_0^1 F_2^{\mathrm{ep}}(x)\mathrm{d}x = \int_0^1 x\left(\frac{4}{9}[u(x) + \bar{u}(x)] + \frac{1}{9}[d(x) + \bar{d}(x)]\right)\mathrm{d}x = \frac{4}{9}f_u + \frac{1}{9}f_d$$

$$\int_0^1 F_2^{\mathrm{en}}(x)\mathrm{d}x = \int_0^1 x\left(\frac{4}{9}[d(x) + \bar{d}(x)] + \frac{1}{9}[u(x) + \bar{u}(x)]\right)\mathrm{d}x = \frac{4}{9}f_d + \frac{1}{9}f_u$$

$$\star f_u = \int_0^1 [xu(x) + x\bar{u}(x)]\mathrm{d}x \quad \text{is the fraction of the proton momentum}$$

carried by the up and anti-up quarks

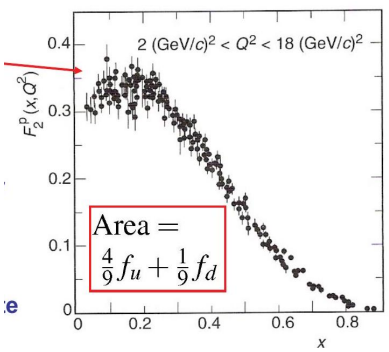
Experimentally

$$\int F_2^{\mathrm{ep}}(x)\mathrm{d}x \approx 0.18$$

$$\int F_2^{\mathrm{en}}(x)\mathrm{d}x \approx 0.12$$

$$f_u \approx 0.36 \quad f_d \approx 0.18$$

- In the proton, as expected, the up quarks carry twice the momentum of the down quarks
- The quarks carry just over 50% of the total proton momentum. The rest is carried by gluons (which being neutral doesn't contribute to electron-nucleon scattering).



Valence and Sea Quarks

- As we are beginning to see the proton is complex..

-The parton distribution function $u^{\mathrm{p}}(x) = u(x)$ includes contributions from the "valence" quarks and the virtual quarks produced by gluons: the "sea"

- Resolving into valence and sea contributions:

$$\begin{array}{ll} u(x) = u_{\mathrm{V}}(x) + u_{\mathrm{S}}(x) & d(x) = d_{\mathrm{V}}(x) + d_{\mathrm{S}}(x) \\ \bar{u}(x) = \bar{u}_{\mathrm{S}}(x) & \bar{d}(x) = \bar{d}_{\mathrm{S}}(x) \end{array}$$

-The proton contains two valence up quarks and one valence down quark and would expect:

$$\int_0^1 u_{\mathrm{V}}(x)\mathrm{d}x = 2 \quad \int_0^1 d_{\mathrm{V}}(x)\mathrm{d}x = 1$$

- But no a priori expectation for the total number of sea quarks!

- But sea quarks arise from gluon quark/anti-quark pair production and with $m_u = m_d$ it is reasonable to expect

$$u_S(x) = d_S(x) = \bar{u}_S(x) = \bar{d}_S(x) = S(x)$$

-With these relations (7) and (8) become

$$F_2^{\mathrm{ep}}(x) = x\left(\frac{4}{9}u_{\mathrm{V}}(x) + \frac{1}{9}d_{\mathrm{V}}(x) + \frac{10}{9}S(x)\right) \quad F_2^{\mathrm{en}}(x) = x\left(\frac{4}{9}d_{\mathrm{V}}(x) + \frac{1}{9}u_{\mathrm{V}}(x) + \frac{10}{9}S(x)\right)$$

$$\frac{F_2^{\mathrm{en}}(x)}{F_2^{\mathrm{ep}}(x)} = \frac{4d_{\mathrm{V}}(x) + u_{\mathrm{V}}(x) + 10S(x)}{4u_{\mathrm{V}}(x) + d_{\mathrm{V}}(x) + 10S(x)}$$

-The sea component arises from processes such as $g \to \bar{u}u$. Due to the $1/q^2$ dependence of the gluon propagator, much more likely to produce Iow energy gluons. Expect the sea to comprise of low energy $q/\bar{q}$

-Therefore at low x expect the sea to dominate:

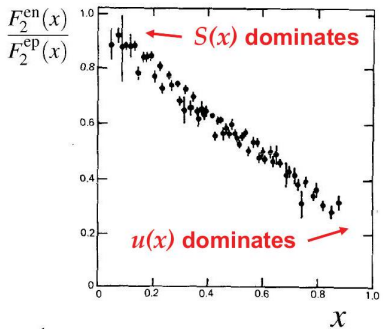
$$\frac{F_2^{\mathrm{en}}(x)}{F_2^{\mathrm{ep}}(x)} \to 1 \quad \text{as} \quad x \to 0$$

Observed experimentally

- At high x expect the sea contribution to be small

$$\frac{F_2^{\mathrm{en}}(x)}{F_2^{\mathrm{ep}}(x)} \to \frac{4d_{\mathrm{V}}(x) + u_{\mathrm{V}}(x)}{4u_{\mathrm{V}}(x) + d_{\mathrm{V}}(x)} \quad \text{as} \quad x \to 1$$

Note: $u_{\mathrm{V}} = 2d_{\mathrm{V}}$ would give ratio 2/3 as $x \to 1$



Experimentally $F_2^{en}(x)/F_2^{ep}(x) \to 1/4 \quad$ as $\quad x \to 1$

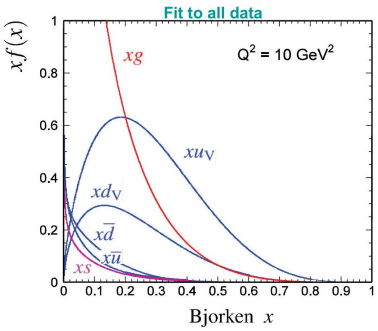
$$\to d(x)/u(x) \to 0 \quad \text{as} \quad x \to 1$$

This behaviour is not understood.

Parton Distribution Functions

Ultimately the parton distribution functions are obtained from a fit to all experimental data including neutrino scattering (see handout 10)

-Hadron-hadron collisions give information on gluon pdf $g(x)$



Note:

- Apart from at large x

$$u_V(x) \approx 2d_V(x)$$

- For $x < 0.2$

gluons dominate

- In fits to data assume

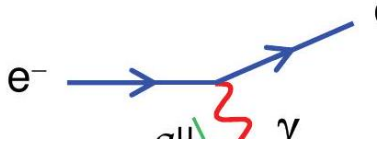
$$u_s(x) = \bar{u}(x)$$

- $\bar{d}(x) > \bar{u}(x)$ not understood exclusion principle?
- Small strange quark component $s(x)$

(Try Question 12)

Scaling Violations

- In last 40 years, experiments have probed the proton with virtual photons of ever increasing energy
- Non-point like nature of the scattering becomes

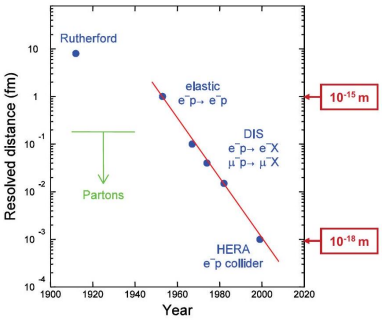


apparent when $\lambda_\gamma \sim$ size of scattering centre

e$^-$

$$\lambda_\gamma = \frac{h}{|\vec{q}|} \sim \frac{1\text{GeVfm}}{|\vec{q}|(\text{GeV})}$$

- Scattering from point-like quarks gives rise to Bjorken scaling: no q^2 cross section dependence
- IF quarks were not point-like, at high q^2 (when the wavelength of the virtual photon $\sim$ size of quark) would observe rapid decrease in cross section with increasing q^2.
- To search for quark sub-structure want to go to highest q^2



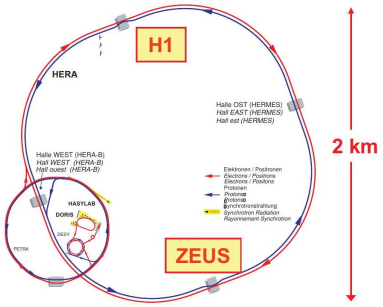
HERA e $^{\pm}$p Collider: 1991-2007

ˆ DESY (Deutsches Elektronen-Synchroton) Laboratory, Hamburg, Germany

$e^{\pm} \xrightarrow{27.5\text{GeV}} 820\text{GeV P} \quad \sqrt{s} = 300\text{GeV}$

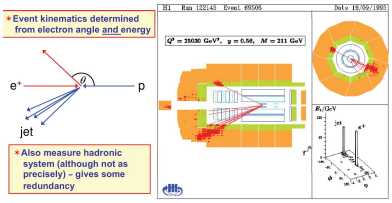


⋆ Two large experiments: H1 and ZEUS



⋆ Probe proton at very high Q^2 and very low x

Example of a High Q Event in H1



$F_2\left(x, Q^2\right)$ **Results**

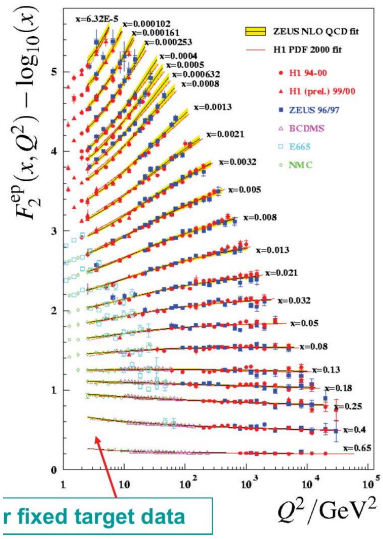
⋆ No evidence of rapid decrease of cross section at highest Q^2

$$\Rightarrow R_{\text{quark}} < 10^{-18} \text{ m}$$

For $x > 0.05$, only weak dependence of F_2 on Q^2: consistent with the expectation from the quark-parton model

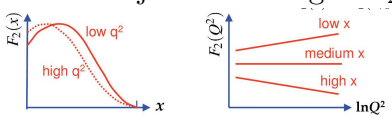
⋆ But observe clear scaling violations, particularly at low x

$$F_2\left(x, Q^2\right) \neq F_2(x)$$



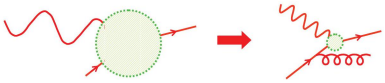
Origin of Scaling Violations

⋆ Observe "small" deviations from exact Bjorken scaling $F_2(x) \to F_2\left(x, Q^2\right)$



⋆ At high Q^2 observe more low x quarks

⋆ "Explanation": at high Q^2 (shorter wave-length) resolve finer structure: i.e. reveal quark is sharing momentum with gluons. At higher Q^2 expect to "see" more low x quarks



QCD cannot predict the x dependence of $F_2\left(x, Q^2\right)$

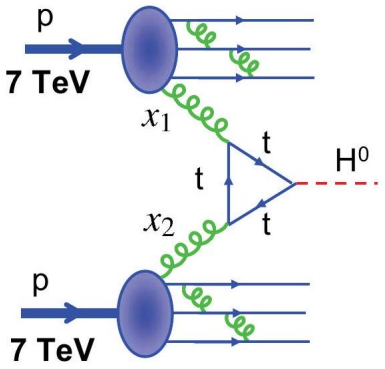
⋆ But QCD can predict the Q^2 dependence of $F_2\left(x, Q^2\right)$

Proton-Proton Collisions at the LHC

⋆ Measurements of structure functions not only provide a powerful test of QCD, the parton distribution functions are essential for the calculation of cross sections at pp and $\mathrm{p\overline{p}}$ colliders.

- Example: Higgs production at the Large Hadron Collider LHC)2009-)

-The LHC will collide 7TeV protons on 7TeV protons
-However underlying collisions are between partons
-Higgs production the LHC dominated by "gluon-gluon fusion"



- Cross section depends on gluon PDFs

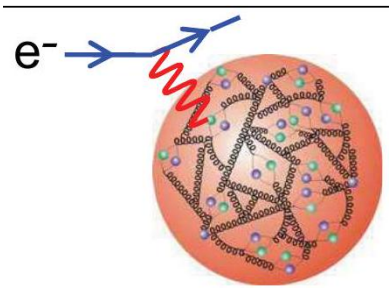
$$\sigma(pp \to HX) \sim \int_0^1 \int_0^1 g\left(x_1\right) g\left(x_2\right) \sigma(gg \to H) \mathrm{d}x_1 \, \mathrm{d}x_2$$

- Uncertainty in gluon PDFs lead to a $\pm 5\%$ uncertainty in Higgs production cross section
- Prior to HERA data uncertainty was $\pm \mathbf{25}\%$

Summary

- At very high electron energies $\lambda \ll r_p$: the proton appears to be a sea of quarks and gluons.
- Deep Inelastic Scattering = Elastic scattering from the quasi-free constituent quarks

$\Rightarrow$ Bjorken Scaling $F_1\left(x, Q^2\right) \to F_1(x)$ point-like scattering



$\Rightarrow$ Callan-Gross $\quad F_2(x) = 2xF_1(x)$
Scattering from spin-1/2

- Describe scattering in terms of parton distribution functions $u(x), d(x), \ldots$ which describe momentum distribution inside a nucleon
- The proton is much more complex than just uud - sea of anti-quarks/gluons
- Quarks carry only 50% of the protons momentum - the rest is due to low energy gluons
- We will come back to this topic when we discuss neutrino scattering...

1.8.3 H7: Symmetries and the Quark Model

Introduction/Aims

$\star$ Symmetries play a central role in particle physics; one aim of particle physics is to discover the fundamental symmetries of our universe

$\star$ In this handout will apply the idea of symmetry to the quark model with the aim of:

- Deriving hadron wave-functions
- Providing an introduction to the more abstract ideas of colour and QCD (handout 8)
- Ultimately explaining why hadrons only exist as $\bar{q}q$ (mesons) qq (baryons) or $\bar{q}\bar{q}\bar{q}$ (anti-baryons)
- introduce the ideas of the **SU**(2) and SU(3) symmetry groups which play a major role in particle physics (see handout 13)

Symmetries and Conservation Laws

$\star$ Suppose physics is invariant under the transformation

$$\psi \to \psi' = \hat{U}\psi \quad \text{e.g. rotation of the coordinate axes}$$

- To conserve probability normalisation require

$$\langle\psi|\psi\rangle = \langle\psi'|\psi'\rangle = \langle\hat{U}\psi|\hat{U}\psi\rangle = \left\langle\psi\left|\hat{U}^\dagger\hat{U}\right|\psi\right\rangle$$
$$\Rightarrow \hat{U}^\dagger\hat{U} = 1 \quad \text{i.e. } \hat{U} \text{ has to be unitary}$$

- For physical predictions to be unchanged by the symmetry transformation, also require all QM matrix elements unchanged

$$\langle\psi|\hat{H}|\psi\rangle = \left\langle\psi'|\hat{H}|\psi'\right\rangle = \left\langle\psi\left|\hat{U}^\dagger\hat{H}\hat{U}\right|\psi\right\rangle$$

i.e. require

$$\hat{U}^\dagger\hat{H}\hat{U} = \hat{H}$$

$\times\hat{U}$
$\hat{U}\hat{U}^\dagger\hat{H}\hat{U} = \hat{U}\hat{H} \quad \rightarrow \hat{H}\hat{U} = \hat{U}\hat{H}$
therefore

$$[\hat{H}, \hat{U}] = 0$$

$\hat{U}$ commutes with the Hamiltonian
$\star$ Now consider the infinitesimal transformation (ε small)

$$\hat{U} = 1 + i\varepsilon\hat{G}$$

)$\hat{G}$ is called the generator of the transformation)

- For $\hat{U}$ to be unitary

$$\hat{U}\hat{U}^\dagger = (1 + i\varepsilon\hat{G})\left(1 - i\varepsilon\hat{G}^\dagger\right) = 1 + i\varepsilon\left(\hat{G} - \hat{G}^\dagger\right) + O\left(\varepsilon^2\right)$$

neglecting terms in $\varepsilon^2 \quad UU^\dagger = 1 \quad \Rightarrow \quad \hat{G} = \hat{G}^\dagger$
i.e. $\hat{G}$ is Hermitian and therefore corresponds to an observable quantity G ! - Furthermore, $[\hat{H}, \hat{U}] = 0 \quad \Rightarrow [\hat{H}, 1 + i\varepsilon\hat{G}] = 0 \quad \Rightarrow [\hat{H}, \hat{G}] = 0$
But from QM

$$\frac{\mathrm{d}}{\mathrm{d}t}\langle\hat{G}\rangle = i\langle[\hat{H}, \hat{G}]\rangle = 0$$

i.e. G is a conserved quantity.

$$\text{Symmetry} \iff \text{Conservation Law}$$

$\star$ For each symmetry of nature have an observable conserved quantity
Example: Infinitesimal spatial translation $x \rightarrow x + \varepsilon$
i.e. expect physics to be invariant under $\psi(x) \rightarrow \psi' = \psi(x + \varepsilon)$

$$\psi'(x) = \psi(x + \varepsilon) = \psi(x) + \frac{\partial\psi}{\partial x}\varepsilon = \left(1 + \varepsilon\frac{\partial}{\partial x}\right)\psi(x)$$

but $\quad \hat{p}_x = -i\frac{\partial}{\partial x} \Rightarrow \psi'(x) = (1 + i\varepsilon\hat{p}_x)\,\psi(x)$
The generator of the symmetry transformation is $\hat{p}_x \Rightarrow p_x$ is conserved
-Translational invariance of physics implies momentum conservation!

- In general the symmetry operation may depend on more than one parameter

$$\hat{U} = 1 + i\vec{\varepsilon}\cdot\vec{G}$$

For example for an infinitesimal 3D linear translation:

$$\vec{r} \longrightarrow \vec{r} + \vec{\varepsilon}$$

$$\rightarrow \quad \hat{U} = 1 + i\vec{\varepsilon}\cdot\vec{p} \quad \vec{p} = (\hat{p}_x, \hat{p}_y, \hat{p}_z)$$

- So far have only considered an infinitesimal transformation, however a finite transformation can be expressed as a series of infinitesimal transformations

$$\hat{U}(\vec{\alpha}) = \lim_{n\to\infty}\left(1 + i\frac{\vec{\alpha}}{n}\cdot\vec{G}\right)^n = e^{i\vec{\alpha}\cdot\vec{G}}$$

Example: Finite spatial translation in 1D: $x \to x + x_0$ with $\hat{U}(x_0) = e^{ix_0\hat{p}_x}$

$$\begin{aligned}\psi'(x) = \psi(x + x_0) = \hat{U}\psi(x) = \exp\left(x_0\frac{\mathrm{d}}{\mathrm{d}x}\right)\psi(x) \quad \left(p_x = -i\frac{\partial}{\partial x}\right)\\ = \left(1 + x_0\frac{\mathrm{d}}{\mathrm{d}x} + \frac{x_0^2}{2!}\frac{\mathrm{d}^2}{\mathrm{d}x^2} + \ldots\right)\psi(x)\\ = \psi(x) + x_0\frac{\mathrm{d}\psi}{\mathrm{d}x} + \frac{x_0^2}{2}\frac{\mathrm{d}^2\psi}{\mathrm{d}x^2} + \ldots\end{aligned}$$

i.e. obtain the expected Taylor expansion

Symmetries in Particle Physics: Isospin

-The proton and neutron have very similar masses and the nuclear force is found to be approximately charge-independent, i.e.

$$V_{pp} \approx V_{np} \approx V_{nn}$$

-To reflect this symmetry, Heisenberg (1932) proposed that if you could "switch off" the electric charge of the proton

There would be no way to distinguish between a proton and neutron

- Proposed that the neutron and proton should be considered as two states of a single entity; the nucleon

$$p = \begin{pmatrix}1\\0\end{pmatrix} \quad n = \begin{pmatrix}0\\1\end{pmatrix}$$

⋆ Analogous to the spin-up/spin-down states of a spin- 1/2 particle

ISOSPIN

⋆ Expect physics to be invariant under rotations in this space

-The neutron and proton form an isospin doublet with total isospin $I = 1/2$ and third component $I_3 = \pm 1/2$

Flavour Symmetry of the Strong Interaction

We can extend this idea to the quarks:

⋆ Assume the strong interaction treats all quark flavours equally (it does)

- Because $m_u \approx m_d$:

The strong interaction possesses an approximate flavour symmetry i.e. from the point of view of the strong interaction nothing changes if all up quarks are replaced by down quarks and vice versa.

- Choose the basis

$$u = \begin{pmatrix} 1 \\ 0 \end{pmatrix} \quad d = \begin{pmatrix} 0 \\ 1 \end{pmatrix}$$

- Express the invariance of the strong interaction under $u \leftrightarrow d$ as invariance under "rotations" in an abstract isospin space

$$\begin{pmatrix} u' \\ d' \end{pmatrix} = \hat{U} \begin{pmatrix} u \\ d \end{pmatrix} = \begin{pmatrix} U_{11} & U_{12} \\ U_{21} & U_{22} \end{pmatrix} \begin{pmatrix} u \\ d \end{pmatrix}$$

The 2×2 unitary matrix depends on 4 complex numbers, i.e. 8 real parameters But there are four constraints from $\hat{U}^\dagger \hat{U} = 1$

$\Rightarrow \quad 8 - 4 = 4$ **independent matrices**

- In the language of group theory the four matrices form the U(2) group
- One of the matrices corresponds to multiplying by a phase factor

$$\hat{U}_1 = \begin{pmatrix} 1 & 0 \\ 0 & 1 \end{pmatrix} e^{i\phi}$$

not a flavour transformation and of no relevance here.

- The remaining three matrices form an SU(2) group (special unitary) with $\det U = 1$
- For an infinitesimal transformation, in terms of the Hermitian generators $\hat{G}$

$$\hat{U} = 1 + i\varepsilon \hat{G}$$

- $\det U = 1 \Rightarrow \mathrm{Tr}(\hat{G}) = 0$
- A linearly independent choice for $\hat{G}$ are the Pauli spin matrices

$$\sigma_1 = \begin{pmatrix} 0 & 1 \\ 1 & 0 \end{pmatrix} \quad \sigma_2 = \begin{pmatrix} 0 & -i \\ i & 0 \end{pmatrix} \quad \sigma_3 = \begin{pmatrix} 1 & 0 \\ 0 & -1 \end{pmatrix}$$

- The proposed flavour symmetry of the strong interaction has the same transformation properties as SPIN!
- Define ISOSPIN: $\vec{T} = \frac{1}{2}\vec{\sigma} \quad \hat{U} = e^{i\vec{\alpha}\cdot\vec{T}}$
- Check this works, for an infinitesimal transformation

$$\hat{U} = 1 + \frac{1}{2} i\vec{\varepsilon} \cdot \vec{\sigma} = 1 + \frac{i}{2}\left(\varepsilon_1\sigma_1 + \varepsilon_2\sigma_2 + \varepsilon_3\sigma_3\right) = \begin{pmatrix} 1 + \frac{1}{2}i\varepsilon_3 & \frac{1}{2}i\left(\varepsilon_1 - i\varepsilon_2\right) \\ \frac{1}{2}i\left(\varepsilon_1 + i\varepsilon_2\right) & 1 - \frac{1}{2}i\varepsilon_3 \end{pmatrix}$$

Which is, as required, unitary and has unit determinant

$$U^\dagger U = I + O\left(\varepsilon^2\right) \quad \det U = 1 + O\left(\varepsilon^2\right)$$

Properties of Isopin

- Isospin has the exactly the same properties as spin

$$[T_1, T_2] = iT_3 \quad [T_2, T_3] = iT_1 \quad [T_3, T_1] = iT_2$$
$$\left[T^2, T_3\right] = 0 \quad T^2 = T_1^2 + T_2^2 + T_3^2$$

As in the case of spin, have three non-commuting operators, T_1, T_2, T_3 and even though all three correspond to observables, can't know them simultaneously. So label states in terms of total isospin I and the third component of isospin I_3

NOTE: isospin has nothing to do with spin - just the same mathematics

- The eigenstates are exact analogues of the eigenstates of ordinary angular momentum $|s, m\rangle \to |I, I_3\rangle$

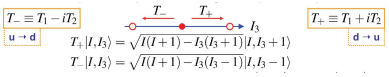
$$\text{with} \quad T^2 |I, I_3\rangle = I(I+1) |I, I_3\rangle \quad T_3 |I, I_3\rangle = I_3 |I, I_3\rangle$$

- In terms of isospin:

$$u = \begin{pmatrix} 1 \\ 0 \end{pmatrix} = \left|\frac{1}{2}, +\frac{1}{2}\right\rangle \quad d = \begin{pmatrix} 0 \\ 1 \end{pmatrix} = \left|\frac{1}{2}, -\frac{1}{2}\right\rangle$$
$$\xrightarrow[+\frac{1}{2}]{d} I_3 \quad \text{I}$$

- In general $\quad I_3 = \frac{1}{2}(N_u - N_d)$

- Can define isospin ladder operators - analogous to spin ladder operators



Step up/down in I_3 until reach end of multiplet $\quad T_+|I, +I\rangle = 0 \quad T_-|I, -I\rangle = 0$

$$\underline{\left| T_+ u = 0 \quad T_+ d = u \quad T_- u = d \quad T_- d = 0 \right.}$$

- Ladder operators turn $u \to d$ and $d \to u$

⋆ Combination of isospin: e.g. what is the isospin of a system of two d quarks, is exactly analogous to combination of spin (i.e. angular momentum)

$$\left|I^{(1)}, I_3^{(1)}\right\rangle \left|I^{(2)}, I_3^{(2)}\right\rangle \to |I, I_3\rangle$$

- I_3 additive: $\quad I_3 = I_3^{(1)} + I_3^{(2)}$

- I in integer steps from $\left|I^{(1)} - I^{(2)}\right|$ to $\left|I^{(1)} + I^{(2)}\right|$

⋆ Assumed symmetry of Strong Interaction under isospin transformations implies the existence of conserved quantites

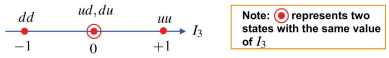
- In strong interactions I_3 and I are conserved, analogous to conservation of J_Z and J for angular momentum

Combining Quarks

Goal: derive proton wave-function

- First combine two quarks, then combine the third
- Use requirement that fermion wave-functions are anti-symmetric

Isospin starts to become useful in defining states of more than one quark.
e.g. two quarks, here we have four possible combinations:



- We can immediately identify the extremes (I_3 additive)

$$uu \equiv \left|\frac{1}{2},\frac{1}{2}\right\rangle\left|\frac{1}{2},\frac{1}{2}\right\rangle = |1,+1\rangle \quad dd \equiv \left|\frac{1}{2},-\frac{1}{2}\right\rangle\left|\frac{1}{2},-\frac{1}{2}\right\rangle = |1,-1\rangle$$

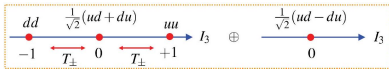
To obtain the $|1,0\rangle$ state use ladder operators

$$T_-|1,+1\rangle = \sqrt{2}|1,0\rangle = T_-(uu) = ud + du$$
$$\Rightarrow |1,0\rangle = \frac{1}{\sqrt{2}}(ud+du)$$

The final state, $|0,0\rangle$, can be found from orthogonality with $|1,0\rangle$

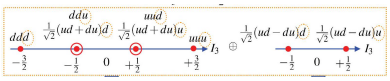
$$\Rightarrow \quad |0,0\rangle = \frac{1}{\sqrt{2}}(ud-du)$$

- From four possible combinations of isospin doublets obtain a triplet of isospin 1 states and a singlet isospin 0 state $2 \otimes 2 = 3 \oplus 1$



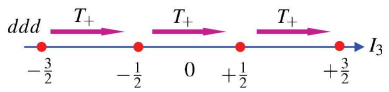
- Can move around within multiplets using ladder operators
- note, as anticipated $I_3 = \frac{1}{2}(N_u - N_d)$
- States with different total isospin are physically different - the isospin 1 triplet is symmetric under interchange of quarks 1 and 2 whereas singlet is anti-symmetric

⋆ Now add an additional up or down quark. From each of the above 4 states get two new isospin states with $I_3' = I_3 \pm \frac{1}{2}$



6

- Use ladder operators and orthogonality to group the 6 states into isospin multiplets, e.g. to obtain the $I = \frac{3}{2}$ states, step up from ddd
  ⋆ Derive the $I = \frac{3}{2}$ states from $ddd \equiv \left|\frac{3}{2},-\frac{3}{2}\right\rangle$



$$T_+\left|\frac{3}{2},-\frac{3}{2}\right\rangle = T_+(ddd) = (T_+d)\,dd + d\,(T_+d)\,d + dd\,(T_+)\,d$$
$$\sqrt{3}\left|\frac{3}{2},-\frac{1}{2}\right\rangle = udd + dud + ddu$$
$$\left|\frac{3}{2},-\frac{1}{2}\right\rangle = \frac{1}{\sqrt{3}}(udd + dud + ddu)$$
$$T_+\left|\frac{3}{2},-\frac{1}{2}\right\rangle = \frac{1}{\sqrt{3}}T_+(udd + dud + ddu)$$
$$2\left|\frac{3}{2},+\frac{1}{2}\right\rangle = \frac{1}{\sqrt{3}}(uud + udu + uud + duu + udu + duu)$$
$$\left|\frac{3}{2},+\frac{1}{2}\right\rangle = \frac{1}{\sqrt{3}}(\text{ uиd } + \text{ udu } + \text{ duи })$$
$$T_+\left|\frac{3}{2},+\frac{1}{2}\right\rangle = \frac{1}{\sqrt{3}}T_+(uud + udu + duu)$$
$$\sqrt{3}\left|\frac{3}{2},+\frac{3}{2}\right\rangle = \frac{1}{\sqrt{3}}(uu + uu + uu)$$
$$\left|\frac{3}{2},+\frac{3}{2}\right\rangle = \text{ uuu}$$

- From the 6 states on previous page, use orthoganality to find $\left|\frac{1}{2},\pm\frac{1}{2}\right\rangle$ states
- The 2 states on the previous page give another $\left|\frac{1}{2},\pm\frac{1}{2}\right\rangle$ doublet
- The eight states uu, uиd, udu, udd, duu, dud, ddu, ddd are grouped into an isospin quadruplet and two isospin doublets

$$2 \otimes 2 \otimes 2 = 2 \otimes (3 \oplus 1) = (2 \otimes 3) \oplus (2 \otimes 1) = 4 \oplus 2 \oplus 2$$

- Different multiplets have different symmetry properties

$\left|\frac{3}{2},+\frac{3}{2}\right\rangle =$ иии
$\left|\frac{3}{2},+\frac{1}{2}\right\rangle = \frac{1}{\sqrt{3}}(ud + udu + duu)$
$\left|\frac{3}{2},-\frac{1}{2}\right\rangle = \frac{1}{\sqrt{3}}(ddu + dud + udd)$
A quadruplet of states which are symmetric under the interchange of any two quarks
$\left|\frac{3}{2},-\frac{3}{2}\right\rangle = ddd$
$\left|\frac{1}{2},-\frac{1}{2}\right\rangle = -\frac{1}{\sqrt{6}}(2ddu - udd - dud)$
$\left|\frac{1}{2},+\frac{1}{2}\right\rangle = \frac{1}{\sqrt{6}}(2uud - udu - duu)$
$\Big\}\ \mathbf{M}_S$
Mixed symmetry.
Symmetric for $1 \hookrightarrow 2$
$\left|\frac{1}{2},-\frac{1}{2}\right\rangle = \frac{1}{\sqrt{2}}(udd - dud)$
$\left|\frac{1}{2},+\frac{1}{2}\right\rangle = \frac{1}{\sqrt{2}}(udu - duu)$

Mixed symmetry. Anti-symmetric for $1 \leftrightharpoons 2$

- Mixed symmetry states have no definite symmetry under interchange of quarks $1 \leftrightarrow 3$ etc.

Combining Spin

- Can apply exactly the same mathematics to determine the possible spin wave-functions for a combination of 3 spin-half particles

$$\left|\frac{3}{2},+\frac{3}{2}\right\rangle = \uparrow\uparrow\uparrow$$
$$\left|\frac{3}{2},+\frac{1}{2}\right\rangle = \frac{1}{\sqrt{3}}(\uparrow\uparrow\downarrow + \uparrow\downarrow\uparrow + \downarrow\uparrow\uparrow)$$
$$\left|\frac{3}{2},-\frac{1}{2}\right\rangle = \frac{1}{\sqrt{3}}(\downarrow\downarrow\uparrow + \downarrow\uparrow\downarrow + \uparrow\downarrow\downarrow)$$
$$\left|\frac{3}{2},-\frac{3}{2}\right\rangle = \downarrow\downarrow\downarrow$$
$$\left|\frac{1}{2},-\frac{1}{2}\right\rangle = -\frac{1}{\sqrt{6}}(2\downarrow\downarrow\uparrow - \uparrow\downarrow\downarrow - \downarrow\uparrow\downarrow)$$
$$\left|\frac{1}{2},+\frac{1}{2}\right\rangle = \frac{1}{\sqrt{6}}(2\uparrow\uparrow\downarrow - \uparrow\downarrow\uparrow - \downarrow\uparrow\uparrow)$$

$\mathrm{M_S}$

$$\left.\begin{array}{l}\left|\frac{1}{2},-\frac{1}{2}\right\rangle = \frac{1}{\sqrt{2}}(\uparrow\downarrow\downarrow - \downarrow\uparrow\downarrow)\\ \left|\frac{1}{2},+\frac{1}{2}\right\rangle = \frac{1}{\sqrt{2}}(\uparrow\downarrow\uparrow - \downarrow\uparrow\uparrow)\end{array}\right\} \quad \mathbf{M_A}$$

- Can now form total wave-functions for combination of three quarks

Baryon Wave-functions (ud)

⋆ Quarks are fermions so require that the total wave-function is anti-symmetric under the interchange of any two quarks

⋆ the total wave-function can be expressed in terms of:

$$\psi = \phi_{\text{flavour}}\ \chi_{\text{spin}}\ \xi_{\text{colour}}\ \eta_{\text{space}}$$

⋆ The colour wave-function for all bound qqq states is anti-symmetric (see handout 8)

- Here we will only consider the lowest mass, ground state, baryons where there is no internal orbital angular momentum.
- For $\mathrm{L} = 0$ the spatial wave-function is symmetric $(-1)^{\mathrm{L}}$.

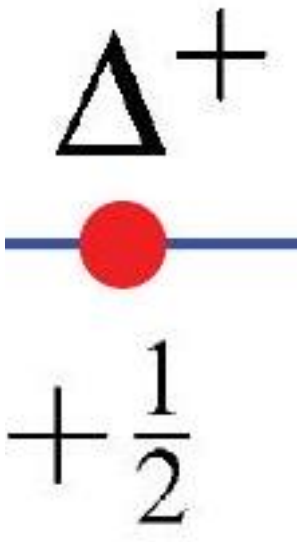
$$\Rightarrow \xi_{\text{colour}}\ \eta_{\text{space}} \quad \begin{array}{c}\text{anti-symmetric}\\ \phi_{\text{flavour}}\ \chi_{\text{spin}} \qquad \text{symmetric}\end{array} \Big\} \text{ Overall anti-symmetric}$$

- Two ways to form a totally symmetric wave-function from spin and isospin states:

(1) combine totally symmetric spin and isospin wave-functions $\phi(S)\chi(S)$ ddd $\frac{1}{\sqrt{3}}(ddu + dud + udd)$ $\frac{1}{\sqrt{3}}(uud + udu + duu)$ иии

$-\frac{3}{2}$

Δ^0



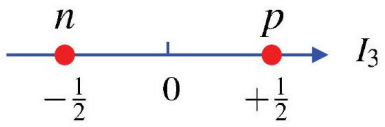
$\xrightarrow[+\frac{3}{2}]{\Delta^{++}} I_3$

2 combine mixed symmetry spin and mixed symmetry isospin states

- Both $\phi(M_S)\,\chi(M_S)$ and $\phi(M_A)\,\chi(M_A)$ are sym. under inter-change of quarks $1 \leftrightarrow 2$
- Not sufficient, these combinations have no definite symmetry under $1 \leftrightarrow 3, \ldots$
- However, it is not difficult to show that the (normalised) linear combination:

$$\frac{1}{\sqrt{2}}\phi(M_S)\,\chi(M_S) + \frac{1}{\sqrt{2}}\phi(M_A)\,\chi(M_A)$$

is totally symmetric (i.e. symmetric under $1 \leftrightarrow 2; 1 \leftrightarrow 3; 2 \leftrightarrow 3$)



- The spin-up proton wave-function is therefore:

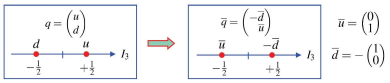
$$|p\uparrow\rangle = \tfrac{1}{6\sqrt{2}}(2uud - udu - duu)(2\uparrow\uparrow\downarrow - \uparrow\downarrow\uparrow - \downarrow\uparrow\uparrow) + \tfrac{1}{2\sqrt{2}}(udu - duu)(\uparrow\downarrow\uparrow - \downarrow\uparrow\uparrow)$$

$$|p\uparrow\rangle = \frac{1}{\sqrt{18}})2u\uparrow u\uparrow d\downarrow - u\uparrow u\downarrow d\uparrow - u\downarrow u\uparrow d\uparrow +$$
$$2u\uparrow d\downarrow u\uparrow - u\uparrow d\uparrow u\downarrow - u\downarrow d\uparrow u\uparrow +$$
$$2d\downarrow u\uparrow u\uparrow - d\uparrow u\downarrow u\uparrow - d\uparrow u\uparrow u\uparrow)$$

NOTE: not always necessary to use the fully symmetrised proton wave-function, e.g. the first 3 terms are sufficient for calculating the proton magnetic moment

Anti-quarks and Mesons (u and d)

⋆ The u, d quarks and $\bar{u}, \bar{\mathrm{d}}$ anti-quarks are represented as isospin doublets



- Subtle point: The ordering and the minus sign in the anti-quark doublet ensures that anti-quarks and quarks transform in the same way (see Appendix I). This is necessary if we want physical predictions to be invariant under $u \leftrightarrow d; \bar{u} \leftrightarrow \bar{d}$
- Consider the effect of ladder operators on the anti-quark isospin states

e.g

$$T_+\bar{u} = T_+\begin{pmatrix}0\\1\end{pmatrix} = \begin{pmatrix}0 & 1\\0 & 0\end{pmatrix}\begin{pmatrix}0\\1\end{pmatrix} = \begin{pmatrix}1\\0\end{pmatrix} = -\bar{d}$$

-The effect of the ladder operators on anti-particle isospin states are:

$$T_+\bar{u} = -\bar{d} \quad T_+\bar{d} = 0 \quad T_-\bar{u} = 0 \quad T_-\bar{d} = -\bar{u}$$

Compare with

$$T_+u = 0 \quad T_+d = u \quad T_-u = d \quad T_-d = 0$$

Light ud Mesons

Can now construct meson states from combinations of up/down quarks



- Consider the $q\bar{q}$ combinations in terms of isospin

$$|1,+1\rangle = \left|\frac{1}{2},+\frac{1}{2}\right\rangle\overline{\left|\frac{1}{2},+\frac{1}{2}\right\rangle} = -u\bar{d}$$
$$|1,-1\rangle = \left|\frac{1}{2},-\frac{1}{2}\right\rangle\overline{\left|\frac{1}{2},-\frac{1}{2}\right\rangle} = d\bar{u}$$

The bar indicates this is the isospin representation of an anti-quark
To obtain the $I_3 = 0$ states use ladder operators and orthogonality

$$\begin{aligned} T_-|1,+1\rangle &= T_-[-u\bar{d}] \\ \sqrt{2}|1,0\rangle &= -T_-[u]\bar{d} - uT_-[\bar{d}] \\ &= -d\bar{d} + u\bar{u} \\ \Rightarrow \quad |1,0\rangle &= \frac{1}{\sqrt{2}}(u\bar{u} - d\bar{d}) \end{aligned}$$

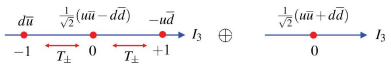
- Orthogonality gives:

$$|0,0\rangle = \frac{1}{\sqrt{2}}(u\bar{u} + d\bar{d})$$

⋆ To summarise:



□
Triplet of $I = 1$ states and a singlet $I = 0$ state



-You will see this written as, $2 \otimes \overline{2} = 3 \oplus 1$

Quark doublet

- To show the state obtained from orthogonality with $|1,0\rangle$ is a singlet use ladder operators

$$T_+|0,0\rangle = T_+\frac{1}{\sqrt{2}}(u\bar{u}+d\bar{d}) = \frac{1}{\sqrt{2}}(-u\bar{d}+u\bar{d}) = 0$$

similarly $\quad T_-|0,0\rangle = 0$

⋆ A singlet state is a "dead-end" from the point of view of ladder operators

SU(3) Flavour

⋆ Extend these ideas to include the strange quark. Since $m_s > m_u, m_d$ don't have an exact symmetry. But m_s not so very different from m_u, m_d and can treat the strong interaction (and resulting hadron states) as if it were symmetric under $u \leftrightarrow d \leftrightarrow s$

- NOTE: any results obtained from this assumption are only approximate as the symmetry is not exact.
- The assumed uds flavour symmetry can be expressed as

$$\begin{pmatrix} u' \\ d' \\ s' \end{pmatrix} = \hat{U}\begin{pmatrix} u \\ d \\ s \end{pmatrix} = \begin{pmatrix} U_{11} & U_{12} & U_{13} \\ U_{21} & U_{22} & U_{23} \\ U_{31} & U_{32} & U_{33} \end{pmatrix}\begin{pmatrix} u \\ d \\ s \end{pmatrix}$$

- The 3×3 unitary matrix depends on 9 complex numbers, i.e. 18 real parameters There are 9 constraints from $\hat{U}^\dagger\hat{U} = 1$

Can form $18 - 9 = 9$ linearly independent matrices

These 9 matrices form a U(3) **group.**

- As before, one matrix is simply the identity multiplied by a complex phase and is of no interest in the context of flavour symmetry
- The remaining 8 matrices have $\det U = 1$ and form an SU(3) group
- The eight matrices (the Hermitian generators) are: $\vec{T} = \frac{1}{2}\vec{\lambda} \quad \hat{U} = e^{i\vec{\alpha}\cdot\vec{T}}$

⋆ In SU(3) flavour, the three quark states are represented by:

$$u = \begin{pmatrix} 1 \\ 0 \\ 0 \end{pmatrix} \quad d = \begin{pmatrix} 0 \\ 1 \\ 0 \end{pmatrix} \quad s = \begin{pmatrix} 0 \\ 0 \\ 1 \end{pmatrix}$$

⋆ In SU(3) uds flavour symmetry contains SU(2) ud flavour symmetry which allows us to write the first three matrices:

$$\lambda_1 = \begin{pmatrix} \sigma_1 & 0 \\ 0\,0 & 0 \end{pmatrix} \quad \lambda_2 = \begin{pmatrix} \sigma_2 & 0 \\ 0\,0 & 0 \end{pmatrix} \quad \lambda_3 = \begin{pmatrix} \sigma_3 & 0 \\ 0\,0 & 0 \end{pmatrix}$$

i.e. $\mathbf{u} \leftrightarrow \mathbf{d}$ $\lambda_1 = \begin{pmatrix} 0 & 1 & 0 \\ 1 & 0 & 0 \\ 0 & 0 & 0 \end{pmatrix}$ $\lambda_2 = \begin{pmatrix} 0 & -i & 0 \\ i & 0 & 0 \\ 0 & 0 & 0 \end{pmatrix}$ $\lambda_3 = \begin{pmatrix} 1 & 0 & 0 \\ 0 & -1 & 0 \\ 0 & 0 & 0 \end{pmatrix}$

- The third component of isospin is now written $I_3 = \frac{1}{2}\lambda_3$

$$\text{with} \quad I_3 u = +\frac{1}{2}u \quad I_3 d = -\frac{1}{2}d \quad I_3 s = 0$$

- I_3 "counts the number of up quarks - number of down quarks in a state
- As before, ladder operators $T_\pm = \frac{1}{2}(\lambda_1 \pm i\lambda_2)$ d
- Now consider the matrices corresponding to the $\mathbf{u} \leftrightarrow \mathbf{s}$ and $\mathbf{d} \leftrightarrow \mathbf{s}$

$$\mathbf{u} \leftrightarrow \mathbf{s} \quad \lambda_4 = \begin{pmatrix} 0 & 0 & 1 \\ 0 & 0 & 0 \\ 1 & 0 & 0 \end{pmatrix} \quad \lambda_5 = \begin{pmatrix} 0 & 0 & -i \\ 0 & 0 & 0 \\ i & 0 & 0 \end{pmatrix}$$

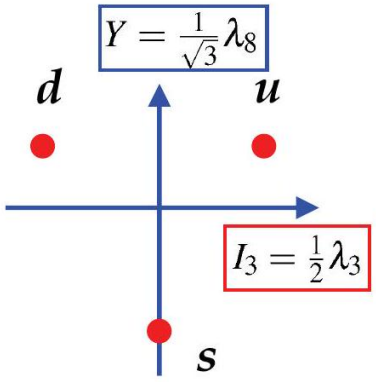
$$\mathrm{d} \leftrightarrow \mathbf{s} \quad \lambda_6 = \begin{pmatrix} 0 & 0 & 0 \\ 0 & 0 & 1 \\ 0 & 1 & 0 \end{pmatrix} \quad \lambda_7 = \begin{pmatrix} 0 & 0 & 0 \\ 0 & 0 & -i \\ 0 & 0 & 0 \\ 0 & 0 & -1 \end{pmatrix} \quad \begin{pmatrix} 0 & 0 & 0 \\ 0 & 1 & 0 \\ 0 & 0 & -1 \end{pmatrix}$$

- Hence in addition to $\lambda_3 = \begin{pmatrix} 1 & 0 & 0 \\ 0 & -1 & 0 \\ 0 & 0 & 0 \end{pmatrix}$ have two other traceless diagonal matrices
- However the three diagonal matrices are not be independent.
- Define the eighth matrix, λ_8, as the linear combination:

$$\lambda_8 = \frac{1}{\sqrt{3}} \begin{pmatrix} 0 & 0 & 0 \\ 0 & 1 & 0 \\ 0 & 0 & -1 \end{pmatrix} + \frac{1}{\sqrt{3}} \begin{pmatrix} 1 & 0 & 0 \\ 0 & 0 & 0 \\ 0 & 0 & -1 \end{pmatrix} = \frac{1}{\sqrt{3}} \begin{pmatrix} 1 & 0 & 0 \\ 0 & 1 & 0 \\ 0 & 0 & -2 \end{pmatrix}$$

which specifies the "vertical position" in the 2D plane

"Only need two axes (quantum numbers)
to specify a state in the 2D plane": $(\mathrm{I}_3, \mathrm{Y})$

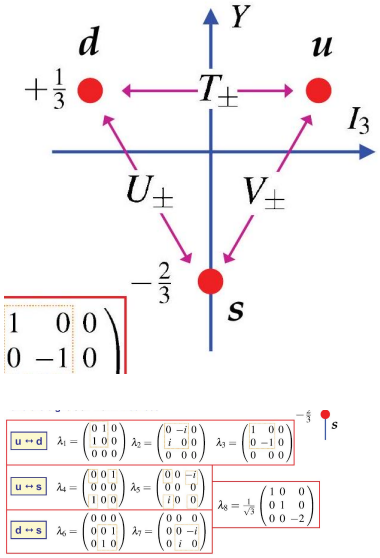


⋆ The other six matrices form six ladder operators which step between the states

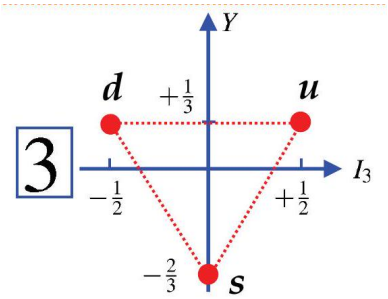
$$T_\pm = \tfrac{1}{2}(\lambda_1 \pm i\lambda_2)$$
$$V_\pm = \tfrac{1}{2}(\lambda_4 \pm i\lambda_5)$$
$$U_\pm = \tfrac{1}{2}(\lambda_6 \pm i\lambda_7)$$

with $I_3 = \tfrac{1}{2}\lambda_3$ $\quad Y = \tfrac{1}{\sqrt{3}}\lambda_8$

and the eight Gell-Mann matrices



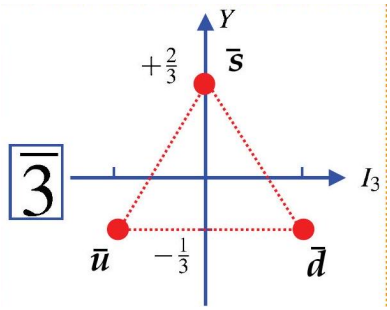
Quarks and anti-quarks in SU(3) Flavour



Quarks
$I_3 u = +\frac{1}{2}u; \quad I_3 d = -\frac{1}{2}d; \quad I_3 s = 0$

$$Yu = +\frac{1}{3}u; \quad Yd = +\frac{1}{3}d; \quad Ys = -\frac{2}{3}s$$

-The anti-quarks have opposite **SU**(3) flavour quantum numbers



Anti-Quarks

$$I_3\bar{u} = -\frac{1}{2}\bar{u}; \quad I_3\bar{d} = +\frac{1}{2}\bar{d}; \quad I_3\bar{s} = 0$$

$$Y\bar{u} = -\frac{1}{3}\bar{u}; \quad Y\bar{d} = -\frac{1}{3}\bar{d}; \quad Y\bar{s} = +\frac{2}{3}\bar{s}$$

SU(3) Ladder Operators

- SU(3) uds flavour symmetry contains ud, us

and ds $SU(2)$ symmetries

- Consider the $u \leftrightarrow S$ symmetry "V-spin" which has the associated $s \to u$ ladder operator

$$V_+ = \frac{1}{2}(\lambda_4 + i\lambda_5) = \frac{1}{2}\begin{pmatrix} 0 & 0 & 1 \\ 0 & 0 & 0 \\ 1 & 0 & 0 \end{pmatrix} + \frac{i}{2}\begin{pmatrix} 0 & 0 & -i \\ 0 & 0 & 0 \\ i & 0 & 0 \end{pmatrix} = \begin{pmatrix} 0 & 0 & 1 \\ 0 & 0 & 0 \\ 0 & 0 & 0 \end{pmatrix}$$

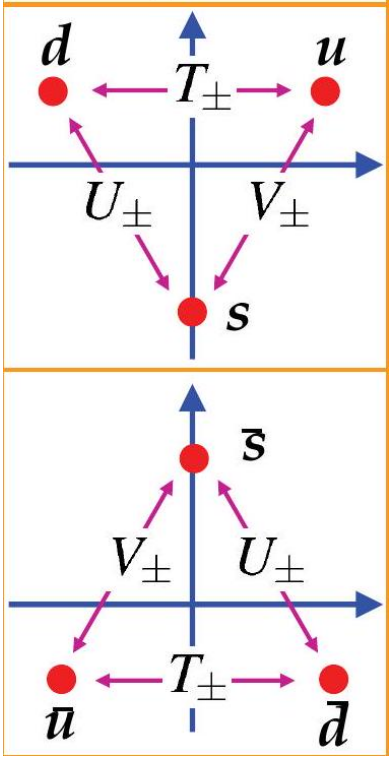
$$\text{with} \quad V_+ s = \begin{pmatrix} 0 & 0 & 1 \\ 0 & 0 & 0 \\ 0 & 0 & 0 \end{pmatrix}\begin{pmatrix} 0 \\ 0 \\ 1 \end{pmatrix} = \begin{pmatrix} 1 \\ 0 \\ 0 \end{pmatrix} = +u$$

⋆ The effects of the six ladder operators are:

$T_+d = u; \quad T_u = d;$	$T_+\bar{u} = -\bar{d}; \quad T_\bar{d} = -\bar{u}$
$V_+s = u; \quad V_u = s;$	$V_+\bar{u} = -\bar{s}; \quad V_\bar{s} = -\bar{u}$
$U_+s = d; \quad U_d = s;$	$U_+\bar{d} = -\bar{s}; \quad U_\bar{s} = -\bar{d}$

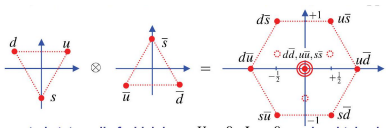
all other combinations give zero
SU(3) LADDER OPERATORS

$$T_\pm = \frac{1}{2}(\lambda_1 \pm i\lambda_2)$$
$$V_\pm = \frac{1}{2}(\lambda_4 \pm i\lambda_5)$$
$$U_\pm = \frac{1}{2}(\lambda_6 \pm i\lambda_7)$$

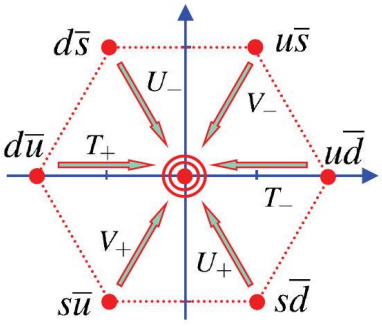


Light (uds) Mesons

- Use ladder operators to construct uds mesons from the nine possible $q\bar{q}$ states



-The three central states, all of which have $Y = 0; I_3 = 0$ can be obtained using the ladder operators and orthogonality. Starting from the outer states can reach the centre in six ways



- Only two of these six states are linearly independent.
- But there are three states with $Y = 0; I_3 = 0$

-Therefore one state is not part of the same multiplet, i.e. cannot be reached with ladder ops.

- First form two linearly independent orthogonal states from:

$$|u\bar{u}\rangle - |d\bar{d}\rangle \quad |u\bar{u}\rangle - |s\bar{s}\rangle \quad |d\bar{d}\rangle - |s\bar{s}\rangle$$

⋆ If the SU(3) flavour symmetry were exact, the choice of states wouldn't matter. However, $m_s > m_{u,d}$ and the symmetry is only approximate.

- Experimentally observe three light mesons with m $\sim$ 140MeV: π^+, π^0, π^- - Identify one state (the π^0) with the isospin triplet (derived previously)

$$\psi_1 = \frac{1}{\sqrt{2}}(u\bar{u} - d\bar{d})$$

- The second state can be obtained by taking the linear combination of the other two states which is orthogonal to the π^0

$$\psi_2 = \alpha(|u\bar{u}\rangle - |s\bar{s}\rangle) + \beta(|d\bar{d}\rangle - |s\bar{s}\rangle)$$

with orthonormality: $\langle\psi_1|\psi_2\rangle = 0; \quad \langle\psi_2|\psi_2\rangle = 1$

$$\psi_2 = \frac{1}{\sqrt{6}}(u\bar{u} + d\bar{d} - 2s\bar{s})$$

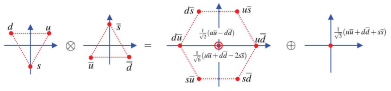
- The final state (which is not part of the same multiplet) can be obtained by requiring it to be orthogonal to ψ_1 and ψ_2

$$\psi_3 = \frac{1}{\sqrt{3}}(u\bar{u} + d\bar{d} + s\bar{s})$$

⋆ It is easy to check that ψ_3 is a singlet state using ladder operators

$$T_+\psi_3 = T_-\psi_3 = U_+\psi_3 = U_-\psi_3 = V_+\psi_3 = V_-\psi_3 = 0$$

which confirms that $\psi_3 = \frac{1}{\sqrt{3}}(u\bar{u} + d\bar{d} + s\bar{s})$ is a "flavourless" singlet
-Therefore the combination of a quark and anti-quark yields nine states which breakdown into an OCTET and a SINGLET



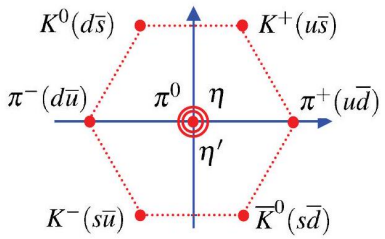
- In the language of group theory: $3 \otimes \overline{3} = 8 \oplus 1$

⋆ Compare with combination of two spin-half particles $2 \otimes 2 = 3 \oplus 1$
TRIPLET of spin-1 states: $|1,-1\rangle, |1,0\rangle, |1,+1\rangle$ spin-0 SINGLET: $|0,0\rangle$

- These spin triplet states are connected by ladder operators just as the meson uds octet states are connected by SU(3) flavour ladder operators

-The singlet state carries no angular momentum - in this sense the SU(3) flavour singlet is "flavourless"

PSEUDOSCALAR MESONS ($L = 0,\ \mathrm{S} = 0,\ \mathrm{J} = 0, \mathrm{P} = -1$)



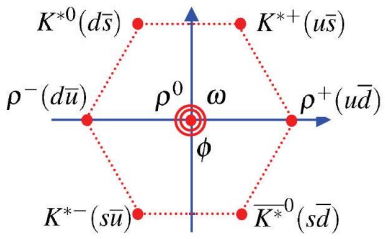
- Because SU(3) flavour is only approximate the physical states with $I_3 = 0, Y = 0$ can be mixtures of the octet and singlet states.

Empirically find:

$$\pi^0 = \frac{1}{\sqrt{2}}(u\bar{u} - d\bar{d})$$
$$\eta \approx \frac{1}{\sqrt{6}}(u\bar{u} + d\bar{d} - 2s\bar{s})$$
$$\eta' \approx \frac{1}{\sqrt{3}}(u\bar{u} + d\bar{d} + s\bar{s})$$

singlet

VECTOR MESONS ($L = 0, S = 1, J = 1, P = -1$)



- For the vector mesons the physical states are found to be approximately "ideally mixed":

$$\rho^0 = \frac{1}{\sqrt{2}}(u\bar{u} - d\bar{d})$$
$$\omega \approx \frac{1}{\sqrt{2}}(u\bar{u} + d\bar{d})$$
$$\phi \approx s\bar{s}$$

MASSES

$\pi^\pm$: 140MeV
π^0 : 135MeV
$K^\pm$: 494MeV $\quad K^0/\bar{K}^0$: 498MeV
η : 549MeV
η' : 958MeV

$\rho^\pm$: 770MeV $\quad \rho^0$: 770MeV

$$K^{*\pm}: 892\text{MeV} \quad K^{*0}/\overline{K}^{*0}: 896\text{MeV}$$

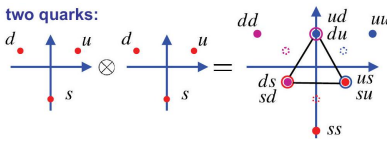
$$\omega: 782\text{MeV} \quad \phi: 1020\text{MeV}$$

Combining uds Quarks to form Baryons

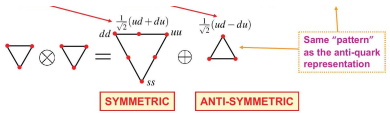
⋆ Have already seen that constructing Baryon states is a fairly tedious process when we derived the proton wave-function. Concentrate on multiplet structure rather than deriving all the wave-functions.

⋆ **Everything we do here is relevant to the treatment of colour**

- First combine two quarks:



⋆Yields a symmetric sextet and anti-symmetric triplet: $3 \otimes 3 = 6 \oplus \overline{3}$

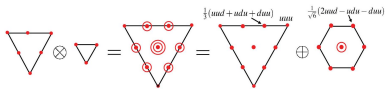


- Now add the third quark:

$$\nabla \otimes \nabla \otimes \nabla = \left[\nabla^{+}\Delta\right]_{\otimes} \nabla$$

- Best considered in two parts, building on the sextet and triplet. Again concentrate on the multiplet structure (for the wave-functions refer to the discussion of proton wave-function).

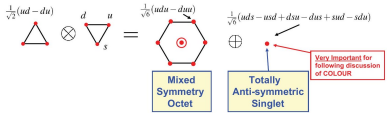
(1) Building on the sextet: $3 \otimes 6 = 10 \oplus 8$



Decuplet

(2) Building on the triplet:

- Just as in the case of uds mesons we are combining $\overline{3} \times 3$ and again obtain an octet and a singlet



- Can verify the wave-function $\psi_{\text{singlet}} = \frac{1}{\sqrt{6}}(uds - usd + dsu - dus + sud - sdu)$ is a singlet by using ladder operators, e.g.

$$T_{+}\psi_{\text{singlet}} = \frac{1}{\sqrt{6}}(uus - usu + usu - uus + suu - suu) = 0$$

- In summary, the combination of three uds quarks decomposes into

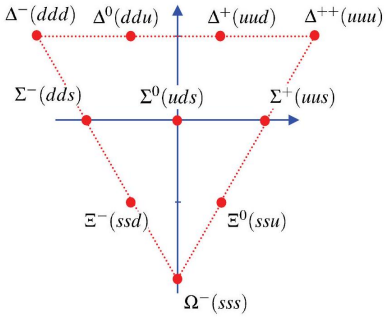
$$3 \otimes 3 \otimes 3 = 3 \otimes (6 \oplus \overline{3}) = 10 \oplus 8 \oplus 8 \oplus 1$$

Baryon Decuplet

⋆ The baryon states (L = 0) are:

- the spin 3/2 decuplet of symmetric flavour and symmetric spin wave-functions $\phi(S)\chi(S)$

BARYON DECUPLET ($L = 0,\ \mathrm{S} = 3/2,\ \mathrm{J} = 3/2, \mathrm{P} = +1$)
Mass in MeV



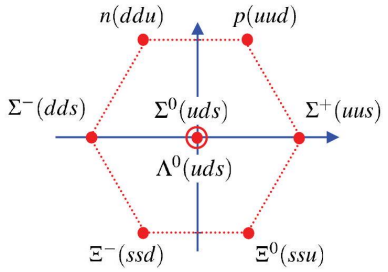
$\Delta(1232)$
$\Sigma(1318)$
$\Omega(1672)$
⋆ If SU(3) flavour were an exact symmetry all masses would be the same (broken symmetry)

Baryon Octet

⋆ The spin 1/2 octet is formed from mixed symmetry flavour and mixed symmetry spin wave-functions

$$\alpha\phi\left(M_S\right)\chi\left(M_S\right) + \beta\phi\left(M_A\right)\chi\left(M_A\right)$$

See previous discussion proton for how to obtain wave-functions
BARYON OCTET ($L = 0,\ \mathrm{S} = 1/2,\ \mathrm{J} = 1/2, \mathrm{P} = +1$)



Mass in MeV
939
$\Sigma(1193)$
Λ (1116)
$\Xi(1318)$
NOTE: Cannot form a totally symmetric wave-function based on the anti-symmetric flavour singlet as there no totally anti-symmetric spin wave-function for 3 quarks

Summary

⋆ **Considered SU(2) ud and SU(3) uds flavour symmetries**

⋆ Although these flavour symmetries are only approximate can still be used to explain observed multiplet structure for mesons/baryons

- In case of SU(3) flavour symmetry results, e.g. predicted wave-functions should be treated with a pinch of salt as $m_s \neq m_{u/d}$

⋆ Introduced idea of singlet states being "spinless" or "flavourless"
⋆ In the next handout apply these ideas to colour and QCD...

Appendix: the SU(2) **anti-quark representation**

- Define anti-quark doublet $\bar{q} = \binom{-\bar{d}}{\bar{u}} = \binom{-d^*}{u^*}$

Non-examinable

- The quark doublet $q = \binom{u}{d}$ transforms as $q' = Uq$

$$\begin{pmatrix} u' \\ d' \end{pmatrix} = U \begin{pmatrix} u \\ d \end{pmatrix} \underset{\text{conjugate}}{\text{Complex}} \begin{pmatrix} u'^* \\ d'^* \end{pmatrix} = U^* \begin{pmatrix} u^* \\ d^* \end{pmatrix}$$

- Express in terms of anti-quark doublet

$$\begin{pmatrix} 0 & -1 \\ 1 & 0 \end{pmatrix} \bar{q}' = U \begin{pmatrix} 0 & -1 \\ 1 & 0 \end{pmatrix} \bar{q}$$

- Hence $\bar{q}$ transforms as

$$\bar{q}' = \begin{pmatrix} 0 & 1 \\ -1 & 0 \end{pmatrix} U^* \begin{pmatrix} 0 & -1 \\ 1 & 0 \end{pmatrix} \bar{q}$$

- In general a 2×2 unitary matrix can be written as

$$U = \begin{pmatrix} c_{11} & c_{12} \\ -c_{12}^* & c_{11}^* \end{pmatrix}$$

- Giving

$$\begin{aligned} \bar{q}' &= \begin{pmatrix} 0 & 1 \\ -1 & 0 \end{pmatrix} \begin{pmatrix} c_{11}^* & c_{12}^* \\ -c_{12} & c_{11} \end{pmatrix} \begin{pmatrix} 0 & -1 \\ 1 & 0 \end{pmatrix} \bar{q} \\ &= \begin{pmatrix} c_{11} & c_{12} \\ -c_{12}^* & c_{11}^* \end{pmatrix} \\ &= U\bar{q} \end{aligned}$$

-Therefore the anti-quark doublet $\bar{q} = \binom{-\bar{d}}{\bar{u}}$ transforms in the same way as the quark doublet $q = \binom{u}{d}$

NOTE: this is a special property of SU(2) and for SU(3) there is no analogous representation of the anti-quarks

1.8.4 H8: Quantum Chromodynamics

The Local Gauge Principle

(see the Appendices A, B and C for more details)

⋆ All the interactions between fermions and spin-1 bosons in the SM are specified by the principle of LOCAL GAUGE INVARIANCE

⋆ To arrive at QED, require physics to be invariant under the local phase transformation of particle wave-functions

$$\psi \to \psi' = \psi e^{iq\chi(x)}$$

⋆ Note that the change of phase depends on the space-time coordinate: $\chi(t, \vec{x})$

- Under this transformation the Dirac Equation transforms as

$$i\gamma^\mu \partial_\mu \psi - m\psi = 0 \Rightarrow i\gamma^\mu \left(\partial_\mu + iq\partial_\mu \chi\right)\psi - m\psi = 0$$

-To make "physics", i.e. the Dirac equation, invariant under this local phase transformation FORCED to introduce a massless gauge boson, A_μ.

- The Dirac equation has to be modified to include this new field:

$$i\gamma^\mu \left(\partial_\mu - qA_\mu\right)\psi - m\psi = 0$$

-The modified Dirac equation is invariant under local phase transformations if:

$$A_\mu \to A'_\mu = A_\mu - \partial_\mu \chi$$

⋆ For physics to remain unchanged - must have GAUGE INVARIANCE of the new field, i.e. physical predictions unchanged for $A_\mu \to A'_\mu = A_\mu - \partial_\mu \chi$

⋆ Hence the principle of invariance under local phase transformations completely specifies the interaction between a fermion and the gauge boson (i.e. photon):

$$\begin{aligned} & i\gamma^\mu \left(\partial_\mu \psi - qA_\mu\right)) \\ & \implies \text{interaction vertex:} \quad i\gamma^\mu q A_\mu \end{aligned} \qquad \text{(seep.111)}$$

QED!

⋆ The local phase transformation of QED is a unitary U(1) transformation

$$\psi \to \psi' = \hat{U}\psi \quad \text{i.e.} \quad \psi \to \psi' = \psi e^{iq\chi(x)} \quad \text{with} \quad U^\dagger U = 1$$

Now extend this idea...

From QED to QCD

⋆ Suppose there is another fundamental symmetry of the universe, say "invariance under SU(3) local phase transformations"

- i.e. require invariance under $\psi \to \psi' = \psi e^{ig\vec{\lambda}\cdot\vec{\theta}(x)}$ where

$\vec{\lambda}$ are the eight 3×3 Gell-Mann matrices introduced in handout 7
$\vec{\theta}(x)$ are 8 functions taking different values at each point in space-time
$\Rightarrow$ 8 spin-1 gauge bosons
$\psi = \begin{pmatrix} \psi_1 \\ \psi_2 \\ \psi_3 \end{pmatrix}$ wave function is now a vector in COLOUR SPACE

$\star$ QCD is fully specified by require invariance under $SU(3)$ local phase transformations
Corresponds to rotating states in colour space about an axis whose direction is different at every space-time point
$\Longrightarrow$ interaction vertex: $-\frac{1}{2} i g_s \lambda^a \gamma^\mu$

- Predicts 8 massless gauge bosons - the gluons (one for each λ)

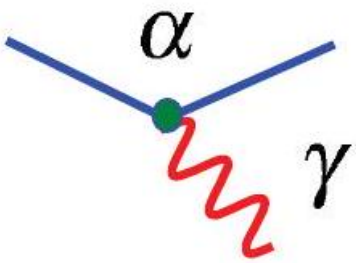
$\star$ Also predicts exact form for interactions between gluons, i.e. the 3 and 4 gluon vertices - the details are beyond the level of this course

Colour in QCD

$\star$ The theory of the strong interaction, Quantum Chromodynamics (QCD), is very similar to QED but with 3 conserved "colour" charges

In QED:

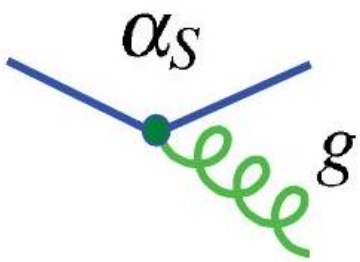
- the electron carries one unit of charge - e
- the anti-electron carries one unit of anti-charge $+e$
- the force is mediated by a massless "gauge



boson" - the photon

In QCD:

- quarks carry colour charge: r, g, b
- anti-quarks carry anti-charge: $\bar{r}, \bar{g}, \bar{b}$
- The force is mediated by massless gluons



⋆ In QCD, the strong interaction is invariant under rotations in colour space

$$r \leftrightarrow b; r \leftrightarrow g; b \leftrightarrow g$$

i.e. the same for all three colours

SU(3) colour symmetry

-This is an exact symmetry, unlike the approximate uds flavour symmetry discussed previously.

Represent r, g, b SU(3) colour states by:

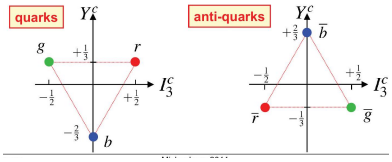
$$r = \begin{pmatrix} 1 \\ 0 \\ 0 \end{pmatrix}; \quad g = \begin{pmatrix} 0 \\ 1 \\ 0 \end{pmatrix}; \quad b = \begin{pmatrix} 0 \\ 0 \\ 1 \end{pmatrix}$$

⋆ Colour states can be labelled by two quantum numbers:

- I_3^c colour isospin
- Y^c colour hypercharge

Exactly analogous to labelling u,d,s flavour states by I_3 and Y

⋆ Each quark (anti-quark) can have the following colour quantum numbers:



Colour Confinement

- It is believed (although not yet proven) that all observed free particles are "colourless"

-i.e. never observe a free quark (which would carry colour charge)

- consequently quarks are always found in bound states colourless hadrons

⋆ **Colour Confinement Hypothesis:**

only colour singlet states can

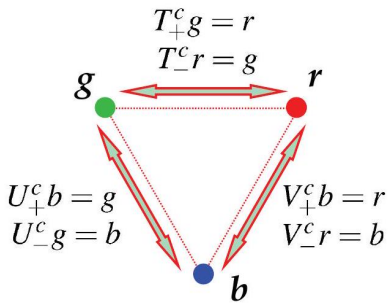
exist as free particles

⋆ All hadrons must be "colourless" i.e. colour singlets

⋆ To construct colour wave-functions for hadrons can apply results for SU(3) flavour symmetry to **SU**(3) colour with replacement

$$u \to r$$
$$d \to g$$
$$s \to b$$

⋆ just as for uds flavour symmetry can define colour ladder operators



Colour Singlets

⋆ It is important to understand what is meant by a singlet state

⋆ Consider spin states obtained from two spin 1/2 particles.

- Four spin combinations: $\uparrow\uparrow, \uparrow\downarrow, \downarrow\uparrow, \downarrow\downarrow$
- Gives four eigenstates of $\hat{S}^2, \hat{S}_z$

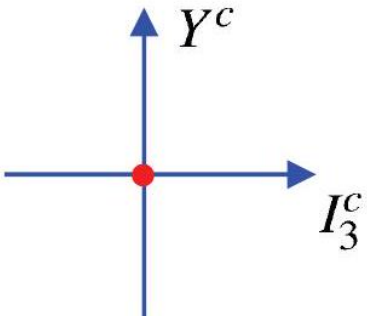
$(2 \otimes 2 = 3 \oplus 1)$

$$|1, +1\rangle = \uparrow\uparrow$$
$$|1, 0\rangle = \frac{1}{\sqrt{2}}(\uparrow\downarrow + \downarrow\uparrow)$$
$$|1, -1\rangle = \downarrow\downarrow$$

⋆ The singlet state is "spinless": it has zero angular momentum, is invariant under SU(2) spin transformations and spin ladder operators yield zero

$$S_\pm |0, 0\rangle = 0$$

- In the same way COLOUR SINGLETS are "colourless" combinations:
- they have zero colour quantum numbers $I^c_3 = 0, Y^c = 0$
- invariant under SU(3) colour transformations
- ladder operators $T_\pm, U_\pm, V_\pm$all yield zero

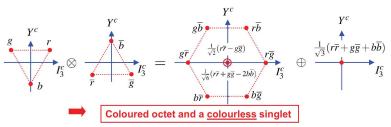


NOT sufficient to have $I^c_3 = 0, Y^c = 0$: does not mean that state is a singlet

Meson Colour Wave-function

⋆ Consider colour wave-functions for $q\bar{q}$

⋆ The combination of colour with anti-colour is mathematically identical to construction of meson wave-functions with uds flavour symmetry



- Colour confinement implies that hadrons only exist in colour singlet states so the colour wave-function for mesons is:

$$\psi_c^{q\bar{q}} = \frac{1}{\sqrt{3}}(r\bar{r} + g\bar{g} + b\bar{b})$$

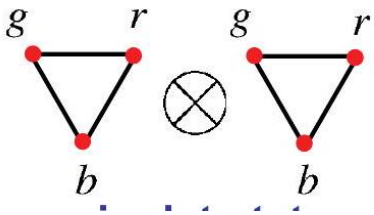
⋆ Can we have a $qq\bar{q}$ state? i.e. by adding a quark to the above octet can we form a state with $Y^c = 0; I_3^c = 0$. The answer is clear no.

$qq\bar{q}$ bound states do not exist in nature.

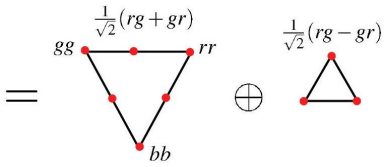
Baryon Colour Wave-function

⋆ Do qq bound states exist? This is equivalent to asking whether it possible to form a colour singlet from two colour triplets?

- Following the discussion of construction of baryon wave-functions in SU(3) flavour symmetry obtain

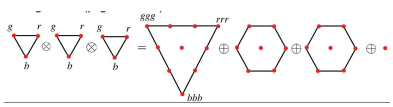


- No qq colour singlet state



- Colour confinement ⇒ bound states of qq do not exist

BUT combination of three quarks (three colour triplets) gives a colour singlet state (pages 235-237)



⋆ The singlet colour wave-function is:

$$\psi_c^{qqq} = \frac{1}{\sqrt{6}}(rgb - rbg + gbr - grb + brg - bgr)$$

Check this is a colour singlet...

- It has $I_3^c = 0, Y^c = 0$: a necessary but not sufficient condition
- Apply ladder operators, e.g. T_+ (recall $T_+ g = r$)

$$T_+ \Psi_c^{qqq} = \frac{1}{\sqrt{6}}(rrb - rbr + rbr - rrb + brr - brr) = 0$$

-Similarly $T_- \psi_c^{qqq} = 0; \quad V_\pm \psi_c^{qqq} = 0; \quad U_\pm \psi_c^{qqq} = 0;$

Colourless singlet - therefore qqq bound states exist!

$\Rightarrow$ **Anti-symmetric colour wave-function**

Allowed Hadrons i.e. the possible colour singlet states

$q\bar{q}, qqq$

$q\bar{q}q\bar{q}, qqqq\bar{q}$

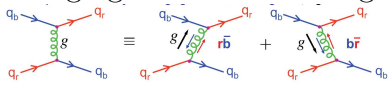
Mesons and Baryons

Exotic states, e.g. pentaquarks

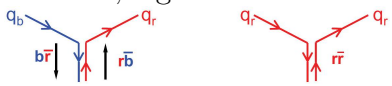
To date all confirmed hadrons are either mesons or baryons. However, some recent (but not entirely convincing) "evidence" for pentaquark states

Gluons

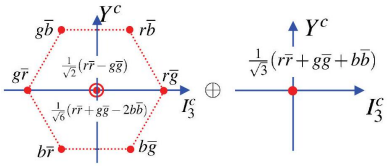
- In QCD quarks interact by exchanging virtual massless gluons, e.g.



⋆ Gluons carry colour and anti-colour, e.g.



⋆ Gluon colour wave-functions (colour + anti-colour) are the same as those obtained for mesons (also colour + anti-colour)



⋆ So we might expect 9 physical gluons:

OCTET: $r\bar{g}, r\bar{b}, g\bar{r}, g\bar{b}, b\bar{r}, b\bar{g}, \frac{1}{\sqrt{2}}(r\bar{r} - g\bar{g}), \frac{1}{\sqrt{6}}(r\bar{r} + g\bar{g} - 2b\bar{b})$ SINGLET: $\frac{1}{\sqrt{3}}(r\bar{r} + g\bar{g} + b\bar{b})$

BUT, colour confinement hypothesis:

only colour singlet states can exist as free particles

Colour singlet gluon would be unconfined. It would behave like a strongly interacting photon $\Rightarrow$ infinite range Strong force.

⋆ Empirically, the strong force is short range and therefore know that the physical gluons are confined. The colour singlet state does not exist in nature!

NOTE: this is not entirely ad hoc. In the context of gauge field theory (see minor option) the strong interaction arises from a fundamental SU(3) symmetry. The gluons arise from the generators of the symmetry group (the Gell-Mann λ matrices). There are 8 such matrices $\Rightarrow$ 8 gluons. Had nature "chosen" a U(3) symmetry, would have 9 gluons, the additional gluon would be the colour singlet state and QCD would be an unconfined long-range force.

NOTE: the "gauge symmetry" determines the exact nature of the interaction $\Rightarrow$ FEYNMAN RULES

Gluon-Gluon Interactions

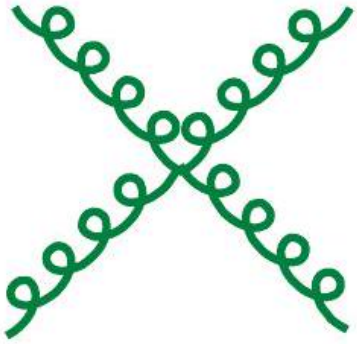
⋆ In QED the photon does not carry the charge of the EM interaction (photons are electrically neutral)

⋆ In contrast, in QCD the gluons do carry colour charge

$\Longrightarrow$ Gluon Self-Interactions

⋆ Two new vertices (no QED analogues)

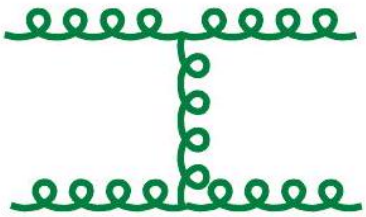
triple-gluon vertex



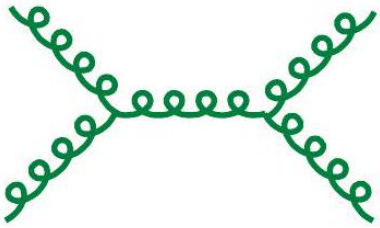
quartic-gluon vertex

- In addition to quark-quark scattering, therefore can have gluon-gluon scattering

e.g. possible way of arranging



the colour flow



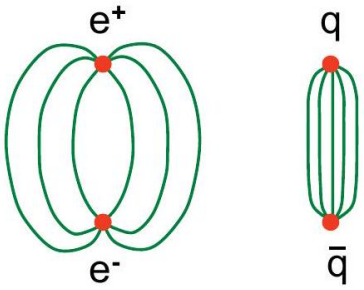
Gluon self-Interactions and Confinement

⋆ Gluon self-interactions are believed to give rise to colour confinement

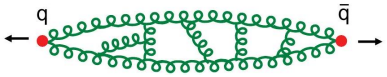
⋆ Qualitative picture:

- Compare QED with QCD

-In QCD “gluon self-interactions squeeze lines of force into a flux tube"



⋆ What happens when try to separate two coloured objects e.g. $q\bar{q}$



- Form a flux tube of interacting gluons of approximately constant energy density $\sim$ 1GeV/fm

$$\Rightarrow V(r) \sim \lambda r$$

- Require infinite energy to separate coloured objects to infinity - Coloured quarks and gluons are always confined within colourless states - In this way QCD provides a plausible explanation of confinement - but not yet proven (although there has been recent progress with Lattice QCD)

Hadronisation and Jets

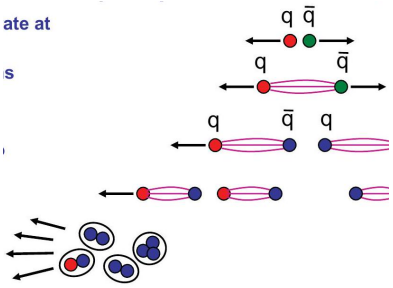
⋆ Consider a quark and anti-quark produced in electron positron annihilation

i) Initially Quarks separate at high velocity

ii) Colour flux tube forms between quarks

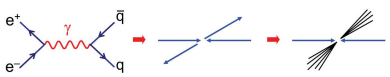
iii) Energy stored in the flux tube sufficient to produce q $\bar{q}$ pairs

iv) Process continues until quarks pair up into jets of colourless hadrons



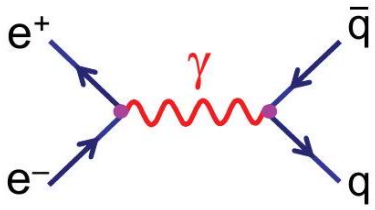
⋆ This process is called hadronisation. It is not (yet) calculable.

⋆ The main consequence is that at collider experiments quarks and gluons observed as jets of particles



QCD and Colour in e^+e^- Collisions

⋆e^+e^-colliders are an excellent place to study QCD



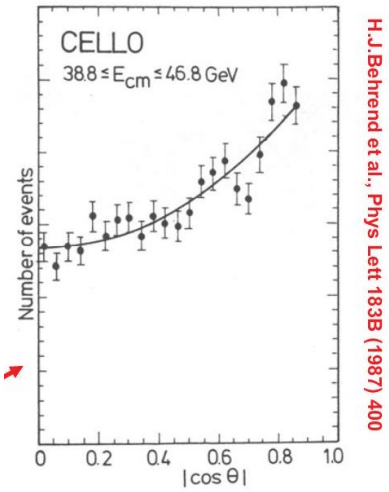
⋆ Well defined production of quarks

- QED process well-understood
- no need to know parton structure functions
- – experimentally very clean - no proton remnants

⋆ In handout 5 obtained expressions for the $e^+e^- \to \mu^+\mu^-$cross-section $\sigma = \frac{4\pi\alpha^2}{3s}$ $\frac{\mathrm{d}\sigma}{\mathrm{d}\Omega} = \frac{\alpha^2}{4s}(1+\cos^2\theta)$

- In e^+e^-collisions produce all quark flavours for which $\sqrt{s} > 2m_q$
- In general, i.e. unless producing a $q\bar{q}$ bound state, produce jets of hadrons
- Usually can't tell which jet came from the quark and came from anti-quark

Angular distribution of jets $\propto (1+\cos^2\theta)$ Quarks are spin 1/2



⋆ Colour is conserved and quarks are produced as $r\bar{r}, g\bar{g}, b\bar{b}$
⋆ For a single quark flavour and single colour

$$\sigma\left(e^+e^- \to q_i\bar{q}_i\right) = \frac{4\pi\alpha^2}{3s}Q_q^2$$

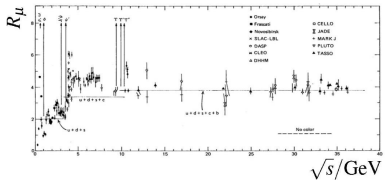
- Experimentally observe jets of hadrons:

$$\sigma\left(e^+e^- \to \text{ hadrons }\right) = 3\sum_{u,d,s,..}\frac{4\pi\alpha^2}{3s}Q_q^2$$

Factor 3 comes from colours

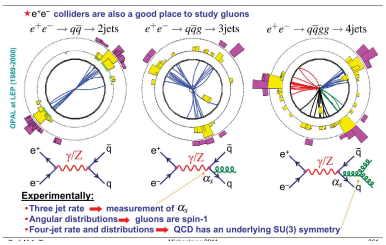
- Usual to express as ratio compared to $\sigma\left(e^+e^- \to \mu^+\mu^-\right)$

$$R_\mu = \frac{\sigma\left(e^+e^- \to \text{ hadrons }\right)}{\sigma\left(e^+e^- \to \mu^+\mu^-\right)} = 3\sum_{u,d,s,..} Q_q^2$$



$\underline{\mathbf{u}, \mathrm{d}, \mathbf{s}, \mathbf{c}}: R_\mu = \frac{10}{3}$
$\underline{\mathbf{u}, \mathrm{d}, \mathbf{s}, \mathbf{c}, \mathrm{b}}: R_\mu = \frac{11}{3}$
$\star$ Data consistent with expectation with factor 3 from colour

Jet production in e+e- Collisions



The Quark - Gluon Interaction

- Representing the colour part of the fermion wave-functions by:

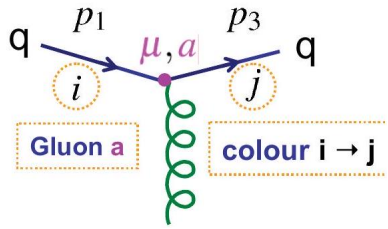
$$r = c_1 = \begin{pmatrix} 1 \\ 0 \\ 0 \end{pmatrix} \quad g = c_2 = \begin{pmatrix} 0 \\ 1 \\ 0 \end{pmatrix} \quad b = c_3 = \begin{pmatrix} 0 \\ 0 \\ 1 \end{pmatrix}$$

- Particle wave-functions $u(p) \longrightarrow c_i u(p)$

-The QCD qqg vertex is written:

$$\bar{u}\left(p_3\right) c_j^\dagger \left\{-\frac{1}{2} i g_s \lambda^a \gamma^\mu\right\} c_i u\left(p_1\right)$$

- Only difference w.r.t. QED is the insertion of the 3×3
- Isolating the colour part:



$$c_j^\dagger \lambda^a c_i = c_j^\dagger \begin{pmatrix} \lambda_{1i}^a \\ \lambda_{2i}^a \\ \lambda_{3i}^a \end{pmatrix} = \lambda_{ji}^a$$

-Hence the fundamental quark - gluon QCD interaction can be written

$$\bar{u}(p_3)\, c_j^\dagger \left\{ -\frac{1}{2} i g_s \lambda^a \gamma^\mu \right\} c_i u(p_1) \equiv \bar{u}(p_3) \left\{ -\frac{1}{2} i g_s \lambda_{ji}^a \gamma^\mu \right\} u(p_1)$$

Feynman Rules for QCD

External Lines	incoming quark	$u(p)$	$\longrightarrow$
	outgoing quark	$\bar{u}(p)$	$\longrightarrow$
spin 1/2	incoming anti-quark	$\bar{v}(p)$	$\longrightarrow$
	outgoing anti-quark	$v(p)$	$\bullet \leftarrow$
	incoming gluon	$\varepsilon^\mu(p)$	elel
sk	outgoing gluon	$\varepsilon^\mu(p)^*$	ee

- Internal Lines (propagators)

spin 1 gluon
$\frac{-ig_{\mu\nu}}{q^2}\delta^{ab}$



$a, b = 1, 2, \ldots, 8$ are gluon colour indices

Vertex Factors

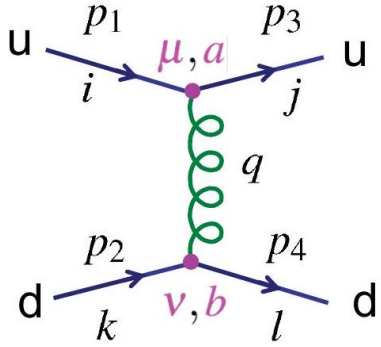
spin 1/2 quark

$$-ig_s \frac{1}{2} \lambda_{ji}^a \gamma^\mu$$

i, j = 1, 2, 3 are quark colours, λ^a $a = 1, 2, ..8$ are the Gell-Mann SU(3) matrices
+3 gluon and 4 gluon interaction vertices
Matrix Element $-iM$ = product of all factors

Matrix Element for quark-quark scattering

⋆ Consider QCD scattering of an up and a down quark



-The incoming and out-going quark colours are labelled by $i, j, k, l = \{1, 2, 3\}$ (or $\{r, g, b\}$)

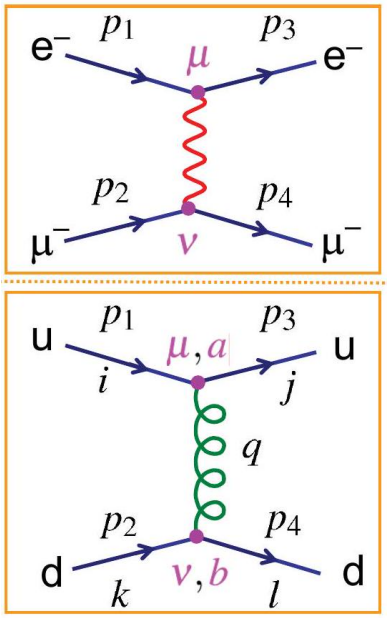
- In terms of colour this scattering is $ik \to jl$
- The 8 different gluons are accounted for by the colour indices $a, b = 1, 2, \ldots, 8$
- NOTE: the δ-function in the propagator ensures $a = b$, i.e. the gluon "emitted" at a is the same as that "absorbed" at b

$\star$ Applying the Feynman rules:
$-iM = \left[\bar{u}_u(p_3)\left\{-\frac{1}{2}ig_s\lambda^a_{ji}\gamma^\mu\right\}u_u(p_1)\right]\frac{-ig_{\mu\nu}}{q^2}\delta^{ab}\left[\bar{u}_d(p_4)\left\{-\frac{1}{2}ig_s\lambda^b_{lk}\gamma^\nu\right\}u_d(p_2)\right]$ where summation over a and b (and μ and v) is implied.
$\star$ Summing over a and b using the δ-function gives:

$$M = -\frac{g_s^2}{4}\lambda^a_{ji}\lambda^a_{lk}\frac{1}{q^2}g_{\mu\nu}\left[\bar{u}_u(p_3)\gamma^\mu u_u(p_1)\right]\left[\bar{u}_d(p_4)\gamma^v u_d(p_2)\right]$$

QED
$-iM = \left[\bar{u}(p_3)ie\gamma^\mu u(p_1)\right]\frac{-ig_{\mu\nu}}{q^2}\left[\bar{u}(p_4)ie\gamma^\nu u(p_2)\right]$
$M = -e^2\frac{1}{q^2}g_{\mu\nu}\left[\bar{u}(p_3)\gamma^\mu u(p_1)\right]\left[\bar{u}(p_4)\gamma^v u(p_2)\right]$
QCD
$M = -\frac{g_s^2}{4}\lambda^a_{ji}\lambda^a_{lk}\frac{1}{q^2}g_{\mu v}\left[\bar{u}_u(p_3)\gamma^\mu u_u(p_1)\right]\left[\bar{u}_d(p_4)\gamma^v u_d(p_2)\right]$
$\star$ QCD Matrix Element = QED Matrix Element with:

- $e^2 \to g_s^2$ or equivalently $\alpha = \frac{e^2}{4\pi} \to \alpha_s = \frac{g_s^2}{4\pi}$



- QCD Matrix Element includes an additional "colour factor"

$$C(ik \to jl) \equiv \frac{1}{4}\sum_{a=1}^{8}\lambda^a_{ji}\lambda^a_{lk}$$

Evaluation of QCD Colour Factors

- QCD colour factors reflect the gluon states that are involved

$\lambda^1 = \begin{pmatrix} 0 & 1 & 0 \\ 1 & 0 & 0 \\ 0 & 0 & 0 \end{pmatrix}$	$\lambda^4 = \begin{pmatrix} 0 & 0 & 1 \\ 0 & 0 & 0 \\ 1 & 0 & 0 \end{pmatrix}$	$\lambda^6 = \begin{pmatrix} 0 & 0 & 0 \\ 0 & 0 & 1 \\ 0 & 1 & 0 \end{pmatrix}$	$\lambda^3 = \begin{pmatrix} 1 & 0 & 0 \\ 0 & -1 & 0 \\ 0 & 0 & 0 \end{pmatrix}$
$\lambda^2 = \begin{pmatrix} 0 & -i & 0 \\ i & 0 & 0 \\ 0 & 0 & 0 \end{pmatrix}$	$\lambda^5 = \begin{pmatrix} 0 & 0 & - \\ 0 & 0 & 0 \\ i & 0 & 0 \end{pmatrix}$	$\lambda^7 = \begin{pmatrix} 0 & 0 & 0 \\ 0 & 0 & -i \\ 0 & i & 0 \end{pmatrix}$	$\lambda^8 = \frac{1}{\sqrt{3}} \begin{pmatrix} 1 & 0 & 0 \\ 0 & 1 & 0 \\ 0 & 0 & -2 \end{pmatrix}$
$r\bar{b}, b\bar{r}$	$g\bar{b}, b\bar{g}$	$\frac{1}{\sqrt{2}}(r\bar{r} - g\bar{g}) \frac{1}{\sqrt{6}}(r\bar{r} + g\bar{g} - 2b\bar{b})$	

Gluons: $r\bar{g}, g\bar{r}$

(1) Configurations involving a single colour

$\mathbf{r} \underbrace{a}_{i=1}$ · Only matrices with non-zero entries in 11 position are inv

$$C(rr \to rr) = \tfrac{1}{4} \sum_{a=1}^{8} \lambda^a_{11} \lambda^a_{11} = \tfrac{1}{4} \left(\lambda^3_{11} \lambda^3_{11} + \lambda^8_{11} \lambda^8_{11} \right)$$

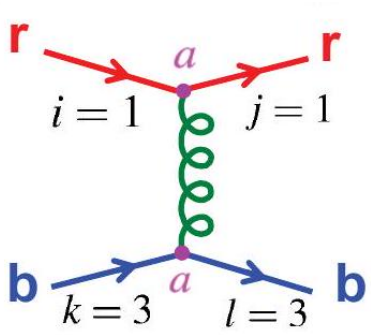
$\mathbf{r} \overbrace{k=1}^{a}{}_{l=1} \mathbf{r}$

$$= \frac{1}{4} \left(1 + \frac{1}{3} \right) = \frac{1}{3}$$

Similarly find

$$C(rr \to rr) = C(gg \to gg) = C(bb \to bb) = \frac{1}{3}$$

Other configurations where quarks don't change colour e.g. $rb \to rb$



- Only matrices with non-zero entries in 11 and 33 position are involved

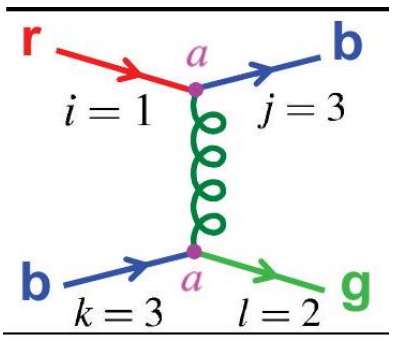
$$C(rb \to rb) = \frac{1}{4} \sum_{a=1}^{8} \lambda^a_{11} \lambda^a_{33} = \frac{1}{4} \left(\lambda^8_{11} \lambda^8_{33} \right)$$
$$= \frac{1}{4} \left(\frac{1}{\sqrt{3}} \cdot \frac{-2}{\sqrt{3}} \right) = -\frac{1}{6}$$

Similarly $C(rb \to rb) = C(rg \to rg) = C(gr \to gr) = C(gb \to gb) = C(br \to br) = C(bg \to bg) = -\frac{1}{6}$

3. Configurations where quarks swap colours e.g. $rg \to gr$
   $r \quad g \quad \mathbf{r}$
   $_{i=1\}^{a}{}_{k=2} j=2$

- Only matrices with non-zero entries in 12 and 21 position
  $C(rb \to br) = C(rg \to gr) = C(gr \to rg) = C(gb \to bg) = C(br \to rb) = C(bg \to gb) = \frac{1}{2}$

(4. Configurations involving 3 colours e.g. $rb \to bg$



Colour Factors: Quarks vs Anti-Quarks

- Recall the colour part of wave-function:
- The QCD qqg vertex was written:

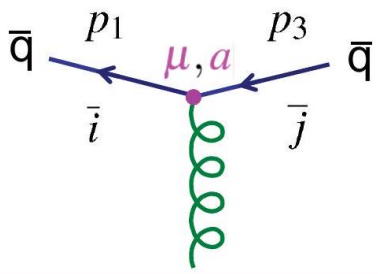
$$r = c_1 = \begin{pmatrix} 1 \\ 0 \\ 0 \end{pmatrix} \quad g = c_2 = \begin{pmatrix} 0 \\ 1 \\ 0 \end{pmatrix} \quad b = c_3 = \begin{pmatrix} 0 \\ 0 \\ 1 \end{pmatrix}$$

$$\bar{u}(p_3)\, c_j^{\dagger} \left\{ -\frac{1}{2} i g_s \lambda^a \gamma^\mu \right\} c_i u(p_1)$$

⋆ Now consider the anti-quark vertex

- The QCD qqg vertex is:

$$\bar{v}(p_1)\, c_i^{\dagger} \left\{ -\frac{1}{2} i g_s \lambda^a \gamma^\mu \right\} c_j v(p_3)$$



Note that the incoming anti-particle now enters on the LHS of the expression

- For which the colour part is

$$c_i^\dagger \lambda^a c_j = c_i^\dagger \begin{pmatrix} \lambda^a_{1j} \\ \lambda^a_{2j} \\ \lambda^a_{3j} \end{pmatrix} = \lambda^a_{ij}$$

i.e indices ij are swapped with respect to the quark case

- Hence

$$\bar{v}(p_1) c_i^\dagger \left\{ -\frac{1}{2} i g_s \lambda^a \gamma^\mu \right\} c_j v(p_3) \equiv \bar{v}(p_1) \left\{ -\frac{1}{2} i g_s \lambda^a_{ij} \gamma^\mu \right\} v(p_3)$$

- c.f. the quark - gluon QCD interaction

$$\bar{u}(p_3) c_j^\dagger \left\{ -\frac{1}{2} i g_s \lambda^a \gamma^\mu \right\} c_i u(p_1) \equiv \bar{u}(p_3) \left\{ -\frac{1}{2} i g_s \lambda^a_{ji} \gamma^\mu \right\} u(p_1)$$

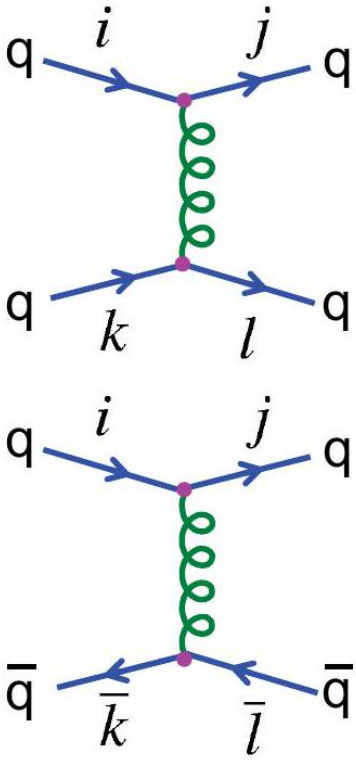
⋆ Finally we can consider the quark - anti-quark annihilation

$$\text{q}p_1 \text{ QCD vertex: } \bar{v}(p_2) c_k^\dagger \left\{ -\frac{1}{2} i g_s \lambda^a \gamma^\mu \right\} c_i u(p_1)$$

$$\bar{q}\ \vec{k}\ p_2^\dagger \lambda^a c_i = \lambda^a_{ki}$$

$$\bar{v}(p_2) c_k^\dagger \left\{ -\frac{1}{2} i g_s \lambda^a \gamma^\mu \right\} c_i u(p_1) \equiv \bar{v}(p_2) \left\{ -\frac{1}{2} i g_s \lambda^a_{ki} \gamma^\mu \right\} u(p_1)$$

- Consequently the colour factors for the different diagrams are:

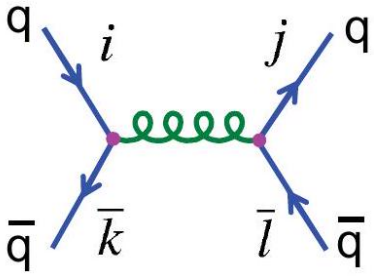


$$C(\bar{k} \to j\bar{l}) \equiv \frac{1}{4} \sum_{a=1}^{8} \lambda^a_{ji} \lambda^a_{kl}$$

e.g.

$$C(ik \to jl) \equiv \frac{1}{4}\sum_{a=1}^{8} \lambda^a_{ji}\lambda^a_{lk}$$

$$C(rr \to rr) = \frac{1}{3}$$
$$C(rg \to rg) = -\frac{1}{6}$$
$$C(rg \to gr) = \frac{1}{2}$$
$$C(r\bar{r} \to r\bar{r}) = \frac{1}{3}$$
$$C(r\bar{g} \to r\bar{g}) = -\frac{1}{6}$$
$$C(r\bar{r} \to g\bar{g}) = \frac{1}{2}$$

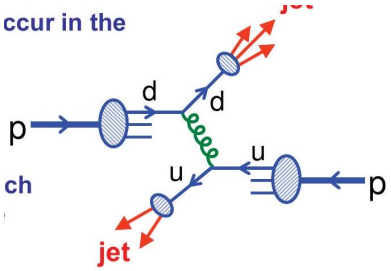


$$C(i\bar{k} \to j\bar{l}) \equiv \frac{1}{4}\sum_{a=1}^{8} \lambda^a_{ki}\lambda^a_{jl}$$

$$C(r\bar{r} \to r\bar{r}) = \frac{1}{3}$$
$$C(r\bar{g} \to r\bar{g}) = \frac{1}{2}$$
$$C(r\bar{r} \to g\bar{g}) = -\frac{1}{6}$$

Quark-Quark Scattering

- Consider the process $u + d \to u + d$ which can occur in the high energy proton-proton scattering
- There are nine possible colour configurations of the colliding quarks which are all equally likely.
- Need to determine the average matrix element which is the sum over all possible colours divided by the number of possible initial colour states



$$\langle |M_{fi}|^2 \rangle = \frac{1}{3} \cdot \frac{1}{3} \sum_{i,j,k,l=1}^{3} |M_{fi}(ij \to kl)|^2$$

- The colour average matrix element contains the average colour factor

$$\langle |C|^2 \rangle = \frac{1}{9} \sum_{i,j,k,l=1}^{3} |C(ij \to kl)|^2$$

- For $qq \to qq$ $\quad rr \to rr, .. \quad rb \to rb, .. \quad rb \to br, ..$

$$\langle |C|^2 \rangle = \frac{1}{9} \left[3 \times \left(\frac{1}{3}\right)^2 + 6 \times \left(-\frac{1}{6}\right)^2 + 6 \times \left(\frac{1}{2}\right)^2 \right] = \frac{2}{9}$$

- Previously derived the Lorentz Invariant cross section for $e^- \mu^- \to e^- \mu^-$ elastic scattering in the ultra-relativistic limit (handout 6).

QED

$$\frac{d\sigma}{dq^2} = \frac{2\pi\alpha^2}{q^4} \left[1 + \left(1 + \frac{q^2}{s} \right)^2 \right]$$

- For ud $\to$ ud in QCD replace $\alpha \to \alpha_s$ and multiply by $\langle |C|^2 \rangle$

QCD

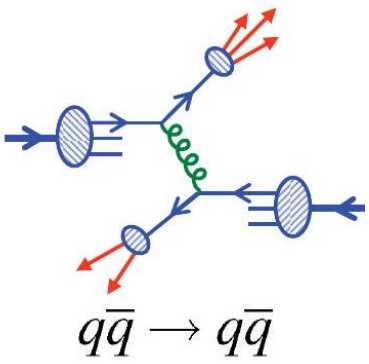
$$\frac{d\sigma}{dq^2} = \frac{2}{9} \frac{2\pi\alpha_S^2}{q^4} \left[1 + \left(1 + \frac{q^2}{\hat{s}} \right)^2 \right]$$

Never see colour, but enters through colour factors. Can tell QCD is SU(3)

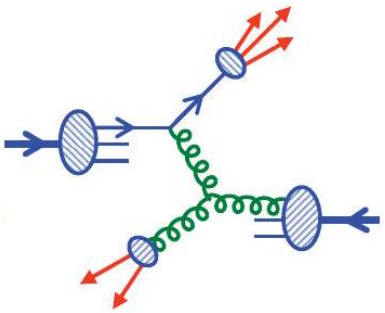
-Here $\hat{S}$ is the centre-of-mass energy of the quark-quark collision

-The calculation of hadron-hadron scattering is very involved, need to include parton structure functions and include all possible interactions

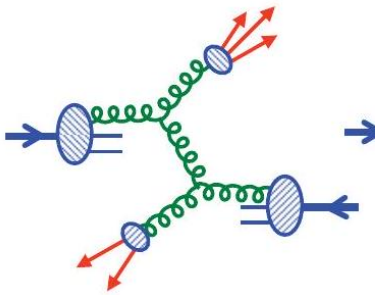
e.g. two jet production in proton-antiproton collisions



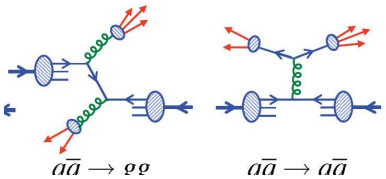
$q\bar{q} \to q\bar{q}$



$qg \to qg$



$gg \to gg$



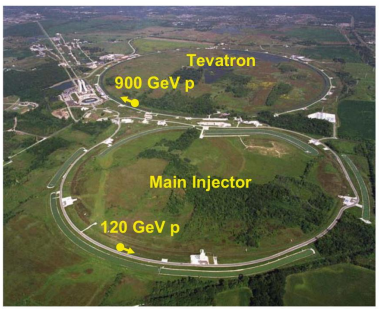
$q\bar{q} \to q\bar{q}$

e.g. $p\bar{p}$ collisions at the Tevatron

$\star$ Tevatron collider at Fermi National Laboratory (FNAL)

- located 40 miles from Chigaco, US
- started operation in 1987 (will run until 2009/2010)

$\star p\bar{p}$ collisions at $\sqrt{s} = 1.8$TeV c.f. 14TeV at the LHC



Two main accelerators:

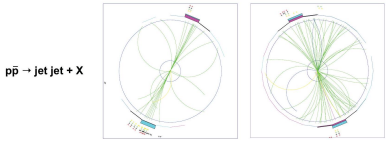
⋆ Main Injector

- Accelerates 8GeVp to 120GeV
- also $\bar{p}$ to 120GeV
- Protons sent to Tevatron & MINOS

•$\bar{p}$ all go to Tevatron
⋆ Tevatron

- 4 mile circumference
- accelerates $p/\bar{p}$ from 120GeV to 900GeV

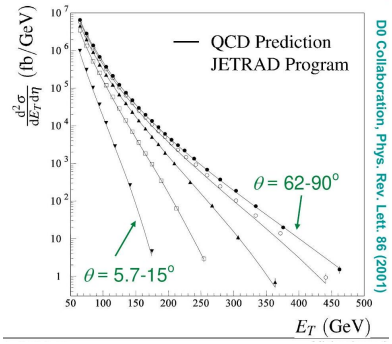
⋆ Test QCD predictions by looking at production of pairs of high energy jets



⋆ Measure cross-section in terms of

- "transverse energy" $E_T = E_{\text{jet}} \sin\theta$
- "pseudorapidity" $\eta = \ln\left[\cot\left(\frac{\theta}{2}\right)\right]$

...don't worry too much about the details here, what matters is that...



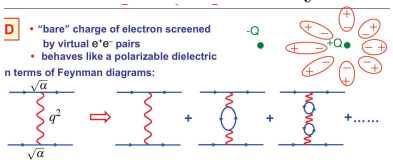
⋆ QCD predictions provide an excellent description of the data
⋆ NOTE:

- at low E_T cross-section is dominated by low x partons i.e. gluon-gluon scattering
- at high E_T cross-section is dominated by high x partons i.e. quark-antiquark scattering

Running Coupling Constants

by virtual e^+e^-pairs

- behaves like a polarizable dielectric ⋆ In terms of Feynman diagrams:

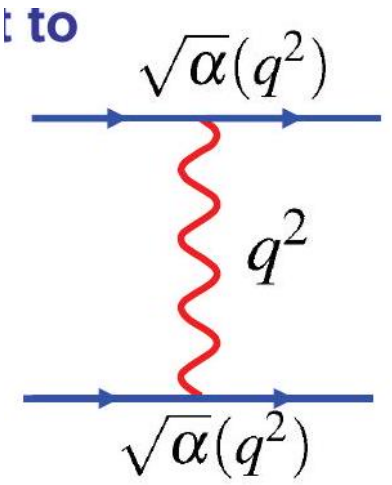


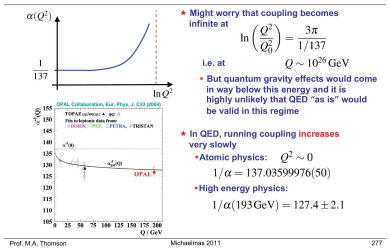
⋆ Same final state so add matrix element amplitudes: $M = M_1 + M_2 + M_3 + \ldots$

⋆ Giving an infinite series which can be summed and is equivalent to a single diagram with "running" coupling constant

$$\alpha\left(Q^2\right) = \alpha\left(Q_0^2\right) / \left[1 - \frac{\alpha\left(Q_0^2\right)}{3\pi} \ln\left(\frac{Q^2}{Q_0^2}\right)\right]$$

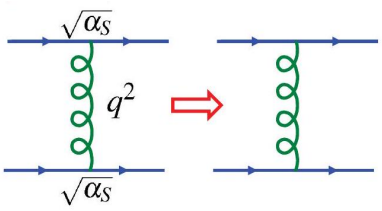
Note sign
$Q^2 \gg Q_0^2$

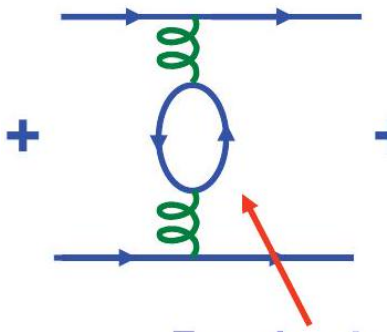




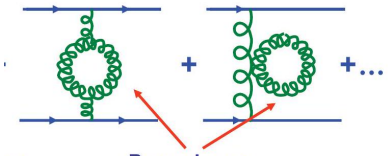
Running of α_s

Similar to QED but also have gluon loops





Fermion Loop



Boson Loops

⋆ Remembering adding amplitudes, so can get negative interference and the sum can be smaller than the original diagram alone

⋆ Bosonic loops "interfere negatively"

$$\alpha_S\left(Q^2\right) = \alpha_S\left(Q_0^2\right) / \left[1 + B\alpha_S\left(Q_0^2\right) \ln\left(\frac{Q^2}{Q_0^2}\right)\right]$$

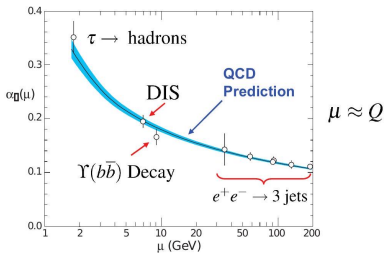
$$\text{with} \quad B = \frac{11N_c - 2N_f}{12\pi} \quad \begin{cases} N_c = \text{ no. of colours} \\ N_f = \text{ no. of quark flavours} \end{cases}$$

$$N_c = 3; N_f = 6 \Longrightarrow B > 0$$

$$\Longrightarrow \alpha_S \text{ decreases with } Q^2$$

⋆ Measure α_s in many ways:

- jet rates
- DIS
- tau decays
- bottomonium decays
  -..+ -
- As predicted by QCD, α_S decreases with Q^2



$\mu \approx Q$

⋆ At low Q^2: α_S is large, e.g. at $Q^2 = 1\text{GeV}^2$ find $\alpha_S \sim 1$

- Can't use perturbation theory! This is the reason why QCD calculations at Iow energies are so difficult, e.g. properties hadrons, hadronisation of quarks to jets,...

⋆ At high Q^2 : α_S is rather small, e.g. at $Q^2 = M_Z^2$ find $\alpha_S \sim 0.12$

$\Rightarrow$ **Asymptotic Freedom**

- Can use perturbation theory and this is the reason that in DIS at high Q^2 quarks behave as if they are quasi-free (i.e. only weakly bound within hadrons)

Summary

$\star$ Superficially QCD very similar to QED
$\star$ But gluon self-interactions are believed to result in colour confinement
$\star$ All hadrons are colour singlets which explains why only observe
Mesons
Baryons
$\star$ A low energies $\alpha_S \sim 1$
$\Rightarrow$ Can't use perturbation theory!
Non-Perturbative regime
$\star$ Coupling constant runs, smaller coupling at higher energy scales

$$\alpha_S(100\text{GeV}) \sim 0.1$$

$\Rightarrow$ Can use perturbation theory
Asymptotic Freedom

- Where calculations can be performed, QCD provides a good description of relevant experimental data

Appendix A1: Electromagnetism

(Non-examinable)
$\star$ In Heaviside-Lorentz units $\varepsilon_0 = \mu_0 = c = 1$ Maxwell's equations in the vacuum become

$$\vec{\nabla} \cdot \vec{E} = \rho; \quad \vec{\nabla} \wedge \vec{E} = -\frac{\partial \vec{B}}{\partial t}; \quad \vec{\nabla} \cdot \vec{B} = 0; \quad \vec{\nabla} \wedge \vec{B} = \vec{J} + \frac{\partial \vec{E}}{\partial t}$$

$\star$ The electric and magnetic fields can be expressed in terms of scalar and vector potentials

$$\vec{E} = -\frac{\partial \vec{A}}{\partial t} - \vec{\nabla}\phi; \quad \vec{B} = \vec{\nabla} \wedge \vec{A} \tag{A1}$$

$\star$ In terms of the 4 -vector potential $A^\mu = (\phi, \vec{A})$ and the 4 -vector current $j^\mu = (\rho, \vec{J})$ Maxwell's equations can be expressed in the covariant form:

$$\partial_\mu F^{\mu v} = j^v \tag{A2}$$

where $F^{\mu\nu}$ is the anti-symmetric field strength tensor

$$F^{\mu v} = \partial^\mu A^v - \partial^v A^\mu = \begin{pmatrix} 0 & -E_x & -E_y & -E_z \\ E_x & 0 & -B_z & B_y \\ E_y & B_z & 0 & -B_x \\ E_z & -B_y & B_x & 0 \end{pmatrix} \tag{A3}$$

- Combining (A2) and (A3)

$$\partial_\mu \left(\partial^\mu A^v - \partial^v A^\mu\right) = j^v \tag{A4}$$

which can be written $\Box^2 A^\mu - \partial^\mu \left(\partial_v A^v\right) = j^\mu$
where the D'Alembertian operator

$$\Box^2 = \partial_v \partial^v = \frac{\partial^2}{\partial t^2} - \vec{\nabla}^2 \tag{A5}$$

- Acting on equation (A5) with ∂_v gives

$$\begin{aligned}\partial_v j^v =& \partial_\nu \partial_\mu \partial^\mu A^v - \partial_\mu \partial_\nu \partial^v A^\mu = 0 \\ & \frac{\partial \rho}{\partial t} + \vec{\nabla} \cdot \vec{J} = 0 \quad \text{Conservation of Electric Charge}\end{aligned}$$

- Conservation laws are associated with symmetries. Here the symmetry is the GAUGE INVARIANCE of electro-magnetism

Appendix A2: Gauge Invariance (Non-examinable)

⋆ The electric and magnetic fields are unchanged for the gauge transformation:

$$\vec{A} \to \vec{A}' = \vec{A} + \vec{\nabla}\chi; \quad \phi \to \phi' = \phi - \frac{\partial \chi}{\partial t}$$

where $\chi = \chi(t, \vec{x})$ is any finite differentiable function of position and time ⋆ In 4-vector notation the gauge transformation can be expressed as:

$$A_\mu \to A'_\mu = A_\mu + \partial_\mu \chi$$

⋆ Using the fact that the physical fields are gauge invariant, choose χ to be a solution of
⋆ In this case we have

$$\partial^\mu A'_\mu = \partial^\mu \left(A_\mu + \partial_\mu \chi\right) = \partial^\mu A_\mu + \Box^2 \chi = 0$$

⋆ Dropping the prime we have a chosen a gauge in which

$$\boxed{\partial_\mu A^\mu = 0} \qquad \boxed{\text{The Lorentz Condition}}$$

⋆ With the Lorentz condition, equation (A5) becomes:

$$\Box^2 A^\mu = j^\mu \tag{A7}$$

⋆ Having imposed the Lorentz condition we still have freedom to make a further gauge transformation, i.e.

$$A_\mu \to A'_\mu = A_\mu + \partial_\mu \Lambda$$

where $\Lambda(t, \vec{x})$ is any function that satisfies

$$\Box^2 \Lambda = 0 \tag{A8}$$

⋆ Clearly (A7) remains unchanged, in addition the Lorentz condition still holds:

$$\partial^\mu A'_\mu = \partial^\mu \left(A_\mu + \partial_\mu \Lambda\right) = \partial^\mu A_\mu + \Box^2 \Lambda = \partial^\mu A_\mu = 0$$

Appendix B: Local Gauge Invariance

(Non-examinable)

⋆ The Dirac equation for a charged particle in an electro-magnetic field can be obtained from the free particle wave-equation by making the minimal substitution

$$\vec{p} \to \vec{p} - q\vec{A}; \quad E \to E - q\phi \quad (q = \text{ charge }) \qquad \text{(seep.113)}$$

In QM: $i\partial_\mu \to i\partial_\mu - qA_\mu$ and the Dirac equation becomes

$$\gamma^\mu \left(i\partial_\mu - qA_\mu\right)\psi - m\psi = 0 \qquad \text{(B1)}$$

- In Appendix A2: saw that the physical EM fields where invariant under the gauge transformation

$$A_\mu \to A'_\mu = A_\mu - \partial_\mu \chi \qquad (2)$$

⋆ Under this transformation the Dirac equation becomes

$$\gamma^\mu \left(i\partial_\mu - qA_\mu + q\partial_\mu\chi\right)\psi - m\psi = 0$$

which is not the same as the original equation. If we require that the Dirac equation is invariant under the Gauge transformation then under the gauge transformation we need to modify the wave-functions

$$\psi \to \psi' = \psi e^{iq\chi}$$

⋆ To prove this, applying the gauge transformation:

$$A_\mu \to A'_\mu = A_\mu - \partial_\mu\chi \quad \psi \to \psi' = \psi e^{iq\chi}$$

to the original Dirac equation gives

$$\gamma^\mu \left(i\partial_\mu - qA_\mu + q\partial_\mu\chi\right)\psi e^{iq\chi} - m\psi e^{iq\chi} = 0 \qquad \text{(B2)}$$

But

$$i\partial_\mu\left(\psi e^{iq\chi}\right) = ie^{iq\chi}\partial_\mu\psi - q\left(\partial_\mu\chi\right)e^{iq\chi}\psi$$

Equation (B2) becomes

$$\begin{aligned} &\gamma^\mu e^{iq\chi}\left(i\partial_\mu - qA_\mu + q\partial_\mu\chi - q\partial_\mu\chi\right)\psi - m\psi e^{iq\chi} = 0 \\ \Rightarrow \quad &\gamma^\mu e^{iq\chi}\left(i\partial_\mu - qA_\mu\right)\psi - m\psi e^{iq\chi} = 0 \\ \Rightarrow \quad &\gamma^\mu\left(i\partial_\mu - qA_\mu\right)\psi - m\psi = 0 \end{aligned}$$

which is the original form of the Dirac equation

Appendix C: Local Gauge Invariance 2

(Non-examinable)

⋆ Reverse the argument of Appendix B. Suppose there is a fundamental symmetry of the universe under local phase transformations

$$\psi(x) \to \psi'(x) = \psi(x)e^{iq\chi(x)}$$

⋆ Note that the local nature of these transformations: the phase transformation depends on the space-time coordinate $x = (t, \vec{x})$

⋆ Under this transformation the free particle Dirac equation

$$\begin{aligned} i\gamma^\mu\partial_\mu\psi - m\psi &= 0 \\ \text{becomes } i\gamma^\mu\partial_\mu\left(\psi e^{iq\chi}\right) - m\psi e^{iq\chi} &= 0 \\ ie^{iq\chi}\gamma^\mu\left(\partial_\mu\psi + iq\psi\partial_\mu\chi\right) - m\psi e^{iq\chi} &= 0 \\ i\gamma^\mu\left(\partial_\mu + iq\partial_\mu\chi\right)\psi - m\psi &= 0 \end{aligned}$$

Local phase invariance is not possible for a free theory, i.e. one without interactions

⋆ To restore invariance under local phase transformations have to introduce a massless "gauge boson" A^μ which transforms as

$$A_\mu \to A'_\mu = A_\mu - \partial_\mu\chi$$

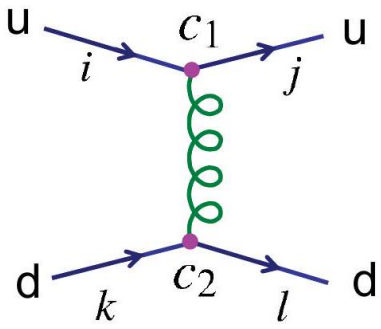
and make the substitution

$$\partial_\mu \to D_\mu = \partial_\mu + iqA_\mu$$

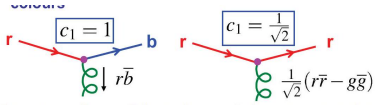
Appendix D: Alternative evaluation of colour factors

"Non-examinable" but can be used to derive colour factors.

⋆ The colour factors can be obtained (more intuitively) as follows:



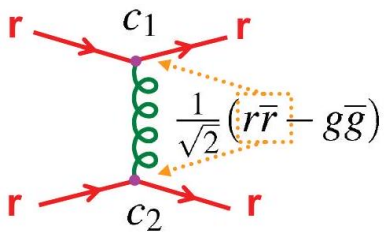
- Write $C(ik \to jl) = \frac{1}{2}c_1c_2$
- Where the colour coefficients at the two vertices depend on the quark and gluon colours



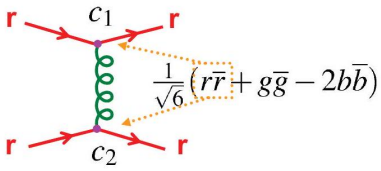
- Sum over all possible exchanged gluons conserving colour at both vertices

Configurations involving a single colour

e.g. $rr \to rr$: two possible exchanged gluons



$c_1 = c_2 = \frac{1}{\sqrt{2}}$



$c_1 = c_2 = \frac{1}{\sqrt{6}}$

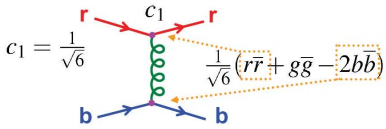
$$C(rr \to rr) = \frac{1}{2}\left(\frac{1}{2} + \frac{1}{6}\right) = \frac{1}{3}$$

e.g. $bb \to bb$: only one possible exchanged gluon

$$\mathrm{b} \to \int_{c_2}^{c_1} \mathrm{b}$$

b

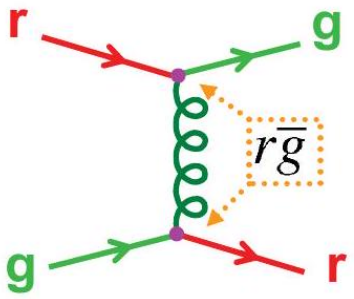
Other configurations where quarks don't change colour



$c_2 = -\frac{2}{\sqrt{6}}$

$$C(rb \to rb) = \frac{1}{2}\left(-\frac{1}{\sqrt{6}}\frac{2}{\sqrt{6}}\right) = -\frac{1}{6}$$

Configurations where quarks swap colours



$$c_1 = c_2 = 1$$

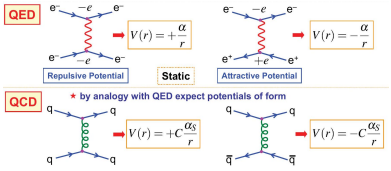
$$C(rg \to gr) = \frac{1}{2}$$

Appendix E: Colour Potentials

- Previously argued that gluon self-interactions lead to $a+\lambda r$ long-range potential and that this is likely to explain colour confinement

- Have yet to consider the short range potential - i.e. for quarks in mesons and baryons does QCD lead to an attractive potential?

-Analogy with QED: (NOTE this is very far from a formal proof)



⋆ Whether it is a attractive or repulsive potential depends on sign of colour factor
⋆ Consider the colour factor for a q $\bar{q}$ system in the colour singlet state:

$$\psi = \frac{1}{\sqrt{3}}(r\bar{r} + g\bar{g} + b\bar{b})$$

with colour potential $\langle V_{q\bar{q}} \rangle = \langle \psi | V_{\rm QCD} | \psi \rangle$

$$\langle V_{q\bar{q}} \rangle = \frac{1}{3}\left(\langle r\bar{r} | V_{\rm QCD} | r\bar{r} \rangle + \ldots + \langle r\bar{r} | V_{\rm QCD} | b\bar{b} \rangle + \ldots \right)$$

$$\langle r\bar{r} | V_{\rm QCD} | r\bar{r} \rangle = -C(r\bar{r} \to r\bar{r})\frac{\alpha_S}{r}$$

e term arising from $r\bar{r} \to r\bar{r}$

- Have 3 terms like $r\bar{r} \to r\bar{r}, b\bar{b} \to b\bar{b}, \ldots$ and 6 like $r\bar{r} \to g\bar{g}, r\bar{r} \to b\bar{b}, \ldots$

$$\langle V_{q\bar{q}} \rangle = -\frac{1}{3}\frac{\alpha_S}{r}[3 \times C(r\bar{r} \to r\bar{r}) + 6 \times C(r\bar{r} \to g\bar{g})] = -\frac{1}{3}\frac{\alpha_S}{r}\left[3 \times \frac{1}{3} + 6 \times \frac{1}{2}\right]$$

$$\langle V_{q\bar{q}} \rangle = -\frac{4}{3}\frac{\alpha_S}{r} \quad \text{NEGATIVE} \Rightarrow \text{ATTRACTIVE}$$

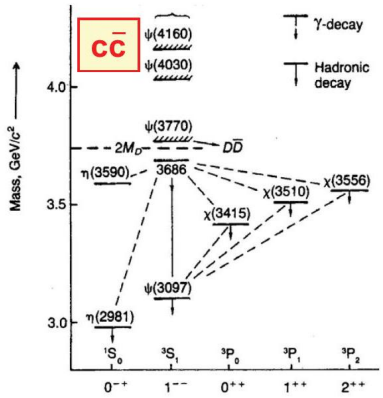
- The same calculation for a q $\bar{q}$ colour octet state, e.g. $r\bar{g}$ gives a positive repulsive potential: $C(r\bar{g} \to r\bar{g}) = -\frac{1}{6}$

⋆ Whilst not a formal proof, it is comforting to see that in the colour singlet $q\bar{q}$ state the QCD potential is indeed attractive.
(question 15)
⋆ Combining the short-range QCD potential with the linear long-range term discussed previously:

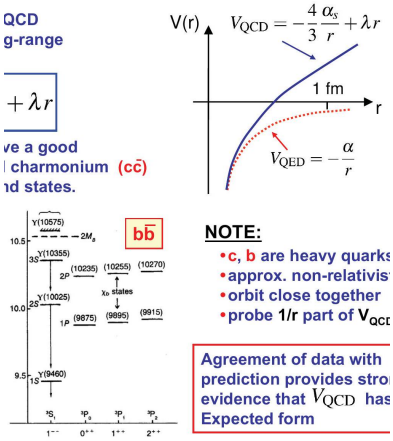
$$V_{\rm QCD} = -\frac{4}{3}\frac{\alpha_s}{r} + \lambda r$$

⋆ This potential is found to give a good description of the observed charmonium (c c-)

and bottomonium ($b\bar{b}$) bound states.



JpC



NOTE:

- c, b are heavy quarks
- approx. non-relativistic
- orbit close together • probe $1/r$ part of $\mathrm{V_{QCD}}$

Agreement of data with prediction provides strong evidence that V_{QCD} has the Expected form

1.8.5 H9: The Weak Interaction and V-A

Parity

⋆ The parity operator performs spatial inversion through the origin:

$$\psi'(\vec{x},t) = \hat{P}\psi(\vec{x},t) = \psi(-\vec{x},t)$$

- applying $\hat{P}$ twice: $\hat{P}\hat{P}\psi(\vec{x},t) = \hat{P}\psi(-\vec{x},t) = \psi(\vec{x},t)$

$$\text{so} \quad \hat{P}\hat{P} = I \quad \rightarrow \quad \hat{P}^{-1} = \hat{P}$$

- To preserve the normalisation of the wave-function

$$\langle\psi|\psi\rangle = \langle\psi'|\psi'\rangle = \left\langle \psi \left| \hat{P}^\dagger \hat{P} \right| \psi \right\rangle$$
$$\hat{P}^\dagger \hat{P} = I \quad \Rightarrow \quad \hat{P} \quad \text{Unitary}$$

- But since $\hat{P}\hat{P} = I \quad \hat{P} = \hat{P}^\dagger \quad \Rightarrow \quad \hat{P}$ Hermitian

which implies Parity is an observable quantity. If the interaction Hamiltonian commutes with $\hat{P}$, parity is an observable conserved quantity

- If $\psi(\vec{x}, t)$ is an eigenfunction of the parity operator with eigenvalue P

$$\hat{P}\psi(\vec{x}, t) = P\psi(\vec{x}, t) \quad \rightarrow \quad \hat{P}\hat{P}\psi(\vec{x}, t) = P\hat{P}\psi(\vec{x}, t) = P^2\psi(\vec{x}, t)$$

since $\hat{P}\hat{P} = I$
$P^2 = 1$
$\Rightarrow$ Parity has eigenvalues $P = \pm 1$
$\star$ QED and QCD are invariant under parity

- Experimentally observe that Weak Interactions do not conserve parity

Intrinsic Parities of fundamental particles:

Spin-1 Bosons

- From Gauge Field Theory can show that the gauge bosons have $P = -1$

$$P_\gamma = P_g = P_{W^+} = P_{W^-} = P_Z = -1$$

Spin- $1/2$ **Fermions**

- From the Dirac equation showed (handout 2):

Spin 1/2 particles have opposite parity to spin 1/2 anti-particles

- Conventional choice: spin 1/2 particles have $P = +1$

$$P_{e^-} = P_{\mu^-} = P_{\tau^-} = P_v = P_q = +1$$

and anti-particles have opposite parity, i.e.

$$P_{e^+} = P_{\mu^+} = P_{\tau^+} = P_{\bar{v}} = P_{\bar{q}} = -1$$

$\star$ For Dirac spinors it was shown (handout 2) that the parity operator is:

$$\hat{P} = \gamma^0 = \begin{pmatrix} 1 & 0 & 0 & 0 \\ 0 & 1 & 0 & 0 \\ 0 & 0 & -1 & 0 \\ 0 & 0 & 0 & -1 \end{pmatrix}$$

Parity Conservation in QED and QCD

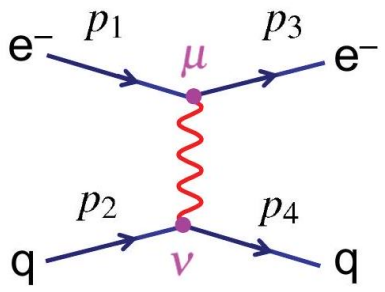
- Consider the QED process $e^- q \to e^- q$

-The Feynman rules for QED give:

$$-iM = \left[\bar{u}_e\left(p_3\right) ie\gamma^\mu u_e\left(p_1\right)\right] \frac{-ig_{\mu v}}{q^2} \left[\bar{u}_q\left(p_4\right) ie\gamma^v u_q\left(p_2\right)\right]$$

- Which can be expressed in terms of the electron and quark 4-vector currents:

$$M = -\frac{e^2}{q^2} g_{\mu\nu} j_e^\mu j_q^v = -\frac{e^2}{q^2} j_e \cdot j_q$$



with

$$j_e = \bar{u}_e\left(p_3\right)\gamma^\mu u_e\left(p_1\right) \text{ and } j_q = \bar{u}_q\left(p_4\right)\gamma^\mu u_q\left(p_2\right)$$

⋆ Consider the what happen to the matrix element under the parity transformation

- Spinors transform as

$$u \xrightarrow{\hat{P}} \hat{P}u = \gamma^0 u$$

- Adjoint spinors transform as

$$\bar{u} = u^\dagger\gamma^0 \xrightarrow{\hat{P}} (\hat{P}u)^\dagger\gamma^0 = u^\dagger\gamma^{0\dagger}\gamma^0 = u^\dagger\gamma^0\gamma^0 = \bar{u}\gamma^0$$
$$\bar{u} \xrightarrow{\hat{P}} \bar{u}\gamma^0$$

- Hence

$$j_e = \bar{u}_e\left(p_3\right)\gamma^\mu u_e\left(p_1\right) \xrightarrow{\hat{P}} \bar{u}_e\left(p_3\right)\gamma^0\gamma^\mu\gamma^0 u_e\left(p_1\right)$$

⋆ Consider the components of the four-vector current

$0:\quad j_e^0 \xrightarrow{\hat{P}} \bar{u}\gamma^0\gamma^0\gamma^0 u = \bar{u}\gamma^0 u = j_e^0$
since $\gamma^0\gamma^0 = 1$
$j_e^k \xrightarrow{\hat{P}} \bar{u}\gamma^0\gamma^k\gamma^0 u = -\bar{u}\gamma^k\gamma^0\gamma^0 u = -\bar{u}\gamma^k u = -j_e^k$
since $\gamma^0\gamma^k = -\gamma^k\gamma^0$
$k = 1, 2, 3:$
-The time-like component remains unchanged and the space-like components change sign

- Similarly $\quad j_q^0 \xrightarrow{\hat{P}} j_q^0 \quad j_q^k \xrightarrow{\hat{P}} -j_q^k \quad k = 1,2,3$

⋆ Consequently the four-vector scalar product
$j_e \cdot j_q = j_e^0 j_q^0 - j_e^k j_q^k \xrightarrow{\hat{P}} j_e^0 j_q^0 - \left(-j_e^k\right)\left(-j_q^k\right) = j_e \cdot j_q \quad k = 1,3$

$$\text{or} \quad j^\mu \xrightarrow{\hat{P}} j_\mu$$
$$j^\mu . j^\nu \xrightarrow{\hat{P}} j_\mu . j_\nu$$
$$\xrightarrow{\hat{P}} j^\mu . j^\nu$$

QED Matrix Elements are Parity Invariant
Parity Conserved in QED

- The QCD vertex has the same form and, thus,

Parity Conserved in QCD

Parity Violation in β-Decay

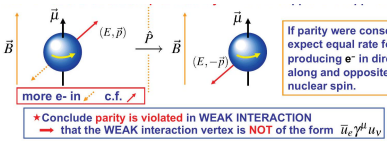
⋆ The parity operator $\hat{P}$ corresponds to a discrete transformation $x \to -x$, etc. ⋆ Under the parity transformation:

Vectors
change sign
$$\begin{cases} \vec{r} \xrightarrow{\hat{P}} -\vec{r} \\ \vec{p} \xrightarrow{\hat{P}} -\vec{p} \end{cases}$$
$$\left(p_x = \frac{\partial}{\partial x}, \text{ etc.}\right)$$
Axial-Vectors
$$\begin{cases} \vec{L} \xrightarrow{\hat{P}} \vec{L} \\ \vec{\mu} \xrightarrow{\hat{P}} \vec{\mu} \end{cases}$$
$$(\vec{L} = \vec{r} \wedge \vec{p})$$
$$(\vec{\mu} \propto \vec{L})$$

⋆ 1957: C.S.Wu et al. studied beta decay of polarized cobalt-60 nuclei:

$$^{60}\text{Co} \to {}^{60}Ni^* + e^- + \bar{\nu}_e$$

⋆ Observed electrons emitted preferentially in direction opposite to applied field



Bilinear Covariants

⋆ The requirement of Lorentz invariance of the matrix element severely restricts the form of the interaction vertex. QED and QCD are "VECTOR" interactions:

$$j^\mu = \bar{\psi}\gamma^\mu\phi$$

⋆ This combination transforms as a 4-vector (Handout 2 appendix V)

⋆ In general, there are only 5 possible combinations of two spinors and the gamma matrices that form Lorentz invariant currents, called "bilinear covariants":

Type	Form	Components	"Boson Spin"
SCALAR	$\bar{\psi}\phi$	1	0
PSEUDOSCALAR	$\bar{\psi}\gamma^5\phi$	1	0
VECTOR	$\bar{\psi}\gamma^\mu\phi$	4	1
AXIAL VECTOR	$\bar{\psi}\gamma^\mu\gamma^5\phi$	4	1
TENSOR	$\bar{\psi}\left(\gamma^\mu\gamma^\nu - \gamma^\nu\gamma^\mu\right)\phi$	6	2

⋆ Note that in total the sixteen components correspond to the 16 elements of a general 4×4 matrix: "decomposition into Lorentz invariant combinations"

⋆ In QED the factor $g_{\mu\nu}$ arose from the sum over polarization states of the virtual photon (2 transverse +1 longitudinal, 1 scalar) $= (2\ \mathrm{J}+1)+1$

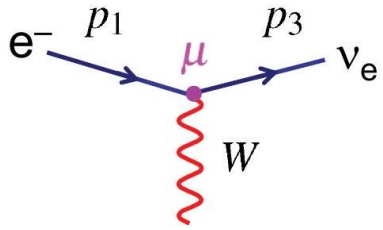
⋆ Associate SCALAR and PSEUDOSCALAR interactions with the exchange of a SPIN-0 boson, etc. - no spin degrees of freedom

V-A Structure of the Weak Interaction

⋆ The most general form for the interaction between a fermion and a boson is a linear combination of bilinear covariants

⋆ For an interaction corresponding to the exchange of a spin-1 particle the most general form is a linear combination of VECTOR and AXIAL-VECTOR

⋆ The form for WEAK interaction is determined from experiment to be VECTOR - AXIAL-VECTOR (**V** - **A**)



$$j^\mu \propto \bar{u}_{\nu_e}\left(\gamma^\mu - \gamma^\mu\gamma^5\right)u_e$$

⋆ Can this account for parity violation?

⋆ First consider parity transformation of a pure AXIAL-VECTOR current

$$j_A = \bar{\psi}\gamma^\mu\gamma^5\phi \quad \text{with} \quad \gamma^5 = i\gamma^0\gamma^1\gamma^2\gamma^3; \quad \gamma^5\gamma^0 = -\gamma^0\gamma^5$$

$$j_A = \bar{\psi}\gamma^\mu\gamma^5\phi \xrightarrow{\hat{P}} \bar{\psi}\gamma^0\gamma^\mu\gamma^5\gamma^0\phi = -\bar{\psi}\gamma^0\gamma^\mu\gamma^0\gamma^5\phi$$

$$j^0_A \overset{\hat{P}}{=} \vec{P}\ -\bar{\psi}\gamma^0\gamma^0\gamma^0\gamma^5\phi = -\bar{\psi}\gamma^0\gamma^5\phi = -j^0_A$$

$$j^k_A \overset{\longrightarrow}{=\!=} -\bar{\psi}\gamma^0\gamma^k\gamma^0\gamma^5\phi = +\bar{\psi}\gamma^k\gamma^5\phi = +j^k_A \quad k=1,2,3 \quad \text{or } j^\mu_A \xrightarrow{\hat{P}} -j_{A\mu}$$

- The space-like components remain unchanged and the time-like components change sign (the opposite to the parity properties of a vector-current)

$$j_A^0 \xrightarrow{\hat{P}} -j_A^0; \quad j_A^k \xrightarrow{\hat{P}} +j_A^k; \quad j_V^0 \xrightarrow{\hat{P}} +j_V^0; \quad j_V^k \xrightarrow{\hat{P}} -j_V^k$$

- Now consider the matrix elements

$$M \propto g_{\mu v} j_1^\mu j_2^v = j_1^0 j_2^0 - \sum_{k=1,3} j_1^k j_2^k$$

- For the combination of a two axial-vector currents

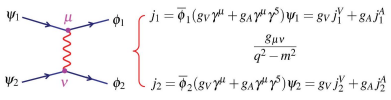
$$j_{A1} \cdot j_{A2} \xrightarrow{\hat{P}} \left(-j_1^0\right)\left(-j_2^0\right) - \sum_{k=1,3} \left(j_1^k\right)\left(j_2^k\right) = j_{A1} \cdot j_{A2}$$

- Consequently parity is conserved for both a pure vector and pure axial-vector interactions
- However the combination of a vector current and an axial vector current

$$j_{V1} \cdot j_{A2} \xrightarrow{\hat{P}} \left(j_1^0\right)\left(-j_2^0\right) - \sum_{k=1,3} \left(-j_1^k\right)\left(j_2^k\right) = -j_{V1} \cdot j_{A2}$$

changes sign under parity - can give parity violation!

⋆ **Now consider a general linear combination of VECTOR and AXIAL-VECTOR** (note this is relevant for the Z-boson vertex)



$$M_{fi} \propto j_1 \cdot j_2 = g_V^2 j_1^V \cdot j_2^V + g_A^2 j_1^A \cdot j_2^A + g_V g_A \left(j_1^V \cdot j_2^A + j_1^A \cdot j_2^V\right)$$

- Consider the parity transformation of this scalar product

$$j_1 \cdot j_2 \xrightarrow{\hat{P}} g_V^2 j_1^V \cdot j_2^V + g_A^2 j_1^A \cdot j_2^A - g_V g_A \left(j_1^V \cdot j_2^A + j_1^A \cdot j_2^V\right)$$

- If either g_A or g_V is zero, Parity is conserved, i.e. parity conserved in a pure VECTOR or pure AXIAL-VECTOR interaction
- Relative strength of parity violating part $\propto \frac{g_V g_A}{g_V^2 + g_A^2}$

Chiral Structure of QED (Reminder)

⋆ Recall (Handout 4) introduced CHIRAL projections operators

$$P_R = \frac{1}{2}\left(1+\gamma^5\right); \quad P_L = \frac{1}{2}\left(1-\gamma^5\right)$$

project out chiral right- and left- handed states

⋆ In the ultra-relativistic limit, chiral states correspond to helicity states

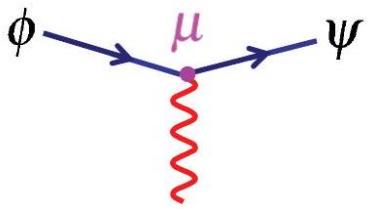
⋆ Any spinor can be expressed as:

$$\psi = \frac{1}{2}\left(1+\gamma^5\right)\psi + \frac{1}{2}\left(1-\gamma^5\right)\psi = P_R\psi + P_L\psi = \psi_R + \psi_L$$

-The QED vertex $\bar{\psi}\gamma^\mu\phi$ in terms of chiral states:

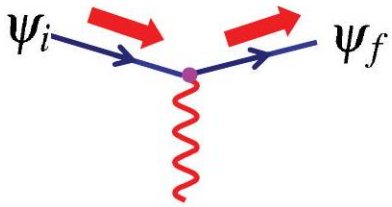
$$\bar{\psi}\gamma^\mu\phi = \bar{\psi}_R\gamma^\mu\phi_R + \bar{\psi}_R\gamma^\mu\phi_L + \bar{\psi}_L\gamma^\mu\phi_R + \bar{\psi}_L\gamma^\mu\phi_L$$

conserves chirality, e.g.



$$\begin{aligned}\bar{\psi}_R\gamma^\mu\phi_L &= \frac{1}{2}\psi^\dagger\left(1+\gamma^5\right)\gamma^0\gamma^\mu\frac{1}{2}\left(1-\gamma^5\right)\phi \\ &= \frac{1}{4}\psi^\dagger\gamma^0\left(1-\gamma^5\right)\gamma^\mu\left(1-\gamma^5\right)\phi \\ &= \frac{1}{4}\bar{\psi}\gamma^\mu\left(1+\gamma^5\right)\left(1-\gamma^5\right)\phi = 0\end{aligned}$$

⋆ In the ultra-relativistic limit only two helicity combinations are non-zero



Helicity Structure of the WEAK Interaction

- The charged current ($\mathbf{W}^\pm$) weak vertex is:

$$\frac{-ig_w}{\sqrt{2}}\frac{1}{2}\gamma^\mu\left(1-\gamma^5\right)$$

⋆ Since $\frac{1}{2}\left(1-\gamma^5\right)$ projects out left-handed chiral particle states:

$$\bar{\psi}\frac{1}{2}\gamma^\mu\left(1-\gamma^5\right)\phi = \bar{\psi}\gamma^\mu\phi_L \qquad \text{(question16)}$$

⋆ Writing $\bar{\psi} = \bar{\psi}_R + \bar{\psi}_L$ and from discussion of QED, $\bar{\psi}_R\gamma^\mu\phi_L = 0$ gives

$$\bar{\psi}\frac{1}{2}\gamma^{\mu}\left(1-\gamma^{5}\right)\phi = \bar{\psi}_{L}\gamma^{\mu}\phi_{L}$$

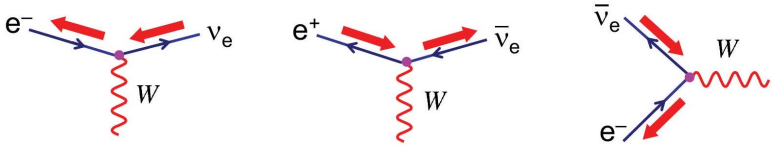
Only the left-handed chiral components of particle spinors and right-handed chiral components of anti-particle spinors participate in charged current weak interactions

⋆ At very high energy ($E \gg m$), the left-handed chiral components are helicity eigenstates:

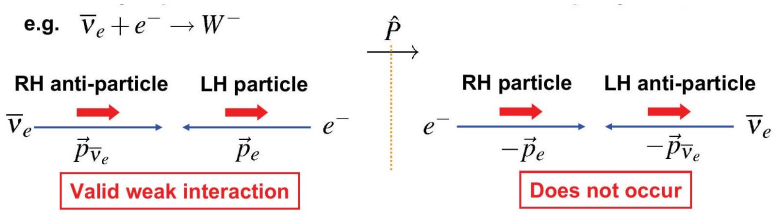
$$\frac{1}{2}\left(1-\gamma^{5}\right)u \rightharpoonup$$
$$\frac{1}{2}\left(1-\gamma^{5}\right)v \rightharpoondown$$

LEFT-HANDED PARTICLES Helicity $= -1$
RIGHT-HANDED ANTI-PARTICLES Helicity $= +1$

In the ultra-relativistic limit only left-handed particles and right-handed antiparticles participate in charged current weak interactions e.g. In the relativistic limit, the only possible electron - neutrino interactions are:

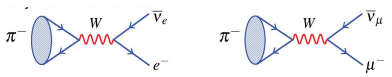


⋆ The helicity dependence of the weak interaction $\longleftrightarrow$ parity violation



Helicity in Pion Decay

⋆ The decays of charged pions provide a good demonstration of the role of helicity in the weak interaction



EXPERIMENTALLY:

$$\frac{\Gamma\left(\pi^{-}\to e^{-}\bar{\upsilon}_{e}\right)}{\Gamma\left(\pi^{-}\to \mu^{-}\bar{\upsilon}_{\mu}\right)} = 1.23\times 10^{-4}$$

- Might expect the decay to electrons to dominate - due to increased phase space.... The opposite happens, the electron decay is helicity suppressed

⋆ Consider decay in pion rest frame.

- Pion is spin zero: so the spins of the $\bar{\upsilon}$ and μ are opposite
- Weak interaction only couples to RH chiral anti-particle states. Since neutrinos are (almost) massless, must be in RH Helicity state
- Therefore, to conserve angular mom. muon is emitted in a RH HELICITY state



- But only left-handed CHIRAL particle states participate in weak interaction
  ⋆ The general right-handed helicity solution to the Dirac equation is

$$u_\uparrow = N \begin{pmatrix} c \\ e^{i\phi}S \\ \frac{|\vec{p}|}{E+m}c \\ \frac{|\vec{p}|}{E+m}e^{i\phi}S \end{pmatrix} \quad \text{with} \quad c = \cos\frac{\theta}{2} \text{ and } \quad s = \sin\frac{\theta}{2}$$

- project out the left-handed chiral part of the wave-function using

$$P_L = \frac{1}{2}\left(1-\gamma^5\right) = \frac{1}{2}\begin{pmatrix} 1 & 0 & -1 & 0 \\ 0 & 1 & 0 & -1 \\ -1 & 0 & 1 & 0 \\ 0 & -1 & 0 & 1 \end{pmatrix}$$

giving

$$P_L u_\uparrow = \frac{1}{2}N\left(1-\frac{|\vec{p}|}{E+m}\right)\begin{pmatrix} c \\ e^{i\phi}S \\ -c \\ -e^{i\phi}S \end{pmatrix} = \frac{1}{2}N\left(1-\frac{|\vec{p}|}{E+m}\right)u_L$$

In the limit $m \ll E$ this tends to zero

- similarly

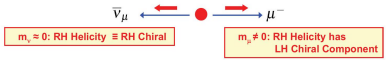
$$P_R u_\uparrow = \frac{1}{2}N\left(1+\frac{|\vec{p}|}{E+m}\right)\begin{pmatrix} c \\ e^{i\phi}S \\ c \\ e^{i\phi} \end{pmatrix} = \frac{1}{2}N\left(1+\frac{|\vec{p}|}{E+m}\right)u_R$$

In the limit $m \ll E$, $\quad P_R u_\uparrow \to u_R$

$u_\uparrow = P_R u_\uparrow + P_L u_\uparrow = \frac{1}{2}\left(1+\frac{|\vec{p}|}{E+m}\right)u_R + \frac{1}{2}\left(1-\frac{|\vec{p}|}{E+m}\right)u_L$

RH Helicity | RH Chiral | LH Chiral

- In the limit $E \gg m$, as expected, the RH chiral and helicity states are identical - Although only LH chiral particles participate in the weak interaction the contribution from RH Helicity states is not necessarily zero!



Expect matrix element to be proportional to LH chiral component of RH Helicity electron/muon spinor

$$M_{fi} \propto \frac{1}{2}\left(1-\frac{|\vec{p}|}{E+m}\right) = \frac{m_\mu}{m_\pi + m_\mu}$$

⋆ Hence because the electron mass is much smaller than the pion mass the decay $\pi^- \to e^-\bar{\nu}_e$ is heavily suppressed.

⋆ The V-A nature of the charged current weak interaction vertex fits with experiment

EXAMPLE charged pion decay

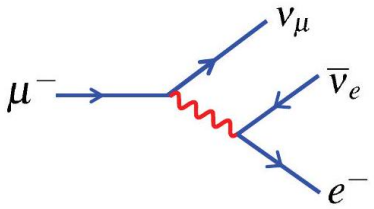
(question 17)

- Experimentally measure: $\frac{\Gamma\left(\pi^- \to e^- \bar{\nu}_e\right)}{\Gamma\left(\pi^- \to \mu^- \bar{\nu}_\mu\right)} = (1.230 \pm 0.004) \times 10^{-4}$
- Theoretical predictions (depend on Lorentz Structure of the interaction)

$$\text{V-A } \left(\bar{\psi}\gamma^\mu\left(1-\gamma^5\right)\phi\right) \text{ or V + A } \left(\bar{\psi}\gamma^\mu\left(1+\gamma^5\right)\phi\right) \Rightarrow \frac{\Gamma\left(\pi^- \to e^-\bar{\nu}_e\right)}{\Gamma\left(\pi^- \to \mu^-\bar{\nu}_\mu\right)} \approx 1.3 \times 10^{-4}$$

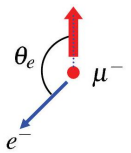
$$\text{Scalar } (\bar{\psi}\phi) \text{ or Pseudo-Scalar } \left(\bar{\psi}\gamma^5\phi\right) \Rightarrow \frac{\Gamma\left(\pi^- \to e^-\bar{\nu}_e\right)}{\Gamma\left(\pi^- \to \mu^-\bar{\nu}_\mu\right)} = 5.5$$

EXAMPLE muon decay



e.g. TWIST expt: $6 \times 10^9 \mu$ decays Phys. Rev. Lett. 95 (2005) 101805
Measure electron energy and angular distributions relative to muon spin direction. Results expressed in terms of general $S + P + V + A + T$ form in "Michel Parameters"

$$\rho = 0.75080 \pm 0.00105$$



e^-
V-A Prediction: $\rho = 0.75$

Weak Charged Current Propagator

⋆The charged-current Weak interaction is different from QED and QCD in that it is mediated by massive W-bosons (80.3GeV)
⋆ This results in a more complicated form for the propagator:

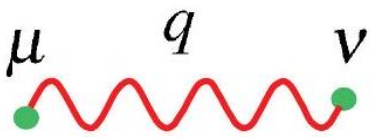
- in handout 4 showed that for the exchange of a massive particle:

$$\underset{\frac{1}{q^2}}{\text{massless}} \longrightarrow \underset{\frac{1}{q^2-m^2}}{\text{massive}}$$

- In addition the sum over W boson polarization states modifies the numerator

W-boson propagator

$$\text{spin } 1\mathbf{W}^\pm \quad \frac{-i\left[g_{\mu v} - q_\mu q_v / m_W^2\right]}{q^2 - m_W^2}$$



⋆ However in the limit where q^2 is small compared with $m_W = 80.3\text{GeV}$ the interaction takes a simpler form.

- -boson propagator ($q^2 \ll m_W^2$)

$$\frac{ig_{\mu v}}{m_W^2}$$

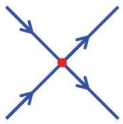
- The interaction appears point-like (i.e no q^2 dependence)

Connection to Fermi Theory

- In 1934, before the discovery of parity violation, Fermi proposed, in analogy with QED, that the invariant matrix element for β-decay was of the form:

$$M_{fi} = G_{\text{F}} g_{\mu v} \left[\bar{\psi}\gamma^{\mu}\psi\right] \left[\bar{\psi}\gamma^{\nu}\psi\right]$$

where $G_{\text{F}} = 1.166 \times 10^{-5}\text{GeV}^{-2}$



- Note the absence of a propagator: i.e. this represents an interaction at a point

⋆ After the discovery of parity violation in 1957 this was modified to

$$M_{fi} = \frac{G_{\text{F}}}{\sqrt{2}} g_{\mu\nu} \left[\bar{\psi}\gamma^{\mu}\left(1-\gamma^5\right)\psi\right] \left[\bar{\psi}\gamma^{\nu}\left(1-\gamma^5\right)\psi\right]$$

(the factor of $\sqrt{}2$ was included so the numerical value of G_{F} did not need to be changed)
⋆ Compare to the prediction for W-boson exchange

$$M_{fi} = \left[\frac{g_W}{\sqrt{2}}\bar{\psi}\frac{1}{2}\gamma^{\mu}\left(1-\gamma^5\right)\psi\right] \frac{g_{\mu\nu} - q_{\mu}q_v/m_W^2}{q^2 - m_W^2} \left[\frac{g_W}{\sqrt{2}}\bar{\psi}\frac{1}{2}\gamma^{\nu}\left(1-\gamma^5\right)\psi\right]$$

which for $q^2 \ll m_W^2$ becomes:

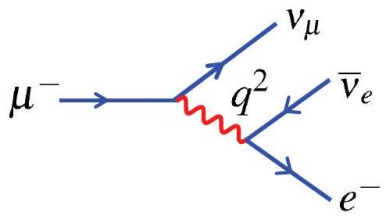
$$M_{fi} = \frac{g_W^2}{8m_W^2} g_{\mu v} \left[\bar{\psi}\gamma^{\mu}\left(1-\gamma^5\right)\psi\right] \left[\bar{\psi}\gamma^{v}\left(1-\gamma^5\right)\psi\right]$$

$$\frac{G_{\text{F}}}{\sqrt{2}} = \frac{g_W^2}{8m_W^2}$$

Still usually use G_{F} to express strength of weak interaction as the is the quantity that is precisely determined in muon decay

Strength of Weak Interaction

⋆ Strength of weak interaction most precisely measured in muon decay



- Here $q^2 < m_\mu(0.106\text{GeV})$
- To a very good approximation the W-boson propagator can be written

$$\frac{-i\left[g_{\mu v} - q_\mu q_v/m_W^2\right]}{q^2 - m_W^2} \approx \frac{ig_{\mu v}}{m_W^2}$$

- In muon decay measure g_W^2/m_W^2
- Muon decay

$G_\text{F} = 1.16639(1) \times 10^{-5}\text{GeV}^{-2}$

$$\boxed{\frac{G_\text{F}}{\sqrt{2}} = \frac{g_W^2}{8m_W^2}}$$

⋆ To obtain the intrinsic strength of weak interaction need to know mass of W-boson: $m_W = 80.403 \pm 0.029\text{GeV}$
(see handout 14)

$$\alpha_W = \frac{g_W^2}{4\pi} = \frac{8m_W^2 G_\text{F}}{4\sqrt{2}\pi} = \frac{1}{30}$$

The intrinsic strength of the weak interaction is similar to, but greater than, the EM interaction! It is the massive W-boson in the propagator which makes it appear weak. For $q^2 \gg m_W^2$ weak interactions are more likely than EM.

Summary

⋆ Weak interaction is of form Vector - Axial-vector (V-A)

$$\frac{-ig_w}{\sqrt{2}}\frac{1}{2}\gamma^\mu\left(1-\gamma^5\right)$$

⋆ Consequently only left-handed chiral particle states and right-handed chiral anti-particle states participate in the weak interaction
MAXIMAL PARITY VIOLATION
Weak interaction also violates Charge Conjugation symmetry
⋆ At low q^2 weak interaction is only weak because of the large W-boson mass

$$\frac{G_\text{F}}{\sqrt{2}} = \frac{g_W^2}{8m_W^2}$$

⋆ Intrinsic strength of weak interaction is similar to that of QED

1.8.6 H10: Leptonic Weak Interactions and Neutrino Deep Inelastic Scattering

Aside: Neutrino Flavours

⋆ Recent experiments (see Handout 11) ⇒ neutrinos have mass (albeit very small)

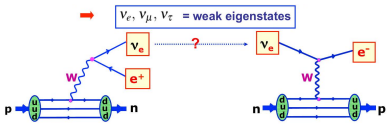
⋆ The textbook neutrino states, v_e, v_μ, v_τ, are not the fundamental particles; these are v_1, v_2, v_3

⋆ Concepts like "electron number" conservation are now known not to hold.

⋆ So what are v_e, v_μ, v_τ?

⋆ Never directly observe neutrinos - can only detect them by their weak interactions. Hence by definition v_e is the neutrino state produced along with an electron.

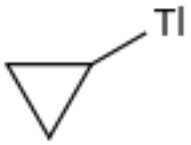
Similarly, charged current weak interactions of the state v_e produce an electron



⋆ Unless dealing with very large distances: the neutrino produced with a positron will interact to produce an electron. For the discussion of the weak interaction continue to use v_e, v_μ, v_τ as if they were the fundamental particle states.

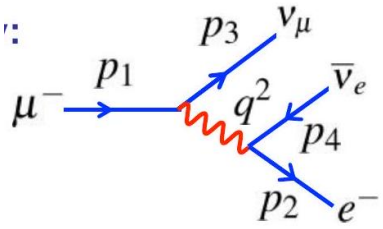
Muon Decay and Lepton Universality

⋆ The leptonic charged current ($\mathbf{W}^\pm$) interaction vertices are:



W

⋆ Consider muon decay:



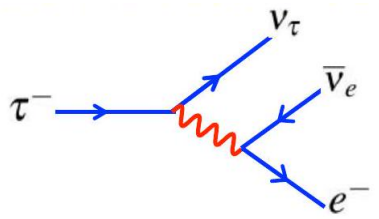
-It is straight-forward to write down the matrix element

$$M_{fi} = \frac{g_W^{(e)} g_W^{(\mu)}}{8m_W^2} \left[\bar{u}\left(p_3\right)\gamma^\mu\left(1-\gamma^5\right)u\left(p_1\right)\right] g_{\mu\nu} \left[\bar{u}\left(p_2\right)\gamma^\nu\left(1-\gamma^5\right)v\left(p_4\right)\right]$$

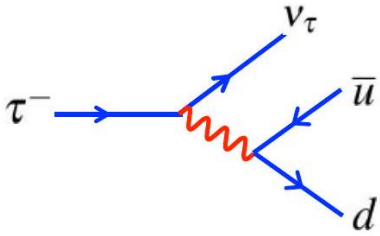
Note: for lepton decay $q^2 \ll m_W^2$ so propagator is a constant $1/m_W^2$ i.e. in limit of Fermi theory

-Its evaluation and subsequent treatment of a three-body decay is rather tricky (and not particularly interesting). Here will simply quote the result

-The muon to electron rate $\Gamma(\mu \to e\nu v) = \frac{G_F^e G_F^\mu m_\mu^5}{192\pi^3} = \frac{1}{\tau_\mu}$ with $G_F = \frac{g_W^2}{4\sqrt{2}m_W^2}$ - Similarly for tau to electron $\Gamma(\tau \to e\nu v) = \frac{G_F^e G_F^\tau m_\tau^5}{192\pi^3}$ -However, the tau can decay to a number of final states:



$$\mathrm{Br}(\tau \to evv) = 0.1784(5)$$



-Recall total width (total transition rate) is the sum of the partial widths

$$\Gamma = \sum_i \Gamma_i = \frac{1}{\tau}$$

-Can relate partial decay width to total decay width and therefore lifetime:

$$\Gamma(\tau \to e\nu v) = \Gamma_\tau Br(\tau \to e\nu v) = Br(\tau \to e\nu v)/\tau_\tau$$

-Therefore predict

$$\tau_\mu = \frac{192\pi^3}{G_{\mathrm{F}}^e G_{\mathrm{F}}^\mu m_\mu^5} \quad \tau_\tau = \frac{192\pi^3}{G_{\mathrm{F}}^e G_{\mathrm{F}}^\tau m_\tau^5}\,\mathrm{Br}(\tau \to evv)$$

-All these quantities are precisely measured:

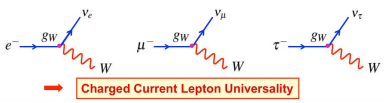
$$m_\mu = 0.1056583692(94)\mathrm{GeV} \qquad \tau_\mu = 2.19703(4) \times 10^{-6}\ \mathrm{s}$$
$$m_\tau = 1.77699(28)\mathrm{GeV} \qquad \tau_\tau = 0.2906(10) \times 10^{-12}\ \mathrm{s}$$
$$Br(\tau \to evv) = 0.1784(5)$$

$$\frac{G_{\mathrm{F}}^\tau}{G_{\mathrm{F}}^\mu} = \frac{m_\mu^5 \tau_\mu}{m_\tau^5 \tau_\tau} Br(\tau \to evv) = 1.0024 \pm 0.0033$$

-Similarly by comparing

$$\mathrm{Br}(\tau \to evv) \text{ and}$$
$$\frac{G_{\mathrm{F}}^e}{G_{\mathrm{F}}^\mu} = 1.000 \pm 0.004$$

⋆ Demonstrates the weak charged current is the same for all leptonic vertices



Neutrino Scattering

-In handout 6 considered electron-proton Deep Inelastic Scattering where a virtual photon is used to probe nucleon structure

-Can also consider the weak interaction equivalent: Neutrino Deep Inelastic Scattering where a virtual W-boson probes the structure of nucleons

$\Rightarrow$ additional information about parton structure functions

- provides a good example of calculations of weak interaction cross sections.

⋆ Neutrino Beams:

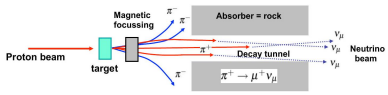
· Smash high energy protons into a fixed target $\Rightarrow$ hadrons

-Focus positive pions/kaons

-Allow them to decay $\pi^+ \to \mu^+ v_\mu + K^+ \to \mu^+ v_\mu (BR \approx 64\%)$

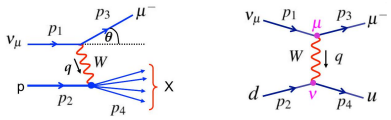
-Gives a beam of "collimated" v_μ

·Focus negative pions/kaons to give beam of $\bar{v}_\mu$



Neutrino-Quark Scattering

⋆ For v_μ-proton Deep Inelastic Scattering the underlying process is $v_\mu d \to \mu^- u$



⋆ In the limit $q^2 \ll m_W^2$ the **W**-boson propagator is $\approx i g_{\mu\nu}/m_W^2$

-The Feynman rules give:

$$-iM_{fi} = \left[-i\frac{g_W}{\sqrt{2}}\bar{u}(p_3)\gamma^\mu \frac{1}{2}\left(1-\gamma^5\right)u(p_1)\right]\frac{ig_{\mu v}}{m_W^2}\left[-i\frac{g_W}{\sqrt{2}}\bar{u}(p_4)\frac{1}{2}\gamma^v\left(1-\gamma^5\right)u(p_2)\right]$$

$$M_{fi} = \frac{g_W^2}{2m_W^2}g_{\mu v}\left[\bar{u}(p_3)\gamma^\mu \frac{1}{2}\left(1-\gamma^5\right)u(p_1)\right]\left[\bar{u}(p_4)\frac{1}{2}\gamma^v\left(1-\gamma^5\right)u(p_2)\right]$$

-Evaluate the matrix element in the extreme relativistic limit where the muon and quark masses can be neglected

In this limit the helicity states are equivalent to the chiral states and

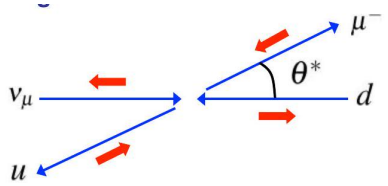
$$\frac{1}{2}\left(1-\gamma^5\right)u_\uparrow(p_1) = 0 \quad \frac{1}{2}\left(1-\gamma^5\right)u_\downarrow(p_1) = u_\downarrow(p_1)$$
$$\Longrightarrow M_{fi} = 0 \quad \text{for } u_\uparrow(p_1) \text{ and } u_\uparrow(p_2)$$

-Since the weak interaction "conserves the helicity", the only helicity combination where the matrix element is non-zero is

$$M_{fi} = \frac{g_W^2}{2m_W^2}g_{\mu v}\left[\bar{u}_\downarrow(p_3)\gamma^\mu u_\downarrow(p_1)\right]\left[\bar{u}_\downarrow(p_4)\gamma^v u_\downarrow(p_2)\right]$$

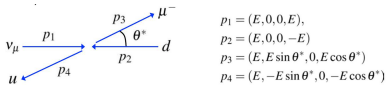
NOTE: we could have written this down straight away as in the ultra-relativistic limit only LH helicity particle states participate in the weak interaction.

⋆ Consider the scattering in the C.o.M frame



Evaluation of Neutrino-Quark Scattering ME

- Go through the calculation in gory detail (fortunately only one helicity combination) · In the $v_\mu d$ CMS frame, neglecting particle masses:



-Dealing with LH helicity particle spinors. From handout 3 (p.80), for a massless particle travelling in direction (θ, ϕ):

$$u_\downarrow = \sqrt{E}\begin{pmatrix} -s \\ ce^{i\phi} \\ s \\ -ce^{i\phi} \end{pmatrix} \quad c = \cos\frac{\theta}{2}; \quad s = \sin\frac{\theta}{2}$$

-Here $(\theta_1, \phi_1) = (0, 0); (\theta_2, \phi_2) = (\pi, 0); (\theta_3, \phi_3) = (\theta^*, 0)\,; (\theta_4, \phi_4) = (\pi - \theta^*, \pi)$
giving:

$$u_\downarrow(p_1) = \sqrt{E}\begin{pmatrix} 0 \\ 1 \\ 0 \\ -1 \end{pmatrix}; u_\downarrow(p_2) = \sqrt{E}\begin{pmatrix} -1 \\ 0 \\ 1 \\ 0 \end{pmatrix}; u_\downarrow(p_3) = \sqrt{E}\begin{pmatrix} -s \\ c \\ s \\ -c \end{pmatrix}; u_\downarrow(p_4) = \sqrt{E}\begin{pmatrix} -c \\ -s \\ c \\ s \end{pmatrix}$$

-To calculate

$$M_{fi} = \frac{g_W^2}{2m_W^2} g_{\mu v} \left[\bar{u}_\downarrow(p_3)\gamma^\mu u_\downarrow(p_1)\right]\left[\bar{u}_\downarrow(p_4)\gamma^v u_\downarrow(p_2)\right]$$

need to evaluate two terms of form

$$\begin{aligned}
\bar{\psi}\gamma^0\phi &= \psi^\dagger\gamma^0\gamma^0\phi = \psi_1^*\phi_1 + \psi_2^*\phi_2 + \psi_3^*\phi_3 + \psi_4^*\phi_4 \\
\bar{\psi}\gamma^1\phi &= \psi^\dagger\gamma^0\gamma^1\phi = \psi_1^*\phi_4 + \psi_2^*\phi_3 + \psi_3^*\phi_2 + \psi_4^*\phi_1 \\
\bar{\psi}\gamma^2\phi &= \psi^\dagger\gamma^0\gamma^2\phi = -i\left(\psi_1^*\phi_4 - \psi_2^*\phi_3 + \psi_3^*\phi_2 - \psi_4^*\phi_1\right) \\
\bar{\psi}\gamma^3\phi &= \psi^\dagger\gamma^0\gamma^3\phi = \psi_1^*\phi_3 - \psi_2^*\phi_4 + \psi_3^*\phi_1 - \psi_4^*\phi_2
\end{aligned}$$

-Using

$$u_\downarrow(p_1) = \sqrt{E}\begin{pmatrix} 0 \\ 1 \\ 0 \\ -1 \end{pmatrix}; u_\downarrow(p_2) = \sqrt{E}\begin{pmatrix} -1 \\ 0 \\ 1 \\ 0 \end{pmatrix}; u_\downarrow(p_3) = \sqrt{E}\begin{pmatrix} -s \\ c \\ s \\ -c \end{pmatrix}; u_\downarrow(p_4) = \sqrt{E}\begin{pmatrix} -c \\ -s \\ c \\ s \end{pmatrix}$$

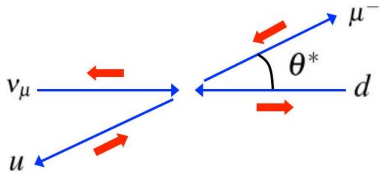
$$\begin{aligned}
\Longrightarrow \quad & \bar{u}_\downarrow(p_3)\gamma^\mu u_\downarrow(p_1) = 2E(c, s, -is, c) \\
& \bar{u}_\downarrow(p_4)\gamma^v u_\downarrow(p_2) = 2E(c, -s, -is, -c)
\end{aligned}$$

$$\Longrightarrow M_{fi} = \frac{g_W^2}{2m_W^2} 4E^2\left(c^2 + s^2 + s^2 + c^2\right) = \frac{g_W^2\hat{s}}{m_W^2} \quad \hat{s} = (2E)^2$$

⋆ Note the Matrix Element is isotropic

$$M_{fi} = \frac{g_W^2}{m_W^2}\hat{s}$$

we could have anticipated this since the helicity combination (spins anti-parallel)



has $S_z = 0 \Rightarrow$ no preferred polar angle

⋆ As before need to sum over all possible spin states and average over all possible initial state spin states. Here only one possible spin combination ($LL \rightarrow$ LL) and only 2 possible initial state combinations (the neutrino is always produced in a LH helicity state)

$$\left\langle |M_{fi}|^2 \right\rangle = \frac{1}{2} \cdot \left| \frac{g_W^2}{m_W^2}\hat{s}^2 \right.$$

The factor of a half arises because half of the time the quark will be in a RH states and won' t participate in the charged current Weak interaction

⋆ From handout 1, in the extreme relativistic limit, the cross section for any $2 \rightarrow 2$ body scattering process is

$$\frac{\mathrm{d}\sigma}{\mathrm{d}\Omega^*} = \frac{1}{64\pi^2\hat{s}} \left\langle |M_{fi}|^2 \right\rangle$$

$$\frac{\mathrm{d}\sigma}{\mathrm{d}\Omega^*} = \frac{1}{64\pi^2\hat{s}} \left\langle |M_{fi}|^2 \right\rangle = \frac{1}{64\pi\hat{s}} \frac{1}{2} \left(\frac{g_W^2 \hat{s}}{m_W^2} \right)^2 = \left(\frac{g_W^2}{8\sqrt{2}\pi m_W^2} \right)^2 \hat{s}$$

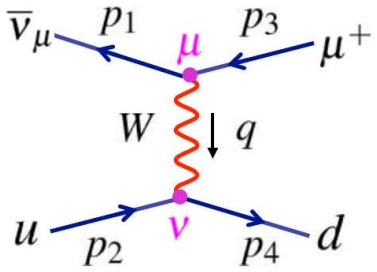
$$\text{using } \frac{G_\mathrm{F}}{\sqrt{2}} = \frac{g_W^2}{8m_W^2} \quad \frac{\mathrm{d}\sigma}{\mathrm{d}\Omega^*} = \frac{G_\mathrm{F}^2}{4\pi^2}\hat{s}$$

⋆ Integrating this isotropic distribution over $\mathrm{d}\Omega^*$

$$\Rightarrow \sigma_{vq} = \frac{G_\mathrm{F}^2 \hat{s}}{\pi} \tag{1}$$

-cross section is a Lorentz invariant quantity so this is valid in any frame

Antineutrino-Quark Scattering



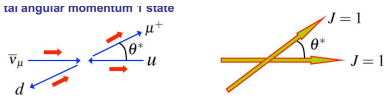
In the ultra-relativistic limit, the charged-current interaction matrix element is:

$$M_{fi} = \frac{g_W^2}{2m_W^2} g_{\mu v} \left[\bar{v}\left(p_1\right) \gamma^\mu \frac{1}{2} \left(1 - \gamma^5\right) v\left(p_3\right) \right] \left[\bar{u}\left(p_4\right) \gamma^v \frac{1}{2} \left(1 - \gamma^5\right) u\left(p_2\right) \right]$$

⋆ In the extreme relativistic limit only LH Helicity particles and RH Helicity antiparticles participate in the charged current weak interaction:

$$\Rightarrow M_{fi} = \frac{g_W^2}{2m_W^2} g_{\mu v} \left[\bar{v}_\uparrow (p_1) \gamma^\mu v_\uparrow (p_3)\right] \left[\bar{u}_\downarrow (p_4) \gamma^v u_\downarrow (p_2)\right]$$

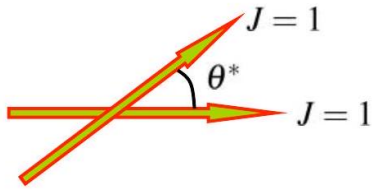
⋆ In terms of the particle spins it can be seen that the interaction occurs in a total angular momentum 1 state



⋆ In a similar manner to the neutrino-quark scattering calculation obtain:

$$\frac{\mathrm{d}\sigma_{\bar{v}q}}{\mathrm{d}\Omega^*} = \frac{\mathrm{d}\sigma_{vq}}{\mathrm{d}\Omega^*} \frac{1}{4} \left(1 + \cos\theta^*\right)^2$$

-The factor $\frac{1}{4}\left(1 + \cos\theta^*\right)^2$ can be understood in terms of the overlap of the initial and final angular momentum wave-functions



⋆ Similarly to the neutrino-quark scattering calculation obtain:

$$\frac{\mathrm{d}\sigma_{\bar{v}q}}{\mathrm{d}\Omega^*} = \frac{G_\mathrm{F}^2}{16\pi^2} \left(1 + \cos\theta^*\right)^2 \hat{s}$$

⋆ Integrating over solid angle:

$$\mathrm{d}\Omega = \mathrm{d}\phi \sin\theta \mathrm{d}\theta \rightarrow \mathrm{d}\phi \mathrm{d}(\cos\theta)$$

$$\int \left(1 + \cos\theta^*\right)^2 \ \mathrm{d}\Omega^* = \int \left(1 + \cos\theta^*\right)^2 \ \mathrm{d}\left(\cos\theta^*\right) \mathrm{d}\phi = 2\pi \int_{-1}^{+1} \left(1 + \cos\theta^*\right)^2 \ \mathrm{d}\left(\cos\theta^*\right) = \frac{16\pi}{3}$$

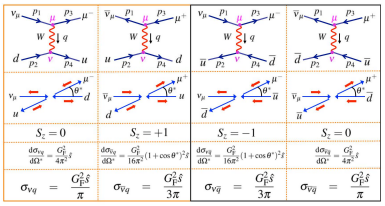
$$\sigma_{\bar{v}q} = \frac{G_\mathrm{F}^2 \hat{s}}{3\pi}$$

⋆ This is a factor three smaller than the neutrino quark cross-section

$$\frac{\sigma_{\bar{v}q}}{\sigma_{vq}} = \frac{1}{3}$$

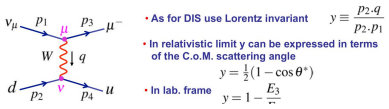
(Anti)neutrino-(Anti)quark Scattering

-Non-zero anti-quark component to the nucleon ⇒ also consider scattering from $\bar{q}$ -Cross-sections can be obtained immediately by comparing with quark scattering and remembering to only include LH particles and RH anti-particles



Differential Cross Section do/dy

⋆ Derived differential neutrino scattering cross sections in C.o.M frame, can convert to Lorentz invariant form



- In relativistic limit y can be expressed in terms of the C.o.M. scattering angle

$$y = \frac{1}{2}\left(1 - \cos\theta^*\right)$$

$$y = 1 - \frac{E_3}{E_1}$$

- In lab. frame

⋆ Convert from $\frac{\mathrm{d}\sigma}{\mathrm{d}\Omega^*} \to \frac{\mathrm{d}\sigma}{\mathrm{d}y}$ using

$$\frac{\mathrm{d}\sigma}{\mathrm{d}y} = \left|\frac{\mathrm{d}\cos\theta^*}{\mathrm{d}y}\right| \frac{\mathrm{d}\sigma}{\mathrm{d}\cos\theta^*} = \left|\frac{\mathrm{d}\cos\theta^*}{\mathrm{d}y}\right| 2\pi \frac{\mathrm{d}\sigma}{\mathrm{d}\Omega^*} = 4\pi \frac{\mathrm{d}\sigma}{\mathrm{d}\Omega^*}$$

-Already calculated (1)

$$\frac{\mathrm{d}\sigma}{\mathrm{d}\Omega^*} = \frac{G_\mathrm{F}^2}{4\pi^2}\hat{s}$$

- Hence:

$$\frac{\mathrm{d}\sigma_{vq}}{\mathrm{d}y} = \frac{\mathrm{d}\sigma_{\bar{v}\bar{q}}}{\mathrm{d}y} = \frac{G_\mathrm{F}^2}{\pi}\hat{s}$$

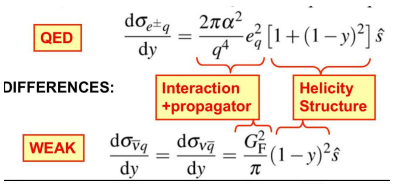
$$\text{and} \quad \frac{\mathrm{d}\sigma_{\bar{v}q}}{\mathrm{d}\Omega^*} = \frac{\mathrm{d}\sigma_{v\bar{q}}}{\mathrm{d}\Omega^*} = \frac{G_\mathrm{F}^2}{16\pi^2}\left(1 + \cos\theta^*\right)^2 \hat{s}$$

$$\text{becomes} \quad \frac{\mathrm{d}\sigma_{\bar{v}q}}{\mathrm{d}y} = \frac{\mathrm{d}\sigma_{v\bar{q}}}{\mathrm{d}y} = \frac{G_\mathrm{F}^2}{4\pi}\left(1 + \cos\theta^*\right)^2 \hat{s}$$

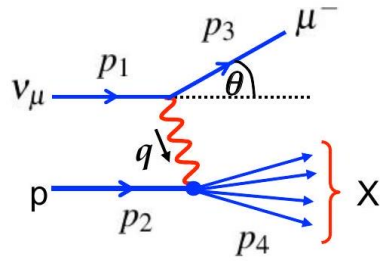
$$\text{from} \quad y = \frac{1}{2}\left(1 - \cos\theta^*\right) \to 1 - y = \frac{1}{2}\left(1 + \cos\theta^*\right)$$

$$\text{and hence} \quad \frac{\mathrm{d}\sigma_{\bar{v}q}}{\mathrm{d}y} = \frac{\mathrm{d}\sigma_{v\bar{q}}}{\mathrm{d}y} = \frac{G_\mathrm{F}^2}{\pi}(1-y)^2\hat{s}$$

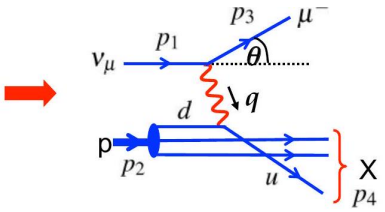
⋆ For comparison, the electro-magnetic $e^\pm q \to e^\pm q$ cross section is:



Parton Model For Neutrino Deep Inelastic Scattering



Scattering from a proton with structure functions



Scattering from a point-like quark within the proton

- Neutrino-proton scattering can occur via scattering from a down-quark or from an anti-up quark

-In the parton model, number of down quarks within the proton in the momentum fraction range $x \to x + \mathrm{d}x$ is $d^p(x)\mathrm{d}x$. Their contribution to the neutrino scattering cross-section is obtained by multiplying by the $\nu_\mu d \to \mu^- u$ cross-section derived previously

$$\frac{\mathrm{d}\sigma^{\nu p}}{\mathrm{d}y} = \frac{G_\mathrm{F}^2}{\pi}\hat{s}d^p(x)\mathrm{d}x$$

where $\hat{s}$ is the centre-of-mass energy of the $\nu_\mu d$

- Similarly for the $\bar{u}$ contribution

$$\frac{\mathrm{d}\sigma^{\nu p}}{\mathrm{d}y} = \frac{G_\mathrm{F}^2}{\pi}\hat{s}(1-y)^2\bar{u}^p(x)\mathrm{d}x$$

⋆ Summing the two contributions and using $\hat{s} = xS$

$$\Rightarrow \frac{\mathrm{d}^2\sigma^{\nu p}}{\mathrm{d}x\ \mathrm{d}y} = \frac{G_\mathrm{F}^2}{\pi}sx\left[d^p(x) + (1-y)^2\bar{u}^p(x)\right]$$

⋆ The anti-neutrino proton differential cross section can be obtained in the same manner:

$$\frac{\mathrm{d}^2\sigma^{\bar{\nu}}p}{\mathrm{d}x\ \mathrm{d}y} = \frac{G_\mathrm{F}^2}{\pi}sx\left[(1-y)^2u^p(x) + \bar{d}^p(x)\right]$$

⋆ For (anti)neutrino - neutron scattering:

$$\frac{\mathrm{d}^2\sigma^{\nu n}}{\mathrm{d}x\ \mathrm{d}y} = \frac{G_\mathrm{F}^2}{\pi}sx\left[d^n(x) + (1-y)^2\bar{u}^n(x)\right]$$
$$\frac{\mathrm{d}^2\sigma^{\bar{\nu}}n}{\mathrm{d}x\ \mathrm{d}y} = \frac{G_\mathrm{F}^2}{\pi}sx\left[(1-y)^2u^n(x) + \bar{d}^n(x)\right]$$

-As before, define neutron distributions functions in terms of those of the proton

$$u(x) \equiv u^{\mathrm{p}}(x) = d^{\mathrm{n}}(x); \quad d(x) \equiv d^{\mathrm{p}}(x) = u^{\mathrm{n}}(x)$$
$$\bar{u}(x) \equiv \bar{u}^{\mathrm{p}}(x) = \bar{d}^{\mathrm{n}}(x); \quad \bar{d}(x) \equiv \bar{d}^{\mathrm{p}}(x) = \bar{u}^{\mathrm{n}}(x)$$
$$\frac{\mathrm{d}^2\sigma^{\nu p}}{\mathrm{d}x\ \mathrm{d}y} = \frac{G_{\mathrm{F}}^2}{\pi} sx\left[d(x) + (1-y)^2\bar{u}(x)\right] \tag{2}$$
$$\frac{\mathrm{d}^2\sigma^{\bar{\nu}} p}{\mathrm{d}x\ \mathrm{d}y} = \frac{G_{\mathrm{F}}^2}{\pi} sx\left[(1-y)^2 u(x) + \bar{d}(x)\right] \tag{4}$$
$$\frac{\mathrm{d}^2\sigma^{\nu n}}{\mathrm{d}x\ \mathrm{d}y} = \frac{G_{\mathrm{F}}^2}{\pi} sx\left[u(x) + (1-y)^2\bar{d}(x)\right] \tag{5}$$
$$\frac{\mathrm{d}^2\sigma^{\bar{\nu}} n}{\mathrm{d}x\ \mathrm{d}y} = \frac{G_{\mathrm{F}}^2}{\pi} sx\left[(1-y)^2 d(x) + \bar{u}(x)\right]$$

⋆ Because neutrino cross sections are very small, need massive detectors. These are usually made of Iron, hence, experimentally measure a combination of proton/neutron scattering cross sections

⋆ For an isoscalar target (i.e. equal numbers of protons and neutrons), the mean cross section per nucleon:

$$\frac{\mathrm{d}^2\sigma^{\nu N}}{\mathrm{d}x\ \mathrm{d}y} = \frac{1}{2}\left(\frac{\mathrm{d}^2\sigma^{\nu p}}{\mathrm{d}x\ \mathrm{d}y} + \frac{\mathrm{d}^2\sigma^{\nu n}}{\mathrm{d}x\ \mathrm{d}y}\right)$$
$$\Rightarrow \frac{\mathrm{d}^2\sigma^{\nu N}}{\mathrm{d}x\ \mathrm{d}y} = \frac{G_{\mathrm{F}}^2}{2\pi} sx\left[u(x) + d(x) + (1-y)^2(\bar{u}(x) + \bar{d}(x))\right]$$

-Integrate over momentum fraction x

$$\frac{\mathrm{d}\sigma^{\nu N}}{\mathrm{d}y} = \frac{G_{\mathrm{F}}^2}{2\pi} s\left[f_q + (1-y)^2 f_{\bar{q}}\right] \tag{6}$$

where f_q and $f_{\bar{q}}$ are the total momentum fractions carried by the quarks and by the anti-quarks within a nucleon

$$f_q \equiv f_d + f_u = \int_0^1 x[u(x) + d(x)]\mathrm{d}x; \quad f_{\bar{q}} \equiv f_{\bar{d}} + f_{\bar{u}} = \int_0^1 x[\bar{u}(x) + \bar{d}(x)]\mathrm{d}x$$

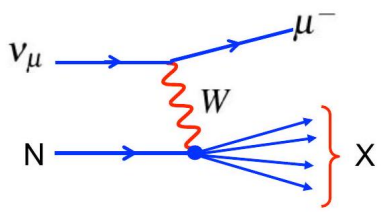
-Similarly

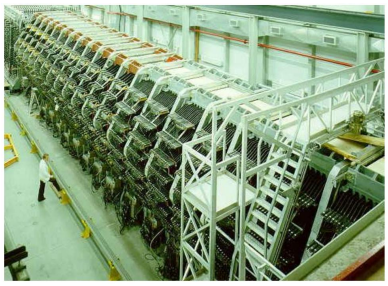
$$\frac{\mathrm{d}\sigma^{\bar{\nu}} N}{\mathrm{d}y} = \frac{G_{\mathrm{F}}^2}{2\pi} s\left[(1-y)^2 f_q + f_{\bar{q}}\right] \tag{7}$$

e.g. CDHS Experiment (CERN 1976-1984)

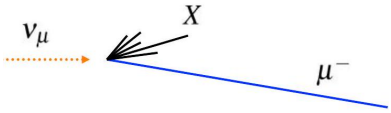
-1250 tons

- Magnetized iron modules - Separated by drift chambers Study Neutrino Deep Inelastic Scattering

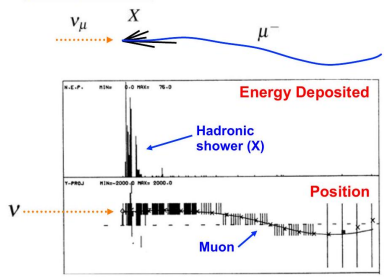




Experimental Signature:



Example Event:



-Measure energy of X
E_X
· Measure muon momentum from curvature in B-field

$$E_\mu$$

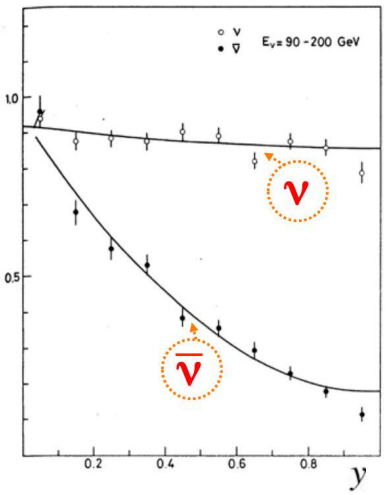
⋆ For each event can determine neutrino energy and y !

$$E_v = E_X + E_\mu$$

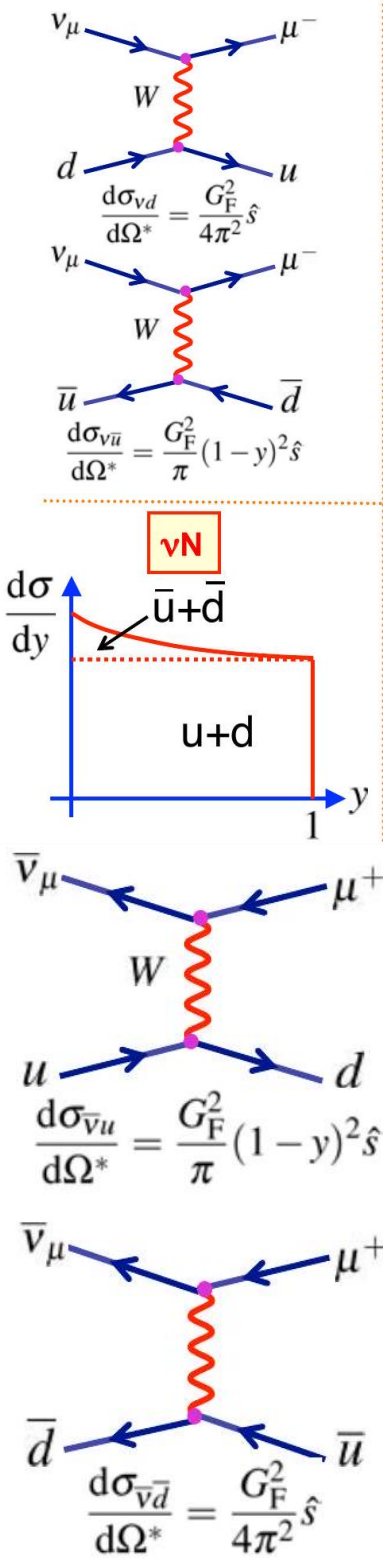
$$E_\mu = (1-y)E_v \longrightarrow y = \left(1 - \frac{E_\mu}{E_v}\right)$$

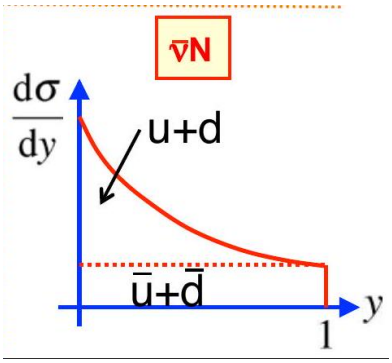
Measured y Distribution

-CDHS measured y distribution

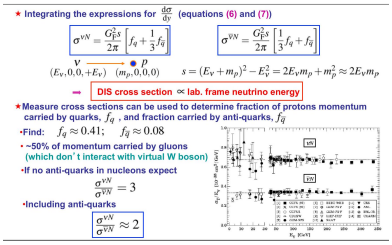


- Shapes can be understood in terms of (anti)neutrino (anti)quark scattering





Measured Total Cross Sections



$$\sigma^{\nu N} = \frac{G_F^2 s}{2\pi}\left[f_q + \tfrac{1}{3} f_{\bar{q}}\right] \quad \sigma^{\bar{\nu} N} = \frac{G_F^2}{2\pi}\left[\tfrac{1}{3} f_q + \right.$$

$$(E_\nu, 0, 0, +E_\nu) \quad (m_p, 0, 0, 0) \quad s = (E_\nu + m_p)^2 - E_\nu^2 = 2E_\nu$$

$$\Rightarrow \text{ DIS cross section } \propto \text{ lab. frame neutrino energy}$$

$\star$ Measure cross sections can be used to determine fraction of protons momentum carried by quarks, f_q, and fraction carried by anti-quarks, $f_{\bar{q}}$

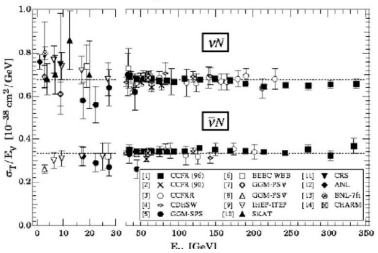
-Find: $f_q \approx 0.41$; $f_{\bar{q}} \approx 0.08$

- $\sim 50\%$ of momentum carried by gluons (which don't interact with virtual W boson) -If no anti-quarks in nucleons expect

$$\frac{\sigma^{\nu N}}{\sigma^{\bar{\nu} N}} = 3$$

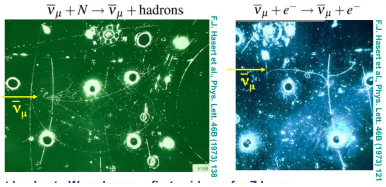
-Including anti-quarks

$$\frac{\sigma^{\nu N}}{\sigma^{\bar{\nu} N}} \approx 2$$

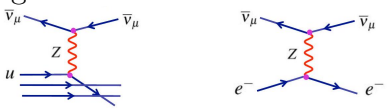


Weak Neutral Current

⋆ Neutrinos also interact via the Neutral Current. First observed in the Gargamelle bubble chamber in 1973. Interaction of muon neutrinos produce a final state muon



⋆ Cannot be due to W exchange - first evidence for Z boson



Summary

⋆ Derived neutrino/anti-neutrino - quark/anti-quark weak charged current (CC) interaction cross sections

⋆ Neutrino - nucleon scattering yields extra information about parton distributions functions:

- v couples to d and $\bar{u}; \bar{v}$ couples to u and $\bar{d}$

$\Rightarrow$ investigate flavour content of nucleon

- can measure anti-quark content of nucleon

$v\bar{q}$ suppressed by factor $(1-y)^2$ compared with vq
$\bar{v}q$ suppressed by factor $(1-y)^2$ compared with $\bar{v}\bar{q}$

⋆ Further aspects of neutrino deep-inelastic scattering (expressed in general structure functions) are covered in Appendix II

⋆ Finally observe that neutrinos interact via weak neutral currents (NC)

Appendix I

-For the adjoint spinors $\bar{u} = u^\dagger \gamma^0$ consider

$$\overline{\frac{1}{2}\left(1-\gamma^5\right)u} = \left[\frac{1}{2}\left(1-\gamma^5\right)u\right]^\dagger \gamma^0 = u^\dagger \frac{1}{2}\left(1-\gamma^5\right)\gamma^0 = u^\dagger \gamma^0 \frac{1}{2}\left(1+\gamma^5\right) = \bar{u}\frac{1}{2}\left(1+\gamma^5\right)$$

$$\frac{1}{2}\left(1-\gamma^5\right)u_\uparrow = 0 \quad \Rightarrow \quad \bar{u}\frac{1}{2}\left(1+\gamma^5\right) = 0$$

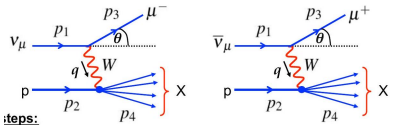
Using the fact that γ^5 and γ^μ anti-commute can rewrite ME:

$$M_{fi} = \frac{g_W^2}{2m_W^2} g_{\mu v}\left[\bar{u}\left(p_3\right)\frac{1}{2}\left(1+\gamma^5\right)\gamma^\mu u\left(p_1\right)\right]\left[\bar{u}\left(p_4\right)\frac{1}{2}\left(1+\gamma^5\right)\gamma^v u\left(p_2\right)\right]$$

$$\Longrightarrow M_{fi} = 0 \quad \text{for} \quad \bar{u}_\uparrow\left(p_3\right) \text{ and } \quad \bar{u}_\uparrow\left(p_4\right)$$

Appendix II: Deep-Inelastic Neutrino Scattering

Two steps:



- First write down most general cross section in terms of structure functions
- Then evaluate expressions in the quark-parton model

QED Revisited

$\star$ In the limit $s \gg M^2$ the most general electro-magnetic deep-inelastic cross section (from single photon exchange) can be written (Eq. 2 of handout 6)

$$\frac{\mathrm{d}^2\sigma_{e^\pm p}}{\mathrm{d}x\ \mathrm{d}Q^2} = \frac{4\pi\alpha^2}{Q^4}\left[(1-y)\frac{F_2\left(x,Q^2\right)}{x} + y^2 F_1\left(x,Q^2\right)\right]$$

- For neutrino scattering typically measure the energy of the produced muon $E_\mu = E_v(1-y)$ and differential cross-sections expressed in terms of $\mathrm{d}x\ \mathrm{d}y$ - Using $Q^2 = (s-M^2)\,xy \approx sxy \Rightarrow \frac{\mathrm{d}^2\sigma}{\mathrm{d}x\ \mathrm{d}y} = \left|\frac{\mathrm{d}Q^2}{\mathrm{d}y}\right| \frac{\mathrm{d}^2\sigma}{\mathrm{d}x\ \mathrm{d}Q^2} = sx\frac{\mathrm{d}^2\sigma}{\mathrm{d}x\ \mathrm{d}Q^2}$
- In the limit $s \gg M^2$ the general Electro-magnetic DIS cross section can be written

$$\frac{\mathrm{d}^2\sigma^{e^\pm p}}{\mathrm{d}x\ \mathrm{d}y} = \frac{4\pi\alpha^2 s}{Q^4}\left[(1-y)F_2\left(x,Q^2\right) + y^2 x F_1\left(x,Q^2\right)\right]$$

-NOTE: This is the most general Lorentz Invariant parity conserving expression * For neutrino DIS parity is violated and the general expression includes an additional term to allow for parity violation. New structure function $F_3\left(x,Q^2\right)$

$v_\mu p \to \mu^- X$

$$\frac{\mathrm{d}^2\sigma^{vp}}{\mathrm{d}x\ \mathrm{d}y} = \frac{G_\mathrm{F}^2 s}{2\pi}\left[(1-y)F_2^{vp}\left(x,Q^2\right) + y^2 x F_1^{vp}\left(x,Q^2\right) + y\left(1-\frac{y}{2}\right)xF_3^{vp}\left(x,Q^2\right)\right]$$

-For anti-neutrino scattering new structure function enters with opposite sign
$\bar{v}_\mu p \to \mu^+ X \quad \frac{\mathrm{d}^2\sigma^{\bar{v}p}}{\mathrm{d}x\ \mathrm{d}y} = \frac{G_\mathrm{F}^2 s}{2\pi}\left[(1-y)F_2^{\bar{v}p}\left(x,Q^2\right) + y^2 x F_1^{\bar{v}p}\left(x,Q^2\right) - y\left(1-\frac{y}{2}\right)xF_3^{\bar{v}p}\left(x,Q^2\right)\right]$

- Similarly for neutrino-neutron scattering

$$v_\mu n \to \mu^- X \quad \frac{\mathrm{d}^2\sigma^{vn}}{\mathrm{d}x\ \mathrm{d}y} = \frac{G_\mathrm{F}^2 s}{2\pi}\left[(1-y)F_2^{vn}\left(x,Q^2\right) + y^2 x F_1^{vn}\left(x,Q^2\right) + y\left(1-\frac{y}{2}\right)xF_3^{vn}\left(x,Q^2\right)\right]$$

$$\bar{v}_\mu n \to \mu^+ X \quad \frac{\mathrm{d}^2\sigma^{\bar{v}n}}{\mathrm{d}x\ \mathrm{d}y} = \frac{G_\mathrm{F}^2 s}{2\pi}\left[(1-y)F_2^{\bar{v}n}\left(x,Q^2\right) + y^2 x F_1^{\bar{v}n}\left(x,Q^2\right) - y\left(1-\frac{y}{2}\right)xF_3^{\bar{v}n}\left(x,Q^2\right)\right]$$

Neutrino Interaction Structure Functions

⋆ In terms of the parton distribution functions we found (2):

$$\frac{\mathrm{d}^2\sigma^{\nu p}}{\mathrm{d}x\ \mathrm{d}y} = \frac{G_\mathrm{F}^2}{\pi} sx\left[d(x) + (1-y)^2\bar{u}(x)\right]$$

-Compare coefficients of y with the general Lorentz Invariant form (p.321) and assume Bjorken scaling, i.e. $F\left(x, Q^2\right) \to F(x)$

$$\frac{\mathrm{d}^2\sigma^{\nu p}}{\mathrm{d}x\ \mathrm{d}y} = \frac{G_\mathrm{F}^2 s}{2\pi}\left[(1-y)F_2^{\nu p}(x) + y^2 x F_1^{\nu p}(x) + y\left(1-\frac{y}{2}\right)xF_3^{\nu p}(x)\right]$$

-Re-writing (2) $\frac{\mathrm{d}^2\sigma^{\nu p}}{\mathrm{d}x\ \mathrm{d}y} = \frac{G_\mathrm{F}^2}{2\pi}s\left[2xd(x) + 2x\bar{u}(x) - 4xy\bar{u}(x) + 2xy^2\bar{u}(x)\right]$
and equating powers of y

$$\left.\begin{aligned} 2xd + 2x\bar{u} &= F_2 \\ -4x\bar{u} &= -F_2 + xF_3 \\ 2\bar{u} &= F_1 - xF_3/2 \end{aligned}\right\}$$

$$F_2^{\nu p} = 2xF_1^{\nu p} = 2x[d(x) + \bar{u}(x)]$$
$$xF_3^{\nu p} = 2x[d(x) - \bar{u}(x)]$$

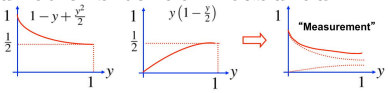
NOTE: again we get the Callan-Gross relation $F_2 = 2xF_1$

No surprise, underlying process is scattering from point-like spin-1/2 quarks ⋆ Substituting back in to expression for differential cross section:

$$\frac{\mathrm{d}^2\sigma^{\nu p}}{\mathrm{d}x\ \mathrm{d}y} = \frac{G_\mathrm{F}^2 s}{2\pi}\left[\left(1-y+\frac{y^2}{2}\right)F_2^{\nu p}(x) + y\left(1-\frac{y}{2}\right)xF_3^{\nu p}(x)\right]$$

⋆ Experimentally measure F_2 and F_3 from y distributions at fixed x

- Different y dependencies (from different rest frame angular distributions) allow contributions from the two structure functions to be measured



⋆Then use $F_2^{\nu p} = 2x[d(x) + \bar{u}(x)]$ and $F_3^{\nu p} = 2[d(x) - \bar{u}(x)]$
Determine $d(x)$ and $\bar{u}(x)$ separately

⋆ Neutrino experiments require large detectors (often iron) i.e. isoscalar target

$$F_2^{\nu N} = 2xF_1^{\nu N} = \frac{1}{2}\left(F_2^{\nu p} + F_2^{\nu n}\right) = x[u(x) + d(x) + \bar{u}(x) + \bar{d}(x)]$$
$$xF_3^{\nu N} = \frac{1}{2}\left(xF_3^{\nu p} + xF_3^{\nu n}\right) = x[u(x) + d(x) - \bar{u}(x) - \bar{d}(x)]$$

⋆ For electron - nucleon scattering:

$$F_2^{ep} = 2xF_1^{ep} = x\left[\frac{4}{9}u(x) + \frac{1}{9}d(x) + \frac{4}{9}\bar{u}(x) + \frac{1}{9}\bar{d}(x)\right]$$
$$F_2^{en} = 2xF_1^{en} = x\left[\frac{4}{9}d(x) + \frac{1}{9}u(x) + \frac{4}{9}\bar{d}(x) + \frac{1}{9}\bar{u}(x)\right]$$

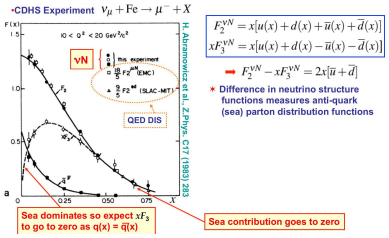
- For an isoscalar target

$$F_2^{eN} = \frac{1}{2}\left(F_2^{ep} + F_2^{en}\right) = \frac{5}{18}x[u(x) + d(x) + \bar{u}(x) + \bar{d}(x)]$$
$$\Rightarrow F_2^{\nu N} = \frac{18}{5}F_2^{eN}$$

- Note that the factor $\frac{5}{18} = \frac{1}{2}\left(q_u^2 + q_d^2\right)$ and by comparing neutrino to electron scattering structure functions measure the sum of quark charges

$$\text{Experiment:} \quad 0.29 \pm 0.02$$

Measurements of $F_2(x)$ and $F_3(x)$



Valence Contribution

⋆ Separate parton density functions into sea and valence components

$$u(x) = u_V(x) + u_S(x) = u_V(x) + S(x)$$
$$d(x) = d_V(x) + d_S(x) = d_V(x) + S(x)$$
$$\bar{u}(x) = \bar{u}_S(x) = S(x)$$
$$\bar{d}(x) = \bar{d}_S(x) = S(x)$$
$$\Rightarrow \quad F_3^{\nu N} = [u(x) + d(x) - \bar{u}(x) - \bar{d}(x)] = u_V(x) + d_V(x)$$

⋆ Area under measured function $F_3^{\nu N}(x)$ gives a measurement of the total number of valence quarks in a nucleon!

$$\text{expect} \int_0^1 F_3^{\nu N}(x)\mathrm{d}x = 3 \quad \text{“Gross - Llewellyn-Smith sum rule”}$$

Experiment: 3.0 ± 0.2

-Note: $F_2^{\bar{\nu}p} = F_2^{\nu n}; F_2^{\bar{\nu}n} = F_2^{\nu p}; F_3^{\bar{\nu}p} = F_3^{\nu n}; F_3^{\bar{\nu}n} = F_3^{\nu p}$ and anti-neutrino structure functions contain same pdf information

1.9 Properties of Typical Particles

1.9.1 p, n, α-Particle

p

(???)

основные реакции

n

(?? properties??)

основные реакции

α-Particle

полезно понять ее свойства.

обзор свойств

основные реакции

1.9.2 Other Typical Mesons

K мезоны

мотивация изучать эту частицу

обзор свойств

основные реакции

смешивание K-онов

ρ мезон

и зачем там он?

мотивация изучать эту частицу

основные свойства

основные реакции

μ мезон

и зачем там он?

мотивация изучать эту частицу

какие-то его распады что-то для слабого взаимодействия дают.

основные свойства

основные реакции

распад мюона

Масса мюона: $m_\mu = 105.66$МВ, масса электрона $m_e = 0.511$М В; высвобождаемая при распаде мюона энергия, которую мог бы получить электрон: $m_\mu - m_e = 105.15$ МэВ. Здесь обсудим распад

$$\mu^- \to e^- + \bar{\nu}_e + \nu_\mu$$

Как и в бета-распаде нейтрона, здесь участвуют 4 фермиона. Напрашивается предположение, что матричный элемент распада мюона должен быть похож на матричный элемент распада нейтрона. Если это так, то можно вычислить ожидаемое распределение по энергии электрона E в системе покоя мюона, равно как и время жизни мюона (см. [4]). Энергетическое

распределение будет зависеть от спиральности нейтрино (параметр λ в книге [4]); пренебрегая массой электрона по сравнению с его энергией, можно получить [4]:

$$\frac{I(E)}{dE} \sim \frac{\tilde{G}^2 m_\mu^2 E^2}{48\pi^3}\left[|1-\lambda|^2 \times 6\left(1-2\frac{E}{m_\mu}\right)+|1+\lambda|^2\left(3-4\frac{E}{m_\mu}\right)\right]$$

где $\tilde{G}$ - константа связи для μ -распада. Наблюдаемое распределение хорошо согласуется с (1.65) при $\lambda = +1$, что означает, что мюонное нейтрино должно иметь, как и мюон, отрицательную спиральность.

В литературе до начала 70-х годов использовалась следуюшая форма за- писи проинтегрированног по углам энергетического распределения электронов (см. [1]):

$$\frac{I(E)}{dE} = \frac{m_\mu^5}{16\pi^3}\tilde{G}^2 x^2\left[1-x+\frac{2}{3}\rho\left(\frac{4}{3}x-1\right)\right]$$

где параметр ρ называется параметром Мишеля и

$$x = \frac{E_e}{m_\mu/2}$$

Параметр Мишеля сыграл известную роль в определении структуры гамильтониана слабого взаимодействия; было выполнено много экспериментов по его измерению. Он оказался близок к значению $\rho = 0.75$, что и должно было быть для $V-A$ структуры 4 -фермионного взаимодействия и соответствует $\lambda = +1$ Для времени жизни мю-мезона имеем: что приводит к извлекаемому из данных о времени жизни мюона $\tau_\mu \approx 2.19\cdot 10^{-6}$сек значению $\tilde{G}$, совпадаюпему (с точностью не хуже 2%) со Значением векторной константы связи для ядерного распада.

Все это говорит о том, что слабое взаимодействие между фермионами не зависит от того, является ли фермион адроном или нет.

Полная вероятность распада (размерные соображения). Из соображений размерности: константа слабого взаимодействия G имеет размерность $[m]^{-2}$; обратное время жизни имеет размерность $[m]^{+1}$; т.о. полная вероятность распада должна быть пропорциональна $m_\mu^5 G^2$.

Особо заслуживают внимания разные области энергетического спектра электронов: (1) энергия электрона вблизи максимально возможной, (2) энергия электрона далека от максимально возможной. Вблизи этих пределов, как видно из рисунков 1.2, 1.3, электроны вылетают преимущественно против и по направлению спина мюона соответственно. Это означает, что угловое распределение электронов распада по отношению к направлению спина мюона имеет характер $(1-\mathbf{P}_\mu \mathbf{n}_e)$ $(\mathbf{n}_e = \mathbf{k}_e/k_e,$ где $\mathbf{k}_e$ - вектор импульса электрона) и $(1+\mathbf{P}_\mu \mathbf{n}_e)$ соответственно. Здесь $\mathbf{P}_\mu$ - вектор поляризации мюона.

Итак, угловое распределение электронов в разных частях энергетического спектра должно быть различным.

Важно, что эффективное 4-фермионное взаимодействие локально, т.е. орбитальных угловых моментов нет (все частицы - в S -волне).

Экспериментально установленное равенство векторных констант связи во взаимодействиях, отвечающих за распад μ -мезона и за бета-распад ядер само по себе удивительно, тем более на фоне того, что в случае распада μ -мезона псевдовекторная константа связи равна векторной, но в случае β -распада примерно на 25% больше ее. Правда, разница здесь в том, что μ -мезон не участвует в сильных взаимодействиях, тогда как протон и нейтрон достаточно сильно связаны с π -мезоном: псевдоскалярной частицей. Поэтому можно было бы ожидать, что даже если бы обсуждаемые константы были бы одинаковы в эффективном гамильтониане, все же сильное взаимодействие между нуклонами и пионом

может привести к эффектам экранирования и изменить измеряемые эффективные константы (что и происходит). С другой стороны, именно равенство псевдовекторной и векторной констант связи в распаде μ -мезона и привело, во-первых, к формулировке идеи универсального 4-фермионного взаимодействия (независимо от того, имеем ли дело с фермионами-адронами или нет), и во-вторых - к идее (Герштейн и Зельдович, позднее - Фейнман и Гелл-Манн), сохраняющегося векторного тока.

π мезон

и зачем там он?

мотивация изучать эту частицу

какие-то его распады что-то для слабого взаимодействия дают.

основные свойства

основные реакции

распад пиона

Масса пиона: $m_{\pi^\pm} = 139.57\text{M}_\ni\text{B}, m_{\pi^0} = 134.9764\text{M}$ В. Лептонный распад: $\pi^+ \to l^+ + \nu$; высвобождаемая при распаде пиона энергия, которая делится между лептоном и нейтрино: 139.06 МэВ при распаде с испусканием позитрона, и 33.91 МэВ при распаде с испусканием мюона (т.е. электрон релятивистский, мюон - нет).

Этот двухчастичный распад, помимо всего прочего, интересен тем, что может идти только за счет "малых" компонент лептонных волновых функций, что виднс из рис. 1.4. В рамках идеи об универсальном $V-A$ взаимодействии для времени жизни пиона по отнопению к распаду (1.73) можно получить выражение (см. где m - масса испускаемого лептона (электрона или мюона), m_π - масса пиона, а коэффициент a - характеризующий полную вероятность распада - может быть разным в распадах на мюон и на электрон (например. из-за дополнительных поправок). Этот процесс инициируется аксиально-векторным током, не изменяющим странность.

Отсюда для отношения вероятностей распада пиона на мюон и нейтрино и на электрон и нейтрино имеем (если дополнительная константа a одна и та же; из эксперимента оказалось, что $|a| \approx 0.92 m_\pi$) :

$$R\left(\frac{\pi \to e + \nu_e}{\pi \to \mu + \nu_\mu}\right) = \left(\frac{m_e}{m_\mu}\right)^2 \frac{\left(m_\pi^2 - m_e^2\right)^2}{\left(m_\pi^2 - m_\mu^2\right)^2} = 1.3 \cdot 10^{-4}$$

что хорошо согласуется с экспериментальными данными. Отношение фазовых объемов для распадов по указанным каналам есть

$$\frac{\left(m_\pi^2 - m_e^2\right)^2}{\left(m_\pi^2 - m_\mu^2\right)^2} \cdot \frac{m_\pi^2 + m_e^2}{m_\pi^2 + m_\mu^2} \approx 3.5$$

Первый множитель в (1.75) обусловлен действием правил отбора при $V-A$ связи (см. рис. 1.4)с учетом того, что у нейтрино всегда отрицательная спиральность, у антинейтрино - всегда положительная.

Частичное сохранение аксиально-векторного тока

Вернемся к распаду пиона на лептоны и запишем соответствующий матричный элемент в форме [10]:

$$< 0 \left| J_A^\alpha \right| \pi >\sim \frac{q^\alpha}{(2\pi)^3/2} F_\pi \left(m_\pi^2\right)$$

где J_A^α - псевдовекторная часть адронного тока, α - обычный индекс 4-мерных векторов, $F_\pi\left(q^2\right)$ - пионный формфактор (который для распада пиона нужно брать при $q^2 = m_\pi^2$), определяющий время жизни пиона. Величину $F_\pi\left(q^2 = m_\pi^2\right)$ можно связать с пион-нуклонной константой связи (см. например в [4]).

Если бы аксиально-векторный ток сохранялся (как сохраняется слабый векторный ток), то было бы верно соотношение

$$q_\alpha J_A^\alpha \sim \frac{m_\pi^2}{(2\pi)^3/2} F_\pi \left(m_\pi^2\right) = 0$$

то есть, константа $F_\pi\left(q^2 = m_\pi^2\right)$ должна была бы быть равной нулю, что означает, что пион был бы стабильным!

Конечность времени жизни пиона по отношению к распаду на мюон (или электрон) и нейтрино означает, т. о., что аксиально-векторный ток не может сохраняться при ненулевой массе пиона; однако, он мог бы сохраняться, например, в пределе безмассового пиона (когда $m_\pi^2 = 0$).

Если принять гипотезу о том, что аксиально-векторный ток строго сохраняется только в пределе нулевой массы пиона (или нуклона, или при одновременном стремлении к нулю и массы нуклона, и массы пиона), но при конечной (но малой) величине q^2 пропорциональна, например, пионному полю, то (в координатном представлении): где $\varphi(x)$ - пионное поле в точке x, что оказывается возможным получить упомянутую выше связь между константами аксиально-векторной связи, массой пиона и пион-нуклонной константой связи для сильного взаимодействия. Соответствующая формула называется соотношением Гольдбергера-Треймана. Вначале она была получена методами дисперсионных соотношений, а затем - в рамках гипотезы ЧСАТ.

Гипотеза о частичном сохранении слабого аксиально-векторного тока в англоязычной литературе сокрашенно обозначается как PCAC-гипотеза (в русскоязычной встречается и такое обозначение, и аббревиатура «ЧСАТ-гипотеза»).

η мезон

мотивация изучать эту частицу

основные свойства

основные реакции

1.9.3 Photons, Z and W-bosons

Гамма-квант (γ) - фотон большой энергии, т.е. квант гамма-пзлучения. Условно гамма-квантами считают фотоны с энергией больше 10 кэВ. Гамма-кванты могут испускаться (поглощаться) атомными ядрами при переходах из одного квантового состояния в другое, при превращениях элементарных частиц, торможении заряженных частиц высокой энергін, синхротронном излучении. Примером процесса с участием элементарных частиц, в котором рождаются гамма-кванты, является аннигиляция (уничтожение) электрона e- и позитрона e^+с образованием двух фотонов: $e^- + e^+ \to 2\gamma$. Если аннигилируют практически неподвижные

е е $^-$и e^+, то фотоны уносят энергію, равную сумме энергий покоя е $^-$и е $^+$, т.е. энергию $2mc^2 = 2 \cdot 0.511$М э = 1.022М э, где m - масса электрона и позитрона. Фотоны разлетаются в противоположные стороны п каждый уносіт энергию 0.511 МэВ.

обзор свойств

основные реакции

Распад Z -бозона на пару нейтрино у киселева из ктп.

Вершина взаимодействия левого нейтрино с Z -бозоном определяется зарядом $Q = 0$ и проекцией слабого изспина $t_3 = \frac{1}{2}$

$$-\frac{e}{2\sin\theta_W \cos\theta_W} \mathcal{Z}_\mu \left[\bar{\nu}_L \gamma^\mu \nu_L\right]$$

так что матричный элемент распада, который описывается диаграммой на рис. 18, равен

$$\mathrm{i}\mathfrak{M} = -\mathrm{i}\frac{e}{2\sin\theta_W \cos\theta_W} \varepsilon_\mu^{\mathcal{Z}} \left[\bar{u}_L(k) \gamma^\mu v_L\left(k'\right)\right]$$

где $\varepsilon_\mu^{\mathcal{Z}}$ - вектор поляризации Z -бозона с импульсом $p : \varepsilon_\mu^{\mathcal{Z}} \cdot p = 0$, - как и должно быть для массивного поля, $\left(\varepsilon_\mu^{\mathcal{Z}}\right)^2 = -1$.

Возведем матричный элемент в квадрат и просуммируем по поляризациям нейтрино, так что

$$\begin{aligned}\sum \left[\bar{u}_L(k) \gamma_\mu v_L\left(k'\right)\right] \left[\bar{v}_L\left(k'\right) \gamma_\nu u_L(k)\right] &= \frac{1}{2} \operatorname{tr}\left\{\gamma^\mu \left(1 - \gamma_5\right) \not{k}' \gamma^\nu \not{k}\right\} = \\ &= 2k'_\mu k_\nu - 2g_{\mu\nu}\left(k' \cdot k\right) + 2k'_\nu k_\mu - \\ &- 2\mathrm{i}\hat{\varepsilon}_{\mu\mu'\nu\nu'} \left(k'\right)^{\mu'} k^{\nu'}\end{aligned}$$

Усреднение по поляризациям Z -бозона даст

$$\frac{1}{3} \sum \varepsilon_{\mathcal{Z}}^\mu \varepsilon_{\mathcal{Z}}^{*\mu} = \frac{1}{3}\left(-g^{\mu\nu} + \frac{p^\mu p^\nu}{m_{\mathcal{Z}}^2}\right)$$

Произведение этих факторов равно

$$\frac{1}{3}\left(4\left(k' \cdot k\right) + \frac{1}{m_{\mathcal{Z}}^2}\left(4\left(p \cdot k'\right)\left(p \cdot k\right) - 2p^2\left(k' \cdot k\right)\right) = \frac{2}{3} m_{\mathcal{Z}}^2\right.$$

где мы воспользовались приближением безмассового нейтрино,

$$\left(k' + k\right)^2 = 2\left(k' \cdot k\right) = m_{\mathcal{Z}}^2$$

и вычислили скалярные произведения

$$2\left(p \cdot k'\right) = 2\left(k' + k\right) \cdot k' = 2\left(k \cdot k'\right) = m_{\mathcal{Z}}^2$$

и

$$2(p \cdot k) = 2\left(k' + k\right) \cdot k = 2\left(k' \cdot k\right) = m_{\mathcal{Z}}^2$$

В итоге, усредненный квадрат матричного элемента

$$\left\langle|\mathfrak{M}|^2\right\rangle = \frac{4\pi\alpha_{\mathrm{em}}}{4\sin^2\theta_W \cos^2\theta_W} \frac{2}{3} m_{\mathcal{Z}}^2$$

задает дифференциальную ширину распада

$$\mathrm{d}\Gamma = \frac{\langle|\mathfrak{M}|^2\rangle}{2m_{\mathcal{Z}}}\mathrm{d}\mathfrak{p}_f$$

где интегрирование по фазовому объему в случае квадрата матричного элемента, который не зависит от углов, для двух безмассовых частиц в конечном состоянииумы уже вычисляли

$$\int \mathrm{d}\mathfrak{p}_f = \frac{1}{8\pi}$$

так что ширина Z -бозона при распаде на все безмассовые ароматы нейтрино pasta

$$\Gamma[\nu] = N_{[\nu]}\frac{\alpha_{\mathrm{em}}}{24\sin^2\theta_W\cos^2\theta_W}m_{\mathcal{Z}}$$

Экспериментально можно найти полную ширину Z -бозона и измерить бренчинги (относительные вероятности) распада мод, в которых нет нейтрино, а регистрируются заряженные лептоны и адроны.

Тогда недостающие каналы следует интерпретировать как распады Z -бозона на все типы легких

нейтрино. Эмпирически находят с высокой точностью $N_{[\nu]} \approx 3$, что, конечно, подтверждает гипотезу о трех поколениях лептонов.

Подчеркнем, что столь точные выводы можно было сделать только с учетом однопетлевых квантовых поправок.

В частности, значение константы электромагнитного взаимодействия $\alpha_{\text{ем}}$ необходимо было рассчитать с помощью ренормгруппы на виртуальностях, равных массе Z -бозона, где $\alpha_{\mathrm{em}}(m_{\mathcal{Z}}) \approx 1/129$, что, конечно, заметно отличается от значения постоянной тонкой структуры, которая измерена в электромагнитных переходах в атоме $\alpha_{\mathrm{em}} \approx 1/137$, где вирпуальность соответствует энергии связи электрона в атоме.

Что касается значения угла Вайнберга, то на масштабе виртуальности $m_{\mathcal{Z}}$ его вполне можно установить из отношения масс W и Z -бозонов.

1.9.4 Neutrinos

What neutrino can be?

Is the neutrino a goldstone particle? by Volkov D.V., Akulov, V.P.

1.9.5 The Higgs Boson

(????)

1.10 Mathematics and physics for particle physics

(??? add useful formulas)

1.10.1 Algebras for particles (???)

(коротко основные идеи, пока они в записи по алгебре)

1.11 Some Important Experiments

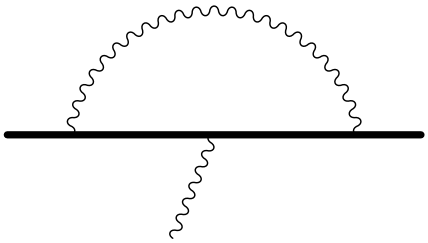
(???? write later)

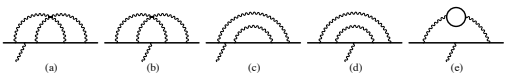
1.12 Derivation of Some Typical Properties of Some Particles

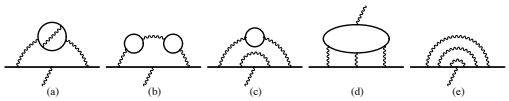
1.12.1 Muon's anomalous magnetic moment

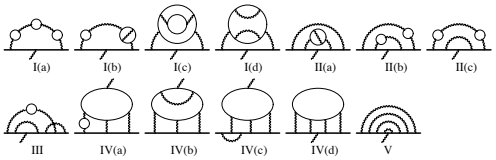
(????)

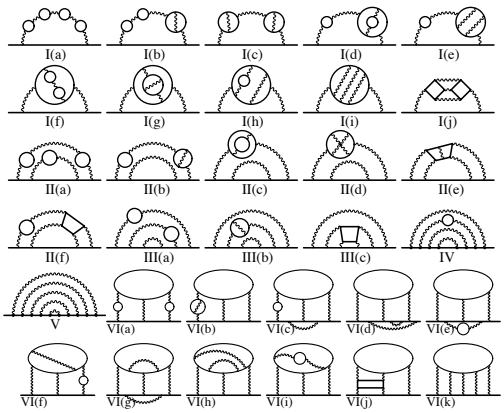
(впишу суть той статьи, тут важно додумать много!)











Part II
Particle Physics Fundamentals and Standard Model

2 General Understanding of Particles and Their Interactions

(сюда мб всего окуня выгружу потом)

2.1 QFT Templates for Particle Physics (!??!??)

(суть теории поля и КТП для этого раздела. выпишу потом мб.)

2.2 Description of Decays and Scatterings

(?? write how to do it)

2.3 α-decay

(???)

2.4 β-decay

(окей, пока тут, но вообще, подробно об этом в ядерной физике)

Это радиоактивного распада, обусловленный слабым взаимодействием и изменяющий заряд ядра на единицу без изменения массового числа.

При этом распаде ядро излучает бета-частицу (электрон или позитрон), а также нейтральную частицу с полуцелым спином (электронное антинейтрино или электронное нейтрино).

мотивация

наверное, изучая бета распад мы можем изучить слабое взаимодействие и посчитать константу ферми. интересно, как???

вкратце свойства и формулы

Бета-распад нейтрона:

$$n \to p + e^- + \bar{\nu}_e$$

Бета распад - пример слабого взаимодействия.

Матричный элемент выведен ниже и равен:

$$\begin{aligned}\mathcal{M} = (\bar{u}_{p,n.r.} u_{n,n.r.}) \cdot \left[C_S \bar{u}_e \left(1 + \alpha_S \gamma_5\right) v_{\bar{\nu}} + C_V \bar{u}_e \left(1 + \alpha_V \gamma_5\right) \gamma^0 v_{\bar{\nu}}\right] + \\ + (\bar{u}_{p,n.r.} \boldsymbol{\sigma} u_{n,n.r.}) \cdot \left[C_A \bar{u}_e \left(1 + \alpha_A \gamma_5\right) \gamma_5 \gamma v_{\bar{\nu}} + 2 C_T \bar{u}_e \left(1 + \alpha_T \gamma_5\right) \boldsymbol{\sigma} v_{\bar{\nu}}\right]\end{aligned}$$

в разрешенные фермиевские переходы могут давать вклады взаимодействия скалярного и векторного типов, а в гамов-теллеровские переходы - аксиально-векторные и тензорные взаимодействия.

Во времена установления вида гамильтониана бета-распада, для обратного бета-распада ядра ^{14}O (это распад фермиевского типа и при этом $\left|M^{(+)}_{F,nucl}\right|^2 = 2\Big)$:

$$^{14}O \to \left(\beta^+\right) \to^{14} N^*$$

были проведены аккуратные вычисления функции $f\left(Z, E_{\max}\right)$, экспериментальные измерения времени жизни и энергии $E_{\max}$, что позволило найти численную величину константы Ферми [1,3]

$$G_F^2 = \frac{1}{2} \cdot \left[|C_S|^2 \left(1 + |\alpha_S|^2\right) + |C_V|^2 \left(1 + |\alpha_V|^2\right)\right]$$

По состоянию на 60-е годы 20-го века ее принятое значение было [1] $G_F = (1.418 \pm 0.004) \cdot 10^{-49}$ эрг$\cdot$ см ^{3}; позже (80-е годы) это значение было уточнено и

$$\text{составило [3]} G_F = 1.43582(4) \cdot 10^{-49} {}^{\circ}_{\ni \mathrm{p}} \cdot \mathrm{cm}^3 = 1.6632(4) \cdot 10^{-5} \left(\Gamma_{\ni} \mathrm{B/c}^2\right)^{-2}.$$

1. Из изучения энергетического спектра электронов или позитронов для разрешенных β -распадов (графики Кюри) было установлено, что эффективный гамильтониан β - распада не зависит от энергии продуктов распада.

2. Из измерений времен жизни и электрон-нейтринной корреляции в распадах типа Ферми и Гамова-Теллера была установлена доминантность V и A взаимодействий.

3. Из опытов по измерению времен жизни ядер по отношению к бета-распаду Для фермиевских и Гамов-Теллеровских переходов, а также из измерений времени жизни нейтрона, были определены численные значения констант G_F и G_{GT}

4. Из опытов по определению поляризации электронов β-распада было установлено, что $C_i = C_i'$, то есть четность в бета-распаде не сохраняется.

5. Из опытов по определению корреляции между направлением поляризации распадающегося ядра и направлением вылета электронов было установлено, что относительный знак C_V и C_A отрицателен.

6. Уже из наблюдений, перечисленных в п.п. 1 и 2, а также в результате тонких опытов, выполненных позже, по поиску эффектов от интерференционных членов Фирца, было установлено, что нет фундаментальных S и T членов в эффективном гамильтониане β -распада.

Все это суммируется в следующем виде матричного элемента для распада нейтрона (см. [3]): $M = \frac{G_F}{\sqrt{2}} \int d^3x \bar{\psi}_p \gamma_\mu \left(1 - \lambda\gamma_5\right) \psi_n \bar{\psi}_e \gamma^\mu \left(1 - \gamma_5\right) \psi_{\bar{\nu}_e}$ где $\lambda \equiv |C_A/C_V| = 1.25$

обзор механизма распада

β^+ **распад**

β^- **распад**

K **захват**

?

«сверхразрешенные» переходы

переходы между двумя членами одного и того же изотопического мультиплета;

типирование от строковского, мб такого и нет

разрешенные

типирование от строковского, мб такого и нет

запрещенные 1-го порядка

типирование от строковского, мб такого и нет

запрещенные 2-го порядка

типирование от строковского, мб такого и нет

мотивация изучать графики Кюри

Изучение графиков Кюри для разрешенных бета-переходов атомных ядер сыграло важную роль в установлении общего вида эффективного гамильтониана слабого взаимодействия. Именно: оказалось, что графики Кюри для таких бетапереходов действительно имеют характер прямых линий, что означает независи- мость этого гамильтониана от энергии электронов.

Позднее (в $80-\mathrm{x}-90-\mathrm{x}$ годах) эти графики привлекли внимание в связи с проблемой прямой экспериментальной оценки массы нейтрино и были использованы при анализе данных о бета-распаде ядер трития. (Тритий был выбран потому, что у него величина $\mathrm{E}_{\max}$ - наименьшая из других, удобных для экспериментов, β -активных ядер.)

появление графиков Кюри

График Кюри[5] (известен также как график Ферми) — диаграмма, используемая для изучения бета-распада. Это энергетическая зависимость квадратного корня из количества излучённых бета-частиц с данной энергией, делённая на функцию Ферми. Для разрешённых (и некоторых запрещённых) бета-распадов график Кюри линеен (прямая линия, наклонённая в сторону роста энергии). Если нейтрино имеют конечную массу, то график Кюри вблизи точки пересечения с осью энергии отклоняется от линейного, благодаря чему появляется возможность измерить массу нейтрино.

(зачем они?)

Бета-распад нейтрона:

$$n \to p + e^{-} + \bar{\nu}_e$$

1.1) Рассмотрим вероятность перехода в единицу времени из начального состояния в конечное для реакции (1.1), когда электрон имеет импульс q_e в интервале dq_e. Согласно квантовой механике, она определяется квадратом матричного элемента:

$$\frac{\delta W\left(q_e\right)}{\delta t} = I\left(q_e\right) dq_e = \text{Norm } \cdot \sum | < f|H|i > |^2 \delta\left(E_f - E_i\right)$$

где $I\left(q_e\right) dq_e$ есть интенсивность испускаемого потока электронов с импульсами q_e, лежашими в интервале dq_e. Суммирование в (1.2) идет по всем конечным состояниям таким, что электрон имеет указанный импульс; подразумевается также, что по начальным спиновым состояниям нейтрона выполнено усреднение. Дельтафункция обеспечивает выполнение закона сохранения энергии; далее будем работать в приближении, когда уносимой нуклоном отдачи энергией пренебрегаем (но импульс отдачи у него есть и поэтому направления импульсов электрона и нейтрино, вообще говоря, могут быть некоррелированы). Сумму по конечным состояниям можно заменить интегралом, так как конечные состояния электрона, нейтрино и протона лежат в области непрерывного спектра; вычисления будем здесь делать в фиксированной системе отсчета - системе покоя нейтрона:

$$\frac{\delta W\left(q_e\right)}{\delta t} = I\left(q_e\right) dq_e = Norm \cdot q_e^2 dq_e \int d\Omega_e d^3 q_\nu \delta\left(E_f - E_i\right) | < f|H|i > |^2$$

Закон сохранения энергии, в нашем приближении, можно записать как

$$m_n = E_e + E_\nu + \frac{p^2}{2m_p} + m_p \approx E_e + E_\nu + m_p, \quad E_e + E_\nu \approx m_n - m_p \equiv E_{\max}$$

то есть, $E_\nu = E_{\max} - E_e$ и для безмассовых нейтрино дополнительно: $E_\nu = q_\nu$. Теперь формулу (1.3) (для безмассового нейтрино и в пренебрежении как отдачей протона, так и кулоновским взаимодействием между электроном и протоном) можно переписать как

$$\frac{\delta W(q_e)}{\delta t} = I(q_e)\, dq_e =$$
$$= N_{orm} \cdot q_e^2 dq_e \int d\Omega_e E_\nu^2 dE_\nu d\Omega_\nu \delta(E_{\max} - E_e - E_\nu) \mid < f|H|i > \mid^2$$

и после интегрирования по энергии нейтрино (где помогает δ -функция) получаем

$$I(q_e)\, dq_e = \text{Norm} \cdot q_e^2 dq_e (E_{\max} - E_e)^2 \int d\Omega_e d\Omega_\nu \mid < f|H|i > \mid^2$$

то есть, дифференциальный спектр электронов $I(q_e)$ имеет вид

$$I(q_e) = \text{Norm} \cdot q_e^2 (E_{\max} - E_e)^2 \int d\Omega_e d\Omega_\nu \mid < f|H|i > \mid^2$$

Иногда удобно анализировать подобные формулы, взяв их в такой форме, где спектр зависит от безразмерных параметров. Например, можно выразить энергии в единицах массы электрона:

$$I(\varepsilon_e) = \left(\text{Norm } \cdot m_e^4\right) \cdot \varepsilon_e \sqrt{(\varepsilon_e^2 - 1)} (\varepsilon_{\max} - \varepsilon_e)^2 \int d\Omega_e d\Omega_\nu \mid < f|H|i > \mid^2$$
$$\varepsilon_e = \frac{E_e}{m_e}, \quad \varepsilon_{\max} = \frac{E_{\max}}{m_e},$$

где использованы соотношения $q_e E_e dE_e = q_e^2 dq_e, q_e = \sqrt{E_e^2 - m_e^2}$, чтобы в выражении для энергетического спектра оставить в качестве аргумента только энергию электрона.

Если квадрат матричного элемента $\mid < f|H|i > \mid^2$ распада устроен так, что он не зависит от направления вылета электрона и нейтрино, то его можно вынести изпод знака интеграла и интегрирование по углам даст просто константу (если даже он зависит от этих направлений, но известным образом, то можно выполнить интегрирование по углам и получить некую иную константу, что дальнейшихх рассуждений принципиально не меняет). Более того: если $\mid < f|H|i > \mid^2$ не зависит также и от энергии электрона, то вся форма спектра целиком будет определяться фак- тором $q_e^2 (E_{\max} - E_e)^2$! наоборот: если форма спектра электронов соот- ветствует зависимости $q_e^2 (E_{\max} - E_e)^2$, то можно считать, что $\mid < f|H|i > \mid^2$ не зависит от энергии электрона. Чтобы узнать, так это в действительности или нет, строится график зависимости величины $\mathcal{F}(E_e) \equiv \sqrt{I(q_e)}/q_e$ от энергии электрона: т.н. график Кюри.

К обсуждению графика Кюри придется еше вернуться, но в связи с другими вопросами. Здесь же пора обсудить, как этот график выглядел бы, если бы нейтрино имело массу (малую по сравнению с массой электрона, например). Как видно из предыдущего, производная $d\mathcal{F}(E)/dE = \text{const}$ при $E \to E_{\max}$, если масса нейтрино нулевая (см. рис. 1.1).

Предположим, что масса нейтрино отлична от нуля и равна m_ν. Тогда, при сделанных ранее предположениях об отдаче нуклона, максимально возможное значение энергии электрона будет иным и равным $E'_{\max} = m_n - m_p - m_\nu \equiv E_{\max} - m_\nu$, т.е. граница спектра электронов

сдвинется (рис. 1.1). Но как будет приближаться функция $\mathcal{F}(E)$ к этой границе? Вернемся к интегралу в формуле (1.3):

$$\int d\Omega_e d\Omega_\nu q_\nu^2 dq_\nu \delta\left(E_{\max} - E_e - E_\nu\right)$$

где d^3q_ν выписан в сферических координатах. Перепишем его с заменой переменных и учетом того, что $q_\nu dq_\nu = E_\nu dE_\nu$; оставим только часть, связанную с интегрированием по энергии нейтрино:

$$\int q_\nu^2 dq_\nu \delta\left(E_{\max} - E_e - E_\nu\right) = \int q_\nu E_\nu dE_\nu \delta\left(E_{\max} - E_e - E_\nu\right) = \\ = E_\nu \sqrt{E_\nu^2 - m_\nu^2}\Big|_{E_\nu = E_{\max} - E}$$

Подставив сюда вместо $E_{\max}$ новое значение граничной энергии, а именно, $E'_{\max}$, Имеем:

$$I\left(q_e; m_\nu\right) \sim q_e^2 \left(E'_{\max} - E_e + m_\nu\right) \cdot \sqrt{\left(E'_{\max} - E_e + 2m_\nu\right)\left(E'_{\max} - E_e\right)} = \\ = q_e^2 \left(x + m_\nu\right) \sqrt{\left(x + 2m_\nu\right) x}$$

где $x = E'_{\max} - E_e$. Отсюда, производная функции $\mathcal{F}(x) \equiv \sqrt{I\left(q_e; m_\nu\right)}/q_e$ есть:

$$\frac{d\mathcal{F}(x)}{dx} \sim \frac{\left(x + m_\nu\right)^2 + x\left(x + 2m_\nu\right)}{2x^{3/4}\left(x + 2m_\nu\right)^{3/4}\left(x + m_\nu\right)^{1/2}}, \left(\lim_{x\to 0} \frac{d\mathcal{F}(x)}{dx} = \infty\right.$$

то есть, энергетический спектр электронов вблизи граничной энергии выглядит на графике Кюри примерно так, как показано на рис. 1.1.

примеры графиков Кюри

(мб вставлю, тут картинка, тип наклонная линия влево, под ней как корень зависимость становится вблизи нуля по ординате)

(пока все равно не понимаю, не вижу смысла вставлять)

матричный элемент β-распада

(мб вначало перекину, ибо это то, чем по факту мы пользуемся, скорее всего)

(тут берем теорию, которую где-то в дополнениях или здесь приведу. По сути мы стартуем с просто хз чего, если не понимать, откуда это вообще взялось?)

В 4-фермионной теории Ферми в задаче имеются 4 фермиона. Наиболее общий вид матричного элемента, удовлетворяющего требованиям лоренцинвариантности, независимости от энергии электрона 1 и сохранения CPT есть

$$\mathcal{M} = \sum_i \left\{C_i \left(\bar{u}_p \Gamma_i u_n\right)\left(\bar{u}_e \Gamma^i v_{\bar{\nu}}\right) + C'_i \left(\bar{u}_p \Gamma_i u_n\right)\left(\bar{u}_e \gamma_5 \Gamma^i v_{\bar{\nu}}\right)\right\}$$

О чем свидетельствуют графики Кюри для разрешенных β -распадов.

Здесь обозначены:

$$\Gamma_I = \left(1, \gamma_5, \gamma_\mu, \gamma_5\gamma_\mu, \sigma_{\mu\nu}\right), \text{i.e. } \Gamma_I = (S, P, V, A, T); \\ \sigma_{\mu\nu} = \tfrac{i}{2}\left(\gamma_\mu\gamma_\nu - \gamma_\nu\gamma_\mu\right)$$

где S, P, V, A, T означают, соответственно, скаляр, псевдоскаляр, вектор, аксиальный вектор (псевдовектор) и тензор по отношению к лоренцевым преобра- зованиям.

Формулу для $\mathcal{M}$ можно записать в форме (обозначения кн. Бьеркена и Дрелла [4]):

$$\mathcal{M} = \sum_i C_i \left[\bar{u}_p\left(p_p\right)\Gamma_i u_n\left(p_n\right)\right]\left\{\bar{u}_e\left(p_e\right)\left[1+\alpha_i\gamma_5\right]\Gamma^i v_{\bar{\nu}}\left(p_{\bar{\nu}}\right)\right\} + \text{h.c.}$$

где явно видно, что члены, пропорциональные $\alpha_i\gamma_5$, нарушают пространственную четность P (обозначение h.c. означает «эрмитово сопряженное выражение»).

Эрмитово-сопряженные члены матричного элемента соответствуют, например, обратному β -распаду: $p \to n + \bar{e} + \nu_e$; при этом:

$$\begin{aligned}
\bar{u}_p \ldots u_n &\to \bar{u}_n \ldots u_p \\
\bar{u}_e \ldots v_\nu &\to \bar{u}_\nu \ldots v_{\bar{e}} \\
\alpha_i &\to +\alpha_i, i = A, V \\
\alpha_i &\to -\alpha_i, i = S, P, T
\end{aligned}$$

Вспомним, что в бета-распаде нуклоны - нерелятивистские и это можно с пользой для понимания применить к нашему матричному элементу. В самом деле, возьмем нерелятивистское представление для нуклонных биспиноров:

$$u_p = \begin{pmatrix} \phi \\ \chi \end{pmatrix} \approx \begin{pmatrix} u_p^g \\ 0 \end{pmatrix}, u_p^g \equiv u_{p,n.r.}$$

Теперь комбинации $\bar{u}_p\Gamma_i u_n$ в нерелятивистском приближении и во взятом здесь представлении γ -матриц легко выписать:

$$\begin{aligned}
&\bar{u}_p \cdot \mathbf{1} \cdot u_n = \bar{u}_p^g \cdot \mathbf{1} \cdot u_n^g \equiv < 1 > \\
&\bar{u}_p \cdot \gamma_5 \cdot u_n = 0 \\
&\bar{u}_p \cdot \gamma_\mu \cdot u_n = \delta_{0\mu} \cdot u_p^{+g} u_n^g \equiv \delta_{0\mu} \cdot < 1 > \\
&\bar{u}_p \cdot \gamma_5\gamma_\mu \cdot u_n = \left\{ \begin{array}{c} 0, \mu = 0 \\ u_p^{+g}\sigma_i u_n^g \equiv < \sigma_i >, \mu = i \end{array} \right\} \\
&\bar{u}_p \cdot \sigma_{\mu\nu} \cdot u_n = \left\{ \begin{array}{c} 0, \mu = 0 \text{или } \nu = 0 \\ u_p^{+g}\sigma_k u_n^g \equiv < \sigma_k >, \mu = i, \nu = j; \quad i,j,k : \text{cycl} \end{array} \right\}
\end{aligned}$$

Остается все это подставить в формулу (1.15) и после простой выкладки полу- чить:

$$\begin{aligned}
\mathcal{M} = &\left(\bar{u}_{p,n.r.} u_{n,n.r.}\right) \cdot \left[C_S \bar{u}_e \left(1+\alpha_S\gamma_5\right) v_{\bar{\nu}} + C_V \bar{u}_e \left(1+\alpha_V\gamma_5\right)\gamma^0 v_{\bar{\nu}}\right] + \\
&+ \left(\bar{u}_{p,n.r.}\boldsymbol{\sigma} u_{n,n.r.}\right) \cdot \left[C_A \bar{u}_e \left(1+\alpha_A\gamma_5\right)\gamma_5\gamma v_{\bar{\nu}} + 2C_T \bar{u}_e \left(1+\alpha_T\gamma_5\right)\boldsymbol{\sigma} v_{\bar{\nu}}\right]
\end{aligned}$$

В итоге

$$\begin{aligned}
\mathcal{M} = &\left(\bar{u}_{p,n.r.} u_{n,n.r.}\right) \cdot \left[C_S \bar{u}_e \left(1+\alpha_S\gamma_5\right) v_{\bar{\nu}} + C_V \bar{u}_e \left(1+\alpha_V\gamma_5\right)\gamma^0 v_{\bar{\nu}}\right] + \\
&+ \left(\bar{u}_{p,n.r.}\boldsymbol{\sigma} u_{n,n.r.}\right) \cdot \left[C_A \bar{u}_e \left(1+\alpha_A\gamma_5\right)\gamma_5\gamma v_{\bar{\nu}} + 2C_T \bar{u}_e \left(1+\alpha_T\gamma_5\right)\boldsymbol{\sigma} v_{\bar{\nu}}\right]
\end{aligned}$$

Первая часть матричного элемента - по отношению к нуклонам есть истинный скаляр, т.е. здесь не меняется ни спин, ни четность P конечных состояний нуклонов (или конечных состояний ядер при их β -распаде) по отношению к начальным.

Собирая вместе выписанные в (1.30) и (1.31) вклады и учитывая вес (1.40), имеем для квадрата модуля полного матричного элемента бета-распада:

$$\begin{aligned}
|M|^2 = \frac{4E_eE_{\bar{\nu}}}{2m} \times \Big\{ &\overline{< \mathbf{1} >^2} \cdot \left[|C_S|^2 \left(1+|\alpha_S|^2\right) \times \left(1 - \beta_e \cdot \beta_{\bar{\nu}} \cos\theta_{e\bar{\nu}}\right) + \right. \\
&\left. + |C_V|^2 \left(1+|\alpha_V|^2\right) \times \left(1 + \beta_e \cdot \beta_{\bar{\nu}} \cos\theta_{e\bar{\nu}}\right)\right] + \\
&+ \overline{|<\sigma>|^2} \cdot \left[|C_A|^2 \left(1+|\alpha_A|^2\right) \times \left(1 - \frac{1}{3} \times \beta_e \cdot \beta_{\bar{\nu}} \cos\theta_{e\bar{\nu}}\right) + \right. \\
&\left. +4\,|C_T|^2 \left(1+|\alpha_T|^2\right) \times \left(1 + \frac{1}{3} \times \beta_e \cdot \beta_{\bar{\nu}} \cos\theta_{e\bar{\nu}}\right)\right] \Big\}
\end{aligned}$$

Интерференционные члены Фирца, которые явно зависят от энергии электрона, в формуле (1.41) опушены: многочисленные экспериментальные данные по н. разрешенным распадам показали, что графики Кюри для этих распадов являются прямолинейными, то есть в их матричных элементах нет зависимости от энергии электрона.

Поэтому фирцевские члены равны нулю:

$$\mathrm{Re}\left[\left(1+\alpha_{\mathrm{A}}^{*}\alpha_{\mathrm{T}}\right)\mathrm{C}_{\mathrm{A}}^{*}\mathrm{C}_{\mathrm{T}}\right]=\mathrm{Re}\left[\left(1+\alpha_{\mathrm{S}}^{*}\alpha_{\mathrm{V}}\right)\mathrm{C}_{\mathrm{S}}^{*}\mathrm{C}_{\mathrm{V}}\right]=0$$

Проинтегрировав по импульсам и углам вылета нейтрино и по азимутальному углу вылета электрона, легко получить формулу для энергетического и углового распределения интенсивности $I\left(q_e\right)$ потока электронов в бета-распаде. Ее принято записывать в виде (см. например [1,10])

$$\frac{I\left(q_e\right)}{d\cos\theta_e}=\frac{1}{4\pi^3}q_e^2\left(E_{\max}-E_e\right)^2\cdot\xi\cdot\left(1+a\beta_e\cos\theta_e\right)$$

Где

$$\xi=\frac{1}{2}\overline{\left|M_F^{\mathrm{nucl}}\right|^2}\left[\left|C_S\right|^2\left(1+\left|\alpha_S\right|^2\right)+\left|C_V\right|^2\left(1+\left|\alpha_V\right|^2\right)\right]+$$
$$+\frac{1}{6}\overline{\left|M_{GT}^{\mathrm{nucl}}\right|^2}\left[\left|C_A\right|^2\left(1+\left|\alpha_A\right|^2\right)+\left|C_T\right|^2\left(1+\left|\alpha_T\right|^2\right)\right]$$

h

$$\xi\cdot a=\frac{1}{2}\overline{\left|M_F^{nucl}\right|^2}\left[\left|C_V\right|^2\left(1+\left|\alpha_V\right|^2\right)-\left|C_S\right|^2\left(1+\left|\alpha_S\right|^2\right)\right]+$$
$$+\frac{1}{6}\overline{\left|M_{GT}^{nucl}\right|^2}\left[\left|C_T\right|^2\left(1+\left|\alpha_T\right|^2\right)-\left|C_A\right|^2\left(1+\left|\alpha_A\right|^2\right)\right]$$

Здесь вместо средних $\overline{<1>^2}$ и $\overline{|<\sigma\rangle|^2}$ введены т. н. ядерные матричные Элементы $\overline{\left|M_F^{nucl}\right|^2}$ и $\overline{\left|M_{GT}^{nucl}\right|^2}$, поскольку при рассмотрении ядерного бета-распада надо принять во внимание, что в начальном состоянии нуклоны находятся в ядре, а в конечном состоянии - либо также в ядре, либо- вылетая из него - испытывают воздействие сильного взаимодействия с ядром остатком.

Формулы (1.43)-(1.45) уже почти готовы для проведения обсуждения экспериментальных данных. Однако перед этим нужно внимательнее поглядеть на ядерные матричные элементы $\overline{\left|M_F^{\mathrm{nucl}}\right|^2}$ и $\overline{\left|M_{GT}^{\mathrm{nucl}}\right|^2}$.

переходы Ферми при β-распаде

Иными словами, если распад идет только за счет этой части матричного элемента, То и такие переходы называются переходами Ферми; здесь ΔT - величина изме- нения изоспина адрона.

Часть, отвечаюшая за переходы типа Ферми, содержит скалярное (S) и векторное (V) взаимодействия. При вычислении квадрата модуля матричного элемента возникают слагаемые типа «скаляр-скаляр» $(S-S)$, «скаляр-вектор» $(S-V)$ и «вектор-вектор» $(V-V)$. Вид $S-S$ и $V-V$ членов следующий:

$$S-S\to 4E_eE_{\bar{\nu}}\times\left(1+\left|\alpha_S\right|^2\right)\times\left(1-\frac{p_e\cdot p_{\bar{\nu}}\cos\theta_{e\bar{\nu}}}{E_eE_{\bar{\nu}}}\right)$$
$$V-V\to 4E_eE_{\bar{\nu}}\times\left(1+\left|\alpha_V\right|^2\right)\times\left(1+\frac{p_e\cdot p_{\bar{\nu}}\cos\theta_{e\bar{\nu}}}{E_eE_{\bar{\nu}}}\right)$$

где $E_e, E_{\bar{\nu}}$ и $p_e, p_{\bar{\nu}}$ -энергии и импульсы электрона и антинейтрино соответственно, $\theta_{e\bar{\nu}}$ - угол разлета электрона и антинейтрино.

Видно, что вклад скалярной части максимален, когда антинейтрино и элекгрон разлетаются в противоположные стороны (при этом вклад векторной части минимален и равен нулю), а

для вклада векторной части ситуация обратная: он максимален, когда импульсы электрона и антинейтрино направлены в одну и ту ке сторону (при этом вклад скалярной части минимален и равен нулю).

Вклад интерференционного члена $S-V$(интерференционный член Фир- ца) не зависит от угла $\theta_{e\bar{\nu}}$ и равен

$$S-V \to 2\,\mathrm{Re}\left[C_S C_V^*\left(1+\alpha_S\alpha_{\mathrm{V}}^*\right)\right]\times\left(\frac{m}{E_e}\right)$$

где m есть масса электрона. Собирая все вместе имеем для усредненного по ядерным состояниям (для распада нейтрона - по спинам нуклонов) квадрата матричного элемента для переходов типа Ферми (здесь учтено, что отношения p_e/E_e и $p_{\bar{\nu}}/E_{\bar{\nu}}$ есть не что иное, как скорости этих частиц, β_e и $\beta_{\bar{\nu}}$, т. е. $\bar{\beta}\equiv \mathrm{p}/E$)

$$\begin{aligned}2m\overline{|M_F|^2} = 4E_eE_{\bar{\nu}}\times\Big\{&\left|C_S\right|^2\left(1+\left|\alpha_S\right|^2\right)\times\left(1-\beta_e\cdot\beta_{\bar{\nu}}\cos\theta_{e\bar{\nu}}\right)+\\&+\left|C_V\right|^2\left(1+\left|\alpha_V\right|^2\right)\times\left(1+\beta_e\cdot\beta_{\bar{\nu}}\cos\theta_{e\bar{\nu}}\right)+\\&+2\,\mathrm{Re}\left[\mathrm{C_S C_V^*}\left(1+\alpha_{\mathrm{S}}\alpha_{\mathrm{V}}^*\right)\right]\times\left(\frac{\mathrm{m}}{\mathrm{E_e}}\right)\Big\}\end{aligned}$$

переходы Гамова-Теллера при β-распаде

Вторая часть матричного элемента содержит матричный элемент от оператора спина, взятый между конечным и начальным состояниями ядерной системы; это - аксиальный вектор. Он может менять спин, но не более, чем на 1. Однако, четность он не меняет. Поэтому такие переходы характеризуются правилами отбора

$$|\Delta J|=1,0;\text{переход } 0\to 0\text{запрешен };\Delta P=0,\Delta T=0,\pm 1$$

переходы этого типа называются переходами Гамова-Теллера.

Выполнив аналогичные выкладки для Гамов-Теллеровской части полного матричного элемента (в которой фигурируют аксиально-векторные (A) и тензорные (T) вклады), получим:

$$\begin{aligned}2m\overline{|M_{G-T}|^2} = 4E_eE_{\bar{\nu}}\times 3\Bigg\{&\left|C_A\right|^2\left(1+\left|\alpha_A\right|^2\right)\times\left(1-\frac{1}{3}\times\beta_e\cdot\beta_{\bar{\nu}}\cos\theta_{e\bar{\nu}}\right)+\\&+4\left|C_T\right|^2\left(1+\left|\alpha_T\right|^2\right)\times\left(1+\frac{1}{3}\times\beta_e\cdot\beta_{\bar{\nu}}\cos\theta_{e\bar{\nu}}\right)\\&+4\,\mathrm{Re}\left[\mathrm{C_A C_T^*}\left(1+\alpha_{\mathrm{A}}\alpha_{\mathrm{T}}^*\right)\right]\times\left(\frac{\mathrm{m}}{\mathrm{E_e}}\right)_{\text{зависимость от энерги|и электр}}\end{aligned}$$

Из полученных результатов видно, что электрон-антинейтринная корреляция для S и A членов такова, что антинейтрино и электрон предпочитают разлетаться В разные стороны, но в случае преобладания A -члена эта корреляция заметно слабее. Для V и T членов она такова, что эти лептоны предпочитают вылетать в одну сторону, но для T -члена она (корреляция) тоже заметно слабее, чем д,для V -члена.

Посмотрим теперь на «ядерную» часть, определяющую «веса», с которыми вклады, отвечающие за переходы Ферми и Гамова-Теллера, входят в полный квадрат модуля матричного элемента, определяющего вероятности β-распадов.

спектры при бета-распаде

правило сумм

Введем обозначения $M^{(-)}_{F,\mathrm{nucl}}\sim \mathrm{I}_+$, $\mathrm{M}^{(+)}_{\mathrm{nucl}}\sim \mathrm{I}_-$, $\mathrm{M}^{(-)}_{\mathrm{GT,nucl}}\sim \mathrm{I}_+\sigma$, $\mathrm{M}^{(+)}_{\mathrm{GT,nucl}}\sim \mathrm{I}_-\sigma$ Пользуясь коммутационными соотношениями (1.46) и считая, что ядерные состояния отвечают модели

независимых нуклонов, можно увидеть, что для фермиевских переходов справедливо следуюшее правило сумм:

$$\sum_{\text{final state}} \left(\left| M^{(-)}_{F,\text{nucl}} \right|^2 - \left| M^{(+)}_{F,\text{nucl}} \right|^2 \right) = N - Z$$

где N - число нейтронов в ядре с атомным номером A и Z - заряд этого ядра (очевидно, $A = N + Z$)

Аналогичное правило сумм можно вывести и для Гамов-Теллеровских перехо- Дов:

$$\sum_{\text{final state}} \left(\left| M^{(-)}_{GT,nucl} \right|^2 - \left| M^{(+)}_{GT,nucl} \right|^2 \right) = 3(N - Z)$$

время жизни при бета-распаде

Имея формулу

$$\frac{I(q_e)}{d\cos\theta_e} = \frac{1}{4\pi^3} q_e^2 (E_{\max} - E_e)^2 \cdot \xi \cdot (1 + a\beta_e \cos\theta_e)$$

для энергетического спектра и угловой зависимости вылета электронов от β -распада, нетрудно проинтегрировать ее по углу, чтобы получить не зависяшую от угла форму спектра (ср. с формулой (1.7)) :

$$I(q_e) = \frac{\xi}{2\pi^3} q_e^2 (E_{\max} - E_e)^2$$

и время жизни по отношению к бета-распаду:

$$\frac{1}{\tau} = \frac{\xi}{2\pi^3} \int_0^{q_{e,\max}} dq_e q_e^2 (E_{\max} - E_e)^2 = \left(\frac{m_e^5 \cdot \xi}{2\pi^3} f(q_{e,\max}) \right.$$
$$f(q_{e,\max}) = -\frac{\eta}{4} - \frac{1}{12}\eta^3 + \frac{1}{30}\eta^5 + \frac{1}{4}\sqrt{\eta^2+1} \ln\left[\eta + \sqrt{\eta^2+1}\right]$$
$$\eta = \frac{q_{e,\max}}{m_e} = \sqrt{\frac{E^2_{\max}}{m_e^2} - 1} \equiv (\beta_e \cdot \gamma_e)$$

то есть, η есть не что иное, как произведение скорости электрона (в единицах скорости света) на его релятивистский гамма-фактор.

Для справки: строго говоря, в приложении формулы (1.51) именно к ядру, следует учесть как электромагнитные поправки в ядерной части матричных элементов, так и искажение электронных волновых функций в кулоновском поле ядра (что не делалось здесь для упрошения формул), а также - некоторые другие поправки. В результате, интеграл по импульсу электрона содержит еше некоторую функцию $F(Z, E_e)$, зависяшую от заряда ядра и энергии электрона. Поэтому в книгах о бета-распаде интеграл, стояший в формуле (1.51), нормированный на комбинацию констант связи, часто записывают в иной форме (с несколько иными обозначениями, чем здесь), а именно, как

$$f(Z, E_{\max}) = \int_1^{E_{\max}} pE (E_{\max} - E) F(Z, E) dE$$

константа Ферми из бета-распада

Во времена установления вида гамильтониана бета-распада, для обратного бета-распада ядра ^{14}O (это распад фермиевского типа и при этом $\left| M^{(+)}_{F,nucl} \right|^2 = 2$) :

$$^{14}O \to \left(\beta^+\right) \to ^{14} N^*$$

были проведены аккуратные вычисления функции $f\left(Z, E_{\max}\right)$, экспериментальные измерения времени жизни и энергии $E_{\max}$, что позволило найти численную величину константы Ферми [1,3]

$$G_F^2 = \frac{1}{2} \cdot \left[|C_S|^2 \left(1 + |\alpha_S|^2\right) + |C_V|^2 \left(1 + |\alpha_V|^2\right) \right]$$

По состоянию на $60-$е годы 20-го века ее принятое значение было [1]$G_F = (1.418 \pm 0.004) \cdot 10^{-49}$ эрг·см ^{3}; позже ($80-$ е годы) это значение было уточнено и

$$\text{составило } [3] G_F = 1.43582(4) \cdot 10^{-499\text{p}} \cdot \text{cm}^3 = 1.6632(4) \cdot 10^{-5} \left(\Gamma_\ni \text{B/c}^2\right)^{-2}$$

Затем, имея в виду тот факт, что для чистого перехода типа Ферми коэффициент a, определяющий угловое распределение электронов по отношению к направлению вылета нейтрино есть

$$a = \frac{|C_V|^2 \left(1 + |\alpha_V|^2\right) - |C_S|^2 \left(1 + |\alpha_S|^2\right)}{2G_F^2}$$

экспериментаторы провели соответствующие измерения для ядер, испытывающих чисто фермиевские переходы и нашли, что они почти целиком обусловлены векторным взаимодействием. Например, для распада

$$^{35}Ar \to (\beta^+) \to ^{35} Cl$$
$$\text{оказалось, что } a = 0.97 \pm 0.14 [1].$$

Итак, измерения времени жизни для ядер, испытывающих чисто фермиевские переходы, а также измерения позитрон-нейтринной корреляции, дали возможность определить константу взаимодействия и установить векторный характер фермиевской части гамильтониана слабого взаимодействия:

$$G_F = \frac{1}{\sqrt{2}} \sqrt{|C_V|^2 \left(1 + |\alpha_V|^2\right)}$$

Аналогично, из экспериментальных исследований электрон-нейтринных корреляций для Гамов-Теллеровских переходов было установлено, что за такие чистые переходы почти целиком отвечает аксиально-векторное взаимодействие.

Затем, хорошо определив полные вероятности фермиевских распадов ядер типа ^{14}O, ^{10}C и т. д. (для которых можно достаточно точно рассчитать ядерные матричные элементы) а также измерив время жизни нейтрона (которое определяется комбинацией $G_F^2 + 3G_{GT}^2$), экспериментаторы определили величину отношения

$$\frac{G_F^2 + 3G_{GT}^2}{2G_F^2} \to \frac{G_{GT}^2}{G_F^2}$$

(Об этом довольно подробно рассказано в кн. [1]). Все это позволило установить, что

$$\lambda \equiv \left| \frac{C_A}{C_V} \right| \approx 1.25$$

причем отличие величины λ от 1 вызвано эффектами сильного взаимодействия (подробнее см. в кн. [3]); надо также иметь в виду, что все, непосредственно определяемые из эксперимента константы, являются перенормированными.

угловые распределения при бета-распаде

учет поляризаций электронов

как-то там усреднение можно сделать, написано слишком фигово, чтобы я пробовал это переписать.

Следующий цикл опытов по установлению вида гамильтониана слабого взаимодействия был связан с измерениями поляризации электронов в бета-распадах как чисто фермиевского, так и чисто Гамов-Теллеровского типов. Это было необходимо для ответа на вопрос, какова величина коэффициентов α_i в формуле (1.15). Оказалось, что в разрешенных β -распадах спиральность электрона равна $-1(v/c)$ а спиральность позитронов равна $+1(v/c)$; измерения электрон-нейтринных угловых корреляций позволили установить, что спиральность электронного нейтрино равна -1, а спиральность соответствующего антинейтрино равна $+1$. Все это вопервых, говорит о том, что коэффициенты C_i и C_i' для V и A членов в (1.13) равны и, во-вторых, что константы связи для скалярного и тензорного членов малы По абсолютной величине (см. [2] и [11]): $\frac{C_S}{C_V} = -0.001 \pm 0.006$, $\frac{C_T}{C_A} = -0.0004 \pm 0.0003$ Таким образом, указаний на присутствие фундаментальных S и T взаимодействий в гамильтониане бета-распада нет. Однако, это не означает, что в характеристиках тех или иных конкретных реакций нет характерных для них проявлений: они встречаются и своим появлением обязаны т. н. индуцированным взаимодействиям (псевдоскалярному и пр.).

Ответ на вопрос о том, какова относительная фаза между константами C_V и C_A, был найден в экспериментах по бета-распаду поляризованных ядер. Оказалось (см. [1]), что достаточно измерять корреляцию между направлением вылета электрона и направлением поляризации распадаюшегося ядра. Было установлено, что эта относительная фаза равна π, то есть относительный знак между константами C_V и C_A равен -1.

Главный итог этих исследований суммируется в простой формуле: взаимодействие, ответственное за бета-распад, имеет $V - A$ характер.

сохранение векторного тока при бета-распаде

Если посмотреть внимательно на форму матричного элемента β -распада для векторной части взаимодействия (1.69), то можно заметить ее большое сходство с электромагнитной вершиной протона (см. [4]); отличие лишь в том, что последняя не меняет электрический заряд адрона (3-ю компоненту изоспина), а векторная часть слабого тока - меняет:

$$\frac{G}{\sqrt{2}}\bar{\psi}_p\gamma_\mu\psi_n = \frac{G}{\sqrt{2}}\bar{\Psi}\gamma_\mu\tau_+\Psi$$

где Ψ - волновая функция нуклона, оператор изоспина обозначен как τ и для изоспиноров есть не что иное, как матрицы Паули, действующие в изоспиновом пространстве. Соответственно, τ_+ есть не что иное, как повышающий оператор изоспина (см. формулы 1.46) :

$$\tau_+ = \frac{1}{2}(\tau_1 + i\tau_2)$$

Итак, идея Герштейна и Зельдовича состояла в том, что векторный ток в β - распаде может быть получен из электромагнитного тока поворотом в изотопическом пространстве, то есть - из изовекторной части обычного электромагнитного тока:

$$j_\mu^3 \to j_\mu^+ = \frac{G}{e\sqrt{2}}\left(j_\mu^1 + ij_\mu^2\right)$$

Поскольку электромагнитный ток сохраняется, то и слабый векторный ток Должен также сохраняться:

$$q^\mu j_\mu^+ = 0$$

где q^μ - разность 4-импульсов начального и конечного адронов. Иными словами: «лептонный ток $\bar{\psi}_e \gamma_\mu (1-\gamma_5) \psi_\nu$ взаимодействует с «повышаюшей» компонентой сохраняюшегося изотопического тока, который, по аналогии с электродинамикой, рассматривают как ток перехода» [4]. Эта идея впервые связала электромагнитные явления с явлениями, происходящими за счет слабого взаимодействия (его векторной части) и позднее блестяпе подтвердилась. Она позволила также связать возникающие в теории слабого взаимодействия формфакторы (их появление обусловлено конечностью размеров адронов и их составной природой) с электромагнитными формфакторами адронов (см. также [2]). Гипотеза о сохранении слабого векторного тока в англоязычной Гипс крашее литературе сокрашенно обозначается как CVC-гипотеза (в русскоязычной встречается и такое обозначение, и аббревиатура «СВТ-гипотеза»).

Роль волновых функций начального и конечного состояний

Вернемся к вопросам, рассмотренным в связи с графиком Кюри. Как уже обсуждалось, проинтегрировав по углу вылета электрона, получим энергетический спектр:

$$I(q_e) = \frac{\xi}{2\pi^3} \cdot q_e^2 (E_{\max} - E_e)^2$$

вид которого уже знаком, а выполнив еше одно интегрирование, получим полное обратное время жизни по отношению к этому распаду:

$$\frac{1}{\tau} = \frac{\xi}{2\pi^3} \cdot \int_0^{q_{\max}} dq_e q_e^2 (E_{\max} - E_e)^2$$

Вообше говоря, применяя всю эту феноменологию именно к ядру (достаточно сложному), необходимо было бы учесть искажение волновых функций электрона кулоновским полем ядра (что не учитывалось при выводе предыдущих формул), электромагнитные поправки в ядерной части матричного элемента (где используются волновые функции нуклонов) и т.п.

Как результат таких поправок, под интегралом по q_e появляется, как дополнительный множитель, некоторая дополнительная функция $F(Z, E_e)$, которая зависит от заряда ядра и энергии электрона. Эта функция называется функцией Ферми; она табулируется. Поэтому в теории ядерного бета-распада интеграл в (1.100) записывают в форме

$$f(Z, E_{\max}) = \int_0^{q_{\max}} q_e E_e (E_{\max} - E_e) F(Z, E_e) dE_e$$

Второе обстоятельство этого же плана: даже если пренебречь кулоновскими эффектами, волновые функции нуклонов (начального и конечного состояний) можно считать свободными только д,ля распада нейтрона (или обратного бетараспада протона) в пустоте. При анализе β -распада ядер нужно использовать нуклонные волновые функции из полных волновых функций начальных и конечных ядер! Качественные следствия:

β -распад в среде (полная вероятность, энергетический спектр и прочие характеристики) при β -распаде ядер или адронов в среде могут, в принципе, отличаться от аналогичных характеристик распада в пустоте. β -распад одного и того же ядра (полная вероятность, энергетический спектр и прочие характеристики) при его распаде в составе нейтрального

атома может, в принципе, отличаться характеристик его распада, когда атом полностью ионизован.

Происходит это из-за изменения электронных волновых функций и величины гоступного фазового объема для электрона конечного состояния. Яркий пример тому дается в следуюшем параграфе.

Бета распад в сверхсильных внешних полях

.

Внешнее магнитное поле существенно изменяет характер движения заряженных частиц. Это должно сказаться на структуре фазового пространства (не все области его становятся равнодоступными для электрона конечного состояния), и тем самым должно оказать влияние на характеристики бета-распада (см. книгу [6] а также обзор [7]). Кроме того, внешнее магнитное поле создает в пространстве выделенное направление, что должно сказаться и на спиновой структуре распада. Как показали расчеты (см. [6]), это действительно происходит. Квантующие свойства магнитного поля приводят к резонансному характеру спектра электронов от бета-распада (потому, что электрон после распада может оказаться на Плоской замкнутой орбите врашения в магнитном поле). В полях с напряженностью, близкой к H_c, средний радиус $< R >$ орбиты можно оценить как

$$< R^2 >= (2n+1)\frac{H}{H_c}\left(\frac{\hbar}{m_e c}\right)^2$$

где n главное квантовое число, и при $n = 0, H = H_c$ имеем $R \approx \hbar/(m_e c)$. Энергетический спектр становится сушественно нелинейным:

$$E = mc^2\sqrt{\left(1 + 2n\frac{H}{H_c}\right)}$$

когда $p_z = 0$, причем в "основном" состоянии ($n = 0$) спин электрона ориентирован строго против направления магнитного поля.

(чет тут происходит, я хз вообще)

2.5 Weak Interactions

(main part about it!!)

(???? I unfortunately forgot, there did I take this theory???)

обзор слабого взаимодействия

Характерной особенностью слабого взаимодействия от более сильных - сильного и электромагнитного - является то, что оно нарушает целый ряд законов сохранения: пространственной четности P, зарядовой четности C, комбинированной четности CP, странности, чарма и т. Д.

Другой характерной чертой слабого взаимодействия, которая н обусловлено его название "слабое", является то, что процессы, инициированные им, протекают медленнее, чем сильные и электромагнитные, имеют меньшие вероятности.

Следует подчеркнуть, однако, что слабое взаимодействие действительно слабо лишь при сравнительно низких энергиях взаимодействующих частиц.

При энергиях же сталкивающихся частиц, превышающих же порядка слабое взаимодействие становится даже несколько Сильнее электромагнитного.

В 1960х годах была построена единая теория электромагнитного взаимодействий, которая получила замечательные экспериментальные подтверждения в 1970х-1980х годах.

1.

Классическая теория бета распада

.

Четырехфермионное взаимодействие

.

Экспериментальные данные для установления структуры эффективного гамильтониана

V A теория

CBT

Поскольку электромагнитный ток сохраняется, то и слабый векторный ток Должен также сохраняться:

$$q^{\mu} j_{\mu}^{+} = 0$$

где q^{μ} - разность 4-импульсов начального и конечного адронов. Иными словами: «лептонный ток $\bar{\psi}_e \gamma_\mu (1 - \gamma_5) \psi_\nu$ взаимодействует с «повышаюшей» компонентой сохраняюшегося изотопического тока, который, по аналогии с электродинамикой, рассматривают как ток перехода» [4]. Эта идея впервые связала электромагнитные явления с явлениями, происходящими за счет слабого взаимодействия (его векторной части) и позднее блестяпе подтвердилась. Она позволила также связать возникающие в теории слабого взаимодействия формфакторы (их появление обусловлено конечностью размеров адронов и их составной природой) с электромагнитными формфакторами адронов (см. также [2]). Гипотеза о сохранении слабого векторного тока в англоязычной Гипс крашее литературе сокрашенно обозначается как CVC-гипотеза (в русскоязычной встречается и такое обозначение, и аббревиатура «CBT-гипотеза»).

ЧСАТ

Вернемся к распаду пиона на лептоны и запишем соответствующий матричный элемент в форме [10]:

$$< 0 \left| J_A^{\alpha} \right| \pi > \sim \frac{q^{\alpha}}{(2\pi)^3/2} F_{\pi} \left(m_{\pi}^2 \right)$$

где J_A^{α} - псевдовекторная часть адронного тока, α - обычный индекс 4-мерных векторов, $F_{\pi}\left(q^2\right)$ - пионный формфактор (который для распада пиона нужно брать при $q^2 = m_{\pi}^2$), определяющий время жизни пиона. Величину $F_{\pi}\left(q^2 = m_{\pi}^2\right)$ можно связать с пион-нуклонной константой связи (см. например в [4]).

Если бы аксиально-векторный ток сохранялся (как сохраняется слабый векторный ток), то было бы верно соотношение

$$q_{\alpha} J_A^{\alpha} \sim \frac{m_{\pi}^2}{(2\pi)^3/2} F_{\pi} \left(m_{\pi}^2 \right) = 0$$

то есть, константа $F_{\pi}\left(q^2 = m_{\pi}^2\right)$ должна была бы быть равной нулю, что означает, что пион был бы стабильным!

Конечность времени жизни пиона по отношению к распаду на мюон (или электрон) и нейтрино означает, т. о., что аксиально-векторный ток не может сохраняться при ненулевой массе пиона; однако, он мог бы сохраняться, например, в пределе безмассового пиона (когда $m_{\pi}^2 = 0$).

Если принять гипотезу о том, что аксиально-векторный ток строго сохраняется только в пределе нулевой массы пиона (или нуклона, или при одновременном стремлении к нулю и

массы нуклона, и массы пиона), но при конечной (но малой) величине q^2 пропорциональна, например, пионному полю, то (в координатном представлении): где $\varphi(x)$ - пионное поле в точке x, что оказывается возможным получить упомянутую выше связь между константами аксиально-векторной связи, массой пиона и пион-нуклонной константой связи для сильного взаимодействия. Соответствующая формула называется соотношением Гольдбергера-Треймана. Вначале она была получена методами дисперсионных соотношений, а затем - в рамках гипотезы ЧСАТ.

Гипотеза о частичном сохранении слабого аксиально-векторного тока в англоязычной литературе сокрашенно обозначается как PCAC-гипотеза (в русскоязычной встречается и такое обозначение, и аббревиатура «ЧСАТ-гипотеза»).

структура лагранжиана слабого взаимодействия

Почти одновременно с «ноябрьской революцией» 1974 года, когда было открыто новое квантовое число чарма и очарованные частицы, были открыты и нейтральные токи, а вскоре было понято, как можно построить перенормированную калибровочно-инвариантную теорию поля и была реанимирована старая идея Вайнберга о способе объединения электромагнитного и слабого взаимодействия, что оформилось в современной электрослабой теории Вайнберга-Салама.

Многое из того понимания, что до этого времени было достигнуто, сохранилось в новой теории, многое изменилось в свете новых представлений. Современное состояние физики слабых взаимодействий и сама электрослабая теория рассматривается в других курсах. Поэтому здесь остановимся только на отдельных аспектах современного понимания физики слабых взаимодействий. В этой вводной части следуем книге.Л.Б.Окуня [5]. - Общий вид лагранжиана:

$$\mathcal{L}^W = \mathcal{L}^{ch}(x) + \mathcal{L}^{\text{neutr}}(x)$$

- Взаимодействие заряженных токов:

$$\mathcal{L}^{ch}(x) = \frac{G}{\sqrt{2}} j^{\alpha+}(x) j_\alpha(x)$$

Заряженный ток $j^\alpha(x)$ уменьшает заряд частиц на единицу. Эрмитово сопряженный ток $j^{\alpha+}(x)$ увеличивает заряд на единицу. - Взаимодействие нейтральных токов:

$$\mathcal{L}^{\text{neutr}}(x) = \frac{G\rho}{\sqrt{2}} j^{0+}(x) j_0(x)$$

Нейтральный ток $j^0(x)$ не меняет заряд. Множитель ρ в единой электрослабой теории равен 1. Множитель $1/\sqrt{2}$ - по традиции. Константа G размерная, ее величина

$$G \approx \frac{10^{-5}}{m_p^2}$$

Токи взаимодействуют локально; константа G для разных токов - одна и та же (универсальное слабое взаимодействие).

Заряженные токи всегда левые

Всегда, когда из опыта удавалось выяснить пространственно-временную структуру заряженных токов, она имела вид

$$\overline{\text{final}}\, \mathcal{O}_\alpha^L \text{init}\ , \mathcal{O}_\alpha^L = \gamma_\alpha (1 + \gamma_5)\,,$$

(то есть, в ур. (1.84) имеем разность векторного ($V \sim \gamma_\alpha$) и аксиально-векторного ($A \sim \gamma_5\gamma_\alpha$) операторов), или:

$$\mathcal{O}_\alpha^L = \gamma_\alpha\left(1+\gamma_5\right) = \frac{1}{2}\left(1-\gamma_5\right)\gamma_\alpha\left(1+\gamma_5\right)$$

то есть,

$$\overline{\text{final}}\,\mathcal{O}_\alpha^L\text{init} \;= 2\overline{\text{final}}_{\;L}\gamma_\alpha\text{init}_{\;L},$$

где индекс L указывает на то, что в этот ток входят только левые компоненты биспиноров (далее вместо final, init пипем просто f, i) :

$$\bar{f}_L = \bar{f}\cdot\frac{1}{2}\left(1-\gamma_5\right)$$
$$i_l = \frac{1}{2}\left(1+\gamma_5\right)\cdot i$$

Если записать все это в терминах "малых"и "больших" компонент, то:

$$\psi = \begin{pmatrix}\phi\\ \chi\end{pmatrix}, \chi = \frac{\sigma\mathrm{p}}{E+m}\phi, \quad \psi_L = \frac{1}{2}\left(1+\gamma_5\right)\psi \to \frac{1}{2}\begin{pmatrix}\phi-\chi\\ \chi-\phi\end{pmatrix}$$

Теперь в явном виде посмотрим на $\phi-\chi$:

$$\phi-\chi = \left(1-\frac{\sigma\mathbf{p}}{E+m}\right)\phi$$

что в ультрарелятивистском пределе есть:

$$\phi-\chi \approx (1-\sigma\mathbf{n})\phi; \mathbf{n}\equiv\frac{\mathbf{p}}{|\mathbf{p}|}; \phi-\chi\approx\left(1-\sigma_z\right)\phi = \begin{pmatrix}0&0\\0&1\end{pmatrix}\phi$$

если ось Z направлена вдоль импульса частицы. Отсюда видно, что если $\phi =$

$$\begin{pmatrix}1\\0\end{pmatrix}, \text{то } \psi_L = 0, \text{если же } \phi = \begin{pmatrix}0\\1\end{pmatrix}, \text{то } \psi_L = \phi$$

Птак, в заряженном токе участвуют только левые компоненты биспиноровых операторов. В пределе скоростей частиц, стремяшихся к скорости света, в заряженный ток входят только частицы с левыми спиральностями и античастиIы с правыми спиральностями.

Образно говоря, слабые токи, меняющие заряд, есть заряженные левовинтовые токи.

Нейтральные токи

Их искали долго! Нашли только в 1974 году. Это была пара тройка событий, зарегистрированных в в пузырьковой камере в ЦЕРН.

(Кстати, это пример того, когда даже единичное, но однозначно интерпретируемое событие, имеет ценность, т.е. не всегда столь важно, велика ли статистическая выборка. . .)

Сегодня нейтральные токи уже не столько предмет исследования, сколько инструмент для изучения других явлений и объектов.

Как известно, из унитарности S матрицы следует, что если есть неупругие п роцессы, то непременно должно существовать упругое рассеяние. Но т огда должно существовать и упругое рассеяние нейтрино на адроне (например, протоне); такое рассеяние обеспечить за счёт заряженных т оков практически невозможно (соответствующие диаграммы в низшем порядке теории возмущений отсутствуют).

Уже поэтому нейтральные токи должны были бы существовать!

Вот почем у было приложено так много усилий для поиска реакций, обусловленных нейтральными токами!

В общем виде, структура нейтрального тока имеет вид:

$$j^0_\alpha = \sum_i \left(g^i_L \bar{\psi}_i \mathcal{O}^L_\alpha \psi_i + g^i_R \bar{\psi}_i \mathcal{O}^R_\alpha \psi_i \right), i = \nu_e, \nu_\mu, \nu_\tau, e, \mu, \tau, u, c, t, d, s, b;$$
$$\mathcal{O}^L_\alpha = \gamma_\alpha \left(1 + \gamma_5\right), \quad \mathcal{O}^R_\alpha = \gamma_\alpha \left(1 - \gamma_5\right)$$

g^i_L, g^i_R - численные коэффициенты, которые в электрослабой теории определяются зарядами частиц:

$$g^i_L = \frac{1}{2}, g^i_R = 0, \quad i = \nu_e, \nu_\mu, \nu_\tau$$
$$g^i_L = -\frac{1}{2} + \xi, \quad g^i_R = \xi, \quad i = e, \mu, \tau$$
$$g^i_L = \frac{1}{2} - \frac{2}{3}\xi, \quad g^i_R = -\frac{2}{3}\xi, \quad i = u, c, t$$
$$g^i_L = -\frac{1}{2} + \frac{1}{3}\xi, \quad g^i_R = \frac{1}{3}\xi, \quad i = d, s, b$$
$$\xi = \sin^2 \theta_W$$

где θ_W - угол Вайнберга. Численно, фактор ξ около $0.2 \div 0.25$. Итак: нейтральные токи содержат как левые, так и правые компоненты биспиноров. Образно говоря, они связывают "левый" и "правый" миры. (См. также [3]).)

3 Physics of Hadrons

(?????????? there are a lot of theory, I'll write later)

4 Particles by Tong

Recommended Books and Resources

There are a number of textbooks and semi-popular books that hit roughly the right level. First the semi-popular:

- Tini Veltman, "Facts and Mysteries in Elementary Particle Physics"

A straightforward book describing the essentials of the particle physics with some historical anecdotes thrown in for colour. Veltman won the Nobel prize with Gerard 't Hooft for demonstrating the renormalisability of the Standard Model.

- Abraham Pais, "Inward Bound"

A spectacularly detailed book, covering discoveries in particle physics throughout the 20^{th} century by a scientist who had a ringside seat for many of the key developments. Pais was no slouch as a physicist, providing important classification schemes for particles, naming both "baryons" and "leptons" and, with Gell-Mann, the first to understand the mixing of neutral kaons. On the flip side, he also coined the wildly inappropriately modest name "The Standard Model". (And he didn't even capitalise it.)

- Leon Lederman, "The God Particle"

To get anything out of this book you first have to get past the appalling title and then past the grating voice in which every story is buried neck deep in wisecracks, delivered with the all the subtlety of a dinner party bore after a line of cocaine. Still, given that Lederman is one of the great experimental particle physicists of the past century, it is sometimes worth the effort.

If you want more mathematical meat, then there are a few books that require a knowledge of quantum mechanics but fall short of using the full machinery of quantum field theory. Two good ones are:

- Halzen and Martin, "Quarks and Leptons"
- David Griffiths, "Introduction to Elementary Particles"

4.1 1 Introduction

The purpose of these lectures is to address one of the oldest questions in science: what are we made of? What are the fundamental building blocks of the universe from which you, me, and everything else are constructed?

In the twentieth century, progress in addressing this question was nothing short of spectacular. By the time the dust had settled, we were left with a remarkably simple picture: every experiment that we've ever performed can be explained in terms of a collection of particles interacting through a handful of forces. The theory which ties all of this together is the pinnacle of 350 years of scientific endeavour. It is, by any measure, the most successful scientific theory of all time. Yet we give it a rubbish name: it is called the Standard Model.

These lectures have two, intertwined narratives. The main thread describes the contents and structure of the Standard Model. The language in which the Standard Model is written is known as quantum field theory, and much of our initial focus will be on describing this framework, and the way it forces upon us certain inescapable facts about the universe. As we proceed, the emphasis will be on the key theoretical ideas that underpin the Standard Model and more detailed descriptions of the particles and the forces that make up our world.

Many of the ideas that we will meet are abstract and counterintuitive and they took physicists many decades to understand. It is striking that, at nearly every step, what ultimately lead physicists in the right direction was experiment. Sometimes these experiments simply confirmed that theorists were on the right path, but more often they came as a surprise, forcing physicists in entirely new directions.

The second thread of these lectures is to describe these experimental advances, and attempt to connect them to the more theoretical ideas. With this goal in mind, each chapter ends with an accompanying "Interlude" in which we take a more historical tour through the subject, describing some of the key experimental results, along with some of the confusions that plagued the physicists of the time.

Finally, it is clear that the Standard Model is not the last word, and we will see what questions it fails to answer. In the last section we raise some of the outstanding open problems and speculate a little on what lies beyond.

In the remainder of this extended introduction, we will give a whirlwind tour of the Standard Model, painting the big picture by omitting many many details. As these
lectures progress, we will fill in the gaps. Much of the theory sits on an excellent footing, in the sense that we now know that some aspects of the laws of physics could not be any different: many details are forced upon us by mathematical consistency alone. In contrast, other parts of the theory remain mysterious and it is unclear why the world appears one way, rather than another.

The Structure of the Atom

Before our forefathers understood atoms, or nuclei, or elementary particles, they understood chemistry. And this is where our story starts.

Our modern, scientific understanding of the structure of matter begins with the chemist John Dalton and his "law of multiple proportions". This is the observation that, when mixing elements together to form different compounds, you should do so in integer amounts. So, for example, you can combine carbon and oxygen to form one type of gas, but it you want to make a different type of gas then you need exactly double the amount of oxygen.

That's surprising. It's not, for example, what happens when you bake. If you've discovered the perfect recipe for sourdough, then you don't double the amount of flour and suddenly find that you've got bread for a bagel. That's not the way things work. Dalton understood the importance of his observation which he interpreted, correctly, as evidence for the old ideas of Leucippus and Democritus who argued that matter is made of indivisible objects called atoms.

These days, the idea of atoms is sewn into the names that we give to the gases. Add carbon and oxygen in equal measure and you get carbon monoxide CO. Double the oxygen and you get carbon dioxide CO_2. But there's no such thing as $CO_{\sqrt{2}}$ because you can't have $\sqrt{2}$ oxygen atoms attached to each carbon atom.

A fuller picture came with Mendelev's arrangement of the elements in the pattern known as the periodic table. In 1867, he placed the elements in (roughly) order of their mass, grouped together based on their observed properties. Mendelev realised that the gaps in his table were opportunities, rather than flaws: they were elements that were yet to be discovered. In this way, he predicted the existence of germanium, gallium and scandium. It would not be the last time that a theorist was able to predict the existence of a new, seemingly fundamental, particle.

From the perspective of a chemist, the periodic table is important because it places elements in groups with similar behaviour. Those elements on the left of the table go fizz when you put them in water. Those on the right don't. However, from the perspective

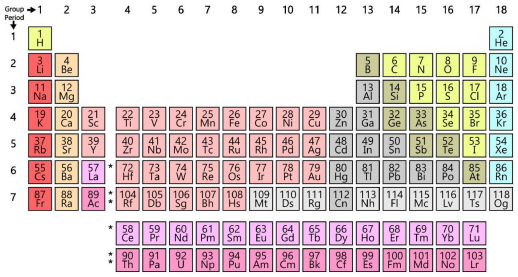


Figure 1. The periodic table of elements. (Image from Wikipedia.) We can now do better.

of fundamental physics, the importance of the periodic table can be found in the clues it gives us for what lies beneath. By Mendelev's time, it had long been understood that elements are made of atoms. The name atom was optimistically derived from the Greek "atomos", meaning "indivisible". The order in the periodic table suggests a structure to the atoms. The elements are labelled by two numbers. The atomic number Z is an integer and tells where the atom sits in the table. The atomic weight A tells us the mass of the atom and, for the first few elements in the table, is very close to an integer. We now know that both of these numbers have their origin in the fact that atoms are very much divisible.

Concrete progress came in 1897 when JJ Thomson discovered the particle that we now call the electron. He announced the discovery to a stunned lecture room at the Royal Institution in London. Thomson later recalled that one of the distinguished scientists in the audience told him that he thought the whole thing was a hoax.

It took another 35 years to unravel the full structure of the atom, with much of the work done by Ernest Rutherford and his colleagues. By the time the dust had settled, it was clear that each atom consists of a nucleus, surrounded by a somewhat blurry cloud of electrons. The nucleus itself is comprised of two further particles, the proton and neutron. The atomic number Z counts the number of protons in the nucleus; the atomic weight A counts (roughly) the combined number of protons and neutrons.

The electrons carry electric charge. By convention, the charge is taken to be negative, an annoying choice that you can blame on Benjamin Franklin, one of the founding fathers of the US. The protons carry positive charge. The neutrons are, as their name suggests, neutral. Remarkably, but importantly, the magnitude of the charge of the proton is exactly the same as the electron; they differ only in sign. Atoms contain an equal number of electrons and protons and so are themselves neutral.

The nucleus sits at the heart of the atom, but is tiny in comparison. Atoms have a typical size of 10^{-10} m, while the nuclei have a typical size of 10^{-15} to 10^{-14} m. Rutherford himself used the analogy of a fly in the centre of a cathedral. Despite its small size, the nucleus contains nearly all the mass of the atom. This is because the protons and neutrons are much heavier than the electron. We will learn more about the properties of particles later, but for now we'll just mention that the mass of the electron is

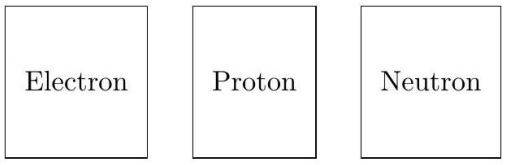
$$m_{\text{electron}} \approx 9.1 \times 10^{-31} \text{ kg}$$

(The kilogram is a useful unit when weighing humans. Less so for elementary particles. We'll meet a better unit shortly.) Both the proton and neutron are roughly 2000 times heavier. Or, more accurately,

$$\begin{aligned} m_{\text{proton}} &\approx 1837 m_{\text{electron}} \\ m_{\text{neutron}} &\approx 1839 m_{\text{electron}} \end{aligned}$$

The fact that the masses of the proton and neutron are so close remains something of a mystery. As we will later see, it is related to the fact that two smaller particles called quarks have almost negligible masses but this, in turn, is not something that we can explain from more fundamental arguments. Nonetheless, the approximate equality $m_{\text{proton}} \approx m_{\text{neutron}}$ is important and is the reason that the atomic weights A are so close to integers for the light elements. For now, these numbers simply tell us that the electrons contribute less than 0.1% of the mass of an atom.

The story above paints a much simpler picture of the structure of matter than that proposed by Mendelev. At the fundamental level, the complicated periodic table can be replaced by something significantly simpler. It would appear that we need just three particles to explain the elements. They are:



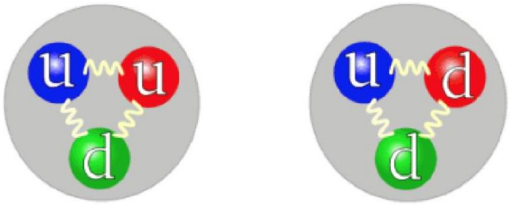


Figure 2. The proton, shown on the left, contains two up quarks and a down quark. The neutron, shown on the right, contains two down and an up.

Sadly physicists had less than 100 days to enjoy this simple picture! The neutron was the last of the three particles to be discovered. That happened in May 1932. In August of the same year, anti-matter was found and subsequent discoveries then came thick and fast. We now know that the sub-atomic world contains many riches beyond the three obvious particles that can be found in atoms.

The Structure of the Structure of the Atom

The history of how we understood the structure of matter is long, complicated and confusing and will be told in part as these lectures progress. But, at first blush, the end result seems to be not much more complicated than that of the rosy picture that scientists had in early 1932. For all we can tell, the electron remains as a fundamental particle. In contrast, neither the proton nor the neutron are fundamental. Each contains smaller particles known as quarks. A cartoon version (we'll do better later) says that the proton and neutron each consist of three quarks that, in turn, come in two different varieties. They are called the up quark and the down quark. The names are not particularly evocative: there is nothing "up" nor "down" about either of the quarks.

The proton contains two up quarks and a down quark, while the neutron contains two down quarks and an up. Both quarks have fractional electric charge. In units in which the electron has charge -1 , the up quark has charge $+\frac{2}{3}$ and the down quark charge $-\frac{1}{3}$. This then gives the familiar charges of the proton ($\frac{2}{3}+\frac{2}{3}-\frac{1}{3}=+1$) and the neutron $\left(-\frac{1}{3}-\frac{1}{3}+\frac{2}{3}=0\right)$.

In addition, there is a further, neutral particle called the neutrino. This is not one of the building blocks from which we're made but, as we shall see, has an important role to play in the universe. The neutrino carries no electric charge and is much lighter than all the other particles. It is usually introduced with the epithet "elusive": it barely
interacts and can travel through a lightyear of lead with only a 50% chance of hitting anything.

This, then, leaves us with our new periodic table, a world with just four particles:

Electron	Down Quark	Up Quark	Neutrino

One might have thought this was a good place to stop. However, at this stage, something strange happens. For reasons that we don't understand, Nature chose to take this pattern of four particles and repeat it twice over. The total number of particles of this type that we know about in the Universe isn't 4, but 12 .

In addition to the electron, there are two further particles. They behave like the electron in every possible way. For example, they have the same electric charge and, as we will see later, the same interactions with other forces. The only way in which they differ from the electron is that they're heavier. They are called the muon and the tau (pronounced to rhyme with "now"). They have masses

$$m_{\text{muon}} \approx 207 m_{\text{electron}}$$
$$m_{\text{tau}} \approx 3483 m_{\text{electron}}$$

Similarly, there are two extra neutrinos and four extra quarks. The neutrinos inherit their name from the corresponding electron-like particle: we talk of "electron neutrinos" and "muon neutrinos" and "tau neutrinos". The quarks in the second group are called strange and charm. There was a brief time when physicists toyed with the idea of naming the third group of quarks beauty and truth. The latter was subsequently rejected out of a well-placed sense of embarrassment, but the names that remain in their place, bottom and top, are astonishingly dull [1]. This, then, is the final pattern of particles that we find ourselves with:

Electron 1	Down Quark 9	Up Quark 4	Electron Neutrino ~10^{-6}
Muon 207	Strange Quark 186	Charm Quark 2495	Muon Neutrino ~10^{-6}
Tau 3483	Bottom Quark 8180	Top Quark 340,000	Tau Neutrino ~10^{-6}

The numbers in the table are the masses of the particles, written as multiples of the electron mass. (Hence the electron itself is assigned mass 1.) The masses of the neutrinos are known to be very small but, otherwise are only constrained within a window and not yet established individually.

Each horizontal line of this diagram is called a generation. Hence, each generation consists of an electron-like particle, two quarks, and a neutrino. The statement that each generation behaves the same means that, among other things, the electric charges of all electron-like particles in the first column are -1 (in appropriate units); the electric charges of all quarks in the second column are $-\frac{1}{3}$ and all those in the third column $+\frac{2}{3}$. All neutrinos are electrically neutral.

We understand aspects of this horizontal pattern very well. In particular, various mathematical consistency conditions tell us that the particles must come in a collective of four particles, and their properties are largely fixed. In particular, we understand why the particles have the electric charges that they do: this is forced upon us by the mathematics and they simply can't be anything else. We'll describe this more in Section 4.

We don't, however, understand the observed pattern of masses. More importantly, we don't understand the vertical direction in the pattern at all. We don't understand why there are 3 generations in the world and not, say, 17. Nonetheless, we know from both particle physics and from cosmological observations that there are no more than 3 light neutrino species and measurements of the way the Higgs decays tells us that it
doesn't couple to anything heavier than the top. It seems likely that we're stuck with these three generations and nothing else.

The 12 particles listed above are all the "matter particles" that we have so-far discovered in the universe. Each has some fairly intricate properties that we will learn as these lectures progress. In particular, each particle has a corresponding anti-particle, and both the particles and anti-particles decompose further into "left-handed" and "right-handed" pieces. We will describe all this in Section 2.

[1] Nearly everyone now refers to the b quark as bottom. One exception is LHCb , an important experiment at CERN devoted to the study of b quarks. They prefer the older name, presumably because they would rather be LHC-beauty than LHC-bottom. The obvious suggestion that they embrace both names and rebrand themselves LHCbb has gone sadly unheeded.

Forces

All the particles that we described above interact through a handful of forces. It's usually said that there are four fundamental forces at play in the universe. In fact, by any logical count, we should say that there are five forces, with the interaction of the Higgs boson providing the fifth.

The traditional four forces of Nature are:

- Gravity: This was the first force to be discovered and, in many ways, the one we understand least. The effects of gravity are very familiar: it's the reason why apples fall from trees and tides wash in and out. It's the reason why planets orbit stars, and stars form galaxies, and the reason why these are all dragged inexorably apart by the expansion of the universe. Our best theory of gravity was given to us by Einstein: it is the theory of General Relativity.

- Electromagnetism: Like gravity, this force is familiar because it manifests itself in the macroscopic world, where it is harnessed for much of modern technology. On the atomic level, it is the electromagnetic force, acting between the electrons in an atom, that give rise to the chemical properties of the elements.

- Strong Nuclear Force: This force has no counterpart in classical physics. It is responsible for binding quarks together inside protons and neutrons and, subsequently, for binding protons and neutrons together as nuclei.

- The Weak Nuclear Force: Another force that manifests itself only on very small scales. Its primary role is to allow certain particles to decay into other particles. For example, beta radiation, in which a neutron decays into a proton, electron and anti-neutrino occurs because of the weak force.

The story above contains a little bit of a lie. At the fundamental level (meaning at the shortest distance scales), the force of electromagnetism should be replaced by something called hypercharge. It's not dissimilar to electromagnetism, but it differs in details. What we observe as electromagnetism is some mix of hypercharge and the weak force.

Finally, the "fifth force" is:

- The Higgs Force: Again, a force which has no classical analog. Its role, however, is rather dramatic: it allows all the elementary particles described in the table above to get a mass.

Each of these five forces will be described in considerable detail as the lectures progress. Section 2 describes the matter particles and their interaction with electromagnetism; Section 3 describes the strong force; and Section 4 describes the weak force and the Higgs boson. Finally, we will turn to gravity in Section 5.

4.1.1 1.1 Quantum Fields

Ironically, the theory of particle physics is not a theory of particles. It's a theory of fields. A field is a fluid-like object which is spread throughout all of space. A field can take a different value at every point in space, and that value can change with time.

The most familiar examples are the electric and magnetic field which are associated to the electromagnetic force. These comprise of a pair of vectors, which exist at every point in the universe. Mathematically, the electric and magnetic field are functions $\mathbf{E}(\mathbf{x}, t)$ and $\mathbf{B}(\mathbf{x}, t)$, which can take different values at different points $\mathbf{x}$ in space and points t in time. Like all fluids, the electromagnetic field can ripple. These ripples are what we call light waves.

Things get more interesting when we introduce quantum mechanics into the mix. In the 1920s, physicists understood that, on the smallest distance scales, the universe doesn't follow the common sense laws that Newton gave us. Instead, it's much more mysterious and counter-intuitive, and follows the rules of quantum mechanics. One of the key consequences of quantum mechanics is that energy isn't something smooth and continuous. Instead, energy can only be parcelled in discrete lumps. That's what the word "quantum" means: discrete, or lumpy.

The real fun happens when we try to combine the ideas of quantum mechanics with fields. One implication is that the electromagnetic waves that make up light are not continuous. Instead light is made up of particles called photons. The photons are ripples of the electromagnetic field tied into little parcels of energy due to quantum mechanics.



Figure 3. This is not what physicists mean by a field. It's what a farmer means by a field. Or a normal person.

The surprise is that the paradigm above holds for all other particles too. First, each of the forces described above has a field associated to it. And, when quantum mechanics is taken into account, ripples of the field become particles. The names of the particles associated to each of the forces are:

- Electromagnetism: As described above, the particle is the photon. In particle physics, photons are denoted by the greek letter γ (gamma). This comes originally from high-energy photons known as "gamma rays", but is now used to describe photons of any energy.
- Strong Nuclear Force: The field associated to this force is called the Yang-Mills field. The corresponding particles are gluons.
- Weak Nuclear Force: The field is another variant of the Yang-Mills type. The corresponding particles are the W and Z bosons.
- The Higgs Force: The associated particle is called, unsurprisingly, the Higgs boson. It was discovered at CERN in 2012, the last of the Standard Model particles to be found experimentally.
- Gravity: The force of gravity is rather special. Einstein's theory of general relativity teaches us that the gravitational field is actually space and time itself. Ripples of space and time are called gravitational waves and were first observed by the LIGO detector in 2015 . The associated quantum particles, known as gravitons, have not been observed experimentally. Given the weakness of gravitational interactions, it seems unlikely that this situation will change any time soon.

So each force is associated to a field and an associated quantum particle. But, so too, are the matter particles. For example, spread throughout the room you're sitting in, and in fact

throughout the entire universe, there exists something called the electron field. The ripples in this fluid get tied into little knots, or little bundles of energy, by the rules of quantum mechanics. And those bundles of energy are the particles that we call electrons. Every electron is a ripple of the same underlying field, like waves are ripples of the same underlying ocean.

There is also a muon field, and a tau field, together with six different kinds of quark fields and three kinds of neutrino fields. The Standard Model of particle physics is a theory describing how 12 matter fields interact with 5 fields of force. If one field - say the electron field - starts to move and sway, then it causes the gravitational field and the electromagnetic field to move. These, in turn kickstart the quark fields, and so on. All of these fields are engaged in an intricate, harmonious dance, swaying backwards and forwards, to a music that we call the laws of physics.

This can be contrasted with our view of classical physics. There we have two very different objects: particles and fields. At times, they make fairly awkward bedfellows. But there is a beautiful unification in the quantum world: everything is field. The particles are emergent objects.

The Implications of Quantum Fields

The world of quantum fields can, at times, be difficult to get our heads around. It is often easier to resort to the language of particles and, for the most part, this is what we will do in these lectures. Nonetheless, there are times when the particle picture breaks down and it is only when we think in terms of fields that things make sense. Here we describe a number of implications of the field theoretic picture. We'll see many more as the lectures progress.

Implication 1: First, and most importantly, field theories allow us to write laws of physics consistent with locality. If you shake an electron, it doesn't immediately affect a second electron sitting elsewhere. Instead the shaking electron produces a perturbation in the neighbouring electromagnetic field. This then propagates outwards, until it reaches the second electron. In this manner, there is no "action-at-a-distance", and causality is ingrained in the very structure of field theory.

Implication 2: The second consequence of quantum fields is the following: all particles of a given type are the same.

For example, two electrons are identical in every way, regardless of where they came from and what they've been through. The same is true of every other fundamental particle. Suppose, for example, that we capture a proton from a cosmic ray which we identify as coming from a supernova lying 8 billion lightyears away. We compare this proton with one freshly minted in a particle accelerator here on Earth. And the two are exactly the same! How is this possible? Why aren't there errors in proton production? How can two objects, manufactured so far apart in space and time, be identical in all respects? The answer is that there's a sea of proton "stuff" that fills the universe. This is the proton field or, if you look closely enough, the quark field. When we make a proton we dip our hand into this sea and mould a particle. It's not surprising that protons forged in different parts of the universe are identical: they're made of the same stuff.

Implication 3: The field perspective allows us to simply interpret situations where the number of particles changes. For example, beta decay is a process in which the neutron decays,

$$n \to p + e + \bar{\nu}_e$$

The decay products are a proton p, and electron e and an electron neutrino $\bar{\nu}_e$. (The bar on the $\bar{\nu}_e$ tell us that it's actually an anti-neutrino; we'll describe anti-matter in Section 2.) In terms of the underlying quarks, the down quark decays into an up quark

$$d \to u + e + \bar{\nu}_e$$

From a particle perspective, this is somewhat confusing. You might be tempted to view the decay above by thinking that a proton, electron and anti-neutrino are sitting inside the neutron, perhaps bound together by some mysterious force and just waiting to get out. (Or, equivalently, that the down quark is made of an up quark, electron and anti-neutrino.) But that's not the right way to think about the neutron (or the down quark.) Indeed, we've stated above that the down quark is a fundamental constituent of matter, and that would be difficult to believe if it contained other objects.

Happily, these confusions evaporate when we think in terms of fields. The particle that we call the down quark is a ripple of the down quark field. But there's no reason to think that this ripple can last forever. Instead, it can decay, but only at the cost of exciting three other fields: those of the up quark, electron and neutrino. The reason why these three particular fields get excited, and no others, is due to the detailed interactions of the various fields. These rules will be described as these lectures progress.

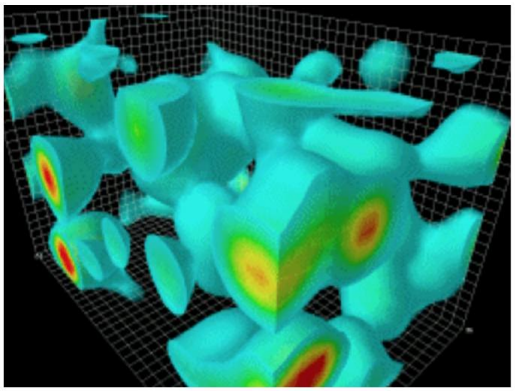


Figure 4. The vacuum of space is an interesting and complicated place. This picture is taken from the QCD simulation of Derek Leinweber

Implication 4: There is one last idea that will be useful to have in the back of your mind: the existence of quantum fields means that empty space, also known as the vacuum, is not a dull place. It is filled with quantum fields which, even when left alone, are not necessarily calm. An example is shown in Figure 4, depicting a computer simulation of empty space. What's shown is a typical configuration of the gluon field in the vacuum. The true vacuum is, in fact, much more complicated even than that shown in the picture. The vacuum doesn't have just a single field configuration but is something more murky: a quantum superposition of infinitely many different field configurations, each appearing with some probability. In quantum field theory, the vacuum of space is an interesting place. It froths with quantum uncertainty.

The take-home message for these lectures is that the vacuum of space is not some inert, boring substance. The bubbling fields breathe life into the vacuum and mean that it is able to respond to things happening within it. This phenomenon, as we shall see, lies at the heart of some of the more subtle effects of quantum fields.

4.1.2 1.2 Natural Units

Before we get going, we should introduce the units that we use to quantitatively describe the sub-atomic world. Usually in physics, we introduce different units for length, time and mass. For example, the SI units are meters, seconds and kilograms respectively. However, at

the fundamental level these concepts are not as different as they first appear and the laws of physics provide a way to translate between them.

For example, there is a speed limit in place in the universe. No particle can travel faster than

$$c = 299792458 \text{ ms}^{-1} \approx 3 \times 10^8 \text{ ms}^{-1} \tag{1.1}$$

All particles with mass are obliged to travel slower than this speed, while all massless particles are obliged to travel at exactly this speed. The most familiar massless particle is the photon and for this reason c is referred to as the speed of light.

The speed of light allows us to translate freely between units of length and units of time. Given a length scale L, there is a natural time scale $T = L/c$, which is the time it takes light to cross the distance L.

In fact, the existence of a constant speed in the universe is hinting at something deeper: the concepts of space and time are not as distinct as we first thought. To put this in perspective, here's an analogy. I might decide that I'm going to measure all horizontal distances in centimeters, and all vertical distances in inches. I then proudly reveal a new fundamental constant of nature C which translates between the two,

$$C \approx 0.394 \text{ Inches cm}^{-1}$$

This is clearly a dumb thing to do. If I have a ruler marked in cm to measure horizontal distances, then I can always rotate it and use it to measure vertical distances in cm as well. The rotational symmetry in the world means that there is no fundamental difference between distances in the horizontal and vertical directions.

But exactly the same story holds for the speed of light. The theory of special relativity tells us that there is a symmetry between space and time, albeit one that only becomes apparent when you travel fast. If you move close to the speed of light you experience strange effects like time dilation and length contraction, which can be explained by a rotation of time into space and vice versa. What this means is that, at the fundamental level, we should measure time and space using the same units. If we choose to measure time in seconds, then we should measure length in light-seconds, the distance that light travels in a second. With this choice, the speed of light is simply

$$c = 1$$

A corollary of this is that mass is now measured in the same units as energy. This is because Einstein's famous formula $E = mc^2$ becomes simply $E = m$. In these lectures, we will specify the masses of elementary particles in units of energy. If, for some reason, you want to get the mass in, say, kilograms, then you simply need to reinstate the factor of the speed of light in $m = E/c^2$ and use the value $c \approx 3 \times 10^8$ ms^{-1}.

A similar story arises when we consider quantum mechanics. The fundamental constant in quantum mechanics is Planck's constant,

$$\hbar = 1.054571817 \times 10^{-34}\text{Js}$$

It has units of energy $\times$ time. What this constant is really telling is us that, at the fundamental level there is a close connection between energy and time. A process with energy E will typically take place in a time $T = \hbar/E$. In this way, we can translate between units of energy and units of time, and these concepts are not as distinct as our ancestors believed. To highlight this, we choose units so that

$$\hbar = 1$$

The choice $c = \hbar = 1$ is referred to as natural units. It means that there's only one dimensionful quantity left, which we usually take to be energy. Any measurement whether it's of length, time or mass - can be expressed in terms of energy.

A Sense of Scale

The SI unit of energy is a Joule and is not particularly appropriate for the sub-atomic world. Instead, we use the electronvolt (eV) which is the energy an electron picks up when accelerated across 1 volt. This is

$$1\text{eV} \approx 1.6 \times 10^{-19}\ \text{J}$$

The electronvolt is the energy scale appropriate for atomic physics. For example, the energy that binds an electron to a proton to form a hydrogen atom is $E \approx 13.6\text{eV}$. For elementary particles, we will need a somewhat larger unit of energy. We typically use $\text{MeV} = 10^6\text{eV}$ or $\text{GeV} = 10^9\text{eV}$. The LHC, our best current collider, runs at an energy scale measured in $\text{TeV} = 10^{12}\text{eV}$. (It's worth pointing out that this is actually closer to a Joule than it is to an electronvolt!)

The masses of the 12 matter particles cover a range from eV to GeV . They are:

Electron 0.5 MeV	Down Quark 4 MeV	Up Quark 2 MeV	Electron Neutrino < 0.1eV
Muon 106 MeV	Strange Quark 87 MeV	Charm Quark 1.3 GeV	Muon Neutrino < 0.1eV
Tau 1.8 GeV	Bottom Quark 4.2 GeV	Top Quark 170 GeV	Tau Neutrino < 0.1eV

The entries for neutrinos are upper bounds on the mass. Meanwhile, the masses of the 5 force-carrying particles are

Photon massless
Graviton massless
Gluon ~ 200MeV
W and Z Bosons $80, 91$GeV
Higgs Boson 125 GeV

For each of these particles, there is an associated length scale. We get this by transforming energy E into a length using the fundamental constants of Nature c and $\hbar$,

$$\lambda = \frac{\hbar c}{E} \tag{1.2}$$

This is known as the Compton wavelength. Roughly speaking, it can be viewed as the size of the particle. For example, for the electron the Compton wavelength is $\lambda_e \approx 2 \times 10^{-12}$ m. Perhaps somewhat surprisingly, the heavier a particle is, the smaller its Compton wavelength.

The Biggest and the Smallest

There are two further length scales that we should mention before delving into details of the subatomic world. One is associated to the strength of the gravitational force. Newton's constant is given by

$$G_N \approx 6.67 \times 10^{-11} \text{ m}^3 \text{ kg}^{-1} \text{ s}^{-2}$$

In natural units, Newton's constant has dimensions of [Energy] $^{-2}$. Putting back the factors of $\hbar$ and c, we can derive an energy scale known as the Planck mass

$$M_{\rm pl} = \sqrt{\frac{\hbar c}{8\pi G}} \approx 2 \times 10^{18}\text{GeV}$$

(The factor of 8π is conventional, and is sometimes dropped.) This is an enormous energy scale, fifteen orders of magnitude larger than the scales that appear in the Standard Model. The corresponding length scale is the Planck length

$$L_{\rm pl} = \sqrt{\frac{8\pi\hbar G}{c^3}} \approx 8 \times 10^{-35} \text{ m}$$

This, in turn, is a tiny length scale, 15 orders of magnitude smaller than the scale that we have explored at our best particle colliders. The Planck scale is where both quantum mechanics and gravity become important. It seems likely that space and time cease to make sense at these scales, although it's not clear exactly what this means.

On the other end of the spectrum, the largest size that we can talk about is the entire observable universe,

$$L_{\rm universe} \approx 9 \times 10^{26} \text{ m}$$

The corresponding energy scale is

$$H \approx 2 \times 10^{-33}\text{eV}$$

This energy scale is closely related to the so-called "Hubble constant" that measures how fast the universe is expanding, albeit written in the unusual units of electronvolts. Clearly, it's a tiny energy scale. A particle with the mass of H would have the same size as the entire universe.

This, then, is the playground of physics. The goal of physics is to understand everything that can happen at lengths in the range

$$10^{-34} \text{ m} < L < 10^{26} \text{ m}$$

or, equivalently, at energies in the range

$$10^{-33}\text{eV} < E < 10^{27}\text{eV}$$

It turns out that there is quite a lot of interesting things in this window! And, underlying many of them, is the Standard Model.

4.1.3 A Interlude: The Road to Discovery

Throughout these lectures, our focus will be on explaining the key ideas and concepts that underlie the subatomic world. This means that we will describe our current understanding viewed through the lens of the Standard Model. Yet this theory took many decades to build, years in which physicists were mostly bewildered and confused. It's important to ask: how did we arrive at this point?

The answer to this question is almost entirely: experiment. While there were many groundbreaking theoretical observations, at each step the important progress was only made in response to a novel experimental discovery. After each section of these lectures, we will have a short interlude in which we describe this experimental progress. This will also provide an opportunity to present a more historical approach to the subject of particle physics. The hope is that these interludes will serve to ground some of the ideas that we meet in the main thread, and place them in more concrete context.

In this first interlude, we explain the beginnings of particle physics. We describe the discoveries that resulted in the comforting and familiar picture of matter as made of just three particles: the electron, proton and neutron.

A. 1 Ray Physics

Before particle physics was the study of fields, it was the study of rays. By the end of the 1800s, several kinds of "rays" had been found, each seemingly exhibiting different properties. It took several decades to distill the properties of these rays (do they undergo diffraction? can they be bent by electric or magnetic fields?) and, ultimately, to understand their particle constituents.

Cathode Rays

Take a glass tube, and remove most of the air. If you drop a large voltage across the tube, a faint glow can be seen at one end, a result of rays emitted by the cathode (the negatively charged electrode) hitting the glass wall. In many ways the discovery of these cathode rays, first observed in 1869 by the German physicists Hittorf and Plücker, marks the beginning of modern day particle physics.

A number of properties of cathode rays were soon established, including the fact that they travel in straight lines, as revealed by the shadow cast by objects placed in their path, but their trajectory can be deflected by both electric and magnetic fields. We now know that cathode rays are beams of accelerated electrons.

With hindsight, these early discharge tubes can be viewed as the world's first particle accelerators. The electrons were accelerated to energies of around 10^5eV. In contrast, in the last electron-positron accelerator at CERN, known as LEP, electrons were accelerated to energies of around 2×10^{11}eV. Its successor, the LHC, accelerates protons to energies of 6×10^{12}eV. Evidently, the increase of energy by 7 orders of magnitude took 150 years of hard work. There are reasons to believe that the next 7 orders of magnitude will be even more challenging.

X-Rays

One recurring theme of particle physics is how one discovery paves the way for the next. The first example occurred in November 1895, when Wilhelm Röntgen was playing with cathode rays. He covered the glass tube with thin black cardboard and noticed that, when the tube was turned on, a paper screen painted with a chemical called barium platinocyanide would give a faint green glow, even when placed up to a meter away from the apparatus. He concluded that the tube was emitting some invisible rays, which he dubbed X-rays.

Röntgen's subsequent investigations showed that X-rays were not the same as the cathode rays from which they originated since they travelled much further in air. He also realised that X-rays could be used to develop photographic plates, and his first paper includes the astonishing photograph of his wife's hand shown to the right. His wife's perfectly reasonable response: "I have seen my death".

Röntgen's paper resulted in enormous excitement, both among other scientists and the general public. Rather like Einstein in later years, everyone wanted a piece of Röntgen. However, it appears that he was less than impressed with the whole show and worked hard to stay out of the limelight. A sole newspaper interview from this time reveals a Dirac-like level of brevity:



Hand des Anatomen Geheimrath von Kölliker. Im Physikalischen Institut der Universität Würzburg mit X-Strahlen aufgenommen von Professor Dr. *W. C. Röntgen.*

Interviewer: What did you think?
Röntgen: I did not think; I investigated.
Interviewer: What is it?
Röntgen: I don't know.

The nature of X-rays remained mysterious for a long time. The suggestion that they may be short wavelength electromagnetic waves was not generally accepted since no one succeeded in observing X-ray diffraction. This changed in 1912, when Max Laue (later von Laue) realised that the crystal lattice of solids had the right separation needed to observe diffraction of X-rays, opening up the entire field of X-ray crystallography.

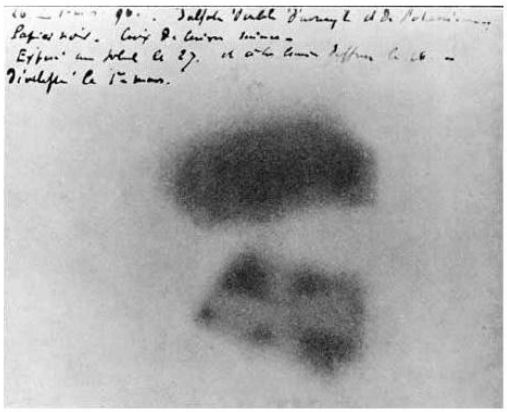
Uranic Rays

Among the many people to be inspired by Röntgen's discovery was a French physicist named Henri Becquerel. For some years, he had held a fascination with phosphorescent materials and decided to explore the connection to X-rays. Ironically, in the end his discovery had nothing to do with X-rays.

Uranium salts had long been known to have phosphorescent properties. Becquerel's experiment involved exposing uranium to sunlight for several hours. With the uranium suitably excited, he observed that it emitted rays which, rather like X-rays, created silhouetted images

on photographic plates wrapped in thick, black paper.

Becquerel's breakthrough came because of the weather. The final days of February 1896 were dark and overcast in Paris. With no sunlight available, Becquerel stored his experiment in the drawer of his desk and got on with other things, like a spot of shopping. By March 1st the sky remained cloudy and, perhaps bored, perhaps inspired, Becquerel decided to develop the photographic plate anyway, expecting to find nothing. Instead, to his astonishment,



there appeared the clear image of a copper cross that had been placed between the plate and the uranium source. Becquerel's photograph is shown to the right.

Becquerel's desk drawer discovery showed that all his careful preparation, exposing uranium to sunlight, had nothing to do with the uranic rays that it emitted. This was, to say the least, disconcerting. If the rays were emitted without any prompting from an external energy source like the Sun then where did their energy come from? It was tempting to think that the whole thing violated the conservation of energy.

α, β and γ Rays

Soon after Becquerel's breakthrough, three further radioactive elements - thorium, polonium and radium - were discovered by Marie Curie (née Skłodowska) and her husband Pierre. The next step was to try to characterise the rays that were emitted. This was done by one of the early heroes of particle physics: Ernest Rutherford.

Rutherford was the first to realise that uranium emitted not one, but two different types of radiation. He called these α-rays and β-rays:

- α-rays: Alpha radiation is easily absorbed. Indeed, we now know that all α-rays would have been absorbed by the black paper wrapping the photographic plate in Becquerel's original experiment and so were not detected. Over a period of 13 years, from 1895 to 1908, it slowly became clear that α particles are four times heavier than hydrogen, with charge $+2$. In other words, they are what we now know to be the nucleus of a helium atom.

- β-rays: Beta radiation is more penetrating. In time, it was identified with a stream of electrons. This will be described below.

Later, Villard discovered that radium emitted yet a different kind of radiation, one that he naturally called. . .

- γ-rays: Another, very penetrating form of radiation. This was later found to be highly energetic electromagnetic waves.

Around the turn of the century, the situation was rather confusing. There were cathode rays and x-rays and α and β and γ rays. not to mention a number of false discoveries that

were purely illusory. Getting to the heart of these phenomena would, ultimately, require an understanding of electromagnetism and the strong and weak nuclear forces.

A. 2 The Electron

Cathode rays were the first to be discovered and, subsequently, the first to be understood in terms of a constituent particle. This particle is, of course, the electron.

The claim that rays are composed of particles means that their properties can be understood using Newtonian mechanics in which the particles are endowed with a mass m and electric charge e. In 1885, Hendrik Lorentz wrote down the equation of motion for such a particle moving in the presence of an electric field $\mathbf{E}$ and magnetic field $\mathbf{B}$. A particle with velocity $\mathbf{v}$ will experience an acceleration $\mathbf{a}$ given by

$$m\mathbf{a} = e(\mathbf{E} + \mathbf{v} \times \mathbf{B}) \tag{A.1}$$

The first goal was therefore to measure the deflection of the cathode rays due to electric and magnetic fields. This measurement was performed by J.J. Thomson in 1897. Two other physicists, Wiechert and Kaufmann made similar measurements using only magnetic fields around the same time. However, as you can see from the equation of motion, the deflection of the rays cannot tell us about m and e individually: it only tells us about the ratio e/m.

Fortuitously, the same ratio e/m had arisen in an entirely different context the year before. This came from the discovery that the atomic spectral lines can be split in the presence of a magnetic field, a phenomenon known as the Zeeman effect. Lorentz himself analysed this effect using the equation (A.1) and, happily, the value of e/m that was needed to explain the observed splitting was close to that later found in cathode rays.

But the ratio e/m for cathode rays came with a surprise: it was significantly larger than the value for other known ions. (Thomson's measurement of e/m gave a value that was 770 times larger than that of a hydrogen ion - the particle that would later be rebranded as a proton. We now know that the correct value of the ratio is around 1836.) But the question remained: is this because the electric charge e of the particle is very big, or because the mass m is very small. To resolve this issue, one had to find a way to measure either e or m individually.

The prevailing viewpoint at the time was the right one: that the mass of the particle was unusually small. Indeed, there was already some indication of how small it had to be, since the electric charge on a hydrogen ion had been estimated to reasonable accuracy. This in itself was no mean feat. It was fairly straightforward to measure the electric charge on, say, a mole of ions. The difficulty is in figuring out how many atoms are in a mole. Or, in other words, in figuring out Avogadro's number $N \approx 6 \times 10^{23}$. (See the final question on this Statistical Mechanics Example Sheet if you want to challenge yourself.) A number of ingenious ways to determine N were proposed, resulting in a ballpark figure for e, the minimum unit of electric charge carried by what we now call the proton. One of the best estimates (out by a factor of 20 or so) was proposed by the Irish physicist Stoney, who also coined the name electron, for this "atom of electricity".

A more direct measurement of the electric charge was first achieved by J.J. Thomson, and this is the reason that he, rather than Wiechert or Kauffman, is primarily remembered as the discover of the electron. He didn't study cathode rays, but he turned instead to the photoelectric effect. This occurs when UV light is shone on a material, causing electrons to be emitted, but at much slower velocities than those in cathode rays. Thomson measured the ratio e/m of these emitted particles and found that it agreed with his earlier measurements of cathode rays. But this time he could go further, employing a preliminary version of a detector known as the cloud chamber. This chamber contains supersaturated vapour which condenses into little droplets,

or clouds, as a ray passes through and ionises the atoms. In this way, the path of the emitted object can be tracked.

In 1899, with his new cloud chamber toy in hand, Thomson was able to determine the number of negatively charged ions that formed due to photoelectric emission simply by counting the droplets along the path. He was also able to determine the overall electric charge by counterbalancing the effect of gravity with an electric field. In this way, he measured the charge on each individual droplet, getting within 30% of the electric charge that we know today. This was the first time that the cloud chamber gave rise to a major breakthrough in physics. It would not be the last.

A more precise measurement, employing a similar technique but using oil droplets rather than a cloud chamber, was performed in 1909 by Millikan and Fletcher. They again balanced gravitational and electric forces, but were able to observe individual droplets, deducing that the charge was always quantised in units of 1.6×10^{-19} Coulombs. Their measurement was within less that 1% of the modern value. Famously, Millikan struck a dubious bargain with his student Fletcher and the resulting paper was published under Millikan's name alone. No doubt he felt bad as he collected his Nobel prize twelve years later.

A. 3 The Proton

The discovery of the proton went hand in hand with the discovery of the nucleus itself. The key experiment is one of the most famous in physics. Working in Manchester in 1909, Hans Geiger and his undergraduate assistant Ernest Marsden were firing alpha particles at thin sheets of metal and measuring how they bounced off. One day Rutherford entered the room and, according to Marsden, suggested "see if you can get some effect of α-particles directly reflected".

The results were startling and entirely unexpected. About 1 alpha particle in 8000 was reflected back in the direction from which it came. In later years, Rutherford recounted his surprise in a well known quote:
"It was quite the most incredible event that has ever happened to me in my life. It was almost as incredible as if you fired a 15 -inch shell at a piece of tissue paper and it came back and hit you."

But what did it mean?
The prevailing theories for the structure of the atom could not account for these experiments. Of course, physicists knew that atoms contained electrons, and there was acceptance that there had to be a compensating positive charge, but theories of the structure of the atom - whether based on plum puddings, planetary systems, or vortices - were put forward with little evidence.

The Gieger-Marsden experiment held the key. That it was Rutherford himself who understood its consequences is, in some ways, rather surprising. Rutherford was not known to hold much love for theoretical physics. He is reported to have said of relativity, "Oh, that stuff. We never bother with that in our work." and he was never a strong proponent of Bohr's founding work on quantum theory. My favourite Rutherford quote, capturing both his attitude to theorists, and his personality, is

> "How can a fellow sit down at a table and calculate something that would take me - me - six months to measure in a laboratory?"

Nonetheless, when needed, Rutherford showed himself to be no mean theorist. In 1911, he postulated that each atom contains a heavy, almost point-like object at the centre, carrying positive charge Q. He computed that an α-particle, repelled by the electrostatic Coulomb force, would be deflected by an angle θ with probability

$$\sigma(\theta) = \frac{Q^2 q^2}{4m^2 v^2 \sin^4(\theta/2)} \tag{A.2}$$

Here q, m and v are the charge, mass and velocity of the α-particle. This formula is now known as the Rutherford cross-section. You can find a derivation in the lecture notes on Dynamics and Relativity. The formula agrees with the experimental data with impressive accuracy.

As with many great discoveries in science, there was no small amount of luck involved. On the experimental side, the alpha particles used in the experiment were fast enough to blast through the electrons of the atom without care, but slow enough to be deflected from the nucleus before they experienced the strong nuclear force. On the theoretical side, Rutherford deduced his formula using Newtonian classical mechanics. But the correct calculation of the cross-section requires quantum mechanics and in nearly all cases this differs from the classical result. The Coulomb force law turns out to be the exception - it is the one force where classical and quantum results for scattering agree! (You can learn more about this in the scattering theory section of the lectures on Topics in Quantum Mechanics.)

With Rutherford's explanation of the nucleus, there was still work to be done. At the time, all elements were labelled by their atomic weight A which, at least for light elements, was close to an integer. Listing all the elements in order then gives two numbers: A, their weight and Z, their place in the list. The first few elements are shown in Table 1.

	H	He	Li	Be	B	C	N	O
Z	1	2	3	4	5	6	7	8
A	1	4	7	9	11	12	14	16

Table 1. The first few elements

But the question remained: what is the physical meaning of Z ? In particular, if you're just given the list of known elements, how do you know you've got them all? For example, it might be tempting to think that A is really telling us the rightful place in the list, with two missing elements with $A = 2$ and 3 that are just waiting to be found.

The suggestion that Z should be equated with the positive electric charge of the nucleus did not have an auspicious start. It was first made by van den Broek, a Dutch real estate lawyer who was pushing some new and improved 3d version of Mendelev's periodic table. His accounting of the elements never took off, but his suggestion that Z measures the electric charge was rapidly accepted. Moreover, Rutherford's scattering formula (A.2) gives a clear way to measure the charge Q of the nucleus. These, and other experiments, ultimately led to the complete periodic table that we know and love today [2].

From here it was a short step to the idea that the hydrogen nucleus - originally called the H -particle - was a building block of all nuclei. The issue was finally put to rest some years later when Rutherford demonstrated that H-particles were emitted by other nuclei - specifically nitrogen - when bombarded by α-particles. The name "proton" was coined by Rutherford at this time.

A. 4 The Neutron

In 1911, the nucleus was discovered. By 1920, there was no doubt about the existence of the proton. But it took until 1932 for the other constituent of the nucleus, the neutron, to be

found.

In the decade between the discoveries of the proton and neutron, physics changed beyond anyone's wildest imagination. Quantum mechanics was formulated and the basics of quantum field theory were laid down. These ideas provide the foundation for nearly everything that we discuss in these lectures - both experimental and theoretical. Yet the discovery of the neutron owed only little to these new developments. The neutron took so long to find simply because it's hard to see. For this reason, the neutron still carries an air of that pre-quantum world, less exotic than, say, anti-matter whose origin story is so closely tied to developments in quantum theory. Yet, astonishingly, there was less than a 100 days between the discovery of the two particles!

You might wonder why physicists didn't stay up at night, puzzled by the difference between the atomic number Z and the mass A of the nucleus. It's because they had a very convincing explanation. They thought that the nucleus must consist of A protons with $A - Z$ electrons to cancel the charge. Moreover, there was an extremely good reason to think that the nucleus contained electrons. This was beta decay. The electrons emitted in beta decay are far more energetic than the orbiting electrons in the atom, and this meant that they had to have their origin in the nucleus. But if electrons were being emitted from the nucleus, then obviously they must have been there all along. That's simply common sense. Of course, we now know that common sense isn't always the best guide when it comes to the sub-atomic world.

If you knew where to look, the advent of quantum mechanics did make it increasingly difficult to believe in electrons in the nucleus. Trapped inside a cell the size of a nucleus, the Heisenberg uncertainty relation means that the electron necessarily has energy greater than 40 MeV , significantly larger than nuclear binding energies and making it untenable that the electron could remain in place. Further trouble came with the discovery of spin. (We describe spin in more detail in Section 2.1.) If both the proton and electron have spin 1/2 then, regardless of whether spins add or subtract, a nucleus with A protons and $A - Z$ electrons should have integer spin when Z is even and halfinteger spin when Z is odd. But that's not what's seen. Nitrogen, for example, has $Z = 7$ but was long known to have integer spin. Opinions differed on what to make of this. So ingrained was the idea that the nucleus contains protons and electrons that Fermi and Rasetti even wrote a paper suggesting that the mismatch should cast doubt on the idea of spin.

Still, when the breakthrough came it owed essentially nothing to new-fangled quantum ideas and everything to experiment. The first hint that something new was afoot came in 1930 in Berlin. Walther Bothe and Herbert Becker took alpha rays from a polonium source and directed them on beryllium. They found that the beryllium gen-
erated a new radiation of great penetrating power which they concluded, incorrectly, must be gamma rays. Over the next couple of years the experiment was repeated and improved, notably by Iréne Curie who was sitting on the world's most powerful source of polonium, a gift from her mother. Together with her husband Fréderic Joliot (by that time both doubled-barrelled Curie-Joliot's), they directed this beam of supposed gamma rays at parafin and found that it could eject protons at huge velocities. But still they stuck with the gamma ray interpretation.

The Curie-Joliot experiment was the watershed moment. Their interpretation was not, it's fair to say, universally embraced. Apparently the Italian physicist Ettore Majorana responded to the news with the exclamation

[02] A physicist called Henry Moseley deserves special credit here. When Mendelev originally proposed his periodic table he found gaps, allowing him to successfully predict the existence of three new elements. Moseley, using X-ray techniques to determine the atomic number Z, successfully predicted seven more!

Moseley, like many physicists of that time, was drafted into the Great War. Geiger and Marsden, for example, found themselves both posted to the Western front, fighting on opposite sides. Both survived. Moseley was not so lucky and the man widely recognised as England's most promising young physicist was killed in the battle of Gallipoli by a bullet in the head. He was 27 years old.

"What fools! They have discovered the neutral proton, and they do not recognise it!"

In Cambridge, Rutherford and James Chadwick, his second-in-command, held similar sentiments. There was too much amiss for the radiation to be gamma rays. Less than three weeks later, Chadwick discovered the neutron.

In fairness, Chadwick had been searching for something like a neutron for over a decade. He didn't originally envisage a new elementary particle, but instead a closely knit bound state of a proton and electron, much smaller than a hydrogen atom so that it could fit inside the nucleus. That meant he was well prepared when the Curie-Joliot result came in. His short paper studies the penetrating power of the radiation. The Bothe-Becker-Curie-Joliot interpretation was that the original alpha rays react as

$$^9\text{Be} + \alpha \longrightarrow {}^{13}C + \gamma$$

But the properties of the carbon nucleus were known well enough to put an upper bound on the energy of the emitted gamma ray. Whatever was coming out of this reaction was much more powerful. Chadwick found the correct conclusion: he was seeing something entirely new

$$^9\text{Be} + \alpha \longrightarrow {}^{12}C + n$$

Chadwick had found the neutron.

4.2 2 A First Look at Quantum Fields

In this section we look in more detail at some of the key features of quantum fields and their interactions. We illustrate these properties with the simplest quantum force, electromagnetism. Or, to give it its fancy name, quantum electrodynamics.

4.2.1 2.1 Matter Fields and Force Fields

We'll meet a bewildering number of names in these lectures, each of them classifying particles according to various properties. But one classification is more important than all others: every type of particle falls into one of two classes called

- Bosons
- Fermions

The distinction between these two kinds of particles lies in the quantum world. Fermions have the property that no two particles can occupy the same quantum state. Roughly speaking, this means that you can't put two fermions on top of each other. This property is known as the Pauli exclusion principle. In contrast, there is no such restriction on bosons. You can pile up as many of them as you like, one on top of the other.

(A mathematical aside: if you've done a little quantum mechanics then it's very easy to describe the difference between bosons and fermions. Two identical particles are described by a wavefunction $\psi(\mathbf{x}_1, \mathbf{x}_2)$ which tells you the probability amplitude to find the two particles at positions $\mathbf{x}_1$ and $\mathbf{x}_2$. If the particles are bosons then, when you swap their positions, the wavefunction remains unchanged: $\psi(\mathbf{x}_2, \mathbf{x}_1) = \psi(\mathbf{x}_1, \mathbf{x}_2)$. In contrast, if the particles are fermions then the wavefunction picks up a minus sign when you swap them: $\psi(\mathbf{x}_2, \mathbf{x}_1) = -\psi(\mathbf{x}_1, \mathbf{x}_2)$. This means, in particular, that if you try to bring the two particles together at some point $\mathbf{x}_1 = \mathbf{x}_2 = \mathbf{x}$, then $\psi(\mathbf{x}, \mathbf{x}) = 0$ for fermions, so there is vanishing probability that the two particles sit on top of each other.)

All the matter particles in the universe - electrons, quarks and neutrinos - are fermions. All the force carrying particles are bosons. In fact, this is more or less a definition of what we mean

by a "matter" particle vs a "force" particle. The matter particles obey the Pauli exclusion principle; the force particles do not.

The distinction between bosons and fermions has a couple of familiar consequences. Electrons are fermions and therefore obey the Pauli exclusion principle. This is ultimately responsible for the structure of the periodic table. The electrons can't all sit
close to the nucleus, but fill up successive atomic shells, with the electrons in the outer shell - known as valence electrons - largely responsible for the chemical properties of the element.

Photons are bosons, and this means that the Pauli exclusion principle does not apply. A laser is an example of a system in which many photons sit in the same quantum state.

2.1.1 Spin

Particles are endowed with a number of other properties. The most familiar of these is the mass of the particle, but it is not the only one.

Particles also have an inherent angular momentum that we call spin. It's not a bad analogy to think of elementary particles as spinning about some axis, much like the Earth spins. But spin is a quantum mechanical property and if you push the spinningEarth analogy too far then it breaks down. For example, if you ask questions like "how fast is the surface of the particle moving" then you'll get nonsensical answers. Furthermore, there's no way to spin up a particle like a basketball; the magnitude of the spin is something that is fixed and unchanging. You can, however, change the orientation of the axis along which the particle spins.

Like many phenomena in the atomic world, spin is quantised. That means that the spin can't take arbitrary values, but comes in discrete amounts. These are [3]

$$s = 0, \frac{1}{2}\hbar, \hbar, \frac{3}{2}\hbar, 2\hbar, \ldots \tag{2.1}$$

In natural units, we just say that a particle has spin 0 , or spin $\frac{1}{2}$, and so on. Each particle in nature has a spin with a value taken from this list.

Particles that have a half-integer spin come with a rather strange property. If you rotate them by 360° then they don't quite come back the same as they were before! Instead, their quantum wavefunction comes back to minus itself. This means that you have to rotate the particle by 720° before it comes back to the same state. This is one of the more surprising facts about elementary particles and is a clear departure from our every day experience with classical objects.

There is a deep theorem, originally framed by Pauli, which states that the spin determines whether a particle is a boson or fermion:

The Spin-Statistics Theorem: Particles with integer spin are bosons. Particles with half-integer spin are fermions.

This theorem follows when you combine the laws of quantum mechanics with the rules of special relativity. (The word "statistics" in the name of the theorem is not particularly helpful. Its origin lies in the fact that you get different answers when you count the number of possible states in which bosons or fermions can sit, and this counting is referred to as the "statistics" of the particle. We won't need this interpretation in these lectures. You can learn more in the lectures on Statistical Physics.)

The spins of all the known elementary particles in Nature are:

- Spin 0: The Higgs Boson.

[3] I've been a little bit sloppy here. Strictly speaking, the total spin of the particle is $\sqrt{s(s+\hbar)}$ with s taking one of the values listed in (2.1).

- Spin $\frac{1}{2}$: All matter particles, i.e. the electron, muon and tau, together with the six types of quarks and three neutrinos.
- Spin 1: The photon, gluon and W and Z bosons. In other words, the particles associated to electromagnetism and the weak and strong nuclear forces.
- Spin 2: The graviton.

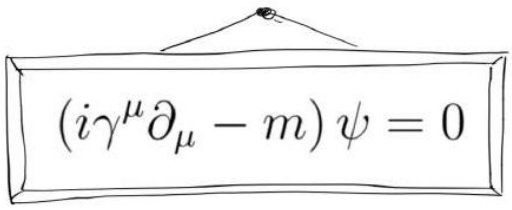
The remaining properties of particles mostly specify their interactions under the various forces. A familiar example is the electric charge, which determines the strength of a particle's interaction with electromagnetism. We'll describe the electric charge of all particles in Section 2.2, and the interactions with other forces in subsequent sections.

Finally, all of the properties described above, including the fermionic/bosonic nature of the particle, are really properties of the underlying field, which are subsequently inherited by the particle.

2.1.2 The Dirac Equation

All fields with spin $\frac{1}{2}$ - which, as we've just seen, means all fields associated to matter particles - are described by the Dirac equation.

We won't explain the mathematics behind the Dirac equation in these lectures, but it's so beautiful that it would be a shame not to show it to you. I've put it in a picture frame to highlight that it's here for decoration as much as anything else.



Here ψ is the quantum field; it depends on space and time. It also has four components, so it's similar to a vector but differs in a subtle way. It is known as a spinor. For what it's worth, the parameter m is the mass of the particle, while ∂_μ denotes derivatives and γ^μ are a bunch of 4×4 matrices. If you want to understand what the Dirac equation really means, you can find details in the lectures on Quantum Field Theory.

Dirac originally wrote his equation to describe the electron. But, rather wonderfully, it turns out that this same equation describes muons, taus, quarks and neutrinos. This is part of the rigid structure of quantum field theory. Any particle with spin $\frac{1}{2}$ must be described by the Dirac equation: there is no other choice. It is the unique equation consistent with the principles of quantum mechanics and special relativity.

The Dirac equation encodes all the properties of particles with spin $\frac{1}{2}$. Given such a particle, once you fix the orientation of the spin there are two possible states in which the particle can sit. Roughly speaking, it can spin clockwise or it can spin anti-clockwise. We call these two states "spin up" and "spin down".

The Pauli exclusion principle states that no two fermions can sit in the same quantum state. But the quantum state is determined by both the position and the spin of the electron. This means that an electron with spin down can be in the same place as an electron with spin up, because their spins differ. If you've done some basic chemistry, this should be familiar: both the hydrogen and helium atoms have electrons sitting in the orbit that sits closest to the nucleus. The two electrons in helium necessarily have different spins to satisfy the exclusion principle. But, by the time you get to the third element in the periodic table, lithium, there is no longer room for an additional electron in the closest orbit and the third electron is forced to sit in the next one out.

2.1.3 Anti-Matter

The real pay-off from the Dirac equation comes when you solve it. The most general solution has an interesting property: there is a part which describes the original particles, like the electron. But there is a second part that describes particles with the same
mass but with the opposite electric charge. The electron has negative charge, so these other particles must have positive charge. These positively charged electrons are called positrons: they are examples of anti-matter.

If a particle and anti-particle collide, both are annihilated. Typically, the energy is released in high energy photons. We denote the electron as $e^-$and the positron as e^+. Their annihilation usually results in the emission of two photons. (The emission of a single photon is not consistent with the conservation of both energy and momentum. For example, in the centre of mass frame, conservation of momentum would mean that the emitted photon would have nowhere to go.) The annihilation process is described by the reaction

$$e^- + e^+ \to \gamma + \gamma$$

The end result of all this is that the Dirac equation actually describes four different types of single particle states: a particle with either spin up or spin down, and an anti-particle with either spin up or spin down. The fact that there are four such states is related to the fact that the field ψ is a vector-like object with four components.

Dirac wrote down his equation in 1928. After a few years of confusion, Dirac himself suggested that these novel solutions should be interpreted as anti-matter. In 1931, he wrote
"A hole, if there were one, would be a new kind of particle, unknown to experimental physics, having the same mass and opposite charge to an electron."

This bold proposal, was confirmed experimentally just one year later, a development that we will describe in more detail in Section B.) The prediction of anti-matter remains one of the great triumphs of theoretical physics. We now know that all the matter particles in Nature have corresponding anti-particles. In all cases, the conserved charges of the anti-particles are equal and opposite to those of the particles.

The Fallacy of the Dirac Sea

Although Dirac's genius led him to predict anti-particles, the argument that got him there was somewhat flawed.

Dirac's mistake was to misinterpret the meaning of ψ in his equation! He originally wrote down the Dirac equation as a relativistic generalisation of the Schrödinger equation, with ψ viewed as the wavefunction of a single particle. We now know that this is not the right interpretation: ψ should be viewed as a quantum field, whose excitations describe many particles, rather than the wavefunction for a single particle.

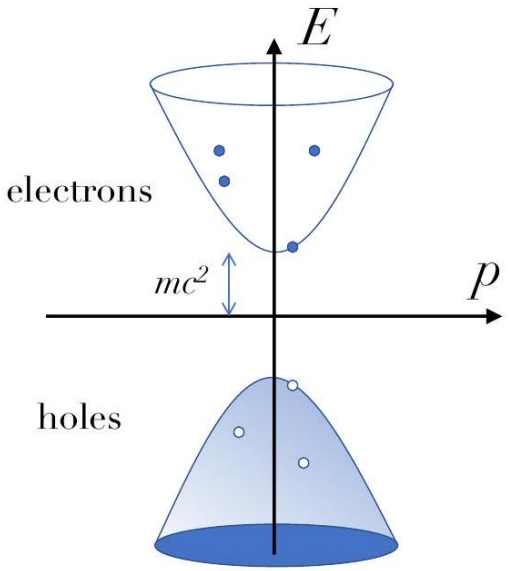


Figure 5. The filled Dirac sea, shown in blue, with holes interpreted as anti-matter.

We can explain what's going on here in a little more detail. The famous Einstein equation $E = mc^2$ tells us the energy of a particle of mass m when the particle is at rest. If the particle is moving with momentum p, then the correct formula is

$$E = \sqrt{p^2c^2 + m^2c^4} \tag{2.2}$$

where, for once, we've left the factors of c in the equation rather than setting $c = 1$. If you solve the Dirac equation, with ψ viewed as a wavefunction, then you find the two sets of solutions, but with energy

$$E = \pm\sqrt{p^2c^2 + m^2c^4}$$

The positive energy solutions are identified as, say, electrons. But what to do with the negative energy solutions? Note that as the particle moves faster, so p increases, and the negative energy solutions become more and more negative. This is problematic. If something can lower its energy then it usually does. But clearly we don't observe any particles getting faster and faster.

Dirac found a clever, but not altogether convincing, trick to escape from this conclusion. He suggested that the negative energy states were already filled by electrons. Because electrons are fermions, the Pauli exclusion principle means that no other electron is allowed to sit in these states, blocking the possibility for electrons to lose energy by tumbling to ever-lower states. This situation is shown in Figure 5.

In this picture, the vacuum of the universe consists of an infinite number of electrons. This is called the Dirac sea. One might worry about why we don't feel the infinite electric charge, but since this situation represents the ground state of the universe, Dirac argued that we reset the clock and say that this is what we mean by neutral. Any charge is now measured relative to this ground state.

Dirac's picture suggests that something novel may happen. We could excite an electron out of the Dirac sea, and into the positive energy states. This is shown in Figure 5. To do this, we need to inject a minimum of $E = 2mc^2$ energy into the system, to bridge the gap between the lower and upper bands in the figure. But if we can somehow achieve this, then we have created an electron out of the vacuum. But we have also created a hole, an absence of an electron, in the sea of negative energy states. In a zen-like manoeuvre, we now attribute properties to this

absence. Like the excited electron, it can freely move around. Because there's an absence of charge, relative to the vacuum it will appear to have positive charge. Finally, if the electron and the hole come into contact, the electron can drop back down into the negative energy state. It will appear as if the electron and hole have annihilated, releasing at least energy $E = 2mc^2$ in the process.

Dirac's picture of anti-particles is ingenious. But, ultimately, it's not the right way to think about things. If you view the object ψ not as a single-particle wavefunction, but rather as a quantum field, then the energy of both particles and anti-particles turns out to be positive. There is no need to invoke an infinity of electrons, disappearing to the bottom of the sea. Instead, there are no negative energy states: simply particles and anti-particles.

Moreover, it turns out that bosons also have anti-particles. But now there is no counterpart to the Dirac sea argument because bosons don't obey the Pauli exclusion principle. Meanwhile, bosonic anti-particles arise just as straightforwardly in quantum field theory as fermionic anti-particles.

Although Dirac's clever argument is not the right one for fundamental physics, it does turn out to have its uses elsewhere because it's a good description of what happens in solid materials. Any solid is made of atoms, and some number of electrons typically disassociate themselves from the nuclei and wander around which, in the quantum world, means that they fill up the lowest energy levels provided by the surrounding solid. In this context, this is called the Fermi sea but it is conceptually identical to Dirac's sea. When an electron is excited out of this sea, it leaves behind a hole. This hole - which is the absence of an electron - behaves in many ways like a particle with

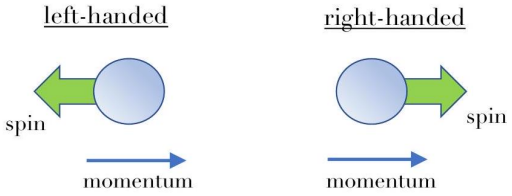


Figure 6. The handedness of a massless particle is determined by the relative direction of its spin and momentum.

positive electric charge. Indeed, there are some materials in which electricity appears to be conducted by positively charged particles. These aren't protons! They are holes.

There is a lesson here which is repeated over and over again in the history of science: a good idea tends to find a place in the world, even if it's not where it was originally intended.

2.1.4 Massless Particles

For massless particles, the story of spin needs to be slightly retold. Before we jump into the details, it's natural to ask: why bother? What spin $\frac{1}{2}$ particles in Nature are massless?

The answer to this question is shocking: all of them! One of the most striking features of the Standard Model is that, at the fundamental level, all the matter particles are massless. In fact, more than that, it turns out that it's not possible to incorporate masses into the theory without first doing some damage to some aspects of the weak force. This damage is achieved by the Higgs boson which, ultimately, is why the fundamental particles appear to have mass. We will describe all of this in Section 4. But, in preparation for that, it will be useful to explain here what becomes of spin when particles are massless.

Solving the Dirac equation, one finds that as a particle gets faster, its spin necessarily becomes oriented along the direction of motion. For massless particles, which travel at the

speed of light, there are two options: either the spin points in the same direction as the particle is travelling, or it points in the opposite direction. When the spin points in the same direction, the particle is said to be right-handed. When it points in the opposite direction, it is said to be left-handed. This is shown in Figure 6.

This distinction is quantified using something called helicity. If the particle moves with momentum $\mathbf{p}$ and the spin points in the direction $\mathbf{s}$ then the helicity is defined to be

$$h = \frac{\mathbf{s}\cdot\mathbf{p}}{|\mathbf{p}|}$$

Right-handed particles have helicity $+\frac{1}{2}$; left-handed particles have helicity $-\frac{1}{2}$.
Such a distinction doesn't make sense for massive particles. One can simply overtake the particle and look back to see it moving in the opposite direction, but with the spin remaining the same, so its helicity appears to be flipped. However, you can never overtake a massless particle because it travels at the speed of light, and this means that everyone agrees on the helicity of a massless particle.

In fact, one can go further. It turns out that, for massless particles, it is possible to have "half a Dirac fermion". This is a particle where only, say, the left-handed helicity exists. There is no particle at all with right-handed helicity. The anti-particle would then exhibit the opposite behaviour, only existing in the right-handed state, never lefthanded. A particle with these properties is known as a Weyl fermion. This idea will play a key role when we discuss the weak force.

I should stress that such Weyl fermions, with fixed helicity, are only possible for massless particles. The particles that we observe, such as electrons, do ultimately have a mass and they achieve this by gluing together two Weyl fermions to form a complete Dirac fermion, with both kinds of spin. We'll learn more about how this happens in Section 4.

4.2.2 2.2 Quantum Electrodynamics

The Dirac equation described in the previous section tells us that matter particles necessarily come with anti-particles. But for these particles to subsequently do something, they must interact. Those interactions happen through forces.

The simplest force in particle physics is electromagnetism. In large part, it is simplest because we have some classical intuition for this force: it is the same force understood many centuries ago by Coulomb, Ampére, Faraday and Maxwell, albeit dressed by some quantum bells and whistles.

The force is mediated by two fields, the electric field $\mathbf{E}(\mathbf{x},t)$ and the magnetic field $\mathbf{B}(\mathbf{x},t)$. Each of these is a vector field, meaning that at every point in space $\mathbf{x}$ and for every time t, the field is specified by both a magnitude and a direction.

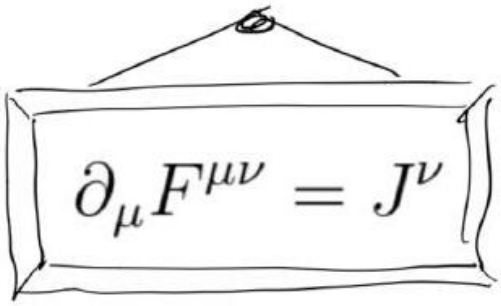
The equations that describe the dynamics of the electric and magnetic fields are known as the Maxwell equations. We won't need them in these lectures but, for completeness, here they are:

$$\begin{aligned} \nabla\cdot\mathbf{E} &= \tfrac{\rho}{\epsilon_0} \quad , \quad \nabla\times\mathbf{E} = -\tfrac{\partial\mathbf{B}}{\partial t} \\ \nabla\cdot\mathbf{B} &= 0 \quad , \quad \nabla\times\mathbf{B} = \mu_0\left(\mathbf{J} + \epsilon_0\tfrac{\partial\mathbf{E}}{\partial t}\right) \end{aligned} \tag{2.3}$$

The fields $\mathbf{E}$ and $\mathbf{B}$ react to the presence of electric charge density ρ and electric currents $\mathbf{J}$, while ϵ_0 and μ_0 are two constants that characterise the strength of the electric and magnetic forces in a way that we will describe more below.

The equations, as written above, hide the full beauty of the Maxwell equations. A better formulation encodes both the electric and magnetic fields in a 4×4 antisymmetric matrix called the field strength, which takes the form $F_{\mu\nu} = \partial_\mu A_\nu - \partial_\nu A_\mu$. Only then do the Maxwell

equations reveal their true simplicity, in a way that deserves hanging in a frame,



You can learn more about the Maxwell equations and their classical solutions in the lectures on Electromagnetism. Famously, among the solutions to these equations are electromagnetic waves, including visible light. When you look at these solutions through the lens of quantum mechanics, you find that they decompose into particles, known as photons.

A photon can come in two different states that we call polarisation. These are entirely analogous to the "spin up" and "spin down" states of the electron. (The fact that both spin 1/2 and spin 1 particles have two internal states is something of a coincidence. For example, it's only true in three spatial dimensions; the counting is different in other dimensions.)

The theory describing the electromagnetic field interacting with the electron field is known as quantum electrodynamics, or QED for short. It is the theory describing light interacting with matter, and ultimately underpins large swathes of science, including condensed matter physics and chemistry. Happily, it is also the simplest component of the Standard Model.

The Strength of the Interaction

Take two particles carrying electric charge Q_1 and Q_2 and hold them some distance r apart. The relevant solution to the Maxwell equations tells us that the particles experience a force given by

$$F = \frac{Q_1 Q_2}{4\pi\epsilon_0 r^2} \tag{2.4}$$

This is called the Coulomb force. The force is repulsive if the two particles carry charge of the same sign; it is attractive if they carry charges of opposite sign.

This formula shows us that the constant ϵ_0 characterises the strength of the Coulomb force. If the value of ϵ_0 was smaller, then Coulomb force would be more powerful. If you look up ϵ_0, you'll find some unhelpful number quoted with unit of Farads per metre. A more useful measure of the strength of the electric force comes from the dimensionless quantity known as the fine structure constant,

$$\alpha = \frac{e^2}{4\pi\epsilon_0\hbar c} \tag{2.5}$$

where e is the electric charge of the electron. It turns out that the value of the fine structure constant is roughly

$$\alpha \approx \frac{1}{137}$$

This is the cleanest way to characterise the strength of the electric force. In particular, in natural units with $\hbar = c = 1$, two electrons held a distance r apart experience a force given by

$$F = \frac{\alpha}{r^2}$$

Maxwell's equations also contain a second constant, μ_0, which characterises the strength of the magnetic interaction. It turns out that this is not independent from ϵ_0. One of the great discoveries of Maxwell is that the two constants are related by

$$\epsilon_0\mu_0 = \frac{1}{c^2}$$

with c the speed of light. As a side remark, note that if the strength of the electric force $1/\epsilon_0$ were weaker, then the strength of the magnetic force $1/\mu_0$ would necessarily be stronger.

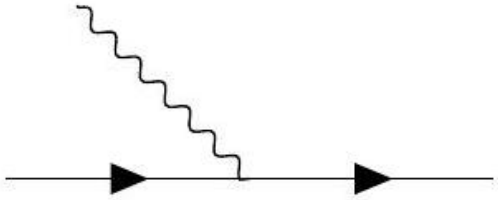
2.2.1 Feynman Diagrams

There are some simple cartoons that allow us to figure out what processes are allowed in quantum electrodynamics (and, indeed, in the other forces). These cartoons are called Feynman diagrams.

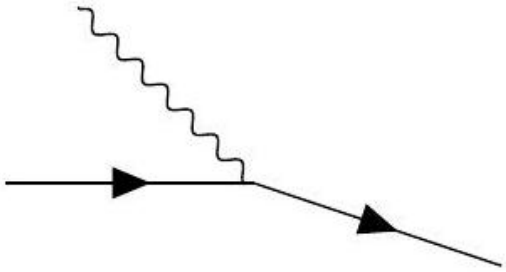
We will take time to run horizontally, from left to right [4]. We then draw electrons as solid lines with a forward pointing arrow, like this $\longrightarrow$.

Positrons are depicted as solid lines with a backwards pointing arrow, like this $\longleftarrow$. We'll see the utility of the backwards-arrow notation below. It suggests that it may be possible to think of anti-particles as particles that move backwards in time. There is mathematical sense in which this statement is correct, but it shouldn't be taken too literally.

Finally, photons are depicted as wavy lines like this
There is just a single interaction between the electron and photon, from which all other processes can be built. This can be viewed as an electron absorbing a photon, and scattering off in a different direction. It looks like this



The point where the photon hits the electron is referred to as a vertex.
Conservation of momentum means that the electron necessarily moves off in a different direction after absorbing the photon. So you might have thought that it would be better to draw the Feynman diagram like this



Indeed, sometimes we'll draw diagrams like this. However, the Feynman diagrams should not be read too literally: the paths aren't the actual paths of particles in spacetime. They should be viewed in a more topological fashion, like the London underground map. We'll say more below about what Feynman diagrams are, and what they aren't.

[04] This is the convention used in the Quantum Field Theory lectures, but it's not universal. Some authors prefer time to flow upwards.

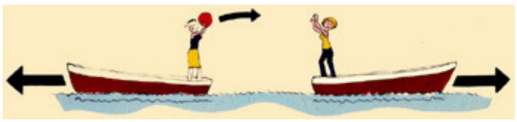
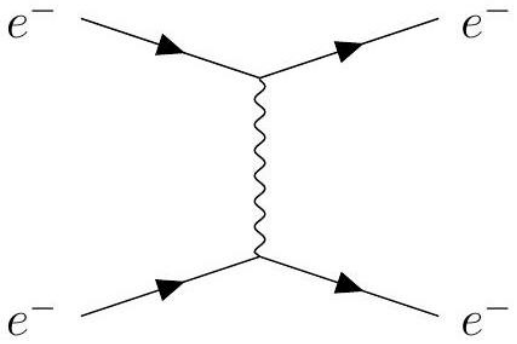


Figure 7. This is not a good analogy for virtual particles.

Now the game is as follows: you can describe any process by stitching together the Feynman diagram building blocks above. You can orient the different legs of the diagrams in any way you wish. You just have to make sure that the arrows on the solid lines follow each other. Any process that you can draw can happen, provided that it is allowed on grounds of energy and momentum conservation.

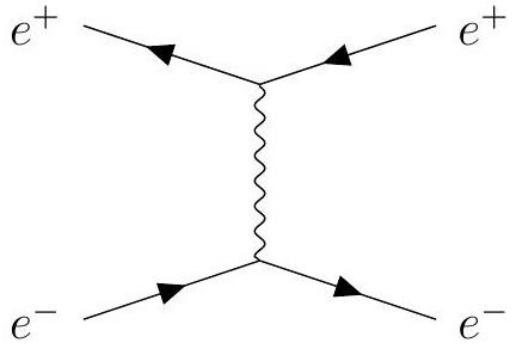
Let's look at some examples. Here is a Feynman diagram describing one electron scattering off another



I've added the name of the particle to the external legs, a practice that will prove useful as we progress. Note that the electrons don't just bounce off each other; there is no direct contact between them. Instead, the electrons scatter by exchanging a photon. Particles that appear only in internal legs of Feynman diagrams, like the photons above, are referred to as virtual particles. This is a lesson that we'll see repeated later: all forces can be understood by the exchange of virtual bosonic particles.

In some ways, Feynman diagrams are a little too evocative, and we should be careful not to interpret the diagram above too literally. For example, you shouldn't think of one electron as recoiling as it emits a virtual photon, which is then absorbed by the second, resulting in a repulsive force from Newton's third law, like two people in boats throwing a ball back and forth between themselves. This will then leave you puzzled about how such particle exchange can possibly lead to an attractive force.

Yet in quantum field theory, there is no problem with virtual particles describing an attractive force. Indeed, the Feynman diagram for the scattering of an electron off a positron is almost identical to the one above:

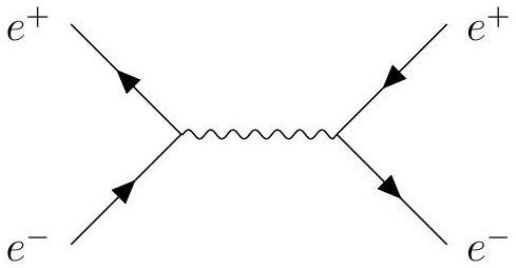


Translating this diagram into mathematics gives the attractive Coulomb force, but this isn't easily captured by the people-in-the-boat analogy. (If you get to the point where you start thinking about people in boats throwing boomerangs backwards and forwards then you might

realise that the analogy has clearly been stretched too far.)

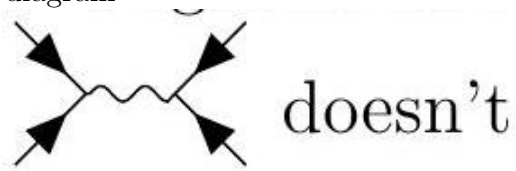
In fact, what's really going on here is that both of the scattering diagrams above are a reformulation of the familiar result from classical physics in which one electron experiences a force due to the electric field of another. If you translate the diagram above into mathematics, you will find that it is simply a rewriting of the Coulomb force law (2.4). Viewed this way, the "virtual particles" are merely a handy device to capture the behaviour of the underlying field. If we were to think in terms of fields, then we have no need to discuss virtual particles. Moreover, there are situations - like for the strong force - where the concept of virtual particles is not useful, while the fields remain.

For the scattering of an electron off a positron, there is a second, qualitatively different diagram that also contributes.



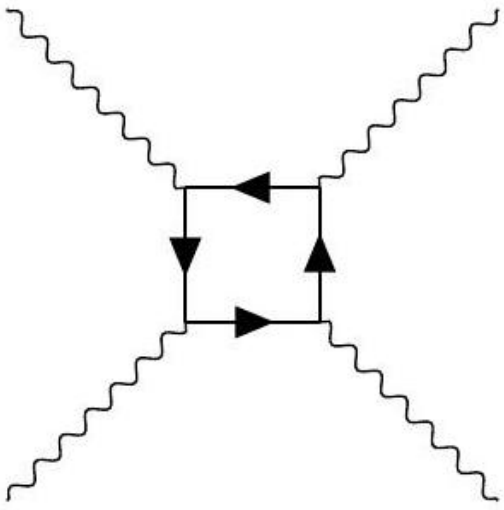
This has the interpretation of the electron-positron pair annihilating into a virtual photon, which then turns back into a pair of particles. It turns out that this diagram doesn't contribute to the Coulomb force (2.4), which holds only in the non-relativistic limit where velocities of all particles are low, but does change the scattering behaviour at higher energies. For our purposes, however, it is useful simply to illustrate the utility
of the forwards/backwards arrow notation for particles and anti-particles: they capture the conservation of electric charge.

The total electric charge of an electron-positron pair is zero, which allows them to annihilate into a (virtual) photon. In contrast, such a process isn't possible for the scattering of two electrons, because their charge is non-zero. In the diagrammatic language, we see this because the corresponding Feynman diagram



have the arrows matching up, and so is illegal.

There are also interesting processes that we can construct with photons on the external legs. For example, here is a diagram that corresponds to one photon scattering off another



Famously, light doesn't scatter off itself in the classical world. This is important, for it allows us to see! But it's no longer true in the quantum world. The diagram above can be viewed as a light scattering off a particle-anti-particle pair which briefly appear as a vacuum fluctuation. The probability for such a process is small, which is why we don't notice this process every day. But, although small, it is non-zero, and light-by-light scattering has been observed in particle colliders.

2.2.2 What is a Feynman Diagram Really?

All quantum processes have an element of randomness. Particle physics is no different. If you collide two particles together at high energies, there are many possibilities for what may emerge. Quantum field theory allows us to assign probabilities - or, more precisely, quantum amplitudes - to all of these possibilities.

However, there's a hitch. Quantum field theory is hard, and the expressions for these probabilities are ridiculously complicated. In many situations, we have no idea how to compute them. However, for QED we can make progress based on the observation that the interaction strength, as captured by the fine structure constant $\alpha \approx 1/137$, is small. This means that we can expand the complicated probabilities in a perturbative expansion, rather like Taylor expanding a function.

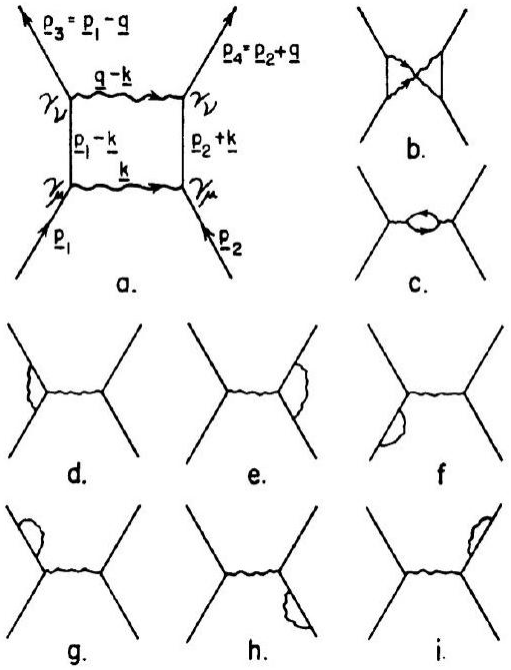
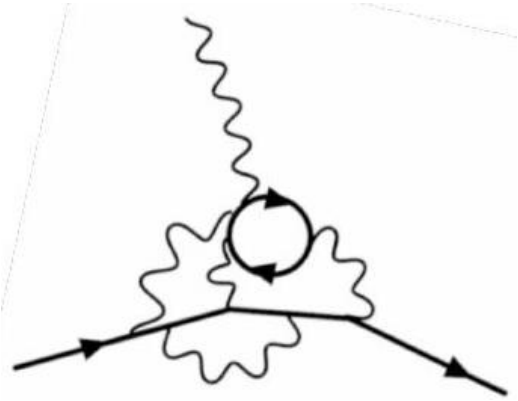


Figure 8. A handful of Feynman diagrams, taken from Feynman's original paper.

The Feynman diagrams are a pictorial way of capturing this perturbative expansion. Suppose that you want to compute the probability for some process to happen, for example the electron-positron scattering described above. The process itself is defined by the external legs of the diagram - these are what tell you, for example, that you start with two particles and end up with two particles. Given this data, you should now write down all possible Feynman diagrams. The diagrams that we drew above are the simplest diagrams, but there are an infinite number of diagrams contributing to any process with an increasingly complicated structure of internal lines. For example, the original vertex can be dressed with all sorts of other lines, to give things that look like this:



Some examples of Feynman diagrams for $e^- + e^+$scattering are shown in Figure 8
So far, this procedure doesn't sound very helpful. We have to write down an infinite number of ever more elaborate diagrams to describe any process. Moreover, there are rules which translate each diagram into a mathematical expression, usually involving
some very complicated and challenging integrals. What saves us is the fact that the more complicated a diagram, the less important it is in some process. To compute the importance of any diagram, you need simply to count the number of vertices. While the exact contribution of any diagram may be very difficult to compute, the happy news is that it is proportional to

$$\alpha^{\#\text{ of vertices}}$$

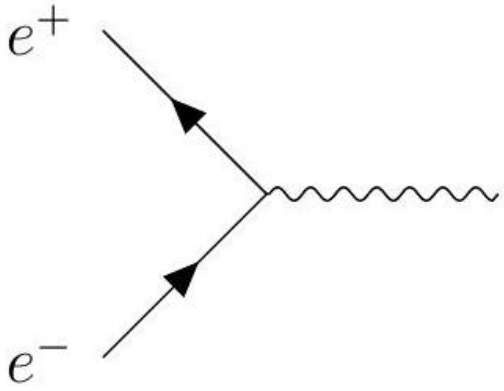
So, for example, a diagram with a single vertex will mean that the probability is something in the ballpark of 1/137. Meanwhile, the the elaborately dressed vertex shown above contributes something proportional to α^9. With $\alpha \approx 1/137$, this kind of diagram barely changes the answer, and so can be safely neglected. The light-by-light scattering diagram that we showed earlier comes in at α^4, explaining why we don't observe this phenomena in every day experience.

There is one important lesson to take from this: the utility of Feynman diagrams is intimately connected to the weakness of the electromagnetic interaction. In situations where the interactions between fields are strong, Feynman diagrams are not the right way to think about the physics.

If you want to learn more about how to unmask Feynman diagrams, and turn them back into the underlying equations, then you can find details in lectures on Quantum Field Theory.

Some Examples

To illustrate these ideas, we can compute the relative probabilities that an electron and positron will annihilate to a bunch of photons. First, we need to address a subtlety. It's possible to draw a diagram representing an annihilation to a single photon:



This would appear to be proportional to α. However, if you calculate this diagram, you'll find that it's vanishing. This is because although it is consistent with charge conservation, it's

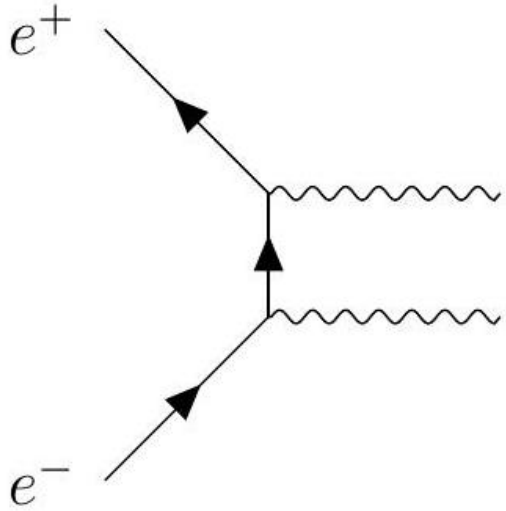
not consistent with the conservation of energy and momentum. To see this, consider the frame in which the electron and positron have equal and opposite momenta. The outgoing photon must then have vanishing momentum, but non-vanishing energy, and this isn't possible.

It's worth pointing out that this diagram can occur as a sub-diagram in other processes. For example, we already used it in electron-positron scattering, In this case, the intermediate photon is virtual and it turns out that there's no requirement for virtual particles to obey the usual energy-momentum relations. You can handwave this away by saying that virtual particles can borrow energy for some period of time by virtue of (the slightly dodgy version of) the Heisenberg uncertainty relation: $\Delta E \Delta t \sim \hbar$.

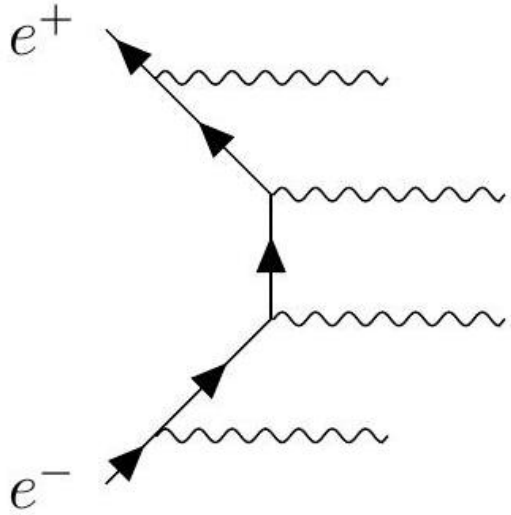
Back to the annihilation of an electron and positron, the simplest process results in two photons:

$$e^+ + e^- \to \gamma + \gamma$$

This is described by the following Feynman diagram:



From our discussion above, we know that this is proportional to α^2. But other processes are possible. For example, the pair could annihilate to any number $n > 1$ of photons. For example, the diagram for annihilation to four photons is



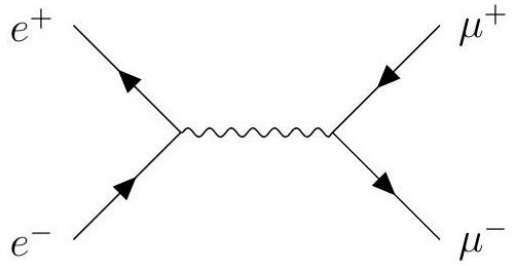
This probability for such a diagram is proportional to α^4. This means that the probability of getting four photons our of a collision is suppressed by a factor of α^2 relative to the probability of getting two photons.

2.2.3 New Particles From Old

Electrons are not the only particles that experience the force of electromagnetism. Any particle that carries electric charge also interacts with the photon. In particular this means that all fermions, except for the neutrinos, feel the force of electromagnetism.

We can easily extend our Feynman diagrams to include these extra particles. By convention, we depict any fermion with a forward arrow $\rightarrow$ and any anti-fermion with a backward arrow $\leftarrow$, but now we must label these lines with the particle name to show what particle we're talking about. Every particle with electric charge will have an interaction vertex of the form $\xrightarrow{h}$. When evaluating Feynman diagrams, these vertices contribute a factor of $Q^2\alpha$ to the probabilities, where Q is the charge of the particle, in units where the electron has $Q = -1$.

This brings new opportunities. For example, we can collide an electron and positron, but now produce new particles such as a muon-anti-muon pair as shown in the diagram below.



We still have to worry about energy and momentum conservation when evaluating this diagram. If, in the centre of mass frame, the energy of the incoming electron-positron pair is less than $2mc^2$, the rest mass of the muon-anti-muon pair, then the muons cannot be produced. However, when the incoming energy exceeds this threshold, then we can start to produce new particles from old ones. The same kind of process allows us to produce any charged particles from the collision of electrons and positrons. This, of course, is the basis for particle colliders.

4.2.3 2.3 Renormalisation

At the fundamental level our world is built not from particles, but from fields. Moreover, as we stressed in the introduction, these fields froth and foam in the uncertain quantum world. This gives rise to an important phenomenon known as renormalisation.

Let's consider a single electron. It gives rise to an electric field which, like the force, varies as an inverse square law,

$$\mathbf{E} = \frac{e}{4\pi\epsilon_0 r^2}\hat{\mathbf{r}}$$

where $\hat{\mathbf{r}}$ is the unit vector pointing radially outwards. Clearly the electric field gets bigger and bigger as we approach the position $r = 0$ of the particle. But what is happening to the electron field near this point? It turns out, that both electric and electron fields start thrashing wildly as we get near to $r = 0$.

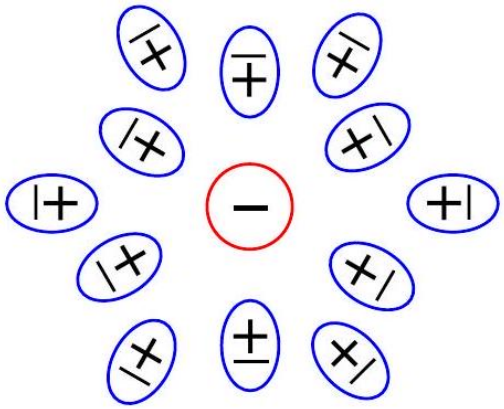
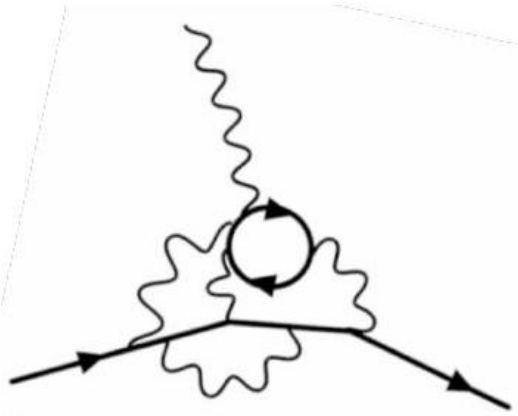


Figure 9. The renormalisation of electric charge.

While it's challenging to talk about quantum fields, we can build some intuition by reverting to the language of particles. As we get closer to the electron, the electric field gets stronger and, as a result, the energy density stored in the field gets larger and larger. At some point - a distance of around 10^{-12} m - the energy density is so large that an electron-positron pair can be produced from the vacuum.

There is a general rule in quantum field theory that anything that can happen does, in fact, happen. This means a single electron is surrounded by a swarm of particle-antiparticle pairs, continually popping in and out of the vacuum. As we get closer still, muons, taus and even quarks will also appear in the mix. We learn that any simple picture you may have of a single particle giving rise to the electric field is really very far from the truth: it is impossible to enforce any kind of social distancing in the quantum world.

This story should really be viewed in terms of quantum fields. When we talk of a swarm of particle-antiparticle pairs, it is really a metaphor for the quantum field being excited in a tangled and elaborate fashion. Just as the vacuum is something complicated in quantum field theory, so too is the notion of a single particle.



In the language of Feynman diagrams, these particle-anti-particle pairs are captured by the diagrams that include loops of particles, like the one shown on the right.

The excited quantum field has an important consequence for the strength of the electromagnetic interaction. Again, we can understand this in the language of particles. The swarm of particle-anti-particle pairs will not be oriented randomly around the electron. Instead, the positrons, which carry positive charge, will be attracted to the

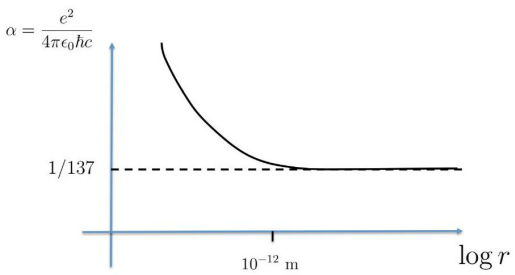


Figure 10. The renormalisation of fine structure constant.

electron in the centre, while the electrons will be repelled, as shown in Figure 9. The net effect is that as you get closer to the electron, you find more and more negative charges outside you. Which must mean that the original charge must have been bigger than we see. This is an effect known as screening. This swarm of particle-anti-particle pairs is actually hiding the true charge of the electron in the centre.

In fact, an excellent analogy of this phenomenon arises in metals. Take a positive charge and place it in a metal. The mobile electrons will enthusiastically cluster around, screening the positive charge so that it can't be detected at large distances. This is very similar to what happens with the electron in the vacuum and is one of many situations in which ideas in particle physics are mirrored in condensed matter physics.

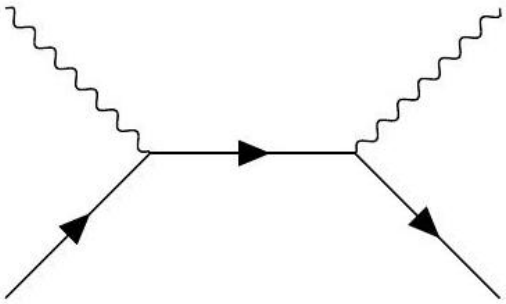
Because the effective charge of the electron gets bigger at shorter distances, so too does the interaction strength as captured by the fine structure constant (2.5). In fact, we learn that the fine structure constant is very badly named, since it's not in fact constant at all. At distances larger than $r \gtrsim 10^{-12}$ m, it plateaus to the usually quoted value of $\alpha \approx 1/137$. But as you go to smaller scales, the strength of the electromagnetic interaction increases logarithmically. For example, the strength of the interaction has been well measured at the scale of the weak force, which is roughly $r \approx 10^{-17}$ m, where it is found to be $\alpha \approx 1/127$. A sketch of the variation of the fine structure constant often referred to as running - is shown in Figure 10.

The lesson of renormalisation as described above is a general one. It turns out that none of the dimensionless physical constants of nature are, in fact, constant. All of them depend on the distance scale you're looking at.

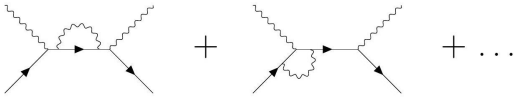
2.3.1 The Long, Confusing History of Renormalisation

While the description of renormalisation described above is fairly straightforward, the mathematics underlying it is not. For this reason, our forefathers had to travel a long and tortuous road to make sense of quantum field theory in general, and the issue of renormalisation in particular.

The story starts in the late 1920s, soon after the original development of quantum mechanics. The quantum pioneers - Heisenberg, Dirac, Pauli and others - tried to apply their ideas to the interaction of light and matter. They tried to ask very simple questions, like the probability for a photon to scatter off an electron. While they didn't have the diagrammatic tools later introduced by Feynman, they did understand that we could approach the problem in a perturbative expansion, starting with a process which we now draw like this:



They found that this calculation gave pretty good agreement with the experiments. But then they tried to do better, and compute the leading corrections. In diagrammatic language, this means evaluating diagrams like this



However, here they ran into a problem. Each of these subsequent diagrams was proportional to α^4, as expected. But the proportionality constant was infinity. That made it very hard to argue that the contribution from these diagrams was smaller than the first.

The quantum heroes worked on this problem for well over a decade but made little progress. Looking back, many of their ideas were simply too crazy. Having forged one revolution they were, like Che Guevara, all keen for the next. Bohr wanted to get rid of energy conservation. Heisenberg wanted to make spacetime non-commutative. Pauli wanted to invade Bolivia. Yet the answer they were seeking did not, ultimately, require an overhaul of the foundations of physics. It needed a different approach.

The war intervened and, as life returned to normal, a new generation of physicists took up the challenge, foremost among them Tomonaga in Japan, and Schwinger, Feynman and Dyson in the US. They were helped in no small way by a new experimental result, discovered by Willis Lamb. The eponymous Lamb shift is a tiny, but detectable change to the energy levels of hydrogen due to the problematic one-loop Feynman diagrams. Their solution was a slow-burn revolution, one that took many decades to play out as the power of quantum field theory became clear. However, at the time it didn't feel like a revolution. It felt like a con. Their solution was this:

$$\infty - \infty = \text{ finite}$$

In other words, they found a mathematical procedure that allowed you to subtract one infinity from another, leaving an unambiguous finite answer. They called this process renormalisation. The results were nothing short of spectacular.

The poster boy for renormalisation is a quantity known as the magnetic moment of the electron. If you place an electron in a magnetic field, then the spin of the particle will precess, as shown in figure. The speed at which the spin precesses is characterised by a dimensionless number g known as the electron's magnetic moment.

In the grand scheme of things, this number is not particularly important. However, it has played a key role

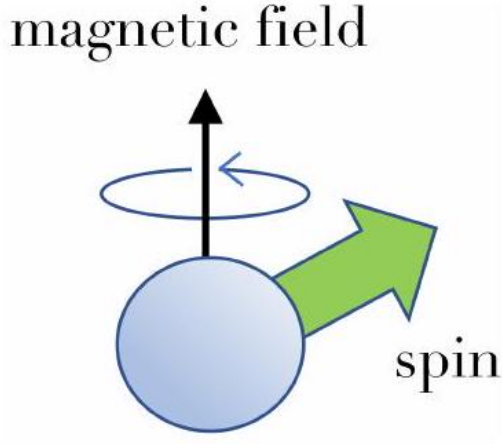


Figure 11. The precession of a spin

in the development of quantum field theory because it is a quantity that we can determine with some accuracy, both experimentally and theoretically. After many decades of painstaking work, the experimental result for the electron magnetic moment is

$$g_{\text{expt}} = 2.0023193043617 \pm 3$$

Meanwhile, after many decades of extraordinarily challenging calculations, evaluating increasingly complex Feynman diagrams up to corrections of order α^5, the theoretical result is

$$g_{\text{theory}} = 2.00231930436\ldots$$

The agreement is awe inspiring. In most areas of science you jump up and down with joy if you get the first digit right. In economics you don't even need that. Yet here there is agreement between theory and experiment to 12 significant figures [5] !

Despite this runaway success, there was something a little disquieting about renormalisation. The idea that you can take one infinity away from another, to leave something finite was not mathematically legitimate. This was Feynman's take:

> "The shell game that we play to find [the answer] is technically called renormalization. But no matter how clever the word, it is what I would call a dippy process! Having to resort to such hocus-pocus has prevented us from proving the theory of quantum electrodynamics is mathematically self- consistent. .... I suspect that renormalization is not mathematically legitimate."

The physical meaning of renormalisation took several more decades to uncover. And it came from an unusual place: the attempt to understand boiling water! In particular, when water is close to the critical point, it turns out that the physics can be understood using very similar Feynman diagram techniques to those employed in particle physics. But this time there are no infinities. That's because when you get to the place in the calculation where infinities might rear their head, you need to remember that water isn't infinitely divisible, but is made of atoms. When you take this into account, the infinities in the diagrams simply aren't there.

But the same should also be true of quantum field theories in particle physics. There is no reason to think that our theories are valid to arbitrarily high energies, or arbitrarily short distance scales. A modern perspective on renormalisation absorbs this lesson. Just as Newtonian mechanics comes with a health warning, stating that you shouldn't trust it in extreme situations - when speeds become too large, masses become too heavy, or particles

become too small - so too does quantum field theory. No quantum field theory should be trusted to arbitrarily small distance scales, or arbitrarily high energies. That would be hubris. Instead, we should admit that there is an energy scale beyond which our theory no longer applies. This energy is called the cut-off. For

the Standard Model, the cut-off is somewhere above 1 TeV . Simply injecting a little humility into the proceedings, and admitting that we don't yet understand everything, is sufficient to remove the infinities.

But now there is a new problem. We must make sure that no physical answer depends on our choice of the cut-off. After all, the cut-off is an expression of our ignorance, the limit of our current knowledge. It would be very unsatisfactory if something physical like, say, the electron mass depended on what we don't know about physics at high energies.

It took many scientists many years to figure out how to include a level of our ignorance in the theory, without anything depending on our ignorance. The different parts of the story were finally pieced together in the early 1970s by Kenneth G. Wilson. His work is surely the most influential piece of theoretical physics in the latter part of the 20^{th} century, and now has applications from particle physics to biological physics to gravitational physics. Wilson's insight was that nothing you can physically measure depends on the choice of cut-off providing that physical quantities are not constant: they must change depending on the scale at which you explore the world. This is way that we introduced renormalisation in the previous section. Moreover, the complicated and dubious calculations which seemingly gave $\infty - \infty =$ finite can be reinterpreted in a more palatable way as telling us how quantities change with scale.

This new approach is sometimes referred to as the Wilsonian renormalisation group, to distinguish it from the older approach of Feynman and others. You can read more about this in the lectures on Statistical Field Theory.

The upshot of this is that if you do quantum field theory carefully, there are no infinites. But neither are there (dimensionless) constants of Nature. Instead, one key lesson of quantum field theory is that the universe in which we live is organised by scale. If you want to write down a theory of our world, then you need to explicitly state the scale at which the theory holds. Change the scale, and you must change the theory. Or, at the very least, you must change the parameters of the theory.

There is a final twist to this. The Feynman quote on the previous page is from 1985, fifteen years after Wilson did his crucial work and three years after Wilson was awarded the Nobel prize. I don't know why Feynman still held that opinion at that time. It is conceivable that he was unaware of the importance of Wilson's work. After all, the detailed calculations are not wildly different from those Feynman himself did decades earlier, and perhaps he did not appreciate the all-important change of emphasis. Or perhaps he simply didn't like the truth getting in the way of a good story.

4.2.4 B Interlude: Looking to the Sky

Radioactivity was a gift to physicists. Beta decay provided the first insights into the weak force, a topic we will return to in Section 4, while beams of alpha particles which can reach energies up to 5 MeV - were used as a microscope to peek into the nucleus for the first time. As we learned in Interlude A, both the proton and the neutron were discovered by bombarding other elements with alpha particles.

[05] The same calculations for the magnetic moment of the muon give $g_{\text{theory}} = 2.00233183602$ and $g_{\text{expt}} = 2.00233184122$. Although the agreement is impressive, it fails at the 10^{th} significant figure. This is one of the very few discrepancies between theory and experiment. If this disagreement is borne out, it may be due to the effects of new particles, beyond those of the Standard Model. If nothing else, this discrepancy should serve to show just how astonishingly good the Standard Model really is: there are surely no other areas of science where people have sleepless nights over a failure in the 10^{th} digit.

But 5 MeV can only get you so far. Looking inwards requires higher energies. The smaller the distance scale you want to explore, the higher the energy you need. Ultimately, progress was made by constructing particle accelerators, but physicists first made use of another of Nature's gifts: cosmic rays.

The Rise of the Balloon

Our world is constantly bombarded by charged particles from the cosmos. These particles - which are collectively known as cosmic rays - are mostly protons or helium nuclei, with the occasional electron and heavier nuclei thrown in for good measure. They travel enormous distances before reaching us, originating far outside our galaxy in supernova explosions or in the accretion discs which surround supermassive black holes in the centre of other galaxies.

When cosmic rays hit the upper atmosphere, they create a shower of new particles, many of which survive the journey down to Earth where they can be detected. Theodore Wulf was the first to realise that there was something interesting to be explored. In 1910 he built a simple electrometer to detect ionised particles in the atmosphere. At the time, it was thought that this ionising radiation was emitted by the Earth. Wulf had the simple but brilliant idea to test this by climbing the Eiffel tower to perform his experiment. He found that the amount of radiation did indeed drop, but nowhere near as quickly as one would expect. Something was afoot.

The challenge was accepted two years later by Victor Hess. Needing to get to greater heights, he took up ballooning. At a height of 1 km , he found that the radiation was more or less the same as on Earth. At a height of 5 km , he found the radiation was nine times greater. To test various hypotheses, he flew in the day and he flew at night. He even flew during a solar eclipse. He concluded that either there was some unknown substance hiding in the upper atmosphere, or the radiation had an extraterrestrial source. He called it ultraradiation.

The name didn't stick. In Caltech, Robert Millikan (of oil drop fame) turned his attention to this new phenomenon. He had a better name: cosmic rays. More importantly, he also had resources and a team of brilliant experimenters who could explore their implications.

With hindsight, it's very clear why cosmic ray showers provided such an opportunity for particle physics. Radioactivity offers alpha particles with energies up to 5 MeV . Cosmic rays have no such limitations. A plot of the energy vs the flux of cosmic rays is shown to the right. As you can see, cosmic rays with energies of 1 GeV are common place, but energies extend up to 10^{11} GeV , way beyond what we can create in colliders. To find interesting physics, we just need to have our detec-

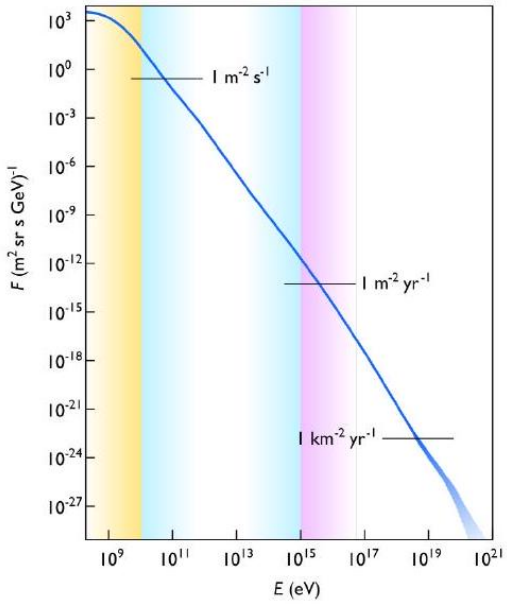


Figure 12. The distribution of cosmic ray energies. Image from Wikipedia.

B. 1 The Positron

In May 1931, after struggling for some years with the meaning of the negative energy solutions of his equation, Dirac finally made the bold leap and predicted the existence of anti-electrons. In September 1932, Carl Anderson announced the discovery of a new particle, with the same mass as the electron, but opposite charge. He later named this particle the positron. Rather surprisingly, the discovery of anti-matter owed essentially nothing to its earlier theoretical prediction.

Anderson's interest was in cosmic rays. Unlike Hess, however, he had no intention of getting in a balloon. With a good detector, he needed to climb no higher than his third storey office to study the showers from cosmic rays.

Anderson's detector was the cloud chamber. We already briefly met a preliminary version of the cloud chamber in Section A. 2 when describing J.J. Thomson's discovery of the electron. In the intervening years, it was perfected and was usually referred to as the Wilson cloud chamber after its inventor, C.T.R. Wilson. When a charged particle passes through the chamber, it leaves behind a path of ionised gas particles, around which droplets subsequently condense. The result is that an elementary particle leaves behind a misty trail, visible to the naked eye, like the contrails left by a plane in sky.

Working at Caltech under the guidance of Millikan, Anderson built a cloud chamber sitting within a magnetic field of 25,000 Gauss. The purpose of the magnetic field was

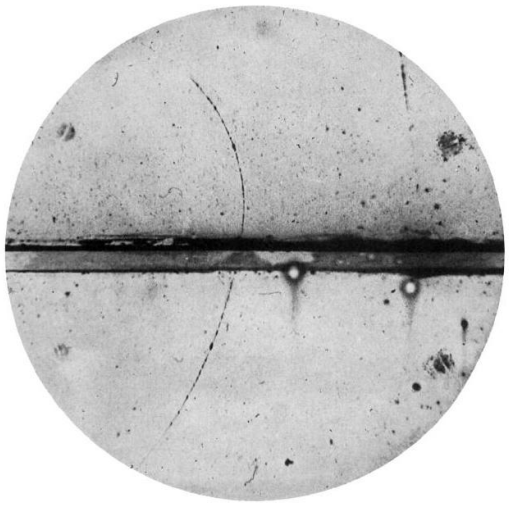


Figure 13. Anderson's first published picture of a positron. You can see the layer of lead running through the middle. The positron entered the cloud chamber at the bottom left, was slowed by the lead, with the trail visibly more curved after it exited. Somewhat unusually, this positron arose from a cosmic ray collision below the detector.

to bend the trajectory of a charged particle, allowing one to get a handle on the ratio e/m of charge to mass. Anderson found trajectories bending in both directions. Those that bent in one direction were clearly negatively charged electrons, coming down from the sky. But what about those that bent in the other direction? They were too light to be protons. However, they could have been electrons coming up from the ground. It seemed unlikely because, as Milikan pointed out: "Everyone knows that cosmic ray particles go down. They don't go up except in very rare circumstances".

To better understand what was going on, Anderson placed a thin, horizontal layer of lead in the the cloud chamber. This wasn't thick enough to stop the particles completely, but it did cause them to lose a significant amount of energy as they passed through. This meant that the particle would be travelling more slowly after it passed through the lead, and so its trail would bend in a tighter curve. In this way, Anderson was able to determine the direction of the particle and, hence, its charge. He found, in the words of his original paper, an "easily deflectable positive".

Anderson's results were soon confirmed by others, notably Patrick Blackett and Giuseppe Occhialini in Cambridge. Indeed, the week before Anderson dropped his bombshell, Blackett and Occhialini published a paper in Nature entitled "Photography of Penetrating Corpuscular Radiation" in which they boasted about their new toy, a cloud chamber in a high magnetic field, rigged up to work only when an accompanying

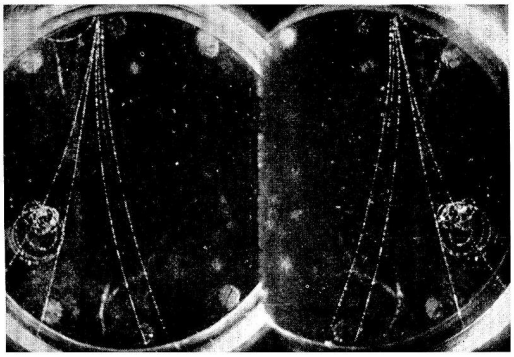


Figure 14. This cloud chamber track, showing electrons and positrons veering in opposite directions, was taken by Anderson and his student Seth Neddermeyer in 1936. They were still avoiding balloons, but climbed to Pike's Peak in the Rocky mountains, 4300 m above sea level, where, as they stated in the abstract, "the proportion of such tracks is considerably greater than at Pasadena."

Geiger counter triggered. They illustrated their paper with a few uninspiring photographs to show that the machine worked. It was only after they heard of Anderson's result that they realised they focussed on the wrong images: among their photographic plates were positrons in "great abundance". The pain of this oversight must have been felt even more acutely given that they were colleagues of Dirac. As a (very!) small compensation, they did quickly find something that Anderson had missed: the creation of electron-positron pairs within the chamber.

Later, when asked if they were aware of Dirac's theory when performing their experiment, Blackett replied that he ...

> "... could not recall but that it did not matter anyway because nobody took Dirac's theory seriously."

This seemed to be the prevailing attitude, at least among experimenters. Neither Anderson's original discovery paper, nor a longer paper published in 1933 in which he introduces the name positron, mentions the theory of Dirac [6]. Anderson later recalled:

"The Dirac work was not an important ingredient in deciding which way the experiments should be carried out or what should be done experimentally."

Rutherford, begrudging as always towards theorists, took things one grumpy step further: "It seems to me that in some way it is regrettable that we had a theory of the positive electron before the beginning of the experiments. Blackett did everything possible not to be influenced by theory, but the way of anticipating results must inevitably be influenced to some extent by theory. I would have liked it better if the theory had arrived after the experimental fact had been established."

B. 2 Expecting a Meson

At this point our story of discovery gets somewhat out of sync with the main thread of the lecture notes. To understand what happened next, we must first make some comments on the strong nuclear force. We will describe the theory underlying this force in much more detail in Section 3.

[06] As a slightly bitchy aside, it appears that theory wasn't Anderson's strong point. His longer paper on the positron ends with the "the proton will then in all probability be represented as a complex particle consisting of a neutron and positron".

The first hint that a new force was needed to explain the structure of the nucleus came from (who else?) Rutherford. In 1917, he started a series of experiments, following the set-up of Geiger and Marsden but replacing their sheets of metal with hydrogen.

The charge on a hydrogen nucleus is almost 80 times smaller than that of the gold used in the original Geiger-Marsden experiment. This means that the Coulomb repulsion is significantly smaller and the α particle can get much closer to the nucleus. Rutherford noted that the scattering of α-particles no longer agreed with his formula (A.2) that had worked so successfully in the past. Nor did it agree with a more detailed study by Darwin that assumes a Coulomb repulsion, but allows for scattering of the nucleus as well as the α-particle.

We now know that this is because the α-particle and hydrogen nucleus get close enough to experience the strong force. However, the world wasn't quite ready for a new force and Rutherford originally suggested that the effect could be explained by some deformation of the α-particle.

As time went on, this interpretation became increasingly untenable. At a meeting at the Royal Society in 1929, Rutherford stated clearly
"The hydrogen and helium nucleus appears to be surrounded by a field of force of unknown origin"

But what are the properties of this force field?
The key insight was made in 1934 by the Japanese physicist Hideki Yukawa. He realised that if there were a new spin 0 particle [7] of mass m then it would give rise to a potential energy between particles which varies with the separation r as

$$V(r) \sim \frac{e^{-r/R}}{r}$$

This is now known as the Yukawa potential. It has the property that it quickly goes to zero for $r \gg R$, where the range R of the potential is inversely related to the mass as

$$R = \frac{\hbar}{mc}$$

This is the same relationship between energy and length that we met earlier in when describing the Compton wavelength (1.2). The data available at the time suggested that the strong force had a range of about $R \approx 2 \times 10^{-15}$ m. This meant that if you wanted to explain the strong force in terms of some field, you should be looking for a new particle approximately 200 times heavier than the electron, or

$$m \approx 100\text{MeV}$$

The idea languished until 1937, when just such a particle was found.

B. 3 The Muon and the Pion

The discovery of the muon didn't happen overnight. There was no smoking gun event that people could point to and shout "Eureka". Instead it was more of a slow burn as, from 1934 to 1937, an increasing number of cosmic ray tracks had absorption properties that didn't seem to fit theoretical expectations.

The prime driver in these discoveries was, once again, Carl Anderson, now working with his recently-graduated student, Seth Neddermeyer. As they understood more about cosmic rays, they found tracks that didn't lose energy as quickly as theorists predicted. But it wasn't clear whether the theorists should be trusted, or whether the data contained something more interesting.

[07] This is draped in a little bit of hindsight. Yukawa's original paper suggests a massive spin 1 particle, but

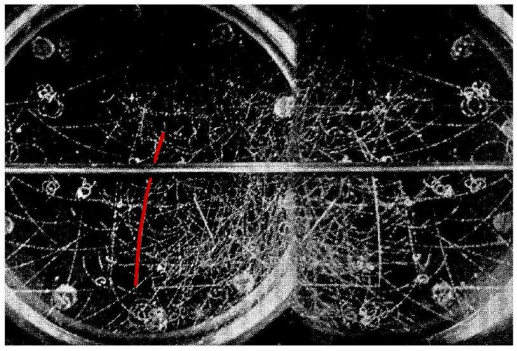


Figure 15. A cloud chamber picture from the same 1936 paper as Figure 14. The track daubed in red by my ipad pen was difficult to interpret as either an electron or a proton.

Already in 1936, Anderson and Neddermeyer published results which didn't conform to expectations. They pointed out that the red track shown in Figure 15 is too ionizing to be identified as an electron, but travels further than expected from a proton. In 1937, they finally bit the bullet, concluding that "there exist particles of unit charge but with a mass ... larger than that of a normal free electron and much smaller than that of a proton."

By 1939, the data seemed to suggest that this new particle had a mass 200 times heavier than the electron. The connection to Yukawa's proposed particle was obvious and a number of names were suggested for this new particle, including "yukon". Physical Review, pedantic as ever, insisted on "mesotron". Physicists ultimately converged on "meson", with the meso- from the Greek "mid".

However, as time went on, less and less about this new meson made sense. Models of nuclear binding worked much better with a particle that was slightly heavier and decayed significantly quicker. More brutally, experiments in 1946 showed that the interaction of the new meson with nuclei was around 10^{12} times weaker than that predicted by Yukawa's theory. That was too large a discrepancy to overlook!

Resolution

Happily the situation was resolved not long after. The discovery was made in 1947 in Bristol, England by a group of scientists led by Cecil Powell. Whenever Powell's collaborators are mentioned, people always include Giuseppe Occhialini (who recall, just missed out on the discovery of the positron) and sometimes César Lattes. But

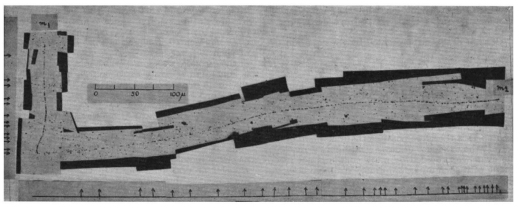


Figure 16. The discovery of the charged pion. It enters in the top left (labelled $m_{1 $), slows in the bromide and comes to rest, before decaying into a muon that flies off to the right (labelled m_2) and an anti-neutrino which is invisible in the picture. The caption in the paper starts with the comment "Observation by Mrs I. Roberts".}

only looked at the contribution from the first component, analogous to focussing on the just the electrostatic potential and ignoring magnetic fields. Later, in 1937 with Sakata, he developed the theory with a massive spin 0 field.

they rarely mention the fourth author on the paper, a poor graduate student by the name of Hughes Muirhead. And they certainly never mention the people behind the scenes who did the hard work: a team of women who painstakingly studied the images under microscopes to find the interesting events [8].

The discovery made by Powell's team was possible, as always, because they had a new piece of kit. Powell developed a new way of detecting particles by coating a glass plate with a photographic emulsion. When a charged particle passes through, it activates the emulsion, leaving behind a trail of silver bromide. They exposed their photographic plates to cosmic rays at high altitude, in balloons and on mountains, including Jungfraujoch and Kilimanjaro. When developed, the plates revealed a new meson, one both heavier and more short-lived, which decays quickly to the earlier meson. The V-shaped tracks were first found by Marietta Kurz, but these sat towards the edge of the emulsion and so were considered incomplete. A few days later, two clear L-shaped tracks were found by Irene Roberts. This was the long-sought meson.

Now, of course, we had two "mesons", rather than one. It quickly became clear that the particle discovered by Roberts had the properties expected of Yukawa's meson and, as we explain in the next section, can be viewed as the glue that binds together the proton and neutron in the nucleus. This became known as the π-meson, or pion. It is

not an elementary particle but is, we now know, composed of quarks. Meanwhile, the particle discovered by Anderson and Neddermeyer is something new entirely, completely unrelated to the nuclear force. It became known as the μ-meson although, as time passed, the word meson was dropped. It is now simply the muon.

The muon-pion mix-up, which lasted a decade, is entirely due to a coincidence in their mass. We now know that the mass and lifetime of the two is

$$\begin{aligned} \pi^{\pm}: &\quad M \approx 140\text{MeV and } T \approx 2\times 10^{-8}\text{ s} \\ \mu^{\pm}: &\quad M \approx 106\text{MeV and } T \approx 2\times 10^{-6}\text{ s} \end{aligned}$$

The pion decays primarily as $\pi^- \longrightarrow \mu^- + \bar{\nu}_\mu$ and $\pi^+ \longrightarrow \mu^+ + \nu_\mu$. (You'll have to wait until we discuss the weak force in Section 4 to understand how this decay occurs.) Moreover, as we explain in Section 3.4, we have a good understanding of the pion in terms of its constituent quarks. We even understand why it has the mass that it does. In contrast, the muon remains a mystery, a repetition of the electron at a higher scale whose existence is as surprising to us today as in the 1940s.

B. 4 The Beginning of the Deluge

Cosmic rays had still more surprises in store for physicists searching for elementary particles. The first came later in 1947, when George Rochester and Clifford Butler, working in Blackett's laboratory in Manchester, made a careful study of around 5000 photographs that they had taken over the previous year. Among them they discovered two with peculiar features.

The first, shown on the left of Figure 17, contains a forked track, seemingly appearing from nowhere. This is due to a neutral invisible particle which subsequently decays into two charged particles which are either muons or pions. The second, shown on the right of Figure 17, shows a marked kink, strongly suggesting that a charged particle decayed into a different charged particle (again, either a muon or pion), but also an invisible neutral particle which left without leaving a track. These new particles were estimated to have masses between $770m_e$ and $1600m_e$. They were dubbed V-particles on account of the V-shaped tracks that they left.

It was not long before further V-particles were discovered, some lighter than the proton, some heavier. Indeed, at some point it seemed like there would be no end to these new particles.

[08] Actually, this statement was true when I wrote it, but then I decided to edit the Wikipedia page.

In collecting his Nobel prize in 1955, Willis Lamb quipped
"The finder of a new elementary particle used to be rewarded by a Nobel Prize, but such a discovery now ought to be punished by a $\$10,000$ fine. ″

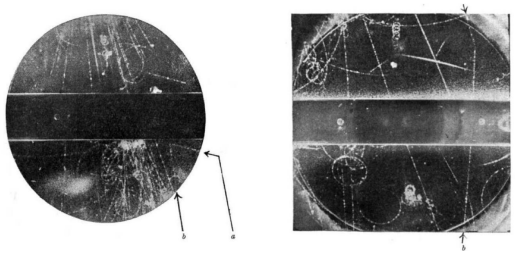


Figure 17. The discovery of kaons. A neutral kaon decays on the left, a charged kaon on the right.

For the next decade or so, particle physics entered a phase of taxonomy. The goal was to classify particles, first in terms of their mass and lifetimes, and then in terms of their decays, looking for patterns that would bring some order to the mess. It took many years before the things fell nicely into place and it was appreciated that all these particles could be understood in terms of yet smaller constituents called quarks. The V-particles shown in Figure 17 are now called kaons and were the first particles seen that contain a strange quark. We will tell the story of quarks in the next section.

The discovery of V-particles marks the beginning of a new era in theoretical physics. It also marks the end of an era in experimental physics. By the mid-1950's the energies and fluxes from accelerators were more than competitive with those in cosmic rays, and man-made muons, pions and V-particles were readily available. We will chart the rise of accelerator and detector technology in Interlude C.

4.3 3 The Strong Force

In the middle of the 20^{th} century, the number of seemingly "fundamental" particles exploded. The electron, proton and neutron had long been known. These were joined, in 1947, by a new particle called the pion, whose role was to keep the proton and neutron bound inside the nucleus.

The discovery of the pion was welcomed: it had long been expected, and its role in the universe was understood. The discovery, the same year, of another particle called the kaon was more confusing. As was the subsequent discovery of the rho meson, the eta, the eta prime, the delta, the lambda and the xi. Before long, physicists were running out of Greek and Roman letters to name these particles. A glance through the current particle data book includes particles with enticing names like $Z_c(3900)$.

By the end of the 1960s, there were hundreds of seemingly elementary particles and the situation looked hopelessly complicated. It was clear that these particles could not all be fundamental, but it was difficult to see any simple underlying explanation. In despair, Freeman Dyson declared
"I am acutely aware of the fact that the marriage between mathematics and physics, which was so enormously fruitful in past centuries, has recently ended in divorce."

Yet Dyson accepted defeat too soon. The answer was discovered in the early 1970s. In part, the answer lay in the existence of constituent particles called quarks. But, equally as important, were the peculiar and unprecedented properties of the force that binds these quarks together. This is the strong nuclear force.

4.3.1 3.1 Yang-Mills Theory

Both the strong and weak nuclear forces share a common property with electromagnetism: the force is carried by a field of spin 1 . In the case of electromagnetism, this field is described by the Maxwell equations. For the two nuclear forces, it is described by a generalisation of the Maxwell equations known as the Yang-Mills equations.

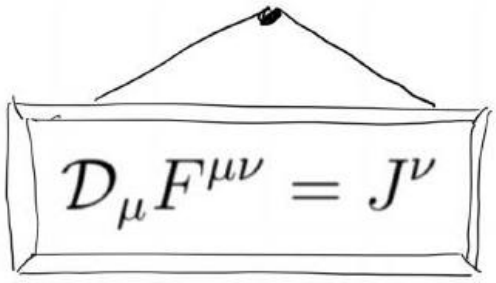
It's not so easy to write down a consistent generalisation of the Maxwell equations. In fact, it turns out that there's more or less a unique way to do it. This is based on a mathematical framework known as group theory. Here we'll give a baby version of this.

Yang-Mills theory is, like its predecessor, based on electric fields $\mathbf{E}(\mathbf{x}, t)$ and magnetic fields $\mathbf{B}(\mathbf{x}, t)$. Each of these is again a 3 -dimensional vector,

$$\mathbf{E} = (E_x, E_y, E_z) \quad \text{and} \quad \mathbf{B} = (B_x, B_y, B_z)$$

This is the essence of what it means for a field to be spin 1. The novelty in Yang-Mills theory is that each component of these vectors is now a matrix at each point in space and time, rather than just a number. There are different versions of Yang-Mills theory for different kinds of matrices. There is a Yang-Mills theory based on 2×2 matrices, and one based on 3×3 matrices and so on for each integer N. However, once you decided on the size of the matrix, everything else is fixed.

To write the classical equations of motion, it's best to again bundle the "electric" and "magnetic" fields into a 4×4 matrix $F_{\mu\nu}$, each component of which is now itself an $N \times N$ matrix: i.e a matrix of matrices. The Yang-Mills equations of motion are one of the key equations of physics, and fully deserving of their place in a frame



Here $\mathcal{D}_\mu$ is something like a partial derivative with respect to space and time, but one that also includes some commutator of matrices. (It's known as a covariant derivative.) On the right-hand side sits J^ν, the analog of the electric current which, as we will see shortly, arises from quarks. The Yang-Mills equations are very similar to the Maxwell equations. Indeed, if you choose 1×1 matrices, which are just numbers, then the Yang-Mills equations reduce to the Maxwell equations.

To specify any force described by Yang-Mills theory, we just need to say how big the matrices are. Nature is kind to us: she has chosen to make use only of the simplest matrices.

- Electromagnetism: 1×1 matrices
- Weak Nuclear Force: 2×2 matrices
- Strong Nuclear Force: 3×3 matrices

Isn't that nice!

Before we go on, I should confess that the above discussion was a little imprecise in places. A correct statement is that there exists a version of Yang-Mills theory for every Lie group. Everywhere that I said "size of matrix", you should replace this with "choice of Lie group" where a "Lie group" is a fancy mathematical object. Matrices provide some simple examples

of some Lie groups, but there are also others. Happily, all the groups that we need in particle physics can be reduced to matrices. A more grown-up version of the above list then characterises each force by a group. For what it's worth, they are: [9]

- Electromagnetism: $U(1)$
- Weak Nuclear Force: $SU(2)$
- Strong Nuclear Force: $SU(3)$

For the rest of this section, we will focus on $SU(3)$ Yang-Mills, relevant for the strong force. The theory of the strong force, interacting with quarks, is known as Quantum Chromodynamics, or QCD for short. The 3×3 matrix-valued electric and magnetic fields are sometimes called chromoelectric and chromomagnetic fields.

3.1.1 Gluons and Asymptotic Freedom

If you solve the Maxwell equations, you find waves propagating at the speed of light. These are light waves. As we have seen, in the quantum theory, these waves are comprised of massless spin 1 particles called photons. The massless nature of the photon is the reason light waves travel at the speed of light.

Similarly, if you solve the classical Yang-Mills equations, you again find waves travelling at the speed of light. In analogy with electromagnetism, we might expect that, in the quantum theory, there are massless particles associated to these waves. But no such massless particles are seen in the world. What's going on?

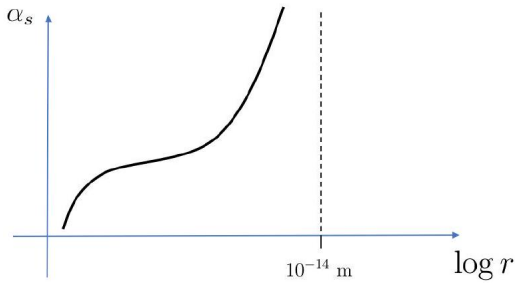


Figure 18. The renormalisation of coupling for the strong force.

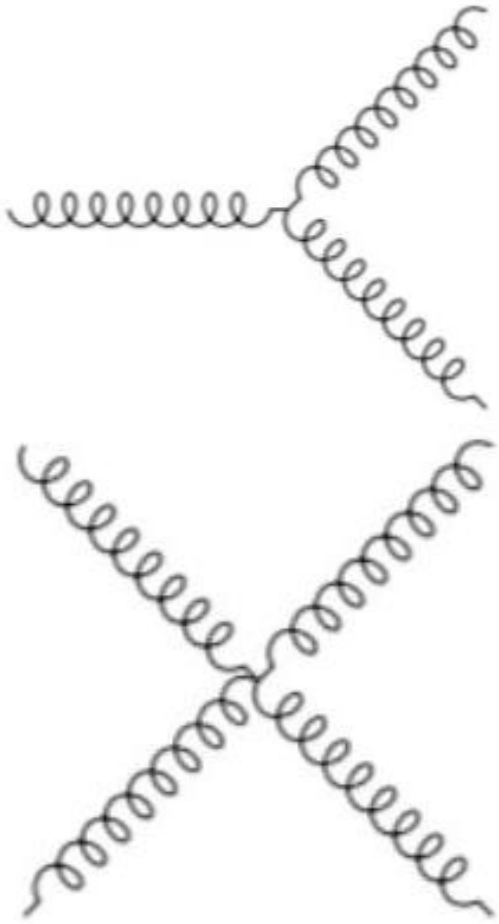
The answer to this question lies in a subtle property of Yang-Mills theory, which means that the quantum theory looks very different from its classical counterpart. There are spin 1 particles associated to the $SU(3)$ Yang-Mills theory and these are called gluons. But, rather surprisingly, gluons turn out to be massive rather than massless.

To understand this, we first need to appreciate a key difference between Yang-Mills theory and Maxwell theory. The Maxwell equations are linear. One consequence of this is that light wave pass right through each other. In contrast, the Yang-Mills equations are non-linear. (This is not obvious in the framed equation on the previous page. It is hidden in the meaning of

[09] A little matrix knowledge can be a confusing thing at this stage. The strong nuclear force is associated to the group $SU(3)$, which consists of 3×3 complex, unitary matrices of determinant 1 . This means that the matrix U must obey $U^\dagger U = \mathbb{1}$ and $\det U = 1$ to be in $SU(3)$. But this isn't the kind of 3×3 matrix that make up the components of the chromoelectric and chromomagnetic fields. Instead, these are Hermitian matrices, namely 3×3 matrices which obey $E_x = E_x^\dagger$. There is, however, a relationship between these kinds of matrices: the exponential of a Hermitian matrix, like e^{iE_x}, is in the group $SU(3)$. Mathematically, this is the difference between a Lie group and a Lie algebra.

the covariant derivative $\mathcal{D}_\mu$.) This means that two classical waves in Yang-Mills will typically scatter off each other in some complicated fashion.

When we turn to the quantum theory, the non-linearity translates to an interaction vertex in the Feynman diagrams for gluons. We depict gluons using curly lines like this ellee. There are, it turns out, two interaction vertices: one where three gluons interact, and another where four gluons interact:



Just as in QED, there is a dimensionless coupling constant that characterises the strength of this interaction. For QED, this was the fine structure constant α. For the strong force, the coupling is denoted α_s. And, importantly, just like for QED, the value of this coupling depends on the distance scale (or, equivalently, energy scale) at

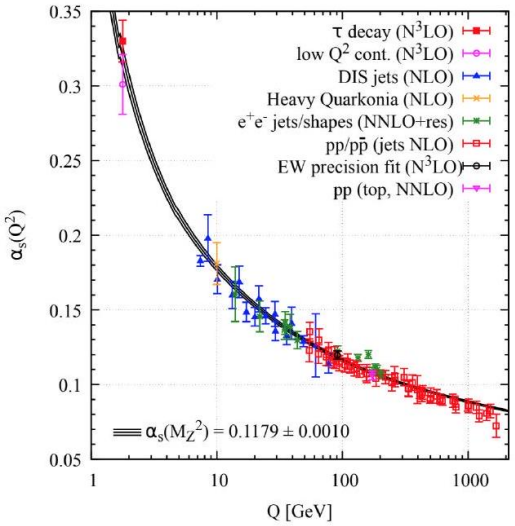


Figure 19. The running of coupling for the strong force, now plotted against energy scale. This figure is taken from the review of QCD by the Particle Data Group.

which it's measured. This is the story of renormalisation that we met previously in Section 2.3. But here is where there's a crucial difference between electromagnetism and the strong force: as we go to larger distances, the strong force gets stronger, not weaker. A sketch of the coupling is shown in Figure 18. (This should be contrasted with the running of the fine structure constant, as shown in Figure 10.) The experimental data for the running of the strong coupling is shown in Figure 19, now plotted against energy scale E, which is inversely related to length by $E = 1/r$.

How can we understand this intuitively? For electromagnetism, there was a simple physical picture in which the electric charge gets screened by particle-anti-particle pairs, and so appears smaller as we go to longer distances. For the strong force, the gluons themselves are doing the screening. Except they anti-screen, meaning that they cause the force to get stronger the further out we go!

In fact there is an intuitive way to understand this, although it's rather subtle. A clue can be found lurking back in the theory of electromagnetism. Recall that the Maxwell equations contain two parameters: $1/\epsilon_0$ characterises the strength of the electric force, while $1/\mu_0$ characterises the strength of the magnetic force. But these are not independent. They are related by

$$\epsilon_0 \mu_0 = \frac{1}{c^2} \tag{3.1}$$

with c the speed of light. This means that if the strength of the electric force gets weaker, then the magnetic force necessarily gets stronger, and vice versa.

There is a similar story for Yang-Mills. But now the gluons are doing the screening, and couple to both the chromoelectric and the chromomagnetic fields. It turns out that, because they are spin 1 particles, they screen the chromomagnetic fields more strongly than they screen the chromoelectric fields. In other words, the chromomagnetic part of the Yang-Mills interaction gets weaker as we go to larger distances. The relation (3.1) then tells us that the chromoelectric part of the interaction necessarily gets stronger. The upshot is that gluons anti-screen. If you want the gory details, the calculation can be found in Section 2.4 of the lectures on Gauge Theory.

So what is the strength of the strong force? At the energy scale $E \approx 100$GeV, corresponding to a distance scale of $r \sim 10^{-17}$ m, we have

$$\alpha_s \approx 0.1 \quad \text{when} \quad E \approx 100\text{GeV}$$

Even at these fairly high energies, the strength of the force is an order of magnitude larger than QED. If we go to higher energies, or shorter distances, α_s decreases. In fact, as we go to arbitrarily high energies, the strength of the strong force vanishes, $\alpha_s \to 0$. This phenomenon is known as asymptotic freedom: it means that at high energies, or short distance scales, the strong force essentially disappears!

However, outside of particle colliders, everything that we observe in the world takes place at distance scales significantly larger than 10^{-17} m, and the strong force only gets stronger as we go to larger distances. But here there is another surprise. According to naive calculations, by the time you get to around $r \sim 10^{-15}$ m, or an energy scale of $E \sim 100$MeV, the coupling constant appears to get infinitely large!

Above, I used the phrase "naive" calculations, because I have in mind the kind of perturbative Feynman diagram calculations that we described in the previous section. But, as we stressed, these diagrams only make sense when the coupling is small. As soon as the coupling is around $\alpha_s \approx 1$, the very complicated Feynman diagrams, involving lots of loops, are just as important as the simple Feynman diagrams and we have no control over the calculation. But this is exactly what happens in QCD! At very short distances, we're fine and we can do calculations. But at long distances, the theory becomes very challenging. The separation between "easy" and "hard" turns out to be around $r \sim 10^{-14}$ m to 10^{-15} m, but is usually expressed in terms of an energy scale known as the strong coupling scale, or Lambda-QCD,

$$\Lambda_{\text{QCD}} \approx 200\text{MeV}$$

This is a characteristic energy scale of QCD. At energies $E \gg \Lambda_{\text{QCD}}$, the strong force is not particularly strong and we can trust Feynman diagrams. But by the time we get to energies Λ_{QCD}, the strong force lives up to its name. Most phenomena that are due to the strong force have an energy somewhere in the ballpark of Λ_{QCD}

Before we describe some of these phenomena, it's worth pausing to mention that something unusual has happened here. The strength of the strong force, like QED, is characterised by a dimensionless coupling α_s. But the phenomena of renormalisation means that this coupling depends on scale, and the upshot of this is that we ultimately exchange a dimensionless number, α_s, for a dimensionful scale Λ_{QCD}.

3.1.2 The Mass Gap

When we try to study the strong force on energy scales $E < \Lambda_{\text{QCD}}$, corresponding to distance scales, $r > 10^{-14}$ m, we have a problem. The strong coupling means that the fields are wildly fluctuating on these scales, and our favourite method of Feynman diagrams is no longer useful. This also means that the classical equations of motion are no guide at all for what the quantum theory might look like.

The gluon is the first casualty of strong coupling. As we explained at the beginning of this section, the classical Yang-Mills equations suggest that the gluon should be massless. But the strong coupling effects change this. Instead, the gluon - which is a ripple of the Yang-Mills fields - has mass, given by

$$m_{\text{gluon}} \approx \Lambda_{\text{QCD}}$$

This is sometimes referred to as the Yang-Mills mass gap. The "gap" here is one between the ground state and the first excited state. For theories of massless particles, there is no gap because we can have particles of arbitrarily low energy. But for massive particles, the minimum amount of energy needed is $E = mc^2$.

To say that the Yang-Mills mass gap is difficult to prove would be something of an understatement. Demonstrating the mass gap is generally regarded as one of the major open problems in theoretical physics. Indeed, a million dollar Clay mathematics prize awaits anyone who succeeds. Although we do not have any rigorous (or even semirigorous) derivations of the mass gap, there is no doubt that it is a property of YangMills. Our best theoretical evidence comes from computer simulations which, in this context, are called lattice simulations, reflecting the fact that spacetime is approximated by a grid, or lattice, or points. These simulations show unambiguously that the gluon is massive. You can read more about the lattice, and other approaches to Yang-Mills, in the lectures on Gauge Theory.

Finally, and most importantly, the existence of a mass gap is consistent with experiment, where no massless gluon is seen. Moreover, while the strong force is strong, it is also short-ranged. The characteristic energy scale $\Lambda_{\rm QCD}$ corresponds to a distance scale which in natural units (remember $\hbar = c = 1$) is

$$R_{\rm QCD} = \frac{1}{\Lambda_{\rm QCD}} \approx 5 \times 10^{-15} \text{ m}$$

To understand how this scale affects the world around us, we first need to throw in the final key ingredient: quarks.

4.3.2 3.2 Quarks

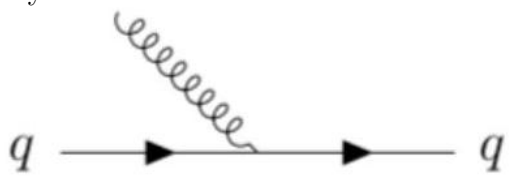
Usually in physics, we can get by without memorising lots of random names. The strong force is the exception, leaving us looking more like botanists than physicists. First, there are the many hundreds of names of different particles. But more important are names of groups of particles, each classifying a different property.

To kick things off, the fermions in the Standard Model are divided into two different types

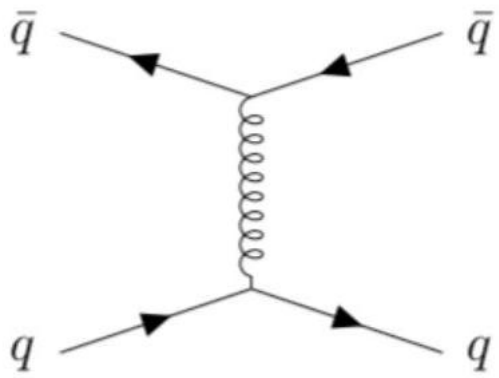
- Quarks: These are particles that feel the strong force.
- Leptons: These are particles that don't.

The leptons are the electron, muon, tau and three species of neutrino. (The name comes from the Greek $\lambda\epsilon\pi\tau o\zeta$ meaning small.) Leptons don't interact with the $SU(3)$ Yang-Mills field, and we will ignore them for the rest of this section. In contrast, the six quarks - up, down, strange, charm, bottom and top - do feel the strong force.

In the language of Feynman diagrams, we denote the quarks as a solid line, with an arrow distinguishing quark from anti-quark. This is the same kind of line that we previously used to denote leptons, so we add a label q to show that it's a quark. The interaction between quarks and gluons is then described by the interaction vertex



When evaluating these Feynman diagrams, each vertex contributes a factor of the strong coupling, α_s. We can then use the Feynman diagrams to compute, say, the force between a quark and anti-quark. This comes from the following diagram:



If the quark and anti-quark are separated by a distance $r \ll R_{\rm QCD}$, then evaluating this diagram results in an attractive force that is very similar to the Coulomb force (2.4),

$$F(r) \sim \frac{\alpha_s}{r^2} \quad \text{when } r \ll R_{QCD} \tag{3.2}$$

Here α_s itself also depends on r, albeit logarithmically. We already saw a sketch of this dependence in Figure 18.

However, there's a catch: if the distance between the quarks is too big - bigger than R_{QCD} - then the language of Feynman diagrams stops working. As we increase the separation between quarks to distances greater than $R_{\rm QCD}$, the Coulomb-like expression (3.2) stops being the right one, and it instead changes to

$$F(r) \sim \text{ constant} \quad \text{when } r \gg R_{QCD} \tag{3.3}$$

A constant force may not seem like much. But it gets exhausting. This is better seen if we look at the associated energy needed to separate a quark and anti-quark by distance R. For short distances, the energy takes the same form as in electrostatics,

$$V(r) \sim -\frac{\alpha_s}{r} + \text{ constant} \quad \text{when } r \ll R_{QCD}$$

But when the quarks experience a constant force, the energy grows linearly

$$V(r) \sim \Lambda_{\rm QCD}^2 r \quad \text{when } r \gg R_{QCD}$$

Clearly if you want to separate the quark-anti-quark pair by a long distance, then it costs an increasing amount of energy. In particular, it costs an infinite amount of energy to separate them an infinite distance. But taking, say, the anti-quark a long way away is tantamount to leaving the quark on its own. In other words, a solitary quark requires infinite energy! Quarks do not want to be alone: they only occur in bound states with other quarks or anti-quarks. This phenomenon is called confinement.

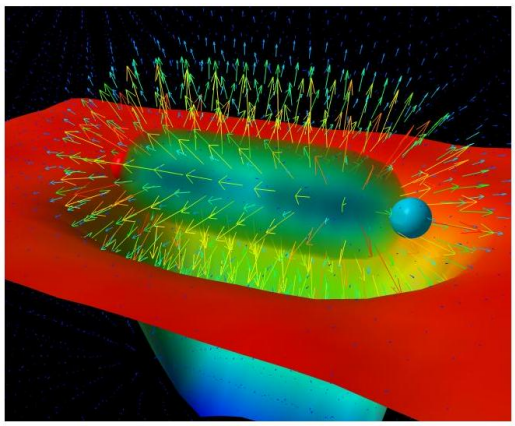
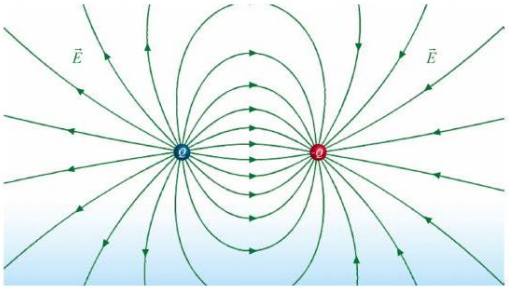


Figure 20. The chromoelectric flux tube between a quark and anti-quark in a meson state, from the QCD simulation of Derek Leinweber

Confinement, like the Yang-Mills mass gap, has so-far resisted a rigorous mathematical derivation. But we again have very clear evidence from numerical simulations, together with a handful of less-than-rigorous mathematical arguments, that confinement occurs. Moreover, this also gives us some intuition for what's going on.

First, let's recall what happens in electrostatics. If we separate a positive and negative electric charge by some distance r, then an electric field is set up between the two. The form of this electric field is shown on the right, and ultimately is responsible for the $F \sim 1/r^2$ Coulomb force law that the charges experience.

In Yang-Mills theory, the chomoelectric field takes a



similar form if the quark and anti-quark are separated by a distance $r \ll R_{QCD}$. But as you increase the separation of the quark and antiquark beyond the critical distance R_{QCD}, the form of the field changes. Instead of the field lines spreading out, the mass of the gluon forces them to bunch together into string-like configurations called flux tubes. This can be clearly seen in the computer simulation of QCD shown in Figure 20. It's as if the quark and anti-quark are joined by a piece of string. If you want to separate them further, you have to stretch the flux tube and this costs an energy $V(r) \sim r$ proportional to its length. This is responsible for the confinement of quarks.

3.2.1 Colour

The property that determines how particles experience the electromagnetic force is electric charge. The analogous property for the strong force is called colour [10]. Needless to say, this has nothing to do with the colour that we see. It is merely a label given by physicists who grew up without the classical education needed to name things in Greek or Latin.

While electric charge is just a number, colour charge is a little more involved: it is best thought of as a 3-dimensional vector $\boldsymbol{\omega}$ of fixed length. Here it's 3-dimensional because the Yang-Mills fields for the strong force are 3×3 matrices. This vector doesn't point in the three

dimensions of space, but instead is something more abstract. If it points in different directions, we think of the quark as carrying a different colour. The exact translation between the vector and colour is pretty arbitrary, but we could take

$$\text{red: } \boldsymbol{\omega} = \begin{pmatrix} 1 \\ 0 \\ 0 \end{pmatrix} \quad \text{green: } \boldsymbol{\omega} = \begin{pmatrix} 0 \\ 1 \\ 0 \end{pmatrix} \quad \text{blue: } \boldsymbol{\omega} = \begin{pmatrix} 0 \\ 0 \\ 1 \end{pmatrix}$$

But the vector doesn't have to point exactly in one of these directions. For example, we could consider a vector $\boldsymbol{\omega} = \frac{1}{\sqrt{2}} \begin{pmatrix} 1 \\ 1 \\ 0 \end{pmatrix}$ which should be thought of as a combination (or, in quantum language, a superposition) of red and green. Fortunately, we don't extend the colour analogy so far as to call this "muddy brown".

3.2.2 A First Look at Mesons and Baryons

Each quark carries a colour-vector $\boldsymbol{\omega}$, while the leptons do not. Confinement means that we do not see individual quarks, but they only appear in bound states so that the total colour charge vanishes. Any such composite particle, held together by the strong force, is referred to as a hadron. There are two ways in which hadrons can form,

- Mesons: These contain a quark and anti-quark. If the quark has colour vector $\boldsymbol{\omega}_1$ and the anti-quark colour vector $\boldsymbol{\omega}_2$, then they can combine as $\boldsymbol{\omega}_2^\dagger \cdot \boldsymbol{\omega}_1$ to form a colour-neutral state. Schematically, this looks like

$$\text{meson } = \bar{r}r + \bar{g}g + \bar{b}b$$

which should be read as "(anti-red)red + (anti-green)green + (anti-blue)blue". The flux tube for such a meson is shown in Figure 20.

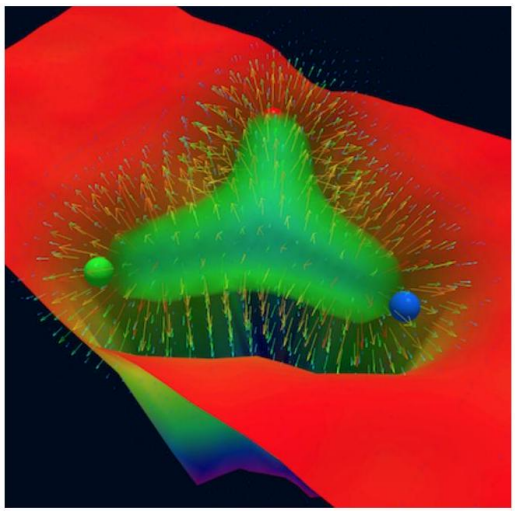


Figure 21. The flux tube between three quarks in a baryon state, from the QCD simulation of Derek Leinweber

[010] Scientists in the US work in units $u = 1$.

- Baryons: These contain three quarks. If the three quarks have colour vectors $\boldsymbol{\omega}_1$, $\boldsymbol{\omega}_2$ and $\boldsymbol{\omega}_3$ then they combine as the triple product $\boldsymbol{\omega}_1 \cdot (\boldsymbol{\omega}_2 \times \boldsymbol{\omega}_3)$ to form a colour neutral state. Schematically, this looks like

$$\text{baryon} = rbg$$

The fact that the baryon contains 3 quarks, rather than any other number, can be traced to the 3×3 matrices that describe the strong force. The flux tube for a baryon is shown in Figure 21.

To understand the collection of hadrons that emerges after confinement, we first need to look at the masses of quarks. In particular, we should compare the masses to the characteristic scale of the strong interactions, $\Lambda_{QCD} \approx 200\text{MeV}$.

Three of the quarks have masses smaller than Λ_{QCD}.

$$\begin{aligned} m_{\text{down}} &= 5\text{MeV} \\ m_{\text{up}} &= 2\text{MeV} \\ m_{\text{strange}} &= 95\text{MeV} \end{aligned}$$

The up and down quark have masses significantly smaller than Λ_{QCD}, while the strange quark is only slightly smaller. Recall from our discussion in 1.2 that the Compton wavelength, $\lambda = \hbar/mc$, can be thought of as the size of a particle. Any particle with $m < \Lambda_{QCD}$ necessarily has its size $\lambda > R_{QCD}$. That means that there's no way to bring two of these quarks closer than R_{QCD}, so these light quarks will only experience the confining force (3.3).

In contrast, the three heavier quarks have masses

$$\begin{aligned} m_{\text{charm}} &= 1.3\text{GeV} \\ m_{\text{bottom}} &= 4.2\text{GeV} \\ m_{\text{top}} &= 170\text{GeV} \end{aligned}$$

These are all much heavier than Λ_{QCD}. These three quarks all have Compton wavelength $\lambda \ll R_{QCD}$, so it makes sense for them to come close enough to experience the Coulomb-like force (3.2). This means that we might expect the spectrum of hadrons containing charm, bottom and top quarks to be a little different from those containing only the lighter quarks. Indeed, this turns out to be the case.

4.3.3 3.3 Baryons

We'll kick thing off with baryons, containing three quarks. To start, suppose that we have only the up and down quark to work with. There are various ways that we can combine these quarks. First, recall that the each quark has spin $\frac{1}{2}$. When combining quarks, we need to figure out what to do with their spins.

3.3.1 Protons and Neutrons

Suppose that we have two spins in one direction, and the third spin in the opposite direction. This will result in a baryon of spin $\frac{1}{2} + \frac{1}{2} - \frac{1}{2} = \frac{1}{2}$. There are two choices, which result in the two most familiar baryons: the proton (p) and the neutron (n). Their quark content and masses are

$$\begin{aligned} n(ddu) \quad m_n &\approx 939.57\text{MeV} \\ p(uud) \quad m_p &\approx 938.28\text{MeV} \end{aligned}$$

These are the two lightest spin $\frac{1}{2}$ baryons. Recall that the down quark has charge $-1/3$ and the up quark charge $+2/3$, so the proton has charge $+1$ while the neutron has no electric charge.

Already, there is something of a surprise here. The up and down quarks each have mass of a few MeV . Yet the proton and neutron each have mass of around 1000 MeV . How is this possible given that the proton and neutron are supposed to contain three quarks each?

The answer to this is simple: when we say that the proton and neutron each contain three quarks, we are hiding a more painful truth. The proton and neutron, and indeed all other hadrons, are in reality enormously complicated objects. The most accurate description is in terms of complicated, strongly interacting fields. In a particle language, we could describe them as containing many hundreds of quarks, anti-quarks and gluons, all interacting in a complicated fashion. The statement that the proton and neutron are composed of three quarks is really shorthand for the fact that they contain three more quarks than anti-quarks. These three additional quarks are sometimes called valence quarks, to distinguish them from the surrounding sea of quark-anti-quark pairs.

To put this in perspective, we could ask the following hypothetical question: suppose that the quarks were actually massless. What would the mass of the proton be? The surprising answer is that the mass of the proton would be more or less unchanged, still weighing in at a little less than 940 MeV ! The same is true of the neutron. The masses of the proton and neutron care almost nothing about the mass of the three valence quarks: instead they are entirely dominated by the strong coupling scale $\Lambda_{\rm QCD}$ and their mass is few times $\Lambda_{\rm QCD}$.

You may have heard it said that the Higgs is responsible for all the mass in the universe. This is a fairly blatant lie. Later, in Section 4, we will learn that all elementary particles, including the quarks, do indeed get their mass from the Higgs boson. But the overwhelming majority mass in atoms is contained in the protons and neutrons that make up the nucleus, and this mass has nothing to do with the Higgs boson. It is entirely due to the urgent thrashing of strongly interacting quantum fields.

The irrelevance of the quark masses also has a more subtle implication. The masses of the proton and neutron are almost equal, despite the fact that the down quark is twice as heavy as the up. This reflects the fact that, at least as far as the strong interaction is concerned, the two particles behave almost identically. If we do an experiment with protons that is mediated by the strong force, then the same experiment performed with neutrons will yield exactly the same answer. This almost-symmetry of nature is referred to as isospin. Note, however, that it only holds for the strong force. The proton and neutron do not behave the same under the electromagnetic force, since the proton is charged while the neutron is not. Neither, it turns out, do they behave the same under the weak force.

There is, however, one place where the masses of the quarks are important. The fact that the down quark is heavier than the up quark does contribute a tiny amount to the mass and is the reason that the neutron is very slightly heavier than the proton. This
is important because it means that beta decay proceeds by a neutron decaying into a proton, rather than the other way around. We'll learn more about this in Section 4 where we discuss the weak force.

3.3.2 Delta Baryons

We could ask: why can't we have a baryon with, say, three up quarks? The answer to this lies in the Pauli exclusion principle. The full explanation is a little subtle, but the upshot is that we can have three up quarks in a baryon, but only if all their spins point in the same direction. (At first glance this might seem the wrong way around since, in chemistry, the Pauli exclusion principle dictates that electrons in the same orbital state have opposite spins. But quarks have that additional colour degree of freedom, and there is an anti-symmetry there which, in turn,

requires a symmetric alignment of spins.)

When all the spins point in the same direction, the baryon itself has spin $\frac{1}{2} + \frac{1}{2} + \frac{1}{2} = \frac{3}{2}$ baryon. Now there are four choices, all of which are known as Delta (Δ) baryons. These particles have more or less equal mass, but different charges

$$\left.\begin{array}{ll} \Delta^{++} & (\text{uuu}) \\ \Delta^{+} & (\text{uud}) \\ \Delta^{0} & (\text{udd}) \\ \Delta^{-} & (\text{ddd}) \end{array}\right\} \quad m \approx 1232\text{MeV}$$

Here the superscripts,,,+++ 0 and - specify the electric charge of the particle.
We don't see Δ baryons floating around in the world. They have a lifetime of around 10^{-24} seconds, after which they decay, typically into a proton or neutron together with a meson called a pion. For example,

$$\Delta^{++} \to p + \pi^{+} \quad \text{and} \quad \Delta^{-} \to n + \pi^{-}$$

The lifetime of 10^{-24} seconds is much shorter than we can measure and particles with such short lifetimes are called, quite reasonably, unstable. Even when moving close to the speed of light Δ baryons don't travel far enough to register directly in particle detectors. Instead, they reveal themselves in more indirect means as so-called resonances in certain experiments. We'll describe this further in Interlude C.1.

The lifetime of the Δ baryons is actually the characteristic timescale of the strong force: $T_{QCD} = R_{QCD}/c \approx 10^{-24}$ seconds. If anything happens due to the strong force, it usually happens on roughly this timescale.

3.3.3 Strangeness

Let's now consider baryons that we can construct from the first three quarks: up, down and strange.

We'll first consider baryons with spin $\frac{1}{2}$. In addition to the proton and neutron, we now have four further baryons that contain a single strange quark, called sigma (Σ) baryons

$$\begin{array}{ll} \Sigma^{-}(dds) & m \approx 1197\text{MeV} \\ \Sigma^{0}(dus) & m \approx 1193\text{MeV} \\ \Sigma^{+}(uus) & m \approx 1189\text{MeV} \end{array}$$

and the lambda (Λ) baryon

$$\Lambda^{0}(dus) \quad m \approx 1116\text{MeV}$$

Again, the superscript labels the electric charge of the baryon. You may have noticed that the quark content of the Σ^0 and Λ^0 are the same. The difference lies in the details of the wavefunctions for the up and down quarks. (Technically, some different minus signs mean that all Σ baryons have isospin 1 , while the Λ has isospin 0 .)

There are also two types of baryons that contain two strange quarks, called cascade, or xi (Ξ) baryons

$$\begin{array}{ll} \Xi^{-}(dss) & m \approx 1322\text{MeV} \\ \Xi^{0}(uss) & m \approx 1315\text{MeV} \end{array}$$

None of these baryons are familiar from our everyday experience. This is because they again decay, typically to protons and pions. However, here there is a surprise: although these new baryons have a mass in the same ballpark as the Δ 's, they live for significantly longer. In particular, the $\Sigma^{\pm}$, the Λ^0 and the $\Xi^{0,-}$ all live for a whopping 10^{-10} seconds.

Now, 10^{-10} seconds may not sound like much. Indeed, it's difficult to imagine having a rich and fulfilling life in this time. But it's an aeon compared to the 10^{-24} seconds that the Δ baryons live. This is a puzzle: why do these new baryons have a such a comparatively long life, even though their masses are comparable to the Δ ?

A partial answer to this is to invoke a new conservation law. We know that electric charge is conserved in all interactions. It turns out that there is another quantity strangeness - which is conserved. Or, at the very least, almost conserved. Strangeness is simply a count of the number of strange quarks.

Here "almost conserved" means conserved by the strong interaction. The strong interactions cannot change the number of strange quarks and so particles like $\Sigma^{\pm}$, Λ^0 and $\Xi^{0,-}$ do not decay straight away. The decay only proceeds through the weak interaction, and this takes significantly longer. We'll describe how these decays occur in Section 4. In contrast, particles like the Δ baryons decay directly through the strong interaction, and this happens much faster. (As an aside: there's always one complication. It turns out that, among the collection of strange baryons, there is one which is unstable: the $\Sigma^0 \to \Lambda^0 + \gamma$ with a lifetime of around 10^{-20} seconds. But this is allowed by the strong force because the number of strange quarks is unchanged. The Λ^0, as we've seen, then waits another 10^{-10} seconds before it too decays.)

As a general rule of thumb, hadrons can decay through one of the three forces: strong (like the Δ' 's), electromagnetic (like Σ^0) or weak (like $\Sigma^{\pm}, \Lambda^0$ and Ξ.). The lifetimes of these particles reflect the decay process:

- Strong decay: $\sim 10^{-22}$ to 10^{-24} seconds.
- Electromagnetic decay: $\sim 10^{-16}$ to 10^{-21} seconds.
- Weak decay: $\sim 10^{-7}$ to 10^{-13} seconds.

Where you sit within each range depends on other factors, such as the relative masses of the parent and daughter particles. Particles that live for up to 10^{-10} seconds are referred to (I think, somewhat tongue in cheek) as stable. In contrast, any particle that lasts 10^{-20} seconds or shorter is, like the Δ baryon, referred to as unstable or a resonance.

It should be clear from the discussion, however, that there's nothing very qualitatively different between a stable particle like the Λ and a resonance like the Δ. Both will decay in less than the blink of an eye. But a lifetime of 10^{-10} seconds mean that, with good technology, you can take a photograph of the particle's track in a cloud chamber or bubble chamber. You can see many such photographs in Interludes B and C. When a particle leaves such a vivid trace, it's hard to deny its existence. In contrast, we're never going to take a photograph of something that lasts 10^{-20} seconds. But that doesn't mean that it's any less real! It just leaves its signature in more subtle ways.

3.3.4 The Eightfold Way

There is a clear pattern to the masses of the spin $\frac{1}{2}$ baryons. To highlight this, we can place the 8 baryons in the following shape:

$$\begin{array}{ccccc} & n(ddu) & & p(uud) & \\ \Sigma^-(dds) & & \Sigma^0, \Lambda^0(dus) & & \Sigma^+(uus) \\ \Xi^-(dss) & & \Xi^0(uss) & & \end{array}$$

The particles are arranged in rows of increasing strangeness and, correspondingly, in increasing mass. The particles in the top row have $m \approx 940$MeV; those in the second row $m \approx 1190$Mev; and those in the final row $m \approx 1320$MeV. Meanwhile, particles in the same \diagonal have equal charge.

We see that adding a strange quark increases the mass of a baryon by roughly 140 ± 10 MeV . This can be largely, but not entirely, accounted for by the mass of the strange quark, $m_{\text{strange}} \approx 95\text{MeV}$.

Recall that there is an approximate symmetry, relating up and down quarks, called isospin. If we squint, we could enhance this to a larger, and even more approximate, symmetry relating up, down and strange quarks. This subsumes the previous isospin symmetry, but isn't quite as a good because the strange quark is significantly heavier than the other two. Indeed, it only holds if we're willing to pretend that 1320MeV $\approx$ 940 MeV . Nonetheless, it is true that, at least as far as the strong force is concerned, all 8 baryons in the table have more or less the same properties. For example, a given meson will scatter off all 8 in pretty much the same way. The symmetry, first proposed by Gell Mann and, independently, Ne'eman in 1961 is called $SU(3)$ flavor symmetry or, more poetically, the eightfold way.

The $SU(3)$ flavor symmetry relating the three lightest quarks is not to be confused with the $SU(3)$ colour symmetry that underlies the strong force. It's just that the number 3 appears a bunch of times in the Standard Model. (Don't read anything mystic into this. It's just a small number.) With decades of hindsight, the eightfold way appears more accidental than fundamental. Nonetheless, it was important historically as a useful organising principle in cataloging the many hundreds of hadrons that were discovered.

The same almost-symmetry is sitting within the baryons of spin $\frac{3}{2}$. These can be placed in the following pattern, again organised by increasing strangeness

$$\begin{array}{cccc} \Delta^-(ddd) & \Delta^0(ddu) & & \Delta^+(duu) \\ \Sigma^{\star -}(dds) & \Sigma^{\star 0}(dus) & \Delta^{++}(uuu) & \\ & & & \Sigma^{\star +}(uus) \\ & \Xi^{\star -}(dss) & & \Xi^{\star 0}(uss) \end{array}$$

Once again, the masses in each row are roughly constant: $m \approx 1232\text{MeV}$ in the first row; $m \approx 1385\text{MeV}$ in the second; $m \approx 1533\text{MeV}$ in the third; and with the Ω^- weighing in at $m \approx 1672\text{MeV}$. In each case, the increase is again roughly 140 to 150 Mev and is due to the extra strange quark.

Notice that the middle 7 baryons in this table have the same quark content as the spin $\frac{1}{2}$, strangeness 1 , baryons that we met previously. These should be thought of excitations of these previous baryons, with the spin of one of the constituent quarks flipped, changing the overall spin from $\frac{1}{2}$ to $\frac{3}{2}$.

The real novelties in the table above are the three outliers, in which all quarks are the same. As we mentioned above, the Pauli exclusion principle prohibits the existence of spin $\frac{1}{2}$ baryons with three identical quarks, so they appear here for the first time. Two are particularly important: the $\Delta^{++}$was the first particle to be found without charge ± 1 (or 0) and helped enormously in piecing together the story of the underlying quarks. The Ω^-baryon, meanwhile, holds a special place in the history of science because GellMann used the simple quark model described above to predict its mass and properties before it was discovered experimentally. He therefore followed Mendeleev and Dirac in predicting the existence of a "fundamental" particle of nature (where, as should by now be clear, the meaning of the word "fundamental" is time-dependent).

There are eight baryons with spin $\frac{1}{2}$, and ten baryons with spin $\frac{3}{2}$, with the former lending its name to the "eightfold way" used to describe the whole enterprise. But, underlying this set-up are just 3 quarks - up, down and strange - and, as we mentioned above, an approximate

$SU(3)$ symmetry that rotates them. Why do we start with the number 3 , and end up with 8 and 10 baryons respectively? In fact, there is a good reason for this, although it's difficult to explain without going into the mathematics of group theory. It turns out that any group has a bunch of different ways in which it
can express itself, known as representations. And these representations come only with very specific numbers. Although it's not obvious, the numbers 8 and 10 are naturally associated to the group $SU(3)$.

Finally, I mention that, in principle, it should be possible to calculate the masses of the proton, neutron and all other baryons directly from our knowledge of QCD dynamics. While this is somewhat beyond what we can do with pen and paper, we can simulate QCD on a computer, and get pretty accurate predictions for the masses of baryons that we've seen above, certainly good to the 5% level. The same is true for the mesons that we will meet in the next section. There is now no doubt that the complexity seen in the hadron spectrum can be entirely explained by the dynamics of QCD.

More Baryons

The lists above do not exhaust the baryons that have been discovered. There are further baryons containing charm and bottom quarks. For example, in addition to the Σ^+, comprised of uus, there is also a Σ_c^+comprised of uuc and Σ_b^+comprised of uub, and similar stories for many of the other baryons. It is, however, difficult to argue for any approximate symmetry among these baryons, since the mass of the heavy quarks is much greater than those of the lighter quarks and greater than Λ_{QCD}.

There are also excited states of all these baryons, in which the quarks orbit each other, not dissimilar to the way in which the electrons orbit the proton in the excited states of the hydrogen atom.

There are not, however, baryons containing top quarks. The top quark is so heavy that such baryons are predicted to decay in around 10^{-25} seconds, even faster than the characteristic timescale $T_{QCD} \approx 10^{-23}$ seconds of the strong force. This means that such "top baryons" decay before they even form. Needless to say, none have been observed.

4.3.4 3.4 Mesons

We now turn to mesons, bound states of a quark and an anti-quark. Many hundreds have been discovered. Here we describe some of the most important.

3.4.1 Pions

We will again start by assuming that we've only got up and down quarks to play with. Once again, we can put the quark spins in the same direction, or in opposite directions.

We start by putting the spin of the quark and anti-quark in opposite directions. This results in mesons with spin 0 . There are three such mesons that we can build from the up and down quarks, known as pions. Their masses and quark content are given by

$$\begin{array}{cll} & \pi^+(\bar{d}u) & m \approx 139\text{MeV} \\ \pi^0 & \frac{1}{\sqrt{2}}(\bar{u}u - \bar{d}d) & m \approx 135\text{MeV} \\ & \pi^-(\bar{u}d) & m \approx 139\text{MeV} \end{array}$$

The $\pi^-$is the anti-particle of $\pi^+$and the two have exactly the same mass. The neutral pion, π^0 is a combination of up and down quarks as shown. It has no electric charge, but a very similar mass to the $\pi^\pm$. The similar masses reflect the isospin symmetry which says that, as far as the strong force is concerned, the up and down quarks have the same properties.

Despite their similar masses, the neutral and charged pions have rather different lifetimes. The neutral pion decays through the electromagnetic force to two photons

$$\pi^0 \to \gamma + \gamma$$

It has a lifetime of around 10^{-17} seconds. In contrast, the charged pions $\pi^+$and π^- decay through the weak force. We'll see in Section 4 that they typically decay to a muon and a neutrino

$$\pi^+ \to \mu^+ + \nu_\mu \quad \text{and} \quad \pi^- \to \mu^- + \bar{\nu}_\mu$$

They live for 10^{-8} seconds, an eternity in the subatomic world and much longer than any of the baryons except the proton and neutron.

There is one, very important characteristic that distinguishes mesons from baryons. Mesons, made of a quark and anti-quark, have integer spin and are therefore bosons. Baryons, made of three quarks, have half integer spin and are therefore fermions.

Back at the beginning of Section 2, we explained that fermions are "matter particles" while bosons are "force particles". It should come as no surprise to learn that baryons, like protons and neutrons, are matter particles. After all, you're made up of them. But it may be less familiar to hear that mesons, like the pion, are force particles. What force do they mediate?

The answer to this is quite lovely: the pions give rise to an attractive force between the baryons. In particular, they give rise to an attractive force between any collection of protons and neutrons. It is this force that binds the protons and neutrons together inside the nucleus.

The existence of a scalar particle, mediating the interaction between protons and neutrons, was predicted by Yukawa in 1935, more than a decade before the pion was discovered. Yukawa observed that a massive scalar particle would give rise to a Coulombtype force, but with an exponential suppression due to the mass. The potential energy between any two particles takes the form

$$V(r) \sim -\frac{e^{-mr}}{r} \tag{3.4}$$

This is called the Yukawa potential. When $m = 0$, it agrees with the more familiar Coulomb potential. For very small distances, $r \ll 1/m$, it is more or less the same as the Coulomb potential. But the force drops off very quickly at distances $r \gg 1/m$. Yukawa had the simple insight that the force that binds the nucleus together should exert itself over distances comparable to the size of the nucleus. From this, he predicted the mass of the pion to be around 200 times the mass of the electron, or about 100 MeV . As we see, he was not far off.

The force that binds the nucleus together is usually simply referred to as the strong nuclear force. But it would be better to give it a different name - say "mesonic force", or "Yukawa force" - to highlight the fact that it is really a residual, secondary effect. At the fundamental level the strong force is mediated by gluons and binds quarks together. But it binds them together in two ways: one to create baryonic matter particles, and another to create mesonic force particles. The upshot is that there are two layers to the strong force: we start with one force and a set of matter particles gluons interacting with quarks - and end up with a very different force and a new set of matter particles - the mesonic force interacting with protons and neutrons. In this sense, both the particles in the nucleus, and the force that holds them together, are emergent phenomena, arising from something more fundamental underneath.

We might, then wonder: do similar transformations await us as we go to yet smaller scales? Could there be some other, very different degrees of freedom on the smallest scales, from which the Standard Model emerges. The answer, of course, is: we don't know.

3.4.2 The Eightfold Way Again

Let's now throw the strange quark into the mix. In addition to the three pions, there are five further spin 0 mesons we can build. (Actually six, but one of these, the η' has slightly different properties so we'll postpone its discussion for now.) These are a
collection of particles called kaons

$$\begin{array}{ll} K^+(\bar{s}u) & m \approx 494\text{MeV} \\ K^0(\bar{s}d) & m \approx 498\text{MeV} \\ \bar{K}^0(\bar{d}s) & m \approx 498\text{MeV} \\ K^-(\bar{u}s) & m \approx 494\text{MeV} \end{array}$$

The charged kaons are, like the charged pions, relatively long lived: their lifetime is around 10^{-8} seconds. They too decay via the weak force.

The lifetime of the neutral kaons is a somewhat more complicated story: rather curiously they appear to have two different lifetimes, either 10^{-7} seconds or 10^{-10} seconds, depending on how you count! That's kind of weird. Moreover, rather unexpectedly, it turns out to be an indirect hint of one of the deepest properties of the Standard Model: the fundamental laws of physics are not the same if you run them forwards and backwards in time! We will postpone discussion of this topic to Section 4.3.4.

Finally, there is one meson that is a combination of up, down and strange quarks called, uninspiringly, the eta (η) meson. Its mass and quark content are

$$\eta : \quad \frac{1}{\sqrt{6}}(\bar{u}u + \bar{d}d - 2\bar{s}s) \quad m \approx 548\text{MeV}$$

This is similar in spirit to the π^0 meson: for each type of quark there is also an antiquark sitting within the meson. This allows it to decay quickly, in 10^{-19} seconds, to two photons.

Together with the pions, these 8 mesons sit in a pretty pattern governed by the eightfold way symmetry relating the three fundamental quarks. We again construct rows of increasing strangeness, where a strange anti-quark $\bar{s}$ counts as negative strangeness:

$$K^0\ (\bar{s}d) \qquad K^+\ (\bar{s}u)$$

$$\pi^-\ (\bar{u}d) \qquad \pi^0, \eta \qquad \pi^+\ (\bar{d}u)$$

$$K^-\ (\bar{u}s) \qquad \bar{K}^0\ (\bar{d}s)$$

We haven't written the quark content of the π^0 and η only in an attempt to keep table looking vaguely aesthetic.

Viewed purely in terms of masses, the eightfold way looks less convincing for the mesons than for the baryons. An additional strange quark or anti-quark now costs roughly 350 MeV , and the kaons and η are two to three times heavier than the pions. Despite this, it turns out that the masses of all these mesons are well understood theoretically, with the eightfold way an important part of the derivation.

Although I won't recount the full story here, there is part of it that is worth highlighting. Recall that the masses of the proton and neutron are set almost entirely by Λ_{QCD}, rather than the masses of the up and down quark. Indeed, as we mentioned previously, if the up and down quarks were massless then the mass of the proton and neutron would remain pretty much unchanged. At first glance, it looks like the same might be true of the mesons above. After all, the mass of the pions is much closer to $\Lambda_{QCD} \approx 200\text{MeV}$ than to m_{up} and m_{down} , which are a few MeV . However, it turns out that this guess is completely wrong! If the mass of the up and down quarks vanish, then the mass of the pions would also vanish! Similarly, if the mass of the up, down and strange quarks all vanished, then all 8 mesons above would have vanishing mass.

This may seem like a theoretical curiosity since, in the real world, the masses of the quarks are distinctly not zero. Nonetheless, it turns our that this simple observation is enough to govern many of the properties of these mesons. You can read more about this beautiful story in the chapter on chiral symmetry breaking in the lectures on Gauge Theory.

There is one final spin 0 meson that is a bit of a loner. It is even given a rubbish name. The eta-prime (η') meson has quark content and mass given by

$$\eta' \frac{1}{\sqrt{3}}(\bar{u}u + \bar{d}d + \bar{s}s) \quad m \approx 958\text{MeV}$$

The eta-prime is significantly heavier than the other 8 mesons, despite having a very similar quark content to the eta meson. There is again a beautiful story behind this associated to the so-called axial anomaly, one of the more subtle and deep aspects of quantum field theory. This too is described in the lectures on Gauge Theory.

More Mesons

So far we have only discussed spin 0 mesons, in which the spins of the constituent quark and anti-quark point in opposite directions. We could also arrange for these spins to be aligned. In this case, we end up with mesons of spin 1 .

For example, there is a collection of three spin 1 mesons containing only the up and down quarks. These are called rho mesons, and can be viewed as excitations of the three pions. They have masses ~ 770MeV and decay quickly to pairs of pions.

There are many many further mesons, including excitations of those already mentioned, and mesons that involve the charm and bottom quark. Once again, the top quark decays too quickly and does not form mesons.

Two sets of these mesons deserve a special mention. The first is charmonium, a bound state of charm and anti-charm quark. It also goes by the dual name J $-$ psi(J/ψ),

$$J/\psi(\bar{c}c) \quad m \approx 3.1\text{GeV}$$

Its lifetime is around 10^{-21} seconds. The discovery of this particle in 1974 was the first glimpse of the charm quark and will be described in Section C.3.

There are a collection of lighter mesons that contain just a single charm quark. These are called (somewhat peculiarly) D-mesons. The lightest are:

$$D^0(c\bar{u})m \approx 1865\text{MeV}$$
$$D^+(c\bar{d})m \approx 1869\text{MeV}$$

These are remarkably long lived particles, with the D^+living 10^{-12} seconds, and the D^0 about half this time. The long lifetime is because these particles decay only through a somewhat subtle property of the weak force. We will learn more about this in Section 4.3.

Similarly, the bottom quark was first discovered in bottomonium, also known as the upsilon (Υ)

$$\Upsilon(\bar{b}b) \quad m \approx 9.5\text{GeV}$$

This has a lifetime of 10^{-20} seconds. Once again, it is neither the lightest nor the longest lived meson containing a b-quark. The lightest B-mesons are

$$B^+(u\bar{b}) \text{ and } B^0(d\bar{b}) \quad m \approx 5280\text{MeV}$$

Despite being significantly heavier, they actually live (very) slightly longer than the Dmesons, with a lifetime of around 1.5×10^{-12} seconds. Again, this is down to intricacies of the weak force.

C Interlude: The Rise of the Machine

From the 1920s onwards, it became clear that the alpha particles emitted in radioactivity, with their 5 MeV of energy, would not suffice to understand the nucleus. As we saw in Interlude B, in the short term most discoveries would come courtesy of cosmic rays. But, long term, new accelerator technology was needed.

The cathode ray tube is, in many ways, the first particle accelerator, albeit one built before the constituents were even known to be particles. The key idea is a simple one: if you drop a large voltage over some distance then charged particles will pick up speed. You can then use the resulting beam to smash into other things, as Röntgen did in his discovery of X-rays.

A variant of this idea was taken forward by John Cockcroft and Ernest Walton. Working in Cambridge in 1932, under the ever watchful eye of Rutherford, they built a voltage multiplier capable of accelerating protons to 700 keV . They then used this to great effect, inducing the first artificial transmutation of a nucleus,

$$p + {}^7\mathrm{Li} \longrightarrow 2\alpha$$

In more popular terminology, they succeeded in splitting the atom. These days, the "high-tension laboratory", where Cockcroft and Walton performed their later experiments, has been converted into the "Cockcroft lecture theatre", where we teach Newtonian mechanics and special relativity to first year undergraduates.

Both the cathode ray tube and the Cockcroft-Walton accelerator are linear accelerators: the charged particles move in a straight line. The next great breakthrough - due to Ernest Lawrence - was a simple one: make the particles bend.

C. 1 The Cyclotron

Lawrence was inspired by a simple fact in classical mechanics. Take a charged particle of mass m and charge q, restricted to move in the $(\ x, y\ )$-plane, with a magnetic field B in the z-direction. If you give the particle an initial kick of speed v, then it moves in a circle and comes back to its starting position in time

$$T = \frac{2\pi m}{qB} \tag{C.1}$$

The lovely fact is that this time doesn't depend on the speed v ! If you set the particle off with a bigger velocity, then it will travel in a bigger circle, but always come back in the same time.

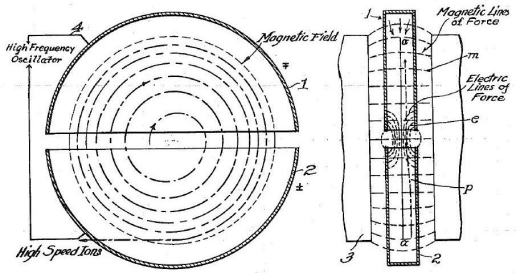


Figure 22. The principle behind the cyclotron, from Ernest Lawrence's 1934 patent application.

This is the key principle behind the cyclotron. The charged particles move perpendicular to a fixed magnetic field. They are trapped in two boxes, called dees, so named because they are shaped like the letter D. The two dees are placed back to back, with a small gap between them

like so: GD. A voltage is placed across the gap, ensuring that the particles are accelerated every time they cross from one dee to the other. The rub, of course, is that first they cross the gap in one direction, then in the other. This means that if you want them to be accelerated each time, rather than decelerated, then you have to flip the polarity of the voltage in the time it takes them to travel a semi-circle. The good news, as we've seen in (C.1), is that this time doesn't depend on how fast the particles are going. This means that you can tune the AC voltage to a frequency, resonant with the particles and the particles will speed up, travelling in ever wider circles until they spit out the end where they can be used for whatever purpose is needed.

A prototype cyclotron, known as the 9 -inch, was first constructed in Berkeley in 1930. By 1932, Lawrence and his student, Stanley Livingston, had succeeded in building an 11-inch machine that could reach energies of 1 MeV and were able to quickly reproduce the Cockcroft-Walton results splitting the atom. For the rest of the 1930s, Lawrence exhibited a single-minded focus on reaching higher and higher energies. By 1936 he reached 8 MeV , by 193920 MeV . Indeed, such was his desire to reach higher energies, it seemed to barely occur to Lawrence that he should, perhaps, occasionally pause to do some science with his machines.

Furthermore, there is a limit to how far the key equation (C.1) can be pushed. As protons reach energies of around 25 MeV , the effects of special relativity have to
be taken into account and their mass starts to increase with velocity. This knocks the timing, since the faster protons now take slightly longer to make their orbit. To compensate, one has to tune the magnetic field to keep the timing in sync. This kind of machine, still with particles spiralling outwards but with a varying magnetic field, goes by the catchy name of a synchrocylclotron, or SC for short.

Soon after the war, flush with money from the military, Lawrence completed his first SC, a 184 -inch monster machine with a magnet that weighed 10,000 tons and accelerated alpha particles to 380 MeV , later increased to 720 MeV . The question was: what to do with it?

The Neutral Pion

The neutral pion π^0 holds two claims to fame. It was the first particle to be predicted on grounds of symmetry. And it was the first particle to be discovered in a collider on Earth, rather than in a cosmic ray shower.

First the experimental situation. Recall from Interlude B. 3 that the charged pion was discovered in cosmic ray showers by Powell and his team in 1947. In fact, rather embarrassingly, by that point Lawrence's SC had been producing pions for over a year. But, such was the focus on reaching higher energies, no one had put any thought into building detectors. It was only when Cécil Lattes, one of Powell's collaborators, moved to Berkeley in 1948 that they placed photographic emulsion plates in the accelerator and found pions in great numbers.

The neutral pion is a different matter altogether. Since it carries no electric charge, it leaves no tracks and neither cloud chambers nor photographic emulsions can be used to find it. Instead, it can only be seen by more indirect means through its decay to two photons

$$\pi^0 \longrightarrow \gamma + \gamma$$

The smoking gun is the detection of two simultaneous photons, whose energy, momentum and angular momentum correlations can be traced to the decay of a single particle. The neutral pion was discovered in this manner in 1950 by Steinberger, Panofski and Steller, using the Berkeley SC.

Next, the theory. In Section 3 we explained the eightfold way, the idea that there is an approximate symmetry between the up, down and strange quarks which leads to patterns in the masses of baryons and mesons. We also briefly mentioned a precursor to this idea, first pointed out in the early 1930's by Heisenberg. This is the idea that, at

least as far as the strong force is concerned, the neutron and proton behave in almost identical fashion. They have similar mass. Moreover, the binding force between nn, pp and *np* is more or less the same. Even with the very limited experimental data of the early 1930s, Heisenberg intuited that this was important. At the time the symmetry between the proton and neutron was called isotopic spin [11], these days shortened to just isospin.

However, the idea of isospin runs into trouble when you appreciate the obvious: the proton and neutron have different electric charges. If the strong force is mediated by charged pions $\pi^{\pm}$alone, as was thought by the late 1930s (recall, people still thought that the muon was responsible at this point!) then charge conservation meant that the interactions experienced by the proton and neutron would necessarily be different. The way out was suggested by the theorist Nicholas Kemmer in 1938: you get to keep isospin symmetry, but only if there exists a third, neutral pion π^0.

Resonances

Neutral particles are not the only ones that are hard to see. Any hadron or meson that decays through the strong force, rather than the weak force, will have a lifetime of around 10^{-24} seconds. That's not a huge amount of time, even by the standards of particle physics. Even allowing for relativistic time dilation, these particles are not going to travel far enough to snap a photograph of them. Instead, we need more indirect methods to detect them.

The method of choice is to observe the effect of these new particles on the old. To explain this I first need to introduce a new concept: that of cross-section.

When two elementary particles come close to each other, there is some probability that they will interact. This interaction may result in them scattering off each other, or transforming - even if only briefly - into some other particle. Roughly speaking, the cross-section is the probability that they interact in some way, rather than pass through each other.

We can also speak less roughly. The cross-section, as the name suggests, is actually an area. As such it can't quite be a probability (which must be dimensionless) but it's closely related. The idea is that the cross-section is the area - or size - that the particles present to each other as they approach. As an analogy, if you're throwing balls in an attempt to hit some target, it's the cross-sectional area of the target that

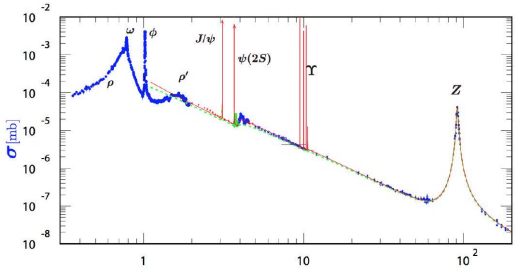


Figure 23. A collection of data from many experiments studying $e^{+} e^{-} \longrightarrow$ hadrons. The horizontal axis is the centre of mass energy, measured in GeV . A number of different mesons can be clearly seen at low energy, with the Z-boson at high energy. This plot was taken from the particle data group plots of cross-sections and related quantities.}

will determine your success. A barn door has a bigger cross-section than a beer can. This, in turn, means that games where you try to hit a barn door are somewhat less entertaining

[011] This is, of course, a daft name. A much better name would be isobaric spin, since isobars are elements with the same atomic mass but different combinations of protons and neutrons.

than those where you try to hit a beer can.

Importantly, the cross-section for some interaction depends on the energy of the colliding particles. Typically, in particle physics one finds that the cross-section drops as the energy of the incoming particles increases. But, every now and then, one sees a pronounced bump in the cross-section. This bump is called a resonance and is the telltale sign that there's a new, third particle, appearing in the story.

The bumps appear when the energy of the incoming particles is tuned to the mass of some new particle. This allows for a new interaction, in which the two incoming particles briefly morph into the new one which will then, typically, subsequently decay. These decay products may be the original particles, in which case it will just look like they've scattered off each other, or they may be something new entirely.

The early data on resonances is not particularly clean. (We'll give an example below.) However, the idea is clearly illustrated in Figure 23 which collects together the results of many decades worth of experiments of e^+e^-collisions, where the end products are hadrons. The horizontal axis depicts the (log of the) energy, measured in GeV . The vertical axis depicts the (log of the) cross-section. You can see the overall downwards trend of the cross-section as the energy increases, but most striking are the various
peaks. At lower energies these peaks correspond to meson states that we met in the last section. Way up, at close to 100 GeV , we see the Z-boson that mediates the weak force. We'll discuss this more in the following section.

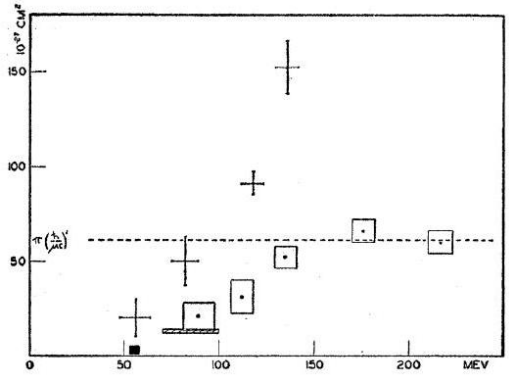
The shape of the resonance contains a lot of information about the underlying particle. The energy at which the resonance occurs tells us the mass of the particle. Meanwhile, the width of the resonance tells us its lifetime: the bigger the width, the quicker the particle decays. Returning to Figure 23, you can see that the width is barely discernible on the red spikes in the middle. This is because, as we saw in the last section, these are the lightest states containing charm and bottom quarks respectively. The presence of these new quarks limits their decay options, resulting in a much longer lifetime than might naively be expected.

Many of the particles that we'll meet as these lectures progress were detected through their resonance effect on scattering. You can read more about the basics of resonances in quantum mechanical scattering in the lectures on Topics in Quantum Mechanics.

Delta Baryons

The first novel particle detected as a resonance was the collection of four Δ-baryons. Viewed through today's lens of the quark model, they are Δ^{++}(uuu), Δ^+(uud), Δ^0 (udd) and Δ^-(ddd). Each has mass 1232 MeV and a lifetime of around 5×10^{-24} seconds.

The year was 1952, the place Chicago. Enrico Fermi and his team had built a synchrocyclotron, based on the principles introduced by Lawrence. They extracted a beam of pions from the machine and directed it at hydrogen gas to watch how the pions scattered off protons. They didn't see anything as distinctive as a bump. They did, however, see a rise in the crosssection. Most strikingly, there was a clear difference in



the cross-sections for π^+(shown as crosses in the data to the right) and π^-(shown as rectangles) [12]. This needed an explanation.

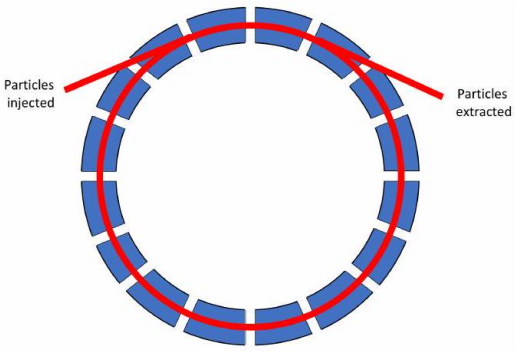
In fact, this effect had been anticipated earlier by a theorist called Keith Brueckner. He looked at the three scattering processes

$$\pi^+ + p \longrightarrow \pi^+ + p$$
$$\pi^- + p \longrightarrow \pi^- + p$$
$$\pi^- + p \longrightarrow \pi^0 + n$$

By invoking a set of intermediate states, which we now call the Δ-baryons, he argued that the processes could proceed through the creation of Δ^{++}or Δ^0 and should occur with relative probabilities in the ratio $9:2:1$. This was what the Chicago team observed. Further analysis of the angular distribution of the scattering showed that the intermediate states must have spin $3/2$. Historically, the discovery of the Δ^{++}, with its striking $+2$ charge, played an important role in elucidating the underlying structure of quarks.

C. 2 The Synchrotron

Cylcotrons, with the particles spiralling outwards, can reach energies no higher than 1 GeV or so. The next phase in accelerator development was the synchrotron. Here, particles travel in a circle of fixed radius. Their path is again bent by magnets, and accelerated in the gaps between the magnetics by electric fields. To keep the particle travelling in a circle, the magnetic field must be synchronised with the particle's velocity, so that the magnetic field becomes stronger as the parti-



cles pick up speed. A cartoon picture of the synchrotron is shown on the right.

The development of the synchrotron brought many new technical challenges, including the difficult issue of stabilising the beam. Key to the whole endeavour is the concept of phase stability, in which an alternating voltage is placed over the gaps acts to ensure that all particles converge on the same speed, with the faster ones slowing slightly and the tardy ones picking

[012] This figure is taken from the paper Total Cross Sections of Positive Pions in Hydrogen" by Anderson, Fermi, Long, and Nagle.

up speed. This results in particles sitting in bunches, rather than the continuous beam of the earlier cyclotron.

Another difference from the cyclotron is that you don't get to start the particles from rest. They must be injected into the synchrotron at some other accelerator. This, then, is the fate of accelerators upon retirement: they become injection machines for the next generation.

The early proton synchrotrons had the cool names, before the push for dull acronyms became too strong to ignore. In Brookhaven, the Cosmotron reached energies of 3 GeV ; in Berkeley, the Bevatron 6 GeV . These began a long succession of machines, culminating more than half a century later, with the Tevatron at Fermilab reaching 1 TeV and the LHC at CERN reaching 13 TeV .

More Anti-Matter

The 6 GeV reached by the bevatron was not chosen arbitrarily. It was built with a particular science case in mind: the creation of anti-protons. The 6 GeV threshold allows their production through

$$p + p \longrightarrow p + p + p + \bar{p}$$

The first proton on the left-hand side was in the beam; the second proton on the lefthand side was sitting in a fixed copper target. The resulting debris mostly consists of pions, with the occasional anti-proton lying within. The challenge was to find them.

You might have thought that the best way to detect anti-protons would be to watch them annihilate with protons. In fact, it turned out to be significantly simpler to identify them through their mass and charge. To this end, the experimenters first set up a series of magnets, designed to deflect unwanted positively charged particles and focus only negatively charged particles with very specific momentum into the detectors. The first set of detectors consisted of scintillation counters, an instrument for measuring the photons emitted by the ionised tracks left by a charged particle. Two scintillation counters were placed 12 m apart. Both anti-protons and pions in the beam had the same momentum, which meant that the heavier protons were slower and so took longer to travel the 12 m between the detectors. A whole 10^{-8} seconds longer. That was the first clue.

Next, the beam entered a pair of Cerenkov detectors. These detect an effect known as Cerenkov radiation which is emitted when particles travel through a material faster than light can travel through that material. The first Cerenkov detector fired whenever the particle was travelling too fast to be an anti-proton. The second Cerenkov detector had a special design which meant that it fired only for a small window of velocities, tuned to that of the anti-proton, and so failed to fire for the faster mesons.

With this elaborate set-up, over the course of two weeks in October 1955, Emilio Segrè and his team of Owen Chamberlain, Clyde Wiegand and Tom Ypsilantis found 60 anti-protons, nestled among 3.5 million pions. They announced the discovery at a press conference on October 19^{th} 1955.

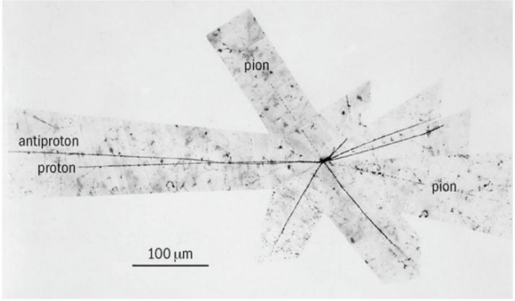


Figure 24. A photographic emulsion showing $p \bar{p}$ annihilation. The original (in vertical orientation) can be found in the 1956 Nuovo Cimento paper "On the Observation of an Antiproton Star in Emulsion Exposed at the Bevatron" by Chamberlain et. al.}

This story also has some human twists. Indeed, as machines got bigger, so too did the opportunity for machinations. The clever magnetic lens design used in the experiment was due to an Italian physicist, Oreste Piccioni who, at the time, was a visitor in Berkeley. Although the group lead by Segrè adopted this design, they were reluctant to allow Piccioni to join their team when he returned to Berkeley full time in the summer of 1955. Instead, Piccioni joined a rival team, also searching for the anti-proton, lead by Edward Lofgren.

The two teams took it in turns to use the bevatron, two weeks on, two weeks off. The machine broke in the middle of Segrè's second run and they could take no data. When the machine was finally repaired, nice-guy Lofgren yielded his time to allow Segrè to complete his run. Two weeks later they announced the discovery of the anti-proton. Four years after that, Segrè and Chamberlain collected their Nobel prize. Nice guys, it turns out, rarely fared well in the increasingly ruthless world of experimental particle physics.

However, there was some joy for both Lofgren and Piccioni. One year later, they were among the team who discovered the anti-neutron through the annihilation processes

$$p + \bar{p} \longrightarrow n + \bar{n}$$

It appears, however, that this brought little comfort to Piccioni. Some years later, he sued Segré and Chamberlain for $\$125,000$ of their Nobel prize money. The case made it to the US supreme court, before being dismissed.

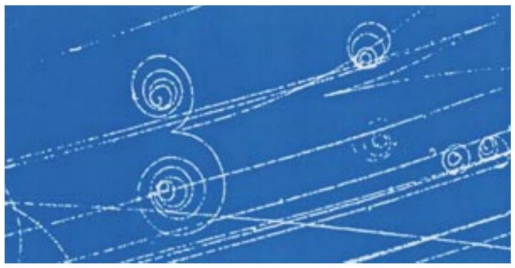


Figure 25. This bubble chamber photograph, taken at the Lawrence Berkeley Laboratory, shows a high energy γ ray colliding with an electron to produce an $e^{+}e^{-}$pair, which spiral in opposite directions. The original electron receives a huge kick and flies off to the right. At some point it emits a gamma ray which then turns into a second e^+e^-pair, this time with higher energy, visible as the V signature to the right of the picture.}

Mesons and Baryons in Bubbles

The next leap forward was in detector technology. In the 1950s, Donald Glaser proposed the idea of a bubble chamber, a successor to the cloud chamber. The detector is filled with a liquid - ideally liquid hydrogen - that is kept under pressure at constant temperature, slightly below its boiling point. Just before the particles pass through, the pressure is reduced by a small amount, lowering the boiling point so that the liquid is super-heated, meaning that it remains in the liquid phase even though the temperature is above boiling. As a charged particle passes through, it gives the liquid the nudge it needs to start boiling, leaving behind a trail of bubbles. Examples of the particles' graceful arcs, as they spiral in an applied magnetic field, can be seen in Figures 25 and 26.

In addition, this was a time of increased automation. The number of events that could be recorded in a bubble chamber was far greater than in previous detectors. Teams of highly skilled, poorly paid women, scouring photographic emulsions for interesting forks and kinks just wasn't going to cut it anymore. Instead, both analysis and data storage required the use of computers. Experiments could be done in one institution, and analysed elsewhere.

Results came quickly. First, a collection of vector (i.e. spin 1) mesons were discovered, starting with the ρ and ω. The η meson was discovered at Johns Hopkins university, using data borrowed from Berkeley. (η translates to the letter H, which is short for "Hopkins" apparently.)

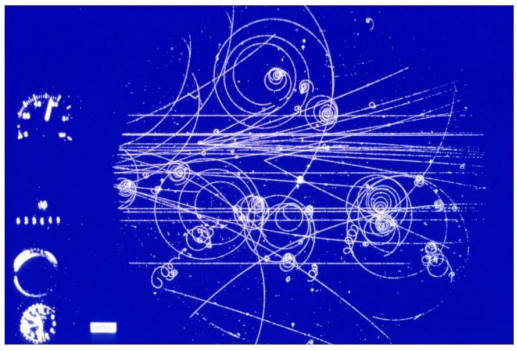


Figure 26. This photo was taken in 1960 at CERN. A stream of π^{-}mesons enter from the left. One of these pions hits a proton in the liquid hydrogen spraying new particles. Among these is a neutral Λ baryon, which doesn't leave a track but reveals its existence a little to right as it decays into a proton and pion, producing the characteristic V shape seen in the middle of the picture. The results of this decay have high energy and travel in straight line. Other, lower energy charged particles spiral in the magnetic field.}

Baryons were also seen in quantity, both long-lived strange baryons and, indirectly, shorter lived resonances. An important breakthrough happened in 1964, when the Ω^- baryon was discovered. The Ω^-contains three strange quarks and its mass, lifetime and decay modes had been predicted earlier using the quark model.

The Ω^-discovery is shown in Figure 27. An incoming kaon collides with a proton in the liquid, yielding

$$K^-(\bar{u}s) + p(uud) \longrightarrow \Omega^-(sss) + K^+(u\bar{s}) + K^0(d\bar{s})$$

There is then a succession of further baryon decays, with

$$\begin{aligned}
\Omega^-(sss) &\longrightarrow \Xi^0(uss) + \pi^-(\bar{u}d) \\
\Xi^0(uss) &\longrightarrow \Lambda^0(uds) + 2\gamma \\
\Lambda^0(uds) &\longrightarrow p(uud) + \pi^-(\bar{u}d)
\end{aligned}$$

Each of these decays changes strangeness by -1 , and so happens only through the weak force. Correspondingly, the lifetime is around 10^{-10} seconds for each, long enough for them to leave a trail a bubbles.

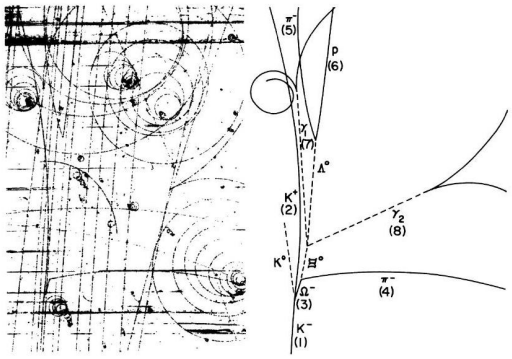


Figure 27. The original bubble chamber picture, and an accompanying line tracing, showing the discovery of the $\Omegaˆ{-
$baryon. This is taken from the 1964 paper "Observation of a hyperon with strangeness minus three" by Barnes et. al. Here "et al" refers to an additional 30 authors, heralding the large collaborations that were to come.}

C. 3 Quarks

The cornucopia of hadrons discovered throughout the 50s and 60s gave enough clues to lead to the quark model. The observed masses and lifetimes could be roughly accounted for by postulating three different types of constituent spin $\frac{1}{2}$ particles - up, down and strange - each of which carries three different internal degrees of freedom called colour. But that still left open the question of whether these quarks were real entities, or just mathematical accounting tricks.

Most physicists at the time assumed that quarks were merely a useful fiction. Their concern was the obvious one: if quarks are real, then why don't we observe them in isolation, where their fractional electric charge would stand out like a sore thumb. Gell-Mann ends the 1964 paper in which he first proposed quarks with the sentence

> "A search for stable quarks of charge $-\frac{1}{3}$ or $+\frac{2}{3}$ and/or stable di-quarks of charge $-\frac{2}{3}$ or $+\frac{1}{3}$ at the highest energy accelerators would help to reassure us of the non-existence of real quarks.

Zweig, who independently had the same idea in the same month - January 1964 referred to quarks as "aces" and was marginally more optimistic. The final sentence of his paper reads "There is also the outside chance that the model is a closer approximation to nature than we may think, and that fractionally charged aces abound within us."

The situation was resolved by a series of experiments that, although initially designed to study resonances of the proton, turned out to be perfectly placed to instead explore its inner structure. These experiments, which ran from 1967 to 1973, took place at the Stanford Linear Accelerator, better known as SLAC, a 3 km long machine that accelerated electrons to 20 GeV , effectively by getting them to surf the crest of an electromagnetic wave.

The SLAC experiments didn't see anything as striking as fractional electric charge. Indeed, their data was, at first, murky and complicated. However, over the course of several years it became increasingly apparent that their results could only be explained if the electrons were scattering off some point-like constituent inside the proton and neutron. As we now explain, these experiments involve a process known as ...

Deep Inelastic Scattering

By the mid 1960s, it was apparent that the proton is not a point-like object but has a size of around 10^{-15} m. This was seen, for example, in the elastic scattering of electrons off protons. Here, the word "elastic" means that the electron has the same energy after the collision as before. For example, the Geiger-Marsden experiment that uncovered the structure of the atom involved the elastic scattering of alpha particles off the nucleus.

In contrast, in inelastic scattering, the electron collides with more destructive force, knocking the proton into a higher excited state, such as a spin $\frac{3}{2}$ baryon, or breaking it apart completely. This process can roughly be characterised as

$$e + p \longrightarrow e + \text{ other stuff}$$

where we don't too much care about the other stuff. We care only about what happens to the electron. If the electron comes in at very high energies then it buries deep into the proton where it can probe whatever lies inside.

If, as was originally thought, the proton was structureless, then the cross-section for electron-proton scattering should rapidly decrease with energy. And this is indeed seen in elastic scattering. However, when the electron energy gets high enough to enter the inelastic regime, something different occurs. The first clue that something was afoot was simply that more electrons were scattered at low angles than expected. However, when the data was plotted in a particular way, something more surprising stood out.

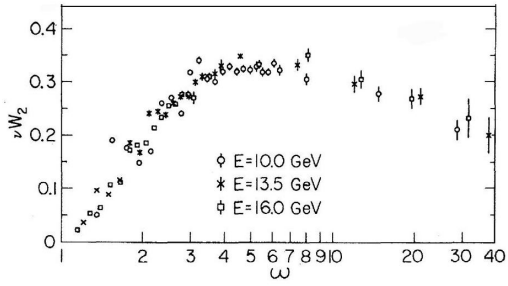


Figure 28. It's neither pretty, nor obvious, but this data provided the first hint of the existence of quarks. The proton structure function is plotted on the vertical axis, while $\omega = 1/x$ is on the horizontal axis. This graph is taken from the 1969 paper "Observed Behavior of Highly Inelastic Electron-Proton Scattering".

To explain this, I need to first describe a little bit of scattering theory. The crosssection for electron-proton scattering depends on an object called the proton structure function. And this, in turn, depends on the energy E of the incoming electron, the energy E' of the outgoing electron and the angle θ by which the electron is deflected. In general, any cross-section depends on these variables in two combinations

$$\nu = E - E' \quad \text{and} \quad q^2 = 4EE'(1 - \cos\theta)$$

The surprise was that, at high energies, the proton structure function doesn't depend on both ν and q^2 : it depends only on the dimensionless ratio

$$x = \frac{q^2}{2M\nu}$$

where M is the mass of the proton. The initial data, shown in Figure 28, plots the proton structure function for scattering by a small angle ($\theta = 6^\circ$ in this case.) The fact that the

data for three different energies all lie on the same curve is showing that the structure function depends only on the combination x. This is known as Bjorken scaling, after the theorist Bjorken who first suggested this behaviour (and first suggested that the experimenters plot their data in this unlikely manner.)

The question, of course, is what does scaling mean? The intuitive idea, largely due to Feynman, is that scaling is telling us directly that the electron is scattering off a point-like object inside the proton. Very roughly speaking, this is because the
proton structure function doesn't depend on any scale, because x is a dimensionless variable. But the only object with no scale is a point. (Feynman's original argument is characteristically creative and involves going to a frame of reference in which the point-like object in the proton has infinite momentum.)

Feynman referred to the point-like objects inside the proton as partons, noticeably avoiding the term "quark" in his original paper. I do not know if this was for the purposes of scientific agnosticism or scientific antagonism. (Gell-Man and Feynman were colleagues, collaborators and, perhaps above all, rivals!) Either way, the omission was appropriate. Simple models in which the proton and neutron are each composed of three quarks do not provide a good fit to the data. This is because, as we explained in the previous section, the proton and neutron are themselves enormously complicated objects. The cartoon picture in which they each contain three quarks is a long way from reality and ignores the morass of gluons and quark-anti-quark pairs that also sit inside. Deep inelastic scattering provides the tool to probe this complexity. Good fits to the data could only be achieved by including partons that are gluons and quark-anti-quark pairs, in addition to the three valence quarks.

Deep inelastic scattering also provides a method to indirectly test the electric charges carried by the partons. It turns out that the cross-section is proportional to the sum of the squares of the charges of the partons. For a proton, with uud quarks, this sum gives $\left(\frac{2}{3}\right)^2 + \left(\frac{2}{3}\right)^2 + \left(-\frac{1}{3}\right)^2 = 1$, while for a neutron with udd, it is $\left(\frac{2}{3}\right)^2 + \left(-\frac{1}{3}\right)^2 + \left(-\frac{1}{3}\right)^2 = \frac{2}{3}$. The simplest quark model then predicts that the cross-section for neutrons should be $\frac{2}{3}$ that of protons. After taking into the account the many subtleties described above, this is confirmed by experiment.

Although the parton model provided a good explanation for the experimental results, there was one mystery that remained. The partons that lead to exact scaling behaviour are free particles. Subsequent deviations from scaling suggested that there were some interactions between the partons, but these were necessarily small. Yet how could partons be confined within the proton if the interactions were so small? This issue was resolved by the discovery of asymptotic freedom in Yang-Mills like theories by Gross, Wilczek and, independently, Politzer in 1973.

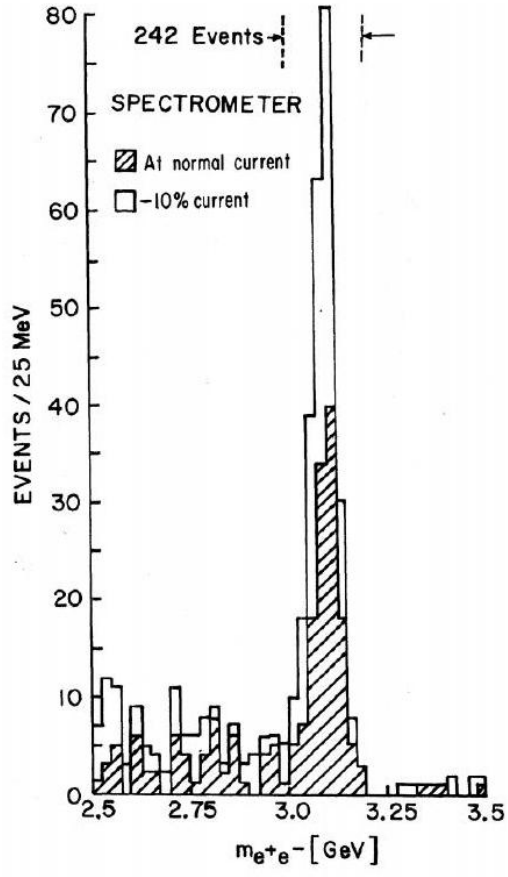
Charmed

In November 1974, a new quark was found. This was the charm. It came as a surprise to many physicists and went a long way towards cementing belief in the quark model.

The discovery was made simultaneously on the West coast in SLAC and on the East coast in Brookhaven. Since both teams got to name the particle, it now goes by the double-barrelled J/ψ.

The J/ψ weighs in at 3.1 GeV , with a lifetime of almost 10^{-20} seconds. This is much longer than expected for a particle that is so heavy, a fact that reveals itself in the very narrow resonance shown on the right.

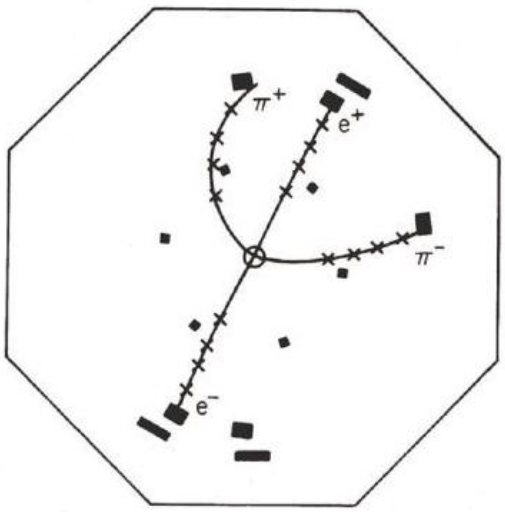
It didn't take long to understand that this resonance is so narrow because it contains a new quark-anti-quark pair, bound as $\bar{c}c$ meson. It is now also known as charmonium. In fact, in many ways the charmed mesons are easier to understand than their lighter cousins. Because the charm



quark is so heavy (about 1.3 GeV), it has a very small Compton wavelength. This means that two charm quarks in a meson sit so closely together that they are in the asymptotically free regime of QCD, where the coupling strength is fairly small. This makes it easier to understand their properties.

Within a few weeks of the original J/ψ discovery, a collection of further resonances had been found, all agreeing well with theoretical expectations. These new resonances were found only at SLAC so their name took preference, and they are called ψ'. In a cute twist, the reconstructed event decay of a ψ' takes the eponymous form shown on the right.

While most physicists had not expected the charm quark, there were some who had previously argued for its existence on



theoretical grounds. The most compelling was due to Glashow, Iliopoulos and Maiani (or GIM) who, in 1970, analysed a subtle property of the weak force known as flavour changing neutral currents. (We'll describe some basic properties of the weak force in Section 4.) An example of this phenomenon is the decay $K^0 \longrightarrow \mu^+ + \mu^-$. This happens very rarely, but it was difficult to

understand why: theoretical expectations suggest that a process involving the exchange of an up quark and W-boson should give a much larger decay rate. The GIM mechanism proposed the existence of a charm quark, with charge +2/3, and showed that this gives a contribution to the decay almost exactly cancels the contribution from the up quark.

After the discovery of the charm quark, many things fell into place. The key ideas underlying the Standard Model, from asymptotic freedom of the strong force, to symmetry breaking of the weak force (described in Section 4) had all been developed previously. But the discovery of the charm quark prompted a synthesis of these ideas, with all phenomena described by four quarks, two charged leptons, and two neutrinos, coupled through forces associated to $SU(3) \times SU(2) \times U(1)$. The inappropriately modest name Standard Model dates from this time. For this reason, physicists who lived through the discovery of charm sometimes refer to this period as the November Revolution.

Colliders

The discovery of charm also involved an important experimental leap: colliders.
All the accelerators that we've discussed so far take a beam of particles and smash it into a fixed target. This has the obvious advantage that it's easy to hit a fixed target. But it also has a disadvantage because conservation of momentum means that any particles you create fly off at close to the speed of light. It's not so much the fact they're moving that's the problem, but that much of the beam energy is wasted because it goes into the kinetic energy of the final product. If you succeed in accelerating particles of mass m to an energy E which then hits a fixed target, then the energy available to create new particles is $\sqrt{2mE}$. Clearly it would be better if we could make use of more of that precious beam energy.

These problems go away in a collider. This consists of two beams with equal and opposite momentum, which are then brought together at one or more intersection points where the collision takes place.

Needless to say, the technological hurdles in getting this to work are formidable. Not least is the problem of luminosity, meaning the number of collision events taking place. The density of particles in each beam is significantly less than that of a fixed target and, correspondingly, the number of collisions is greatly reduced. To compensate for this, each beam should consist of many pulses of particles, with collisions happening repeatedly and often. This, in turn, requires that the beams have long lifetimes. Typical numbers involve beam lifetimes of several hours, allowing them to circulate 10^{10} times or so. These accelerators also go by the name of storage rings.

The discovery of charm at Brookhaven used a standard fixed target experiment. A beam of electrons ploughed into a beryllium target, and they found their J particle as the huge peak in the centre of mass energy of e^+e^-pairs.

In contrast, the SLAC team used an e^+e^-collider, called SPEAR, short for the Stanford Positron Electron Asymmetric Rings. These storage rings took electrons and positrons from the linear collider and brought them into head-on collisions. They discovered their ψ particle as a resonance in the cross-section for $e^+ + e^- \longrightarrow$ hadrons.

As an aside, the acronym "asymmetric" in the acronym SPEAR dates from an earlier proposal in which $e^+$and e^-were accelerated in different rings. After a budget cut, the design changed to a single ring, but the acronym stayed.

Round Three

Back in 1932, there were 100 days where physicists could revel in a simplistic world containing only electrons, protons and neutrons. Then the discovery of positrons burst their bubble.

In the 1970s, physicists had a little over a year in which they could believe in a nice symmetrical world with two generations of fermions, each containing two quarks, an electron-type particle and a neutrino. Late in 1975, a group working at the SPEAR experiment found something odd and entirely unexpected. Their original paper doesn't beat around the bush, opening with the blunt statement:
"We have found 64 events of the form

$$e^+ + e^- \longrightarrow e^\pm + \mu^\mp + \geq 2 \text{ undetected particles}$$

for which we have no conventional explanation."
The paper suggests that these events could be due to a new charged, heavy lepton or to a new charged heavy boson. It took some years to realise that the former is the case: the original e^+e^-pair collide to form what we now call the tau leptons,

$$e^+ + e^- \longrightarrow \tau^+ + \tau^-$$

The taus subsequently decay as, for example,

$$\tau^- \longrightarrow \nu_\tau + e^- + \bar{\nu}_e \quad \text{and} \quad \tau^+ \longrightarrow \bar{\nu}_\tau + \mu^+ + \nu_\mu$$

giving rise to the observed signature.
The discovery of the τ lepton upset the balance. It would be another 20 years until it was restored, with the bottom quark, top quark and tau neutrino filling out the set. The bottom quark was discovered not long after. In 1977, a fixed target experiment at Fermilab found a strong, narrow resonance at 9.5 GeV , the upsilon Υ with quark content $\bar{b}b$.

Finding the top quark was another matter. A rough guesstimate for its mass can be made by a quick glimpse at the first five quarks:

$$\begin{array}{lll} m_d = 4.7\text{MeV} & m_s = 96\text{MeV} & m_b = 4.2\text{GeV} \\ m_u = 2.2\text{MeV} & m_c = 1.3\text{GeV} & m_t = ? \end{array}$$

Given this pattern, what would you guess for m_t ? Perhaps 40 GeV ? In the 1970's, a couple of e^+e^-colliders failed to find the top quark at 30 GeV . In the 1980's, a p^+p^- collider failed to find it at 80 GeV . By this time it was clear that the top quark was so heavy that it would not form a detectable $\bar{t}t$ meson state like J/ψ or Υ. This is because (see Section 4) it could decay directly to a W-boson through

$$t \longrightarrow W^+ + b \quad \text{and} \quad \bar{t} \longrightarrow W^- + \bar{b}$$

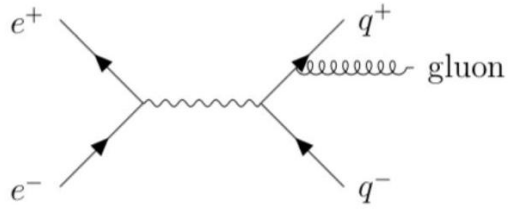
This decay happens in a shorter time scale than that associated to the strong force. This means that, if we want to find the top quark, we need to find clear evidence for the decay products that it leaves behind.

Because the top quarks are created as $\bar{t}t$ pairs, they will decay to $\bar{b}b$ pairs, together with a W^+W^-pair. The W-bosons themselves then decay, sometimes to quarks $W^\pm \to \bar{q}q$ and sometimes to leptons $W^\pm \to l^\pm\nu$ where $l = e, \mu$ or τ. The question is: how to see these decay products?

We know what charged leptons look like, and we know that neutrinos are just going to escape unnoticed. So the real question is: how do we see the quarks? Because these are confined, we can't see quarks directly. However, when quark-anti-quark pairs are formed from collisions, something rather dramatic happens. Each one of the pair flies off in a different direction but, because they hate to be alone, they pull further quark-anti-quark pairs from the vacuum as they go. The end result is that each quark morphs into a collection of hadrons, all moving in roughly the same direction. This is called a jet and the phenomenon of quarks turning into a multitude of mesons and baryons is called hadronisation.

Jets were first seen in SPEAR e^+e^-collisions in 1975 and proved yet more evidence for the reality of quarks. With a lot of work, it is sometimes possible to go backwards and, from the jet, reconstruct the kind of quark that started it.

As an aside to our main story, in the late 1970s, the first indirect evidence for the existence of the gluon came through a process associated to the following Feynman diagram:



One of the emitted quarks radiates a gluon, but the gluon can no more live on its own than the quarks. The result is 3 jets; two from the quarks, one from the gluon.

Back to the story of the top, the cleanest signature of top production occurs when both W bosons decay into leptons, giving two leptons and two jets

$$t\bar{t} \longrightarrow l^+ + l^- + \nu + \bar{\nu} + \bar{b} + b$$

This has a low background from other processes, but happens only rarely in top decay as well. Another option is that one of the W-bosons decays into leptons and the other into quarks, giving

$$t\bar{t} \longrightarrow \begin{array}{l} l^+ + \nu + \bar{q} + q + \bar{b} + b \\ \text{or} \quad l^- + \bar{\nu} + \bar{q} + q + \bar{b} + b \end{array}$$

which has a single lepton, and four jets. This process, which is depicted in Figure 29, happens more often, but also has a higher background. The final decay, with no lepton and six jets gets swamped by the background.

After a number of hints in the early 1990s, the discovery of the top quark was finally announced in 1995. It was found at the Tevatron in Fermilab, a p^+p^-collider that reached energies of 1 TeV . Collisions took place at two similar but complimentary detectors, situated in different places around the ring, and were analysed by two independent rival collaborations known as D$\varnothing$ (pronounced dee-zero) and CDF . A top-quark event from the CDF collaboration is shown on the next page.

The top took so long to track down because it was much heavier than anyone had anticipated. It finally weighed in at

$$m_t = 170\text{GeV}$$

This remains the heaviest fundamental particle that we know. Why is it so much heavy? We have, I think it's fair to say, no idea. Surely it is telling us something important.

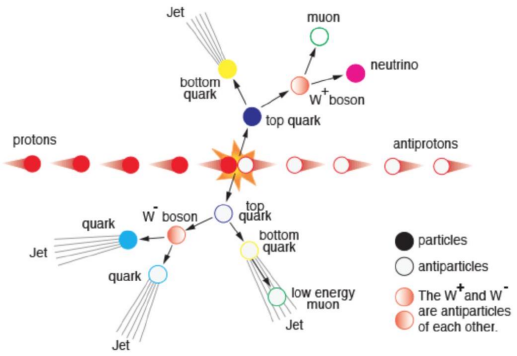
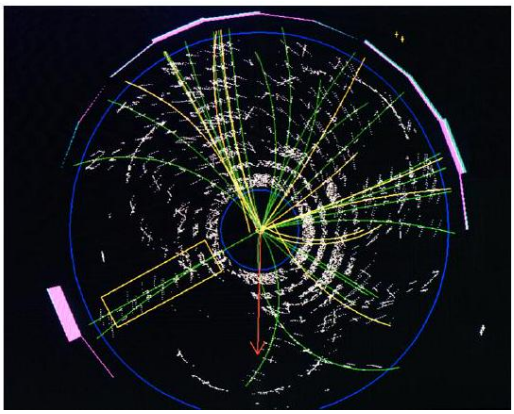


Figure 29. A schematic picture of a top quark event, taken from the Fermilab website.

With the tau, bottom and top quark in place, all that was left was the tau neutrino. This was discovered by the DONUT experiment at Fermilab in 2000. They used the Tevatron to create a beam of neutrinos which included ν_τ. These were then directed at nuclear emulsion targets where they collided with iron nuclei. The tell-tale sign of a ν_τ neutrino is the creation of a τ lepton, which leaves a small 1 mm track in the



emulsion. Four such events were seen.

4.4 4 The Weak Force

It is now time to turn to the weak force. For many years, there was just one manifestation of the weak force, namely beta decay

$$n \to p + e^- + \bar{\nu}_e$$

We now know that this can be understood in terms of the down quark decaying into an up quark, electron and anti-electron neutrino

$$d \to u + e^- + \bar{\nu}_e$$

There is nothing in the strong force or electromagnetism that would allow one type of quark to morph into another. We need to invoke something new.

That "something new" turns out to be something old and familiar. Nature has a tendency to re-use her good ideas over and over again, and the weak force is no exception. Like the strong force, it too is described by Yang-Mills theory. The difference is that the matrices are now 2×2 instead of 3×3. However, as we'll see in this section, it's not just the strengths of the forces that differ and the weak and strong forces manifest themselves in a very different manner.

The three forces of Nature together provide the foundation of the Standard Model. In mathematical language these forces are characterised by a group

$$G = SU(3) \times SU(2) \times U(1)$$

where the 3×3 matrix fields of $SU(3)$ describe the strong force, and the 2×2 matrix fields of $SU(2)$ describe the weak force. However, rather surprisingly the fields of $U(1)$ do not describe the force of electromagnetism! Instead, they describe an "electromagnetism-like" force that is called hypercharge. The combination of SU(2) and $U(1)$ is sometimes referred to as electroweak theory. We will learn in Section 4.2 how electromagnetism itself lies within.

The weak force has few obvious manifestations in our everyday life and, in many ways, is the most intricate and subtle of all the forces. It is intimately tied to the Higgs boson and, through that, the way in which elementary particles get mass. Moreover, both the most beautiful parts of the Standard Model, and those aspects that we understand least, are to be found in the weak force.



Figure 30. Parity violation of Chien-Shiung Wu.

4.4.1 4.1 The Structure of the Standard Model

When describing the strong force, we saw that it affects some particles (we call these quarks) while leaving other untouched (we call these leptons). Our first task now should be to describe which particles are affected by the weak force.

You might think that we could simply list those particles that feel the weak force. But, as we will see, things are not quite so straightforward. It turns out that the weak force acts on all the particles in the universe. But it does so by acting on exactly half of each particle!

4.1.1 Parity Violation

There is one defining characteristic of the weak force and hypercharge that differentiates them from the strong force (and from electromagnetism). They do not respect the symmetry of parity.

This fact was discovered by Chien-Shiung Wu, on a cold winters day in New York City in December 1956. Wu's experiment was technically challenging but conceptually very simple. She placed a bunch of Cobalt atoms in a magnetic field and watched them die. Cobalt undergoes beta decay

$$^{60}\mathrm{Co} \to {}^{60}\mathrm{Ni} + e^- + \bar{\nu}_e + 2\gamma$$

with a half-life of around 5.3 years. The two photons arise because cobalt first decays to an excited state of the nickel nucleus, which subsequently decays down to its ground state emitting two gamma rays. The whole point of the magnetic field was to make sure that the nucleon spins of the atoms were aligned. Wu discovered that the electrons were preferentially emitted in the opposite direction to the nucleon spin

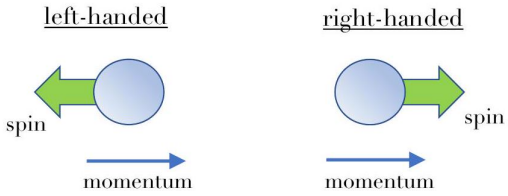


Figure 31. The handedness of a massless particle is determined by the relative direction of its spin and momentum.

This may sound innocuous but we now realise that it was one of the most significant discoveries in all of particle physics. The key point is that when we say the nuclei spins in a given direction, we mean in a right-handed sense. Take your right-hand and curl your fingers round in the way the nuclei are spinning: then your thumb points in the "direction of spin" which, as Wu observed, is opposite to the motion of the electrons.

Now suppose that, for some bizarre reasons, Wu looked at her experiment reflected in a mirror. The directions of the electrons would remain unchanged but the spin of the nuclei would be reversed, because right-hands are reflected into left-hands. This means that, viewed in a mirror, Wu would have come to the opposite conclusion: the electrons would be preferentially emitted in the same direction as the nuclei spin.

To put this in context, stare at the two photographs of Wu and her experiment shown in Figure 30. If you look closely you can tell which photograph is the original and which is flipped about an axis. (For example, one way to do this is to note that the writing is only legible on the left-hand picture.) Wu discovered that the same is true of the laws of physics at a fundamental level: you can tell if you're looking directly at sub-atomic particles or viewing them reflected in a mirror. There are things that can happen in a mirror that cannot happen in our world! This property is known as parity violation.

How can we write down theories which violate parity, meaning that they describe a world which looks different when reflected mirror? The key is something that we learned back in Section 2.1.4: any massless spin $\frac{1}{2}$ particle decomposes into two pieces, called left-handed and right-handed. Recall that a right-handed particle is one whose spin is aligned with its momentum, while a left-handed particle has spin and momentum anti-aligned. This distinction only makes sense for massless particles since they travel at the speed of light and so all observers, regardless of their own motion, agree on the direction of spin and momentum.

To write down a theory which violates parity is then straightforward: we simply need to ensure that the left-handed particles experience a different force from the right-handed particles.

The weak force accomplishes this in the most extreme way possible: only left-handed particles experience the weak force. Right-handed particles do not feel it at all. For reasons that we now explain, this is the key property of the weak force and one of the key properties of the Standard Model.

There are quite a few things that we will need to unpick regarding the weak force. Not least is the fact that, as stressed above, the distinction between left-handed and right-handed particles is only valid when the particles are massless. A remarkable and shocking consequence of parity violation is that, at the fundamental level, all elementary spin $\frac{1}{2}$ particles are indeed massless. The statement that elementary particles like electrons, quarks and neutrinos - are fundamentally massless seems to be in sharp contradiction with what we know about these particles! We learn in school that electrons and quarks have mass. Indeed, in the introduction to these lecture notes we included a table with the masses of all elementary particles. How can this possibly be reconciled with the statement that they are, at heart, massless? Clearly we have a little work ahead of us to explain this. We'll do so in Section 4.2 where we introduce

the Higgs boson.

4.1.2 A Weak Left-Hander

We're now in a position to explain how the three forces of the Standard Model act on the matter particles. The short-hand mathematical notation for the forces is

$$G = SU(3) \times SU(2) \times U(1)$$

Let's first recall some facts from the previous chapter. The strong force is associated to the " $SU(3)$ " term in the equation above. As we explained in Chapter 3, the analog of the electric and magnetic fields for the strong force are called gluons, and are described by 3×3 matrices. (This is what the " 3 " in $SU(3)$ means.) Correspondingly, each quark carries an additional label, that we call colour that comes in one of three variants which we take to be red, green or blue.

While quarks come in three, colour-coded varieties, the leptons - i.e. the electron and neutrino - do not experience the strong force and hence they come in just a single, colourless variety. In the introduction, we said that each generation contains four particles: two quarks and two leptons. However, a better counting, including colour,

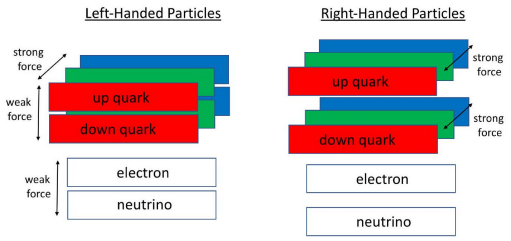


Figure 32. The jigsaw of the Standard Model. Only quarks experience the strong force. Only left-handed particles experience the weak.

shows that each generation really contains 8 particles (strictly 8 Dirac spinors). There are $3 + 3$ from the two quarks, and a further $1 + 1$ from the two leptons.

The next step in deconstructing the Standard Model is to note that each spin $\frac{1}{2}$ particle should really be decomposed into its left-handed and right-handed pieces. Only the left-handed pieces then experience the weak force $SU(2)$. If we were to follow the path of the strong force, you might think that we should introduce some new degree of freedom, analogous to colour, on which the weak force would act. A sort of weak colour. Like pastel. In fact, that's not necessary. The "weak colour" is already there in the particles we have.

This is illustrated in Figure 32. The right-handed particles are the collection of coloured quarks and colourless leptons. The left-handed particles are the same, except now the weak force acts between the up and down quark, and between the electron and neutrino. In other words, the names of distinct particles - up/down for quarks and electron/neutrino for leptons - are precisely the "weak colour" label we were looking for! We've denoted this in the figure by placing the weak doublets in closer proximity.

This should strike you as odd. For the strong force, the red, blue and green quarks all act in the same way. We say that there is a symmetry between them. However, it's very hard to make the same argument for the "weak colour" label. The electron and neutrino are very different beasts. If we're really introducing "weak colour" in analogy with actual colour, surely there should a symmetry between them. What's going on?

This brings us to our second striking fact: at the fundamental level, there is no distinction between a left-handed electron and left-handed neutrino! Nor is there a distinction between a

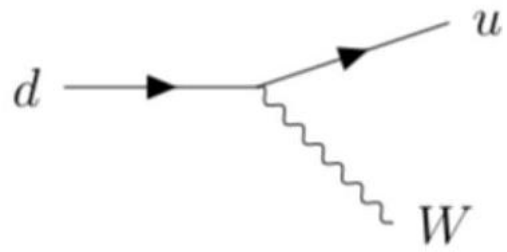
left-handed up quark and left-handed down-quark. These particles share all their properties. However, as the story of the Standard Model plays out, the Higgs field intervenes. In addition to giving the elementary particles mass, the Higgs fields also leaves the electron/neutrino and up/down pairs with the distinctive characteristics that we observe. This aspect of the Standard Model is called symmetry breaking and will be described in Section 4.3.2.

Gauge Bosons

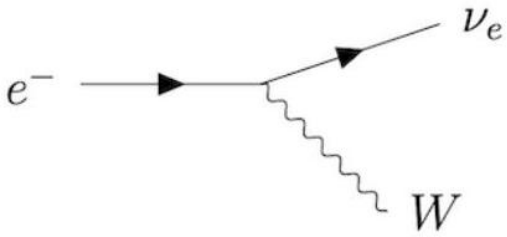
As with the other forces that we've met, there are spin 1 particles associated to the weak force. These are the analogs of the photon for electromagnetism and the gluon for the strong force. The spin 1 particles associated to the weak force are called W-bosons and Z-bosons. We'll see the difference between the W and Z later when we discuss the Higgs.

The type of spin 1 particles - like the photon, gluon, W and Z - that mediate forces are rather special and collectively go by the name of gauge bosons. (Here "gauge" is pronounced to rhyme with "wage".) The kind of Yang-Mills type theories that underly these are called gauge theories.

We can draw Feynman diagrams associated to the weak force. The W-boson interacts with the quarks, changing a down into an up like this

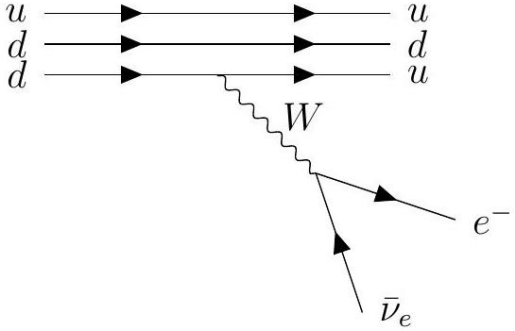


Note that the colour of the quark remains unchanged. For example, a red down-quark will turn into a red up-quark. Similarly, the W-boson interacts with the leptons like this.



In each case, the conservation of electric charge tells us that the W-boson must carry charge -1 . We'll describe this in more detail later.

Already from these diagrams, we can start to understand how beta decay works. Recall that the quark content of the neutron is udd, while that of the proton is uud. One of the down quarks in a neutron decays into an up quark by emitting a W-boson. This is subsequently followed by the decay of the W-boson into an electron and antineutrino.



Note that we get an anti-neutrino rather than a neutrino because the arrow is now running backwards in time. We see that beta decay doesn't proceed through a direct interaction between

quarks and leptons. It's mediated by the W-boson, in the same way that the electromagnetic force is mediated by the photon.

The fact that the down quark decays into an up quark, and not the other way round, can be traced to the fact that the down quark is (marginally) the heavier of the two. Moreover, the W-boson is heavier than the combination of the electron and neutrino (now the difference is not so marginal) so this decay too is allowed. These facts, like so many other things, come from the Higgs boson. By now, you should probably be getting the feeling that the Higgs plays an important part in all of this!

Hypercharge

Shortly we'll see how electric charge emerges in this story. But first, we need to understand its counterpart at a more fundamental level. This is something called hypercharge and is associated to the $U(1)$ factor in the Standard Model. It is a force that is closely related to electromagnetism. However, the various particles don't have the same charges under hypercharge as they do electric charge. Importantly, hypercharge does not respect parity and left-handed and right-handed particles carry different charges. These hypercharges are listed in Table 2, together with a summary of how the strong and weak forces act.

We've normalised the hypercharges in the standard way so that they come in units of 1/6. However, this is just convention and there's nothing deep in this choice. We could just as well multiply everything by a factor of six, so all hypercharges are integer. Notice that one advantage of the current normalisation is that the hypercharge for the

Particles		Strong	Weak	Hypercharge
Left-handed	quarks	yes	yes	$+1/6$
	leptons	no	yes	$-1/2$
Right-handed	up quark	yes	no	$+2/3$
	down quark	yes	no	$-1/3$
	electron	no	no	-1
	neutrino	no	no	0

Table 2. The Standard Model forces acting on each of the fermions in a single generation.

right-handed particles coincide with their electromagnetic charge. This, as we shall see, is no coincidence. However, the hypercharges for the left-handed particles are rather different.

Before we move, I should mention that there is one caveat. (Isn't there always!) We don't yet have direct evidence for the existence of the right-handed neutrino and there is a possibility that it doesn't exist! Indeed, many people would say that the right-handed neutrino should not be included in the list of particles in the Standard Model. From the table you can see that the right-handed neutrino is neutral under all three of the forces in the Standard Model and this makes it very challenging to detect. We'll see the indirect evidence for its existence in Section 4.4 where we describe more about neutrinos in general.

4.1.3 A Perfect Jigsaw

The particles and forces listed in Table 2 summarise 150 years of work (dated from Röntgen's discovery of X-rays), dedicated to understanding the structure of matter at the most fundamental level. The first thing that comes to mind when you see it is: what a mess! The individual elements comprise some of the most gorgeous objects in theoretical physics - the Dirac, Maxwell and Yang-Mills equations. And yet any semblance of elegance would seem to

have been jettisoned at the last, with the different components thrown together in this strange higgledy-piggledy fashion. Why this collection of forces and particles? In particular, why this strange collection of hypercharges?

Happily, there is a wonderful and astonishing answer to these questions. The beautiful truth is simply: it could barely have been any other way.

The reason for this has its roots in Wu's observation that the world does not respect the symmetry of parity. As we explained above, we can account for this in the Standard Model by ensuring that left-handed fermions experience different forces from righthanded fermions. However, it turns out that this is not quite as straightforward to achieve as I've made out.

To explain why, I need to tell you a few further facts about the mathematics underlying quantum field theory. Quantum field theories in which left- and right-handed fermions experience different forces are called chiral theories. It turns out that chiral theories are particularly fragile objects, always teetering on the brink of mathematical inconsistency. Put bluntly, most chiral theories that you write down don't make any sense. If you write down a random collection of particles, with left- and right-handed components experiencing different forces, it is overwhelming likely that the equations will spit back stupid, and obviously wrong answers like " $1 = 0$ ".

If you want to write down a sensible chiral quantum field theory then there are a bunch of hoops that you have to jump through. These hoops are mathematical consistency conditions that the different forces must obey if the theory is to be sensible. One simple way of obeying these consistency condition is to ensure that left- and righthanded particles feel the same force but such theories don't exhibit parity violation. If you want to write down a theory with parity violation, you're obliged to work harder and find a delicate balance between the forces experienced by the left-handed particles and those experienced by the right-handed particles.

I won't describe all the consistency conditions, but here's a taster. Let's call the hypercharge of each fermion $\tilde{Q}_f$ where f labels the fermion. Then one consistency condition reads

$$\sum_{\text{left-handed}} \tilde{Q}_f^3 = \sum_{\text{right-handed}} \tilde{Q}_f^3 \tag{4.1}$$

To check that this works for one generation of the Standard Model particles listed in Table 2, you have to remember that each quark comes with three colours, while the left-handed fermions are really a pair under the weak force. We then have

$$3 \times 2 \times \left(\frac{1}{6}\right)^3 + 2 \times \left(-\frac{1}{2}\right)^3 = 3 \times \left(\frac{2}{3}\right)^3 + 3 \times \left(-\frac{1}{3}\right)^3 + (-1)^3 + 0^3$$

A successful solution to the mathematical consistency conditions, like the one above, is known technically as quantum anomaly cancellation. It's not a particularly enlightening name. For now, I can only tell you that underlying these conditions are some of the
deepest and most powerful ideas from the mathematics of topology. Indeed, the subject of "quantum anomalies" is currently where the fields of mathematics and physics have their richest intersection. (You can read more about quantum anomalies, in their full technical glory, in chapter 3 of the lecture notes on Gauge Theory.)

Viewed through the lens of quantum anomalies, the Standard Model morphs from a seeming mess into a perfect jigsaw. The forces act on the various particles so that the mathematical consistency conditions are satisfied. If you try to change any small piece, the whole thing falls apart and ceases to be a sensible physical theory.

I should stress that the Standard Model is not the only chiral gauge theory. If you allow for entirely different forces, or different collections of particles, then you can write down other such theories. But the Standard Model is, arguably, the simplest chiral gauge theory. Although, at

first glance, the Standard Model looks like a jumble of random forces and particles, it is instead a beautiful and surprising theoretical construct. You just have to look at it the right way.

Hypercharge and Fermat's Last Theorem

It's difficult to explain the quantum anomaly consistency conditions at a deeper level without getting into the full mathematics. But here's a quick calculation that I'm particularly fond of that will hopefully give a sense of what's going on. Take the set of particles listed in Table 2, and assign them the properties under the strong and weak force that are listed. But allow them to have almost arbitrary values $\tilde{Q}_f$ of hypercharge. The "almost" is there because I'll impose two restrictions. First, we'll take the righthanded neutrinos to be neutral. (This can be motivated on the grounds that we're not really sure that they exist!) Second, we'll take the hypercharges $\tilde{Q}_f$ to be rational numbers, of the form p/q where p and q are integers. There are good theoretical reasons to think that charges should be quantised in this way. Then we ask the question: what values of hypercharges satisfy the mathematical consistency conditions?

It turns out that some of the hypercharges can be immediately related to others through the consistency conditions. And some remain arbitrary. If you follow through the calculation, and do some fairly complicated change of variables, the equation (4.1) ends up turning into the equation

$$X^3 + Y^3 = Z^3$$

where X, Y and Z must all be integers. This is a very famous equation! Fermat's last theorem tells us that the equation has no non-trivial solutions. There are, however, trivial solutions like $1^3 + 0^3 = 1^3$. If you take this trivial solution and plug it back into the complicated change of variables, you'll discover the set of hypercharges listed in Table 2. These hypercharges may look random, but they're related to some very deep and beautiful mathematics. In particular, they're related to Fermat's last theorem!

Further Generations

As we explained in the introduction, the pattern of particles listed in Table 2 is repeated twice more. The second generation consists of the strange and charm quarks, together with the muon and muon-neutrino. The third generation consists of the bottom and top quarks, together with the tau and tau-neutrino.

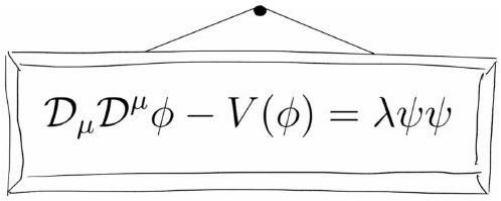
We don't understand why there are three generations. However, the quantum consistency conditions tell us that each generation must come in a complete set. For example, there was a 20 year gap between the discovery of the tau lepton in 1975 and the discovery of the top quark in 1995. (The bottom quark was discovered in 1977). Yet no one doubted that the top quark was there because mathematical consistency required it. The whole theory doesn't make any sense without the top quark.

4.4.2 4.2 The Higgs Field

Finally, it's time to introduce the famous Higgs boson. This is, it turns out, the simplest particle in the Standard Model. But the way in which it interacts with other fields is, by far, the most intricate. And, as we shall see, it is ultimately the Higgs boson that ties everything else together.

The Higgs boson is the simplest particle because it has spin 0 . Indeed, it is the only fundamental particle that we know of without spin. Fields without spin are also referred to as scalar fields.

Recall that spin $\frac{1}{2}$ fields are described by the Dirac equation and spin 1 fields by the Maxwell or Yang-Mills equations. Both were pretty enough to be put in picture frames in earlier chapters. Any spin 0 field, like the Higgs boson, is described by the KleinGordon equation. It's nowhere near as beautiful as earlier equations, largely because it is too simple: it lacks the subtleties and surprises that make the Dirac and Yang-Mills equations so special. Nonetheless, it would be slightly churlish to deny it a place on the wall so, for what it's worth, here is the Klein-Gordon equation



In this equation, $V(\phi)$ is the Higgs potential while the terms on the right-hand-side describe the couplings to the fermions in the theory. Both of these will be described in more detail below.

As we've alluded to earlier in these lectures, the Higgs field plays a number of roles and we'll elaborate on these as we go along. For now we mention only that the Higgs field does not experience the strong force, but it does feel both the weak force and hypercharge. We should therefore augment Table 2 listing the forces experienced by each particle with one further entry:

Particle	Strong	Weak	Hypercharge
Higgs	no	yes	+1/2

Table 3. The forces experienced by the Higgs boson

Note that, because the Higgs field has no spin, it doesn't decompose further into leftand right-handed pieces. It just is.

Like all other fields, ripples of the Higgs field give rise to particles. This is the Higgs boson, the last of the Standard Model particles to be discovered. It weighs in at a mass

$$m_H \approx 125\text{GeV}$$

making it the second heaviest particle in the Standard Model, after the top quark.
However, the real importance of the Higgs lies not in the particle (although that's certainly interesting!) but, as we'll now explain, more in a property of the field itself.

4.2.1 The Higgs Potential

Given that the Higgs field is simpler than all the others, why does it play such an important role? Well, there's something that a spin 0 field can do that higher spin fields cannot: they can "turn on" in the vacuum.

To understand what this means, recall that in the introduction we gave some intuition for a quantum field as an object that's constantly fluctuating. More precisely, the vacuum of space should be viewed as a quantum superposition of many different field configurations. An example of a typical configuration of the gluon field in the vacuum is reproduced in Figure 33. Given this, it would seem that all fields "turn on" in the vacuum. However, importantly, for any field with spin the average of all these field fluctuations always vanishes in the vacuum.

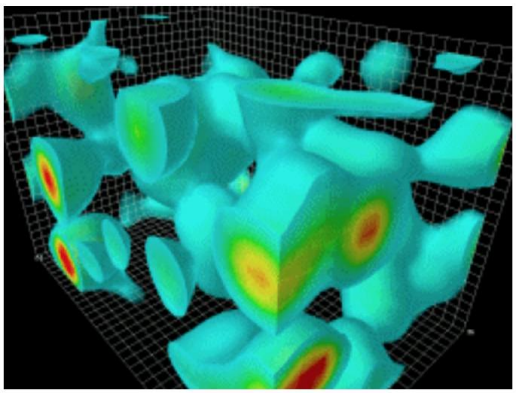


Figure 33. The fluctuations of a quantum field, taken from the simulations of Derek Leinweber.

The reason for this is simple: if a field with spin has a non-zero average, then it has to point in some direction. For example, if the average of the electric field **E** is non-vanishing then it picks out a direction in space. But the vacuum of space must look the same in every direction, so the average must be zero. (This statement is a little quick, but there are mathematical theorems that make it more precise.)

However, a scalar field is spinless, so doesn't point in any particular direction even when turned on. If we denote the field as $\phi(\mathbf{x}, t)$ then it's possible that, even in the vacuum, the average of all the fluctuations doesn't vanish, so

$$\langle \phi(\mathbf{x}, t) \rangle = \text{ constant } \neq 0$$

where the angular brackets denote the average. In technical language, we say that the field condenses, a term that has its origin in the study of phase transitions and the condensation of water from vapour.

This new possibility brings up two immediate questions. What determines whether the field condenses? And what are the consequences if it does? Here we'll answer the first of these questions, postponing the second to Section 4.2.2.

The fate of a scalar field is not something that we get to chose. It is determined dynamically by the theory. Any scalar field experiences a potential energy that we call $V(\phi)$. This is a function that tells us how much energy it costs for the field to take certain values. Roughly speaking, there are two different shapes that these potentials take in theories of particle physics. These are shown in Figure 34.

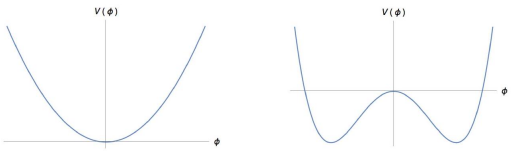


Figure 34. Two possible shapes for the potential for a scalar field. The Higgs field has a potential like that shown on the right, so that the field condenses, with $\langle \phi \rangle \neq 0$ in the vacuum.

In the vacuum, the scalar field sits at the minimum of the potential. If the potential has the shape shown on the left of Figure 34, then $\langle \phi \rangle = 0$ in the vacuum. However, if the potential has the shape shown on the right of Figure 34, then $\langle \phi \rangle \neq 0$ in the vacuum, and more interesting things happen. It turns out that the potential for the Higgs field in the Standard Model has the shape shown on the right, and this is what endows the Higgs with its power. (This statement is roughly true. A more accurate depiction of the Higgs potential will be given in Section 4.3.2.)

This, of course, brings up another interesting question: why does the Higgs potential in our world have the shape on the right, and not the shape on the left? We don't know the answer to that. At present, it is an input into the Standard Model and, hopefully, will be explained by some more complete theory in the future.

Here we are focussing on the question of whether the minimum of $V(\phi)$ sits at $\phi = 0$, or $\phi \neq 0$. But another question that we could ask is the value of $V(\phi)$ itself at the minimum. In the context of particle physics, this plays no role: it is just like any other potential energy, where only potential differences really matter and you can always add a constant to $V(\phi)$ without changing the physics. However, once we include gravity into the mix, the value of the potential energy becomes very important and contributes towards the cosmological constant. We'll say more about this in Section 5.3.1.

The Higgs Expectation Value

The upshot of the discussion above is that, even in the vacuum, the Higgs field averages to something non-vanishing. That something non-vanishing turns out to have the dimensions of energy. It is

$$\langle \phi \rangle \approx 246\text{GeV} \tag{4.2}$$

This is known as the Higgs vacuum expectation value. It is one of the key fundamental scales in the universe.

So what are the consequences of this? Well, they are pretty dramatic: the vacuum expectation value (4.2) turns out to give a mass to everything that it touches. This is known as the Higgs mechanism or the Higgs effect. The particles that get masses include both the W-bosons and Z-bosons that mediate the weak and hypercharge, together with all the spin 1/2 matter particles of the Standard Model. We'll postpone a discussion of fermion masses to Section 4.3, but the punchline is simply that the quarks, electrons and neutrinos get the masses that we advertised back in Section 1. Here, we will begin by focussing on the masses of the W -bosons and Z -bosons and some of their consequences. But first we will attempt, and largely fail, to give some intuition for why the Higgs field gives mass to particles at all.

Analogies for the Higgs Mechanism

The result of the Higgs expectation value $\langle \phi \rangle \neq 0$ is utterly startling. The Higgs field is like the ancient king Midas, but instead of turning everything to gold it makes everything massive. (Both make things heavier.) Why?

This is not an easy question to answer at the level of these lectures. What's perhaps unusual about this is that it's not at all difficult to understand the Higgs effect at the level of equations. Indeed, it's one of the simpler calculations in quantum field theory, but that doesn't change the fact that you do first need to learn quantum field theory. Largely, the difficulty in translating from equations to everyday language lies in the fact that the Higgs effect is really a phenomenon that is to do with fields rather than particles and we simply don't have much intuition for how these objects behave.

If we want to avoid the mathematics, we're obliged to rely on analogy. And, sadly, good analogies that relate the Higgs boson to more familiar, everyday phenomena are hard to come by. Here, for example, is a bad analogy. We could say that the Higgs field is like some kind of treacle. If you drag a spoon through treacle, you experience more resistance than if you drag it through water. Something similar happens with the elementary particles that interact with the Higgs. As we've seen, at the fundamental level all matter particles (as well as the W -boson and Z -boson) are actually massless and so should travel at the speed of light. But as they

move in the vacuum, they have to plough through the Higgs field and this slows them down, effectively giving them a mass.

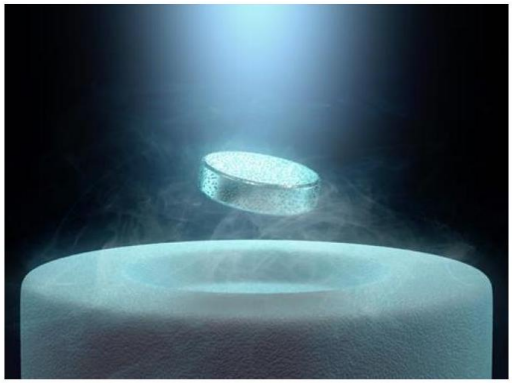


Figure 35. A superconductor and the Higgs boson are described by identical mathematics. (Image taken from the Royal Society of Chemistry).

In fact, this isn't a totally terrible analogy. But if you try to push it any further it will quickly break down. For example, the reason that the spoon slows down is because of friction forces, which means that it continually loses energy to the treacle. In contrast, there's no friction force going on with the Higgs, nor any constant transfer of energy from the particle to the Higgs field. The analogy just stops working at this point.

There is, however, one completely excellent analogy for the Higgs effect, although not one that's particularly everyday. This can be found in phenomenon of superconductivity. In certain metals (for example, aluminum or lead) the electrical resistivity plummets to zero as they are cooled to low temperatures. At the same time, the metal expels any magnetic field, giving rise to dramatic technological applications like levitating trains.

The theory behind superconductivity is well understood. First, the electrons bind together into pairs. This, already, is somewhat surprising since the electrostatic Coulomb force repels two electrons and so it seems unlikely that they would want to bind together. However, in a metal the sound waves (also known as phonons) give a second, attractive force between electrons and in favourable conditions this can win over, causing the electrons to bind. While the individual electrons have spin, the bound state can be spinless (rather like the mesons, formed of two quarks, that we met in Section 3.) It turns out that the potential for this bound state looks like the right-hand graph in Figure 34, and it condenses. The result is that, inside a superconductor, the photon gets a mass and this underlies behind all the subsequent phenomena, including the resistance free conduction and the expulsion of magnetic fields.

On a mathematical level, the analogy between the Higgs effect and superconductivity is exact: the key aspects of the equations describing the two are identical. It is a manifestation of the remarkable unity of physics, where the same ideas crop up in diverse situations.

4.2.2 W and Z Bosons

There are gauge bosons associated to all three forces in the Standard Model. Because the Higgs doesn't experience the strong force, the associated gauge bosons - which we named gluons in Section 3 - are unaffected by the Higgs boson. This is why we could discuss them earlier without dealing with all these subtleties.

In contrast, both the $SU(2)$ weak force and the $U(1)$ hypercharge interact with the Higgs. Which means that they get a mass. The result is three, massive spin 1 bosons:

$$W^{\pm}\text{bosons: } M_W \approx 80\text{GeV}$$
$$Z \text{ boson: } M_Z \approx 91\text{GeV}$$

Here the $W^+$and W^-particles are distinguished by their $\pm$electric charge. They are the anti-particles of each other. In contrast, the Z-boson is neutral. It is its own anti-particle. Note that both masses are a factor of 3 or so below the Higgs expectation value (4.2). This is not a coincidence: the expectation value sets the scale of the masses, with the reduction due to the strength with which the Higgs field interacts with these spin 1 bosons.

The fact that the force-carrying particles become massive greatly changes the properties of the force. Instead of the familiar $V \sim 1/r$ Coulomb potential of electromagnetism (or the less familiar $V \sim r$ confining force of QCD), the massive W - and Z -bosons give a potential energy between particles that takes the form

$$V(r) \sim \frac{e^{-Mr}}{r} \tag{4.3}$$

where r is the distance between two particles, while M is the mass of the W or Z boson. We've met a force of this kind before: it takes the same form as the Yukawa force (3.4) that is mediated by pions, and binds the protons and neutrons together in a nucleus. These forces have the characteristic feature that they become negligibly small for distances $r \gg 1/M$.

When, in Section 3, we discussed the force mediated by mesons, their mass was $m \approx 140$MeV and the force extended over a distance $\approx 2\times10^{-15}$ m. Which, of course, is the size of the nucleus.

For the weak force, the masses of the force-carrying particles are almost 1000 times heavier than the meson, so the distance over which the weak force acts is almost a 1000 times smaller than the size of the nucleus. That's a pretty small distance scale! Indeed, it's so small that it means our old Newtonian way of thinking about forces as acting between particles really isn't particularly useful anymore. Unlike electromagnetism and the strong force, there are no examples where the weak force can be viewed of as an attractive force that make things stick together. There are no atoms or mesons of the weak force. Instead, as we've already seen, the primary role of the weak force is one of decay. Its job is to rent asunder that which the strong put together. This affects the neutron through beta decay and many other particles whose lives are cut tragically short by the weak force. We will describe this in more detail shortly.

The One That Got Away

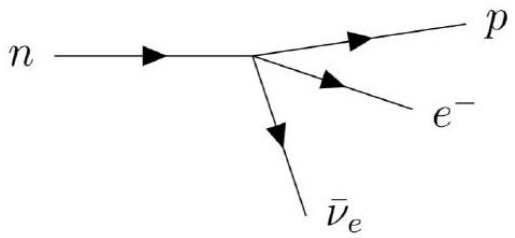
There's one final, very important twist to the story above. As we've seen, the gauge bosons associated to both the $SU(2)$ weak force and the $U(1)$ hypercharge interact with the Higgs. However, there's one special combination of these gauge bosons where the weak interaction is precisely cancelled by the hypercharge interaction. In other words, one combination of spin 1 bosons manages escape the attention of the Higgs and therefore remains massless. This is the photon.

This gives us a new perspective on the familiar electromagnetic force. Electromagnetism is not one of the three fundamental forces in the Standard Model, but instead is a combination of the weak force and hypercharge. It is special, because it is the only combination uncontaminated by the Higgs boson.

For this reason, the $SU(2) \times U(1)$ weak and hypercharge forces are referred to collectively as the electroweak theory. It is sometimes said that they are a unification of the weak and electromagnetic forces. While it's certainly true that the weak and electromagnetic forces are intricately interwoven, it's not quite correct to say that they're "unified". Indeed, it might be better to say that they're divided by the Higgs: the weak force became mired in the Higgs condensate, while the electromagnetic force is the one that got away.

4.2.3 Weak Decays

Enrico Fermi was the first person to understand beta decay. In 1934, just 18 months after the discovery of the neutron, he proposed a simple quantum field theory in which a neutron can decay into a proton, an electron and an anti-neutrino. The associated Feynman diagram is

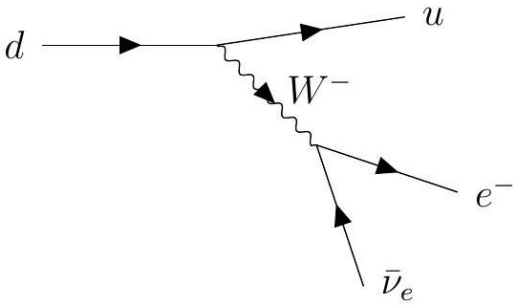


Thus, right from the beginning, the story of the weak force was one of decay.
Fermi's theory was one of the great breakthroughs of particle physics. Not only did it give a correct explanation for beta decay, but it was the first time that a quantum field theory was written down in which a particle of one type can transmute into something else. Any idea that the neutron was composed of a proton plus electron (or, as was also suggested, the proton was composed of a neutron + positron) were consigned to the waste bin.

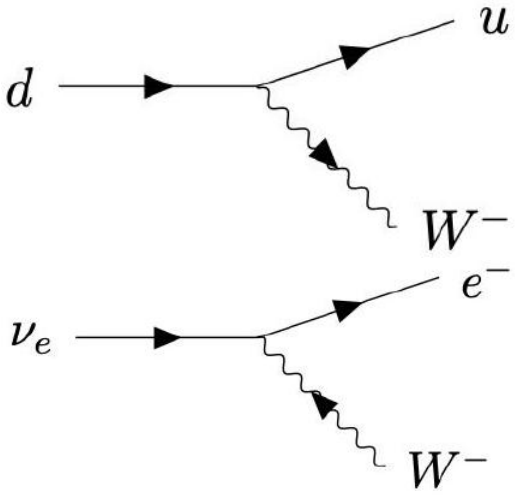
It took several more decades to understand what things look like if we zoom in a little further. The structure of the electroweak theory in its essentially complete form was first understood by Steven Weinberg, but many others got close including Sheldon Glashow, Abdus Salam and John Ward.

W-bosons

We know that if we zoom into the neutron and proton we find quarks. Beta decay occurs when a down quark changes into an up quark. However, this process doesn't happen through a direct interaction of four fermions: it is mediated by the W-boson, and looks like this.



Let's unpack this a little. There are two vertices that involve the W -bosons. The relevant sub-diagrams look like this:



We've met both of these before, except this time we've specified that it's the W^-boson involved in the process. This is needed to ensure the conservation of electric charge. As usual, diagrams with W^+can be formed by flipping the arrows or, equivalently, replacing particles with anti-particles.

There are a few things to say about beta decay when mediated by a W-boson. First, the reason that down quarks decay into up quarks, rather than the other way around, is because the mass of the down quarks is heavier than the masses of the decay products

$$m_d > m_u + m_e + m_{\nu_e}$$

We'll explain more about how these masses arise from the Higgs field in Section 4.3, but at this stage I'll simply point out that we don't currently have any understanding of why the masses are ordered this way rather than some other way. Nonetheless, this is crucial for beta decay to take place while conserving energy. The remaining energy $\Delta E = m_d c^2 - m_u c^2 - m_e c^2 - m_\nu c^2$ goes into the kinetic energy of the decay products.

If the masses had been ordered in some other way, then we would have a world in which, say, the electron could decay into a down and anti-up quark, together with a neutrino. Indeed, you can easily write down a Feynman diagram for such a process, but it's forbidden in our world because of energy conservation.

However, this begs a new question. The first sub-diagram in beta decay looks like a down quark decaying to an up quark and a W^-boson. But the W^-boson is way heavier than the up and down quark. Hence, energy conservation would suggest that such a decay is impossible. However, internal particles in diagrams - sometimes called virtual particles - are not subject to the same strict rules of energy conservation as external legs. (We described a similar idea in Section 2 when we first introduced Feynman diagrams.) Although beta decay proceeds through the creation of a Wboson, the existence of this W-boson is fleeting. Heuristically, we sometimes say that the W-boson briefly borrows some energy from the vacuum, and this is allowed by the Heisenberg uncertainty principle as long as it is paid back in a suitably short period of time. A better explanation is to admit that all is fields, and the kind of random fluctuations needed to create the W-boson are part and parcel of quantum field theory.

Whatever words we choose to drape around this, the fact that the intermediate Wboson is much heavier than any of the incoming or outgoing particles has consequence: it reduces the probability for the decay to take place and this in turn means that the lifetime of particles that decay through the weak force can be much larger than other timescales in particle physics. In fact, the lifetime of particles depends both on the mass of the W-boson and the mass differences between the initial and final particles.

So, for example, the half-life of a neutron is around 10 minutes, a very human number, while the half-life of uranium is around 4.5 billion years. And, of course, most nuclei do not decay at all, with the strong force providing a safe haven that stabilises the neutron.

That Time, Before We Were Born, When We Nearly All Died

As something of an aside, there's a wonderful race-against-the-clock story from the early universe that someone should turn into a Hollywood movie.

A long long time ago - a few fractions of a second after the big bang to be precise - protons and neutrons lived together in happy equilibrium. Beta decay happened, but so too did inverse beta decay and the two reactions were in a delicate balance. However, this state of harmony could not last forever. At around 2 seconds after the big bang, an imbalance kicked in and the inverse beta decay no longer occurred.

From then on, the neutrons were on their own. If any were to die, there was nothing to replace them. With a half-life of just 10 minutes, they needed to quickly find a sanctuary before

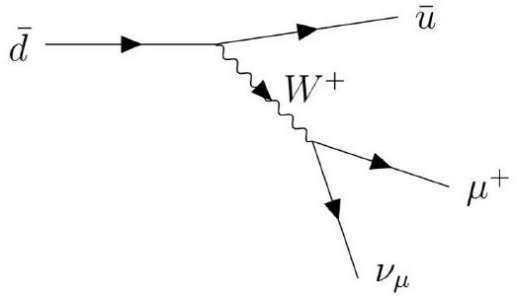
they were all killed off by beta decay, a fate which would leave the later universe a very dull place to live.

The refuge was obvious: they should bind together with a proton to form a deuterium nucleus, or with a couple of protons to form a helium nucleus. Sadly the early universe back then was a hot and violent place, and every time the neutrons tried to bind together with a proton, the resulting nucleus was quickly smashed apart. For some time, the fate of neutrons - and all future life - hung in the balance. The neutrons needed to wait long enough for the universe to cool so that they could form nuclei, but time was not on their side. Eventually, around 6 minutes after the big bang, the temperature dropped sufficiently and the first stable deuterium nuclei formed, followed quickly by helium. The universe was saved, leaving a future that could be filled with atoms and stories.

The scary part about the above tale is that the 6 minutes needed for nuclei to form seems to have nothing to do with the 10 minutes needed for neutrons to decay. They come from entirely different pieces of physics. We should all feel very lucky to have survived this perilous time in history. You can learn more about the calculations underlying this in the lectures on Cosmology.

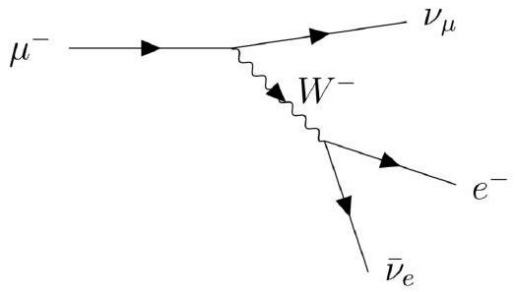
Pion Decay

Neutrons are not the only victim of the weak force. A world without the weak force would be awash with pions which, as we saw in Chapter 3, are the lightest of the
particles formed from quarks. The vast majority of the time (something like 99.99%) charged pions $\pi^+ = u\bar{d}$ decay through the weak force to muons. This occurs through the Feynman diagram:



The resulting $\bar{u}$ anti-up quark then combines with the other up quark in the pion, and the two rapidly decay into photons. The lifetime of the charged pion is about 10^{-8} second.

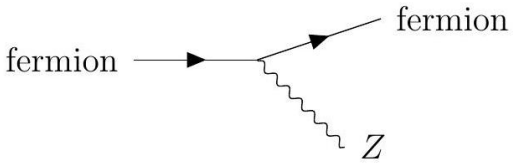
The resulting muons don't live too long either although, as we already saw in Interlude C , they hang around longer than the pions. Their demise is also due to the weak force and they decay to electrons and neutrinos through the process



The lifetime of the muon is around 2×10^{-6} seconds. All other particles involving quarks and leptons from the second and third generation have the same fate, decaying through the weak force to the more familiar particles from the first generation.

Z-Bosons

The Feynman diagrams involving Z-bosons are similar to those involving photons that we met in Section 2 in the sense that they don't change the type of fermion with which they interact:



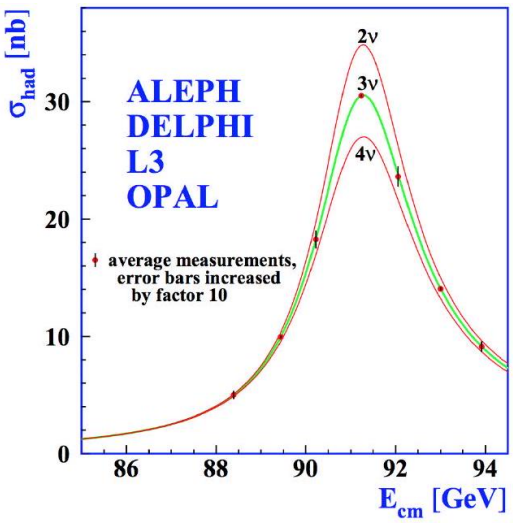


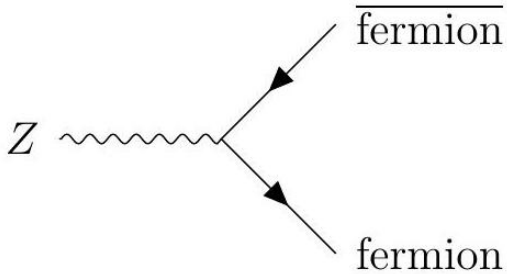
Figure 36. The Z-boson seen as a resonance in $e^{+}e^{-}$scattering. The three graphs show the shape of the graph that would be seen if there were 2,3 or 4 species of neutrinos. The data points fall beautifully on the middle option. This plot was taken from a joint paper, combining many different experimental results.}

The fermion on the two legs is the same, but now can be either u, d, ν_e or e^-. Similar Feynman diagrams involving higher generations of fermions also exist for both W and Z interactions.

The effects of the Z-boson are less immediately dramatic than those of the W. There are a number of processes that have been key for us in unravelling the structure of the weak force. In particular, Z-interactions allow neutrinos to scatter off any other lepton or quark, and this is one of the key ways in which these particles are detected.

Second, there is an important story involving the lifetime of the Z-boson. This gives our best current understanding to the question: how many generations of fermions are there? Of course, we've discovered three. But are there more to be found?

A very nice experiment involving the Z-boson strongly suggests that that we've found them all. This comes from looking at how the Z-boson decays. As we've seen, this can occur through a diagram of the form



where the fermion-anti-fermion pair can be either quarks or leptons. All that's needed is that

the mass of the final two fermions is less than the 91 GeV mass of the Z.

About 20% of the time, the Z-boson decays to a pair of neutrinos. As we'll explain in more detail, the neutrinos are extremely light with a mass less than $\lesssim$ 1eV. If there were more generations of fermions they would, as we've seen in Section 4.1.3, necessarily include further neutrinos. But, assuming that these additional neutrinos are not widly heavier than the first three, they would affect the lifetime of the Z-boson and so could be detected indirectly.

A careful experimental study of the lifetime of the Z-boson then gives a striking result. The number N_ν of neutrinos that the Z decays into is

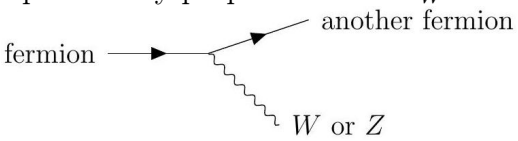
$$N_\nu = 2.994 \pm 0.008$$

If you're looking for an integer, this is the same thing as 3 . If there are further generations to be found, then the neutrinos must be so heavy that they don't affect the lifetime of the Z-boson. In other words, any further neutrino must be something like 10^9 times heavier than the three that we know and love. Similar arguments come from the study of the Higgs decays.

The Fermi Constant

For both QED and QCD we made a big deal out of the coupling constants and the way they change as you look at different energy scales. But, so far, we've made no comment about the strength of the coupling for the weak force.

There is such dimensionless coupling which we write as α_W. It's analogous to the fine structure constant α in QED. Whenever you see a Feynman diagram like the one below, it contributes to a process with probability proportional to α_W :



Rather surprisingly, the value of α_W is not particularly small. Like all coupling constants, it changes with scale. At the scale of 100 GeV , it takes the value

$$\alpha_W \approx \frac{1}{30}$$

This is somewhat larger than $\alpha \approx 1/137$ of electromagnetism! So why is the weak force so weak?

The answer, like everything to do with the weak force, lies in the Higgs mechanism. The weak coupling constant runs under renormalisation group and, like the strong force, actually increases as we look at lower energies. However, the Higgs ruins all of this. At the scale of the Higgs condensate, the coupling freezes to roughly the value $\alpha_W \approx 1/30$. More importantly, the W and Z bosons get a mass at this scale and this greatly limits the range over which the weak force can operate to roughly distances $r \sim 1/M_W$. We saw this already in the effective Yukawa-type force (4.3) that arises from the exchange of massive W and Z bosons. Ultimately the reason that the weak force is so weak is because the distance over which it operates is so small, rather than the intrinsic weakness of the force itself.

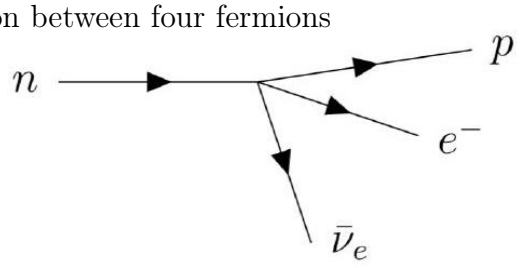
We can make this more quantitative. It's often more useful to characterise the strength of the weak force using a dimensionful coupling constant

$$G_F = \frac{\pi}{\sqrt{2}} \frac{\alpha_W}{M_W^2} \tag{4.4}$$

where the strange value of $\pi/\sqrt{2}$ is there for historical purposes. G_F is called the Fermi constant and takes the value

$$G_F \approx 1.166 \times 10^{-5}\text{GeV}^{-2}$$

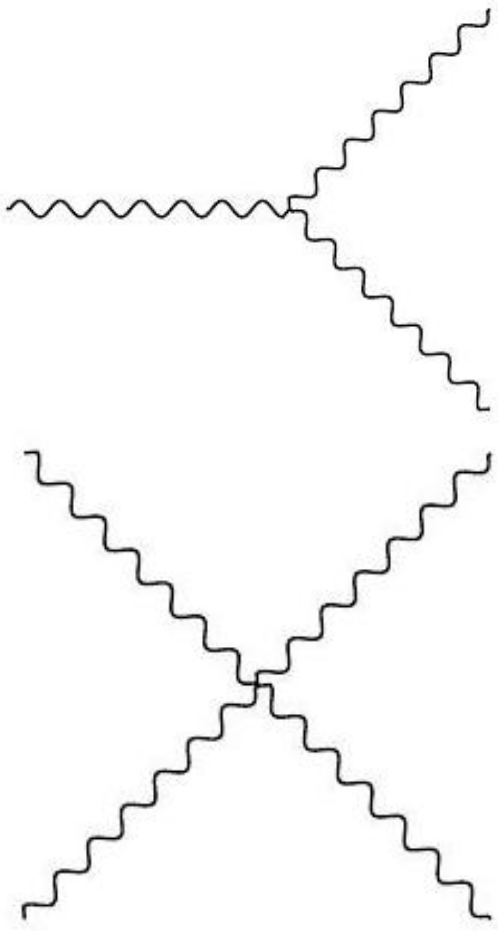
To understand the importance of this coupling, let's go back to our favourite beta decay. If we squint and ignore the W-boson, we return to Fermi's original theory where the process looks like a direct interaction between four fermions



The probability of such a decay is characterised by G_F which, as we see from the definition (4.4), incorporates both the original weak coupling constant α_W and the
finite range of the W-boson due to its mass. More precisely, to get a probability we should construct a dimensionless object out of G_F so the probability of any low-energy event with $E^2 \ll G_F^{-1}$ is really $\sim G_F E^2$. Because G_F^{-1} is so big, any weak process that happens at low energy is suppressed. This is why the weak force is weak.

W and Z Self-Interactions

To complete our collection of Feynman diagrams, I'll finish by pointing out that there are interactions between the $W^{\pm}$and Z bosons themselves. This follows because, just like for gluons, the underlying equations describing the weak force are the Yang-Mills equations, whose defining property is the presence of interaction terms between spin 1 particles. These Feynman diagrams take the form



where each leg can be any $W^{\pm}$or Z boson, as long as charge conservation is obeyed at the vertex. These diagrams are mostly important in higher order corrections to the kinds of processes that I've described above.

4.4.3 4.3 Flavours of Fermions

In this section, we will describe how the quarks and leptons interact with the Higgs field. The six quarks are often referred to as flavours. As we will see, the structure of flavour is, in many ways, the most fiddly and poorly understood part of the Standard Model. It is certainly where the vast majority of the parameters in the Standard Model reside and, most likely, the best place to look for clues about what lies beyond.

4.3.1 Yukawa Interactions

The Higgs field talks to quarks and leptons through Yukawa interactions.
There is room for confusion in this name. The original interactions postulated by Yukawa were designed to explain how neutrons and protons bind together inside a nucleus, with a scalar field providing the mediating force. We now known that the scalar particle Yukawa had in mind is the pion and, as explained in Section 3, is composed of two quarks.

However, Yukawa's basic idea - that a scalar field can interact with two fermions - is reprised in the Standard Model with the Higgs field arising as the fundamental scalar, and the name "Yukawa interactions" has been co-opted in this new context. More precisely, the Yukawa interactions in the Standard Model couple the Higgs field to one left-handed fermion and one right-handed fermion.

Like all forces, there are dimensionless numbers that tell us the strength of the interaction between the Higgs field and the fermions. These dimensionless numbers are called Yukawa couplings and we will denote them by λ. The Higgs field then gives a mass to each fermion that is directly proportional to the strength of the Yukawa coupling,

$$\text{mass} = \frac{\lambda}{\sqrt{2}} \times 246\text{GeV} \tag{4.5}$$

where 246 GeV is the value of the Higgs expectation value (4.2) that we met earlier. The factor of $1/\sqrt{2}$ in this formula is just convention.

Each fermion has a different Yukawa coupling, and hence a different mass. The Yukawa couplings for the various quarks are:

$$\begin{aligned}
\text{top}: &\quad \lambda \approx 1 &&\Rightarrow m_t \approx 173\text{GeV}\\
\text{bottom}: &\quad \lambda \approx 2.5\times 10^{-2} &&\Rightarrow m_b \approx 4.2\text{GeV}\\
\text{charm}: &\quad \lambda \approx 7.5\times 10^{-3} &&\Rightarrow m_c \approx 1.3\text{GeV}\\
\text{strange}: &\quad \lambda \approx 5.5\times 10^{-4} &&\Rightarrow m_s \approx 96\text{MeV}\\
\text{up}: &\quad \lambda \approx 1.3\times 10^{-5} &&\Rightarrow m_u \approx 2.2\text{MeV}\\
\text{down}: &\quad \lambda \approx 2.7\times 10^{-5} &&\Rightarrow m_d \approx 4.7\text{MeV}
\end{aligned}$$

Meanwhile, the Yukawa couplings for the electron and its cousins are

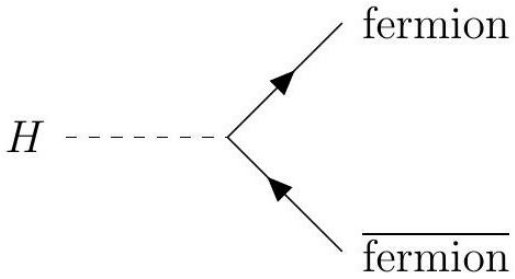
$$\begin{aligned}
\text{tau}: &\quad \lambda \approx 1\times 10^{-2} &&\Rightarrow m_\tau \approx 1.8\text{GeV}\\
\text{muon}: &\quad \lambda \approx 6.1\times 10^{-4} &&\Rightarrow m_\mu \approx 106\text{MeV}\\
\text{electron}: &\quad \lambda \approx 2.9\times 10^{-6} &&\Rightarrow m_e \approx 0.5\text{MeV}
\end{aligned}$$

Although we've reduced the masses of the various quarks and leptons to dimensionless coupling constants λ, we currently have no understanding of why the Yukawa couplings take these values. The Yukawa couplings span 5 orders of magnitude in order to explain the quark

masses, and a further order of magnitude to explain the electron mass. We don't know why. Is it coincidence that the top Yukawa coupling is almost exactly one? Again, we simply don't know. All of these are, from the perspective of the Standard Model, fundamental constants and we have no deeper understanding of them.

You may have noticed that we haven't yet discussed neutrinos. These have masses at least six orders of magnitude smaller than the electron, or 10^{-12} times smaller than the top quark. Thankfully there is a plausible reason for this vast discrepancy in mass, but we postpone the discussion until Section 4.4.

The fact that the masses of all fermions derive from the Higgs field has a consequence that could only be tested after the Higgs boson was discovered. The Higgs boson couples to all fermions with the Feynman diagram interaction



The strength of this interaction is dictated by the same Yukawa coupling λ that determines the mass of the fermion. This means that once the Higgs boson is produced, we have an entirely different way of measuring the Yukawa couplings by determining the relative probability that the Higgs boson decays to various fermion-anti-fermion pairs. So far, decays to the top and bottom quarks and the tau have been measured, all in agreement with theoretical expectations.

4.3.2 Symmetry Breaking

Symmetry is one of the key concepts in particle physics. For example, the $SU(3)$, $SU(2)$ and $U(1)$ labels that we've been using to describe the three forces are really mathematical expressions of symmetry. Until now, we've somewhat underplayed the idea of symmetry in these lectures, largely because it's a fairly formal mathematical idea and analogies tend to get bogged down in useless diversions. However, in describing how fermions get a mass we have a chance to elaborate on this. At the same time, we'll also get a better understanding of how electromagnetism emerges from the electroweak force.

For an example of symmetry, we can first look to the strong force. As we've seen, each quark comes with a colour: red, green or blue. But there is a symmetry underlying the choice of colours. To see this, you take a collection of particles and swap all the colours around,

$$\text{red} \longrightarrow \text{green} \longrightarrow \text{blue} \longrightarrow \text{red}$$

The end result will then look identical to the set-up we started with. This happens for the proton because it has a collection of quarks with one colour of each and that
doesn't change under a permutation of colours. Meanwhile, as we described in Section 3.2, a meson has a quantum superposition of colours $\bar{r}r + \bar{g}g + \bar{b}b$, so that too remains unchanged.

What's the analogous statement for the weak force? We've seen that "weak colour" is the up/down and electron/neutrino label for left-handed particles. This means that, at the fundamental level there is a symmetry that swaps

$$\text{up} \longleftrightarrow \text{down}$$

and

$$\text{electron} \longleftrightarrow \text{neutrino}$$

for left-handed particles. Under such an exchange, all physics should remain the same. Now, although there is such a symmetry at the fundamental level, it certainly doesn't manifest itself in our world. If you were to exchange all the electrons in your body for neutrinos, bad things would happen. So what's going on? What happened to this fundamental symmetry of nature?

The answer is that the symmetry is broken by the Higgs boson. To understand this, we first note that the Higgs experiences the $SU(2)$ weak force. This means that the Higgs too must have a "weak colour" label, something that we've neglected to mention so far. The Higgs field is actually a pair of complex-valued Higgs fields

$$\phi = \begin{pmatrix} \phi_1 \\ \phi_2 \end{pmatrix}$$

where the two fields ϕ_1 and ϕ_2 are mixed by the weak force.
Because there are actually two Higgs fields, the potential $V(\phi)$ should really be plotted in 3d. We have drawn this in Figure 37. Note that the shape of the potential doesn't change if you rotate it around the vertical axis, and this reflects the symmetry of the weak force. There's no sense in which the potential prefers the ϕ_1 direction to the ϕ_2 direction: both are on the same footing. If you slice this potential along any direction, then you get the 1d graph that we previously drew on the right-hand side of Figure 34.

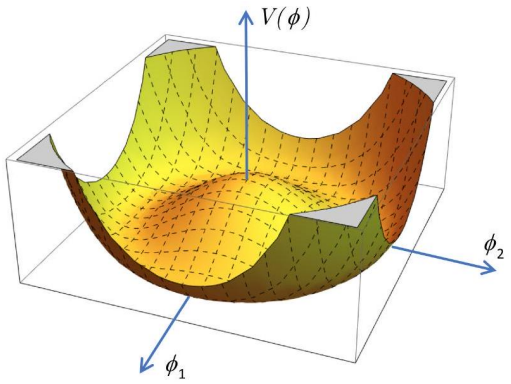


Figure 37. A better depiction of the Higgs potential. This is sometimes called the "mexican hat" potential for its sombrero-like quality.

This new 3d potential doesn't have isolated minima. Instead, there is a ring of minima, all lying at some fixed distance $\sqrt{\phi_1^2 + \phi_2^2}$ from the origin. In the vacuum, the Higgs field must sit somewhere in this valley. But where? Nothing tells the Higgs field where to sit and, moreover, because of the symmetry, any choice is as good as any other. Nonetheless, like a ball on a roulette wheel, the Higgs must choose somewhere to sit. And choose it does. Because it doesn't matter where the Higgs field sits, we may as well decide that it lies along the ϕ_1 axis, although any other position

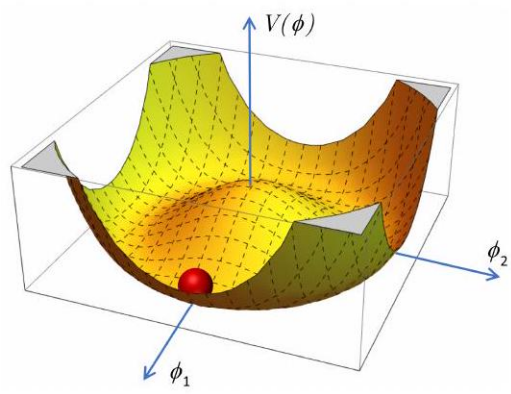


Figure 38. The choice of Higgs expectation value breaks the symmetry

would be just as good. This is shown in the figure to the right.

Once the Higgs field has nestled in place, it's no longer true that the ϕ_1 direction is the same as the ϕ_2 direction, because the Higgs field sits in one of these directions and not the other. We say that the symmetry has been broken. More precisely, we say that the symmetry has been spontaneously broken.

Ultimately, this is the reason why electrons and neutrinos (and up and down quarks) behave so very differently in our world. The laws of physics endow the left-handed versions of the particles with identical properties. But then the Higgs field comes along and spoils it, choosing to sit in one place and rather than another. The ϕ_1 direction
in which the Higgs field sits coincides with the "electron direction" for leptons, and the "down quark" direction for quarks. The ϕ_2 direction is where the neutrino and up quark live.

Finally, we can complete the story of how electromagnetism emerges from the electroweak force. The photon is the combination of the weak and hypercharge forces that does not fall into the clutches of the Higgs boson. The right-handed particles know nothing about the weak force, so for them the coupling to the photon (which we call electric charge) is identical to the coupling to hypercharge. Indeed, if you look at Table 2 you'll see that the hypercharge for the right-handed particles is the same as their electric charge.

However, the left-handed particles feel both the weak and hypercharge and the resulting electric charge is a combination of both. How that combination plays out depends on whether the particle is aligned with the Higgs field, or orthogonal to the Higgs field. For those left-handed particles that are aligned with the Higgs field, the resulting electric charge is

$$\text{electric charge} \;=\; \text{hypercharge} \;-\frac{1}{2}$$

while for those that lie orthogonal to the Higgs field, the electric charge is

$$\text{electric charge} \;=\; \text{hypercharge} \;+\frac{1}{2}$$

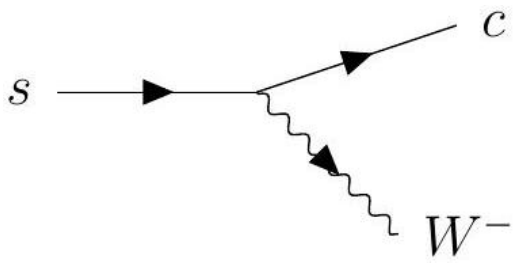
We can now check what this means for the left-handed quarks and leptons by looking back at Table 2. After symmetry breaking, the left-handed quark splits into two particles with electric charges $\frac{1}{6} \mp \frac{1}{2} = -\frac{1}{3}$ and $+\frac{2}{3}$. These, of course, are the charges of the down and up quark respectively. Meanwhile, the left-handed leptons also split into two, now with charges $-\frac{1}{2} \mp \frac{1}{2} = -1$ and 0 . These are the electric charges of the electron and neutrino.

4.3.3 Quark Mixing

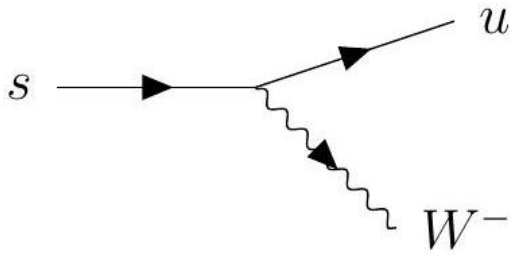
We've now described all the forces of the Standard Model. However, within the structures that we've outlined above, there are certain particle interactions that we cannot explain. We can't,

for example, explain the decay of hadrons that contain quarks from the higher generations.

To see the problem, consider the kaon K^-, whose quark content is $\bar{u}s$. We stated in Section 3.4 that kaons decay with a lifetime of around 10^{-8} seconds. But where do they go? Within the strong and electromagnetic forces, there's no way for quarks to change their type, so it must be a weak interaction that does the job. But the weak interaction that we've described above doesn't allow quarks to change generation. For a strange quark, we have the Feynman diagram



But then we're left with a charmed quark and there's nowhere for that to go. Instead, for a kaon to decay we would need an interaction that mixes the generations, like this:



If such a decay was possible then the resulting up quark could annihilate with the $\bar{u}$ in the kaon, while the W^-can decay into, say, an electron and anti-neutrino in the usual way.

So what are we missing? Is it possible for the weak force to mediate decays that change quarks from one generation into another? The answer to the second question is: yes. The answer to the first question is that we're missing something rather subtle about the meaning of the word "particle"!

So far, we have been using two, somewhat different meanings of the word "particle" and tacitly assuming that they coincide. These are:

- A particle is an excitation of the field that has a fixed energy. Or, because $E = mc^2$, an equivalent way of saying this is that we can assign a specific mass to the particle. In the language of quantum mechanics, we say that it is an energy eigenstate.

- A particle is the object that interacts with a particular force. This is really pertinent only for the weak force which, as we've seen, turns one particle into a different particle: say the down quark into an up quark.

The subtlety comes about because, for the weak force, these two ideas of what it means to be a particle don't quite agree. The excitations of the field with a fixed energy aren't the same thing as the excitations of the field that have a specific interaction with the weak force. Another way of saying this is to recall that the mass of the particle comes from the Higgs field. So what's really going on here is a mismatch between the way the Higgs interacts with fermions and the way the W -bosons interact with fermions. The two interactions are not quite aligned.

Let's keep our original names for quarks $-u, d, s$, etc - for the particles that have a definite mass. We'll then denote the particles that experience the weak force with primes $-u', d', s'$ and so on. It turns out that we can always simply define the up-sector quarks to be aligned,

$$u = u' \text{ and } c = c' \text{ and } t = t' \tag{4.6}$$

But the down-sector quarks are then misaligned. It's simplest to explain what's going on if we first ignore the bottom quark. The misalignment is then given by

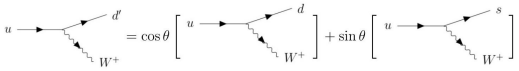
$$\begin{aligned} d' &= d\cos\theta + s\sin\theta \\ s' &= s\cos\theta - d\sin\theta \end{aligned} \tag{4.7}$$

Here θ is known as the Cabbibo angle. It is a fundamental parameter of Nature, an example of what's called a mixing angle. We'll see many more of these shortly. The Cabbibo angle is measured experimentally to be

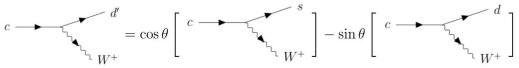
$$\sin\theta \approx 0.22 \quad \Rightarrow \quad \theta_c \approx \frac{\pi}{14} \approx 13^\circ$$

Why this number and no other? We don't know! We don't currently have any deeper explanation for this.

The formulae (4.7) might remind you of the equations for a rotation, and that's exactly the right way to think about it. The (d', s') quarks that feel the weak force are rotated relative to the (d, s) quarks that interact with the Higgs. This phenomenon is called quark mixing. It means that the Feynman diagrams that we previously wrote down for the weak force should be amended. The correct Feynman diagram involving the up quark is

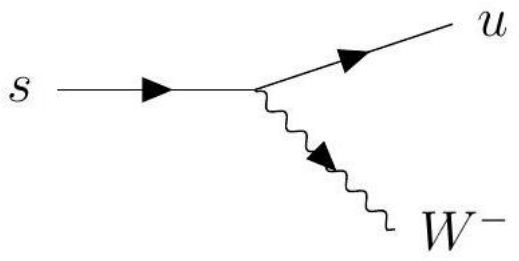


and similarly for the charm quark



How should we think about this? It seems to say that if, for example, a charm quark decays by emitting a W-boson, then the end product is both a strange quark and a down quark, in some combination. But, of course, we're in a quantum world here. And just as a particle can be in two places at the same time, or a cat both dead and alive, the decay product of a charm is indeed a quantum superposition of a down quark and a strange. As usual, this manifests itself in our experiments as probability. We get probabilities by taking the square of a Feynman diagram: so the probability of $c \to s + W^+$is proportional to $\cos^2\theta$ while the probability of $c \to d + W^+$is proportional to $\sin^2\theta$.

The phenomenon of quark mixing resolves our earlier puzzle: it's now quite possible for a meson like the kaon to decay, because there is an escape route for the strange quark, with Feynman diagrams like this now allowed:



The only price we pay is that the probability for such events to happen is reduced by $\sin^2\theta \approx 0.05$. This results in an increased lifetime for mesons containing strange quarks.

This story repeats with the addition of an extra generation. Now there is mixing between the down, strange and bottom quarks, and the simple rotation (4.7) is replaced by a more complicated matrix equation

$$\begin{pmatrix} d' \\ s' \\ b' \end{pmatrix} = \begin{pmatrix} V_{ud} & V_{us} & V_{ub} \\ V_{cd} & V_{cs} & V_{cb} \\ V_{td} & V_{ts} & V_{tb} \end{pmatrix} \begin{pmatrix} d \\ s \\ b \end{pmatrix} \tag{4.8}$$

The 3×3 matrix is known as the Cabbibo-Kobayashi-Maskawa (or CKM) matrix. The upper-left 2×2 sub-matrix agrees with the Cabbibo mixing (4.7), but now we have the possibility of mixing between all three quarks.

You might reasonably ask: what made the up-sector special? Why is the up-sector aligned, as in (4.6), while the down-sector has the complicated CKM matrix? The answer is that this is just a choice. There's some freedom in the equations to guarantee a partial alignment between the weak and Higgs forces. The convention is to pick the up-sector to be aligned because then the misalignment looks simple for the relatively
light strange mesons, with no need to invoke the charm quark in the argument. But if you were feeling a little perverse, there's nothing to stop you redefining everything with the down-sector aligned and the up-sector askew, or even some combination of the two.

The components of the CKM matrix have been accurately measured experimentally. It turns out that some of the elements can be complex numbers and we'll explain the significance of this in Section 4.3.4. For now, we give just the absolute values of each element which are roughly

$$\begin{pmatrix} |V_{ud}| & |V_{us}| & |V_{ub}| \\ |V_{cd}| & |V_{cs}| & |V_{cb}| \\ |V_{td}| & |V_{ts}| & |V_{tb}| \end{pmatrix} \approx \begin{pmatrix} 0.97 & 0.22 & 0.004 \\ 0.22 & 0.97 & 0.04 \\ 0.009 & 0.04 & 0.999 \end{pmatrix}$$

You can see the Cabbibo angle sitting there in $V_{us} = \sin\theta \approx 0.22$. The full CKM matrix extends the Cabbibo angle to a 3×3 matrix. Not all the elements of this matrix are independent. (The matrix can be shown to be "unitary".) It turns out that there are 4 independent parameters in the CKM matrix.

Just like we have no understanding of why the Cabbibo angle takes its particular value, nor do we have any good understanding of the CKM matrix. As you can see, it's not far from a diagonal matrix, with the Cabbibo terms being the only ones that aren't tiny. We don't know why.

It's worth pausing to take in a bigger perspective here. In the first part of this chapter, we described how the matter content of the Standard Model interacts with the different forces. There we found a beautiful consistent picture - a perfect jigsaw in which the interactions were largely forced upon us by the consistency requirements of the theory. For a theoretical physicist, it is really the dream scenario. This, however, contrasts starkly with the story of flavour. Even focussing solely on the quarks, we find that there are 6 Yukawa couplings that determine their mass, plus a further 4 entries of the CKM matrix that determine their mixing. And none of these parameters are fixed, or understood at a deeper level.

Somewhat ironically, much of this complexity can be traced to the simplicity of the Higgs. The strong and electroweak forces are described by Yang-Mills type theories, and these come with mathematical subtleties that are ultimately responsible for the quantum consistency conditions that constrain their interactions. But there are no such subtle constraints for the Higgs boson. It is a simple, spin 0 particle, that can do as it pleases and the result is the plethora of extra parameters that we've seen.

Turning this on its head, there is a possibility that the flavour sector of the Standard Model may well offer a unique opportunity. The structure of quark masses, together with the CKM matrix, surely contains clues for what lies beyond the Standard Model. Why the hierarchy of masses? Why these values of the CKM matrix? Moreover, there is a peculiar pattern: with $V_{us} = \sin\theta$, the other remaining values of the CKM matrix are not far from $V_{cb} \approx \sin^2\theta$ and $V_{ub} \approx \sin^3\theta$. Is this coincidence, or telling us something deep and important? We don't know. But hopefully, one day, we will find out.

4.3.4 CP Violation and Time Reversal

There is one last surprise waiting for us in the CKM matrix. We started this chapter by describing how the symmetry of parity is not respected in the microscopic world: the laws of physics look different when reflected in the mirror. As we saw, this was a pivotal moment in the history of particle physics, giving an important clue about the chiral structure of the Standard Model.

The violation of parity goes hand in hand with the violation of another symmetry, know as charge conjugation. We could ask: are the laws of physics the same for particles and anti-particles? And the answer is no. Anti-particles do not feel the same forces as particles. Moreover, this follows immediately from parity violation: the weak interaction involves left-handed neutrinos, or right-handed anti-neutrinos. So if you just change a particle to an anti-particle - say a left-handed neutrino to a left-handed anti-neutrino - then it doesn't experience the weak force anymore.

However, it remains a logical, and indeed compelling, possibility that the laws of physics are invariant under the simultaneous action of parity and charge conjugation. This symmetry is called CP, the C for "charge conjugation" and the P for "parity". A universe that exhibited CP symmetry would have the property that the laws of physics look the same if we swap all particles with anti-particles and look at them reflected in the mirror.

So are the laws of physics actually invariant under CP? You may not be surprised to hear that the answer is no.

CP violation was discovered in 1964. We describe the experimental evidence in Interlude D.2, focussing here on the theory. While violation of parity has an enormous effect on the theoretical underpinnings of the Standard Model, the violation of CP appears to be almost an afterthought: it turns out that the laws of physics violate CP if the CKM matrix contains a complex number! It does, and so CP is violated.

There is a way to quantify how much CP is violated in the Standard Model. From the CKM matrix, one can define a single number called the Jarlskog invariant, J. The maximum theoretical value it can take is $J \leq 1/2\sqrt{3} \approx 0.3$. Its experimentally measured value is $J \approx 3 \times 10^{-5}$. We see that the CP violation, at least as manifested among quarks, is really very small.

The experimental consequences of CP violation among quarks are, to put it mildly, rather subtle. It shows up in the decay of certain neutral mesons involving higher generations (like the kaon $K^0 = d\bar{s}$). We'll explain this in more detail in Section D.2.

Why should we care about CP violation? Well, there are two reasons. The first is that our universe is, rather fortunately, full of matter but with very little anti-matter. It's thought that this imbalance occurred naturally in the early universe, but for this to happen there have to be processes where matter and anti-matter behave differently. This, it turns out, requires CP violation. So although small, it may well have had extraordinarily large consequences. We'll discuss this further in Section 5.3.3.

There's also a twist to this tale. It turns out that a world with just two generations of fermions has no room for CP violation in the CKM matrix! In that case, the only quark mixing comes from the Cabbibo angle (4.7) and there's no complex number in sight. So, while it may seem like the bottom and top quark aren't much good for anything today, without them we may well find ourselves in a universe with as much matter as anti-matter.

Time Reversal

The second reason that CP symmetry is important is because it's closely related to yet another symmetry, that of time reversal.

A theory is said to obey the symmetry of time reversal if there's no way to distinguish

between the laws of physics running forwards in time and running backwards. Of course, in our macroscopic everyday world, the arrow of time is obvious. Underlying this is the concept of entropy which characterises the tendency for things to become disordered and muddled for the simple reason that there's more ways to be messy than to be neat. Ultimately, the entropic arrow of time can be traced to initial conditions. For a reason that we don't fully understand, the universe started off neat and tidy, so that it could ultimately descend into disorder, creating interesting structures like galaxies, planets and life along the way.

This entropic arrow of time is a powerful idea, largely because it doesn't depend on what's happening on the microscopic scale. In particular, it cares little for whether the laws of physics at the fundamental level are time reversal invariant. Nonetheless, it's interesting to ask whether time reversal is a symmetry of the world. If we were able to take a movie of interactions of fundamental particles, then play it backwards, would we notice the difference?

It turns out that the answer to this question is very closely tied to CP violation. The three symmetries of parity, charge conjugation and time reversal are an intwined triumvirate. There is a theorem that states that all laws of physics must be invariant under the combination of all three symmetries, what is known as CPT, with T standing for "time reversal". This means that if you make a movie of some dance performed by fundamental particles, then it's guaranteed to look the same if you watch it played backwards, in a mirror, with all particles exchanged for anti-particles.

The CPT theorem tells us that if CP is violated, then so too is T, for only then can the combination CPT be saved. The upshot is that the experimental discovery of CP violation is, admittedly indirectly, telling us that the laws of physics must look different running forwards and backwards in time. In other words, even at the microscopic level, there is an arrow of time in the universe.

Now, that sounds like a very big deal. Nonetheless, it's striking how little impact this fact has, not just on our daily lives, but on our deeper understanding of physics. As we mentioned above, it is likely that CP violation or, equivalently, time reversal violation is responsible for the preponderance of matter over anti-matter in the universe and that's not something to sneeze at. But that happened a long time ago! Has the violation of time reversal really not had any significant consequences since?! Moreover, it's not even straightforward to give a clear description of the microscopic process that runs differently forwards and backwards in time. The experimental observation of CP violation is described in Section D.2, and involve some rather subtle aspects of meson decay. We'll do slightly better in Section 4.4 when we discuss possible CP violating effects in neutrinos where an interpretation in terms of time reversal is easier to come by.

However, on the theoretical level it's interesting to compare the effects of parity violation with the effects of time reversal violation. At first glance, they seem very similar: one is a flip of spatial coordinates, $\mathbf{x} \to -\mathbf{x}$, the other a flip of time $t \to -t$. Yet the discovery of parity violation had profound consequences, leading immediately to the need for chiral matter, the associated delicate consistency conditions between
left- and right-handed fermions that, ultimately, gives us much of the structure of the Standard Model. This stands in sharp contrast to the theoretical consequences of time reversal violation which imply only that a single parameter, buried within the CKM matrix, is a complex rather than a real. It makes you wonder if there's something that we're missing!

4.3.5 Conservation Laws

Some things never change. In physics, we call these conservation laws. They comprise some of the most useful and powerful laws of nature. Among the conservation laws that we learn early in our physics education are the conservation of energy, momentum, angular momentum, and electric charge.

The familiar conservation laws listed above are all exact. No known process violates these laws. Moreover, they are sewn in the mathematical fibre of quantum field theory at such a deep level that it seems likely that they are here to stay.

In addition to these exact conservation laws, we have a number of "almost conservation" laws, together with a couple of "probably almost conservation" laws. These are the subject of this section.

First, the "almost conservation" laws. These are things that are conserved if you ignore one kind of force or another, but ultimately do not hold when you consider the whole of the Standard Model. For example, the electromagnetic and strong interactions don't change the type of quark. This means that the number of up quarks, down quarks and strange quarks are each individually conserved by any electromagnetic or strong process. Of course, as soon as the weak interaction kicks in, the down quark can decay into an up quark as we have seen repeatedly in this section. But because the weak force is, as the name suggests, weak, these decays can take a long time. This means that there will be situations where we can ignore weak decays and view the number of up and down quarks - or, equivalently, the number of protons and neutrons - as an effectively conserved quantity. This almost conservation law is sometimes called isospin and was mentioned briefly in Section 3.

As we saw in the last section, a strange quark can decay only through the weak force and, even then, only through the process of quark mixing. This causes yet further suppression in decays of mesons containing strange quarks, and this is seen in the relatively long lifetimes of the kaons where now "relatively long" means around 10^{-8} seconds. Again, we can think of this as an "almost conservation" of a quantity called strangeness. Combining isospin with strangeness gives the eightfold way that we described in Section 3.

There is a similar story in the lepton sector. If we ignore the weak force, the number of electrons, muons, taus and their associated neutrinos are all unchanging. When we include the weak force, the muon and tau can both decay. Moreover, as we will see in the next section, the neutrinos also undergo a mixing process, analogous to the one we've seen for quarks, so the individual neutrino species are not, ultimately, conserved quantities either.

Nonetheless, when the dust settles there do seem to be two exact conservation laws that follow from the Standard Model as described so far.

- Conservation of quark number

If you start with one kind of quark, it can decay into a different kind, usually ending up as the up quark since this is the lightest. But, if we count quarks as +1 and anti-quarks as -1 , then the total number of quarks can't change.

Confinement means that we don't see individual quarks, but rather the protons, neutrons and mesons that they bind into. The mesons contain a quark and antiquark, and so there's no such thing as meson conservation. But the conservation of quark number means that the number of baryons (again, counting anti-baryons as -1) can't change. For this reason, "conservation of quark number" is usually referred to as baryon conservation.

We see a good example of this in beta decay. The neutron decays, but leaves behind a proton. The total number of baryons before and after is the same.

- Conservation of lepton number

Just as the total number of quarks can't change, neither can the total number of leptons. Again, we see this in beta decay. The neutron decays into a proton, electron and anti-neutrino. It creates an electron, which changes the lepton number by +1 , but this is accompanied by an anti-neutrino which, because of the "anti-" contributes -1 to lepton number. The overall lepton number remains unchanged.

So the laws of physics seem to give two conserved quantities, baryon conservation and lepton conservation. And it's a true statement that we've never observed any process in which either these conservation laws are violated. Nonetheless, there are good reasons to think that they are not true conservation laws of nature. For this reason, I'll call them "probably almost conservation laws".

There are two reasons to think that baryon number and lepton number are not exactly conserved. While theoretically sound, neither of these is going to be high on an experimenters list of things to do. However, as I explain below, there are at least two experiments that might, with some level of optimism, tell us more in the future.

Reason 1: Electroweak Instantons

The first reason that baryon and lepton number are not likely to be precisely conserved quantities is, in many ways, the most subtle since it hinges on some of the deeper ideas relating geometry and quantum field theory. When we first met Feynman diagrams in Section 2.2, we explained that they were a way to give approximate answers to questions in quantum field theory. But there are some effects in quantum field theory that Feynman diagrams miss completely! These effects are, in some sense, smaller than any given Feynman diagram. (They are also closely related to the ideas of quantum anomalies that we discussed in Section 4.1.3.) And, in the Standard Model, there is such an effect that can turn a baryon into a lepton.

This process is due to an object known as an electroweak instanton. It turns out that it can't turn a proton into a positron: the proton is absolutely stable in the Standard Model. However, it can turn a collection of three baryons into three leptons. (The factor of three is actually related to the existence of three generations!) This means, for example, that the ^{3}He nucleus is unstable to decay into three leptons, say a couple of positrons and an anti-neutrino.

Now, we haven't ever observed such a decay. And for good reason. If you compute how long it would take for a helium nucleus to decay by this process, you get a silly number: something like 10^{173} years. Our universe has lasted around 10^{10} years. Clearly, it's unrealistic to think that we would ever observe this process. Nonetheless, strictly speaking in the Standard Model the baryon and lepton numbers are not individually conserved. Instead, there is only a single conserved quantity

$$\text{Conserved quantity } = (\text{ number of baryons }) - (\text{ number of leptons })$$

This quantity is usually called simply $B - L$.

Reason 2: Black Holes

Black holes aren't black. Hawking taught us long ago that they slowly emit radiation due to quantum effects. While there is much that we don't understand about quantum gravity, the existence of Hawking radiation stands out as one of the few robust and trustworthy calculations that we can do. The prediction of this radiation follows from the known laws of physics, and doesn't rely on any speculative ideas about what lies beyond.

If we wait long enough (and, again, we're talking ridiculously long times here), any black hole will eventually evaporate and disappear. So we can ask: what became of the stuff that we threw in?

First, the black hole can't destroy electric charge. If you throw, say, an electron into a black hole then the black hole itself now carries the electric charge. Moreover, this is visible outside of the event horizon because the black hole emits an electric field. That electric field can't just disappear. So, as the black hole evaporates, it must eventually spit out a charged particle - maybe an electron, maybe an anti-proton - which carries the electric charge. The

process of black hole evaporation must respect conservation of electric charge. Similarly, black hole evaporation respects the conservation laws of energy, momentum and angular momentum.

In contrast, there is nothing to prevent black holes from destroying baryons and leptons. When a black hole forms from the collapse of a star, it will typically contain around 10^{57} protons, and roughly the same number of electrons. But there's nothing like an electric field outside the black hole that tells you how many baryons and leptons are sitting inside. Furthermore, as the black hole evaporates there's no reason that it should spit out these particles intact. In fact, the vast majority of the mass of a black hole will be emitted in gravitational and electromagnetic radiation rather than baryons or leptons. In this way, we expect black hole evaporation to respect neither baryon number nor lepton number conservation.

Before we go on, I should stress an important point. There is an interesting and long standing problem about whether the information of what's thrown into a black hole is lost. We think that the answer is no. But, importantly, this isn't in contradiction with the violation of conservation laws!

To see why this is, consider the analogy of burning a book. In principle, the information written on the pages isn't lost: it's encoded in some impossibly complicated way in the correlations of the light and smoke that are emitted, and in the cinders that remain. Although the information is retained, the individual letters in the book are clearly lost.

In this analogy, the baryons in a black hole are like the letters. If you're clever enough and persistent enough, you may be able to detect that baryons were once present in the subtle correlations of the photons emitted by the black hole. But that doesn't change the fact that the baryons themselves have, almost certainly, gone for good.

Possible Experiments

No experimenter is lining up to test either of the theoretical arguments above. Nonetheless, the reasoning relies only on known, established laws of physics and tells us that, unlike electric charge, there is no fundamental reason for the conservation of lepton or baryon number. One might then wonder whether the violation of these conservation laws can be seen in some less extreme circumstance, one that could be tested here on Earth. There are two classes of ongoing experiments designed to test this.

Proton Decay

As mentioned above, within the Standard Model, the proton is absolutely stable. Nonetheless, it may well be that there is some physics beyond the Standard Model that causes protons to decay. Obviously, if we ever observed such a thing it would give us an important clue for what's happening on the next level.

So far, all we have are lower bounds. From our failure to detect proton decay in experiments we can infer that the lifetime of the proton is greater than around 10^{34} years. This is already quite an impressive statement, since its significantly longer than the age of the universe which is about 10^{10} years! But every litre of water contains about 10^{25} hydrogen atoms, so if you take 100 million litres of water, stare at it for a year, and fail to see a proton decay then you start to get close to the bound. There are a number of experiments around the world doing exactly this. The best current bounds come from the super-Kamiokande water Cerenkov detector in Japan. (We'll learn more about this detector in Section D. 4 when we discuss experiments on neutrino oscillations.)

Neutrinoless Double Beta Decay

There is a rare, but well understood phenomena in which two neutrons in a nucleus simultaneously decay to two protons. This is called double beta decay.

For example, ^{48}Ca is a rare isotope of calcium, making up less than 0.2% of the naturally occurring element. It consists of 20 proton and 28 neutrons. A standard beta-decay process would take ^{48}Ca to ^{48}Sc, but this isotope of scandium has a smaller binding energy than calcium and so the beta decay process doesn't happen. Instead, ^{48}Ca decays through the much rarer double beta decay process

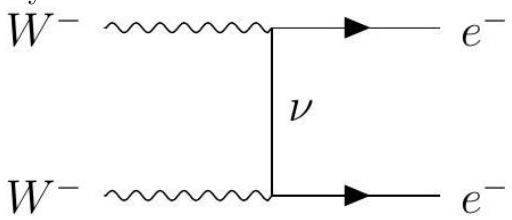
$$^{48}\text{Ca} \longrightarrow {}^{48}\text{Ti} + 2e^- + 2\bar{\nu}_e$$

The half-life is long: about 10^{20} years.

The double beta decay was first observed in the 1980s. As you can see, it violates neither baryon nor lepton number. However, it does raise the possibility for an even rarer occurrence: double beta decay without neutrinos. This would be a decay process of the form

$$^{48}\text{Ca} \longrightarrow {}^{48}\text{Ti} + 2e^-$$

With no neutrinos in the final state, lepton number is violated in this process. From the perspective of Feynman diagrams, the two neutrons would decay to protons by emitting two W^-bosons. These subsequently behave as follows:



Note that there's no arrow on the intermediate neutrino. Moreover, it's not possible to draw an arrow that lines up with both the external electron legs. Such a diagram is only valid if there's no way to distinguish between a neutrino and an anti-neutrino; indeed, this is what the observation of neutrinoless double beta decay would mean. We'll see how this might come about in the next section.

Despite many ongoing experiments around the world, neutrinoless double beta decay has yet to be observed. If it were seen, it would be a very big deal. Indeed, as we explain in the next section, it would give a key insight into the nature of neutrinos.

4.4.4 4.4 Neutrinos

No one would accuse a neutrino of being gregarious. They interact less than a first year undergraduate mathematics student forced to sit next to their theoretical physics professor at a matriculation dinner (to give a weirdly specific yet shudderingly memorable analogy).

For example, in the time it takes you to read this sentence, around 100 trillion neutrinos will have passed through your body. Most of them came from the Sun, but a significant minority have a cosmic origin, and have been streaming through the universe, uninterrupted since the first few seconds after the Big Bang. Moreover, in contrast to photons, the number of neutrinos hitting you doesn't change appreciably as day turns into night. The neutrinos from the Sun will happily pass right through the Earth and out the other side. This is vividly demonstrated in the picture of the Sun at night shown in Figure 39.

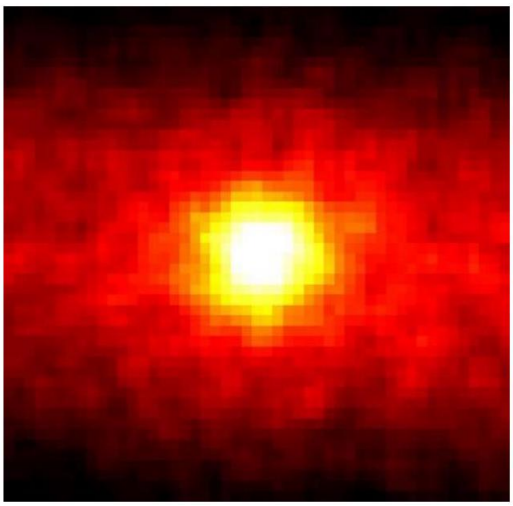


Figure 39. The Sun at night. This is a picture, taken by Super-Kamiokande, shows the neutrino flux coming from the Sun. The utterly remarkable fact is that the picture was taken at night, with the neutrinos passing through the Earth before hitting the detector.

There are two reasons why neutrinos are so intangible. The first is that they are the only particle to interact solely through the weak force. And, as we've seen, the weak force is weak. The second reason is that their mass is much much smaller than any other fermion which means that on the rare occasion that they do interact, they don't deliver much of a punch. The purpose of this section is to describe some properties of neutrinos in more detail.

4.4.1 Neutrino Masses

There is much that we don't know about neutrino masses. But we do know that the masses are not zero.

At the moment, we have no direct measurement of the mass of each neutrino. But we do have some precious information. First, we know that one neutrino must have a mass greater than

$$m_\nu \gtrsim 0.05\text{eV}$$

We'll explain how we know that neutrinos have a mass this big in Section 4.4.2.
Second, constraints from cosmology give us an upper bound on the sum of all neutrino masses. This comes from the imprint that neutrinos in the early universe leave on the cosmic microwave background radiation. (We'll say more about the intersection of

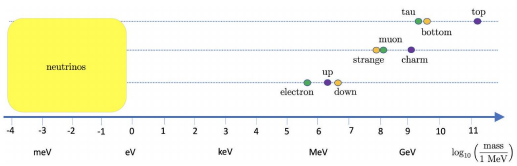


Figure 40. Fermion masses, arranged by generation. The charged leptons are green, the $-1/3$ quarks are orange, and the charge $+2/3$ quarks are purple. The neutrinos are way off to the left.

cosmology and particle physics in Section 5.3.). This bound is

$$\sum_\nu m_\nu \lesssim 0.25\text{eV}$$

There are still lots of possibilities consistent with these bounds. It may even be, for example, that one neutrino is massless while others have mass ~ 0.1eV or so. Still, our ignorance notwithstanding, a rough summary of the masses of all fermions is shown in Figure 40. Even with our limited knowledge, it's clear that neutrinos aren't like the other particles. There is six orders of magnitude separating the mass of the top quark from the mass of the electron. Then there is a gap of another six order of magnitude before we get to the neutrinos. The first question we should ask is: why?

We don't have a definitive answer to this question. But we do have a plausible answer. As I will now explain, there are a number of different possibilities for the way that neutrinos get a mass, but some of these offer a clear explanation for why neutrino masses are so much smaller than those of the charged fermions. To understand this, we will need to delve once again into some intricacies of quantum field theory and the Dirac equation.

Let's first recall some facts that we learned previously. A massless fermion can come in one of two kinds: left-handed or right-handed. Furthermore, if a particle has one orientation then it's anti-particle necessarily has the opposite. Applied to neutrinos, this means that the particles that interact through the weak force, which are necessarily the particles we detect in beta decay and other processes, are:

- A left-handed neutrino
- A right-handed anti-neutrino

When we refer to a "left-handed neutrino" below, this is shorthand for "left-handed neutrino and the right-handed anti-neutrino". They come together as a pair. You can't have one without the other.

In contrast, we've never observed the parity counterparts of these objects. This means that we've seen neither a right-handed neutrino nor a left-handed anti-neutrino in experiments. When we talk about a "right-handed neutrino" below, this will be shorthand for "right-handed neutrino and the left-handed anti-neutrino". Again, these come as an entwined pair.

The final important fact that we need is that massive particles arise by gluing together a left-handed fermion with a right-handed fermion. So the fact that neutrinos have a mass suggests that we should have both left- and right-handed neutrinos in the game, even though we can only directly observe the left-handed ones. However, nothing with neutrinos is as straightforward as it seems. One of the reasons they're special is because, as we saw in Section 4.1 (see, in particular, Table 2) the putative right-handed neutrino doesn't feel any force at all. It's this latter fact that is special to neutrinos and, as we now explain, opens up a new opportunity.

A Mass From the Higgs

First, it is quite feasible that neutrinos get a mass from the same mechanism as all other fermions, namely through interactions with the Higgs boson.

Recall that the interactions of all fermions with the Higgs field are characterised by a dimensionless number called a Yukawa coupling. The mass of the fermion is then given by (4.5)

$$\text{mass} = \frac{\lambda}{\sqrt{2}} \times 246\text{GeV} \tag{4.9}$$

where 246 GeV is the energy scale at which the Higgs settles down. The values of the Yukawa couplings range from $\lambda \approx 1$ for the top quark to $\lambda \approx 3 \times 10^{-6}$ for the electron.

This same story now repeats for the neutrinos. All you have to do is tune the value of the Yukawa coupling to $\lambda \approx 10^{-12}$, or whatever is needed to explain the three masses. In the context of neutrinos, this standard mechanism for generating mass is called a Dirac mass.

I stress that there's nothing logically wrong with this approach. The Yukawa couplings for charged fermions already range from 1 to 10^{-6} and so you may not feel unhappy by stretching the range down to 10^{-12}. But it does feel like the vastly different masses of neutrinos are crying out for a different explanation. Happily, one exists.

A Mass Without the Higgs and the Seesaw Mechanism

For all other fermions, the need for a Higgs field to induce a mass can be traced to the fact that the left-handed and right-handed particles experience different forces. The same is true for neutrinos, but with the key additional fact that the right-handed neutrino experiences no force at all.

But the lack of any force brings a level of freedom that other fermions do not enjoy. This is because the force that a particle experiences is used to distinguish between the particle and its anti-particle. For example, the difference between an electron and a positron lies in its electric charge. A particle that experiences no force - like the right-handed neutrino - may well be its own anti-particle.

We now tie this observation together with some facts about fermions. First, a fermion gets mass only by coupling together a left-handed and right-handed piece. Second, if we have a right-handed massless particle, then its anti-particle is left-handed. Third, if the particle experiences no force, then it can be its own anti-particle. When the dust settles, all of this means that the right-handed neutrino is unique among particles because it can get a mass without interacting with the Higgs field. It does so by interacting with itself! This kind of mass is called a Majorana mass, named after the Italian theorist Ettore Majorana who first realised this possibility in 1937.

We will discuss some consequences of the Majorana mass below but there is one important point that we flag up immediately. Forces are not the only way to distinguish particles from anti-particles: the conservation laws that we mentioned in Section 4.3.5 provide another. Recall that if we have a theory with conservation of lepton number, we count electrons and neutrinos as +1 and positrons and anti-neutrinos as -1 . The converse of this statement is that if a neutrino is the same as an anti-neutrino, then there can be no conservation of lepton number!

This gives the smoking gun for a Majorana mass: in any theory where neutrinos have a Majorana mass, lepton number is not conserved. As explained in Section 4.3.5, we would then expect to see neutrinoless double beta decay. This is one reason why those ongoing experiments are so important: they will greatly help complete our understanding of the neutrino sector of the Standard Model.

So we learn that neutrinos can get masses in two ways:

- A Dirac mass m, from left-handed and right-handed neutrinos interacting with the Higgs field.
- A Majorana mass M, from the right-handed neutrino coupling to itself.

Of course, when we do experiments on a neutrino, we measure just one mass. Which one do we see? The answer is rather nice. It is the combination [13],

$$\text{mass } = \left| -\frac{M}{2} \pm \frac{1}{2}\sqrt{M^2 + 4m^2} \right| \tag{4.10}$$

The $\pm$ sign here is telling us that we should see two particles, each their own antiparticle, with different masses.

Now comes the key idea. The Dirac mass m comes from the Higgs mechanism, so is given by (4.9) for some unknown Yukawa coupling λ. But the Majorana mass M is unrelated to the Higgs mechanism and could be very large, $M \gg m$, perhaps coming from some unknown physics at a high energy scale that we have yet to understand. If this is true, the two masses in (4.10) are approximately

$$\text{mass } \approx M \quad \text{and} \quad \frac{m^2}{M} \tag{4.11}$$

The particle with mass M is essentially the right-handed neutrino and is very heavy. We have yet to detect this in any experiment. Meanwhile, the other particle, which can be identified with the left-handed neutrino that we observe experimentally, has mass m^2/M. The key point is that the Dirac mass need not be particularly small; it could take the same kind of value as the other quarks and leptons. But if the Majorana mass is bigger still, with $M \gg m$, then we would see a tiny neutrino mass m^2/M. If this is the way Nature works, then the tiny value of the observed neutrino mass comes about not because the Dirac mass m is very small, but because the Majorana mass M is very large. This in known as the seesaw mechanism.

As an example, here are some sample numbers. Suppose that the Dirac mass of the neutrino is as high as 100 GeV , comparable to the mass of the top quark. If the Majorana mass is around $M \approx 10^{15}$GeV which, as we will discuss in Section 5.1.1, is the scale of grand unified theories, then we naturally get a neutrino mass of the right order of magnitude $\sim 10^{-2}$eV.

A Mass Without a Right-Handed Neutrino at all!

The seesaw mechanism provides a very natural explanation for why neutrinos are so much lighter than everything else. However, we are notably relying on physics at a high energy scale, way beyond our current reach, and this mechanism clearly predicts the existence of a new particle of a big mass M that we have still to discover.

There's something a little unsettling about this. Because, at the end of the day, we introduced the right-handed neutrino only to find that it has a very high mass and can be ignored, leaving behind the light left-handed neutrino that we actually detect in experiments. But if the right-handed neutrino is so heavy that we can't see it, then surely there should be a way to describe the physics that it leaves behind without the need to invoke it!

Indeed, there is. Here is the way that it works. Although the left-handed neutrino experiences the weak force, it has the property, unique among all the fermions, that it can bind together with the Higgs field to produce something that is neutral under all forces. (You can see this if you compare the charges of fermions in Table 2 with the charges of the Higgs field in Table 4.2.) This means that although we can't introduce a Majorana mass for the left-handed neutrino alone, we can introduce a Majorana mass for the left-handed-neutrino-Higgs combo.

Clearly, this mass once again involves the Higgs field. However, it's different from the Yukawa terms that give the other fermions a mass. First, it involves only the lefthanded neutrino, not the right-handed. Second, like any Majorana mass, it violates conservation of lepton number and so will give rise to neutrinoless double beta decay. And finally, and perhaps most importantly, it involves two interactions with the Higgs field and not just one [14]. This means that if $\langle\phi\rangle = 246$GeV is the expectation value of the Higgs field, the Majorana mass of the left-handed neutrino will be proportional to ϕ^2. But this doesn't have the right dimensions to be a mass! This means that we must introduce another scale M, so that the resulting mass

[013] This formula comes from solving a quadratic equation. Specifically, it comes from finding the eigenvalues of the matrix $\begin{pmatrix} 0 & m \\ m & M \end{pmatrix}$ where the off-diagonal terms are the Dirac mass and the term in the lower-right is the Majorana mass.

of the left-handed neutrino is roughly ϕ^2/M. This is the same form as we saw in the seesaw mechanism (4.11).

From this perspective, the mysterious new scale M is associated to some novel physics at a high energy that we don't yet understand. It could be the mass of the right-handed neutrino as in the seesaw mechanism, or it could be something else entirely. Either way, the irony of the seesaw mechanism remains: detecting a very small Majorana mass for the neutrino is clearly pointing to some new physics at a very high scale!

Some Other Way?

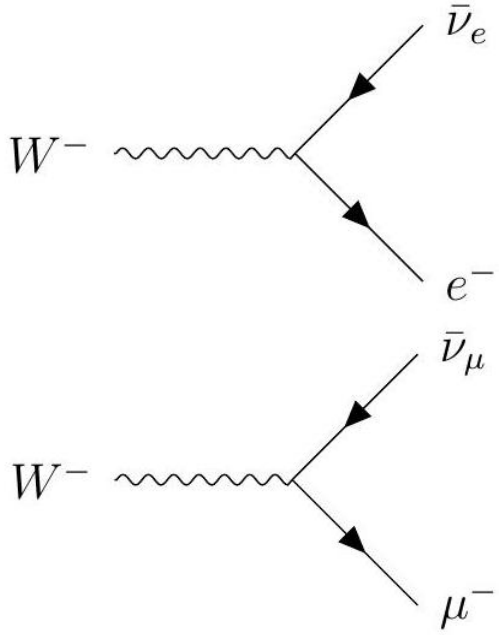
Above we've sketched the most plausible scenarios for neutrinos to get a mass. However, they're not the only possibilities. One could, for example, introduce further scalar fields that act like the Higgs boson, but carry different quantum numbers. If these too get an expectation value, it's possible to arrange for the neutrinos to get a mass. As you can see, our need to better understand the neutrino sector of the Standard Model has some urgency.

4.4.2 Neutrino Oscillations

So far we have described the different ways in which neutrinos can get a mass. But we haven't yet explained how we know that they have mass. After all, it's not like we can simply collect a bunch of neutrinos in a jar and weigh it. Instead, our information comes in a less direct manner.

We have met the key piece of physics already. In Section 4.3.3, we described how the assignment of mass to quarks is misaligned with the way the weak force acts on the quarks. This resulted in the phenomenon of quark mixing, described by the CKM matrix.

An entirely analogous phenomenon is at play in the lepton sector. It's simplest to explain what's going on by starting with two neutrinos, ignoring the third for now. To this end, we'll consider just ν_e and ν_μ. These are defined to be the neutrinos that couple to the electron and muon respectively, as in the following diagrams



But, just as with quarks, the ν_e and ν_μ particles that appear in these interactions are not the particles that have a well defined mass. Instead, there is a mixing and the neutrinos that have a specific mass are ν_1 and ν_2 defined by

[014] In more precise language of effective field theory, it is a dimension 5 operator built out of Standard Model fields, in contrast to the dimension 4 Yukawa terms.

$$\nu_1 = \nu_e \cos\theta + \nu_\mu \sin\theta$$
$$\nu_2 = \nu_\mu \cos\theta - \nu_e \sin\theta$$

This is entirely analogous to the quark mixing that we saw in (4.7). It turns out that $\theta \approx 33^\circ$ for leptons, so that $\sin\theta \approx 0.55$. This is somewhat larger than $\theta_{\text{Cabbibo}} \approx 22^\circ$ that we saw in quark mixing. This, it turns out, is what storytellers call "foreshadowing".

At this stage of the argument, however, there's a slight change of perspective. In the context of quarks, when we hold a meson in our hand (metaphorically speaking) we know that it has a definite mass. The mixing then shows up because this meson interacts through the weak force with quarks of other generations

For neutrinos, this situation is reversed. If we've got a beam of neutrinos then it came from some phenomenon involving the weak force, usually associated in some way to beta decay. This means that we know our experiment emitted a neutrino like, say, ν_e with definite flavour but, at least if $\theta \neq 0$, this neutrino does not have a definite mass. What happens next is quite wonderful. The kind of particles that happily travel along without adventure are those with definite mass (known, in the language of quantum mechanics, as energy eigenstates.) But ν_e doesn't have this property. And this has a dramatic effect: as the beam travels some distance, the neutrinos oscillate from ν_e to ν_μ and then back again.

There is a fairly simple formula that describes how this happens. Suppose that the difference in the masses of ν_1 and ν_2 is

$$\Delta m^2 = m_2^2 - m_1^2$$

measured in eV. If the neutrinos have kinetic energy E (measured in GeV) and travel a distance L (measured in km) then the probability that ν_e transforms into ν_μ is given by

$$P(\nu_e \to \nu_\mu) = \sin^2(2\theta)\sin^2\left(1.27 \times \frac{L\Delta m^2}{E}\right) \tag{4.12}$$

The fact that this probability depends on sine functions is telling us that the change of flavour is an oscillation, in the sense that it goes back and forth. The formula contains two fundamental parameters: the mixing angle θ and the difference in masses Δm^2. To see oscillations, both need to be non-zero. The formula also contains two parameters that can vary from one experiment to another: the energy E of the beam and the length travelled L. In principle, by varying E and L, and seeing how one kind of neutrino morphs into another, we can determine the mixing angle θ and mass difference Δm^2.

We explain more about how these experiments are done in Section D.4. Here, instead, we focus on the results. For reasons that will become clear, I'll first describe what we know about the mixing angles and only then turn to the masses.

Neutrino Mixing Angles

With three generations, neutrino mixing is described by introducing a 3×3 matrix, entirely analogous to the CKM matrix that we met for quarks in (4.8). This is

$$\begin{pmatrix} \nu_e \\ \nu_\mu \\ \nu_\tau \end{pmatrix} = \begin{pmatrix} U_{e1} & U_{e2} & U_{e3} \\ U_{\mu 1} & U_{\mu 2} & U_{\mu 3} \\ U_{\tau 1} & U_{\tau 2} & U_{\tau 3} \end{pmatrix} \begin{pmatrix} \nu_1 \\ \nu_2 \\ \nu_3 \end{pmatrix} \tag{4.13}$$

On the left-hand side we have neutrinos ν_e, ν_μ and ν_τ that interact with their counterpart electrons through the weak force; On the right-hand side we have neutrinos ν_1, ν_2 and ν_3 that have definite mass. Relating them is a 3×3 matrix is known as the Pontecorvo-Maki-Nakagawa-Sakata (PMNS) matrix, or simply the neutrino mixing matrix.

The components of the PMNS matrix have now been measured to reasonable accuracy. The absolute values are roughly

$$\begin{pmatrix} |U_{e1}| & |U_{e2}| & |U_{e3}| \\ |U_{\mu 1}| & |U_{\mu 2}| & |U_{\mu 3}| \\ |U_{\tau 1}| & |U_{\tau 2}| & |U_{\tau 3}| \end{pmatrix} \approx \begin{pmatrix} 0.8 & 0.5 & 0.1 \\ 0.3 & 0.5 & 0.7 \\ 0.4 & 0.6 & 0.6 \end{pmatrix}$$

Some values are known fairly well; others less well. There are, for example, error bars of ± 0.1 on $U_{\tau 2}$.

The first thing to note is that the PMNS matrix is strikingly different from the CKM matrix describing the mixing of quarks [15]. In the quark sector, the CKM matrix was close to being the unit matrix, with just small off-diagonal elements. This meant that there was close alignment between the masses and the weak force.

But we see no such thing in the neutrino sector. The mixing is pretty much as big as it can be! Once again, we see that, in quantitative detail, the neutrinos really behave nothing like the charged fermions.

We do not have an explanation for the structure of the PMNS matrix. Indeed, its form came as a surprise to theorists. Surely it is telling us something important. It's just we don't yet know what!

[15] Recall that $\begin{pmatrix} d' \\ s' \\ b' \end{pmatrix} = \begin{pmatrix} V_{ud} & V_{us} & V_{ub} \\ V_{cd} & V_{cs} & V_{cb} \\ V_{td} & V_{ts} & V_{tb} \end{pmatrix} \begin{pmatrix} d \\ s \\ b \end{pmatrix}$ with $\begin{pmatrix} |V_{ud}| & |V_{us}| & |V_{ub}| \\ & |V_{cd}| & |V_{cb}| \\ & |V_{cs}| & \end{pmatrix} \approx \begin{pmatrix} 0.97 & 0.22 & 0. \\ 0.22 & 0.97 & 0 \\ 0.009 & 0.04 & 0. \end{pmatrix}$

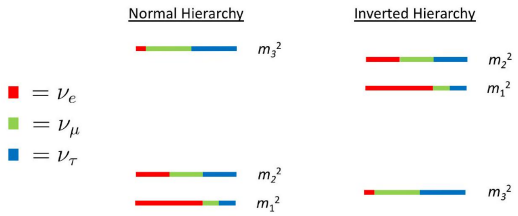


Figure 41. A colour coded description of the possible ordering of neutrino masses.

Neutrino Mass Differences

The mixing angles are a surprise. They tell us that each of the particles ν_1, ν_2 and ν_3 that have definite mass are not closely associated to the particles ν_e, ν_μ and ν_τ that have definite weak interaction.

Inverting the relation (4.13), we can make the following statements about the neutrinos ν_1, ν_2 and ν_3 that have definite masses:

- ν_1 acts like an electron neutrino two thirds of the time, and as a muon or tau neutrino the other third.
- ν_2 acts like any one of the three neutrinos one third of the time.
- ν_3 acts like a tau neutrino 45% of the time and like a muon neutrino 45% of the time. The remaining 10%, it acts like an electron neutrino.

With this in place, we can now describe what we know about the mass differences. First, ν_1 is known to be lighter than ν_2 and the squares of their mass differ by

$$m_2^2 - m_1^2 \approx 7.4 \times 10^{-5}\text{eV}^2$$

The difference in their masses is of order $\sim 10^{-2}$eV, an order of magnitude smaller than the biggest mass. We also know the difference between the masses of ν_3 and ν_2 but, crucially, we don't yet know which one is heavier! We have

$$m_3^2 - m_2^2 = \pm 2.5 \times 10^{-3}\text{eV}^2$$

Of course, if we could measure the mass difference between m_1 and m_3.then we would be able to resolve this $\pm$ ambiguity. As it stands, we just don't know the order of the masses.

The two possibilities are shown in Figure 41. Given the pattern seen in all other fermions, one might expect that the electron neutrino ν_e would be the lightest. Since the ν_e has the biggest overlap with ν_1, this would mean that ν_1 is lightest. This is referred to as the normal hierarchy. But, as we've seen, very little about the neutrinos follows our expectation. So another possibility is that ν_3, which contains very little of the electron neutrino, is the lightest. This is called the inverted hierarchy.

CP Violation Among Neutrinos

Neutrino mixing provides another forum in which the Standard Model can exhibit CP violation. And, as we described in Section 4.3.4, this also entails an opportunity for the violation of time reversal invariance.

In the quark sector, the violation of CP symmetry shows up as a complex number in the CKM matrix. The same is true in the neutrino sector. It turns out that if the neutrinos have only a Dirac mass, then there is a single complex number while if the neutrinos have a Majorana mass then there is an opportunity to introduce two more.

We do not currently have a good handle on these complex numbers. (Indeed, we have no handle whatsoever on the CP violation coming from Majorana masses.) However, preliminary results suggest that the complex numbers are non-vanishing and there is CP violation in the neutrino sector.

The good news is that, although difficult to measure, CP violation in the neutrino sector is conceptually rather more straightforward than in the quark sector. In particular, CP simply exchanges all left-handed neutrinos with right-handed anti-neutrinos. This means that if CP is preserved, the following probabilities are equal

$$CP \Rightarrow \quad P(\nu_\alpha \to \nu_\beta) = P(\bar{\nu}_\alpha \to \bar{\nu}_\beta)$$

where you can replace ν_α and ν_β with your favourite choice of flavour from ν_e, ν_μ and ν_τ. To detect CP violation, we (simply!) have to do an experiment that shows the probability for a neutrino to change flavour is not the same as the probability for its anti-particle to do the same thing.

Similarly, the violation of time reversal is also easier to state among neutrinos. In a world that is time-reversal symmetric, the probability of a neutrino morphing into a different one would coincide with the probability that this process is reversed,

$$T \Rightarrow \quad P(\nu_\alpha \to \nu_\beta) = P(\nu_\beta \to \nu_\alpha)$$

This is an experiment that could, in principle, be performed to discover a violation of time reversal invariance in our world.

Finally, as we discussed in Section 4.3.4, there is a mathematical theorem that says the laws of physics must be invariant under the combination CPT. In the language of neutrinos, this theorem tells us that

$$CPT \Rightarrow \quad P(\nu_\alpha \to \nu_\beta) = P(\bar{\nu}_\beta \to \bar{\nu}_\alpha) \tag{4.14}$$

A mathematical theorem is all well and good but it's nice to confront it with experiment. While the expectation is that CP and time reversal will both be found wanting in the neutrino sector, if it was found that the probabilities (4.14) don't coincide, that would surely rock our understanding of physics.

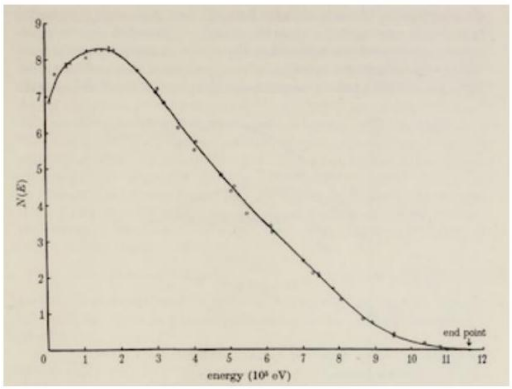
4.4.5 D Interlude: Big Science for Weak Things

For many decades, there was just one known manifestation of the weak force: beta decay. Much of our early understanding of the weak force came from careful study of this phenomenon.

We described some of the initial flurry of discovery in Interlude A. Radiation was found, largely by accident, in the darkness of Becquerel's desk drawer in 1896. By 1898, Rutherford had determined that the radiation from uranium consists of two different types $-\alpha$ rays and β rays - characterised by their penetrating power. And by 1900 it was understood that β rays were composed of the newly discovered particle called the electron. The next step was to further study the properties of these rays.

That, it turns out, was not easy. It had long been understood that α particles are emitted from the nucleus with a fixed velocity, and the general expectation was that the same would be true of β rays. However, the experiments were significantly harder. The leading experts in this game were Hahn, Meitner, and von Baeyer. Their first experiment confirmed that electrons were emitted with a uniform velocity; their second suggested a spread of velocities; their third a collection of distinct, but fixed, velocities. The situation was, to put it mildly, confusing.

The fog finally lifted in 1914. James Chadwick had completed his PhD under Rutherford and gone to work with Geiger in Berlin. (We met an older version of Chadwick in Section A. 4 where we recounted his discovery of the neutron.) While the earlier experiments had used somewhat temperamental photographic plates to detect electrons, Chadwick used the counter recently invented by his postdoc mentor. His experiments made it clear that the electrons were emitted with a range of



different velocities. A typical plot of energies is shown in the figure on the right [16].

1914 was not a great year to be an Englishman working in Berlin. Shortly after finishing his experiment, Chadwick was arrested and interned in the stables of a racecourse where he would spend the rest of the war, the monotony broken only by regular

Offener Brief an die Crunpe der Radioaktiven bei der Gauvereins-Tagung zu Tubingen.

Abstract

Liabe Radioaktive Damen und Herren, Wie der Ueberbringer dieser Zeilen, den ich huldvollst ansuhören bitte, Ihnen des näheren auseinandersetsen wird, bin ich angesichts

[016] This was taken from a paper by G. J. Neary entitled "The β-Ray Spectrum of Radium E". (Radium E is now known as ^{210}Bi.)

der "falschen" Statistik der N- und Li-6 Kerne, sorie des kontimierlichen beta-Spektrums auf oinen versweifelten Ausweg verfallen um den "Wechselsats" (1) der Statistik und den Energiesats su retten. Maimlich die Möglichkeit, es koinnten alektrisch neutrale Teilahen, die iah Neutronen nemnen will, in den Kernen existieren, welche den Spin 1/2 haben und das Ausschliessungisprinsip befolgen und die von Lichtquanten musserdem noch dadurch unterscheiden, dass sie Mist mit Lichtgeschwindigkeit laufen. Die Masse der Neutronen Suste von ders alben Orossenordrung wie die Elaktronenmasse sein und selafalls nicht grosser als 0,Ol. Protonenmasse.- Das kontimierliche wan Spaktrum wire dann verstindlich unter der Annahme, dass beim betw-Zerfall mit dem klektron jureils noch ein Neutron emittiert asil derart, dass die Summe der Energien von Meutron und klektron konstant ist.

Figure 42. Liebe Radioacktive Damen und Herren.

deliveries of Nature and the occasional piece of scientific apparatus to help him pass the time.

Chadwick's work was not the end of the story, and a great deal of to-ing and fro-ing took place, largely between Lisa Meitner's group in Berlin and the pair of Chadwick and Charles Ellis, now back in Cambridge. But by the late 1920s, the situation was decisively settled: the spectrum of beta rays was continuous.

What to make of this? It was in sharp distinction to both alpha rays and gamma rays, where the radiation was emitted with a definite energy. Moreover, the emission of alpha and gamma rays was well understood as the transition between different states, just like the clean spectra of atoms. What could a continuous spectrum possibly mean?

D. 1 The Neutrino

Two proposals were put forward in 1930. Bohr, ever the revolutionary, was keen to ditch energy conservation. Pauli, however, had a different idea: a new, hitherto undetected, particle. If two particles were emitted in beta decay, then the energy could be shared among them in different ways. There would then be no reason for the electron that we observe to carry a unique energy.

Pauli's first made this proposal public, just days after a messy divorce, in a famous "Dear Radioactive Ladies and Gentleman" letter sent to a conference in Tubingen. This is shown in Figure 42. The first paragraph translates as

"I have come upon a desperate way out regarding the 'wrong' statistics of the N - and Li 6 -nuclei, as well as to the continuous β-spectrum, in order to save the 'alternation law' of statistics and the energy law. To wit, the possibility that there could exist in the nucleus electrically neutral particles, which I shall call neutrons, which have spin 1/2 and satisfy the exclusion principle and which are further distinct from light-quanta in that they do not move with light velocity. The mass of the neutrons should be of the same order of magnitude as the electron mass and in any case not larger than 0.01 times the proton mass. The continuous β-spectrum would then become understandable from the assumption that in β-decay a neutron is emitted along with the electron, in such a way that the sum of the energies of the neutron and the electron is constant."

It is clear from the letter that Pauli is trying to solve two problems at once. We now know that these two problems in fact require two new particles. The first problem was described in Section A. 4 and arose from the prevailing view that the nucleus is comprised of A protons with $A-Z$ electrons making up the charge difference. Pauli doesn't dissent from this viewpoint, but proposes that there are further neutral particles in the nucleus which ensures that the nucleon spin agrees with the sum of its constituents. As we saw, this problem was solved in 1932 by the discovery of the neutron.

The second problem addressed by Pauli is the one of interest here. The continuous spectrum of β-decay is resolved if a light, neutral particle is also emitted. Pauli calls this the neutron,

but obviously that name was later taken. The Italian name neutrino was coined by Fermi in 1933.

Detection

Pauli was unduly nervous about his proposed neutrino. Indeed, his letter continues "I don't feel secure enough to publish anything about this idea, so I first turn confidently to you, dear Radioactives, with a question as to the situation concerning experimental proof. . ."

The neutrino hypothesis was accepted long before the particle was seen directly in experiment. It was an integral part of Fermi's theory of beta decay, which agreed too well with the observed phenomenology. Moreover, the same theory made it clear how difficult a direct detection would be. As we've mentioned previously, a typical neutrino emitted in beta decay will interact only once as it travels through a light-year of lead.

The resolution to this problem is not to focus on a single neutrino. Instead, you need to go to a place where there are many. This was the goal of a team lead by Clyde Cowan and Fred Reines, working at the Los Alamos lab. Originally their idea was to detect the neutrinos emitted in a nuclear explosion, but they soon realised that a nuclear reactor offered a better (and presumably safer) alternative. Because of the ghostly nature of neutrinos, they named their original experiment "project poltergeist".

They set up their experiment in the Savannah reactor site, a nuclear reservation in South Carolina, USA. The nuclear reactor emits a flux of 10^{13} neutrinos per cm^2 per second, through beta decay

$$n \longrightarrow p + e^{-} + \bar{\nu}_e$$

The experimental challenge is to take the resulting neutrinos and observe the inverse process

$$\bar{\nu}_e + p \longrightarrow n + e^{+}$$

The bad news is that such processes are extremely rare. The good news is that both products n and e^+have a distinctive signature. The experimental set-up consisted of two tanks, each holding 200 litres of water. These provide the targets for the neutrinos. The resulting positron quickly annihilates with an electron in the water, emitting two gamma rays. Slightly later, the neutron is captured. To aid this process, Cowan and Rienes dissolved cadmiun salts in the water. These are known to efficiently capture neutrons, emitting a third gamma ray in the process with a well understood energy spectrum. The signature of neutrinos is then two coincidental pulses of gamma rays, the first a pair; the second, delayed by a few milliseconds, a single photon, all of which were registered by liquid scintillators which surrounded the two tanks.

The experiment ran for almost 1400 hours and, when the reactor was on, detected roughly 3 coincidental pulses an hour.

Announcing a major discovery must be both exciting and nerve-wracking. Announcing the discovery to Wolfgang Pauli, not known to suffer fools gladly, doubly so. But on June 14$^{\text{th}}$ 1956, Cowan and Rienes sent Pauli a telegram that read:

> "We are happy to inform you that we definitely detected neutrinos from fission fragments by observing inverse beta decay of protons. Observed cross section agrees well with the expected six times ten to minus forty four square centimeters"

For some reason, Pauli's reply was never sent. It exists only in the form of a draft discovered later in his papers and reads: "Thanks for the message. Everything comes to him who knows how to wait."

The Muon Neutrino

It had long been known that when charged pions decay to a muon, they also emit a second spin 1/2 particle with all the properties (or lack thereof) of a neutrino.

$$\pi^+ \longrightarrow \mu^+ + \nu_\mu \quad \text{and} \quad \pi^- \longrightarrow \mu^- + \bar{\nu}_\mu$$

We now know, of course, that this is a different kind of neutrino from the one that appears in beta decay. The question is: how to tell ν_μ and ν_e apart?

One way is to run the inverse beta decay experiment again. What do you see if this neutrino collides with a proton? The two obvious possibilities are:

$$\nu_\mu + p \stackrel{?}{\rightarrow} n + \mu^+$$
$$\text{or} \quad \nu_\mu + p \stackrel{?}{\rightarrow} n + e^+$$

If the muon neutrino ν_μ is, in reality, the same object as the electron neutrino ν_e, then both of these processes should occur, presumably with comparable frequency. In contrast, if ν_μ is truly distinct from ν_e, then you would expect to see only the first process and not the second.

At this stage, accelerators once again come to the fore. A synchrotron can accelerate protons to, say, 30 GeV which, upon a collision with a fixed target, create a beam of pions. 25 meters down the road, these pions decay into a beam of muons and neutrinos. At this point, you need to put some shielding in place to remove the muons, leaving behind just the neutrinos. In the original experiment, performed at Brookhaven in 1962 by Lederman, Schwartz, Steinberger, and others, this shielding was achieved by 5,000 tonnes of steel from a decommissioned battleship (often falsely claimed to be the USS Missouri, which seems unlikely given that this ship, although mothballed in the late '50s, was subsequently reactivated and even served in the gulf war).

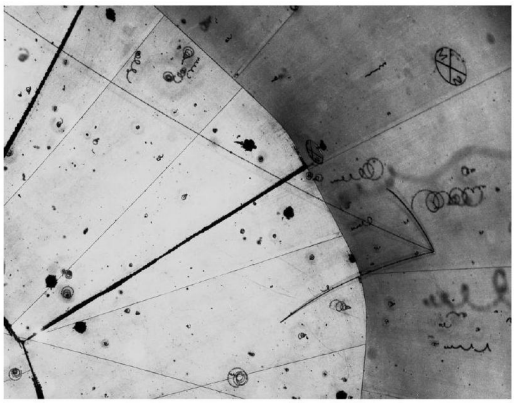


Figure 43. Muonic inverse beta decay, seen in a bubble chamber. The neutrino entered from the right where it hit a proton at the vertex where three lines meet. The proton is the short line moving up and to the left; the pion the slightly longer line moving down and to the left. The longest line of all, exiting top-left, is the muon. This image was taken at Argonne National Laboratory.

Waiting on the other side of the battleship, was a novel kind of detector known as spark chamber. This consists of an array of plates, sitting at a high voltage, with gas between them. When a charged particle passes through it ionises the gas which, when it hits the plates, leaves a trail of visible sparks. One can easily distinguish the track a muon from the much lighter electron.

One advantage of using accelerators is that the neutrino cross-section increases with energy. As Pais puts it, while you need a lightyear of lead to stop an MeV neutrino, a few million miles will do the job for a GeV neutrino. And, indeed, the 30 GeV machine was just sufficient to see the desired result: after several months of experiments, starting with roughly 10^{17} protons hitting the target, 29 anti-muons were seen and no positrons. This means that the subscript matters: ν_μ is indeed different from ν_e.

In subsequent years, muonic inverse beta decay could be seen in bubble chambers. The first such example is shown in Figure 43.

D. 2 Not P and Not CP Either

We started Chapter 4 with a description of parity violation, since this sets the scene for much of the subsequent structure of the Standard Model. As we reviewed there, parity violation was first seen in the realm of atomic physics through the beta decay
of cobalt atoms. But, prior to this, there was a hint of parity violation in the world of particle physics.

Heavy mesons provide the setting to see violation of both parity and of CP. Here "heavy" means mesons that include strange, charm or bottom quarks. The lightest of these is, of course, the strange quark and this is where the phenomena were first observed.

The story starts with what we now call the charged kaon, $K^+ = \bar{s}u$, which weighs in at 494 MeV . Back in the 1950s, before quarks were understood, this particle was seen in experiments. But it had an unusual property: sometimes it decayed to two pions, and sometimes it decayed to three pions. In fact, this difference was so striking that, at the time, it was assumed that the experiments must be seeing two different particles. They gave these particles names θ and τ. Both names have since been retired and, in the case of τ, upcycled into the name of a lepton, but back in the 1950s these were two of the most interesting particles around. They decayed as

$$\theta^+ \longrightarrow \pi^+ + \pi^0$$
$$\tau^+ \longrightarrow \pi^+ + \pi^+ + \pi^-$$

But then there was a surprising coincidence that needed an explanation: as far as the experiments could tell, $\theta^+$and τ^+had exactly the same mass and lifetime! Why on earth would that be? This was known as the theta-tau puzzle.

Of course, we know now the resolution to the theta-tau puzzle: it's that both particles have the same mass because they're actually the same particle - the kaon K^+. But physicists in the 1950s were reluctant to draw this obvious conclusion because it violated one of their cherished principles of physics: that the world should be invariant under parity.

It's not so easy to explain why this is the case without going into the mathematics. But it turns out that the decay to two pions looks identical when reflected in the mirror, while the decay to three pions does not. This isn't because of any obvious reason due to the directions in which the pions fly out. Instead, it shows up only in the subtle fact that the wavefunction of three pions differs by a minus sign upon reflection.

Given this experimental observation, parity could be conserved only if $\theta^+$and τ^+ were genuinely different particles, with θ^+staying unchanged when reflected in a mirror, while τ^+picked up a minus sign in its wavefunction. Conversely, if you want to identify the $\theta^+$and $\tau^+$and say that they're the same particle, then you can do so only if you sacrifice the symmetry of parity.

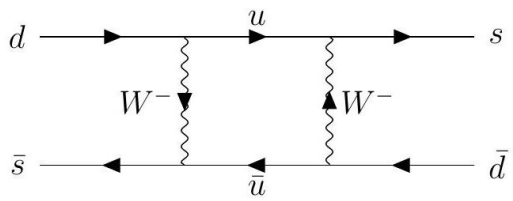
Needless to say, the argument above is somewhat subtle and was far from enough to convince physicists that parity was indeed broken in the weak interaction. The first physicists to take this possibility seriously were T.D. Lee and C.N. Yang (yes, Yang-Mills Yang) who, in 1956, did a systematic analysis of parity symmetry in various experiments. They came to the conclusion that, while there was overwhelming evidence for parity in the strong and electromagnetic forces,

the jury was still out when it came to the weak force. They also proposed the experiment involving the decay of cobalt atoms that was subsequently performed by their colleague, C.S. Wu.

Wu's experiment showed that parity isn't just violated in the weak force a little: it is violated as much as it possibly could be. This spurred particle physicists to find other pieces of evidence. Confirmation came quickly from showing that muons arising from $\pi^+ \longrightarrow \mu^+ + \nu_\mu$ decay are polarised in a manner that can only be explained by parity violation. Moreover, the signature was so stark that even though the experiment was initiated after hearing of Wu's results, it was completed before she had finished. In the end, the two papers establishing parity violation in very different ways were published back to back.

Neutral Kaons and CP

Kaons also played a starring role in the discovery of CP violation. This time it was the neutral kaon $K^0 = d\bar{s}$ and its anti-particle $\bar{K}^0 = \bar{d}s$ that were of interest. The phenomenon of quark mixing that we met in Section 4.3.3 means that heavy, neutral mesons of this type have an interesting property: over time, the particle can change into its anti-particle and then back again! This happens through a Feynman diagram of the form



As we learned when discussing quark mixing, those intermediate u and $\bar{u}$ quarks could also be replaced by c and $\bar{c}$, or t and $\bar{t}$.

This means that as a K^0 wends along its merry way, it's constantly switching between a K^0 and $\bar{K}^0$. The actual particles that we observe are some mix of the two. But what mix? Here's where things get interesting.

Under CP symmetry, a K^0 switches with a $\bar{K}^0$ (because particles swap with antiparticles). So if the kaon was to arrange itself in accord with CP, the right mix would simply be

$$K_1^0 = K^0 + \bar{K}^0$$
$$K_2^0 = K^0 - \bar{K}^0$$

Then K_1^0 reflects into itself under CP, while K_2^0 reflects into minus itself. (These words make more sense when written as quantum mechanical equations! The right statement is that the two combinations above are CP eigensates.)

Moreover, just as parity conservation (if it existed!) would dictate the possible decays of particles, so too would CP conservation. CP symmetry means that we should see the two different species of kaons decay in different ways

$$K_1^0 \longrightarrow \pi^0 + \pi^0$$
$$K_2^0 \longrightarrow \pi^0 + \pi^0 + \pi^0$$

So do we?

The K^0 and $\bar{K}^0$ do indeed mix into two different combinations and, experimentally, these are distinguished by their lifetime. There is a long-lived neutral kaon that is called K_L and a short-lived neutral kaon that is called K_S. At first glance it seems as if all is good, since these two different combinations decay as

$$K_S^0 \longrightarrow \pi^0 + \pi^0 \text{ in around } 10^{-10} \text{ s}$$
$$K_L^0 \longrightarrow \pi^0 + \pi^0 + \pi^0 \text{ in around } 5 \times 10^{-8} \text{ s}$$

This makes it look like we can identify $K_S^0 = K_1^0$ and $K_L^0 = K_2^0$, in which case CP would be preserved.

However, a careful examination shows that this isn't quite the case. In 1964, Christenson, Cronin, Fitch and Turlay created a beam of neutral kaons, and let it travel for 18 m . Travelling at close to the speed of light, it takes around 6×10^{-8} s to travel 18 m , meaning that the short-lived K_S^0 kaons had long since departed and the beam contained only K_L^0 kaons. The goal was to see if they did, indeed, all decay to three pions as expected by CP.

They did not. Of the roughly 23,000 decays, they found 45 decaying into two pions (both $\pi^0 + \pi^0$ and, more commonly, $\pi^+ + \pi^-$). This is only 0.2% of the sample, but was enough to show that CP is not a symmetry of our world. The kaon states that have a definite mass are not quite the K_1^0 and K_2^0 states compatible with CP, but instead take the form

$$K_S^0 \approx K_1^0 - 0.002 K_2^0$$
$$K_L^0 \approx K_2^0 + 0.002 K_1^0$$

That tiny extra 0.002 piece is the sign of CP violation.
The signature of CP violation in quarks is remarkably subtle. The effect is stronger in mesons that contain bottom quarks, but the essence of the idea remains the same. Recall from Section 4.3.3 that among the indirect implications of this result is the statement that the laws of physics are not invariant under time reversal. It seems surprising that the observable consequences of something so profound can only currently be seen in something so subtle and seemingly insignificant as the decay of certain mesons.

D. 3 The Bosons of the Weak Force

Before the discovery of the W-boson, there was beta decay. Before the discovery of the Z-boson, there were neutral currents. This is the name given to the process in which a neutrino sneaks in, gives a charged lepton a gentle kick, and then quietly leaves again. For example,

$$\nu_e + e^- \longrightarrow \nu_e + e^-$$

Since we don't actually see the neutrino, the signal is rather subtle: the electron simply flies off without warning.

The first detection of neutral currents came in 1973 at CERN. A proton synchrotron (known simply as the PS) was used to create a beam of muon neutrinos which then entered an enormous bubble chamber, given the poetic name Gargamelle. You can see the discovery picture in Figure 44.

By this time, the theory of the weak force, with its W - and Z -bosons, was in place and it was possible to get a ballpark figure for their mass. But to find them required a machine that could reach the required energy. Something just shy of a 100 GeV or so should do it.

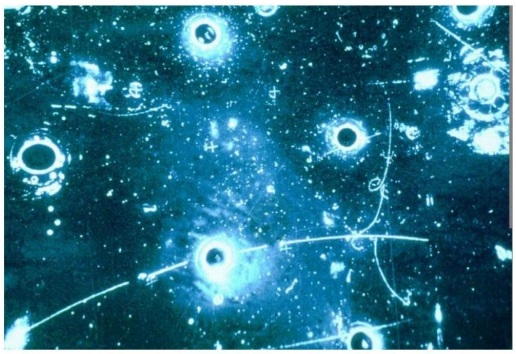
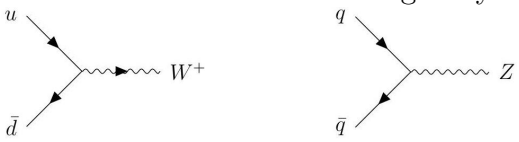


Figure 44. The first detection of neutral currents. The neutrino came in somewhere at the top and sent an electron barreling downwards, creating a shower of $e^{+
e^{-}$pairs, with their tell-tale spiral tracks. A black and white version of this appears in the discovery paper "Search for Elastic Muon-Neutrino Electron Scattering". The same journal contains a second paper with evidence for neutral currents from hadrons.}

The W and Z Bosons

By 1976, CERN had turned on its latest machine, uninspiringly named the Super Proton Synchrotron or SPS. The proton beam reached 300 GeV before colliding into a fixed target. Sadly, as we mentioned before, much of the energy in fixed target machines ends up in the kinetic energy of the final product so only $\sqrt{2m_pE}$ of the energy, or about 25 GeV in this case, is available to do something useful. And that's not enough.

In the same year that the SPS turned on, Rubbia, Cline and McIntyre wrote a paper proposing to add a counter-rotating beam of anti-protons to CERN's newest accelerator. The centre-of-mass energy is then 300+300 = 600GeV. It turns out that around half the momentum in a proton is carried by the gluons, with the remainder split evenly between the three valence quarks. That means that each valence quark carries roughly 1/6 of the energy, so 600 GeV should be sufficient to create both W and Z-bosons through Feynman diagrams of the form



where q and $\bar{q}$ can be any quark-anti-quark pair.

Not everyone in CERN was overjoyed at the prospect of their new toy undergoing such an extensive overhaul so soon after turning on but Carlo Rubbia was, by all accounts, a persuasive if not particularly likeable man. The argument that he might move to Fermilab and do the experiment there was perhaps the decisive one and the SPS was upgraded to the SppS, or Super Proton-Anti-Proton Synchrotron. A key part of the design was an idea to focus the beam known as stochastic cooling, introduced by Simon van der Meer.

The first collisions occurred in December 1981 and were recorded in two detectors known as UA1 and UA2, the "UA" standing for "underground area", referencing the fact that both beam and detectors sit 100 m below the surface. The goal was to see the decay products.

First, the W-boson. This decays about 70% of the time to quark-anti-quark pairs, such as $W^+ \to u\bar{d}$, and these appear in the detector as jets. But jets are ten a penny in $p\bar{p}$ collisions. For this reason, you need to focus on the 30% of the time that the W-boson decays as $W^+ \to \bar{l}\nu$ or $W^- \to l\bar{\nu}$ with the lepton l either an electron or muon.

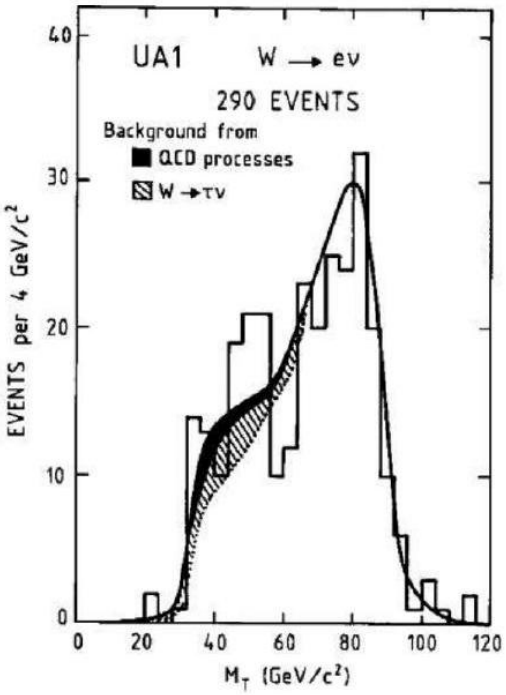
If the W-boson was sitting at rest when it decayed, we would get back-to-back leptons with momentum $\mathbf{p}_l = -\mathbf{p}_\nu$. Of course, you miss the neutrino in the detector, so you should see the electron or muon fly off with its kinetic energy [17] given by $|\mathbf{p}_l| = M_W/2$, half the mass energy

of the W-boson.

In reality, the W-boson usually isn't at rest when it decays, but travelling at some unknown velocity aligned with the direction of the beam. Furthermore if the lepton also travels in the same direction of the beam, then you're simply going to miss it: there's too much going on down there and no detector. The trick, therefore, is to look at the transverse momentum $\mathbf{p}_T$ of the lepton, meaning the momentum orthogonal to the beam. This obeys $|\mathbf{p}_T| \leq M_W/2$, with equality occurring only when you're lucky, and the W-boson was at rest and the lepton emerges perpendicular to the beam. However, one can show that the expected distribution of $|\mathbf{p}_T|$ from many W-boson decays takes a specific shape, peaking at $M_W/2$ and then quickly dropping off.

Using this method, the first clear signs of the W-boson were seen in January 1983. The discovery was announced soon afterwards. The figure on the right shows that data collected by UA1 between 1982 and 1985. The data is plotted using a variable related to $\mathbf{p}_T$ called transverse mass, a slightly odd name when you first hear it given that mass has no direction.

The search for the Z-boson is cleaner because this time there's no neutrino to miss and you see back-to-back electron-positron pairs. However, the events are rarer, with a frequency of around 10% of the W-bosons decay. For this



reason it took a few months more before the Z-boson was also discovered.

While W- and Z-bosons were first discovered at a $p\bar{p}$ collider, their detailed study came with the next upgrade at CERN. This was the Large Electron Positron Collider, or LEP, a 200 GeV machine built in a new tunnel, some 27 km in circumference. While hadron collisions are a mess, e^+e^-collisions allow for exquisitely precise measurements. It is from this experiment, with its four detectors Aleph, Delphi, Opal, and L3, that we have our most accurate understanding of the weak force. The current values of the masses are now known to be

$$M_W = 80.379 \pm 0.0021\text{GeV} \quad \text{and} \quad M_Z = 91.1876 \pm 0.0021\text{GeV}$$

with comparable precision on their decay widths.

[017] For slowly moving particles, where you can ignore relativity, the kinetic energy is quadratic in the momentum: $E = \frac{1}{2}mv^2 = \frac{1}{2}p^2/m$ where the momentum $p = mv$. But this formula is no longer right when particles move fast. The correct relativistic formula combines the rest mass energy and kinetic energy as $E = \sqrt{m^2c^4 + p^2c^2}$. When particles move extremely fast, with $pc \gg mc^2$, we can neglect the rest mass energy and the kinetic energy is approximately linear in the momentum: $E \approx pc$. This is the formula we've used in the text, with units $c = 1$.

However, there was one last part of the Standard Model that was tantalisingly just out of reach of the LEP machine. This was...

The Higgs Boson

By the end of the last century, the LEP data told us that the Higgs boson must be heavier than 114 GeV . But how much heavier?

To answer this, LEP was dismantled and the Large Hadron Collider, or LHC, constructed in its place, designed to collide two proton beams with a centre of mass energy of 14 TeV . The full CERN accelerator complex is shown in Figure 45 . There are a number of detectors around the ring, the most important of which are ALICE, used for heavy ion collisions, LHCb, used to study B-mesons, and two multi-purpose detectors called ATLAS and CMS. These latter two detectors were the ones to find the Higgs.

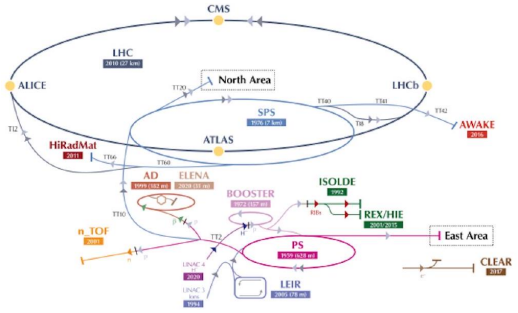
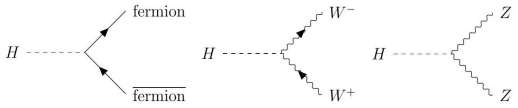


Figure 45. The CERN accelerator complex. You can see the older PS and SPS accelerators which now act as feeders for the LHC.

The Higgs, like the top quark of Interlude C.3, is detected through its decay products. It can decay either into fermions, or into W and Z bosons through diagrams like this



As we explained in Section 4.3, the strength of the interaction is proportional to the mass of the particle, because it comes from the same physics that gives fermions and W and Z bosons a mass in the first place. This means that the Higgs preferentially decays into the particles with higher masses.

The coupling to the top quark is the strongest, but because the top is heavier than the Higgs that decay route woud appear to be ruled out. That means that the decay $H \to b\bar{b}$ is the most common, but it is difficult to distinguish the resulting two jets from the background of a pp collision. The next two decay modes, $H \to W^+W^-$ and $H \to ZZ$, are significantly cleaner since both W and Z can subsequently decay to leptons through $W \to l\bar{\nu}$ and $Z \to l\bar{l}$, giving two lepton and four lepton events respectively where the leptons are either electrons or muons. (Remember, no one sees the neutrino.) The decay through Z-bosons to four leptons is particularly clear and sometimes referred to as the golden channel.

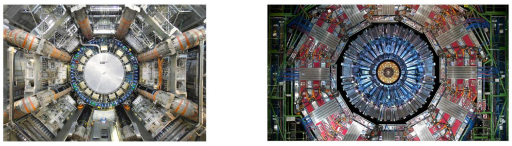
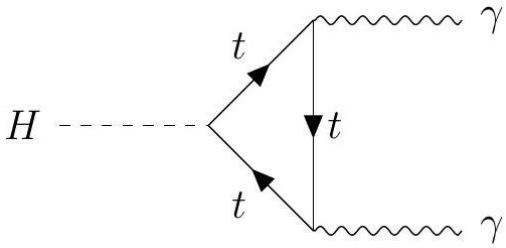


Figure 46. Iconic images of the ATLAS detector, on the left, and CMS, on the right, not to convey any information but simply to let you stare in awe at one of the great engineering feats of all time.

Given that the Higgs decays preferentially to massive particles, it is somewhat ironic that one of the best signals comes from the emission of two photons. These arise from top quarks which, although too heavy to appear directly as decay products, couple so strongly that the one-loop Feynman diagram is comparable to other tree level processes:



On July 4$^{\text{th}}$, 2012, ATLAS and CMS held a joint seminar in which they announced the discovery of the Higgs boson, the final piece of the Standard Model jigsaw. There is nothing as pretty as a bubble chamber photograph to show, merely a small bump above the background for the emission of two photons shown in Figure 47, revealing that the Higgs boson has mass

$$M_H = 125.10 \pm 0.14\text{GeV}$$

Since then, a number of different Higgs decay channels have been seen, all impressively (but, to some, disappointingly) in perfect agreement with expectations from the Standard Model.

There is much that we still don't understand about the Higgs, not least its selfcoupling and more detailed information about the shape of the Higgs potential $V(\phi)$. There is hope that a future e^+e^-collider - perhaps the proposed ILC - could change

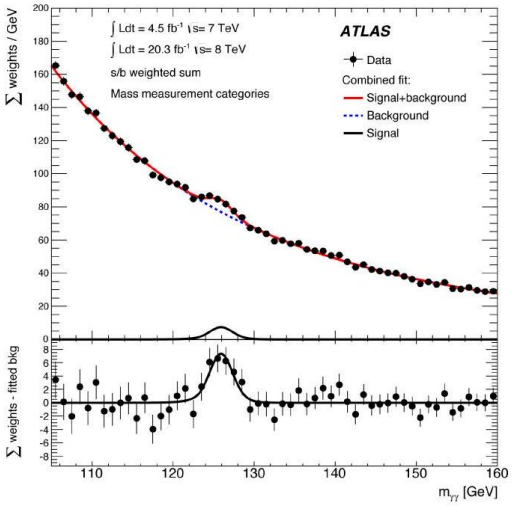


Figure 47. The tiny bump that revealed the Higgs, taken from the ATLAS experiment.

this, allowing us to understand the Higgs sector with the same precision that LEP explored the rest of the electroweak sector.

D. 4 Neutrino Oscillations

We end this interlude the same way in which we began: with neutrinos. We saw how neutrinos were first discovered in Interlude D.1. Now we will learn about their mass, a long and involved story that, as we will see, is still far from complete.

Solar Neutrinos

The first hint that something was awry came when neutrinos failed to escape the Sun. In the late 1960s, Ray Davies built the world's first solar neutrino detector, buried deep underground in the Homestake gold mine in South Dakota. The detector consisted of a large tank filled with a dry-cleaning fluid that, importantly, was rich in chlorine. The neutrinos were detected by a neutrino capture process, which is like stimulated beta decay

$$\nu_e + {}^{37}\mathrm{Cl} \longrightarrow {}^{37}\mathrm{Ar} + e^-$$

These argon atoms were then counted and used as a proxy for the original neutrino.

Neutrinos have the ability to induce such an interaction provided that their energy is greater than $\sim 800\mathrm{keV}$. However, they do so with extraordinarily small probability. We now know that around 10^{11} neutrinos that originate from the Sun stream through a surface area of one square centimetre here on Earth every second. Most, it turns out, aren't powerful enough to induce the reaction above, but there's still about 10^8, per square centimetre, per second, that can do the job. Yet the number of reactions observed in 600 tonnes of cleaning fluid was just a few a day. (Neutrino experiments use the unit of SNU, where 1 SNU means 10^{-36} interactions per target atom per second. The Homestake experiment detected about 2.5 SNU of solar neutrinos.)

There was a problem however. The observed solar neutrinos were a factor of 3 too small. Detailed calculations of the reactions in the Sun, largely performed by John Bachall, showed that the expected flux was around 8 SNU. Where did the other neutrinos go?

The reaction of the larger scientific community to this puzzle was mostly to shrug and move on. To particle physicists, the Sun looked like a ridiculously messy and complicated object; surely those astrophysicists had screwed up the calculations. Meanwhile, the astrophysicists were bewildered at the possibility that you could reliably detect neutrinos; surely the particle physicists had got something wrong in their experiment. After all, could we even be sure that it was detecting neutrinos from the Sun, and not some other source?

However, as time went on the problem became more urgent. Bachall's theoretical models of the Sun passed many impressive tests, leaving little doubt of their accuracy. Meanwhile further experiments confirmed and refined the Homestake results. In Japan, Kamiokande, and later Super-Kamiokande, detected neutrinos at higher energies through Cerenkov radiation emitted in scattering process

$$\nu_e + e^- \longrightarrow \nu_e + e^- \tag{D.1}$$

Importantly, this gave directional information about the incoming neutrinos and showed clearly that they were coming from the Sun. Meanwhile GALLEX in Italy, and SAGE in Russia, both repeated the experiment with gallium rather than chlorine, now relying on the neutrino capture process,

$$\nu_e + {}^{71}\mathrm{Ga} \longrightarrow {}^{71}\mathrm{Ge} + e^-$$

The advantage is that the threshold is somewhat lower than the chlorine reaction, needing only around 200 keV , meaning that many more of the Sun's neutrinos can
partake. Indeed, the number of events seen was significantly higher, at around 75 SNU , but still below the theoretical prediction of 130 SNU. Curiously, the shortfall in these experiments is only around 40%, compared to the 70% seen in the chlorine experiments. This is telling us that the loss of neutrinos is energy dependent. Collectively, these discrepancies between experiment and theory went by the name of the solar neutrino problem.

As the years went on, it became increasingly clear that the resolution to the solar neutrino problem must be found in neutrino oscillations which, as we have seen in Section 4.4, requires that the neutrinos have mass. The question was: how to test this? This requires us to count not just the electron neutrinos emerging from the Sun, but also the muon and tau neutrinos. And this is significantly harder. We can't rely on the obvious neutrino capture process

$$\nu_\mu + n \longrightarrow p + \mu^-$$

because the incoming neutrinos have energies less than the 150 MeV needed to create a muon.

An unambiguous resolution to the solar neutrino problem was provided by the Sudbury Neutrino Observatory (SNO), based in the Creighton nickel mine in Ontario, Canada. One novelty was that their tank was filled with heavy water, D_20, where the hydrogen is replaced by deuterium D. It doesn't take much to split the deuterium nucleus apart; just 2 MeV of energy is enough. Moreover, neutrinos can knock apart a deuterium nucleus in two different ways. A weak interaction involving an intermediate W-boson does the job through a neutrino capture process analogous to those that occur in chlorine or gallium,

$$\nu_e + d \longrightarrow p + p + e^-$$

Only electron neutrinos contribute to such processes. However, the neutrinos can also split the deuterium through a weak interaction involving a Z-boson,

$$\nu + d \longrightarrow n + p + \nu$$

This time there is no charged lepton created, meaning that all three kinds of neutrinos, ν_e, ν_μ and ν_τ contribute.

In addition, SNO measured neutrino scattering events of the form $\nu + e^- \to \nu + e^-$. Electron neutrinos undergo such scattering events through both W-boson and Z-boson interactions, but muon and tau neutrinos only scatter off electrons when an intermediate

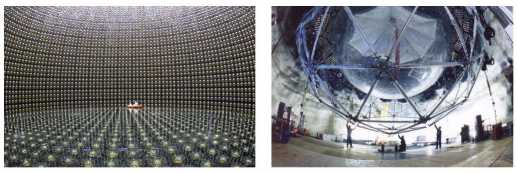


Figure 48. Neutrino detectors tend to look like the lair of a James Bond villain. On the left is a boat cleaning the Super-Kamiokande photosensors as the tank slowly fills up. On the right is the SNO tank, filled with heavy water.

Z-boson is involved. This means that the total rate of such events depends on some combination of the flux of electron, muon and tau neutrinos. (For what it's worth, it turns out to be ν_e flux $+0.15$ times ν_μ and ν_τ flux.)

The upshot is that SNO was able to see everything - electron, muon and tau neutrinos. And once you see everything, nothing is missing. The end result agreed perfectly with theoretical expectations of the nuclear reactions inside the Sun. The electron neutrinos missed by previous experiments had transmuted into muon and tau neutrinos, incontrovertible evidence for neutrino oscillations.

Atmospheric Neutrinos

The story of missing neutrinos was repeated when we looked elsewhere. One key clue came from neutrinos created in the upper atmosphere. Cosmic rays, mostly in the form of protons or helium nuclei, are constantly bombarding the Earth. When they hit the atmosphere they create a constant stream of $\pi^{\pm}$pions. These pions decay to muons

$$\pi^+ \longrightarrow \mu^+ + \nu_\mu \quad \text{and} \quad \pi^- \longrightarrow \mu^- + \bar{\nu}_\mu$$

and the muons then quickly decay to electrons,

$$\mu^+ \longrightarrow e^+ + \nu_e + \bar{\nu}_\mu \quad \text{and} \quad \mu^- \longrightarrow e^- + \bar{\nu}_e + \nu_\mu$$

Indeed, as we saw in Interlude B, this is how both the pion and muon were first discovered. Now, however, our interest lies in the neutrino by-products. These "atmospheric

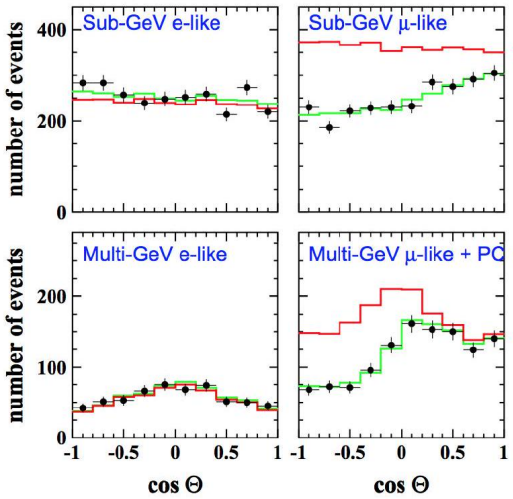


Figure 49. The observed flux of electron neutrinos (on the left) and muon neutrinos (on the right). The top boxes show low-energy neutrinos; the lower boxes high-energy neutrinos. The red line is the theoretical expectation without neutrino oscillations, and the black boxes the data.

neutrinos" have significantly higher energies than solar neutrinos; often around a GeV or higher. Given the decay processes described above, each collision should result in two muon neutrinos (strictly one ν_μ, one $\bar{\nu}_\mu$) for every electron neutrino. The question is: can we find them?

The answer, given by Super-Kamiokande, is interesting and shown in Figure 49. These show plots of the neutrino flux (on the vertical axis) against the angle at which the neutrinos come into the detector (on the horizontal axis). An angle $\cos\theta = 1$, on the far right, means that the neutrinos come directly down. An angle $\cos\theta = -1$, on the far left, means that neutrinos come up, through the Earth.

The data on the left two boxes is for electron neutrinos, both for low-energy events (shown in the top box) and high-energy events (in the bottom box). The red line is the theoretical expectation; the black dots the observed flux. We see that the agreement between experiment and theory works well.

The story is more interesting for muon neutrinos, shown in the two boxes on the right. The number of neutrinos coming straight down agrees perfectly with what we expect, but there's a clear deficit for those that come up through the Earth. Why?

For any other particle, you might think that the Earth is simply getting in the way. But neutrinos pass right through the Earth without any difficulty. (Remember the picture of the Sun at night in Figure 39.) Besides: theorists aren't stupid and had taken the presence of the Earth into account when computing the red line! Instead, the key point is that the muon neutrinos have travelled further, and so had more opportunity to convert into other neutrinos, in this case tau.

Importantly, the atmospheric neutrinos clearly show us that neutrino oscillations depend on the length L that neutrinos travel. We have

$$\text{Straight down: } L = 15 \text{ km} \Rightarrow \text{ No oscillations}$$
$$\text{Straight up: } L = 13000 \text{ km} \Rightarrow \nu_e \text{ unaffected, but } \nu_\mu \to \nu_\tau$$

Meanwhile, for solar neutrinos we have $L = 150$ million km . As we'll now see, this collection of data goes a long way to allowing us to determine neutrino masses.

Getting a Handle on the Masses

Nature is kind, and gives us two sources of neutrinos: solar and atmospheric. As we've seen, these clearly show that something fishy is going on, as neutrinos appear and disappear. But to be sure, we should design our own experiments here on Earth, in which a source of neutrinos is created and subsequently detected elsewhere.

There are now a number of these experiments up and running, with results consistent with the oscillations seen in solar and atmospheric neutrinos. The best results so far have come from the T2K experiment, which directs a beam of muon neutrinos created in Tokai, Japan to the Super-Kamiokande detector located 300 km away. They clearly see ν_e neutrinos in a beam that, at its origin, consisted purely of ν_μ neutrinos. Meanwhile, the OPERA experiment in the Gran Sasso lab in Italy has directly detected ν_τ neutrinos in a ν_μ neutrino beam from CERN, 730 km away.

From this collection of experiments, together with results from solar and atmospheric neutrinos, we can put together the picture of masses and mixing angles that we described in Section 4.4.2.

4.5 5 What We Don't Know

It is often said that each new discovery opens up many more questions than it answers. That's not the case for the Standard Model. The collection of interlinked ideas, bound together in the Standard Model, has brought a synthesis that is unprecedented in science, bringing order to many, seemingly disconnected phenomena and leaving very few threads hanging as a result.

Furthermore, the current experimental situation is one of remarkable harmony. Wielding a broad brush, it is not too inaccurate to say that the Standard Model predicts the correct answer to each and every one of the thousands of particle physics experiments that we've performed.

That's not to say that everything is perfect. There is, as we have recounted in Section 4.4, much still to learn about the neutrino sector. Moreover, if you look in finer detail, then there are a handful of experimental anomalies that seemingly cannot be described by the Standard

Model. The most longstanding of these is the magnetic moment of the muon. Recall that the magnetic moment describes how strongly a particle couples to a magnetic field. Our best theoretical result for the muon is

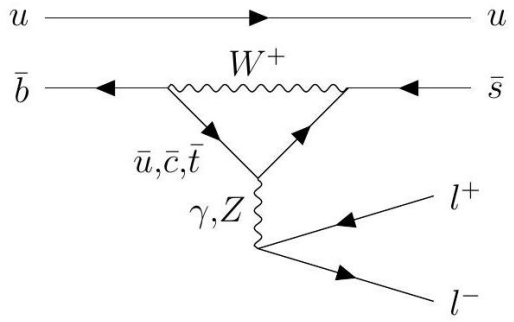
$$g_{\text{theory}} = 2.00233183602$$

while the experimental result is

$$g_{\text{expt}} = 2.00233184122$$

As you can see that, by the time you get to the 9^{th} decimal place, things don't quite match. In any other area of science, you wouldn't care less about a discrepancy in the 9^{th} decimal place. But here it matters. Taken seriously, the deviation between theory and experiment is at the level of 4.2 sigma. Optimistically, this discrepancy might be pointing to extra corrections to g_{expt} , beyond those of the Standard Model. However, there are reasons to be cautious. In particular, the theoretical result involves very difficult numerical simulations to determine contributions from the hadrons and there is some controversy over the accuracy of these results.

There are a number of further niggles too. In nuclear physics, the lifetime of the neutron seems to be slightly different depending on the way in which its measured. In particle physics, a collection of results around B-mesons seem to be slightly discrepant from Standard Model predictions, hinting that electrons, muons and tau leptons may differ in their interactions. The most prominent of these comes from looking at the decays of B-mesons to kaons and a lepton-anti-lepton pair, through a diagram like the following:



These are known as penguin diagrams. (As with the constellations, to see the resemblance you have to squint and reach into the depths of your imagination, before giving up and wondering what these people were smoking. I like to think of the lepton pair as the penguin's beak, but apparently they're the legs.) The quark running in the loop is either (anti) up, charm, or top, while the neutral boson is either a photon or Z. Finally, the end product is, in addition to the kaon, a lepton-anti-lepton pair where either $l = e$ or $l = \mu$.

Since the bottom quark is so heavy, the mass of the leptons is largely irrelevant. This is important because, if we ignore their mass difference, the electron and muon have identical couplings to the weak and electromagnetic forces, a fact that is sometimes called lepton universality. This means that the probability to decay to an electron should be the same as the probability to decay to a muon.

The best current measurements suggest that lepton universality is not respected in this decay: there is a preference to decay to electrons over muons. Taken at face value, it appears that this because something untoward is going on with muons, rather than electrons.

If these anomalies hold up to further analysis, then they are telling us something extremely important: the Standard Model needs replacing. They may, however, be due to random fluctuations and will disappear as the data improves. The B-meson results are currently 3.1 sigma from Standard Model expectations, somewhat short of the 5 sigma gold standard necessary to claim a discovery. At any given time in history there are always number of such mismatches

between theory and experiment. Since the Standard Model was put in place, they have nearly all evaporated upon closer inspection.

These anomalies not withstanding, the current state of affairs is that the Standard Model works extraordinarily well. You have to look very very hard - like the 9^{th} decimal place! - to find clear disagreement between experiment and theory. However, at the same time, it is overwhelmingly clear that the Standard Model is not the last
word in physics and the purpose of this chapter is to describe some of the questions that remain, together with some speculative suggestions for how they may be resolved.

These issues fall into different categories. First, there are a number of unexplained aspects of the Standard Model itself, and these will be described in Section 5.1. Moreover, there is one part of physics that the Standard Model ignores completely: gravity. We will describe how this fits in to the bigger picture in Section 5.2. Finally, if you want some incontrovertible observational evidence that there are things not described by the Standard Model, then we should turn to heavens. In Section 5.3 we describe some of the many puzzles that come from cosmology.

4.5.1 5.1 Beyond the Standard Model

Nearly all the unanswered questions about the Standard Model come from looking more closely at the various constants of Nature and asking why they take the particular values that they do. Here the "constants of Nature" are the parameters that we input into the Standard Model.

For some of these parameters, our understanding is as good as it could possibly be. As explained in Section 4.1.3, the electric charges (or, equivalently, the hypercharges) of the various fermions simply can't be any other way. They are fixed to their values by the stringent requirements of quantum anomaly cancellation. What we would love is to have a similar level of understanding for the other parameters of the Standard Model. Sadly, as we will see, we are a long way from that.

So what are these parameters? Roughly speaking, they fall into three classes (although one could certainly make a more refined classification, especially for the third class). These are:

- Three constants that specify the strengths of the three forces. These are the fine structure constant and its counterpart for the strong and weak force. We'll discuss these in Section 5.1.1.

- Two parameters that specify the Higgs potential. These can be thought of as the mass and expectation value of the Higgs boson. We'll discuss the issues surrounding these in Section 5.1.2.

- Loads of parameters that specify the way the Higgs field interacts with various fermions, usually referred to as the flavour sector. These are the topic of Section 5.1.3.

For quarks, the parameters are six masses (or, equivalently, Yukawa couplings) and a further ten mixing angles that sit in the CKM matrix. (These ten then split further into 9 mixing angles and the phase that gives CP violation.) There is, in addition, one further parameter known as the QCD theta angle that we haven't yet mentioned because, as far as we can tell, it is zero. Nonetheless, zero is a number too and it deserves an explanation.

For leptons the counting is a little more fuzzy. If the neutrinos get a Dirac mass, so that $B - L$ symmetry is preserved, then we again have six masses, or Yukawa, parameters and ten mixing angles in the PMNS matrix. If, however, neutrinos have a component that is a Majorana mass then there are additional parameters (and phases) to specify.

We'll now look at each of these classes of parameters in turn.

5.1.1 Unification

Perhaps the most important fact about all the constants of Nature is that they are very poorly named. They are not constant. Instead, the phenomenon of renormalisation means that the "constants" depend on the energy scale at which you do your experiment. We described this in some detail back in Section 2.3, and again in Section 3.1, when we explained how the fine structure constant, and its counterpart for the strong force, change with energy.

The energy dependence of coupling constants brings important clues when we come to better understand their origin. In particular, we understand well how the coupling constants vary on scales that we've tested - say, up to 10^3GeV. But we could then extrapolate to further energies. Of course, we don't know what lies ahead at further energies, but to get the ball rolling we could simply assume that there's nothing other than the Standard Model, and then see what we find.

What we find is extremely interesting and shown in Figure 50. First let's explain what we're looking at. The forces of the Standard Model are summarised by $U(1) \times SU(2) \times SU(3)$. Corresponding to each of these is a coupling constant α_i where $i = 1, 2, 3$. Note, in particular, that α_1 is the hypercharge coupling, rather than the fine structure constant of electromagnetism which emerges at low-energies from a combination of hypercharge and the weak force. On the horizontal axis is the energy, here called Q, plotted on a logarithmic scale. The part of the graph that we've measured experimentally is way over to the left, with $\log_{10}(Q/\text{GeV}) \lesssim 3$. Everything else is extrapolation.

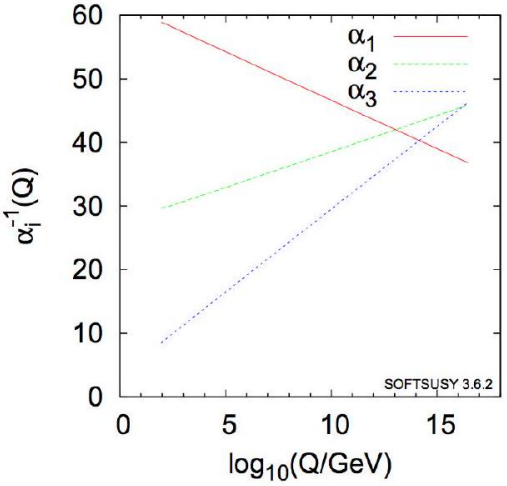


Figure 50. The running of the coupling constants. α_1 is hypercharge; α_2 the weak force and α_3 the strong force. This plot was made by Ben Allanach and taken from the PDG review of GUTs.}

On the vertical axis of Figure 50 is the inverse coupling, α_i^{-1}. The red line decreases with energy, while both the blue and green lines increase. This is telling us that α_1 increases with energy, while both α_2 and α_3 decrease, and this is the expected behaviour given our discussion of asymptotic freedom in Section 3.1.

The most striking aspect of the plot is the way the three lines cluster together as we approach higher energies. Obviously, they don't precisely meet, but nonetheless they lie in the same ballpark. This would appear to be hinting that the three forces are not as different as they appear in our world: perhaps, at a much higher energy scale, they are all unified as one. This idea is know as grand unification. The weak and strong forces meet at a scale

$$M_{\text{GUT}} \approx 10^{16}\text{GeV}$$

which is known as the grand unified scale. At this point, the three coupling constants all converge on a value somewhere around

$$\alpha_{\rm GUT} \approx \frac{1}{40}$$

Even the location of this almost-meeting is important. First, $\alpha_{\rm GUT}$ is nice and small at this point, telling us that the calculation to extrapolate the lines is at least consistent. Second, the scale $M_{\rm GUT}$ lies just below another important scale in nature, namely the

Planck scale

$$M_{\rm pl} \approx 10^{18}{\rm GeV}$$

(This is sometimes referred to as the reduced Planck scale to distinguish it from another contender that differs by a factor of $\sqrt{8\pi}$ and so is closer to 10^{19}GeV.) The Planck scale $M_{\rm pl}$ is where the effects of gravity become important in the quantum regime. We'll have more to say about this later. For now we just mention that the fact $M_{\rm GUT} < M_{\rm pl}$ is important. Had it turned out to be the other way round, then there would be no reason to think that $M_{\rm GUT}$ is interesting: it is a scale that was derived by neglecting the effect of gravity, and that's only an acceptable thing to do at energies less than $M_{\rm pl}$.

If we take the existence of three lines not-quite meeting as evidence of unification, what can we do about it? Is it possible to write down a grand unified theory, or GUT, in which the three forces are unified? The answer is yes. In fact, in many ways the Standard Model is just crying out to be packaged into something simpler! Recall that the mathematical way of describing the three forces is as

$$G_{\rm SM} = SU(3) \times SU(2) \times U(1)$$

where each of these can be roughly thought of as electric and magnetic fields whose individual elements are themselves matrices: 3×3 for the strong force, 2×2 for the weak force and just usual numbers for $U(1)$ hypercharge. But all of these can be packaged nicely inside a bigger matrix. (Or, more precisely, a bigger group.) For example, you can put all of them inside a 5×5 matrix with

$$G_{\rm GUT} = SU(5)$$

Alternatively, they can be packaged into a 10×10 matrix, but where the matrix is now based on real numbers rather than complex numbers

$$G_{\rm GUT} = SO(10)$$

Other options are also available.

In all of these cases, there are new gauge bosons that come as part of the unified force. These are usually called X-bosons, in analogy with the W and Z bosons of the weak force. There are also new scalar fields that condense, giving rise to a Higgs-like mechanism. Unlike the Higgs mechanism of the weak force, this conjectural GUTHiggs should get an expectation value at scale of around $M_{\rm GUT}$. Correspondingly, the X -bosons are heavy with a mass also somewhere in the vicinity of $M_{\rm GUT}$. Needless to say, we would not expect to discover such X-bosons in collider experiments any time soon.

It's not just the forces which have to unify. The matter particles and their other interactions must too. Here too things start off looking rosy. Recall that, including the count over colours, there are 16 fermions in one generation of the Standard Model. It must be possible to package these into the groups mentioned above that unify the forces. (Mathematically, we're looking for representations of $SU(5)$ or $SO(10)$ and these come only in special numbers, special like

the 8 and 10 of the eightfold way are special.) It turns out that the particles of the Standard Model are tailor made to be put together in this way. It seems like everything fits like a glove.

Interestingly, for $SU(5)$ GUTs, the right-handed neutrino remains an outsider, not coupling directly to the forces. Meanwhile, for $SO(10)$ GUTs, the right-handed neutrino also is brought into the fold and, at least at the fundamental level, sits on the same footing as all the other particles.

So far, so good. The last part of grand unified theories is to find a way that the flavour sector drops out nicely, with the Yukawa terms and mixing matrices all falling into place. Here things are less rosy. It's possible, but it's not pretty, typically involving the introduction of yet further fields put together in a fairly baroque way. As with so many other things in the Standard Model, the flavour sector is the one we understand least.

Tweaking the Lines

The coupling constants in Figure 50 get close, but fail to actually meet. However, this plot was made under the assumption that there's nothing new to be found between the energy 10^3GeV that we've probed experimentally and the GUT scale 10^{16}GeV. And that seems unlikely.

If there are new particles to be found, then they contribute to the renormalisation of coupling constants and so change the way the lines run. One obvious suggestion is that these new particles may correct the lines in such a way that they do, in fact, meet after all.

For this to happen, the new particles shouldn't be too heavy otherwise they come in too late to make a difference. One possibility that has been greatly studied is a theory called supersymmetry. We'll say more about this in Section 5.1.2, but for now we'll simply mention that we introduce a bunch of new particles at, say 5×10^3GeV. This tweaks the running of the couplings, to give the result shown in Figure 51. And ...ta-da. The lines now meet perfectly.

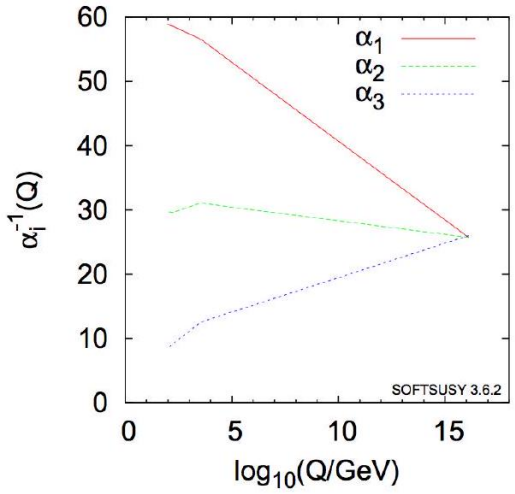


Figure 51. The running of the coupling constants if new supersymmetric particles exist at a low mass. This plot was made by Ben Allanach and taken from the PDG review of GUTs.

However, there's a major problem with this particular supersymmetric scenario. The new particles are so light that some hint of them should have shown up at the LHC by now. They haven't. It's possible to write down theories where supersymmetry still does the job of unification while just evading detection but they look increasingly unlikely.

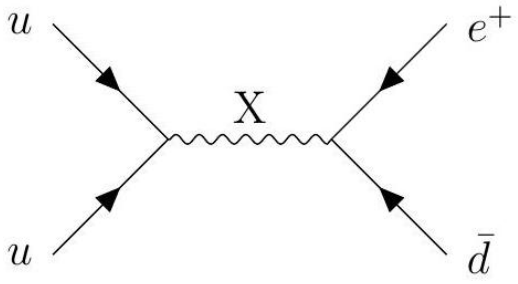
Nonetheless, the idea that there may be further particles out there which point clearly to unification is a tantalising one, and the convergence of the three coupling constants remains one of the major clues we have about physics beyond the Standard Model.

Proton Decay

Although the grand unification scale $M_{\rm GUT}$ is way beyond what we can study experimentally, the idea of grand unification still gives an observable consequence. That is proton decay.

We already discussed proton decay in Section 4.3.5 in the context of the conservation laws. Recall that, within the Standard Model the proton should be absolutely stable. There is a rather exotic process - known as electroweak instantons - that allow three baryons to decay to three leptons but this has never been observed and is unlikely to be any time soon given that calculations give a lifetime of around 10^{173} for a helium nucleus!

However, proton decay is necessarily a consequence of any grand unified theory. This is because the X-bosons gives rise to a Feynman diagram like those of weak decays, but now linking quarks and leptons like so



where, in this example, the X -boson carries electric charge +4/3. The $\bar{d}$ quark then combines with the d quark in the proton to form a pion, hence $p \to e^+ + \pi^0$.

Because the mass of the X-boson is so large, the lifetime of the proton is long. But not all that long! Most GUTs predict a lifetime between 10^{31} and 10^{36} years. Current experimental bounds tell us that the proton lifetime is longer than 10^{34} years, already ruling out the simplest GUTs.

Magnetic Monopoles

All magnets are dipoles, with a north pole and a south pole. Cut a magnet in two, and you'll end up with two dipoles. It's impossible to get, say, a single north pole on its own. If one could find such an object - known as a magnetic monopole - it would have a distinctive radial magnetic field of the form

$$\mathbf{B} = \frac{g}{4\pi}\frac{\hat{\mathbf{r}}}{r^2} \tag{5.1}$$

where g is the magnetic charge.

At first glance, there seems to be little reason to think that magnetic monopoles exist. Indeed, there is even a law of physics that forbids monopoles! One of the Maxwell equations (2.3), governing the theory of electromagnetism, reads

$$\nabla \cdot \mathbf{B} = 0 \tag{5.2}$$

and its sole purpose is to disallow any solution of the form (5.1).

This makes it somewhat surprising that, as the laws of physics evolve beyond electromagnetism, magnetic monopoles re-emerge as one of the most likely candidates for new particles, finding interesting and creative ways to evade the seemingly insurmountable obstacle (5.2). By the time we get to grand unified theories, monopoles become obligatory, appearing as an entirely novel kind of particle known as a soliton. The mass of these magnetic monopoles is

$$M_{\rm monopole} \approx \frac{M_{\rm GUT}}{\alpha_{\rm GUT}}$$

putting them somewhere in the range of 10^{17}GeV, well out of reach of current colliders.

Unlike all heavier particles that we've discussed in these lectures, monopoles would be completely stable. Ironically the same Maxwell equations which once seemed to forbid magnetic monopoles, now forbids them from decaying since they imply the conservation of magnetic charge. Monopoles can only vanish by annihilating with anti-monopoles. This leaves open the possibility that we may, once again, turn to the skies and search for monopoles among cosmic rays. So far, none have been found [18].

It's not just GUTs that give rise to magnetic monopoles. Instead, pretty much any theory that goes beyond the Standard Model will contain magnetic monopoles. They are one of the very few robust predictions for new physics. If you want to learn more about monopoles then you've come to the right place. You can read about their subtle interplay with quantum mechanics in the lectures on Solid State Physics, about their role in quantum field theory in the lectures on Gauge Theory, and about some of their more mathematical aspects in the lectures on Solitons.

5.1.2 The Higgs Potential

Our next pair of parameters are associated to the Higgs potential. Recall from Section 4.2.1 that the Higgs potential $V(\phi)$ determines whether the Higgs boson condenses. In the Standard Model, it takes the very simple form

$$V(\phi) = a|\phi|^2 + b|\phi|^4 \tag{5.3}$$

The two fundamental parameters are a and b.
If $a > 0$ and $b > 0$ then it looks like the graph on the left-hand side of Figure 52. If $a < 0$ and $b > 0$ then it looks like the right-hand side of Figure 52. (If both a and b are less than zero then the potential has no minimum and the Higgs scalar runs away to infinity unless we include further terms of higher powers like $|\phi|^6$.)

As we've seen, the Standard Model has a potential with the shape on the right, meaning that $a < 0$ and $b > 0$. The values of a and b determine both the mass of the Higgs boson m_H and the Higgs expectation value $\langle\phi\rangle$. Roughly speaking, the relationship between these two scales and the parameters in the potential is

$$m_H^2 = |a| \quad \text{and} \quad \langle\phi\rangle^2 = \frac{a}{2b} \tag{5.4}$$

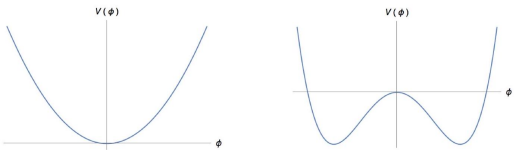


Figure 52. Two possible shapes for the Higgs potential for a scalar field. With $a, b < 0$ we get the shape on the left; with $a < 0$ and $b > 0$ we get the shape on the right.

Much of this section will be devoted to explaining further what the words "roughly speaking" in the previous sentence actually mean. For now, we'll just roll with the equations above and see what they tell us. Experimentally, we know that

[18] A more correct statement is that exactly one has been found! On Valentine's day, 1982, a single event consistent with a magnetic monopole was observed. Nothing similar has been seen since. Given the importance of replicating scientific results, it's difficult to view this as anything more than a tantalising footnote (literally here) in the story of the monopole

$$m_H \approx 125\text{GeV} \text{ and } \langle\phi\rangle \approx 246\text{GeV}$$

This means that the parameters in the potential must take the values

$$a \approx -(125)^2\text{GeV}^2 \quad \text{and} \quad b \approx 0.13$$

For now, the important point to note is that a has dimension of energy-squared, while b is dimensionless. Our interest here lies in a. This is the scale of the Higgs sector which, through Yukawa interactions subsequently sets the mass of all the elementary fermions.

As we've stressed earlier in these lectures, most of the mass of the proton and other hadrons doesn't come from the Higgs sector, but instead from $\Lambda_{\rm QCD} \approx 200$MeV. But this sits on a different footing because $\Lambda_{\rm QCD}$ was, itself, a derived scale: it is the energy at which the dimensionless coupling of the strong force becomes $\alpha_s \approx 1$. This means that $\Lambda_{\rm QCD}$ should be thought of as an emergent energy scale.

In contrast, there is no such story for $\sqrt{|a|} = m_H$. This is an absolute energy scale. In fact, rather remarkably, it is the only fundamental parameter of the Standard Model that is not dimensionless! As we now explain, this means that it comes with certain baggage.

The Higgs Mass

Now we come to the crux of the matter, one that revolves around the "rough speaking" that lead us to the equations (5.4). To understand what the issue is, we need to think a little more deeply about the kind of parameters that make sense in a fundamental theory and how these change at various energy scales due to renormalisation.

To set the scene, I'll introduce some analogies. To this end, here are three objects that should not be viewed as a "fundamental parameters" in a theory.

There sits, in a vault in Paris, a platinum-iridium cylinder that, until 2019, was used as the definition of the kilogram. Clearly it would be ludicrous to take the mass of this object as any kind of input in a fundamental theory of Nature. Even putting aside the facts that the kilogram is very much a human construct, and that the mass of the cylinder is changing over time as it slowly erodes, it is simply silly to think that a huge, complicated object with roughly 10^{24} constituent particles should be important on the tiny distance scales at which our fundamental theory of physics is defined.

This latter criticism can also be levelled at other objects which, at first glance, might appear to be more suitable candidates for fundamental parameters. For example, for many decades the mass of the proton was thought to be a fundamental scale in nature. Of course, we now know that the proton, like the Parisian cylinder, is a horribly complicated object. In particular, the mass of the three valence quarks - two up and a down - contribute a negligible amount to the total mass of the proton. The full mass is often attributed to collection of gluons and sea of quark-anti-quark pairs but, for the purposes of this analogy, we will be better served if we remember what this really means: the mass comes from the wild thrashing of the quantum fields that are excited in complicated ways inside the proton. The mass of the proton is in the ballpark of a few times $\Lambda_{\rm QCD}$ but its exact value is something emergent that depends on lots of messy dynamical processes. For this reason, the mass of the proton is, like the Parisian cylinder, an emergent scale. Neither are good candidates for parameters in a fundamental theory.

And this brings us to our third example of an object which is not a good candidate for a fundamental parameter. This is the mass of the Higgs boson!

Quantum fluctuations mean that, even though the Higgs boson is a fundamental particle, its mass depends on all sorts of complicated and messy dynamics and is ultimately determined, like the mass of the proton, by the behaviour of other quantum fields. In particular, if the fundamental theory has a parameter like a in the potential

(5.3), then its relationship to the mass m_H of the Higgs boson is nothing like as simple as the $m_H^2 = |a|$ equation that we used above. Instead the relationship between the two is much more complicated.

To understand what's going on, first recall our discussion of renormalisation in Section 2.3. There we learned that all parameters in a quantum field theory depend on the distance scale or, equivalently, the energy scale at which an experiment takes place. Moreover, we stressed that all quantum field theories should come with a health warning: there is a minimum distance scale, or maximum energy scale, beyond which they shouldn't be used. This energy scale is called the UV cut-off and we will denote it as Λ_{UV}.

You should think of the UV cut-off as the energy scale at which a given quantum field theory is defined. When you specify the parameters of the theory, you should specify their value at the scale of the cut-off. This is really just the statement of reductionism in physics: small things determine the behaviour of larger things, and a fundamental theory should be defined on the smallest distance scale at which it applies. As you then look at lower energies - or longer distances - you can use renormalisation to figure out how these parameters change.

Now let's return to the Standard Model. It definitely works up to energy scales of 1 TeV so let's be pessimistic and, with the expectation that the Standard Model will cease to give the right answers very soon, take the cut-off to be $\Lambda_{UV} = 1\text{TeV}$. That means that we take the Standard Model to correctly describe the dynamics of quantum fields down to distance scales as small as 10^{-19} m. The fields may well have fluctuations on scales much smaller than that, but we will just admit ignorance about these and proceed.

What now happens if we put a Higgs boson into the mix. Naively the mass of the Higgs boson is given by the formula that we used previously: $m_H = \sqrt{|a|}$. But the Higgs then gets surrounded by a swarm of quantum fluctuations and these change the mass. The upshot is that if a is the fundamental parameter of the theory, then the mass of the Higgs boson that we measure is actually something like

$$m_H^2 \approx \left| a + \mathcal{O}\left(\Lambda_{\rm UV}^2\right) \right| \tag{5.5}$$

where the $\mathcal{O}\left(\Lambda_{\rm UV}^2\right)$ means a contribution that is roughly around $\Lambda_{\rm UV}^2$, but where the exact coefficient (including its sign) depends on the nature and dynamics of all the other fields.

Here's a rather nice analogy. Take a ping pong ball and submerse it in water. What's its mass? According to the International Table Tennis Federation, a ping pong ball should have a mass of exactly 2.7 grams. But the federation rarely promotes matches that take place underwater and there is no suggestion on their website that they understand renormalisation. You can use Newton's equation $F = ma$ to experimentally determine the mass of a ping pong ball in water: just apply a force and measure the acceleration. You'll find that the ping pong ball appears to be roughly 11 times heavier than in air, so closer to 30 g . The reason for this is intuitively simple: when the ping pong ball moves in water, it drags a body of fluid with it. This increases its inertial mass.

This same effect is at play for the Higgs boson. Its mass gets a contribution from the fluctuations of all other quantum fields. This additional contribution is of order $\Lambda_{\rm UV}$ which is much larger than the mass that we actually observe.

What are the consequences of this? The formula (5.5) tells us that the fundamental parameter a in the Higgs potential is not equal to the mass of the Higgs boson. Instead, it too must be something on the scale of the UV cut-off $\Lambda_{\rm UV}$. We call the parameter a the bare mass (squared), while m_H is physical mass of the Higgs boson that we observe. To get the observed physical mass $m_H \approx 125\text{GeV}$ we must add two contributions, a and $\Lambda_{\rm UV}$, both of the same order of magnitude, which then cancel out to leave behind the physical mass.

So what? Well, if we take the cut-off of the Standard Model to be $\Lambda_{\rm UV} \approx 10^3\text{GeV}$, then this seems eminently reasonable. We're just adding two numbers, both of order 1000, to get

something of order 100.

But what if the Standard Model holds to higher energy scales? Suppose that it is trustworthy to energies of order $\Lambda_{UV} \approx 10^4$GeV. Now we add two numbers of order 10,000 to get something left behind that's order 100. Still not preposterous, but you might start to feel a little uneasy.

And what if we really push things? Suppose that the Standard Model actually holds all the way up to the GUT scale of $\Lambda_{UV} \approx M_{\rm GUT} \approx 10^{16}$GeV. Now we must take the fundamental parameter in the Higgs potential to be $a \approx (10^{16}\text{GeV})^2$ so that this cancels almost precisely the contribution from the quantum fluctuations, leaving behind a measly Higgs boson mass of 125 GeV . If you were to change a by just one part in a billion, you would end up with a Higgs boson mass that is 5 orders of magnitude higher than we observe! By this stage, the situation appears to be ridiculously untenable

We have a bunch of different names for this state of affairs. We say that the parameter a in the Higgs potential should be finely tuned. It's a good name and describes the issue well. Alternatively, we say that the Higgs mass m_H that we observe is unnatural; the quantum fluctuations want to push the mass to higher and higher energy scales, but this is cancelled - to what may feel like unreasonable accuracy - by the contribution from the bare mass. This seems to be a less useful name as it's hard to see how something in nature can be unnatural. But it does at least stress how jarring the situation is.

This whole set of ideas also goes under the umbrella of the hierarchy problem. Why is there a large hierarchy of scales between the Higgs mass and the UV cut-off, when theory suggests that they should be the same order of magnitude?

Recall that the UV cut-off $\Lambda_{\rm UV}$ is really an expression of our ignorance: we confess that our quantum field theory - in this case the Standard Model - is incomplete and does not include relevant physics at energies beyond $\Lambda_{\rm UV}$. The hierarchy problem is really the statement that the mass of the Higgs boson is pushed by quantum corrections to whatever is the highest mass scale in the game. Yet, somehow, the observed mass remains happily at 125 GeV .

The hierarchy problem in this brutal form is only a problem for the parameter a in the Higgs potential. All other parameters in the Standard Model are dimensionless and do not suffer the same fate. They change only very mildly (logarithmically to be precise) under renormalisation. It is only the Higgs mass that is so very sensitive to physics at higher energy scales.

Solutions to the Hierarchy Problem

The hierarchy problem motivated an enormous amount of research in the 1980's, 90 's and early 2000's. The favoured explanation was the obvious one: keep the UV cut-off $\Lambda_{\rm UV}$ low enough that you don't need to invoke a silly level of fine-tuning. But this, in turn, means that there should be some new physics, invalidating the Standard Model, that comes in at some low scale, like a few TeV .

This new physics can't just be anything. Add a few new particles at the TeV scale and you'll see that they just make the problem worse, adding yet more quantum fluctuations that increase the mass of the Higgs boson. Instead, you must find a way to add some new fields to the Standard Model that stabilise the mass of the Higgs somewhere in near 100 GeV , solving the problem once and for all. There are a number of ways to achieve this. Here I describe some, roughly in descending order of popularity.

- Supersymmetry: This is a proposed, novel symmetry of Nature in which every bosonic field has a fermionic counterpart, and vice versa, with each boson/fermion pair experiencing the same forces.

Clearly, we don't see supersymmetry among the particles that we know. The idea is that supersymmetry is, like many symmetries, broken so that the additional fields - so called superpartners - only appear when we reach some new mass scale, say a few TeV .

There are a number of reasons to be enamoured of supersymmetry. First, it solves the hierarchy problem by dint of the fact that bosons and fermions contribute with opposite signs to the mass of the Higgs, ensuring that all quantum fluctuations cancel above the supersymmetry scale. Second, as we saw previously, the presence of supersymmetry causes the three coupling constants to meet perfectly at the unification scale. Moreover, there are reasons to think that supersymmetry may be an important ingredient in quantum gravity, which would mean that it should certainly be present by the time we get to the Planck scale. All in all, TeV scale supersymmetry leads to a nice, comforting story.

- Technicolour: The Standard Model contains just one other mass scale, $\Lambda_{\rm QCD}$. But, as we described above, this is associated to the strong coupling dynamics of QCD and so doesn't suffer from a hierarchy problem. Perhaps the mass of the Higgs emerges in a similar way.
  In such scenarios, the Higgs particle is not fundamental at all, but rather appears as a composite of two, new fermions, bound together into a meson by a new force called, in analogy with strong force, technicolour.

- Something Else: There are quite alternative proposals. Among them is the idea that Higgs as a (pseudo)-Nambu-Goldstone boson (I won't explain what this means!) or, more creative suggestions, such as extra dimensions of space which manage to dilute quantum corrections at the TeV scale.

Each of these ideas provides a viable solution to the hierarchy problem, but only by introducing some observable deviation from the Standard Model at the TeV scale. But now we have a collider - the LHC - that can reach these scales. And nothing is seen. The Higgs boson appears, as far as we can tell, as a genuinely elementary particle and there is, as yet, no hint of new particles that could stabilise its mass. This makes it increasingly unlikely that any of the "natural" solutions described above are implemented in Nature. Of course, it's certainly possible that, say, supersymmetry is still out there, but just pushed up to a higher scale, with an accompanying need
for some amount of fine tuning to the Higgs mass. But the motivation starts to look increasingly shaky.

So what are we to make of this? Admittedly, the hierarchy problem has a different flavour from other major open problems in physics. Is there really anything wrong with just stating that the parameter a is (to give an extreme example) defined at the GUT scale $\Lambda_{\rm UV} = M_{\rm GUT}$ and fine tuned to 15 significant figures so that it perfectly cancels out the contributions to the Higgs mass from quantum fluctuations of order $\Lambda_{\rm UV}$? It certainly seems odd, but perhaps that's just the way it is.

We can look elsewhere in physics to get some guidance. In particular, quantum field theory isn't just useful for particle physics: it is the right language to describe large swathes of solid state physics (also known as condensed matter physics), which is the study of how various materials behave. This arena provides many hundreds, if not thousands, of examples of quantum field theories (or, relatedly, statistical field theories) where we can test our logic. In that framework, we can ask: do we find quantum materials where we have light scalar excitations, like the Higgs boson? Here "light" means with a mass significantly smaller than the UV cut-off which, in solid state physics, is usually supplied by the underlying lattice of the material.

The answer to this question is a resounding no! Or, stated more accurately, within the realm of solid state physics if there is a light scalar excitation then there is always a good reason behind it. These reasons are often similar to the ones invoked for the hierarchy problem, like the scalar is really made of two underling fermions, or it is a (pseudo)-Nambu-Goldstone boson. (I still won't explain what this last phrase means.) The upshot is that in other realms

where quantum field theory is useful, the logic of naturalness is a very good guide: if you see a scalar field that is unnaturally light, then you should search for an explanation because it will tell you something important and interesting about the system.

At the risk of belabouring this point with a long detour, there is one particular condensed matter system that is worth looking at more closely. This is superconductivity which, as we already mentioned in Section 4.2.1, has a mathematical description that is almost identical to that of the Higgs boson. Usefully, the hierarchy problem also makes an appearance in superconductors, although it's not in the guise of a light scalar field but, as I now explain, something more subtle. As you cool a metal, it undergoes a phase transition to become a superconductor. This happens at the critical temperature T_c which is typically a few degrees Kelvin. The phase transition happens discontinuously, meaning that the metal changes abruptly to a superconductor just like water
changes abruptly to ice. This is sometimes called a first order phase transition. But theoretical expectations tell us that the phase transition should be smooth and continuous, what's called a second order phase transition. This isn't seen in experiment because it turns out that you have to tune the temperature T to ridiculous accuracy before you notice that the transition is actually continuous, something like

$$\frac{T - T_c}{T_c} \approx 10^{-9}$$

Why would you have to tune the temperature so close to T_c before you can see the real physics of the second order phase transition? It's a very unusual state of affairs and in most other systems you only need $(T - T_c)/T_c \approx 1$ before you can see the true nature of the phase transition. The fine-tuning of temperature needed for a superconductor turns out to be entirely analogous to that of the lightness of the Higgs boson. The 10^{-9} accuracy is a small number and deserves an explanation. And, in this case, there is a very good explanation: the would-be Higgs boson in a superconductor is composed of two electrons bound together at an energy scale which emerges mathematically in a manner that is similar to way $\Lambda_{\rm QCD}$ emerges in the strong force. You can trace the existence of the small number 10^{-9} to this underlying dynamics. It's an explanation that is close in spirit to the technicolour proposal for the Higgs boson. But, as far as we can tell, the same story is not what's going on for the Higgs. (If you want more details about the relationship between phase transitions and renormalisation group, you can read about it in the lectures on Statistical Field Theory.)

All of this is to say that our experience with quantum field theory tells us that we should be nervous about the fine-tuning underlying the Higgs. Still, there is a vast difference between meV scale at which effective quantum field theories in condensed matter are valid, and the TeV scale or higher of particle physics. And Nature seems to be telling us very clearly that there is nothing wrong with fine tuning at these very high energy scales, even though it flies in the face of how we understand quantum field theory. It seems to me, and many others, that this is a problem one should take seriously because it tells us that we're not thinking about quantum field theory in the right way. But I don't know a better one!

There is one last word on this. The word is anthropic. It gives me a slight shudder just thinking about it so I'm going to postpone further discussion to Section 5.3.1.

5.1.3 A Bit of Flavour and Strong CP

In the late 1800 's, one of the great unsolved mysteries was the spectrum of hydrogen. Only a few lines were known when, in 1885, Balmer noted that their wavelength λ
could be fitted to the remarkably simple formula

$$\lambda \approx 10^{-7} \left(\frac{1}{4} - \frac{1}{n_2^2} \right)^{-1} \text{ m}$$

with $n_2 = 3, 4, 5, 6$. Three years later, Rydberg generalised this to the formula

$$\lambda \approx 10^{-7} \left(\frac{1}{n_1^2} - \frac{1}{n_2^2} \right)^{-1} \text{ m}$$

with n_1 and n_2 both integers. (The simplest $n_1 = 1$ lines lie in the ultra-violet and took another 20 years to discover.)

The Balmer formula provides one of the rare examples in science where fitting data, with no understanding of the underlying physics, gives a strong hint of something important underneath. Indeed, the presence of integers in Balmer's formula foreshadowed one of the greatest paradigm shifts in science: the need for quantum mechanics. Ironically, Bohr would later claim that he had completely forgotten about the Balmer formula when he constructed his quantum model of the atom, and only later realised that the two matched perfectly!

If you were to wonder what collection of today's unexplained experimental data has the best chance of a Balmer-like breakthrough, the answer is obvious: it is everything to do with flavour. There are a few dozen parameters that describe the masses and mixing angles of three generations of quarks and leptons. There are clear patterns among them but, so far, we have little idea what those patterns are telling us.

It is not for want of trying. There are many theories that have tried to explain what's observed, many of them revolving around some kind of new, approximate symmetry, sometimes referred to as family symmetries. Some of these theories are pretty(ish), some baroque. None of them are overwhelmingly compelling, in large part because there are so many options available. For this reason, I won't describe any of these in detail.

The Strong CP Problem

There is, however, one parameter in the Standard Model that deserves special attention. It is a parameter of the strong force known as the QCD theta angle, or θ_{QCD}.

It is not so straightforward to describe, at the level of these lectures, how θ_{QCD} changes the dynamics of the strong force, not least because it is a quantum parameter, in the sense that it has no classical counterpart at all. If you want all the gory details, you can read about theta angles in the lectures on Gauge Theory.

The main reason that the QCD theta angle is interesting is that it doesn't exist! As far as we can tell, $\theta_{\text{QCD}} = 0$. Strictly our best experimental bound is

$$\theta_{\text{QCD}} < 10^{-10}$$

There are a few questions to unpack here.
First, why should we care about something that doesn't exist?! The point is that the Standard Model is a remarkably restrictive framework. We can't just write down random interactions willy nilly. There are only very special interactions that are allowed, and each of them comes with a parameter. The game that we play is to write down all possible interactions and then determine their associated parameter by experiment. This is what leads us to the couple of dozen parameters or so listed at the beginning of this section. The theta angle is special because it is the only one of these parameters that appears to vanish. And that is crying out for an explanation.

Next: what would the consequences be if θ_{QCD} were not to vanish? It turns out that this is the one opportunity for the strong force to violate the symmetries of parity P , charge conjugation C and time reversal T .

Recall from Section 4.3.4 that weak force respects neither parity nor CP but, as far as we can tell, both are respected by the strong force and electromagnetism. In a world where $\theta_{\rm QCD} \neq 0$, the strong force would also break these symmetries. It does so by endowing the neutron with an electric dipole moment. This means that although the neutron is neutral, the distribution of the quarks inside would be shifted slightly so that one side of the neutron is slightly positively charged with a compensating negative charge on the other side. This means that the neutron carries a little arrow, pointing in the direction of the charge imbalance. This is in addition to another arrow, pointing in the direction in which the neutron spins and it turns out that these two arrows are either aligned or anti-aligned. When one acts with parity, or charge conjugation, or time reversal, one of the arrows flips, while the other does not. This means that these symmetries are broken since, for example, the neutron appears different when viewed in a mirror.

Although all three symmetries are broken when $\theta_{\rm QCD} \neq 0$, physicists tend to focus on CP . The unexplained fact that $\theta_{\rm QCD} = 0$ is known as the strong CP problem.

Before we turn to putative explanations for this problem, there is one final question I'd like to address. What does it have to do with flavour physics? The question of flavour is all about how fermions couple to the Higgs boson, while the strong CP
problem appears to be, as the name suggests, firmly in the camp of QCD. Here's where things get a little complicated because the story that I told above isn't entirely accurate.

The fuller truth is that in the Standard Model the masses of the six quarks are actually complex numbers rather than real numbers. Each has a magnitude and a phase

$$M_q = m_q e^{i\chi_q}$$

where the label q runs over the six different quarks. What we observe is the magnitude m_q. The complex phases χ_q have almost no effect on the physics. They do just one thing: they contribute to the QCD theta angle! In fact, what we measure is not the QCD theta angle directly, but rather

$$\bar{\theta} = \theta_{\rm QCD} + \sum_q \chi_q$$

It is this sum of angles that is observed experimentally to vanish: $\bar{\theta} = 0$. In other words, the strong CP problem involves both QCD and flavour physics, entwined in some interesting fashion.

There are a number of prospective solutions to the strong CP problem. Here I'll just mention one, which goes by the name of the Peccei-Quinn theory. The key idea is both simple and dramatic: one takes the parameter $\theta_{\rm QCD}$ and promotes it to a dynamical field.

This means that we no longer get to chose the value of $\theta_{\rm QCD}$. Instead its value can fluctuate. This is only progress if we can explain why we don't observe the fluctuations and why, moreover, the field prefers to sit at the value such that $\bar{\theta} = 0$.

The new field $\theta_{\rm QCD}$ is, like the Higgs boson, a scalar field and its preferred value will be set by some potential, analogous to the $V(\phi)$ potential that we saw before. Here there is a very nice story. It turns out that the rest of the Standard Model fields have something to say about this potential. In particular, the dynamics of the gluons generates a potential for $\theta_{\rm QCD}$. And this potential has the property that its minimum sits at the place where $\bar{\theta} = \theta_{\rm QCD} + \sum_q \chi_q = 0$. In other words, if $\theta_{\rm QCD}$ was dynamical, it would want to arrange itself so that there is no CP violation in the strong force. This, it would seem, is a very compelling solution to the strong CP problem.

What about the second issue? Now that $\theta_{\rm QCD}$ is dynamical, why do we not see its fluctuations? Here things are less rosy. First, it's not clear that the simple dynamical mechanism described above is really sufficient to set $\bar{\theta} = 0$ to one part in 10^{10} as required by experiment.

Second, with a new field comes a new particle which, in the case of $\theta_{\rm QCD}$ is referred to as the axion. There have been many decades of searches for the axion, with nothing yet seen. There are many further experiments underway, aiming to improve the bounds the axion mass and interaction strength or, in the dream scenario, actually find the thing!

While the Peccei-Quinn theory, and the accompanying axion, remains the most popular explanation for the strong CP problem, the lack of clear experimental support means that it is not the only game in town. Whatever the ultimate reason, the fact that the strong force prefers to respect the discrete symmetries of our world, even though it has a clear opportunity to violate them, is one of the key clues for physics beyond the Standard Model.

4.5.2 5.2 Gravity

There is one force that is obviously missing from the Standard Model. This is gravity, both the most obvious force at play in the world around us and yet, in many ways, the one we understand least.

There are two good reasons why gravity is not included in the Standard Model. The first is that the force of gravity is entirely inconsequential for anything to do with particle physics. To get some sense for this, we can look at the theory of gravity first written down by Newton. Any two objects, with masses m_1 and m_2, sitting a distance r apart, will feel a force

$$F_{\rm Newton} = \frac{Gm_1m_2}{r^2} \tag{5.6}$$

where G is Newton's gravitational constant

$$G \approx 6.67 \times 10^{-11}\ {\rm m}^3\ {\rm kg}^{-1}\ {\rm s}^{-2} \tag{5.7}$$

It is a remarkable fact that this takes exactly the same form as the Coulomb force between any two electrically charged objects that we met earlier in (2.4),

$$F_{\rm Coulomb} = \frac{Q_1Q_2}{4\pi\epsilon_0 r^2}$$

This gives us an opportunity to compare the strengths of gravity and electromagnetism on the subatomic scale. For example, a hydrogen atom consists of a single electron orbiting a proton, held in place by the Coulomb force. The size of the hydrogen atom is about 5×10^{-11} m, known as the Bohr radius. But there should also be atoms held together by the gravitational force. We could consider an electron orbiting a single neutron, held in place by Newton's force (5.6). The question is: how big would this gravitationally bound atom be?

The answer is pretty stunning: a gravitationally bound atom would have a size that is substantially larger than our observable universe. Gravity isn't just a little weaker than the other forces. It's much much weaker than the other forces. Another way of saying this is to take two electrons and compare their gravitational attraction to their Coulomb repulsion. The answer is

$$\frac{F_{\rm Newton}}{F_{\rm Coulomb}} \approx 10^{-43}$$

No one cares about the gravitational force acting on a single elementary particle. However, gravity has a trick up its sleeve. All the other forces of nature have both positive and negative charges which cause particles to attract into effectively neutral objects on small distance scales. This happens most dramatically for the strong force, where quarks are confined into protons and neutrons. It then happens again for electromagnetism where electrons and protons are bound into neutral atoms. This means that by the time you get to the macroscopic

world in which we live, these forces have done their job and their effects are no longer manifest. In contrast, there is no negative mass and so nothing to shield us from the effect of gravitation. As you pile more and more particles together, the Coulomb force becomes diluted, while the gravitational force only grows. This is why gravity is the force that seems to dominate our lives.

We do have a good understanding of why gravity is special in this way. The three forces in the Standard Model are associated to spin 1 fields. (The Higgs force, of course, is associated to a spin 0 field.) Gravity is unique because it is associated to a spin 2 field. And in contrast to all other forces, spin 2 fields can only have "positive charge", where the charge is what we call mass.

Spin 2 fields are, it turns out, special in many ways. While we could conceive of theories with many different spin 1 forces, that's not possible for spin 2 fields. There is just one way to introduce a fundamental spin 2 field into the laws of physics and it is utterly remarkable. The spin 2 field, it turns out, must be spacetime itself!

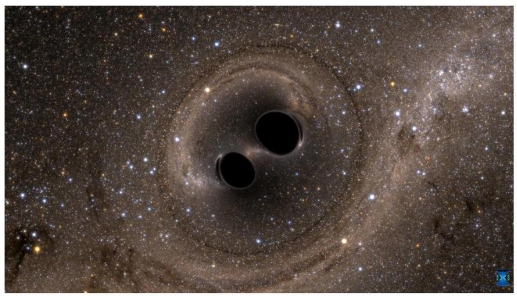
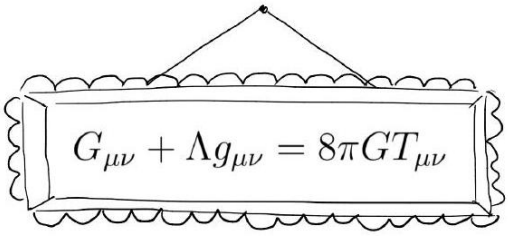


Figure 53. A computer simulation of two black holes, about to collide. The background field of stars is distorted by the curvature of spacetime in the vicinity of the black holes.

The connection between space, time and gravity is Einstein's great insight and the resulting theory goes by the name of General Relativity. It would take us too far from our main narrative to describe general relativity in any great detail, but if any equation deserves being placed in a picture frame, it is Einstein's:



This equation replaces Newton's gravitational force law (5.6). It relates the curvature of spacetime, captured in the $G_{\mu\nu}$ and $g_{\mu\nu}$ on the left-hand side, to the energy distribution of other fields, captured in the $T_{\mu\nu}$ on the right-hand side. There are two gravitational constants in the Einstein equations. The first is Newton's constant G, which retains its place as a fundamental constant of nature in general relativity. The second, Λ, is known as the cosmological constant. We will have more to say about this in Section 5.3.1.

The Einstein equations replicate the familiar results of Newton's force law, from apples falling from trees, to the orbits of the planets around the sun. But they do so much more besides. They tell us how light bends as it passes heavy objects, giving rise to the distortion of the background field of stars, how black holes form as the density of matter becomes too great, and how collisions of these black holes can cause detectable ripples of the spacetime continuum known as gravitational waves. Furthermore, the

Einstein equations provide, for the first time, a framework in which we can think about the dynamics of the entire universe, giving rise to the field of Cosmology. For any physics on the very largest scales, the Einstein equations hold sway.

5.2.1 Quantum Gravity

Above I said that there are two reasons that gravity is not included in the Standard Model. The first is that gravity is inconsequential for particle physics. The second is that we don't really know how to do it.

General relativity is a classical theory. It does not incorporate the effects of quantum mechanics. In contrast, everything else that we've described in these lectures is all about quantum mechanics. The question is: can we incorporate general relativity into the quantum world? This is the problem of quantum gravity.

It's usually stated that naive attempts to combine quantum mechanics and general relativity fail miserably. That's not quite true. Naive attempts to combine the two theories actually work very well. Up to a point. For example, any simple minded approach to quantum gravity clearly shows that, on some level, spacetime acts just like any other quantum field. Small fluctuations of spacetime are tied up into little knots by the framework of quantum mechanics, resulting in a new kind of massless particle known as a graviton. Just as light waves are made of many underlying photons, so too are gravitational waves made of gravitons.

We've never detected an individual graviton. Indeed, because gravity is so very weak we only succeeded in detecting gravitational waves in 2015. Building an experiment to see individual gravitons is not technologically feasible in the forseeable future. To put this in perspective, we first detected light when eyes evolved. Fossil records clearly show the existence of eyes in the Ediacaran period and from then it took something like 550 million years before we were able to detect the underlying photons. I'm not promising that it will take us a similar timescale to detect gravitons, but it's as good a guess as any.

Although it's something of an academic exercise, we can also compute Feynman diagrams for gravitons to see they interact with each other under the rules of quantum mechanics. Again, all is good, but now there's a catch. The calculations make sense provided that the energies of the gravitons are not too large.

We can actually anticipate the problem from the few facts that we know about gravity. The strength of the gravitational force is governed by Newton's constant (5.7). This is what plays the role of the fine structure constant in electromagnetism or
analogous quantities for the strong and weak force. Except there's a crucial difference: the strengths of all the other forces are governed by dimensionless numbers. In contrast, there's no way to get a dimensionless number out of Newton's constant. Instead, if we include some factors of $\hbar$ and c, we get a scale:

$$G = \frac{\hbar c}{8\pi M_{\rm pl}^2}$$

where $M_{\rm pl}$ is the Planck mass,

$$M_{\rm pl} \approx 10^{18}{\rm GeV}$$

This is telling us that the strength of the gravitational force depends strongly on the energy of the process. If two particles scatter with energy E, then gravitational effects will scale as

$$\text{Strength of Gravity } \sim \left(\frac{E}{M_{\rm pl}}\right)^2 \sim GE^2$$

In some sense, you knew this already. Newton's equation (5.6) tells us that the gravitational force between two objects scales as Gm_1m_2 which is just the formula above with the masses in place of the energy. This formula also gives another perspective on why gravitational forces are so weak in the world of particle physics, where our most powerful accelerators can reach energies of $E \sim 10^3$GeV, many orders of magnitude below the Planck scale.

This argument means that any naive theory of quantum gravity will give sensible answers providing that we look at energies $E \ll M_{\rm pl}$, where we can use Feynman diagrams and simple perturbation theory. But, as the energy increases to somewhere near the Planck scale, the gravitational interaction becomes strong and our Feynman diagram expansion ceases to work. In this simple minded approach, quantum gravity only becomes challenging when we reach energies close to the Planck scale. In technical, and slightly old-fashioned, terms general relativity is said to be non-renormalisable.

Before we proceed, it's worth thinking a little more about the size of the Planck scale. Back at the beginning of these lectures, I commented that the SI unit for energy, the Joule, is not particularly useful in the subatomic realm. Instead we define the much smaller unit of an electronvolt. But, by the time we get to the Planck scale, even the Joule is too small! We have

$$M_{\rm pl} \approx 10^9 \text{ J}$$

That's a seriously large amount of energy. It is, for example, greater than the kinetic energy of all the cars in a formula one race! In particle physics, when we talk about reaching a certain energy scale we really mean energy density. Physics at the Planck scale involves energies of $M_{\rm pl}$ squeezed into a region of size $L_{\rm pl}^3$, where $L_{\rm pl} \approx 10^{-34}$ m. These are silly numbers. There is, as we will see below, good reason to believe this is the highest energy density allowed by the laws of physics.

An Analogy: Fermi's Theory of the Weak Force

We've encountered a situation very similar to gravity elsewhere in these lectures. Recall from Section 4.2.3 that Fermi's original theory of the weak force included a dimensionful coupling known as the Fermi constant (4.4), whose value is roughly

$$G_F \approx \frac{\alpha_W}{M_W^2} \tag{5.8}$$

where $\alpha_W \approx 1/30$ while $M_W \approx 80$GeV is the W-boson mass. If you don't know about W- and Z-bosons, and work purely within the Fermi theory then everything is fine provided that you only look at low energy processes. But, from this perspective, the strength of the weak force depends on energy as

$$\text{Strength of Weak Force } \sim \alpha_W \left(\frac{E}{M_W}\right)^2 \sim G_F E^2$$

As you approach energies closer to M_W then Fermi's theory stops working and must be replaced by something else. That something else is, of course, the W- and Z-bosons.

If we take this lesson seriously, it suggests a similar fate for gravity, with general relativity the low-energy approximation to something more fundamental. If we were to push the analogy with (5.8) yet further, we might expect that Newton's constant arises from a combination of a dimensionless coupling $\alpha_{\rm grav}$ and a fundamental scale $M_{\rm grav}$, so that

$$G_N \approx \frac{\alpha_{\rm grav}}{M_{\rm grav}^2}$$

with general relativity breaking down as we approach energies $M_{\rm grav}$. In such a scenario, we would see some new physics emerging at the energy scale $M_{\rm grav}$, possibly manifesting itself

as new particles. Note that, if this is the way things pan out, then we can't be sure about the scale $M_{\rm grav}$ because it's related to $M_{\rm pl}$ by a dimensionless coupling $\alpha_{\rm grav}$. Assuming that $\alpha_{\rm grav}$ isn't ridiculously small, it would appear natural that $M_{\rm grav}$ is somewhere in the ballpark of the Planck scale $M_{\rm p1}$.

The discussion above is, appropriately for these lectures, very much a particle physicist's perspective on quantum gravity, focussing on scattering of gravitons and what happens at high energies. But Einstein's theory is, at heart, a theory of geometry and this suggests different approaches to quantum gravity where, for example, spacetime sits in a superposition of all possible geometries, much like a particle in a double slit experiment follows all possible trajectories. This brings new conceptual issues to the table, but the problem described above remains, now in the guise of difficulties when spacetime fluctuates on very small scales,

$$L_{\rm pl} = \frac{1}{M_{\rm pl}} \approx 10^{-34}\ {\rm m}$$

It may well be that the very notion of space and time need replacing when we get to such small distance scales.

The Unreasonable Effectiveness of Classical Gravity

The analogy with Fermi's theory of the weak force gives us a useful way of thinking about what a dimensionful coupling, like G_N, means in quantum theories. But general relativity is a considerably deeper and more subtle theory than Fermi's and it has a number of tricks up its sleeve.

In particular, Fermi's theory of the weak force only works for energies $E \ll M_W$. For any energies higher than that, you need to use the gauge theory of W- and Z-bosons. But that's not the way things work for gravity. General relativity will give you the right answer to any quantum question at energies $E \ll M_{\rm pl}$. But if you throw together two particles at energies $E \gg M_{\rm pl}$, then general relativity will also give you the right answer. That's because, if you throw particles together at very high energies, then you simply form a black hole!

Black holes are nature's way of putting a limit on the amount of matter than can be squeezed into some small amount of space. They have two key features: at the centre of the black hole is the singularity. According to general relativity, this is a region where the curvature of spacetime becomes infinitely large. What that really means is that we shouldn't trust general relativity near the singularity and it should be replaced by a theory of quantum gravity. But, happily, we don't need a theory of quantum gravity to understand many features of black holes because the singularity is shielded from view by the second feature of a black hole: the event horizon. This is a surface that can be thought of as the edge of the black hole. If you venture through the event horizon of a black hole then you're in trouble: you will never escape and will be dragged inexorably towards the singularity. In this scenario, you will need to very
quickly develop a fully fledged theory of quantum gravity if you want to know what fate awaits you. If, however, you are less foolhardy and remain outside the event horizon then you can get by quite happily with our naive theory of quantum gravity.

That's not to say that there aren't interesting quantum gravity effects associated to the event horizon. If you study quantum field theory in the presence of a black hole, you find Hawking radiation, the process in which the black hole emits (mostly) photons and gravitons and slowly evaporates. It is a striking effect, and not without its own puzzles, but these too can seemingly be understood largely within a naive approach to quantum gravity, without the need for the full theory at the Planck scale.

The size of the event horizon is called the Schwarzschild radius. A black hole of mass M has Schwarzschild radius

$$R_s = 2GM \sim \frac{M}{M_{\rm pl}^2}$$

This simple equation turns one of the key ideas of particle physics on its head. Throughout these lectures, going to higher and higher energies has been tantamount to looking on smaller and smaller distance scales, with energy and distance related, in natural units, by $\lambda \sim 1/E$. But, when gravitational effects become important, we see that going to higher energies gives rise to bigger black holes. If we scatter two particles at energies $E \gg M_{\rm pl}$, then we make a black hole of size $R \sim E/M_{\rm pl}^2 \gg L_{\rm pl}$. This is how nature evades energy densities smaller than the Planck scale.

This means that, provided we don't do anything stupid, like jump into a black hole, we understand perfectly well what happens in very high energy scattering. You form a big black hole which slowly evaporates over gazillions of years. We never need any knowledge of the fundamental theory of quantum gravity to figure out the physics.

All of this is to say that the applications of a full theory of quantum gravity to scattering appear strangely limited. It is needed only in a small window of energies $E \sim M_{\rm pl}$. For energies $E \ll M_{\rm pl}$, a naive theory of quantum gravity will do the job, and for energies $E \gg M_{\rm pl}$, classical general relativity will do the job, at least until the resulting black hole has had enough time to evaporate down to size $R \sim L_{\rm pl}$. In final stages of the black hole's life, we will again need to resort to a detailed theory of quantum gravity to understand what happens.

Of course, not all of physics is to do with scattering. As we mentioned above, if we really want to understand what happens inside a black hole at the singularity then we surely need quantum gravity. Furthermore, a very similar kind of singularity arises in
general relativity at the Big Bang. If we follow the evolution of the universe back in time, then general theorems of Hawking and Penrose tell us that we will necessarily meet a singularity where general relativity breaks down. This means that if we want to answer the all-important question of how the universe began then we surely need a decent theory of quantum gravity. But it is rather hard to find any lingering effects of the Big Bang in our current universe. This is isn't simply because it happened a long time ago. Rather it is because there was a period of rapid expansion in the early universe known as inflation which dilutes any specific effects due to the singularity. It appears, once again, that Nature wishes to thwart us in our attempts to see directly the effects of quantum gravity.

This is not to say that quantum gravity is uninteresting. The questions of how singularities are resolved, both cosmological and those inside black holes, are important ones. Moreover, a closer look at how quantum theory meshes with gravity opens up a number of subtle conceptual issues, including how information escapes from black holes, how we should think about observers in an accelerating universe, and the seeming holographic nature of gravity. Moreover, there is the striking fact that, in string theory, we do have a fully fledged theory of quantum gravity, one that has intricate connections with various quantum field theories. All of these, however, are topics for other lectures.

4.5.3 5.3 Cosmology

There are more things in heaven and earth, Horatio, Than are dreamt of in your Standard Model.

Hamlet was wrong about the earth. As we've seen, we are painfully short of experiments that cannot be explained by the Standard Model. But he was right about the heavens. When we look to the sky, it becomes clear that there is much we don't understand.

Our shocking lack of understanding becomes apparent when we audit the energy budget of our universe. This reveals that the particles of the Standard Model comprise just 5% of the

total energy. All the things that we can see - stars, galaxies, planets, light itself - and all the things that we can detect through more indirect means - inert dust, neutrinos, gravitational waves - make up just a tiny fraction of the energy that is out there.

The vast majority of the energy in the universe is dark, which simply means that it doesn't interact (as far as we can tell) with the particles in the Standard Model. This "missing" energy can be further characterised as having two very different properties:

- Roughly 25% of the energy of the universe comprises of some new particles (or, better, new fields) that are not included in the Standard Model. This is called dark matter.
- The remaining 70% is a cosmological constant, sometimes called dark energy.

For reasons that we won't get into here, there's reason to believe that the short list above accounts for everything. There are very likely surprises in store for us in both dark energy and dark matter, but there is not some extra energy out there that we've missed completely. That's because, in the framework of cosmology, the total energy doesn't actually have to add up to 100% ! Any deviation from 100% shows up as some overall curvature to the universe. But the universe is, as far as we can tell, exactly flat and that tallies nicely with our other observations which show that the energy hits the magical 100% threshold.

In this final section, we will elaborate on some of the puzzles of cosmology that are likely to have the biggest impact on particle physics. We will be fairly brief. Many more details can be found in the lectures on Cosmology.

5.3.1 The Cosmological Constant

The vast majority of energy in the universe is rather strange. It is best described as an anti-gravity force field, spread thinly throughout space, causing everything to repel everything else. We refer to this force field as dark energy.

We can't detect this dark energy here on earth. Nor can we see its effects within our solar system, nor even within our galaxy. Instead it is only when we look out at vast distance scales when the effects of dark energy become apparent as it manifests itself in the way the universe expands.

We've known that the universe is expanding since the 1920s. This is a straightforward prediction of Einstein's equations of general relativity, albeit one that was not embraced by theorists until the observational data made the case overwhelming. But around the turn of the last century, we learned something striking. The expansion of the universe is speeding up over time. We live not just in an expanding universe, but in an accelerating universe. This is despite the fact that the galaxies in the universe are all mutually attracted to each other through gravity which should cause the expansion to slow. But there is something else at play that overwhelms the natural gravitation attraction of galaxies at very large scales. This something else is dark energy.

In some sense, we understand dark energy very well. The Einstein equations of general relativity allow for exactly one additional term, with a single parameter Λ known as the cosmological constant. This extra term has exactly the right effect, changing the dynamics of spacetime to give the observed acceleration of the universe. All we have to do is set the cosmological constant to take the value,

$$\Lambda \approx \left(10^{-29}\text{eV}\right)^2$$

A better way of thinking about this is in terms of the density of dark energy which, in natural units (where length is equivalent to inverse energy) has dimensions of energy to the power 4 . To get this, we should multiply by $M_{\rm pl}$, giving the energy density

$$\rho_\Lambda \approx \Lambda M_{\rm pl}^2 \approx \left(10^{-3}{\rm eV}\right)^4 \tag{5.9}$$

Just plug these values of the cosmological constant into the Einstein equations and you're done: the expansion of the universe then matches perfectly with what we observe.
(Before we go on, I should mention that this last sentence might not be quite true. There is currently a discrepancy between two different methods of measuring the expansion of the universe. The first, and arguably the cleanest, looks at the cosmic microwave background radiation, the afterglow of the Big Bang, and infers how the universe has subsequently evolved. The second looks at distant supernovae which are bright enough (and, apparently, uniform enough) to accurately measure both their distance and their recession velocity. These two results give answers that differ that level of 10% or so and it is difficult to reconcile them in any straightforward way. It may be, of course, that there is some unknown systematic in one of the experiments that gives a skewed result. Or it may be that there is something deep going on that we've missed. This is known as the Hubble tension.)

The Energy of the Vacuum

Although we have the equations to describe the accelerated expansion of the universe, there is a level of disquiet about the cosmological constant. This derives from the fact that we actually have a good understanding of the physics underlying the cosmological constant and this seems to be in conflict with the observed value.

The cosmological constant is, it turns out, something very familiar in physics: it is the vacuum energy. Recall that we're taught in high school that the overall value of the energy doesn't matter. Instead, only energy differences are important. That's true in all situations except for in cosmology. Gravity responds to all kinds of energy including the energy of empty space and this appears as the cosmological constant in the Einstein equations where it affects the overall expansion of the universe.

In some ways, this is a good thing. The cosmological constant isn't just some random number that we've plucked out of thin air to account for the expansion of the universe. Instead it's something that should arise naturally from our other laws of physics. And this gives us the opportunity to calculate it from what we know about particle physics.

This is where the narrative takes something of a left turn. The vacuum energy in quantum field theory is something interesting. Recall that one of the characteristic features of quantum field theory is that the vacuum isn't a dull place: the quantum fields froth with quantum fluctuations. We showed an example of the quantum field vacuum way back in Figure 4. And all of those fluctuations contribute to the vacuum energy. If the vacuum has fluctuations on some maximum energy scale E, then we typically expect a ground state energy density of order E^4.

That's problematic. We know that the Standard Model of particle physics holds up to the energy scale of a TeV or so. But this strongly suggests that the vacuum energy density should be at least

$$\rho_{\rm SM} = \left(10^{12}{\rm eV}\right)^4$$

This is not particularly close to the observed value. It is 60 orders of magnitude greater than the observed value ρ_Λ. More generally, the contribution of any quantum field to the vacuum energy density is naturally of order $\rho_{\rm QFT} \sim \Lambda_{\rm UV}^4$, where $\Lambda_{\rm UV}$ is the UV cut-off.

In the cosmological context, a vacuum energy density of order a TeV or higher gives ridiculous results. A cosmological constant this large would give a universe that expands so quickly that it is not conducive to forming nuclei or atoms, let alone galaxies and life. The huge dis-

crepancy between the expected value of ρ_{QFT} and the observed value of ρ_Λ is known as the cosmological constant problem.

The cosmological constant problem is entirely analogous to the hierarchy problem that surrounds the Higgs mass that we discussed in Section 5.1.2. In both cases, quantum corrections seem to naturally push the value of some quantity to be much higher than we observe. This happens only for the Higgs mass and the cosmological constant because these are the only two dimensionful parameters in the known laws of physics. (Strictly speaking, we also have the Planck mass $M_{\rm pl}$, but this can be thought as setting the scale relative to which all other parameters are measured.)

The cosmological constant problem is sometimes referred to as the worst prediction in the history of physics. The people making this claim clearly haven't studied the history of physics. (Rayleigh-Jeans law anyone?) Nonetheless, the prediction is clearly nothing to be proud of. The solution to the ultra-violet catastrophe inherent in the Rayleigh-Jeans law ultimately resulted in the greatest paradigm shift in the history of science: the discovery of quantum mechanics. It's not clear if the cosmological constant problem will result in a similar upheaval to our understanding of physics or whether, with some small twist of our head, the question will unravel as we realise that we've been looking at things the wrong way. For now, it's fair to say that we have just one solution to the cosmological constant problem. This is the idea that, in addition to the contribution from quantum field fields, there is another contribution to the cosmological constant, so that the two add up to give the observed value (5.9)

$$\rho_\Lambda = \rho_{\rm SM} + \rho_{\text{something else}}$$

Clearly the additional contribution $\rho_{\text{something else}}$ must cancel the contribution from the Standard Model to 60 significant figures, leaving behind the tiny cosmological constant that we observe. This is another example of fine tuning. It is the same kind of idea that we met in equation (5.5) when discussing the mass of the Higgs boson.

It is quite possible that there is some missing principle that we've failed to grasp that makes fine tuning less silly than it first appears. The task of finding such a mechanism is made considerably harder when we realise that there have been a number of times in the history of the universe when $\rho_{\rm SM}$ abruptly changed while, presumably, $\rho_{\text{something}}$ else did not. This occurs at a phase transition. For example, there was a time in the early universe when things were so hot that quarks and gluons were not confined inside baryons and mesons. As the universe cooled, confinement kicked in and, at that time, the vacuum energy of the Standard Model jumped by around $\Delta\rho_{\rm SM} \sim (100{\rm MeV})^4$. Still earlier, the electroweak phase transition, where the Higgs boson first condensed, resulted in a change of $\Delta\rho_{QFT} \sim (100{\rm GeV})^4$. This means that any putative cancellation mechanism must conspire to give a tiny cosmological constant ρ_Λ at the end of the life of the universe, not at the beginning.

Before we muddy the waters yet further, it's worth mentioning that the observed vacuum energy (5.9) is pretty much in the same ballpark as the neutrino masses. Is this coincidence? Probably. Certainly it's hard to know what to make of it. But, given our evident confusion about the cosmological constant, it's worth bearing in mind.

The A-Word

As we saw above, a naive application of quantum field theory suggests a ludicrous value for the cosmological constant, one that results in an expansion so fast that not even atoms have a chance to form from their underlying constituents. Given this, we could ask the following question: what is the maximum value of the cosmological constant that still allows complex structures to evolve? For example, what is the maximum allowed value of Λ that

allows galaxies to form?

It turns out that the upper bound on Λ depends on the strength of the initial seeds from which the galaxies grew. (We'll mention these briefly later in this section.) However, if we fix this initial condition, then we can ask again: how big can the cosmological constant be?

The answer is quite striking: the scale of the vacuum energy is pretty much the maximum it could be. If ρ_Λ were bigger by an order of magnitude or so, then no galaxies would form, presumably making it rather more difficult for life to find a comfortable foothold in the universe.

What to make of this observation? One possibility is to shrug and move on. Another is to weave an elaborate story. Suppose that our observable universe is part of a much larger structure, a "multiverse" in which different domains exhibit different values of the fundamental parameters, or perhaps even different laws of physics. In this way, the cosmological constant is not a fundamental parameter which we may hope to predict, but rather an environmental parameter, no different from, say, the distance between the Earth and the Sun. We should not be shocked by its seemingly small value because, were it any higher, we wouldn't be around to comment on it. Such reasoning goes by the name of the anthropic principle.

The anthropic explanation for the cosmological constant may be correct. But, in the absence of any testable predictions, it is not clear what to make of it and further philosophising tends to be more of a distraction than a help.

A Rebranding: Dark Energy

Given our manifest befuddlement about all things Λ, it is prudent to wonder if perhaps the accelerated expansion of the universe has nothing to do with a cosmological constant at all! It is quite possible that the cosmological constant in the Einstein equations is $\Lambda = 0$. If this is the case, then we need to look for another explanation for the accelerated expansion. It is not difficult to find such explanations, although none of them are particularly compelling. For example, a scalar field with a ridiculously low mass (around 10^{-33}eV or so), rolling down a potential can do the job should we wish.

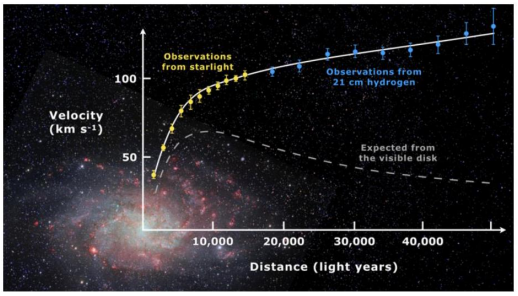


Figure 54. The rotation curve of galaxy M33. Image taken from Wikipedia.

I should stress that these new explanations in no way alleviate the cosmological constant problem. Finding a mechanism that sets the cosmological constant to zero is no easier than finding a mechanism that sets it to the observed value. Furthermore, one typically introduces many more fine tuning issues in whatever new dynamics is then introduced to drive the accelerated expansion.

Nonetheless, the history of particle physics has taught us that we shouldn't be too hasty in following our preconceived ideas about how the universe should be. To avoid committing to the cosmological constant explanation, the mysterious 70% of the energy in the universe is often referred to as dark energy.

5.3.2 Dark Matter

Dark matter comprises around 25% of the energy density of the universe. Unlike dark energy, it is conceptually quite straightforward: it is simply some new, heavy particles that are not accounted for in the Standard Model. Or, at a fundamental level, some new quantum fields.

We know very little about the properties of dark matter, beyond the fact that it does not interact with light. We do not know if it is a single species of particle, or many. We do not know if it consists of several decoupled sectors, or just one. Given the wonderful complexity of the Standard Model, it seems reasonable to assume that there is still rather a lot to learn about dark matter.

All we know about dark matter comes from its gravitational interactions. Yet the combined evidence is overwhelming. Here are some highlights:



Figure 55. On the left, the Abell S1063 cluster. The smeared blue lines are background galaxies, distorted by gravitational lensing. On the right, the bullet cluster.

- The beautiful spiral galaxies that we see in the sky seem to be spinning too fast! The attractive gravitational force from all the stars in the galaxy, does not come close to reproducing the necessary centripetal force to stop the galaxy from flying apart. Moreover, if you measure the spectral lines of hydrogen far from the visible edge of the galaxy, you find that it continues to rotate at a roughly constant speed for quite some distance. All of this can be explained by simple Newtonian dynamics, but only if there is much more mass in the galaxy than is visible. To account for the observations, there should be a roughly spherical cloud of dark matter surrounding the galaxy.

The rotation curve for a nearby galaxy, together with the predicted curve if there is only the visible matter, is shown in Figure 54.

- A galaxy cluster is a collection of 100 to 1000 galaxies, bound together by gravity. A clever argument, known as the virial theorem, gives a relationship between the speed of the galaxies and their separation (or, more precisely, their kinetic energy and potential energy). From this, one can extract the mass of the galaxy. The answer is a couple of hundred times greater than the visible mass.

- A classic prediction of general relativity is that light bends as it passes heavy objects. Furthermore, the image gets distorted, a phenomenon known as gravitational lensing. Sometimes this happens in a spectacular fashion, as shown in the picture on the left of Figure 55 where the image of a background galaxy is distorted into the blue arcs by the cluster in the foreground. Even small distortions of this kind allow us accurately determine the mass of the cluster in the
foreground. You will not be surprised to hear that the mass greatly exceeds that seen in visible matter.

The bullet cluster, shown in the right of Figure 55, provides a particularly dramatic example of gravitational lensing. This picture shows two sub-clusters of galaxies which are thought to

have previously collided. There are three types of matter shown in the picture: stars which you can see, hot gas which is observed in x-rays and is shown in pink, and the distribution of mass detected through gravitational lensing shown in blue. The stars sit cleanly in two distinct sub-clusters because individual galaxies have little chance of collision. In contrast, most of the ordinary matter sits in clouds of hot gas which interact fairly strongly as the clusters collide, slowing the gas and leaving it displaced from the stars as shown in the figure. But most of the matter, as detected through gravitational lensing, is dark and this, like the galaxies, has glided past each other seemingly unaffected by the collision. The interpretation is that dark matter interacts weakly, both with itself and with ordinary matter.

- The observations described above show clearly that, on the scale of both galaxies and clusters of galaxies, there is more matter than can be detected by electromagnetic radiation. This alone is not sufficient to tell us that dark matter must be composed of some new unknown particle. For example, it could be in the form of failed stars ("jupiters"). There is, however, compelling evidence that this is not the case, and dark matter is something more exotic.

The primary evidence comes from Big Bang nucleosynthesis, an impressively accurate theory of how the light elements were forged in the early universe. It turns out that the relative abundance of different elements depends on the total amount of baryon matter. In particular, the amount of deuterium compared to everything else depends in a delicate way on the total amount of ordinary matter. This tells us that the total amount of ordinary matter is just a few percent of the total energy density.

- In Section 5.3.4, we'll describe the cosmic microwave background, a photograph of the fireball that filled the universe when it was very much younger. The flickering of this fireball shows that some spots were hot and others cold. As the universe evolved, these initial fluctuations provided that seeds that later grew into the clusters, galaxies and stars that we see around us.

It turns out, however, that this cannot be achieved by ordinary matter alone. There simply isn't time, largely because ordinary matter couples to photons and
this causes a pressure which suppresses gravitational collapse. But dark matter doesn't know about the photons, so there is nothing to stop it forming gravitational wells into which visible matter can subsequently fall. The whole story of the formation of galaxies only works because of the existence of dark matter.

Moreover, the existence of dark matter also leaves a distinct imprint in the ripples of the cosmic microwave background (specifically in the relative heights of the first and second peak of the power spectrum).

Taken individually, one might have thought that there could be some alternative explanation for these pieces of evidence. For example, faced just with the galaxy rotation curves, one might try to tinker with Newton's equations of motion to get something that fits. But that will then leave us unable to explain, say how the light elements were forged in Big Bang nucleosynthesis. And yet all of the problems above are resolved by the simple admission that there are particles (or, strictly speaking, quantum fields) in the universe that are not accounted for in the Standard Model.

Clearly we should try to understand these fields and, ultimately, enlarge the Standard Model to embrace them. This is not so straightforward because all our evidence for dark matter comes from gravitational interactions alone. In an attempt to change this, there are many ongoing experiments designed to detect dark matter here on earth. All of these rely on the hope that there is some non-gravitational interaction between dark matter and Standard Model fields,

perhaps through the weak force or perhaps through some new, as yet undiscovered force. These experiments are increasingly impressive at pushing the boundaries and one can only hope that they will one day make a key discovery.

There is one reason for optimism here. This is because the abundance of dark matter and ordinary matter is not wildly different. There is more dark matter by a factor of 5 , but not a factor of 500 or 5 billion. The most plausible explanation for this is if dark matter and ordinary matter were in equilibrium together in the early universe, before they subsequently decoupled. But such equilibrium can only be maintained if there are some non-gravitational interactions between them.

In particular, there is one tantalising hint. If one assumes that dark matter has a mass of around the TeV scale associated to the weak force, and moreover interacts with the strength of the weak force, then the relative abundances come up just about right. However, if it were to interact directly through the weak force at this scale then we must ask why it hasn't shown itself at the LHC. Maybe this tantalising hint is merely a red herring.

5.3.3 Baryogenesis

The universe contains lots of matter but very little anti-matter. How did this asymmetry come to be?

One possibility is that it is an initial condition on the universe. Another is that the universe started with equal amounts of matter and anti-matter, but somehow a small dynamical shift took place that preferred one over the other. This latter process is known as baryogenesis.

We don't have an established theory of baryogenesis, but there are a set of three criteria that must be obeyed, known as the Sakharov conditions. These are:

- The first criterion is the most obvious: particle number cannot be a conserved quantity. Here "particle number" refers to particles minus anti-particles. In a symmetric universe, the total particle number would start off at zero. We want it to end up at something non-zero.

In the Standard Model, both baryon number and lepton number are almost conserved although, as we saw in Section 4.3.5, in extreme conditions only $B - L$ is strictly conserved. The early universe certainly counts as an extreme condition. The need for baryogenesis suggests that we need interactions that break the symmetry $B - L$. For example, a Majorana mass for neutrinos will do the job.

- The symmetry CP must also be broken. As we've seen in Section 4.3.4, CP relates the behaviour of particles to anti-particles, but for baryogenesis to occur their behaviour must be different.

We've seen that CP is violated in the quark sector, but this is not enough to give rise to the necessary level of baryogenesis. It remains to be seen whether CP violation in the lepton sector is sufficient to do the job, or whether baryogenesis requires interactions beyond those discussed in these lectures.

- The final criterion is the least obvious: the early universe must deviate from thermal equilibrium.

A deviation from thermal equilibrium occurs when the universe undergoes a first order phase transition. (You can read more about phase transitions in the lectures on Statistical Physics and Statistical Field Theory.) The Standard Model does not appear to offer the opportunity

for such a violent event at the necessary energy scales. This suggests that we should need some new physics to induce baryogenesis.

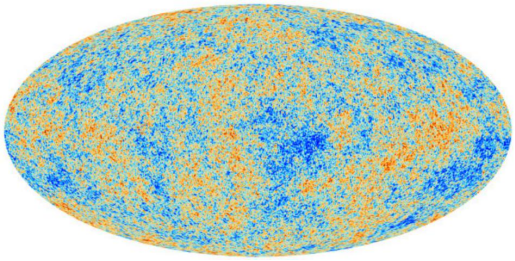


Figure 56. Look and weep, Ansel Adams.

There are many models of baryogenesis on the market, but currently no smoking gun experiment or observation that will determine which, if any, is correct.

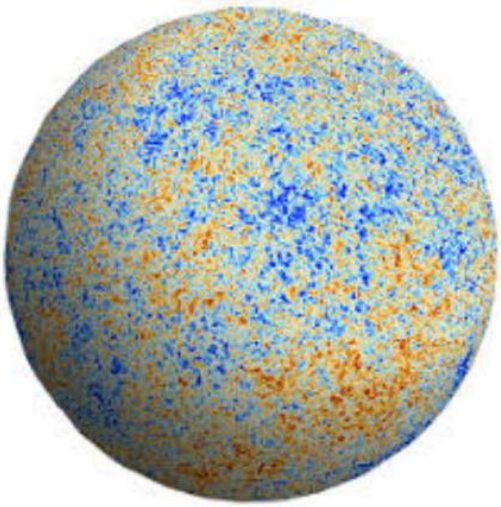
5.3.4 Primordial Fluctuations

Most reasonable people agree that the greatest movie ever made is Ghostbusters. Sadly the world contains no small number of unreasonable people, those who prefer their movies to have a less intellectual bent, or those who put less stock in powerful acting performances and groundbreaking cinematography. It is difficult to argue that the opinion of these people is any less valid just because it is wrong. Art is not like science. There is no immutable, underlying truth that determines what is the right and wrong.

Until, that is, we come to photography. No one, reasonable or otherwise, can disagree about the greatest photograph ever taken. All other candidates pale into insignificance when faced with the collective endeavours of a bunch of radio horns and a handful of satellites who, between them, achieved the seemingly impossible feat of taking a photograph of the Big Bang.

First, I should tell you what the Big Bang theory entails. It is not a theory that tells us how the universe started. The question "how did the universe start?" has a very straightforward answer which is "we don't know". Instead, the Big Bang theory tells us what the universe was like when it was very much younger. The theory starts with the observation that there was a time - 13.8 billion years ago to be precise when the universe was so hot that matter, atoms and even nuclei melted and all of space was filled with a fireball. When I say that we've taken a photograph of the Big Bang, I mean that we've taken a photograph of this fireball, capturing the light that
has travelled through the universe uninterrupted for almost 14 billion years. This light is known as the cosmic microwave background, or CMB for short.

The clearest photograph that we have was taken by the Planck satellite and is shown in Figure 56. This is a panoramic shot, containing information from each point in the sky which is then depicted in 2 d much like a map of the Earth. A better setting for the CMB is shown in figure to the right. We sit in the centre of this sphere. If we look far enough away, roughly 20 billion light years in any direction,



then we see the CMB.

In the early universe, the fireball reached extreme temperatures, almost certainly the most extreme temperatures the universe has ever seen. But, as the universe expanded, the fireball cooled and it is now a tepid 2.73 Kelvin. This temperature is almost uniform across the sky, but there are small fluctuations at the level of 1 part in 10^5. These hot and cold spots are depicted in red and blue in the photograph. These fluctuations have been imprinted in the CMB for 14 billion years, and so contain a wealth of information about what the universe was like when it was much younger. This information is usually plotted as a function of angular scale, as shown in Figure 57. From the positions of the peaks and troughs, we can determine much about the age and contents of the universe. For example, the position of the first peak contains information about the age of the universe, while the relative height of the first and second peaks contains information about the amount of dark matter in the universe.

Here, however, our interest is rather different. The question that we wish to ask is: where did those temperature fluctuations come from originally? This is question for which we're fairly confident that we have the answer. And it is nothing short of astonishing.

Inflation

The answer involves a process known as inflation, a period of rapid accelerated expansion when the universe was very young. Here "very young" means when the universe was, at most 10^{-11} second old, but most likely it occurred much earlier than this. (In this counting, 10^{-30} seconds counts as "much younger" than 10^{-11} seconds!)

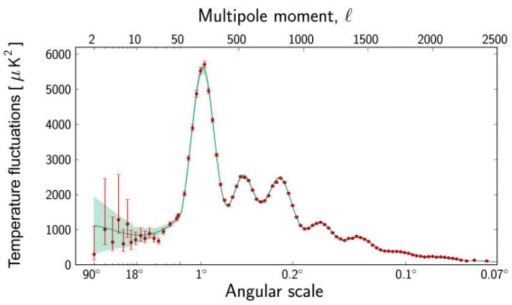


Figure 57. The dependence of the CMB temperature fluctuations with angular scale.

The original reasons for postulating the existence of an inflationary phase had nothing to do with the fluctuations. Instead, such a phase would resolve two unanswered questions about the universe we live in.

The first is: why is the universe so flat? It turns out that a flat universe is dynamically unstable, like a pencil balanced on its tip. Any small overall curvature at the beginning of the universe would have grown over time yet, after 14 billion, the universe appears as flat as a metaphorical and cosmological pancake. Why? Inflation gives an answer to this question. A brief phase of rapid expansion, stretches out any curvature that may have once existed, like pulling a membrane taut. This nicely explains why we find ourselves living in a flat universe.

The second is: why is the CMB so uniform? We can stare out at the sky in one direction and detect photons from the CMB, photons that have travelled roughly 20 billion light years uninterrupted. We can then turn around and see photons that have travelled 20 billion light years from the opposite direction. The properties of these photons are basically the same: in particular, both exhibit identical temperatures of 2.73 Kelvin. The fact that these two far flung reaches of the universe have the same temperature is a puzzle. Usually when two systems sit at the same temperature it's because they've had the opportunity to interact, exchange energy, and settle down to thermal equilibrium. But those two patches of the universe have had no such opportunity simply because they're too far away. Light from one region of space hasn't had
time to reach the other: indeed, we're sitting in the middle and it's only now that we can see both regions. So how could they possibly sit at the same temperature?

There is a more nuanced version of this second issue. This arises, somewhat ironically, when we appreciate that the CMB is not completely uniform after all but contains the tiny fluctuations shown in the photograph. There are fluctuations in both the temperature and the polarisation of light and, importantly, these two different types of fluctuations are correlated. These correlations - which go by the uninspiring name of "TE correlations" - are the kind of the type that would arise through simple and well understood dynamical processes in the early universe, such as photons scattering off electrons. But observations reveal that there are correlations over patches of the sky that were, apparently, never in causal contact with each other. That's a worry. Taken naively, it's telling us that there were dynamical processes in the early universe that occurred faster than the speed of light and that violates one of the key tenets of physics.

The TE correlations are, by far, the strongest argument for inflation. If we want to preserve some of our most cherished notions of physics, like locality and causality, then it tells us very clearly that those far flung patches of the sky must, in fact, have been in causal contact back in the day. Inflation is the mechanism that allows this to happen. In the very early universe, two patches of space could be near. But inflation then takes those patches and stretches them to enormous distances, until they sit on opposite sides of the observable universe. Yet they retain, in the CMB, the correlation that gives the game away that they were once playmates.

The arguments given above strongly suggest that inflation happened. The next question is: what caused it? Here we're on less sound footing. The good news is that when general relativity is coupled to quantum fields, one naturally gets the rapid expansion that we need for inflation. Indeed, we've already seen how to do it: the vacuum energy, or cosmological constant, does the job. The accelerated phase of inflation in the early universe is conceptually identical to the accelerated phase that we now find ourselves in, but with two differences. The first difference is quantitative: the effective cosmological constant in the early universe must have been many many orders of magnitude larger than what we see today. The second difference is that the original period of inflation must, ultimately, have come to a halt. The real challenge in constructing a viable model is therefore figuring out how to get inflation to stop!

This, it turns out, is not so difficult. Indeed, if there's bad news in the story of inflation, it is that it's too easy to write down models that do the job which means that
every Tong, Dick and Harry has their own theory of inflation, with hundreds now on the market and very little to decide between them. None of these models are particularly exotic and nearly

all include the same basic ingredient: a scalar field. The idea is that the inflaton, unlike the Higgs boson, had not yet settled to the minimum of its potential energy in the early universe, so its value changes over time. Correspondingly, so too does the vacuum energy that drives inflation.

None of the models for inflation stand out as being overly compelling. Indeed, in many ways they all look somewhat artificial. One might wonder if perhaps we could identify the inflaton with the Higgs boson itself, and there have been attempts to do so, but it's not a particularly natural fit. This means that while there is good evidence that the process of inflation took place, our knowledge is limited when it comes to the detailed underlying dynamics. Before we beat ourselves up about this too much, it's worth remembering that we're talking about a process that happened something like 10^{-30} seconds after the Big Bang. The fact that we haven't yet got all the details pinned down isn't terribly surprising.

Inflationary Perturbations

All of which brings us to the main topic of this section: where did the ripples in the CMB come from? These ripples contain correlations over large distance scales which means that, if they are to have a local and causal origin, then they must have been laid down during the inflationary period itself. Happily, inflation provides a remarkable origin story for these fluctuations.

The ripples arise simply from the realisation that the inflaton is a quantum field. In fact, we started these lectures by explaining that the vacuum of space is not a dull place since the quantum fields cannot stay still: they froth and bubble with quantum jitters. During inflation, the universe expands so quickly that these quantum fluctuations get caught in the act and are stretched from the microscopic scale, to distances that span the entire visible universe. These are what we see imprinted as hot and cold spots in the CMB: they are nothing less than quantum fluctuations that took place just fractions of a second after the Big Bang and are then frozen in place by the rapid expansion of the universe.

This may be one of the most extraordinary ideas in all of science, connecting our understanding of physics on the very smallest scales with that on the very largest. It passes many checks. A statistical analysis of the CMB fluctuations shows that they agree perfectly with those expected from a weakly interacting quantum field. Moreover, as we get better data on the fluctuations, so we begin to get a handle on

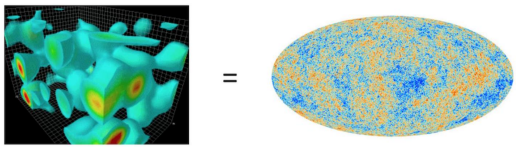


Figure 58. The ripples in the CMB are quantum vacuum fluctuations, laid down in the first few fractions of a second after the Big Bang.

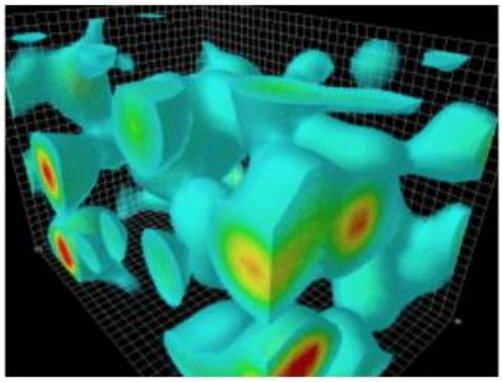
the dynamics of the inflaton field in the very early universe. We're currently at a stage where many putative models of inflation can be ruled out, although there are many that still survive. The hope is that further study of the CMB will yield precious clues about the interactions of these quantum fields in the first few moments after the Big Bang.

Remarkably, there is one further chapter to this story. Rather than asking where the ripples in the CMB came from, we could ask what subsequently happened to them. Here too we find an astonishing answer. The quantum fluctuations resulted in temperature variations in the CMB, with some places hotter and others colder. As the universe expanded and cooled, these hot and cold spots became the gravitational wells into which matter fell. First protons and

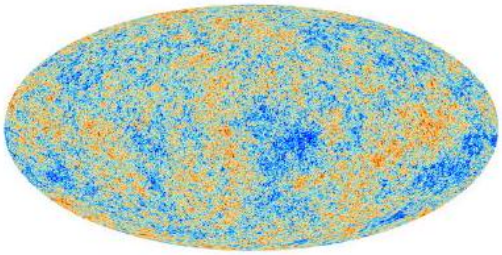
electrons, which subsequently bound together into hydrogen dust and a smattering of other light elements. Over time, this dust gathered, and the pressure grew until finally, after 500 million years or so, these balls of dust ignited and became stars.

This means that the quantum fluctuations from when the universe was in its infancy later became the seeds from which galaxies grew. This is backed up by observation: a statistical analysis of the galaxies in our universe matches impressively with an analysis of the CMB fluctuations. For example, the large peak in Figure 57 manifests itself in a particular way in which galaxies cluster in the sky (known, boringly as "baryon acoustic oscillations").

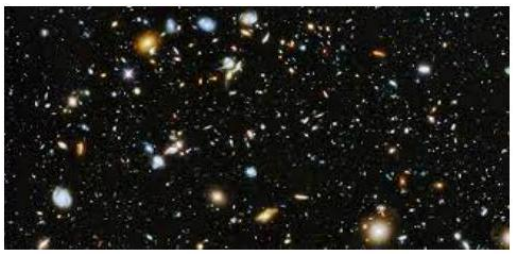
Putting the pieces together, we can draw a direct line from this:



to this:



to this:



It is one of the most remarkable stories in all of science, but there are many details still to be written. Hopefully, in the future we will understand better how the quantum fields involved in this story fit with those of the Standard Model.

5 Leptons and Quarks by Okun

5.1 1 Introduction

The weak interaction is responsible for a large number of physical processes: nuclear β-decay, numerous decays of elementary particles, reactions induced by neutrinos from accelerators and nuclear reactors, and also some subtle effects involving parity violation in γ-decays of nuclei and in atomic optical spectra. All known leptons and hadrons are subject to the weak interaction. It plays an important role in such astrophysical phenomena as the sun's burning and supernova explosions. Some of the weak processes were already put to use (for example, the angular asymmetry in the muon decay is a promising new tool in chemistry). Mainly, however, our interest

in the weak interaction is rooted not in its possible applications but in the hope that its study will ultimately yield a unified theory of elementary particles and of the interactions between them. And although it would be very difficult today to predict any practical consequences of such a unified theory, there can be no doubt of their utmost importance.

In contrast to "stronger" interactions, namely the strong and electromagnetic, the weak interaction violates a number of conservation laws. Among the quantum numbers that are not conserved are space parity P, charge conjugation parity C, combined inversion parity CP, strangeness, charm, and some others.

The standard theory of weak interactions is based on the analogy with the electromagnetic interaction which is produced by the electromagnetic current coupled to the photon (see fig. 1.1). Likewise, the weak interaction is postulated to result from weak currents being coupled to the so-called intermediate bosons $\mathrm{W}^+, \mathrm{W}^-, \mathrm{Z}$. Intermediate bosons have not yet been found experimentally; however, this does not point to a defect in the theory since the expected masses are of the order of 100 GeV , the energies of the existing accelerators being well below their production thresholds. The W^+ and W^-bosons are coupled to charged currents which change the charges of particles involved. Such are the currents $\bar{e}\nu_\mathrm{e}$ or $\bar{\mu}\nu_\mu$ and their hermitian conjugate currents $\bar{\nu}_\mathrm{e}e$ and $\bar{\nu}_\mu\mu$. The last two currents, for instance, interact

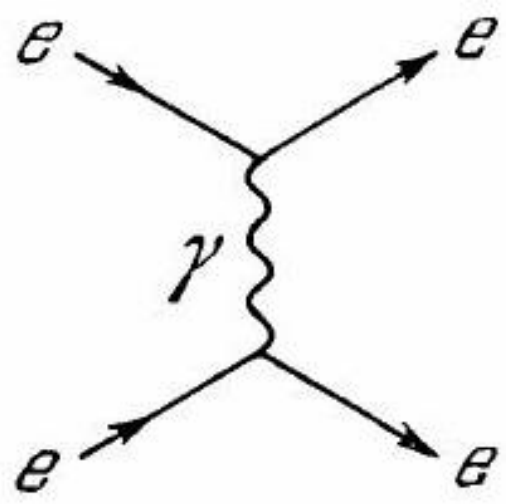


Fig. 1.1.

by exchanging a virtual W-boson and yield the muon decay $\mu \to \mathrm{e}\bar{\nu}_\mathrm{e}\nu_\mu$ (fig. 1.2). The Z^0 bosons are created by neutral currents of the types $\bar{e}e, \bar{\nu}_\mu\nu_\mu, \bar{\mu}\mu$, and so on, involving identical ingoing and outgoing particles. Neutral currents are responsible, for example, for the scattering $\nu_\mu\mathrm{e} \to \nu_\mu\mathrm{e}$ (fig. 1.3). Both the charged and the neutral currents include a leptonic and a hadronic part. At present we know six leptons which are naturally grouped into three pairs:

$$\begin{array}{lll} \nu_\mathrm{e} & \nu_\mu & \nu_\tau \\ \mathrm{e}^- & \mu^- & \tau^-, \end{array}$$

so that each lepton has its neutrino counterpart. Each lepton enters the charged current j with the appropriate neutrino:

$$j_\ell = \bar{e}\nu_\mathrm{e} + \bar{\mu}\nu_\mu + \bar{\tau}\nu_\tau.$$

This current emits W^+bosons and absorbs W^-bosons. The hermitian conjugate current $j_\ell{}^+$

$$j_\ell^+ = \bar{\nu}_\mathrm{e}e + \bar{\nu}_\mu\mu + \bar{\nu}_\tau\tau$$

emits W^-bosons and absorbs W^+bosons. The neutral leptonic current j_ℓ^0 contains six terms: $\bar{\nu}_e\nu_e, \bar{\nu}_\mu\nu_\mu, \bar{\nu}_\tau\nu_\tau, \bar{e}e, \bar{\mu}\mu, \bar{\tau}\tau$.

The two leptonic currents given above are responsible for the processes involving both leptons ($e^-, \mu^-, \tau^-, \nu_e, \nu_\mu, \nu_\tau$) and antileptons (e^+, $\mu^+, \tau^+, \bar{\nu}_e, \bar{\nu}_\mu, \bar{\nu}_\tau$). This follows from the properties of the relevant operators. For example, the operator $\bar{e}$ creates an electron and annihilates a positron, while the operator e creates a positron and annihilates an electron. Operators of other particles act in a similar manner.

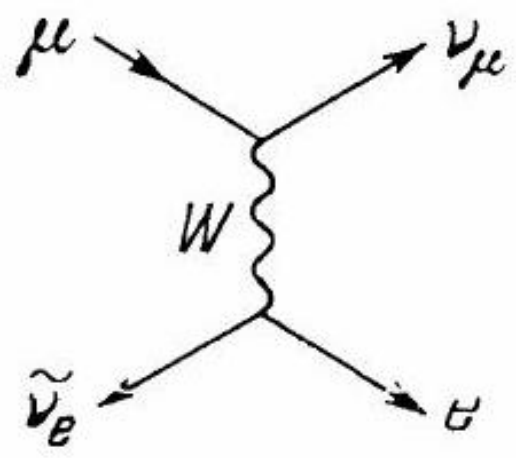


Fig. 1.2.

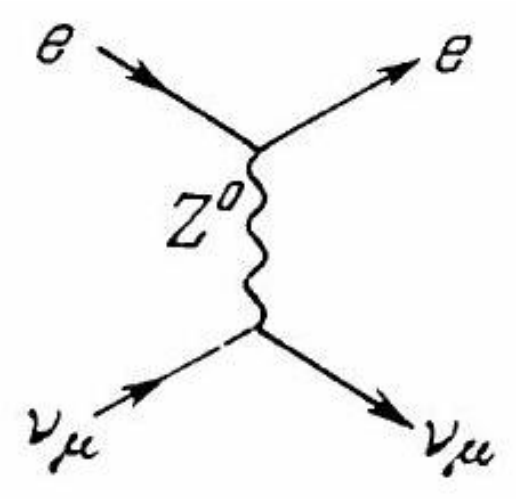


Fig. 1.3.

5.1.1 1.1. Quark currents

Hadrons are represented in weak currents by quarks. According to quark theory, all known hadrons consist of quarks of five types (five flavors): u, d, s, c and b . Theoretical arguments, however, point to the existence of a sixth quark t, so that in analogy to the six leptons, the six quarks form three pairs:

u c t
d s b.

We recall that the charges of quarks u, c, and t are $+\frac{2}{3}$, and those of quarks d, s, and b are $-\frac{1}{3}$. The quark structure is uud for the proton, udd for the neutron, udd̄ for the π^+meson, and so on. Strange particles include s-quarks (for instance, $\Lambda = \text{uds}, \text{K}^+ = \text{us}$), and charmed particles include c-quarks (for example, $\text{D}^+ = \text{cd}, \text{F}^+ = \text{cs}$). Particles with hidden charm, such as the J/ψ meson, are represented by c c̄. The structure of the Υ-meson is bb̄.

No hadrons with single b-quarks have so far been found ⋆, and only very scant indirect information is available on the weak interaction of the b - and t-quarks (see Chapter 15). Our knowledge of the first two pairs of quarks is, on the other hand, quite substantial. We know, first of all, that a quark may enter charged currents both with its paired partner and with a partner from another pair. For instance, in addition to the currents $\bar{u}d$ and $\bar{c}s$, the current $\bar{u}s$ exists as well. If it did not, strange particles would be absolutely stable whereas in fact they undergo decays; for example, the current $\bar{u}d$ is responsible for neutron decay (fig 1.4), while the $\bar{u}s$ current is responsible for the decay of the Λ-hyperon (fig. 1.5).

If it is assumed that each of the upper quarks can go over to any of the lower quarks, then in the general case the charged hadronic current j_h must contain nine terms: $\bar{u}d, \bar{u}s, \bar{u}b, \bar{c}d, \bar{c}s, \bar{c}b, \bar{t}d, \bar{t}s, \bar{t}b$; the picture is similar for

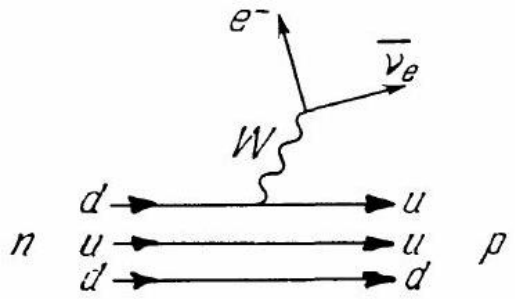


Fig. 1.4.

the hermitian conjugate current j_h^+. As for the neutral hadronic current j_h^0, it must have six terms: $\bar{u}u, \bar{d}d, \bar{s}s, \bar{c}c, \bar{b}b, \bar{t}t$. There are no neutral currents transforming quarks of one type into quarks of a different type, such as $\bar{d}s$, $\bar{u}c$, and so on (see Chapter 2).

5.1.2 1.2. On the color of weak currents

In addition to flavor, quarks are characterized by color. The same flavor characterizes three non-identical quarks differing in a quantum number quoted as color, so that we shall refer to yellow (y), blue (b), and red (r) u-quarks, d-quarks, and so on. The total number of quarks is therefore 18. Physical hadrons are singlets in color space, and are termed colorless or white. Color symmetry is absolute, and weak quark currents are, just as hadrons, white. This means, for example, that $\bar{u}d$ is in fact a sum of three terms:

$$\bar{u}d = \bar{u}^i d_i = \bar{u}^1 d_1 + \bar{u}^2 d_2 + \bar{u}^3 d_3,$$

where suffices 1, 2, 3 stand for yellow, blue, and red colors, respectively. The same is true for other quark currents. Hereafter, unless stated otherwise, summation over color suffices in quark currents is omitted.

[0⋆]B mesons containing single b-quarks were discovered in 1980, see footnote on p. 5.

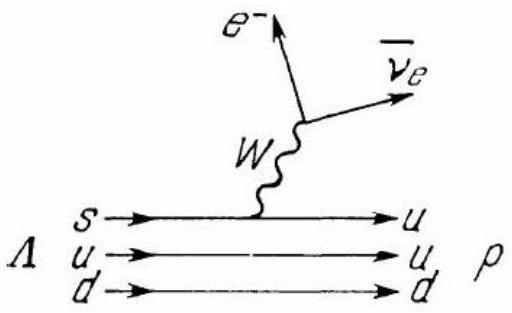


Fig. 1.5.

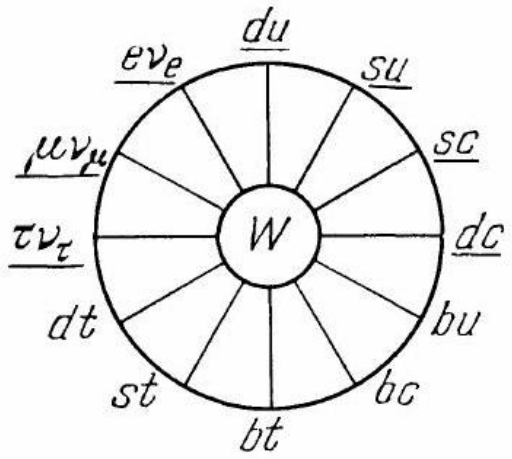


Fig. 1.6.

5.1.3 1.3. Currents and processes

The theory thus contains twelve charged currents coupled to W-bosons (see fig. 1.6) and twelve neutral currents coupled to Z -bosons (fig. 1.7). Underlined in figs. 1.6 and 1.7 are the currents verified by experiment ⋆.

A symbol du in fig. 1.6 denotes either the current $\bar{d}u$ or the hermitian conjugate current $\bar{u}d$; the same is true for other currents in this figure. In some cases this condensed notation proves convenient.

As each of the twelve currents can interact with each current of the diagram, the total number of possible interactions must equal 78 both for fig. 1.6 and for fig. 1.7. So far only fourteen such current × current interactions are experimentally detected for charged currents, and seven for

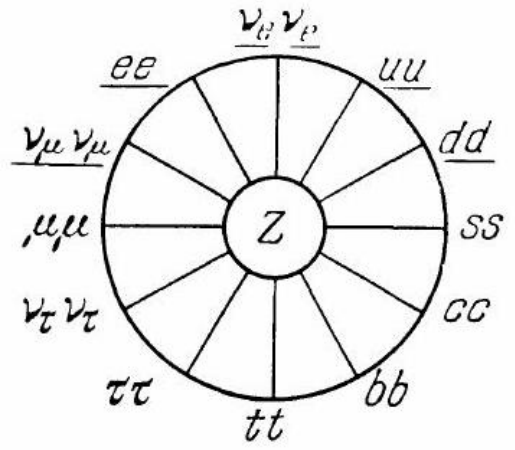


Fig. 1.7.

neutral ones. Let us make a list of these interactions, indicating in square brackets the processes in which they are experimentally observed. These processes are usually classified into three groups: pure leptonic, semi-leptonic (involving both leptons and hadrons), and non-leptonic (involving hadrons only). Four leptonic, seven semi-leptonic, and three non-leptonic interactions were found for charged currents:
$(e\nu_{\rm e})\,(e\nu_{\rm e})$ $[\bar\nu_{\rm e}{\rm e}\to\bar\nu_{\rm e}{\rm e}]$,
$(e\nu_{\rm e})\,(\mu\nu_\mu)$ $[\mu\to{\rm e}\nu\nu]$, $(e\nu_{\rm e})\,(\tau\nu_\tau)$ $[\tau\to{\rm e}\nu\nu]$, $(\mu\nu_\mu)\,(\tau\nu_\tau)$ $[\tau\to\mu\nu\nu]$,
$(e\nu)(ud)$ $[{\rm n}\to{\rm pe}\nu]$, $(e\nu)(us)$ $[{\rm K}\to{\rm e}\nu\pi]$, $(e\nu)(cs)$ $[{\rm D}\to{\rm e}\nu{\rm K}]$,
$(\mu\nu)(ud)$ $[\pi\to\mu\nu]$, $(\mu\nu)(us)$ $[{\rm K}\to\mu\nu]$, $(\mu\nu)(cs)$ $[{\rm D}\to\mu\nu{\rm K}]$, $(\tau\nu)(ud)$ $[\tau\to\rho\nu]$,
$(ud)(du)$ [P-odd nuclear forces],
$(ud)(su)$ $[\Lambda\to{\rm p}\pi]$, $(ud)(cs)$ $[{\rm D}\to{\rm K}\pi\pi]$.
(Where the subscripts of neutrinos and the antiparticle bar $^-$were not essential, they were dropped in order to avoid overloading the formulas).

In the case of neutral currents, two leptonic, four semi-leptonic, and three non-leptonic interactions were found:
$(\nu_\mu\nu_\mu)\,(ee)$ $[\nu_\mu{\rm e}\to\nu_\mu{\rm e}]$, $(\nu_{\rm e}\nu_{\rm e})\,(ee)$ $[\bar\nu_{\rm e}{\rm e}\to\bar\nu_{\rm e}{\rm e}]$,
$(\nu_\mu\nu_\mu)\,(dd), (\nu_\mu\nu_\mu)\,(uu)$ $[\nu_\mu+$ nucleus $\to\nu_\mu+$ hadrons, $\nu_\mu{\rm p}\to\nu_\mu{\rm p}]$, $(ee)(uu), (ee)(dd)$ [e + p $\to$ e+ hadrons, photons in bismuth],
$(dd)(dd), (uu)(uu), (dd)(uu)$ [P-odd nuclear forces].
In two of the above cases, the same physical phenomenon results both from charged and from neutral currents. These are the scattering process $\bar\nu_{\rm e}{\rm e}\to\bar\nu_{\rm e}{\rm e}$, and the nuclear parity-violating interaction between nucleons. A special analysis is required to separate the contributions of charged and neutral currents to these processes.

Each of the 156 interactions shown in figs. 1.6 and 1.7 generates a number of related processes. We have already mentioned that according to quantum field theory, field operators describe the production and annihilation of both particles and antiparticles. Hence, the same interaction results in several processes. Thus, the interaction $(\mu\nu)(ud)$ is responsible for muon capture $\mu^-{\rm p}\to{\rm n}\nu$, decay of the π-meson $\pi^+\to\mu^+\nu$, neutrino reactions of the type $\nu_\mu+$ nucleon $\to\mu^-+$hadrons, and so on.

Figs. 1.6 and 1.7 obviously invite the following questions:
(i) What are the couplings between different currents?

[0]*Decays of Υ''' mesons into B and $\bar B$ mesons containing single b-quarks were observed in the reaction ${\rm e}^+{\rm e}^-\to\Upsilon'''\to{\rm B}\overline{\rm B}$ in 1980, with charmed mesons dominating the decay products of B-mesons. The observed decays of B mesons seem to be caused by the interactions (bc) $(e\nu), (bc)(\mu\nu)$, and $(bc)(ud)$. This means that one more current, namely, bc, should be underlined in fig. 1.6.

(ii) What is the space-time structure of the different currents and what are its experimental corollaries?
(iii) What properties are anticipated for W - and Z -bosons?

5.1.4 1.4. About the outline of this book

The first two questions are discussed in Chapters 1 through 17, devoted mostly to a phenomenological analysis of a number of weak processes at low energies (below the production threshold of W - and Z -bosons). The second part of the book treats the high-energy physics of weak interactions (at energies above the production threshold of W - and Z -bosons, i.e. in the range that the experimenters plan to reach in the eighties). The idea of a unified electroweak interaction, as stated in the standard model of electroweak interaction, makes the backbone of this part of the book.

In the low-energy limit, the fact that current interactions are mediated by intermediate bosons, is immaterial. We are thus justified in referring to an effective local interaction between currents. For instance, for muon decay, the non-local graph reduces to a local four-fermion interaction graph (see fig. 1.8). This local (i.e. occurring in a single world-point) four-fermion interaction is characterized by the Fermi constant $G \cong 10^{-5} m_{\mathrm{p}}^{-2}$. (The system of units employed throughout the book assumes $\hbar = c = 1$.) The same coupling constant characterizes (although with some qualifications) the remaining 155 four-fermion interactions. The next chapter deals with the form of the effective four-fermion lagrangian of the weak interaction in more detail.

The first part of the book is thus devoted to the applications of the theory of four-fermion weak interactions. The second part starts with exposing the

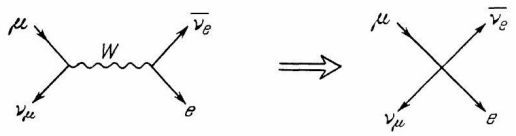


Fig. 1.8.

weak spots of the four-fermion theory and presents the gauge theory of the unified electroweak interaction. Then we discuss the corollaries of this last theory.

From the purely theoretical point of view it would be more logical, of course, to choose another, deductive approach. Namely, the book should have started with presenting the SU(2)× U(1) symmetry and its spontaneous breaking, writing down the lagrangian of the electroweak interaction and discussing the properties of intermediate bosons, and only then should the results of the theory for low-energy processes have been described. I am of the opinion, however, that the presentation must be based on the phenomena which have been investigated not only theoretically but experimentally as well.

With the plan of the book as chosen here, the reader gradually assimilates important elements of the theory, such as particle states with a definite helicity. He will learn about the experiments from which the main parameters of the theory have been extracted. He will recognize the inherent contradictory nature of the four-fermion theory and the need to introduce the vector and scalar intermediate bosons.

Naturally, the book will unavoidably take on an archaic appearance after the W-, Z-, and especially H-bosons will have been found experimentally. But if it helps to bring us closer to these discoveries, I shall consider its mission fulfilled.

5.2 2 Structure of weak currents

In the introduction we gave a qualitative "bird's eye view" of the weak interaction. Let us discuss now the quantitative description of weak currents. It was mentioned above that the low-energy behavior of weak processes is represented very well by an effective four-fermion lagrangian comprising two terms:

$$\mathcal{L}^{\mathrm{w}}(x) = \mathcal{L}^{\mathrm{ch}}(x) + \mathcal{L}^{\mathrm{n}}(x).$$

Here $\mathcal{L}^{\mathrm{ch}}$ is the Lagrangian of the interaction of charged currents, and $\mathcal{L}^{\mathbf{n}}$ is that for neutral currents:

$$\mathcal{L}^{\mathrm{ch}}(x) = \sqrt{\frac{1}{2}} G j^{\alpha+}(x) j_{\alpha}(x)$$
$$\mathcal{L}^{\mathrm{n}}(x) = \rho \sqrt{\frac{1}{2}} G j^{0\alpha}(x) j^{0}_{\alpha}(x)$$

where $j^{\alpha}(x)$ is the charged current (it decreases the particle charge by unity), $j^{+\alpha}(x)$ the hermitian conjugate current (increasing the particle charge by unity), and $j^{0\alpha}$ a neutral current (it is diagonal, i.e. transforms the particle into itself). As mentioned in the introduction, $G \cong 10^{-5} m_{\mathrm{p}}^{-2}$, and the factor $\sqrt{\frac{1}{2}}$ is a tribute to tradition. According to the standard theory of the electroweak interaction (see Chapter 22) the dimensionless parameter ρ equals unity. This prediction agrees with the experimental data within $\simeq \pm 3\%$ accuracy.

The interaction of currents in the lagrangians $\mathfrak{L}^{\mathrm{ch}}$ and $\mathfrak{L}^{\mathrm{n}}$ is local, that is the interaction takes place only when the operators of the two currents act at the same world-point. The four-fermion weak interaction is sometimes referred to as the universal interaction; this implies that different currents interact with the same coupling constant G. This statement of universality calls for serious qualifications which will be given later in this chapter.

5.2.1 2.1. Left-handed charged currents

Whenever the space-time structure of a charged current yielded to experimental determination, it was found to be of the type

$$\bar{f} O^{\mathrm{L}}_{\alpha} i,$$

where i and f, the operators of the initial and final particles, are Dirac bispinors, $\bar{f} = f^{+}\gamma_0$, and the matrix O^{L}_{α} is of the form

$$O^{\mathrm{L}}_{\alpha} = \gamma_{\alpha}\left(1 + \gamma_5\right), \quad \alpha = 0, 1, 2, 3.$$

The reader is reminded that $\gamma^{\alpha} = (\gamma^0, \gamma), \gamma_{\alpha} = (\gamma_0, -\gamma)$, where

$$\gamma^0 = \gamma_0 = \begin{pmatrix} 1 & 0 \\ 0 & -1 \end{pmatrix}, \quad \gamma = \begin{pmatrix} 0 & \sigma \\ -\sigma & 0 \end{pmatrix},$$
$$\gamma_5 = \gamma^5 = -i\gamma^0\gamma^1\gamma^2\gamma^3 = -\begin{pmatrix} 0 & 1 \\ 1 & 0 \end{pmatrix}$$

(the properties of Dirac matrices γ are given in the appendix). The quantity $\bar{f} O^{\mathrm{L}}_{\alpha} i$ is the difference between a vector $V(\gamma_{\alpha})$ and an axial vector $A(\gamma_5\gamma_{\alpha})$. Consequently, the interaction of charged currents is referred to as the universal $V - A$ interaction.

By virtue of the anticommutation of the matrices γ_5 and γ_{α},

$$O_\alpha^{\mathrm{L}} = \gamma_\alpha\,(1+\gamma_5) = \frac{1}{2}\,(1-\gamma_5)\,\gamma_\alpha\,(1+\gamma_5)\,.$$

We can write, therefore,

$$\bar{f} O_\alpha^{\mathrm{L}} i = 2 f_{\mathrm{L}} \gamma_\alpha i_{\mathrm{L}},$$

where

$$i_{\mathrm{L}} = \frac{1}{2}\,(1+\gamma_5)\,i, \quad \bar{f}_{\mathrm{L}} = \bar{f}\frac{1}{2}\,(1-\gamma_5)\,.$$

The suffix L indicates that i_{L} and f_{L} are the so-called left-handed components o Dirac bispinors. In order to clarify this term, consider a wave function

$$\psi_L = \frac{1}{2}\,(1+\gamma_5)\,\psi,$$

where ψ satisfies the Dirac equation

$$(\hat{p} - m)\psi = (E\gamma_0 - \boldsymbol{p}\cdot\boldsymbol{\gamma} - m)\,\psi = 0$$

(as usual, $\hat{a} \equiv a^\alpha \gamma_\alpha = a^0\gamma_0 - \boldsymbol{a}\cdot\boldsymbol{\gamma}$ for any 4-vector a^α). Expressing the bispinor ψ via two-component spinors φ and χ,

$$\psi = \begin{pmatrix}\varphi\\ \chi\end{pmatrix},$$

we obtain that the Dirac equation yields a relationship between χ and φ :

$$\chi = \frac{\boldsymbol{\sigma}\cdot\boldsymbol{p}}{E+m}\varphi.$$

Now the explicit form of the matrix γ_5 yields that

$$\psi_{\mathrm{L}} = \frac{1}{2}\,(1+\gamma_5)\,\psi = \frac{1}{2}\begin{pmatrix} 1 & -1\\ -1 & 1\end{pmatrix}\begin{pmatrix}\varphi\\ \chi\end{pmatrix} = \frac{1}{2}\begin{pmatrix}\varphi-\chi\\ \chi-\varphi\end{pmatrix}$$

that is ψ_L contains the combination $\varphi-\chi$ and not the combination $\varphi+\chi$. Taking the above expression for χ, we obtain that

$$\varphi - \chi = \left(1 - \frac{\boldsymbol{\sigma}\cdot\boldsymbol{p}}{E+m}\right)\varphi.$$

In the ultra-relativistic limit, that is for $E \gg m$ and $v = |\boldsymbol{p}|/E \to 1$, we obtain

$$\varphi - \chi \cong (1 - \boldsymbol{\sigma}\cdot\boldsymbol{n})\varphi,$$

where $\boldsymbol{n} = \boldsymbol{p}/|\boldsymbol{p}|$ is a unit vector in the direction of the particle momentum. If a coordinate axis z is directed along $\boldsymbol{n}$, then

$$(\varphi - \chi) \cong (1 - \sigma_z)\,\varphi = \begin{pmatrix} 0 & 0\\ 0 & 1\end{pmatrix}\varphi.$$

Now let us take into account that the two-component spinor $\varphi = \binom{1}{0}$ represents a particle with a spin along z, and $\varphi = \binom{0}{1}$ a particle with the opposite direction of spin. Consequently, $\psi_{\mathrm{L}} = 0$ if $\varphi = \binom{1}{0}$, and $\psi_{\mathrm{L}} \neq 0$ if $\varphi = \binom{0}{1}$, so that ψ_{L} represents a particle with spin in the direction opposite to that of its momentum. Such particles are said to possess left-handed helicity, or left-handed polarization. A particle is said to possess right-handed helicity, or

polarization, if its spin is directed along its momentum. The concept of helicity is not Lorentz invariant if the particle mass is non-zero. The helicity of such a particle depends upon the motion of the observer's frame of reference. For example, it will change sign if we try to catch up with the particle at a speed above its velocity. Overtaking a particle is the more difficult, the higher its velocity, so that helicity becomes a better quantum number as velocity increases. It is an exact quantum number for massless particles (neutrinos and photons).

The above space-time structure of charged currents means that only left-handed components of bispinor operators are involved. This means further that at $v \to 1$, particles have only left-handed helicity, and antiparticles only right-handed helicity.

5.2.2 2.2. Breaking of P - and C-invariance

The $V - A$ nature of the charged current implies that the weak interaction is not invariant with respect to space inversion. Indeed, this operation affects the signs of V - and A-terms in an opposite manner, so that the terms $VV^+$and AA^+in a lagrangian $(V - A)(V - A)^+ = VV^+ + AA^+ - VA^+ - AV^+$do not change sign while $VA^+$and AV^+do. P-violation in weak interactions is manifested by a number of physical effects, and among them by $\boldsymbol{P}$-odd $\boldsymbol{J}\cdot\boldsymbol{p}$-type correlations between the particle momentum $\boldsymbol{p}$ and its spin or the spin of another particle, $\boldsymbol{J}$. We recall that under space inversion, $\boldsymbol{p} \to -\boldsymbol{p}, \boldsymbol{J} \to +\boldsymbol{J}$, P-odd correlations of this type were first found experimentally in 1956 in β-decay and in decays of elementary particles.

Furthermore, the product $(V-A)(V-A)^+$is not invariant with respect to charge conjugation since this operation does not affect the signs of the terms in $\mathrm{VV}^+ + AA^+$, but reverses those of the terms in $\mathrm{VA}^+ + AV^+$. Violation of charge conjugation invariance is best seen in the neutrino: charge conjugation invariance demands that a weak process emitting a left-handed neutrino be transformed to a weak process emitting a left-handed antineutrino; this latter, however, is stated by the $V - A$ theory to be non-existent.

Breaking of CP invariance is a more delicate problem (see Chapter 12). CP may be broken by the complex coefficients with which the twelve currents of fig. 1.6 enter the total charged current j.

5.2.3 2.3. Universality of the charged current

It has been mentioned above that according to the theory, three leptonic pairs enter the weak current in a symmetrical manner, and the total leptonic current has the form

$$j_\alpha^\ell = \bar{e}O_\alpha^{\mathrm{L}}\nu_{\mathrm{e}} + \bar{\mu}O_\alpha^{\mathrm{L}}\nu_\mu + \bar{\tau}O_\alpha^{\mathrm{L}}\nu_\tau.$$

A quark current can be written in a similar manner:

$$j_\alpha^{\mathrm{h}} = \bar{d}'O_\alpha^{\mathrm{L}}u + \bar{s}'O_\alpha^{\mathrm{L}}c + \bar{b}'O_\alpha^{\mathrm{L}}t,$$

where d', s', b' are orthonormalized linear combinations of d−, s−, and b-quarks. Nine coefficients characterizing these combinations can be expressed, in the most general form, in terms of three Euler angles $\theta_1, \theta_2, \theta_3$ and one phase factor δ. These coefficients will be written in their explicit form in Chapter 15; now it is sufficient to mention that if $b' = b$, that is if transitions bu and $\bar{b}c$ can be neglected, we are left with a single angle θ
characterizing mixing of d - and s-quarks:

$$d' = d\cos\theta + s\sin\theta$$
$$s' = -d\sin\theta + s\cos\theta$$

The angle θ is called the Cabibbo angle. (Sometimes we shall replace θ with θ_{C}.) Experimental data on decays of strange particles yield $\theta \cong 13^{\circ}$.

The following correspondence is therefore found between leptons and quarks in weak interactions:

$$\begin{pmatrix} \nu_{\mathrm{e}} & \nu_{\mu} & \nu_{\tau} \\ e & \mu & \tau \end{pmatrix} \leftrightarrow \begin{pmatrix} u & c & t \\ d' & s' & b' \end{pmatrix};$$

(obviously, the correspondence

$$\begin{pmatrix} \nu_{\mathrm{e}} & \nu_{\mu} & \nu_{\tau} \\ e & \mu & \tau \end{pmatrix} \leftrightarrow \begin{pmatrix} u' & c' & t' \\ d & s & b \end{pmatrix},$$

where u', c', t' are linear combinations of u−, c−, t-quarks, would be absolutely equivalent). The variety of weak decays of hadrons stems from the fact that quark doublets do not include particles with definite (and non-identical) masses, but rather, their linear combinations. There is no such mixing in the case of leptons if the neutrinos are massless.

Experimenters can go a long way to test the details of the theoretical scheme as presented above. For instance, the coefficient for the term $\bar{\tau} O_{\alpha}^{\mathrm{L}} \nu_{\tau}$ was not measured, and very little is known about experimental values of the parameters θ_2, θ_3 characterizing the admixture of b-quarks to d- and s-quarks, and about the parameter δ characterizing the breaking of CP in the lagrangian $\mathfrak{L}^{\mathrm{ch}}$.

5.2.4 2.4. The neutral current

Two peculiarities of neutral currents stand out when one compares them with charged currents: first, they are diagonal, that is transform a particle into itself, and secondly, they contain, in addition to left-handed components of spinors, right-handed ones as well.

The absence of non-diagonal terms in a neutral current is born out by the fact that experiment does not detect processes which would occur with high decay rates if such terms existed. Here we mean the process $\mu \to \mathrm{ee}$ and a related process $\mu \to \mathrm{e}\gamma$, which would reveal the current $\mu\mathrm{e}$, and also the processes $\mathrm{K} \to \pi \mathrm{e}\bar{\mathrm{e}}, \mathrm{K} \to \pi\mu\bar{\mu}, \mathrm{K} \to \pi\nu\bar{\nu}$ which would reveal the current ds. (The decay $\mathrm{K}^0 \to \mu\bar{\mu}$ recorded with the relative probability of the order of 10^{-8}, results from the joint action of the non-leptonic interaction of charged currents (du)(us) and the electromagnetic interaction.)

That neutral currents comprise both the left-handed and right-handed components, is also an experimental fact (see Chapter 22). In the general case, the neutral current may be written as a sum of twelve terms:

$$j_{\alpha}^{0} = \sum_{i} \left(g_{\mathrm{L}}^{i} \overline{\psi_i} O_{\alpha}^{\mathrm{L}} \psi_i + g_{\mathrm{R}}^{i} \overline{\psi_i} O_{\alpha}^{\mathrm{R}} \psi_i \right)$$

where

$$i = \nu_e, \nu_{\mu}, \nu_{\tau}, \mathrm{e}, \mu, \tau, \mathrm{u}, \mathrm{c}, \mathrm{t},\ \mathrm{d},\ \mathrm{s},\ \mathrm{b},$$
$$O_{\alpha}^{\mathrm{L}} = \gamma_{\alpha}\left(1+\gamma_5\right), \quad O_{\alpha}^{\mathrm{R}} = \gamma_{\alpha}\left(1-\gamma_5\right),$$

and g_{L}^{l} and g_{R}^{l} are numerical coefficients. As shown in Chapter 22, the unified theory of weak and electromagnetic interactions relates coefficients g_{L}^{i} and g_{R}^{i} to the charges of particles:

$$\begin{array}{ll} g_{\mathrm{L}}^{i} = \frac{1}{2}, g_{\mathrm{R}}^{i} = 0 & \text{for } i = \nu_{\mathrm{e}}, \nu_{\mu}, \nu_{\tau}, \\ g_{\mathrm{L}}^{i} = -\frac{1}{2} + \xi, g_{\mathrm{R}}^{i} = +\xi & \text{for } i = \mathrm{e}, \mu, \tau, \\ g_{\mathrm{L}}^{i} = \frac{1}{2} - \frac{2}{3}\xi, g_{\mathrm{R}}^{i} = -\frac{2}{3}\xi & \text{for } i = \mathrm{u}, \mathrm{c}, \mathrm{t}, \\ g_{\mathrm{L}}^{i} = -\frac{1}{2} + \frac{1}{3}\xi, g_{\mathrm{R}}^{i} = +\frac{1}{3}\xi & \text{for } i = \mathrm{d},\ \mathrm{s},\ \mathrm{b}, \end{array}$$

where $\xi = \sin^2\theta_W$, and θ_W is the Weinberg angle. Experiments give:

$$0.20 \lesssim \xi \lesssim 0.25$$

Chapter 22 will show how this value of ξ is derived from the experimental data on elastic and inelastic scattering of ν_μ and $\bar{\nu}_\mu$ by nucleons, and from the cross section of deep-inelastic scattering of electrons on nucleons measured as a function of the longitudinal polarization of electrons. This value of ξ is in agreement with the data on the scattering processes $\nu_\mu e \to \nu_\mu e$ and $\bar{\nu}_e e \to \bar{\nu}_e e$.

This concludes a brief review of the properties of weak currents, and we are now ready to start systematic calculations of weak processes.

5.3 3 Muon decay

The muon decay $\mu \to e\nu\bar{\nu}$ is a process which traditionally opens calculations of weak decays in textbooks. The reason is two-fold. First, this is a pure leptonic process not involving hadrons, and therefore is easily calculated to the end. Second, experimentally this is one of the most thoroughly investigated decays of elementary particles. In this chapter we calculate the electron spectrum, the total decay probability, and finally the angular and spin correlations in polarized muon decays.

5.3.1 3.1. Decay amplitude

Let us consider the decay $\mu^-(p) \to e^-(k)\bar{\nu}_e(q_1)\,\nu_\mu(q_2)$ (quantities in parentheses denote 4 - momenta of the particles). The Feynman graph of this process given in fig. 3.1a is equivalent to that of fig. 3.1b. In this second case the matrix element is of the form

$$M = \sqrt{\frac{1}{2}} G \bar{\nu}_\mu O^\alpha \mu \bar{e} O_\alpha \nu_e$$

where $O_\alpha \equiv O_\alpha^L = \gamma_\alpha(1+\gamma_5)$, and particle symbols stand for their wave functions. By using the Fierz transformation (see appendix) this matrix element can be recast in the form

$$M = -\sqrt{\frac{1}{2}} G \bar{e} O^\beta \mu \bar{\nu}_\mu O_\beta \nu_e.$$

The complex conjugate of this last expression is

$$\begin{aligned} M^* = M^+ &= -\sqrt{\frac{1}{2}} G \nu_e^+ O^{\beta+} \gamma_0 \nu_\mu \mu^+ O_\beta^+ \gamma_0 e \\ &= -\sqrt{\frac{1}{2}} G \nu_e^+ \gamma_0\gamma_0 O^{\beta+} \gamma_0 \nu_\mu \mu^+ \gamma_0\gamma_0 O_\beta^+ \gamma_0 e = -\sqrt{\frac{1}{2}} \bar{\nu}_e O^\beta \nu_\mu \bar{\mu} O_\beta e. \end{aligned}$$

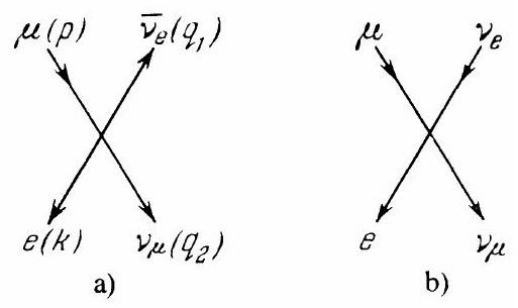


Fig. 3.1.

[We made use of the fact that $\gamma_0 O^{\beta+}\gamma_0 = O^\beta$, because $\gamma_0\left[\gamma_0\left(1+\gamma_5\right)\right]^+\gamma_0 = \gamma_0\left(1+\gamma_5\right)\gamma_0\gamma_0 = \gamma_0\left(1+\gamma_5\right)$, and also

$$\gamma_0\left[\boldsymbol{\gamma}\left(1+\gamma_5\right)\right]^+\gamma_0 = \gamma_0\left(1+\gamma_5\right)\left(-\boldsymbol{\gamma}\right)\gamma_0 = \left(1-\gamma_5\right)\boldsymbol{\gamma} = \boldsymbol{\gamma}\left(1+\gamma_5\right)\Big].$$

Similarly, $\gamma_0 O_\beta^+\gamma_0 = O_\beta$. Therefore,

$$\begin{aligned}|M|^2 = MM^* &= -\frac{1}{2}G^2\bar{\nu}_\mu O^\alpha\mu\bar{e}O_\alpha\nu_{\mathrm{e}}\bar{\nu}_{\mathrm{e}}O^\beta\nu_\mu\bar{\mu}O_\beta e\\ &= -\frac{1}{2}G^2\bar{\nu}_\mu O^\alpha\mu\bar{\mu}O_\beta e\bar{e}O_\alpha\nu_{\mathrm{e}}\bar{\nu}_{\mathrm{c}}O^\beta\nu_\mu\end{aligned}$$

As demonstrated in the appendix, the density. matrix for an unpolarized Dirac particle has the form

$$\sum_s u^k(s)\bar{u}_i(s) = (\hat{p}+m)_i^k,$$

where the summation is over the polarization states of the particle; p is the particle 4-momentum and m its mass; and i, k are bispinor suffices, $i, k = 1, 2, 3, 4$. Using this we obtain

$$\overline{|M|^2} = -\frac{1}{2}G^2\,\mathrm{Tr}\,\hat{q}_2 O^\alpha\left(\hat{p}+m_\mu\right)O_\beta\left(\hat{k}+m_{\mathrm{e}}\right)O_\alpha\hat{q}_1O^\beta.$$

The bar over $|M|^2$ denotes summation over spin states; Tr denotes the trace of the product of matrices to the right of it. Since $\gamma_5\gamma_\alpha = -\gamma_\alpha\gamma_5$, and since $\left(1+\gamma_5\right)^2 = 2\left(1+\gamma_5\right)$,

$$\begin{aligned}\overline{|M|^2} &= -8\cdot\frac{1}{2}G^2\,\mathrm{Tr}\,\hat{q}_2\gamma^\alpha\hat{p}\gamma_\beta\hat{k}\gamma_\alpha\hat{q}_1\gamma^\beta\left(1+\gamma_5\right)\\ &= 8G^2\,\mathrm{Tr}\,\hat{q}_2\hat{k}\gamma_\beta\hat{p}\hat{q}_1\gamma^\beta\left(1+\gamma_5\right) = 32G^2\left(pq_1\right)\mathrm{Tr}\,\hat{q}_2\hat{k}\left(1+\gamma_5\right)\\ &= 128G^2\left(pq_1\right)\left(kq_2\right)\end{aligned}$$

(In deriving this equality, we took into account that $\gamma^\alpha\hat{A}\hat{B}\hat{C}\gamma_\alpha = -2\hat{C}\hat{B}\hat{A}$, $\gamma^\alpha\hat{A}\hat{B}\gamma_\alpha = 4AB$, see Chapter 29.)

5.3.2 3.2. Decay probability

It is now possible to calculate the probability of the muon decay by means of the general expression (see Chapter 29, sect. 4)

$$\mathrm{d}\Gamma = \frac{\overline{|M|^2}}{2\cdot 2m}\,\mathrm{d}\Phi$$

Here $\mathrm{d}\Gamma$ is the differential probability of decay per unit volume of phase space $\mathrm{d}\Phi$, and the factor $\frac{1}{2}$ appears because of the averaging (and not summation) over muon polarizations; the factor $2m$ (where m is the muon mass) appears because of the chosen normalization of wave functions of particles. As shown in the appendix,

$$\mathrm{d}\Phi = (2\pi)^4 \delta^4 (p - k_1 - q_1 - q_2) \frac{\mathrm{d}\boldsymbol{k}}{2E(2\pi)^3} \frac{\mathrm{d}\boldsymbol{q}_1}{2\omega_1(2\pi)^3} \frac{\mathrm{d}\boldsymbol{q}_2}{2\omega_2(2\pi)^3}$$

where E, ω_1, ω_2 are the energies of the electron, $\bar{\nu}_\mathrm{e}$, and ν_μ; $\boldsymbol{k}, \boldsymbol{q}_1$, and $\boldsymbol{q}_2$ stand for their momenta. Neutrinos being not observed, let us integrate over their momenta. This means that we must calculate the integral

$$I_{\alpha\beta} = \int q_{1\alpha} q_{2\beta} \frac{\mathrm{d}\boldsymbol{q}_1}{\omega_1} \frac{\mathrm{d}\boldsymbol{q}_2}{\omega_2} \delta^4 (q_1 + q_2 - q)$$

where $q = p - k$. The anticipated result can be written as a sum of two mutually orthogonal terms:

$$I_{\alpha\beta} = A \left(q^2 g_{\alpha\beta} + 2 q_\alpha q_\beta \right) + B \left(q^2 g_{\alpha\beta} - 2 q_\alpha q_\beta \right)$$

Here $g_{\alpha\beta}$ is a metric tensor (see Chapter 29), q is the total 4-momentum of two neutrinos, and A and B are dimensionless coefficients that we shall now determine. By multiplying both sides of the equality by $q^2 g^{\alpha\beta} - 2 q^\alpha q^\beta$, we obtain

$$\begin{aligned} B \cdot 4q^4 &= \int q_{1\alpha} q_{2\beta} \left(q^2 g^{\alpha\beta} - 2 q^\alpha q^\beta \right) \cdots \\ &= \int \left[q^2 \left(q^1 q^2 \right) - 2 \left(q q_1 \right) \left(q q_2 \right) \right] \cdots = 0 \end{aligned}$$

since $q^2 = (q_1 + q_2)^2 = 2 q_1 q_2, q q_1 = (q_1 + q_2, q_1) = q_1 q_2, q q_2 = (q_1 + q_2, q_2) = q_1 q_2, q_1^2 = q_2^2 = 0$ (the neutrino is massless). By multiplying both sides of the tensor equality by $q^2 g^{\alpha\beta} + 2 q^\alpha q^\beta$, we obtain

$$\begin{aligned} A \cdot 12 q^4 &= q^4 \int \frac{\mathrm{d}\boldsymbol{q}_1}{\omega_1} \frac{\mathrm{d}\boldsymbol{q}_2}{\omega_2} \delta^4 (q_1 + q_2 - q) = q^4 \int \frac{\mathrm{d}\boldsymbol{q}_1}{\omega_1 \omega_2} \delta (2\omega_1 - \omega) \\ &= q^4 \cdot 4\pi \cdot \frac{1}{2} \end{aligned}$$

so that $A = \frac{1}{6}\pi$. (The integral above is taken in the center-of-mass frame of two neutrinos). Finally,

$$I_{\alpha\beta} = \frac{1}{6} \pi \left(q^2 g_{\alpha\beta} + 2 q_\alpha q_\beta \right)$$

where $q = p - k$. Substitution of this result into the expression for the decay width yields

$$\begin{aligned} \mathrm{d}\Gamma &= \frac{G^2}{2 \cdot 2m} \frac{128}{(2\pi)^5 2 \cdot 2} \frac{1}{6} \pi p^\alpha k^\beta \left[q^2 g_{\alpha\beta} + 2 q_\alpha q_\beta \right] \frac{\mathrm{d}\boldsymbol{k}}{2E} \\ &= \frac{G^2}{48\pi^4 m} \left[q^2 (pk) + 2 (qp)(qk) \right] \frac{\mathrm{d}\boldsymbol{k}}{E}. \end{aligned}$$

As the electron mass is negligibly small compared to its energy, we have $qk = (p - k, k) = pk = mE, q^2 = (p - k)^2 = p^2 - 2pk = m^2 - 2mE$. Integration over the electron direction yields 4π, and we obtain

$$\begin{aligned} \mathrm{d}\Gamma &= \frac{G^2}{12\pi^3 m}(pk)\left(p^2 - 2pk + 2p^2 - 2pk\right) E\ \mathrm{d}E \\ &= \frac{G^2}{12\pi^3}\left(3m^2 - 4mE\right) E^2\ \mathrm{d}E = \frac{G^2 m^5}{96\pi^3}(3-2\varepsilon)\varepsilon^2\ \mathrm{d}\varepsilon \end{aligned}$$

where $\varepsilon = E/E_{\max} = 2E/\mathrm{m}$.
The electron spectrum in muon decay, for the most general form of the four-fermion interaction, can be shown to take the form

$$\Gamma(\varepsilon)\mathrm{d}\varepsilon = 12\Gamma\left[(1-\varepsilon) - \frac{2}{9}\rho(3-4\varepsilon)\right]\varepsilon^2\ \mathrm{d}\varepsilon,$$

where the coefficient ρ is called the Michel parameter (the term proportional to ρ gives zero contribution when integrated over the whole range $0 \le \varepsilon \le 1$). Clearly, the spectrum obtained above corresponds to $\rho = 0.75$. Integration over the electron energy yields the total decay width

$$\Gamma = \frac{G^2 m^5}{96\pi^3}\int_0^1 (3-2\varepsilon)\varepsilon^2\ \mathrm{d}\varepsilon = \frac{G^2 m^5}{192\pi^3}$$

After correction for virtual photons, one obtains (see references in Chapter 28)

$$\Gamma = \frac{G^2 m^5}{192\pi^3}\left[1 - \frac{\alpha}{2\pi}\left(\pi^2 - \frac{25}{4}\right)\right].$$

Comparison of this expression with the experimentally measured muon lifetime gives the familiar value of the coupling constant G.

5.3.3 3.3. Decay of polarized muon

Let the spin of a muon in its rest frame be directed along the unit vector $\boldsymbol{\eta}$. The muon density matrix then becomes (see appendix)

$$u^k(s)\bar{u}_i(s) = \frac{1}{2}\left[(\hat{p}+m)\left(1-\gamma_5\right)\hat{s}\right]_i^k,$$

where a 4 -vector s^α has the following properties: $s^2 = -1, sp = 0$. In the muon rest frame, $s^0 = 0, \boldsymbol{s} = \boldsymbol{\eta}$. In the reference frame in which the muon moves with momentum $\boldsymbol{p}$,

$$s^0 = \frac{\boldsymbol{\eta}\cdot\boldsymbol{p}}{m}, \quad s = \boldsymbol{\eta} + \frac{\boldsymbol{p}(\boldsymbol{\eta}\cdot\boldsymbol{p})}{m(E+m)}.$$

If we substitute in the above calculations

$$(\hat{p}+m) \to \frac{1}{2}(\hat{p}+m)\left(1-\gamma_5\hat{s}\right),$$

we will have to substitute $p - ms$ for p in the earlier result

$$\mathrm{d}\Gamma = \frac{G^2}{48\pi^4 m}\left[q^2(pk) + 2(qp)(qk)\right]\frac{\mathrm{d}\boldsymbol{k}}{E}.$$

[This is readily confirmed by considering that part of the trace which comprises the muon density matrix and its neighbor terms

$$\begin{aligned}
&\mathrm{Tr}\cdots(1+\gamma_5)\,(\hat{p}+m)\,(1-\gamma_5\hat{s})\,\gamma_\beta\,(1+\gamma_5)\cdots\\
&\quad=\mathrm{Tr}\cdots(1+\gamma_5)\,(\hat{p}-m\gamma_5\hat{s}+m+\gamma_5\hat{p}\hat{s})\,(1-\gamma_5)\,\gamma_\beta\cdots\\
&\quad=\mathrm{Tr}\cdots(1+\gamma_5)\,(\hat{p}-m\gamma_5\hat{s})\,\gamma_\beta\,(1+\gamma_5)\cdots\\
&\quad=\mathrm{Tr}\cdots(1+\gamma_5)\,(\hat{p}-m\hat{s})\gamma_\beta\,(1+\gamma_5)\cdots\,.
\end{aligned}$$

The terms $m+\gamma_5\hat{p}\hat{s}$ cancelled out since they were multiplied by $(\,1+\gamma_5\,)\times(1-\gamma_5)$. As for the factor $\frac{1}{2}$, it was already taken into account in the expression for the probability indicating averaging over muon polarizations, so that we need not do it a second time.] With muon polarization taken into account,

$$\begin{aligned}
\mathrm{d}\Gamma=&\frac{G^2}{48\pi^4 m}\left\{\left[q^2(pk)+2(qp)(qk)\right]-m\left[q^2(sk)+2(qs)(qk)\right]\frac{\mathrm{d}\boldsymbol{k}}{E}\right\}\\
=&\frac{G^2}{48\pi^4 m}\left\{(pk)\left[(p-k)^2+2\left(p^2-pk\right)\right]\right.\\
&\left.-m(sk)\left[(p-k)^2-2pk\right]\right\}\frac{\mathrm{d}\boldsymbol{k}}{E}\\
=&\frac{G^2m^5}{384\pi^4}[(3-2\varepsilon)+\boldsymbol{\eta}\cdot\boldsymbol{n}(1-2\varepsilon)]\varepsilon^2\;\mathrm{d}\varepsilon\;\mathrm{d}\Omega
\end{aligned}$$

where $\boldsymbol{n}=\boldsymbol{k}/E$ is a unit vector in the direction of the emission of the electron, $\mathrm{d}\Omega=\mathrm{d}\cos\theta\mathrm{d}\varphi$ is an element of the solid angle, and $\cos\theta=\boldsymbol{n}\cdot\boldsymbol{\eta}$. The above derivation uses that $qs=(p-k,s)=-ks$ since $ps=0$; moreover, we take into consideration that in the muon rest frame, $ks=k^0s_0-\boldsymbol{k}\cdot\boldsymbol{s}=-E\boldsymbol{n}\cdot\boldsymbol{\eta}$.

The angular distribution integrated over the electron spectrum takes the form

$$\frac{\mathrm{d}\Gamma(\cos\theta)}{\Gamma}=\frac{1}{2}\left(1-\frac{1}{3}\cos\theta\right)\mathrm{d}\cos\theta$$

The above formulas cover the case when the electron polarization is not measured. If we were interested in the decay probability as a function of electron polarization, k in the expression for $|M|^2$ would have to be replaced by $\frac{1}{2}\,(k-m_\mathrm{e}s_\mathrm{e})$ where s_e is a vector characterizing the electron polarization: $s_\mathrm{e}^2=-1, s_\mathrm{e}k=0$. Explicit expressions for the components of $s_\mathrm{e}, s_\mathrm{e}^0=\boldsymbol{k}\cdot\boldsymbol{\zeta}/m_\mathrm{e}, \boldsymbol{s}_\mathrm{e}=\boldsymbol{\zeta}+(\boldsymbol{k}\cdot\boldsymbol{\zeta})\boldsymbol{k}/m_\mathrm{e}\,(E+m_\mathrm{e})$, demonstrate that the components of s_e normal to $\boldsymbol{n}$ can be neglected, in the ultrarelativistic limit, in comparison to s_e^0 and $\boldsymbol{n}\cdot\boldsymbol{s}_\mathrm{e}=(E/m)(\zeta\cdot\boldsymbol{n})$. We obtain therefore that for $v\to1$,

$$\frac{1}{2}\,(k_\alpha-m_\mathrm{e}s_{\mathrm{e}\alpha})\Rightarrow\frac{1}{2}k_\alpha(1-\zeta\cdot\boldsymbol{n}).$$

We have thus reproduced a well-known property of the weak interaction: the left-handed polarization of the emitted relativistic leptons. The probability of the decay $\mu^-\to\mathrm{e}^-\nu_\mu\bar{\nu}_\mathrm{e}$, with the electron polarization taken into account, is then written as

$$\mathrm{d}\Gamma=\Gamma\frac{1}{2}(1-\zeta\cdot\boldsymbol{n})[(3-2\varepsilon)+\boldsymbol{\eta}\cdot\boldsymbol{n}(1-2\varepsilon)]\varepsilon^2\;\mathrm{d}\varepsilon\;\mathrm{d}\cos\theta.$$

Similar calculations for the decay $\mu^+\to\mathrm{e}^+\nu_\mathrm{e}\bar{\nu}_\mu$ would give

$$\mathrm{d}\Gamma=\Gamma\frac{1}{2}(1+\zeta\cdot\boldsymbol{n})[(3-2\varepsilon)-\boldsymbol{\eta}\cdot\boldsymbol{n}(1-2\varepsilon)]\varepsilon^2\;\mathrm{d}\varepsilon\;\mathrm{d}\cos\theta$$

where ε is the positron energy divided by its maximum energy, and $\boldsymbol{n},\boldsymbol{\zeta},\boldsymbol{\eta}$ are unit vectors in the directions of momentum of the positron, its spin, and the muon spin, respectively.

5.3.4 3.4. Qualitative discussion

A number of results derived in this chapter are very easy to interpret qualitatively, without any calculations. First of all, the fact that $\Gamma \sim G^2 m^5$ follows from dimension-based arguments, since $[\Gamma] = \mu$, and $[G] = \mu^{-2}$, where μ has the dimension of mass. We only use that the probability is

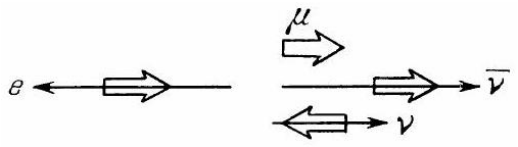


Fig. 3.2.

proportional to G^2 and that the only parameter determining the dynamics of muon decay is the muon mass, since the electron mass can be safely neglected.

Turning to the angular asymmetry, we readily notice that it is neither P nor C-invariant: its signs are different in the left-handed and right-handed reference frames, as well as for the electron and positron in decays of $\mu^-$and μ^+, respectively. Characteristic features of this asymmetry can also be explained. Let us consider an electron with nearly maximum energy ($\varepsilon \sim 1$). In this situation neutrinos (ν and $\bar{\nu}$) must be emitted in the direction opposite to that of the electron (see fig. 3.2) (the phase-space volume of the configuration in which one of them has low momentum, is small). Recalling that the helicities of ν and $\bar{\nu}$ are of opposite signs, we have to conclude that the angular momentum carried by neutrinos is zero. Consequently, the electron must be emitted with its spin parallel to that of the muon. But, the electron helicity being negative, its momentum must be predominantly directed opposite to the muon spin. This is in agreement with the formula derived above for the angular distribution of electrons, which for $\varepsilon \sim 1$ is proportional to ($1 - \boldsymbol{\eta} \cdot \boldsymbol{n}$).

For $\varepsilon \ll 1$, the neutrino and antineutrino move in the opposite directions, with the total spin equal to unity. This time, conservation of angular momentum demands that electrons be emitted along the muon spin direction (see fig. 3.3). Similar arguments will be valid for decays of positive muons.

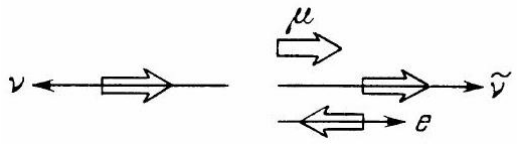


Fig. 3.3.

5.4 4 Strangeness-conserving leptonic decays of hadrons. Properties of the ud current

The interaction between quark and leptonic currents leads to the leptonic decays of hadrons, sometimes referred to as semileptonic decays. In particular, the interaction between currents of light leptons,* $e\nu$ and $\mu\nu$, and the current of light quarks, ud, is responsible for decays of charged π-mesons, for β-decay of the neutron and atomic nuclei, for the capture of $\mu^-$by nuclei, and for the decay $\Sigma \to \Lambda e\nu$. The same interaction operates in reactions involving neutrinos (see chapter 17). In the present chapter we shall discuss the general properties of the ud current. The coefficient with which the ud current enters the total charged current is $\cos\theta$, where θ is

the Cabibbo angle: $\cos\theta \cong 0.97$. When writing expressions for amplitudes of specific processes, we shall single out the factor $\cos\theta$ explicitly, and give them in the form

$$M = \sqrt{\frac{1}{2}} G L_\alpha H^\alpha \cos\theta,$$

where L_α is a leptonic matrix element, and H_α a hadronic matrix element. For instance, we obtain in the case of the process $\nu_\ell + \mathrm{i} \to \mathrm{f} + \ell^{**}$

$$L_\alpha = \langle \ell | \bar{\ell} O_\alpha \nu_\ell \, | \nu_\ell \rangle \, \mathrm{e}^{-ikx} = \bar{u}_\ell O_\alpha u_{\nu_\ell},$$
$$H_\alpha = \langle f | \bar{u} O_\alpha d | i \rangle \mathrm{e}^{-iqx},$$

where i is the initial and f the final hadronic state,

$$k = p_\ell - p_\nu, \quad q = p_\mathrm{f} - p_\mathrm{i}.$$

In the general case, H_α is a sum of a polar and an axial vector:

$$H_\alpha = V_\alpha + A_\alpha,$$

where

$$V_\alpha = \langle f | \bar{u} \gamma_\alpha d | i \rangle \mathrm{e}^{-iqx},$$
$$A_\alpha = \langle f | \bar{u} \gamma_\alpha \gamma_5 d | i \rangle \mathrm{e}^{-iqx}.$$

The matrix elements V_α and A_α are expressed in terms of wave functions of hadrons in i and f states, and of their 4-momenta.

5.4.1 4.1. Isotopic properties of the ud current

The ud current is an isovector, since the u - and d -quarks are isospinors. Its vector component is G even, like the ρ-meson, and the axial component is G odd, like the A_1 or π meson. Matrix elements of these currents (V_α and A_α) must have the same properties. (We recall that the G-transformation is a product of charge conjugation and rotation by 180° around the y-axis in isotopic space. The G-parity of an isomultiplet is readily found by means of the formula $G = C_0(-1)^T$, where C_0 is the charge conjugation parity of the truly neutral component of the multiplet, and T is its isospin.)

5.4.2 4.2. Relationship between the vector current ud and the isovector electromagnetic current

There is a profound relationship between the vector currents $\bar{u}\gamma_\alpha d, \bar{d}\gamma_\alpha u$, and the isovector electromagnetic current of hadrons, $\bar{u}\gamma_\alpha u - \bar{d}\gamma_\alpha d$. The relationship stems from the fact that the three currents form a single isotopic triplet. This becomes clearer when we denote the isodoublet $\binom{u}{d}$ by q. Then

$$\bar{u}\gamma_\alpha d = \bar{q}\gamma_\alpha \tau^+ q, \quad \bar{d}\gamma_\alpha u = \bar{q}\gamma_\alpha \tau^- q,$$
$$\bar{u}\gamma_\alpha u - \bar{d}\gamma_\alpha d = \bar{q}\gamma_\alpha \tau_3 q,$$

[0⋆] We recall that the symbol $e\nu$ stands for one of two currents, $e\nu = \bar{e}O_\alpha\nu_\mathrm{e}$ or $\bar{\nu}_\mathrm{e}O_\alpha e$, and similarly, $\mu\nu = \bar{\mu}O_\alpha\nu_\mu$ or $\bar{\nu}_\mu O_\alpha \mu, ud = \bar{u}O_\alpha d$ or $\bar{d}O_\alpha u$, where $O_\alpha = \gamma_\alpha(1+\gamma_5)$. This contracted notation is used when the discussion is of general character.

⋆⋆ We shall denote, in this chapter and hereafter, charged leptons by the symbol ℓ (for e and μ), using also the symbol ν_ℓ for ν_e and ν_μ.

where

$$\tau^+ = \begin{pmatrix} 0 & 1 \\ 0 & 0 \end{pmatrix}, \quad \tau^- = \begin{pmatrix} 0 & 0 \\ 1 & 0 \end{pmatrix}, \quad \tau_3 = \begin{pmatrix} 1 & 0 \\ 0 & -1 \end{pmatrix}.$$

(For these currents to have identical normalization, the last of them must be divided by $\sqrt{}$ 2. Sometimes $\tau^{\pm}$are defined with an additional factor $\sqrt{}$2.)

We recall that the electromagnetic interaction between u- and d-quarks and the electromagnetic field A_α is of the form

$$eA_\alpha \left(\frac{2}{3}\bar{u}\gamma_\alpha u - \frac{1}{3}\bar{d}\gamma_\alpha d \right) = eA_\alpha \left(\frac{1}{2}\bar{q}\gamma_\alpha \tau_3 q + \frac{1}{6}\bar{q}\gamma_\alpha q \right).$$

The isoscalar current $\bar{q}\gamma_\alpha q$ is not the only isoscalar hadronic current. Indeed, there are isoscalar electromagnetic currents of other quarks: $-\frac{1}{3}\bar{s}\gamma_\alpha s$, $+\frac{2}{3}\bar{c}\gamma_\alpha c$, $-\frac{1}{3}\bar{b}\gamma_\alpha b$, and so on. The current $\bar{q}\gamma_\alpha\tau_3 q$ is, on the other hand, the only isovector current which defines isovector electromagnetic form factors of both the hadrons containing only u- and d-quarks and of all other hadrons, strange, charmed, and so on. In fact, the very existence of isotopic multiplets with non-zero isospin ($T \neq 0$) is caused by the presence of the light quarks, u and/or d, in the corresponding hadrons. Matrix elements of the currents $\bar{q}\tau^+\gamma_\alpha q$ and $\bar{q}\tau_3\gamma_\alpha q$ must be identical because they are in the same isotopic multiplet and also because the strong interaction is isotopically invariant. Specifically, the current $\bar{u}\gamma_\alpha d$ must be conserved like the electromagnetic current:

$$\frac{\partial}{\partial x_\alpha}\bar{u}(x)\gamma_\alpha d(x) = 0.$$

Consequently, all matrix elements of the ud current must be transverse:

$$q^\alpha V_\alpha = 0.$$

Before discussing numerous specific manifestations of the conserved vector current, CVC, let us analyze one important result of this conservation: non-renormalizability of the weak charge.

5.4.3 4.3. Weak charge

When the initial and final hadrons of a semi-leptonic decay belong to the same isotopic multiplet (such as the neutron and proton in the β-decay n $\to$ pe$^-\nu$), we can introduce the concept of the weak charge. The weak charge is defined as the time-like component of the 4 -vector V_α for $q = 0$. The weak charge determines the strength of the weak vector interaction in the static limit. Evidently, the weak charge is a matrix element of the integral

$$\int u^+(x)d(x)\mathrm{d}\boldsymbol{x}.$$

The integral is the generator $\hat{T}^+$of the isotopic group SU(2) and its magnitude for a transition $T_3 \leftrightarrow T_3 + 1$ is determined completely by the
hadron isospin T and its projection T_3. In analogy to a well-known relationship for the angular momentum operator, this integral is equal to

$$\sqrt{T(T+1) - T_3\,(T_3+1)}$$

where T_3 refers to the lower of the two components of the isotopic multiplet. This means, in particular, that the weak charge is unity in the β-decay of a neutron, and equals $\sqrt{}$2 in

the β-decay of the π-meson, $\pi^+ \to \pi^0 e^+ \nu_e$. The weak charge has the same value in the so-called superallowed β-transitions in $^{14}O, ^{26\ m}Al, ^{34}Cl, ^{38\ m}K, ^{42}Sc, ^{46}V, ^{50}Mn, ^{54}Co$. The levels involved in these transitions have $J^P = 0^+$and constitute components of isotriplets. It is essential that in the limit of unperturbed isotopic invariance, the magnitude of the weak charge is unaffected by the structure of the decaying hadron. As a result, the weak charges of the nucleon and quark are identical, just as those of the π-meson and cobalt nucleus (provided we neglect small isotopic non-invariant corrections).

This property of the weak charge is of the same nature as the familiar (and absolutely non-trivial!) additivity of the electric charge. The charge additivity implies that the total electric charge of a system is equal to the sum of charges of the constituent particles, regardless of the form of interaction between the particles.

And although free quarks are never encountered, their weak interaction constant (that of the vector quark current ud) can be found experimentally, precisely because the weak charges of the nucleon and quark are identical. Otherwise we would hardly be justified in factoring out $\cos\theta$.

5.4.4 4.4. Chiral invariance

If the terms representing quark masses in the total quark-gluon lagrangian are omitted, the left-handed and right-handed quark fields become independent, and the degree of symmetry of the lagrangian increases. In particular, the lagrangian is invariant under isotopic transformations separately for the left-handed doublet and for the right-handed doublet,

$$q_{\mathrm{L}} = \begin{pmatrix} u_{\mathrm{L}} \\ d_{\mathrm{L}} \end{pmatrix}, \quad q_{\mathrm{R}} = \begin{pmatrix} u_{\mathrm{R}} \\ d_{\mathrm{R}} \end{pmatrix},$$

respectively, if we neglect the masses m_{u} and m_{d} (this approximation is especially good since both masses are small: $m_{\mathrm{u}} \sim 4\mathrm{MeV}, m_{\mathrm{d}} \sim 7\mathrm{MeV}$). Namely,

$$q_{\mathrm{L}} \to \mathrm{e}^{i\tau\cdot\omega_{\mathrm{L}}/2} q_{\mathrm{L}}, \quad q_{\mathrm{R}} \to \mathrm{e}^{i\tau\cdot\omega_{\mathrm{R}}/2} q_{\mathrm{R}}$$

and the relevant group is $\mathrm{SU}(2)_{\mathrm{L}} \times \mathrm{SU}(2)_{\mathrm{R}}$. This is the so-called chiral symmetry. The strong interaction lagrangian is said to be chiral invariant. The absolute chiral invariance implies conservation both of the vector currents forming the triplet $\bar{q}\gamma_\alpha \tau q$, and of the axial currents forming the triplet $\bar{q}\gamma_\alpha\gamma_5\tau q$. The axial current is conserved, because by definition it is the difference between left-handed and right-handed currents, conserved due to chiral invariance.

It will be shown below that conservation of the axial current could be realized by introducing a triplet of massless mesons with the quantum numbers of π-mesons. The chiral generators $\hat{\boldsymbol{T}}_5 = \int \bar{q}\gamma_0\gamma_5\tau q \, \mathrm{d}\boldsymbol{x}$ thereby transform the states with different numbers of such massless zero-energy π-mesons into one another: nucleon $\to$ nucleon $+\pi \to$ nucleon $+2\pi \cdots$. Such a nonlinear realization of symmetry is usually referred to as the spontaneous breaking of symmetry.

In reality, chiral symmetry is not absolute since pion masses are distinct from zero. Nevertheless, pions are much lighter than other hadrons: $m_\pi^2/m_{\mathrm{p}}^2 \cong 2 \cdot 10^{-2}$, so that the observed deviations from chiral symmetry are proportional to a small parameter (m_π^2 is proportional to $m_{\mathrm{u}} + m_{\mathrm{d}}$). Instead of the rigorously conserved axial current (CAC), we have to deal with the partially conserved axial current (PCAC). Some of the corollaries of PCAC are discussed in chapter 5.

5.5 5 Leptonic decays of pions and nucleons

The following leptonic decays of hadrons will be considered in this chapter: decays of π-mesons ($\pi^+ \to \ell^+\nu$, where ℓ = e or $\mu, \pi^+ \to e^+\nu\pi^0$), β-decay of the neutron $n \to pe^-\bar{\nu}$, and muon capture $\mu^- p \to n\nu$. In addition, we shall briefly discuss the decays $\Sigma \to \Lambda e\nu$ which are also produced by the ud current.

5.5.1 5.1. $\pi \to \ell\nu$ decays

We start with $\pi^+ \to \ell^+\nu$ decay. The quark graph of this decay is shown in fig. 5.1. The vertex marked in the graph by a black dot symbolizes that π^+ consists of u and $\bar{d}$. The vector component V_α of the matrix element H_α is zero, $V_\alpha = 0$, and A_α can be written in the form $A_\alpha = f_\pi \varphi_\pi p_\alpha$, where φ_π is the pion wave function, p_α is the pion 4-momentum, and f_π is a parameter of the dimension of mass (the constant $F_\pi = f_\pi/\sqrt{2}$ is sometimes used instead of f_π). The amplitude for this process is

$$M = \sqrt{\frac{1}{2}} G A_\alpha L^\alpha \cos\theta = \sqrt{\frac{1}{2}} G f_\pi \varphi_\pi p_\alpha \bar{u}_\nu \gamma_\alpha (1+\gamma_5) u_\ell \cos\theta.$$

By using momentum conservation,

$$p_\pi = p_\nu + p_\ell,$$

and the Dirac equation $(\hat{p} - m)u = 0$, let us rewrite M in the form

$$M = \sqrt{\frac{1}{2}} G f_\pi m_\ell \varphi_\pi \bar{u}_\nu (1-\gamma_5) u_\ell \cos\theta.$$

We find that the amplitude is proportional to m_ℓ and vanishes for $m_\ell \to 0$. The reason for this is as follows. It has been mentioned above that helicity is conserved in weak interaction. This fact, and the conservation of angular momentum forbid the spin-zero meson to decay into a left-handed neutrino

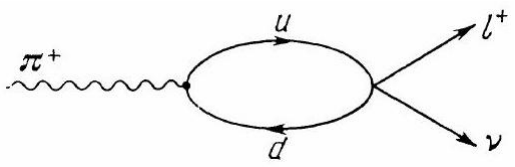


Fig. 5.1.

and a right-handed antilepton. We now find in a straightforward manner

$$\overline{|M|^2} = \frac{1}{2} G^2 f_\pi^2 m_\ell^2 8 (p_\nu p_\ell) \cos^2\theta = 4 G^2 f_\pi^2 m_\ell^2 m_\pi E_\nu \cos^2\theta,$$

where m_π is the pion mass, and E_ν is the neutrino energy in the pion rest frame ($p_\nu p_\ell = (p_\nu, p_\pi - p_\nu) = p_\nu p_\pi = m_\pi E_\nu$). Writing the decay probability in the form

$$\Gamma = \frac{\overline{|M|^2}}{2m} \Phi,$$

where Φ is the phase-space volume

$$\Phi = \int \frac{d\boldsymbol{k}_\nu}{2E_\nu(2\pi)^3} \frac{d\boldsymbol{k}_\ell}{2E_\ell(2\pi)^3} (2\pi)^4 \delta^4 (k_\nu + k_\ell - p_\pi)$$
$$= \frac{1}{4\pi} \int \delta \left(E_\nu + \sqrt{E_\nu^2 + m_\ell^2} - m_\pi \right) \frac{E_\nu dE_\nu}{E_\ell} = \frac{E_\nu}{4\pi m_\pi},$$

we finally obtain

$$\Gamma = \frac{G^2 f_\pi^2 m_\ell^2 E_\nu^2 \cos^2\theta}{2\pi m_\pi} = \frac{G^2 f_\pi^2 m_\ell^2 m_\pi \cos^2\theta}{8\pi} \left(1 - \frac{m_\ell^2}{m_\pi^2}\right)^2.$$

A comparison of this expression with the experimentally measured $\pi \to \mu\nu$ decay rate yields $f_\pi \cong 130$MeV. We shall see later that this quantity enters all relations derived on the basis of PCAC. The ratio of probabilities of $\pi \to e\nu$ and $\pi \to \mu\nu$ is independent of f_π and equals

$$\frac{\Gamma(\pi \to e\nu)}{\Gamma(\pi \to \mu\nu)} = \left(\frac{m_e}{m_\mu}\right)^2 \left(\frac{1 - m_e^2/m_\pi^2}{1 - m_\mu^2/m_\pi^2}\right)^2 \cong 1.3 \cdot 10^{-4}.$$

It must be emphasized that f_π is exactly the same for both decays, because the matrix element of the ud current is a function of only the total 4 -momentum of the leptons, and is independent of the 4-momenta of each individual lepton.

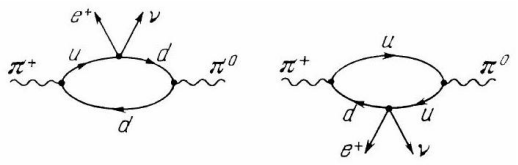


Fig. 5.2.

5.5.2 5.2. $\pi^+ \to \pi^0 e^+ \nu$ decay

The decay $\pi^+ \to \pi^0 e^+ \nu$ is represented by a sum of quark graphs (see fig. 5.2). Its amplitude is

$$M = \sqrt{\frac{1}{2}} G V_\alpha L^\alpha \cos\theta$$

where

$$L_\alpha = \bar{\nu}\gamma_\alpha (1 + \gamma_5) e,$$
$$V_\alpha = (f_+ p_\alpha + f_- q_\alpha) \varphi_2 \varphi_1.$$

Here φ_1 and φ_2 are wave functions of the $\pi^+$and π^0 mesons, p_1 and p_2 are their 4-momenta, $p = p_1 + p_2, q = p_1 - p_2$. In the general case, the scalar dimensionless parameters $f_+$and $f_-$are functions of q^2. We can assume, nevertheless, that the form factors $f_+$and $f_-$are constant in the whole physical range of q^2,

$$f_+(q^2) \cong f_+(0), \quad f_-(q^2) \cong f_-(0),$$

because of the negligibly small release of energy in the π_{e3} decay.
Because of the conservation of the vector current,

$$q^\alpha V_\alpha = 0.$$

This equality must hold in the limit of absolute isotopic invariance, with the electromagnetic interaction switched off. In this limit, $qp = m_{\pi^+}^2 - m_{\pi^0}^2 = 0$ and the transversality condition becomes

$$f_- q^2 = 0.$$

Hence, $f_- = 0$. As for $f_+(0)$, its magnitude is fixed because the vector current ud enters the same triplet as the isovector electromagnetic current. We have demonstrated in chapter 4 that $f_+(0)$ is the weak vector charge whose value in the transition $\pi^+ \to \pi^0 \mathrm{e}^+ \nu$ is $\sqrt{T(T+1) - T_3\,(T_3+1)} = \sqrt{2}$. This value of $f_+(0)$ can easily be estimated from the graphs of fig. 5.2, if we take into account that weak charges in the transitions of quark ($\mathrm{u} \to \mathrm{de}^+\nu$) and antiquark ($\overline{\mathrm{d}} \to \overline{\mathrm{u}}\mathrm{e}^+\nu$) are +1 and -1 , respectively. The matrix element in question is

$$\left\langle \pi^0 = \sqrt{\frac{1}{2}}(u\bar{u} - d\bar{d}) \right| \bar{d}\gamma_0 u \left|\pi^+ = u\bar{d}\right\rangle = \sqrt{2}.$$

Summarizing, the amplitude of the $\pi_{\mathrm{e}3}$ decay is given by

$$M = \sqrt{\frac{1}{2}} G\varphi_1\varphi_2\sqrt{2}p^\alpha \bar{u}_\nu \gamma_\alpha\,(1+\gamma_5)\,u_\ell \cos\theta.$$

Problem: Using this amplitude, calculate the width of the $\pi_{\mathrm{e}3}$ decay. Answer:

$$\Gamma = \frac{G^2\Delta^5}{30\pi^3}\left(1 - \frac{5m_{\mathrm{e}}^2}{\Delta^2} - \frac{3}{2}\frac{\Delta}{m_\pi}\right)\cos^2\theta.$$

Here $\Delta = m_{\pi^+} - m_{\pi^0} \cong 4.5\mathrm{MeV}$; higher powers of the ratios m_{e}/Δ and Δ/m_π were neglected. The calculated probability of the $\pi_{\mathrm{e}3}$ decay comes to approximately 10^{-8} of the total width of the π-meson. The theoretical prediction for $\Gamma\,(\pi^+ \to \pi^0\mathrm{e}^+\nu)$ is confirmed by experiment.

5.5.3 5.3. β-decay of the neutron

Both V_α and A_α are distinct from zero in the decay $\mathrm{n} \to \mathrm{pe}^-\bar{\nu}_{\mathrm{e}}$. In the most general form,

$$V_\alpha = \bar{u}_{\mathrm{p}}\left(f_1\gamma_\alpha + f_2\sigma_{\alpha\beta}q^\beta + f_3 q_\alpha\right)u_{\mathrm{n}}$$
$$A_\alpha = \bar{u}_{\mathrm{p}}\left(g_1\gamma_\alpha + g_2\sigma_{\alpha\beta}q^\beta + g_3 q_\alpha\right)\gamma_5 u_{\mathrm{n}}$$

All six form factors f_i and g_i are functions of q^2, where $q = p_{\mathrm{n}} - p_{\mathrm{p}} = p_{\mathrm{e}} + p_{\bar{\nu}}$. The characteristic scale of q^2 for these functions is of the order of 0.5 GeV^2. The only exception is $g_3\,(q^2)$, whose characteristic scale is much smallet (it is of the order of $m_\pi^2 \cong 0.02\mathrm{GeV}^2$). The energy released in β-decay is in all cases so small that all six form factors can be considered as constants. Experimentally, f_i and g_i as functions of q^2 are found from neutrino experiments

$$\nu_\mu\,(\nu_{\mathrm{e}}) + \mathrm{n} \to \mathrm{p} + \mu^-\,(\mathrm{e}^-)$$
$$\bar{\nu}_\mu\,(\bar{\nu}_{\mathrm{e}}) + \mathrm{p} \to \mathrm{n} + \mu^+\,(\mathrm{e}^+)$$

These experiments are discussed in Chapter 17.

5.5.4 5.4. Vector form factors

Let us consider first the vector form factors f_1, f_2, f_3. The weak charge is found from conservation of the vector current: $f_1(0) = 1$. This can be obtained, of course, by adding quark amplitudes of the graphs of fig. 5.3. In the case under discussion, however, it is simpler to resort to the general formula which gives the weak charge as $\sqrt{T(T+1) - T_3\,(T_3+1)}$. In the

transition n $\to$ p we have $T = \frac{1}{2}, T_3 = -\frac{1}{2}$; consequently, $f_1(0) = 1$, and the weak charge of nucleons is equal to that of the d , u quarks. The data on the neutron β-decay and on superallowed transitions in nuclei (induced precisely by the weak vector charge, see Chapter 4) then yield the value of $\cos\theta$.

Usually the quantity $f_2\sigma_{\alpha\beta}q_\beta$ is called the weak magnetism. The value of f_2 can be predicted by using the similarity of the weak and electromagnetic currents. Indeed, the electromagnetic nucleon vertices are

$$\gamma_\alpha + \frac{1.79}{2m_\mathrm{p}}\sigma_{\alpha\beta}q^\beta \quad \text{for the proton ,}$$

and

$$-\frac{1.91}{2m_\mathrm{p}}\sigma_{\alpha\beta}q^\beta \quad \text{for the neutron.}$$

This means that the isoscalar vertex is

$$\gamma_\alpha - \frac{0.12}{2m_\mathrm{p}}\sigma_{\alpha\beta}q^\beta \quad (\bar{\mathrm{p}}\mathrm{p} + \bar{\mathrm{n}}\mathrm{n}),$$

and the isovector vertex is

$$\gamma_\alpha + \frac{3.7}{2m_\mathrm{p}}\sigma_{\alpha\beta}q^\beta \quad (\bar{\mathrm{p}}\mathrm{p} - \bar{\mathrm{n}}\mathrm{n}).$$

The isovector electromagnetic current enters the same triplet as the weak vector current; hence, the last expression is also valid for V_α. Since $f_1(0) = 1$,

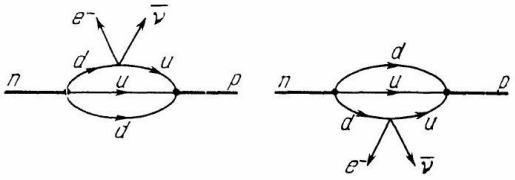


Fig. 5.3.

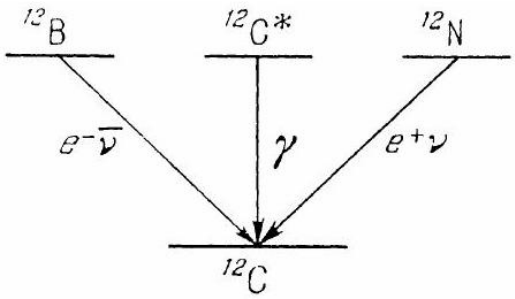


Fig. 5.4.

we obtain $f_2(0) = 3.7/2m_\mathrm{p}$. At the same time this gives $f_3 = 0$. The term $f_3 q_\alpha$ is usually quoted as the effective scalar. This originates in the possibility of expressing this term as a scalar:

$$f_3 q_\alpha \bar{u}_\nu \gamma_\alpha (1 + \gamma_5)\, u_\mathrm{e} = m_\mathrm{e} f_3 \bar{u}_\nu (1 - \gamma_5)\, u_\mathrm{e}.$$

Two facts are responsible for $f_3 = 0$. First of all, f_3 vanishes because of the transversality of V_α ($q^\alpha V_\alpha = 0$ yields $q^2 f_3 = 0$), and secondly, because V_α is G even and the isovector scalar must be G odd. The best experimental restrictions on the value of f_3 are found in μ-capture, $\mu^- \mathrm{p} \to \mathrm{n}\nu$.

Let us return to the weak magnetism. In the β-decay of the neutron, this term is unfortunately very small and therefore very difficult to observe. Its contribution is considerably higher in β-transitions of nuclei with higher energy release. Isotopically symmetric β-transitions of boron and nitrogen nuclei give a good example (see fig. 5.4). In these transitions, weak magnetism is calculated from the matrix element in the radiative decay of the excited level $^{12}\mathrm{C}^*$; this level is in the same isotopic triplet with the ground states of ^{12} B and ^{12} N (all three levels have $J^P = 1^+$).

5.5.5 5.5. Axial form factors

The names given to the three axial form factors are: g_1 axial charge, g_2 weak "electrism", g_3 effective pseudo-scalar. We begin with the term $g_2 \sigma_{\alpha\beta} q_\beta \gamma_5$. This term is similar to the electric dipole moment of the neutron, which is known to be forbidden by the CP invariance of the electromagnetic interaction. Likewise, the weak electric term is also forbidden, being G even while the axial current is G odd. The terms $g_1 \gamma_\alpha \gamma_5$ and $g_3 g_\alpha \gamma_5$ are G odd and therefore allowed. They are related to each other owing to partial conservation of the axial current (PCAC). In the limit of massless pions, the axial current is conserved and matrix elements are transverse:

$$q^\alpha A_\alpha = 0.$$

The term $g_1 \gamma_\alpha \gamma_5$ is in itself not transverse because of the non-vanishing nucleon masses:

$$q_\alpha \bar{u}_\mathrm{p} \gamma_\alpha \gamma_5 u_\mathrm{n} = (m_\mathrm{p} + m_\mathrm{n})\, \bar{u}_\mathrm{p} \gamma_5 u_\mathrm{n}.$$

In order to make it transverse, we multiply it by a transverse expression ($\delta^\alpha_\beta - q^\alpha q_\beta / q^2$). Multiplication of the expression obtained, $\dot{g}_1 \bar{u}_\mathrm{p} \gamma_\beta \gamma_5 \left(\delta^\beta_\alpha - q^\beta q_\alpha / q^2\right) u_\mathrm{n}$, by q^α yields zero. But in addition to the term $g_1 \bar{u}_\mathrm{p} \gamma_\alpha \gamma_5 u_\mathrm{n}$, this expression contains one more term which is easily recognizable as the effective pseudoscalar:

$$-g_1 \bar{u}_\mathrm{p} \gamma_\beta \gamma_5 \frac{q^\beta q_\alpha}{q^2} u_\mathrm{n} = \frac{2 m g_1}{q^2} \bar{u}_\mathrm{p} \gamma_5 u_\mathrm{n} q_\alpha$$

(We have used the equalities $\hat{p}_\mathrm{n} u_\mathrm{n} = m_\mathrm{n} u_\mathrm{n}, \bar{u}_\mathrm{p} \hat{p}_\mathrm{p} = m_\mathrm{p} u_\mathrm{p}$, and the approximation $m_\mathrm{p} = m_\mathrm{n} = m$). We find that the effective pseudoscalar form factor contains a π-meson pole at $q^2 = 0$ (we recall that so far the π-meson is assumed to be massless). Phenomenologically, this pole corresponds to the graph of fig. 5.5. The constants f_π and g which characterize this graph are known. The product $f_\pi q_\alpha$ characterizes the decay $\pi \to \mathrm{e}\nu$, and we have found at the beginning of this chapter that $f_\pi \cong 130\mathrm{MeV}$. The constant g characterizes the π-meson-nucleon strong interaction. If the $\pi\overline{\mathrm{N}}\mathrm{N}$ vertex is written in the form

$$\begin{aligned} g \boldsymbol{\varphi}_\pi \bar{u}_\mathrm{N} \gamma_5 \tau u_\mathrm{N} = g \Big[& \sqrt{2} \varphi_{\pi^-} \bar{u}_\mathrm{p} \gamma_5 u_\mathrm{n} + \sqrt{2} \varphi_{\pi^+} \bar{u}_\mathrm{n} \gamma_5 u_\mathrm{p} \\ & + \varphi_{\pi^0} \bar{u}_\mathrm{p} \gamma_5 u_\mathrm{p} - \varphi_{\pi^0} \bar{u}_\mathrm{n} \gamma_5 u_\mathrm{n} \Big], \end{aligned}$$

then the experimentally obtained value of g is such that $g^2/4\pi \cong 14$. In order to specify the normalization, let us remark that a similar quantity in electrodynamics is $e^2/4\pi = \alpha = \frac{1}{137}$. Some time ago the constant $g^2/4\pi$ was considered to be as fundamental for the strong interaction as $e^2/4\pi$ for the electromagnetic one. Now it is clear that $g^2/4\pi$ is a purely phenomenological

quantity and has nothing to do with the fundamental lagrangian of the strong interaction. Let us recast the π-nucleon vertex in the gradient form:

$$\sqrt{2}g\varphi_\pi \bar{u}_\mathrm{p}\gamma_5 u_\mathrm{n} = -\frac{\sqrt{2}g}{2m}q^\beta \varphi_\pi \bar{u}_\mathrm{p}\gamma_\beta\gamma_5 u_\mathrm{n} = -\sqrt{2}\frac{q^\beta}{f}\varphi_\pi \bar{u}_\mathrm{p}\gamma_\beta\gamma_5 u_\mathrm{n}$$

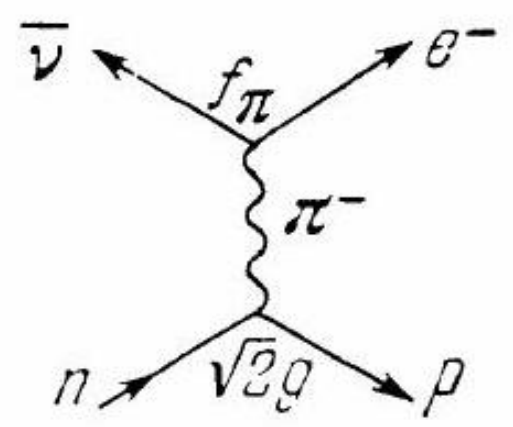


Fig. 5.5.

We have $f = 2$ m/g $\cong$ 140MeV. (The quantity f introduced here must not be confused with f_1, f_2, f_3 and f_π introduced earlier, or with $f = g/2m$ often encountered in the literature). It is clear that the pole term in the amplitude as given by the graph of fig. 5.5 equals

$$-\sqrt{2}\frac{f_\pi}{f}\frac{q_\alpha q^\beta}{q^2}\bar{u}_\mathrm{p}\gamma_\beta\gamma_5 u_\mathrm{n}.$$

On the other hand, multiplication of the matrix element $g_1\bar{u}_\mathrm{p}\gamma_\beta\gamma_5 u_\mathrm{n}$ by $\delta^\beta_\alpha - q_\alpha q^\beta/q^2$ yielded

$$g_1\bar{u}_\mathrm{p}\gamma_\beta\gamma_5 u_\mathrm{n}\left(\delta^\beta_\alpha - q_\alpha q^\beta/q^2\right).$$

Consequently,

$$g_1 = \sqrt{2}\frac{f_\pi}{f}.$$

This is the so-called Goldberger-Treiman relation. Using numerical values of f_π and f, we obtain $g_1 \cong 1.3$ which is in good agreement with the experimental ratio $g_\mathrm{A}/g_\mathrm{V} = 1.25$. (The symbols g_V and g_A are often used in the literature instead of our f_1 and g_1; sometimes g_A stands for $-g_1$). It should be kept in mind that experimental values of f_π and f are found for $q^2 = m_\pi^2$, and g_1 is obtained for $q^2 = 0$. We assume that a shift of $m_\pi^2 \cong 0.02\mathrm{GeV}^2$ has a negligible effect on these quantities.

The pion pole in the matrix element of the axial current appears because of the spontaneous breaking of the chiral symmetry. As has been mentioned in chapter 4, chiral symmetry is realized in a non-linear manner (owing to the non-zero masses of the nucleons), by invoking an isotopic triplet of massless pseudoscalar particles. Such spin-zero massless particles accompanying the spontaneous breaking of symmetry, are called the Goldstone bosons. β-decay gives an example of how the conservation of the axial current (transversality of A_α) is provided by the pole term corresponding to a massless Goldstone meson:

$$-g_1\bar{u}_\mathrm{p}\gamma_\beta\gamma_5 u_\mathrm{n}\frac{q^\beta q_\alpha}{q^2}.$$

Multiplication of this term by the leptonic matrix element yields an expression which is the effective pseudoscalar:

$$-g_1\bar{u}_{\mathrm{p}}\gamma_\beta\gamma_5 u_{\mathrm{n}}\frac{q^\beta q_\alpha}{q^2}L_\alpha = -g_1\frac{2m\cdot m_\ell}{q^2}\bar{u}_{\mathrm{p}}\gamma_5 u_{\mathrm{n}}\bar{u}_\ell\left(1+\gamma_5\right)u_\nu.$$

The effective pseudoscalar is very small in β-decay because of the small electron mass. It is much larger in the case of μ-capture.

The finite mass of the π-meson cannot be ignored any more if the numerical value of the effective pseudoscalar is discussed. Normally one takes account of the pion mass in a most naive manner, by inserting m_π^2 into the propagator "by hand", so that the "constant" in the effective pseudoscalar, $g_{\mathrm{P}} = m_\ell g_3$, becomes

$$g_{\mathrm{P}} = \frac{2mm_\ell g_1}{q^2 - m_\pi^2}.$$

We see that g_{P} is a function of q^2. Practically all energy (of the order of m_μ) in the process $\mu^-\mathrm{p}\to\mathrm{n}\nu$ is carried away by the neutrino, with the nucleon gaining a momentum of the order of m_μ, so that $q^2 \cong -m_\mu^2$. It follows then that $g_{\mathrm{P}}/g_1 \cong -6$. This high value of the effective pseudoscalar is in agreement with experiments on μ-capture.

5.5.6 5.6 The probability of β-decay. Angular correlations

It has been mentioned above that the lagrangian of the interaction between leptonic currents and currents of light quarks is CP invariant. This means, by virtue of the CPT theorem, that the lagrangian is also invariant under time reversal T. The T-invariance of the lagrangian can be shown to result in real form factors f_1, f_2, f_3 and g_1, g_3 entering the matrix element of the β-decay of the neutron. The same is true for the form factors in pion decays.

We have thus completed an analysis of all six form factors in the β-decay of the neutron. The vector and axial charges are the main contributors to this process, so that the decay amplitude can be written in the form

$$M = \sqrt{\frac{1}{2}}G\bar{u}_{\mathrm{p}}\gamma_\alpha\left(1+\alpha\gamma_5\right)u_{\mathrm{n}}\bar{u}_{\mathrm{e}}\gamma^\alpha\left(1+\gamma_5\right)u_\nu\cos\theta,$$

where

$$\alpha = g_1/f_1 = 1.253\pm 0.007.$$

Problem 1: Calculate the $\boldsymbol{e\nu}$ correlation in the decay of the non-polarized neutron.

Answer: The decay probability is proportional to $1+\lambda\boldsymbol{v}_{\mathrm{e}}\cdot\boldsymbol{n}_\nu$ where $\boldsymbol{v}_{\mathrm{e}}$ is the electron velocity vector (as before, in units where $c=1$), $\boldsymbol{n}_\nu$ is the neutrino velocity vector $\left(|\boldsymbol{n}_\nu|^2=1\right)$, and $\lambda = \left(1-\boldsymbol{\alpha}^2\right)/\left(1+3\boldsymbol{\alpha}^2\right)$. For $\alpha\cong 1.25$, $\lambda\cong -0.1$.

Problem 2: Calculate the electron spectrum in the neutron decay.

Answer:

$$\mathrm{d}\Gamma = \frac{G^2\left(1+3\alpha^2\right)\cos^2\theta}{2\pi^3}\left(E_{\mathrm{e}}^2-m_{\mathrm{e}}^2\right)^{1/2}\left(\Delta-E_{\mathrm{e}}\right)^2 E_{\mathrm{e}}\,\mathrm{d}E_{\mathrm{e}}$$

where

$$\Delta = m_{\mathrm{n}} - m_{\mathrm{p}} \cong 1.29\mathrm{MeV}.$$

Problem 3: Calculate the total probability of the neutron decay. Answer: Integration of the preceding equation yields

$$\Gamma = \frac{G^2 \Delta^5 \cos^2 \theta}{60\pi^3} \left(1 + 3\alpha^2\right) 0.47.$$

Problem 4: Calculate the longitudinal polarization of electrons in the neutron decay.

Answer: $P_e = -v_e$, where v_e is the electron velocity.

Problem 5: Calculate the angular distribution of electrons in the decay of the polarized neutron.

Answer: $1 + \rho_e \boldsymbol{v}_e \boldsymbol{\eta}$, where $\boldsymbol{\eta}$ is a unit vector in the direction of the neutron polarization, and

$$\rho_e = -\frac{2\left(\alpha^2 - \alpha\right)}{1 + 3\alpha^2} \cong -0.1 \quad \text{for } \alpha \cong 1.25$$

Problem 6: Calculate the angular distribution of neutrinos in the decay of the polarized neutron.

Answer: $1 + \rho_\nu \boldsymbol{n}_\nu \boldsymbol{\eta}$, where

$$\rho_\nu = \frac{2\left(\alpha^2 + \alpha\right)}{1 + 3\alpha^2} \cong 1$$

Note that $\boldsymbol{\eta}\left[\boldsymbol{p}_e \times \boldsymbol{p}_\nu\right]$-type correlation in the neutron decay must be absent in the Born approximation (by virtue of T-invariance). Indeed, the substitution $t \to -t$ changes sign in each factor of this product; consequently, the whole product is T odd. The coefficient of this correlation is proportional to $\sin\delta$, where $\delta = \arg\alpha$. The experimental value is $\delta = (0.20 \pm 0.19)^\circ$.

5.5.7 5.7. $\Sigma^{\pm} \to \Lambda e^{\pm} \nu$ decays

Being strangeness-conserving, $\Sigma^{\pm} \to \Lambda e^{\pm} \nu$ decays are therefore induced by the ud current. The general form of V_α and A_α for these decays is the same
us for the β-decay of the neutron, but $f_1(0) = 0$ because Σ - and Λ-hyperons ure not in the same isotopic multiplet. This is found most easily if we use the condition $q^\alpha V_\alpha = 0$, which gives

$$\left(m_\Sigma - m_\Lambda\right) f_1\left(q^2\right) + q^2 f_3\left(q^2\right) = 0$$

Hence, $f_1\left(q^2\right) \to 0$ for $q^2 \to 0$. As a result, the term predominant in V_α is $\int \rho_{\alpha\beta} q^\beta$, where $f_2 = \mu_{\Sigma\Lambda}/e$, and the quantity $\mu_{\Sigma\Lambda}$ determines the width of the Σ^0 hyperon with respect to the $\Sigma^0 \to \Lambda^0 \gamma$ decay. ($\Sigma^{\pm} \to \Lambda e^{\pm} \nu$ finds its total electromagnetic analog in $\Sigma^0 \to \Lambda e^+ e^-$.) The contribution of V_α to the total probability of $\Sigma^{\pm} \to \Lambda e^{\pm} \nu$ decays is negligible since $f_2 |\boldsymbol{q}|$ is small ($f_2 \sim 1/m_\Lambda, |\boldsymbol{q}|_{\max} \sim m_\Sigma - m_\Lambda$). As for the axial matrix element A_α, it contains $g_1(0) \neq 0$ so that the probability of $\Sigma^{\pm} \to \Lambda e^{\pm} \nu$ decays is determined by this quantity, identical for both decays. Since $m_{\Sigma^-} - m_\Lambda \cong 82$ MeV and $m_{\Sigma^+} - m_\Lambda \cong 74$MeV, we obtain

$$\frac{\Gamma\left(\Sigma^+ \to \Lambda e^+ \nu\right)}{\Gamma\left(\Sigma^- \to \Lambda e^- \bar{\nu}\right)} = \left(\frac{74}{82}\right)^5 \cong 0.6.$$

Experimental data are in agreement with this prediction.

5.6 6 Leptonic decays of K-mesons and hyperons

Most leptonic decays of strange particles are strangeness changing. The interaction that gives rise to these decays is the coupling of the us current to the leptonic currents $e\nu$ and $\mu\nu$. The following notation is used in the literature for muonic decays of $K^+$and K^0 mesons:

$$\begin{array}{llll} \mathrm{K}^+ \to \mu^+\boldsymbol{\nu} & \left(\mathrm{K}^+_{\mu 2}\right), & \mathrm{K}^+ \to \mu^+\boldsymbol{\nu}\pi^+\pi^- & \left(\mathrm{K}^+_{\mu 4}\right), \\ \mathrm{K}^+ \to \mu^+\boldsymbol{\nu}\pi^0 & \left(\mathrm{K}^+_{\mu 3}\right), & \mathrm{K}^+ \to \mu^+\boldsymbol{\nu}\pi^0\pi^0 & \left(\mathrm{K}^{+\prime}_{\mu 4}\right), \\ \mathrm{K}^0 \to \mu^+\boldsymbol{\nu}\pi^- & \left(\mathrm{K}^0_{\mu 3}\right), & \mathrm{K}^0 \to \mu^+\boldsymbol{\nu}\pi^0\pi^- & \left(\mathrm{K}^0_{\mu 4}\right). \end{array}$$

Similar notation is used for the decays of $\mathrm{K}^-$and $\overline{\mathrm{K}}^0$ mesons. If a decay produces a pair $e\nu$ instead of $\mu\nu$, the symbols change to $\mathrm{K}^+_{e2}, \mathrm{K}^+_{e3}$, and so on. In cases where it is immaterial whether an electron or a muon is emitted, we use the symbols $\mathrm{K}_{\ell 2}$, $\mathrm{K}_{\ell 3}$, $\mathrm{K}_{\ell 4}$ where ℓ denotes a charged lepton ($\ell = \mathrm{e}$ or μ).

No special contracted notation was introduced for leptonic decays of hyperons. The following hyperon decays will be considered in this chapter:

$$\begin{gathered} \Lambda \to \mathrm{p}\ell^-\bar{\nu}, \Xi^- \to \Sigma^0\ell^-\bar{\nu}, \\ \Sigma^- \to \mathrm{n}\ell^-\bar{\nu}, \Xi^0 \to \Sigma^+\ell^-\bar{\nu}, \\ \Xi^- \to \Lambda\ell^-\bar{\nu}, \Omega^- \to \Xi^0\ell^-\bar{\nu}. \end{gathered}$$

6.1. $|\Delta S| = 1$ and $\Delta Q = \Delta S$ rules

All strangeness-changing leptonic decays occur through the us current which changes strangeness by unity; therefore, all these decays must be subject to the selection rule $|\Delta S| = 1$. This rule holds in all the decays listed above.

Decays violating this rule,

$$\begin{gathered} \Xi^- \to \mathrm{n}\ell^-\bar{\nu}, \quad \Xi^0 \to \mathrm{p}\ell^-\bar{\nu}, \\ \Omega^- \to \Lambda^0\ell^-\bar{\nu}, \quad \Omega^- \to \Sigma^0\ell^-\bar{\nu}, \quad \Omega^- \to \mathrm{n}\ell^-\bar{\nu} \end{gathered}$$

have never been observed experimentally.

Another typical prediction of the theory is the selection rule $\Delta Q = \Delta S$ for the change of the charge and strangeness of hadrons. In the $\mathrm{s} \to \mathrm{u}$ transition both the strangeness S and electric charge Q increase by unity; hence, the selection rule is $\Delta Q = \Delta S$. Decays violating this rule,

$$K^0 \to \ell^-\bar{\nu}\pi^+, \quad \overline{\mathrm{K}}^0 \to \ell^+\nu\pi^-, \quad \mathrm{K}^+ \to \ell^-\bar{\nu}\pi^+\pi^+, \quad \Sigma^+ \to \mathrm{n}\ell^+\nu$$

have never been observed. It has to be underlined, though, that both these decays and the above-mentioned decays with $\Delta S > 1$ are forbidden theoretically to an extent much higher than the achieved experimental accuracy. Indeed, the selection rules are violated only in second and higher orders of perturbation theory, so that the anticipated accuracy must be of the order of 10^{-14}.

5.6.1 6.2. SU(3) and SU(2) properties of the us current

The coupling of the us current to the $e\nu$ or $\mu\nu$ current is proportional to $\sin\theta$, where θ is the Cabibbo angle ($\theta \cong 13^\circ$). We shall therefore present the decay amplitudes in the form

$$M = \sqrt{\frac{1}{2}} G H_\alpha L^\alpha \sin\theta$$

where L^α is the leptonic matrix element, $L_\alpha = \bar{u}_\ell \gamma^\alpha (1 + \gamma_5) u_\nu$, and H_α is the hadronic matrix element

$$H_\alpha = \langle f | \bar{u} O_\alpha s | i \rangle,$$

where $O_\alpha = \gamma_\alpha (1 + \gamma_5)$.

We readily find that the currents $\bar{u}O_\alpha d, \bar{d}O_\alpha u, \bar{u}O_\alpha s, \bar{s}O_\alpha u$ are in the same octet

$$\bar{q}^i O_\alpha q_k - \frac{1}{3}\delta^i_k \bar{q}^m O_\alpha q_m,$$

where $q_1 = u, q_2 = d, q_3 = s$. Two more diagonal left-handed currents are in this octet: the isovector current $\sqrt{\frac{1}{2}}\left(\bar{u}O_\alpha u - \bar{d}O_\alpha d\right)$ and the isoscalar one $\sqrt{\frac{1}{6}}\left(\bar{u}O_\alpha u + \bar{d}O_\alpha d - 2\bar{s}O_\alpha s\right)$, participating in the weak interaction of the neutral currents. Also included are strangeness-changing neutral currents $\bar{d}O_\alpha s$ and $\bar{s}O_\alpha d$ which do not take part in the weak interaction. These unequal roles of different components of the current octet should not be

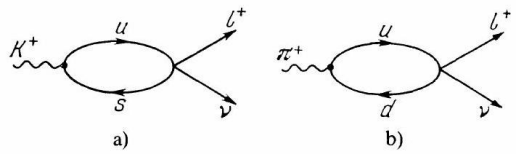


Fig. 6.1.

surprising since the weak interaction is not SU(3) invariant. What we do use is the SU(3) invariance of the strong interaction which enables us to find the relationships between distinct matrix elements of the currents us and ud.

As for the isotopic properties of the us current, it is obviously an isotopic spinor. Indeed, the isospins of the u - and s-quark are $\frac{1}{2}$ and 0 , respectively, so that the us current must change the hadron isospin by $\frac{1}{2}$. We shall discuss this selection rule in more detail when considering K_{e3} decays.

5.6.2 6.3. $K_{\ell 2}$ decays

The $\mathrm{K}^+ \to \ell^+\nu$ decays (fig. 6.1a) are exact analogs of the $\pi^+ \to \ell^+\nu$ decays (fig. 6.1b) in the unbroken SU(3) symmetry approximation. In this approximation, $m_\mathrm{u} = m_\mathrm{d} = m_\mathrm{s}, m_\mathrm{K} = m_\pi$, and the amplitudes of $\mathrm{K}_{\ell 2}$ and $\pi_{\ell 2}$ decays differ only in the factors $\sin\theta$ and $\cos\theta$, respectively. Let us write the $\mathrm{K}_{\ell 2}$ decay amplitude in the form

$$M = \sqrt{\frac{1}{2}} G f_\mathrm{K} p^\alpha \bar{u}_\nu \gamma_\alpha \left(1 + \gamma_5\right) u_\ell \sin\theta,$$

where p is the 4 -momentum of the K -meson. The SU(3) symmetry then yields $f_\mathrm{K} = f_\pi$, and although SU(3) is violated, experimentally f_K is close to f_π. Calculation of the decay probability gives

$$\Gamma(\mathrm{K} \to \ell\nu) = \frac{G^2}{8\pi} f_\mathrm{K}^2 m_\mathrm{K} m_\ell^2 \left(1 - \frac{m_\ell^2}{m_K^2}\right)^2 \sin^2\theta.$$

Assuming $\sin\theta = 0.21$ (see the subsection below on $\mathrm{K}_{\ell 3}$ decays), we obtain from the data on the width $\Gamma\left(\mathrm{K}^+ \to \mu^+\nu\right)$ that $f_\mathrm{K}/f_\pi = 1.27$. The agreement with SU(3) is sufficiently good, especially if one takes into account that SU(3) is violated much more strongly in the masses of the K - and π-mesons.

Note that the ratio of the widths of $\mathrm{K}_{\mathrm{e}2}$ and $\mathrm{K}_{\mu 2}$ decays is much closer to its asymptotic limit, m_e^2/m_μ^2, than in the case of $\pi_{\ell 2}$ decays; this is caused by the phase-space volume being larger in the former case.

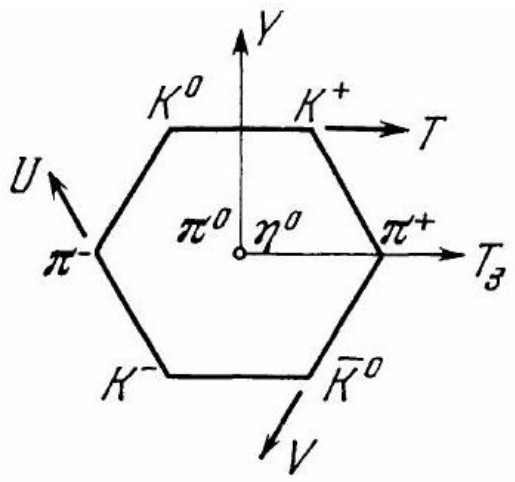


Fig. 6.2.

5.6.3 6.4. K_{t3} decays

L.et us consider first $\mathrm{K}^0_{\ell 3}$ decay. Its amplitude can be written in the form

$$M = \sqrt{\frac{1}{2}} G \sin\theta \left[f_+ \left(q^2\right) p_\alpha + f_- \left(q^2\right) q_\alpha \right] \varphi_\pi \varphi_\mathrm{K} \bar{u}_\nu \gamma^\alpha \left(1 + \gamma_5\right) u_\ell,$$

where $p = p_\mathrm{K} + p_\pi$, and $q = p_\mathrm{K} - p_\pi$ is the 4-momentum carried by leptons. According to the Dirac equation, the f_-term gives a contribution proportional to m_ℓ, and thus can be neglected for $\mathrm{K}_{\mathrm{e}3}$ decay. In the approximation of unbroken SU(3) symmetry, and for $q^2 = 0$, the term proportional to $f_+$is readily related to a similar term in the $\pi_{\mathrm{e}3}$ decay, which yields that in $\mathrm{K}^0_{\ell 3}$ decay, $f^0_+(0) = 1$. It can be demonstrated that the correction to this must be quadratic in the SU(3) symmetry breaking parameter, and therefore be small (this is the so-called Ademollo-Gatto theorem). The equality $f^0_+(0) = 1$ could be obtained in several ways. For instance, a glance at the $T_3 Y$ diagram of the octet of pseudoscalar mesons (fig. 6.2) clearly shows that K^0 and π^+ are the upper and lower components, respectively, of the V-doublet. The $\int u^+(x) s(x) \mathrm{d}^3 x$ operator being the generator in V-space raising the projection of V-spin, the "weak charge" for the $\overline{\mathrm{K}}^0 \to \pi^+$transition is given by

$$f^0_+(0) = \sqrt{V(V+1) - V_3\left(V_3 + 1\right)} = 1.$$

By virtue of the $\Delta T = \frac{1}{2}$ selection rule, $f_+(0)$ for the $\mathrm{K}^+_{\ell 3}$decay must be smaller by a factor of $\sqrt{2}$:

$$f^+_+(0)/f^0_+(0) = 1/\sqrt{2}.$$

This relation must hold to the same accuracy as violation of isotopic invariance of the strong interaction, that is to about one percent. This relation can be derived by using, for example, the well-known ClebschGordan coefficients and assuming formally that lepton pairs in the decays $\mathrm{K}^+ \to \pi^0 \mathrm{e}^+ \nu$ and $\mathrm{K}^0 \to \pi^- \mathrm{e}^+ \nu$ behave as a "spurious particle" with $T = \frac{1}{2}$

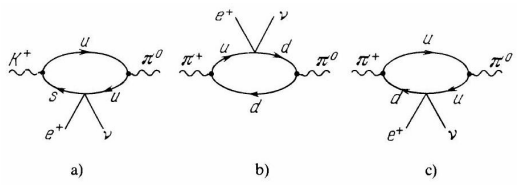


Fig63

and $T_3 = +\frac{1}{2}$ Consequently$f_+^+(0) = 1/\sqrt{2}$ in the approximation of un broken SU(3) symmetryThis is also easily derived if one compares the quark graphs for K_{e3}^+decayfig63aand π_{e3} decayfigs63b and cOnly one graph contributes to K_{e3} decaywhile two graphs must be taken into consideration for π_{e3} decayThis occurs because the isoscalar pair s does not enter the isovector π^0 mesonIf we recall now thatin π_{e3} decay $f_+(0) = \sqrt{2}$ we immediately obtain $f_+^+(0) = 1/\sqrt{2}$ for K_{e3}^+decayExperi mentally$f_+^+(q^2)$ and $f_+^0(q^2)$ are smooth functions of q^2 which are normally written in the linear approximation as

$$f_+^+\left(q^2\right) = f_+^+(0)\left(1 + \lambda_+^+\frac{q^2}{m_\pi^2}\right) \cong \frac{1}{\sqrt{2}}\left(1 + \lambda_+^+\frac{q^2}{m^2}\right)$$
$$f_+^0\left(q^2\right) = f_+^0(0)\left(1 + \lambda_+^0\frac{q^2}{m_\pi^2}\right) \cong 1 + \lambda_+^0\frac{q^2}{m^2}$$

where $\lambda_0^0 = \lambda_+^0 \cong 0.030$ A standard calculation which we suggest as an exercise for the readeryields

$$\Gamma\left(K_{e3}^+\right) = \frac{G^2\sin^2\theta}{768\pi^3}\left|f_+^+(0)\right|^2 m_K^5\left(0.57 + 0.14\lambda_+^+\right).$$

A comparison of this expression with the experimental width of K_{e3}^+decay under the assumption $\sqrt{2}f_+^+(0) = 1$ yields that $\sin\theta \cong 0.21$

5.6.4 $65K_{\mu 3}$ decays

$K_{\mu 3}$ decay is of interest because it could furnish information on the value of $f_-(q_2)$ provided we take for granted the $V - A$ character of the coupling and the μe universality which are fundamental to the standard theory of weak interactionsIn the limit of SU(3) symmetry$f_-(0) = 0$ The Ademollo

- (jatto theorem is not valid, however, with respect to $f_-(0)$, so that SU(3) can be expected to be broken strongly in this case. Thus, it is not impossible that $|\xi(0)| \sim 1$, where

$$\xi\left(q^2\right) = f_-\left(q^2\right)/f_+\left(q^2\right).$$

PCAC serves to derive the relation between the form factors f_K of $K_{\mu 2}$ decay and $f_+\left(m_K^2\right)$ and $f_-\left(m_K^2\right)$ of $K_{\mu 3}$ decay [the last two are taken at a non-physical point in which the pion 4-momentum is zero; hence, $q^2 = \left(p_K\ p_\pi\right)^2 = p_K^2 = m_K^2$]. The expression in question is called the Callan-Treiman formula:

$$f_+^0\left(m_K^2\right) + f_-^0\left(m_K^2\right) = f_K/f_\pi.$$

Using the experimental value of the ratio $f_K/f_\pi = 1.27$, and assuming $f_1^1\left(m_K^2\right) = 1 + 0.03m_K^2/m_\pi^2$, we find $f_-\left(m_K^2\right) \cong -0.1$. In principle, the data on f_-can be extracted from the

results on muon polarization in $K_{\mu 3}$ decay, from the angular and energy distributions of muons and pions and from accurate measurements of the ratio $\Gamma(K_{\mu 3})/\Gamma(K_{e3})$. So far we have no generally accepted value of $\xi(0)$ owing to the small scale of the effect, and the quantity λ_-in the formula $f_-(q^2) = f_-(0)[1 + \lambda_- q^2/m^2]$ is still unknown.

5.6.5 6.6. K_{e4} decays

The decay $K^+ \to \pi^+\pi^- e^+\nu_e$ is the best investigated among the K_{e4} decays. Its amplitude can be written in the form

$$M = \sqrt{\frac{1}{2}} G (V_\alpha + A_\alpha) L^\alpha \sin\theta,$$

where

$$A_\alpha = f_1 (p_1 + p_2)_\alpha + f_2 (p_1 - p_2)_\alpha + f_3 (p - p_1 - p_2)_\alpha$$
$$V_\alpha = f_4 m_K^{-2} \varepsilon_{\alpha\mu\nu\rho} p_\mu p_{1\nu} p_{2\rho}$$

p_1, p_2, p being the momenta of the π^-, π^+, and K mesons, respectively. The form factors f_1, f_2, f_3, f_4 are functions of three scalar variables, pp_1, pp_2, p_1p_2. The contribution of the term f_3 is negligibly small because of the smallness of the electron mass. The contribution of the f_4 term is also small owing to high powers of momentum. An estimate that can be obtained for the form factors f_1 and f_2, assuming them constant and using PCAC, is

$$f_1 \approx f_2 \approx 1/f_\pi.$$

'The K_{e4} decay is especially interesting because it enables us to study in pure form the scattering of pions on pions.

5.6.6 6.7. Leptonic decays of hyperons

Let us derive relations between the amplitudes for leptonic decays of baryons, which follow from the SU(3) symmetry of strong interactions and from the fact that the currents $\bar{u}d$ and $\bar{u}s$ belong to the same octet. Consider the baryon octet with $J^P = \frac{1}{2}^+$(see Chapter 29, sect. 2):

$$B_k^i = \begin{pmatrix} \sqrt{\frac{1}{6}}\Lambda + \sqrt{\frac{1}{2}}\Sigma^0 & \Sigma^+ & p \\ \Sigma^- & \sqrt{\frac{1}{6}}\Lambda - \sqrt{\frac{1}{2}}\Sigma^0 & n \\ \Xi^- & \Xi^0 & -\sqrt{\frac{2}{3}}\Lambda \end{pmatrix}.$$

Here i is the number of the row, and k the number of the column, $i, k = 1, 2, 3$. The trace of B_k^i is zero: $B_i^i = 0$. We shall study the amplitudes

$$\langle B_i^m | j_k^i | B_m^k \rangle \quad \text{and} \quad \langle B_m^k | j_k^i | B_i^m \rangle$$

for the case of

$$j_2^1 = \bar{q}^1 q_2 \equiv \bar{u}d \quad \text{and} \quad j_3^1 = \bar{q}^1 q_3 \equiv \bar{u}s$$

The current j_2^l turns the d-quark into the u-quark, and j_3^l turns s into u . In each amplitude, three octets are to be multiplied, and a scalar thereby obtained. Note that $8 \times 8 = 1 + 8 + 8 + 10 + \overline{10} + 27$ (see Chapter 29), so that two distinct scalars are present in the product $8 \times 8 \times 8$: the symmetrical one, D, and the antisymmetrical one, F. The amplitude in the general form is

$$(D+F)\left\langle B_i^m\right|j_k^i\left|B_m^k\right\rangle+(D-F)\left\langle B_m^k\right|j_k^i\left|B_i^m\right\rangle,$$

where D and F are scalar parameters which in the general case are different for different matrix elements of currents, that is for form factors $f_1, f_2, f_3, g_1,\ g_2, g_3$ (see Chapter 5 where f_l and g_i are defined for β-decay of the neutron). If the initial baryons are described by the matrix B_k^l, the final ones are given by $\bar{B}_i^k$ which is obtained from B_i^k by conjugation of each element and transposition. It is convenient to multiply B by $\bar{B}$ without writing out the explicit expression of the latter. The matrix elements of the current $j_2^1\cos\theta$ are

$$\cos\theta\left\{(D+F)\left[\left(\sqrt{\frac{1}{6}}\bar{\Lambda}^0+\sqrt{\frac{1}{2}}\bar{\Sigma}^0,\Sigma^-\right)+\left(\bar{\Sigma}^+,\sqrt{\frac{1}{6}}\Lambda-\sqrt{\frac{1}{2}}\Sigma^0\right)+(\bar{p}n)\right]\right.$$
$$+(D-F)\left[\left(\bar{\Sigma}^+,\sqrt{\frac{1}{6}}\Lambda^0+\sqrt{\frac{1}{2}}\Sigma^0\right)\right.$$
$$\left.\left.+\left(\sqrt{\frac{1}{6}}\Lambda^0-\sqrt{\frac{1}{2}}\Sigma^0,\Sigma^-\right)+\left(\bar{\Xi}^0\Xi^-\right)\right]\right\}.$$

Here the expression proportional to ($D+F$) is obtained by multiplying the lirst row of B (with bars over the particle symbols) by the second row of the same matrix (this corresponds to the product $\bar{B}_1^m B_m^2$ since the first column B_1^m in matrix $\bar{B}$ is obtained by transposition (and conjugation) of the first row B_m^1 in matrix B). The term proportional to ($D-F$) is obtained by multiplying the second column of matrix B (with bars over the particle symbols) by the first column of the same matrix (this corresponds to the product $\bar{B}_m^2 B_1^m$).

Likewise, we obtain the matrix elements of the current $j_3^1\sin\theta$ by writing out the products of the first row by the third row, and of the third column by the first one:

$$\sin\theta\left\{(D+F)\left[\left(\sqrt{\frac{1}{6}}\Lambda^0+\sqrt{\frac{1}{2}}\bar{\Sigma}^0,\Xi^-\right)+\left(\bar{\Sigma}^+,\Xi^0\right)+\left(\bar{p},-\sqrt{\frac{2}{3}}\Lambda\right)\right]\right.$$
$$\left.+(D-F)\left[\left(\bar{p},\sqrt{\frac{1}{6}}\Lambda^0+\sqrt{\frac{1}{2}}\Sigma^0\right)+\left(\bar{n},\Sigma^-\right)+\left(-\sqrt{\frac{2}{3}}\bar{\Lambda},\Xi^-\right)\right]\right\}$$

The expressions obtained immediately yield six amplitudes for strangenessconserving transitions and six amplitudes for transitions changing strangeness by unity:

$$\begin{array}{llll}
\mathrm{n}\to\mathrm{p}: & (D+F)\cos\theta, & \Lambda\to\mathrm{p}: & -\sqrt{\frac{1}{6}}(D+3F)\sin\theta\\
\Xi^-\to\Xi^0: & (D-F)\cos\theta, & \Xi^-\to\Lambda: & -\sqrt{\frac{1}{6}}(D-3F)\sin\theta\\
\Lambda\to\Sigma^+: & \sqrt{\frac{2}{3}}D\cos\theta, & \Sigma^0\to\mathrm{p}: & \sqrt{\frac{1}{2}}(D-F)\sin\theta\\
\Sigma^-\to\Lambda: & \sqrt{\frac{2}{3}}D\cos\theta, & \Xi^-\to\Sigma^0: & \sqrt{\frac{1}{2}}(D+F)\sin\theta\\
\Sigma^0\to\Sigma^+: & -\sqrt{2}F\cos\theta, & \Sigma^-\to\mathrm{n}: & (D-F)\sin\theta\\
\Sigma^-\to\Sigma^0: & +\sqrt{2}F\cos\theta, & \Xi^0\to\Sigma^+: & (D+F)\sin\theta.
\end{array}$$

Three strangeness-conserving transitions ($\mathrm{n}\to\mathrm{p}, \Sigma^\pm\to\Lambda$) and all the strangeness-changing ones were observed experimentally. (The decay $\Sigma^0\to\mathrm{pe}\,{}^-\bar{\nu}$ cannot be observed since the electromagnetic decay $\Sigma^0\to\Lambda^0\gamma$ is predominant. Nevertheless, it is possible to observe the reaction $\tilde{\nu}_\mu+\mathrm{p}\to\Sigma^0+\mu^+$which has the same matrix element).

We have thus established that the twelve amplitudes are functions of three parameters, D, F, and θ. This is true for each of the six form factors describing baryon decays: f_1, f_2, f_3 and g_1, g_2, g_3. The predominant role in baryon decays is played by the vector form factor $f_1\left(q^2\right)$

and the axial form factor $g_1(q^2)$, where q is the 4 -momentum carried by the leptons. The static limit is a fairly good approximation since $|q| \ll M$, where M is the baryon mass; consequently, we shall consider only the vector and axial charges, $f_1(0)\gamma_\alpha$ and $g_1(0)\gamma_\alpha\gamma_5$. The contributions of other form factors will be neglected.

Let us now discuss the values of the parameters D_{V} and F_{V} giving $f_1(0)$, and D_{A} and F_{A} giving $g_1(0)$. The vector charges $\int \bar{q}\gamma_0 \frac{1}{2}\lambda q \, \mathrm{d}^3x$ are generators of SU(3), so that their matrix elements for transitions between octet states j and k are equal to the structural constants f_{ijk} of SU(3) (see appendix). This means, in our notation, that $F_{\mathrm{v}} = 1, D_{\mathrm{v}} = 0$. This conclusion agrees with that drawn in chapter 5 where the isotopic subgroup SU(2) of SU(3) was considered. Indeed, we had concluded that $f_1(0) = 0$ for the $\Sigma \to \Lambda \mathrm{e}\nu$ decays (and this implies $D_{\mathrm{v}} = 0$), because Σ and Λ belong to different isotopic multiplets. We have also established there that $f_1(0) = 1$ for the β-decay of the neutron (the $T = \frac{1}{2} \to T = \frac{1}{2}$ transition). In the notation of this chapter, this gives $F_{\mathrm{v}} = 1$.

Both D_{A} and F_{A} are distinct from zero and have to be determined by experiment (hereafter the subscript A is omitted). The matrix elements of the fundamental decays are:

$$
\begin{aligned}
\mathrm{n} \to \mathrm{p}\mathrm{e}^-\nu &: [\gamma_\alpha + (D+F)\gamma_\alpha\gamma_5]\cos\theta, \\
\Sigma^\pm \to \Lambda \mathrm{e}^\pm\nu &: \gamma_\alpha\gamma_5\sqrt{\frac{2}{3}}D\cos\theta, \\
\Lambda \to \mathrm{p}\mathrm{e}^-\nu &: -\sqrt{\frac{3}{2}}\left[\gamma_\alpha + \left(F + \frac{1}{3}D\right)\gamma_\alpha\gamma_5\right]\sin\theta, \\
\Sigma^- \to \mathrm{n}\mathrm{e}^-\nu &: -[\gamma_\alpha + (F-D)\gamma_\alpha\gamma_5]\sin\theta, \\
\Xi^- \to \Lambda \mathrm{e}^-\nu &: \sqrt{\frac{3}{2}}\left[\gamma_\alpha + \left(F - \frac{1}{3}D\right)\gamma_\alpha\gamma_5\right]\sin\theta, \\
\Xi^- \to \Sigma^0 \mathrm{e}^-\nu &: \sqrt{\frac{1}{2}}[\gamma_\alpha + (F+D)\gamma_\alpha\gamma_5]\sin\theta, \\
\Xi^0 \to \Sigma^+ \mathrm{e}^-\nu &: [\gamma_\alpha + (F+D)\gamma_\alpha\gamma_5]\sin\theta.
\end{aligned}
$$

The best fit values of $\sin\theta, D$, and F for all available decay rates and the values of the ratio $g_{\mathrm{A}}/g_{\mathrm{V}}$ $(\equiv g_1(0)/f_1(0))$ for the leptonic decays of baryons are: $\sin\theta \cong 0.23, D \cong 0.80, F \cong 0.45$ (note that $g_{\mathrm{A}}/g_{\mathrm{v}}$ measured in neutron decay fixes the sum $F + D = 1.25 \pm 0.01$). Calculation of D/F in the framework of SU(6) symmetry yields $D/F = 3/2$; hence, $D = 0.75, F = 0.5$.

Unfortunately, the value of $g_{\mathrm{A}}/g_{\mathrm{v}}$ has been measured so far only for three decays: $\mathrm{n} \to \mathrm{p}\mathrm{e}^-\nu, \Lambda \to \mathrm{p}\mathrm{e}^-\nu$, and $\Sigma^- \to \mathrm{n}\mathrm{e}^-\nu$. Moreover, there is a discrepancy between two most accurate experimental results concerning the decay of Σ^-. One of them gives $|g_{\mathrm{A}}/g_{\mathrm{v}}| = 0.435 \pm 0.035$, while the other gives $0.17^{+0.07}_{-0.09}$. In both experiments the ratio $|g_{\mathrm{A}}/g_{\mathrm{v}}|$ is obtained from the energy spectra of the neutrons. It seems highly improbable that improved precision of the experiments will reveal serious deviations from the SU(3) picture of semileptonic decays, which by now is well established. Nevertheless, precise measurements of $g_{\mathrm{A}}/g_{\mathrm{v}}$ for a number of decays would be very welcome. It would be interesting, for instance, to see whether $D \cong F$. In this case we must have $g_{\mathrm{A}} \cong 0$ in the $\Sigma^- \to \mathrm{n}\mathrm{e}^-\nu$ decay.

Problem: Derive the expression for the neutron spectrum in the $\Sigma^- \to ne^-\nu$ decay. Assume the neutron to be non-relativistic (i.e. its kinetic energy is negligible compared to that carried away by the electron and neutrino). If we neglect the electron mass, and integrate over the lepton phase space, we obtain

$$\begin{aligned} \mathrm{d}\Gamma &= c\left[g_{\mathrm{V}}^2\delta_0^\alpha\delta_0^\beta + g_{\mathrm{A}}^2\left(-g^{\alpha\beta}+\delta_0^\alpha\delta_0^\beta\right)\right]\left(-g_{\alpha\beta}q^2+q_\alpha q_\beta\right)\mathrm{d}\boldsymbol{q} \\ &= c\left[g_{\mathrm{V}}^2\left(-q^2+q_0^2\right)+g_{\mathrm{A}}^2\left(2q^2+q_0^2\right)\right]\mathrm{d}\boldsymbol{q} \\ &= c\left[g_{\mathrm{V}}^2\boldsymbol{q}^2+g_{\mathrm{A}}^2\left(3\Delta^2-2\boldsymbol{q}^2\right)\right]\mathrm{d}\boldsymbol{q}. \end{aligned}$$

Here $\Delta = m_\Sigma - m_{\mathrm{n}} = q_0, q = (q_0, q)$ is the total 4-momentum of the leptons, and $-\boldsymbol{q}$ is the neutron momentum. By integrating over $\mathrm{d}\boldsymbol{q}(0 \le |\boldsymbol{q}| \le \Delta)$ and comparing the expression obtained $\frac{4}{5}\pi c\,(g_{\mathrm{V}}+3g_{\mathrm{A}}^2)$ to that for the total probability of the decay,

$$\Gamma = \frac{G^2\left(g_{\mathrm{V}}^2+3g_{\mathrm{A}}^2\right)\Delta^5}{60\pi^3}$$

(see Chapter 5), we obtain $c = G^2/48\pi^4$.

5.7 7 Strangeness-changing non-leptonic interactions

In this chapter we shall analyse non-leptonic decays of strange particles: $\mathrm{K} \to 2\pi$, $\mathrm{K} \to 3\pi, \Lambda \to \mathrm{N}\pi, \Sigma \to \mathrm{N}\pi, \Xi \to \Lambda\pi, \Omega \to \Lambda\,\overline{\mathrm{K}}$, and $\Omega \to \Xi\pi$. All these decays are produced by the coupling of *us* - and *du*-currents (this coupling transforms the s-quark into a d-quark). For example, the decay $\mathrm{K}^+ \to \pi^+\pi^0$ is mostly due to the quark graphs of fig. 7.1. Another example is the decay $\Sigma^+ \to \mathrm{n}\pi^+$, which is due mostly to quark graphs of the type illustrated in fig. 7.2. Virtual strong interactions are more essential in non-leptonic than in semi-leptonic interactions discussed in the preceding chapters. The gluon exchanges play a particularly important role.

5.7.1 7.1. Properties of the bare non-leptonic lagrangian

The initial product of currents, sometimes termed the bare non-leptonic lagrangian (a hint at the subsequent "dressing" with gluons), takes the form

$$2\sqrt{2}G\cos\theta\sin\theta\left[\left(\bar{d}_{\mathrm{L}}\gamma_\alpha u_{\mathrm{L}}\right)\left(\bar{u}_{\mathrm{L}}\gamma^\alpha s_{\mathrm{L}}\right)+\left(\bar{u}_{\mathrm{L}}\gamma_\alpha d_{\mathrm{L}}\right)\left(\bar{s}_{\mathrm{L}}\gamma^\alpha u_{\mathrm{L}}\right)\right].$$

(For the sake of brevity, we discuss hereafter mostly the processes which are caused by the first term of this expression, i.e. the term transforming the sto a d-quark.) Let us discuss the properties of this lagrangian. It is CP invariant, but not invariant with respect to P and C separately. It satisfies the condition

$$|\Delta S| = 1,$$

where ΔS is the difference in strangeness of the initial and final states. (Recall that by definition, the strangeness of the s-quark is -1 .) The decays with $|\Delta S| > 1$ are forbidden. These decays (such as $\Xi \to \mathrm{N}\pi, \Omega \to \Lambda\pi$, or $\Omega \to \mathrm{NK}$) are allowed only in higher orders of perturbation theory in weak interactions, and their expected decay rates are smaller by approximately fourteen orders of magnitude than the decay rates of the processes allowed

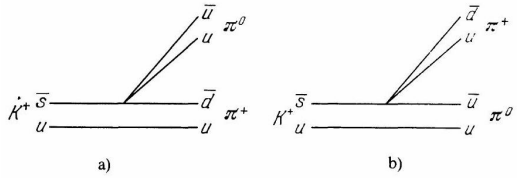


Fig. 7.1.

by the selection rule $|\Delta S| = 1$. None of the forbidden decays are observed, but the experimental upper bounds are too rough compared to the accuracy of the theoretical selection rules.

As for the isospin selection rules, it is easily seen that the $(\bar{d}u)(\bar{u}s)$ interaction, comprising three isospinors and one isoscalar, satisfies the condition

$$\Delta T = \frac{1}{2}, \frac{3}{2}.$$

We shall demonstrate later that experimentally observed transition amplitudes with $\Delta T = \frac{1}{2}$ are greater by approximately an order of magnitude than the amplitudes with $\Delta T = \frac{3}{2}$. No quantitative calculation "to the end" is available so far on the mechanisms of enhancement of amplitudes with $\Delta T = \frac{1}{2}$, and suppression of those with $\Delta T = \frac{3}{2}$. Nevertheless, it is qualitatively clear, that the approximate rule $\Delta T = \frac{1}{2}$ for non-leptonic decays is dynamical in nature. A significant role is played here by virtual gluons. We cannot yet calculate their contribution exactly, so we shall try to obtain an estimate. We shall assume that the contribution of soft gluons (gluons with low q^2) is already covered by the quark wave function of a hadron, and take account of the hard gluons. By virtue of the asymptotic freedom of quantum chromodynamics, this calculation can be realized in the framework of perturbation theory. "Dressing" of the bare non-leptonic lagrangian with hard gluons yields the so-called effective non-leptonic lagrangian (see the end of this chapter) which differs from the bare one both in the value of the

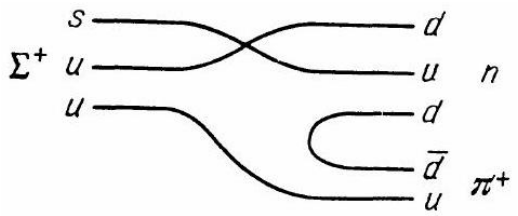


Fig. 7.2.

effective constant in the initial operator expression, and in the appearance of additional operator terms (the so-called Wilson operator expansion).

5.7.2 7.2. The inclusion of hard gluons

Before discussing the contribution of virtual gluons, let us separate the bare lagrangian into two terms,

$$2\left(\bar{d}_{\mathrm{L}}\gamma_\alpha u_{\mathrm{L}}\right)\left(\bar{u}_{\mathrm{L}}\gamma^\alpha s_{\mathrm{L}}\right) = I_3 + I_6,$$

where

$$I_3 = \left(\bar{d}_{\mathrm{L}}\gamma_\alpha u_{\mathrm{L}}\right)\left(\bar{u}_{\mathrm{L}}\gamma^\alpha s_{\mathrm{L}}\right) - \left(\bar{u}_{\mathrm{L}}\gamma_\alpha u_{\mathrm{L}}\right)\left(\bar{d}_{\mathrm{L}}\gamma^\alpha s_{\mathrm{L}}\right),$$
$$I_6 = \left(\bar{d}_{\mathrm{L}}\gamma_\alpha u_{\mathrm{L}}\right)\left(\bar{u}_{\mathrm{L}}\gamma^\alpha s_{\mathrm{L}}\right) + \left(\bar{u}_{\mathrm{L}}\gamma_\alpha u_{\mathrm{L}}\right)\left(\bar{d}_{\mathrm{L}}\gamma^\alpha s_{\mathrm{L}}\right).$$

The first of these terms in antisymmetric, while the second one is symmetric with respect to the permutation $\bar{d} \leftrightarrow \bar{u}$ or $u \leftrightarrow s$. The subscripts 3 and 6 indicate the dimension in color space; their meaning will be clear shortly. Until this section, color variables were omitted because weak currents are color singlets. Here we want to discuss the contribution of color gluons, so that color indices of the quark creation and annihilation operators must be written explicitly. Then,

$$I_{3,6} = \left(\bar{d}^i_{\rm L}\gamma_\alpha u_{{\rm L}i}\right)\left(\bar{u}^k_{\rm L}\gamma^\alpha s_{{\rm L}k}\right) \mp \left(\bar{u}^i_{\rm L}\gamma_\alpha u_{{\rm L}i}\right)\left(\bar{d}^k_{\rm L}\gamma^\alpha s_{{\rm L}k}\right).$$

Let us consider the transition $us \leftrightarrow ud$ (fig. 7.3) realized by I_3 and I_6. In the first case the initial and final states are antisymmetric with respect to the permutation of color indices. Hence, they belong to a color triplet (more precisely, to the anti-triplet $\overline{3}$). In the second case they are symmetric and belong to a sextet (we recall that $3 \times 3 = 6 + \overline{3}$). It is easy to see that the interaction I_3 satisfies the $\Delta T = \frac{1}{2}$ selection rule. Indeed, owing to antisymmetrization, the final state ud (fig. 7.3) is isoscalar ($ud - du$ has $T = 0$), but then $\Delta T = \frac{1}{2}$ since the initial state is an isospinor. In the case of the interaction I_6, the final state $ud + du$ has $T = 1$. Consequently, I_6 includes transitions both with $\Delta T = \frac{1}{2}$ and with $\Delta T = \frac{3}{2}$.

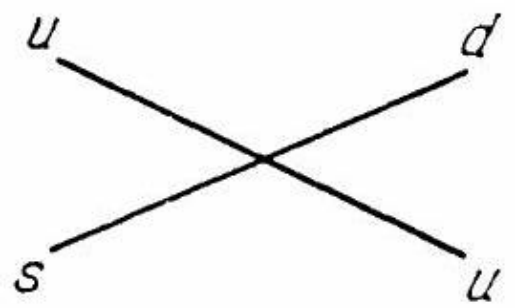


Fig. 7.3.

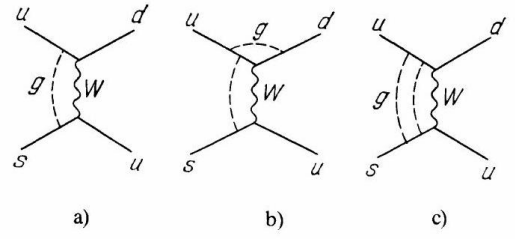


Fig. 7.4.

We shall begin with just those graphs in which a W-boson connects two different quark lines. We mean the graphs of fig. 7.4 and more complex graphs with an infinite number of hard virtual gluons (soft gluons are not shown here and in subsequent graphs). In this case the inclusion of hard virtual gluons does not modify the form of the operators I_3 and I_6 but only changes their coefficients. The result is

$$\sqrt{2}G\left(a_3 I_3 + a_6 I_6\right)\sin\theta\cos\theta.$$

In the leading logarithm approximation,

$$a_i = \left(\frac{\alpha_{\rm s}(\mu)}{\alpha_{\rm s}\left(m_{\rm W}\right)}\right)^{\gamma_t}, \quad i = 3, 6.$$

Here $\alpha_{\rm s}$ is the so-called running coupling constant of the strong interaction, $m_{\rm W}$ is the W-boson mass, μ is the characteristic momentum of quarks in a hadron ($1/\mu$ is the confinement radius), and

$$\gamma_3 = \frac{4}{b}, \quad \gamma_6 = -\frac{2}{b}.$$

We recall that according to quantum chromodynamics, the strong interaction "constant" $\alpha_{\rm s} = g^2/4\pi$ (g is the color charge) is a logarithmic function of the momentum transfer $Q \equiv \sqrt{-q^2}$, and contains the parameter b :

$$\alpha_{\rm s}(Q) = \frac{2\pi}{b\ln(Q/\Lambda)}.$$

Here $\Lambda \sim 100$MeV is a universal constant defining the scale of hadronic dimensions, and the dimensionless constant b is a function of $N_{\rm f}(Q)$, that is of the number of flavors of quarks with masses below Q :

$$b = 11 - \frac{2}{3}N_{\rm f}(Q).$$

If $Q \lesssim m_{\rm c}$ ($m_{\rm c}$ is the mass of the c-quark), then u$-$, d$-$, and s-quarks are operative, $N_{\rm f}(Q) = 3$ and $b = 9$. If $Q \gg m_{\rm c}$, then u-, d-, s-, and c-quarks are operative, $N_{\rm f}(Q) = 4$ and $b = \frac{25}{3}$. If $Q \gg m_{\rm b}$, then u$-$, d$-$, s$-$, c$-$, and b-quarks are operative, $N_{\rm f}(Q) = 5$ and $b = \frac{23}{3}$. The leading logarithm approximation mentioned above assumes that $\alpha_s(\mathrm{Q}) \ll 1$, but that $\alpha_s(Q)\ln(Q/\Lambda)$ is not small. This means that terms of the order of $[\alpha_s(Q)]^{n+1}(\ln(Q/\Lambda))^n$ are neglected, and that the terms of the order of $(\alpha_{\rm s}(Q)\ln(Q/\Lambda))^n$ are summed over to all orders of perturbation theory.

For the estimates in the above expression for a_i we shall assume that $\alpha_{\rm s}(\mu) = 1$. This yields $\mu \cong 140$MeV for $\Lambda \cong 70$MeV. (In this case, $\alpha_{\rm s}(m_\rho) \cong 0.3$, and $\alpha_{\rm s}(2m_{\rm c} \cong 2.5\mathrm{GeV}) \cong 0.2$, which is in agreement with the charmonium data. Some authors derive $\Lambda \cong 350$GeV from the data on deep-inelastic scattering, which yields $\mu \cong 700$MeV.) For $m_{\rm w} \cong 80$GeV and $\Lambda \cong 70$MeV we obtain $\alpha_{\rm s}(\mu)/\alpha_{\rm s}(m_{\rm w}) \cong 10$; hence

$$a_3 \cong 3 \quad \text{and} \quad a_6 = 0.6.$$

This demonstrates that hard gluons enhance the $\Delta T = \frac{1}{2}$ transitions and suppress those with $\Delta T = \frac{3}{2}$. We shall find afterwards, however, that these theoretically predicted enhancement and suppression effects are not sufficient to match the experimentally observed large amplitudes with $\Delta T = \frac{1}{2}$, and small amplitudes with $\Delta T = \frac{3}{2}$.

5.7.3 7.3. The gluonic monopole

One additional class of graphs is possible when virtual gluons are taken into account. This class was not discussed in the preceding pages. We mean the graphs in which a virtual W-boson is emitted and absorbed by the same quark which is coupled to other quarks only by gluons. Elementary graphs of this type are shown in fig. 7.5. Let us now calculate their contribution; note that the result will not be significantly changed when these graphs are

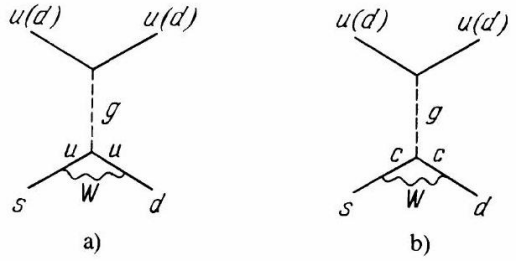


Fig. 7.5.

dressed, in the leading logarithm approximation, by an infinite number of gluons. If we neglect the mixing of d - and s-quarks with b-quarks, the charged currents take the form

$$\bar{u}_{\mathrm{L}}\gamma_\alpha d'_{\mathrm{L}} = \bar{u}_{\mathrm{L}}\gamma_\alpha \left(d_{\mathrm{L}}\cos\theta + s_{\mathrm{L}}\sin\theta\right)$$
$$\bar{c}_{\mathrm{L}}\gamma_\alpha s'_{\mathrm{L}} = \bar{c}_{\mathrm{L}}\gamma_\alpha \left(-d_{\mathrm{L}}\sin\theta + s_{\mathrm{L}}\cos\theta\right)$$

The graphs 5a and 5b would cancel out, therefore, if the masses of u- and c-quarks were identical. Actually $m_{\mathrm{c}} \gg m_{\mathrm{u}}$, and the compensation is realized only for momenta of virtual particles exceeding m_{c}. For lower momenta, the graph 7.5a is predominant. We can then conclude that the sum of the two graphs of fig. 7.5 is approximately equal to the contribution of the first of them, but with the momenta of the virtual particles in the loop cut off at m_{c}. Taking into account that $m_{\mathrm{c}} \ll m_{\mathrm{W}}$, we can reduce the graph in fig. 7.5a to the four-fermion point interaction (see fig. 7.6a). The gap in the fourfermion vertex in fig. 7.6a separates two white $\mathrm{V}-\mathrm{A}$ currents found in parentheses in the expression

$$\sqrt{\frac{1}{2}}G\sin\theta\cos\theta\left(\bar{d}^{\alpha l}\left(O_\mu\right)^\beta_\alpha \delta^k_i u_{\beta k}\right)\left(\bar{u}^{\gamma l}\left(O^\mu\right)^\delta_\gamma \delta^m_l s_{\delta m}\right),$$

where $O_\mu = \gamma_\mu\left(1+\gamma_5\right)$, Greek letters denote Dirac indices ($0,1,2,3$), and Latin letters denote color indices ($1,2,3$). The calculation is conveniently simplified by the Fierz transformation: the operators $\bar{u}$ and u are now in one bracket, and $\bar{d}$ and s in the other one (see fig. 7.6b). By using the relations

$$\left(O_\mu\right)^\beta_\alpha \left(O^\mu\right)^\delta_\gamma = -\left(O_\mu\right)^\delta_\alpha \left(O^\mu\right)^\beta_\gamma$$
$$\delta^k_i\delta^m_l = \frac{1}{3}\delta^m_i\delta^k_l + \frac{1}{2}\boldsymbol{\lambda}^m_i\boldsymbol{\lambda}^k_l$$

(see appendix), and taking into account that fermion operators anticommute, we obtain

$$\left(\bar{d}O_\mu u\right)\left(\bar{u}O^\mu s\right) = \frac{1}{3}\left(\bar{u}O_\mu u\right)\left(\bar{d}O^\mu s\right) + \frac{1}{2}\left(\bar{u}O_\mu\lambda^a u\right)\left(\bar{d}O^\mu\lambda^a s\right)$$

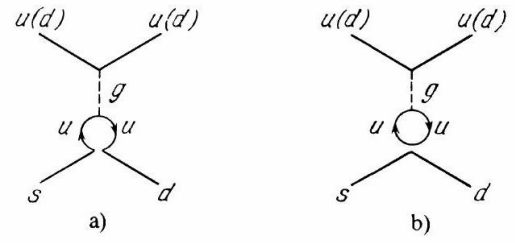


Fig. 7.6.

It is necessary now to calculate the u-quark loop in fig. 7.6b. The upper vertex (emission of a gluon) of this loop is

$$g\bar{u}\frac{\lambda^b}{2}\gamma_\nu u.$$

In loop calculations, we have to find the trace over Dirac and color suffices. Hence, the term $\frac{1}{3}\left(\bar{u}O_\mu u\right)\left(\bar{d}O^\mu s\right)$ of the lower vertex gives zero, and only the part $\frac{1}{2}\left(\bar{u}\gamma_\mu\lambda^a u\right)\left(\bar{d}O^\mu\lambda^a S\right)$ of the term $\frac{1}{2}\left(\bar{u}O_\mu\lambda^a u\right)\left(\bar{d}O^\mu\lambda^a S\right)$ will give a non-zero contribution.

The loop in question is exactly the same (with the exception of additional color matrices) as that found in quantum electrodynamics in the case of vacuum polarization calculations:

$$-\operatorname{Tr}\frac{\lambda^a}{2}\frac{\lambda^b}{2}\int \operatorname{Tr}\gamma_\mu\frac{1}{\hat p+\hat q}\gamma_\nu\frac{1}{\hat p}\frac{\mathrm{d}^4p}{(2\pi)^4}=\frac{\delta^{ab}}{2}\left(q^2g_{\mu\nu}-q_\mu q_\nu\right)\mathscr{P},$$

where $a,b=1,\ldots,8$, and q is the 4 -momentum carried by the gluon (see fig. 7.6b). We have ignored the u-quark mass since $m_{\mathrm{u}}\ll\mu$. The minus sign in front of the above expression comes from the following standard factors (they are discussed in all textbooks on quantum field theory): (-1) for each closed fermion loop, ($+i$) for each fermion propagator, ($-i$) for each propagator of the vector particle, (i) for each vertex, and ($+i$) for the transition in d^4p from $\mathrm{d}p_0$ to $i\,\mathrm{d}p_4$. In addition, the relation between S - and T-matrices, $S=1+iT$, and that between S and the lagrangian, $S=\exp\left(\mathrm{i}\mathcal{L}\mathrm{d}^4x\right)$, must be taken into account.

Up to a dimensionless factor $\mathscr{P}$, the form of the integral is determined by the transversality condition (which demands, in particular, that quadratic divergence be absent). In order to find $\mathscr{P}$, multiply the left-hand and right-hand parts by $g^{\mu\nu}$. This gives

$$\begin{aligned}3q^2\mathscr{P}&=-\int\operatorname{Tr}\gamma_\mu\frac{1}{\hat p+\hat q}\gamma^\mu\frac{1}{\hat p}\frac{\mathrm{d}^4p}{(2\pi)^4}=2\int\operatorname{Tr}\frac{1}{\hat p}\hat q\frac{1}{\hat p}\hat q\frac{1}{\hat p}\frac{1}{\hat p}\frac{\mathrm{d}^4p}{(2\pi)^4}\\&=\frac{1}{(2\pi)^4}\int\frac{\mathrm{d}^4p}{p^6}\left[2(pq)(pq)-q^2p^2\right]\\&=-\frac{q^2}{4\pi^2}\int\frac{\mathrm{d}p^2}{p^2},\end{aligned}$$

since

$$\int\frac{\mathrm{d}^4p}{p^6}2p_\mu p_\nu=\frac{1}{2}g_{\mu\nu}\int\frac{\mathrm{d}^4p}{p^4}$$

Finally,

$$\mathscr{P}=-\frac{1}{12\pi^2}\int\frac{\mathrm{d}p^2}{p^2}=-\frac{1}{12\pi^2}\ln\frac{m_{\mathrm{c}}^2}{\mu^2}$$

where the upper integration limit is chosen to be m_{c}^2 (since the graphs of figs. 7.5a and 7.5b cancel out for $p^2>m_{\mathrm{c}}^2$). The lower integration limit is chosen to be μ^2 because the free quark propagator must be modified at $p^2<\mu^2$ due to confinement. As a result, the contribution of the graph of fig. 7.6a becomes

$$\begin{aligned}&-\sqrt{2}G\sin\theta\cos\theta\frac{g^2}{12\pi^2}\ln\frac{m_{\mathrm{c}}^2}{\mu^2}\left(\bar d_{\mathrm{L}}\gamma_\mu\lambda^a s_{\mathrm{L}}\right)\frac{\delta^{ab}}{2}\left(\bar u\gamma^\mu\frac{\lambda^b}{2}u+\bar d\gamma^\mu\frac{\lambda^b}{2}d\right)\\&=-\sqrt{2}G\sin\theta\cos\theta\frac{\alpha_{\mathrm{s}}(\mu)}{6\pi}\ln\frac{m_{\mathrm{c}}}{\mu}\left(\bar d_{\mathrm{L}}\gamma_\mu\lambda^a s_{\mathrm{L}}\right)\left(\bar u\gamma^\mu\lambda^a u+\bar d\gamma^\mu\lambda^a d\right)\end{aligned}$$

Note that the factor $1/q^2$ in the gluon propagator is cancelled out by the factor q^2 produced by the quark loop. The effective four-fermion interaction described by fig. 7.6a thus looks local from large distances ($r\gg 1/2m_{\mathrm{c}}$). The effective vertex of gluon emission in the $\mathrm{s}\leftrightarrow\mathrm{d}$ transition becomes zero for $q^2=0$ (q is the gluon 4-momentum). So we can refer to it as the monopole vertex. Indeed, it is well-known that in the nuclear monopole transitions, the emission of a real photon with $q^2=0$ is forbidden, and thus an $\mathrm{e}^+\mathrm{e}^-$pair with $q^2>0$ is emitted. (Strictly speaking, the gds vertex is a sum of a monopole, $q^2\gamma_\alpha$, and an anapole, $q^2\gamma_\alpha\gamma_5$).

We must explain now why $\alpha_{\mathrm{s}}(\mu)$, and not $\alpha_{\mathrm{s}}\left(m_{\mathrm{c}}\right)$, was substituted into the above expression. The cut-off of the loop is carried out at the point m_c, so that on the face of it the graphs of fig. 7.6 correspond to $\alpha_s\left(m_c\right)$. It can be demonstrated, however, that if we dress these graphs with additional gluons, a renormalization factor appears: $\left(\alpha_s(\mu)/\alpha_s\left(m_c\right)\right)^{2\gamma_3}$ where $2\gamma_3=8/b=$

$0.96 \cong 1$. Consequently, $\alpha_s(m_c)$ in the expression under consideration is replaced by $\alpha_s(\mu)$ (recall that by our convention, $\alpha_s(\mu) = 1$). Denoting

$$a_R = \frac{1}{6\pi} \ln \frac{m_c}{\mu},$$

we obtain $a_R \cong 0.12$ for $m_c/\mu \cong 10$. Hence, a_R is quite small:

$$a_R \sim \frac{1}{5} a_6 \sim \frac{1}{25} a_3.$$

The contribution of the graphs of the type of fig. 7.6 is nevertheless very substantial because of the specific structure of the operator

$$-\left(\bar{d}_L \gamma_\mu \lambda^a s_L\right)\left(\bar{u}\gamma^\mu \lambda^a u + \bar{d}\gamma^\mu \lambda^a d\right)$$

In fact, this operator is a sum of two terms,

$$-\left(\bar{d}_L \gamma_\mu \lambda^a s_L\right)\left(\bar{u}_L \gamma^\mu \lambda^a u_L + \bar{d}_L \gamma^\mu \lambda^a d_L\right)$$
$$-\left(\bar{d}_L \gamma_\mu \lambda^a s_L\right)\left(\bar{u}_R \gamma^\mu \lambda^a u_R + \bar{d}_R \gamma^\mu \lambda^a d_R\right).$$

The first of these terms involves only left-handed spinors and, because of the smallness of the coefficient a_R, is much less important than I_3 and I_6 which have the same helicity structure. Therefore, as a crude approximation, the contribution of this operator can be neglected. The second operator (we denote it by I_R) contains both the left-handed and right-handed spinors. In a number of cases this may considerably enhance the contribution of I_R to the amplitude of non-leptonic decays. This phenomenon will be demonstrated in Chapter 9.

5.7.4 7.4. Effective non-leptonic lagrangian

Now let us collect all the terms of the simplified effective non-leptonic quark interaction with $\Delta S = 1$:

$$\tilde{\mathcal{L}}_{\text{eff}}(\Delta S = 1) = \sqrt{2} G \sin\theta \cos\theta \left[a_3 I_3 + a_6 I_6 + a_R I_R\right],$$

where

$$I_{3,6} = \left(\bar{d}_L \gamma_\alpha u_L\right)\left(\bar{u}_L \gamma^\alpha s_L\right) \mp \left(\bar{u}_L \gamma_\alpha u_L\right)\left(\bar{d}_L \gamma^\alpha s_L\right),$$
$$I_R = -\left(\bar{d}_L \gamma_\alpha \lambda s_L\right)\left(\bar{u}_R \gamma^\alpha \lambda u_R + \bar{d}_R \gamma^\alpha \lambda d_R\right),$$
$$a_3 \cong 3, \quad a_6 \cong 0.6, \quad a_R \cong 0.12.$$

Similarly to I_3, the operator I_R is an isotopic spinor and therefore results only in transitions with $\Delta T = \frac{1}{2}$.

If in addition to the u - and d-quarks the upper lines in figs. 7.5 and 7.6 symbodize s-quarks as well, and if the dressing of these graphs with an infinite number of gluons were also included, then the total effective non-leptonic lagrangian would have the form given by Shifman, Vainshtein and Zakharov

$$\mathcal{L}_{\text{eff}}(\Delta S = 1) = \sqrt{2} G \sin\theta \cos\theta \sum_{i=1}^{6} c_i O_l,$$

where O_i are four-fermion operators which transform as irreducible representations of the isospin group SU(2) and the flavor group $SU(3)_f$:

$$O_1 = \bar{d}_L \gamma_\mu s_L \bar{u}_L \gamma^\mu u_L - \bar{u}_L \gamma_\mu s_L d_L \gamma^\mu u_L \quad \left(\{8f\}, \Delta T = \frac{1}{2}\right),$$

$$
\begin{aligned}
O_2 = \;& \bar{d}_{\mathrm{L}}\gamma_\mu s_{\mathrm{L}}\bar{u}_{\mathrm{L}}\gamma^\mu u_{\mathrm{L}} + \bar{u}_{\mathrm{L}}\gamma_\mu s_{\mathrm{L}}\bar{d}_{\mathrm{L}}\gamma^\mu u_{\mathrm{L}} + 2\bar{d}_{\mathrm{L}}\gamma_\mu s_{\mathrm{L}}\bar{d}_{\mathrm{L}}\gamma^\mu d_{\mathrm{L}} \\
& +2\bar{d}_{\mathrm{L}}\gamma_\mu s_{\mathrm{L}}\bar{s}_{\mathrm{L}}\gamma^\mu s_{\mathrm{L}} \\
O_3 = \;& \bar{d}_{\mathrm{L}}\gamma_\mu s_{\mathrm{L}}\bar{u}_{\mathrm{L}}\gamma^\mu u_{\mathrm{L}} + \bar{u}_{\mathrm{L}}\gamma_\mu s_{\mathrm{L}}\bar{d}_{\mathrm{L}}\gamma^\mu u_{\mathrm{L}} + 2d_{\mathrm{L}}\gamma_\mu s_{\mathrm{L}}\bar{d}_{\mathrm{L}}\gamma^\mu d_{\mathrm{L}} \\
& -3\bar{d}_{\mathrm{L}}\gamma_\mu s_{\mathrm{L}}\bar{s}_{\mathrm{L}}\gamma^\mu s_{\mathrm{L}} \qquad \left(\{27\}, \Delta T = \tfrac{1}{2}\right), \\
O_4 = \;& \bar{d}_{\mathrm{L}}\gamma_\mu s_{\mathrm{L}}\bar{u}_{\mathrm{L}}\gamma^\mu u_{\mathrm{L}} + \bar{u}_{\mathrm{L}}\gamma_\mu s_{\mathrm{L}}\bar{d}_{\mathrm{L}}\gamma^\mu u_L \qquad \left(\{27\}, \Delta T = \tfrac{3}{2}\right), \\
& -\bar{d}_{\mathrm{L}}\gamma_\mu s_{\mathrm{L}}\bar{d}_{\mathrm{L}}\gamma^\mu d_{\mathrm{L}} \qquad \left(\{8\}, \Delta T = \tfrac{1}{2}\right), \\
O_5 = \;& \bar{d}_{\mathrm{L}}\gamma^\mu\lambda^a s_{\mathrm{L}}\left(\bar{u}_{\mathrm{R}}\gamma_\mu\lambda^a u_{\mathrm{R}} + \bar{d}_{\mathrm{R}}\gamma^\mu\lambda^a d_{\mathrm{R}} + \bar{s}_{\mathrm{R}}\gamma^\mu\lambda^a s_{\mathrm{R}}\right) \qquad \left(\{8\}, \Delta T = \tfrac{1}{2}\right).
\end{aligned}
$$

The characteristic numerical values of the coefficients c_i (for parameter values of $\mu = 0.14\mathrm{GeV}, m_{\mathrm{W}} = 100\mathrm{GeV}, m_{\mathrm{c}} = 2\mathrm{GeV}$, and $\alpha_{\mathrm{s}}(\mu) = 1$) are:

$$
\begin{aligned}
& c_1 = -2.75, \quad c_2 = 0.06, \quad c_3 = 0.08, \quad c_4 = 0.39 \\
& c_5 = -0.14, \quad c_6 = -0.05
\end{aligned}
$$

Clearly, $I_3 = -O_1, 15I_6 = 3O_2 + 2O_3 + 10O_4$. The operator I_{R} would be identical to O_5 if the upper lines in the graphs of figs. 7.5 and 7.6 represented not only u- and d- but s-quarks as well. (Terms of the type $(ds)(\bar{s}s)$ were ignored so far, since they cannot contribute to simple quark diagrams representing decays of strange particles. This will be shown later.) The operator O_6 corresponds to the as yet undiscussed graph of fig. 7.7, involving the exchange of two gluons, and to more complicated graphs in which the gluons connecting the quark lines form a white system. The result is almost unaltered when O_6 is taken into account. Namely, O_5 is replaced by the combination $O_5 + \frac{3}{16}O_6$ (the factor $\frac{3}{16}$ is easily obtained by means of the Fierz transformation).

The effective lagrangian $\mathsf{C}_{\mathrm{eff}}$ ($\Delta S = 1$) will be applied in chapters 9 and 10 to a dynamic analysis of non-leptonic decays of hyperons and K -mesons. Before doing that, however, we devote chapter 8 to kinematic (independent of dynamics) properties of hyperon-decay amplitudes.

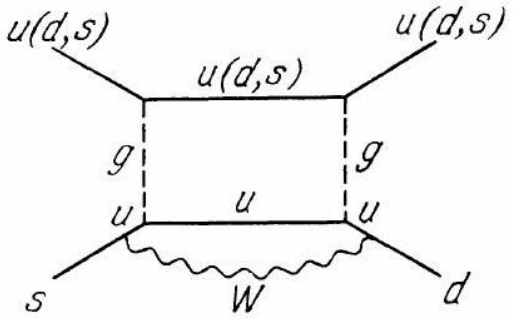


Fig. 7.7.

5.8 8 Phenomenology of non-leptonic decays of hyperons

5.8.1 8.1. Relativistically invariant amplitude

The non-leptonic decay $\mathrm{B}_1 \to \mathrm{B}_2 + \pi$ of a baryon with $J^P = \frac{1}{2}^+$is characterized by its amplitude M which is given, in the most general form, as

$$M = Gm_\pi^2\bar{u}_2\left(A + B\gamma_5\right)u_1.$$

Here u_1 and u_2 are spinor wave functions of the initial and final baryons, and φ_π is the π-meson wave function. The multiplier m_π^2, where m_π is the charged pion mass, is inserted "by hand" in order to obtain a correct dimension and reasonable order of magnitude of the amplitude. Indeed, if we divide the nuclear time of the order of 10^{-24} s by $G^2m_\pi^4 \sim 10^{-14}$, the result is

a time of the order of 10^{-10} s, that is the characteristic lifetime of hyperons. The dimensionless coefficients A and B are numbers (complex numbers in the general case; see below). Making use of the Dirac equation one can easily show that the expression $\bar{u}_2\,(A + B\gamma_5)\,u_1$ is the most general Lorentz-invariant characterizing the vertex $\bar{B}_2 B_1 \pi$. By taking into account that φ_π is a pseudoscalar, we conclude that P-parity is not conserved by amplitude A and conserved by B. Obviously, A corresponds to the S -wave, that is to zero orbital momentum ($l = 0$) of the system $B_2\pi$, and B corresponds to the P-wave ($l = 1$).

A standard calculation gives for the decay width

$$\Gamma = \frac{G^2 m_\pi^4}{8\pi} q \left\{ \left[\frac{(M+m)^2 - \mu^2}{M^2} \right] |A|^2 + \left[\frac{(M-m)^2 - \mu^2}{M^2} \right] |B|^2 \right\},$$

where q is the momentum of the decay products in the rest frame of the decaying hyperon ($q = |q|$), $M(m)$ is the mass of the decaying (produced) baryon, μ is the mass of the pion (π^0 or $\pi^\pm$) which is produced in the decay in question, and m_π is the mass of the charged pion.

5.8.2 8.2. Non-relativistic form of the amplitude

Let us express the four-component Dirac spinors u_1 and u_2 in terms of the two-component Pauli spinors ψ_1 and ψ_2 :

$$u_1 = \begin{pmatrix} \psi_1 \\ \chi_1 \end{pmatrix} = \begin{pmatrix} \psi_1 \\ 0 \end{pmatrix}$$
$$u_2 = \begin{pmatrix} \psi_2 \\ \chi_2 \end{pmatrix} = \sqrt{\frac{E+m}{2E}} \begin{pmatrix} \psi_2 \\ \boldsymbol{\sigma} \cdot \boldsymbol{q} \psi_2 / \sqrt{E+m} \end{pmatrix}.$$

We obtain

$$M \sim \psi_2^+ (S + P \boldsymbol{\sigma} \cdot \boldsymbol{n}) \psi_1$$

where $\boldsymbol{n} = \boldsymbol{q}/|\boldsymbol{q}|$, and S and P are amplitudes of the S - and P -waves, respectively. It is easy to see that

$$\frac{P}{S} = \sqrt{\frac{E-m}{E+m}} \frac{B}{A}.$$

(The normalization of the amplitudes S and P will not be taken into consideration.)

5.8.3 8.3. Spin correlations in hyperon decays

Consider the decay

$$\Lambda \to p + \pi^-.$$

Let $\boldsymbol{\eta}$ and $\boldsymbol{\zeta}$ be unit vectors characterizing the polarization of the Λ-hyperon and the proton, respectively, in the rest frames of each of these particles:

$$\psi_1 \psi_1^+ = \frac{1}{2}(1 + \boldsymbol{\eta} \cdot \boldsymbol{\sigma}),$$
$$\psi_2 \psi_2^+ = \frac{1}{2}(1 + \zeta \cdot \boldsymbol{\sigma}).$$

Let $\boldsymbol{n}$ be a unit vector in the direction of the proton momentum in the Λ-hyperon rest frame. Let us find the decay probability as a function of $\boldsymbol{\eta}$,
ζ, and $\boldsymbol{n}$:

$$
\begin{aligned}
W(\boldsymbol{\eta},\zeta,\boldsymbol{n}) \sim & |M|^2 \sim \mathrm{Tr}(1+\zeta\cdot\boldsymbol{\sigma})(S+P\boldsymbol{\sigma}\cdot\boldsymbol{n})(1+\boldsymbol{\eta}\cdot\boldsymbol{\sigma}) \\
& \times (S^*+P^*\boldsymbol{\sigma}\cdot\boldsymbol{n}) \\
\sim & \left\{|S|^2(1+\boldsymbol{\eta}\cdot\zeta)+|P|^2(1+2(\boldsymbol{\eta}\cdot\boldsymbol{n})(\zeta\cdot\boldsymbol{n})-\boldsymbol{\eta}\cdot\zeta\right. \\
& \left.+\left(SP^*+S^*P\right)(\boldsymbol{\eta}\cdot\boldsymbol{n}+\zeta\cdot\boldsymbol{n})+i\left(SP^*-S^*P\right)\zeta[\boldsymbol{\eta}\cdot\boldsymbol{n}]\right\} \\
\sim & \{1+\alpha(\boldsymbol{\eta}\cdot\boldsymbol{n}+\zeta\cdot\boldsymbol{n})+\beta\zeta[\boldsymbol{\eta}\cdot\boldsymbol{n}]+\gamma\boldsymbol{\eta}\cdot\zeta \\
& +(1-\gamma)(\boldsymbol{\eta}\cdot\boldsymbol{n})(\zeta\cdot\boldsymbol{n})\}
\end{aligned}
$$

Here

$$
\alpha=\frac{SP^*+S^*P}{|S|^2+|P|^2},\quad \beta=i\frac{SP^*-S^*P}{|S|^2+|P|^2},\quad \gamma=\frac{|S|^2-|P|^2}{|S|^2+|P|^2}.
$$

(It is easily found that $\alpha^2+\beta^2+\gamma^2=1$). The following relations were used to calculate the trace (see appendix):

$$
\begin{aligned}
\sigma_i\sigma_k &= \delta_{ik}+i\varepsilon_{ikl}\sigma_l \\
\mathrm{Tr}\,\sigma_i\sigma_k &= 2\delta_{ik} \\
\mathrm{Tr}\,\sigma_i\sigma_k\sigma_l &= 2i\varepsilon_{ikl} \\
\mathrm{Tr}\,\sigma_i\sigma_k\sigma_l\sigma_m &= 2\left(\delta_{ik}\delta_{lm}+\delta_{im}\delta_{kl}-\delta_{il}\delta_{km}\right).
\end{aligned}
$$

Let us analyze the expression for $W(\boldsymbol{\eta},\boldsymbol{\zeta},\boldsymbol{n})$. The decay probability in the S-wave is zero if $\boldsymbol{\eta}$ and $\boldsymbol{\zeta}$ are antiparallel. This result is quite natural: with zero orbital momentum, the proton spin must be in the same direction as that of the Λ-hyperon. This is not true for the P-wave: the probability is maximum when the proton spin is directed along the vector $2\boldsymbol{n}(\boldsymbol{\eta}\cdot\boldsymbol{n})-\boldsymbol{\eta}$.

If the proton polarization is not measured, we put $\zeta=0$. In this case the angular distribution of protons takes the form $1+\alpha\boldsymbol{\eta}\cdot\boldsymbol{n}$. The P-odd angular asymmetry is a result of interference between the S - and P -waves. If the decaying hyperon is not polarized, then $\boldsymbol{\eta}=0$ and the decay probability is proportional to $1+\alpha\zeta\cdot n$. This means that the proton is polarized longitudinally (its spin is directed along its momentum), and that the degree of this polarization is $\boldsymbol{\alpha}$. As can be readily found from the expression for $W(\boldsymbol{\eta},\boldsymbol{\zeta},\boldsymbol{n})$, the proton polarization is given by

$$
\boldsymbol{P}=\frac{\boldsymbol{n}(\alpha+\boldsymbol{\eta}\cdot\boldsymbol{n})+\beta[\boldsymbol{\eta}\cdot\boldsymbol{n}]+\gamma[\boldsymbol{n}[\boldsymbol{\eta}\cdot\boldsymbol{n}]]}{1+\alpha\boldsymbol{\eta}\cdot\boldsymbol{n}}.
$$

(The decay probability $W(\boldsymbol{P},\boldsymbol{\zeta})$ is proportional to $1+\boldsymbol{\zeta}\cdot\boldsymbol{P}$ and reaches a maximum for $\boldsymbol{\zeta}\|\boldsymbol{P}$.)

The nucleon polarization along the normal to the plane containing the vectors $\boldsymbol{\eta}$ and $\boldsymbol{n}$, is proportional to $\mathrm{Im}\,SP^*$ and is non-vanishing only for the non-zero relative phases, Δ, of the S - and P -wave amplitudes:

$$
\alpha=\frac{2|S||P|\cos\Delta}{|S|^2+|P|^2},\quad \beta=-\frac{2|S||P|\sin\Delta}{|S|^2+|P|^2}.
$$

We show below that Δ can be expressed as a function of pion-proton scattering phases, provided time-reversal invariance holds.

5.8.4 8.4. Isotopic amplitudes and the $\Delta T = \frac{1}{2}$ rule

The initial state in the $\Lambda\to \mathrm{p}+\pi^-$decay has $T=0$, while the final state is a superposition of $T=\frac{1}{2}$ and $T=\frac{3}{2}$:

$$p\pi^- = \sqrt{\frac{1}{3}}\psi_{3/2} - \sqrt{\frac{2}{3}}\psi_{1/2}.$$

Similarly, we have for the $\Lambda \to \mathrm{n} + \pi^0$ decay:

$$n\pi^0 = \sqrt{\frac{2}{3}}\psi_{3/2} + \sqrt{\frac{1}{3}}\psi_{1/2}.$$

If the $\Delta T = \frac{1}{2}$ rule were absolute, the transitions would be only to the state $\psi_{1/2}$, so that the ratio of the amplitudes Λ^0_- and Λ^0_0 describing the decays $\Lambda^0 \to \mathrm{p}\pi^-$and $\Lambda^0 \to \mathrm{n}\pi^0$, respectively, would be

$$\frac{\Lambda^0_-}{\Lambda^0_0} = -\sqrt{2},$$

valid both for A and for B amplitudes. As a result, the correlation coefficients α, β, γ for the two decays would be identical, with the following ratio for the decay rates:

$$\Gamma\left(\Lambda \to \mathrm{p}\pi^-\right) : \Gamma\left(\Lambda \to \mathrm{n}\pi^0\right) = 2.$$

All these predictions are well confirmed experimentally (see appendix).
In order to derive the corollaries of the $\Delta T = \frac{1}{2}$ rule for decays of Σ-hyperons, it will be convenient to introduce the concept of the spurion, S ,
and consider the reactions

$$\begin{aligned}
\mathrm{S}\Sigma^+ \to \mathrm{p}\pi^0\Sigma^+_0 &= \left(\sqrt{\frac{2}{3}}\psi_{3/2} - \sqrt{\frac{1}{3}}\psi_{1/2}|H|\sqrt{\frac{1}{3}}\varphi_{3/2} + \sqrt{\frac{2}{3}}\varphi_{1/2}\right) \\
&= \frac{1}{3}\sqrt{2}\left(\Sigma_{3/2} - \Sigma_{1/2}\right), \\
\mathrm{S}\Sigma^+ \to \mathrm{n}\pi^+\Sigma^+_+ &= \left(\sqrt{\frac{1}{3}}\psi_{3/2} + \sqrt{\frac{2}{3}}\psi_{1/2}|H|\sqrt{\frac{1}{3}}\varphi_{3/2} + \sqrt{\frac{2}{3}}\varphi_{1/2}\right) = \left\langle\psi_{3/2}\right| H \left|\varphi_{3/2}\right\rangle = \Sigma_{3/2}. \\
&= \frac{1}{3}\left(\Sigma_{3/2} + 2\Sigma_{1/2}\right), \\
\mathrm{S}\Sigma^- \to \mathrm{n}\pi^-\Sigma^-_-
\end{aligned}$$

Here ψ and φ are the isotopic wave functions of the pion-nucleon and spurion- $\sum$ systems, respectively. (The isotopic properties of the spurion are identical to those of the K^0 meson; but the spurion is a fictitious particle which carries neither energy nor momentum. Introduction of the spurion allows one to operate with the isotopically invariant interaction hamiltonian H.) Consequently, the three observed amplitudes are given in terms of two isotopic amplitudes $\Sigma_{3/2}$ and $\Sigma_{1/2}$, which yields the triangle relation,

$$\Sigma^+_+ + \sqrt{2}\Sigma^+_0 = \Sigma^-_-,$$

both for the S - and P -wave amplitudes of Σ decays. The amplitudes as given by experiment are schematically presented in fig. 8.1. The triangle in the figure is not closed because of the transitions with $\Delta T = \frac{3}{2}$. It is of great interest that the triangle is almost right-angled, and that its legs are almost on the coordinate axes. This will be taken up again in the next chapter when the dynamics of hyperon decays is discussed.

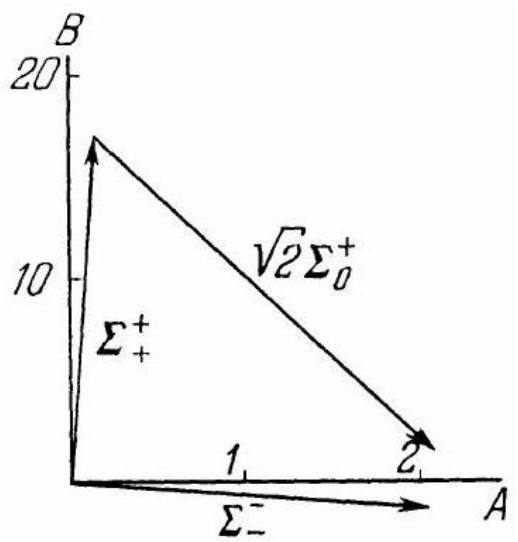


Fig. 8.1.

By using the spurion we easily establish that the $\Delta T = \frac{1}{2}$ rule leads to the relations

$$M\left(\Xi^- \to \pi^-\Lambda^0\right) : M\left(\Xi^0 \to \pi^0\Lambda^0\right) = \sqrt{2},$$
$$M\left(\Omega^- \to \Xi^0\pi^-\right) : M\left(\Omega^- \to \Xi^-\pi^0\right) = \sqrt{2}.$$

We shall see in chapter 9 .that in the latter case, theory predicts, and experiment confirms, that the admixture of $\Delta T = \frac{3}{2}$ causes a considerable deviation from $\sqrt{2}$.

5.8.5 8.5 Phases of the S - and P -wave amplitudes

We shall demonstrate that the phases of S - and P -wave amplitudes for hyperon decay to a given isotopic state are equal to the phases of the scattering of decay products in this isotopic state. This statement is based on the unitarity of the S-matrix and on its symmetry. This last property follows from the invariance of the lagrangian with respect to time reversal T. (Here we neglect very weak violation of CP invariance (or T-invariance, by virtue of the CPT theorem) which results in small phases of S- and P -wave amplitudes, even in the case of no interaction in the final state).

The proof will be obtained in the most general form, so that it may be used in other cases as well: decays of K -mesons, neutrino reactions, and so on. First of all we want to find a relation between the matrix elements of the direct and inverse reactions. This relation is a result of the unitarity of the S-matrix,

$$SS^+ = 1,$$

provided the amplitudes of these reactions connecting the initial states i and final states f are small. Let us separate S into two terms,

$$S = S^0 + S^1$$

where $|S^0| \gg |S^1|$. The terms S^0 and S^1 are chosen to satisfy the conditions:

$$S^0_{fi} = 0, \quad S^0_{ii'} \neq 0, \quad S^0_{ff'} \neq 0$$
$$S^1_{fi} \neq 0, \quad S^1_{ii'} = 0, \quad S^1_{ff'} = 0$$

where i, i' (f, f') are states from a group of initial (final) states. Therefore,

$$S_{fi} = S^1_{fi}, \quad S_{ii'} = S^0_{ii'}, \quad S_{ff'} = S^0_{ff'}$$

The unitarity condition is now expressed by

$$\left(S^0 + S^1\right)^+ \left(S^0 + S^1\right) = 1.$$

Neglecting the terms $S^1 S^{1+}$, we obtain

$$\begin{aligned} S^{0+} S^0 &= 1, \\ S^{0+} S^1 + S^{1+} S^0 &= 0, \end{aligned}$$

whence

$$S^1 = -S^0 S^{1+} S^0$$

or

$$S^1_{fi} = -S^0_{ff'} S^{1+}_{f'i'} S^0_{i'i}.$$

Using now the definition of hermitian conjugation and the equality $S^1_{fi} = S_{fi}$, we derive

$$S_{fi} = -S^0_{ff'} S^*_{i'f'} S^0_{i'i}.$$

If the states i and f are diagonal (i.e. $i' = i, f' = f$), then

$$S^0_{i'i} = \delta_{i'i} \mathrm{e}^{2i\delta_d}, \quad S^0_{ff'} = \delta_{ff'} \mathrm{e}^{2i\delta_f},$$

where δ_i and δ_f are scattering phases in the initial and final states, respectively. In this case

$$S_{fi} = -\mathrm{e}^{+2i\left(\delta_1 + \delta_f\right)} S^*_{if}.$$

Note that so far we have used only the unitarity of the S-matrix and the weakness of the interaction inducing the transitions between i and f (this last property was used when $S^1 S^{1+}$ was ignored).

Let us take into account now that in the case of T-reversibility the S-matrix must be symmetric,

$$S_{fi} = S_{if}.$$

Substitution of this condition into the preceding expression yields

$$S_{fi} = -\mathrm{e}^{+2i\left(\delta_l + \delta_f\right)} S^*_{fi},$$

or

$$\arg S_{f_l} = \delta_f + \delta_l + \frac{1}{2}\pi.$$

We now take into consideration that the amplitudes M differ from the corresponding elements of S by a factor i. Moreover, $\delta_i = 0$ in the decay of a particle. This immediately gives

$$\arg M_{fi} = \delta_f.$$

It then follows that for the amplitudes of hyperon decay into channels with given l and T

$$S_T = \pm\,|S_T|\,\mathrm{e}^{i\delta_S^T},$$
$$P_T = \pm\,|P_T|\,\mathrm{e}^{i\delta_\mathrm{P}^T}.$$

The relative phase of S- and P-wave amplitudes, Δ, equals: $\Delta = \delta_S - \delta_P + n\pi$. (We recall that the correlation $\zeta[\boldsymbol{\eta}\cdot\boldsymbol{n}]$ is proportional to $\sin\Delta$.)

5.8.6 8.6. SU(3) relation between amplitudes of hyperon decays

Let us derive a relation between the S -wave amplitudes of hyperon decays. We assume that the predominant part of the non-leptonic interaction, satisfying the $\Delta T = \frac{1}{2}$ rule, is a component of an octet. In accordance with this hypothesis we consider the spurion to be the sixth component of the octet ($\propto \lambda_6$), like the K^0 meson. The SU(3)-invariant amplitude, describing processes

$$\mathrm{S} + \mathrm{B} \to\ \mathrm{B} + \mathrm{P},$$

in which both the fictitious particle S and the real particles (baryons B and pseudoscalar mesons P) are components of octets, can be written in the most general form as

$$A = \sum_{i=1}^{9} A_i J_i,$$

where A_i are numbers and J_i are SU(3) scalars constructed from octet wave functions. Nine such scalars can be formed in the general case:

$$\begin{array}{lll} J_1 = (S\bar{B}\tilde{P}B), & J_4 = (SB\bar{B}\tilde{P}), & J_7 = (S\bar{B})(B\tilde{P}), \\ J_2 = (SB\tilde{P}\bar{B}), & J_5 = (S\tilde{P}\bar{B}B), & J_8 = (SB)(\bar{B}\tilde{P}), \\ J_3 = (S\bar{B}B\tilde{P}), & J_6 = (S\tilde{P}B\bar{B}), & J_9 = (S\tilde{P})(\bar{B}B), \end{array}$$

where parentheses stand for "trace"; for instance, $(SB) = S_k^i B_k^i, (S\bar{B}\tilde{P}B) = S_k^i \bar{B}_l^k \tilde{P}_m^l B_i^m$. The nine scalars are related by a linear constraint:

$$\sum_{i=1}^{6} J_i = \sum_{i=7}^{9} J_i,$$

which will not be used here. We now easily obtain from the explicit from of the meson and baryon octets the formulas

$$A\left(\Lambda_-^0\right) = \sqrt{\frac{1}{6}}\left(A_1 + A_3 - 2A_4\right),$$
$$A\left(\Xi_-^-\right) = \sqrt{\frac{1}{6}}\left(A_2 - 2A_3 + A_4\right),$$
$$A\left(\Sigma_0^+\right) = \sqrt{\frac{1}{2}}\left(A_1 - A_3\right),$$
$$A\left(\Sigma_+^+\right) = A_1 + A_7,$$
$$A\left(\Sigma_-^-\right) = A_3 + A_7.$$

Later we shall need the transformation properties of octet matrices and invariants J_i under charge conjugation. These are

$$B = B_k^i \xrightarrow{C} B_C = \bar{B}_i^k = \tilde{\bar{B}},$$
$$P \xrightarrow{C} \tilde{P},$$
$$S \xrightarrow{C} S,$$

so that

$$J_1 \to J_1, \quad J_3 \leftrightarrow J_5$$
$$J_2 \to J_2, \quad J_4 \leftrightarrow J_6$$
$$J_9 \to J_9, \quad J_7 \leftrightarrow J_8$$

The amplitude $A = \sum A_i J_i$ corresponds to transitions with $P = -1$ and $CP = +1$, and hence with $C = -1$. Consequently,

$$A \xrightarrow{C} -A.$$

This yields

$$A_1 = A_2 = A_9 = 0, \quad A_3 = -A_5, \quad A_4 = -A_6, \quad A_7 = -A_8$$

By using the relation $A_1 = A_2 = 0$, we obtain

$$A\left(\Lambda_-^0\right) + 2A\left(\Xi_-^-\right) = \sqrt{3}A\left(\Sigma_0^+\right)$$

This is the so-called Lee-Sugawara equation, supported rather well by experiment. It should also be mentioned that a similar relation between P -wave amplitudes was also found experimentally, although it is not predicted by SU(3) symmetry (under C-conjugation

$$B = \sum_{i=1}^{9} B_i J_i \to +B$$

and none of the nine amplitudes B_i vanish).

5.9 9 Dynamics of non-leptonic decays of hyperons

In this chapter we calculate amplitudes for several non-leptonic decays of hyperons. Calculations are based on the quark model of hadrons and on the total effective non-leptonic lagrangian

$$\mathcal{L}_{\text{eff}} = \sqrt{2}G \sin\theta \cos\theta \sum_{i=1}^{6} c_i O_i.$$

Explicit expressions for the operators O_t and the values of the coefficients c_t in the above expression were given at the end of Chapter 7. The present chapter deals mostly with decays of the Λ-hyperon. Decays of the Ω-hyperon are discussed at the end of the chapter.

5.9.1 9.1. Quark graphs

The weak interaction of quarks responsible for the non-leptonic decays of hyperons can be of two types: scattering (fig. 9.1) or decay (fig. 9.2). Let us consider, for instance, decays of the Λ-hyperon. Quark graphs describing these decays can be divided into two classes: external (fig. 9.3) and internal graphs (figs. 9.4 and 9.5). The s-quark decay in external graphs occurs as if the decay were isolated, i.e. the quark emits a free π-meson made up of a quark and an antiquark produced in the weak vertex. Creation of the π-meson in internal graphs is more complex

and requires participation of other quarks. So far we cannot calculate these more complicated graphs. It is readily apparent, however, that they possess a spectacular property: they allow only transitions with $\Delta T = \frac{1}{2}$. To understand the mechanism forbidding the transitions with $\Delta T = \frac{3}{2}$, just look at the simplified effective lagrangian $\tilde{\mathscr{L}}$ derived in chapter 7 . We recall that this lagrangian consists of three terms:

$$\tilde{\mathcal{E}}_{\text{eff}} = \sqrt{2}G\,(a_3 I_3 + a_6 I_6 + a_R I_R)\sin\theta\cos\theta,$$

Dynamics of non-leptonic decays of hyperons

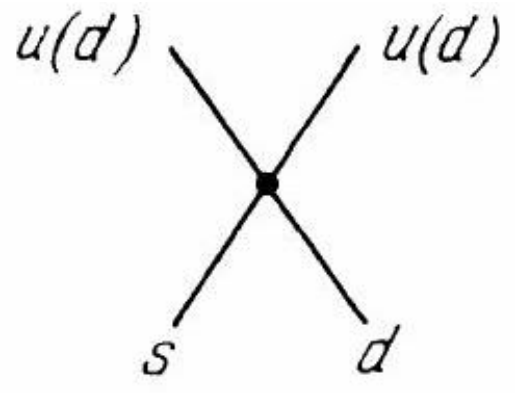


Fig. 9.1.

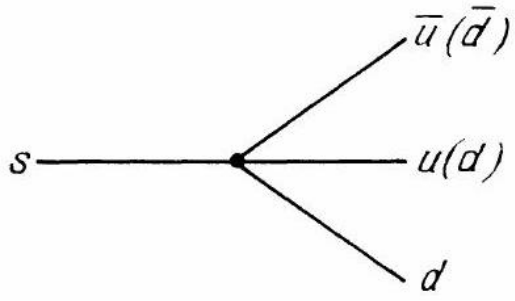


Fig. 9.2.

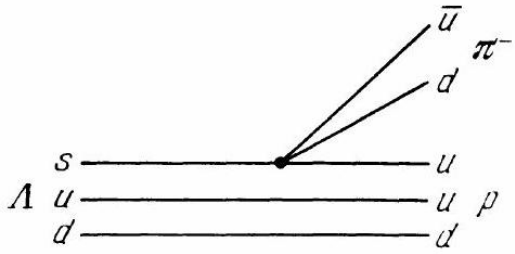


Fig. 9.3.

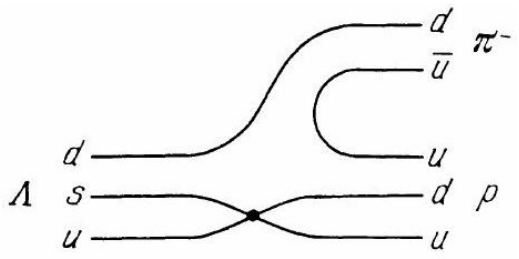


Fig. 9.4.

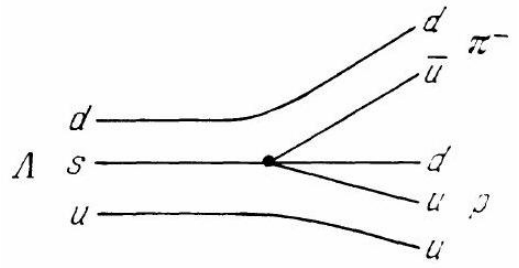


Fig. 9.5.

where

$$I_{3,6} = \bar{u}_{\rm L}\gamma_\alpha s_{\rm L}\bar{d}_{\rm L}\gamma^\alpha u_{\rm L} \mp \bar{d}_{\rm L}\gamma_\alpha s_{\rm L}\bar{u}_{\rm L}\gamma^\alpha u_{\rm L}$$
$$I_{\rm R} = -\bar{d}_{\rm L}\gamma_\alpha\lambda^a s_{\rm L}\left(\bar{u}_{\rm R}\gamma^\alpha\lambda^a u_{\rm R} + \bar{d}_{\rm R}\gamma^\alpha\lambda^a d_{\rm R}\right)$$
$$a_3 \approx 3, \quad a_6 \approx 0.6, \quad a_{\rm R} \approx 0.12$$

Among the three terms, only I_6 allows transitions with $\Delta T = \frac{3}{2}$, while I_3 and $I_{\rm R}$ are pure isotopic spinors and therefore allow transitions only with $\Delta T = \frac{1}{2}$. But it is precisely I_6 which cannot contribute to the internal graphs. The point is, the operator I_6 is symmetrized over quark pairs. (Both initial and final quarks are symmetrized in the case of scattering (figs. 9.1 and 9.4), and only final quarks are symmetrized in the case of decay (figs. 9.2 and 9.5)). At the same time, any pair of quarks in a white baryon is in the color-antisymmetric state and forms an antitriplet $\overline{3}$. Note that owing to this reason, three "symmetric" operators O_2, O_3 (the only O -operator with $\Delta T = \frac{3}{2}$) and O_4, of the total effective lagrangian do not contribute to internal graphs. Among the remaining operators, O_1 is predominant in these graphs (because of a large value of c_1).

5.9.2 9.2. Factorization of external diagrams for the decay $\Lambda^0 \to p\pi^-$

Let us turn now to the calculation of external graphs. We consider the decay $\Lambda^0 \to p\pi^-$and determine the contribution of each term of the operators O_i to the amplitudes. If we assume that quarks forming the π-meson in fig. 9.3 do not interact with quarks in the initial and final baryons, then the decay amplitude is factorized into a product of two matrix elements. This becomes especially lucid if we take the term $\bar{d}_{\rm L}\gamma_\alpha u_{\rm L}\bar{u}_{\rm L}\gamma^\alpha s_{\rm L}$:

$$\left\langle \pi^- p\right| \bar{d}_{\rm L}\gamma_\alpha u_{\rm L}\bar{u}_{\rm L}\gamma^\alpha s_{\rm L}|\Lambda\rangle = \left\langle \pi^-\right| \bar{d}_{\rm L}\gamma_\alpha u_{\rm L}|0\rangle\langle p|\bar{u}_{\rm L}\gamma^\alpha s_{\rm L}|\Lambda\rangle.$$

Both factors are already familiar:

$$\left\langle \pi^- \right| \bar{d}_{\rm L}\gamma_\alpha u_{\rm L}|0\rangle = \frac{1}{2}\langle\pi|d\gamma_\alpha\gamma_5 u|0\rangle = \frac{1}{2}f_\pi\varphi_\pi k_\alpha,$$

where φ_π is the π-meson wave function, k_α is its 4 -momentum, and $f_\pi \approx 0.95 m_\pi$ is a well-known constant characterizing the decays $\pi \to e\nu$ and $\pi \to \mu\nu$. As for the matrix element $\langle\bar{p}|\bar{u}_{\rm L}\gamma_\Lambda s_{\rm L}|\Lambda\rangle$, it determines the amplitude of Λ-hyperon β-decay, and is written in the form

$$\langle p|\bar{u}_{\rm L}\gamma_\alpha s_{\rm L}|\Lambda\rangle = \frac{1}{2}\langle p|\bar{u}\gamma_\alpha\left(1+\gamma_5\right)s|\Lambda\rangle = +\frac{1}{2}\bar{u}_{\rm p}\left(g_{\rm V}\gamma_\alpha + g_{\rm A}\right)\gamma_\alpha\gamma_5\Big) u_\Lambda.$$

By virtue of SU(3) symmetry, $g_{\rm V} = -3/\sqrt{6}, g_{\rm A}/g_{\rm V} = F + \frac{1}{3}D$ (see chapter 6). The experimental value of $g_{\rm v}$ in the decays $\Lambda \to p\ell\nu$ does not contradict
the theoretical value; as for the ratio $g_{\rm A}/g_{\rm v}$, experiment gives 0.62 ± 0.05. We thus obtain

$$\begin{aligned}\left\langle \pi^- p\right| \bar{d}_{\rm L}\gamma_\alpha u_{\rm L}\bar{u}_{\rm L}\gamma^\alpha s_{\rm L}|\Lambda\rangle &= -\frac{1}{8}\sqrt{6}f_\pi k_\alpha\bar{u}_{\rm p}\left(\gamma_\alpha + \frac{g_{\rm A}}{g_{\rm V}}\gamma_\alpha\gamma_5\right)u_\Lambda\varphi_\pi \\ &= -\frac{1}{8}\sqrt{6}f_\pi\bar{u}_{\rm p}[(m_\Lambda - m_p) \\ &\qquad - \left(m_\Lambda + m_{\rm p}\right)\frac{g_{\rm A}}{g_{\rm V}}\gamma_5\Big] u_\Lambda\varphi_\pi.\end{aligned}$$

Let us recall now the general form of the amplitude for non-leptonic hyperon decay (it was given at the beginning of chapter 8):

$$M = Gm_\pi^2\bar{u}_2\left(A + B\gamma_5\right)u_1\varphi_\pi.$$

We see that the contributions of the term $\sqrt{2}G\bar{d}_L\gamma_\alpha u_L\bar{u}_L\gamma^\alpha s_L \sin\theta\cos\theta$ to the amplitudes A and B of the decay $\Lambda^0 \to p\pi^-$are, respectively,

$$\begin{aligned}A\left(\Lambda_-^0\right): &\quad -\tfrac{1}{4}\sqrt{3}\sin\theta\cos\theta\tfrac{f_\pi(m_\Lambda - m_{\rm p})}{m_\pi^2}, \\ B\left(\Lambda_-^0\right): &\quad +\tfrac{1}{4}\sqrt{3}\sin\theta\cos\theta\tfrac{f_\pi(m_\Lambda - m_{\rm p})}{m_\pi^2}\tfrac{g_{\rm A}}{g_{\rm V}}.\end{aligned}$$

In order to find the amplitude corresponding to the term $\bar{u}_{\rm L}\gamma_\alpha u_{\rm L}\bar{d}_{\rm L}\gamma^\alpha s_{\rm L}$ we must permute the operators $\bar{u}_{\rm L}$ and $d_{\rm L}$. This is conveniently carried out by means of the Fierz transformation (see Chapter 29):

$$\begin{aligned}&\delta_k^i\left[\gamma_\mu\left(1+\gamma_5\right)\right]_\beta^\alpha\delta_m^l\left[\gamma^\mu\left(1+\gamma_5\right)\right]_\delta^\gamma \\ &= +\frac{1}{3}\delta_m^i\left[\gamma_\mu\left(1+\gamma_5\right)\right]_\delta^\alpha\delta_k^l\left[\gamma^\mu\left(1+\gamma_5\right)\right]_\beta^\gamma \\ &+ \frac{1}{2}\left(\lambda^a\right)_m^i\left[\gamma_\mu\left(1+\gamma_5\right)\right]_\delta^\alpha\left(\lambda^a\right)_k^l\left[\gamma^\mu\left(1+\gamma_5\right)\right]_\beta^\gamma.\end{aligned}$$

Here Greek letters denote Dirac indices, Latin letters denote colors, and the plus signs result from anticommutation of spinor operators. According to color conservation, the contribution of the second term vanishes, $\left(\langle\pi|\bar{d}_{\rm L}\gamma_\alpha\lambda^{\rm a}u_{\rm L}|0\rangle = 0\right)$, and we obtain

$$\left\langle \pi^- p\right| \bar{u}_L\gamma_\alpha u_L\bar{d}_L\gamma^\alpha s_L|\Lambda\rangle = \frac{1}{3}\left\langle \pi^- p\right| \bar{d}_L\gamma_\alpha u_L\bar{u}_L\gamma^\alpha s_L|\Lambda\rangle.$$

It is apparent that the terms $\bar{d}_{\rm L}\gamma_\alpha d_{\rm L}d_{\rm L}\gamma^\alpha s_{\rm L}, \bar{d}_{\rm R}\gamma_\alpha d_{\rm R}d_{\rm L}\gamma^\alpha s_{\rm L}$, and $\bar{d}_{\rm R}\gamma_\alpha\lambda^a d_{\rm R}\bar{s}_{\rm L}\gamma^\alpha\lambda^a s_{\rm L}$ do not contribute to the external graph of the decay $\Lambda^0 \to p\pi^-$since they do not contain the $\bar{u}$-quark required to form the π^- meson. In order to calculate the contributions of the terms $\bar{u}_{\rm R}\gamma_\alpha u_{\rm R}\bar{d}_{\rm L}\gamma^\alpha s_{\rm L}$
and $\bar{u}_{\rm R}\gamma_\alpha\lambda^a u_{\rm R}\bar{d}_{\rm L}\gamma^\alpha\lambda^a s_{\rm L}$, we shall use the Fierz transformations

$$\delta_k^l \left[\gamma_\mu \left(1+\gamma_5\right)\right]_\beta^\alpha \delta_m^l \left[\gamma^\mu \left(1-\gamma_5\right)\right]_\delta^\gamma$$
$$= -2\left[\frac{1}{3}\delta_m^i \left(1+\gamma_5\right)_\delta^\alpha \delta_k^l \left(1-\gamma_5\right)_\beta^\gamma + \frac{1}{2}\left(\lambda^a\right)_m^i \left(1+\gamma_5\right)_\delta^\alpha \left(\lambda^a\right)_k^l \left(1-\gamma_5\right)_\beta^\gamma\right]$$
$$\left(\lambda^a\right)_k^i \left[\gamma_\mu \left(1+\gamma_5\right)\right]_\beta^\alpha \left(\lambda^a\right)_m^l \left[\gamma^\mu \left(1-\gamma_5\right)\right]_\delta^\gamma$$
$$= -2\left[\frac{16}{9}\delta_m^i \left(1+\gamma_5\right)_\delta^\alpha \delta_k^l \left(1-\gamma_5\right)_\beta^\gamma - \frac{1}{3}\left(\lambda^a\right)_m^i \left(1+\gamma_5\right)_\delta^\alpha \left(\lambda^a\right)_k^l \left(1-\gamma_5\right)_\beta^\gamma\right]$$

(The minus signs in front of these two expressions take account of the anticommutation of spinor operators.) Carrying out factorization and taking into account conservation of color, we obtain

$$\left\langle \pi^- p\right| \bar{u}_\mathrm{R}\gamma^\alpha u_\mathrm{R}\bar{d}_\mathrm{L}\gamma^\alpha s_\mathrm{L}|\Lambda\rangle = -\frac{2}{3}\left\langle \pi^-\right| \bar{d}_\mathrm{L}u_\mathrm{R}|0\rangle\langle p|\bar{u}_\mathrm{R}s_\mathrm{L}|\Lambda\rangle,$$
$$\left\langle \pi^- p\right| u_\mathrm{R}\gamma^\alpha\lambda^a u_\mathrm{R}\bar{d}_\mathrm{L}\gamma^\alpha\lambda^a s_\mathrm{L}|\Lambda\rangle = -\frac{32}{9}\left\langle \pi^-\right| \bar{d}_\mathrm{L}u_\mathrm{R}|0\rangle\langle p|\bar{u}_\mathrm{R}s_\mathrm{L}|\Lambda\rangle.$$

5.9.3 9.3. Enhancement of the contribution of right-handed quarks

Now compare the "right-handed" amplitude

$$\left\langle \pi^-\right| \bar{d}_\mathrm{L}u_\mathrm{R}|0\rangle\langle p|\bar{u}_\mathrm{R}s_\mathrm{L}|\Lambda\rangle$$

comprising creation and annihilation operators of the right-handed quarks (which are present in O_5 and O_6) with the "left-handed" amplitude

$$\left\langle \pi^-\right| \bar{d}_\mathrm{L}\gamma_\alpha u_\mathrm{L}|0\rangle\langle p|\bar{u}_\mathrm{L}\gamma^\alpha s_\mathrm{L}|\Lambda\rangle,$$

which does not comprise the right-handed quarks (this type of amplitude is generated by the operators O_1, O_2, O_3, O_4). The former is a product of scalars while the latter is a product of vectors. In order to reduce them to identical form, we shall use the relation

$$\left\langle \pi^-\right| \bar{d}\gamma_\alpha\gamma_5 u|0\rangle = \frac{m_\mathrm{u}+m_\mathrm{d}}{m_\pi^2}\left\langle \pi^-\right| \bar{d}\gamma_5 u|0\rangle k_\alpha.$$

In order to verify this equality, it is sufficient to multiply it by k_α and use the Dirac equation for quarks. We recall that $k = k_\Lambda - k_\mathrm{p}, k^2 = m_\pi^2$; at the same time, $k = k_\mathrm{d} + k_{\bar{\mathrm{u}}} = k_\mathrm{s} - k_\mathrm{u}$. The last equality enables us to write

$$k_\alpha\langle p|\bar{u}\left(\gamma^\alpha + \gamma^\alpha\gamma_5\right)s|\Lambda\rangle = \langle p|\bar{u}\left[\left(m_\mathrm{s}-m_\mathrm{u}\right) - \left(m_\mathrm{s}+m_\mathrm{u}\right)\gamma_5\right]s|\Lambda\rangle$$
$$= m_\mathrm{s}\langle p|\bar{u}\left(1-\gamma_5\right)s|\Lambda\rangle.$$

(Here the u-quark mass is neglected compared to that of the s-quark. Recall that $m_\mathrm{s} \approx 150\mathrm{MeV}, m_\mathrm{u} \approx 4\mathrm{MeV}, m_\mathrm{d} \approx 7\mathrm{MeV}$). We thus find that the "right-handed" amplitudes contain a large multiplier

$$\chi = \frac{m_\pi^2}{\left(m_\mathrm{u}+m_\mathrm{d}\right)m_\mathrm{s}} \approx 12.$$

One can easily find that

$$A(\text{ "right-handed" }) = -\chi A(\text{ "left-handed" }),$$
$$B(\text{ "right-handed" }) = \chi B(\text{ "left-handed" }).$$

It is now possible to give the final result for the contribution of the external graph to the amplitude for the decay $\Lambda^0 \to \mathrm{p}\pi^-$taking into account all terms of the effective non-leptonic lagrangian $\mathcal{L}$:

$$\begin{aligned} A\left(\Lambda_-^0\right) =& \frac{1}{4}\sqrt{3}\sin\theta\cos\theta\frac{f_\pi\left(m_\Lambda - m_\mathrm{p}\right)}{m_\pi^2}\left[\frac{2}{3}c_1 - \frac{4}{3}c_2 - \frac{4}{3}c_3 - \frac{4}{3}c_4\right. \\ & \left. -\frac{32}{9}\chi c_5 - \frac{2}{3}\chi c_6\right], \\ B\left(\Lambda_-^0\right) =& -\frac{1}{4}\sqrt{3}\sin\theta\cos\theta\frac{f_\pi\left(m_\Lambda + m_\mathrm{p}\right)}{m_\pi^2}\frac{g_\mathrm{A}}{g_\mathrm{V}} \\ & \times\left[\frac{2}{3}c_1 - \frac{4}{3}c_2 - \frac{4}{3}c_3 - \frac{4}{3}c_4 + \frac{32}{9}\chi c_5 + \frac{2}{3}\chi c_6\right]. \end{aligned}$$

Substitution of the values $c_1 = -2.75, c_2 = 0.06, c_3 = 0.08, c_4 = 0.39, c_5 = -0.14, c_6 = -0.05$ yields

$$\begin{aligned} A\left(\Lambda_-^0\right) &\approx 0.44, \\ B\left(\Lambda_-^0\right) &\approx 7.4. \end{aligned}$$

Experimental data give

$$\begin{aligned} A\left(\Lambda_-^0\right) &= 1.47 \pm 0.01, \\ B\left(\Lambda_-^0\right) &= 9.98 \pm 0.24. \end{aligned}$$

Agreement proves better for amplitude B than for A. It is possible that internal graphs neglected in the above calculations are important in the case of A.

5.9.4 9.4. $\Lambda^0 \to \mathbf{n}\boldsymbol{\pi}^0$ decay

Similar calculations for the decay $\Lambda^0 \to \mathrm{n}\pi^0$ readily yield

$$\begin{aligned} \left\langle\pi^0 n\right| u_L\gamma_\alpha u_L\bar{d}_L\gamma^\alpha s_L|\Lambda\rangle &= \left\langle\pi^0\right| \bar{u}_L\gamma_\alpha u_L|0\rangle\langle n|\bar{d}_L\gamma^\alpha s_L|\Lambda\rangle, \\ \left\langle\pi^0 n\right| \bar{d}_L\gamma_\alpha u_L\bar{u}_L\gamma^\alpha s_L|\Lambda\rangle &= \frac{1}{3}\left\langle\pi^0\right| \bar{u}_L\gamma_\alpha u_L|0\rangle\langle n|\bar{d}_L\gamma^\alpha s_L|\Lambda\rangle, \\ \left\langle\pi^0 n\right| \bar{d}_\mathrm{L}\gamma_\alpha d_\mathrm{L}\bar{d}_\mathrm{L}\gamma^\alpha s_\mathrm{L}|\Lambda\rangle &= \frac{4}{3}\left\langle\pi^0\right| \bar{d}_\mathrm{L}\gamma_\alpha d_\mathrm{L}|0\rangle\langle n|\bar{d}_\mathrm{L}\gamma^\alpha s_\mathrm{L}|\Lambda\rangle, \\ \left\langle\pi^0 n\right| \bar{d}_\mathrm{R}\gamma_\alpha\lambda^a d_\mathrm{R}\bar{d}_\mathrm{L}\gamma^\alpha\lambda^a s_\mathrm{L}|\Lambda\rangle &= -\frac{32}{9}\left\langle\pi^0\right| \bar{d}_\mathrm{L}d_\mathrm{R}|0\rangle\langle n|\bar{d}_\mathrm{R}s_\mathrm{L}|\Lambda\rangle, \\ \left\langle\pi^0 n\right| \left(\bar{d}_\mathrm{R}\gamma_\alpha d_\mathrm{R} + \bar{u}_\mathrm{R}\gamma_\alpha u_\mathrm{R}\right)\bar{d}_\mathrm{L}\gamma^\alpha s_\mathrm{L}|\Lambda\rangle &= -\frac{2}{3}\left\langle\pi^0\right| \bar{d}_\mathrm{L}d_\mathrm{R}|0\rangle\langle n|\bar{d}_\mathrm{R}s_\mathrm{L}|\Lambda\rangle. \end{aligned}$$

These relations make it possible to write out the final expression for the contribution of the external graphs of fig. 9.6 to the amplitudes for $\Lambda^{(0)} \to \mathrm{n}\pi^0$ decay:

$$\begin{aligned} A\left(\Lambda_0^0\right) =& \frac{\sqrt{3}}{4\sqrt{2}}\sin\theta\cos\theta\frac{f_\pi\left(m_\Lambda - m_\mathrm{p}\right)}{m_\pi^2}\left[-\frac{2}{3}c_1 + \frac{4}{3}c_2 + \frac{4}{3}c_3 - \frac{8}{3}c_4\right. \\ & \left. +\frac{32}{9}\chi c_5 + \frac{2}{3}\chi c_6\right], \\ B\left(\Lambda_0^0\right) =& -\frac{\sqrt{3}}{4\sqrt{2}}\sin\theta\cos\theta\frac{f_\pi\left(m_\Lambda + m_\mathrm{p}\right)}{m_\pi^2}\frac{g_\mathrm{A}}{g_\mathrm{V}} \\ & \times\left[-\frac{2}{3}c_1 + \frac{4}{3}c_2 + \frac{4}{3}c_3 - \frac{8}{3}c_4 - \frac{32}{9}\chi c_5 - \frac{2}{3}\chi c_6\right]. \end{aligned}$$

Let us find now the contribution of operator O_4 giving rise to transitions with $\Delta T = \frac{3}{2}$:

$$A\left(\Lambda_-^0\right) + \sqrt{2}A\left(\Lambda_0^0\right) = -\sqrt{3}\sin\theta\cos\theta\frac{f_\pi\left(m_\Lambda - m_\mathrm{p}\right)}{m_\pi^2}c_4 = -0.17$$
$$B\left(\Lambda_-^0\right) + \sqrt{2}B\left(\Lambda_0^0\right) = +\sqrt{3}\sin\theta\cos\theta\frac{f_\pi\left(m_\Lambda + m_\mathrm{p}\right)}{m_\pi^2}\frac{g_\mathrm{A}}{g_\mathrm{V}}c_4$$
$$= +1.32.$$

(The right-hand sides of these expressions would be exactly zero if the $\Delta T = \frac{1}{2}$ rule were strict.) The experimental values are

$$A\left(\Lambda_-^0\right) + \sqrt{2}A\left(\Lambda_0^0\right) = -0.09 \pm 0.03$$
$$B\left(\Lambda_-^0\right) + \sqrt{2}B\left(\Lambda_0^0\right) = -0.66 \pm 0.81$$

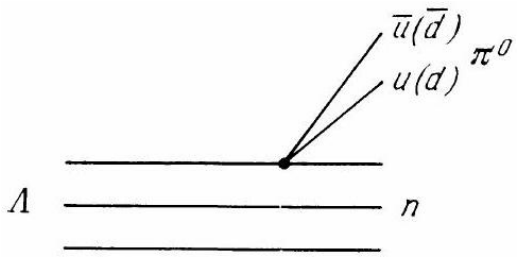


Fig. 9.6.

We see that the theory gives for the S -wave a somewhat milder suppression of the amplitude with $\Delta T = \frac{3}{2}$ than is found experimentally. Although the sign in the case of the P -wave is different from the predicted one, this is not really a contradiction because experimental error is very large. It would be very interesting to obtain more accurate experimental data since the theoretical prediction for the amplitudes with $\Delta T = \frac{3}{2}$ is very reliable because of the absence of a contribution from the internal diagrams. Indeed, the predicted amplitude may vary by a factor of 2 but its sign is unambiguous.

5.9.5 9.5. Ω-hyperon decays

Let us consider now the decays

$$\Omega^- \to \Xi^0\pi^-,$$
$$\Omega^- \to \Xi^-\pi^0.$$

The ratio of the rates for these two decays would be exactly 2 if the $\Delta T = \frac{1}{2}$ rule were strict. Let us calculate this ratio taking into account the contribution of the operator O_4 giving rise to transitions with $\Delta T = \frac{3}{2}$ in external graphs (figs. 9.7 and 9.8). Two waves participate in the decay of the Ω-hyperon which has $J^P = \frac{3}{2}^+$: P($l = 1$) and D($l = 2$). The scale of the P-wave amplitude is approximately identical to that in decays of hyperons with $J^P = \frac{1}{2}^+$. As for the D -wave amplitude, it must be small because it contains a factor $(kR)^2 \ll 1$ due to the centrifugal barrier. Consequently, we take into account only the P -wave amplitude. By retracing the line of arguments followed in the above case of the Λ-hyperon, we easily obtain

$$\frac{\Gamma\left(\Omega^{-} \rightarrow \Xi^{0} \pi^{-}\right)}{\Gamma\left(\Omega^{-} \rightarrow \Xi^{-} \pi^{0}\right)} \simeq \frac{\left|P\left(\Omega_{-}^{-}\right)\right|^{2}}{\left|P\left(\Omega_{0}^{-}\right)\right|^{2}}$$
$$\simeq 2 \frac{\left|c_{1}+2 c_{2}+2 c_{3}+2 c_{4}-\frac{16}{3} \chi c_{5}-\chi c_{6}\right|^{2}}{\left|-c_{1}+2 c_{2}+2 c_{3}-4 c_{4}-\frac{16}{3} \chi c_{5}-\chi c_{6}\right|^{2}}$$
$$\simeq 2.94$$

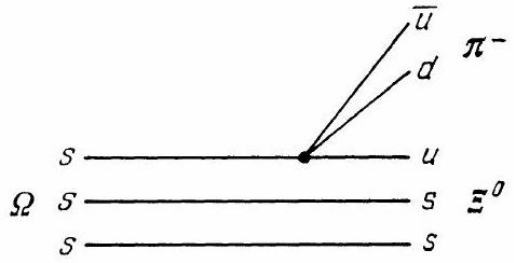


Fig. 9.7.

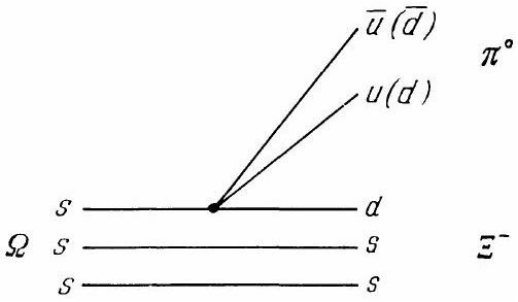


Fig. 9.8.

A preliminary experimental result for this ratio is 2.93 ± 0.45. An analysis of Λ-hyperon decays has demonstrated that the theoretical value of $\chi\left(c_{5}+c_{6}\right)$ is perhaps underestimated, while that of c_4 overestimated. It is reasonable to expect therefore, that the experimental value for the ratio $\Gamma\left(\Omega^{-} \rightarrow \Xi^{(0} \pi^{-}\right) : \Gamma\left(\Omega^{-} \rightarrow \Xi^{-} \pi^{0}\right)$ will be close to 2.5 when accuracy is improved. Note that χ would increase by a factor of 1.5 if quark masses were smaller, by the same factor, than the currently accepted values (namely, if they were $m_{\mathrm{u}} \approx 3 \mathrm{MeV}, m_{\mathrm{d}} \approx 5 \mathrm{MeV}, m_{\mathrm{s}} \approx 100 \mathrm{MeV}$). Incidentally, with a lower mass of the s-quark it would be clearer why nature demonstrates such a good SU(3) $\times$ SU(3) chiral symmetry.

5.10 10 Non-leptonic decays of K-mesons

In this chapter we discuss decays of charged and neutral K -mesons into two and three pions: $\mathrm{K} \rightarrow 2\pi$ and $\mathrm{K} \rightarrow 3\pi$. Before going into the problems connected with the isotopic selection rules and quark dynamics, we have to analyze restrictions imposed on these decays by conservation of CP parity. (Small effects in which CP invariance is broken will be discussed in Chapter 12).

5.10.1 10.1. K_1^0 and K_2^0 mesons

Consider the decay of a neutral kaon into two pions, $\pi^0\pi^0$ or $\pi^+\pi^-$. The $\pi^0\pi^0$ system is CP even: $CP\left(\pi^{0} \pi^{0}\right)=\left(CP\left(\pi^{0}\right)\right)^{2}=(-1)^{2}=+1$. The same is true for the $\pi^+\pi^-$system:

$$CP\left(\pi^+\pi^-\right) = C\left(\pi^+\pi^-\right) P\left(\pi^+\pi^-\right) = (-1)^l(-1)^l = +1.$$

(Here l is the orbital momentum of the system $\pi^+\pi^-; l = 0$ in K-meson decays). Because of this, and by virtue of the conservation of CP parity, only a CP-even system can decay into two pions. However, neither K^0 nor $\overline{\mathrm{K}}^0$ have definite CP parity:

$$CP\left|K^0\right\rangle = \left|\bar{K}^0\right\rangle,$$
$$CP\left|\bar{K}^0\right\rangle = \left|K^0\right\rangle.$$

As a result, two pions are produced in the decay of a linear superposition of K^0 and $\overline{\mathrm{K}}^0$:

$$K_1^0 = \frac{K^0 + \bar{K}^0}{\sqrt{2}}.$$

Its CP-parity is $+1$:

$$CP\left|K_1^0\right\rangle = +\left|K_1^0\right\rangle.$$

An orthogonal superposition

$$K_2^0 = \frac{K^0 - \bar{K}^0}{\sqrt{2}}$$

is CP odd ($CP\left|K_2^0\right\rangle = -\left|K_2^0\right\rangle$), and will decay into two pions only in interactions violating CP invariance.

Consider now decays into three pions: $CP\left|\pi^0\pi^0\pi^0\right\rangle = -\left|\pi^0\pi^0\pi^0\right\rangle$ so that the decay of K_1^0 into three neutral pions is forbidden while the decay $\mathrm{K}_2^0 \to 3\pi^0$ is allowed. The CP parity of the system $\pi^+\pi^-\pi^0$ is a function of the orbital state of the pions. The total angular momentum $\boldsymbol{J}$ of the three pions in the decay $\mathrm{K} \to 3\pi$ is zero. We can write J as a sum,

$$J = I + L,$$

where $\boldsymbol{l}$ is the orbital momentum of the pair $\pi^+\pi^-$, and $\boldsymbol{L}$ is the orbital momentum of the π^0 meson with respect to the center of mass of the pair $\pi^+\pi^-$. From $J = 0$ we obtain $L = l$. The pair $\pi^+\pi^-$is CP even irrespective of l, and the π^0 meson is CP odd, so that

$$CP\left|\pi^+\pi^-\pi^0\right\rangle = (-1)^{l+1}\left|\pi^+\pi^-\pi^0\right\rangle$$

The system $\pi^+\pi^-\pi^0$ can therefore be produced with even l in the decay of the K_2^0 meson, and with odd l in the decay of the K_1^0 meson. Non-zero orbital momenta suppress the decay amplitude; hence,

$$\left|M\left(\ \mathrm{K}_1^0 \to \pi^+\pi^-\pi^0\right)\right| \ll \left|M\left(\ \mathrm{K}_2^0 \to \pi^+\pi^-\pi^0\right)\right|.$$

Consequently, predominant decays must be $\mathrm{K}_1^0 \to 2\pi$ and $\mathrm{K}_2^0 \to 3\pi$. The former violate and the latter conserve P-parity. The corresponding interactions in the effective non-leptonic lagrangian are of the same order of magnitude (see chapters 7 and 9). Thus, the ratio of decay rates for $\mathrm{K}_1^0 \to 2\pi$ and $\mathrm{K}_2^0 \to 3\pi$ is determined by the ratio of phase-space volumes in these decays, and therefore by the energy release in the two cases. As a result, the decay rate of $\mathrm{K}_1^0 \to 2\pi$ is larger by approximately three orders of magnitude than the decay rate of $\mathrm{K}_2^0 \to 3\pi$.

Let us turn now to isotopic relations between different charged channels of non-leptonic decays.

5.10.2 10.2. Isotopic relations for K → 2π decays

Two pions can be found in the states with $T = 0, 1$, and 2 . Let one pion be described by an isotopic vector $\boldsymbol{a}$ and another by an isotopic vector $\boldsymbol{b}$. The state with $T = 0$ is described by an isoscalar $\boldsymbol{a} \cdot \boldsymbol{b} = a_i b_i$. The state with $T = 1$ is represented by an isovector $a_i b_t \varepsilon_{ijk}$, that is by $[\boldsymbol{a} \times \boldsymbol{b}]$. The states
with $T = 2$ are represented by a symmetric tensor of rank two with zero trace:

$$a_i b_j + a_j b_i - \frac{2}{3}\delta_{ij}(\boldsymbol{a} \cdot \boldsymbol{b}).$$

(This tensor has five independent components.) The tensor and the scalar are symmetrical with respect to permutation of the vectors $\boldsymbol{a}$ and $\boldsymbol{b}$, and the vector is anti-symmetrical. Two pions produced in the K-meson decay have $l = 0$ and are in a spatially symmetrical state; consequently, they cannot be in the isospin-antisymmetric state by virtue of the generalized Bose principle and therefore cannot have $T = 1$. This means that the two pions can have $T = 0, 2$ in the $\mathrm{K}_1^0 \to 2\pi$ decay, and only $T = 2$ in the decay $\mathrm{K}^+ \to \pi^+\pi^0$ ($T = 0$ is impossible in this last case since $T_3 = 1$).

Let us now apply the $\Delta T = \frac{1}{2}$ rule. Were it an exact rule, two pions could not be in a state with $T = 2$ in the decay of the K -meson having isospin $\frac{1}{2}$. Consequently, the decay $\mathrm{K}^+ \to \pi^+\pi^0$ would be forbidden, and the decays $\mathrm{K}_1^0 \to 2\pi$ would be to the state of two pions with $T = 0$. From the wave function of this state

$$a_i b_i = a_+ b_- + a_- b_+ + a_0 b_0,$$

where subscripts indicate charge states of pions, we readily conclude that

$$\frac{\Gamma\left(\mathrm{K}_1^0 \to \pi^+\pi^-\right)}{\Gamma\left(\mathrm{K}_1^0 \to \pi^0\pi^0\right)} = 2.$$

Experimentally this ratio is close to 2.2 , and the decay $\mathrm{K}^+ \to \pi^+\pi^0$ is not completely forbidden even if suppressed by a factor of several hundred as compared to the decays $\mathrm{K}_1^0 \to 2\pi$. The deviation from the $\Delta T = \frac{1}{2}$ rule is caused in both cases by transitions with $\Delta T = \frac{3}{2}$ produced owing to the term $I_6\left(O_4\right)$ in the effective non-leptonic lagrangian.

By using "spurions" with $T = \frac{1}{2}$ and $T = \frac{3}{2}$ and the table of the ClebschGordan coefficients (see appendix, Chapter 29, sect. 2.5), we easily derive the following relations (it is essential that the wave function of two π-mesons is symmetrized over the relevant isotopic variables):

$$\begin{aligned}
M\left(\mathrm{K}_1^0 \to \pi^+\pi^-\right) &= \sqrt{\frac{2}{3}} A_0 \mathrm{e}^{i\delta_0} + \sqrt{\frac{1}{3}} A_2 \mathrm{e}^{i\delta_2} \\
M\left(\mathrm{K}_1^0 \to \pi^0\pi^0\right) &= \sqrt{\frac{1}{3}} A_0 \mathrm{e}^{i\delta_0} - \sqrt{\frac{2}{3}} A_2 \mathrm{e}^{i\delta_2} \\
M\left(\mathrm{K}^+ \to \pi^+\pi^0\right) &= \frac{1}{2}\sqrt{3} A_2 \mathrm{e}^{i\delta_2}
\end{aligned}$$

where A_0 and A_2 are real amplitudes of transitions to states with $T = 0$ and $T = 2$, respectively, and δ_0 and δ_2 are phases of the $\pi\pi$ scattering in these
states. (These phases are taken into account in correspondence with the relations derived in chapter 8.) The ratio for widths becomes

$$\begin{aligned}
\frac{\Gamma\left(\mathrm{K}_1^0 \to \pi^+\pi^-\right)}{\Gamma\left(\mathrm{K}_1^0 \to \pi^0\pi^0\right)} &= \frac{p_\pm}{p_0}\left[2 + 6\sqrt{2}\frac{A_2}{A_0}\cos\left(\delta_2 - \delta_0\right)\right], \\
\frac{\Gamma\left(\mathrm{K}^+ \to \pi^+\pi^0\right)}{\Gamma\left(\mathrm{K}_1^0 \to 2\pi\right)} &= \frac{3}{4}\left(\frac{A_2}{A_0}\right)^2.
\end{aligned}$$

Using the ratio of phase-space volumes equal to the ratio of momenta $p_{\pm}/p_0 = 0.986$, and using also the data on S-wave $\pi\pi$ scattering, $\delta_0 - \delta_2 = 53^0 \pm 6^0$, we find that the two ratios are in agreement with experiment if $A_2/A_0 = 4.5 - 4.6\%$.

5.10.3 10.3. Quark graphs for $K^{\pm} \to \pi^{\pm}\pi^0$ decays

As an example, let us calculate the amplitude of the $K^{\pm} \to \pi^{\pm}\pi^0$ decays on the basis of the effective non-leptonic interaction O_4 (we recall that the remaining terms of the effective non-leptonic lagrangian discussed in chapter 7 are subject to the $\Delta T = \frac{1}{2}$ selection rule and therefore make no contribution to the $K^+ \to \pi^+\pi^0$ decay). In order to avoid dealing with the $\bar{s}$-quark and to operate only with the s-quark, let us consider only the $K^- \to \pi^-\pi^0$ decay whose amplitude is equal to that of $K^+ \to \pi^+\pi^0$.

It is quite apparent that annihilation-type graphs shown in fig. 10.1 make no contribution to the amplitude. Indeed, the π^0 mesons in graphs 10.1a and 10.1b are produced with opposite signs (from $u\bar{u}$ in fig. 10.1a and from $d\bar{d}$ in fig. 10.1b). We now take into account that two pions produced in the decay are in a symmetric state (this corresponds to the up-down symmetry of the graphs). It is then immediately apparent that the two graphs 10.1a and 10.1 b cancel each other out.

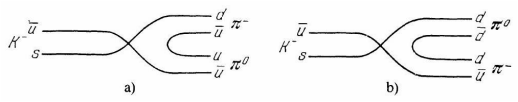


Fig. 10.1.

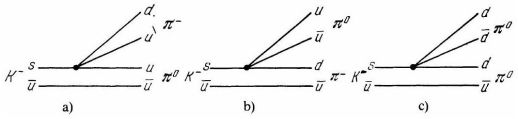


Fig. 10.2.

Let us consider now the external graphs in which an s-quark emits a pion (see fig. 10.2). We recall (see the end of chapter 7) that

$$O_4 = \bar{d}_{\mathrm{L}}\gamma_\alpha u_{\mathrm{L}}\bar{u}_{\mathrm{L}}\gamma^\alpha s_{\mathrm{L}} + \bar{u}_{\mathrm{L}}\gamma_\alpha u_{\mathrm{L}}\bar{d}_{\mathrm{L}}\gamma^\alpha s_{\mathrm{L}} - \bar{d}_{\mathrm{L}}\gamma_\alpha d_{\mathrm{L}}\bar{d}_{\mathrm{L}}\gamma^\alpha s_{\mathrm{L}}.$$

First factorize the amplitude corresponding to the graph of fig. 10.2a. The contribution of the first term of O_4 to the amplitude is

$$\left\langle \pi^-\pi^0 \right| \bar{d}_{\mathrm{L}}\gamma_\alpha u_{\mathrm{L}}\bar{u}_{\mathrm{L}}\gamma^\alpha s_{\mathrm{L}} \left| K^- \right\rangle_{\mathrm{a}} = \left\langle \pi^- \right| \bar{d}_{\mathrm{L}}\gamma_\alpha u_{\mathrm{L}}|0\rangle \left\langle \pi^0 \right| \bar{u}_{\mathrm{L}}\gamma^\alpha s_{\mathrm{L}} \left| K^- \right\rangle .$$

The contribution of the second term of O_4 to the amplitude of fig. 10.2a can be found by means of the Fierz transformation (see appendix and chapters 7 and 9):

$$\left\langle \pi^-\pi^0 \right| \bar{u}_{\mathrm{L}}\gamma_\alpha u_{\mathrm{L}}\bar{d}_{\mathrm{L}}\gamma^\alpha s_{\mathrm{L}} \left| K^- \right\rangle_{\mathrm{a}} = \frac{1}{3} \left\langle \pi^-\pi^0 \right| \bar{d}_{\mathrm{L}}\gamma_\alpha u_{\mathrm{L}}\bar{u}_{\mathrm{L}}\gamma^\alpha s_{\mathrm{L}} \left| K^- \right\rangle .$$

Obviously, the contribution of the third term of O_4 to the amplitude of fig. 10.2a is zero: this term contains no u-quark operators. The total contribution of operator O_4 to the amplitude corresponding to graph 10.2a is

$$\begin{aligned}\left\langle \pi^-\pi^0\right| O_4 \left|K^-\right\rangle_{\rm a} &= \frac{4}{3}\left\langle \pi^-\right| \bar{d}_{\rm L}\gamma_\alpha u_{\rm L}|0\rangle \left\langle \pi^0\right| \bar{u}_{\rm L}\gamma^\alpha s_{\rm L}\left|K^-\right\rangle \\ &= \frac{1}{3}\left\langle \pi^-\right| \bar{d}\gamma_\alpha\gamma_5 u|0\rangle \left\langle \pi^0\right| \bar{u}\gamma^\alpha s\left|K^-\right\rangle .\end{aligned}$$

A similar analysis in the case of the graph of fig. 10.2b yields

$$\begin{aligned}\left\langle \pi^-\pi^0\right| \bar{d}_{\rm L}\gamma_\alpha u_{\rm L}\bar{u}_{\rm L}\gamma^\alpha s_{\rm L}\left|K^-\right\rangle_{\rm b} &= \frac{1}{3}\left\langle \pi^-\pi^0\right| \bar{u}_{\rm L}\gamma_\alpha u_{\rm L}\bar{d}_{\rm L}\gamma^\alpha s_L\left|K^-\right\rangle_{\rm b} \\ &= \frac{1}{3}\left\langle \pi^0\right| \bar{u}_{\rm L}\gamma_\alpha u_{\rm L}|0\rangle \left\langle \pi^-\right| \bar{d}_{\rm L}\gamma^\alpha s_{\rm L}\left|K^-\right\rangle .\end{aligned}$$

Hence,

$$\left\langle \pi^-\pi^0\right| O_4 \left|K^-\right\rangle_{\rm b} = \frac{1}{3}\left\langle \pi^0\right| \bar{u}\gamma_\alpha\gamma_5 u|0\rangle \left\langle \pi^-\right| \bar{d}\gamma^\alpha s\left|K^-\right\rangle .$$

Consider finally the amplitude corresponding to the graph of fig. 10.2c.
Only the last term of O_4 contributes to it:

$$\begin{aligned}\left\langle \pi^-\pi^0\right| O_4 \left|K^-\right\rangle_{\rm c} &= -\left\langle \pi^-\pi^0\right| \bar{d}_{\rm L}\gamma_\alpha d_{\rm L}\bar{d}_{\rm L}\gamma^\alpha s_{\rm L}\left|K^-\right\rangle_{\rm c} \\ &= -\frac{4}{3}\left\langle \pi^0\right| \bar{d}_{\rm L}\gamma_\alpha d_{\rm L}|0\rangle \left\langle \pi^-\right| \bar{d}_{\rm L}\gamma^\alpha s_{\rm L}\left|K^-\right\rangle \\ &= -\frac{1}{3}\left\langle \pi^0\right| \bar{d}\gamma_\alpha\gamma_5 d|0\rangle \left\langle \pi^-\right| \bar{d}\gamma^\alpha s\left|K^-\right\rangle\end{aligned}$$

Taking into account now that

$$\begin{aligned}\left\langle \pi^0\right| \bar{u}\gamma_\alpha\gamma_5 u|0\rangle &= -\left\langle \pi^0\right| \bar{d}\gamma_\alpha\gamma_5 d|0\rangle = \frac{1}{2}\sqrt{2}\left\langle \pi^-\right| \bar{d}\gamma_\alpha\gamma_5 u|0\rangle \\ \left\langle \pi^-\right| \bar{d}\gamma_\alpha s\left|K^-\right\rangle &= \sqrt{2}\left\langle \pi^0\right| \bar{u}\gamma_\alpha s\left|K^-\right\rangle\end{aligned}$$

we notice that graphs 10.2a, 2b, and 2c give identical contributions. Finally,

$$\begin{aligned}\left\langle \pi^-\pi^0\right| O_4 \left|K^-\right\rangle =& \left\langle \pi^-\pi^0\right| O_4 \left|K^-\right\rangle_{\rm a} + \left\langle \pi^-\pi^0\right| O_4 \left|K^-\right\rangle_{\rm b} \\ &+ \left\langle \pi^-\pi^0\right| O_4 \left|K^-\right\rangle_{\rm c} \\ =& \left\langle \pi^-\right| \bar{d}\gamma_\alpha\gamma_5 u|0\rangle \left\langle \pi^0\right| \bar{u}\gamma^\alpha s\left|K^-\right\rangle \\ =& \sqrt{\frac{1}{2}} f_\pi k_{1\alpha}\left[f_+\left(k+k_2\right)^\alpha + f_-\left(k-k_2\right)^\alpha\right] \\ =& \sqrt{\frac{1}{2}} f_\pi\left[f_+\left(m_{\rm K}^2 - m_\pi^2\right) + f_- m_\pi^2\right]\end{aligned}$$

These expressions take into account the relations (see chapters 5 and 6)

$$\begin{aligned}\left\langle \pi^-\right| \bar{d}\gamma_\alpha\gamma_5 u|0\rangle &= f_\pi k_{1\alpha}, \\ \left\langle \pi^0\right| \bar{u}\gamma^\alpha s\left|K^-\right\rangle &= \sqrt{\frac{1}{2}}\left(f_+\left(k+k_2\right)^\alpha + f_-\left(k-k_2\right)^\alpha\right),\end{aligned}$$

where k is the momentum of the K -meson, and k_1 and k_2 are momenta of the $\pi^-$and π^0 mesons, respectively. In the case of $K^- \to \pi^-\pi^0$ decay, $k = k_1 + k_2$. If we neglect m_π^2 in comparison to $m_{\rm K}^2$ (moreover, we take into account that $f_- < f_+ = 1$), then

$$\left\langle \pi^-\pi^0\right| O_4 \left|K^-\right\rangle \approx \sqrt{\frac{1}{2}} f_\pi m_{\rm K}^2$$

Recalling that

$$\mathcal{L}_{\text{eff}} = \sqrt{2}G \sin\theta \cos\theta \sum_{i=1}^{6} c_i O_i,$$

where $c_4 = 0.39$ (see the end of Chapter 7), we obtain for the decay amplitude

$$\begin{aligned} M\left(\mathrm{K}^{\pm} \to \pi^{\pm}\pi^0\right) &= \left\langle \pi^-\pi^0 \right| \mathfrak{L}_{\text{eff}} \left| K^- \right\rangle \\ &= \sqrt{2}Gc_4 \sin\theta\cos\theta \left\langle \pi^-\pi^0 \right| O_4 \left| K^- \right\rangle \\ &= Gm_{\mathrm{K}}^2 f_\pi c_4 \sin\theta\cos\theta. \end{aligned}$$

Experimentally

$$\left| M\left(\mathrm{K}^+ \to \pi^+\pi^0\right) \right| \approx 0.05 G m_{\mathrm{K}}^2 m_\pi$$

We find that the experimental value of c_4 is smaller by a factor of 1.5 than the value calculated in the framework of the theory taking account of hard virtual gluons (i.e. of corrections for strong interactions at small distances). Recall that the data on the $\Lambda \to \mathrm{N}\pi$ decays also indicate that c_4 is smaller by the same factor of 1.5 than the result of theoretical calculations. These calculations are unsatisfactory possibly because only the main logarithmic terms are taken into account. Furthermore, the contribution of intermediate distances is neglected (large distances are covered by the meson wave functions).

We have thus discussed the $\mathrm{K}^+ \to \pi^+\pi^0$ decay due to transitions with $\Delta T = \frac{3}{2}$. The $\mathrm{K_S} \to 2\pi$ decays dominated by transitions with $\Delta T = \frac{1}{2}$ can be analyzed in a similar manner. It can be shown, in particular, that the main contribution to the $\mathrm{K_S^0} \to \pi^+\pi^-$decay is made by the operators O_5 and O_6 and that the theoretical value of the amplitude obtained fits well the corresponding experimental data.

5.10.4 10.4. $K \to 3\pi$ decays

In a general case, three pions may form a state with $T = 0, 1, 2$, and 3 :

$$3 \times 3 \times 3 = 1 + 3 + 3 + 3 + 5 + 5 + 7.$$

Let us denote isotopic functions of pions by $\boldsymbol{a}, \boldsymbol{b}, \boldsymbol{c}$. A state with $T = 0$ is written as $\boldsymbol{a}[\boldsymbol{bc}]$; it is anti-symmetric and therefore can comprise only three different pions with odd orbital momenta l and L (see the beginning of this chapter). Such a state could be produced in a suppressed (as yet unobserved) decay $\mathrm{K_1^0} \to \pi^+\pi^-\pi^0$. The state with $T = 3$ is completely symmetrical. Two states with $T = 2$ have mixed symmetry. One of the three states with $T = 1$ is completely symmetrical, and the remaining two have mixed symmetry. The symmetrical state with $T = 1$ is predominant in the $\mathrm{K} \to 3\pi$ decay because of the $\Delta T = \frac{1}{2}$ rule and low energy release:

$$A = a(bc) + b(ca) + c(ab)$$

Decays of the K^+meson are represented by the component A_+:

$$A_+ = a_+(bc) + b_+(ca) + c_+(ab)$$

and decays of the $\mathrm{K_2^0}$ meson by the component A_0 :

$$A_0 = a_0(\boldsymbol{bc}) + b_0(\boldsymbol{ca}) + c_0(\boldsymbol{ab}).$$

Recast A_+in the form

$$\begin{aligned} A_+ = &+ a_+b_+c_- + a_+b_-c_+ + a_+b_0c_0 \\ &+ b_+c_+a_- + b_+c_-a_+ + b_+c_0a_0 \\ &+ c_+a_+b_- + c_+a_-b_+ + c_+a_0b_0 \end{aligned}$$

This yields the ratio of decay widths of the K^+meson:

$$\begin{aligned} \frac{\Gamma\left(K^+ \to \pi^+\pi^-\pi^-\right)}{\Gamma\left(K^+ \to \pi^0\pi^0\pi^+\right)} &= \frac{\left|2a_+b_+c_-\right|^2 + \left|2b_+c_+a_-\right|^2 + \left|2c_+a_+b_-\right|^2}{\left|a_+b_0c_0\right|^2 + \left|b_+c_0a_0\right|^2 + \left|c_+a_0b_0\right|^2} \\ &= \frac{12}{3} = \frac{4}{1} \end{aligned}$$

In the explicit form A_0 is written as

$$\begin{aligned} A_0 = &+ a_0b_+c_- + a_0b_-c_+ + a_0b_0c_0 \\ &+ b_0c_+a_- + b_0c_-a_+ + b_0c_0a_0 \\ &+ c_0a_+b_- + c_0a_-b_+ + c_0a_0b_0 \end{aligned}$$

This yields the relation between the K_2^0 meson decay widths:

$$\begin{aligned} &\Gamma\left(K_2^0 \to \pi^+\pi^-\pi^0\right) : \Gamma\left(K_2^0 \to \pi^0\pi^0\pi^0\right) \\ &= \left\{\left|a_0b_+c_-\right|^2 + \left|a_0b_-c_+\right|^2 + \left|b_0c_+a_-\right|^2\right. \\ &\left. + \left|b_0c_-a_+\right|^2 + \left|c_0a_+b_-\right|^2 + \left|c_0a_-b_+\right|^2\right\} : \left|3a_0b_0c_0\right|^2 \\ &= 6 : 9 = 2 : 3. \end{aligned}$$

Making use of the spurion, we easily obtain

$$M\left(\ K^0 \to\ A_0\right) : M\left(\ K^+ \to A_+\right) = 1 : \sqrt{2}.$$

If we now take into account that

$$M\left(\ K^0 \to\ A_0\right) = -M\left(\bar{K}^0 \to\ A_0\right)$$

and

$$K_2^0 = \sqrt{\frac{1}{2}}\left(K^0 - \bar{K}^0\right),$$

we conclude that

$$M\left(\ K_2^0 \to\ A_0\right) = M\left(\ K^+ \to A_+\right),$$

that is total widths of three-pion decays of the $K^+$and K^0 mesons must be equal. Finally,

$$\begin{aligned} \Gamma\left(K^+ \to \pi^+\pi^+\pi^-\right) : \Gamma\left(K_2^0 \to \pi^0\pi^0\pi^0\right) : \Gamma\left(K_2^0 \to \pi^+\pi^-\pi^0\right) : \\ : \Gamma\left(K^+ \to \pi^0\pi^0\pi^+\right) = 4 : 3 : 2 : 1 \end{aligned}$$

Before these ratios are compared to experimental values, we must take into account the differences in phase-space volumes due to differences in masses of $K^+$and K^0 mesons and $\pi^\pm$and π^0 mesons. Ratios of the phase-space volumes are

$$1 : 1.44 : 1.28 : 1.15.$$

This taken into account, the ratios $4 : 1$ and $3 : 2$ are satisfied with approximately 5% accuracy. The ratio

$$\Gamma\left(\mathrm{K}^+ \to \pi^+\pi^+\pi^-\right) : \Gamma\left(\mathrm{K}_2^0 \to \pi^+\pi^-\pi^0\right) = 2$$

is more sensitive to transitions with $\Delta T = \frac{3}{2}$. Experiment gives approximately 2.5 .

5.11 11 Neutral K-mesons in vacuum and in matter

Neutral K-mesons are a unique physical system which appears to have been created by nature specially to demonstrate, in the most impressive manner, a number of spectacular phenomena.

Two degenerate levels (K^0 and $\overline{\mathrm{K}}^0$) are mixed by the strangeness-violating weak interaction. This mixing produces two levels K_1^0 and K_2^0 with small mass difference ($\Delta m \simeq 0.5 \cdot 10^{10}$ s^{-1}) but very different lifetimes ($\tau_1 \simeq 10^{-10}$ s, $\tau_2 \simeq 5 \cdot 10^{-8}$ s). The maximum breaking of P - and C-parity occurs in the decays of these two levels. Both the interaction and decays of neutral K -mesons are characterized by spectacular quantum-mechanical effects. If the K-mesons did not exist, they should have been invented "on purpose", in order to teach students the principles of quantum mechanics. In particular, K-mesons make it possible to realize in the laboratory, and over large distances, a number of gedanken experiments, such as, for example, the Einstein-Podolsky-Rosen experiment. And the last but not the least significant phenomenon is the breaking of CP parity in decays of K^0 mesons, which we shall discuss in the next chapter. The subject of the present chapter is the difference in masses of K_1^0 and K_2^0 mesons, and interference effects in decays of these particles.

5.11.1 11.1. $K^0 \leftrightarrow \bar{K}^0$ transitions and the $K_1^0 - K_2^0$ mass difference

Most elementary particles have corresponding antiparticle counterparts, with the same mass, lifetime, and spin, but with opposite sign of charge (electric, baryonic, or leptonic). The electron-positron, proton-antiproton, and neutron-antineutron are examples of such pairs. The truly neutral particles which are identical to their antiparticles (the photon, π^0, η^0, ω^0, etc.) form a much smaller class of particles. The neutral K -mesons are at the junction of these two classes. On the one hand, K^0 and $\overline{\mathrm{K}}^0$ are not identical: the former has positive strangeness and the latter negative, so that in strong

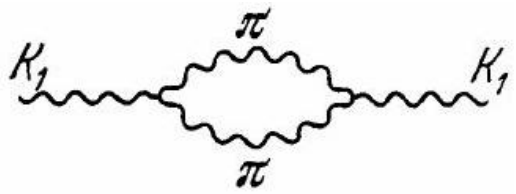


Fig. 11.1.

interactions with nuclei K^0 and $\overline{\mathrm{K}}^0$ are just as different as the neutron n and antineutron $\overline{\mathrm{n}}$. On the other hand, non-conservation of strangeness in weak interactions allows $\mathrm{K}^0 \leftrightarrow \overline{\mathrm{K}}^0$ transitions while the transition $\mathrm{n} \leftrightarrow \overline{\mathrm{n}}$ is ruled out because of conservation of baryonic charge.

The mixing of two degenerate levels in vacuum must result in level splitting. The levels with definite CP parity,

$$K_1^0 = \frac{K + \bar{K}^0}{\sqrt{2}} \quad \text{and} \quad K_2^0 = \frac{K - \bar{K}^0}{\sqrt{2}},$$

would have definite masses and lifetimes if CP invariance were strict. In fact, this invariance is broken but the corresponding corrections to mass and lifetime are negligibly small. The

lifetime difference between K_1^0 and K_2^0 occurs because K_1^0 decays into two pions while only three-pion decays are allowed for K_2^0 (see chapter 10). Let us consider the graphs of figs. 11.1 and 11.2. The imaginary parts of these graphs are proportional to $\Gamma(K_1 \to 2\pi)$ and $\Gamma(K_2 \to 3\pi)$, respectively. The real parts contribute to the masses of the K_1 and K_2 mesons. If we assume that by order of magnitude the real parts are comparable to the imaginary ones, then $|\Delta m_{12}| \equiv |m_2 - m_1| \sim \Gamma_1 \sim G^2 m_\pi^5$. It is essential to emphasize that the mass difference Δm_{12} would not vanish even if, for instance, pions were twice as massive as they actually are and consequently the decays $K_1 \to 2\pi$ and $K_2 \to 3\pi$ were kinematically forbidden.

It should be instructive to regard the masses of the K_1^0 and K_2^0 mesons as mean values of the hamiltonian over the states K_1^0 and K_2^0 :

$$
\begin{aligned}
m_1 = \langle K_1 | H | K_1 \rangle &= \left\langle \frac{K+\bar{K}}{\sqrt{2}} \middle| H \middle| \frac{K+\bar{K}}{\sqrt{2}} \right\rangle \\
&= \frac{1}{2}[\langle K|H|K\rangle + \langle \bar{K}|H|\bar{K}\rangle + \langle K|H|\bar{K}\rangle + \langle \bar{K}|H|K\rangle], \\
m_2 = \langle K_2 | H | K_2 \rangle &= \left\langle \frac{K-\bar{K}}{\sqrt{2}} \middle| H \middle| \frac{K-\bar{K}}{\sqrt{2}} \right\rangle \\
&= \frac{1}{2}[\langle K|H|K\rangle + \langle \bar{K}|H|\bar{K}\rangle - \langle K|H|\bar{K}\rangle - \langle \bar{K}|H|K\rangle].
\end{aligned}
$$

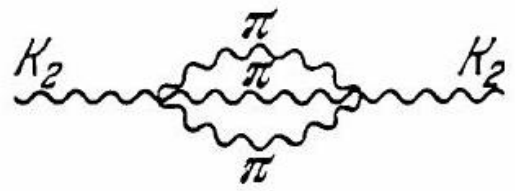


Fig. 11.2.

We see that

$$m_1 - m_2 = \langle K|H|\bar{K}\rangle + \langle \bar{K}|H|K\rangle,$$

that is the mass difference between K_1^0 and K_2^0 mesons is due to $K \leftrightarrow \overline{K}$ transitions which change strangeness by 2 . Such transitions with $|\Delta S| = 2$ are absent in the weak lagrangian in the discussed quark theory of the weak interaction (see fig. 11.3). The mass difference Δm_{12} is very sensitive to such transitions. It would "respond" to them even if the constant G_2 (see fig. 11.3) were smaller by seven orders of magnitude than the Fermi constant G. Indeed, let us analyze the contribution of the graph in fig. 11.3 to the amplitude of the $K^0 \leftrightarrow \overline{K}^0$ transition (fig. 11.4). Factorization of the contributions of loops readily yields

$$\Delta m_{12} \sim G_2 f_K^2 m_K,$$

where $f_K \simeq 165\text{MeV}$ is a constant characterizing the decay amplitude of $K \to \mu\nu$, and m_K is the K-meson mass. Hence, G_2 is smaller by at least seven orders of magnitude than the Fermi constant G.

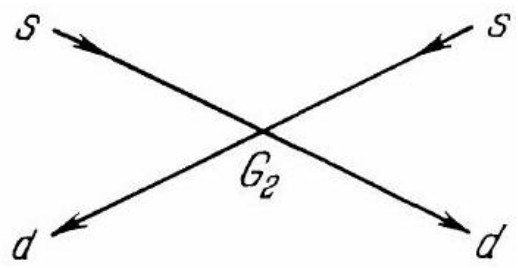


Fig. 11.3.

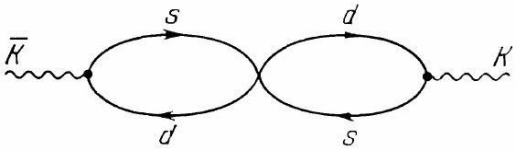


Fig. 11.4.

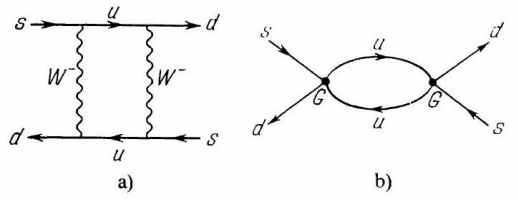


Fig. 11.5.

5.11.2 11.2. Glashow-Iliopoulos-Maiani mechanism

In the theory under discussion, ss $\leftrightarrow$ dd transitions can, and must, arise in the second order of perturbation theory in G (fig. 11.5). Fig. 11.5a shows how this transition goes via exchange of W-bosons; the same process is shown in fig. 11.5b in the local four-fermion limit. Obviously, the graph of fig. 11.5b is quadratically divergent and yields the effective constant of the ss $\leftrightarrow$ dd transition, of the order of $G^2\Lambda^2$, where Λ is the cutoff energy. As clearly follows from fig. 11.5a, this cutoff energy is of the order of m_{W}, that is of the mass of the intermediate boson. But as follows from the preceding section, the quantity $G_2 \sim G^2 m_{\mathrm{W}}^2$ is by many orders of magnitude larger than is allowed by the experimental value of Δm_{12}.

It is very interesting that the theory of the weak interaction which is our subject here, copes with this difficulty by mutual compensation of the graphs containing virtual u- and c-quarks. The mechanism of this compensation is often abbreviated as GIM, by the first letters of the authors' names. It must be emphasized that Glashow, Iliopoulos and Maiani have published their paper several years before charmed particles were discovered, and greatly stimulated the experimental effort to detect these particles.

With the c-quarks taken into account, we must consider not just one square of fig. 11.5a, but four such squares (fig. 11.6). We recall that the

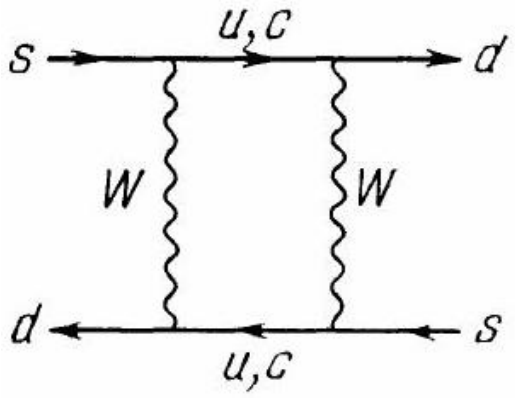


Fig. 11.6.

charged current emitting W-bosons is $\bar{u}d' + \bar{c}s'$ where

$$d' = d\cos\theta + s\sin\theta, \quad s' = -d\sin\theta + s\cos\theta$$

(We have neglected the contribution of the b - and t -quarks; its inclusion is straightforward (see Chapter 15)). Now it is easily verified that contributions of all four squares in fig. 11.6 are proportional to $\sin^2\theta\cos^2\theta$, with the plus sign in the case of $u\bar{u}$ and $c\bar{c}$, and with minus in the case of $u\bar{c}$ and $c\bar{u}$. The four graphs of fig. 11.6 therefore completely cancel one another for momenta of virtual quarks much greater than m_{c}. A non-zero contribution arises from the low-momentum range, because $m_{\mathrm{c}} \neq m_{\mathrm{u}}$:

$$\mathfrak{L}_{\Delta S=2} = G_2\bar{s}\gamma_\alpha\left(1+\gamma_5\right)d\cdot\bar{s}\gamma^\alpha\left(1+\gamma_5\right)d$$

where

$$G_2 = \frac{1}{16\pi^2}G^2\left(m_{\mathrm{c}}-m_{\mathrm{u}}\right)^2\sin^2\theta\cos^2\theta = \frac{1}{16\pi^2}G^2m_{\mathrm{c}}^2\sin^2\theta\cos^2\theta$$

It is now simple to calculate the mass difference between the K_1^0 and K_2^0 mesons:

$$\Delta m_{12} \equiv m_2 - m_1 \simeq \frac{4m_{\mathrm{c}}^2\cos^2\theta}{3\pi m_\mu^2}\Gamma\left(\mathrm{K}^+\to\mu^+\nu\right)$$

A comparison with the observed value of Δm_{12} yields that the c-quark mass is of the order of 1 GeV .

5.11.3 11.3. Oscillations of strangeness

Let us consider the behaviour of K^0 mesons in vacuum. Assume that at $t = 0$ we have pure K^0 mesons produced, for example, in the reaction $\pi^- + \mathrm{p} \to \mathrm{K}^0 + \Lambda$. No $\overline{\mathrm{K}}^0$ mesons are present at $t = 0$. Take into account now that

$$K = \frac{K_1+K_2}{\sqrt{2}}, \quad K_1 = \frac{K+\bar{K}}{\sqrt{2}}, \quad K_2 = \frac{K-\bar{K}}{\sqrt{2}}.$$

After a time t we then have

$$\frac{1}{2}\left[(K+\tilde{K})\mathrm{e}^{-im_1t-\Gamma_1t/2} + (K-\tilde{K})\mathrm{e}^{-im_2t-\Gamma_2t/2}\right]$$

If K_1^0 and K_2^0 mesons were stable ($\Gamma_1 = \Gamma_2 = 0$), then after $t = \pi/(m_2 - m_1)$ the beam would consist exclusively of $\overline{K}^0$ mesons. After another such interval the beam's strangeness would again become positive. Such oscillations of strangeness superposed over exponential damping due to $\Gamma_{1,2} \neq 0$
are indeed observed experimentally. For instance, they are observed in leptonic decays of neutral kaons.

We recall that the $\Delta Q = \Delta S$ rule forbids the decays $K^0 \to e^- \bar{\nu} \pi^+$and $\overline{K}^0 \to e^+ \nu \pi^-$and allows only

$$K^0 \to e^+ \nu \pi^- \quad \text{and} \quad \overline{K}^0 \to e^- \bar{\nu} \pi^+.$$

The oscillations of strangeness can therefore be observed by recording the number of electrons and positrons produced in K_{e3} decays. Indeed,

$$N_{e^+}(t) \propto N_K(t) = \frac{1}{4}\left[e^{-\Gamma_1 t} + e^{-\Gamma_2 t} + 2e^{-(\Gamma_1+\Gamma_2)/2}\cos(m_2 - m_1)\,t\right],$$
$$N_{e^-}(t) \propto N_{\tilde{K}}(t) = \frac{1}{4}\left[e^{-\Gamma_1 t} + e^{-\Gamma_2 t} - 2e^{-(\Gamma_1+\Gamma_2)/2}\cos(m_2 - m_1)\,t\right].$$

Experiments of this type make it possible to determine Δm_{12}. Another possibility to observe oscillations of strangeness consists in recording interactions of K -mesons in plates of materials placed atross the beam path. The point is, that the strong interactions of K^0 and $\bar{K}^0$ mesons are essentially different. For example, slow $\overline{K}^0$ mesons are effectively absorbed in collisions with protons, producing hyperons:

$$\overline{K}^0 + p \to \Lambda^0 + \pi^+.$$

At the same time, conservation of strangeness in strong interactions forbids absorption of K^0 mesons resulting in production of hyperons.

The "two-facedness" of neutral kaons is a purely quantum-mechanical property. The K^0 (or $\overline{K}^0$) meson is a superposition of K_1^0 and K_2^0, which, in their turn, are superpositions of K^0 and $\overline{K}^0$. The results of measurements depend on the character of the measurement process. If these are 2π or 3π decays, that is decays into channels with definite values of CP parity, then K_1^0 and K_2^0 are recorded. If these are decays of the type of $K^0 \to e^+ \nu \pi^-$ and $\overline{K}^0 \to e^- \bar{\nu} \pi^+$which proceed differently for the particle and its antiparticle, K^0 and $\bar{K}^0$ are recorded.

In a sense, neutral kaons resemble the electron spin in mutually perpendicular magnetic fields. The strangeness and CP parity are similar to spin projections on the x and z axes. Once the spin projection on z is fixed, the projection on x is uncertain, and vice versa. The state with the spin projection on the z-axis equal to $+\frac{1}{2}$ is a linear superposition of states with projections on the x-axis equal to $+\frac{1}{2}$ and $-\frac{1}{2}$. Kaon decays into chargesymmetric ($2\pi, 3\pi$) and charge-asymmetric states ($e^+\nu\pi^-, e^-\tilde{\nu}\pi^+$) play the role of mutually perpendicular magnetic fields H_z and H_x.

5.11.4 11.4. Regeneration

Differences in nuclear properties of K^0 and $\overline{K}^0$ mesons result in an extremely interesting phenomenon called regeneration. Assume that at $t = 0$ we have a beam consisting of K^0 mesons only. Decays $K_1^0 \to 2\pi$ will take place in this beam during time $t \sim \tau_1 \equiv 1/\Gamma_1$. These decays will stop after $\tau_1 \ll t \ll \tau_2$ where $\tau_2 = 1/\Gamma_2$, since all K_1^0 mesons will decay and leave a pure beam of K_2^0 mesons. If the beam is now directed at a plate, say a copper plate, $K_1^0 \to 2\pi$ decays will reappear behind the plate. What happens is the regeneration of K_1^0 mesons in matter.

Let us find the regeneration amplitude f_{21}. Denote the amplitude of the $\mathrm{K}^0\left(\overline{\mathrm{K}}^0\right)$ meson scattering on a nucleus by $f(\bar{f})$. After scattering, a K_2^0 meson transforms into a linear superposition of K_2^0 and K_1^0 :

$$K_2^0 = \sqrt{\frac{1}{2}}\left(K^0 - \bar{K}^0\right) \Rightarrow \sqrt{\frac{1}{2}}\left(fK^0 - \bar{f}\bar{K}^0\right)$$
$$= \frac{1}{2}\left[f\left(K_1^0 + K_2^0\right) - \bar{f}\left(K_1^0 - K_2^0\right)\right] = \frac{1}{2}(f+\bar{f})K_2^0 + \frac{1}{2}(f-\bar{f})K_1^0.$$

Hence,

$$f_{21} = \frac{1}{2}(f - \bar{f})$$

and we would have $f_{21} = 0$ if $f = \bar{f}$.
When K_1^0 mesons travel at a non-zero angle with respect to the incident beam of K_2^0 mesons, regeneration on different nuclei in the plate is incoherent (usually such incoherent regeneration is called diffractional). If, however, a K_1^0 meson travels forward, the amplitudes of regeneration on nuclei along the beam axis add up coherently. Consider a plate $\mathrm{d}x$ thick, and a K_2^0 beam incident on it from the left (fig. 11.7). The K_1^0 wave arriving at point A from a ring with radius ρ and volume $2\pi\rho\ \mathrm{d}\rho\ \mathrm{d}x$, is equal to

$$f_{21}N2\pi\rho\ \mathrm{d}\rho\ \mathrm{d}x\frac{\mathrm{e}^{ik_1 r}}{r},$$

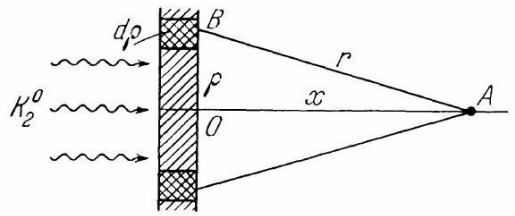


Fig. 11.7.

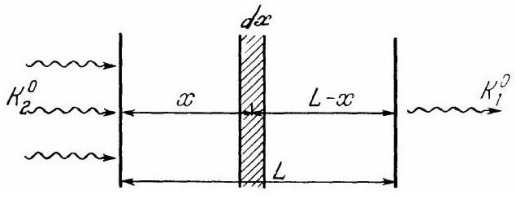


Fig. 11.8.

where N is the number of nuclei per 1 cm^3, and k_1 is the K_1^0 meson momentum. Making use of the equality $r\ \mathrm{d}r = \rho\mathrm{d}\rho$ and integrating over r, we obtain

$$\frac{2\pi i}{k_1}f_{21}(0)N\ \mathrm{d}x\mathrm{e}^{ik_1 x} = i\lambda f_{21}(0)N\ \mathrm{d}x\mathrm{e}^{ik_1 x},$$

where $\lambda = 2\pi/k_1$. (Only the lower limit of integration at $r = x$, corresponding to regeneration at zero angle, makes a non-zero contribution; hence, $f_{21}(0)$ appears in the above expression. At the upper limit the integral vanishes because of the oscillation in the integrand.) If we take

into account that f_{21} is small and if we neglect the reverse transformation $\mathrm{K}_1^0 \to \mathrm{K}_2^0$, we easily derive a similar formula for a plate with finite thickness L (fig. 11.8). The K_1^0 wave generated in the $\mathrm{d}x$ thick layer at a distance x from the left-hand side of the plate, will reach the right-hand side of the plate with the amplitude $\mathrm{d}a_1$:

$$\mathrm{d}a_1 = iN\lambda f_{21}\ \mathrm{d}x \exp\left[ik_2 x + ik_1(L-x) - \frac{L-x}{2\Lambda} - \frac{L}{2u}\right].$$

The first term in the exponent describes propagation of the K_2^0 wave till depth x, and the second term represents propagation of the K_1^0 wave from x to the right-hand side of the plate; the third term gives damping of the K_1^0 wave due to decays of K_1^0 mesons (Λ is the decay length, $\Lambda = \tau_1 \gamma v$, where τ_1 is the $\mathrm{K}_\mathrm{Y}^\mathrm{Q}$ lifetime, $\boldsymbol{v}$ is its velocity, $\gamma = (1-\boldsymbol{v}^2)^{-1/2}$), and the fourth term describes absorption of mesons in the plate (u is the collision length, identical for K_1^0 and K_2^0).

The energy of the K -meson scattered forward remains practically unaltered so that

$$k_1^2 + m_1^2 = k_2^2 + m_2^2,$$

whence

$$k_1 - k_2 = (m_1 - m_2)\frac{m}{k}.$$

By integrating $\mathrm{d}a_1$ over x from 0 to L and taking the squared modulus of the expression obtained, we find the intensity of the coherent K_1^0 wave,

$$|a_1|^2 = \frac{4\,|f_{21}(0)|^2\, N^2\Lambda^2\lambda^2}{1+4\delta^2}\left|\mathrm{e}^{-i\delta l} - \mathrm{e}^{-l/2}\right|^2 \mathrm{e}^{-L/u},$$

where two dimensionless quantities are used:

$$l = \frac{L}{\Lambda} \quad \text{and} \quad \delta = (m_2 - m_1)\,\tau_1.$$

Consider now the diffraction regeneration of K_1^0 mesons. The differential cross section of regeneration is

$$\frac{\mathrm{d}\sigma_{21}}{\mathrm{d}\Omega} = |f_{21}|^2.$$

The intensity of K_1^0 mesons created within the layer of thickness $\mathrm{d}x$ and having travelled the distance $L-x$ is

$$\mathrm{d}\left(\frac{\mathrm{d}n_1}{\mathrm{d}\Omega}\right) = |f_{21}|^2 N\ \mathrm{d}x \exp\left[-\frac{L-x}{\Lambda} - \frac{L}{u}\right].$$

Integration over x yields

$$\frac{\mathrm{d}n_1}{\mathrm{d}\Omega} = |f_{21}|^2 N\Lambda\left(1-\mathrm{e}^{-l}\right)\mathrm{e}^{-L/u}$$

The ratio of coherent to diffraction intensity is

$$R = \frac{|a_1|^2}{\mathrm{d}n_1/\mathrm{d}\Omega} = \frac{4N\Lambda\lambda^2\left|\mathrm{e}^{-i\delta l} - \mathrm{e}^{-l/2}\right|^2}{(1-\mathrm{e}^{-l})\,(1+4\delta^2)}$$

and is independent of f_{21}. The intensity of diffraction regeneration at zero angle is found by extrapolation. Measurement of R makes it possible to determine Δm_{12} with high accuracy.

The interference of K_1^0 waves which regenerated in two (or more) plates has been measured in a number of experiments. Among other things, these experiments yielded the sign of Δm_{12} and established that K_2^0 is heavier than K_1^0.

5.12 12 Violation of CP invariance

5.12.1 12.1. $\mathrm{K}_\mathrm{L}^0 \to \pi^+\pi^-$decay

Cristensen, Cronin, Fitch and Turlay have found in 1964 that long-lived neutral K-mesons decay into $\pi^+\pi^-$with a small relative width ($B \simeq 2 \cdot 10^{-3}$). This discovery signified that decays of K_2^0 mesons violate CP invariance. Violation of CP invariance means that, if K_1^0 (K_2^0) denote, as before, the states with $CP = +1(-1)$, the long-lived neutral K -meson is not identical to K_2^0. It has no definite CP parity and is represented by a superposition of K_1^0 and K_2^0 :

$$K_\mathrm{L}^0 = \frac{1}{\sqrt{1+|\varepsilon|^2}}\left(K_2^0 + \varepsilon K_1^0\right)$$

(subscript L for "long"). The short-lived meson is denoted by K_S^0 (S for "short"). Experiments have demonstrated that the complex parameter ε is small ($|\varepsilon| \simeq 2.3 \cdot 10^{-3}$, see below) so that $|\varepsilon|^2$ will be hereafter neglected. If the amplitudes of the $\mathrm{K}_\mathrm{L} \to \pi^+\pi^-$and $\mathrm{K}_\mathrm{S} \to \pi^+\pi^-$decays are denoted by $\langle \pi^+\pi^- \mid K_\mathrm{L}\rangle$ and $\langle \pi^+\pi^- \mid K_\mathrm{S}\rangle$, it is convenient to introduce a complex parameter

$$\eta_{+-} \equiv |\eta_{+-}|\, \mathrm{e}^{i\phi_{+-}} = \frac{\langle \pi^+\pi^- \mid K_\mathrm{L}\rangle}{\langle \pi^+\pi^- \mid K_\mathrm{S}\rangle}.$$

The experimental values are $|\eta_{+-}| \simeq 2.3 \cdot 10^{-3}, \phi_{+-} \simeq 45°$.
Phenomenologically it is natural to distinguish between two possible mechanisms of CP violation in $\mathrm{K}_\mathrm{L}^0 \to \pi^+\pi^-$decay. The first of these is a direct CP-odd decay $\mathrm{K}_2^0 \to \pi^+\pi^-$, due to the CP-non-invariant interaction with $|\Delta S| = 1$ (S stands for strangeness). The strength of this interaction must be weaker by at least three orders of magnitude than that of the weak non-leptonic interaction. Hence, it was called the milliweak interaction. The second mechanism reduces the $\mathrm{K}_\mathrm{L}^0 \to \pi^+\pi^-$decay to a CP-invariant decay of the $\varepsilon\mathrm{K}_1^0$ component contained in K_L^0. In this case violation of CP is



Fig. 12.1.

totally restricted to the mixing $\mathrm{K}_2^0 \leftrightarrow \mathrm{K}_1^0$ which forms states with definite masses and lifetimes K_L^0 and K_S^0. This mechanism is referred to as the superweak mixing (see below, p. 97). Obviously, in this case (neglecting $|\varepsilon|^2$ terms)

$$\left\langle \pi^+\pi^- \mid K_\mathrm{L}^0\right\rangle = \varepsilon \left\langle \pi^+\pi^- \mid K_1^0\right\rangle = \varepsilon \left\langle \pi^+\pi^- \mid K_\mathrm{S}\right\rangle.$$

Hence,

$$\eta_{+-} = \varepsilon.$$

The mixing $\mathrm{K}_2^0 \leftrightarrow \mathrm{K}_1^0$ and the subsequent decay $\mathrm{K}_1^0 \to \pi^+\pi^-$can be represented in perturbation theory by a graph of fig. 12.1. Here $i\mu_{21}$ is non-diagonal CP-odd "mass". If K_2^0

and K_1^0 have no common decay channels (this is assumed by the mechanism under discussion), then $i\mu_{21}$ is pure imaginary by virtue of CPT invariance (i.e. the hermiticity of the interaction hamiltonian transforming K_2 into K_1). As one easily finds from the graph of fig. 12.1,

$$\eta_{+-} = \frac{i\mu_{21}}{m_2 - m_1 - \frac{1}{2}i\,(\Gamma_2 - \Gamma_1)} = \frac{i\mu_{21}}{(m_\mathrm{L} - m_\mathrm{S}) - \frac{1}{2}i\,(\Gamma_\mathrm{L} - \Gamma_\mathrm{S})},$$

whence

$$\tan\phi_{+-} = \frac{2\,(m_\mathrm{L} - m_\mathrm{S})}{\Gamma_\mathrm{S} - \Gamma_\mathrm{L}} \simeq 0.96$$
$$\phi_{+-} \simeq 44^0$$

The mechanism of $K_2^0 \leftrightarrow K_1^0$ mixing thus yields the phase value, ϕ_{+-}, in agreement with experiment.

5.12.2 12.2. Other observed $\boldsymbol{CP}$ violating effects

We shall see that the mechanism of superweak mixing is quite adequate to describe two other CP-odd effects observed experimentally.

Let us denote the CP-odd decay amplitude for $\mathrm{K}_\mathrm{L}^0 \to \pi^0\pi^0$ by $\langle\pi^0\pi^0 \mid K_\mathrm{L}\rangle$, and introduce a parameter

$$\eta_{00} = \frac{\langle\pi^0\pi^0 \mid K_\mathrm{L}\rangle}{\langle\pi^0\pi^0 \mid K_\mathrm{S}\rangle}.$$

As follows from the preceding section,

$$\eta_{00} \equiv |\eta_{00}|\,\mathrm{e}^{i\phi_{00}} = \eta_{+-} = \varepsilon,$$

if the $K_2^0 \leftrightarrow K_1^0$ mixing mechanism is responsible for the CP breaking. The experimental accuracy of η_{00} measurements is poorer than that of η_{+-}:

$$|\eta_{00}| : |\eta_{+-}| = 1.03 \pm 0.04, \quad \phi_{00} - \phi_{+-} = 10^0 \pm 6^0.$$

The equality $\eta_{00} = \eta_{+-}$thus holds within experimental errors.
The $\mathrm{K}_2^0 \leftrightarrow \mathrm{K}_1^0$ mixing results in a charge asymmetry of leptonic decays of the K_L^0 meson. Denote the parameter of this asymmetry by δ :

$$\delta = \frac{\Gamma\,(\mathrm{K}_\mathrm{L}^0 \to \mathfrak{l}^+\nu\pi^-) - \Gamma\,(\mathrm{K}_\mathrm{L}^0 \to \mathfrak{l}^-\tilde{\nu}\pi^+)}{\Gamma\,(\mathrm{K}_\mathrm{L}^0 \to \mathfrak{l}^+\nu\pi^-) + \Gamma\,(\mathrm{K}_\mathrm{L}^0 \to \mathfrak{l}^-\tilde{\nu}\pi^+)}.$$

We shall take into account that $K_\mathrm{L} = K_2 + \varepsilon K_1 = \sqrt{\frac{1}{2}}[K(1+\varepsilon) - \bar{K}\times(1-\varepsilon)]$, and apply the $\Delta Q = \Delta S$ rule which states that the $\mathrm{K} \to \ell^+$and $\overline{\mathrm{K}} \to \ell^-$decays are allowed while $\mathrm{K} \to \ell^-$and $\overline{\mathrm{K}} \to \ell^+$are forbidden. Also taking into account that $\Gamma\,(\mathrm{K} \to \ell^+) = \Gamma\left(\overline{\mathrm{K}} \to \ell^-\right)$, we obtain

$$\delta = \frac{|1+\varepsilon|^2 - |1-\varepsilon|^2}{|1+\varepsilon|^2 + |1-\varepsilon|^2} \simeq 2\,\mathrm{Re}\,\varepsilon.$$

Experimental values of charge asymmetry are available both for the K_{e3} and for $\mathrm{K}_{\mu3}$ decays. Within the experimental error, the values of δ coincide; the mean asymmetry parameter is $\delta = (3.3 \pm 0.12)\cdot 10^{-3}$ which must be compared with $\sqrt{2}\,|\eta_{+-}| \simeq 3.2\cdot 10^{-3}$. The agreement is again good.

All the CP-odd decays listed above are among the decays of K_L^0 mesons. In spite of a thorough search, no violation of CP was detected in decays or interactions of other particles.

This exceptional behavior of K_L^0 mesons is based on the enhancement of CP-odd effects in K_L^0 decays; this will be shown in the next section.

5.12.3 12.3. Superweak mixing

The parameter $i\mu_{21}$ was defined above as the non-diagonal mass,

$$i\mu_{21} = \langle K_1 | H | K_2 \rangle ,$$

where H is the hamiltonian of the CP-non-invariant interaction giving rise to the $K_1 \leftrightarrow K_2$ transitions. Let us find the selection rules for this hamiltonian, and its effective strength. In doing this, we shall not decide in advance on whether the hamiltonian is a primary one or whether it appears as an effective hamiltonian in higher orders of the perturbation theory with respect to a primary CP-non-invariant interaction (see Chapter 15, sect. 4). It is apparent that H changes strangeness by 2 :

$$|\Delta S| = 2.$$

Indeed,

$$\begin{aligned} i\mu_{21} = \langle K_1 | H | K_2 \rangle &= \frac{1}{2}\langle K + \bar{K} | H | K - \bar{K} \rangle \\ &= \frac{1}{2}[\langle K|H|K\rangle - \langle \bar{K}|H|\bar{K}\rangle + \langle \bar{K}|H|K\rangle - \langle K|H|\bar{K}\rangle] \\ &= \frac{1}{2}[\langle \bar{K}|H|K\rangle - \langle K|H|\bar{K}\rangle]. \end{aligned}$$

The last equality appears because the particle and antiparticle have equal masses (which in the general case are complex if decays are taken into account):

$$\langle K|H|K\rangle = \langle \bar{K}|H|\bar{K}\rangle.$$

We recall that the mass difference $\Delta m_{LS} = m_L - m_S$ is also caused by transitions with $|\Delta S| = 2$ (see chapter 11):

$$\Delta m_{LS} = m_L - m_S = -\frac{1}{2}[\langle K|H|\bar{K}\rangle + \langle \bar{K}|H|K\rangle].$$

However, Δm_{LS} involves the sum and not the difference of amplitudes of the $K \to \overline{K}$ and $\overline{K} \to K$ transitions.

Assume that the $K \leftrightarrow \overline{K}$ transitions occur because of the effective fourfermion interaction turning a pair of s-quarks into a pair of d-quarks and vice versa (see figs. 12.2 and 12.3). Then the CP-invariant part of this interaction contributes to Δm_{LS}, and the CP-non-invariant part to $i\mu_{21}$. The former is proportional to $\mathrm{Re}\, G_2$, the real part of the constant G_2, while the latter is proportional to the imaginary part, $\mathrm{Im}\, G_2$. Taking into account that

$$|\mu_{21}| \sim 3 \cdot 10^{-3} |\Delta m_{LS}| ,$$

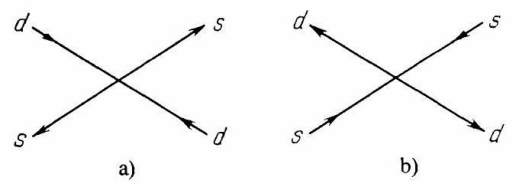


Fig. 12.2.

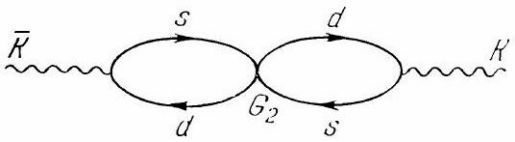


Fig. 12.3.

we conclude that

$$|\mathrm{Im}\, G_2| \sim 3 \cdot 10^{-3}\, |\mathrm{Re}\, G_2|\,.$$

We have established in Chapter 11 that $|\mathrm{Re}\, G_2| \sim 10^{-6} - 10^{-7}G$ where G is the universal Fermi coupling constant. Now we have to conclude that $\mathrm{Im}\, G_2 \sim 10^{-9}G$. An interaction with such a small coupling constant is referred to as superweak. Attempts to observe the superweak interaction in decays with $|\Delta S| = 2$, for instance, in the decay $\Xi^- \to n\pi^-$, are futile because the expected relative width is of the order of 10^{-18}. Despite its superweakness, this interaction gives rise, nevertheless, to effects of the order of 10^{-3} in decays of the K_L^0 meson. This is caused by the resonant enhancement, due to the closeness in masses of the K_L^0 and K_S^0 mesons (see fig. 12.1 and the expression for $\boldsymbol{\eta}_{+-}$).

Possible manifestations of the milliweak C-even but P - and CP-odd interaction with $|\Delta S| = 1$ must be searched for, first of all, by experimentally cheeking the equality $\eta_{+-} = \eta_{00}$ (see Chapter 15 , sect. 4).

5.12.4 12.4. On decays of the K_S^0 meson

As a result of the $K_2 \leftrightarrow K_1$ mixing, the wave function of the short-lived kaon becomes

$$K_S^0 = \frac{1}{\sqrt{1+|\varepsilon|^2}}\left(K_1^0 + \varepsilon K_2^0\right) \simeq K_1^0 + \varepsilon K_2^0.$$

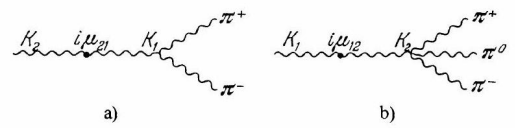


Fig. 12.4.

Note that the sign and the magnitude of ε is the same here as in the case of the K_L^0 meson ($K_L^0 = K_2^0 + \varepsilon K_1^0$). The states K_L^0 and K_S^0 are, therefore, not orthogonal. In order to ascertain that ε is the same in K_L^0 and K_S^0, consider the decays $K_S^0 \to \pi^0\pi^0\pi^0$ and $K_S^0 \to \pi^+\pi^-\pi^0$ (in

the second case we mean a decay into a CP-odd state $\pi^+\pi^-\pi^0$ with zero orbital momenta ($l = L = 0$, see chapter 10)). A comparison of figs. 12.4a and byields

$$\eta_{+-} = \frac{\langle \pi^+\pi^- \mid K_{\rm L}\rangle}{\langle \pi^+\pi^- \mid K_{\rm S}\rangle} = \frac{i\mu_{21}}{m_2 - m_1 - \frac{1}{2}i\,(\Gamma_2 - \Gamma_1)} = \varepsilon$$
$$\eta_{+-0} = \frac{\langle \pi^+\pi^-\pi^0 \mid K_{\rm S}\rangle}{\langle \pi^+\pi^-\pi^0 \mid K_{\rm L}\rangle} = \frac{i\mu_{12}}{m_1 - m_2 - \frac{1}{2}i\,(\Gamma_1 - \Gamma_2)}$$

Taking into account that $i\mu_{21} = -i\mu_{12}$, we obtain $\eta_{+-0} = \varepsilon$. Likewise,

$$\eta_{000} \equiv \frac{\langle \pi^0\pi^0\pi^0 \mid K_{\rm S}\rangle}{\langle \pi^0\pi^0\pi^0 \mid K_{\rm L}\rangle} = \varepsilon.$$

Unfortunately, the expected values are far beyond the capabilities of experiment. The experimental upper bounds are very high, $|\eta_{+-0}|^2 < 0.12$, $|\eta_{000}|^2 < 0.28$, for the following reason. The $\mathrm{K}^0_{\rm L} \to 2\pi$ decay forbidden by CP invariance competes more or less successfully with the decay $\mathrm{K_L} \to 3\pi$ suppressed by the phase-space volume. On the other hand, the decay $\mathrm{K_S} \to 3\pi$, forbidden by CP and suppressed by the phase-space volume, cannot compete with the intensive decay $\mathrm{K_S} \to 2\pi$, so that very high statistics is necessary to find this decay.

A search for $\mathrm{K_S} \to 3\pi$ decays is of interest for finding out whether a P-even but C - and CP-odd interaction with $|\Delta S| = 1$ can exist. This interaction could give rise to direct decays $\mathrm{K_1} \to 3\pi$.

5.12.5 12.5. Violation of time-reversal invariance and the neutron dipole moment

Any reasonable physical theory must be CPT invariant. This means that decays of the $\mathrm{K}^0_{\rm L}$ meson violate not only CP invariance but time-reversal
invariance, T, as well. Indeed, an analysis of the CP-odd decays of $\mathrm{K}^0_{\rm L}$ mesons indicates that the time reversibility in them is violated (violation of CPT and conservation of T would mean a pure imaginary transition parameter μ_{21} and would shift the phase of ε by 90°).

A search for time irreversibility was conducted, in addition to $\mathrm{K}^0_{\rm L}$ decays, in many other processes. The maximum experimental progress was achieved in a search for the electric dipole moment of the neutron, $d_{\rm n}$: since 1964, when the $\mathrm{K}^0_{\rm L} \to \pi^+\pi^-$decay was discovered, the upper bound on $d_{\rm n}$ was lowered by more than four orders of magnitude. It is customary to write $d_{\rm n}$ as a product of the elementary electric charge e by a distance l :

$$d_{\rm n} = el.$$

At the present moment, we know that $l \lesssim 10^{-24}$ cm. This is smaller by approximately ten orders of magnitude than the corresponding length in the neutron magnetic moment.

Why should $d_{\rm n} \neq 0$ signify that not only P - but T-invariance as well are violated? In order to answer that, let us recall the behavior of a number of physical quantities under space inversion P and time reversal T :

	$\boldsymbol{P}$	$\boldsymbol{T}$
coordinates	$\boldsymbol{r} \to -\boldsymbol{r}$	$\boldsymbol{r} \to \boldsymbol{r}$
time	$t \to t$	$t \to -t$
momentum	$\boldsymbol{p} \to -\boldsymbol{p}$	$\boldsymbol{p} \to -\boldsymbol{p}$
energy	E $\to$ E	E $\to$ E
angular momentum	$\boldsymbol{J} \to \boldsymbol{J}$	$\boldsymbol{J} \to -\boldsymbol{J}$
vector potential	$\boldsymbol{A} \to -\boldsymbol{A}$	$\boldsymbol{A} \to -\boldsymbol{A}$
scalar potential	$\varphi \to \varphi$	$\varphi \to \varphi$
electric field	$\boldsymbol{E} \to -\boldsymbol{E}$	$\boldsymbol{E} \to \boldsymbol{E}$
magnetic field	$\boldsymbol{H} \to \boldsymbol{H}$	$\boldsymbol{H} \to -\boldsymbol{H}$

(The signs are conveniently found by means of the relations $\boldsymbol{p} = m\ \mathrm{d}\boldsymbol{r}/\mathrm{d}t$, $\boldsymbol{J} = \boldsymbol{r} \times \boldsymbol{p}, \boldsymbol{E} = \nabla\varphi, \boldsymbol{H} = \nabla \times \boldsymbol{A}$). Both the magnetic $\boldsymbol{\mu}$ and electric $\boldsymbol{d}$ dipole moments of a particle must be directed along the particle spin, because the spin is the only vector quantity characterizing the particle. Hence, $\boldsymbol{\mu} \sim \boldsymbol{J}$ and $\boldsymbol{d} \sim \boldsymbol{J}$. We find therefore that the magnetic dipolemagnetic field interaction, $\boldsymbol{J} \cdot \boldsymbol{H}$, is P - and T-invariant, while the electric dipole-electric field interaction, $\boldsymbol{J} \cdot \boldsymbol{E}$, is P - and T-non-invariant.

What is the expected value of d_n ? If the superweak interaction $i \operatorname{Im} G_2(\bar{s}d)(\bar{s}d)$, where $\operatorname{Im} G_2 \sim 10^{-9}$G, is the only source of CP violation, then d_n is immeasurably small, namely $l < 10^{-38}$ cm. This estimate is based on the argument that in addition to the superweak interaction, the second order of the weak interaction must also contribute to d_n in order to ensure
$\Delta S = 0$ (and non-conservation of P-parity). Consequently, $l \sim G^2 m^5 \operatorname{Im} G_2$ where m is a mass of the order of one GeV .

However, it seems highly improbable for the superweak interaction (provided it exists) to have only one component, that with $|\Delta S| = 2$. The regularity observed so far is: the weaker the interaction is, the higher the number of conservation laws it breaks. It is therefore logical to expect the superweak interaction to comprise, along with a component with $|\Delta S| = 2$, a P-odd and CP-odd component with $\Delta S = 0$. In this case $l \sim m \operatorname{Im} G_2 \sim 10^{-28}$ cm. If CP invariance is violated because of the phase δ in the matrix of nine charged currents (see Chapter 15), then $l \ll 10^{-33}$ cm. Models in which CP invariance breakdown occurs in the interaction of several Higgs bosons give a value of d_n close to the current experimental limit.

5.12.6 12.6. Gedanken experiments

Physicists were inclined to believe in the absolute character of CP invariance until the $\mathrm{K}_\mathrm{L}^0 \to \pi^+\pi^-$decay was discovered, and at first many were surprised by the CP breakdown. But nowadays people are surprised why the violation of CP is so weak. The principal significance of the discovery of CP non-invariance should nevertheless not be underestimated: we have found out that there are absolute differences between particles and antiparticles, between left and right, and that the microscopic world has its own arrow of time.

Even before CP non-invariance was discovered, a story popular in science fiction books pictured a spaceship of aliens communicating with the Earth and moving towards it. The terrestrials try to determine whether the aliens are built of matter or antimatter. They find that this cannot be done in a CP-invariant world. One cannot distinguish between an electron and a positron, or the left-handed and the right-handed if only information and not material samples are exchanged. This gedanken ship analogy is not a modern invention. Indeed, Galileo illustrated his relativity principle by means of a ship sailing smoothly along the coast. No mechanical experiments aboard the ship can establish whether the ship is at rest or in motion. A 17th century ship demonstrated the invariance of nature's laws with respect to galilean transformations, while the 20th century spaceship demonstrates this with respect to

CP transformations. It is of course sufficient to throw a glance at the shore to determine that the ship is moving; and it is sufficient to send a beam of light with left-handed polarization to the spaceship to reach an agreement about what is matter and what is antimatter. Indeed, one can then make use of the left-handed polarization of
electrons and right-handed polarization of positrons in β-decay in order to solve the matter-antimatter alternative. However, the light with left-handed polarization is precisely a terrestrial sample mentioned above. The rules of the game forbid looking at the shoreline or sending a sample.

In reality, nature is CP non-invariant so that no sample exchange is necessary. For instance, one could use the fact that $\mathrm{K}_{\mathrm{L}}^{0}$ mesons are the same whether obtained in a laboratory accelerator or in an "anti-laboratory anti-accelerator". The $\mathrm{K}_{\mathrm{L}}^{0}$ mesons decay more often into positrons than into electrons. This is an absolute difference between particles and antiparticles. Now it becomes elementary to make use of the longitudinal polarization and give an absolute definition of left and right.

The Σ^{+}hyperon and its antiparticle, $\bar{\Sigma}^{-}$, give another interesting example of the absolute difference between a particle and its antiparticle. The total widths are identical by virtue of CPT invariance:

$$\Gamma\left(\Sigma^{+}\right)=\Gamma\left(\bar{\Sigma}^{-}\right).$$

It follows from the CP non-invariance, however, that

$$\Gamma\left(\Sigma^{+}\rightarrow \mathrm{p}\pi^{0}\right)\neq\Gamma\left(\bar{\Sigma}^{-}\rightarrow \overline{\mathrm{p}}\pi^{0}\right),$$
$$\Gamma\left(\Sigma^{+}\rightarrow \mathrm{n}\pi^{+}\right)\neq\Gamma\left(\bar{\Sigma}^{-}\rightarrow \overline{\mathrm{n}}\pi^{-}\right).$$

We leave the proof to the reader as an exercise. We only hint that redistribution among channels is caused by interference of phases due to CP non-invariance, and phases due to scattering of decay products on one another (see Chapter 8). The former change sign, and the latter do not under particle-antiparticle conjugation.

5.13 13 Decays of the τ-lepton

The third charged lepton (after e and μ) called triton or τ-lepton (triton means third in Greek) was discovered in colliding $\mathrm{e}^{+}\mathrm{e}^{-}$beams at Stanford, in 1975. We know now that the τ mass is approximately 1780 MeV , its spin is $\frac{1}{2}$, and that its decays, as those of the muon, are mediated by the $V-A$ interaction.

5.13.1 13.1. ν_{τ} neutrino

All known decays of the τ-lepton are accompanied by neutrino emission. According to the theory outlined in the present book, this neutrino is different from ν_{e} and ν_{μ}, being a specific ν_{τ} neutrino. Experiments show that $\nu_{\tau}\neq\nu_{\mu}$ (otherwise τ-leptons would be produced copiously by muon neutrino beams). So far the possibility of $\nu_{\tau}=\nu_{\mathrm{e}}$ is not ruled out experimentally (because ν_{e} beams are much less intense than beams of ν_{μ}) but seems very unlikely. The experimental upper bound on the ν_{τ} mass is: $m_{\nu_{\tau}}<250\mathrm{MeV}$. As follows from the theory of the hot universe, $m_{\nu_{\tau}}<10-30\mathrm{eV}$ (see Chapter 27).

So far τ-leptons were produced only in colliding $\mathrm{e}^{+}\mathrm{e}^{-}$beams in the reaction

$$\mathrm{e}^{+}\mathrm{e}^{-}\rightarrow\gamma\rightarrow\tau^{+}\tau^{-}.$$

It has been found, for instance, that τ-leptons are the products of ψ' meson decay:

$$\mathrm{e}^+\mathrm{e}^- \to \gamma \to \psi' \to \tau^+\tau^-.$$

We shall consider now the main decays of the $\tau^\pm$leptons (only τ^-will be discussed for the sake of brevity).

5.13.2 13.2. Decays $\tau^- \to \mu^- \bar{\nu}_\mu \nu_\tau$ and $\tau^- \to \mathrm{e}^- \bar{\nu}_\mathrm{e} \nu_\tau$

These decays are absolutely similar to the $\mu^- \to \mathrm{e}^- \nu_\mathrm{e} \nu_\mu$ decay. The respective decay rates are obtained from the muon decay rate (see chapter 3) by $m_\mu \to m_\tau$ substitution:

$$\Gamma(\tau \to \mathrm{e}\bar{\nu}\nu) = \Gamma(\tau \to \mu\bar{\nu}\nu) = \frac{G^2 m_\tau^5}{192\pi^3} = \left(\frac{m_\tau}{m_\mu}\right)^5 \Gamma(\mu \to \mathrm{e}\bar{\nu}\nu)$$
$$\simeq 6.2 \cdot 10^{11}\ \mathrm{s}^{-1}.$$

Experimentally, the Michel parameter for these decays is $\rho = 0.73 \pm 0.15$, in good agreement with the $V - A$ interaction.

5.13.3 13.3. Semi-hadronic decays. General remarks

As is well known, the asymptotic freedom of QCD (quantum chromodynamics) enables calculation of the cross section for the process $\mathrm{e}^+\mathrm{e}^- \to \gamma \to$ hadrons at $s \to \infty$

$$R = \frac{\sigma\left(\mathrm{e}^+\mathrm{e}^- \to \gamma \to \text{ hadrons }\right)}{\sigma\left(\mathrm{e}^+\mathrm{e}^- \to \gamma \to \mu^+\mu^-\right)} = 3\sum_f Q_f^2 \left(1 + \frac{\alpha_\mathrm{s}}{\pi} + \cdots\right),$$

where the factor 3 is the number of colors, Q_f is the charge of the f th quark, and the summation covers all flavors that can be produced at a given energy, and α_s is the QCD running coupling constant. Below the charm production threshold, $R \simeq 3\left(Q_\mathrm{u}^2 + Q_\mathrm{d}^2 + Q_\mathrm{s}^2\right) \simeq 2$.

We will estimate the total width of the decays of the type $\tau \to \nu_\tau +$ hadrons relying on the analogy with the annihilation $\mathrm{e}^+\mathrm{e}^- \to$ hadrons. In the case of τ-lepton decay, we have to take into account the interactions $\left(\bar{\nu}_\tau \tau\right)\left(\bar{d}u\right)\cos\theta$ and $\left(\bar{\nu}_\tau \tau\right)\left(\bar{s}u\right)\sin\theta$. A quark estimate is obtained by neglecting all quark masses:

$$\frac{\Gamma\left(\tau \to \nu_\tau + \text{ hadrons }\right)}{\Gamma\left(\tau \to \nu_\tau \mu \bar{\nu}_\mu\right)} \simeq \frac{\Gamma\left(\tau \to \nu_\tau \mathrm{d}\bar{\mathrm{u}}\right) + \Gamma\left(\tau \to \nu_\tau \mathrm{s}\bar{\mathrm{u}}\right)}{\Gamma\left(\tau \to \nu_\tau \mu \bar{\nu}_\mu\right)} \simeq 3.$$

If the deviation from the asymptotic freedom value is taken into account, this ratio changes to nearly 4 . The expected lifetime of the τ-lepton is then

$$\tau_\tau \simeq \frac{1}{6\Gamma\left(\tau \to \nu_\tau \mu \bar{\nu}_\mu\right)} \simeq \frac{1}{3.1 \cdot 10^{12}\ \mathrm{s}^{-1}} \simeq 2.6 \cdot 10^{-13}\ \mathrm{s}.$$

So far, only the upper bound was found experimentally:

$$\tau_\tau \lesssim 10^{-12}\ \mathrm{s}.$$

Consider now individual channels of the semi-hadronic decays. It seems natural to list them in the order of accuracy with which the corresponding decay rates can be calculated at the present time.

The amplitude of the $\tau \to \pi\nu_\tau$ decay is related directly to that of the $\pi \to \mu\nu$ decay provided the weak interaction lagrangian includes the universal charged current. The amplitude of the $\tau \to \rho\nu$ decay is related directly to that of the $\rho \to \mathrm{e}^+\mathrm{e}^-$decay, owing to the isotopic properties of the ud current. For the same reason, the amplitudes of the $\tau \to \nu + 2n\pi$ decays and

the electromagnetic annihilation $e^+e^- \to 2n\pi$ are related for a given invariant mass of the $2n\pi$ system. As for the τ-lepton decays with emission of an odd number of pions, $\tau \to \nu + (2n+1)\pi$, they are coupled to the axial ud current and so represent a unique source of pseudoscalar and axial-vector meson states.

5.13.4 13.4. Decay $\tau \to \pi\nu_\tau$

Compare $\pi \to \mu\nu$ and $\tau \to \pi\nu$ decay graphs (see figs. 13.1 and 13.2).
Both decays are due to the same $W\pi^-$interaction which, in quark terms, reduces to the W-boson coupling to the axial ud current (fig. 13.3). The $\tau \to \pi\nu_\tau$ decay amplitude is given by

$$M = \sqrt{\frac{1}{2}} G f_\pi k^\alpha \varphi_\pi \bar{u}_{\nu_\tau} \gamma_\alpha (1+\gamma_5) u_\tau \cos\theta,$$

where k is the π-meson 4 -momentum. It is important to note that both here and in the $\pi \to \mu\nu$ decay amplitude, the factor f_π is the same, that is independent of the type of leptons involved in the decay. This is emphasized in figs. 13.1-13.3 by the presence of intermediate W-bosons. The universal-

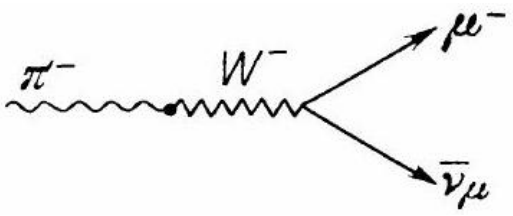


Fig. 13.1.

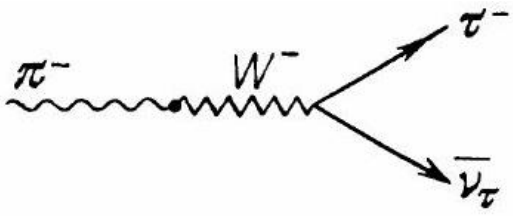


Fig. 13.2.

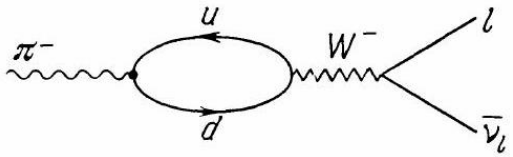


Fig. 13.3.

ity is broken by corrections of the order of α, if virtual photons are taken into account (fig. 13.4), because the τ and μ masses are different. If these corrections are neglected, f_π is a function of k^2 only, with $k^2 = m_\pi^2$ for both decays, since in both cases the π-meson is on the mass shell.

The decay width is

$$\Gamma\left(\tau \to \pi\nu_\tau\right) \frac{\overline{|M|^2}}{2 \cdot 2m_\tau}\Phi,$$

where Φ is the phase-space volume:

$$\Phi = \int \frac{\mathrm{d}\boldsymbol{k}_\nu}{2E_\nu(2\pi)^3}\frac{\mathrm{d}\boldsymbol{k}_\pi}{2E_\pi(2\pi)^3}(2\pi)^4\delta^4\left(k_\nu + k_\pi - k_\tau\right) = \frac{E_\nu}{4\pi m_\tau}.$$

The squared modulus of the matrix element averaged over the τ-lepton polarizations is

$$\begin{aligned}\frac{1}{2}\overline{|M|^2} &= \frac{1}{2}\cdot\frac{1}{2}G^2 f_\pi^2 m_\tau^2 \operatorname{Tr}\left(\hat{k} + m_\tau\right)\left(1 - \gamma_5\right)\hat{k}_\nu\left(1 + \gamma_5\right)\cos^2\theta \\ &= 2G^2 f_\pi^2 m_\tau^2\left(k_\tau k_\nu\right)\cos^2\theta = 2G^2 f_\pi^2 m_\tau^3 E_\nu \cos^2\theta.\end{aligned}$$

Finally, we obtain

$$\begin{aligned}\Gamma\left(\tau \to \pi\nu_\tau\right) &= \frac{G^2 f_\pi^2 m_\tau E_\nu^2 \cos^2\theta}{4\pi} = \frac{G^2 f_\pi^2 m_\tau^3 \cos^2\theta}{16\pi}\left(1 - \frac{m_\pi^2}{m_\tau^2}\right)^2 \\ &\simeq \frac{12\pi^2 f_\pi^2 \cos^2\theta}{m_\tau^2}\Gamma(\tau \to \mu\bar{\nu}\nu) \simeq 0.6\Gamma(\tau \to \mu\bar{\nu}\nu)\end{aligned}$$

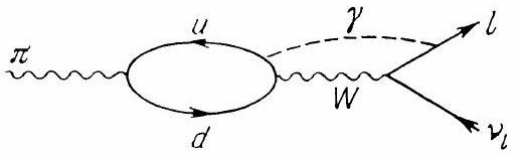


Fig. 13.4.

The $\tau \to \nu_\tau \mathrm{K}$ decay rate is obtained from the above expression by substituting $f_\pi \to f_\mathrm{K}, m_\pi \to m_\mathrm{K}, \cos\theta \to \sin\theta$.

5.13.5 13.5. Decay $\tau \to \rho\nu_\tau$

The $\tau \to \rho\nu_\tau$ decay amplitude can be written as

$$M = \sqrt{\frac{1}{2}}Gg_\rho\varphi_\alpha\bar{u}_{\nu_\tau}\gamma^\alpha\left(1 + \gamma_5\right)u_\tau\cos\theta.$$

Here g_ρ is a scalar parameter of the dimension of m^2 (its magnitude will be discussed later), and φ_α is the ρ-meson wave function; φ_α is a four-vector satisfying the transversality condition: $p^\alpha\varphi_\alpha = 0$ where p is the ρ-meson 4-momentum. This condition indicates that the time component of φ_α in the ρ-meson rest frame is zero. Hence, the ρ-meson density matrix is also transverse on the mass shell (see appendix, Chapter 29, sect. 4.3):

$$\varphi_\alpha\varphi_\beta^* = -g_{\alpha\beta} + \frac{p_\alpha p_\beta}{m_\rho^2}.$$

We now find $\overline{|M|^2}$:

$$\begin{aligned}
\overline{|M|^2} =& \frac{1}{2}G^2 g_\rho^2 \cos^2\theta \left(\frac{p_\alpha p_\beta}{m_\rho^2} - g_{\alpha\beta}\right) \\
& \times \operatorname{Tr} \hat{p}_\nu \gamma^\alpha (1+\gamma_5)(\hat{p}_\tau + m_\tau)\gamma^\beta (1+\gamma_5) \\
=& G^2 g_\rho^2 \cos^2\theta \left[\frac{1}{m_\rho^2}\operatorname{Tr}\hat{p}_\nu\hat{p}\hat{p}_\tau\hat{p} + 2\operatorname{Tr}\hat{p}_\nu\hat{p}_\tau\right] \\
=& \frac{4G^2 g_\rho^2 \cos^2\theta}{m_\rho^2}\left[2(p_\nu p)(p_\tau p) + m_\rho^2 (p_\nu p_\tau)\right] \\
=& \frac{4G^2 g_\rho^2 \cos^2\theta}{m_\rho^2}(p_\nu p_\tau)\left[2p_\tau p + m_\rho^2\right] \\
=& \frac{4G^2 g_\rho^2 \cos^2\theta}{m_\rho^2}(p_\nu p_\tau) m_\tau^2 \left(1 + 2\frac{m_\rho^2}{m_\tau^2}\right).
\end{aligned}$$

(We have used the equality $p_\nu^2 = (p_\tau - p)^2 = -2p_\tau p + m_\tau^2 + m_\rho^2 = 0$). Taking into account that the phase-space volume is

$$\Phi = \frac{p_\nu p_\tau}{4\pi m_\tau^2} = \frac{1}{8\pi}\left(1 - \frac{m_\rho^2}{m_\tau^2}\right),$$

we obtain

$$\begin{aligned}
\Gamma(\tau \to \rho\nu_\tau) &= \frac{1}{2}\overline{|M|^2}\frac{\Phi}{2m_\tau} = \frac{G^2 g_\rho^2 \cos^2\theta}{4\pi m_\rho^2 m_\tau}(p_\nu p_\tau)^2\left(1 + 2\frac{m_\rho^2}{m_\tau^2}\right) \\
&= \frac{1}{16\pi}G^2\left(\frac{g_\rho}{m_\rho}\right)^2 m_\tau^3 \cos^2\theta \left(1 - \frac{m_\rho^2}{m_\tau^2}\right)^2\left(1 + 2\frac{m_\rho^2}{m_\tau^2}\right) \\
&\simeq \frac{1}{16}G^2\left(\frac{g_\rho}{m_\rho}\right)^2 m_\tau^3 \cos^2\theta
\end{aligned}$$

We turn now to the parameter g_ρ. In order to find it, compare the quark graphs of a weak decay $\tau \to \rho\nu$ and an electromagnetic decay $\rho \to \mathrm{e}^+\mathrm{e}^-$ (fig. 13.5). The sum of graphs (b) and (c) gives the amplitude for $\rho^0 \to \mathrm{e}^+\mathrm{e}^-$ decay, normally written in the form

$$M = \frac{m_\rho^2}{\gamma}\varphi_\alpha \frac{4\pi\alpha}{q^2}\bar{u}_\mathrm{e}\gamma^\alpha u_\mathrm{e} = \frac{4\pi\alpha}{\gamma}\varphi_\alpha \bar{u}_\mathrm{e}\gamma^\alpha u_\mathrm{e}.$$

Here γ is a dimensionless constant, q is the 4-momentum of a virtual photon, $q^2 = m_\rho^2$. It is now easy to obtain

$$\begin{aligned}
\frac{1}{3}\overline{|M|^2} &= \left(\frac{4\pi\alpha}{\gamma}\right)^2 \frac{1}{3}\left(-\delta_{\alpha\beta} + \frac{p_\alpha p_\beta}{m_\rho^2}\right)\operatorname{Tr}\hat{p}_1\gamma^\alpha\hat{p}_2\gamma^\beta \\
&= \left(\frac{4\pi\alpha}{\gamma}\right)^2 \frac{8}{3}p_1 p_2 = \frac{4}{3}\left(\frac{4\pi\alpha}{\gamma}\right)^2 m_\rho^2
\end{aligned}$$

(the factor $\frac{1}{3}$ corresponds to averaging over the ρ-meson polarizations). The expression for the width is

$$\Gamma\left(\rho^0 \to \mathrm{e}^+\mathrm{e}^-\right) = \frac{1}{2m_\rho}\left(\frac{4\pi\alpha}{\gamma}\right)^2 \frac{4}{3}m_\rho^2 \frac{1}{8\pi} = \frac{4}{3}\pi\alpha^2\frac{m_\rho}{\gamma^2}.$$

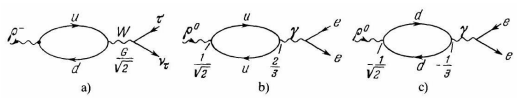


Fig. 13.5.

With standard values of $\Gamma(\rho^0 \to e^+e^-) \simeq 6.5\text{keV}$ and $m_\rho \simeq 770\text{MeV}$, we obtain

$$\frac{\gamma^2}{4\pi} = \frac{\alpha^2}{3}\frac{m_\rho}{\Gamma(\rho \to e^+e^-)} \simeq 2.1.$$

A detailed theoretical fit of the cross-section data for the e^+e^-annihilation yields a somewhat larger value:

$$\frac{\gamma^2}{4\pi} = 2.36 \pm 0.18$$

In order to express g_ρ in terms of γ, let us return again to the graphs of fig. 13.5 and recall that

$$\rho^0 = \sqrt{\frac{1}{2}}(u\bar{u} - d\bar{d}), \quad \rho^+ = u\bar{d}$$

Taking into account that the charges of the u - and d-quark are $\frac{2}{3}$ and $-\frac{1}{3}$, respectively, we obtain

$$\frac{m_\rho^2}{\gamma} = \sqrt{\frac{1}{2}}\left[\frac{2}{3} - \left(-\frac{1}{3}\right)\right] I = \sqrt{\frac{1}{2}} I$$

for the net contribution of graphs 13.5 b and c , and

$$g_\rho = I$$

for that of graph 13.5a, where I is the result of integration over the loop. Hence, $g_\rho/m_\rho = \sqrt{2}m_\rho/\gamma$.

Substitution of the expression derived above into that for $\Gamma(\tau \to \rho\nu)$ yields

$$\begin{aligned}
\Gamma(\tau \to \rho\nu) &= \frac{G^2\cos^2\theta}{8\pi\gamma^2} m_\tau^3 m_\rho^2 \left(1 - \frac{m_\rho}{m_\tau^2}\right)^2 \left(1 + \frac{2m_\rho^2}{m_\tau^2}\right) \\
&= 6\pi\frac{4\pi}{\gamma^2}\cos^2\theta \left(\frac{m_\rho}{m_\tau}\right)^2 0.91\Gamma(\tau \to e\bar{\nu}_e\nu_\tau) \\
&= 1.46\Gamma(\tau \to e\tilde{\nu}\nu) \quad \text{for } \gamma^2/4\pi = 2.1 \\
&= 1.30\Gamma(\tau \to e\tilde{\nu}\nu) \quad \text{for } \gamma^2/4\pi = 2.36 \\
&= 1.18\Gamma(\tau \to e\tilde{\nu}\nu) \quad \text{for } \gamma^2/4\pi = 2.60
\end{aligned}$$

5.13.6 13.6. Decays $\tau \to \nu_\tau + 2n\pi$

The relation between the decays $\tau \to \rho\nu_\tau$ and $\rho \to e^+e^-$derived above is a particular case of a more general relationship between the $\tau^- \to \nu_\tau(2n\pi)^-$ decays and the electromagnetic annihilation $e^+e^- \to (2n\pi)^0$. This relationship appears because the components of the same vector-isovector current are operative in both cases: $\bar{d}\gamma_\alpha u$ in the τ-decay, and $\sqrt{\frac{1}{2}}\left(\bar{u}\gamma_\alpha u - \bar{d}\gamma_\alpha d\right)$ in the case of e^+e^-annihilation. No other currents contribute to it. This is easily demonstrated

if we take into account that the $2n\pi$ system is G-even while the isoscalar electromagnetic current $\sqrt{\frac{1}{2}}\left(\bar{u}\gamma_\alpha u + \bar{d}\gamma_\alpha d\right)$ and the weak axial current $\bar{d}\gamma_\alpha\gamma_5 u$ are G-odd.

Introduce the notation:

$$v_\alpha = \left\langle (2n\pi)^0 \right| \frac{2}{3}\bar{u}\gamma_\alpha u - \frac{1}{3}\bar{d}\gamma_\alpha d|0\rangle,$$
$$v_\alpha^+ = \left\langle (2n\pi)^+ \right| \bar{u}\gamma_\alpha d|0\rangle.$$

Arguments similar to those which served to show above that $g_\rho = \sqrt{2}m_\rho^2/\gamma$, yield that $|v_\alpha^+| = \left|\sqrt{2}v_\alpha\right|$. The 4 -vector v_α is a function of the invariant mass of the $2n\pi$ system, which we denote by $\sqrt{s}$, and (if $n > 1$) of other kinematic variables characterizing this system. The annihilation amplitude is

$$M\left(\mathrm{e}^+\mathrm{e}^- \to 2n\pi\right) = \frac{4\pi\alpha}{q^2}\bar{u}_\mathrm{e}\gamma^\alpha u_\mathrm{e} \cdot v_\alpha.$$

The standard formula for the cross section yields

$$\sigma\left(\mathrm{e}^+\mathrm{e}^- \to 2n\pi\right) = \int \left(\frac{4\pi\alpha}{q^2}\right)^2 \frac{1}{4\cdot 2s}\,\mathrm{Tr}\,\hat{p}_1\gamma^\alpha\hat{p}_2\gamma^\beta v_\alpha v_\beta^*\,\mathrm{d}\Phi,$$

where p_1 and p_2 are 4 -momenta of the electron and positron, $\mathrm{d}\Phi$ is the phase-space volume, $q = p_1 + p_2$, and $q^2 = s$. Because of the transversality of the current ($q^\alpha v_\alpha = 0$), we have

$$\int v_\alpha v_\beta^*\,\mathrm{d}\Phi = \pi\left(q_\alpha q_\beta - g_{\alpha\beta}q^2\right)\rho\left(q^2\right)$$

This expression is a definition of the dimensionless spectral density $\rho\left(q^2\right)$.

Calculation of the trace gives

$$\begin{aligned}\sigma\left(\mathrm{e}^+\mathrm{e}^- \to 2n\pi\right) =& \frac{(4\pi\alpha)^2}{8s^3}4\pi\left[2p_1^\alpha p_2^\beta - g^{\alpha\beta}\left(p_1p_2\right)\right] \\ &\times\left(q_\alpha q_\beta - q^2 g_{\alpha\beta}\right)\rho(s) \\ =& \frac{(4\pi\alpha)^2}{2s^3}\left[2\left(p_1q\right)\left(p_2q\right) + \left(p_1p_2\right)q^2\right]\pi\rho(s) \\ =& \frac{(4\pi\alpha)^2}{2s}\pi\rho(s)\end{aligned}$$

(Here we use the equality $p_1 + p_2 = q$ whence $p_1p_2 = p_1q = p_2q = \frac{1}{2}q^2$.)
If we define the quantity $R(s)$ in a standard manner,

$$\sigma(s) = \frac{4\pi\alpha^2}{3s}R(s),$$

then ρ can be expressed via R :

$$\rho(s) = \frac{R(s)}{6\pi^2}.$$

In the case of a one-particle state (such as the ρ-meson, provided we neglect its width) we have

$$\mathrm{d}\Phi = \frac{(2\pi)^4}{(2\pi)^3}\delta^4\left(q - p_1 - p_2\right)\delta\left(q^2 - m_\rho^2\right)\mathrm{d}^4q$$

and

$$\pi\rho(s) = 2\pi\delta\left(q^2 - m_\rho^2\right)\frac{m_\rho^2}{\gamma^2}$$

so that

$$\sigma\left(\mathrm{e}^+\mathrm{e}^- \to \rho\right) = 16\pi^3\frac{\alpha^2}{\gamma^2}\delta\left(s - m_\rho^2\right) = 12\pi^2\frac{\Gamma\left(\rho \to \mathrm{e}^+\mathrm{e}^-\right)}{m_\rho}\delta\left(s - m^2\rho\right).$$

This last equality is based on the expression derived earlier:

$$\Gamma\left(\rho \to \mathrm{e}^+\mathrm{e}^-\right) = \frac{4\pi\alpha^2}{3\gamma^2}m_\rho$$

(Recall that the Breit-Wigner formula for the $\mathrm{e}^+\mathrm{e}^- \to \rho \to 2\pi$ annihilation is

$$\sigma\left(\mathrm{e}^+\mathrm{e}^- \to \rho \to 2\pi\right) = \frac{3\pi}{m_\rho^2}\frac{\Gamma(\rho \to \mathrm{ee})\Gamma}{\left(E - m_\rho\right)^2 + \frac{1}{4}\Gamma^2}.$$

If $\Gamma \to 0$,

$$\frac{\frac{1}{2}\Gamma}{\left(E - m_\rho\right)^2 + \frac{1}{4}\Gamma^2} \Rightarrow \pi\delta\left(E - m_\rho\right) = 2\pi m_\rho\delta\left(s - m_\rho^2\right)$$

We find therefore that the result obtained above is in agreement with the Breit-Wigner formula as well).

We turn now to τ-lepton decay:

$$M\left(\tau \to \nu_\tau + 2n\pi\right) = \sqrt{\frac{1}{2}}G\cos\theta\bar{u}_{\nu_\tau}\gamma^\alpha\left(1 + \gamma_5\right)u_\tau \cdot v_\alpha^+.$$

The rate of decay into the $2n\pi$ system with mass $\sqrt{s}$ is

$$\begin{aligned}\mathrm{d}^3\Gamma =& \frac{G^2\cos^2\theta}{2 \cdot 2m_\tau}\operatorname{Tr}\hat{p}_\nu\gamma^\alpha\left(1 + \gamma_5\right)\left(\hat{p}_\tau + m_\tau\right)\gamma^\beta\left(1 + \gamma_5\right)\pi\left(q_\alpha q_\beta - g_{\alpha\beta}q^2\right)\\ &\times\rho(s)\frac{\mathrm{d}\boldsymbol{p}_\nu}{2E_\nu(2\pi)^3}\end{aligned}$$

where $q = p_\tau - p_\nu$, averaging was carried out over polarizations of the τ-lepton, and $\rho(s)$ is the same as in $\mathrm{e}^+\mathrm{e}^- \to 2n\pi$ annihilation. After calculation of the trace and integration over the neutrino angle we obtain

$$\begin{aligned}\mathrm{d}\Gamma &= \frac{G^2\cos^2\theta}{2\pi m_\tau}\left[2p_\nu^\alpha p_\tau^\beta - g^{\alpha\beta}\left(p_\nu p_\tau\right)\right]\left(\dot{q}_\alpha q_\beta - g_{\alpha\beta}q^2\right)\rho(s)E_\nu\mathrm{d}E_\nu\\ &= \frac{G^2\cos^2\theta}{2\pi m_\tau}\left[2\left(p_\nu q\right)\left(p_\tau q\right) + \left(p_\nu p_\tau\right)q^2\right]\rho(s)E_\nu\mathrm{d}E_\nu\\ &= \frac{G^2\cos^2\theta}{2\pi m_\tau}\left(p_\nu p_\tau\right)\left(2p_\tau q + q^2\right)\rho(s)E_\nu\mathrm{d}E_\nu\\ &= \frac{G^2\cos^2\theta}{2\pi}\left(m_\tau^2 + 2s\right)\rho(s)E_\nu^2\ \mathrm{d}E_\nu\\ &= \frac{G^2\cos^2\theta}{2\pi}\left(3m_\tau - 4E_\nu\right)m_\tau\rho(s)E_\nu^2\ \mathrm{d}E_\nu\end{aligned}$$

(here we take into account that $p_\nu q = p_\nu p_\tau, 2p_\tau q = m_\tau^2 + q^2, s = m_\tau^2 - 2E_\nu m_\tau$). Going over to the variable s, we obtain

$$\mathrm{d}\Gamma(\tau \to \nu + 2n\pi) = \frac{G^2 \cos^2\theta}{2\pi} \frac{(m_\tau^2 + 2s)\,(m_\tau^2 - s)^2}{8m_\tau^3} \rho(s)\mathrm{d}s$$

The formula for $\mathrm{d}\Gamma(\tau \to \nu + 2n\pi)$ must be compared with that for $\sigma\,(\mathrm{e}^+\mathrm{e}^- \to 2n\pi)$. Both these quantities are expressed, for a given number of
pions and a given value of s, via the same $\rho(s)$. In order to find the total decay rate $\Gamma(\tau \to \nu + 2n\pi)$, we have to substitute $\rho(s)$ from $\sigma\,(\mathrm{e}^+\mathrm{e}^- \to 2n\pi\ )$ into $\mathrm{d}\Gamma$ and numerically integrate over $\mathrm{d}s$.

Let us check the formula for $\mathrm{d}\Gamma$ using the decay $\tau \to \rho\nu$ as an example, In the case of this decay, $\rho(s) = 2\delta\left(q^2 - m_\rho^2\right) m_\rho^2/\gamma^2$ and

$$\Gamma = \frac{G^2 \cos^2\theta}{8\pi\gamma^2} \frac{\left(m_\tau^2 + 2m_\rho^2\right)\left(m_\tau^2 - m_\rho^2\right)^2 m_\rho^2}{m_\tau^3},$$

which coincides with the result of the preceding section. Let us check our general formula for $\mathrm{d}\Gamma$ in the case of free quarks:

$$\begin{aligned}\int v_\alpha^+ v_\beta^{+*}\,\mathrm{d}\Phi \Rightarrow 3\int \mathrm{Tr}\,\hat{p}_2\gamma_\alpha\hat{p}_1\gamma_\beta \frac{\mathrm{d}\boldsymbol{p}_1}{2E_1}\frac{\mathrm{d}\boldsymbol{p}_2}{2E_2}\frac{\delta^4(p_1+p_2-q)}{(2\pi)^2}\\ = 3\cdot\frac{1}{6}\pi\left(q^2 g^{\mu\nu} + 2q^\mu q^\nu\right)\frac{1}{4\pi^2}\left(g_{\mu\alpha}g_{\nu\beta} + g_{\mu\beta}g_{\nu\alpha} - g_{\mu\nu}g_{\alpha\beta}\right)\\ = 3\frac{1}{6\pi}\left(q_\alpha q_\beta - q^2 g_{\alpha\beta}\right) = 2\pi\rho\left(q^2\right)\left(q_\alpha q_\beta - g_{\alpha\beta}q^2\right),\end{aligned}$$

whence $\rho = \frac{3}{2}\,(1/6\pi^2)$ (the factor 3 appears from summation over quark colors). The total decay rate for $\tau \to \nu + 2n\pi$ then becomes

$$\begin{aligned}\Gamma &\simeq \int_0^{m_\tau/2} 3\frac{G^2\cos^2\theta}{24\pi^3} m_\tau\,(3m_\tau - 4E_\nu)\,E_\nu^2\,\mathrm{d}E_\nu\\ &= \int_0^1 \frac{G^2 m^5\cos^2\theta}{192\pi^3} 3(3-2\varepsilon)\varepsilon^2\,\mathrm{d}\varepsilon = \frac{3}{2}\frac{G^2 m_\tau^5\cos^2\theta}{192\pi^3}.\end{aligned}$$

This result is in agreement with the quark estimate obtained at the beginning of this chapter. Indeed, when quark masses are neglected, the vector current supplies half of the hadronic width of the τ-lepton. Another half comes from the axial current. (These currents do not interfere in the expression for the decay rate since the vector current gives rise to an even number of pions while the axial current gives rise to an odd number.)

It is interesting to compare quark estimates for the $\tau \to \nu + 2n\pi$ decay and for the $\mathrm{e}^+\mathrm{e}^- \to 2n\pi$ reaction. In the latter case we must separate an isovector part R_1 out of the total

$$R = R_1 + R_0 = 3\left(Q_\mathrm{u}^2 + Q_\mathrm{d}^2\right) = \frac{5}{3},$$

that is to pass from non-interfering quark contributions to non-interfering isotopic ones. Taking into account quark charges, we find that the amplitudes of currents with $T = 1, (\bar{u}u - \bar{d}d)$, and of those with $T = 0, (\bar{u}u + \bar{d}d)$,
are in the proportion of $3:1$, and the corresponding probabilities $9:1$. Consequently,

$$R_1 = \frac{9}{10}R = \frac{3}{2}.$$

Recalling the relation $R = 6\pi^2\rho$ we find that our new estimate is the same as the earlier one.

5.13.7 13.7. Decays $\tau \to \nu_\tau + (2n+1)\pi$

As we have mentioned above, these decays are due to the axial current $\bar{d}\gamma_\alpha\gamma_5 u$. Consider the amplitude

$$a_\alpha = \langle (2n+1)\pi | \bar{d}\gamma_\alpha\gamma_5 u | 0 \rangle.$$

After calculations similar to those of the preceding section we arrive at

$$\begin{aligned}
&\mathrm{d}\Gamma(\tau \to \nu_\tau + (2n+1)\pi) \\
&\quad = \frac{G^2\cos^2\theta}{2\pi m_\tau}\left[2p_\nu^\alpha p_\tau^\beta - g^{\alpha\beta}(p_\nu p_\tau)\right] \\
&\quad \times \left[\left(q_{\alpha\beta} - g_{\alpha\beta}q^2\right)\rho_\mathrm{t}(s) + q_\alpha q_\beta \rho_\ell(s)\right] E_\nu \mathrm{d}E_\nu \\
&\quad = \frac{G^2\cos^2\theta}{2\pi}\left[\left(m_\tau^2 + 2s\right)\rho_\mathrm{t}(s) + m_\tau^2\rho_\ell(s)\right] E_\nu^2\,\mathrm{d}E_\nu \\
&\quad = \frac{G^2\cos^2\theta}{2\pi}\left[\left(m_\tau^2 + 2s\right)\rho_\mathrm{t}(s) + m_\tau^2\rho_\ell(s)\right] \frac{\left(m_\tau^2 - s\right)^2}{8m_\tau^3}\,\mathrm{d}s
\end{aligned}$$

The following notation is used above:

$$\int a_\alpha a_\beta^*\,\mathrm{d}\Phi = 2\pi\left[\left(q_\alpha q_\beta - g_{\alpha\beta}q^2\right)\rho_\mathrm{t}(s) + q_\alpha q_\beta\rho_\ell(s)\right]$$

(The coefficient 2 is introduced to make the normalization of the axial current spectral density identical to that of the vector current). In the approximation of the rigorously conserved axial current (i.e. $m_\mathrm{u} = m_\mathrm{d} = 0$), $m_\pi = 0, \rho_\ell = 0$. The conservation of the axial current being only partial, we have $\rho_\ell \neq 0$. In the case of $n = 0$ (the $\tau \to \pi + \nu$ decay)

$$\begin{aligned}
a_\alpha &= \langle \pi | \bar{d}\gamma_\alpha\gamma_5 u | 0 \rangle = f_\pi q_\alpha \\
\int a_\alpha a_\beta^*\,\mathrm{d}\Phi &= f_\pi^2 q_\alpha q_\beta 2\pi\delta\left(q^2 - m_\pi^2\right)
\end{aligned}$$

whence

$$\rho_\mathrm{t} = 0, \quad 2\rho_\ell = 2f_\pi^2\delta\left(s - m_\pi^2\right).$$

Substitution of these expressions into that for $\mathrm{d}\Gamma$ yields

$$\Gamma(\tau \to \nu_\tau + \pi) = \frac{G^2\cos^2\theta}{16\pi} m_\tau^3 f_\pi^2 \left(1 - \frac{m_\pi^2}{m_\tau^2}\right)^2,$$

which coincides with the result obtained at the beginning of this chapter. The same result could be derived in the limit of pure chiral symmetry when

$$q_\alpha a_\alpha = 0, \quad m_\pi = 0,$$

if we neglect terms of the order of m_π^2. In this case

$$\rho_\ell = 0, \quad 2\rho_\mathrm{t} = 2f_\pi^2\delta(s) + \text{ contributions of } 3\pi, 5\pi, \ldots$$

It is easy to demonstrate that we again obtain the familiar result for $\Gamma(\tau \to \pi\nu_\tau)$. As for the states $3\pi, 5\pi, \ldots$ and possible resonances in these systems, their contribution can be shown to satisfy the so-called Weinberg sum rules:

$$\int (\rho - \rho_t)\, ds = 0$$
$$\int (\rho - \rho_t)\, s\, ds = 0$$

which are based on $\rho_t(s) \to \rho(s)$ for $s \to \infty$ in the chiral limit (we recall that $2\pi\rho\,(q_\alpha q_\beta - g_{\alpha\beta}q^2) = \int v_\alpha^+ v$

Further study of $\tau \to 3\pi + \nu_\tau$ decays will help to finally resolve the problem of the existence and properties of the axial A_1 meson ($m_{A_1} \simeq 1100\text{MeV}, \Gamma_{A_1} \simeq 300\text{MeV}$; the main decay channel: $A_1 \to \rho\pi$). The second Weinberg sum rule has no contribution from the π-meson (in the $m_\pi = 0$ limit); saturated with ρ and A_1 mesons, it gives the relation

$$\frac{m_\rho^4}{\gamma_\rho^2} = \frac{m_{A_1}^4}{\gamma_{A_1}^2}.$$

Therefore,

$$\frac{\Gamma(\tau \to \rho\nu_\tau)}{\Gamma(\tau \to A_1\nu_\tau)} = \frac{\left(m_\tau^2 + 2m_\rho^2\right)\left(m_\tau^2 - m_\rho^2\right)^2 m_{A_1}^2}{\left(m_\tau^2 + 2m_{A_1}^2\right)\left(m_\tau^2 - m_{A_1}^2\right)^2 m_\rho^2} \simeq 2.7.$$

5.13.8 13.8. Decays $\tau \to \nu_\tau + \mathbf{K} + n\pi$

The $\tau \to \nu_\tau + K + n\pi$ decay rates are proportional to $\sin^2\theta_C$ where θ_C is the Cabibbo angle. Compared to pure pion decays, they are therefore very much suppressed. Decay-rate calculations are similar to those given above, and in some cases relations can be derived on the basis of the SU(3) symmetry of the strong interaction. On the whole, the $\tau \to \nu_\tau + K + n\pi$ decays must come to about $4 - 5\%$ of all semi-hadronic decays of the τ-lepton.

5.13.9 13.9. Summary of results

To conclude this chapter, we list the theoretical values of partial widths, B.

Decay channel	$B(\%)$	Basis of the estimate
$e\bar{\nu}\nu$	17	QCD + $(V-A)$ for Γ_{tot}
$\pi\nu$	10	$\pi \to \mu\nu$ decay
$\rho\nu$	23	CVC $+e^+e^- \to$ hadrons
$A_1\nu$	9	Weinberg sum rules
$(K + n\pi)\nu$	3	$\tan^2\theta$
(3 or 5π) ν	$\frac{11}{100}$	remainder

5.14 14 Decays of charmed particles

Decays of charmed particles are due to the product of currents

$$(\bar{s}c\cos\theta - \bar{d}c\sin\theta)\,(\bar{\nu}_e e + \bar{\nu}_\mu\mu + \bar{\nu}_\tau\tau + \bar{u}d\cos\theta + \bar{u}s\sin\theta) + \text{ h.c.}$$

(color and Lorentz indices are omitted). It can be seen from this expression that decays of charmed non-strange particles must produce predominantly strange particles. This applies both to leptonic and non-leptonic decays.

5.14.1 14.1. Leptonic and non-leptonic decays

Leptonic decays of charmed particles can be described in the following manner:

$$\begin{array}{llllll} c \to s\ell^+\nu_\ell & \cos^2\theta, & \Delta S = \Delta C, & \mathrm{D} \to \ell^+\nu\overline{\mathrm{K}}, & \mathrm{F} \to \ell^+\nu, \\ c \to d\ell^+\nu_\ell & \sin^2\theta, & \Delta S = 0, & \mathrm{D} \to \ell^+\nu, & \mathrm{F} \to \ell^+\nu\mathrm{K}. \end{array}$$

Here we give, from left to right: quark decays responsible for leptonic decays of charmed particles, the appropriate Cabibbo factors suppressing decay rates, selection rules, and examples of decays in question. Note that decays into $\tau^+\nu$ are also kinematically allowed for the F and D^+mesons, and that

$$\frac{\Gamma\left(\mathrm{F}^+ \to \tau^+\nu\right)}{\Gamma\left(\mathrm{F}^+ \to \mu^+\nu\right)} = \left(\frac{m_\tau}{m_\mu}\right)^2 \left(\frac{1 - m_\tau^2/m_{\mathrm{F}}^2}{1 - m_\mu^2/m_{\mathrm{F}}^2}\right)^2 \simeq 17,$$
$$\frac{\Gamma\left(\mathrm{D}^+ \to \tau^+\nu\right)}{\Gamma\left(\mathrm{D}^+ \to \mu^+\nu\right)} = \left(\frac{m_\tau}{m_\mu}\right)^2 \left(\frac{1 - m_\tau^2/m_{\mathrm{D}}^2}{1 - m_\mu^2/m_{\mathrm{D}}^2}\right)^2 \simeq 2.5.$$

The last two decays ($\mathrm{D} \to \tau\nu$ and $\mathrm{D} \to \mu\nu$) are suppressed by the factor $\sin^2\theta$ (we recall that $m_{\mathrm{F}} \simeq 2040\mathrm{MeV}, m_\tau \simeq 1780\mathrm{MeV}, m_{\mathrm{D}^+} \simeq 1868\mathrm{MeV}, m_{\mathrm{D}^0} \simeq 1863\mathrm{MeV}$).

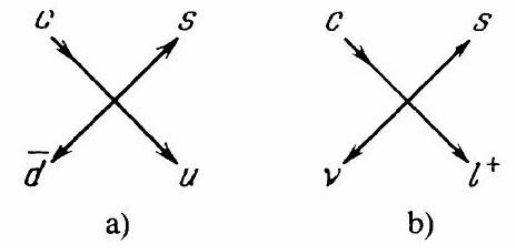


Fig. 14.1.

Creation of charmed particles in neutrino experiments and the subsequent decay of these particles result in the so-called dileptonic events. For example,

$$\nu_\mu + \mathrm{d} \to {}_1 \xrightarrow{\mathrm{C}+\mu^-} {}^{\mathrm{s}\mu^+} \nu_\mu \quad \text{or} \quad \mathrm{se}^+\nu_\mathrm{e}.$$

Such dileptonic events were observed in high-energy neutrino experiments:

$$\nu + \text{ nucleus } \to \mu^- + \mu^+ + \ldots,$$

where the ellipsis stands for the remaining particles created in the reaction; some of these may even escape detection. Dileptons will be discussed in more details in chapter 17.

The three types of non-leptonic decays may be described in the following manner:

$$\begin{array}{llllll} \mathrm{c} \to \ \mathrm{us}\,\overline{\mathrm{d}}, & \cos^4\theta, & \Delta S = \Delta C, & \mathrm{D} \to \ \overline{\mathrm{K}} + n\pi, & \mathrm{F} \to \eta\pi & \ldots \\ \mathrm{c} \to \mathrm{ud}\,\overline{\mathrm{d}}, \mathrm{us}\overline{\mathrm{s}}, & \cos^2\theta\sin^2\theta, & \Delta S = 0, & \mathrm{D} \to n\pi, & \mathrm{F} \to \ \mathrm{K}\pi & \ldots \\ \mathrm{c} \to \mathrm{ud}\overline{\mathrm{s}}, & \sin^4\theta, & \Delta S = -\Delta C, & \mathrm{D} \to \ \mathrm{K} + n\pi, & \mathrm{F} \to \mathrm{KK} & \ldots \end{array}$$

If we neglect decays proportional to $\sin^2\theta$, and assume approximately $\cos^2\theta \simeq 1$, then it can be estimated on the basis of the simple quark graphs of fig. 14.1 that

$$\Gamma(\mathrm{c} \to \mathrm{su}\,\overline{\mathrm{d}}) : \Gamma\left(\mathrm{c} \to \ \mathrm{s}\ell^+\nu\right) : \Gamma\left(\mathrm{c} \to \ \mathrm{s}\mu^+\nu\right) \simeq 3 : 1 : 1,$$

where the factor 3 stems from summation over colors of the $u\,\overline{\mathrm{d}}$ pair.

5.14.2 14.2. The role of virtual gluons

The branching ratio of non-leptonic decays is slightly enhanced if virtual gluons are taken into account (fig. 14.2).

This enhancement must not be as large as in the case of non-leptonic decays of strange particles. Two factors are responsible here. First, the Compton wavelength of the c-quark is much smaller than that of the

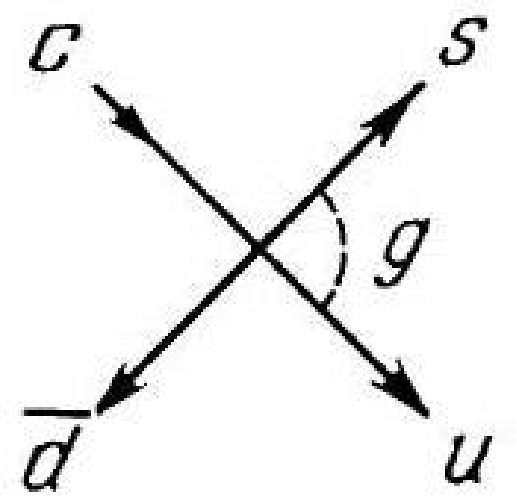


Fig. 14.2.

s-quark: $1/m_{\rm c} \ll 1/m_{\rm s}$, and the asymptotic freedom results in smaller $\alpha_{\rm s}$ at smaller distances. Second, monopole-type transitions (see chapter 7) are practically absent. Their amplitudes are proportional to $\sin\theta\cos\theta$ (see fig. 14.3); moreover, they are considerably suppressed because the masses of the d- and s-quarks are close to one another, much closer than those of the uand c-quarks (compare figs. 14.3 and 14.4).

In the case of cd $\to$ us as well as su $\to$ ud transitions, virtual gluons enhance amplitudes in the $\overline{3}_{\rm c}$ channel and suppress those in the $6_{\rm c}$ channel (the subscript c indicates that color is meant). In the case of the su $\to$ ud transition, the enhancement coefficient is close to 3 and that of suppression close to 0.6 , while in the case of the cd $\to$ us transition they are $\simeq 2^{1/2}$ and $\simeq 2^{-1/4}$, respectively. On the whole, the total decay rate of non-leptonic decays of the c-quark increases only slightly, as compared to the estimate based on the bare quark graph. As for the lifetime of, for instance, D-mesons, it can be estimated on the basis of the above arguments as being

$$1/\tau_{\rm D} \simeq (5-10)\Gamma({\rm c}\to {\rm se}\nu) \simeq (5-10)\left(\frac{\bar{m}_{\rm c}}{m_\mu}\right)^5 \Gamma(\mu\to {\rm e}\bar{\nu}\nu),$$

where $\bar{m}_{\rm c}$ is the effective mass of the decaying c-quark. Recalling now $\tau_\mu \simeq 2\cdot 10^{-6}$ s, and assuming $\overline{\rm m}_{\rm c} \simeq 1.5$GeV, we obtain

$$\tau_D \simeq (3-6)\cdot 10^{-13}\ {\rm s}.$$

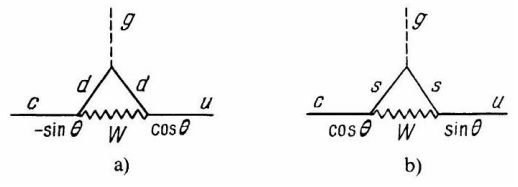


Fig. 14.3.

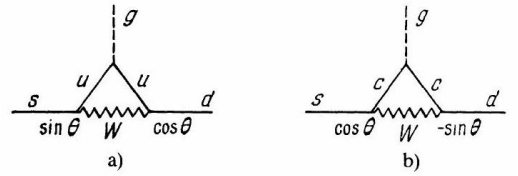


Fig. 14.4.

This estimate is obviously very sensitive to the choice of $\bar{m}_{\mathrm{c}}$, and fairly crude: for instance, the result is identical for the $\mathrm{D}^+, \mathrm{D}^0$ and F mesons and charmed baryons*.

5.14.3 14.3. Selection rules for $T-, U-$, and $V-$ spin

Let us see now what isospin and SU(3) symmetry selection rules govern the main ($\propto \cos^4\theta$) non-leptonic decays of charmed particles. Obviously, $\Delta T = 1$ in the $\mathrm{c} \to \mathrm{uds}$ decay. One of the corollaries of this is that, for example, the reaction

$$\mathrm{F}^+ \to \pi^+\pi^0$$

is forbidden (isospin of $\mathrm{F}^+$is zero, while for the $\pi^+\pi^0$ S-wave, $T = 2$).
The interaction $(\bar{u}d)(\bar{s}c)$ is transformed under the group $\mathrm{SU}(3)_{\mathrm{f}}$ as

$$8 \times 3 = 3 + \overline{6} + 15 \quad (t : \times t^{\cdot} = t^{\cdot} + t.. + t : \cdot)$$

(see appendix, Chapter 29, sect. 2.7). The state $\overline{6}$ of three quarks us $\overline{\mathrm{d}}$ is antisymmetric with respect to $u \leftrightarrow s$ exchange. Hence, these quarks form an antisymmetric color antitriplet $\overline{3}_{\mathrm{c}}$, and the corresponding amplitudes are enhanced by virtual gluons. Sometimes this effect is referred to as the sextet enhancement. The sextet enhancement of charmed particle decay is an analog of the octet enhancement in decays of strange particles. (We recall that in the interaction $(\bar{d}u)(\bar{u}s)$, the enhanced octet is 8_{f} ($\underline{8} \times 8 = 1 + 8_{\mathrm{f}} + 8_{\mathrm{d}} + 10 + \overline{10} + 27$), antisymmetrical with respect to the $\overline{\mathrm{d}} \leftrightarrow \overline{\mathrm{u}}$ and $\mathrm{u} \leftrightarrow \mathrm{s}$ exchange. This 8_{f} octet corresponds to the color antitriplets of the initial and

final quarks). As a result of the $\overline{\mathrm{u}} \leftrightarrow \overline{\mathrm{s}}$ antisymmetrization, the sextet transitions satisfy the $\Delta V = 0$ rule (for the definition of V-spin see appendix, Chapter 29, sect. 2.7). This rule would mean, for example, that the decay

$$\mathrm{D}^+ \to \overline{\mathrm{K}}^0\pi^+$$

[0]*After this book had been written, experimental data were obtained showing that the D^+ meson lifetime is several times that of the D^0 meson. It is possible that in addition to the c-quark decay, an essential process in the decay of the D^0 and F^+mesons is the annihilation of quarks of which these mesons consist: $c\overline{\mathrm{u}} \to \mathrm{s}\overline{\mathrm{d}}$ for D^0 and $c\overline{\mathrm{s}} \to \mathrm{ud}$ for F^+(the annihilation $c\,\overline{\mathrm{d}} \to \mathrm{ud}$ for the D^+meson is Cabibbo-suppressed).

is forbidden. This is easily shown by taking into account that the D^+meson has zero V-spin, $\pi^+$and $\overline{K}^0$ are components of a V-doublet, and that by virtue of the generalized Bose principle the S -wave $\pi\overline{K}^0$ system has $V = 1$.

It must be emphasized that the $\Delta V = 0$ rule must be very strongly violated, much more so than the $\Delta T = \frac{1}{2}$ rule for non-leptonic decays of strange particles, since the sextet enhancement is weaker than the octet one (we have already mentioned this fact). This conclusion is consistent with the experimental data. Thus, the decay $D^+ \to \overline{K}^0\pi^+$which is forbidden owing to V conservation, has $B \simeq 1.5 \pm 0.6\%$, while the V-allowed decay $D^0 \to K^-\pi^+$has $B \simeq 2.2 \pm 0.6\%$. No straightforward comparison of these figures is possible since these widths are relative and not absolute quantities. However, it is unlikely that the total widths of $D^+$and D^0 differ very much; therefore, the absolute widths of the V-allowed and V-forbidden decays probably differ not more than by an order of magnitude.

The following relations between amplitudes of two-particle decays can be derived on the basis of only the SU(3) invariance of the strong interaction, without taking into account the sextet enhancement:

$$M\left(D^0 \to \overline{K}^0\pi^0\right) = -\sqrt{3}M\left(D^0 \to \overline{K}^0\eta^0\right),$$
$$M\left(D^0 \to K^-\pi^+\right) + \sqrt{2}M\left(D^0 \to \overline{K}^0\pi^0\right) = M\left(D^+ \to \overline{K}^0\pi^+\right),$$
$$M\left(F^+ \to \overline{K}^0 K^+\right) - \sqrt{\frac{3}{2}}M\left(F^+ \to \pi^+\eta^0\right) = M\left(D^+ \to \overline{K}^0\pi^+\right).$$

So far these relations were not tested experimentally.
Let us consider now the non-leptonic interaction with $\Delta S = 0$,

$$\cos\theta \sin\theta \left[-\bar{u}O_\alpha d \cdot \bar{d}O^\alpha c + \bar{u}O_\alpha s \cdot \bar{s}O^\alpha c\right], \quad O_\alpha = \gamma_\alpha(1+\gamma_5).$$

This interaction is a component of the U-vector with $U_3 = 0$; therefore for this interaction

$$\Delta U = 1, \quad \Delta U_3 = 0.$$

This yields, in particular, that the reactions $D^0 \to K^0\overline{K}^0, \pi_U\pi_U, \eta_U\eta_U$, where

$$\pi_U = \frac{1}{2}\left(\pi^0 - \sqrt{3}\eta^0\right), \quad \eta_U = \frac{1}{2}\left(\eta^0 + \sqrt{3}\pi^0\right),$$

are forbidden. It can readily be shown that the sextet component in the weak non-leptonic lagrangian satisfies the rule $\Delta T = \frac{1}{2}$ for decays with $\Delta S = 0$. In its turn, this leads to the relations

$$\Gamma\left(F^+ \to K^0\pi^+\right) \simeq 2\Gamma\left(F^+ \to K^+\pi^0\right),$$
$$\Gamma\left(D^0 \to \pi^+\pi^-\right) \simeq 2\Gamma\left(D^0 \to \pi^0\pi^0\right),$$

which must be strongly violated in experiment.

5.15 15 Weak decays of b- and t-quarks

Weak decays of the b - and t -quarks occur because they participate in the weak charged current. In the general form, this current is given by

$$j_\mu = \sum_i \overline{\boldsymbol{\alpha}}^i_L \gamma_\mu V^{ik} \boldsymbol{\kappa}^k_L$$

where $\alpha^1 = u, \alpha^2 = c, \alpha^3 = t; \kappa^1 = d, \kappa^2 = s, \kappa^3 = b; \alpha$ (for the Greek $\alpha\nu\omega$ meaning top) symbolizes "top" quarks, and κ (for the Greek $\kappa\alpha\tau\omega$ meaning bottom) symbolizes "bottom" quarks;

$$\bar{\alpha}_{\mathrm{L}} = \bar{\alpha}\frac{1}{2}(1-\gamma_5), \quad \kappa_{\mathrm{L}} = \frac{1}{2}(1+\gamma_5)\kappa;$$

V is a unitary 3×3 matrix. If V were a unit matrix, $V^{ik} = \delta^{ik}$, the structure of the charged current would be $\bar{u}d + \bar{c}s + \bar{t}b$. The s- and b-quarks would then be stable, and with them the strange particles and b-hadrons. We know, however, that in reality these particles are unstable. Therefore we need to consider the matrix V in the most general form. In the case of six quarks this matrix has four parameters and is called the Kobayashi-Maskawa matrix.

5.15.1 15.1. Unitary $n \times n$ matrix

For the sake of generality, let us consider the current in which $n\alpha$-quarks are transformed into nk-quarks. Let us find the number of parameters which in this case determine the form of the unitary current matrix V. In the general case, the matrix V comprises n^2 complex numbers or $2n^2$ real parameters. The unitarity condition

$$V^+V = 1$$

reduces the number of parameters to n^2. Indeed, we have n conditions of the type

$$V_{1k}V^+_{k1} = V_{1k}V^*_{1k} = 1$$

$$V = \begin{pmatrix} 1 & 1 & 1 & 1 & x \\ \cdot & \cdot & \cdot & \cdot & 1 \\ \cdot & \cdot & \cdot & \cdot & 1 \\ \cdot & \cdot & \cdot & \cdot & 1 \\ \cdot & \cdot & \cdot & \cdot & 1 \end{pmatrix}$$

Fig. 15.1.

on the diagonal, as well as $\frac{1}{2}n(n-1)$ conditions of the type $\mathrm{Re}\, V_{1k}V^*_{2k} = 0$ and $\frac{1}{2}n(n-1)$ conditions of the type $\mathrm{Im}\, V_{1k}V^*_{2k} = 0$, the last two sets of equations resulting from the condition

$$V_{1k}V^+_{k2} = V_{1k}V^*_{2k} = V_{2k}V^*_{1k} = V_{2k}V^+_{k1} = 0.$$

Of the remaining n^2 parameters, $2n-1$ are non-physical phases which can be "eliminated" by redefining, or "rotating", the (unobservable) phases of $n\alpha$-quarks and ($n-1$) κ-quarks. The total number of such non-physical phases is $2n-1$, and not $2n$, since one of the matrix elements of V cannot be " κ-rotated" as it is already " α-rotated" (in fig. 15.1 this matrix element is at the intersection of the upper row and the right-hand column). The total number of physical parameters is equal therefore to

$$n^2 - (2n-1) = (n-1)^2.$$

Let us find now how many of these $(n-1)^2$ parameters are angles of orthogonal rotations, and how many are phase factors. The number of independent rotations in an n-dimensional space is $n_\theta = \frac{1}{2}n(n-1)$, and therefore the number of physical phase parameters is

$$n_\delta = (n-1)^2 - \frac{1}{2}n(n-1) = \frac{1}{2}(n-1)(n-2).$$

Let us consider the simplest examples:

$$
\begin{aligned}
&n = 2, \text{ four unitary matrices } (1, \tau), \quad n_\theta = 1, n_\delta = 0,\\
&n = 3, \text{ nine unitary matrices } (1, \lambda), \quad n_\theta = 3, n_\delta = 1,\\
&n = 4, \text{ sixteen unitary matrices}, \quad n_\theta = 6, n_\delta = 3.
\end{aligned}
$$

5.15.2 15.2. Angles $\boldsymbol{\theta}_1, \boldsymbol{\theta}_2, \boldsymbol{\theta}_3$ and phase $\boldsymbol{\delta}$

Let us construct the V-matrix explicitly for the case of six quarks (u, c, t, d, s, b). The angles $\theta_1, \theta_2, \theta_3$ can be chosen in several ways. We shall use the Euler angles and the notation usually adopted in the literature.

Consider a triad of coordinates (z, y, x) and a triad of quarks (d, s, b) put in correspondence with it. Now we make three rotations: by an angle θ_3 around the z-axis (fig. 15.2), then by an angle θ_1 around a new x-axis, and then by an angle θ_2 around a new z-axis. The sequence of these rotations is described by a product of three matrices:

$$
\begin{pmatrix} 1 & 0 & 0 \\ 0 & c_2 & s_2 \\ 0 & -s_2 & c_2 \end{pmatrix}
\begin{pmatrix} c_1 & s_1 & 0 \\ -s_1 & c_1 & 0 \\ 0 & 0 & 1 \end{pmatrix}
\begin{pmatrix} 1 & 0 & 0 \\ 0 & c_3 & s_3 \\ 0 & -s_3 & c_3 \end{pmatrix},
$$

where $c_l = \cos\theta_l, s_l = \sin\theta_l$. Now we only need to insert the phase factor $\mathrm{e}^{t\delta}$. Clearly, it cannot be put either at the beginning or at the end, since in these positions it will be non-physical, being identifiable with the unobservable phase of one of the quarks. The result will be non-trivial if we write, for example,

$$
(\bar{u}, \bar{c}, \bar{t})
\begin{pmatrix} 1 & 0 & 0 \\ 0 & c_2 & s_2 \\ 0 & -s_2 & c_2 \end{pmatrix}
\begin{pmatrix} c_1 & s_1 & 0 \\ -s_1 & c_1 & 0 \\ 0 & 0 & \mathrm{e}^{\iota\delta} \end{pmatrix}
\begin{pmatrix} 1 & 0 & 0 \\ 0 & c_3 & s_3 \\ 0 & -s_3 & c_3 \end{pmatrix}
\begin{pmatrix} d \\ s \\ b \end{pmatrix}.
$$

Multiplication of these matrices yields

$$
(\bar{u}, \bar{c}, \bar{t})
\begin{pmatrix} c_1 & s_1 c_3 & s_1 s_3 \\ -s_1 c_2 & c_1 c_2 c_3 - \mathrm{e}^{\iota\delta} s_2 s_3 & c_1 c_2 s_3 + \mathrm{e}^{\iota\delta} s_2 c_3 \\ s_1 s_2 & -c_1 s_2 c_3 - \mathrm{e}^{\iota\delta} c_2 s_3 & -c_1 s_2 s_3 + \mathrm{e}^{\mathrm{i}\delta} c_2 c_3 \end{pmatrix}
\begin{pmatrix} d \\ s \\ b \end{pmatrix}.
$$

The matrix can be simplified if we assume that all $s_\iota \ll 1$:

$$
V = \begin{pmatrix} 1 & s_1 & s_1 s_3 \\ -s_1 & 1 & s_3 + s_2 \mathrm{e}^{\iota\delta} \\ s_1 s_2 & -s_2 - s_3 \mathrm{e}^{\iota\delta} & \mathrm{e}^{\iota\delta} \end{pmatrix}.
$$

So far no b-hadrons with single b-quarks have been found (this statement reflects the state of the art at the beginning of 1979), and not even

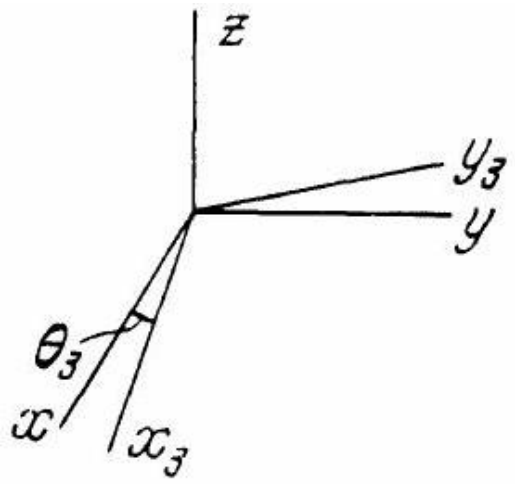


Fig. 15.2.

quarkonium, tf , has been observed; nevertheless, it can be said even at this juncture that the b- and t-quarks are unstable, that is $s_3 \neq 0, s_2 \neq 0$. We shall give substantiation to this statement in the next section.*

5.15.3 15.3. Metastability of the b-quark

If we had $s_2 = s_3 = 0$, the b-quark would be absolutely stable, and with it the lightest of the B -hadrons, such as the mesons $B^- = b\bar{u}$ and $B^+ = \bar{b}u$. The anticipated masses of these mesons are of the order of 5 GeV . A search for stable particles with such masses in pp collisions has been unsuccessful. Moreover, the upper bound on the cross section of production of $B^{\pm}$with lifetime above 10^{-8} s was found to be approximately 10^{-37} cm^2, which is by an order of magnitude smaller than the cross section of the reaction $pp \to \Upsilon + \ldots$. The anticipated cross section of B^+B^-pair production must not be so small; hence, these experiments indicate that $\tau_B \lesssim 10^{-8}$ s. This means in its turn, that s_3 and/or $s_2 \gtrsim 10^{-4}$.

Possible values of s_3 can also be derived from the comparison of values of the Cabibbo angle found from $\cos\theta$ (in nuclear β-decay) and from $\sin\theta$ (in non-leptonic decays of K -mesons and hyperons). It is easy to show that in the transition from four to six quarks

$$\cos\theta \Rightarrow c_1$$
$$\sin\theta \Rightarrow s_1 c_3$$

The Fermi coupling constant G_μ for the muon decay can be obtained from the experimentally measured muon lifetime τ_μ if we use the theoretical expression for the decay rate:

$$\tau_\mu^{-1} = \frac{G_\mu^2 m_\mu^5}{192\pi^3} f\left(\frac{m_e^2}{m^2}\right)\left[1 - \frac{\alpha}{2\pi}\left(\pi^2 - \frac{25}{4}\right)\right],$$

where

$$f(x) = 1 - 8x + 8x^3 - x^4 + 12x^2 \ln(1/x).$$

This yields

$$G_\mu = (1.16632 \pm 0.00004) \cdot 10^{-5}\text{GeV}^{-2}$$
$$= (1.43582 \pm 0.00004) \cdot 10^{-49}\text{erg} \cdot \text{ cm}^3.$$

On the other hand, the data on superallowed β-transitions $0^+ \to 0^+$in nuclei yield

$$G_\beta = (1.398 \pm 0.003) \cdot 10^{-49}\text{erg} \cdot \text{ cm}^3,$$

whence $c_1 = G_\beta/G_\mu = 0.974 \pm 0.003, s_1 = 0.227 \pm 0.013$. (the uncertainty in G_β reflects the experimental errors and, to approximately the same degree, theoretical ambiguity in covering radiative, Coulomb, and weak corrections, the last of which takes into account the second order of perturbation theory in weak interactions). If we compare $s_1 = 0.227 \pm 0.013$ with the value $\sin\theta = 0.219 \pm 0.011$ yielded by analyzing leptonic decays of K-mesons and hyperons, we can derive from the equality $c_3 = \sin\theta/s_1$, that c_3 is in the interval $0.87 - 1.00$, the mean value being $c_3 = 0.965$. Hence,

$$s_3 \simeq 0.25 \pm 0.25.$$

5.15.4 15.4. Contribution of t-quarks to $\mathbf{K^0 \leftrightarrow \overline{K}^0}$ transitions

Let us analyze the contribution of the u−, c−, and t -quarks to transitions with $|\Delta S| = 2$ (fig. 15.3). The integrand for the loop comprises a weighted sum of three propagators:

$$\begin{aligned}
&(1-\gamma_5)\left[V_{11}^+V_{12}\frac{1}{\hat{k}-m_\text{u}}+V_{12}^+V_{22}\frac{1}{\hat{k}-m_\text{c}}+V_{13}^+V_{32}\frac{1}{\hat{k}-m_\text{t}}\right](1+\gamma_5)\\
&=2\hat{k}\left[V_{11}^+V_{12}\frac{1}{k^2-m_\text{u}^2}+V_{12}^+V_{22}\frac{1}{k^2-m_\text{c}^2}+V_{13}^+V_{32}\frac{1}{k^2-m_\text{t}^2}\right](1+\gamma_5)\\
&=2\hat{k}\left[V_{12}^+V_{22}\left(\frac{1}{k^2-m_\text{c}^2}-\frac{1}{k^2-m_\text{u}^2}\right)\right.\\
&\qquad\left.+V_{13}^+V_{32}\left(\frac{1}{k^2-m_\text{t}^2}-\frac{1}{k^2-m_\text{u}^2}\right)\right](1+\gamma_5)\\
&\simeq 2\hat{k}\left[V_{21}^*V_{22}\frac{m_\text{c}^2}{k^2\left(k^2-m_\text{c}^2\right)}+V_{31}^*V_{32}\frac{m_\text{t}^2}{k^2\left(k^2-m_\text{t}^2\right)}\right](1+\gamma_5)\\
&\simeq -2\hat{k}s_1\left[\frac{m_\text{c}^2}{k^2\left(k^2-m_\text{c}^2\right)}+s_2\left(s_2+s_3\text{e}^{\iota\delta}\right)\frac{m_\text{t}^2}{k^2\left(k^2-m_\text{t}^2\right)}\right](1+\gamma_5)\,.
\end{aligned}$$

The above transformations were based on the unitarity of the V-matrix $\left(V_{11}^+V_{12}+V_{12}^+V_{22}+V_{13}^+V_{32}=0\right)$ and on the equality $(1-\gamma_5)(1+\gamma_5)=0$; we have neglected the u-quark mass and used the simplified form of the V-matrix valid in the case of all $s_i \ll 1$ (see above).

[0]*According to the data obtained at the e^+e^-colliding beam facility PETRA, the lower bound on the t -quark mass is $\simeq 18$GeV. As for the discovery of mesons comprising single b-quarks see footnote on p. 5.

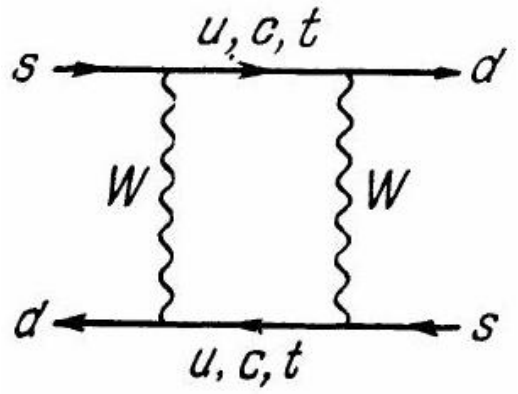


Fig. 15.3.

Discussing the Glashow-Iliopoulos-Maiani scheme in chapter 11, we gave an expression for Δm_{LS} taking into account contributions of only u- and c-quarks. Now it is not difficult to demonstrate, by calculating integrals corresponding to the loop in fig. 15.3, that inclusion of the t-quark into the picture results in multiplication of the above expression by a correction factor $\mathrm{Re}\, r$, where

$$r = 1 + x^2\xi + 2x \ln \xi,$$

in which $\xi = m_{\mathrm{t}}^2/m_{\mathrm{c}}^2$ and $x = s_2\left(s_2 + s_3 \mathrm{e}^{\mathrm{i}\delta}\right)$ (in deriving the expression for r we made use of the equalities

$$m_{\mathrm{c}}^2 \int_0^\infty \frac{\mathrm{d}k^2}{\left(k^2 + m_{\mathrm{c}}^2\right)^2} = 1, \quad m_t^2 \int_0^\infty \frac{\mathrm{d}k^2}{\left(k^2 + m_{\mathrm{t}}^2\right)^2} = 1,$$
$$m_{\mathrm{t}}^2 \int_0^\infty \frac{\mathrm{d}k^2}{\left(k^2 + m_{\mathrm{t}}^2\right)\left(k^2 + m_{\mathrm{c}}^2\right)} = \frac{m_{\mathrm{t}}^2}{m_{\mathrm{t}}^2 - m_{\mathrm{c}}^2} \ln \frac{m_{\mathrm{t}}^2}{m_{\mathrm{c}}^2} \simeq \ln \frac{m_{\mathrm{t}}^2}{m_{\mathrm{c}}^2},$$

and assumed that $m_{\mathrm{c}}^2/m_{\mathrm{t}}^2 \ll 1$).
If the "dressing" of the graph of fig. 15.3 with virtual gluons is taken into account, then the first two terms in r are multiplied by $\simeq 0.6$, and the third by $\simeq 0.4$. Keeping this in mind, let us recall the contribution of the bare graph of fig. 11.6 with u - and c-quarks only. This contribution (see p. 90) is equal to $\simeq 2.10^7 \left(m_{\mathrm{c}}/m_\mu\right)^2\ \mathrm{s}^{-1}$, which is to be compared with the experimental value $\Delta m_{\mathrm{LS}} \simeq 5 \cdot 10^9\ \mathrm{s}^{-1}$. By using the known value $m_{\mathrm{c}} \simeq 1.3\mathrm{GeV}$, we find that the contribution of t-quarks is essential: $\mathrm{Re}(r-1) \gtrsim 1$. This means, in turn, that angle θ_2 cannot be very small.

The value of $\mathrm{Im}\, r$ determines the violation of CP invariance in the $\mathrm{K}^0 - \overline{\mathrm{K}}^0$ system. In particular, we find for the parameter $i\mu_{12}$ characterizing the transitions $\mathrm{K}_2 \leftrightarrow \mathrm{K}_1$ (see chapter 12):

$$\frac{\mu_{12}}{\Delta m_{LS}} = \frac{\mathrm{Im}\, r}{\mathrm{Re}\, r}.$$

Experimentally, this ratio is about $2 \cdot 10^{-3}$. Consequently,

$$s_2 s_3 \sin\delta \gtrsim 10^{-3}$$

for not too high values of $m_{\mathrm{t}}/m_{\mathrm{c}}$. From this we can conclude that the lifetime of b -hadrons does not exceed 10^{-12} s.

It must be emphasized that if the angle θ_3 is sufficiently small, the experimentally observed smallness of CP-odd effects does not necessarily require that phase δ be small. For example,

if $s_3 \simeq 10^{-3}$ and $s_2 \simeq s_1$, then $\delta \simeq 1$. (This variant will be eliminated once it is established experimentally that the relative widths of the $b \to u\ell\bar{\nu}, b \to ud\bar{u}$, or $b \to us\bar{c}$ decays are not vanishingly small.) If, however, $s_3 \simeq s_2 \simeq s_1$, then $\delta \simeq 10^{-2}$.

Note that all CP-noninvariant amplitudes are proportional to $s_1 s_2 s_3 \delta$, both in the decays of charmed particles and in the decays of the b - and t -hadrons. (They must vanish if at least one of the angles θ_i is zero.) *

5.15.5 15.5. Cascade decays of b - and t-hadrons

It has been mentioned above that the b-quark must decay mostly owing to the interaction

$$\left(s_3 + s_2 e^{i\delta}\right)(\bar{c}b)\left(\bar{d}u + \bar{s}c + \bar{e}\nu_e + \bar{\mu}\nu_\mu + \bar{\tau}\nu_\tau\right).$$

The expected lifetime of B-mesons obtained by scaling the muon lifetime, must then be of the order of 10^{-14} s. This scaling takes into account the factor $(m_b/m_\mu)^5 \simeq (4.750/105)^5 \simeq 2 \cdot 10^8$ and a factor of about 5 corresponding to five channels, two of which are color-tripled (but four out of nine are especially strongly suppressed by the phase space); it is also assumed that $\left|s_3 + s_2 e^{i\delta}\right| \simeq 0.5$. B-mesons must then produce cascade decays, in accordance with the quark decay cascade. For example,

$$b \to c\mu^- \bar{\nu} \quad \begin{matrix} \\ \hookrightarrow s\mu^+ \nu \end{matrix}, \qquad B^- \to D^0\mu^- \bar{\nu}. \quad \begin{matrix} \\ \hookrightarrow K^- \mu^+ \nu. \end{matrix}$$

In particular, such cascade decays must produce the so-called trimuon events in neutrino experiments.

As a rule, decays of t -hadrons must produce b-hadrons (see the expression for the V matrix) and therefore the decay cascade must include one additional step.

5.16 16 Neutrino-electron interactions

In this and in the subsequent chapter we discuss neutrino reactions. These reactions played an important role both in establishing the properties of weak interaction and in the determination of the parton structure of nucleons. This chapter deals with reactions occurring in neutrino-electron collisions. It is preferable to begin the discussion with these processes since they are much simpler from a theoretical point of view than neutrino-nucleon interactions. Unfortunately, they are much less studied experimentally, owing to a sort of "complementarity principle".

5.16.1 16.1. Kinematics of $\nu + e \to \nu + \ell$ reactions

Before calculating cross sections, we consider the kinematics of reactions. We start with the reaction

$$\nu(k_1) + e(p_1) \to \nu(k_2) + \ell(p_2),$$

where ν is the electron or muon neutrino or antineutrino, and ℓ(e or μ) is a charged lepton. Quantities in parentheses are 4 -momenta of the particles involved: $k_1^2 = k_2^2 = 0, p_1^2 = m^2, p_2^2 =$

^{0*} It is interesting to note that the phase δ enters the amplitude of the CP-violating K -meson decays not only through the box diagram of fig. 15.3, which gives superweak $K_2^0 - K_1^0$ mixing, but also through a milliweak transition between s - and d -quarks with an emission of a gluon. This milliweak transition with $|\Delta S| = 1$ and $\Delta T = 1/2$ is described by the graphs of fig. 7.5 (and 7.6) (p. 53) with virtual u-, c- and t-quarks. The interplay of the two mechanisms leads to an interesting prediction: $|\eta_{+-} - \eta_{00}| \simeq 2 \cdot 10^{-5}$. This quantity may be even larger if CP is violated by Higgs bosons (for references see Chapter 28).

μ^2, where m is the electron mass and μ is the mass of the final lepton. In the laboratory reference frame

$$k_i = \omega_i, \boldsymbol{k}_i, \quad p_i = E_i, \boldsymbol{p}_i, \quad i = 1, 2.$$

In the center of mass

$$k_i = \omega_i^0, \boldsymbol{k}_i^0, \quad p_i = E_i^0, \boldsymbol{p}_i^0, \quad i = 1, 2$$
$$\boldsymbol{k}_1^0 + \boldsymbol{p}_1^0 = 0, \quad \boldsymbol{k}_2^0 + \boldsymbol{p}_2^0 = 0 \quad \text{(see fig. 16.1)} .$$

Introduce the standard invariants s and t. As usual, s is the total squared

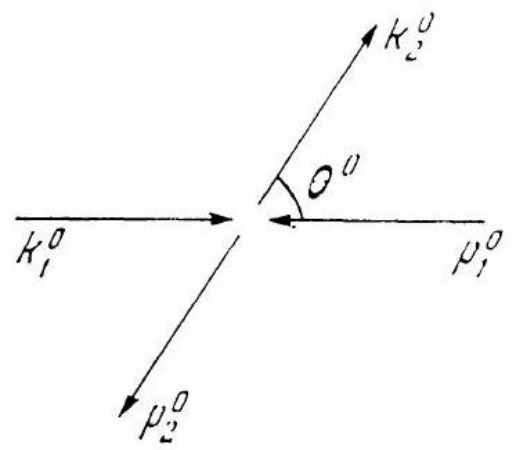


Fig. 16.1.

energy in the center-of-mass frame:

$$\begin{aligned}
s &= (k_1 + p_1)^2 = \left(\omega_1^0 + E_1^0\right)^2 = 2m\omega_1 + m^2 \\
&= (k_2 + p_2)^2 = \left(\omega_2^0 + E_2^0\right)^2, \\
\omega_1^0 &= \frac{(k_1, k_1 + p_1)}{\sqrt{s}} = \frac{k_1 p_1}{\sqrt{s}} = \frac{s - m^2}{2\sqrt{s}}, \quad E_1^0 = \frac{s + m^2}{2\sqrt{s}}, \\
\omega_2^0 &= \frac{(k_2, k_2 + p_2)}{\sqrt{s}} = \frac{(k_2 p_2)}{\sqrt{s}} = \frac{s - \mu^2}{2\sqrt{s}}, \quad E_2^0 = \frac{s + \mu^2}{2\sqrt{s}}.
\end{aligned}$$

The threshold for the $\nu\mathrm{e} \to \nu\mu$ reaction is

$$s = \mu^2, \quad \omega_1 = \frac{\mu^2 - m^2}{2m} \approx 11\mathrm{GeV}.$$

In the case of elastic scattering, $\mu = \mathrm{m}$:

$$\omega_2^0 = \omega_1^0 = \omega^0 = \frac{s - m^2}{2\sqrt{s}}, \quad E_1^0 = E_2^0 = E^0 = \frac{s + m^2}{2\sqrt{s}}.$$

The 4 -momentum transfer squared is defined in the standard manner:

$$\begin{aligned}
t &= (k_1 - k_2)^2 \\
&= -2\omega_1^0\omega_2^0\left(1 - \cos\theta^0\right) = -2\omega_1\omega_2(1 - \cos\theta) = (p_1 - p_2)^2 \\
&= 2m^2 - 2E_1^0 E_2^0\left(1 - v_1^0 v_2^0 \cos\theta^0\right) \\
&= -2mE_2 + m^2 + \mu^2 = (\mu - m)^2 - 2mT,
\end{aligned}$$

where $T = E_2 - \mu$ is the kinetic energy of the recoil lepton in the laboratory reference frame,

$$v_1^0 = \frac{|\boldsymbol{p}_1^0|}{E_1^0} = \frac{s - m^2}{s + m^2}, \quad v_2^0 = \frac{|\boldsymbol{p}_2^0|}{E_2^0} = \frac{s - \mu^2}{s + \mu^2}.$$

In the case of elastic scattering

$$v_1^0 = v_2^0 = v^0 = \frac{s - m^2}{s + m^2}$$

Determine now the physical region of T. The minimum value of T corresponds to $\theta^0 = 0$; consequently, $t = 0$, and

$$T_{\min} = \frac{(\mu - m)^2}{2m}.$$

In the case of elastic scattering $T_{\min} = 0$. The maximum value of T corresponds to $\theta^0 = \pi$,

$$T_{\max} = \frac{(\mu - m)^2 + 4\omega_1^0\omega_2^0}{2m}.$$

In the case of elastic scattering

$$T_{\max} = \frac{2\left(\omega^0\right)^2}{m} = \frac{\left(s - m^2\right)^2}{2sm} = \frac{2m\omega_1^2}{2m\omega_1 + m^2} = \frac{\omega_1}{1 + m/2\omega_1}.$$

Neglecting the m/μ ratio, we obtain for the $\nu e \to \nu\mu$ reaction:

$$T_{\max} \simeq s/2m.$$

In addition to the relations

$$2p_1k_1 = s - m^2, \quad 2p_2k_2 = s - \mu^2$$

two more relations are useful:

$$2p_1k_2 = s + t - \mu^2, \quad 2p_2k_1 = s + t - m^2.$$

The experimental observation of the processes in question, and their analysis against the background of other processes, are very difficult because cross sections are small and only one particle, namely the recoil lepton, is recorded. The energy of the impinging neutrino, ω_1, can be found by measuring the energy E_2 of the recoil lepton and its emission angle with respect to the neutrino beam, θ :

$$2E_2\omega_1\left(1 - v_2\cos\theta\right) = \mu^2 - m^2 + 2m\left(\omega_1 + m - E_2\right).$$

The result for elastic ν e scattering at high energies ($\omega_1 \gg m, E_2 \gg m$) is

$$\omega_1 \simeq \frac{2mE_2}{2m - \theta^2 E_2}$$

(note that at high energies the kinematically allowed angles θ are small: $\theta \lesssim \sqrt{m/\omega_1}$). Determination of ω_1 by the above formula facilitates identification of an event as ν e scattering, provided characteristic neutrino energies in the beam are known in advance (at least roughly).

5.16.2 16.2. Cross section of the $\nu_\mu e^- \to \nu_e \mu^-$reaction

The theory of the $\nu_\mu e^- \to \mu^- \nu_e$ and $\bar{\nu}_e e^- \to \mu^- \bar{\nu}_\mu$ reactions is especially simple because in contrast to elastic ν e scattering, only charged currents are involved (see fig. 16.2). We begin with the reaction

$$\nu_\mu (k_1) + e (p_1) \to \nu_e (k_2) + \mu^- (p_2) .$$

Quantities in parentheses are 4 -momenta of the particles. The process amplitude is

$$M = \sqrt{\frac{1}{2}} G \left[\bar{u}_{\nu_e} \gamma_\alpha (1 + \gamma_5) u_e\right] \left[\bar{u}_\mu \gamma^\alpha (1 + \gamma_5) u_{\nu_\mu}\right] .$$

The calculation of the squared amplitude summed over spin variables is standard (see chapter 3); the result is

$$\overline{|M|^2} = 128 G^2 (p_1 k_1) (p_2 k_2) .$$

As dictated by the crossing symmetry, this expression is absolutely identical to that for muon decay.

The cross section is given by the formula

$$\sigma = \frac{1}{2 \cdot 4 (k_1 p_1)} \int \overline{|M|^2} \frac{d\boldsymbol{k}_2}{(2\pi)^3 2\omega_2} \frac{d\boldsymbol{p}_2}{(2\pi)^3 2E_2} (2\pi)^4 \delta^4 (k_2 + p_2 - k_1 - p_1) .$$

Averaging of $|M|^2$ in the integrand is carried out over polarizations of the initial electron and not over those of the neutrino since the latter is longitudinally polarized. Calculating now the center-of-mass phase-space

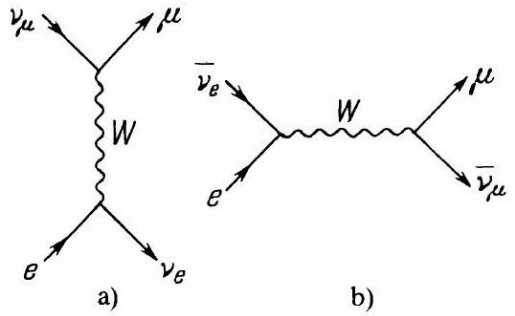


Fig. 16.2.

volume, we obtain

$$\begin{aligned} d\sigma &= -\overline{|M|^2} \frac{(p_2 k_2)}{(p_1 k_1) s} \frac{d\cos\theta^0}{64\pi} \\ &= -\frac{2G^2}{\pi} \frac{(p_1 k_1) (p_2 k_2) (p_2 k_2)}{(p_1 k_1) s} d\cos\theta^0 = -\frac{2G^2}{\pi} \left(\omega_2^0\right)^2 d\cos\theta^0 . \end{aligned}$$

We find that the cross section in the center-of-mass reference frame is isotropic. Making use of the expression $dt = 2\omega_1^0 \omega_2^0 d\cos\theta^0$, we obtain

$$\begin{aligned} d\sigma &= -\frac{\overline{|M|^2}}{(p_1 k_1)^2} \frac{dt}{128\pi} = -\frac{G^2 (p_1 k_1) (p_2 k_2)}{\pi (p_1 k_1)^2} dt = -\frac{G^2}{\pi} \frac{s - \mu^2}{s - m^2} dt \\ &= \frac{G^2}{\pi} \frac{s - \mu^2}{s - m^2} 2m \, dT . \end{aligned}$$

The total cross section is found by integration over $\mathrm{d}\cos\theta^0$ (or $\mathrm{d}t$, or $\mathrm{d}T$):

$$\sigma = \frac{4G^2}{\pi}\left(\omega_2^0\right)^2 = \frac{G^2}{\pi}\frac{\left(s-\mu^2\right)^2}{s}.$$

The cross section vanishes at the threshold. In the case $s \gg \mu^2$ we have

$$\sigma \approx \frac{G^2 s}{\pi}.$$

5.16.3 16.3. Cross section of the $\bar{\nu}_{\mathrm{e}}\mathbf{e}^- \to \bar{\nu}_\mu \boldsymbol{\mu}^-$reaction

Calculation of $\overline{|M|^2}$ for the reaction

$$\bar{\nu}_{\mathrm{e}}\left(k_1\right) + \mathrm{e}^-\left(p_1\right) \to \bar{\nu}_\mu\left(k_2\right) + \mu^-\left(p_2\right)$$

need not be repeated. It is sufficient to make a substitution $k_1 \leftrightarrow k_2$ in the expression for $|M|^2$ for the reaction $\nu_\mu \mathrm{e}^- \to \nu_{\mathrm{e}}\mu^-$. This substitution is based on the two reactions being coupled by the crossing operation: emission of ν_{e} is substituted by absorption of $\bar{\nu}_{\mathrm{e}}$, and absorption of ν_μ by emission of $\bar{\nu}_\mu$. Consequently,

$$\overline{|M|^2} = 128G^2\left(p_1k_2\right)\left(p_2k_1\right),$$

and the differential cross section becomes

$$\begin{aligned}\mathrm{d}\sigma &= -\frac{2G^2}{\pi}\frac{\left(p_1k_2\right)\left(p_2k_1\right)\left(p_2k_2\right)}{\left(p_1k_1\right)s}\,\mathrm{d}\cos\theta^0 \\ &= -\frac{2G^2}{\pi}\frac{\left(\omega_2^0\right)^2 E_1^0 E_2^0}{s}\left(1+v_1^0\cos\theta^0\right)\left(1+v_2^0\cos\theta^0\right)\mathrm{d}\cos\theta^0\end{aligned}$$

Note that

$$\left.\frac{\mathrm{d}\sigma\left(\nu_\mu \mathrm{e} \to \mu\nu_{\mathrm{e}}\right)}{\mathrm{d}\cos\theta^0}\right|_{\theta^0=0} = \left.\frac{\mathrm{d}\sigma\left(\nu_{\mathrm{e}}\mathrm{e} \to \mu^-\bar{\nu}_\mu\right)}{\mathrm{d}\cos\theta^0}\right|_{\theta^0=0} = -\frac{2G^2}{\pi}\left(\omega_2^0\right)^2.$$

In the invariant notation

$$\begin{aligned}\mathrm{d}\sigma &= -\frac{G^2}{\pi}\frac{\left(p_1k_2\right)\left(p_2k_1\right)}{\left(p_1k_1\right)^2}\,\mathrm{d}t = -\frac{G^2}{\pi}\frac{\left(s+t-\mu^2\right)\left(s+t-m^2\right)}{\left(s-m^2\right)^2}\,\mathrm{d}t \\ \left.\frac{\mathrm{d}\sigma}{\mathrm{d}t}\left(\nu_\mu \mathrm{e} \to \nu_{\mathrm{e}}\mu\right)\right|_{t=0} &= \left.\frac{\mathrm{d}\sigma}{\mathrm{d}t}\left(\tilde{\nu}_{\mathrm{e}}\mathrm{e} \to \tilde{\nu}_\mu\mu\right)\right|_{t=0}.\end{aligned}$$

Integration over θ^0 from 0 to π yields

$$\sigma = \frac{4G^2}{\pi}\left(\omega_2^0\right)^2\frac{E_1^0E_2^0}{s}\left(1+\frac{1}{3}v_1^0v_2^0\right) = \frac{G^2}{\pi}\frac{4\left(\omega_2^0\right)^2}{s}\left(E_1^0E_2^0+\frac{1}{3}\omega_1^0\omega_2^0\right).$$

The reaction $\nu_\mu \mathrm{e} \to \nu_{\mathrm{e}}\mu$ has been observed experimentally only recently, owing to its high threshold value and low cross section. This observation has not yielded any principally new data on weak interactions since the amplitude of this reaction is trivially related to the thoroughly analyzed amplitude of the $\mu \to \mathrm{e}\bar{\nu}_{\mathrm{e}}\nu_\mu$ decay. Nevertheless, several reasons justify a discussion of the reactions $\nu_\mu \mathrm{e} \to \nu_{\mathrm{e}}\mu$ and $\bar{\nu}_\mu \mathrm{e} \to \bar{\nu}_{\mathrm{e}}\mu$ in this book: first, cross sections of these processes are usually not given in books devoted to weak interactions; second, similar formulas are used in the framework of the parton model to calculate production cross sections of heavy quarks (c, b, t) in neutrino experiments; third, these formulas can be used in the $\mu = m$ limit to analyse ν e $\to \nu$ e elastic scattering.

5.16.4 16.4. Elastic νe and $\bar{\nu}$ e scattering induced by the charged current

Neutrino elastic scattering on electrons is caused by neutral currents in the case of ν_μ and $\bar{\nu}_\mu$, and by a combination of neutral and charged current in the case of ν_e and $\bar{\nu}_\mathrm{e}$. We begin with the idealized case of the elastic

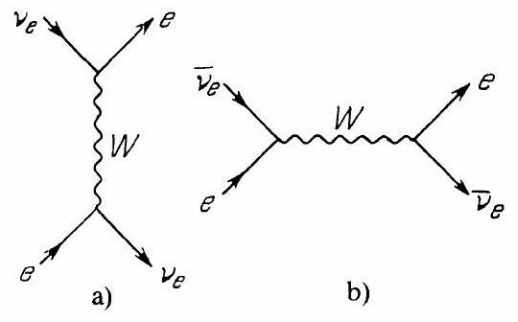


Fig. 16.3.

scattering cross sections of the processes $\nu_\mathrm{e}\mathrm{e} \to \nu_\mathrm{e}\mathrm{e}$ and $\bar{\nu}_\mathrm{e}\mathrm{e} \to \bar{\nu}_\mathrm{e}\mathrm{e}$, ignoring for a moment neutral currents. We shall obtain cross sections in the form in which they were written in textbooks before the discovery of neutral currents. They are of more than just historical interest, however. Cross sections for neutrino interactions with light quarks are of a very similar form. Moreover, it is very convenient to use this simple case as a basis for discussing the behavior of neutrino processes at high energies ($s \gg m^2$).

Let us start with the graphs of fig. 16.3. These graphs reduce to the four-fermion graphs of fig. 16.4 at sufficiently low energies, i.e. for $s \ll m_\mathrm{W}^2$ (the case of $s \sim m_\mathrm{W}^2$ being unfeasible for laboratory neutrino experiments). Assuming $\mu = m$, we easily derive from the formulas obtained above:

$$\frac{\mathrm{d}\sigma_{\nu\mathrm{e}}}{\mathrm{d}t} = -\frac{G^2}{\pi}, \quad \frac{\mathrm{d}\sigma_{\bar{\nu}\mathrm{e}}}{\mathrm{d}t} = -\frac{G^2}{\pi}\frac{(s+t-m^2)^2}{(s-m^2)^2}, \quad 0 > t > -\frac{(s-m^2)^2}{s}$$

$$\sigma_{\nu\mathrm{e}} = \frac{G^2}{\pi}\frac{(s-m^2)^2}{s} = \frac{2G^2}{\pi}\frac{m\omega_1}{1+m/2\omega_1},$$

$$\sigma_{\bar{\nu}\mathrm{e}} = \frac{G^2}{3}\frac{(s-m^2)^3 - [(s-m)^2m^2/s]^3}{(s-m^2)^2} = \frac{G^2}{3\pi}(s-m^2)\left[1-\left(\frac{m^2}{s}\right)^3\right]$$

$$= \frac{2G^2m\omega_1}{3\pi}\left[1-\left(\frac{m/2\omega_1}{1+m/2\omega_1}\right)^3\right].$$

$\nu_e\bar{\nu}_e x_\nu^e \bar{\nu}_{\bar{e}}^e$.

Fig. 16.4.

The formulas are simplified for $s \gg m^2$:

$$\frac{\mathrm{d}\sigma_{\nu\mathrm{e}}}{\mathrm{d}t} \approx -\frac{G^2}{\pi}, \quad \frac{\mathrm{d}\sigma_{\bar{\nu}\mathrm{e}}}{\mathrm{d}t} \approx -\frac{G^2}{\pi}\left(1+\frac{t}{s}\right)^2, \quad 0 \geq t \geq -s,$$

$$\sigma_{\nu\mathrm{e}} \approx \frac{G^2 s}{\pi} \approx \frac{G^2 2m\omega_1}{\pi} \approx 1.68\cdot 10^{-41}\,(E_\nu/\mathrm{GeV})\,\mathrm{cm}^2,$$

$$\sigma_{\bar{\nu}\mathrm{e}} \approx \frac{G^2 s}{3\pi} \approx \frac{G^2 2m\omega_1}{3\pi} \approx 0.56\cdot 10^{-41}\,(E_\nu/\mathrm{GeV})\,\mathrm{cm}^2.$$

This behavior of cross sections is easily understood in qualitative terms. The linear dependence of the cross section on s stems from the dimension of G : the only other dimensional parameter available to us at $s \to \infty$ is the total energy in the center-of-mass frame. The isotropy of νe scattering in this frame is equally clear. Indeed, the total angular momentum J of both the ingoing and outgoing ν and e is zero so that, for the point interaction, all directions of scattering are equally good (see fig. 16.5 where long arrows symbolize momenta, and short ones spins of the particles). Mutual orientations of spins and momenta shown in fig. 16.5 are characteristic for the charged current. Indeed, it includes only the left-handed components of the neutrino and of the electron. The configuration of spins and momenta in $\bar{\nu}$e scattering is shown in fig. 16.6; it is clear that in this case the total angular momentum J of the colliding electron and neutrino equals unity and is directed along the momentum of the ingoing neutrino: $J_z = 1$. Owing to conservation of J_z, only one of the three possible final states of $\bar{\nu}$e ($J_z = \pm 1, 0$) is realized. This corresponds to the coefficient $\frac{1}{3}$ in the expression for $\sigma_{\bar{\nu}\mathrm{e}}$. (Note that the ν_{e}e and $\bar{\nu}$e cross sections are equal for $\omega_1 \ll m$:

$$\sigma_{\nu\mathrm{e}} = \sigma_{\bar{\nu}\mathrm{e}} = \frac{4G^2\omega_1^2}{\pi}.$$

In this limiting case the cross section is determined by the available energy only, and does not include the electron mass).

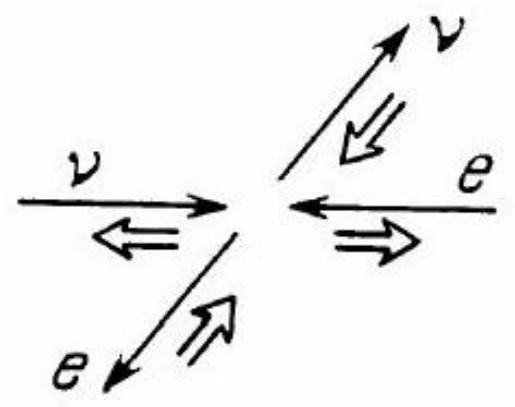


Fig. 16.5.

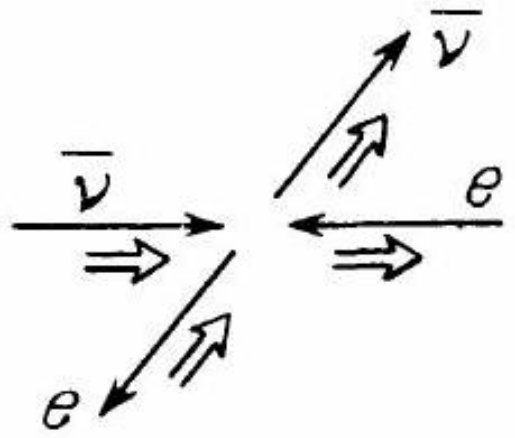


Fig. 16.6.

The cross sections for ν e and $\bar{\nu}$ e scattering for $s \gg m^2$ being different, a question arises concerning a violation of the Pomeranchuk theorem in this case (the theorem states the equality of cross sections in the interaction of a particle and its antiparticle with a given target at asymptotically high energies). The answer to this question is that in a certain sense the energies for which ν e scattering was discussed so far, were superlow: $s \ll m_{\mathrm{W}}^2 \ll G^{-1}$. The quantity Gs is a natural dimensionless parameter for the four-fermion interaction. As long as $Gs \ll 1$, the amplitude is purely real, and only one partial wave is present (the interaction is point-like). The Pomeranchuk theorem is applicable in the range $Gs \gg 1$ where multiparticle inelastic processes are important and many partial waves are involved. Expressions for cross sections derived in this chapter are not valid in this range.

5.16.5 16.5. Cross sections for the νe and $\bar{\nu}$ e scattering: general formulas

With neutral currents taken into account (see chapter 22) the ν e scattering amplitude takes the form

$$M = \sqrt{\frac{1}{2}} G \bar{u}_{\mathrm{e}_2} \left[g_{\mathrm{L}} \gamma_\alpha \left(1+\gamma_5\right) + g_{\mathrm{R}} \gamma_\alpha \left(1-\gamma_5\right) \right] u_{\mathrm{e}_1} \cdot \bar{u}_{\nu_2} \gamma_\alpha \left(1+\gamma_5\right) u_{\nu_1}.$$

Here $\nu = \nu_{\mathrm{e}}$ or ν_μ (scattering of $\bar{\nu}_{\mathrm{e}}$ and $\bar{\nu}_\mu$ is discussed at the end of this section). As will be shown in chapter 22, the constants g_L and g_R in the case of the stndard model of the electroweak interaction could be written in the form

$$\left.\begin{array}{l} g_{\mathrm{L}} = \frac{1}{2} + \sin^2\theta_{\mathrm{W}} \\ g_{\mathrm{R}} = \sin^2\theta_{\mathrm{W}} \\ g_{\mathrm{L}} = -\frac{1}{2} + \sin^2\theta_{\mathrm{W}} \\ g_{\mathrm{R}} = \sin^2\theta_{\mathrm{W}} \end{array}\right\} \text{ for } \nu_{\mathrm{e}} \text{ e scattering}$$

(We recall that $g_{\mathrm{V}} = g_{\mathrm{L}} + g_{\mathrm{R}}, g_{\mathrm{A}} = g_{\mathrm{L}} - g_{\mathrm{R}}$.) The total amplitude of ν_μe scattering is due to the coupling of the neutral currents $\bar{\nu}_\mu \nu_\mu$ and $\bar{e}e$; the ν_{e}e
scattering amplitude is the sum of two terms, one of which is a product of neutral currents $\bar{\nu}_{\mathrm{e}}\nu_{\mathrm{e}}$ and $\bar{e}e$, and the other term is a product of charged currents $\bar{\nu}_{\mathrm{e}}$e and $\bar{e}\nu_{\mathrm{e}}$. In writing the total amplitude, the Fierz transformation was used for the last of these terms:

$$\bar{\nu}_{\mathrm{e}} \gamma_\alpha \left(1+\gamma_5\right) e \cdot \bar{e} \gamma^\alpha \left(1+\gamma_5\right) \nu_{\mathrm{e}} = \bar{e} \gamma_\alpha \left(1+\gamma_5\right) e \nu_{\mathrm{e}} \gamma^\alpha \left(1+\gamma_5\right) \nu_{\mathrm{e}}.$$

(The charged current corresponds therefore to the coefficients $g_L = 1$, $g_{\mathrm{R}} = 0$). For $\overline{|M|^2}$ we obtain

$$\overline{|M|^2} = 128 G^2 \left[g_{\mathrm{L}}^2 \left(p_1 k_1\right)^2 + g_{\mathrm{R}}^2 \left(p_1 k_2\right)^2 - g_{\mathrm{L}} g_{\mathrm{R}} m^2 \left(k_1 k_2\right) \right].$$

Here the terms proportional to g_{L}^2 and g_{R}^2 are the same as in scattering due to the charged currents $\nu_{\mathrm{e}} e \to \nu_{\mathrm{e}} e$ and $\bar{\nu}_{\mathrm{e}} e \to \bar{\nu}_{\mathrm{e}} e$, respectively (see above). It is convenient to use the Fierz transformation when calculating interference terms proportional to $g_L g_R$. For example, the first interference term is conveniently written in the form

$$g_L g_R \bar{u}_{e_2} \gamma_\alpha \left(1+\gamma_5\right) u_{e_1} \bar{u}_{\nu_2} \gamma^\alpha \left(1+\gamma_5\right) u_{\nu_1} \bar{u}_{\nu_1} \left(1-\gamma_5\right) u_{e_2} \bar{u}_{e_1} \left(1+\gamma_5\right) u_{\nu_2}.$$

Both interference terms give identical contributions. Taking into account that $p_1 k_1 = m\omega_1, p_1 k_2 = m\omega_2 = m\left(\omega_1 - T\right), k_1 k_2 = p_1 p_2 - m^2 = T \cdot m$, the final expression for the cross section for ν e scattering becomes:

$$\frac{\mathrm{d}\sigma}{\mathrm{d}T} = \frac{2G^2 m}{\pi}\left[g_{\mathrm{L}}^2 + g_{\mathrm{R}}^2\left(1 - \frac{T}{\omega_1}\right)^2 - g_{\mathrm{L}} g_{\mathrm{R}} \frac{mT}{\omega_1^2}\right].$$

(Recall that m is the electron mass, T is the electron kinetic energy after scattering in the laboratory frame, and ω_1 is the energy of the ingoing neutrino.) The interference term tends to zero in the $\omega_1 \gg m$ limit. This is a natural result since the interference of left-handed and right-handed helicity states must vanish for ultra-relativistic particles.

The following symmetry arguments could be used to obtain cross sections for $\bar{\nu}_{\mathrm{e}}$e and $\bar{\nu}_{\mu}$e scattering. The $\bar{\nu}\mathrm{e}^- \to \bar{\nu}\mathrm{e}^-$scattering amplitude is equal to that for $\nu\mathrm{e}^+ \to \nu\mathrm{e}^+$. But the left-handed and right-handed components must change places when going from the electrons to the positron. Hence,

$$\frac{\mathrm{d}\sigma_{\overline{\nu e}}}{\mathrm{d}T} = \frac{2G^2 m}{\pi}\left[g_{\mathrm{R}}^2 + g_{\mathrm{L}}^2\left(1 - \frac{T}{\omega_1}\right)^2 - g_{\mathrm{L}} g_{\mathrm{R}} \frac{mT}{\omega_1^2}\right].$$

5.16.6 16.6. Other effects of the νe interaction

The neutrino-electron interaction must result in a number of processes, for instance, in $\mathrm{e}^+\mathrm{e}^- \to \nu\bar{\nu}$ annihilation (fig. 16.7). It is practically impossible

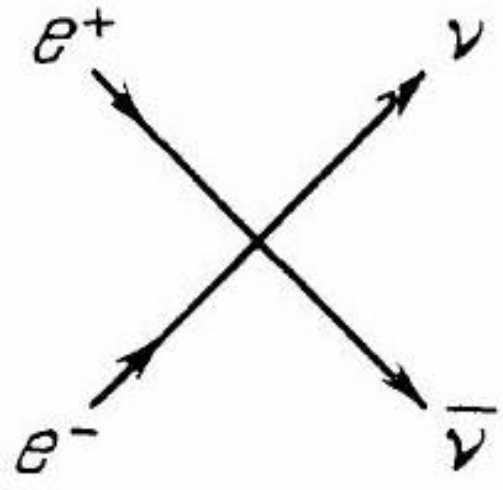


Fig. 16.7.

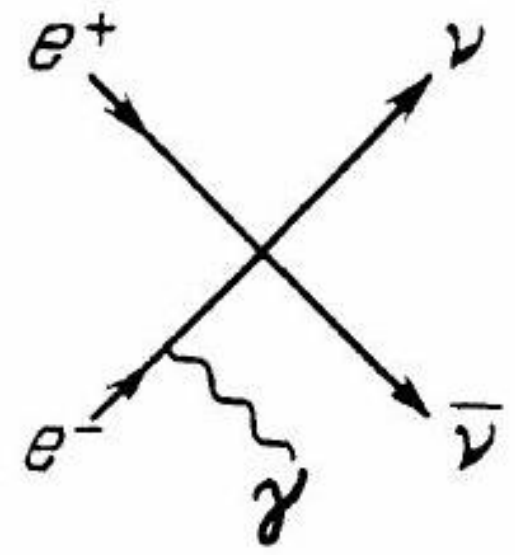


Fig. 16.8.

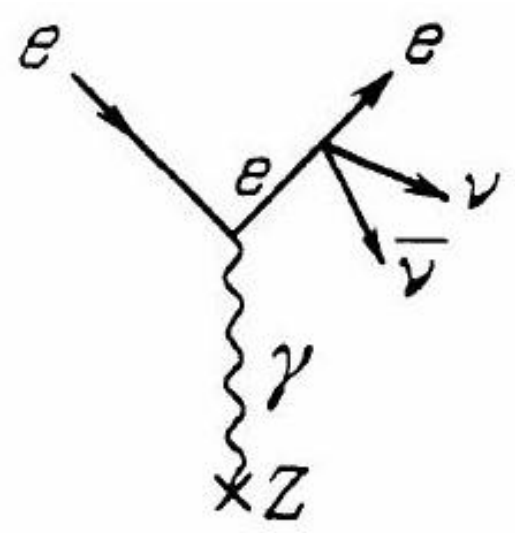


Fig. 16.9.

to observe this process in laboratory conditions. Hopefully, bremsstrahlung photons accompanying this annihilation (fig. 16.8) may be detected in the future in colliding high-energy beams of $e^+$and e^-. The process of bremsstrahlung neutrino emission (fig. 16.9) must play an important role in the dynamics of hot stars. This process may be significant, despite its small cross section, because the small interaction cross section of the neutrino allows it to leave the star much more easily than a photon.

To conclude this chapter, let us turn to the neutrino-muon interaction.

5.16.7 16.7. Creation of muon pairs by neutrinos in the Coulomb field of the nucleus

The diagonal interaction $G_{\mu\mu}(\bar{\nu}\mu)(\bar{\mu}\nu)$ must result in the elastic scattering $\nu\mu \to \nu\mu$. There being no muonic targets, this process cannot be observed

directly in experiments. Information about this interaction can be extracted by studying the process

$$\nu + Z \to \nu + \mu^+ + \mu^- + Z$$

taking place in the Coulomb field of a nucleus with charge Z (fig. 16.10). The cross section for this process can be estimated rather easily at asymptotically high energies if calculations are carried out in two steps. The first step consists in calculating the muon pair production cross section in the neutrino collision with a real photon, $\nu\gamma \to \nu\mu^+\mu^-$. It is found to be

$$\sigma_\phi \approx \frac{2\alpha G_{\mu\mu}^2 s}{9\pi^2}\left(\ln\frac{s}{4\mu^2}\right).$$

Here $G_{\mu\mu}$ is the interaction constant: $G_{\mu\mu}\left(\bar{\nu}_\mu\gamma_\alpha\left(1+\gamma_5\right)\mu\right)\left(\bar{\mu}\gamma^\alpha\left(1+\gamma_5\right)\nu_\mu\right)$, $s = (k+q)^2$ where k and q are the neutrino and photon 4-momenta, respectively, and μ is the muon mass. This expression is valid for $s \gg 4\mu^2$.

At the second stage the cross section obtained must be multiplied by the probability of finding a virtual photon γ in the Coulomb field of the nucleus with such 4-momenta q that the total energy of ν and γ in their center-of-mass frame is $\sqrt{}$ s. It can be shown that this probability is

$$\mathrm{d}^2 n\left(q^2, s\right) \approx \frac{Z^2\alpha}{\pi}\frac{\mathrm{d}q^2}{q^2}\frac{\mathrm{d}s}{s}.$$

Integration over the photon mass (over $\mathrm{d}q^2$) yields

$$\mathrm{d}n(s) = \frac{Z^2\alpha}{\pi}\,\mathrm{d}s\ln\frac{Q_{\max}^2}{Q_{\min}^2}.$$

Here $Q_{\min}$ is determined by the threshold of the $\nu\gamma_{\mathrm{v}} \to \nu\mu^+\mu^-$reaction (the subscript v indicates that the photon is virtual). If we take into account that the energy transferred by the photon is much smaller than its momentum ($q_0 \sim q^2/2M$ where M is the nucleus mass) then the threshold condition

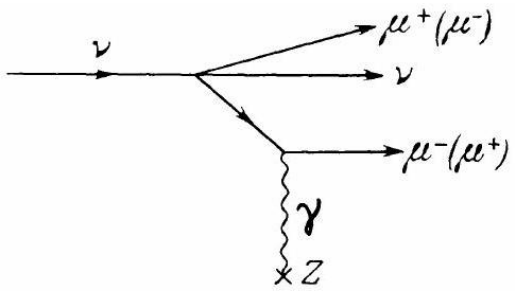


Fig. 16.10.

takes the form

$$4\mu^2 = \left(k + q_{\min}\right)^2 \approx 2kq_{\min} \approx -2\boldsymbol{k}\cdot\boldsymbol{q}_{\min} \le 2\omega Q_{\min},$$

where ω is the neutrino energy in the laboratory reference frame, and $Q = |\boldsymbol{q}|$.

The quantity $Q_{\max}$ characterizes the maximum momentum that can be transferred to the nucleus without causing it to disintegrate (this requirement means that the process must occur in the Coulomb field of the nucleus as a whole). By order of magnitude, $1/Q_{\max}$ is equal to the nucleus radius:

$$Q_{\max} = m_\pi A^{-1/3},$$

where m_π is the π-meson mass, and A is the total number of nucleons in the nucleus. Finally,

$$\sigma\left(\nu \mathrm{Z} \to \nu\mu^+\mu^- \mathrm{Z}\right) = \int_{4\mu}^{2\omega Q_{\max}} \sigma_\phi n(s) \mathrm{d}s \approx \frac{2Z^2\alpha^2 G_{\mu\mu}^2(2\omega) m_\pi A^{-1/3}}{9\pi^3} \ln\frac{2\omega m_\pi A^{-1/3}}{4\mu^2}$$

This expression holds only when the logarithm is substantially greater than unity, that is when the energy is high enough above threshold. We see that the modulus of the photon effective mass is of the order of $Q_{\max} = m_\pi A^{-1/3}$. Numerical calculations of the cross section $\sigma\left(\nu \mathrm{Z} \to \nu\mu^+\mu^- \mathrm{Z}\right)$, not for the asymptotic but for really feasible neutrino energies, are available in the literature. According to these calculations the production cross section for a muon pair in a neutrino beam with energy 50 GeV colliding with an iron nucleus ($Z = 26, A = 56$) is approximately $3 \cdot 10^{-40}$ cm$^2 \left(G_{\mu\mu}/G\right)^2$. (Our asymptotic formula gives the cross section smaller by a factor of about 1.5. One of the factors causing this difference is the fact that the value of the radius assumed in the numerical calculation was not exactly equal to $m_\pi A^{-1/3}$.)

So far the process in question has not been observed. The data available yield only an upper bound for $G_{\mu\mu} : G_{\mu\mu} \lesssim 7G$. Observation of the process $\nu_\mu \mathrm{Z} \to \mu^+\mu^-\nu\mathrm{Z}$, measurement of $G_{\mu\mu}$ and of the ratio of the vector to axial constants in the expression $G_{\mu\mu}\bar{\nu}\gamma_\alpha\left(1+\gamma_5\right)\nu\bar{\mu}\left[\gamma_\alpha + \left(g_\mathrm{A}/g_\mathrm{v}\right)\gamma_\alpha\gamma_5\right]\mu$ (to simplify the expressions we have assumed $g_\mathrm{A}/g_\mathrm{V} = 1$) are of great interest from the standpoint of testing μ-e universality.

5.17 17 Neutrino-nucleon interactions

This chapter is mostly devoted to neutrino-nucleon interactions which are due to charged currents (to specify the analysis, we single out the reactions produced by the muon neutrino).

5.17.1 17.1. Kinematics

The process of the neutrino-nucleon interaction is usually described in terms of kinematic variables shown in fig. 17.1 where $k = (E, \boldsymbol{k})$ and $k' = (E', \boldsymbol{k'})$ are the 4 -momenta of the initial and final lepton, p is the nucleon 4 momentum, p' is the 4-momentum of the final hadron state h , and $q = k - k' = p' - p$ is the 4 -momentum carried by the W -boson. Usually three invariant variables, ν, Q^2 and W, are introduced.

$$\nu = qp/m = E - E',$$

where m is the nucleon mass. Consequently, ν is the total energy carried away by the final hadrons (in the literature the symbol ν sometimes stands for qp).

$$Q^2 \equiv -q^2 = -\left(k - k'\right)^2 = 2EE'\left(1 - v'\cos\theta\right)$$

where θ is the angle between the muon and neutrino momenta in the laboratory reference frame, v' is the muon velocity ($v' \simeq 1$ at high energies).

$$W^2 = \left(p'\right)^2 = (p+q)^2 = m^2 + 2m\nu - Q^2.$$

Thus, W is the mass of the final hadron state. We observe that the variable W^2 is an explicit function of ν and Q^2. Distinct kinematic regions are shown in fig. 17.2 in the ($Q^2, \nu m$) plane. The line $W = m$ corresponds to quasi-elastic scattering reactions (h = N):

$$\nu_\mu + \mathrm{n} \to \mu^- + \mathrm{p},$$
$$\bar{\nu}_\mu + \mathrm{p} \to \mu^+ + \mathrm{n}.$$

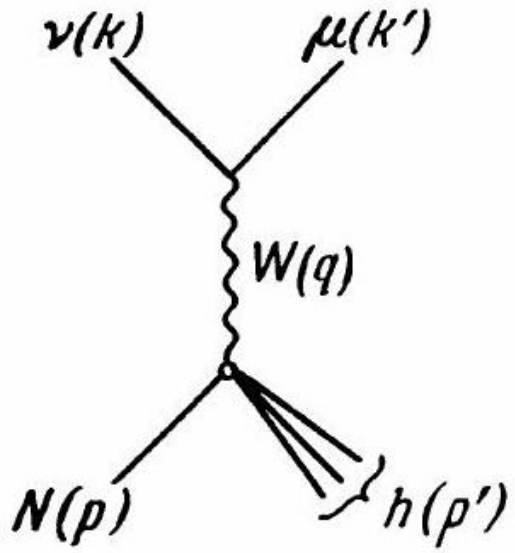


Fig. 17.1.

To the left of this line, the region is kinematically forbidden. The line $W = m + m_\pi$ traces the threshold of inelastic reactions of the type

$$\nu + \mathrm{N} \to \mu + \mathrm{N} + \pi.$$

Dashed lines correspond to production of a number of hadronic resonances ($\mathrm{h} = \mathrm{N}^*, \Delta$), for instance

$$\nu_\mu + \mathrm{p} \to \mu^- + \Delta^{++}.$$

The hatched area gives the lower left-hand part of the deep-inelastic region. In this region both ν and Q^2 are large and multiple production of hadrons takes place.

5.17.2 17.2. Quasi-elastic scattering

The quasi-elastic scattering cross section at low energies (for instance, that of the reactor-produced neutrino) is written without difficulty by analogy with the ν e-scattering cross section (see Chapter 16):

$$\sigma\left(\bar{\nu}_\mathrm{e}\mathrm{p} \to \mathrm{ne}^+\right) = \frac{G^2\left(g_\mathrm{V}^2 + 3g_\mathrm{A}^2\right)E^2}{\pi}$$

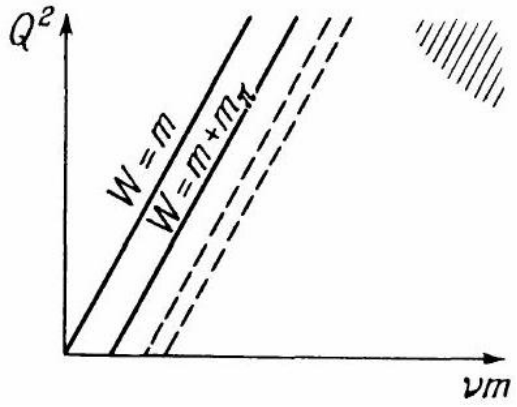


Fig. 17.2.

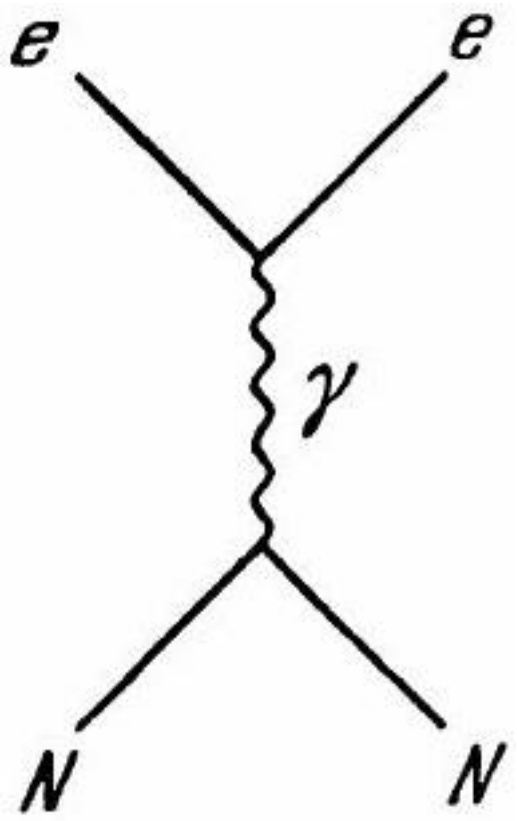


Fig. 17.3.

(we have assumed above that $m_{\rm p} \gg E \gg m_{\rm e}$). The constants $g_{\rm V}$ and $g_{\rm A}$ are those of the neutron β-decay: $g_{\rm V} = 1, g_{\rm A} = 1.25$. If nucleons were structureless point-like particles, the quadratic growth of the cross section would change to be linear at $E \gg m_{\rm p}$. However, when E is of the order of 1 GeV , the nucleon form factor becomes effective and cuts off high values of Q^2. Experiment indicates that both the vector and axial form factors are dipole in form, namely

$$g_{\rm V}^2 \frac{1}{\left(1 + Q^2/m_{\rm V}^2\right)^2}, \quad g_{\rm A}^2 \frac{1}{\left(1 + Q^2/m_{\rm A}^2\right)^2},$$

with $m_{\rm V} \simeq 0.84$GeV and $m_{\rm A} \simeq 0.9$GeV. As a result, beginning with energies of the order of 1 GeV , the neutrino-nucleon quasi-elastic interaction cross section asymptotically tends to

the level of approximately 10^{-38}cm^2. (Let us remark that approximately the same axial form factor with the same value of m_A was found in the case of $\nu_\mu p \to \mu^- \Delta^{++}$).

It is important to emphasize that by virtue of the isotopic properties of the ud current the vector form factor in quasi-elastic neutrino reactions must coincide with the electromagnetic isovector form factor of the nucleon, measured in experiments on scattering of electrons by nucleons (fig. 17.3). Experiment confirms this prediction of the theory. Experiments on deepinelastic scattering have demonstrated a still more profound relationship between electromagnetic and weak processes. This is discussed in the next section.

5.17.3 17.3. Partons

The experiments on deep-inelastic electroproduction carried out of Stanford in 1967 have led to the discovery that the cross section at high Q^2 and ν does not decrease with increasing Q^2, and is a function of the dimensionless

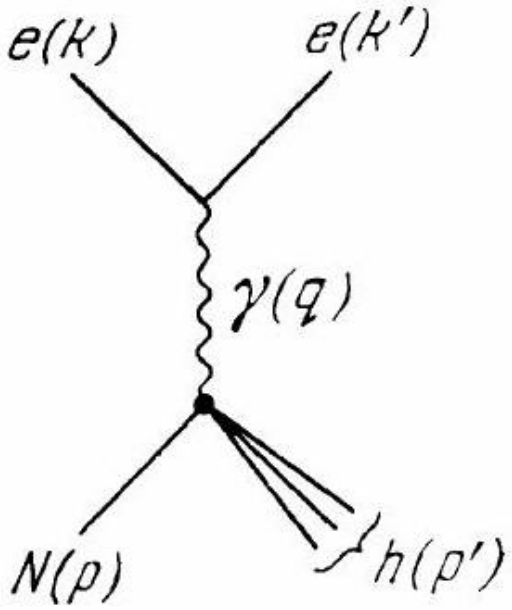


Fig. 17.4.

variables $x = Q^2/2m\nu$ and $y = 2m\nu/s$, where $s = (k+p)^2$ (kinematic variables are defined as in the case of neutrino reactions (compare figs. 17.1 and 17.4)). In a sense, this discovery resembled that of the atomic nucleus in the Rutherford-Marsden experiments when it was found that the cross section of α-particle scattering by an atom at high momentum transfer is not small. In the case of α-particle scattering, high momentum is transferred to a "point-like" atomic nucleus; in the case of electroproduction, high momentum is transferred to point-like particles forming the nucleon. Feynman coined for these parts of the nucleon the name "partons".

The partons in the nucleon are quarks (and gluons). Mostly, nucleons consist of three quarks, called valence quarks. However, according to the uncertainty relation, the three valence quarks could be joined for short duration by quark-antiquark pairs. Such pairs form the so-called quarkantiquark sea. In addition, gluons are also present in the nucleon. The momentum of a fast nucleon is therefore carried by quarks, antiquarks, and gluons. Deep-inelastic scattering occurs when a lepton collides with a quark or an antiquark. By virtue of the asymptotic freedom of quantum chromodynamics, at high Q^2 and ν a light quark can be considered in the zero approximation as a free and practically massless particle.

5.17.4 17.4. Kinematics of lepton-parton collisions

Let us consider a collision of a fast nucleon and a lepton. As compared to the quark longitudinal momentum, its transverse momentum at high energies can be neglected. Denote the quark 4 -momentum by xp where p is the nucleon 4 -momentum, and $0 \leq x \leq 1$. First find $\hat{s}$, that is the squared center-of-mass total energy of the lepton and quark:

$$\hat{s} = (xp + k)^2 \simeq x \cdot 2pk \simeq x \cdot s.$$

As a result of the collision, the quark momentum changes to

$$k + px - k' = q + px.$$

The parton mass being zero, we obtain

$$(q + px)^2 = q^2 + x \cdot 2pq = 0$$

hence,

$$x = -\frac{q^2}{2pq} = \frac{Q^2}{2\nu m}.$$

We find that in terms of the parton model, the quantity x introduced in the preceding section has a straightforward interpretation. The quantity y also has a simple meaning. Indeed, $y = 2m\nu/s = 2pq/2pk = \nu/E$, that is y gives the fraction of the initial neutrino energy carried away by the hadrons. Denoting the lepton scattering angle in the lepton-quark center-of-mass frame by $\hat{\theta}$, we obtain

$$\begin{aligned} y = \frac{2m\nu}{s} = \frac{Q^2}{x \cdot s} = -\frac{(k - k')^2}{x \cdot s} = -\frac{\hat{t}}{\hat{s}} \\ = \frac{\hat{s}(1 - \cos\theta)}{2\hat{s}} = \frac{1 - \cos\hat{\theta}}{2} = \sin^2\frac{1}{2}\hat{\theta} \end{aligned}$$

What is the mechanism by which the elastic scattering of a lepton by a quark results in the inelastic scattering of the lepton by the nucleon? Let us resort to an analogy: imagine an atom instead of a nucleon, and one of the electrons of this atom instead of the parton. A knocked-out electron is a result of the inelastic ionization of the atom. The emitted electron is observable; but what is the fate of a knocked-out parton (quark)? The lepton-quark collision occurs at a small distance (Q^2 is high) where quarks are nearly free; as the quarks move away, however, they interact more and more strongly, exchanging soft gluons and producing $q\bar{q}$ pairs in vacuum. As a result, a fast colored quark generates a white hadron jet. This very complicated process, closely related to the mechanism of color confinement, is referred to as the hadronic fragmentation of the parton.

5.17.5 17.5. Lepton-parton collision cross sections

The partons being point-like particles, the lepton-parton interaction is described by the same formulas as the lepton-lepton interaction. We recall that the νe and $\bar{\nu}e$ charged current scattering cross sections for the total
center-of-mass energy $\sqrt{s}$ are equal, respectively, to

$$\frac{\mathrm{d}\sigma}{\mathrm{d}y} = \frac{G^2 s}{\pi} \quad \text{for } \nu\mathrm{e} \to \nu\mathrm{e}$$

and

$$\frac{\mathrm{d}\sigma}{\mathrm{d}y} = \frac{G^2 s}{\pi}(1-y)^2 \quad \text{for } \bar{\nu}\mathrm{e} \to \bar{\nu}\mathrm{e},$$

where $y = E_2/\omega$. These differential cross sections are plotted in fig. 17.5. We easily notice that cross sections for collisions of ν and $\bar{\nu}$ with quarks and antiquarks differ only in the trivial factors $\cos^2\theta_\mathrm{C}$ and $\sin^2\theta_\mathrm{C}$ (θ_C is the Cabibbo angle) and in the substitution $s \to sx$:

Processes

$\nu_\mu \mathrm{d} \to \mathrm{u}\mu^-$,	$\bar{\nu}_\mu \overline{\mathrm{d}} \to \overline{\mathrm{u}}\mu^+$	$\cos^2\theta_\mathrm{C}$	$\cos^2\theta_\mathrm{C}$
$\nu_\mu \mathrm{s} \to \mathrm{u}\mu^-$,	$\bar{\nu}_\mu \overline{\mathrm{s}} \to \overline{\mathrm{u}}\mu^+$	$\sin^2\theta_\mathrm{C}$	$\sin^2\theta_\mathrm{C}$
$\nu_\mu \overline{\mathrm{u}} \to \overline{\mathrm{d}}\mu^-$,	$\bar{\nu}_\mu \mathrm{u} \to \mathrm{d}\mu^+$	$(1-y)^2\cos^2\theta_\mathrm{C}$	$\frac{1}{3}\cos^2\theta_\mathrm{C}$
$\nu_\mu \overline{\mathrm{u}} \to \overline{\mathrm{s}}\mu^-$,	$\bar{\nu}_\mu \mathrm{u} \to \mathrm{s}\mu^+$	$(1-y)^2\sin^2\theta_\mathrm{C}$	$\frac{1}{3}\sin^2\theta_\mathrm{C}$
$\nu_\mu \mathrm{u} \to \mathrm{d}\mu^+$,	$\bar{\nu}_\mu \overline{\mathrm{u}} \to \overline{\mathrm{d}}\mu^-$	0	0
$\nu_\mu \mathrm{u} \to \mathrm{s}\mu^+$,	$\bar{\nu}_\mu \overline{\mathrm{u}} \to \overline{\mathrm{s}}\mu^-$	0	0
$\nu \mathrm{u} \to \mathrm{d}\mu^-$,	$\bar{\nu}_\mu \overline{\mathrm{u}} \to \overline{\mathrm{d}}\mu^+$	0	0
$\nu \mathrm{u} \to \mathrm{s}\mu^-$,	$\bar{\nu}_\mu \overline{\mathrm{u}} \to \overline{\mathrm{s}}\mu^+$	0	0

Here $\sigma = \int_0^1 (\,\mathrm{d}\sigma/\mathrm{d}y)\mathrm{d}y$. Also note that the factors $\frac{1}{3}$ appear because $\int_0^1 (1-y)^2\,\mathrm{d}y = \frac{1}{3}$. Selection rules in the last two rows stem from electric charge conservation, and those in the two preceding rows from leptonic charge conservation.

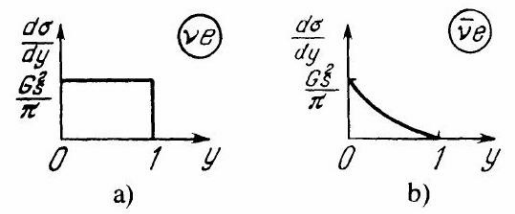


Fig. 17.5.

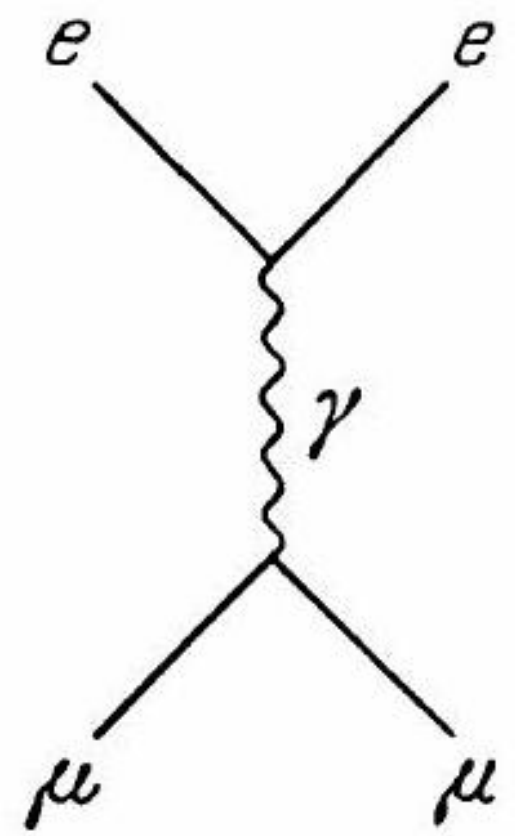


Fig. 17.6.

Now let us consider the electromagnetic cross sections. The electron-muon scattering differential cross section (see fig. 17.6) has the form

$$\frac{\mathrm{d}\sigma^{\gamma}}{\mathrm{d}y} = \frac{4\pi\alpha^2}{2s}\frac{s^2+u^2}{t^2} = \frac{2\pi\alpha^2}{s}\frac{1+(1-y)^2}{y^2}.$$

The cross section for electron scattering by a u - (or $\bar{u}$-) quark differs from the above expression by a factor of $\frac{4}{9}$, and that by $\mathrm{d}-, \mathrm{s}-, \mathrm{d}-$, and $\bar{\mathrm{s}}$-quarks by a factor of $\frac{1}{9}$. (Let us trace the relationship between the cross sections of the $\mathrm{e}^-\mu^- \to \mathrm{e}^-\mu^-$and $\nu\mathrm{e} \to \nu\mathrm{e}$ processes. Four helicity configurations, LL, RR, LR, and RL, contribute to the former. Their contributions do not interfere at $v \to c$ and are proportional to s^2 for LL and RR, and to u^2 for LR and RL. The factor t^2 in the denominator appears because of the photon propagator, and s because of the relativistic normalization of the cross section. The coefficient $2\pi\alpha^2$ is easily obtained if we compare the contributions of LL to the cross sections of $\nu\mathrm{e}$ and $\mathrm{e}\mu$ scattering. Namely, $(G/\sqrt{2})^2$ is replaced by $(4\pi\alpha)^2/t^2 2^5$, since $\gamma_\mu = \frac{1}{2}\gamma_\mu(1+\gamma_5) + \frac{1}{2}\gamma_\mu(1-\gamma_5)$, and because averaging takes place over spin states of the initial electron but not over those of the neutrino. Hence, the contribution of the LL configuration is $4\pi\alpha^2 s/4t^2$, and the total contribution of LL + RR is twice as large).

5.17.6 17.6. Parton distributions

In order to give a formula for the cross section for the deep-inelastic lepton-nucleon interaction, we need the distributions of quarks and antiquarks in nucleons. The number of u-quarks in the range from x to $x + \mathrm{d}x$ is usually denoted by $u(x)\mathrm{d}x/x$ (and sometimes by $u(x)\mathrm{d}x$). In our notation, $xu(x)\mathrm{d}x/x = u(x)\mathrm{d}x$ is the fraction of the total proton momentum carried by

u-quarks with values of x within the dx interval. Similarly,
$d(x)$ and $s(x)$ describe the corresponding quantities for d - and s-quarks, and $\bar{u}(x), \bar{d}(x)$, and $\bar{s}(x)$ for the respective antiquarks (all this for the proton!).

The isotopic symmetry (symmetry with respect to the $T_3 \to -T_3$ operation) states that in the neutron, $u(x)$ refers to d-quarks, $d(x)$ to u-quarks, $s(x)$ to s-quarks, and $\bar{u}(x), \bar{d}(x), \bar{s}(x)$ to $\overline{\mathrm{d}}, \overline{\mathrm{u}}$, and $\overline{\mathrm{s}}$-quarks, respectively.

A number of sets of six quark and antiquark distribution functions, $q_i(x)$, can be found in the literature. These sets are basically similar and differ only in minor details. All were obtained by processing the deep-inelastic experimental data by means of parton formulas given in the next section. One of such sets is schematically shown in fig. 17.7.

Denote the total relative momentum carried by all u-quarks in the proton by $U \equiv fu(x)\mathrm{d}x$, and introduce similar symbols for all other quarks and antiquarks. The distributions shown in fig. 17.7 correspond to the following values of the total relative momenta:

$$U \simeq 0.28, \quad D \simeq 0.15, \quad \bar{U} \simeq \bar{D} \simeq 0.03, \quad S \simeq \bar{S} \simeq 0.01.$$

The sum of relative momenta of all quarks and antiquarks are, respectively:

$$\begin{aligned} Q = U + D + S &\equiv \int_0^1 [u(x) + d(x) + s(x)]\mathrm{d}x \\ &\equiv \int_0^1 q(x)\mathrm{d}x \cong 0.44 \\ \bar{Q} = \bar{U} + \bar{D} + \bar{S} &\equiv \int_0^1 [\bar{u}(x) + \bar{d}(x) + \bar{s}(x)]\mathrm{d}x \\ &\equiv \int_0^1 \bar{q}(x)\mathrm{d}x \cong 0.07 \end{aligned}$$

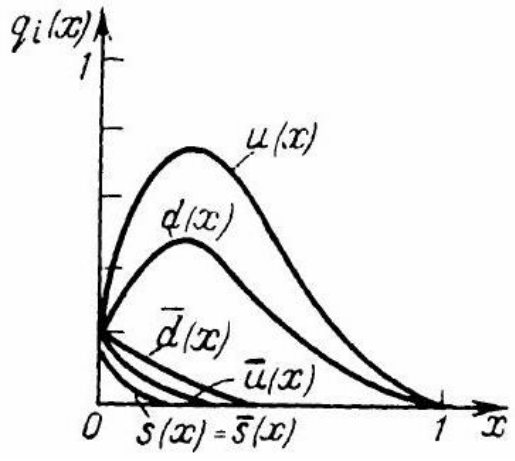


Fig. 17.7.

so that approximately one half of the proton momentum is carried by quarks and antiquarks, and the other half by gluons. Usually the quark-antiquark ratio is characterized by $\alpha = \bar{Q}/(Q + \bar{Q})$ or by $B = (Q - \bar{Q})/(Q + \bar{Q}) = 1 - 2\alpha$. High-energy neutrino experiments yield

$$\alpha \simeq 0.15, \quad B \simeq 0.70.$$

The same experiments demonstrate that

$$q(x) - \bar{q}(x) \sim \sqrt{x}(1-x)^n, \quad \text{where } n \cong 3.5$$
$$\bar{q}(x) + \bar{s}(x) \sim (1-x)^m, \quad \text{where } m \cong 6.5$$

Note that quark distributions must satisfy the following obvious conditions:

$$\int_0^1 [u(x) - \bar{u}(x)]\frac{\mathrm{d}x}{x} = 2$$
$$\int_0^1 [d(x) - \bar{d}(x)]\frac{\mathrm{d}x}{x} = 1$$
$$\int_0^1 [s(x) - \bar{s}(x)]\frac{\mathrm{d}x}{x} = 0$$

The right-hand sides of these equations yield the number of u, d, and s valence quarks in the proton.

5.17.7 17.7. Cross sections of deep-inelastic processes

Let us write down the cross sections $\mathrm{d}^2\sigma/\mathrm{d}x\ \mathrm{d}y$ of some deep-inelastic processes occurring in collisions of leptons with the proton (p), neutron (n), and "mean nucleon" (N) (the last of these refers to a nucleus with an equal number of protons and neutrons):

$$\begin{aligned}
\mathrm{ep} \to \mathrm{eh}: &\quad \tfrac{2\pi\alpha^2}{s}\tfrac{1+(1-y)^2}{x^2y^2}\left[\tfrac{4}{9}(u(x)+\bar{u}(x)) + \tfrac{1}{9}(d(x)\right. \\
&\quad \left. +\bar{d}(x)) + \tfrac{1}{9}(s(x)+\bar{s}(x))\right] \\
\mathrm{en} \to \mathrm{eh}: &\quad \tfrac{2\pi\alpha^2}{s}\tfrac{1+(1-y)^2}{x^2y^2}\left[\tfrac{4}{9}(d(x)+\bar{d}(x)) + \tfrac{1}{9}(u(x)\right. \\
&\quad \left. +\bar{u}(x)) + \tfrac{1}{9}(s(x)+\bar{s}(x))\right]
\end{aligned}$$

$$\begin{aligned}
\nu\mathrm{p} \to \mu^-\mathrm{h}: &\quad \tfrac{G^2 s}{\pi}\left[d(x) + s(x) + \bar{u}(x)(1-y)^2\right], \\
\nu\mathrm{p} \to \mu^+\mathrm{h} &\quad \tfrac{G^2 s}{\pi}\left[u(x)(1-y)^2 + \bar{d}(x) + \bar{s}(x)\right], \\
\nu\mathrm{n} \to \mu^-\mathrm{h}: &\quad \tfrac{G^2 s}{\pi}\left[u(x) + s(x) + \bar{d}(x)(1-y)^2\right], \\
\bar{\nu}\mathrm{n} \to \mu^+\mathrm{h}: &\quad \tfrac{G^2 s}{\pi}\left[d(x)(1-y)^2 + \bar{u}(x) + \bar{s}(s)\right], \\
\nu\mathrm{N} \to \mu^-\mathrm{h}: &\quad \tfrac{G^2 s}{2\pi}[u(x) + d(x) + 2s(x) \\
&\quad +(\bar{u}(x) + \bar{d}(x))(1-y)^2], \\
\bar{\nu}\mathrm{N} \to \mu^+\mathrm{h}: &\quad \tfrac{G^2 s}{2\pi}\left[(u(x) + d(x))(1-y)^2\right. \\
&\quad \left. +\bar{u}(x) + \bar{d}(x) + 2\bar{s}(x)\right].
\end{aligned}$$

These expressions hold at energies substantially above the production threshold of charmed particles. It is for this reason that they do not contain $\cos^2\theta_\mathrm{C}$ or $\sin^2\theta_\mathrm{C}$. By integrating over $\mathrm{d}x$ and $\mathrm{d}y$ we obtain the total cross sections of the $\bar{\nu}$ and ν interaction with the "mean nucleon":

$$\sigma\left(\bar{\nu}\mathrm{N} \to \mu^+\mathrm{h}\right) \cong \frac{G^2 s}{2\pi}\left[\frac{1}{3}(Q+S) + (\bar{Q} - \bar{S})\right] \cong \frac{G^2 s}{\pi}0.10$$
$$\sigma\left(\nu\ \mathrm{N} \to \mu^-\mathrm{h}\right) \cong \frac{G^2 s}{2\pi}\left[(Q+S) + \frac{1}{3}(\bar{Q} - \bar{S})\right] \cong \frac{G^2 s}{\pi}0.22$$

The ratio of these cross sections is close to 0.5 . Note that it would be nearly $\frac{1}{3}$ if nucleons contained no antiquarks.

5.17.8 17.8. Production of strange and charmed particles

This section is devoted to the production of a hadronic "spray" containing one strange or one charmed particle. Denote by h_s ($h_{\bar{s}}$) a final hadronic state containing a single strange particle

with strangeness $S = -1 (S = +1)$ and an arbitrary number of ordinary hadrons (π-mesons and nucleons). Let
us consider the cross sections $\mathrm{d}^2\sigma/\mathrm{d}x\ \mathrm{d}y$ of the following processes:

$$\begin{aligned}
\nu\mathrm{p} \to \mu^-\mathrm{h}_{\bar{\mathrm{s}}}: &\quad \tfrac{G^2 s}{\pi}\bar{u}(x)(1-y)^2\sin^2\theta_\mathrm{C}\\
\nu\mathrm{n} \to \mu^-\mathrm{h}_{\bar{\mathrm{s}}}: &\quad \tfrac{G^2 s}{\pi}\bar{d}(x)(1-y)^2\sin^2\theta_\mathrm{C}\\
\bar{\nu}\mathrm{p} \to \mu^+\mathrm{h}_{\mathrm{s}}: &\quad \tfrac{G^2 s}{\pi}u(x)\sin^2\theta_\mathrm{C}\\
\bar{\nu}\mathrm{n} \to \mu^+\mathrm{h}_{\mathrm{s}}: &\quad \tfrac{G^2 s}{\pi}d(x)\sin^2\theta_\mathrm{C}
\end{aligned}$$

We notice that in $\bar{\nu}$-beams, strange particles are produced on u- and d -quarks, and in ν-beams on $\overline{\mathrm{u}}$ - and $\overline{\mathrm{d}}$-quarks. The momentum carried by quarks is much larger than that of antiquarks, so that production of strange particles must be much more abundant in antineutrino beams. This conclusion is born out by experiment.

We shall discuss now the production of charmed particles. Denote the final hadronic state, containing a single charmed particle with $C = +1 (C = -1)$, by $\mathrm{h_c}\,(\mathrm{h}_{\bar{\mathrm{c}}})$. We have for $\mathrm{d}^2\sigma/\mathrm{d}x\ \mathrm{d}y$:

$$\begin{aligned}
\nu\mathrm{p} \to \mu^-\mathrm{h_c}: &\quad \tfrac{G^2 s}{\pi}\left[d(x)\sin^2\theta_\mathrm{C} + s(x)\cos^2\theta_\mathrm{C}\right],\\
\nu\mathrm{n} \to \mu^-\mathrm{h_c}: &\quad \tfrac{G^2 s}{\pi}\left[u(x)\sin^2\theta_\mathrm{C} + s(x)\cos^2\theta_\mathrm{C}\right],\\
\bar{\nu}\mathrm{p} \to \mu^+\mathrm{h}_{\bar{\mathrm{c}}}: &\quad \tfrac{G^2 s}{\pi}\left[\bar{d}(x)\sin^2\theta_\mathrm{C} + \bar{s}(x)\cos^2\theta_\mathrm{C}\right](1-y)^2,\\
\bar{\nu}\mathrm{n} \to \mu^+\mathrm{h}_{\bar{\mathrm{c}}}: &\quad \tfrac{G^2 s}{\pi}\left[\bar{u}(x)\sin^2\theta_\mathrm{C} + \bar{s}(x)\cos^2\theta_\mathrm{C}\right](1-y)^2.
\end{aligned}$$

The formulas are valid only at energies so high that the c-quark mass can be neglected, that is when $x \gg m_\mathrm{c}^2/s$. At smaller x, the threshold supression of the cross section takes place. The corresponding formulas are easily derived by using the expression for the cross section of the $\nu_\mu\mathrm{e} \to \mu^-\nu_\mathrm{e}$ and $\bar{\nu}_\mathrm{e}\mathrm{e} \to \mu^+\nu_\mu$ processes (see chapter 16).

We see that a neutrino beam is a better generator of charmed particles than a beam of antineutrinos. Production of charmed particles by a neutrino beam on the "mean nucleon" must come to about 10% of the total cross section, that is to $\simeq \sin^2\theta_\mathrm{C} + 2S/(U+D)$. It has been mentioned in chapter 14 that the production and subsequent decay of the charmed quark results in so-called dileptonic events. In most cases these events involve a strange particle since the c-quark decay mostly produces the s-quark.

5.17.9 17.9. Phenomenology of deep-inelastic processes

Consider now the general form of the cross section of the deep-inelastic neutrino-nucleon interaction without resorting to the parton model. We shall use only the argument that the weak interaction is due to the product of two left-handed currents, leptonic and hadronic. In calculating the squared modulus of the amplitude, we deal with the product of the leptonic and hadronic tensors. The leptonic tensor is written in the form

$$\begin{aligned}
L^{\mu\nu} &= \frac{1}{8}\,\mathrm{Tr}\,\gamma^\mu\,(1 \pm \gamma_5)\,\hat{k}\gamma^\nu\,(1 \pm \gamma_5)\,\hat{k}'\\
&= k^\mu k'^\nu + k^\nu k'^\mu - g^{\mu\nu}kk' \pm i\varepsilon^{\mu\nu\alpha\beta}k_\alpha k'_\beta.
\end{aligned}$$

Here the upper sign (+) refers to the neutrino and the lower sign (-) to the antineutrino (see the momentum notation in fig. 17.1). If we neglect the muon mass, then those terms of the hadronic tensor $H_{\mu\nu}$ which are proportional to $q_\mu = (k-k')_\mu$ and q_ν give zero after multiplication by $L^{\mu\nu}$. Only three terms give non-zero contributions, and the cross section can be written as

$$\frac{\mathrm{d}^2\sigma}{m\ \mathrm{d}Q^2\ \mathrm{d}\nu} = \frac{G^2}{\pi(2mE)^2} L^{\mu\nu} H_{\mu\nu}$$
$$= \frac{G^2}{\pi(2mE)^2} L^{\mu\nu} \left[-W_1 g_{\mu\nu} + W_2 \frac{p_\mu p_\nu}{m^2} - \frac{i}{2m^2} W_3 \varepsilon_{\mu\nu\rho\sigma} p^\rho q^\sigma \right],$$

where p is the nucleon 4 -momentum, m is its mass, E is the neutrino energy, $2mE = s - m^2$, and W_1, W_2, W_3 are dimensionless functions of $Q^2 = -q^2$ and $\nu = qp/m$. Multiplication of the tensors yields

$$\frac{\mathrm{d}^2\sigma}{m\ \mathrm{d}Q^2\ \mathrm{d}\nu} = \frac{G^2}{(2mE)^2} \left[W_1 Q^2 + W_2 \frac{2(pk)\,(pk') - m^2\,(kk')}{m^2} \right.$$
$$\left. \mp W_3 \frac{(pk)\,(qk') - (pk')\,(qk)}{m^2} \right]$$
$$= \frac{G^2}{2\pi m^2} \frac{E'}{E} \left[2W_1 \sin^2 \frac{1}{2}\theta + W_2 \cos^2 \frac{1}{2}\theta \right.$$
$$\left. \mp W_3 \frac{E + E'}{m} \sin^2 \frac{1}{2}\theta \right]$$
$$\cong \frac{G^2}{\pi s^2} \left[W_1 Q^2 + W_2 \frac{s(s - 2m\nu)}{2m^2} \mp W_3 \frac{Q^2(s - \nu m)}{2m^2} \right].$$

(We have made use of the fact that $Q^2 = 4EE' \sin^2 \frac{1}{2}\theta, s \cong 2mE, qk' = -qk = +kk' = -\frac{1}{2}q^2 = +\frac{1}{2}Q^2$.) For high Q^2 and ν, that is in the range of scaling invariance (the so-called Bjorken scaling), the quantities W_1, $W_2\nu/m, W_3\nu/m$ are functions of a single dimensionless variable $x = Q^2/2m\nu$:

$$W_1 = F_1(x),$$
$$\frac{\nu}{m} W_2 = F_2(x),$$
$$\frac{\nu}{m} W_3 = F_3(x).$$

We then easily obtain that in this case

$$\frac{\mathrm{d}^2\sigma^{\nu,\tilde{\nu}}}{\mathrm{d}x\ \mathrm{d}y} = \frac{G^2 s}{2\pi} \left[F_1(x) x y^2 + F_2(x)(1 - y) \mp F_3(x) x y \left(1 - \frac{1}{2} y \right) \right].$$

This expression coincides with the parton cross sections for the "mean nucleon" if

$$2xF_1(x) = F_2(x) = q(x) + \bar{q}(x),$$
$$-xF_3(x) = q(x) - \bar{q}(x).$$

(We have neglected the contribution of the s-quarks.) The first of these formulas is referred to as the Callan-Gross relation. It is a corollary of the quark spin being equal to $\frac{1}{2}$.

5.17.10 17.10. The parton model and quantum chromodynamics

According to quantum chromodynamics, scaling is not absolute even for $Q^2 \to \infty, \nu \to \infty$, and $F_i(x)$ must be a logarithmic function of Q^2. The necessity of this violation of scaling is easily understood if we take into account that quarks are not completely free and may emit bremsstrahlung gluons. Indeed, the strong-interaction constant α_s falls off only logarithmically as Q^2 increases. This violation of scaling results in the total momentum of quarks being a slowly decreasing function, and that of gluons and antiquarks a slowly increasing function of Q^2.

5.18 18 Renormalizability

The preceding chapters were devoted to weak processes at low energies ($Gs \ll 1$), and the calculations were limited to first order perturbation theory in the Fermi constant G. Now we start considering weak processes at high energies ($Gs \gtrsim 1$). The structure of the weak interaction was unimportant at low energies, but at high energies (at short distances) the situation is different and the intermediate vector bosons $W^{\pm}$and Z^0 mentioned at the beginning of the book now play a crucial role. We shall present the standard model of the unified electromagnetic and weak interaction (Chapter 21) based on intermediate vector bosons (Chapter 23) and on scalar (so-called Higgs) bosons (Chapter 24). This standard model gives a very good description of all data on neutral currents (Chapter 22).

Before considering the standard model, however, we shall discuss separately its main components. The present chapter deals with the requirement of renormalizability, which states that all divergences in the theory must be removable by renormalizing several physical quantities (charges and masses). This in turn requires that the cross sections of physical processes (calculated in the framework of perturbation theory) decrease sufficiently rapidly as the momentum transfer increases. This decrease is provided by the intermediate bosons $W^{\pm}$and Z^0. To achieve this, the bosons must represent gauge fields of a non-abelian group (Chapter 19) and acquire masses through spontaneous symmetry breaking (Chapter 20).

5.18.1 18.1. Why do we need renormalizability?

One could say, with a measure of snobbishness, that the requirement of renormalizability of a theory is imposed by the "handycraft" approach. The purpose of renormalizability is to give meaning to perturbation theory calculations. But why should nature worry about weak processes being adequately represented by perturbation theory? After all, perturbation theory is not more than a "poor man's" method of calculation.

At least two arguments exist which support both perturbation theory and renormalizability. The first is purely empirical: were perturbation theory invalid, one would see no basis for explaining why the vector constant in neutron β-decay is equal to the muon decay constant times $\cos\theta_C$. This equality would be violated by a large contribution due to virtual particles.

This line of reasoning can be countered, of course, by declaring this equality as absolutely accidental; but does this equality not form the foundation of the very idea of Cabibbo universality? The small width of the $K \to \mu^+\mu^-$decay, and the small difference, Δm_{LS}, of the K_L and K_S meson masses are two additional empirical manifestations of the smallness of the higher orders of perturbation theory. However, both the $K_L \to 2\mu$ decay rate and Δm_{LS} are almost independent of the physics at small distances. This became clear after the discovery of the fourth quark and after the confirmation of the Glashow-Illiopoulos-Maiani scheme. The fact is, according to this scheme, that the smallness of these effects is due to the compensation of contributions of the u- and c-quarks.

Another argument in favor of perturbation theory is of an aesthetic nature: in spite of its "non-aristocratic", "earthbound" origin (and possibly owing to it), the renormalizable theory of weak interactions is very much alive, beautiful, and enables us to obtain a number of predictions.

Renormalizability of quantum electrodynamics is known to give high accuracy in calculations of electron-photon interactions, by "burying" all ultraviolet divergences in the renormalized mass and charge of electron. This cannot be done in the case of the four-fermion interaction, since the number of ultraviolet-divergent amplitudes is infinite. This results from the m^{-2} dimension of the constant G. Therefore, a factor G is added in the next order of perturbation theory, together with the energy squared of virtual particles, E^2, which makes the product dimensionless, and has to be cut off "by hand" at a threshold Λ^2.

5.18.2 18.2. Unitarity limit

The divergence of integrals over the energy of virtual particles is closely related to the use of cross sections yielded by perturbation theory in the case of four-fermion interactions (for example, ν e scattering and $e^+e^- \to \nu\bar{\nu}$ annihilation). The fact that these processes proceed in a channel with fixed angular momentum results in violation of the unitarity condition at a certain value of energy which is called the unitarity limit.

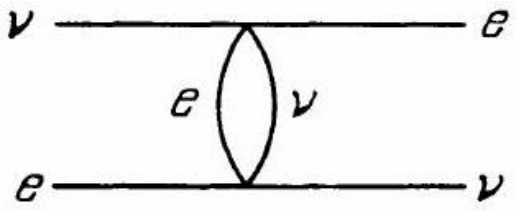


Fig. 18.1.

For example, the unitarity condition for the ν e scattering amplitude with $J = 0, f_0$, is: $|\mathrm{Re}\, f_0|^2 \leq \mathrm{Im}\, f_0 - |\mathrm{Im}\, f_0|^2$. Its right-hand side is at a maximum if $\mathrm{Im}\, f_0 = \frac{1}{2}$, which gives $|\mathrm{Re}\, f_0| \leq \frac{1}{2}$. In the lowest order of perturbation theory $f_0 = Gs/2\sqrt{2}\pi$ (only charged currents are taken into account here for the sake of simplicity) and therefore $Gs < \sqrt{2}\pi$. The energy $\sqrt{s} = \sqrt{\sqrt{2}\pi/G} \simeq 600\mathrm{GeV}$ is the unitarity limit energy for "standard" νe scattering.

The unitarity limit energy for $\bar{\nu}$ e scattering is of approximately the same order of magnitude. At energies above the unitarity limit, higher angular momenta must become important, owing to the second (fig. 18.1) and higher orders in G of perturbation theory. In the general case, the contribution of higher orders to the low-energy amplitude will not be small. Perturbation theory will be effective if the weak cross sections stop increasing long before the unitarity limit is reached.

5.18.3 18.3. Intermediate bosons

The above situation is realized if the weak interaction is mediated by the intermediate W-boson (fig. 18.2). In this case the differential cross section takes the form

$$\frac{\mathrm{d}\sigma}{\mathrm{d}|t|} = \frac{G^2}{\pi} \frac{m_{\mathrm{W}}^4}{(m_{\mathrm{W}}^2 + |t|)^2},$$

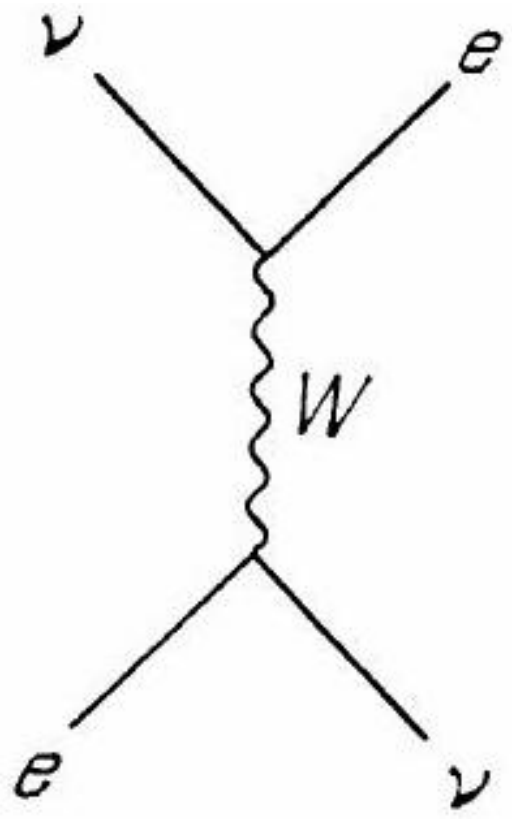


Fig. 18.2.

where the denominator corresponds to the propagator of the W-boson, and the numerator can easily be written if we demand that the "four-fermion expression"

$$\frac{\mathrm{d}\sigma}{\mathrm{d}|t|} = \frac{G^2}{\pi},$$

which gives $\sigma = G^2 s/\pi$ when integrated over $|t|$ from 0 to s, be valid at $t \to 0$. As for the total cross section corresponding to the graph of fig. 18.2, it is

$$\sigma = \int_0^s \frac{\mathrm{d}\sigma}{\mathrm{d}|t|}\mathrm{d}|t| = \frac{G^2 m_{\mathrm{W}}^2}{\pi}.$$

We see that introduction of the intermediate boson with mass m_{w} stops the growth of the weak interaction at energies of the order of m_{w}.

The coupling constant of the W-boson with the weak current being dimensionless, like electric charge, it would seem logical for the theory operating with W -bosons to be renormalizable, like quantum electrodynamics.

This is not the case, however, owing to several serious differences between the W-boson and the photon: the W-boson is massive, it is charged, and (the point of paramount importance) it is coupled to a non-conserved current. The axial current of fermions is not conserved because fermion masses are distinct from zero; and the vector current is not conserved because of the non-zero mass difference between currentproducing particles. Additionally, beyond the lowest order of perturbation theory, the weak fermion current would not be conserved even if the fermion masses were zero. To demonstrate that this is so, it is sufficient to compare a weak vertex $\bar{\nu}\mathrm{eW}^-$with an electromagnetic vertex $\bar{\mathrm{e}}\gamma$ (fig. 18.3).

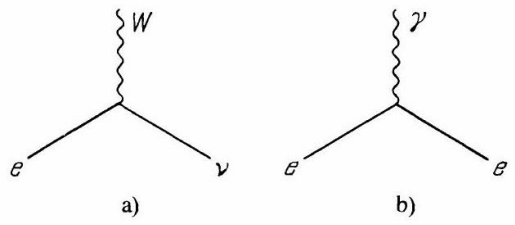


Fig. 18.3.

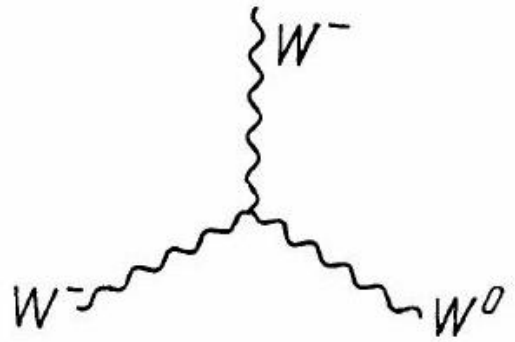


Fig. 18.4.

After emission of a photon, an electron conserves its electric charge and can emit new photons with the same efficiency. As for the weak charge, it is not transferred from the electron to the neutrino, and the neutrino cannot emit another W^-meson since this is forbidden by conservation of the electric (vertex $\bar{e}\nu W^-$) or leptonic charge ($\bar{e}^+\nu W^-$).

This means that emission of a W^-boson in the graph of fig. 18.3a is accompanied by the sudden disappearance of the weak charge responsible for the emission of the W^-boson. In order to avoid this, we have to assume that the weak charge is transferred to the W^-boson (see fig. 18.3a) which now can emit a W^-boson via the process shown in fig. 18.4. But this requires the existence, together with charged $W^\pm$bosons, of neutral W^0 bosons as well. (In one special class of theories the role of the W^0 boson is played by the photon; such theories are not discussed in this book). Before we resume the discussion of neutral bosons, let us analyse in more detail what is wrong with a non-conserved current.

5.18.4 18.4. Wave function of the vector boson

Let us consider the wave function of a vector particle represented by a four-dimensional vector A_α. This vector must satisfy the condition $k_\alpha A^\alpha = 0$ where k is the momentum of the vector boson. In the boson rest frame this condition has a very simple meaning. In this frame $k_0 A_0 = mA_0 = 0$ and hence $A_0 = 0$, that is the wave function of the vector particle is represented by a three-dimensional vector $\boldsymbol{A}$ and thus has three independent spatial components. From the normalization condition, namely $\boldsymbol{A}^2 = 1$, we obtain $A^2 = -1$. Let us now find what form the vector A will take if the boson moves, say, along the z-axis. Its 4 -momentum then is

$$k = (k_x, k_y, k_z, E) = (0, 0, |\boldsymbol{k}|, E),$$

where

$$E = \sqrt{m^2 + k^2}.$$

Obviously, a 4-vector A_α satisfying the conditions $A^2 = -1$ and $Ak = 0$, can be represented as a sum of a longitudinal and a transverse term

$$A_\alpha = L_\alpha \cos\theta + T_\alpha \sin\theta$$

where θ is the angle between the vector $\boldsymbol{A}$ in the particle rest frame and the z-axis,

$$\begin{aligned} L_\alpha &= \frac{1}{m}(0, 0, E; |\boldsymbol{k}|), \\ T_\alpha &= (t_x, t_y, 0, 0)\,, \\ t_x^2 + t_y^2 &= 1. \end{aligned}$$

The longitudinal vector L_α, with both of its components increasing with increasing energy, behaves dangerously at high energies. If this growth of longitudinal components is not suppressed, it will result in the growth of matrix elements and, finally, in non-renormalizability of the theory. To guard against this, we need conservation of the current responsible for the boson emission. Conservation of the current, $\partial_\alpha j^\alpha(x) = 0$, means that the boson emission vertex, $L_\alpha \Gamma^\alpha$, is transverse: $k_\alpha \Gamma^\alpha = 0$. Let us write L_α in the following form:

$$L_\alpha = \frac{k_\alpha}{m} + \delta_\alpha$$

where

$$\delta_\alpha = L_\alpha - \frac{k_\alpha}{m} = \frac{E - |\boldsymbol{k}|}{m}(0, 0, 1, -1) = \frac{m}{E + |\boldsymbol{k}|}(0, 0, 1, -1).$$

If the boson emission vertex is transverse, then for $m \to 0$ the transverse component is eliminated:

$$\Gamma^\alpha A_\alpha = \Gamma^\alpha T_\alpha \sin\theta + \Gamma^\alpha \delta_\alpha \cos\theta$$

and the amplitude has no terms increasing with energy as E/m.

5.18.5 18.5. Digression on the photon mass

It will be instructive in this connection to discuss the problem of the photon mass. If the photon possessed a mass m_γ, then by virtue of the conservation of the electromagnetic current the amplitudes of all physical processes would contain no terms of the ω/m_γ type (where ω is the photon frequency) which tend to infinity for $m_\gamma \to 0$, and would only have correction terms of the m_γ/ω type tending to zero for $m_\gamma \to 0$. With the current conserved,
there is therefore a continuous transition to the zero mass limit. The non-zero photon mass would be revealed in a number of phenomena. For example, with $m_\gamma \neq 0$, the field of a magnetic dipole $\boldsymbol{m}$ would have an additional Yukawa-type exponential factor:

$$A = \frac{\boldsymbol{m} \cdot \boldsymbol{r}}{r^3}\,(1 + m_\gamma r)\,\mathrm{e}^{-m_\gamma r}$$

Schrödinger has concluded that, with the field of the earth extending over 10^4 km, the Compton wave length of the photon

$$\lambda_\gamma = \frac{1}{m_\gamma} \gtrsim 10^4 \text{ km}$$

Launchings of satellites have raised this bound to 30000 km , and space probe measurements of Jupiter's magnetic field increase this estimate by another order of magnitude.

The non-zero photon mass would also change the Coulomb potential:

$$V(r) = \frac{Q\mathrm{e}^{-m_\gamma r}}{r}.$$

As a result, the field inside a charged sphere would not be zero. This field was searched for by Plimpton and Lowton who measured the potential difference in two concentric spheres with radii $R_1 = 75$ cm and $R_2 = 60$ cm . At $V_1 = 3000$ V they obtained $V_1 - V_2 \lesssim 10^{-6}$ V. It is easy to show that

$$\frac{V_1 - V_2}{V_1} \simeq \frac{1}{6} m_\gamma^2 \left(R_1^2 - R_2^2\right)$$

The lower bound found from this estimate is lower than those given above, namely $\lambda_\gamma \gtrsim 10$ km.

The best restriction on the photon mass ($\lambda_\gamma \gtrsim 10^{22}$ cm) is derived from observations of galactic magnetic fields.

But let us return to intermediate vector bosons.

5.18.6 18.6. Vector boson propagator

The longitudinal part of the vector boson wave function is an increasing function of energy, and corresponds to a term in the propagator of the virtual vector boson which also increases with increasing energy. The propagator of a vector particle is obtained from the Proca equation,

$$\partial^\mu F_{\mu\nu} + m^2 A_\nu = j_\nu,$$

where

$$F_{\mu\nu} = \partial_\mu A_\nu - \partial_\nu A_\mu$$

By taking the derivative of the left-hand and right-hand sides, we obtain

$$\partial^\nu \partial^\mu F_{\mu\nu} + m^2 \partial^\nu A_\nu = \partial^\nu j_\nu$$

As $F_{\mu\nu}$ is antisymmetric, this equation yields

$$\partial^\nu A_\nu = \frac{\partial^\nu j_\nu}{m^2}$$

Let us rewrite the initial equation, $\partial^\mu \partial_\mu A_\nu - \partial_\nu \partial^\mu A_\mu + m^2 A_\nu = j_\nu$, in the form

$$\left[(\partial_\mu)^2 + m^2\right] A_\nu = j_\nu + \frac{\partial_\nu \partial_\mu j^\mu}{m^2} = \left(g_{\mu\nu} + \frac{\partial_\nu \partial_\mu}{m^2}\right) j^\mu$$

which yields the propagator in the form

$$D_{\mu\nu} = -\frac{g_{\mu\nu} - k_\mu k_\nu / m^2}{k^2 - m^2}$$

Pay attention to the common minus sign in the vector particle propagator. It is this sign that leads to repulsion of like charges.

Unless the contribution of the term $k_\mu k_\nu / m^2$ vanishes owing to the transversality of the vertices, it immediately results in non-renormalizability of a theory containing massive vector bosons. Therefore we have to introduce, along with charged bosons, neutral vector bosons, and envisage conservation of the current coupled to these bosons. A theory which to a certain degree possesses the required properties was proposed by Yang and Mills as long ago as 1954, without any relation to the weak interaction. This theory is treated in the next chapter.

5.19 19 Gauge invariance

This chapter is mostly devoted to a discussion of the Yang-Mills theory which describes an isotopic triplet of massless vector fields coupled to a conserved current. Before presenting the theory, we shall remark on the classification of symmetries and shall also discuss several theories more simple than that of Yang and Mills. All symmetries can be separated into two large groups: global symmetries and local symmetries.

5.19.1 19.1. Global abelian symmetry U(1)

The simplest example of global symmetry is charge conservation, expressed as the invariance of the lagrangian with respect to transformations of the type

$$\psi \to \psi' = \mathrm{e}^{i\alpha Q}\psi$$
$$\bar{\psi} \to \bar{\psi}' = \bar{\psi}\mathrm{e}^{-i\alpha Q}$$

where Q is the charge of the particle described by the field ψ, and α is an arbitrary number independent of space-time coordinates of the particle. Not only the electric charge Q, but other charges as well (baryonic charge B, leptonic charge L, etc.) may play the part of the above charge. The group of these phase transformations is called U(1).

Various transformations of the group U(1) commute. Such groups are called abelian. If the parameter α is independent of x_μ, the group is called global. We have thus defined the global abelian symmetry U(1).

5.19.2 19.2. Global non-abelian symmetry SU(2)

Another example of global symmetry is the usual isotopic invariance. Under the isotopic transformation, SU(2),

$$\psi \to \psi' = \mathrm{e}^{i\boldsymbol{\alpha}\cdot\boldsymbol{T}}\psi$$
$$\bar{\psi} \to \bar{\psi}' = \bar{\psi}\mathrm{e}^{-i\boldsymbol{\alpha}\cdot\boldsymbol{T}}$$

where $\boldsymbol{T}$ are matrices, and $\boldsymbol{\alpha}$ are, as before, parameters independent of coordinates. The values of $\boldsymbol{\alpha}$ are identical be it in Moscow, New York, or on the moon. This is the reason for referring to the symmetry as global. In the case of the simplest non-trivial isotopic multiplet (i.e. doublet)

$$\psi = \begin{pmatrix}\psi^1\\ \psi^2\end{pmatrix}, \quad \boldsymbol{T} = \frac{1}{2}\boldsymbol{\tau}$$

where τ stands for three Pauli matrices

$$\tau_1 = \begin{pmatrix}0 & 1\\ 1 & 0\end{pmatrix}, \quad \tau_2 = \begin{pmatrix}0 & -i\\ i & 0\end{pmatrix}, \quad \tau_3 = \begin{pmatrix}1 & 0\\ 0 & -1\end{pmatrix}$$

The symmetry SU(2) is called non-abelian since the matrices τ are noncommuting.

5.19.3 19.3. Local abelian symmetry

Let us consider now the lagrangian of quantum electrodynamics which describes electrons, photons, and their interaction:

$$\mathcal{L} = \bar{\psi}(i\hat{\partial} + e\hat{A} - m)\psi - \frac{1}{4}F_{\mu\nu}F^{\mu\nu}.$$

This lagrangian is readily shown to be invariant with respect to the transformation

$$\psi \to \psi' = \mathrm{e}^{i\alpha(x)}\psi \equiv S\psi, \quad \bar{\psi} \to \bar{\psi}' = \bar{\psi}\mathrm{e}^{-i\alpha(x)} \equiv \bar{\psi}S^{+}$$

where $\alpha(x)$ is a parameter depending on the world point x. Under this transformation

$$A_\mu \to A'_\mu = A_\mu + \frac{1}{e}\frac{\partial\alpha(x)}{\partial x^\mu} \equiv A_\mu - \frac{i}{e}\left(\frac{\partial}{\partial x^\mu}S\right)S^{+}$$

The field strength,

$$F_{\mu\nu} = \frac{\partial}{\partial x^\mu}A_\nu - \frac{\partial}{\partial x^\nu}A_\mu,$$

is invariant with respect to this transformation. It should be emphasized that in the case of non-zero photon mass the local $U(1)$ symmetry would be broken since the term $m_\gamma^2 A_\mu A^\mu$ does not transform into itself after $\partial_\mu\alpha(x)/e$ has been added to A_μ.

We find that local invariance requires that the conserved charge be a source of a massless vector field. In this respect the photon-generating electric charge is radically different from the baryonic, leptonic, and muonic charges which, as far as we know, generate no specific massless fields, that is, there exist no baryonic, leptonic or muonic "photons". Hence, these charges correspond to global and not to local U(1) symmetries.

The observable transverse components of the photon field, $A_x(k)$ and $A_y(k)$, are not transformed under gauge transformations (we assume here that the photon momentum is directed along the z-axis); only non-physical longitudinal components of the photon 4 -vector, $A_z(k)$ and $A_t(k)$, are transformed. Unobservability of these components is a result of conservation of the vector current.

From a purely formal point of view, local invariance can be achieved with a non-physical longitudinal field only, without introducing observable vector fields and without interpreting the longitudinal field as a non-physical component of the vector field. We shall use, however, the terminology generally accepted in the literature, and refer to a theory as a local one only if it involves a massless vector gauge field.

5.19.4 19.4 Digression on baryonic and leptonic photons

We have made the remark above that baryonic photons do not exist. This statement calls for clarification.

It is not difficult to show that if baryonic photons exist, their interaction with baryons must be extremely weak: $\alpha_\mathrm{B} \leq 10^{-47}$ (this should be compared to $\alpha = \frac{1}{137}$ for ordinary photons). This restriction stems from the equality of the inertial and gravitational mass verified to an accuracy of 10^{-12} in experiments pioneered by Eötvös. Indeed, baryonic photons would produce a sort of "Coulomb" field around the earth, repulsing baryons away from it. For a given body, the force of this repulsion would be proportional to the number of baryons in this body and not to its mass, and would be different in, for example, a lead and copper sphere with identical masses. The force applied to the i th body with mass M_i containing A_i
nucleons is

$$F = \kappa\frac{M_i M}{r^2} + \alpha_\mathrm{B}\frac{A_i A}{r^2} = \kappa\frac{M_i M}{r^2}\left\{1 + \frac{\alpha_\mathrm{B}}{\kappa}\left(\frac{A}{M}\right)\left(\frac{A_i}{M_i}\right)\right\}$$

where M is the earth mass, A is the number of nucleons in the earth ($M/A \simeq m_\mathrm{p}$), and $\kappa = 6\cdot 10^{-39} m_\mathrm{p}^{-2}$ is the gravitational constant where m_p is the proton mass. The nucleon mass in the lead nucleus is greater than that in the copper nucleus by approximately 1MeV ($(M_\mathrm{Pb}/A_\mathrm{Pb} - M_\mathrm{Cu}/A_\mathrm{Cu}) = 1$
).

Experiment gives

$$\frac{\alpha_{\rm B}}{\kappa m_{\rm p}}\left[\frac{A_{\rm Cu}}{M_{\rm Cu}}-\frac{A_{\rm Pb}}{M_{\rm Pb}}\right]<10^{-12}$$

whence

$$\alpha_{\rm B}<10^{-9}\kappa m_{\rm p}^2\le 10^{-47}.$$

A similar argument is possible for the constant α_L of the interaction between hypothetical leptonic "photons" and electrons. In this case

$$\frac{\alpha_{\rm L}}{\kappa m_{\rm p}}\left[\frac{Z_{\rm Cu}}{M_{\rm Cu}}-\frac{Z_{\rm Pb}}{M_{\rm Pb}}\right]<10^{-12}$$

where Z is the charge of the nucleus; hence,

$$\alpha_{\rm L}\le 10^{-49}$$

As for the constant α_μ of interaction between hypothetical muonic "photons" and the muonic charge, the corresponding upper bound is many orders of magnitude higher than for $\alpha_{\rm B}$ and $\alpha_{\rm L}$, owing to the muon instability.

It is natural to conclude on the basis of the above estimates that massless vector particles coupled to the leptonic and baryonic charges do not exist. These charges are possibly coupled to some massive vector particles.

5.19.5 19.5. Local SU(2) symmetry

Let us now return to Yang-Mills theory which is a local realization of isotopic invariance. The theory is invariant with respect to local isotopic rotations:

$$\psi\to\psi'=S\psi,$$
$$\bar\psi\to\bar\psi'=\bar\psi S^{+}.$$

Here $S=\mathrm{e}^{i\boldsymbol{\alpha}(x)\cdot\boldsymbol{T}}$, where $\boldsymbol{T}$ are three matrices of isotopic rotations, and $\boldsymbol{\alpha}(x)$ denotes three parameters of these rotations which in the general case are different in different world points. Realization of such symmetry requires the existence of a triplet of massless vector fields A_μ coupled to fields ψ.

The lagrangian has the form

$$\mathcal{L}=\bar\psi(i\hat D-m)\psi-\frac{1}{4}\boldsymbol{G}_{\mu\nu}\cdot\boldsymbol{G}^{\mu\nu},$$

where $D_\alpha=\partial_\alpha-igA_\alpha$ is the covariant, or generalized, derivative (or simply the long derivative, in the lingo of some students). In contrast to the abelian case, A_α is a matrix,

$$(A_\alpha)_i^k=\sum_1^3\boldsymbol{A}_\alpha(\boldsymbol{T})_i^k.$$

Let us consider a field transforming under a specific representation of the group SU(2). This representation determines the specific form of the matrices $\boldsymbol{T}$ and therefore, of A_α. If the field ψ is an isodoublet, then

$$(T_a)_\alpha^\beta=\left(\frac{1}{2}\tau_a\right)_\alpha^\beta,\quad \alpha,\beta=1,2,$$

and if the field ψ is an isotriplet, then

$$(T_a)_i^k = \varepsilon_{iak},$$

where $a, i, k = 1, 2, 3$.
The isovector of the field strength has the form

$$G_{\mu\nu} = \boldsymbol{G}_{\mu\nu}\boldsymbol{T} = \partial_\mu A_\nu - \partial_\nu A_\mu - ig\left[A_\mu A_\nu - A_\nu A_\mu\right].$$

(Usually the matrices chosen for matrices $\boldsymbol{T}$ are $\boldsymbol{T} = \frac{1}{2}\boldsymbol{\tau}$.) This expression which we shall clarify later, shows that in contrast to the abelian case, the field strength of a non-abelian gauge field is a non-linear function of the field. (The commutator $A_\mu A_\nu - A_\nu A_\mu$ is zero in the abelian case.) As a result, the lagrangian of a free Yang-Mills field contains, along with $(A)^2$ terms, terms $(A)^3$ and $(A)^4$. In contrast to the usual photons, Yang-Mills photons have isovector "charges"; these photons are self-emitting, and thus behave as "radiating light".

Gravitons, that is quanta of the gravitation field, have a similar property. The source of gravitons is known to be the energy-momentum tensor. Therefore even massless particles, such as photons, interact with the gravitational field, the stronger the higher their energy is. The photon-graviton interaction vertex is shown in fig. 19.1a. Since the graviton has energy and momentum, it might also emit gravitons (fig. 19.1b). The usual abelian

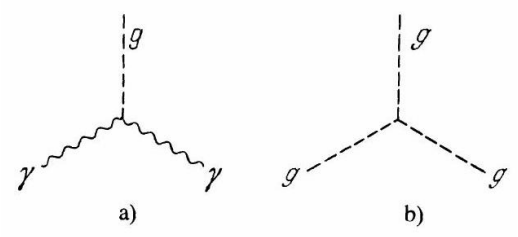


Fig. 19.1.

photon has no such triple vertex, $\gamma\gamma\gamma$, while for non-abelian photon the vertex $A^+A^-A^0$ is non-vanishing. This vertex represents scattering of A^+ and A^-"photons" on the A^0 field, $A^+A^- \to A^0$ annihilation, and other processes related to the above-mentioned process through crossing symmetry. Recall that we needed a vertex of just this type in order to provide conservation of the weak current in higher orders of perturbation theory (see chapter 18).

How are A_μ and $F_{\mu\nu}$ transformed? In order to find how the A_μ field is transformed, consider, for instance, the expression $\bar\psi\hat D\psi = \bar\psi(\hat\partial - ig\hat A)\psi$. Let $\psi' = S\psi, \bar\psi' = \bar\psi S^+$. What should be the form of A' for the expression $\bar\psi\hat D\psi$ to be gauge-invariant, that is for the gauge transformation to give

$$\bar\psi\hat D\psi \to \bar\psi'\hat D'\psi' = \bar\psi\hat D\psi?$$

Obviously the necessary and sufficient condition for this is

$$A_\mu \to A'_\mu = SAS^+ - \frac{i}{g}\left(\partial_\mu S\right)S^+.$$

(Recall that in the abelian case

$$A_\mu \to A'_\mu = A_\mu - \frac{i}{g}\left(\partial_\mu S\right)S^+.\Big)$$

Thus the non-abelian field is first isotopically rotated and only after that "elongated" by the term $-(i/g)(\partial_\mu S)S^+$. When the gauge matrix $S = \exp(i\boldsymbol{\alpha}(x)\boldsymbol{T})$ is nearly a unit matrix, that is when the angle of rotation $\boldsymbol{\alpha}(x)$ is small, the explicitly isovector form of field transformation gives a clearer picture than the matrix form used above. In this case $S = 1 + i\boldsymbol{\alpha}(x)\boldsymbol{T}$:

$$A_\mu \to A'_\mu = A_\mu - \boldsymbol{\alpha} \times \boldsymbol{A}_\mu + \frac{1}{g}\frac{\partial \boldsymbol{\alpha}}{\partial x^\mu}.$$

(We have used above that

$$\begin{aligned} SA_\mu S^+ &= (1 + i\boldsymbol{\alpha}\cdot\boldsymbol{T})(A_\mu \cdot T)(1 - i\boldsymbol{\alpha}\cdot\boldsymbol{T}) = A_\mu \boldsymbol{T} + i[\boldsymbol{T}\boldsymbol{\alpha}, \boldsymbol{T}A_\mu] \\ &= (A_\mu)_l T_l + i\alpha_i (A_\mu)_k [T_i T_k] \\ &= \left[(A_\mu)_l - \alpha_i (A_\mu)_k \varepsilon_{ikl}\right] T_l = (A_\mu - \boldsymbol{\alpha} \times A_\mu)\boldsymbol{T}, \end{aligned}$$

and also that for small $\boldsymbol{\alpha}$: $(\partial S/\partial x^\mu)S^+ = i\boldsymbol{T}\partial\boldsymbol{\alpha}(x)/\partial x^\mu$.)
As for the field strength $G_{\mu\nu}$, it immediately follows from the definition

$$G_{\mu\nu} = \partial_\mu A_\nu - \partial_\nu A_\mu - ig[A_\mu A_\nu - A_\nu A_\mu]$$

that

$$G_{\mu\nu} \to G'_{\mu\nu} = SG_{\mu\nu}S^+$$

We see that $\boldsymbol{G}_{\mu\nu}$ is transformed as a usual isovector. In particular, for small $\boldsymbol{\alpha}$ we have: $\boldsymbol{G}_{\mu\nu} \to \boldsymbol{G}'_{\mu\nu} = \boldsymbol{G}_{\mu\nu} - \boldsymbol{\alpha} \times \boldsymbol{G}_{\mu\nu}$. The field strength $G_{\mu\nu}$ is constructed in such a clever manner that it is transformed in the same way by the global and by the local isotopic rotations.

5.19.6 19.6. Panegyric to Yang-Mills theory

We are quite used to symmetries imposing certain restrictions on masses of particles and on the corresponding coupling constants. For example, isotopic invariance of strong interactions requires that the proton and neutron masses be equal, and that their interaction with π-mesons be described by the same coupling constant. A spectacular property of non-abelian gauge symmetry is that in addition to restricting masses and coupling constants of particles, this symmetry determines the dynamics of interactions of gauge fields (non-linear terms of the $(A)^3$ and $(A)^4$ types). Non-abelian gauge fields carry "isotopic charge" which determines their self-interaction as well as their interaction with other fields. The form of these interactions is given unambiguously by gauge symmetry.

In this sense Yang-Mills theory very much resembles general relativity theory in which the dynamics of the gravitational interaction is determined to a great extent by the requirement of invariance with respect to the most general transformations of coordiantes. Hence, the similarity of non-linear interactions of non-abelian photons and gravitons mentioned above, is only one of the specific manifestations of the profound similarity of these two theories. Yang-Mills theory is a sufficiently simple model in which to attempt to understand some consequences of quantization in such an essentially non-linear theory as the general theory of relativity. More and
more attention is being paid nowadays to the development of the quantum theory of gravitation.

In the sixties Yang-Mills theory was subjected to a thorough theoretical scrutiny. The rules for constructing Feynman graphs were formulated, and renormalizability was proved. In Yang-Mills theory the renormalizability is a corollary of the constant g being dimensionless, of the conservation of isotopic currents, and of the masslessness of non-abelian photons.

Today Yang-Mills fields, which at the beginning were considered as a mere theoretical curiosity, have become the central object of theoretical studies. In fact, all our hopes of arriving

at the theory of elementary particles are pivoted on non-abelian gauge fields. This is valid for the unified theory of weak and electromagnetic interactions, for the gluonic theory of strong interactions, and finally, for the possible future synthesis of these theories. (Recall that the theory of colored gluons coupled to colored quarks possesses the local SU(3) symmetry.)

At this juncture a thoughtful reader should have interrupted the panegyric to put the natural question: how are masses taken into account?

5.19.7 19.7. How to take masses into account?

The first question to appear is how to introduce into the theory the masses of intermediate bosons. Indeed, we know from experiment that these particles must have finite (and quite large!) masses, while Yang-Mills gauge fields are massless. It would seem innocuous at first glance to insert a term m^2A^2 into the lagrangian "by hand". We have established in the discussion of the photon mass that this causes no harm in the case of abelian gauge fields. There is a "soft" transition from $m = 0$ to $m \neq 0$ for the photon, and quantum electrodynamics remains renormalizable.

One easily finds that this is not the case for non-abelian gauge fields: introduction of mass "by hand" destroys renormalizability. Let us consider the amplitude for the emission of n photons:

$$A^{\alpha_1}A^{\alpha_2}\dots A^{\alpha_n}M_{\alpha_1\alpha_2\dots\alpha_n}$$

where A^i is the wave function of the i th photon.
In the abelian case the matrix element $M_{\alpha_1\alpha_2\dots\alpha_n}$ is transverse with respect to any combination of indices. For instance,

$$k^{\alpha_1}M_{\alpha_1\alpha_2\dots\alpha_n} = 0$$
$$k^{\alpha_1}k^{\alpha_2}M_{\alpha_1\alpha_2\dots\alpha_n} = 0$$

and so on.

Moreover, k_i^2 may be zero or non-zero, that is photons may be real as well as virtual. In contrast to this, in the non-abelian case, transversality for any of the "photons" is realized only if all the remaining "photons" are real (are on the mass shell), so that in the amplitude their emission is taken into account explicitly by their wave functions:

$$k^{\alpha_1}M_{\alpha_1\alpha_2\alpha_3\dots\alpha_n}A^{\alpha_2}A^{\alpha_3}\dots A^{\alpha_n} = 0$$

In all other cases transversality is absent; in particular,

$$k^{\alpha_1}k^{\alpha_2}M_{\alpha_1\alpha_2\alpha_3\dots\alpha_n}A^{\alpha_3}\dots A^{\alpha_n} \neq 0$$

This is caused by the isotopic charge of non-abelian photons. By definition, a virtual non-abelian photon transfers this charge from one part of a Feynman graph to another. In essence, by considering a graph in which one of the photons is virtual, we consider only a segment of a physical graph in which the isotopic current is not conserved and therefore transversality is absent. (This is not so for usual (abelian) photons because they are electrically neutral.)

Recall now the expression for the longitudinal part of the wave function of a massive vector particle:

$$L_\alpha = \frac{k_\alpha}{m} + \delta_\alpha, \quad \delta_\alpha = \frac{m}{E + |\boldsymbol{k}|}(0, 0, 1, -1),$$

where $m, E, \boldsymbol{k}$ are the mass, energy, and momentum of the particle, and k_α is its 4 - momentum. It then follows that the amplitude for emission of n longitudinal abelian photons

tends to zero as $(m/E)^n$ for $E \to \infty$. In contrast to this, the amplitude for emission of n longitudinal non-abelian photons is proportional to $(m/E)^{-n+2}$, and for $n > 2$ grows to infinity for $E \to \infty$. Indeed, by multiplying the matrix element by "photon" wave functions A^l, we can retain the δ_α term only in one of them, and therefore have to retain the term k_α/m in the rest of the wave functions. Consequently, we shall have at high energies:

$$\frac{m}{E}\left(\frac{E}{m}\right)^{n-1} = \left(\frac{E}{m}\right)^{n-2}$$

This means that in the non-abelian case we again deal with the nonrenormalizable theory.

Although the gauge origin of intermediate bosons made it possible to improve the high-energy behavior of amplitudes by slightly slowing down their growth, the power of energy is reduced only by two. This growth will
be eliminated completely if the introduction of a non-zero mass for intermediate bosons is accompanied by the appearance of additional fields whose contribution cancels the divergence in question. Such a "soft" introduction of the intermediate boson mass is a feature of the spontaneous breaking of gauge symmetry to be discussed in the next chapter.

5.20 20 Spontaneous symmetry breaking

The purpose of this chapter is to introduce W-boson masses by means of the Higgs mechanism of spontaneous breaking of local SU(2) symmetry. This method of mass introduction does not upset the renormalizability of the theory. Spontaneous symmetry breaking results from the degeneracy of the vacuum.

We begin with several simpler examples of spontaneous breaking of various symmetries: discrete, global and local U(1), and global SU(2).

5.20.1 20.1. Spontaneous breaking of discrete symmetry

Let us look first at the simplest case: the ordinary, scalar real field with the lagrangian

$$\mathcal{L} = \frac{1}{2}\left(\frac{\partial\varphi}{\partial x_\mu}\right)^2 - \frac{1}{2}m^2\varphi^2 - \frac{1}{4}\lambda^2\varphi^4$$

and the hamiltonian

$$H = \frac{1}{2}\left(\frac{\partial\varphi}{\partial t}\right)^2 + \frac{1}{2}\left(\frac{\partial\varphi}{\partial x}\right)^2 + \frac{1}{2}m^2\varphi^2 + \frac{1}{4}\lambda^2\varphi^4,$$

where m is the mass of particles described by the field φ, λ being a dimensionless constant characterizing the interaction between these particles. Consider a field which is constant in time and space. For this field

$$H(\varphi) = V(\varphi) \equiv \frac{1}{2}m^2\varphi^2 + \frac{1}{4}\lambda^2\varphi^4.$$

The function $V(\varphi)$ is plotted in fig. 20.1. It has a minimum at $\varphi = 0$ which means that there is no field in vacuum (in the minimum-energy state). The expression for the lagrangian and fig. 20.1 show that the lagrangian is symmetric with respect to a discrete transformation $\varphi \to -\varphi$.

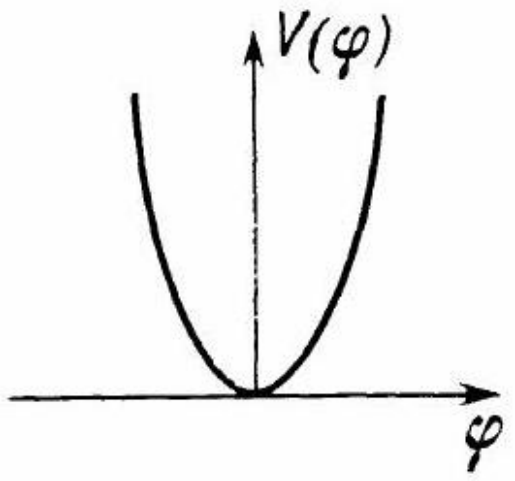


Fig. 20.1.

Now let us consider the same lagrangian but with a different sign in front of m^2. At first glance, we obtain a particle for which $E^2 = \boldsymbol{p}^2 - m^2$ and which therefore moves at a speed exceeding that of light:

$$v = \frac{|\boldsymbol{p}|}{E} = \frac{\sqrt{E^2 + m^2}}{E} > 1.$$

In the literature such particles are called tachyons. In fact no tachyon is implied since the state with $\varphi = 0$ is not the vacuum any more. In order to demonstrate this, let us turn to $V(\varphi)$. Fig. 20.2 gives the potential energy

$$V(\varphi) = -\frac{1}{2}m^2\varphi^2 + \frac{1}{4}\lambda^2\varphi^4.$$

We see that at $\varphi = 0$ this function has a maximum, not a minimum. Small perturbations of the field φ in the vicinity of $\varphi = 0$ cannot therefore be considered as particles. Here the system is unstable, tending to slip into one of the stable minima, $\varphi = m/\lambda$ or $\varphi = -m/\lambda$. Instead of a single vacuum at $\varphi = 0$, as in the usual case of positive sign in front of $\frac{1}{2}m^2$, the system has two degenerate vacua at $\varphi = \pm m/\lambda$. We call them degenerate because they have equal energies.

By adding a constant to $V(\varphi)$ (this does not change the field equations!) we rewrite it in a form in which the degenerate vacua are found at the points where $V(\varphi) = 0$. The new expression for $V(\varphi)$ takes the form (fig. 20.3)

$$V(\varphi) = \frac{1}{4}\lambda^2\left(\varphi^2 - \eta^2\right)^2,$$

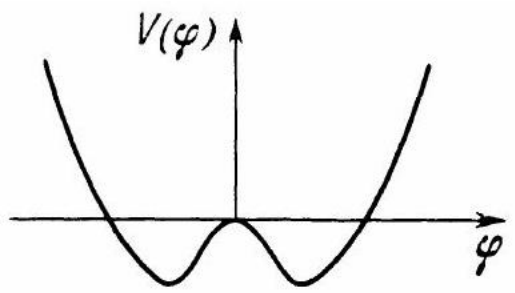


Fig. 20.2.

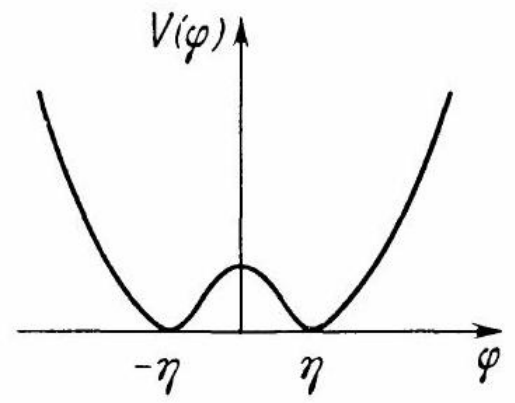


Fig. 20.3.

where $\eta = m/\lambda$. It seems more logical to consider $V(\varphi)$ as shown in fig. 20.3 and not as in fig. 20.2, since in the latter case the energy density of the vacuum is $-m^4/4\lambda^2$. This is a fantastically high negative energy (10^{41}GeV/cm^3 for $\lambda \simeq 1$ and $m \simeq 1\text{GeV}$) as compared with the mean energy density in the universe, 10^{-6}GeV/cm^3 (one proton per cubic meter, i.e. 10^{-30} g/cm^3). It can be concluded from the observed data on the expansion of the universe that the vacuum energy density (the so-called cosmological term in Einstein's equations) is unlikely to be much larger than the observed density of matter (hardly by a factor more than 10). Therefore in what follows we shall use the form $V(\varphi) = \frac{1}{4}\lambda^2\left(\varphi^2 - \eta^2\right)^2$.

The choice of a specific vacuum is decided by microscopic perturbations in the first moments of the life of the universe. But after the system has spontaneously "slipped" into one of the vacua, it cannot change to another one. The amplitude of a below-barrier transition from the state $\varphi = +\eta$ to the state $\varphi = -\eta$ is zero. It has the form e^{iS} where S is the action. In the case in question the action is imaginary (the transition is below-barrier, that is classically forbidden) and infinitely large (since the action must be found as an integral over the whole space of the universe), so that we obtain $e^{-\infty}$.

Could it be possible to realize the transition to another vacuum in only a part of the universe? For example, could we create the new vacuum in a volume of about 1 m^3, in laboratory conditions? Unfortunately, it is very difficult to generate even a very small bubble of the new vacuum, and even a small bubble is unstable. It must collapse on a nuclear time scale, emitting mesons. This would happen because the interface between the two vacua must be a wall with very high surface density σ of the order of $\lambda\eta^3$ and with thickness δ of the order of $1/\lambda\eta$. For $\lambda \simeq 1$ and $\eta = 1\text{GeV}$, we obtain $\delta \simeq 10^{-14}$ cm, and $\sigma \simeq 1$ kg/cm^2. These estimates are easily derived if we minimize the wall energy density which is equal to the sum of two terms:

$$\sigma \simeq \left\{\frac{1}{2}\left(\frac{\partial\varphi}{\partial x}\right)^2 + V(\varphi)\right\}\delta.$$

By substituting into it the estimates

$$\left(\frac{\partial\varphi}{\partial x}\right)^2 \simeq \left(\frac{\eta}{\delta}\right)^2 \quad \text{and} \quad V(\varphi) \simeq \lambda^2\eta^4$$

we find that the minimum of δ is reached at $\delta \simeq 1/\lambda\eta$, so that $\sigma \simeq \lambda\eta^3$.
In the case $V(\varphi) = \frac{1}{4}\lambda^2\left(\varphi^2 - \eta^2\right)^2$ we therefore encounter a lagrangian with mirror symmetry (with respect to the $\varphi \to -\varphi$ transformation) and a vacuum (let it be $\varphi = \eta$) which has no such symmetry. This is a typical example of the so-called spontaneous symmetry breaking.

Abdus Salam once gave an illustration of spontaneous breaking of a discrete symmetry. Imagine a banquet with guests seated at a large round table. A person could equally well take a serviette from his right or from his left. But this symmetry is spontaneously broken once one of the guests decides to pick up the serviette, say, on his left; other guests are left no choice. Obviously, the symmetric state is unstable, especially with hungry guests.

If we write the field φ in the form $\varphi = \eta + \chi$, then χ will describe excitations of the field (particles) with respect to the vacuum $\varphi = \eta$. In the new variables the lagrangian does not possess the mirror symmetry:

$$\begin{aligned}\mathcal{L} &= \frac{1}{2}\left(\frac{\partial\varphi}{\partial x_\mu}\right)^2 - \frac{1}{4}\lambda^2\left(\varphi^2 - \eta^2\right)^2 \\ &= \frac{1}{2}\left(\frac{\partial\chi}{\partial x_\mu}\right)^2 - \lambda^2\eta^2\chi^2 - \lambda^2\eta\chi^3 - \frac{1}{4}\lambda^2\chi^4\end{aligned}$$

Note that the field χ is not tachyonic: its mass μ is equal to $\sqrt{2}\lambda\eta$, and the mass term has the usual sign (minus in the lagrangian and plus in the hamiltonian).

5.20.2 20.2. Spontaneous breaking of global $U(1)$ symmetry

Spontaneous breaking of a continuous (not discrete) global symmetry produces massless particles, the so-called Goldstone bosons. Let us analyze this effect by considering the lagrangian

$$\mathcal{L} = \left|\frac{\partial\varphi}{\partial x_\mu}\right|^2 - V(|\varphi|),$$

where φ is a complex scalar field

$$V(|\varphi|) = \frac{1}{2}\lambda^2\left(|\varphi|^2 - \frac{1}{2}\eta^2\right)^2.$$

(The coefficient $\frac{1}{2}$ of η^2 is introduced to reduce the number of factors $\sqrt{2}$ in further formulas). This lagrangian is invariant with respect to the global U(1) gauge transformation

$$\varphi \to \varphi' = \varphi e^{i\alpha}.$$

The potential $V(|\varphi|)$ is plotted in fig. 20.4. In this situation we deal with an infinite number of degenerate vacua. The shape of the $V(\varphi)$ potential surface in fig. 20.4 resembles that of a bottom of a beer bottle. All the vacua satisfy the condition $\varphi = \eta/\sqrt{2}$, and lie in the trough. We choose the gauge phase value $\alpha = 0$ common for the whole world, and present φ in the form:

$$\varphi(x) = (\eta + \chi(x) + i\psi(x))/\sqrt{2}.$$

Here $\chi(x)$ and $\psi(x)$ are two real fields describing the excitations of the system with respect to the stable vacuum $\varphi = \eta/\sqrt{2}$. The choice of a stable vacuum breaks the $U(1)$ invariance by fixing the phase of the function φ (fig. 20.5). In the new variables our lagrangian has the form

$$\mathcal{L} = \frac{1}{2}\left(\frac{\partial\chi}{\partial x_\mu}\right)^2 + \frac{1}{2}\left(\frac{\partial\psi}{\partial x_\mu}\right)^2 - \frac{1}{8}\lambda^2\left(\chi^2 + 2\eta\chi + \psi^2\right)^2.$$

This lagrangian contains a massive scalar field χ (its mass is $\mu = \lambda\eta$) and a massless scalar field ψ (massless because of the absence of a term proportional to ψ^2). As we see from fig. 20.5, the field χ describes small radial oscillations of the system with respect to a point $\varphi = \eta/\sqrt{2}$, and the field ψ describes tangential oscillations (along the vacuum trough). The field ψ is

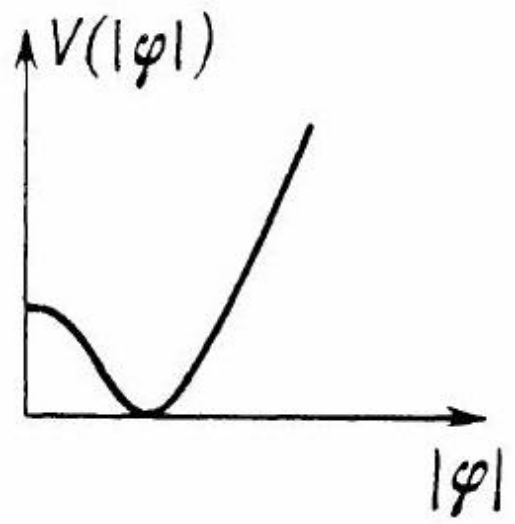


Fig. 20.4.

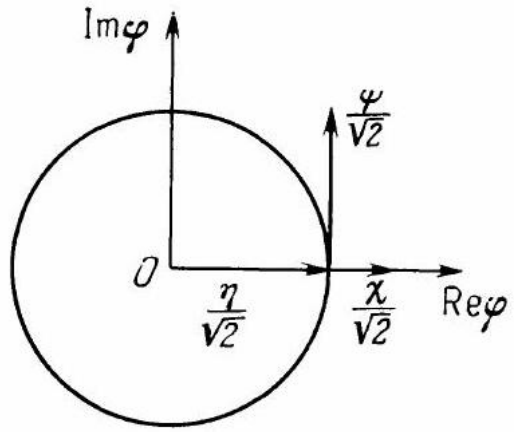


Fig. 20.5.

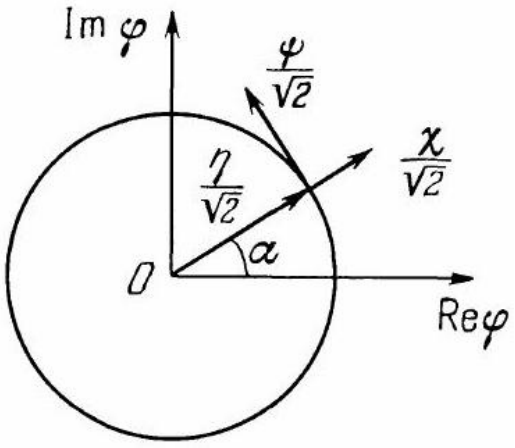


Fig. 20.6.

called the Goldstone field, and particles corresponding to this field are Goldstone bosons.

Different values of the gauge phase α define different vacuae and different physical fields (see fig. 20.6).

5.20.3 20.3. Spontaneous breaking of global SU(2) symmetry

The lagrangian in this case is

$$\mathcal{L} = \left(\frac{\partial\bar{\varphi}}{\partial x_\mu}\right)\left(\frac{\partial\varphi}{\partial x_\mu}\right) - V(\bar{\varphi}\varphi).$$

The field φ is now an isotopic doublet similar to the K-meson doublet:

$$\varphi = \begin{pmatrix}\varphi_+\\ \varphi_0\end{pmatrix},$$

and $\bar{\varphi}\varphi$ is an isotopic scalar: $\bar{\varphi}\varphi = \varphi_+^*\varphi_+ + \varphi_0^*\varphi_0$. In fact we deal with four real scalar fields since $\varphi_0 \neq \tilde{\varphi}_0$. Spontaneous breaking of the isotopic
symmetry produces one massive field and three Goldstone massless fields, all of them scalar and real.

We are now very close to what will be necessary to construct a renormalizable model of the weak interaction, and the spontaneous breaking of local symmetry.

5.20.4 20.4. Spontaneous breaking of abelian gauge symmetry

We shall write the lagrangian with local abelian symmetry and degenerate vacuum in the form:

$$\mathcal{L} = |D_\mu\varphi|^2 - \frac{1}{2}\lambda^2\left(|\varphi|^2 - \frac{1}{2}\eta^2\right)^2 - \frac{1}{4}F_{\mu\nu}F^{\mu\nu},$$

where φ is a complex scalar field, $D_\mu = \partial_\mu - ieA_\mu$, $F_{\mu\nu} = \partial_\mu A_\nu - \partial_\nu A_\mu$, and A_μ is the 4 -vector potential of the photon field. We shall write $\varphi(x) = \phi(x)\exp(i\theta(x))$ and choose $\theta(x)$ in such a manner that $\phi(x)$ is real at all world points. Now we make use of the gauge transformation to eliminate the phase $\theta(x)$, and introduce a field $\chi(x)$ which describes excitations in the vicinity of the stable vacuum $\eta/\sqrt{2}$: $\phi(x) = (\eta + \chi(x))/\sqrt{2}$.

After spontaneous symmetry breaking the lagrangian changes to

$$\mathcal{L} = \frac{1}{2}\left(\frac{\partial\chi}{\partial x_\mu}\right)^2 - \frac{1}{8}\lambda^2\chi^2(2\eta+\chi)^2 + e^2A_\mu^2(\eta+\chi)^2 - \frac{1}{4}F_{\mu\nu}F^{\mu\nu},$$

and describes a real scalar field χ with mass $\mu = \lambda\eta$ and a massive vector field A_μ with mass $m = e\eta$. All non-linear interactions of these fields ($\chi^3, \chi^4, A^2\chi, A^2\chi^2$) are renormalizable since the dimensions of the corresponding coupling constants are m^1 and m^0, respectively.

We observe that spontaneous symmetry breaking resulted in a redistribution of fields: one of the two real fields forming the complex scalar field was transformed into the third (longitudinal) component of the vector particle which in its turn was transformed from a massless two-component Maxwell photon into a massive three-component Proca boson. Note that this did not alter the total number of scalar and vector components: $2 + 2 = 3 + 1$.

The above example illustrates the general fact that the spontaneous breaking of local symmetry does not produce Goldstone bosons, but that the vector gauge field becomes massive. In field theory this effect is called
the Higgs effect and the scalar particles described by the field χ are called Higgs bosons.

A non-relativistic analog of the Higgs effect was known for a long time. It is the magnetic field penetration into a superconductor. As a result of the spontaneous breaking of gauge symmetry, the magnetic field gains a mass whose inverse value characterizes the depth of field

penetration into the superconductor. A phenomenological description of this phenomenon is given by the Ginzburg-Landau equation.

This is a good moment to emphasize that in recent years field theory has come into very close contact with the non-relativistic theory of phase transitions in many-body systems, and borrowed a number of fruitful ideas. The very idea of spontaneous symmetry breaking (a seemingly negligible cause triggering an avalanche-like phase transition), has its origin in statistical physics (recall, e.g., spontaneous magnetization of ferromagnets).

Another significant trend is the growing interpenetration of the theory of elementary particles and cosmology. On one hand, the knowledge of particle properties leads to a more reliable relativistic statistical picture of the first moments of the big bang (see Chapter 27). On the other hand, it becomes clearer that these first moments have determined not only the cosmological pattern of the world as a whole but, possibly, the properties of the microcosm as well, by fixing the physical vacuum in which elementary particles have to exist.

5.20.5 20.5. On the conservation of electric charge

The fact that the charged scalar field φ of the above example gained a non-zero vacuum-expectation value implies non-conservation of the electric charge. This will be shown more clearly if we imagine that the field φ interacts with leptons, that is with electrons and neutrinos:

$$\sqrt{2}f\left(\bar{e}\nu\varphi + \bar{\nu}e\varphi^{+}\right).$$

As a result of spontaneous symmetry breaking this term generates a "non-diagonal mass" $f\eta$ transforming an electron into a neutrino,

$$f\eta(\bar{e}\nu + \bar{\nu}e),$$

and an interaction violating electric charge conservation:

$$f\chi(\bar{e}\nu + \bar{\nu}e)$$

(we recall that the field χ is neutral). It has already been mentioned above that non-conservation of electric charge creates a non-zero photon mass: $m_\gamma = e\eta$. As for the scalar field, its mass $\mu = \lambda\eta$ cannot be much larger than the photon mass. An important point is that if we want the lagrangian to be physically meaningful, the upper bound on λ must be of the order of unity (otherwise the simplest graph representing $\chi + \chi \to \chi + \chi$ scattering contradicts unitarity). This restriction on λ means that $\mu \lesssim \eta$ and, as a result, $\mu \simeq m_\gamma$ (recall that $m_\gamma = \sqrt{4\pi\alpha}\eta \approx \eta$). We have therefore constructed a theory in which a massive vector field (photon) is coupled to a non-conserved current (electric current). It can be shown that this theory is renormalizable and that it manifests reasonable behaviour at asymptotically high energies, which distinguishes it from theories in which the vector field mass is introduced into the lagrangian "by hand" from the very beginning.

The mass term added directly to the massless lagrangian is called the hard mass term. The mass appearing because of spontaneous symmetry breaking is called the soft mass. The theory with the hard mass is non-renormalizable, while that with the soft mass is renormalizable. The renormalizability in the soft case is due to the possibility of neglecting the η^2 term in the hamiltonian in the high-energy limit. This can be expressed in a different manner, by saying that the dangerous terms including longitudinal components of the massive vector field are compensated by the contribution of the Higgs bosons.

Experimentally, conservation of electric charge has been verified with an accuracy much lower than that of baryonic charge conservation: the lower limit of the electron lifetime with respect to $e \to \nu\gamma$ type decays is of the order of 10^{22} years, while the lower limit of the proton

lifetime with respect to $p \to \mu\pi$ type decays is of the order of 10^{30} years. It is then natural to ask what restriction on the constant f of the interaction $\sqrt{2}f\,(\bar{e}\nu\varphi + \bar{\nu}e\varphi^+)$ follows from the fact that $\tau_e > 10^{22}$ years. The answer is quite unexpected. Namely, it can be shown that the theory of spontaneous breaking of local U(1) symmetry discussed in this and earlier sections, cannot be used at all as a realistic model of electric charge non-conservation; it cannot be enforced on nature. It is essential that as follows from the existing upper bound on the photon mass, $m_\gamma \lesssim 10^{-22}$ cm^{-1}, the quantity $\eta = m_\gamma/e$ is also of the order of 10^{-22} cm^{-1}, and the mass of the neutral Higgs boson μ is nearly the same or even smaller. Under terrestrial conditions, even with practically static fields, we have to deal with frequencies much higher than these values of m_γ, μ and η. All these quantities can therefore be neglected under such conditions, so that the Higgs boson and the longitudinal component of the photon, γ_l, are emitted coherently as a practically massless charged scalar particle φ (see fig. 20.7). However, the excellent

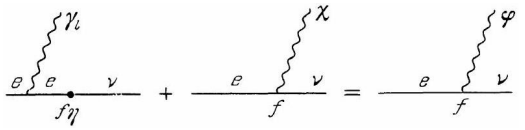


Fig. 20.7.

agreement of quantum electrodynamics with experiment absolutely excludes the possibility of the existence of such a practically massless charged particle. Indeed, creation of pairs of such particles by photons would be observed as the most spectacular of all electromagnetic effects.

Hence, non-conservation of the electric charge is not achievable in a soft manner: the practical masslessness of the photon is an insurmountable obstacle. In contrast to photons, intermediate bosons are very heavy particles, so that the soft mechanism of mass generation for these bosons is quite possible.

As the last step to constructing a renormalizable theory of weak interactions, we shall discuss the spontaneous breaking of non-abelian gauge symmetry, in which massless non-abelian photons become massive and turn into both neutral and charged intermediate bosons.

5.20.6 20.6. Spontaneous breaking of local SU(2) symmetry

Consider the lagrangian

$$\mathcal{L} = |D_\mu\varphi|^2 - \frac{1}{2}\lambda^2\left(|\varphi|^2 - \frac{1}{2}\eta^2\right)^2 - \frac{1}{4}\boldsymbol{G}_{\mu\nu}\boldsymbol{G}^{\mu\nu}.$$

Here $\varphi = \begin{vmatrix} \varphi^+ \\ \varphi_0 \end{vmatrix}$ is an isotopic spinor, $|\varphi|^2 = \varphi_+^*\varphi_+ + \varphi_0^*\varphi_0$,

$$D_\mu\varphi = \left(\partial_\mu - \frac{1}{2}ig\boldsymbol{\tau}\cdot\boldsymbol{A}_\mu\right)\varphi,$$

$$\begin{aligned} G_{\mu\nu} &= \boldsymbol{G}_{\mu\nu}\cdot\boldsymbol{T} = \partial_\mu A_\nu - \partial_\nu A_\mu - ig\,[A_\mu A_\nu - A_\nu A_\mu] \\ &= (\partial_\mu\boldsymbol{A}_\nu - \partial_\nu\boldsymbol{A}_\mu + g\,[\boldsymbol{A}_\mu\times\boldsymbol{A}_\nu])\,\boldsymbol{T}. \end{aligned}$$

This lagrangian is locally SU(2) invariant, and describes the infinitely degenerate vacuum at $\varphi = \eta/\sqrt{2}$. Let us use the local invariance and choose φ in the form

$$\varphi = \frac{1}{\sqrt{2}}\begin{pmatrix} 0 \\ \eta + \chi \end{pmatrix}.$$

With this choice of gauge, three of four real scalar fields are sent to the vector sector to be kept there forever; then we choose the vacuum at $|\varphi| = \eta/\sqrt{2}$, thereby spontaneously breaking the symmetry. Only one Higgs field χ is left, and the three vector fields became massive. The lagrangian now takes the form

$$\mathcal{L} = \frac{1}{2}\left(\frac{\partial\chi}{\partial x_\mu}\right)^2 + \frac{1}{8}g^2\left|\boldsymbol{\tau}\cdot\boldsymbol{A}\begin{pmatrix}0\\ \eta+\chi\end{pmatrix}\right|^2 - \frac{1}{8}\lambda^2\chi^2(2\eta+\chi)^2 - \frac{1}{4}\boldsymbol{G}_{\mu\nu}\boldsymbol{G}^{\mu\nu}.$$

The second term can be rewritten explicitly, taking into account that

$$\boldsymbol{\tau}\cdot\boldsymbol{A} = \tau_+A_- + \tau_-A_+ + \tau_3A_3,$$

where

$$\begin{aligned}
\tau_+ &= (\tau_1 + i\tau_2)/\sqrt{2} = \sqrt{2}\begin{pmatrix}0 & 1\\ 0 & 0\end{pmatrix},\\
\tau_- &= (\tau_1 - i\tau_2)/\sqrt{2} = \sqrt{2}\begin{pmatrix}0 & 0\\ 1 & 0\end{pmatrix},\\
A_+ &= (A_1 + iA_2)/\sqrt{2}, \quad A_- = (A_1 - iA_2)/\sqrt{2}.
\end{aligned}$$

Then

$$\begin{aligned}
\frac{1}{8}g^2\left|\boldsymbol{\tau}\cdot\boldsymbol{A}\begin{pmatrix}0\\ \eta+\chi\end{pmatrix}\right|^2 &= \frac{1}{8}g^2\left|A_3\begin{pmatrix}0\\ -\eta-\chi\end{pmatrix} + A_-\sqrt{2}\begin{pmatrix}\eta+\chi\\ 0\end{pmatrix}\right|^2\\
&= \frac{1}{8}g^2\left(A_3^2 + 2A_-A_+\right)(\eta+\chi)^2
\end{aligned}$$

The masses of the three vector particles (A_-, A_+, and A_3) are thus shown to be identical and equal to $\frac{1}{2}g\eta$.

This concludes the preliminaries to the presentation of the standard unified model of electromagnetic and weak interactions.

5.21 21 Standard model of the electroweak interaction

To begin the description of the standard unified model of electroweak interactions, we shall first write down the model lagrangian containing the vector and scalar fields, and the fields of the electron and electron neutrino as representatives of fermions. At the end of the chapter we shall discuss the addition of other leptons and quarks. We pay maximum attention to obtaining a relationship between the masses of the intermediate bosons m_{w} and m_{Z}, the fine structure constant α, and the Fermi constant G.

The first papers presenting what is now called the standard variant of the model appeared in the 60's. Since then, hundreds and possibly even thousands of papers were devoted to the study and development of this model. Several dozens of modified versions were suggested but the initial structure proved to be in better agreement with nature than the numerous sophisticated modifications.

We shall see in the next chapter that the standard model fits well the experimental data on neutral currents. We must emphasize that the model could easily be altered by the introduction of additional intermediate bosons and/or new leptons (besides τ and ν_τ), all within the same fundamental ideas. These ideas will be tested by means of the next generation of colliding beams facilities which would refute or confirm the existence of the W- and Z-bosons with masses of the order of 80 to 100 GeV , as well as that of massive scalar bosons.

5.21.1 21.1. Main features of the model

It is impossible to construct a renormalizable theory of weak interactions without including the photon. This occurs because in the general case the electromagnetic interaction of massive vector bosons is not renormalizable. To make it renormalizable, one should introduce the photon and intermediate bosons on an equal basis, as gauge fields, and then give masses spontaneously to intermediate bosons leaving the photon massless (the latter means strict conservation of electric charge). Accordingly, the standard model is based on local $\mathrm{SU}(2)\times\mathrm{U}(1)$ symmetry corresponding to four gauge fields, two of them charged and two neutral. Let us denote the three fields corresponding to non-abelian SU(2) symmetry by $\boldsymbol{A}=\{A_1,A_2,A_3\}$ and the field corresponding to abelian U(1) symmetry by B. We shall see later that the photon and Z-boson are two orthogonal superpositions of the fields A_3 and B, and the bosons $\mathrm{W}^+$and $\mathrm{W}^-$of the fields A_1 and A_2.

We shall include first only the lightest leptons, that is the electron and electron neutrino. The remaining leptons and quarks will be included only after we establish the properties of the simplified model. Two aspects are important when fermions are included: first, we have to take into account parity non-conservation, that is introduce coupling of gauge fields both to vector and to axial currents; second, conservation of currents coupled to gauge fields must not be violated. The two requirements can be satisfied by assuming that the lagrangian includes massless fermions with completely independent left-handed and right-handed components, $\psi_{\mathrm{L,R}}=\frac{1}{2}\left(1\pm\gamma_5\right)\psi$. Assume now that ν_{L} and e_{L} form an isotopic doublet

$$L=\begin{pmatrix}\nu_{\mathrm{L}}\\ e_{\mathrm{L}}\end{pmatrix},$$

while ν_{R} and e_{R} are isotopic singlets. We have put the left-handed fermions in the isotopic doublet so that they could emit (owing to their non-zero isospin) $\mathrm{W}^{\pm}$bosons. We have thus satisfied the conditions forced on us by experiment: the weak charged current contains left-handed spinors. Righthanded components of spinors will be put into an isosinglet, in order to avoid right-handed charged currents. The isotopic invariance of the lagrangian now demands the fermions to be massless: indeed, the mass term $m\bar{e}e=m\left(\bar{e}_{\mathrm{L}}e_{\mathrm{R}}+\bar{e}_{\mathrm{R}}e_{\mathrm{L}}\right)$ cannot be inserted "by hand" since this would violate isotopic invariance.

Finally, we introduce into the lagrangian an isotopic doublet of scalar fields,

$$\varphi=\begin{pmatrix}\varphi^+\\ \varphi^0\end{pmatrix}$$

(together with antiparticles, this makes four fields: $\varphi^+,\varphi^0,\varphi^-,\bar{\varphi}^0$). After developing a non-zero vacuum-expectation value, the field $\left(\varphi^0+\bar{\varphi}^0\right)/\sqrt{2}$ will give masses to the W - and Z -bosons and the electron.

Returning to the gauge fields, we must add that the field B interacts with the hypercharge Y of the particles, defined as twice the mean charge of the multiplet, $Y=2\langle Q\rangle$. It is easy to see that

$$\begin{array}{ll}Y=-1 & \text{for } \nu_{\mathrm{L}} \text{ and } e_{\mathrm{L}},\\ Y=-2 & \text{for } e_{\mathrm{R}},\\ Y=0 & \text{for } \nu_{\mathrm{R}},\\ Y=1 & \text{for } \varphi^+\text{and } \varphi^0.\end{array}$$

We must emphasize that the above isospin and hypercharge have nothing in common with the isospin and hypercharge of the usual hadrons. In a certain sense, the isotopic group discussed in this chapter has a more profound physical meaning than the usual isotopic invariance of strong interactions, since weak isotopic charges are sources of vector particles. At the same

time, from the viewpoint of the quark-gluon theory, the usual isotopic invariance merely reflects the "accidental" smallness of the u- and d-quark masses as compared to their kinetic energies in hadrons.

Having made these preliminary remarks, we shall explicitly write down the lagrangian.

5.21.2 21.2. Nine terms of the lagrangian

The full expression for the lagrangian of our system has nine terms:

$$\begin{aligned}\mathcal{L} = &-\frac{1}{4}\boldsymbol{G}_{\mu\nu}\boldsymbol{G}^{\mu\nu} - \frac{1}{4}F_{\mu\nu}F^{\mu\nu} + i\bar{L}\hat{D}L + i\bar{e}_{\mathrm{R}}\hat{D}e_{\mathrm{R}} \\ &+ i\bar{\nu}_{\mathrm{R}}\hat{D}\nu_{\mathrm{R}} + |D_\mu\varphi|^2 - \frac{1}{2}\lambda^2\left(|\varphi|^2 - \frac{1}{2}\eta^2\right)^2 \\ &- f_{\mathrm{e}}\left(\bar{L}e_{\mathrm{R}}\varphi + \bar{e}_{\mathrm{R}}L\varphi^\dagger\right) - f_{\nu_{\mathrm{e}}}\left(\bar{L}\nu_{\mathrm{R}}\varphi_{\mathrm{c}} + \bar{\nu}_{\mathrm{R}}L\varphi_{\mathrm{c}}^\dagger\right).\end{aligned}$$

The notation and the meaning of each term will now be clarified. We begin with the covariant derivative

$$D_\mu = \partial_\mu - ig\boldsymbol{T}\cdot\boldsymbol{A}_\mu - ig'\frac{1}{2}YB_\mu.$$

The values of Y for the fields included in the expression for D_μ were listed above. The second term in D_μ vanishes in the case of isoscalar fields with $T = 0$ (e_{R} and ν_{R}). For isospinor fields with $T = \frac{1}{2}$(φ and L), $\boldsymbol{T} = \frac{1}{2}\tau$.

The field strengths of the gauge fields are

$$G_{\mu\nu} = \partial_\mu A_\nu - \partial_\nu A_\mu - ig\left[A_\mu A_\nu - A_\nu A_\mu\right] = G_{\mu\nu}\boldsymbol{T},$$

where $A_\mu = A_\mu\cdot\boldsymbol{T}$; $F_{\mu\nu} = \partial_\mu B_\nu - \partial_\nu B_\mu$. The term $i\bar{L}\hat{D}L$ describes both the free motion of the left-handed fermions and their interaction with gauge fields:

$$\bar{L}\hat{D}L = \left(\bar{\nu}_{\mathrm{L}}\bar{e}_{\mathrm{L}}\right)\hat{D}\begin{pmatrix}\nu_{\mathrm{L}}\\ e_{\mathrm{L}}\end{pmatrix}$$

where $\hat{D} = D_\mu\gamma^\mu = \hat{\partial} - \frac{1}{2}\,\mathrm{ig}\,\boldsymbol{\tau}\cdot\hat{\boldsymbol{A}} + \frac{1}{2}ig'\hat{B}$.

For the right-handed electron we obtain

$$\bar{e}_{\mathrm{R}}\hat{D}e_{\mathrm{R}} = \bar{e}_{\mathrm{R}}\left(\hat{\partial} + ig'\hat{B}\right)e_{\mathrm{R}},$$

and for the right-handed neutrino,

$$\bar{\nu}_{\mathrm{R}}\hat{D}\nu_{\mathrm{R}} = \bar{\nu}_{\mathrm{R}}\hat{\partial}\nu_{\mathrm{R}}.$$

The right-handed neutrino has zero isospin and zero hypercharge, and therefore does not interact with the gauge fields. The quantity $D_\mu\varphi$ in the sixth term has the form

$$D_\mu\varphi = \left(\partial_\mu - \frac{1}{2}ig\boldsymbol{\tau}\cdot\boldsymbol{A}_\mu - \frac{1}{2}ig'B_\mu\right)\varphi.$$

The expression for $|D_\mu\varphi|^2$ represents an isotopic scalar:

$$|D_\mu\varphi|^2 = \left(D_\mu\varphi\right)_i^*\left(D^\mu\varphi\right)^i$$

This term describes both the free motion of scalar fields and their interaction with the gauge fields $\boldsymbol{A}_\mu$ and B_μ. When the field φ acquires a vacuumexpectation value equal to $\eta/\sqrt{2}$ (see

the seventh term), the sixth term gives masses to intermediate bosons, in analogy to what has been described in chapter 20. The eighth and ninth terms describe the interaction of fermions with scalar fields. After the field φ acquires a non-zero vacuum-expectation value, these terms give non-zero masses to fermions: the term with f_{e} to the electron, and that with $f_{\nu_{\mathrm{e}}}$ to the neutrino.

The isospinor φ_{c} included in the term containing $f_{\nu_{\mathrm{e}}}$ is the charge conjugate of the isospinor φ, and has the form:

$$\varphi_{\mathrm{c}} = \begin{pmatrix} \bar{\varphi}^0 \\ -\varphi^- \end{pmatrix}.$$

The minus sign in the isospinor appears because of the charge conjugation matrix in isotopic space:

$$(\varphi_{\mathrm{c}})_i = \varphi^{*k}\varepsilon_{ik}.$$

If we want the neutrino mass to be zero, we must set $f_{\nu_{\mathrm{e}}} = 0$ (the experimental upper bound is $m_{\nu_{\mathrm{e}}} \leq 30\mathrm{eV}$). If $m_{\nu_{\mathrm{e}}} = 0$, the right-handed neutrino is completely isolated from other particles and does not take part either in strong, electromagnetic or weak interactions. However, ν_R is
allowed to participate in gravitational interactions, with gravitons transforming into $\nu_{\mathrm{R}}\bar{\nu}_{\mathrm{R}}$ pairs. Produced by this mechanism, ν_{R} and $\bar{\nu}_{\mathrm{R}}$ would be absolutely "sterile" but would be deflected by gravitational fields. Another possibility is the absence of right-handed neutrinos in nature.

It is easy to show that all nine terms of the lagrangian obey local isotopic invariance and local hypercharge conservation. The lagrangian contains no constants with dangerous dimension (m to negative powers), and already in the pioneer papers it was conjectured that it is renormalizable. It proved to be far from elementary, however, to demonstrate the validity of this hypothesis. The proof was given by 't Hooft (1971). A discussion of this proof goes beyond the scope of this book.

Making use of the gauge invariance of the lagrangian (see chapter 20), let us apply the phase transformation $\exp\left(\frac{1}{2}i\tau\boldsymbol{\theta}(x)\right)$ to the isospinor φ, giving it the form

$$\varphi = \frac{1}{\sqrt{2}}\begin{pmatrix} 0 \\ \eta + \chi(x) \end{pmatrix},$$

where η is a real constant entering the lagrangian, and χ is a real scalar field. After going to a new vacuum, the field $\chi(x)$ represents excitations over this vacuum, namely massive scalar mesons with mass $\lambda\eta$. The other three components of the field φ are now "serving" as longitudinal components of massive $\mathrm{W}^+, \mathrm{W}^-$and Z -bosons.

5.21.3 21.3. Masses of W - and Z-bosons

In order to clarify how the masses of these bosons appear in the model, let us consider the terms proportional to η, in the expression for $D_\mu\varphi$:

$$\begin{aligned} D_\mu\varphi &= \left(\partial_\mu - \frac{1}{2}ig\tau\cdot A_\mu - \frac{1}{2}ig'B_\mu\right)\begin{pmatrix} 0 \\ (\eta+\chi)/\sqrt{2} \end{pmatrix} \\ &\Rightarrow \frac{1}{4}\sqrt{2}i\left(gA_{3\mu} - g'B_\mu\right)\begin{pmatrix} 0 \\ \eta \end{pmatrix} - \frac{1}{2}igA_\mu^-\begin{pmatrix} \eta \\ 0 \end{pmatrix}. \end{aligned}$$

Then the term $|D_\mu\varphi|^2$ yields the mass terms of the intermediate bosons

$$\frac{1}{8}\eta^2\left(gA_{3\mu} - g'B_\mu\right)^2 + \frac{1}{4}\eta^2 g^2 A^- A^+.$$

The following notation will be convenient for further analysis:

$$\bar{g} = \sqrt{g^2 + g'^2}, \quad g/\bar{g} = \cos\theta_{\mathrm{W}}, \quad g'/\bar{g} = \sin\theta_{\mathrm{W}}.$$

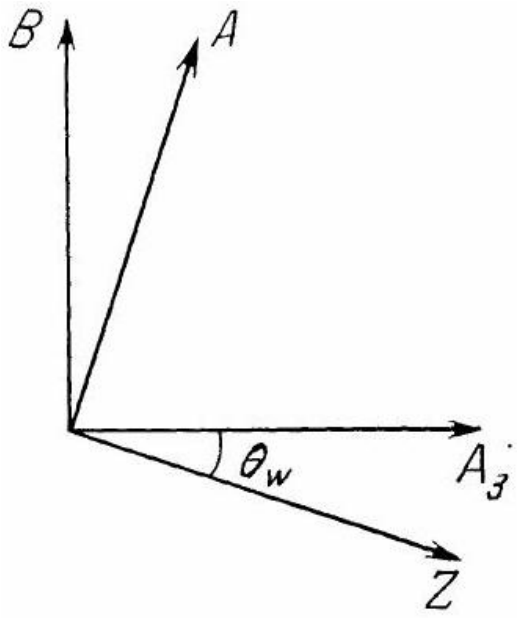


Fig. 21.1.

The parameter θ_{w} is called the Weinberg angle. Let us introduce the mutually orthogonal fields of the intermediate boson Z and the photon A (fig. 21.1). Furthermore, we shall use new symbols for charged bosons:

$$W^{\pm} \equiv A^{\pm} = \sqrt{\frac{1}{2}}\,(A_1 \pm iA_2)\,.$$

With new notation, the mass terms of the intermediate bosons are rewritten in the form:

$$\frac{1}{8}\bar{g}^2\eta^2 Z^2 + \frac{1}{4}g^2\eta^2\,|W_\mu|^2\,.$$

A comparison with standard expressions for mass terms in the lagrangian,

$$\frac{1}{2}m_{\mathrm{Z}}^2 Z^\mu Z_\mu, \quad m_{\mathrm{W}}^2 W^\mu W_\mu^*,$$

yields

$$m_{\mathrm{Z}} = \frac{1}{2}\bar{g}\eta, \quad m_{\mathrm{W}} = \frac{1}{2}g\eta, \quad \frac{m_{\mathrm{W}}}{m_{\mathrm{Z}}} = \cos\theta_{\mathrm{W}}.$$

As for the photon A, its mass remains zero.

If the Higgs sector of the lagrangian is even more complicated, the formulas for m_{W}^2 and m_{Z}^2 must be altered. It is obvious, however, that even in the case of several Higgs multiplets the parameter $\rho = \bar{g}^2 m_{\mathrm{W}}^2/g^2 m_{\mathrm{Z}}^2 = m_{\mathrm{W}}^2/m_{\mathrm{Z}}^2\cos^2\theta_{\mathrm{W}}$ which characterizes the strength of the four-fermion interaction of the neutral axial currents (see chapter 2) would remain equal to unity if all Higgs multiplets were doublets. The relation $\rho = 1$ would be invalid if some of the scalar multiplets have isospin larger than $\frac{1}{2}$.

We should emphasize that expressions for the photon and Z -boson,

$$A = B\cos\theta_{\rm W} + A_3\sin\theta_{\rm W},$$
$$Z = -B\sin\theta_{\rm W} + A_3\cos\theta_{\rm W},$$

where $\tan\theta_{\rm W} = g'/g$, are not related to the structure of the Higgs sector and are determined only by the structure of gauge fields. This is so because the photon representing a linear combination of fields B and A_3 does not interact, and this is normal for the photon, with neutral particles (and in particular, with φ^0 and $\bar{\varphi}^0$), while a combination orthogonal to this and representing the Z -boson is coupled both to charged and neutral particles. Let us discuss the couplings of the photon and of the Z -boson in more detail.

5.21.4 21.4. Relation between electric charge and the constants g and g'

As we can see from the expression for D_μ, the interaction of neutral gauge fields with hypercharge Y and isospin projection T_3 has the form

$$-ig'\frac{1}{2}YB - igT_3A_3.$$

Making use of the equality

$$Q = T_3 + \frac{1}{2}Y$$

where Q is electric charge in units of e, we transform the above expression to

$$\begin{aligned}
-ig'\frac{1}{2}YB - igT_3A_3 &= -ig'\left(\frac{1}{2}Y + T_3\right)B + i\left(g'B - gA_3\right)T_3 \\
&= -ig'QB - i\bar{g}T_3Z \\
&= -i\frac{g'g}{\bar{g}}QA + i\frac{g'^2}{\bar{g}}QZ - i\bar{g}T_3Z \\
&= -i\bar{g}\left(T_3 - Q\sin^2\theta_{\rm W}\right)Z - i\frac{g'g}{\bar{g}}QA.
\end{aligned}$$

This expression is universal. In particular, it is valid both for the left-handed and for the right-handed spinors, and of course for scalar particles. The expression shows that a neutral particle (one with $Q = 0$) is coupled only to the Z-boson but not to the photon. Therefore the Z-boson becomes massive when φ^0 acquires a non-zero vacuum-expectation value, and the photon remains massless (see the preceding section). Obviously, the last term in this expression, $-i\left(g'g/\bar{g}\right)QA$, describes the photon coupling to the electric charge, whence $g'g/\bar{g} = e = \sqrt{4\pi\alpha}$. This relation can be rewritten in the form

$$e = g\sin\theta_{\rm W}, \quad e = g'\cos\theta_{\rm W}, \quad e = \bar{g}\sin\theta_{\rm W}\cos\theta_{\rm W},$$

or

$$\frac{1}{e^2} = \frac{1}{g^2} + \frac{1}{g'^2}$$

We conclude that interactions of all gauge fields are determined by the electric charge e and one free parameter, namely the Weinberg angle. In particular, the "charge" characterizing the coupling of the left-handed or right-handed spinor to the Z -boson is equal to

$$-\frac{e}{\sin\theta_{\rm W}\cos\theta_{\rm W}}\left(T_3 - Q\sin^2\theta_{\rm W}\right),$$

where T_3 and Q are the particle isospin projection and particle charge.
The fact that both weak and electromagnetic interactions are characterized by the same charge e is the most conclusive demonstration of the standard model being a unified theory of weak and electromagnetic interactions. The theory is not yet completed because it contains a free parameter θ_{W} which is not calculated or predicted theoretically (we shall see in chapter 22 that experimentally $\theta_{\mathrm{W}} \cong 30^\circ$). The free parameter θ_{W} appears because the symmetry group of the weak interaction is a direct product of two simple groups, SU(2) and U(1). The arbitrary choice of θ_{W} could be eliminated if we assumed both groups to be subgroups of a larger group (see Chapter 25).

5.21.5 21.5. Relation between the vacuum-expectation value η and the Fermi constant G

In order to find the relation between η and G, let us consider the interaction of charged currents shown in fig. 21.2. The term $i\bar{L}\hat{D}L$ in the lagrangian yields for the vertices of this graph:

$$\begin{aligned} &-\tfrac{1}{2}ig\left(\bar{\nu}_{\mathrm{L}}\bar{e}_{\mathrm{L}}\right)\left[\tau_-\hat{W}^- + \tau_+\hat{W}^+\right]\binom{\nu_{\mathrm{L}}}{e_{\mathrm{L}}} \\ &= -\tfrac{1}{2}\sqrt{2}ig\left(\bar{e}_{\mathrm{L}}\hat{W}^-\nu_{\mathrm{L}} + \bar{\nu}_{\mathrm{L}}\hat{W}^+e_{\mathrm{L}}\right) \end{aligned}$$

(recall that $\tau_\pm = \sqrt{2}\begin{pmatrix} 0 & 1 \\ 0 & 0 \end{pmatrix}$). The amplitude corresponding to fig. 21.2 can now be found by means of the standard rules for Feynman graphs:

$$M = \frac{1}{2}g^2\left(\bar{e}_{\mathrm{L}}\gamma^\alpha\nu_{\mathrm{L}}\right)\left(\bar{\nu}_{\mathrm{L}}\gamma^\beta e_{\mathrm{L}}\right)\frac{g_{\alpha\beta} - q_\alpha q_\beta/m_{\mathrm{W}}^2}{m_{\mathrm{W}}^2 - q^2}$$

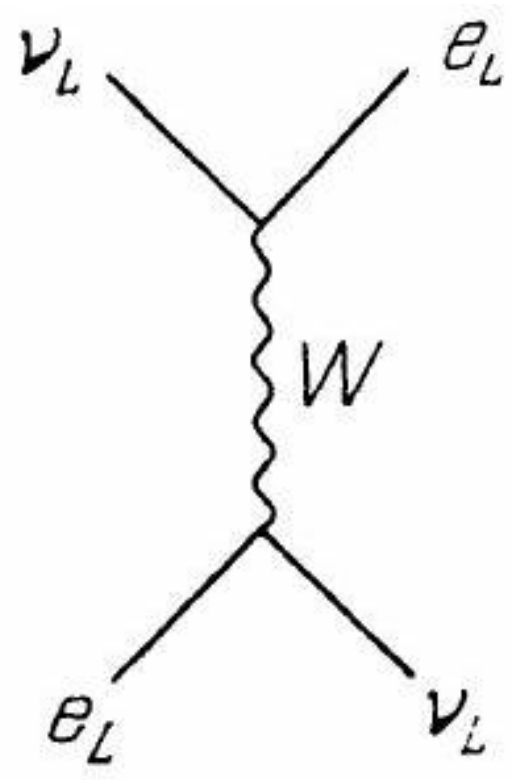


Fig. 21.2.

In the low-energy limit this expression becomes

$$M = \frac{g^2}{2m_{\mathrm{W}}^2} \left(\bar{e}_{\mathrm{L}} \gamma^\alpha \nu_{\mathrm{L}}\right) \left(\bar{\nu}_{\mathrm{L}} \gamma_\alpha e_{\mathrm{L}}\right),$$

which must be compared to the standard amplitude for ν e scattering obtained by multiplying charged currents,

$$M = \sqrt{\frac{1}{2}} G \left(\bar{e} \gamma^\alpha \left(1 + \gamma_5\right) \nu\right) \left(\bar{\nu} \gamma_\alpha \left(1 + \gamma_5\right) e\right).$$

The comparison yields:

$$\frac{g^2}{8m_{\mathrm{W}}^2} = \frac{G}{\sqrt{2}}.$$

It must be emphasized that this relation is much more general than the specific model in which it was derived. Recalling an expression derived earlier,

$$m_{\mathrm{W}}^2 = \frac{1}{4} g^2 \eta^2,$$

we find that

$$\frac{1}{\eta^2} = \sqrt{2} G, \quad \frac{1}{\eta} = \left(\sqrt{2} G\right)^{1/2},$$

or $\eta = 246\mathrm{GeV}$.

5.21.6 21.6. More about the masses of the W - and Z -bosons

By using the formulas

$$\frac{g^2}{8m_{\mathrm{w}}^2} = \frac{G}{\sqrt{2}} \quad \text{and} \quad g^2 = \frac{4\pi\alpha}{\sin^2 \theta_{\mathrm{w}}}$$

we obtain for the W -boson mass

$$m_{\mathrm{W}} = \frac{1}{\sin \theta_{\mathrm{W}}} \left(\frac{\pi\alpha}{\sqrt{2} G}\right)^{1/2} = \frac{37.3}{\sin \theta_{\mathrm{W}}} \mathrm{GeV}$$

Note that this relation is independent of the structure of the Higgs sector. Assuming the scalar fields to be isodoublet fields, we obtain the following expression for the Z -boson mass:

$$m_{\mathrm{Z}} = \frac{m_{\mathrm{W}}}{\cos \theta_{\mathrm{W}}} = \frac{37.3}{\sin \theta_{\mathrm{W}} \cos \theta_{\mathrm{W}}} = \frac{74.6}{\sin 2\theta_{\mathrm{W}}} \mathrm{GeV}$$

The minimum masses of the W - and Z -bosons are therefore 37.3 and 74.6 GeV , respectively. No wonder they were not found at the existing accelerators.

5.21.7 21.7. Electron mass

The next term of the lagrangian to be considered is

$$f_{\mathrm{e}} \left(\bar{L} e_{\mathrm{R}} \varphi + \bar{e}_{\mathrm{R}} L \varphi^+\right)$$

giving the mass of the electron. Substitution of

$$\varphi = \frac{1}{\sqrt{2}} \begin{pmatrix} 0 \\ \eta + \chi \end{pmatrix}$$

yields

$$\sqrt{\frac{1}{2}} f_{\mathrm{e}} \left(\bar{e}_{\mathrm{L}} e_{\mathrm{R}} + \bar{e}_{\mathrm{R}} e_{\mathrm{L}} \right) (\eta + \chi) = \sqrt{\frac{1}{2}} f_{\mathrm{e}} \bar{e} e (\eta + \chi)$$

The first term gives the electron a mass which is found to be $m_{\mathrm{e}} = f_{\mathrm{e}} \eta / \sqrt{2}$. There are no predictions about the value of f_{e} which is a serious shortcoming indicating that the theory is incomplete. The experimental value of f_{e} is very small,

$$f_{\mathrm{e}} = \frac{\sqrt{2} m_{\mathrm{e}}}{\eta} \simeq 3 \cdot 10^{-6}$$

So far we cannot understand how such a small parameter can appear in the theory. The constant f_{e} characterizes both the electron mass and its interaction with the field χ :

$$\sqrt{\frac{1}{2}} f_{\mathrm{e}} \bar{e} e (\eta + \chi) = m_{\mathrm{e}} \bar{e} e + (\sqrt{2} G)^{1/2} m_{\mathrm{e}} \chi \bar{e} e$$

We see that Higgs scalar bosons interact with particles the more strongly, the greater the masses of these particles.

Now it will be appropriate to mention how other leptons and quarks are included in the standard model.

5.21.8 21.8. Introduction of other leptons and quarks

All that we have said above concerning the electron and its neutrino, is valid for the muon and its neutrino. The leptonic sector of the lagrangian is expanded by including a doublet ($\nu_{\mu \mathrm{L}}, \mu_{\mathrm{L}}$) and two singlets $\nu_{\mu \mathrm{R}}$ and μ_{R}. Similarly, we add a doublet ($\nu_{\tau \mathrm{L}}, \tau_{\mathrm{L}}$) and two singlets $\nu_{\tau \mathrm{R}}$ and τ_{R}. If $m_{\nu_\mu} = 0$, $m_{\nu_\tau} = 0$, then $f_{\nu_\mu} = 0$ and $f_{\nu_\tau} = 0$ respectively. From what we have said about the electron mass, we obtain that $f_{\mathrm{e}} : f_\mu : f_\tau = m_{\mathrm{e}} : m_\mu : m_\tau$.

Addition of quarks to the standard model is carried out in a similar manner: left-handed particles form isodoublets, and right-handed ones form isosinglets. Three new aspects must be taken into account, however, when quarks are introduced into the model: first, quark hypercharges differ from those of leptons because of the quark fractional charges; second, not only f_{u}-type constants must be non-zero but f_{d}-type ones must be non-vanishing as well; third, the Cabibbo-like angles must be included.

The last of these three aspects will now be discussed for the four quarks, $\mathrm{u}, \mathrm{d}, \mathrm{s}, \mathrm{c}$ (to cover the b - and t -quarks would only entail algebraic complications, see Chapter 15).

Four left-handed quarks form two isodoublets,

$$\begin{pmatrix} u \\ d' \end{pmatrix}_{\mathrm{L}}, \quad \begin{pmatrix} c \\ s' \end{pmatrix}_{\mathrm{L}}$$

where

$$d' = d \cos \theta_{\mathrm{C}} + s \sin \theta_{\mathrm{C}}$$
$$s' = -d \sin \theta_{\mathrm{C}} + s \cos \theta_{\mathrm{C}}$$

and θ_{C} is the Cabibbo angle ($\theta_{\mathrm{C}} \cong 15^\circ$). This choice of left-handed quarks is based on the form of the quark charged current known from the experimental data:

$$\bar{u}_{\rm L}\gamma_\alpha d'_{\rm L} + \bar{c}_{\rm L}\gamma_\alpha s'_{\rm L}.$$

The right-handed quarks are represented by four singlets. Different choices are possible here: $u_{\rm R}, d'_{\rm R}, s'_{\rm R}, c_{\rm R}$, or $u_{\rm R}, d_{\rm R}, s_{\rm R}, c_{\rm R}$, or any other
orthogonal set. This arbitrariness takes place because right-handed quarks enter only the neutral current. We have shown above that the coupling to the Z-boson is completely determined by the quantity $T_3 - Q\sin^2\theta_{\rm W}$, so that we obtain two combinations,

$$\bar{u}_{\rm R}\gamma_\alpha u_{\rm R} + \bar{c}_{\rm R}\gamma_\alpha c_{\rm R}, \quad \bar{d}_{\rm R}\gamma_\alpha d_{\rm R} + s_{\rm R}\gamma_\alpha s_{\rm R},$$

invariant with respect to Cabibbo rotations

$$\bar{d}'_{\rm R}\gamma_\alpha d'_{\rm R} + \bar{s}'_{\rm R}\gamma_\alpha s'_{\rm R} = \bar{d}_{\rm R}\gamma_\alpha d_{\rm R} + \bar{s}_{\rm R}\gamma_\alpha s_{\rm R}.$$

This is also valid for neutral currents of left-handed quarks,

$$\bar{u}_{\rm L}\gamma_\alpha u_{\rm L} + \bar{c}_{\rm L}\gamma_\alpha c_{\rm L} \quad \text{and} \quad \bar{d}'_{\rm L}\gamma_\alpha d'_{\rm L} + \bar{s}'_{\rm L}\gamma_\alpha s'_{\rm L}$$

This explains why the neutral currents, in contrast to charged currents, conserve the type (flavor) of quarks. They are diagonal in flavor indices. Then why cannot we choose d′ and s′ as quarks, instead of d and s , and thus get rid of the Cabibbo angle? The answer to this question is related to quark masses and therefore to their interactions with scalar (Higgs) bosons. Contrary to the leptonic case in which the interactions of the Higgs bosons with e and μ are characterized by two constants $f_{\rm e}$ and f_μ, the interaction of the Higgs bosons with d′ and s′ contains three terms:

$$\begin{aligned}
&\sqrt{\frac{1}{2}} f_{\rm d'} \left(\bar{d}'_{\rm L} d'_{\rm R} + \bar{d}'_{\rm R} d'_{\rm L}\right)(\eta+\chi) = \sqrt{\frac{1}{2}} f_{\rm d'} \bar{d}' d' (\eta+\chi),\\
&\sqrt{\frac{1}{2}} f_{\rm s'} \left(\bar{s}'_{\rm L} s'_{\rm R} + \bar{s}'_{\rm R} s'_{\rm L}\right)(\eta+\chi) = \sqrt{\frac{1}{2}} f_{\rm s'} \bar{s}' s' (\eta+\chi),\\
&\sqrt{\frac{1}{2}} f_{\rm d's'} \left(\bar{s}'_{\rm L} d'_{\rm R} + \bar{s}'_{\rm R} d'_{\rm L} + \bar{d}'_{\rm R} s'_{\rm L} + \bar{d}'_{\rm L} s'_{\rm R}\right)(\eta+\chi)\\
&= \sqrt{\frac{1}{2}} f_{\rm d's'} \left(\bar{s}' d' + \bar{d}' s'\right)(\eta+\chi).
\end{aligned}$$

Rotation by the Cabibbo angle transforms the expression

$$\sqrt{\frac{1}{2}} \left[f_{\rm d'} \bar{d}' d' + f_{\rm s'} \bar{s}' s' + f_{\rm d's'} \left(\bar{s}' d' + \bar{d}' s'\right)\right] \eta$$

to a diagonal form:

$$m_{\rm d} \bar{d} d + m_{\rm s} \bar{s} s$$

where $m_{\rm d}$ and $m_{\rm s}$ are the masses of the d - and s-quarks. Comparison of the last two expressions yields

$$\begin{aligned}
m_{\rm d} &= \sqrt{\frac{1}{2}} \left(f_{\rm d'} \cos^2\theta_{\rm C} + f_{\rm s'} \sin^2\theta_{\rm C} - 2 f_{\rm d's'} \cos\theta_{\rm C} \sin\theta_{\rm C}\right) \eta,\\
m_{\rm s} &= \sqrt{\frac{1}{2}} \left(f_{\rm d'} \sin^2\theta_{\rm C} + f_{\rm s'} \cos^2\theta_{\rm C} + 2 f_{\rm d's'} \cos\theta_{\rm C} \sin\theta_{\rm C}\right) \eta,\\
\tan 2\theta_{\rm C} &= \frac{2 f_{\rm d's'}}{f_{\rm s'} - f_{\rm d'}}.
\end{aligned}$$

We see that the Cabibbo angle appears because $f_{d's'} \neq 0$.
There is a complete degeneracy with respect to flavors, as long as quarks interact only with gluons. Introduction of photons and Z -bosons separates the space of "up" quarks (with $Q = \frac{2}{3}$) from the space of "down" quarks (with $Q = -\frac{1}{3}$). Within each of these two groups degeneracy still persists. Introduction of the interaction with the Higgs bosons (H-bosons) removes this degeneracy and fixes a certain direction in each of these spaces. The interaction with the W-bosons singles out some other direction in the space of the d - and s-quarks; the difference in these two directions (H and W) is characterized by the Cabibbo angle.

A question is in order: why rotate only the d - and s-quarks, but not the uand c-quarks? The answer is: it is sufficient to rotate either d and s , or u and c, while simultaneous rotation of all of them yields no new observable phenomena. Indeed, the expression for the charged current is a function of only the difference in these rotation angles. Let us prove this statement. Let us assume the u-, d-, s-, c-quarks to have definite masses. Introduce the superpositions

$$\begin{aligned} d' &= d\cos\alpha + s\sin\alpha, \\ s' &= -d\sin\alpha + s\cos\alpha, \\ u' &= u\cos\beta + c\sin\beta, \\ c' &= -u\sin\beta + c\cos\beta, \end{aligned}$$

and consider a charged current of the type $\bar{u}'\gamma_\alpha d' + \bar{c}'\gamma_\alpha s'$. After elementary manipulations we obtain

$$\begin{aligned} \bar{u}'_{\mathrm{L}}\gamma_\alpha d'_{\mathrm{L}} + \bar{c}'_{\mathrm{L}}\gamma_\alpha s'_{\mathrm{L}} =& \bar{u}_{\mathrm{L}}\gamma_\alpha d_{\mathrm{L}}\cos\theta_{\mathrm{C}} + \bar{u}_{\mathrm{L}}\gamma_\alpha s_{\mathrm{L}}\sin\theta_{\mathrm{C}} \\ &+ \bar{c}_{\mathrm{L}}\gamma_\alpha s_{\mathrm{L}}\cos\theta_{\mathrm{C}} - \bar{c}_{\mathrm{L}}\gamma_\alpha d_{\mathrm{L}}\sin\theta_{\mathrm{C}}, \end{aligned}$$

where $\theta_{\mathrm{C}} = \alpha - \beta$. This result is a special case of a more general analysis given in Chapter 15, where we considered a unitary $n \times n$ matrix in flavor space, describing the weak charged current.

If the theory in question is correct, the key point of the "flavor" physics is the interaction of Higgs fields. Specific properties of different types of hadrons stem from the properties of the quark mass matrix, that is from the properties of the constants f. Small values of f for the u- and d-quarks make their masses small and thus result in the standard isotopic invariance. It is essential that the masses m_{u} and m_{d} may be very different. It will be sufficient for both to be much smaller than μ_c, where $1/\mu_c$ is the size of the hadron determined by the confinement radius. Comparatively large masses of the c-quarks result in striking peculiarities in the behavior of charmonium and charmed particles. Were it not for the differences in interactions of various quarks with Higgs bosons, we would find in nature SU(N) invariance of strong interactions (where N is the total number of distinct quark "flavors"), slightly violated by virtual photons (and intermediate bosons). So far the spectrum of quark and lepton masses, that is the pattern of the constants f, is not understood at all. There is no doubt that the experimental discovery of Higgs bosons would be an important step to solving this key problem of elementary particle physics.

5.22 22 Neutral currents

The prediction of neutral currents constituted the main contribution of the unified electroweak model to the domain of weak interactions at low energies, that is energies of the existing accelerators. Neutral currents in neutrino-nucleon interactions were discovered in 1973. Since then total cross sections of these processes, cross sections of some inelastic channels, and elastic cross sections were measured both for ν_μ and for $\bar{\nu}_\mu$. All these data agree with predictions of the standard model for $\theta_{\mathrm{w}} \cong 30°$.

The subject of the present chapter is a detailed discussion of the neutrinoelectron and neutrino-nucleon interactions. In addition, we shall discuss the effects due to the interference of the weak and electromagnetic interaction in neutrinoless processes: $e^+e^- \to \mu^+\mu^-$annihilation, scattering of electrons on nucleons, parity violation in atoms. At the end of the chapter we shall touch on the problem of parity violation in atomic nuclei.

5.22.1 22.1. Scattering of ν_e and $\overline{\nu}_e$ on the electron

It has been established in Chapter 21 that the "charge" characterizing the coupling of the "particle" to the Z-boson is $-\bar{g}\,(T_3 - \xi Q)$. Here we introduce the notation $\xi = \sin^2\theta_w$, with a view to shortening the subsequent formulas. The word "particle" is in quotation marks because in the case of leptons and quarks we consider separately the left-handed and right-handed components as having different values of T and T_3. The coupling to the Z -boson of the (ν_L, e_L) doublet has the form

$$i\bar{g}\frac{1}{2}\nu_L\hat{Z}\nu_L + i\bar{g}\left(-\frac{1}{2}+\xi\right)\bar{e}_L\hat{Z}e_L$$

and that of the singlet e_R :

$$i\bar{g}\xi\bar{e}_R\hat{Z}e_R.$$

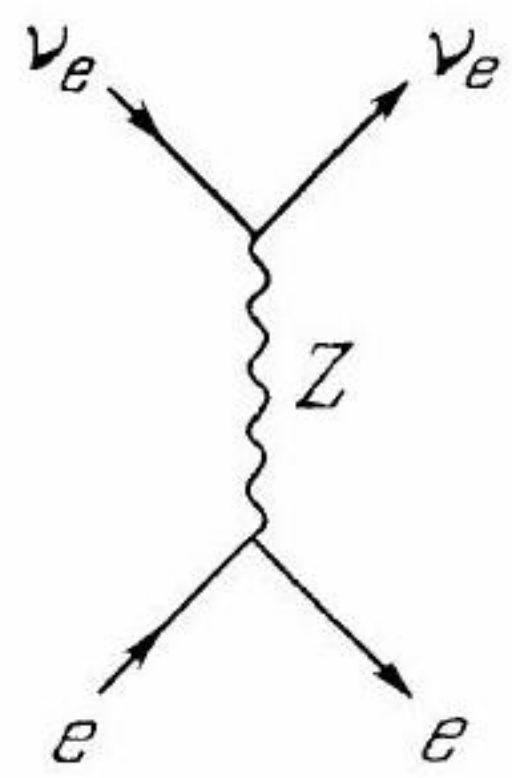


Fig. 22.1.

On the whole, the electron vertex has the form:

$$i\bar{g}\left[\left(-\frac{1}{2}+\xi\right)\bar{e}_L\gamma_\alpha e_L + \xi\bar{e}_R\gamma_\alpha e_R\right]Z^\alpha = i\bar{g}\left[-\frac{1}{2}\bar{e}_L\gamma_\alpha e_L + \xi\bar{e}\gamma_\alpha e\right]Z^\alpha.$$

The effective lagrangian of ν_e e scattering due to the exchange of the Z -boson is represented by the graph of fig. 22.1; at energies much smaller than the Z -boson mass, it takes the form:

$$2\sqrt{2}G\left(\bar{\nu}_{eL}\gamma^{\alpha}\nu_{eL}\right)\left[\left(-\frac{1}{2}+\xi\right)\bar{e}_{L}\gamma_{\alpha}e_{L}+\xi\bar{e}_{R}\gamma_{\alpha}e_{R}\right].$$

(Here we have taken into account that $\bar{g}^2/m_Z^2 = \rho g^2/m_W^2 = 4\sqrt{2}G\rho$ and that in the standard model $\rho = 1$ (see p. 190). Recalling that the squared total neutral current includes twice the product of the neutrino and electron currents, it is then easy to reconstruct the normalization of the four-fermion lagrangian $\mathfrak{L}^n$ given on p . 9). The contribution of this lagrangian to the total amplitude of ν_e e scattering is summed up with that of the effective lagrangian due to exchange of the W-boson (fig. 22.2). This second contribution is

$$\frac{g^2}{m_W^2}\frac{1}{2}\left(\bar{e}_{L}\gamma_{\alpha}\nu_{L}\right)\left(\bar{\nu}_{L}\gamma^{\alpha}e_{L}\right)=2\sqrt{2}G\left(\bar{e}_{L}\gamma_{\alpha}e_{L}\right)\left(\bar{\nu}_{L}\gamma^{\alpha}\nu_{L}\right).$$

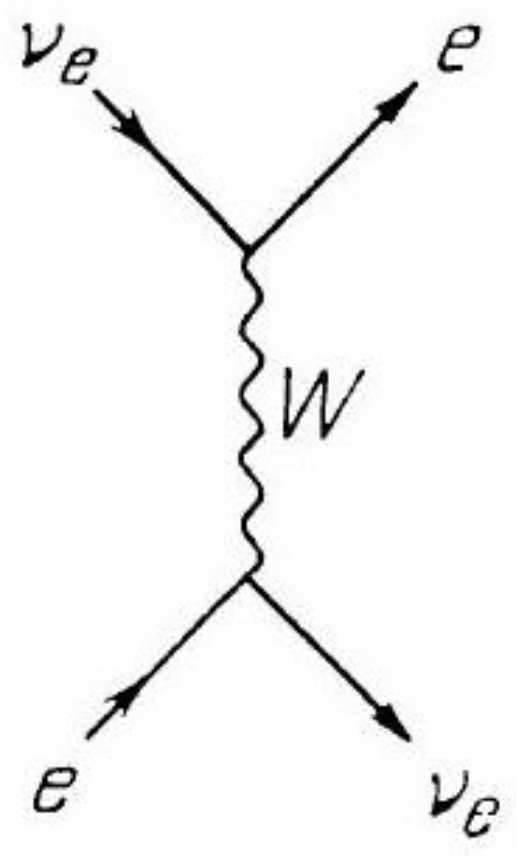


Fig. 22.2.

Here the factor $\frac{1}{2}$ appears because the vertex of W emission has the form

$$\sqrt{\frac{1}{2}}ig\bar{e}_{L}\hat{W}\nu_{eL}.$$

A point of special interest is the sign of the expression obtained by means of the Fierz transformation. Recall that this transformation changes the sign of the $V-A$ amplitude. However, the Fierz transformation does not change the sign of the effective $V-A$ lagrangian, since anticommutation of spinor operators supplies an additional minus sign.

The total contribution of the graphs of figs. 22.1 and 22.2 is then

$$2\sqrt{2}G\left(\bar{\nu}_{\mathrm{eL}}\gamma^\alpha\nu_{\mathrm{eL}}\right)\left[\left(\frac{1}{2}+\xi\right)\bar{e}_{\mathrm{L}}\gamma_\alpha e_{\mathrm{L}}+\xi\bar{e}_{\mathrm{R}}\gamma_\alpha e_{\mathrm{R}}\right].$$

Standard calculations (see chapter 16) demonstrate that this interaction corresponds to the cross sections

$$\sigma_{\nu_{\mathrm{e}}\mathrm{e}}=\frac{G^2 s}{\pi}\left[\left(\frac{1}{2}+\xi\right)^2+\frac{1}{3}\xi^2\right],$$
$$\sigma_{\tilde{\nu}_{\mathrm{e}}\mathrm{e}}=\frac{G^2 s}{\pi}\left[\frac{1}{3}\left(\frac{1}{2}+\xi\right)^2+\xi^2\right].$$

The last expression does not contradict the data obtained in experiments with reactor-produced antineutrinos. No data are available yet on ν_{e}e scattering.

5.22.2 22.2. Scattering of ν_μ and $\overline{\nu}_\mu$ on the electron

In the theory without neutral currents, the muon neutrino is not scattered by the electron in the first order in G because there is no $\bar{\mathrm{e}}\nu_\mu W$ vertex and therefore there is no graph similar to that of fig. 22.2. The theory with neutral currents predicts a process (see the graph in fig. 22.3) which goes via the exchange of the Z-boson.

We have already discussed the invariance of all intermediate boson couplings with respect to the $\nu_{\mathrm{e}} \leftrightarrow \nu_\mu$ and $\mathrm{e} \leftrightarrow \mu$ substitution. Consequently, the effective lagrangian corresponding to the graph of fig. 22.3 has the same form as that for fig. 22.1, namely:

$$2\sqrt{2}G\left(\bar{\nu}_{\mu\mathrm{L}}\gamma^\alpha\nu_{\mu\mathrm{L}}\right)\left[\left(-\frac{1}{2}+\xi\right)\bar{e}_{\mathrm{L}}\gamma_\alpha e_{\mathrm{L}}+\xi\bar{e}_{\mathrm{R}}\gamma_\alpha e_{\mathrm{R}}\right].$$

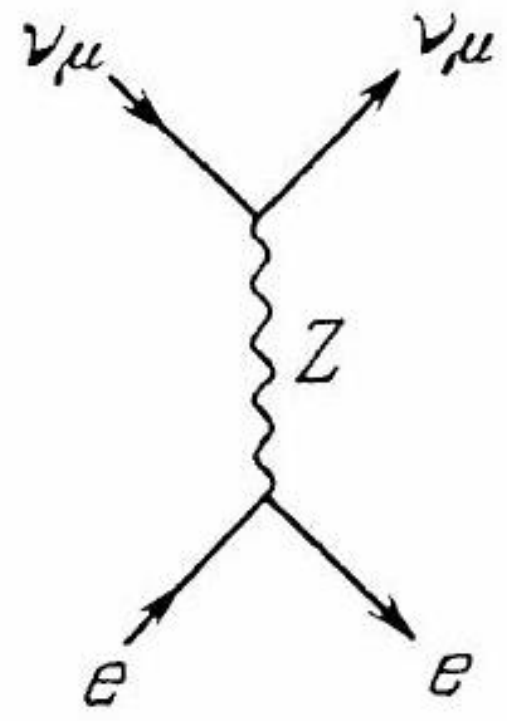


Fig. 22.3.

This interaction corresponds to the cross sections

$$\sigma_{\nu_\mu e} = \frac{G^2 s}{\pi}\left[\left(-\frac{1}{2}+\xi\right)^2 + \frac{1}{3}\xi^2\right],$$
$$\sigma_{\tilde{\nu}_\mu e} = \frac{G^2 s}{\pi}\left[\frac{1}{3}\left(-\frac{1}{2}+\xi\right)^2 + \xi^2\right].$$

Within experimental error, the data on ν_μ e scattering are in agreement with these expressions for $\xi \cong \frac{1}{4}$.

5.22.3 22.3. Annihilation $e^+e^- \to \mu^+\mu^-$

Annihilation may proceed in lower order of perturbation theory both via a virtual photon and via a virtual Z-boson (figs. 22.4 and 22.5). The graph in fig. 22.4 corresponds to production of a $\mu^+\mu^-$pair with negative C-parity (since the photon is C-odd). The graph in fig. 22.5 represents production of $\mu^+\mu^-$in a superposition of states with $C = +1$ and $C = -1$, because the Z -boson vertex contains both the axial and the vector interaction. Interference of states with $C = \pm 1$ must result in charge asymmetry in the distribution of $\mu^+$and μ^-(with respect to the e^+momentum in the center $\to$ f-mass frame of the colliding $e^+$and e^-). Let us calculate this effect. The amplitude corresponding to the sum of graphs in figs. 22.4 and 22.5 , is

$$\begin{aligned} M =& \frac{e^2}{q^2}\left[\bar{\mu}(p)\gamma_\alpha \mu\left(-p'\right)\right]\left[\bar{e}\left(-k'\right)\gamma^\alpha e(k)\right] \\ &+ \frac{\bar{g}^2}{q^2 - m_Z^2}\left[\left(-\frac{1}{2}+\xi\right)\bar{\mu}_L(p)\gamma_\alpha \mu_L\left(-p'\right) + \xi\bar{\mu}_R(p)\gamma_\alpha \mu_R\left(-p'\right)\right] \\ &\times\left[\left(-\frac{1}{2}+\xi\right)\bar{e}_L\left(-k'\right)\gamma^\alpha e_L(k) + \xi\bar{e}_R\left(-k'\right)\gamma^\alpha e_R(k)\right]. \end{aligned}$$

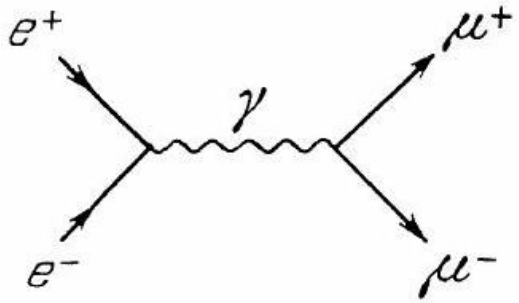


Fig. 22.4.

Here $\bar{\mu}(p)$ is the wave function of the created $\mu^-$with 4-momentum p; $\mu\left(-p'\right)$ is the wave function of the created $\mu^+$with 4 -momentum p'; $e(k)$ is the wave function of the annihilated $e^-$with 4 -momentum k; $\bar{e}\left(-k'\right)$ is the wave function of the annihilated $e^+$with 4 -momentum k'. Minus signs in front of k' and p' appear because of crossing. Neglecting the e and μ masses as compared to their energies, we have dropped the term

$$-\frac{q_\alpha q_\beta}{m_Z^2\left(q^2 - m_Z^2\right)}$$

in the Z -boson propagator.
Let us introduce the notation

$$x = \frac{\bar{g}^2}{e^2}\frac{q^2}{q^2 - m_{\mathrm{Z}}^2} \quad \left(x = -\frac{2\sqrt{2}G}{\pi\alpha}q^2 \quad \text{for } q^2 \ll m_{\mathrm{Z}}^2\right).$$

Omitting the arguments of the wave functions, M can now be written in the form:

$$\begin{aligned} M =& \frac{4\pi\alpha}{q^2}\left\{(\bar{\mu}_{\mathrm{L}}\gamma_\alpha\mu_{\mathrm{L}})(\bar{e}_{\mathrm{L}}\gamma^\alpha e_{\mathrm{L}})\left[1 + x\left(-\frac{1}{2} + \xi\right)^2\right] + (\bar{\mu}_{\mathrm{R}}\gamma_\alpha\mu_{\mathrm{R}})(\bar{e}_{\mathrm{R}}\gamma^\alpha e_{\mathrm{R}})\right. \\ &\times\left[1 + x\xi^2\right] + \left[(\bar{\mu}_{\mathrm{L}}\gamma_\alpha\mu_{\mathrm{L}})(\bar{e}_{\mathrm{R}}\gamma^\alpha e_{\mathrm{R}}) + (\bar{\mu}_{\mathrm{R}}\gamma_\alpha\mu_{\mathrm{R}})(\bar{e}_{\mathrm{L}}\gamma^\alpha e_{\mathrm{L}})\right] \\ &\times\left.\left[1 + x\xi\left(-\frac{1}{2} + \xi\right)\right]\right\}. \end{aligned}$$

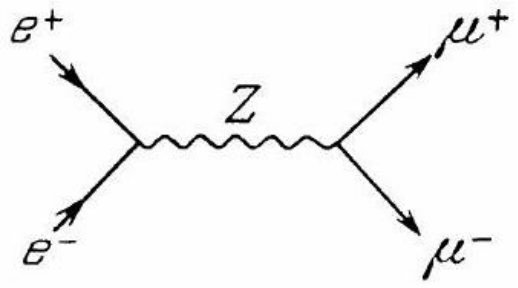


Fig. 22.5.

Let us introduce the new variables:

$$\begin{aligned} s &= (k' + k)^2 = (p' + p)^2 = q^2, \\ t &= (p - k)^2 = -\frac{1}{2}s(1 - \cos\theta) = -2pk = -2p'k', \\ u &= (p' - k)^2 = -\frac{1}{2}s(1 + \cos\theta) = -2p'k = -2pk' \end{aligned}$$

where θ is the angle between the momenta of the $e^-$and μ^-in the center-of-mass frame, and calculate $\overline{|M|^2}$, with the bar over $|M|^2$ denoting summation over the spins of $\mathrm{e}^+, \mathrm{e}^-, \mu^+$, and μ^-. Note that in this calculation the four terms contained in M do not interfere, since they correspond to different helicities of the initial and (or) final particles.

The Fierz transformation of the term $(\bar{\mu}_L\gamma_\alpha\mu_L)(\bar{e}_R\gamma^\alpha e_R)$ yields:

$$\begin{aligned} (\bar{\mu}_{\mathrm{L}}\gamma_\alpha\mu_{\mathrm{L}})(\bar{e}_{\mathrm{R}}\gamma^\alpha e_{\mathrm{R}}) &= 2(\mu_{\mathrm{L}}e_{\mathrm{R}})(e_{\mathrm{R}}\mu_{\mathrm{L}}) \\ &= \frac{1}{2}(\bar{\mu}(1 - \gamma_5)e)(\bar{e}(1 + \gamma_5)\mu), \end{aligned}$$

whence

$$\begin{aligned} |(\bar{\mu}_{\mathrm{L}}\gamma_\alpha\mu_{\mathrm{L}})(\bar{e}_{\mathrm{R}}\gamma^\alpha e_{\mathrm{R}})|^2 \Rightarrow \frac{1}{4}\operatorname{Tr}\hat{p}'(1 - \gamma_5)\hat{k}(1 + \gamma_5)\operatorname{Tr}\hat{k}'(1 + \gamma_5)\hat{p}'(1 - \gamma_5) \\ = 4(pk)4(p'k') = 4t^2. \end{aligned}$$

Likewise,

$$|(\bar{\mu}_{\mathrm{R}}\gamma_\alpha\mu_{\mathrm{R}})(\bar{e}_{\mathrm{L}}\gamma^\alpha e_{\mathrm{L}})|^2 \Rightarrow 4t^2.$$

It is not difficult to obtain, by using the Fierz transformation, the relation

$$|(\bar{\mu}_{\mathrm{L}}\gamma_\alpha\mu_{\mathrm{L}})\,(\bar{e}_{\mathrm{L}}\gamma^\alpha e_{\mathrm{L}})|^2 = |(\bar{\mu}_{\mathrm{R}}\gamma_\alpha\mu_{\mathrm{R}})\,(\bar{e}_{\mathrm{R}}\gamma^\alpha e_{\mathrm{R}})|^2 = 4\,(kp')\,4\,(pk') = 4u^2.$$

These results are quite similar to those derived for ν e scattering (see Chapter 16). They can be written down immediately if we consider the Feynman graph in the μ e scattering channel (fig. 22.6), and take into account that the

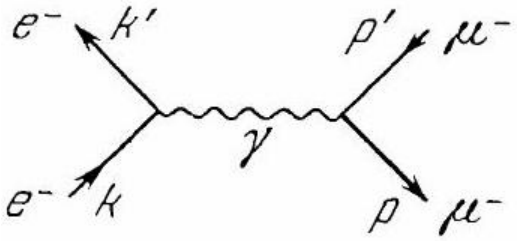


Fig. 22.6.

final result for a collision of two left-handed particles is proportional to the product $(kp')\,(k'p)$. Now let us calculate the cross section:

$$\frac{\mathrm{d}\sigma}{\mathrm{d}\cos\theta} = \frac{\pi\alpha^2}{s^3}\left[au^2 + bt^2\right] = \frac{\pi\alpha^2}{4s}\left[(a+b)\left(1+\cos^2\theta\right) + (a-b)2\cos\theta\right].$$

Here

$$a = \frac{1}{2}\left\{\left[1 + x\left(-\frac{1}{2}+\xi\right)^2\right]^2 + \left[1 + x\xi^2\right]^2\right\},$$

$$b = \left[1 + x\xi\left(-\frac{1}{2}+\xi\right)\right]^2.$$

If $x = 0$, then $a = 1$ and $b = 1$, and our cross section is equal to the well-known cross section of the electromagnetic annihilation $\mathrm{e^+e^-} \to \mu^+\mu^-$:

$$\frac{\mathrm{d}\sigma}{\mathrm{d}\cos\theta} = \frac{\pi\alpha^2}{2s}\left(1+\cos^2\theta\right) \Rightarrow \sigma = \frac{4\pi\alpha^2}{3s}.$$

If $x \neq 0$, then $a - b = \frac{1}{4}\left[x + \frac{1}{2}x^2\left(\frac{1}{2} - 2\xi\right)^2\right]$. If $s \ll m_{\mathrm{Z}}^2$, then $x < 0$ and $a - b \simeq \frac{1}{4}x$, and therefore negative muons must be emitted predominantly in the direction of the initial positron.

Charge asymmetry appears even if Z bosons are ignored, because of the interference of graphs shown in figs. 22.6 and 22.7; it will also appear as a result of the interference of graphs in figs. 22.8 and 22.9, in which the $\mu^+\mu^-$ pairs have different values of C-parity. However, the purely electromagnetic charge asymmetry is a slowly varying function of the energy of the colliding beams, and reaches a maximum for small angles θ. This fact makes it possible to extract the effect of neutral currents.

Experiments of this type are to be run in the colliding $\mathrm{e^+e^-}$beam facilities PETRA 2×19GeV (Hamburg) and PEP 2×15GeV (Stanford). The expected event rate may be several events per hour for storage ring luminosity $L = 10^{31}$ event $/\mathrm{cm}^2\cdot$ s, and the cross section $\sigma = 4\pi\alpha^2/3s \simeq 0.8\cdot10^{-34}$ cm^2 (for $s = 900\mathrm{GeV}^2$).

In principle, the contribution of neutral currents can be detected through longitudinal muon polarization due to parity non-conservation. It appears, however, that this would be a more difficult experiment.

Now we shall turn to neutral current effects in lepton-hadron interactions.

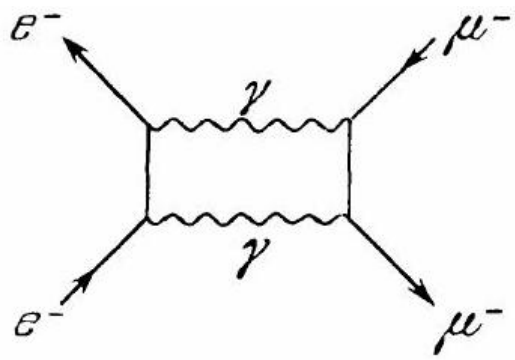


Fig. 22.7.

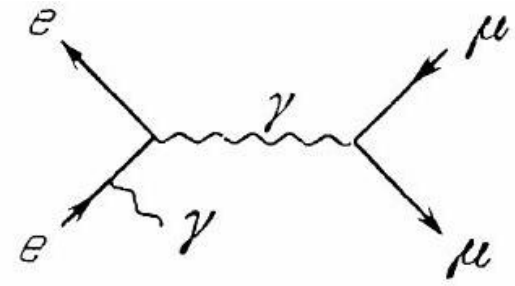


Fig. 22.8.

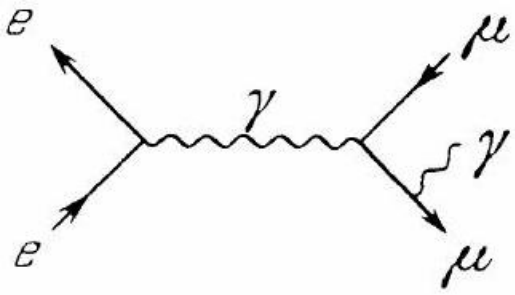


Fig. 22.9.

5.22.4 22.4. Neutral currents and neutrino-nucleon interaction

The interaction of a neutrino with a nucleon could be reduced to its interaction with quarks. Starting with the "Z-charge" equal to $-\bar{g}\,(T_3 - \xi Q)$, we can write the couplings of the u - and d -quarks to the Z -bosons as

$$i\bar{g}\left[\left(\frac{1}{2}-\frac{2}{3}\xi\right)\bar{u}_{\rm L}\hat{Z}u_{\rm L}-\frac{2}{3}\xi\bar{u}_{\rm R}\hat{Z}u_{\rm R}\right],$$
$$i\bar{g}\left[\left(-\frac{1}{2}+\frac{1}{3}\xi\right)\bar{d}_{\rm L}\hat{Z}d_{\rm L}+\frac{1}{3}\xi d_{\rm R}\hat{Z}d_{\rm R}\right].$$

Hereafter we consider only "small" momentum transfer, $|q^2| \ll m_{\rm Z}^2$. In this limit, there is the effective four-fermion interaction

$$2\sqrt{2}G\,(\bar{\nu}_{\rm L}\gamma_\alpha\nu_{\rm L})\left[\left(\tfrac{1}{2}-\tfrac{2}{3}\xi\right)\bar{u}_{\rm L}\gamma^\alpha u_{\rm L}-\tfrac{2}{3}\xi\bar{u}_{\rm R}\gamma^\alpha u_{\rm R}\right.$$
$$\left.+\left(-\tfrac{1}{2}+\tfrac{1}{3}\xi\right)\bar{d}_{\rm L}\gamma^\alpha d_{\rm L}+\tfrac{1}{3}\xi\bar{d}_{\rm R}\gamma^\alpha d_{\rm R}\right]$$

(we recall that $\bar{g}^2/2m_{\rm Z}^2 = 2\sqrt{2}G$, see Chapter 21).

Making use of this equation, we can derive an expression for the cross section for the deep-inelastic interaction. We shall calculate the cross section per "mean nucleon", that is $\frac{1}{2}(\sigma_{\rm p}+\sigma_{\rm n})$. As before, $u(x)/x$ and $d(x)/x$ denote u- and d-quark distribution densities in the proton (in order to simplify formulas we shall neglect, as a crude approximation, the contribution of $\mathrm{s}, \bar{\mathrm{s}}, \bar{\mathrm{u}}$, and $\bar{\mathrm{d}}$). The distribution densities in the "mean nucleon" are identical for the u - and d -quark, and are equal to $(1/2x)[u(x)+d(x)]$. Recall that x stands for the fraction of the total nucleon momentum carried by a quark. The cross sections are given in the parton model in terms of mean quantities (see Chapter 17),

$$U=\int_0^1 u(x)\mathrm{d}x \quad \text{and} \quad D=\int_0^1 d(x)\mathrm{d}x$$

and are equal to

$$\sigma_\nu^{\rm Z}=\frac{G^2 s}{2\pi}(U+D)\left[\left(\frac{1}{2}-\frac{2}{3}\xi\right)^2+\frac{1}{3}\left(\frac{2}{3}\xi\right)^2\right.$$
$$\left.+\left(-\frac{1}{2}+\frac{1}{3}\xi\right)^2+\frac{1}{3}\left(\frac{1}{3}\xi\right)^2\right],$$
$$\sigma_{\bar{\nu}}^{\rm Z}=\frac{G^2 s}{2\pi}(U+D)\left[\frac{1}{3}\left(\frac{1}{2}-\frac{2}{3}\xi\right)^2+\left(\frac{2}{3}\xi\right)^2\right.$$
$$\left.+\frac{1}{3}\left(-\frac{1}{2}+\frac{1}{3}\xi\right)^2+\left(\frac{1}{3}\xi\right)^2\right].$$

These expressions take into account that cross sections for fermions with the same helicities are larger by a factor of three than those for fermions with opposite helicities. It is convenient to consider the ratios of neutral current cross sections, NC, to charged current cross sections, CC. We recall that in the latter case, the cross sections in the approximation under discussion are

$$\sigma_\nu^{\rm W}=\frac{G^2 s}{2\pi}(U+D), \quad \sigma_{\bar{\nu}}^{\rm W}=\frac{1}{3}\frac{G^2 s}{2\pi}(U+D).$$

The above-mentioned ratios are:

$$R_\nu=\frac{\boldsymbol{\sigma}_\nu^{\rm Z}}{\boldsymbol{\sigma}_\nu^{\rm W}}=\frac{1}{2}-\xi+\frac{20}{27}\xi^2$$
$$R_{\bar{\nu}}=\frac{\boldsymbol{\sigma}_{\bar{\nu}}^{\rm Z}}{\boldsymbol{\sigma}_{\bar{\nu}}^{\rm W}}=\frac{1}{2}-\xi+\frac{20}{9}\xi^2$$

Initially the experimental values of R_ν and $R_{\bar\nu}$ were very different ($R_\nu \cong 0.15, R_\nu \cong 0.45$). A trend of convergence has appeared with time, however, and according to the most recent results, $R_\nu = 0.29 \pm 0.01, R_{\bar\nu} = 0.35 \pm 0.05$. This immediately gives

$$\xi = \frac{1}{2}\left(1 + R_{\bar\nu} - 3R_\nu\right) \cong \frac{1}{4}.$$

Recall that $\xi = \sin^2\theta_{\mathrm{W}}$, whence $\theta_{\mathrm{W}} \cong \pm 30^\circ$.

Until now we were discussing only inclusive reactions on heavy nuclei. Reactions on hydrogen were also studied experimentally: elastic, $\nu\mathrm{p} \to \nu\mathrm{p}$ and $\bar\nu\mathrm{p} \to \bar\nu\mathrm{p}$; inelastic, $\nu\mathrm{p} \to \nu\mathrm{X}$ and $\bar\nu\mathrm{p} \to \bar\nu\mathrm{X}$; and exclusive, $\nu\mathrm{p} \to \nu\mathrm{p}\pi^0$, $\nu\mathrm{p} \to \nu\mathrm{n}\pi^+$, and $\nu\mathrm{n} \to \nu\mathrm{p}\pi^-$. The data for all these reactions are in agreement with the value $\xi \cong \frac{1}{4}$. Note that the experiments show the elastic cross section to be different for the neutrino and antineutrino:

$$\frac{\sigma(\bar\nu\mathrm{p} \to \bar\nu\mathrm{p})}{\sigma(\nu\mathrm{p} \to \nu\mathrm{p})} \cong 0.4 \pm 0.2$$

This fact is of special importance. The ratio would be exactly unity for the pure vector or pure axial interaction. Hence, experiment points to the interference of these interactions. This means for any model with a single Z -boson that the Z coupling to quarks does not conserve parity. (With two Z -bosons, one of them could be coupled only to the vector current and the other to the axial one. In this case the cross sections for ν and $\bar\nu$ would differ because of the interference of the vector and axial amplitudes even if parity were conserved).

5.22.5 22.5. Isotopic properties of the neutral current

Isotopic properties of the weak neutral current play an important role in the analysis of weak interactions involving nucleons. This holds both for neutrino reactions and for some other processes: P-odd electron-nucleon interactions and P-odd nuclear forces.

The quark neutral current has the form

$$\sum_q \left(g^q_{\mathrm{L}}\bar q_{\mathrm{L}}\gamma_\alpha q_{\mathrm{L}} - g^q_{\mathrm{R}}\bar q_{\mathrm{R}}\gamma_\alpha q_{\mathrm{R}}\right)$$

where summation covers all quark flavors $q = \mathrm{u}, \mathrm{d}, \mathrm{s}, \ldots$. In the standard model,

$$g^q_{\mathrm{L}} = T_3^{\mathrm{w}} - Q\xi$$
$$g^q_{\mathrm{R}} = -Q\xi$$

where ${T_3}^{\mathrm{w}}$ is the weak isospin of the quark in the left-handed isodoublet, and Q is the quark charge. The values of T_3^{w} and those of T_3 (projection of the usual isospin characterizing hadrons) are identical for the u - and d - quarks which play the decisive role in weak interactions of nucleons:

$$T_3^{\mathrm{w}}(u) = T_3(u) = +\frac{1}{2},$$
$$T_3^{\mathrm{w}}(d) = T_3(d) = -\frac{1}{2}.$$

This enables us to determine the properties of weak neutral currents in the usual isospace: the right-handed current is an isoscalar (term $Q\xi$), while the left-handed current is a superposition of an isoscalar (the term $Q\xi$, and terms T_3^{w} for the s-, c-, and b-quarks) and a component of an isovector (terms T_3^{w} for the u- and d-quarks). Sometimes it is convenient to change from the left-handed and right-handed currents to the vector and axial ones:

$$g_{\rm V}^q = g_{\rm L}^q + g_{\rm R}^q, \quad g_{\rm A}^q = g_{\rm L}^q - g_{\rm R}^q.$$

This gives

$$g_{\rm V}^q = T_3^{\rm w} - 2Q\xi,$$
$$g_{\rm A}^q = T_3^{\rm w}.$$

The axial neutral current of the u- and d-quarks is therefore a pure isovector. This current is in one triplet with the axial charged currents coupled to the $W^+$and W^-bosons. The isoscalar component of the vector current of the u - and d -quarks is proportional to $\sin^2\theta_{\rm w}$. We recall that this component results from the mixing of the isovector and isoscalar intermediate bosons (see chapter 21).

5.22.6 22.6. Parity non-conservation in scattering of electrons by nucleons

Neutral currents must result in breaking of mirror symmetry in electronnucleon (or muon-nucleon) interactions. The effective four-fermion interaction responsible for parity violation is

$$4\sqrt{2}G[g_{\rm L}^{\rm e}\bar{e}_{\rm L}\gamma_\alpha e_{\rm L} + g_{\rm R}^{\rm e}\bar{e}_{\rm R}\gamma_\alpha e_{\rm R}]\sum_q [g_{\rm L}^q\bar{q}_{\rm L}\gamma^\alpha q_{\rm L} + g_{\rm R}^q\bar{q}_{\rm R}\gamma^\alpha q_{\rm R}]$$
$$= -\frac{1}{4}\sqrt{2}G\left[(1-4\xi)\bar{e}\gamma_\alpha e + \bar{e}\gamma_\alpha\gamma_5 e\right]$$
$$\times\sum_q\left[(2T_3 - 4Q\xi)\,\bar{q}\gamma^\alpha q + 2T_3\bar{q}\gamma^\alpha\gamma_5 q\right]$$

The summation is taken over all quark flavors. (We recall that $g_{\rm L}^{\rm e} = -\frac{1}{2} + \xi$, $g_{\rm R}^{\rm e} = \xi$). Terms of two types violate conservation of parity: (i) the product of the axial quark current with the vector electron current, and (ii) the product of the vector quark current with the axial electron current.

The electron-nucleon P-odd interaction was first observed in bismuth atoms (see the next section). Soon the same phenomenon was found in deep-inelastic scattering of polarized electrons when the asymmetry

$$A = \frac{{\rm d}\sigma_{\rm R} - {\rm d}\sigma_{\rm L}}{{\rm d}\sigma_{\rm R} + {\rm d}\sigma_{\rm L}}$$

was measured at the Stanford accelerator (R and L denote the left-handed and right-handed polarization, respectively, of the incident electron beam). The result obtained was $A = (-9.5 \pm 1.6)\cdot 10^{-5}\left(Q^2/{\rm GeV}^2\right)$ for scattering by deuterium, ed $\to$ eX with the momentum transfer squared $Q^2 \cong 1.6{\rm GeV}^2$. It is easy to derive a theoretical expression for the asymmetry A if one takes into account that asymmetry is produced by the interference of the large P-even amplitude corresponding to photon exchange (fig. 22.10) and the small P-odd amplitude (Fig. 22.11). By restricting the analysis to the contribution of the valence u- and d-quarks, we obtain by means of standard calculations:

$$A = -\frac{GQ^2}{2\sqrt{2}\pi\alpha}\frac{9}{10}\left[\left(1 - \frac{20}{9}\xi\right) + (1-4\xi)K(y)\right]$$
$$= -1.62\cdot 10^{-4}\left[\left(1 - \frac{20}{9}\xi\right) + (1-4\xi)K(y)\right]\left(\frac{Q}{\rm GeV}\right)^2$$

Here

$$K(y) = \frac{1-(1-y)^2}{1+(1-y)^2},$$

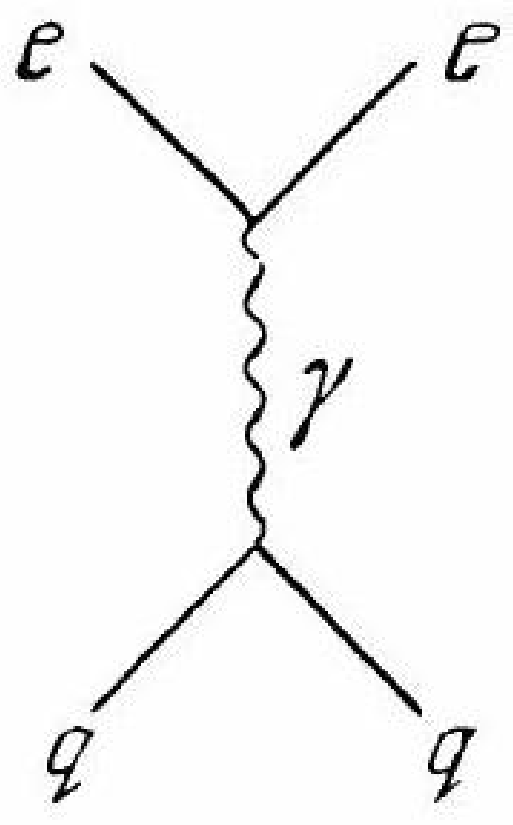


Fig. 22.10.

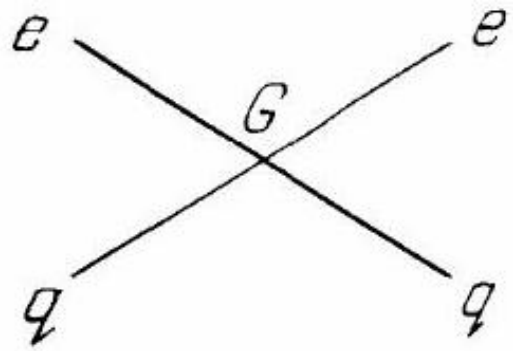


Fig. 22.11.

where $y = 1 - E'/E_0$, and E_0 and E' are the electron energy prior to and after the collision, respectively. (Note that the term $(1 - \frac{20}{9}\xi)$ appears because of the product of the axial electron current with the vector quark current, while the product of the vector electron current with the axial quark current is responsible for the term $(1 - 4\xi)K(y)$.) In the Stanford experiment, $y \cong 0.21$. A comparison of the theoretical expression for A with its experimental value gives $\xi = 0.20 \pm 0.03$.

5.22.7 22.7. Parity non-conservation in atoms

The product of the axial electron current with the vector quark current is responsible for the appearance of the main P-odd term in the interaction between atomic electrons and nucleons of the nucleus. The point is, the vector "Z-charge" of the nucleus is the the sum of vector "Z-charges" of nucleons, and thus may be quite high in heavy nuclei. By using the vector charges of the proton and neutron, and the electron axial charge, we obtain the interaction

$$\sqrt{2}G\left(-\frac{1}{2}\bar{e}\gamma_\alpha\gamma_5 e\right)\left[-\frac{1}{2}\bar{n}\gamma^\alpha n+\left(\frac{1}{2}-2\xi\right)\bar{p}\gamma^\alpha p\right].$$

In the coordinate representation, this interaction is described by a potential

$$V(r)=\frac{G\kappa}{2\sqrt{2}m_\mathrm{e}}[\boldsymbol{\sigma}\cdot\boldsymbol{p}\delta(\boldsymbol{r})+\delta(\boldsymbol{r})\boldsymbol{\sigma}\cdot\boldsymbol{p}],$$

where $\boldsymbol{p}=-i\nabla$ is the momentum operator, m_e is the electron mass,
$\kappa=-\frac{1}{2}$ for the neutron, and
$\kappa=\frac{1}{2}(1-4\xi)$ for the proton.
It was established above that $\xi\cong\frac{1}{4}$. Therefore, we expect that the coefficient κ for the proton in the standard model is much smaller than κ for the neutron, and that for the nucleus, $\kappa\cong-\frac{1}{2}(A-Z)$. The potential V
may produce mixing of atomic levels with different parity. As a result, a P-even level acquires a small P-odd admixture. The amplitude F of this admixture may be estimated as follows:

$$F=\frac{\langle V\rangle}{\Delta E},$$

where $\langle V\rangle$ is the matrix element of the potential V between two mixed levels, and ΔE is the spacing between these levels. In hydrogen $\langle V\rangle$ is typically of the order of $Gva^{-3}\simeq Gm_\mathrm{e}^2\alpha^4$, since the electron velocity $v\simeq\alpha$ and the Bohr radius $a\simeq 1/m_\mathrm{e}$; finally, typical level spacing is $\Delta E\simeq\alpha^2 m_\mathrm{e}$. Therefore, $F\simeq\alpha^2 Gm_\mathrm{e}^2\simeq 10^{-15}$. However, this negligibly small quantity may in some cases be enhanced by specific factors. For instance, let us consider the transition between the hydrogen levels $2\ \mathrm{S}_{1/2}$ and $1\ \mathrm{S}_{1/2}$. In the absence of P-odd effects, this is a magnetic dipole transition with a small amplitude $A(\mathrm{M1})\simeq\alpha^2\mu$, where $\mu=e/2m_\mathrm{e}$ is the Bohr magneton. (The transition is forbidden in the non-relativistic approximation, because of the orthogonality of the wave functions of the ground and excited S-states).

The P-odd admixture must lead to emission, due to the "impure" $2\ \mathrm{S}_{1/2}$ level, of the electric dipole photon as well. The amplitude of this transition is $FA(\mathrm{E1})$, where $A(\mathrm{E1})\simeq ea$ is the amplitude of the $2\mathrm{P}_{1/2}\to 1\ \mathrm{S}_{1/2}$ transition, and F is the mixing amplitude of the levels $2\mathrm{P}_{1/2}$ and $2\ \mathrm{S}_{1/2}$. These levels are known to be split only by the Lamb shift which is of the order of $\alpha^5 m_\mathrm{e}$. As a result, in this case $F\simeq Gm_\mathrm{e}^2/\alpha\simeq 10^{-9}$. The interference of the electric and magnetic transitions must produce circular polarization of photons:

$$P=2F\frac{A(\mathrm{E1})}{A(\mathrm{M1})}\simeq\frac{Gm_\mathrm{e}^2}{\alpha}\left(\frac{ea}{\alpha^2\mu}\right)\simeq\frac{Gm_\mathrm{e}^2}{\alpha^4}\simeq 10^{-3}.$$

Unfortunately, observation of this effect in hydrogen is hindered by the same reasons that render it strong: long lifetime of the $2\ \mathrm{S}_{1/2}$ level, and the background of the adjacent $2\mathrm{P}_{1/2}$ level. The effect may possibly be detected in beams of hydrogen atoms excited to a metastable level. In heavy atoms (Tl, Pb, Bi) the effect is smaller, viz. $P\simeq Gm_\mathrm{e}^2\alpha^2 Z^3(ea/\mu)\simeq 10^{-7}$, but easier to observe.

Parity non-conservation in atomic transitions was first observed early in 1978 by Barkov and Zolotorev (Novosibirsk). They measured the rotation angle of the polarization plane (

$(-3 \pm 0.5) \cdot 10^{-8}$rad) in a linearly polarized laser light after transmission through atomic bismuth vapor. Both the value and the sign of the observed optical activity of bismuth vapor are in agreement with the predictions of the standard electroweak model for $\sin^2\theta_{\rm W} \simeq \frac{1}{4}$.

Another parity non-conservation effect was found at the end of 1978 in Berkeley when a circularly polarized laser beam was passed through thallium vapor; the absorption cross section for right-hand polarized photons was found to be higher than that for left-hand polarized photons, which again is in agreement with the standard electroweak model. While the effect in bismuth is due to parity non-conservation in the real part of the refractive index, in thallium it was measured in the imaginary part.

Parity non-conservation effects are also expected for μ-atoms, but so far experimental accuracy is too low to enable detection.

5.22.8 22.8. P-odd nuclear forces

We shall not discuss in detail the contribution of neutral currents to the nucleon-nucleon weak interaction. The experimentally observed parity nonconservation in nuclear forces may be caused both by charged and by neutral currents. The effect of neutral currents could be ascertained by measuring the isovector component of P-odd nuclear forces. The reason for this is that this term appears with only a small factor, $\sin^2\theta_{\rm C}$, when occurring in the product of charged currents, but is not suppressed when occurring in the product of neutral currents. In particular, the term with $\Delta T = 1$ must appear in the S -wave P-odd isovector vertex $f e_{ikl} \bar{N} \tau_i N \pi_k$ (similar vertices with $\Delta T = 0, 2$ are forbidden by CP conservation).

An analysis of a comparatively large effect of parity non-conservation in the nuclei ^{19} F, ^{41} K, ^{175}Lu and ^{181}Ta, observed in a number of experiments, indicates that f is higher by about an order of magnitude than could be expected in the case of charged currents only. If this interpretation is correct, one must expect considerable, $\cong 0.5\%$, circular polarization of photons emitted in transitions from the excited level $0^+$to the ground level 1^+in the nucleus ^{18} F. (The effect is anticipated to be high, because of the presence of a 0^-level with $T = 1$ close to the level $0^+$with $T = 0$.) Unfortunately, this prediction could be very much suppressed by purely nuclear effects, whose magnitudes are not yet known.

5.23 23 Properties of intermediate bosons

In this chapter we shall calculate partial and full widths of the W - and Z-bosons, and discuss projects for experiments designed to produce these particles.

The masses of intermediate bosons are unambiguously predicted by the standard model of the electroweak interaction provided the Weinberg angle is known:

$$m_{\rm w} = \left(\frac{\pi\alpha}{\sqrt{2}G}\right)^{1/2} \frac{1}{\sin\theta_{\rm w}} = \frac{37.3}{\sin\theta_{\rm w}}\text{GeV},$$
$$m_{\rm z} = \frac{m_{\rm w}}{\cos\theta_{\rm w}} = \frac{74.6}{\sin 2\theta_{\rm w}}\text{GeV}.$$

The neutrino experiments discussed in Chapter 22 yield $\sin\theta_{\rm W} \cong \frac{1}{2}$. This means that $m_{\rm w} \cong 75\text{GeV}, m_{\rm Z} \cong 87\text{GeV}$. If the model is extended by introducing additional bosons, some of them may be much lighter. In this chapter, however, we shall not leave the framework of the standard model.

5.23.1 23.1. Decays of W-bosons

We begin with calculating the width of the $\mathrm{W}^{\pm} \to \mathrm{e}^{\pm}\nu$ decay. We remind the reader that the coupling of the W-boson to the $\bar{\mathrm{e}}\nu$ current is fixed by gauge invariance. It immediately follows from the term

$$i\vec{L}\hat{D}L = i\vec{L}\left(\hat{\partial} - \frac{1}{2}ig\boldsymbol{\tau}\cdot\hat{\boldsymbol{A}} - \frac{1}{2}ig'Y\hat{B}\right)L$$

where

$$L = \begin{pmatrix}\nu_{\mathrm{eL}}\\ e_{\mathrm{L}}\end{pmatrix}, \quad \boldsymbol{\tau}\cdot\boldsymbol{A} = \tau_3 A_3 + \tau_+ W^- + \tau_- W^+,$$

that the We ν vertex has the form

$$\frac{1}{2}\sqrt{2}g\left(\bar{\nu}_{\mathrm{L}}\hat{W}e_{\mathrm{L}} + \bar{e}_{\mathrm{L}}\hat{W}^*\nu_{\mathrm{L}}\right)$$

We make use of the standard formula (see appendix, Chapter 29, sect. 4):

$$\Gamma = \frac{\overline{|M|^2}}{3\cdot 2m_{\mathrm{w}}\cdot 8\pi}$$

Here the factor $\frac{1}{3}$ appears as a result of averaging over spin states of the W-boson, and the bar denotes summation over spin states of the leptons and the W -boson.

$$\begin{aligned}\overline{|M|^2} &= \frac{1}{2}g^2\left(-g^{\alpha\beta} + \frac{k^\alpha k^\beta}{m_{\mathrm{W}}^2}\right)\frac{1}{4}\,\mathrm{Tr}\,\hat{p}_{\mathrm{e}}\gamma_\alpha\hat{p}_\nu\gamma_\beta\left(1+\gamma_5\right)^2\\ &= \frac{1}{2}g^2 4\left(p_{\mathrm{e}}p_\nu\right) = g^2 m_{\mathrm{W}}^2.\end{aligned}$$

The term $k^\alpha k^\beta/m_{\mathrm{W}}^2$ in the W-boson density matrix gives zero contribution since the electron mass was neglected. Then we immediately obtain:

$$\Gamma(\mathrm{W}\to\mathrm{e}\nu) = \frac{g^2 m_{\mathrm{W}}}{48\pi} = \frac{G m_{\mathrm{W}}^3}{6\sqrt{2}\pi} \simeq 180\mathrm{MeV}, \qquad \text{if } m_{\mathrm{W}} \simeq 75\mathrm{GeV}$$

(we have made use of the equality $g^2/2m_{\mathrm{w}}^2 = 4G/\sqrt{2}$).
Compared to the W-boson mass, we can neglect not only the electron mass but also the muon, and τ-lepton masses; consequently,

$$\Gamma\left(\mathrm{W}\to\mathrm{e}\nu_{\mathrm{e}}\right) = \Gamma\left(\mathrm{W}\to\mu\nu_\mu\right) = \Gamma\left(\mathrm{W}\to\tau\nu_\tau\right).$$

Consider hadronic decays of the W -boson. According to the parton model, the total probability of the W-boson decay to a hadronic state with the quantum numbers of the $u\bar{d}$ pair is equal to the probability of decay into this pair calculated with strong interactions switched off. The same is true for the $u\bar{s}, c\bar{s}$, and $c\bar{d}$ pairs. Taking into account the Cabibbo angle θ_{C} and the color factor 3, and neglecting quark masses, we obtain:

$$\begin{aligned}\Gamma(\mathrm{W}\to\mathrm{u}\overline{\mathrm{d}}) = \Gamma(\mathrm{W}\to\mathrm{c}\overline{\mathrm{s}}) &= 3\Gamma(\mathrm{W}\to\mathrm{e}\nu)\cos^2\theta_{\mathrm{C}}\\ \Gamma(\mathrm{W}\to\mathrm{u}\overline{\mathrm{s}}) = \Gamma(\mathrm{W}\to\mathrm{c}\overline{\mathrm{d}}) &= 3\Gamma(\mathrm{W}\to\mathrm{e}\nu)\sin^2\theta_{\mathrm{C}}.\end{aligned}$$

So far we know very little about b - and t -quarks. As an estimate, assume

$$\Gamma(\mathrm{W}\to\mathrm{t}\overline{\mathrm{b}}) = 3\Gamma(\mathrm{W}\to\mathrm{e}\nu).$$

Finally, the total width of the W -boson is (provided no heavier quarks exist)

$$\Gamma^{\mathrm{W}}_{\mathrm{tot}} \cong 12\Gamma(\ \mathrm{W} \to \mathrm{e}\nu) \cong 2.2\mathrm{GeV}.$$

5.23.2 23.2. Decays of Z -bosons

It will be convenient to begin our analysis of Z decays by considering the vertex

$$\frac{1}{2}\bar{g}\bar{\nu}_{\mathrm{eL}}\hat{Z}\nu_{\mathrm{eL}}.$$

The corresponding width is

$$\Gamma\left(\mathrm{Z} \to \nu_{\mathrm{e}}\bar{\nu}_{\mathrm{e}}\right) = \frac{\bar{g}^2 m_{\mathrm{Z}}}{96\pi} = \frac{G m_{\mathrm{Z}}^3}{12\sqrt{2}\pi} \cong 140\mathrm{MeV} \quad \text{for } m_{\mathrm{Z}} \cong 87\mathrm{MeV}$$

(we recall that $\bar{g}/g = m_{\mathrm{Z}}/m_{\mathrm{W}} = 1/\cos\theta_{\mathrm{W}}$ so that

$$\frac{\Gamma\left(\mathrm{Z} \to \nu_{\mathrm{e}}\bar{\nu}_{\mathrm{e}}\right)}{\Gamma\left(\mathrm{W} \to \mathrm{e}\nu_{\mathrm{e}}\right)} = \frac{1}{2\cos^3\theta_{\mathrm{W}}} \cong 0.77 \text{ for } \theta_{\mathrm{W}} = 30^\circ\Big).$$

Obviously, $\Gamma\left(\nu_{\mathrm{e}}\bar{\nu}_{\mathrm{e}}\right) = \Gamma\left(\nu_{\mu}\bar{\nu}_{\mu}\right) = \Gamma\left(\nu_{\tau}\bar{\nu}_{\tau}\right)$. It is not difficult, using the expression for the "Z-charge", $-\bar{g}\left(T_3 - \xi Q\right)$, to write expressions for Z-boson couplings to other leptons and quarks (recall that $\xi = \sin^2\theta_{\mathrm{w}}$):

$$\begin{aligned}
&\bar{g}\left[\left(-\tfrac{1}{2}+\xi\right)\bar{e}_{\mathrm{L}}\hat{Z}e_{\mathrm{L}} + \xi e_{\mathrm{R}}\hat{Z}e_{\mathrm{R}}\right] && \text{(the same for } \mu \text{ and } \tau\text{);}\\
&\bar{g}\left[\left(\tfrac{1}{2}-\tfrac{2}{3}\xi\right)\bar{u}_{\mathrm{L}}\hat{Z}u_{\mathrm{L}} - \tfrac{2}{3}\xi\bar{u}_{\mathrm{R}}\hat{Z}u_{\mathrm{R}}\right] && \text{(the same for c and t);}\\
&\bar{g}\left[\left(-\tfrac{1}{2}+\tfrac{1}{3}\xi\right)\bar{d}_{\mathrm{L}}\hat{Z}d_{\mathrm{L}} + \tfrac{1}{3}\xi\bar{d}_{\mathrm{R}}\hat{Z}d_{\mathrm{R}}\right] && \text{(the same for s and b).}
\end{aligned}$$

From these we obtain:

$$\begin{aligned}
\Gamma(\mathrm{Z} \to \mathrm{e}\bar{\mathrm{e}}) &\simeq \Gamma(\mathrm{Z} \to \mu\bar{\mu}) \simeq \Gamma(\mathrm{Z} \to \tau\bar{\tau})\\
&= \left[(-1+2\xi)^2 + 4\xi^2\right]\Gamma\left(Z \to \nu_{\mathrm{e}}\bar{\nu}_{\mathrm{e}}\right) \simeq 0.5\Gamma\left(\mathrm{Z} \to \nu_{\mathrm{e}}\bar{\nu}_{\mathrm{e}}\right);\\
\Gamma(\mathrm{Z} \to \mathrm{u}\bar{\mathrm{u}}) &\simeq \Gamma(\mathrm{Z} \to \mathrm{c}\bar{\mathrm{c}}) \simeq \Gamma(\mathrm{Z} \to \mathrm{t}\bar{\mathrm{t}})\\
&= 3\left[\left(1-\frac{4}{3}\xi\right)^2 + \left(\frac{4}{3}\xi\right)^2\right]\Gamma\left(\mathrm{Z} \to \nu_{\mathrm{e}}\bar{\nu}_{\mathrm{e}}\right) \simeq \frac{5}{3}\Gamma\left(\mathrm{Z} \to \nu_{\mathrm{e}}\bar{\nu}_{\mathrm{e}}\right);\\
\Gamma(\mathrm{Z} \to\ \mathrm{d}\,\overline{\mathrm{d}}) &\simeq \Gamma(\mathrm{Z} \to\ \mathrm{s}\,\overline{\mathrm{s}}) \simeq \Gamma(\mathrm{Z} \to\ \mathrm{b}\,\overline{\mathrm{b}})\\
&= 3\left[\left(-1+\frac{2}{3}\xi\right)^2 + \left(\frac{2}{3}\xi\right)^2\right]\Gamma\left(\mathrm{Z} \to \nu_{\mathrm{e}}\bar{\nu}_{\mathrm{e}}\right) \simeq \frac{13}{6}\Gamma\left(\mathrm{Z} \to \nu_{\mathrm{e}}\bar{\nu}_{\mathrm{e}}\right).
\end{aligned}$$

The total width of the Z -boson for $\xi = \frac{1}{2}$ is

$$\Gamma^{\mathrm{Z}}_{\mathrm{tot}} \simeq 8\left(3 - 6\xi + 8\xi^2\right)\Gamma\left(\mathrm{Z} \to \nu_{\mathrm{e}}\bar{\nu}_{\mathrm{e}}\right) \simeq 16\Gamma\left(\mathrm{Z} \to \nu_{\mathrm{e}}\bar{\nu}_{\mathrm{e}}\right) \simeq 2.2\mathrm{GeV}.$$

By measuring $\Gamma^{\mathrm{Z}}_{\mathrm{tot}}$ one can find whether the products of Z -boson decays include, in addition to $\nu_{\mathrm{e}}, \nu_{\mu}, \nu_{\tau}$, neutrinos of other types.

5.23.3 23.3. Production of Z -bosons

An optimal method of creation of a Z-particle is to use colliding $\mathrm{e}^+\mathrm{e}^-$ beams:

$$\mathrm{e}^+\mathrm{e}^- \to \mathrm{Z} \to \text{ decay products.}$$

Production of a Z-boson must appear as a resonance at $E = \sqrt{s} = m_Z$, with width $\Gamma \cong 2\text{GeV}$. In a resonance, the cross section for transition to the final state f is given by the Breit-Wigner formula:

$$\sigma = \frac{4\pi(2J+1)}{2 \cdot 2m_{\mathrm{Z}}^2} \frac{\Gamma_{\mathrm{i}}\Gamma_{\mathrm{f}}}{(E-m_{\mathrm{Z}})^2 + \frac{1}{4}\Gamma^2}.$$

Here $J = 1$ is the spin of the Z -boson. The factor $2 \cdot 2$ in the denominator comes from averaging over the electron and positron spins, and

$$\Gamma_{\mathrm{i}} = \Gamma\left(\mathrm{Z} \to \mathrm{e}^+\mathrm{e}^-\right), \quad \Gamma_{\mathrm{f}} = \Gamma(\mathrm{Z} \to \mathrm{f}), \quad \Gamma = \Gamma(\mathrm{Z} \to \text{ all }).$$

Assume that the resonance is realized, that is $(E-m_{\mathrm{Z}})^2 \ll \frac{1}{4}\Gamma^2$, and that we wish to find the total cross section, that is $\Gamma_{\mathrm{f}} = \Gamma$. We have:

$$\sigma = \frac{12\pi}{m_{\mathrm{Z}}^2} \frac{\Gamma(\mathrm{Z} \to \mathrm{e}\bar{\mathrm{e}})}{\Gamma} \cong \frac{0.5}{16} \frac{12\pi}{m_{\mathrm{Z}}^2} \cong 4 \cdot 10^{-32} \text{ cm}^2.$$

It means that colliding electron-positron beams with energy of about 2×45 GeV and luminosity $L = 10^{32}$ event $/\mathrm{s} \cdot \mathrm{cm}^2$ would produce several Z-bosons per second. This would be a veritable Z -boson factory. It should be instructive to compare the resonance cross section of the process

$$\mathrm{e}^+\mathrm{e}^- \to \mathrm{Z} \to \mu^+\mu^-$$

with that of electromagnetic production $\mathrm{e}^+\mathrm{e}^- \to \gamma \to \mu^+\mu^-$at $\sqrt{s} = m_{\mathrm{Z}}$. The former cross section is equal to $(12\pi/m_{\mathrm{Z}}^2)\left(\Gamma_{\mathrm{ee}}/\Gamma\right)^2$, and the latter is $\frac{4}{3}\pi\left(\alpha/m_{\mathrm{Z}}\right)^2$. Their ratio is

$$\frac{9}{\alpha^2}\left(\frac{\Gamma_{\mathrm{ee}}}{\Gamma}\right)^2 \simeq 160.$$

Note that for $\sqrt{s} = m_Z$, the expected energy resolution in colliding beams is of the order of 100 MeV , that is much less than the Z -boson width. Therefore radiative corrections to the above expressions are fairly small, of the order of α, and without large logarithmic terms (as in the case of production of very narrow resonances, such as the J/ψ meson).

5.23.4 23.4. Production of W-bosons

Only non-resonance production of pairs of charged W -bosons is possible in colliding $\mathrm{e}^+\mathrm{e}^-$beams (fig. 23.1). The pair production cross section of W -bosons is smaller than the resonance production cross section of Z -bosons by approximately $3-4$ orders of magnitude. Besides, this process requires even higher energies for the colliding electrons and positrons. It seems more feasible, therefore, to realize production of single W -bosons in colliding $\mathrm{p}\overline{\mathrm{p}}$ or pp beams with energies of several hundreds of GeV or more in each beam, i.e., the inclusive reactions

$$\mathrm{p} + \overline{\mathrm{p}} \to \mathrm{W} + \mathrm{X},$$
$$\mathrm{p} + \mathrm{p} \to \mathrm{W} + \mathrm{X},$$

where X stands for any hadronic state.
These reactions are based on resonance production of W-bosons in quark-antiquark collisions. We have already mentioned in chapter 17 that a fast proton can be treated as an ensemble or partons, that is quarks, antiquarks, and gluons which carry approximately 44,7 , and 49% of its momentum, respectively. The cross section of W production in a collision of a u-quark (from the proton) and a $\overline{\mathrm{d}}$-quark (from the colliding antiproton) is equal to

$$\sigma = \frac{12\pi}{2 \cdot 2 \cdot 3 \cdot 3m_{\mathrm{W}}^2} \frac{\Gamma_l \Gamma}{\left(E - m_{\mathrm{W}}\right)^2 + \frac{1}{4}\Gamma^2}.$$

This formula is quite similar to that describing production of Z -bosons in e^+e^-collisions, and differs by a factor $3 \cdot 3$ in the denominator. This factor appears as a result of averaging over color states of the colliding quarks and antiquarks. (With other conditions equal, the width of the W-decay into colored quarks is three times that of the decay into colorless leptons since the sum over three colors is included. However, the cross section of W production from colored quarks is smaller by a factor of three than that of

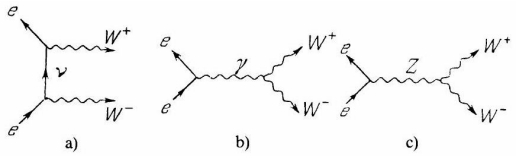


Fig. 23.1.

production from colorless leptons, since a quark of a given color can annihilate into W only with an antiquark of the same color. The reduction factor is three and not nine because one of the factors of three in the denominator is cancelled by a factor of three in the numerator.) Hence, the cross section of resonance W production would be equal to

$$\begin{aligned}\sigma_{\mathrm{res}}(\mathrm{u} + \overline{\mathrm{d}} \to \ \mathrm{W}) &= \frac{12\pi}{9m_{\mathrm{W}}^2} \frac{\Gamma(\ \mathrm{W} \to \mathrm{u}\,\overline{\mathrm{d}})}{\Gamma} \cong \frac{12\pi}{9m_{\mathrm{W}}^2} \frac{3}{12} \\ &= \frac{\pi}{3m_{\mathrm{W}}^2} \cong 6 \cdot 10^{-32}\ \mathrm{cm}^2\end{aligned}$$

Both the proton and antiproton can be viewed as bunches of quarks and antiquarks whose energies form a continuous spectrum. It is therefore convenient to write out the cross section of W production by quarks in the limit in which the quark energy spread is much wider than the W-boson width. In this limit it has the following form:

$$\begin{aligned}\sigma(\mathrm{u} + \overline{\mathrm{d}} \to \ \mathrm{W} \to \mathrm{f}) &= \frac{\pi}{3m_{\mathrm{W}}^2} \frac{\Gamma_{\mathrm{i}}\Gamma_{\mathrm{f}}}{\left(E - m_{\mathrm{W}}\right)^2 + \frac{1}{4}\Gamma^2} \\ &= \frac{4\pi}{3} \frac{\Gamma_{\mathrm{i}}\Gamma_{\mathrm{f}}}{\left(s_{\mathrm{u}\,\overline{\mathrm{d}}} - m_{\mathrm{W}}^2\right)^2 + m_{\mathrm{W}}^2\Gamma^2} \\ &\Rightarrow \frac{4\pi}{3} \frac{\Gamma_{\mathrm{i}}\Gamma_{\mathrm{f}}}{m_{\mathrm{W}}\Gamma} \pi\delta\left(s_{\mathrm{ud}} - m_{\mathrm{W}}^2\right) = \frac{4\pi^2}{3} \frac{\Gamma_{\mathrm{i}}\Gamma_{\mathrm{f}}}{m_{\mathrm{W}}\Gamma s} \delta\left(x_1 x_2 - \tau\right),\end{aligned}$$

where $\Gamma_{\mathrm{i}} = \Gamma(\mathrm{W} \to \mathrm{ud}), s = \left(p_{\mathrm{p}} + p_{\overline{\mathrm{p}}}\right)^2, \tau = m_{\mathrm{W}}^2/s$, the u-quark 4momentum is equal to $x_1 p_{\mathrm{p}}$, and that of the $\overline{\mathrm{d}}$-quark is $x_2 p_{\overline{\mathrm{p}}}; p_{\mathrm{p}}$ and $p_{\overline{\mathrm{p}}}$ are the proton and antiproton 4 -momenta, respectively. Therefore,

$$\begin{aligned}s_{\mathrm{ud}} &= \left(p_{\mathrm{u}} + p_{\overline{\mathrm{d}}}\right)^2 \simeq 2p_{\mathrm{u}}p_{\overline{\mathrm{d}}} = x_1 x_2 \cdot 2p_{\mathrm{p}}p_{\overline{\mathrm{p}}} \\ &\simeq x_1 x_2 \left(p_{\mathrm{p}} + p_{\overline{\mathrm{p}}}\right)^2 = x_1 x_2 s.\end{aligned}$$

Averaging over the u-quark and $\overline{\mathrm{d}}$-quark spectra yields the following cross section of W production in channel i (followed by decay in the channel f):

$$\sigma = \frac{4\pi^2}{3} \frac{\Gamma B_{\mathrm{i}} B_{\mathrm{f}}}{m_{\mathrm{W}}^3} \int u\left(x_1\right) d\left(x_2\right) \delta\left(x_1 x_2 - \tau\right) \mathrm{d}x_1\ \mathrm{d}x_2.$$

Here $B_{\mathrm{i}} = \Gamma_{\mathrm{i}}/\Gamma \equiv \Gamma(\mathrm{W} \to \mathrm{u}\overline{\mathrm{d}})/\Gamma \simeq \frac{1}{4}$. Let us choose the channel $\mathrm{W} \to \mu\nu$ as an example of channel f . Then $B_{\mathrm{f}}\Gamma = \Gamma(\mathrm{W} \to \mu\nu) = Gm_{\mathrm{W}}^3/6\pi\sqrt{2}$. If the integrand included no δ-function, we would have

$$\sigma \simeq \frac{\pi GUD}{28\sqrt{2}} \simeq 2.4 \cdot 10^{-35}\ \mathrm{cm}^2.$$

Recall that $U = \int u(x)\mathrm{d}x \simeq 0.28, D = \int d(x)\mathrm{d}x \simeq 0.15$ (distribution of d-quarks in the antiproton is the same as that of d-quarks in the proton), so that $UD \simeq 0.04$.

Let us change variables from x_1, x_2 to $\tau' = x_1x_2$ and $\xi = x_1 - x_2$. Then $x_{1,2} = \frac{1}{2}\xi \pm \sqrt{\frac{1}{4}\xi^2 + \tau'}$ and

$$\int u\left(x_1\right) d\left(x_2\right) \delta\left(x_1x_2 - \tau\right) \mathrm{d}x_1\ \mathrm{d}x_2 = \int \frac{u\left(x_1\right) d\left(x_2\right)}{\sqrt{\xi^2 + 4\tau'}} \mathrm{d}\xi$$

The variable ξ is the longitudinal momentum of the W -boson in units of the maximum possible momentum, $\frac{1}{2}\sqrt{\ }\mathrm{s}$. It will be convenient to introduce a normalized quantity K, whose values are obtained by numerical integration for various values of τ :

$$K = \frac{1}{UD} \int \frac{u\left(x_1\right) d\left(x_2\right)}{\sqrt{\xi^2 + 4\tau}}\ \mathrm{d}\xi; K\left(\tau = 10^{-2}\right) \simeq 10,$$
$$K\left(\tau = 10^{-1}\right) \simeq 4.$$

The above estimates of the cross section based on the parton model constitute a distant extrapolation from the available experimental data. Quantum chromodynamics predicts deviations from the parton model. In particular, emission of bremsstrahlung gluons must increase the transverse momenta of the annihilating quark and antiquark, and hence the transverse momenta of the W-bosons produced. Nevertheless, QCD calculations show that qualitatively the parton model predictions hold.

In order to have abundant collisions of sufficiently fast quarks, the energy $\sqrt{s}$ of the colliding p and $\overline{\mathrm{p}}$ must be several times larger than the W-boson mass, that is the parameter τ must be $\lesssim \frac{1}{10}$. If two proton beams collide, their energy $\sqrt{s}$ must be still higher since the "sea" antiquarks in the proton are much softer than valence antiquarks in the antiproton.

5.23.5 23.5. Colliding beam projects

At present there is no doubt that clarification of the dynamics of weak interactions calls for colliding beam experiments at energies above the Zand W-boson thresholds.

Projects of colliding lepton beams with energies of the order of 50 to 100 GeV in each beam have been the subject of discussion since the beginning of the late 60's. For instance, the Yerevan project of colliding $\mathrm{e}^+\mathrm{e}^-$beams for 2×100GeV and Budker's idea of colliding $\mu^+\mu^-$beams for 2×250 GeV were debated at the 1969 Yerevan International Conference on Accelerators. In 1975 Richter published a detailed analysis of colliding $\mathrm{e}^+\mathrm{e}^-$ beams with energy 2×100GeV. By Richter's estimates, a machine of this type will cost around 10^9 dollars. Such a machine would be an extremely powerful generator of synchrotron radiation whose industrial application would pay back at least partly the cost of construction. Detailed plans for the LEP project of colliding electron-positron beams, with energy of about 80 GeV in each beam, were discussed at CERN. LEP is a ring about 10 km in diameter, with luminosity of the order of $10^{31} - 10^{32}\ \mathrm{cm}^{-2}\ \mathrm{s}^{-1}$ and energy spread of the order of 0.1%.

The pp and $\overline{\mathrm{p}}\mathrm{p}$ colliders will be built in the following laboratories. An accelerating and storage complex (UNK, for Uskoritel'no Nakopitel'ny Kompleks) with energies of colliding beams equal to 3 TeV is being considered for construction at Serpukhov. The proton-proton storage

ring ISABELLE (2×400GeV) is under construction at Brookhaven. The construction of two $\overline{\mathrm{p}}\mathrm{p}$ colliders, at CERN (2×270GeV) and FNAL (2×1000GeV), will be completed in the eighties.

5.23.6 23.6. DUMAND

It would be interesting to observe creation of W -bosons in a purely leptonic collision. The neutrino energy required to produce a W-boson in a collision $\bar{\nu}\mathrm{e}^- \to \mathrm{W}^-$is

$$E_0 = \frac{m_{\mathrm{W}}^2}{2m_{\mathrm{e}}} \cong 5 \cdot 10^{15}\mathrm{eV}.$$

Such neutrinos can only be found in cosmic rays. The process $\mathrm{e}\nu \to \mathrm{W}$ could yield unique information on the intensity of the flux of cosmic neutrinos.

The project DUMAND (for Deep Underwater Muon and Neutrino Detector), which is now actively discussed, could in principle allow observation of this reaction. The project envisages the construction deep in the ocean of a gigantic cubic lattice of detectors, with the length of the cube edge of about one kilometer. The lattice period is to be about 10 m if the detectors are optical, and about a hundred meters if they are acoustic. The
project would make it possible to work with a water target whose mass exceeds 10^{15} g, and to observe neutrino reactions at very high energies.

Assume the differential flux of neutrinos with energy E to be $j(E)$ neutrino $/\mathrm{cm}^2 \cdot$ s$\cdot$sr. Let us find the number of $\bar{\nu} + \mathrm{e}^- \to \mathrm{W}^-$events per second, n, in a target containing N_{e} electrons:

$$n = 2\pi \int N_{\mathrm{e}} j(E) \frac{\mathrm{d}E}{\mathrm{d}E'} \mathrm{d}E' \sigma\left(E'\right)$$

Here E is the laboratory energy of the neutrino, and E' is the total energy in the center-of-mass frame of the electron and neutrino:

$$E'^2 = 2m_{\mathrm{e}}E \quad \text{and} \quad \frac{\mathrm{d}E}{\mathrm{d}E'} = \frac{E'}{m_{\mathrm{e}}} = \frac{m_{\mathrm{w}}}{m_{\mathrm{e}}}.$$

The factor 2π appears because resonance-energy neutrinos do not enter the detector from the lower hemisphere, being absorbed within the earth. This angular asymmetry is an indication of W-boson production. We now take into account that

$$\begin{aligned} \sigma\left(E'\right) &= \frac{4\pi(2J+1)}{2m_{\mathrm{W}}^2} \frac{\Gamma_i \Gamma}{\left(E' - m_{\mathrm{W}}\right)^2 + \frac{1}{4}\Gamma^2} \\ &\simeq \frac{12\pi^2}{m_{\mathrm{W}}^2} \Gamma(\ \mathrm{W} \to \mathrm{e}\nu) \delta\left(E' - m_{\mathrm{W}}\right) \end{aligned}$$

Then

$$n = 4\sqrt{2}\pi^2 j\left(E_0\right) E_0 G N_{\mathrm{e}}.$$

Therefore, the expected number of events is determined by a single variable, namely by the neutrino flux $j\left(E_0\right)$ at the neutrino energy E_0 corresponding to the W-boson mass: $E_0 = m_{\mathrm{w}}^2/2m_{\mathrm{e}}$. (In the literature the integral flux $\Phi(E)$, obeying a power law, is used:

$$\Phi(E) = \int_E^\infty j(E)\mathrm{d}E = AE^{-\gamma}$$

Hence, in this case $E_0 j\left(E_0\right) = \gamma\Phi\left(E_0\right)$.)

5.24 24 Properties of Higgs bosons

This chapter will discuss in more detail the role played by Higgs bosons (H-bosons) in weak interactions at high energies. We shall also consider the possible mechanisms of creation and decay of these particles.

We have established earlier, when discussing how the electron mass appears in the standard model of the electroweak interaction, that the coupling of the electron to a scalar Higgs boson represented by the real field χ is determined by the value of the electron mass:

$$\frac{m_{\mathrm{e}}}{\eta}(\eta+\chi)\bar{e}e = m_{\mathrm{e}}\bar{e}e + (\sqrt{2}G)^{1/2}m_{\mathrm{e}}\chi\bar{e}e$$

(recall that $\eta = (\sqrt{2}G)^{-1/2} = 246\mathrm{GeV}$). Interaction of H-bosons with other fermions is similar: the coupling is the stronger the heavier the fermion is. H -bosons are coupled weakly to light leptons and light quarks. This conclusion is valid if the theory contains only one isodoublet of scalar mesons, as the standard electroweak model does. With more than one doublet, some of the bosons may have anomalously strong coupling to light particles.

Before considering the reactions involving H-bosons, a few remarks must be made about the expected masses of these particles.

5.24.1 24.1. On the H-boson mass

In contrast to the W - and Z -boson masses, the mass of the H -boson is not fixed by the Weinberg angle and represents a free parameter of the model. The H-boson mass is determined by the potential

$$\begin{aligned} V(\varphi) &= \frac{1}{2}\lambda^2\left(|\varphi|^2 - \frac{1}{2}\eta^2\right)^2 \\ &= \frac{1}{2}\lambda^2\left(|\varphi| - \sqrt{\frac{1}{2}}\eta\right)^2\left(|\varphi| + \sqrt{\frac{1}{2}}\eta\right)^2 = \frac{1}{8}\lambda^2(2\eta+\chi)^2\chi^2 \end{aligned}$$

and equals

$$m_{\mathrm{H}} = \lambda\eta.$$

Nothing was said so far about the dimensionless constant λ. The smaller λ, the lighter H-bosons are. However, λ cannot be very small. Indeed, λ characterizes the nonlinear self-coupling of the field χ which cannot be very small because H -bosons must be coupled, due to exchange by pairs of Z and W-bosons (fig. 24.1a). Hence, even with a small bare constant λ^2, the effective value of λ^2 (taking into account quantum corrections) will not be smaller than a quantity of the order of $\lambda^2_{\mathrm{min}} = e^4 = \alpha^2$, that is $\lambda \geq \alpha$. Consequently, $m_{\mathrm{H}} > \alpha\eta$.

To be more precise, the argument is based not only on the graphs of fig. 24.1 a but also on those of figs. 24.1b, c and other more complicated graphs with a large number of Higgs "whiskers". It can be shown that the sum of these graphs yields an effective potential $\tilde{V}(\varphi)$ of the following type:

$$\tilde{V}(\varphi) = \mu^2|\varphi|^2 + \gamma|\varphi|^4\ln\left(|\varphi|^2/m^2\right).$$

Here $\gamma = 3\left(m_{\mathrm{Z}}^4 + 2m_{\mathrm{W}}^4\right)/16\pi^2\eta^4$ (in the general case when the vector, scalar, and fermion loops are taken into account,

$$\gamma = \frac{3\sum_v m_v^4 + \sum_s m_s^4 - 4\sum_f m_f^4}{16\pi^2\eta^4};$$

however, hereafter we shall neglect the contribution of scalar and fermion loops). The parameters m and μ are renormalization constants and must be chosen in such a manner that $\tilde{V}(|\varphi|^2)$ has a minimum at $|\varphi|^2 = \eta^2$ (recall that $|\varphi|^2 = \frac{1}{2}(\eta+\chi)^2$). The condition $\tilde{V}'(|\varphi|)\Big|_{|\varphi|=\eta/\nu^2} = 0$ gives a relation between μ^2 and m^2 :

$$\gamma \ln \frac{\eta^2}{2m^2} = -\frac{1}{2}\left(\frac{2\mu^2}{\eta^2} + \gamma\right).$$

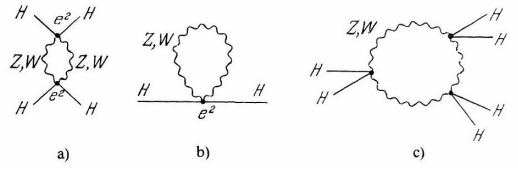


Fig. 24.1.

We easily see that for $\mu^2 > 0$, the potential $\tilde{V}(|\varphi|)$ has another minimum, at $\varphi = 0$. If we demand this minimum to be unstable and the one at $|\varphi|^2 = \frac{1}{2}\eta^2$ to be stable, it is necessary that $\tilde{V}\left(\frac{1}{2}\eta^2\right) < 0$, whence

$$\frac{2\mu^2}{\eta^2} + \gamma \ln \frac{\eta^2}{2m^2} < 0$$

or

$$2\mu^2 < \gamma\eta^2.$$

Let us now find the restriction on the H -boson mass imposed by this inequality:

$$\begin{aligned} m_{\mathrm{H}}^2 = \frac{\mathrm{d}^2\tilde{V}}{\mathrm{d}\chi^2} = \frac{1}{2}\frac{\mathrm{d}^2\tilde{V}}{\mathrm{d}|\varphi|^2} = \mu^2 + 3\gamma\eta^2 \ln\frac{\eta^2}{2m^2} + \frac{7}{2}\gamma\eta^2 \\ = 2\gamma\eta^2 - 2\mu^2 = \gamma\eta^2 + \left(\gamma\eta^2 - 2\mu^2\right) \geq \gamma\eta^2. \end{aligned}$$

Therefore,

$$m_{\mathrm{H}} \geq \sqrt{\frac{3\left(m_{\mathrm{Z}}^4 + 2m_{\mathrm{W}}^4\right)}{16\pi^2\eta^2}} = \frac{\alpha\eta}{4\sin^2\theta_{\mathrm{W}}}\sqrt{3\left(2 + \frac{1}{\cos^4\theta_{\mathrm{W}}}\right)} \cong 7.3\mathrm{GeV}.$$

(This value is obtained for $\sin^2\theta_{\mathrm{w}} = 0.2$). Were this inequality violated in the model with a single Higgs doublet, our physical vacuum (at $|\varphi| = \eta/\sqrt{2}$) would be unstable and sooner or later would spontaneously explode, switching to the stable vacuum with $\varphi = 0$. It must be emphasized, however, that the probability of explosion is exponentially small for $m_{\mathrm{H}} \gtrsim 0.6\mathrm{GeV}$.

5.24.2 24.2. The role of H-bosons at high energies

We cannot indicate the upper bound for the H -boson mass. If, however, it is much larger than those of the W - and Z -bosons, the coupling in the sector of $\mathrm{H}-, \mathrm{W}-$, and Z -particles becomes strong, so that perturbation theory fails at $m_{\mathrm{H}} \gtrsim 1\mathrm{TeV}$. This is easy to understand qualitatively: we recall that λ^2 characterizes not only the self-coupling of the H -boson field (the terms $\lambda^2\chi^4$ and $\lambda^2\eta\chi^3$) but also the interaction between longitudinal components of the $\mathrm{W}^{\pm}$and Z -boson fields and between them and H -bosons. Indeed, all these four fields (${W_3}^+, {W_3}^-, {Z_3}^0$,

and H) are contained in the isodoublet φ whose self-coupling is described by the potential $V(\varphi)$.

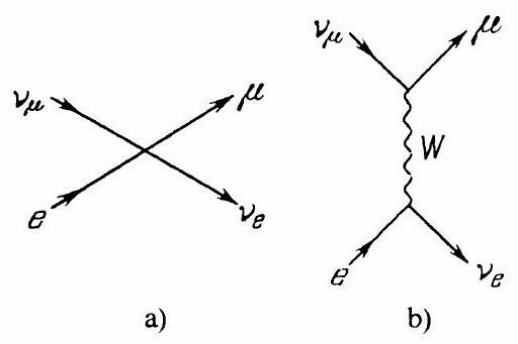


Fig. 24.2.

If $m_{\mathrm{H}} \gtrsim 1\mathrm{TeV}$, then the strong interaction of the H$-$, Z$-$, and W-bosons at energies of the order of 1 TeV may resemble, by the diversity of its manifestations, the resonance region of the usual hadrons in the range around 1 GeV . If, however, $m_{\mathrm{H}} \lesssim m_{\mathrm{W}}$, then perturbation theory must be valid at high energies, and all amplitudes growing with energy will cancel out. The H -bosons play an important role in this compensation. We recall (see chapter 18) that the linear increase of the cross section ($\sigma \propto G^2 s$), corresponding to the graph of fig. 24.2a, is eliminated when the W-boson is included (fig. 24.2b).

However, the processes involving W-bosons continue to grow as s increases. This is illustrated by the cross section corresponding to the graph of fig. 24.3a. For the vector electron current the growth is suppressed when compensation of graphs given in figs. 24.3a and b is taken into account. Note, however, that this compensation is achieved only for the vector electron current but not for the axial one. In the latter case

$$\left.\frac{\mathrm{d}\sigma}{\mathrm{d}t}\right|_{|t|\approx s} \propto \frac{m_{\mathrm{e}}^2 s}{m_{\mathrm{Z}}^4}\frac{1}{s^2},$$

while unitarity requires

$$\left.\frac{\mathrm{d}\sigma}{\mathrm{d}t}\right|_{|t|\approx s} \propto \frac{1}{s^2}.$$

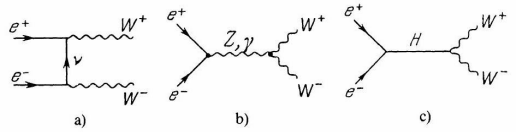


Fig. 24.3.

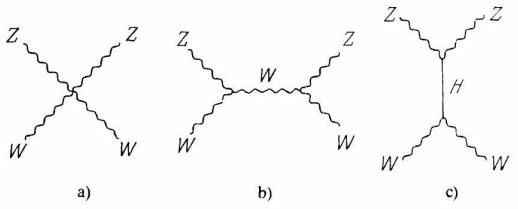


Fig. 24.4.

Addition of a graph with an H-boson (fig. 24.3c) eliminates the term in the amplitude proportional to the electron mass, and results in the desired behavior of the cross section.

Non-renormalizability of the theory without H -bosons manifests itself even better in the scattering of intermediate bosons on one another. It is not difficult to show (see Chapter 19, sect. 7) that the cross section corresponding to the sum of graphs in figs. 24.4a and b grows linearly with s. This growth is suppressed by addition of the H -boson because the graphs in figs. 24.4a, b and c cancel each other out. Therefore, for a very large H-boson mass, the scattering of intermediate bosons may exceed the unitarity limit before the graph 24.4 c becomes effective. This will mean the strong interaction of intermediate bosons.

5.24.3 24.3. Coupling of H-bosons to heavy quarks

An H -boson with mass below that of the Υ-meson could be produced in decays of the Υ-meson or of heavier mesons composed of heavier quarks. Indeed, the quark-H-boson coupling is the stronger the heavier the quark is. Let us compare the decay rates for $\Upsilon \to \mathbf{H} + \gamma$ (fig. 25.5a) and $\Upsilon \to \mu^+\mu^-$

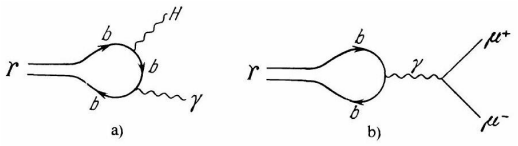


Fig. 24.5.

(fig. 25.5b). It can easily be shown that

$$\frac{\Gamma(\Upsilon \to \mathrm{H}\gamma)}{\Gamma\left(\Upsilon \to \mu^+\mu^-\right)} = \frac{G m_{\mathrm{b}}^2}{\sqrt{2}\pi\alpha}\left(1 - \frac{m_{\mathrm{H}}^2}{m_\Upsilon^2}\right) = 0.008\left(1 - \frac{m_{\mathrm{H}}^2}{m_\Upsilon^2}\right),$$

(the numerical coefficient 0.008 corresponds to $m_{\mathrm{b}} = 4.75\mathrm{GeV}$) which is quite measurable. The main decays of the H -boson must be $\mathrm{H} \to \tau^+\tau^-$and $\mathrm{H} \to \mathrm{c\bar{c}}$, provided its mass is in the range from 7 to 9 GeV . The latter channel implies decays into pairs of charmed particles: $\mathrm{D\overline{D}}, \mathrm{F\overline{F}}, \mathrm{D^*\overline{D}^*}$, and so on. Taking into account the color factor 3, we obtain:

$$\frac{\Gamma(\mathrm{H} \to \mathrm{c\bar{c}})}{\Gamma\left(\mathrm{H} \to \tau^+\tau^-\right)} = \frac{3m_{\mathrm{c}}^2}{m_\tau^2} = \frac{3(1.3)^2}{1.8^2} \cong 1.6.$$

In its turn,

$$\Gamma\left(\mathrm{H} \to \tau^+\tau^-\right) = \frac{1}{8\pi}\sqrt{2} G m_{\mathrm{H}} m_\tau^2 v^3, \qquad \text{where } v = \left(1 - \frac{4m_\tau^2}{m_{\mathrm{H}}^2}\right)^{1/2}.$$

5.24.4 24.4. Coupling of H-bosons to gluons

The gluon mass being zero, there is no direct coupling of H -bosons to gluons. However, there must be an indirect coupling due to quark loops (fig. 24.6). The decay amplitude is

$$M(\mathrm{H} \to 2\ \mathrm{g}) = N_{\mathrm{H}} \frac{\alpha_{\mathrm{s}}\left(m_{\mathrm{H}}\right)}{6\pi} (\sqrt{2}G)^{1/2} \chi G^{1a}_{\mu\nu} G^{\mu\nu}_{2a},$$

where $G^{ia}_{\mu\nu} = k_{i\mu}B^{a}_{i\nu} - k_{i\nu}B^{a}_{i\mu}, i = 1, 2, a = 1, 2, \ldots, 8, k_1$ and k_2 are 4momenta of two gluons, B_1 and B_2 are their wave functions, χ is the H -boson wave function, $\alpha_{\mathrm{s}} = g^2_{\mathrm{s}}/4\pi$ is the chromodynamic running coupling constant (the $\mathrm{H} \to 2$ g decay amplitude is determined by the value of $\alpha(Q)$ for $Q \simeq m_{\mathrm{H}}$), and N_{H} is the number of flavors of heavy quarks. Here we refer to quarks as heavy if their masses satisfy the inequality $m_{\mathrm{q}} > \frac{1}{2}m_{\mathrm{H}}$ where m_{H} is the H -boson mass. It is significant that the contribution of

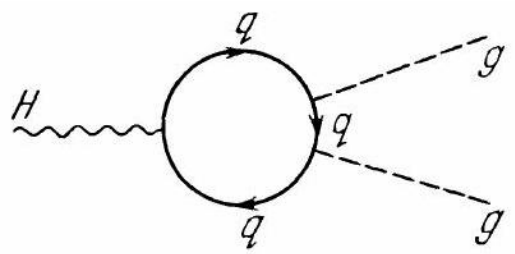


Fig. 24.6.

heavy quarks is independent of the masses of these quarks. Hence, even a comparatively light H -boson is something of a "cash register" of heavy quarks (including quarks so heavy that we cannot hope to produce them even using future accelerators). If N_{H} is sufficiently high, then the decays $\mathrm{H} \to 2\ \mathrm{g} \to$ hadrons become predominant. It is readily obtained that

$$\Gamma(\mathrm{H} \to 2\ \mathrm{g}) = N^2_{\mathrm{H}} \left(\frac{\alpha_{\mathrm{s}}\left(m_{\mathrm{H}}\right)}{\pi}\right)^2 \frac{\sqrt{2}G}{72\pi} m^3_{\mathrm{H}}$$

and therefore,

$$\frac{\Gamma(\mathrm{H} \to 2\ \mathrm{g} \to\ \text{hadrons}\ )}{\Gamma\left(\mathrm{H} \to \tau^+\tau^-\right)} = N^2_{\mathrm{H}} \left(\frac{\alpha_{\mathrm{s}}\left(m_{\mathrm{H}}\right)}{3\pi}\right)^2 \left(\frac{m_{\mathrm{H}}}{m_\tau}\right)^2 \left(1 - \frac{4m_\tau}{m^2_{\mathrm{H}}}\right)^{-3/2}.$$

Note that the H -boson decay into two gluons via the light quark loops is suppressed by an additional factor of the order of $(2m_{\mathrm{q}}/m_{\mathrm{H}})^4$.

The above amplitude $M(\mathrm{H} \to 2\ \mathrm{g})$ can easily be derived on the basis of the expression for the quark loop contribution (fig. 24.7) to the color charge renormalization. This contribution is equal (see Chapter 7) to

$$G^{1a}_{\mu\nu} G^{\mu\nu}_{2a} \frac{\alpha_{\mathrm{s}}}{12\pi} \ln \frac{\Lambda^2}{m^2_{\mathrm{q}}},$$

where Λ is the ultraviolet cut-off constant, and m_{q} is the quark mass. From this we find the transition amplitude of an arbitrary number of H -bosons into two gluons by using the substitution

$$m^2_{\mathrm{q}} \to m^2_{\mathrm{q}} \left(1 + \frac{\chi}{\eta}\right)^2$$

(this substitution takes care of the Higgs-boson origin of the quark mass; we assume that $m_{\rm H} \ll m_{\rm q}$). The amplitude for H $\to$ 2 g is obtained by taking the expansion of the logarithm and retaining only the term linear in χ :

$$M(\mathrm{H} \to 2g) = G^{1a}_{\mu\nu} G^{\mu\nu}_{2a} \frac{\alpha_{\rm s}}{6\pi} \frac{\chi}{\eta}.$$

This amplitude corresponds to one quark loop.

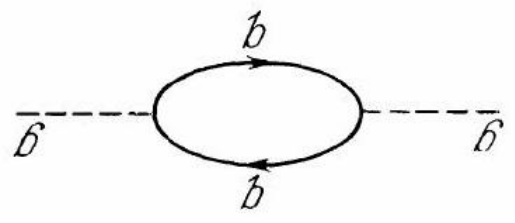


Fig. 24.7.

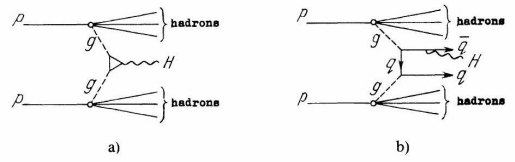


Fig. 24.8.

H -bosons can be produced in high-energy pp and $\bar{\rm p}$p collisions via a reverse reaction: gluon + gluon $\to$ H-boson (fig. 24.8a). The expected cross section for this process is of the order of 10^{-35} cm^2. The process of associated production of a pair of heavy quarks and one H -boson is easier to observe but it has a smaller cross section (fig. 24.8b).

5.24.5 24.5. "Higgs charge" of nucleons

It will be very instructive to discuss the effective constant M which has the dimension of mass and characterizes the H-boson-nucleon coupling vertex, $(M/\eta)\chi\bar{\psi}_{\rm N}\psi_{\rm N}\big)$, for $q^2_{\rm H} = 0$. At first glance, $M = m_{\rm N}$, as in the case of quarks. However, a nucleon is not an elementary particle; it is composite, so that our guess $M = m_{\rm N}$ is wrong. At second glance, it would seem that $M = 2m_{\rm u} + m_{\rm d}$ for the proton and $M = 2m_{\rm d} + m_{\rm u}$ for the neutron, that is M is negligibly small on the hadronic mass scale. Alas, we are wrong again. In reality, the H -boson-nucleon interaction vertex is mostly determined by the interaction of H -bosons with gluons, the respective lagrangian being

$$\mathfrak{L}_{\rm Hgg} = N_{\rm H} \frac{\alpha_{\rm s}}{12\pi} \frac{\chi}{\eta} G^a_{\mu\nu} G^{\mu\nu}_a.$$

(This effective lagrangian differs from a similar expression for the amplitude M(H $\to$ 2 g), corresponding to fig. 24.6, by a factor of $\frac{1}{2}$, taking into account that the gluons are identical). On the other hand, the nucleon mass in the chiral limit is again determined by the contribution of gluons:

$$m_{\rm N}\bar{\psi}_{\rm N}\psi_{\rm N} = \langle N|\theta^\mu_\mu|N\rangle = \langle N|\tilde{\theta}^\mu_\mu|N\rangle.$$

Here $\tilde{\theta}^{\mu}_{\mu}$ is the trace of that part of the operator of the total energy-momentum tensor θ^{μ}_{ν}, which is due to the contribution of light quarks and gluons:

$$\tilde{\theta}^{\mu}_{\mu} = -\frac{\tilde{b}\alpha_{\rm s}}{8\pi} G^{a}_{\mu\nu} G^{\mu\nu}_{a},$$

where $\tilde{b} = 11 - \frac{2}{3}\cdot 3 = 9$. Taking into account that

$$\frac{M}{\eta}\chi\bar{\psi}_{\rm N}\psi_{\rm N} = \langle N|\mathfrak{L}_{\rm Hgg}|N\rangle = \frac{N_{\rm H}}{\eta}\frac{2}{3}\langle N|\frac{\alpha_{\rm s}}{8\pi}G^{a}_{\mu\nu}G^{\mu\nu}_{a}|N\rangle$$
$$= -\frac{N_{\rm H}}{\eta}\frac{2m_{\rm N}}{3\tilde{b}}\bar{\psi}_{N}\psi_{N}$$

we obtain that $M = -\left(2m_{\rm N}/27\right)N_{\rm H} \cong -70{\rm MeV}\cdot N_{\rm H}$. Recall that $N_{\rm H}$ stands for the number of flavors of heavy quarks.

5.24.6 24.6. Digression on the trace of the energy-momentum operator

The result obtained above stems from a spectacular property of the energymomentum tensor. We shall now discuss this property. The trace of the total energy-momentum operator of gluons and quarks is written in the form

$$\theta^{\mu}_{\mu} = \sum_{l} m_{q_l}\bar{q}_l q_l + \sum_{h} m_{q_h}\bar{q}_h q_h - \frac{b\alpha_s}{8\pi}G^{a}_{\mu\nu}G^{\mu\nu}_{a},$$

where $b = 11 - \frac{2}{3}N_l - \frac{2}{3}N_h \equiv \tilde{b} - \frac{2}{3}N_h$, and indices l and h refer to light and heavy quarks, respectively. In contrast to the preceding sections of the present chapter, we define here the u -, d -, and s -quarks whose masses are below μ_c ($1/\mu_c$ is the confinement radius), as light quarks, and all other quarks as heavy. (In the general case, therefore, $N_h \geq N_H$; the equality $N_H = N_h$ then holds only if $m_H \simeq \mu_{\rm c}$).

The last term in the expression for θ^{μ}_{μ} is the contribution of the so-called triangle anomaly. A pertinent image is that of the contribution due to the "shadow cabinet" of gluons and quarks with infinitely high masses, that is the so-called Pauli-Willars particles which regularize (cut off) divergent graphs. These particles have entered the energy-momentum tensor from the lagrangian where they are introduced in order to regularize the theory. The triangle anomalies in question are represented in the graphs of fig. 24.9 (recall that gravitons interact with the energy-momentum tensor). The graphs (a) and (c) of this figure contain physical particles, while the graphs (b) and (d) contain regularizing particles in loops. The graphs (c) and (d) cancel each other out, and heavy quarks drop out if the virtualities of external gluons are small compared to quark masses in the triangle.

Graph 24.9a gives zero contribution to the trace of the energy-momentum tensor since the gluon mass is zero. For light quarks, the graph (c) contains a small factor $m_{\rm q}/\mu_{\rm c}$, where $1/\mu_{\rm c}$ is the confinement radius. Therefore, the regularizing contribution to θ^{μ}_{μ} is not cancelled out for light quarks and gluons.

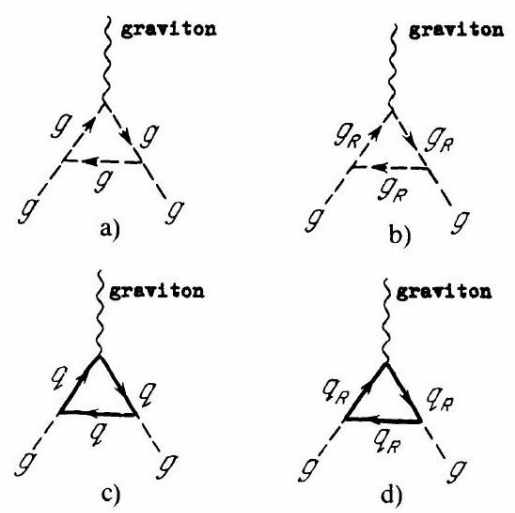


Fig. 24.9.

In the case of the nucleon the matrix elements

$$\langle N|m_{q_h}\bar{q}_h q_h|N\rangle \quad \text{and} \quad \langle N|\frac{2}{3}N_h\frac{\alpha_s}{8\pi}G^a_{\mu\nu}G^{\mu\nu}_a|N\rangle$$

cancel to an accuracy of terms of the order of $(\mu_c/m_{q_h})^2$. If we also use the fact that in the chiral limit $m_{q_l} \to 0$, we come to the conclusion that in this limit the nucleon mass is determined by the contribution of $\tilde{\theta}^\mu_\mu$.

5.24.7 24.7. Coupling of H-bosons to W - and Z-bosons

Obviously, coupling of H -bosons to W - and Z -bosons must be especially strong because of the large masses of the intermediate bosons; this coupling is characterized by the constant α. Consequently, creation of W- and Z -bosons must be accompanied by a rather intensive internal bremsstrahlung of Higgs particles. For example, if $m_H \cong 10\text{GeV}, p\bar{p}$ collisions at $s = 540\text{GeV}$ must produce one Z + H pair per approximately each 300 singly produced Z-bosons.

At the total energy $\sqrt{s} = m_Z + \sqrt{2}m_H$, the e^+e^-beams could be an intensive source of H -bosons, i.e. we mean the process $e^+e^- \to Z + H$ represented by the graph of fig. 24.10. The cross section for this process at $m_H \cong 10\text{GeV}$ is approximately three times the standard electromagnetic

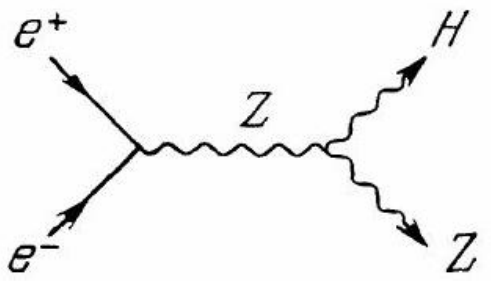


Fig. 24.10.

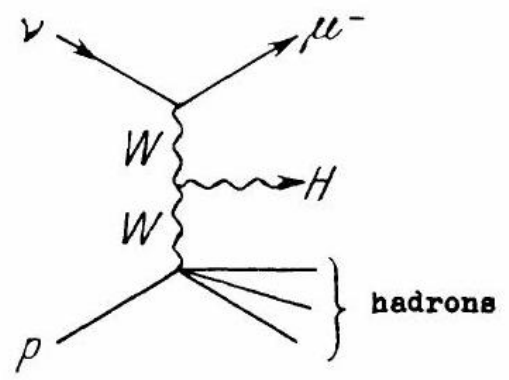


Fig. 24.11.

cross section for $e^+e^- \to \gamma \to \mu^+\mu^-$, equal to $4\pi\alpha^2/3s$, that is it comes to approximately $3 \cdot 10^{-35}$ cm^2.

Production of H -bosons in neutrino experiments must also proceed mostly owing to their strong ($\sim e$) coupling to the W-bosons (fig. 24.11). The cross section for this process must come to approximately $10^{-3}Gs$ of the cross section for the basic process $\nu + p \to \mu^-$+hadrons. The factor Gs is easily derived on the basis of dimensional arguments (see the graph of fig. 24.11).

5.24.8 24.8. Coupling of H-bosons to photons

In the case of a single Higgs doublet the decay $H \to 2\gamma$ must have a small branching ratio. If, however, the number of Higgs particles is considerable, this decay may become important and in principle, even predominant. The decay $H \to 2\gamma$ proceeds via triangular graphs with virtual charged particles (fig. 24.12). We can write the decay amplitude in the form

$$M(H \to 2\gamma) = \frac{\alpha F}{4\pi}(\sqrt{2}G)^{1/2}\chi F^1_{\mu\nu}F_2^{\mu\nu} = \frac{\alpha F}{4\pi}(\sqrt{2}G)^{1/2}m_H^2\chi e_1 e_2.$$

Here $\chi, \boldsymbol{e}_1$, and $\boldsymbol{e}_2$ are wave functions of the H -boson and photons, and m_H is the H -boson mass. The constant F is dimensionless, its value being determined by the contribution of the graph of fig. 24.12. In cases when the virtual particles forming the triangle in fig. 24.12 have unit charges and

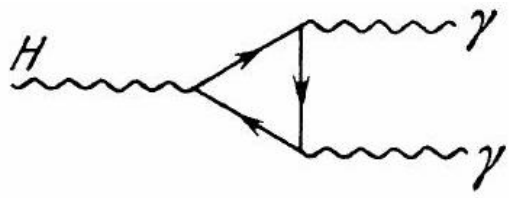


Fig. 24.12.

spins $0, \frac{1}{2}$ and 1 , respectively, the expressions for F are:

$$F_0 = \beta\left(1 - \beta x^2\right),$$
$$F_{1/2} = -2\beta\left[(1-\beta)x^2 + 1\right],$$
$$F_1 = \left[2 + 3\beta + 3\beta(2-\beta)x^2\right].$$

Here $\beta = 4m^2/m_{\mathrm{H}}^2, m$ is the virtual particle mass,

$$x = \arctan \frac{1}{\sqrt{\beta - 1}} \quad \text{for } \beta > 1,$$
$$x = \frac{1}{2}\left(\pi + i \ln \frac{1+\sqrt{1-\beta}}{1-\sqrt{1-\beta}}\right) \quad \text{for } \beta < 1.$$

For $\beta \to 0 : F_0, F_{1/2} \to 0, F_1 \to 2$.
For $\beta \to \infty : F_0 \to -\frac{1}{3}, F_{1/2} \to -\frac{4}{3}, F_1 \to 7$.
Consequently, the contribution of virtual heavy particles to the amplitude $M(\mathrm{H} \to 2\gamma)$ does not tend to zero as their masses increase. The above expressions for F are easily derived if we first calculate the contribution of the scalar, fermion and vector loops to the photonic vacuum polarization, and then carry out a substitution $m \to m\left(1 + \chi(\sqrt{2}G)^{1/2}\right)$ (recall a similar discussion of the H -boson-gluon interactions). In the general case F is the sum $F = \sum_i Q_i^2 F_i$, where Q_i is the charge of the i th virtual particle, and summation is carried out over all virtual particles. With two or more Higgs doublets, the coefficients in this sum are not unity any more, since now the mass of the particle does not fix its coupling to the H -boson. As a result, the amplitude $M(\mathrm{H} \to 2\gamma)$ may be considerably enhanced. By using the expression for $M(\mathrm{H} \to 2\gamma)$ we readily obtain $\Gamma(\mathrm{H} \to 2\gamma) = (\alpha F/4\pi)^2 \times \left(G m_{\mathrm{H}}^3/8\pi\sqrt{2}\right)$.

5.24.9 24.9. General remarks on Higgs bosons

The Higgs mechanism of generation of mass and elimination of divergences is a characteristic element of the electroweak model. This makes the experimental search for Higgs bosons very interesting. Some theorists regard the Higgs mechanism as artificial and are not inclined to believe that it is realized in nature. Of course, a number of important elements are lacking in the present-day picture; in particular, we do not understand what fixes the spectrum of lepton and quark masses, as well as the values of the Cabibbo and Weinberg angles. However, the very idea of the existence of scalar elementary particles does not appear so artificial after we have accepted the existence of elementary particles with spins of $\frac{1}{2}$, 1 (and 2). Supersymmetry schemes developed in recent years include all these particles (and those with spin $\frac{3}{2}$) into one supermultiplet (see Chapter 26), with interactions determined by a single dimensionless constant. It seems natural from this point of view that the number of Higgs particles is not minimal, and that their mass spectrum is very broad.

The so-called grand synthesis (or grand unification) models, which will be considered in Chapter 25, also favor a large number of Higgs bosons.

Two remarks must be made concerning charged H-bosons. First, they must be effectively produced in colliding electron-positron beams. Above the threshold we have:

$$R_{\mathrm{H}} = \frac{\sigma\left(\mathrm{e^+e^-} \to \gamma \to \mathrm{H^+H^-}\right)}{\sigma\left(\mathrm{e^+e^-} \to \gamma \to \mu^+\mu^-\right)} = \frac{1}{4}.$$

Second, semiweak decays of heavy quarks with emission of H -bosons could be possible. If, for instance, the H -boson were lighter than the difference in masses of the b - and c-quarks, we would have

$$\frac{\Gamma\left(\mathrm{b} \to \mathrm{H^-c}\right)}{\Gamma(\mathrm{b} \to \mathrm{c\bar{u}\ d})} \cong \frac{6\pi^2}{G_{\mathrm{F}} m_{\mathrm{b}}^2} \cong 10^5.$$

This chapter was already completed when active discussion began concerning the so-called "technicolor" model. According to this model, Higgs bosons are composite particles built of so-called "techniquarks". "Techniquarks" interact via special "technigluons". The confinement radius for the technicolor interaction is of the order of $1\mathrm{TeV}^{-1}$.

5.25 25 Grand unification

Despite their apparent pomposity, the words "Grand Synthesis", or "Grand Unification" are physical terms, not mere expressions of delight. They represent theoretical models which unify the weak, electromagnetic and strong interactions. This unification becomes possible because the effective constants of these interactions, which depend on momentum transfer owing to polarization of the vacuum, tend to the same limiting value when the momentum transfer increases. According to the guiding idea of grand unification, a single coupling constant characterizes all three interactions at small distances. The grand synthesis models explain why quarks have fractional charges, predict the value of $\sin^2\theta_{\mathrm{w}}$ and, what is especially interesting, predict a qualitatively new phenomenon: instability of the proton. Mostly, we shall discuss a model based on SU(5) symmetry.

5.25.1 25.1. Three generations of fermions

It would seem the most consistent to put all leptons and quarks into a single fundamental multiplet of some group, gauge the corresponding symmetry, and then spontaneously violate this symmetry. This program, however, immediately runs into such unimaginably vast multiplets of intermediate and Higgs bosons that one is forced to begin with a piecemeal approach.

The first step in the outlined direction is the unification on the basis of SU(5) symmetry. The SU(5) model classifies all known fermions into three generations. The scheme starts with the first generation; the subsequent generations are included in an analogous manner. Each generation contains 15 fermion states. Let us discuss the first generation in some detail. It contains three doublets of left-handed quarks and six singlets of right-handed quarks:

$$\begin{pmatrix} u_i \\ d_i \end{pmatrix}_{\mathrm{L}}, \quad u_{i\mathrm{R}}, \quad d_{i\mathrm{R}}$$

(where $i = \mathrm{r}, \mathrm{y}, \mathrm{b}$ are color indices). It also contains a left-handed lepton doublet and a right-handed lepton singlet,

$$\begin{pmatrix} \nu_{\mathrm{e}} \\ e^- \end{pmatrix}_{\mathrm{L}} \quad \text{and} \quad e^-_{\mathrm{R}}$$

(the right-handed neutrino is not included since this particle does not participate even in weak interactions). The second generation contains c, s, ν_μ, and μ, and the third contains $\mathrm{t}, \mathrm{b}, \nu_\tau$, and τ. With the exception of the neutrino, all particles become heavier with each subsequent generation.

Sometimes the upper quarks (u, c, t) are called anoquarks and denoted by α or a (for the Greek $\alpha\nu\omega$ meaning top) while the lower quarks ($\mathrm{d}, \mathrm{s}, \mathrm{b}$) are called catoquarks and denoted by κ or c (for the Greek $\kappa\alpha\tau\omega$ meaning bottom). In this notation, the generation is

$$\begin{pmatrix} \alpha_i \\ \kappa_l \end{pmatrix}_{\mathrm{L}}, \quad \alpha_{i\mathrm{R}}, \quad \kappa_{l\mathrm{R}}, \quad \begin{pmatrix} \nu_\ell \\ \ell^- \end{pmatrix}_{\mathrm{L}}, \quad \ell^-_{\mathrm{R}}.$$

Instead of right-handed particles, it will be convenient to operate with the CP conjugate left-handed antiparticles. All fifteen particles of the generation are then left-handed:

$$\begin{pmatrix} \alpha_i \\ \kappa_i \end{pmatrix}_{\mathrm{L}}, \tilde{\alpha}_{i\ \mathrm{L}}, \tilde{\kappa}_{i\ \mathrm{L}}, \begin{pmatrix} \nu_\ell \\ \ell^- \end{pmatrix}_{\mathrm{L}}, \ell^+_{\mathrm{L}},$$

where $i = \mathrm{r}, \mathrm{y}, \mathrm{b}$ are color indices. We must emphasize that $\ell^+_{\mathrm{L}}$is an antiparticle with respect to $\ell^-_{\mathrm{R}\sim}$and not to ℓ^-_{L}, with a similar statement valid for $\tilde{\alpha}_{i\ \mathrm{L}}$ and $\tilde{\kappa}_{i\ \mathrm{L}}$ (the tilde sign here is short and does not cover the index L; the tilde indicates C-conjugation).

5.25.2 25.2. Quintet and decuplet in SU(5)

A spinor with 15 components is still too large: it corresponds to the group SU(15) and to 224 vector bosons. Therefore the 15 left-handed particles are placed in two multiplets of SU(5) :

$$15 = \overline{5} + 10$$

For the first generation, for example, the quintet is chosen as follows:

$$\bar{Q}^a_{\rm L} = \left(\bar{d}_{\rm r}, \bar{d}_{\rm y}, \bar{d}_{\rm b}, e^-, \nu_{\rm e}\right)_{\rm L}, \quad a = 1, 2, \ldots, 5,$$

or

$$Q_{a\rm R} = \left(d_{\rm r}, d_{\rm y}, d_{\rm b}, e^+, \bar{\nu}_{\rm e}\right)_{\rm R}.$$

As for the decuplet, it transforms as an antisymmetrized product

$$D_{ab} \sim \sqrt{\frac{1}{2}}\left(Q_a Q_b - Q_b Q_a\right).$$

(In analogy to SU(3) where $3 \times 3 = 6 + \overline{3}$, in SU(5) we write $5 \times 5 = 10 + 15$). The antisymmetric matrix describing our decuplet has the form

$$D_{ab} = \frac{1}{\sqrt{2}} \begin{pmatrix} 0 & \bar{u}^{\rm b} & -\bar{u}^{\rm y} & -u_{\rm r} & -d_{\rm r} \\ -\bar{u}^{\rm b} & 0 & \bar{u}^{\rm r} & -u_{\rm y} & -d_{\rm y} \\ \bar{u}^{\rm y} & -\bar{u}^{\rm r} & 0 & -u_{\rm b} & -d_{\rm b} \\ u_{\rm r} & u_{\rm y} & u_{\rm b} & 0 & -e^+ \\ d_{\rm r} & d_{\rm y} & d_{\rm b} & e^+ & 0 \end{pmatrix}_{\rm L}.$$

A useful mnemonic picture can be constructed: each particle of the decuplet consists of two right-handed particles of the quintet, "quintons", and of a gravitino, that is a massless neutral particle with spin $\frac{3}{2}$. (The existence of the gravitino is predicted in the framework of so-called supergravitation, (see Chapter 26.) The spins of the gravitino and two quintons add up as shown in fig. 25.1. Thin arrows in this figure denote particle momenta, and open arrows denote their spins. We see that our composite fermions are left-handed. It is easily verified that colors and charges of these composite fermions are those of the particles in the above decuplet matrix D_{ab}. For instance,

$$D_{12} = \frac{1}{\sqrt{2}}\bar{u}^{\rm b} \sim \frac{d_{\rm r}d_{\rm y} - d_{\rm y}d_{\rm r}}{\sqrt{2}} = \frac{d_i d_k \varepsilon^{ikb}}{\sqrt{2}}.$$

It is not impossible that fig. 1 is not purely mnemonic, but reflects some important physical message, some composite model with dynamics which at

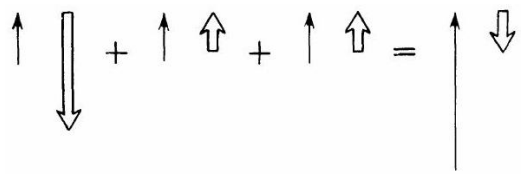


Fig. 25.1.

present is absolutely unclear. However, a more natural explanation of the fact that fundamental particles are grouped into two SU(5) multiplets, is given by SO(10) symmetry (see below).

5.25.3 25.3. 24 vector bosons

The SU(5) group has 24 generators ($5 \times \overline{5} = 24 + 1$). Let us consider a theory in which the SU(5) symmetry is local. Then each of these generators corresponds to a vector boson.

One of the generators of the group is the electric charge. We know that the generator trace is zero (recall the matrices τ in SU(2) and λ in SU(3)). This means that the sum of the charges of particles in an SU(5) multiplet must be zero. Hence,

$$Q_{\mathrm{d_r}} + Q_{\mathrm{d_y}} + Q_{\mathrm{d_b}} = Q_{\mathrm{e}}$$

and in the case of the exact color symmetry $Q_{\mathrm{d}} = -\frac{1}{3}$. Therefore, SU(5) symmetry explains why quarks have fractional charges.

Let us consider now the properties of the 24 vector bosons. In the limit of exact SU(5) symmetry all of them are massless. It is convenient to discuss these bosons looking at the quintet.

The eight bosons giving transitions between three colored quarks are gluons, and they correspond to the subgroup $\mathrm{SU(3)}_c$. The three bosons giving transitions in the lepton sector of the quintet are $\mathrm{W}^+, \mathrm{W}^-, \mathrm{W}^0$, corresponding to the group $\mathrm{SU(2)_L}$. Finally, there is the twelfth boson, B^0, with particle hypercharges as its source; this boson corresponds to the group U(1). The photon and Z^0 boson are (as in the standard electroweak model which is part of the SU(5) model) linear mutually orthogonal superpositions of W^0 and B^0. It is readily shown, when decuplet particles are taken into account, that gluons interact not only with left-handed currents $\bar{d}_{Li}\gamma_\mu \mathrm{d}^k_{\mathrm{L}}$, but also with right-handed currents $\bar{d}_{\mathrm{R}1}\gamma_\mu d^k_{\mathrm{R}}$, and not only with d-quarks but with u-quarks as well. It is also easy to verify that W -bosons interact both with leptons and with quarks.

The remaining twelve vector bosons are much more unusual. They form two charged color triplets:

$$X^i_{+4/3}, \bar{X}^i_{-4/3}, Y^i_{+1/3}, \bar{Y}^i_{-1/3},$$

where $i = \mathrm{r}, \mathrm{y}, \mathrm{b}$ are color indices, and subscripts indicate electric charge.
The bosons X and $\overline{\mathrm{X}}$ are emitted in transitions $\overline{\mathrm{d}} \leftrightarrow \mathrm{e}^-$, and Y and $\overline{\mathrm{Y}}$ in transitions $\overline{\mathrm{d}} \leftrightarrow \nu$. We shall see later, considering transitions in the decuplet
in addition to those in the quintet, that the exchange of X - or Y -bosons results in instability of protons. The X - and Y -boson masses must be very high ($\gtrsim 10^{15}$GeV) in order to make this instability acceptably small. Judging by the enormous spread in particle masses, SU(5) is very badly broken. We shall see, however, that some important features of the symmetry are retained despite this extremely strong symmetry breaking. Under the ruins of the symmetry we shall find the surviving pattern of the coupling constants.

5.25.4 25.4. Running coupling constants

At very short distances when momentum transfer is much larger than the masses of the heaviest vector bosons, SU(5) symmetry is restored and all interactions of vector bosons with other particles (fermions and Higgs bosons) and with one another are determined by a single coupling constant, that is by a single charge g. The term "constant" for this quantity is kept for historical reasons only. In reality it is a logarithmic function of the momentum transfer. At $q \gg 10^{15}$GeV all interactions-weak, strong, and electro-magnetic-are of the same magnitude. As the momentum transfer diminishes, the constants characterizing these interactions diverge from one another. However, broken SU(5) is still valuable because this divergence is logarithmic and hence, not large. Let us consider the charges g_3, g_2, g_1 which correspond to the groups $\mathrm{SU(3)}, \mathrm{SU(2)}, \mathrm{U(1)}$, respectively. The corresponding vertices are:

$$\mathrm{SU}(3): \quad g_3 \boldsymbol{G}_\mu \sum_q \bar{q}\gamma^\mu \frac{1}{2}\boldsymbol{\lambda} q$$

where $\boldsymbol{G}_\mu$ is the octet of gluons, and the sum is taken over all quarks;

$$\mathrm{SU}(2): \quad g_2 \boldsymbol{W}_\mu \left(\sum_q \bar{q}_\mathrm{L}\gamma^\mu \frac{1}{2}\tau q_\mathrm{L} + \sum_\ell \bar{\ell}_\mathrm{L}\gamma^\mu \frac{1}{2}\tau \ell_\mathrm{L} \right),$$

where $\boldsymbol{W}_\mu$ is the triplet of W -bosons, and the sums are taken over all doublets of left-handed quarks and left-handed leptons; and

$$\mathrm{U}(1): \quad g_1 B_\mu \sum_f \bar{f} C_2^{\frac{1}{2}} Y \gamma^\mu f$$

where the sum is taken over all particles: quarks and leptons, singlets and doublets. The coefficient C in the last expression serves to normalize the U(1) current in the same manner as the SU(3) and SU(2) currents. The point is, both matrices $\frac{1}{2}\boldsymbol{\lambda}$ and $\frac{1}{2}\boldsymbol{\tau}$ are generators of the group SU(5), while the diagonal matrix $\frac{1}{2}Y$ is only proportional but not equal to the SU(5) generator. The coefficient C was introduced to normalize $\frac{1}{2}CY$ as $\frac{1}{2}\boldsymbol{\lambda}$ and $\frac{1}{2}\boldsymbol{\tau}$

$$\mathrm{Tr}\left(\frac{1}{2}\tau_i\right)^2 = \frac{1}{2}, \quad \mathrm{Tr}\left(\frac{1}{2}\lambda_a\right)^2 = \frac{1}{2}$$

for any $i = 1, 2, 3$ and any $a = 1, 2, \ldots, 8$. We now demand

$$\mathrm{Tr}\, C^2 \left(\frac{1}{2}Y\right)^2 = \frac{1}{2}.$$

Taking the quintet as an example and using the relation $Q = T_3 + \frac{1}{2}Y$ we find that $\frac{1}{2}Y\left(\bar{d}_\mathrm{L}\right) = +\frac{1}{3}, \frac{1}{2}Y\left(e_\mathrm{L}^-\right) = \frac{1}{2}Y\left(\nu_\mathrm{L}\right) = -\frac{1}{2}$ and therefore

$$\mathrm{Tr}\left(\frac{1}{2}Y\right)^2 = \frac{1}{9}\cdot 3 + \frac{1}{4}\cdot 2 = \frac{5}{6}$$

hence,

$$C^2 = \frac{3}{5}$$

Recall that the standard electroweak model contains the constants g and g' (see Chapter 21) and that

$$g'/g = \tan\theta_\mathrm{W}, \quad g = e/\sin\theta_\mathrm{W}$$

where θ_W is the Weinberg angle. Experiment yields

$$\sin^2\theta_\mathrm{w} \cong 0.2 - 0.25$$

It is easy to see that in our new notation, $g = g_2, g' = g_1 C = g_1\sqrt{\frac{3}{5}}$. Therefore, for $q \gg 10^{15}\mathrm{GeV}$, when $g_1 = g_2, \tan^2\theta_\mathrm{W}^0 = \frac{3}{5}$ and $\sin^2\theta_\mathrm{W} = \frac{3}{8} \simeq 0.38$, which is almost twice the observed value of $\sin^2\theta_\mathrm{w}$ for small transferred momenta. We know that for such momenta ($q \ll 100\mathrm{GeV}$)

$$\alpha_3 \simeq \frac{1}{5}, \quad \alpha_2 \simeq \frac{\alpha}{\sin^2\theta_\mathrm{W}} \simeq \frac{1}{26}, \quad \alpha_1 = \frac{\alpha}{\cos^2\theta_\mathrm{W}}\frac{5}{3} \simeq \frac{1}{67},$$

where we have denoted

$$g_i^2/4\pi = \alpha_i, \quad i = 1, 2, 3$$

Let us find how the α_i change as functions of momentum transfer. These changes are mainly brought about by loops of virtual particles, namely vector bosons (fig. 25.2) and fermions (fig. 25.3) (we neglect Higgs loops). Summation of these loops gives

$$\frac{1}{\alpha_i(M)} - \frac{1}{\alpha_i(\mu)} = \frac{b_i}{2\pi} \ln \frac{M}{\mu}$$

where M and μ are two values of the momentum transfer, both much larger than the masses of the particles whose contribution is taken into account in the calculation. The quantities b_i are determined by the order of the (local)

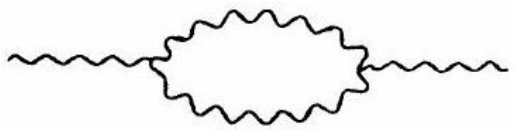


Fig. 25.2.



Fig. 25.3.

group, i.e. by the number of vector bosons, and by the number of fermion flavors. For gluons in $\mathrm{SU}(3)_\mathrm{L}$ we have $b_3 = 11 - \frac{2}{3}N_\mathrm{f}$ where N_f is the number of quark flavors ($b_3 = 7$ if $N_\mathrm{f} = 6$). Here the first term corresponds to fig. 25.2 and the second one to fig. 25.3. In the limit of strict $\mathrm{SU}(5), b_2 = b_3$. However, as a result of the breaking of $\mathrm{SU}(5)$ to $\mathrm{SU}(3) \times \mathrm{SU}(2) \times U(1)$, the loops of fig. 25.2 at $q \ll m_\mathrm{X}, m_\mathrm{Y}$ give for W-bosons $\frac{22}{3}$ instead of 11 (the corresponding term equals $\frac{11}{3}n$ for the $\mathrm{SU}(n)$ group). Consequently, $b_3 - b_2 = \frac{11}{3}$. The boson B_μ interacts with hypercharge while neither gluons nor W-bosons have hypercharge; hence, the loops of fig. 25.2 give no contribution to α_1 as a function of q, so that $b_3 - b_1 = 11$. We see that b_3 and b_2 are positive while b_1 is negative. This means that α_3 and α_2 decrease as the momentum increases (asymptotic freedom) while α_1 increases. Neglecting the threshold effects near m_t, m_W and m_x, it is convenient to plot $1/\alpha_i$

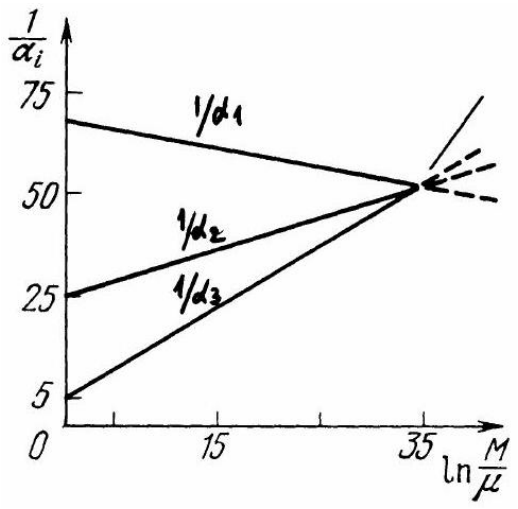


Fig. 25.4.

instead of α_i (see fig. 25.4). Making use of the three equations

$$\frac{1}{\alpha_i(M)} - \frac{1}{\alpha_i(\mu)} = \frac{b_i}{2\pi} \ln \frac{M}{\mu},$$

where

$$\frac{1}{\alpha_1(\mu)} = \frac{3\cos^2\theta_{\mathrm{W}}}{5\alpha}, \qquad \frac{1}{\alpha_2(\mu)} = \frac{\sin^2\theta_{\mathrm{W}}}{\alpha}, \qquad \frac{1}{\alpha_3(\mu)} = \frac{1}{\alpha_{\mathrm{s}}}$$
$$b_1 = -4, \quad b_2 = 3.3, \quad b_3 = 7$$

and assuming unbroken SU(5) symmetry at the point M, that is,

$$\alpha_1(M) = \alpha_2(M) = \alpha_3(M) = \bar{\alpha}(M),$$

we easily find three unknowns: $\ln(M/\mu), \bar{\alpha}(M)$, and $\sin^2\theta_{\mathrm{w}}$. For $\ln(M/\mu)$ we obtain

$$\ln \frac{M}{\mu} = \frac{\pi}{11}\left[\frac{1}{\alpha(\mu)} - \frac{8}{3\alpha_s(\mu)}\right]$$

If we start at $\mu \sim m_{\mathrm{W}}$ and take into account that $\alpha\,(m_{\mathrm{W}}) \cong \frac{1}{129}, \alpha_{\mathrm{s}}\,(m_{\mathrm{W}}) \cong 0.1$, then $\ln\,(M/m_{\mathrm{W}}) \cong 29$ and $M/m_{\mathrm{W}} \cong 4 \cdot 10^{12}$. It is important to emphasize that this result is independent of $\sin^2\theta_{\mathrm{w}}$. We can find $\bar{\alpha}(M)$ just as easily; it is close to 0.02 (see fig. 25.4). The following relation is obtained for $\sin^2\theta_{\mathrm{W}}$:

$$\sin^2\theta_{\mathrm{W}} = \frac{1}{6} + \frac{5}{9}\frac{\alpha}{\alpha_{\mathrm{s}}} \cong 0.20$$

This is strikingly close to the experimental value ($\cong 0.23$). However, a slight discrepancy between theory and the experiment may prove dangerous for the theory if the predicted value is found to lie beyond the experimental errors.

5.25.5 25.5. Unstable proton

Let us turn again to the X - and Y -bosons. The coupling of X -bosons to fermions is written in the form:

$$\sqrt{\frac{1}{2}} g X_{i\mu}\left(\bar{d}^i \gamma^\mu e^+ + \bar{\bar{u}}_{\mathrm{L}m} \gamma^\mu u_{\mathrm{L}k} \varepsilon^{ikm}\right).$$

Note that both $\overline{\tilde{u}}$ and u are covariant color spinors (with lower indices); the term $\bar{d}^i\gamma^\mu e^+$is a sum of two terms: $\bar{d}_{\rm L}\gamma^\mu e^+_{\rm L}$from the quintet and $\overline{e^-_{\rm L}}\gamma^\mu\tilde{d}^i_{\rm L}$
from the decuplet, with the last term being equivalent to $\bar{d}^i_{\rm R}\gamma^\mu e^+_{\rm R}$. The coefficient $\sqrt{\frac{1}{2}}$ in the above expression for the coupling is introduced to normalize the current, responsible for the emission of X-bosons in the same way as the current responsible for the emission of W-bosons. In the last case the factor $\sqrt{\frac{1}{2}}$ is implicitly contained in the isotopic vector $\bar{e}\frac{1}{2}\tau\nu$:

$$\frac{1}{2}\boldsymbol{\tau} = \left\{\frac{1}{2}\begin{pmatrix}1 & 0\\ 0 & -1\end{pmatrix}, \sqrt{\frac{1}{2}}\begin{pmatrix}0 & 1\\ 0 & 0\end{pmatrix}, \sqrt{\frac{1}{2}}\begin{pmatrix}0 & 0\\ 1 & 0\end{pmatrix}\right\}$$

The Y -boson interaction vertex is

$$\sqrt{\frac{1}{2}}gY_{i\mu}\left(\overline{\tilde{d}^j_{\rm L}}\gamma^\mu\nu_{\rm L} + \bar{d}_{{\rm L}m}\gamma^\mu\tilde{u}_{{\rm L}k}\varepsilon^{ikm} + \overline{e^+_{\rm L}}\gamma^\mu u^i_{\rm L}\right).$$

Exchange of X- and Y-bosons obviously results in non-conservation of the baryonic and leptonic charges, due to elementary processes of the type of

$$\overset{\rm x}{\rm x}\,{\rm e}^+\overline{\rm d}, \quad {\rm ud}\overset{\rm Y}{\to}\overline{\rm d}\bar{\nu}, \quad {\rm ud}\overset{\rm Y}{\to}{\rm e}^+\overline{\rm u}.$$

These processes make the proton unstable:

$$\begin{aligned}&{\rm p} = {\rm uud} \to \left({\rm e}^+\overline{\rm d}\ {\rm d}\ \text{or}\ {\rm e}^+\overline{\rm u}{\rm u}\right) \Rightarrow {\rm e}^+\pi^0\left(\eta^0,\rho^0,\omega^0\right)\\ &{\rm p} = {\rm uud} \to {\rm u}\,\overline{\rm d}\bar{\nu} \Rightarrow \bar{\nu}\pi^+\left(\rho^+\right)\end{aligned}$$

Neutrons must undergo similar decays (in nuclei which usually are considered stable):

$${\rm n} = {\rm dd}u \to\ {\rm d}\,\overline{\rm d}\bar{\nu} \Rightarrow \bar{\nu}\pi^0\left(\eta^0,\rho^0,\omega^0\right)$$

We can estimate the proton decay rate by noting that the matrix element is proportional to $g^2/m_{\rm X}^2 \cong \alpha/m_{\rm X}^2$. A dimensional estimate then gives

$$\frac{1}{\tau_{\rm p}} \cong \frac{\alpha^2 m_{\rm p}^5}{m_{\rm X}^4}$$

A quantitative calculation confirms this estimate. The coupling of X - and Y -bosons to the second-generation fermions makes the processes shown in fig. 25.5 possible. The process 25.5 c does not contribute to the proton decay because of the large mass of the c-quark. The processes of figs. 25.5a and b give the following decays:

$$\begin{aligned}&{\rm p} = \ {\rm uud}\ \to \mu^+\bar{\rm s}\ {\rm d} \Rightarrow \mu^+{\rm K}^0,\\ &{\rm p} = \ {\rm uud}\ \to \bar{\nu}_\mu\bar{\rm s}{\rm u} \Rightarrow \bar{\nu}_\mu{\rm K}^+,\\ &{\rm n} = {\rm ddu} \to \bar{\nu}_\mu\bar{\rm s}\ {\rm d} \Rightarrow \bar{\nu}_\mu{\rm K}^0.\end{aligned}$$

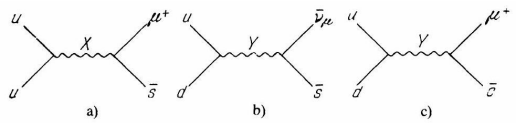


Fig. 25.5.

The probability of the decay with emission of μ^+must be several times lower than that of the decay with emission of e^+. First, the virtual Y-boson does not contribute to the muonic

decay, and second, the phase-space volume is reduced (this reduction is caused by creation of comparatively heavy strange particles). It can be conjectured that muons must be produced in approximately 10% of all proton decays.

The experimental lower bound on the proton lifetime is approximately 10^{30} years. From the relation

$$\tau_{\mathrm{p}} \cong \left(\frac{m_{\mathrm{X}}}{m_{\mathrm{p}}}\right)^4 \frac{1}{\alpha^2 m_{\mathrm{p}}} \gtrsim 10^{37}\ \mathrm{s},$$

we derive that

$$\frac{m_{\mathrm{X}}}{m_{\mathrm{p}}} \gtrsim 10^{14}$$

(here we take into account that $1/\alpha^2 m_{\mathrm{p}} \simeq 10^4 \cdot 10^{-24}$ s). The same estimate is true for Y -bosons. Summarizing, we obtain

$$m_{\mathrm{X}} \simeq m_{\mathrm{Y}} \gtrsim 10^{14}\mathrm{GeV}.$$

We see that this quantity is of the same order of magnitude as the energy $\bar{M}$ at which all three constants α_1, α_2 and α_3, become equal. In order to prevent divergence of these constants at $M > \bar{M}$, the masses of the X- and Y-bosons should not exceed $\bar{M}$. In this case the behavior of all the constants will be determined at $M \gg \bar{M} \cong m_{\mathrm{X}}$ by the coefficient

$$\bar{b} = \frac{11}{3} \cdot 5 - \frac{2}{3} N_{\mathrm{f}} = 14.3.$$

The trend of the unified charge corresponding to this value of $\bar{b}$ is traced by a solid line in the upper right-hand corner of fig. 25.4.

Detailed calculations give $10^{15}\mathrm{GeV} \gtrsim m_{\mathrm{X}} \gtrsim 10^{14}\mathrm{GeV}$ and $\tau_{\mathrm{p}} \simeq 10^{30\pm3}$ years. If additional Higgs fields are introduced into the SU(5) model, the expected value of τ_{p} may exceed 10^{34} years.

In order to prove that $\tau_{\mathrm{p}} > 10^{30}$ years, it is necessary to show that not one of the 10^{30} nucleons in 1.6 tons of matter decay during one year. Experiments of this type are conducted deep underground where the cosmic ray background is sufficiently low. Significant progress will be achieved if the mass will be increased to about $10^3 - 10^5$ tons. The discovery of proton decay would be of crucial importance because it would confirm unambiguously the principal ideas of grand unification.

During the first moments of the big bang 10^{10} years ago, the processes of baryon charge non-conservation were much more abundant, possibly playing a very important role at temperatures of the order of $10^{17} - 10^{10}\mathrm{GeV}$. It is tempting to interpret the existing charge asymmetry of the universe by non-conservation of baryonic charge and violation of CP invariance. A little more will be said about this in Chapter 27.

5.25.6 25.6. Grand Higgs bosons

The SU(5) model is constructed as a spontaneously broken symmetry. This guarantees its renormalizability. At least two multiplets of scalar bosons are necessary for the spontaneous breaking of symmetry. The first of them, a 24 -plet, gives masses to the X - and Y -bosons, and the second, the quintet, gives masses to the W - and Z -bosons and fermions. The scheme of symmetry breaking looks as follows:

$$\mathrm{SU}(5) \xrightarrow{24} \mathrm{SU}(3) \times \mathrm{SU}(2) \times \mathrm{U}(1) \xrightarrow{5} \mathrm{SU}(3) \times \mathrm{U}(1).$$

As a result, we are left with only nine massless fields: eight gluons and the photon. The coupling of vector fields to scalar fields is gauge invariant, and is characterized by a universal charge g. The matrix of vacuum-expectation values, which appear due to spontaneous breaking of SU(5) in the Higgs 24 -plet, has the form

$$v_{24}\cdot\begin{pmatrix}2 & & & & \\ & 2 & & & \\ & & 2 & & \\ & & & -3 & \\ & & & & -3\end{pmatrix}.$$

Hence, SU(3) and SU(2) symmetries remain unbroken. The X - and Y -boson masses are then of the order of gv_{24}, so that v_{24} must be very large, of the order of 10^{15}GeV. At the second stage, the spontaneous symmetry breaking in the Higgs quintet

$$\left(H_{\mathrm{r}}^{-1/3}, H_{\mathrm{y}}^{-1/3}, H_{\mathrm{b}}^{-1/3}, H^{+}, H^{0}\right)$$

takes place, and the neutral component $\sqrt{\frac{1}{2}}\left(H^{0}+\bar{H}^{0}\right)$ gains a non-zero vacuum expectation value $v_5 \simeq 10^2$GeV. At the same time, $\mathrm{H}^{+}, \mathrm{H}^{-}$, and $\sqrt{\frac{1}{2}}\left(H^{0}-\bar{H}^{0}\right)$ transform into the third components of $\mathrm{W}^{+}, \mathrm{W}^{-}$, and Z^{0} bosons, just as in the standard model of electroweak interactions.

Unfortunately, serious problems appear in the Higgs sector of the SU(5) model. The point is that the two multiplets of scalar particles are not isolated but connected by loops of vector fields (fig. 25.6). As a result, there is a threat that a large quantity, αv_{24}, will be added to a small one, v_5. The required hierarchy of vacuum expectation values cannot be preserved without compensations which today appear very artificial.

Let us look now into the masses of fermions. These appear owing to the coupling of the scalar quintet to fermions. It is easy to show that

$$5 \times 10 = 45 + \overline{5},$$
$$10 \times 10 = 50 + 45 + \overline{5}.$$

Hence, the Higgs quintet could give masses both to the α-fermions in the 10 , and to the κ-fermions whose left-handed components belong to the 10 and the right-handed ones to the $\overline{5}$. No doubt, this mechanism does not give a mass to the neutrino. The coupling constants $f_{5,10}$ and $f_{10,10}$ characterizing the interaction of Higgs and fermion multiplets are not fixed by the gauge invariance of the lagrangian; they can be chosen "by hand" so as to provide the best fit to the experimentally observed masses. These constants are different for different fermion generations, with the masses of α-quarks unrelated to those of κ-quarks and leptons. It is easy to show that κ-quarks and leptons have identical masses:

$$m_{\mathrm{d}} = m_{\mathrm{e}}, \quad m_{\mathrm{s}} = m_{\mu}, \quad m_{\mathrm{b}} = m_{\tau}.$$

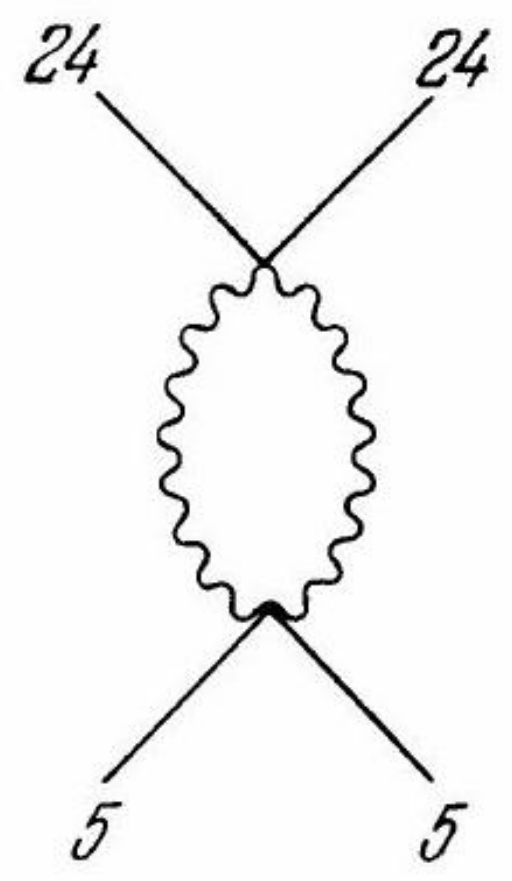


Fig. 25.6.

These relations must be satisfied at momenta of the order of m_{X}. Taking into account the dependence of the masses on the momentum, we can show that

$$\frac{m_\kappa(\mu)}{m_\ell(\mu)} = \left(\frac{\alpha_s(\mu)}{\bar{\alpha}}\right)^{4/b_3} \left(\frac{\bar{\alpha}}{\alpha_1(\mu)}\right)^{1/b_1}$$

where $b_3 = 11 - \frac{2}{3}N_{\mathrm{f}}, b_1 = -\frac{2}{3}N_{\mathrm{f}}$. With μ chosen higher than all thresholds, say $\mu \cong 10\mathrm{GeV}$, we conclude that

$$\frac{m_{\mathrm{d}}}{m_{\mathrm{e}}} = \frac{m_{\mathrm{s}}}{m_\mu} = \frac{m_{\mathrm{b}}}{m_\tau} \cong 2 - 3$$

The ratio m_{b}/m_τ is indeed close to the predicted value, but the agreement for the d - and s-quarks is very poor if the standard values, 7 MeV and 150 MeV , are taken.

The above-mentioned contradictions can be removed by introducing into the SU(5) model additional Higgs fields; this reduces, however, the predictive power of the model.

Among other attempts of grand unification we shall mention some models based on orthogonal and exceptional groups.

5.25.7 25.7. The SO(10) group and other orthogonal groups

SO(10) is a group of orthogonal rotations in a ten-dimensional space (S indicates that the determinant of transformation matrices equals unity). In this case vector particles belong to a 45 -plet, with fermions naturally placed in the spinor representation. In the case of SO(10) the spinor comprises sixteen components so that in addition to fifteen left-handed fermions

we deal with in the SU(5) model, each generation includes the sixteenth fermion, namely the left-handed antineutrino.

The grup SO(10) has SU(5) as a subgroup. The 16-plet of fermions consists of three SU(5) multiplets: $16 = 10 + \overline{5} + 1$. This can be regarded as a natural explanation of the fact that in the framework of SU(5), fermions belong to the reducible representation.

Along with a chain of spontaneous symmetry breakings $SO(10) \to SU(5) \to SU(3) \times SU(2) \times U(1) \to SU(3) \times U(1)$, chains of other types are also possible. Some of them make it possible to obtain, among other things, the value of $\sin^2 \theta_W$ which is closer to the experimental value of this paramenter than that found in the SU(5) model.

The SO(10) model predicts, just as SU(5), the proton instability. Some variants of this model yield the proton lifetime exceeding 10^{34} years. The experiments planned for the first half of the 80 's would be unable to detect such a slow decay.

In addition to the proton decay, another process not conserving the baryonic quantum number ($\Delta B \neq 0$) is discussed in the framework of the SO(10) model, namely neutron-antineutron transitions in vacuum, similar to $K^0 - \overline{K}^0$ oscillations but essentially much slower. A crude dimensional estimate relates the period of oscillations τ_{osc} to the deuteron lifetime τ_{dec} for the decay into pions (in both processes $|\Delta B| = 2$):

$$\tau_{dec} \sim \tau_{osc}^2 m_p.$$

This relation shows that the deuteron lifetime of $\sim 10^{30}$ years corresponds to the neutron oscillation period of about one year. If such oscillations really occur, they could be found in neutron beams of nuclear reactors.

The SO(10) symmetry naturally gives non-zero mass to the neutrino. This occurs because the fermion 16-plet comprises both the left-handed and right-handed components of the neutrino wave function. The estimates of the expected neutrino mass, found in the current literature, lie mostly within the interval $10^{-1} - 10^{-6}$eV.

A large number of papers are devoted to unified gauge theories based on higher-rank orthogonal groups. For instance, the fundamental 64 -component spinor of the group SO(14) comprises four generations of leptons and quarks. The group SO(22) contains, in addition to conventional quarks, the techniquarks mentioned in Chapter 24.

5.25.8 25.8. The exceptional groups

In addition to four series of regular groups

$$A_l = SU(l+1), \quad B_l = SO(2l+1), \quad C_l = Sp(2l), \quad D_l = SO(2l),$$

whose rank l can be arbitrarily high, there are five exceptional Cartan groups: G_2, F_4, E_6, E_7, E_8 (the subscript giving the group rank). Recall that the rank of the group is the number of mutually commuting generators. The groups G_2 and F_4 are not broad enough to include all known flavors and colors of quarks, so that discussions in the literature are mostly restricted to the groups E_6, E_7, and E_8.

The group E_6 has SO(10) as its subgroup. The E_6 model comprises 78 gauge bosons; fermions form a 27 -plet. Two alternative E_6 models are
found in the literature. The first E_6 model includes several generations of fermion 27-plets each of which has the following SO(10) composition: $27 = 16 + 10 + 1$. Each generation thus has 11 new states in addition to the known 16 fermion states: a singlet quark with $Q = -\frac{1}{3}$, a singlet Majorana lepton N^0 and a lepton doublet L^+, L^0. All of them are assumed to be superheavy.

The second E_6 model is more compact: all the known fermions in this model enter, together with several additonal particles, one 27-plet comprising two quarks with $Q = +\frac{2}{3}(u, c)$, four

quarks with $Q = -\frac{1}{3}$(d, s, b, h), four leptons with $Q = -1$ (e, μ, τ, λ), and five leptons with $Q = 0$ ($\nu_e, \nu_\mu, \nu_\tau, \nu_\lambda, \nu_\rho$). We thus find 18 quarks (color taken into account) and nine leptons. The model therefore predicts four so far unobserved particles. What is essential is that there is no t -quark among them! In this model it is difficult to avoid undesirable neutral currents changing quark flavors. Most of the versions of this E_6 model discussed in the literature did not include weak decays of a b-quark into a c-quark (see footnote on p. 5).

The model based on the group E_7 comprises 133 vector bosons, and fermions belong to a 56 -plet containing six color quarks, six color antiquarks, and ten leptons (four charged and six neutral). This model does not include the t -quark if all fermions are assumed to belong to a single 56 -plet. The fatal shortcoming of the model is that the value of $\sin^2\theta_w$ it predicts is at least twice as large as the experimental value.

No detailed investigation of the E_8 model has been undertaken. One of its interesting features is that the dimensions of the fundamental and the adjoint representations are identical: 248 fermions and 248 gauge bosons. The number of scalar particles runs into thousands, which is a frightening prospect.

It should be clear from the contents of this chapter that so far it is impossible to select the best among the competing grand models. The program of grand unification runs into difficulties. The most serious difficulty is the incomplete state of the mechanism of spontaneous symmetry breaking and the related problem of the hierarchies of the vacuum expectation values. A serious shortcoming of the grand unification models is the fact that these models ignore the gravitational interaction. The program of uniting all known types of interaction, including gravity, was given the name of superunification. It will be briefly outlined in the next chapter.

5.26 26 Superunification

5.26.1 26.1. Supersymmetry

Until now we have been discussing multiplets containing either fermions or bosons. By definition, supersymmetry is a symmetry which relates particles with integral spin to those with half-integral spin. For instance, the parameters of the isospin group transformations $\exp(i\boldsymbol{\alpha}\cdot\boldsymbol{\tau})$ are scalars. On the other hand, there are spinors among the parameters of supersymmetric transformations. These transformations turn fermions into bosons and bosons into fermions. Sometimes supersymmetry is referred to as the Fermi-Bose symmetry. When a supersymmetric theory is constructed, spinor generators Q_α are added to the Poincar group generators P_μ and $M_{\mu\nu}$. The simplest supersymmetric lagrangian is given by the sum of free Maxwell and Majorana lagrangians which describe the photons and the truly neutral neutrinos. More complicated supersymmetric lagrangians comprising fields with higher spins ($J > 1$) were also considered. It was found that a number of obstacles which appear when these fields are considered phenomenologically, are eliminated by treating the fields as components of some supersymmetric multiplet.

A local supersymmetry in which the parameters of transformations are functions of coordinates and time, is of special interest. Recall that the local group U(1), related to conservation of electric charge, can be realized only via introduction of massless photons. The local color group SU(3) is realized via an octet of massless gluons. Localization of the Poincar group is realized via gravitons, in the framework of general relativity theory. (If Lorentz rotations are different at different points, this means that these points have accelerations with respect to one another. Invariance with respect to such transformations is possible only by taking the gravitational field into account. This invariance manifests itself, in particular, in that the observer in an elevator car cannot distinguish between effects due to the elevator acceleration and effects due to a uniform gravitational field.)

Both gravitons and massless particles with spin $\frac{3}{2}$, the so-called gravitino, are necessary to realize supersymmetry. A local supersymmetry is called supergravity. Serious efforts are made at present to find out the properties of higher orders of perturbation theory in supergravity. We have already mentioned that the gravitational constant is dimensional, so that from a formal standpoint quantum gravity is non-renormalizable. Indeed, even one-loop graphs lead to divergences in the theory which contains other particles in addition to the gravitons. At the beginning of the 70's, however, it was demonstrated that one-loop graphs in the theory containing gravitons only, are finite. Supergravity, like quantum gravity theory with gravitons only, has no divergences in the one-loop approximation. Moreover, the two-loop approximation is also convergent. A superparticle (multiplet of particles) plays a role identical to that of the graviton in the usual theory of gravitation, so that there are very rigid relationships between properties and interactions of various particles.

The models of the so-called extended supergravity combining the geometric and internal symmetries are of special interest. In these models the Planck mass $m_{\mathrm{P}} = G_{\mathrm{N}}^{-1/2} \cong 10^{19}\mathrm{GeV}$ (where G_{N} is the Newton constant) acts as a natural scale unit of the whole physics of elementary particles. One may hope that extended supergravity is a way to develop the unified theory of all particles and all interactions. Versions of extended supergravity have been discussed, involving n gravitinos ($1 \leq n \leq 8$) and having SO(n) invariance, where SO(n) is a group of orthogonal transformations in n-dimensional space. As n increases, the number of particles with different spins in the multiplet rises as well. For example, for $n = 2$, the theory comprises, in addition to the graviton and two gravitinos, only one particle (with $J = 1$), while for $n = 8$ it comprises one particle with $J = 2$, eight particles with $J = \frac{3}{2}, 28$ with $J = 1, 56$ with $J = \frac{1}{2}$, and 70 with $J = 0$. For $n \geq 9$, the theory already has more than one graviton and also particles with $J > 2$.

It is easy to show that even such a large group as SO(8) is still too narrow to contain all the known fermion and gauge multiplets. Several very interesting papers report SO(8) to have a hidden dynamic symmetry SU(8). The group SU(8) already would be sufficiently broad to comprise not only the SU(5) gauge symmetry but also the three fermion generations.

5.26.2 26.2. Sub-quarks?

What lies behind the large number of quarks, leptons, and other particles which today are considered elementary? In principle, two alternative answers can be given.

Answer One: These particles are indeed elementary; their large number does not spoil the beautiful picture since all of them are components of one superparticle; both the number of these components and the character of the interactions between them are determined by one or several fundamental principles.

Answer Two: The particles that at present are considered elementary are in fact built of some more elementary subparticles. Roughly, the main idea of this approach is: universe-galaxies-stars-atoms-nuclei-quarkssubquarks.

It is then natural to assume that subquarks are the blocks of which not only quarks are built but leptons, gluons, and photons as well. At energies now available (at the achieved momentum transfers) all these particles appear to be elementary, and hence they are very small ($\ll 10^{-15}$ cm). Before the advent of quantum chromodynamics, any theorist would have said that only very heavy particles can be localized at such short distances and that as a result the subquark masses cannot be below several tens of GeV . But now when the idea of confinement has gained so much popularity, it is quite acceptable to picture subquarks as light or even massless particles confined at very short distances. However, by virtue of the uncertainty relation, the kinetic energies of these particles must be high (of the order of the inverse dimension of leptons, photons, etc.). Hence, the intervals between energy levels of such systems consisting of subquarks, that is between masses of the conventional elementary

particles, must be large. But how could we explain in this case the differences of the order of hundreds of MeV , or even several MeV , between the experimentally observed masses of these particles?

5.27 27 Particles and the universe

Some of the fundamental characteristics of elementary particles can be deduced from astrophysical observational data with much higher accuracy than from laboratory experiments. As examples we can mention the upper bounds on the mass of the photon and of different types of neutrinos, restrictions on the mass and lifetimes of hypothetical neutral leptons, the upper bound on the number of different types of neutrino, and finally the arguments in favor of quark confinement derived on the basis of the estimated residual concentration of relic quarks. Some of these restrictions are discussed in the present chapter on the basis of the hot universe model.

5.27.1 27.1. Hot universe

At first glance, the most abundant particles in the surrounding universe are protons and electrons: on average, the universe contains several protons and as many electrons (the universe is electrically neutral) per cubic meter. This is equivalent to a density of approximately $10^{-29} - 10^{-30}$ g/cm^3. In reality, however, the number of photons in the universe is much greater than that of protons, by a factor of approximately 10^9 (400 photons per cm^3). These photons exist in the form of radiation with a temperature of approximately 2.7 K or $2.5 \cdot 10^{-4}$eV, and fill the universe. The total energy of this microwave radiation is smaller by four orders of magnitude than the total mass of protons. It means that although the number of relic photons is large, their role at present is negligible in comparison to that of electrons and protons.

There was a time, however (about 10^{10} years ago), when these photons were highly energetic and to a great extent determined the dynamics of the whole universe.

It has been established, on the basis of the red shift of remote galaxies, that the universe is expanding. This expansion is reminiscent of the growth
of scale on the surface of a balloon when it is being inflated. The distances between any two points in the universe, and with them the photon wavelengths, increase; the universe expands and cools down. Going back in time, we come to the point $t = 0$, corresponding to infinite density and temperature of the universe. Today it is not clear how close to this point we are justified in extrapolating the increasing temperature and density. The extrapolation is probably valid up to $T \simeq 1$MeV, and possibly up to $T \simeq 1$ GeV or even up to the Planck temperature (10^{19}GeV). The hot phase of the evolution of the universe has left us a background of cooled relic photons.

Let us find a relation between the age of the universe, that is the time elapsed since the moment $t = 0$, and its temperature. In general, an analysis of the properties of the expanding universe requires the knowledge of the general theory of relativity. However, the relation in question can be found by means of elementary arguments. Consider a uniform infinite flat universe and a sphere of radius R in this universe. Let a probe particle of mass μ lie on this sphere (see fig. 27.1). Expansion of the universe increases the scale and hence our radius R. This means that $\mathrm{d}R/\mathrm{d}t > 0$. The kinetic energy of the particle in the reference frame connected with the center of the sphere is

$$T_{\text{kin}} = \frac{1}{2}\mu \left(\frac{\mathrm{d}R}{\mathrm{d}t} \right)^2 .$$

Consider now the potential energy of the probe particle. It is determined by the attraction of the particles (both massive and massless) inside the sphere (the matter outside the sphere

has no effect on the particle). The energy of this attraction is

$$U = -G_{\mathrm{N}} \frac{4\pi R^3 \rho \mu}{3R},$$

where $G_{\mathrm{N}} \simeq 6 \cdot 10^{-39} m_{\mathrm{p}}^{-2}$ is Newton's constant and ρ is the mean energy density (we recall that the source of gravitation is energy, not mass).

Let us find now what critical density $\rho = \rho_{\mathrm{c}}$ corresponds to a steady-state expansion when the sum of kinetic and potential energies of the probe

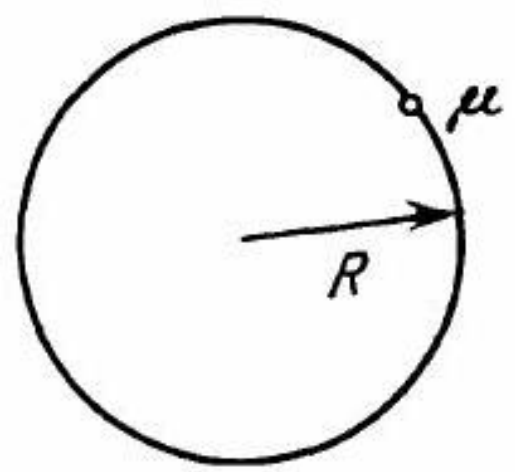


Fig. 27.1.

particle is zero:

$$\frac{\mu}{2} \left(\frac{\mathrm{d}R}{\mathrm{d}t} \right)^2 = G_{\mathrm{N}} \frac{4\pi R^3 \rho \mu}{3R}$$

In this expansion mode

$$\left(\frac{1}{R} \frac{\mathrm{d}R}{\mathrm{d}t} \right)^2 = \frac{8}{3} \pi G_{\mathrm{N}} \rho_c.$$

The quantity $H(t) = (1/R)\mathrm{d}R/\mathrm{d}t$ proves to be independent of R. It is called the Hubble constant and according to observations, $H(t) \simeq 60\mathrm{km/s\cdot}$ Megaparsec $\simeq 18$ km/s· light year (the value 60 km/s· Megaparsec is considered the most likely; in fact, 45 km/s· Megaparsec $< H <$ 120km/s· Megaparsec). The quantity $1/2H \simeq 10^{10}$ years characterizes the age of the Universe. When H is known, it is not difficult to find the critical density ρ_{c} :

$$\rho_{\mathrm{c}} = \frac{3H^2}{8\pi G_{\mathrm{N}}} \simeq 5 \cdot 10^{-30} \ \mathrm{g/cm^3} \simeq 3 m_{\mathrm{p}}/\mathrm{m}^3.$$

The observed density of matter in the universe is quite close to its critical level. If $\rho > \rho_{\mathrm{c}}$, the expansion will ultimately change to contraction. If $\rho < \rho_{\mathrm{c}}$, then the expansion will continue forever.

Let us turn now to the first moments of the big bang when both T_{kin} and $|U|$ were enormously large compared to their current values, while $T_{\mathrm{kin}} + U$ was the same as it is today. Consider a sufficiently hot phase of the universe for which the particle masses in the expression for the density ρ can be neglected in comparison to their momenta. It is clear on the basis of dimensional arguments that in this case $\rho = a/R^4$ where a is a dimensionless constant. Substitution of this expression into the equation

$$\left(\frac{\mathrm{d}R}{\mathrm{d}t}\right)^2 = \frac{8}{3}\pi G_{\mathrm{N}}\rho R^2$$

yields that

$$\frac{\mathrm{d}R}{\mathrm{d}t} = \left(\frac{8}{3}\pi G_{\mathrm{N}}a\right)^{1/2}\frac{1}{R}.$$

Solution of this equation gives

$$R^2 = \left(\frac{32}{3}\pi G_{\mathrm{N}}a\right)^{1/2}t.$$

Returning to the energy density, $\rho = a/R^4$, we obtain

$$\frac{32}{3}\pi G_{\mathrm{N}}\rho t^2 = 1.$$

Let us now consider the relation between ρ and the temperature T of the universe:

$$\rho = 4\sigma\kappa T^4,$$

where $\sigma = \frac{1}{60}\pi^2$ is the Stefan-Boltzmann constant (recall that in our system of units $\hbar = c = 1$). The coefficient κ is a function of T : it depends on the number of types of elementary particles contributing to the total energy density at temperature T. In a universe containing photons only, $\kappa = 1$. With other particles taken into account,

$$\kappa = \kappa(T) = 1 + \frac{7}{8}N_\nu + \frac{7}{4}N_\ell(T) + \ldots,$$

where N_ν is the number of various types of two-component massless neutrino ($\nu_{\mathrm{e}}, \nu_\mu, \nu_\tau, \ldots$), and $N_\ell(T)$ is the number of different fourcomponent leptons for which $2m_{\mathfrak{l}} \ll T$. The ellipsis in the expression for κ stands for the contributions of quarks, gluons (for $T \gtrsim 1\mathrm{GeV}$), and W- and Z-bosons (for $T \gtrsim 100\mathrm{GeV}$). The factor $\frac{7}{8}$ takes into account the difference in densities of the Fermi and Bose distributions for ν and γ, respectively.
(Indeed,

$$\int_0^\infty \frac{z^n\,\mathrm{d}z}{\mathrm{e}^z - 1} - \int_0^\infty \frac{z^n\,\mathrm{d}z}{\mathrm{e}^z + 1} = 2\int_0^\infty \frac{z^n\,\mathrm{d}z}{\mathrm{e}^{2z} - 1} = \frac{1}{2^n}\int_0^\infty \frac{y^n\,\mathrm{d}y}{\mathrm{e}^y - 1},$$

whence

$$\int_0^\infty \frac{z^n\,\mathrm{d}z}{\mathrm{e}^z + 1} \Big/ \int_0^\infty \frac{z^n\,\mathrm{d}z}{\mathrm{e}^z - 1} = 1 - 2^{-n}$$

This gives $\frac{7}{8}$ for $n = 3$).
The contribution of the electron is twice that of the neutrino since the electron has four components. Finally,

$$\frac{128}{3}\pi\sigma\kappa G_{\mathrm{N}}T^4t^2 = 1.$$

This yields the well-known relation of temperature and age of the universe:

$$t(\text{ seconds }) \simeq \frac{1}{T^2\left(\mathrm{MeV}^2\right)}.$$

5.27.2 27.2. Upper bound on the neutrino mass

The theory of the hot universe shows, under the assumption of zero total leptonic charge, that the current number of relic neutrinos is of approximately the same order of magnitude as the number of photons. However,
the detection of the neutrino background is an incomparably more difficult task which so far seems to be unfeasible. The fact that the theory gives us today's concentration of relic neutrinos makes it possible to find the upper bound on the masses of these particles.

Denote the number of muonic neutrinos (photons) in one cm^3 by n_{ν_μ} (n_γ). If $n_{\nu_\mu} \simeq n_\gamma$, then the world contains approximately 10^9 neutrinos per one nucleon. If each neutrino had a mass of, say, 10 eV , the net mass of all neutrinos would be a few times that of all protons in the universe, so that the dynamics of the expansion of the universe would be determined today, as it was several billion years ago, by the gravity effect of these cold and otherwise absolutely passive neutrinos. The neutrino mass cannot be much larger than 10 eV since it would give $\rho \gg \rho_\mathrm{c}$. This in turn would mean that the expansion at the earlier stages of the universe was much faster than in the steady-state case. This conclusion would lead to a contradiction since it would mean that the age of the universe is shorter than that of the oldest rocks on earth (which are several billion years old).

In the above paragraph we have made use of the assumption $n_{\nu_\mu} \simeq n_\gamma$. Let us find an exact ratio of these quantities assuming that only left-handed neutrinos participate in the weak interaction. While ν_μ and γ are in equilibrium, $n_{\nu_\mu} = \frac{3}{4} n_\gamma$ (see the above integrals for the Fermi and Bose distributions at $n = 2$). This ratio remained unaltered even when the neutrino ceased to be in equilibrium with electrons, positrons, and photons. However, annihilation of electrons and positrons increased n_γ by a factor of $1 + \frac{7}{4} = \frac{11}{4}$ by virtue of conservation of entropy (the entropy S is proportional to ρ/T) so that from that time until today $n_{\nu_\mu}/n_\gamma = \frac{3}{4} \cdot \frac{4}{11} = \frac{3}{11}$. The same is true for ν_e and ν_τ. As a result, $m_{\nu_\mathrm{e}} + m_{\nu_\mu} + m_{\nu_\tau} \leqslant 30\mathrm{eV}$. Note that the cosmological limit is comparable with the laboratory upper limit for ν_e and is better than the laboratory upper bounds on the ν_μ and ν_τ masses by four and seven orders of magnitude, respectively.

5.27.3 27.3. Ont the number of possible types of neutrinos

The relation between temperature T and the age t of the universe, established above, is

$$t^2 = \frac{3}{32\pi\sigma\kappa G_\mathrm{N} T^4},$$

where $\sigma = \frac{1}{15}\pi^2$, $G_\mathrm{N} \simeq 6{\cdot}10^{-39} m_\mathrm{p}^{-2}$, and $\kappa = \kappa(T)$ is determined by the number of elementary particles whose masses satisfy the condition $T \gg m$.

At $T \simeq 14\mathrm{MeV}$, when the present ratio of abundances of neutrons (mostly contained in the primordial $^4\mathrm{He}$) and protons (hydrogen) had set on, the coefficient κ was

$$\kappa = 1 + \frac{7}{4} + \frac{7}{8} N_\nu.$$

Here 1 gives the contribution of photons, $\frac{7}{4}$ gives that of electron-positron pairs, and $\frac{7}{8} N_\nu$ that of neutrinos. The last term is proportional to the number of possible types of neutrinos, N_ν. (Note that the equilibrium between neutrinos of different types and photons, electrons, and positrons is maintained by reactions which proceed via neutral currents, for example, $\nu_\mu + \bar{\nu}_\mu \to \mathrm{e}^+ + \mathrm{e}^-$).

We find that at any given temperature, the universe is the younger the greater the number of different types of neutrinos, N_ν, is. In other words, as N_ν is augmented, the time scale contracts, that is the expansion rate of the universe rises:

$$t \to t' = t\sqrt{\kappa/\kappa'}.$$

We shall demonstrate now that the ratio of neutrons to protons is very sensitive to the expansion rate of the universe, so that the observed abundance of ^{4}He is an indicator of the number of different types of neutrinos.

The equilibrium ratio of neutrons to protons at high temperatures is $\exp(-\Delta m/T)$, where $\Delta m = m_{\rm n} - m_{\rm p}$. This equilibrium value is maintained by weak reactions of the type $\mathrm{pe}^- \to \mathrm{n}\nu_{\rm e}, \mathrm{ne}^+ \to \mathrm{p}\bar{\nu}_{\rm e}, \mathrm{n} \to \mathrm{pe}^-\bar{\nu}_{\rm e}$. However, when the characteristic time of these weak reactions, $t_{\rm w}$, becomes large in comparison with $t_{\rm c}$ characterizing the expansion of the universe, the ratio of neutron to proton abundance is "quenched" or "frozen", and does not diminish in the course of a further drop in temperature. Dimensional arguments show that

$$\frac{1}{t_{\rm w}} \simeq G_{\rm F}^2 T^5,$$

where $G_{\rm F} = 10^{-5} m_{\rm p}^{-2}$ is the Fermi constant. By setting $t_{\rm w}$ equal to $t_{\rm c}$ we obtain

$$G_{\rm F}^2 T^5 \simeq \left(\kappa G_{\rm N} T^4\right)^{1/2}.$$

We see that temperature at which neutrons are quenched increases with κ :

$$T_{\rm n} \simeq \kappa^{1/6} G_{\rm N}^{1/6} G_{\rm F}^{-2/3}.$$

As a result, the neutron concentration, $\exp(-\Delta m/T)$, also increases as κ rises.

If we take into account that neutrons are trapped in the primordial ^{4}He, then the abundance (by mass) of the primordial helium was twice the abundance of neutrons. Astrophysical calculations indicate that the abundance of primordial helium was close to 0.24 (this corresponds to $n_{\rm n}/n_{\rm p} \simeq 1/7$). This abundance agrees with a cosmological estimate for $N_\nu = 3$. It is not difficult to show that each additional type of neutrino increases helium abundance by about 1.5%. Several years ago astrophysicists considered it possible that the maximum abundance of the primordial helium was above 30%. However, the upper bound on helium abundance as given in the literature gradually diminishes. Assuming, with a number of authors, that the primordial helium abundance did not exceed 25%, we conclude that nature contains not more than one massless neutrino in addition to $\nu_{\rm e}, \nu_\mu$, and ν_τ.

5.27.4 27.4. Concentration of relic quarks

As long as we are without a consistent theory of confinement, the main argument against the existence of free quarks with fractional charges is their absence in the surrounding matter. The point is, the expected concentration of relic quarks can be estimated in the framework of the theory of the hot universe, and the estimate is found to be very high, much higher than the upper bound imposed by the experiments on the detection of free quarks. We show below how the estimates of this type are obtained.

Assume that a quark confined within a hadron has a mass much smaller than that of a free quark. (Abdus Salam referred to this phenomenon as the Archimedes effect: a quark dipped into a "hadron bathtub" becomes lighter. Absolute confinement corresponds to infinitely heavy free quarks.) Assume for the purpose of estimation that the free quark mass is of the order of 10 GeV (we shall see that the result is not very dependent on $m_{\rm q}$) and consider the universe at $T \simeq 100$GeV. Quarks at this temperature (it was reached 10^{-10} s after the big bang) are in thermodynamical equilibrium with other fundamental particles, namely photons and leptons. At $T \simeq m_{\rm q}$ quarks go out of equilibrium: their production stops, and they begin to burn out. This burning goes through reactions of the type of

$$q + \bar{q} \rightarrow \text{ mesons},$$
$$q + q \rightarrow \bar{q} + \text{ baryon}.$$

These are exothermic reactions: the first releases energy of the order of $2m_{\rm q}$, and the second of the order $m_{\rm q}$. Assume, in analogy to usual exothermic reactions, that σv for these reactions tends, for the quark velocity tending to
zero, to a constant limit σ_0. The quark burning rate is characterized then by $n_{\rm q}\sigma_0$ where $n_{\rm q}$ is the concentration of free quarks. The process slows down, and then stops, when the rate of burning becomes equal to, and then less than, the rate of the cosmological expansion. The temperature at this stage is still comparable, by order of magnitude, with $m_{\rm q}$. Hence,

$$n_{\rm q} \simeq G_{\rm N}^{1/2} T^2/\sigma_0 \simeq G_{\rm N}^{1/2} m_{\rm q}^2/\sigma_0.$$

It will be convenient to consider the ratio of this concentration, $n_{\rm q}$, to the concentration of photons $n_\gamma \simeq T^3 \simeq m_{\rm q}^3$:

$$\frac{n_{\rm q}}{n_\gamma} \simeq \frac{G_{\rm N}^{1/2}}{\sigma_0 m_{\rm q}} \simeq \frac{10^{-18}}{m_{\rm p} m_{\rm q} \sigma_0} \simeq 10^{-21} \quad \text{if } \sigma_0 \simeq m_\pi^{-2}$$

As the universe expands and cools down, the quark and photon concentrations decrease. Their ratio, however, remains constant if the expansion is adiabatic. This ratio, $n_{\rm q}/n_\gamma$, is small because the universe expands slowly, even at $T \simeq 1$GeV, compared to the time scale typical for elementary particles, 1/GeV. A small parameter here is the gravitational constant $G_{\rm N}$ determining the expansion rate of the universe. A large number of quarks merge into hadrons during this slow expansion.

Now we shall take into account that there are 10^9 photons per one proton. Then the ratio of quark to proton abundances must be equal to

$$n_{\rm q}/n_{\rm p} \simeq 10^{-12}$$

Although this is a very small quantity, it is still unacceptably high. It exceeds the abundance of gold, and would make it possible to "haul cartloads" of quarks. After comparing this result with the experimental limit, $n_{\rm q}/n_{\rm p} \lesssim 10^{-27}$, we can hardly avoid the conclusion that there are no free fractionally charged quarks in nature. To lower the quark concentration to an acceptable level, one would have to assign at least atomic (and not nuclear) dimensions to the quark annihilation cross section, σ_0.

5.27.5 27.5. On baryonic asymmetry of the universe

Application of estimates similar to those of the preceding sections, to the annihilation of primordial baryons and antibaryons yields

$$n_{\rm p}/n_\gamma \simeq G_{\rm N}^{1/2} m_{\rm p} \simeq 10^{-18}$$

which is smaller by nine orders of magnitude than the ratio observed in nature. This small value is obtained if one assumes that (i) the initial
baryonic charge of the universe is zero, and (ii) there are no interactions violating conservation of baryonic charge. In order to obtain $n_{\rm p}/n_\gamma \simeq 10^{-9}$ in a world where the baryonic charge is conserved, one has to assume that a small excess of baryonic charge was present from the very beginning, so that $\left(n_{\rm q} - n_{\bar{\rm q}}\right)/n_{\rm q} \simeq 10^{-9}$.

Another point of view appears very attractive. It states that the excess of baryons over antibaryons was produced at the early stages of the evolution of the universe owing to non-conservation of baryonic charge and violation of CP. This idea was first proposed in the middle

of the 60's and has been discussed in a number of recent publications in the framework of grand unification models.

5.28 28. Bibliography

The literature survey given below does not pretend to be complete. It is practically impossible to cover all important publications even if the survey is not too brief.
The literature cited in the survey will help the reader to get a more detailed knowledge of the present state of the problems considered in the book and also, in a number of cases, of the history of these problems. The survey of the literature is divided into the following sections:
28.1. Monographs. Proceedings of Conferences 265
28.1.1. Monographs on the theory of weak interaction 265
28.1.2. Monographs on relativistic quantum theory 265
28.1.3. Group theory (monographs and papers) 266
28.1.4. Conferences, 1960-1982 266
28.2. Decays of leptons and hadrons 267
28.2.1. On the history of weak interactions, 1896-1958 267
28.2.2 Muon decay 268
28.2.3. Strangeness conserving leptonic decays, ... 269
28.2.4. Strangeness changing leptonic decays 269
28.2.5. Non-leptonic decays of strange particles 270
28.2.6. Non-conservation of parity in nuclear forces 272
28.2.7. Neutral K-mesons 272
28.2.8. Violation of CP invariance 274
28.2.9. Charmed quark prior to the discovery of the J/ψ meson 275
28.2.10. Charmed particles after the discovery of the J/ψ meson 276
28.2.11. Decays of the τ-lepton 277
28.2.12. Properties of the b - and t -quarks 277
28.3. Neutrino reactions 278
28.3.1. Neutrino-nucleon interactions. Charged currents 278
28.3.2. Neutrino-nucleon interactions. Neutral currents 279
28.3.3. Neutrino-electron interaction 279
28.3.4. Creation of a muon pair by a neutrino in the Coulomb field of a nucleus 280
28.3.5. Electron-nucleon interaction 280
28.3.6. Phenomenological analysis of data on neutral currents 281
28.4. Weak interactions at high energies 281
28.4.1. Four-fermion interaction and the unitarity limit 281
28.4.2. Gauge symmetry 282
28.4.3. Spontaneous breaking of gauge symmetry 283
28.4.4. Standard model of the electroweak interaction 284
28.4.5. Production and decay of the W- and Z-bosons 285
28.4.6. Future facilities designed to search for the W - and Z -bosons 285
28.4.7. Properties of Higgs bosons 286
28.5. Models of grand and super unification 288
28.5.1. Model based on the group SU(4) $\times$ SU(2) $\times$ SU(2) 288
28.5.2. Model based on the group SU(5) 288
28.5.3. Model based on the group SO(10) 288
28.5.4. Models based on exceptional groups 288
28.5.5. Models of simple unification 289
28.5.6. Reviews of grand unification models 289

28.5.7. Superunification 289
28.6. Particles and the universe 290
28.6.1. The general theory of relativity and the theory of the hot universe 290
28.6.2 The hot universe and leptons 291
28.6.3. The hot universe and quarks 292
28.6.4. Cosmology and spontaneous symmetry breaking 293
28.6.5. Astrophysics and photons 293
28.6.6. Possible non-conservation of the baryonic charge, and baryonic asymmetry of the universe 294
28.6.7. Possible non-conservation of the leptonic charge 295
28.6.8. Concentration of relic monopoles 295
28.6.9. On the conservation of the electric charge 296
28.6.10. Time independence of the fundamental constants 296
28.7. Supplementary bibliography (autumn 1980) 296
28.7.1. Electroweak processes. Review papers 296
28.7.2. Decays of strange particles 297
28.7.3. Violation of CP invariance 297
28.7.4. Decays of c- and b-hadrons 298
28.7.5 Neutral currents 299
28.7.6. Electroweak radiative corrections 300
28.7.7. Virtual Higgs bosons 300
28.7.8. Dynamical symmetry breaking 300
28.7.9. Properties of free neutrinos 301
28.7.10. Neutrino masses in grand unification models 302
28.7.11. Grand unification models and proton decay 302
28.7.12. Various aspects of grand unification 303
28.7.13. Superunification 304
28.7.14. Cosmology and elementary particles. Review papers 305
28.7.15. Neutrino mass and hidden mass in the universe 305
28.7.16. Calculation of $n_{\mathrm{B}}/n_{\gamma}$ 306
28.7.17. Magnetic monopoles and cosmology 306
28.7.18. Search for new particles and interactions 306
28.7.19. Search for deviations from Newton's law 307
28.7.20. Verification of electric charge conservation 307
28.7.21. Future accelerators. 307

5.28.1 28.1. Monographs. Proceedings of conferences

28.1.1. Monographs on the theory of weak interaction

J. M. Gaillard, M. K. Gaillard, D. Haidt, L. Jauneau, O. Nachtman, H. Pietschmann, F. Vannucci, Weak interactions, ed. M. K. Nikolic (Paris, IN2P3, 1977).
D. Bailin, Weak interactions (Sussex University Press, 1977).
J. C. Taylor, Gauge theories of weak interactions (Cambridge University Press, 1976).
R. E. Marshak, Riazuddin, C. P. Ryan, Theory of weak interactions in particle physics (Wiley, 1969).
L. B. Okun, Weak interactions of elementary particles (Pergamon, 1965).

The development of weak interaction theory, ed. P. K. Kabir (Gordon and Breach, 1963). Collection of 39 selected reprints on the theory of weak interactions 1934-1961.

28.1.2. Monographs on relativistic quantum theory

V. B. Berestetsky, E. M. Lifshitz, L. P. Pitaevsky, Relativistic quantum theory, vol. 4 of Course of theoretical physics, translated from Russian by J. B. Syes and J. S. Bell (Pergamon, 1971).

Yu. V. Novozhilov, Vedeniye v teoriyu elementarnikh chastits (Introduction to the theory of elementary particles) (Nauka, Moscow, 1972) (in Russian).

A. I. Akhiezer, V. B. Berestetsky, Quantum electrodynamics, Translated from second Russian edition, ed. G. M. Volkoff (Interscience, 1965).

N. N. Bogolubov, D. V. Shirkov, Introduction to the theory of quantum fields (Wiley, 1959).

J. D. Bjorken and S. D. Drell, Relativistic quantum mechanics, vol. I, Relativistic quantum fields, vol. II (McGraw-Hill, 1965).

R. P. Feynman, Theory of fundamental processes (Benjamin, 1961).

R. P. Feynman, Quantum electrodynamics (Benjamin, 1961).

28.1.3. Group theory (monographs and papers)

G. Racah, Group theory and spectroscopy, Preprint of lectures delivered at the Institute of Advanced Studies, Princeton, spring 1951. Preprint CERN 61-8, 6 March 1961, Geneva.

F. Grsey, in Relativity, groups, and topology, ed. C. De Witt and B. De Witt (Gordon and Breach, 1964).

A. O. Barut and R. Raczka. Theory of group representations and applications (Polish Scientific Publishers, Warszawa, 1977).

K. W. McVoy, Symmetry groups in physics, Rev. Mod. Phys. 37 (1965) 84.

R. E. Behrends, J. Dreitlein, C. Fronsdal, W. Lee, Simple groups and strong interaction symmetries, Rev. Mod. Phys. 34 (1962) 5.

A. Salam, The formalism of Lie groups, in Theoretical physics (IAEA, Vienna, 1963) p. 173.

28.1.4. Conferences, 1960-1982

Rapporteur talks published in the proceedings of regular international conferences are indispensable in following the progress of high-energy physics during the last two decades.

Rochester Conferences on High-Energy Physics. The first seven conferences took place at the University of Rochester, and the subsequent conferences were:
Genve 1958 (VIII), Kiev 1959 (IX), Rochester 1960 (X), Genve 1962 (XI), Dubna 1964 (XII), Berkeley 1966 (XIII), Vienna 1968 (XIV), Kiev 1970 (XV), Batavia 1972 (XVI), London 1974 (XVII), Tbilisi 1976 (XVIII), Tokyo 1978 (XIX), Madison 1980 (XX), Paris (1982) (XXI).

European Conferences on High-Energy Physics

Aix-en-Provence 1961, Sienna 1963, Oxford 1965, Heidelberg 1967, Lund 1969, Amsterdam 1971, Aix-en-Provence 1973, Palermo 1975, Budapest 1977, Genve 1979, Lisbon 1981.

Neutrino Conferences

Moscow 1968, Cortona 1970, Balatonfred 1972, Philadelphia 1974, Balatonfred 1975, Aachen 1976, Baksan Valley 1977, West Lafayette 1978, Bergen 1979, Erice 1980, Hawaii, 1981, Balatonfred, 1982.

Photons and Leptons Conferences

Cambridge 1963, Hamburg 1965, Stanford 1967, Daresbury 1969, Cornwall 1971, Bonn 1973, Stanford 1975, Hamburg 1977, Batavia 1979, Bonn 1981.

5.28.2 28.2. Decays of leptons and hadrons

28.2.1. On the history of weak interactions, 1896-1958

Listed below are some of the papers which played an important role in the genesis of the modern picture of the weak interactions.

A. Becquerel, Compt. Rend. 122 (1896) 501, 509.
The discovery of radiation of salts of uranium (of β-rays of thorium).

E. Rutherford, Phil. Mag., ser. 6, 21 (1911) 669.
The discovery of the atomic nucleus.

J. Chadwick, Nature 129 (1932) 312.
The discovery of the neutron.

W. Pauli, in: Noyaux atomique, VII Conseil de Physique Solvay 1933, Paris, 1934, p. 324.
The hypothesis of the neutrino.

E. Fermi, Z. Phys. 88 (1934) 161.
The theory of β-decay (vector variant).

C. D. Anderson, S. H. Neddermeyer, Phys. Rev. 51 (1937) 894.
The discovery of the muon.

C. M. J. Lattes, H. Muirhead, J. P. S. Occhialini, C. F. Powell, Nature 159 (1947) 694.
The discovery of charged pions.

L. Le Prince-Ringuet, M. Lheritier, Compt. Rend. 219 (1944) 618.
The first observation of the K -meson.

J. D. Rochester, C. C. Butler, Nature 160 (1947) 855.
The first observation of "forks" of decays of neutral strange particles.

B. Pontecorvo, Phys. Rev. 72 (1947) 246.

G. Puppi, Nuovo Cim. 5 (1948) 505.

O. Klein, Nature, 161 (1948) 897.
The hypothesis of the universal weak interaction.

T. D. Lee, C. N. Yang, Phys. Rev. 104 (1956) 254.
Formulation of the problem of parity non-conservation in weak interactions.

E. Ambler, R. W. Hayward, D. D. Hoppes, R. R. Hudson, C. S. Wu, Phys. Rev. 105 (1957) 1413.
The discovery of the P-odd angular asymmetry of electrons in decays of polarized ^{60}Co nuclei.

R. L. Garwin, L. M. Lederman, M. Weinrich, Phys. Rev. 105 (1957) 1415;
J. J. Friedman, V. G. Telegdi, Phys. Rev. 105 (1957) 1681.
The discovery of the muon polarization and electron asymmetry in decays $\pi \to \mu \to$ e.

R. P. Feynman, M. Gell-Mann, Phys. Rev. 109 (1958) 193;
R. E. Marshak, E. C. G. Sudarshan, Phys. Rev. 109 (1958) 1860;
J. J. Sakurai, Nuovo Cim. 7 (1958) 649.
The V - A theory of weak interactions.

28.2.2. Muon decay

L. Michel, Proc. Phys. Soc. A63 (1950) 154, 1371.
Calculation of the spectrum of electrons in muon decay.

A. O. Weissenberg, Muons (North-Holland, Amsterdam, 1966);
J. Feinberg, L. Lederman, Ann. Rev. Nucl. Sci. 13 (1963).
Discussion of the most important experimental data on muons.

S. M. Berman, A. Sirlin, Ann. of Phys. 20 (1962) 20;
A. Sirlin, Rev. Mod. Phys. 50 (1978) 573.
Radiative corrections to muon decay.

28.2.3. Strangeness conserving leptonic decays

S. S. Gershtein, Ya. B. Zeldovich, ZhETF 29 (1955) 698 [JETP 2(1956) 576];
R. P. Feynman, M. Gell-Mann, Phys. Rev. 103 (1958) 193.

Conservation of vector current, non-renormalizability of the vector constant, and prediction of the π_{e3} decay.

M. Gell-Mann, Phys. Rev. 111 (1958) 362.

Weak magnetism.

Y. Nambu, Phys. Rev. Lett. 4 (1960) 380;
Y. Nambu, G. Jona-Lasinio, Phys. Rev. 122 (1961) 345,
V. G. Vaks, A. I. Larkin, ZhETF 40 (1961) 282 [JETP 13 (1961) 192];
J. Goldstone, Nuovo Cim. 19 (1961) 154.

Spontaneous breaking of chiral symmetry and massless bosons.

M. L. Goldberger, S. B. Treiman, Phys. Rev. 110 (1958) 1178, 111 (1958) 354;
Chou Kuang-Chao ZhETF 39 (1960) 703 [JETP 12 (1961) 492].
Effective pseudoscalar and dispersion relations.

M. Gell-Mann, M. Levy, Nuovo Cim. 16 (1960) 705.

The hypothesis of partial conservation of the axial current.

A description of the evolution of the theory of soft pions and partial conservation of the axial current can be found in the review paper:
A. I. Vainshtein and V. I. Zakharov, in Usp. Fiz. Nauk, 100 (1970) 225 [Uspekhi 13 (1970) 73]; and in the monographs:
S. L. Adler, R. F. Dashen, Current algebra and applications to particle physics (Benjamin, 1968);
J. Bernstein, Elementary particles and their currents (Freeman, San Francisco, 1968);
S. B. Treiman, R. Jackiw, D. J. Gross, Lectures on current algebra and its applications (Princeton University Press, 1972).

28.2.4. Strangeness changing leptonic decays

M. Gell-Mann, Proc. Rochester Conf. 8 (1956) 25;
L. B. Okun, ZhETF 34 (1958) 469 [JETP 7 (1958) 322].

Selection rules for semileptonic decays of hadrons, $\Delta Q = \Delta S, |\Delta S| = 1$, $\Delta T = 1/2$, are formulated on the basis of the model in which all hadrons are built of three fundamental baryons with quantum numbers $\mathrm{p}, \mathrm{n}, \Lambda$ (the Sakata model).

N. Cabibbo, Phys. Rev. Lett. 10 (1963) 531.

A unified description of leptonic decays of mesons and baryons on the basis of SU(3) symmetry, with a single parameter, θ_{C}. See also earlier papers:
M. Gell-Mann, M. Levy, Nuovo Cim. 16 (1960) 705;
M. Gell-Mann, Phys. Rev. 125 (1962) 1067.

The current $\bar{p}n\cos\theta + \bar{p}\lambda\sin\theta$ is introduced, and the idea of the modified universality of the weak interaction is formulated.

I. Yu. Kobzarev, L. B. Okun, ZhETF 42 (1962) 1400 [JETP 15 (1962) 970].
The equality of constants of the strangeness-changing vector and axial currents is demonstrated on the basis of SU(3) symmetry of the strong interaction and by comparing decay rates of $\pi_{\mu 2}, \pi_{\mathrm{e}3}$, $\mathrm{K}_{\mu 2}$, $\mathrm{K}_{\ell 3}$.

M. Ademollo, R. Gatto, Phys. Rev. Lett. 13 (1964) 262.

The theorem on the vanishing of first-order corrections in SU(3) breaking to vector vertices.

All the details concerning SU(3) symmetry can be found in
M. Gell-Mann, Y. Ne'eman, The eightfold way (Benjamin, 1964).
C. G. Callan, S. B. Treiman, Phys. Rev. Lett. 16 (1966) 153.

Relations between amplitudes of $K_{\ell 2}$, $K_{\ell 3}$, and $K_{\ell 4}$ decays.

L. M. Chounet, J. M. Gaillard, M. K. Gaillard, Phys. Reports 4C (1972) 199.

A review of leptonic decays of mesons and hyperons.

W. Tannenbaum et al., Phys. Rev. Lett. 33 (1974) 175;
D. Decamp et al., Phys. Lett. 66B (1977) 295.

Experiments on measuring g_A/g_V for $\Sigma^- \to \mathrm{n e^-} \bar{\nu}_\mathrm{e}$ decay.

28.2.5 Non-leptonic decays of strange particles

M. Gell-Mann, A. Pais, Proc. Glasgow Conf., 1954 (Pergamon, London, 1955) p. 342.

The hypothesis of the selection rule $\Delta T = 1/2$.

B. W. Lee, Phys. Rev. Lett. 12 (1964) 83;
H. Sugawara, Progr. Theor. Phys. 31 (1964) 231;
M. Gell-Mann, Phys. Rev. Lett. 12 (1964) 155.

The hypothesis of octet enhancement in the effective non-leptonic strange-ness-changing interaction. The Lee-Sugawara relation is derived.

P. K. Ellias, C. Taylor, Nuovo Cim. 44 (1966) 518;
Y. Hara, Y. Nambu, Phys. Rev. Lett. 16 (1966) 875;
M. Suzuki, Phys. Rev. 144 (1966) 1154;
A. D. Dolgov, V. I. Zakharov, Yad. Fiz. 1 (1968) 352 [Sov. J. Nucl. Phys. 7 (1968) 232].

The relation between the amplitudes of the decays $\mathrm{K} \to 2\pi$ and $\mathrm{K} \to 3\pi$ is derived by the soft pion techniques. The last paper demonstrates that the $\Delta T = 1/2$ rule must be strongly broken ($\simeq 50\%$) in slopes of pion spectra in $\mathrm{K} \to 3\pi$ decays.

T. J. Devlin, J. O. Dickey, Rev. Mod. Phys. 51 (1979) 237.

A review of experimental and theoretical results concerning $\mathrm{K} \to 2\pi$ and $\mathrm{K} \to 3\pi$ decays.

H. Sugawara, Phys. Rev. Lett. 15 (1965) 870;
M. Suzuki, Phys. Rev. Lett. 15 (1965) 486;
Y. Hara, Y. Nambu, T. Schechter, Phys. Rev. Lett. 16 (1966) 875;
S. Badier, C. Bouchiat, Phys. Lett. 20 (1966) 259.

Application of the soft pion techniques to non-leptonic decays of hyperons.

J. Schwinger, Phys. Rev. Lett. 12 (1964) 630;
I. Yu. Kobzarev, L. B. Okun, Yad. Fiz. 1 (1965) 1134 [Sov. J. Nucl. Phys. 1 (1965) 807].

Phenomenological estimates of the matrix elements of the decays $\mathrm{K}^+ \to \pi^+\pi^0$ and $\Lambda^0 \to \mathrm{p}\pi^-$, derived by multiplying hadronic amplitudes for the semi-leptonic decays $\mathrm{K}_{\ell 3}, \pi_{\mu 2}$, and $\Lambda \to \mathrm{p e^-} \bar{\nu}_\mathrm{e}$.

K. Wilson, Phys. Rev. 179 (1969) 1499.

Operator expansion and its application to the $\Delta T = 1/2$ rule.

M. K. Gaillard, B. W. Lee, Phys. Rev. Lett. 33 (1974) 108;
G. Altarelli, L. Maiani, Phys. Lett. 52B (1974) 351.

Hard virtual gluons are shown to enhance amplitudes with $\Delta T = 1/2$ and to suppress those with $\Delta T = 3/2$.

A. I. Vainshtein, V. I. Zakharov, M. A. Shifman, ZhETF 72 (1977) 1275 [JETP 45 (1977) 670].

A gluon-monopole mechanism is suggested for non-leptonic decays satisfying the rule $\Delta T = 1/2$. The total non-leptonic lagrangian is derived.

J. Finjord, Phys. Lett. 76B (1978) 116.

Comparison of the predictions of the gluon-monopole mechanism with the experimental data on decays of the Ω-hyperon.

28.2.6. Non-conservation of parity in nuclear forces

Yu. G. Abov, P. A. Krupchitsky, Yu. A. Oratovsky, Phys. Lett. 12 (1964) 25;

Yu. G. Abov, P. A. Krupchitsky, Yu. A. Oratovsky, Yad. Fiz. 1 (1965) 479 [Sov. J. Nucl. Phys. 1 (1965) 341].

The discovery of the P-odd correlation of the γ-quantum momentum with the neutron spin in the reaction ^{113}Cd(nγ)^{114}Cd.

V. M. Lobashov, V. A. Nazarenko, L. F. Sayenko, L. M. Smotritsky, G. I. Kharkevich, Pis'ma ZhETF 3 (1966) [JETP Lett. 3 (1966) 173].

The discovery of the P-odd circular polarization of γ-quanta in decays of the ^{181}Ta nucleus.

Yu. G. Abov, P. A. Krupchitsky, Usp. Fiz. Nauk 118 (1976) 141 [Uspekhi 19 (1976) 75].

A review of experiments on the study of P-odd nuclear forces.

V. M. Lobashov et al., Nucl. Phys. A197 (1972) 241.

Measurements of circular polarization of photons in the reaction np $\to$ dγ. Theoretical discussion of this effect see in:

G. S. Danilov, Yad. Fiz. 22 (1975) 776 [Sov. J. Nucl. Phys. 22 (1975) 401].

G. V. Danilyan et al., Yad. Fiz. 27 (1978) 42 [Sov. J. Nucl. Phys. 27 (1978) 21].

Non-conservation of parity in nuclear fission.

R. J. Blin-Stoyle, Fundamental interactions and the nucleus (North-Holland, Amsterdam, 1973).

28.2.7 Neutral K-mesons

M. Gell-Mann, A. Pais, Phys. Rev. 97 (1955) 1387.

Introduction of K_1^0 and K_2^0 as the C-even and C-odd superpositions of the states K^0 and $\overline{\mathrm{K}}^0$.

A. Pais, O. Piccioni, Phys. Rev. 100 (1955) 1487.

Theoretical prediction of oscillations in a beam of neutral K-mesons and of the regeneration effect.

K. Lande, E. T. Booth, J. Impeduglia, L. M. Lederman, W. Chinowsky, Phys. Rev. 103 (1956) 1901.

Observation of long-lived neutral K-mesons.

B. L. Ioffe, L. B. Okun, A. P. Rudik, ZhEtF 32 (1957) 396 [JEtP 5 (1957) 328];

L. D. Landau, ZhETF 32 (1957) 405 [JETP 5 (1957) 336];

T. D. Lee, C. N. Yang, R. Oehme, Phys. Rev. 106 (1957) 340.

An analysis of the situation with K_1^0 and K_2^0 taking into account nonconservation of C - and P-parities. K_1^0 and K_2^0 are regarded as states with $CP = +1$ and $CP = -1$, respectively.

L. B. Okun, B. Pontecorvo, ZhETF 32 (1957) 1587 [JETP 5 (1957) 1297].

A small $\mathrm{K}_1^0 - \mathrm{K}_2^0$ mass difference means that there are no transitions with $|\Delta S| = 2$.

L. B. Okun, in Proc. of 1960 Annual Int. Conf. on high-energy physics at Rochester (University of Rochester, 1960) p. 743.

Cutoff value of the order of 1 GeV is obtained by comparing the contribution of the loop in the second order in the weak interaction with the observed small $K_1^0 - K_2^0$ mass difference.

I. Yu. Kobzarev, L. B. Okun, ZhETF 39 (1960) 605 [JETP 12 (1961) 426].

Discussion of possible experiments for determining which is heavier, K_1^0 or K_2^0.

M. L. Good, Phys. Rev. 106 (1957) 591; 110 (1958) 550.

Description of oscillations of K^0 mesons in a medium.

F. Muller et al., Phys. Rev. Lett. 4 (1960) 418.

The first result of measuring the $\mathrm{K}_1^0 - \mathrm{K}_2^0$ mass difference.

C. Geweniger et al., Phys. Lett. 52B (1974) 108. One of the most accurate results for Δm_{LS}.

T. Day, Phys. Rev. 121 (1961) 1204.

Quantum-mechanical reduction of a packet at large distances, exemplified by a $K^0\overline{K}^0$ pair.
See also:
A. Einstein, B. Podolsky, N. Rosen, Phys. Rev. 47 (1935) 777.
G. Feinberg, Phys. Rev. 109 (1958) 1381;
Ya. B. Zeldovich, ZhETF 36 (1959) 1381 [JETP 9 (1959) 984].
The theory of regeneration $K_2^0 \to K_1^0$ on electrons.
W. R. Molzon et al., Phys. Rev. Lett., 41 (1978) 1213.
Experimental observation of the regeneration $K_2^0 e \to K_1^0 e$.

28.2.8. Violation of CP invariance

J. H. Christenson, J. W. Cronin, V. L. Fitch, R. Turlay, Phys. Rev. Lett., 13 (1964) 138.
The discovery of the decay $K_L^0 \to \pi^+\pi^-$.
CPT theorem and its application:
G. Gravert, G. Lders, G. Rollnik, Fortschr. der Phys. 7 (1959) 291.
W. Pauli, in: Niels Bohr and the development of physics, ed. W. Pauli (Pergamon, London, 1955).
L. Wolfenstein, Phys. Rev. Lett. 13 (1964) 562.
The model of superweak violation of CP invariance.
T. T. Wu, C. N. Yang, Phys. Rev. Lett. 13 (1964) 380.
J. S. Bell, J. Steinberger, in: Proc. Int. Conf. on elementary particles, Oxford, 1965 (Rutherford High Energy Lab., Chilton, 1966) p. 193.
A phenomenological analysis of CP violation in decays of K^0-mesons.
For reviews of CP violation see:
Review talks presented at the International Seminar on CP violation, Moscow, 1968, Usp. Fiz. Nauk 95 (1968) No. 3, 4.
L. B. Okun, C. Rubbia, in: Proc. Heidelberg Int. Conf. on elementary particles, ed. H. Filthut (North-Holland, Amsterdam, 1968) p. 299.
K. Kleinknecht, in: Proc. 17th Int. Conf. on high-energy physics, London, 1974 (Rutherford Lab., Chilton, Didcot, 1974) p. 3-23.
The upper bound on the neutron dipole moment:
W. B. Dress et al., Phys. Rev. D15 (1977) 9.
($d_n < e \cdot 3 \cdot 10^{-24}$ cm);
I. S. Altaryev et al., Pis'ma ZhETF 29 (1979) 794 [JETP Lett. 29 (1979) 730]. ($d_n < e \cdot 1.6 \cdot 10^{-24}$ cm).
E. P. Shabalin, Yad. Fiz. 28 (1978) 151 [Sov. J. Nucl. Phys. 28 (1978) 75]; preprint ITEP-87 (1979);
J. Ellis, M. K. Gaillard, Nucl. Phys. B150 (1979) 141.
Estimates of the neutron dipole moment in the six-quark model.
S. Weinberg, Phys. Rev. Lett. 37 (1976) 657;
A. A. Anselm, D. I. D'yakonov, Nucl. Phys. B145 (1978) 271.
Breaking of CP in a model with two quark doublets and two doublets of Higgs bosons.
A. A. Anselm, N. G. Ural'tsev, Yad. Fiz. 30 (1979) 465 [Sov. J. Nucl. Phys. 30 (1979) 240].
Spontaneous breaking of CP invariance in a model with three quark doublets and several multiplets of Higgs fields.
CP-odd gravitational moment of the proton:
I. Yu. Kobzarev, L. B. Okun, ZhEtF 43 (1962) 1904 [JETP 16 (1963) 1343];
T. Leitner, S. Okubo, Phys. Rev. 136 B (1964) 1542;
B. V. Vasilyev, Pis'ma ZhETF 9 (1969) 299 [JETP Lett. 9 (1969) 175].

28.2.9 Charmed quark prior to the discovery of the J/ψ meson

A remark stating that the symmetry between leptons and quarks requires the existence of a fourth quark appeared in the paper which introduced three quarks:
M. Gell-Mann, Phys. Lett. 8 (1964) 214.

See also:
Y. Katayama, K. Matumoto, S. Tanaka, E. Yamada, Progr. Theor. Phys. 28 (1962) 675;
Z. Maki, M. Nakagawa, S. Sakata, Progr. Theor. Phys. 28 (1962) 870.

These papers discuss an extended Sakata model with a fourth fundamental baryon.

Later the four-quark model was discussed by:
Y. Hara, Phys. Rev. B134 (1964) 701,
D. Amati, H. Bacry, J. Nuyts, J. Prentki, Phys. Lett. 11 (1964) 190.

The term "charm" was introduced in:
J. D. Bjorken, S. L. Glashow, Phys. Lett. 11 (1964) 255.

Classification of SU(4) multiplets of mesons and baryons:
V. V. Vladimirsky, preprints ITEP, 1964, no. 262 and 299; 1965, no. 353.

A proposal to search for charmed (in the old terminology, supercharged) particles by looking for multilepton events in neutrino experiments:
L. B. Okun, Phys. Lett. 12 (1964) 250.
S. L. Glashow, J. Iliopoulos, L. Maiani, Phys. Rev. D2 (1970) 1285.

Weak interaction of the (then hypothetical) c-quark and SU(4) symmetry of the strong interaction are used to explain the absence, in experiment, of weak strangeness-changing neutral currents.
(The problem of strange neutral currents became especially acute after the publication of the paper:
B. L. Ioffe, E. P. Shabalin, Yad. Fiz. 6 (1967) 828 [Sov. J. Nucl. Phys. 6 (1968) 603],
which demonstrated that the three-quark model predicts a too high value of the mass difference of the K^0_L and K^0_S mesons, as well as a too high decay rate for $K^0_L \to \mu^+\mu^-$).
Further discussion of this problem:
A. I. Vainshtein, I. B. Khriplovich, Pis'ma ZhETF 18 (1973) 141 [JETP Lett. 18 (1973) 83];
M. K. Gaillard, B. W. Lee, Phys. Rev. D10 (1974) 897;
A. I. Vainshtein, V. I. Zakharov, V. A. Novikov, M. A. Shifman, Yad. Fiz. 23 (1976) 1024 [Sov. J. Nucl. Phys. 23 (1976) 540].

28.2.10 Charmed particles after the discovery of the J/ψ meson
J. J. Aubert et al., Phys. Rev. Lett. 33 (1974) 1404.

An announcement of the discovery of the J -meson by Ting's group.
J. E. Augustin et al., Phys. Rev. Lett., 33 (1974) 1406.

An announcement of the discovery of the ψ-meson by Richter's group.
B. Richter, S. Ting, Nobel Lectures, December 1976, in: Les Prix Nobl en 1976, Stockholm, 1977.
J. Ellis, M. K. Gaillard, D. V. Nanopoulos, Nucl. Phys. B100 (1976) 313;
N. Cabibbo, L. Maiani, Phys. Lett. 73B (1978) 418.
M. B. Voloshin, V. I. Zakharov, L. B. Okun, Pis'ma ZhETF 21 (1975) 403 ['JETP Lett. 21 (1975) 183]; Yad. Fiz. 22 (1975) 166 [Sov. J. Nucl. Phys. 22 (1975) 81];
M. B. Einhorn, C. Quigg, Phys. Rev. D12 (1975) 2015.

Quark graphs and sextet enhancement for non-leptonic decays of charmed particles.
G. Goldhaber et al., Phys. Rev. Lett. 37 (1976) 255.
I. Peruzzi et al., Phys. Rev. Lett. 37 (1976) 569.

The discovery of the D-mesons.
I. Peruzzi et al., Phys Rev. Lett. 39 (1977) 1301.

Measurement of $B\left(\mathrm{D}^0 \to \ \mathrm{K}^-\pi^+\right), B\left(\mathrm{D}^+ \to \overline{\mathrm{K}}^0\pi^+\right)$, and other partial widths of D-mesons.

28.2.11. Decays of the τ-lepton

First experimental evidence of the existence of the τ lepton was obtained at SLAC:
M. L. Perl et al., Phys. Rev. Lett. 35 (1975) 1489;
M. L. Perl et al., Phys. Lett. 63B (1976) 466.

Confirmation of the existence of the τ-lepton:
J. Burmester et al., Phys. Lett. 68B (1977) 297, 301;
R. Brandelik et al., Phys. Lett. 70B (1977) 125.

Summary of experimental data on the τ-lepton:
G. J. Feldman, preprint SLAC-PUB-224 (October 1978); Proc. of the 19th Int. Conf. on high energy physics, 1978, Tokyo, Japan, p. 777.

Theoretical papers:
Y. S. Tsai, Phys. Rev. D4 (1971) 2821; Relation between the decay width of $\tau \to \nu + 2n\pi$ and the annihilation $e^+e^- \to 2n\pi$.
Ya. I. Azimov, L. L. Frankfurt, V. A. Khoze, Usp. Fiz. Nauk 124 (1978) 459 [Uspekhi 21 (1978) 225].

28.2.12. Properties of the b- and t-quarks

S. W. Herb et al., Phys. Rev. Lett 76B (1978) 243.

The discovery of the Υ-meson in the spectrum of dimuons in the reaction p+ nucleus $\to \mu^+\mu^- + \mathrm{X}$.

Ch. Berger et al., Phys. Lett. 76B (1978) 243;
C. W. Darden et al., Phys. Lett. 76B (1978) 246.

Observation of the Υ-meson in colliding e^+e^-beams.
M. Kobayashi, K. Maskawa, Progr. Theor. Phys. 49 (1973) 652.

The general form of the matrix of left-handed charged currents in the six-quark model.
M. K. Gaillard, D. V. Nanopoulos, S. Rudaz, Nucl. Phys. B131 (1977) 285;
R. E. Shrock, L. L. Wang, Phys. Rev. Lett. 41 (1978) 1692.

Phenomenological analysis of the experimental limits for the angles in the Kobayashi-Maskawa matrix.
J. Ellis, M. K. Gaillard, D. V. Nanopoulos, Nucl. Phys. B109 (1976) 213.

An analysis of the effects of CP-violation in the framework of the six-quark model.
D. Cuffs et al., Phys. Rev. Lett. 41 (1978) 363;
R. Vidal et al., Phys. Lett. 77B (1978) 344.

A search for long-lived b-hadrons, with negative result.

5.28.3 28.3. Neutrino reactions

28.3.1. Neutrino-nucleon interactions. Charged currents
C. L. Cowen, H. W. Cruse, F. B. Harrison, A. D. McGuire, F. Reines, Science 124 (1956) 103.
The first measurement of the cross section for the reaction $\bar{\nu}\mathrm{p} \to \mathrm{e}^+\mathrm{n}$ (with reactor antineutrinos).
G. Danby, J. M. Gaillard, K. Goulianos, L. M. Lederman, M. Mistry, M. Schwartz, J. Steinberger, Phys. Rev. Lett. 9 (1962) 36.

The discovery of the muon antineutrino.
J. D. Bjorken, Phys. Rev. 179 (1969) 1547.

The prediction of scaling in deep-inelastic lepton-nucleon interactions.
E. D. Bloom et al., Phys. Rev. Lett. 23 (1969) 930;
M. Breidenbach et al., Phys. Rev. Lett. 23 (1969) 935.
The discovery of scaling in deep-inelastic ep scattering.
The parton model was suggested by R. P. Feynman in 1969 in an unpublished "paper. See:
J. D. Bjorken, E. A. Paschos, Phys. Rev. 185 (1969) 1975;
R. P. Feynman, Photon-hadron interactions (Benjamin, 1972);
R. P. Feynman, in Neutrino 1974, ed. C. Baltay (American Inst. of Phys., New York, 1974) p. 299.
Review papers on high-energy neutrino physics:
C. H. Llewellyn Smith, Phys. Reports 3 (1972) 261;
B. C. Barish. Phys. Reports 39 (1978) p. 279,
J. Steinberger, CERN preprint, Four Lectures presented at the Summer Institute, Cargse, 4-23 July, 1977.

28.3.2 Neutrino-nucleon interactions. Neutral currents

F. J. Hasert et al., Phys. Lett. B46 (1973) 138;
F. J. Hasert et al., Nucl. Phys. B73 (1974) 1.
The discovery of neutral currents in a neutrino experiment in the Gargamelle bubble chamber, at CERN.
A. Benvenuti et al., Phys. Rev. Lett. 32 (1974) 800;
B. Aubert et al., Phys. Rev. Lett. 32 (1974) 1454;
B. C. Barish et al., Phys. Rev. Lett. 34 (1975) 538.
Observation of neutral currents at the Batavia accelerator.
D. Cline et al., Phys. Rev. Lett. 37 (1976) 252, 648;
W. Lee et al., Phys. Rev. Lett. 37 (1976) 186;
H. H. Williams et al., in: Proceedings Topical Conference on neutrino physics at accelerators, Oxford, 1978.
M. Pohl et al., Phys. Lett. 72B (1978) 489.
Observation of neutrino elastic scattering on protons.
V. M. Shekhter, Usp. Fiz. Nauk 119 (1976) 593 [Uspekhi 19 (1976) 645].
A review of neutral currents (experiment and theory).
P. F. Ermolov, A. I. Mukhin, Usp. Fiz. Nauk 124 (1978) 385 [Uspekhi 21 (1978) 185].
A review of neutrino experiments.
M. Holder et al., Phys. Lett. 71B (1977) 222; 72B (1977) 254;
P. Wanderer et al., Phys. Rev. D17 (1978) 1679.
Experimental investigation of inclusive reactions caused by the neutral current at high energies, carried out at CERN and FNAL, respectively.
H. Kluttig et al., Phys. Lett., 77B (1977) 446;
W. Krenz et al., Nucl. Phys., B135 (1978) 45;
O. Erriques et al., Phys. Lett. 73B (1978) 350.
Observation of single pions produced by the neutral neutrino current.

28.3.3. Neutrino-electron interaction

F. Reines et al., Phys. Rev. Lett. 37 (1976) 315.
Observation of $\bar{\nu}_e$ e scattering for reactor anti-neutrinos.
F. T. Avignone III, Z. D. Greenwood, Phys. Rev. D16 (1977) 2383.
Reines' experimental data on $\bar{\nu}_e$ e scattering are re-analyzed.
F. J. Hasert et al., Phys. Lett. 46B (1973) 121.

Observation of the first ν_μe scattering event in the Gargamelle bubble chamber.
H. Faissner et al., Phys. Rev. Lett. 41 (1978) 213;
A. M. Cnops et al., Phys. Rev. Lett. 41 (1978) 357.

Measurement of the ν_μ e scattering cross section. The paper cites earlier publications on the subject.

28.3.4. Creation of a muon pair by neutrino in the Coulomb field of a nucleus

M. S. Marinov, Yu. P. Nikitin, Yu. P. Orevkov, E. P. Shabalin, Yad. Fiz. 3 (1966) 678 [Sov. J. Nucl. Phys. 3 (1966) 497]; Erratum: 15 (1972) 1086
Numerical calculations for $E = 50$GeV.
A. E. Asratyan, M. A. Kubantsev, Yad. Fiz. 25 (1977) 1051 [Sov. J. Nucl. Phys. 25 (1977) 558].
It is shown that detection of the process $\nu Z \to \nu\mu\mu Z$ demands an increase in statistics by two orders of magnitude.

28.3.5. Electron-nucleon interactions

Ya B. Zeldovich, ZhETF 36 (1959) 964 [JETP 9 (1959) 682].
A theoretical analysis of the P-odd electron-nucleon interaction. Prediction of the effect of weak optical activity of atoms. See also:
S. A. Bludman, Nuovo Cim. 9 (1958) 433;
V. N. Baier, I. B. Khriplovich, ZhETF 39 (1960) 1374 [JETP 12 (1960) 959].
M. Bouchiat, C. Bouchiat, Phys. Lett. 48 (1974) 111.
I. B. Khriplovich, Pis'ma ZhETF 20 (1974) 686 [JETP Lett. 20 (1974) 315].
Proposal of experiments to detect optical activity of heavy atoms. In particular, the second of the cited papers suggests an experiment to measure the rotation of the plane of polarization of light in thallium and bismuth vapor.

Theoretical reviews on parity non-conservation in atomic physics.
V. A. Alekseyev, B. Ya. Zeldovich, I. I. Sobelman, Usp. Fiz. Nauk 118 (1976) 385 [Uspekhi 19 (1976) 207];
A. N. Moskalev, R. M. Ryndin, I. B. Khriplovich, Usp. Fiz. Nauk 118 (1976) 409 [Uspekhi 19 (1976) 220].
L. M. Barkov, M. S. Zolotorev, Pis'ma ZhETF 27 (1978) 379; 28 (1978) 544 [JETP Lett. 27 (1978) 357; 28 (1979) 503].
The angle of rotation of the polarization plane of light in bismuth vapor is measured.
P. E. Baird et al., Phys. Rev. Lett. 39 (1977) 798.
L. L. Lewis et al., Phys. Rev. Lett. 39 (1977) 795.

Experiments, respectively, in Seattle and Oxford that detected no rotation of the light polarization plane in Bi .
R. Conti et al., Phys. Rev. Lett. 42 (1978) 343.

Observation of optical activity in thallium.
C. Y. Prescott et al., Phys Lett. 77B (1978) 347.

Observation of parity non-conservation in inelastic scattering of polarized electrons by nucleons.
28.3.6. Phenomenological analysis of data on neutral currents
L. M. Sehgal, Phys. Lett. 71B (1977) 99;
P. Q. Hung, J. J. Sakurai, Phys. Lett. 72B (1977) 208;
L. F. Abbott, R. M. Barnett, Phys. Rev. Lett. 40 (1978) 1303; D. P. Sidhu, P. Langacker, Phys. Rev. Lett. 41 (1978) 732;
J. D. Bjorken, Phys. Rev. D18 (1978) 3239;

J. J. SakuraI, UCLA preprint (1978) TEP/27; Intern. Symp. on high-energy physics with polarized beams and polarized targets, ANL, October 25-28, 1978, 138;
R. M. Barnett, SLAC preprints, 1978, PUB-2131, PUB-2111; Proceedings of the Conference Neutrino-78, Purdue Univ., 1978, ed. E. C. Fowler, p. 699.

Coupling constants of the vector and axial neutral currents are obtained from experimental data, without using the standard model of the electroweak interaction.

5.28.4 28.4. Weak interactions at high energies

28.4.1. Four-fermion interaction and the unitarity limit
W. Heisenberg, Z. Phys. 101. (1936) 533.

It is shown that the weak four-fermion interaction increases with particle energy and becomes strong at energies of the order of 10^3GeV.
L. D. Landau, *ZhETF*10 (1940) 718 (see Collected Papers of L. D. Landau, p. 274. Pergamon Press, 1965).

Introduction of the unitarity limit, in particular, in the case of vector bosons.
D. I. Blokhintsev, Usp. Fiz. Nauk 62 (1957) 49; ZhETF 35 (1958) 53; Nuovo Cim. 9 (1958) 925.
A discussion of the role of weak interactions in electromagnetic processes at energies of the order of 10^3GeV.
B. N. Valuyev, ZhETF 36 (1959) 1578 [JETP 9 (1959) 1121];
B. L. Ioffe, *ZhETF*38 (1960) 1608 [JETP 11 (1960) 1158];
M. A. Markov, Proc. Intern. Conf. on high energy phys. at Rochester, Rochester, 1960 (Interscience) p. 578;
E. P. Shabalin, Yad. Fiz. 6 (1967) 547 [Sov. J. Nucl. Phys. 6 (1967) 399].

A discussion of higher-order effects in weak interactions in $\mu \to e\gamma$ and $\mu \to 3e$ processes, and in the equality of constants of β - and μ-decays.
B. L. Ioffe, L. B. Okun, A. P. Rudik, ZhETF 47 (1964) 1905 [JETP 20 (1965) 1281];
A. D. Dolgov, V. I. Zakharov, L. B. Okun, Yad. Fiz. 14 (1971) 1044; 1247 [Sov. J. Nucl. Phys. 14 (1971) 585, 695];
A. D. Dolgov, L. B. Okun, V. I. Zakharov, Nucl. Phys. B37 (1972) 493, B41 (1972) 197; Phys. Lett. 37B (1972) 298.
A theoretical discussion of weak interactions in colliding e^+e^-beams in the range of the unitarity limit.
See a similar analysis for ν e interactions in:
T. Appelquist, J. D. Bjorken, Phys. Rev. D4 (1971) 3726.

The dispersion theory of weak processes above the unitarity limit was initiated in:
I. Ya. Pomeranchuk, Yad. Fiz. 11 (1970) 852. [Sov. J. Nucl. Phys. 11 (1970) 477].

Further progress see in:
A. D. Dolgov, V. N. Gribov, L. B. Okun, V. I. Zakharov, Nucl. Phys. B59 (1973) 611.

28.4.2. Gauge symmetry

Non-abelian gauge symmetry was introduced in:
C. N. Yang, R. L. Mills, Phys. Rev. 96 (1954) 191.

Further important papers:
R. Utiyama, Phys. Rev. 101 (1956) 1597;
J. J. Sakurai, Ann. of Phys. 11 (1960) 1;
S. L. Glashow, M. Gell-Mann, Ann. of Phys. 15 (1961) 437;
Y. Ne'eman, Nucl. Phys. 26 (1961) 222;

A. Salam, J. C. Ward, Nuovo Cim. 11 (1959) 568; 19 (1961) 165;
J. Schwinger, Phys. Rev. 125 (1962) 397, 1043; 127 (196) 324;
T. W. B. Kibble, J. Math. Phys. 2 (1961) 212.

A modern presentation of gauge field theory, as well as a brief discussion of the history of the problem can be found in the following monographs and review papers:
A. A. Slavnov, L. D. Fadde'ev, Vvedeniye v kvantovuyu teoriyu kalibrovochnikh polei (Introduction to the quantum theory of gauge fields) (Nauka, Moscow, 1978) (in Russian);
V. N. Popov, Kontinual 'niye integraly v kvantovoi teorii polya i statisticheskoi fizike (Path integrals in quantum field theory and statistical physics) (Atomizdat, Moscow, 1976) (in Russian);
S. Coleman, in Laws of hadronic matter, Proc. of the 11th Course, Ettore Majorana Intern. School, ed. A. Zichichi (Academic Press, 1975);
J. Bernstein, Rev. Mod. Phys. 46 (1974) 7;
E. S. Abers, B. W. Lee, Phys. Reports C9 (1973) 1.

The presentation of gauge symmetry in this book is in the spirit of the paper:
A. I. Vainshtein, I. B. Khriplovich, Yad. Fiz. 13 (1971) 199 [Sov. J. Nucl. Phys. 13 (1971) 111].

28.4.3. Spontaneous breaking of gauge symmetry

Higgs effect:
P. W. Higgs, Phys. Rev. Lett. 12 (1964) 132; 13 (1964) 508;
P. W. Higgs, Phys. Rev. 145 (1966) 1156;
F. Englert, R. Brout, Phys. Rev. Lett. 13 (1964) 321;
G. S. Guralnik, C. R. Hagen, T. W. B. Kibble, Phys. Rev. Lett. 13 (1964) 585;
T. W. B. Kibble, Phys. Rev. 155 (1967) 1554.

Non-relativistic analogue of the Higgs effect: non-vanishing photon mass in a superconductor:
V. L. Ginzburg, L. D. Landau, ZhETF 20 (1950) 1064 [Collected Papers of L. D. Landau, p. 546. (Pergamon Press, 1965)].
G. W. ' Hooft, Nucl. Phys. B79 (1974) 276;
A. M. Polyakov, Pis'ma ZhETF 20 (1974) 430 [JETP Lett. 20 (1974) 194].

The magnetic monopole as a classical solution in a theory with spontaneously broken local SU(2) symmetry.
E. B. Bogomolniy, M. S. Marinov, Yad. Fiz. 23 (1976) 676 [Sov. J. Nucl. Phys. 23 (1976) 355].
Calculations of the monopole mass.

28.4.4. Standard model of the electroweak interaction

S. L. Glashow, Nucl. Phys. 22 (1961) 579.
S. Weinberg, Phys. Rev. Lett. 19 (1967) 1264;
A. Salam, in Elementary particle theory, ed. N. Svartholm (Almquist and Wiksell, Stockholm, 1968) 367.

Other papers which discussed the unification of the weak and electromagnetic interactions:
A. Salam, J. C. Ward, Phys. Lett. 13 (1964) 168; Nuovo Cim., 11 (1959) 568.
J. L. Lopes, Nucl. Phys. 8 (1958) 234.
J. Schwinger, Ann. of Phys. 2 (1957) 407.

The history of the problem:
M. Veltman, in Proc. of the 6th Int. Symp. on electron and photon interactions at high energies, Bonn, August 1973, ed. H. Rollnik and W. Pfeil (North-Holland, Amsterdam, 1974)

p. 429.
G. W.'t Hooft, Nucl. Phys. B33 (1971) 173; B35 (1971) 167.
Proof of renormalizability of the standard model.
J. D. Bjorken, C. H. Llewellyn Smith, Phys. Rev. D7 (1973) 887.
Classification of various generalizations of the standard model.
S. L. Glashow, S. Weinberg, Phys. Rev. D15 (1977) 1958.
Introduction of the concept of natural conservation of quantum numbers for the generalized standard model.
A. Sirlin, Rev. Mod. Phys. 50 (1978) 573.
Calculation of corrections of the order of αG to amplitudes of weak decays in the standard model.

28.4.5. Production and decay of the W - and Z-bosons

Early calculations of the production of W-bosons:
L. B. Okun, Yad. Fiz. 3 (1966) 590 [Sov. J. Nucl. Phys. 3 (1968) 426];
Y. Yamaguchi, Nuovo Cim. 43 (1966) 193.
Calculations of the production of W - and Z -bosons in the framework of the parton model:
R. Palmer, E. Paschos, N. Samios, L. L. Wang, Phys. Rev. D14 (1976) 118;
R. F. Peierls, T. L. Trueman, L. L. Wang, Phys. Rev. D16 (1977) 1397;
L. B. Okun, M. B. Voloshin, Nucl. Phys. B120 (1977) 459;
C. Quigg, Rev. Mod. Phys. 49 (1977) 297;
J. D. Bjorken, in Proc. of the Int. Symp. on lepton and photon interactions, Hamburg, 1977.
28.4.6. Future facilities designed to search for the W - and Z-bosons
A. Astbury et al., CERN report, 1978, CERN/SPSC/78-06, SPSC/P92.
A proposed detector for a pp collider with center-of-mass energy of 540 GeV .
Collected papers: The acceleration-storage complex UNK based on the IHEP accelerator, Proc. of the 21st Session of the IHEP coordination council, May 1976 (Serpukhov, 1977) (in Russian).
Proc. of the LEP Summer Study, CERN 79-01, vol. 1, 2, February 14, 1979.
A detailed analysis of physical and technical problems connected with the project of the electron-positron colliding beam facility 2×80GeV.
ISABELLE, A proton-proton colliding beam facility, BNL report 50648 (1977).
DUMAND Project:
V. S. Berezinsky, G. T. Zatsepin, Usp. Fiz. Nauk 122 (1977) 3 [Uspekhi 20 (1977) 361].
A review of the DUMAND project.
V. S. Berezinsky, A. Z. Gazizov, Pis'ma ZhETF 25 (1977) 276 [JETP Lett. 25 (1977) 254].
Theoretical treatment of the reaction $\bar{\nu}e^- \to W^-$in the DUMAND facility.

28.4.7. Properties of Higgs bosons

Early phenomenological discussions of H -bosons as physical particles:
E. B. Bogomol'niy, Yad. Fiz. 18 (1973) 574; 20 (1974) 984 [Sov. J. Nucl. Phys. 18 (1973) 297; 20 (1975) 522];
L. Resnik, M. K. Sundaresan, P. J. S. Watson, Phys. Rev. D8 (1973) 172;
J. Ellis, M. K. Gaillard, D. V. Nanopoulos, Nucl. Phys. B106 (1976) 292.
The lower bound on the H -boson mass:
A. D. Linde, Pis'ma ZhETF 23 (1976) 73 [JETP Lett. 23 (1976) 64];
A. D. Linde, Phys. Lett. 70B (1977) 306;
S. Weinberg, Phys. Rev. Lett. 36 (1976) 294;
P. H. Frampton, Phys. Rev. Lett. 37 (1976) 1378.

The theory of unstable vacuum:
M. B. Voloshin, I. Yu. Kobzarev, L. B. Okun, Yad. Fiz. 20 (1974) 1229 [Sov. J. Nucl. Phys. 20 (1975) 644];
P. H. Frampton, Phys. Rev. D15 (1977) 2922;
S. Coleman, Phys. Rev. D15 (1977) 2929; D16 (1977) 1248 (E);
C. Callan, S. Coleman, Phys. Rev. D16 (1977) 1762.

The role of H -bosons at high energies:
E. B. Bogomol'niy, V. I. Zakharov, L. B. Okun, in: Elementarniye chastitsi (Pervaya shkola fiziki ITEP) [Elementary particles, The First ITEP Physics School] (Atomizdat, Moscow, 1973) No. 1, p. 49 (in Russian);
D. A. Dicus, V. S. Mathur, Phys. Rev. D7 (1973) 311;
B. W. Lee, C. Quigg, H. Thacker, Phys. Rev. Lett. 38 (1977) 883.
M. Veltman, Acta Phys. Polonica B8 (1977) 475; Phys. Lett., 70B (1977) 253.

It is shown that the strong interaction in the Higgs sector gives negligibly small corrections (of the order of $m_{\mathrm{f}}^2/m_{\mathrm{W}}^2$, where m_{f} is the fermion mass) to the effective four-fermion Lagrangian at low energies.
S. Weinberg, Phys. Rev. D19 (1979) 1277.

The relation $m_{\mathrm{W}}^2 = m_{\mathrm{Z}}^2 \cos^2\theta_{\mathrm{W}}$ in the case of strong interactions in the Higgs sector.

Interaction of H -bosons with gluons:
F. Wilczek, Phys. Rev. Lett. 39 (1977) 1304.

This paper also discusses the decays $\Upsilon \to \mathbf{H} + \gamma$.
M. A. Shifman, A. I. Vainshtein, V. I. Zakharov, Phys. Lett. 78B (1978) 443.

This paper also gives a solution of the problem of the Higgs charge of the nucleon.
H. M. Georgi, S. L. Glashow, M. E. Machacek, D. V. Nanopoulos, Phys. Rev. Lett. 40 (1978) 692.
Parton calculations of H -boson production by two gluons in pp collisions.
Interaction of H -bosons with Z - and W -bosons:
B. L. Ioffe, V. A. Khoze, Problems of elementary particle and atomic nucleus physics, Particles and Nucleus 9 (1978) 178 (in Russian);
J. Ellis, M. K. Gaillard, D. V. Nanopoulos Nucl. Phys. B106 (1976) 292;
S. L. Glashow, D. V. Nanopoulos, A. Yildiz, Phys. Rev. 18 (1978) 1724.

Calculations for the process $\mathrm{e^+e^-} \to \mathrm{Z} + \mathrm{H}$. The last paper also calculates the cross section of the associated production of $\mathrm{W} + \mathrm{H}$ and $\mathrm{Z} + \mathrm{H}$ in pp and $\overline{\mathrm{p}}\mathrm{p}$ collisions.

Schemes with two or more doublets of H -bosons.
A. I. Vainshtein, M. B. Voloshin, V. I. Zakharov, M. A. Shifman, Yad. Fiz. 30 (1979) 1368. [Sov. J. Nucl. Phys. 30 (1979) 711]
This paper treats $\mathrm{H} \to 2\gamma$ decays.
F. Wilczek, Phys. Rev. Lett. 39 (1977) 1304; E. Golowich, T. C. Yang, Phys. Lett. 80B (1979) 245.
A discussion of the properties of light H -bosons, including charged ones.
Reviews on H-bosons:
M. K. Gaillard, Comments Nucl. Part. Phys. 8 (1978) 31;
S. Weinberg, Physics Today, 1977, April, p. 42;
A. I. Vainshtein, V. I. Zakharov, M. A. Shifman, Usp. Fiz. Nauk 131 (1980) 537 [Uspekhi 23 (1980)].

Composite Higgs bosons and the model of technicolor:
L. Susskind, reprint SLAC PUB 2142 (June 1978);
S. Dimopoulos, L. Susskind, preprint ITP-626 (Jan. 1979); Nucl. Phys. B155 (1979) 237.
See also:
S. Weinberg, Phys. Rev. D13 (1976) 247;

A. A. Migdal, A. M. Polyakov, ZhETF 51 (1966) 135 [JETP 24 (1967) 91];
J. Schwinger, Phys. Rev. 125 (1962) 397.

5.28.5 28.5. Models of grand and super unification

28.5.1. Model based on the group $\boldsymbol{SU}(\mathbf{4}) \times \boldsymbol{SU}(\mathbf{2}) \times \boldsymbol{SU}(\mathbf{2})$
J. C. Pati, A. Salam, Phys. Rev. D8 (1973) 1240.

28.5.2. Model based on the group SU(5)

H. Georgi, S. L. Glashow, Phys. Rev. Lett. 32 (1974) 438;
H. Georgi, H. R. Quinn, S. Weinberg, Phys. Rev. Lett. 33 (1974) 451;
A. J. Buras, J. Ellis, M. K. Gaillard, D. V. Nanopoulos, Nucl. Phys. B135 (1978) 66.
D. V. Nanopoulos, CERN preprint (1978) TH 2534.
A brief review of the SU(5) model.
C. Jarlskog, F. J. Yndurain, Nucl. Phys. B149 (1979) 29.
T. J. Goldman, D. A. Ross, Phys. Lett. 84B (1979) 208.
A detailed estimate of the lifetime and decay channels of the proton.
E. Gildener, Phys. Rev. D14 (1976) 1667;
K. T. Mahanthappa, D. G. Unger, Phys. Lett. 78B (1978) 604;
S. Weinberg, Phys. Lett. 82B (1979) 387.
The problem of hierarchy of vacuum-expectation values in grand synthesis models.

28.5.3. Model based on the group SO(10)

H. Fritzch, P. Minkowski, Ann. of Phys. 93 (1975) 193;
M. S. Chanowitz, J. Ellis, M. K. Gaillard, Nucl. Phys. B128 (1977) 506;
H. Georgi, D. V. Nanopoulos, Nucl. Phys. B155 (1979) 152.

28.5.4. Models based on exceptional groups

F. Grsey, in: Kyoto Symp. on mathematical problems in theoretical physics, ed. H. Araki (Springer, 1975).
M. Gnaydin, M. Grsey, Phys. Rev. D9 (1974) 3387.
On the role of exceptional groups in the physics of elementary particles.
F. Grsey, P. Sikivie, Phys. Rev. Lett. 36 (1976) 775.
P. Ramond, Nucl. Phys. B126 (1977) 509.
An analysis of representations of the group E_7.
Y. Achiman, B. Stech, Phys. Lett. 77B (1978) 389.
A model based on the group E_6.
V. I. Ogievetsky, V. Yu. Tseitlin, Yad. Fiz. 28 (1978) 1616 [Sov. J. Nucl. Phys. 28 (1978) 832].
Models based on exceptional groups, with the stable proton.
D. I. Dyakonov, Yad. Fiz. 26 (1977) 845 [Sov. J. Nucl. Phys. 26 (1977) 443].
A formula for the Weinberg angle in a unified theory with an arbitrary symmetry group, and with the group E_7 in particular.
28.5.5. Models of simple unification
S. Weinberg, Phys. Rev. D5 (1972) 1962;
J. D. Bjorken, K. Lane, Proc. Int. Conf. Neutrino '77, Moscow (Nauka, Moscow, 1978) vol. 2, p. 412;
H. Fritzsch, preprint CERN (1977) TH 2309, Invited talk at the XII Recontre de Moriond.

28.5.6. Reviews of grand unification models
M. Gell-Mann, P. Ramond, R. Slansky, Rev. Mod. Phys. 50 (1978) 721.
A review with a detailed analysis of representations of exceptional groups and of a number of versions of unified gauge theories.
H. Harari, Phys. Reports 42 (1978) 235.
A review of various schemes of the grand synthesis.
28.5.7. Superunification
Yu. A. Gol'fand, E. P. Likhtman, Pis'ma ZhETF 13 (1971) 452 [JETP Lett. 13 (1971) 323];
J. Gervais, B. Sakita, Nucl. Phys. B34 (1971) 632;
D. V. Volkov, V. P. Akulov, Pis'ma ZhETF 16 (1972) 621 [JETP Lett. 16 (1972) 438];
J. Wess, B. Zumino, Nucl. Phys. B70 (1974) 39. First papers on supersymmetry.
D. Z. Freeman, P. van Nieuwenhuizen, S. Ferrara, Phys. Rev. D13 (1976) 3214;
S. Deser, B. Zumino, Phys. Lett. 62B (1976) 335.
First papers on supergravity.
S. Ferrara, P. van Nieuwenhuizen, Phys. Rev. Lett. 37 (1976) 1669.
First paper on extended supergravity.
A. Salam, J. Strathdee, Fortschr. Phys. 26 (1978) 57;
P. Fayet, S. Ferrara, Phys. Reports C32 (1977) 249;
A. A. Slavnov, Usp. Fiz. Nauk 124 (1978) 487 [Uspekhi 21 (1978) 240];
V. I. Ogiyevetsky, L. Mezinchesku, Usp. Fiz. Nauk 117 (1975) 637 [Uspekhi 18 (1975) 960];
D. Z. Freedman, P. van Nieuwenhuizen, Scientific American 238 (1978) no. 2, 126. Review papers.

5.28.6 28.6. Particles and the universe

28.6.1. The general theory of relativity and the theory of the hot universe
A. Einstein, Ann. der Phys. 49 (1916) 769.
The general theory of relativity.
A. A. Friedmann, Z. Phys. 11 (1922) 377.
A. A. Friedmann, ZhRFKhO 56 (1924) 59 (Reprinted in Usp. Fiz. Nauk 80 (1963) 439 [Uspekhi 6 (1964) 475].
The theory of the non-stationary universe.
E. P. Hubble, Proc. Nat. Acad. Sci. USA 15 (1929) 168. Linear relation between radial velocities of galaxies and distances to these galaxies. According to the initial Hubble estimate, the proportionality coefficient $H = 513 \pm 60$ km/s $\cdot 10^6$ parsec.
G. Gamov, Phys. Rev. 70 (1946) 572.
The hypothesis of the hot universe and an estimate of the expected temperature of the cosmic microwave radiation background.
A. A. Penzias, R. W. Wilson, Astrophys. J. 142 (1965) 419.
The discovery of the cosmic microwave radiation background.
Monographs and reviews on cosmology:
S. Weinberg, The first three minutes, A modern view of the origin of the universe (Basic Books, Inc, New York, 1977);
Ya. B. Zeldovich, Usp. Fiz. Nauk, 89 (1966) 647 [Uspekhi 9 (1967) 602]. Popular presentation of the theory of the hot universe.
Ya. B. Zeldovich, D. I. Novikov, Relativistic astrophysics VII, Structure and evolution of the universe (Chicago Univ. Press, 1980) translated from the Russian.
S. Weinberg, Gravitation and cosmology (Wiley, 1972).
Confrontation of cosmological theories with observational data, Symposium No. 63 IAU (Copernicus Symposium II), held in Cracow, Poland, 10-12 September 1973, ed. by M. Longair

(Reidel, Dordrecht, Holland, 1974).

28.6.2. The hot universe and leptons

S. S. Gershtein, Ya. B. Zeldovich, Pis'ma ZhETF 4 (1966) 174 [JETP Lett. 4 (1966) 120];
R. Cowsik, J. McClelland, Phys. Rev. Lett. 29 (1972) 669;
A. S. Szalay, G. Marx, Astronomy and Astrophysics 49 (1976) 437.

Cosmological bounds on the mass of the neutrino.

M. I. Vysotsky, A. D. Dolgov, Ya. B. Zeldovich, Pis'ma ZhEtF 26 (1977) 200 [JETP Lett. 26 (1977) 188];
A. D. Dolgov, M. I. Vysotsky, Ya. B. Zeldovich, in: Neutrino '77. Proc. of the Int. Conf. on neutrino physics and neutrino astrophysics (Nauka, Moscow) vol. 1, p. 42.
B. W. Lee, S. Weinberg, Phys. Rev. Lett. 39 (1977) 165;
P. Hut, Phys. Lett. 69B (1977) 85;
K. Sato, M. Kobayashi, Progr. Theor. Phys. 58 (1977) 1775;
J. E. Gunn, B. W. Lee, I. Lerche, D. N. Schramm, G. Steigman, Astrophys. J. 223 (1977) 1015.
Cosmological bounds on masses of heavy neutral leptons (both stable and unstable). See also:
D. A. Dicus, E. N. Kolb, V. L. Teplitz, Phys. Rev. Lett. 39 (1977) 168; Astrophys. J., 221 (1978) 327;
D. A. Dicus, E. N. Kolb, V. L. Teplitz, R. V. Wagoner, Phys. Rev. D17 (1978) 1529.
V. F. Shvartsman, Pis'ma ZhETF, 9 (1969) 315 [JETP Lett. 9 (1969) 184].
G. Steigman, D. N. Schramm, J. E. Gunn, Phys. Lett. 66B (1977) 202.

Cosmological restriction on the number of different types of neutrinos derived from the data on the primordial helium abundance, on the basis of the theory of the primordial nucleosynthesis.

Leptons and the hot universe (review paper):
D. N. Schramm, preprint Fermi Institute, 78-25 (1978).

Gravitational interaction of right-handed neutrinos:
M. Gell-Mann, in: La thorie quantique de champs, Deuzime Conseil de Physique, ed. R. Stoops (Bruxelles, 1962) p. 135;
I. Yu. Kobzarev, L. B. Okun, ZhETF 43 (1962) 1904 [JETP 16 (1963) 1343]. See also collected essays dedicated to I. E. Tamm: Problemi teoreticheskoi fiziki (Problems of theoretical physics) (Nauka, Moscow, 1972) p. 219 (in Russian).

Neutrinos and astrophysics:
M. A. Ruderman, Reports on Progress in Physics, 1965, p. 411.

28.6.3. The hot universe and quarks

Ya. B. Zeldovich, L. B. Okun, S. B. Pikelner, Usp. Fiz. Nauk 87 (1965) 115 [Uspekhi 8 (1966) 702].
Estimates of the concentration of relic quarks.
A. De Rujula, R. C. Giles, R. L. Jaffe, Phys. Rev. D17 (1978) 285.

A hypothesis of the existence of free fractionally charged quarks with large mass and large radius.

A review of the search for free fractionally charged quarks:
L. G. Landsberg, Usp. Fiz. Nauk 109 (1973) 695 [Uspekhi 16 (1973) 251].
D. D. Ogorodnikov, I. M. Samoilov, A. M. Solntsev, ZhETF 72 (1977) 1633 [JETP 45 (1977) 857].
Mass-spectroscopic search: less than one quark per 10^{27} nucleons.
G. S. La Rue, W. M. Fairbank, A. F. Hebard, Phys. Rev. Lett. 38 (1977) 1011 (Erratum: p.

1019);
G. S. La Rue, W. M. Fairbank, J. D. Phillips, Phys. Rev. Lett. 42 (1979) 142.
Reports of the detection of fractionally charged particles in small niobium spheres.
G. M. Kukavadze, L. Ya. Memelova, L. Ya. Suvorov, ZhETF 49 (1965) 389 [JETP 22 (1966) 272];
T. Alvger, R. A. Nauman, Phys. Lett. 24B (1967) 647;
R. A. Miller, L. W. Alwarez, W. R. Holley, E. J. Stephenson, Science 196 (1977) 521;
R. F. Smith, J. R. J. Bennet, Nucl. Phys. B149 (1979) 525.
Mass-spectrometric search for anomalously heavy hydrogen (integer-charge quarks).

28.6.4. Cosmology and spontaneous symmetry breaking

T. D. Lee, Phys. Rev. D8 (1973) 1226.
T. D. Lee, G. C. Wick, Phys. Rev. D9 (1974) 2291.
A model of spontaneous breaking of CP invariance.
Ya. B. Zeldovich, I. Yu. Kobzarev, L. B. Okun, ZhEtF 67 (1974) 3 [JETP 40 (1975) 1]; Phys. Lett. 50B (1974) 340.
Spontaneous CP breaking and vacuum domains.
M. B. Voloshin, I. Yu. Kobzarev, L. B. Okun, Yad. Fiz. 20 (1974) 1229 [Sov. J. Nucl. Phys. 20 (1975) 644].
The theory of the unstable vacuum (further references in section 28.4.7 "Properties of the Higgs bosons").
D. A. Kirzhnits, Pis'ma ZhETF 15 (1972) 745 [JETP Lett. 15 (1972)];
D. A. Kirzhnits, A. D. Linde, Phys. Lett. 42B (1972) 471; A. D. Linde, Reports on Progress in Physics 42 (1979) 389.
Restoration of spontaneously broken symmetry in the hot universe.
I. Yu. Kobzarev, in: Elementarniye chastitsi, I. Shkola ITEF (Elementary particles, The First ITEP Physics School) (Atomizdat, Moscow, 1975) no. 3, p. 44.
Review lecture.

28.6.5. Astrophysics and photons

I. Yu. Kobzarev, L. B. Okun, Usp. Fiz. Nauk, 95 (1968) 131 [Uspekhi 11 (1968) 338];
A. S. Goldhaber, M. M. Nieto, Rev. Mod. Phys. 43 (1971) 277.
Reviews discussing the photon mass.
L. Davies, Jr., A. S. Goldhaber, M. M. Nieto, Phys. Rev. Lett. 35 (1975) 1402.
Restriction on the photon mass on the basis of the data on Jupiter's magnetic field: $1/m_\gamma \gtrsim 5 \cdot 10^{10}$ cm.
G. V. Chibisov, Usp. Fiz. Nauk 119 (1976) 551 [Uspekhi 119 (1976) 624].
Restriction on the photon mass on the basis of the data on intergalactic magnetic fields: $1/m_\gamma \gtrsim 10^{22}$ cm.
T. D. Lee, C. N. Yang, Phys. Rev. 98 (1955) 1501;
L. B. Okun, Yad. Fiz. 10 (1969) 358 [Sov. J. Nucl. Phys. 10 (1970) 206].
Geophysical and astrophysical restrictions on the possible properties of hypothetical baryonic, leptonic, and muonic photons, obtained, in particular, from the experiments:
R. V. Eötvös, D. Pekar, E. Fekete, Ann. der Phys. 68 (1922) 11;
R. H. Dicke, P. G. Roll, G. Krotkov, Ann. of Phys. 26 (1964) 442;
V. B. Braginsky, V. I. Panov, ZhETF 61 (1971) 873 [JETP 34 (1972) 463].
28.6.6. Possible non-conservation of the baryonic charge, and baryonic asymmetry of the universe
A. D. Sakharov, Pis'ma ZhETF 5 (1967) 32 [JETP Lett. 5 (1967) 24];

V. A. Kuzmin, Pis'ma ZhETF 12 (1970) 335 [JETP Lett. 12 (1970) 228].

The hypothesis ascribing the observed baryonic asymmetry of the universe to CP non-invariant processes which violate conservation of the baryonic charge at the early stages of the expanding universe.

J. C. Pati, A. Salam, Phys. Rev. Lett. 31 (1973) 661.

Non-conservation of the baryonic charge in the model with integer-charge quarks.

F. Reines, M. F. Crouch, Phys. Rev. Lett. 32 (1974) 493.

J. Learned, F. Reines, A. Soni, Phys. Rev. Lett. 43 (1979) 907.

The experimental lower bound for the proton lifetime.

L. B. Okun, Ya. B. Zeldovich, Comments Nucl. Part. Phys. 6 (1976) 69.

This paper points out that non-conservation of the baryonic charge and CP non-invariance do not result in an excess of baryons over antibaryons, if statistical equilibrium takes place.

A. Yu. Ignatiev, N. V. Krasnikov, V. A. Kuzmin, A. N. Tavkhelidze, Phys. Lett. 76B (1978) 436; see also Neutrino '77, Proc. of the Int. Conf.
on neutrino physics and astrophysics (Nauka, Moscow, 1977) vol. 2, p. 293;
H. Yoshimura, Phys. Rev. Lett. 41 (1978) 281 (Errata: 42 (1979) 746);
S. Dimopoulos, L. Susskind, Phys. Lett. 81B (1979) 416;
D. Toussaint, S. B. Treiman, F. Wilczek, A. Zee, Phys. Rev. D19 (1979) 1036;
D. Toussaint, F. Wilczek, Phys. Lett. 81B (1979) 294;
S. Weinberg, Phys. Rev. Lett. 42 (1979) 850;
A. D. Sakharov, ZhETF 76 (1979) 1172 [JETP 52 (1980) 349];
A. D. Dolgov, Pis'ma ZhETF 29 (1979) 254 [JETP Lett. 29 (1979) 288];
J. Ellis, M. K. Gaillard, D. V. Nanopoulos, Phys. Rev. Lett. 80B (1979) 360 (Erratum: 82B (1979) 464).

A discussion of various mechanisms which enhance or suppress baryonic asymmetry in the hot universe. An attempt to obtain the observed ratio $n_{\rm p}/n_\gamma \simeq 10^{-9}$ on the basis of a number of model lagrangians, including models of grand unification.

D. Cline, C. Rubbia, preprint (1978) Harvard University and University of Wisconsin.

A proposal of an experimental facility which would be capable of recording the decay $p \to \pi^0 e^+$if its probability were greater than 10^{-34} year $^{-1}$.

28.6.7. Possible non-conservation of the leptonic charge

D. Bryman, C. Picciotto, Rev. Mod. Phys. 50 (1978) 11.

A review of the experimental data and theoretical results on the double β-decay.

B. M. Pontecorvo, ZhETF 33 (1958) 549 [JETP 6 (1958) 429];
V. Gribov, B. Pontecorvo, Phys. Lett. 28B (1969) 493;
S. M. Bilen'ky, B. M. Pontecorvo, Usp. Fiz. Nauk 23 (1977) 181 [Uspekhi 20 (1977) 776].

The theory of neutrino oscillations.

28.6.8. Concentration of relic monopoles

T. W. B. Kibble, J. Phys. A9 (1976) 1387.

Ya. B. Zeldovich, M. Yu. Khlopov, Phys. Lett. 79B (1978) 237.

28.6.9. On the conservation of the electric charge

A. A. Pomansky, in: Proc. of the Int. neutrino conference, Aachen, 1976, ed. H. Faissner, H. Reithler, P. Zerwas (Vieweg, Braunschweig, 1977) p. 671;
L. B. Okun, Ya. B. Zeldovich, Phys. Lett. 78B (1978) 597;
M. B. Voloshin, L. B. Okun, Pis'ma ZhETF 28 (1978) 156 [JETP Lett. 28 (1978) 145].

28.6.10. Time independence of the fundamental constants

A. I. Shlyakhter, Nature 264 (1976) 340.

An analysis of the resonance neutron absorption in the natural nuclear pile at Oklo.
The Oklo pile is reviewed in:
Yu. V. Petrov, Usp. Fiz. Nauk 123 (1977) 473 [Uspekhi 20 (1977) 937].

5.28.7 28.7. Supplementary bibliography (autumn 1980)

The list that follows was added in proof. It mostly comprises journal publications of 1980. Unfortunately, it does not include the rapporteur and invited papers presented at the Neutrino-80 Conference (Erice) and the XX International Conference on High Energy Physics (Madison) since the Proceedings of these conferences were not yet available by the time this bibliography was completed.

28.7.1. Electroweak processes. Review papers

S. Weinberg, Rev. Mod. Phys. 52 (1980) 515;
A. Salam, Rev. Mod. Phys. 52 (1980) 525;
S. L. Glashow, Rev. Mod. Phys. 52 (1980) 539;
Nobel Lectures on physics, 1979.
B. Desplanques, Nucl. Phys. A335 (1980) 147. Parity-violating nuclear forces.
P. Depommier, Nucl. Phys. A335 (1980) 97. Rear decays of the pion and muon.
J. Egger, Nucl. Phys. A335 (1980) 87. Verification of conservation of leptonic numbers.
Yu. G. Zdesenko, Particles and Nucleus 11 (1980) Pt. 6, 1369. Double β-decay and conservation of leptonic charge.
M. L. Perl, Annual Rev. Nucl. Particle Sci. 30 (1980), preprint SLAC-PUB2446. December 1979.
τ-lepton.

28.7.2. Decays of strange particles

J. Finjord, M. K. Gaillard, Phys. Rev. D22 (1980) 778. Calculations of non-leptonic and leptonic decays of hyperons.
F. J. Gilman, M. B. Wise, Phys. Rev. D21 (1980) 3150;
M. I. Vysotsky, Lett. Nuovo Cim. 26 (1979) 1979. Analysis of the $K \to \pi e^+ e^-$decay.
R. E. Shrock, M. B. Voloshin, Phys. Lett. 87B (1979) 375. Analysis of the $K_L \to \mu\bar{\mu}$ decay in the six-quark model.
J. Donoghue, E. Golowich, W. Ponce, B. Holstein, Phys. Rev. D21 (1980) 186. Analysis of non-leptonic decays and the $\Delta T = 1/2$ rule.

28.7.3. Violation of CP invariance

M. I. Vysotsky, Yad. Fiz. 31 (1980) 1535 [Sov. J. Nucl. Phys. 31 (1980) 797];
B. Guberina, R. Peccei, Nucl. Phys. B163 (1980) 289.
F. G. Gilman, M. B. Wise, Phys. Lett. 93B (1980) 129. The $K \to \tilde{K}^0$ transition in the six-quark model with gluonic corrections taken into account.
E. Ma, W. A. Simmons, S. F. Taun, Phys. Rev. D20 (1979) 2888. Breaking of CP in systems $D^0 - \tilde{D}^0$ and $B^0 - \tilde{B}^0$ in the six-quark model.
E. P. Shabalin, Yad. Fiz. 32 (1980) 443 [Sov. J. Nucl. Phys. 32 (1980) 228] Estimates of the neutron dipole moment in the six-quark model, with Higgs bosons and strong interaction taken into account.
V. Baluni, Phys. Rev. D19 (1979) 2227;
R. Crewter, P. Di Vecchia, G. Veneziano, E. Witten, Phys. Lett. 88B (1979) 123;
M. A. Shifman, A. I. Vainshtein, V. I. Zakharov, Nucl. Phys. B166 (1980) 493. P - and

T-non-invariant effects due to so-called θ-term in the quantum chromodynamics lagrangian.
B. V. Martemyanov, Yad. Fiz. 30 (1979) 1364 [Sov. J. Nucl. Phys. 30 (1979) 708] Parametrization of CP violation for n quark doublets.
E. Eichten', K. Lane, J. Preskill, Phys. Rev. Lett. 45 (1980) 225; CP violation in models without elementary scalar fields.
M. Bander, D. Silverman, A. Soni, Phys. Rev. Lett. 43 (1979) 242;
A. R. Zhitnitsky, Yad. Fiz. 32 (1980) 434. Analysis of possible CP-odd effects in decays of heavy particles.
J. D. Christenson et al., Phys. Rev. Lett. 43 (1979) 1209; 1212. Measurements of η_{00} and η_{+-}.

28.7.4. Decays of c - and b-hadrons

W. Bacino et al., Phys. Rev. Lett. 45 (1980) 329. Experimental data on the difference in relative widths of semi-leptonic decays of $D^+$and D^0 mesons.
N. Ushida et al., Phys. Rev. Lett. 45 (1980) 1049. Measurement of the D^0 lifetime.
N. Ushida et al., Phys. Rev. Lett. 45 (1980) 1053. Measurement of the D^+, $F^+$and Λ_c^+charmed particle lifetimes.
M. Bander, D. Silverman, A. Soni, Phys. Rev. Lett. 44 (1980) 7;
H. Fritzsch, P. Minkowski, Phys. Lett. 90B (1980) 455;
V. Barger, J. P. Leveille, P. M. Stevenson, Phys. Rev. D22 (1980) 693. Gluonic enhancement of non-leptonic decays of D^0 mesons.
L. Dulyan, A. Khodzamirian, preprint of the Yerevan Physics Inst. 410 (17)-80. The difference in the lifetimes of D^0 and D^+mesons is interpreted in the model of quark graphs corresponding to the c-quark decay.
S. P. Rosen, Phys. Rev. D22 (1980) 776. Corollaries of the $\Delta T = 1$ rule for the decays of charmed mesons.
Y. Tosa, S. Okubo, Phys. Rev. D22 (1980) 168. Analysis of inclusive decays of charmed mesons.
S. P. Rosen, Phys. Rev. Lett. 44 (1980) 1. Sextet enhancement and differences in lifetimes of charmed mesons.
H. Lipkin, Phys. Rev. Lett. 44 (1980) 710. Interaction in final states in decays of charmed mesons.
G. S. Abrams et al., Phys. Rev. Lett. 43 (1979) 481. Observation of the $D^0 \to \pi^+\pi^-$and $D^0 \to K^+K^-$decays. For a discussion of these decays see:
V. Barger, S. Pacvasa, Phys. Rev. Lett. 43 (1979) 812;
L. L. Wang, F. Wilczek, Phys. Rev. Lett. 43 (1979) 816.
H. Georgi, S. Glashow, Nucl. Phys. B167 (1980) 17. An analysis of decays of b -hadrons in models not including the t -quark.
S. K. Bose, E. Paschos, Nucl. Phys. B169 (1980) 384. The $K^0 \to \tilde{K}^0$, $D^0 \to \tilde{D}^0$ and $B^0 \to \tilde{B}^0$ transitions in the eight-quark model.
F. Bucella, L. Oliver, Nucl. Phys. B162 (1980) 237. Phenomenological restrictions on charm-changing neutral currents.

28.7.5 Neutral currents

A. A. Varfolomeyev, Yad. Fiz. 31 (1980) 1268 [Sov. J. Nucl. Phys. 31 (1980) 655] Coherent interaction of the neutrino with a dense medium.

Riazzudin, Phys. Rev. Lett. 45 (1980) 976. Weak neutral currents without electroweak unification.
E. Pasierb, A. S. Gurr, J. Lathrop, F. Reines, H. W. Sobel, Phys. Rev. Lett. 43 (1979) 96. Discovery of neutral currents in the interaction of reactor neutrinos $\tilde{\nu}_e$ with deuterons.

L. M. Barkov, M. S. Zolotorev, Phys. Lett. 85B (1979) 308. New measurements of rotation of the light polarization plane in atomic bismuth vapor are in agreement with earlier results of the same authors and with the standard electroweak theory.

Yu. V. Bogdanov, I. I. Sobelman, I. I. Struk, Pis'ma ZhETF 31 (1980) 234; 556 [JETP Lett. 31 (1980) 214; 522] The expected rotation of the light polarization plane is not observed.

28.7.6. Electroweak radiative corrections

A. Sirlin, Phys. Rev. D22 (1980) 971. Radiative corrections in the SU(2) × U(1) theory.
M. Green, M. Veltman, Nucl. Phys. B169 (1980) 137. Radiative corrections to μ-decay and νe-scattering.
M. Greco, G. Pancheri-Srivastava, Y. Srivastava, Nucl. Phys. B171 (1980) 118. Radiative corrections to the $e^+e^- \to Z^0 \to \mu^+\mu^-$process.
M. Veltman, Phys. Lett. 91B (1980) 95;
F. Antonelli, M. Consoli, G. Corbo, Phys. Lett. 91B (1980) 90. Radiative corrections to $m_{\mathrm{w,Z}}(\Delta m \simeq +3\mathrm{GeV})$.

28.7.7. Virtual Higgs bosons

T. Applequist, C. Bernard, Phys. Rev. D22 (1980) 200;
A. C. Longhitano, Phys. Rev. D22 (1980) 1166. Detailed analysis of the effect of virtual strongly interacting heavy Higgs bosons on weak interactions at low energies.

28.7.8. Dynamical symmetry breaking

S. Raby, S. Dimopoulos, L. Susskind, Nucl. Phys. B169 (1980) 373. A scheme of tumbling symmetries.
G.'t Hooft, Lectures given at the Cargse Summer Institute, 1979. The equality of anomalies for compound massless fermions and subquarks is formulated as a necessary condition for a self-consistent theory of metacolor.
E. Eichten, K. Lane, Phys. Lett. 90B (1980) 125.
P. Di Vecchia, G. Veneziano, preprint TH 2868-CERN, May 1980.
S. Dimopoulos, S. Raby, G. Kane, Nucl. Phys. B182 (1981) 77.
S. Dimopoulos, Nucl. Phys. B168 (1980) 69. Discussion of the properties of technihadrons.

28.7.9. Properties of free neutrinos

J. N. Bahcall, Rev. Mod. Phys. 50 (1978) 881. Review: solar neutrinos.
J. N. Bahcall et al., Phys. Rev. Lett. 45 (1980) 945. The number (2.2± 0.4)SNU experimentally observed by Davis is compared with the theoretical result: (7.5 ± 0.5) SNU (1SNU = $10^{-36}\nu$-captures in ^{37}Cl per one target atom per second).
F. Reines, H. Sobel, E. Pasierb, Phys. Rev. Lett 45 (1980) 1307. Data on neutral and charged currents in the $\tilde{\nu}_e d$ interaction are interpreted as an indication of ν-oscillations.
F. Bohem et al., Phys. Lett. 97B (1980) 310. Experimental search for oscillations of reactor neutrinos. No oscillations were recorded.
V. S. Kozik, V. A. Lyubimov, E. G. Novikov, V. Z. Nozik, E. F. Tretyakov, Yad. Fiz. 32 (1980) 301 [Sov. J. Nucl. Phys. 32 (1980) 154];
V. A. Lyubimov, E. G. Novikov, V. Z. Nozik, E. F. Tretyakov, V. S. Kozik, Phys. Lett. 94B (1980) 266. An estimate of the $\tilde{\nu}_e$ mass from the tritium decay spectrum.
A. De Rujula, M. Lusignoli, L. Maiani, S. Petcov, R. Petronzio, Nucl. Phys. B168 (1980) 54;
V. Barger, K. Whisnant, D. Cline, R. Phillips, Phys. Lett. 93B (1980) 194.

Phenomenological analysis of data on possible neutrino oscillations.
S. M. Bilenky, B. Pontecorvo, Phys. Lett. 95B (1980) 233;
S. M. Bilenky, J. Hosek, S. T. Petcov, Phys. Lett. 94B (1980) 495;
I. Yu. Kobzarev, B. V. Martemyanov, L. B. Okun, M. G. Shchepkin, Yad. Fiz. 32 (1980) 1286 [Sov. J. Nucl. Phys. 32 (1980) 828];
V. Barger, P. Langacker, J. Leveille, S. Pakvasa, Phys. Rev. Lett. 45 (1980) 692. Neutrinos with mixed Dirac and Majorana masses.
B. V. Martem'yanov, M. Yu. Khlopov, M. G. Shchepkin, Pis'ma ZhETF 32 (1980) 484 [JETP Lett. 32 (1980) 464]. Effect of ν oscillations on the $\nu_\mu e$ and $\nu_e e$ scattering.
G. T. Zatsepin, A. Yu. Smirnov, Yad. Fiz. 28 (1978) 1569 [Sov. J. Nucl. Phys. 28 (1978) 807];
A. De Rujula, S. L. Glashow, Phys. Rev. Lett. 45 (1980) 942. Discussion of the photon decays of the neutrino.

28.7.10. Neutrino masses in grand unification models

R. Barbieri, J. Ellis, M. K. Gaillard, Phys. Lett. 90B (1980) 249. Neutrino masses and oscillations is SU(5).
M. Gell-Mann, P. Ramond, R. Slansky, in: Supergravity, ed. P. van Nieuwenhuizen, D. Z. Freeman (North-Holland, Amsterdam, 1979) p. 315; preprint TH 2855-CERN, January 1980;
R. Barbieri, D. V. Nanopoulos, G. Morchio, F. Strocchi, Phys. Lett. 90B (1980) 91.
E. Witten, Phys. Lett. 91B (1980) 81. Neutrino masses in SO(10)
R. N. Mohapatra, G. Senjanovic, Phys. Rev. Lett. 44 (1980) 912. Neutrino mass in the $SU(2) \times SU(2) \times U(1)$ model.

28.7.11. Grand unification models and proton decay

T. Goldman, D. Ross, Nucl. Phys. B171 (1980) 273;
J. Ellis, M. K. Gaillard, D. V. Nanopoulos, S. Rudaz, Nucl. Phys. B176 (1980) 61. Uncertainties in the theoretical precitions of the proton lifetime.
V. S. Berezinsky, A. Yu. Smirnov, Phys. Lett. 97B (1980) 371. A possibility of a practically stable proton in the SU(5) model.
A. Yu. Smirnov, Pis'ma ZhETF 31 (1980) 781 [JETP Lett. 31 (180) 737] Superheavy fermions and proton lifetime.
M. Mahacek, Nucl. Phys. B159 (1979) 37. Channels of proton decay.
G. Segr, H. A. Weldon, Phys. Rev. Lett. 44 (1980) 1737. U(5) model with stable proton.
G. M. Asatryan, S. G. Matinyan, Yad. Fiz. 31 (1980) 1381 [Sov. J. Nucl. Phys. 31 (1980) 711]. Flavor mixing and proton decay.
R. E. Marshak, R. N. Mohapatra, Phys. Rev. Lett. 44 (1980) 1316.
M. V. Kazarnovsky, V. A. Kuz'min, K. G. Chetyrkin, M. E. Shaposhnikov, Pis'ma ZhETF 32 (1980) 88 [JETP Lett. 32 (1980) 82]. Neutron-antineutron oscillations. See also:
V. A. Kuzmin, Pis'ma ZhETF 12 (1970) 335 [JETP Lett. 12 (1970) 228].
F. Wilczeck, A. Zee, Phys. Rev. Lett. 43 (1979) 1571;
S. Weinberg, Phys. Rev. Lett. 43 (1979) 1566. Phenomenological operator analysis of proton decay.

For discussions of various problems associated with the search for proton decay see the quarterly:
Progress in Cosmic Ray Deep Mine Experiments and Baryon Decay Detection experiments. Quarterly News Letter. Wisconsin University, No. 1, February 1980.
28.7.12. Various aspects of grand unification
S. G. Matinyan, Usp. Fiz. Nauk 130 (1980) 3 [Uspekhi 23 (1980) 1] Review of the SU(5) model.
D. V. Nanopoulos, preprint TH 2896-CERN, 1980. Review of the SU(5), SO(10) and E_6 models.

Yu. F. Pirogov, Yad. Fiz. 31 (1980) 547 [Sov. J. Nucl. Phys. 31 (1980) 283] $SU(8)_L \times SU(8)_R$ model.
P. Frampton, S. Nandi, Phys. Rev. Lett. 43 (1979) 1460. SU(9) model.
R. Barbieri, D. V. Nanopoulos, Phys. Lett. 91B (1980) 369. E 6 model.
R. Lednick, V. Tseitlin, Yad. Fiz. 31 (1980) 1036 [Sov. J. Nucl. Phys. 31 (1980) 534] Neutral currents in the E_7 model.
I. Bars, M. Gnaydin, Phys. Rev. Lett. 45 (1980) 859. E_8 model.
J. Ellis, M. K. Gaillard, A. Peterman, C. Sachraida, Nucl. Phys. B164 (1980) 253. Hierarchy of gauge hierarchies.
E. Gildener, Phys. Lett. 92B (1980) 111. The problem of hierarchies.
P. H. Frampton, Phys. Rev. Lett. 43(1979) 1912. On the impossibility of including technicolor into grand unification.
A. Davidson, K. Wali, P. Manheim, Phys. Rev. Lett. 45 (1980) 1135. $SO(10) \times SO(10)$ model including four fermion generations and technicolor.
I. Liede, M. Ross, Nucl. Phys. B167 (1980) 397. Analysis of experimental data on neutral currents points to a contradiction with the SU(5) model.
S. Weinberg, Phys. Lett. 91B (1980) 51. Threshold effects in the dependence of gauge charges on momentum.
N. G. Deshpande, D. Iskandar, Phys. Lett. 87B (1979) 383; Nucl. Phys. B167 (1980) 223. Electroweak models with arbitrary violation of parity in atoms.

28.7.13. Superunification

O. V. Tarasov, A. A. Vladimirov, preprint E2-80-483, Dubna;
L. V. Avdeev, O. V. Tarasov, A. A. Vladimirov, Phys. Rev. Lett. 96B (1980) 94;
M. Grisaru, M. Roek, W. Siegel, Phys. Rev. Lett. 45 (1980) 1063. Vanishing of three loop charge renormalization function in a supersymmetric gauge theory.
R. Kallosh, Nucl. Phys. B165 (1980) 119. Elimination of divergences for the $N = 1$ supergravity in self-dual external fields.
E. S. Fradkin, M. A. Vasiliev, Phys. Lett. 85B (1979) 47;
P. Breitenlohner, M. Sohnius, Nucl. Phys. B165 (1980) 483. Formulation of the $N = 2$ supergravity off the mass shell.
G. Barbiellini et al., preprint DESY 79/67, October 1979. A discussion of the possibilities of experimental search for super-symmetric particles at LEP.
P. Fayet, preprint TH 2864-CERN, May 1980. Possibilities of search for goldstino, photino and gluino with accelerators are discussed.
J. Scherk , Phys. Lett. 88B (1979) 265. Supergravity-based antigravity.
V. I. Ogiyevetsky, E. S. Sokachev, Yad. Fiz. 32 (1980) 862; 870. [Sov. J. Nucl. Phys. 32 (1980) 443; 447] Torsion and curvature in terms of the axial gravitational superfield.
M. Sohnius, K. S. Stelle, P. C. West, Phys. Lett. 92B (1980) 123. SU(4) supersymmetry off the mass shell.
F. A. Berezin, Yad. Fiz. 29 (1979) 1670 [Sov. J. Nucl. Phys. 29 (1979) 857];
A. S. Schwarz, Nucl. Phys. B171 (1980) 154. Attempts of quantum field theory with coordinates and fields treated on an equal footing.
E. Cremmer, B. Julia, Nucl. Phys. B159 (1979) 141; Hidden local SU(8) symmetry in the $N = 8$ supergravity.
T. Curtright, P. Freund, in: Supergravity. Proc. of Super-gravity Workshop at Stony Brook, Sept. 1979, ed. P. van Nieuwenhuizen
and D. Z. Freedman (North-Holland, Amsterdam) 1979, p. 197. Phenomenology of SU(8) symmetry.

J. Ellis, M. K. Gaillard, B. Zumino, Phys. Lett. 94B (1980) 343. SU(5) from broken $N = 8$ supergravity.

28.7.14. Cosmology and elementary particles. Review papers

A. D. Dolgov, Ya. B. Zeldovich, Usp. Fiz. Nauk 130 (1980) 559; Rev. Mod. Phys. 53 (1981) 1.

G. Steigman, Ann. Rev. Nucl. Part. Sci. 29 (1979) 313.
J. Ellis, M. K. Gaillard, D. V. Nanopoulos, preprint TH 2858-CERN, LAPP-TH-19, 1980.

28.7.15. Neutrino mass and hidden mass in the universe

Ya. B. Zeldovich, P. A. Sunyayev, Pis'ma v Astronom. Zhurn. 6 (1980) 451;
A. G. Doroshkevich, Ya. B. Zeldovich, R. A. Sunyayev, M. Yu. Khlopov, Pis'ma v Astronom. Zhurn. 6 (1980) 457; 465.
J. Bond, G. Estatio, J. Silk, preprint Univ. of Calif., 1980.
H. Sato, F. Takahara, preprint RISP-400, 1980.
G. S. Bisnovatiy-Kogan, I. D. Novikov, Astronom. Zhurnal 57 (1980) 899. The role of massive neutrinos is discussed in the formation of galaxy clusters and of their hidden mass. $M \approx m_p/m_\nu$ where M is the mass of so-called pancakes, m_p is the Planck mass, and m_ν is the neutrino mass. An observational estimate of hidden mass in coronas of galaxies see in
J. Einasto, A. Kaasik, E. Saar, Nature 250 (1974) 309.
T. Yanagida, M. Yoshimura, Phys. Rev. Lett. 45 (1980) 71. Majorana masses of the neutrinos and cosmology.

Ya. B. Zeldovich, A. A. Klypin, M. Yu. Khlopov, V. M. Chechetkin, Yad. Fiz. 31 (1980) 1286. [Sov. J. Nucl. Phys. 31 (1980) 664] Astrophysical restrictions on the masses of heavy neutral leptons.
P. Frampton, S. L. Glashow, Phys. Rev. Lett. 44 (1980) 1481. Restrictions on the possible properties of hypotetical long-lived heavy particles.

28.7.16. Calculation of n_B/n_γ
E. Kolb, S. Wolfram, Nucl. Phys. B172 (1980) 224.
V. A. Kuz'min, M. E. Shaposhnikov, Phys. Lett. 92B (1980) 115.
T. Yanagida, M. Yoshimura, Nucl. Phys. B168 (1980) 534. $n_{\rm B}/n_\gamma$ in grand unification models.

28.7.17. Magnetic monopoles and cosmology
J. P. Preskill, Phys. Rev. Lett. 43 (1979) 1365.
P. Langacker, S-Y. Pi, Phys. Rev. Lett. 45 (1980) 1. Monopoles and cosmology.
Y. M. Cho, Phys. Rev. Lett. 44 (1980) 1115. Colored monopoles.
M. Daniel, G. Lazarides, Q. Shafi, Nucl. Phys. 170 (1980) 156. SU(5) monopoles and confinement.
D. M. Scott, Nucl. Phys. 171 (1980) 95; 109. Monopoles in the grand unification theories.
A. D. Linde, Phys. Lett. 96B (1980) 293. Confinement of monopoles at high temperatures.

28.7.18. Search for new particles and interactions
M. Marinelli, G. Morpurgo, Phys. Lett. 94B (1980) 427; 433. Negative results of search for fractionally charged quarks: $n_{\rm q}/n_{\rm B} \lesssim 10^{-21}$.
S. Chaudhuri, D. D. Coon, G. E. Derkits, Jr., Phys. Rev. Lett. 45 (1980) 1374. A new method of search for fractionally charged particles is suggested, with sensitivity $\simeq 10^{-21} - 10^{-24}$ particles per nucleon.
M. Basile et al., Lett. Nuovo Cim. 29 (1980) 251. Quark search experiment in high energy neutrino interactions.

G. Barbiellini et al., preprint DESY 80/42, May 1980. Review of possible experiments on quark and monopole search in colliding LEP beams.
L. B. Okun, Nucl. Phys. B173 (1980) 1.
L. B. Okun, Pis'ma ZhETF 31 (1980) 156 [JETP Lett. 31 (1980) 144]. Hypothesis of the existence of θ-gluons with macroscopic confinement radius.
L. B. Okun, ZhETF 79 (1980) 694 [JETP 52 (1980) 351] Discussion of hypothetical long-range forces.
28.7.19. Search for deviations from Newton's law
R. Spero, J. K. Hoskins, R. Newman, J. Pellam, J. Schultz, Phys. Rev. Lett. 44 (1980) 1645. Dependence $1/r^2$ for the gravity force is verified in the range from 2 to 5 cm .
V. I. Panov, V. N. Frontov, ZhETF 77 (1979) 1701 [JETP 50 (1979) 852]. Independence of the gravitational interaction constant on distance is verified in the range from 0.4 to 10 m to the accuracy of about one per cent.
S. I. Blinninkov, Astrophysics and Space Science 59 (1978) 13. The relation between the mass and radius of white dwarfs excludes variation of G_{N} greater than 10% in the range from 10 m to 1 km .

28.7.20. Verification of electric charge conservation

I. R. Barabanov et al., Pis'ma ZhETF 32 (1980) 384 [JETP Lett. 32 (1980) 359]. Upper bound on ^{71}Ga lifetime with respect to decay $^{71}\mathrm{Ga}_{31}{}^{71}\mathrm{Ge}_{32} + \gamma$ is established: $T \geq 2.3 \cdot 10^{23}$ years.
B. E. Norman, A. G. Seamster, Phys. Rev. Lett. 43 (1979) 1226. T(^{87} Rb $_{37}$ $^{87}\mathrm{Sr}_{38} + \gamma) \geq 1.9 \cdot 10^{18}$ years.

28.7.21. Future accelerators

Proceedings of the Workshop on possibilities and limitations of accelerators and detectors, April 1979, FNAL, Batavia, Ill. USA.

Open Presentation of the Results of the second ICFA Workshop on Possibilities and Limitations of Accelerators and Detectors held October 4-9, 1979 at Les Diablerets, Switzerland.
R. Wilson, Scientific American 242 (1980) No. 1, 26; The next generation of particle accelerators.
D. Cline, C. Rubbia, Phys. Today 33 (1980) No. 8, 44. Antiproton-proton colliders and intermediate bosons.

5.29 29 Appendix (Some useful formulas)

This appendix is a compilation of some notations, definitions and formulas which are frequently mentioned in the text of the book. The appendix is divided into the following sections:
29.1. Pseudoeuclidean metric. 308
29.2. Groups 309
29.2.1. Some definitions 309
29.2.2. The groups SU(n) 310
29.2.3. The group SU(2) 310
29.2.4. Fierz identities for σ-matrices 312
29.2.5. Clebsch-Gordan coefficients, spherical harmonics, and d functions 313
29.2.6. The group SU(3) 314
29.2.7. Fierz identities for λ matrices. 315
29.2.8. SU(3) multiplets. 315
29.3. Properties of Dirac matrices. 318
29.3.1. γ-matrices 318

29.3.2. Trace of γ - matrices 319
29.3.3. Dirac bispinor 320
29.3.4. Four-fermion invariants and Fierz identities for Dirac matrices 321
29.3.5. Derivation of Fierz identities for Dirac matrices. 323
29.4. Rules for the calculation of probabilities. 325
29.4.1. S - and T-matrices 325
29.4.2. Probability and cross sections 326
29.4.3. Particles with non-zero spin. 327

5.29.1 29.1. Pseudoeuclidean metric

Contravariant vector a^μ; examples:

$$x^\mu \equiv x^0, x^1, x^2, x^3 \equiv t, x, y, z \equiv t, \boldsymbol{x}$$
$$p^\mu \equiv p^0, p^1, p^2, p^3 \equiv E, p_x, p_y, p_z \equiv E, \boldsymbol{p}$$

Covariant vector a_μ; examples:

$$x_\mu \equiv x_0, x_1, x_2, x_3 \equiv t, -\boldsymbol{x},$$
$$p_\mu \equiv p_0, p_1, p_2, p_3 \equiv E, -\boldsymbol{p}.$$

Metric tensor:

$$a_\mu = g_{\mu\nu} a^\nu, \quad a^\mu = g^{\mu\nu} a_\nu,$$

where $g_{\mu\nu}$ is a metric tensor with only diagonal components not equal to zero:

$$g^{\mu\nu} = g_{\mu\nu}, \quad g_{00} = -g_{11} = -g_{22} = -g_{33} = 1.$$

Scalar product:

$$\begin{aligned} a^\mu b_\mu &= g^{\mu\nu} a_\mu b_\nu = g_{\mu\nu} a^\mu b^\nu \\ &= a^0 b_0 + a^i b_i = a^0 b_0 - a^i b^i = a^0 b^0 - \boldsymbol{a} \cdot \boldsymbol{b}, \\ \mu, \nu &= 0, 1, 2, 3; \quad i, k = 1, 2, 3. \end{aligned}$$

Example:

$$p^\mu x_\mu = Et - \boldsymbol{p} \cdot \boldsymbol{x}.$$

The momentum operator in the coordinate representation has the form:

$$p^\mu = i\frac{\partial}{\partial x_\mu} = i\frac{\partial}{\partial t}, -i\frac{\partial}{\partial x} = i\frac{\partial}{\partial t}, \frac{1}{i}\frac{\partial}{\partial x}.$$

5.29.2 29.2. Groups

29.2.1. Some definitions.

A group $\mathcal{G}$ is a set of elements in which the operation of associative multiplication and a unit element are defined and for each element the set contains the corresponding inverse element. A group is called an abelian group if all elements commute. The representation G of group $\mathcal{G}$ is defined as a group of linear transformations (of matrices) in a linear space (referred to as the basis of the representation, or a multiplet), whose elements are in one-to-one correspondence with the elements of group $\mathcal{G}$. The groups whose elements are analytical functions of a finite

number of parameters are called Lie groups. The number of independent parameters is called the dimension of the group. The generators of a given representation are operators I_i which realize transformations infinitesimally close to the identity transformation:
$G = 1 + id\omega_i I_i$. The maximum number of mutually commuting generators is called the rank of the group. The number of linearly independent vectors in the basis (the number of components in the multiplet) is called the dimension of the representation (the dimension of a representation is equal to the order of matrices realizing this representation). If a specific choice of basis breaks the representation into a sum of independent subgroups, the representation is called reducible; it is irreducible if this separation cannot be achieved by any choice of basis. Representations are called fundamental if all other representations of the group can be constructed from them by multiplication. The dimension of a regular (adjoint) representation equals the order of the group.

29.2.2. The groups $SU(n)$

SU(n) is a group of complex matrices U satisfying the conditions of unitarity ($U^+U = 1$) and of unimodularity ($\det U = 1$), whose fundamental multiplet is an n-component spinor and whose fundamental representation is given by matrices of order n.

29.2.3. The group $SU(2)$

The fundamental representation of the group SU(2) is given by the matrices

$$U = \exp\left(i\omega_i \frac{1}{2}\sigma_i\right), \quad i = 1, 2, 3,$$

where σ_i are Pauli matrices, and ω_i are three real parameters. The symbol σ_i is used to describe particle spins; in the description of isospin the same matrices are usually denoted by τ_i. Pauli matrices satisfy the commutation relations

$$\left[\frac{1}{2}\sigma_i, \frac{1}{2}\sigma_j\right] = i\varepsilon_{ijk}\frac{1}{2}\sigma_k,$$

where ε_{ijk} is a completely antisymmetric alternating tensor. The components of this tensor are structure constants of the group SU(2). The Pauli matrices are usually taken in the form

$$\sigma_1 = \begin{pmatrix} 0 & 1 \\ 1 & 0 \end{pmatrix}, \quad \sigma_2 = \begin{pmatrix} 0 & -i \\ i & 0 \end{pmatrix}, \quad \sigma_3 = \begin{pmatrix} 1 & 0 \\ 0 & -1 \end{pmatrix}.$$

An arbitrary representation of the group SU(2) has three generators satisfying the condition

$$[I_i, I_j] = i\varepsilon_{ijk} I_k$$

For a regular (three-dimensional) representation,

$$I_1 = \begin{pmatrix} 0 & 0 & 0 \\ 0 & 0 & -i \\ 0 & i & 0 \end{pmatrix},$$

$$I_2 = \begin{pmatrix} 0 & 0 & i \\ 0 & 0 & 0 \\ -i & 0 & 0 \end{pmatrix},$$

$$I_3 = \begin{pmatrix} 0 & -i & 0 \\ i & 0 & 0 \\ 0 & 0 & 0 \end{pmatrix}.$$

Pauli matrices satisfy the following conditions:

$$\sigma_i\sigma_k = \delta_{ik}I + i\varepsilon_{ikl}\sigma_l, \quad \text{where } I = \begin{pmatrix} 1 & 0 \\ 0 & 1 \end{pmatrix},$$

$$\delta_{ik} = \begin{cases} 1 & \text{if} \quad i = k, \\ 0 & \text{if} \quad i \neq k, \end{cases}$$

$$\delta_{ik}\delta_{ik} = 3;$$

$$\varepsilon_{ikl} = \begin{cases} 1 & \text{if} \quad ikl = 123, 312, 231, \\ -1 & \text{if} \quad ikl = 132, 213, 321, \\ 0 & \text{if} \quad i = k, \text{ or } k = l, \text{ or } l = i; \end{cases}$$

$$\varepsilon_{ikl}\varepsilon_{i'k'l} = \begin{Vmatrix} \delta_{ii'} & \delta_{ik'} & \delta_{il'} \\ \delta_{ki'} & \delta_{kk'} & \delta_{kl'} \\ \delta_{li'} & \delta_{lk'} & \delta_{ll'} \end{Vmatrix},$$

$$\varepsilon_{ikl}\varepsilon_{i'k'l} = \begin{Vmatrix} \delta_{ii'} & \delta_{ik'} \\ \delta_{ki'} & \delta_{kk'} \end{Vmatrix} = \delta_{ii'}\delta_{kk'} - \delta_{ik'}\delta_{ki'},$$

$$\varepsilon_{ikl}\varepsilon_{i'kl} = 2\delta_{ii'},$$

$$\varepsilon_{ikl}\varepsilon_{ikl} = 6.$$

Trace of σ-matrices:

$$\begin{aligned} \operatorname{Tr} I &= 2 \\ \operatorname{Tr} \sigma_i &= 0 \\ \operatorname{Tr} \sigma_i\sigma_k &= 2\delta_{ik} \\ \operatorname{Tr} \sigma_i\sigma_k\sigma_l &= 2i\varepsilon_{ikl} \\ \operatorname{Tr} \sigma_i\sigma_k\sigma_l\sigma_m &= 2\left[\delta_{ik}\delta_{lm} + \delta_{im}\delta_{kl} - \delta_{il}\delta_{km}\right]. \end{aligned}$$

29.2.4. Fierz identities for σ-matrices:

$$\begin{aligned} \delta^a_b\delta^c_d &= \frac{1}{2}\delta^a_d\delta^c_b + \frac{1}{2}\boldsymbol{\sigma}^a_d \cdot \boldsymbol{\sigma}^c_b, \\ \boldsymbol{\sigma}^a_b\boldsymbol{\sigma}^c_d &= \frac{3}{2}\delta^a_d\delta^c_b - \frac{1}{2}\boldsymbol{\sigma}^a_d\boldsymbol{\sigma}^c_b, \end{aligned}$$

where

$$\boldsymbol{\sigma} \cdot \boldsymbol{\sigma} = \sigma_i\sigma_i, \quad i = 1, 2, 3$$

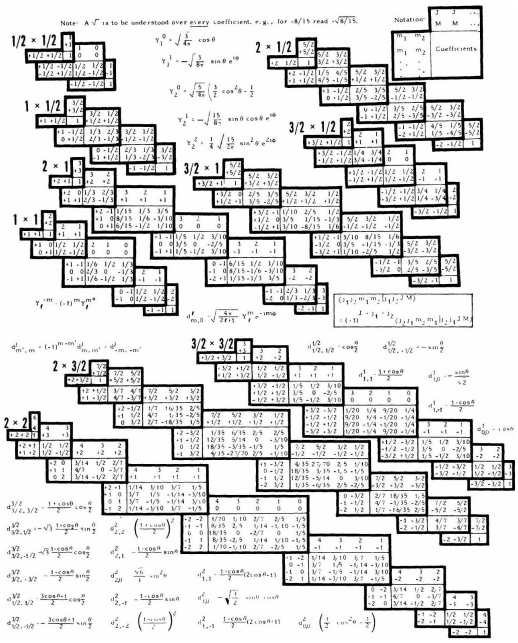
These relations are easily verified by multiplying both equalities by $\delta^a_b\delta^c_d$ and $\delta^a_d\delta^c_b$. It follows from these equalities that

$$\begin{aligned} 3\delta^a_b\delta^c_d + \boldsymbol{\sigma}^a_b \cdot \boldsymbol{\sigma}^c_d &= +\left(3\delta^a_d\delta^c_b + \boldsymbol{\sigma}^a_d \cdot \boldsymbol{\sigma}^c_b\right) \\ \delta^a_b\delta^c_d - \boldsymbol{\sigma}^a_b \cdot \boldsymbol{\sigma}^c_d &= -\left(\delta^a_d\delta^c_b - \boldsymbol{\sigma}^a_d \cdot \boldsymbol{\sigma}^c_b\right) \end{aligned}$$

The first of these expressions, acting on the product of spinors $\psi^b\varphi^d$, yields a state with spin 1 , and the second yields a state with spin 0 . This is in agreement with the form of the operator which gives zero when applied to a state with spin S :

$$\begin{aligned}\boldsymbol{S}^2 - S(S+1) &= \left(\frac{1}{2}\left(\boldsymbol{\sigma}_1 + \boldsymbol{\sigma}_2\right)\right)^2 - S(S+1) \\ &= \frac{3}{2} + \frac{1}{2}\boldsymbol{\sigma}_1 \cdot \boldsymbol{\sigma}_2 - S(S+1) \\ &= \begin{cases} \frac{3}{2} + \frac{1}{2}\boldsymbol{\sigma}_1 \cdot \boldsymbol{\sigma}_2 & \text{for } S = 0 \\ -\frac{1}{2} + \frac{1}{2}\boldsymbol{\sigma}_1 \cdot \boldsymbol{\sigma}_2 & \text{for } S = 1 \end{cases}\end{aligned}$$

29.2.5. Clebsch-Gordan coefficients, spherical harmonics, and dunctions



Sign convention is that of Wigner (Group Theory. Academic Press, New York, 1959), also used by Condon and Shortley (The Theory of Atomic Spectra, Cambridge Univ. Press, New York, 1953), Rose (Elementary Theory of Angular Momentum, Wiley, New York, 1957), and Cohen (Tables of the Clebsch-Gordan Coefficients. North American Rockwell Science Center, Thousand Oaks, Calif., 1974). The signs and numbers in the current tables hase been calculated by computer programs written independently by Cohen and at LBL. (Table extended April 1974.)

29.2.6. The group SU(3)

The fundamental representation of the group SU(3) is given by the matrices

$$U = \exp\left(\frac{1}{2}\lambda_i \omega_i\right), \quad i = 1, 2, \ldots, 8$$

where λ_i are the Gell-Mann matrices, and ω_i are eight real parameters. Usually the matrices λ_i are chosen in the form:

$$\lambda_1 = \begin{pmatrix} 0 & 1 & 0 \\ 1 & 0 & 0 \\ 0 & 0 & 0 \end{pmatrix}, \quad \lambda_2 = \begin{pmatrix} 0 & -i & 0 \\ i & 0 & 0 \\ 0 & 0 & 0 \end{pmatrix}, \quad \lambda_3 = \begin{pmatrix} 1 & 0 & 0 \\ 0 & -1 & 0 \\ 0 & 0 & 0 \end{pmatrix},$$
$$\lambda_4 = \begin{pmatrix} 0 & 0 & 1 \\ 0 & 0 & 0 \\ 1 & 0 & 0 \end{pmatrix}, \quad \lambda_5 = \begin{pmatrix} 0 & 0 & -i \\ 0 & 0 & 0 \\ i & 0 & 0 \end{pmatrix}, \quad \lambda_6 = \begin{pmatrix} 0 & 0 & 0 \\ 0 & 0 & 1 \\ 0 & 1 & 0 \end{pmatrix},$$
$$\lambda_7 = \begin{pmatrix} 0 & 0 & 0 \\ 0 & 0 & -i \\ 0 & i & 0 \end{pmatrix}, \quad \lambda_8 = \frac{1}{\sqrt{3}} \begin{pmatrix} 1 & 0 & 0 \\ 0 & 1 & 0 \\ 0 & 0 & -2 \end{pmatrix}.$$

The matrices λ satisfy the following relations:

$$\begin{aligned} \operatorname{Tr} \lambda_i \lambda_j &= 2\delta_{ij} \\ [\lambda_i \lambda_j] &= 2i f_{ijk} \lambda_k \\ [\lambda_i \lambda_j]_+ &= \frac{4}{3}\delta_{ij} + 2d_{ijk}\lambda_k, \qquad \text{where } i,j,k = 1,2,\ldots,8 \end{aligned}$$

Here f_{ijk} are structure constants of the group $\mathrm{SU}(3), d_{ijk}$ are symmetrical and $f_{\imath jk}$ are antisymmetrical with respect to permutations of any pair of indices. Direct calculations easily give 54 non-zero constants f_{ijk} and 58 non-zero constants d_{ijk} :

ijk	f_{ijk}	ijk	d_{ijk}	ijk	d_{ijk}
123,	1	118	$1/\sqrt{3}$	355	$\frac{1}{2}$
147	$\frac{1}{2}$	146	$\frac{1}{2}$	366	$-\frac{1}{2}$
156	$-\frac{1}{2}$	157	$\frac{1}{2}$	377	$-\frac{1}{2}$
246	$\frac{1}{2}$	228	$1/\sqrt{3}$	448	$-\frac{1}{2}\gamma^3$
257	$\frac{1}{2}$	247	$-\frac{1}{2}$	558	$-\frac{1}{2}\sqrt{3}$
345	$\frac{1}{2}$	256	$\frac{1}{2}$	668	$-\frac{1}{2}\sqrt{3}$
367	$-\frac{1}{2}$	338	$1/\sqrt{3}$	778	$-\frac{1}{2}\gamma^3$
458	$\frac{1}{2}\sqrt{3}$	344	$\frac{1}{2}$	888	$-1/\sqrt{3}$
678	$\frac{1}{2}\sqrt{3}$				

($54 = 9 \times 6$ where 6 is the number of permutations of indices $i \neq j \neq k$, and $58 = 4 \times 6 + 11 \times 3 + 1$). Note that $d_{ijk} = 0$ if the number of indices $2, 5, 7$ is odd. On the other hand, $f_{ijk} = 0$ if the number of these indices is even. These indices, 2,5,7, are special because the corresponding matrices λ are antisymmetric.

29.2.7. Fierz identities for λ matrices

Using the completeness of the nine matrices $\delta^\alpha_\beta, \lambda^\alpha_\beta$, we can write:

$$\begin{aligned} \delta^\alpha_\beta \delta^\gamma_\delta &= A\delta^\alpha_\delta \delta^\gamma_\beta + B\lambda^\alpha_\delta \lambda^\gamma_\beta, \\ \lambda^\alpha_\beta \lambda^\gamma_\delta &= C\delta^\alpha_\delta \delta^\gamma_\beta + D\lambda^\alpha_\delta \lambda^\gamma_\beta, \end{aligned}$$

where A, B, C and D are coefficients to be determined and where

$$\boldsymbol{\lambda} \cdot \boldsymbol{\lambda} = \lambda_i \lambda_i, \quad i = 1,2,\ldots,8.$$

Multiplication of these two equalities by $\delta^\delta_\alpha \delta^\beta_\gamma$ yields

$$3 = 9A, \quad 16 = 9C$$

and multiplication by $\delta^\beta_\alpha\delta^\delta_\gamma$ yields

$$9 = 3A + 16B, \quad 0 = 3C + 16$$

whence

$$\delta^\alpha_\beta\delta^\gamma_\delta = \frac{1}{3}\delta^\alpha_\delta\delta^\gamma_\beta + \frac{1}{2}\boldsymbol{\lambda}^\alpha_\delta \cdot \boldsymbol{\lambda}^\gamma_\beta,$$
$$\boldsymbol{\lambda}^\alpha_\beta \cdot \boldsymbol{\lambda}^\gamma_\delta = \frac{16}{9}\delta^\alpha_\delta\delta^\gamma_\beta - \frac{1}{3}\boldsymbol{\lambda}^\alpha_\delta \cdot \boldsymbol{\lambda}^\gamma_\beta.$$

Now it is not difficult to show that

$$8\delta^\alpha_\beta\delta^\gamma_\delta + 3\lambda^\alpha_\beta \cdot \boldsymbol{\lambda}^\gamma_\beta = +\left(8\delta^\alpha_\delta\delta^\gamma_\beta + 3\boldsymbol{\lambda}^\alpha_\delta \cdot \boldsymbol{\lambda}^\gamma_\beta\right)$$
$$4\delta^\alpha_\beta\delta^\gamma_\delta - 3\boldsymbol{\lambda}^\alpha_\beta \cdot \boldsymbol{\lambda}^\gamma_\delta = -\left(4\delta^\alpha_\delta\delta^\gamma_\beta - 3\boldsymbol{\lambda}^\alpha_\delta \cdot \boldsymbol{\lambda}^\gamma_\beta\right)$$

Applied to the product of two triplet spinors, the first of these expressions selects the state 6 , and the second one selects the state $\overline{3}$ (recall that $3 \times 3 = 6 + \overline{3}$).

29.2.8. SU(3) multiplets

A contravariant three-component spinor t^α is transformed by the matrices $U = \exp\left(\frac{1}{2}i\omega_i\lambda_i\right)$; it is denoted by 3 . A covariant spinor t_α is transformed by complex conjugate matrices $U^* = \exp\left(-\frac{1}{2}i\omega_i\lambda^*_i\right)$; it will be denoted by $\overline{3}$. Representations of higher dimensions can be constructed out of 3 and $\overline{3}$ by
making use of the invariant tensors $\delta^\alpha_\beta, \varepsilon_{\alpha\beta\gamma}$, and $\varepsilon^{\alpha\beta\gamma}$:

$3 \times \overline{3} = 8 + 1$:	singlet, , octet,	$1 \sim t^\alpha t_\beta\delta^\beta_\alpha$; $8 \sim T^\alpha_\beta = t^\alpha t_\beta - \frac{1}{3}\delta^\alpha_\beta\left(t^\gamma t_\gamma\right)$.
$3 \times 3 = 6 + \overline{3}$:	antitriplet,	$\overline{3} \sim T_\gamma = t^\alpha t^\beta\varepsilon_{\alpha\beta\gamma}$;
	sextet,	$6 \sim T^{\alpha\beta} = t^\alpha t^\beta + t^\beta t^\alpha$.
$3 \times 6 = 8 + 10$:		$8 \sim T^\gamma_\delta = t^\alpha t^{\beta\gamma}\varepsilon_{\alpha\beta\delta}$;
	decuplet,	$3 \sim T^\gamma = t_\alpha T^{\alpha\gamma}$;
	$3 \times 6 = 3 + 15$:	$15 \sim T^{\beta\gamma}_\alpha$.
$8 \times 8 = 1 + 8 + 8 + 10 + \overline{10} + 27$:	$\overline{10} \sim T_{\alpha\beta\gamma}$;	
		$27 \sim T^{\gamma\delta}_{\alpha\beta}$.

An arbitrary tensor can be written in the form

$$T^q_p = T^{\beta_1\beta_2\ldots\beta_q}_{\alpha_1\alpha_2\ldots\alpha_p},$$

where symmetrization is carried out separately over all upper and lower indices, and the trace for any pair $\alpha_i\beta_k$ is zero. The total number of components of the multiplet T^q_p is found easily:

$$N = \frac{1}{2}(p+1)(q+1)(p+q+2).$$

Examples of physical SU(3) multiplets:

$$q^\alpha = \begin{pmatrix} u \\ d \\ s \end{pmatrix} \quad \text{quark triplet,}$$
$$\bar{q}_\alpha = (\bar{u}, \bar{d}, \bar{s}) \quad \text{antiquark (anti)triplet,}$$

$$P^{\alpha}_{\beta} = \begin{pmatrix} \sqrt{\frac{1}{6}}\eta^0 + \sqrt{\frac{1}{2}}\pi^0 & \pi^+ & K^+ \\ \pi^- & \sqrt{\frac{1}{6}}\eta^0 - \sqrt{\frac{1}{2}}\pi^0 & K^0 \\ K^- & \tilde{K}^0 & -\frac{2\eta^0}{\sqrt{6}} \end{pmatrix} = \begin{matrix} \text{octet of} \\ \text{pseudo-} \\ \text{scalar} \\ \text{mesons ,} \end{matrix}$$

$$B^{\alpha}_{\beta} = \begin{pmatrix} \sqrt{\frac{1}{6}}\Lambda^0 + \sqrt{\frac{1}{2}}\Sigma^0 & \Sigma^+ & p \\ \Sigma^- & \sqrt{\frac{1}{6}}\Lambda^0 - \sqrt{\frac{1}{2}}\Sigma^0 & n \\ \Xi^- & \Xi^0 & -\sqrt{\frac{1}{6}}2\Lambda^0 \end{pmatrix} \quad \begin{matrix} \text{octet of} \\ \text{baryons.} \end{matrix}$$

When the isotopic subgroup SU(2) of group SU(3) is singled out, it is convenient to plot the particles of the multiplet on the so-called T_3Y diagrams. Examples are given in figs. 29.1, 2, 3.

By combining d and s (or s and u) quarks, instead of u and d, into an SU(2) doublet we single out the U (or V) spin subgroup* of SU(3) (see fig. 29.4). Figs. 29.1-4 demonstrate that particles within one U-multiplet have identical charges. The composition of U-multiplets is obvious in these figures, with the exception of the central particles on the T_3Y diagram for the octet. The point is that the Σ^0 and Λ^0 states possess a definite T-spin but no definite U-spin. It is their linear superpositions

$$\Sigma^0_U = -\frac{1}{2}\Sigma^0 + \frac{1}{2}\sqrt{3}\Lambda^0, \Lambda^0_U = -\frac{1}{2}\sqrt{3}\Sigma^0 - \frac{1}{2}\Lambda^0,$$

that possess definite U-spin: unity for the first and zero for the second.

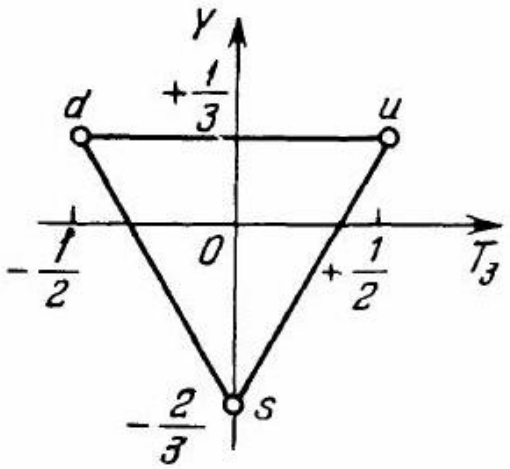


Fig. 29.1

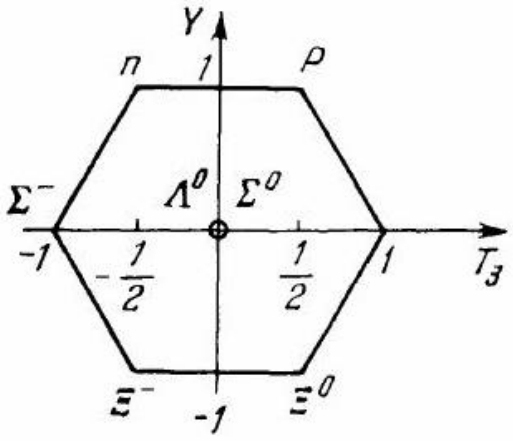


Fig. 29.2

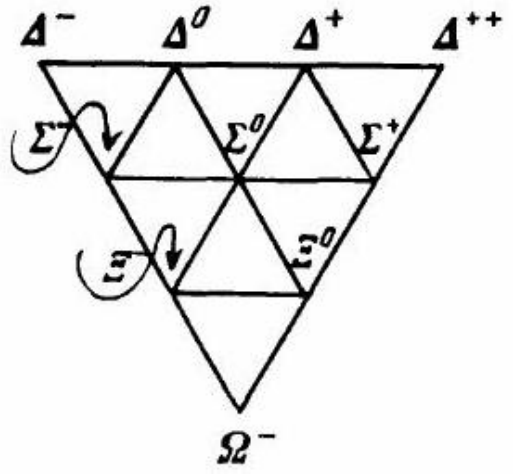


Fig. 29.3

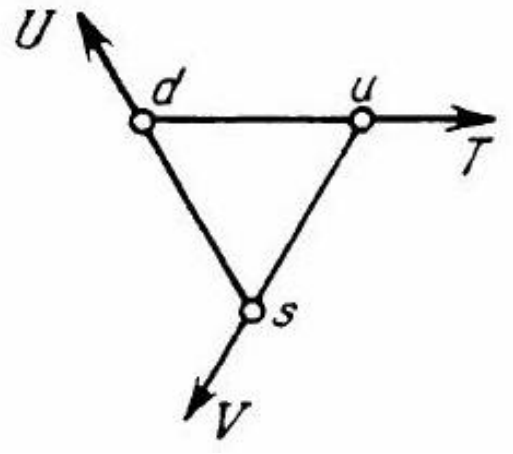


Fig. 29.4

[0]*Sometimes the minus sign is assigned to some of the particles of the SU(3) multiplet in order to make positive the matrix elements of the ladder operators of a given SU(2) subgroup (see J. J. de Swart, Rev. Mod. Phys. 35 (1963) 916).

5.29.3 29.3. Properties of Dirac matrices

29.3.1. γ-Matrices

The matrices γ^μ satisfy the condition

$$\gamma^\mu\gamma^\nu + \gamma^\nu\gamma^\mu = 2g^{\mu\nu}, \quad \mu,\nu = 0,1,2,3.$$

We use the representation

$$\gamma^0 = \begin{pmatrix} 1 & 0 \\ 0 & -1 \end{pmatrix}, \quad \gamma^i = \begin{pmatrix} 0 & \sigma_i \\ -\sigma_i & 0 \end{pmatrix}, \quad i = 1,2,3.$$

The last three matrices can be written in vector form:

$$\gamma = \begin{pmatrix} 0 & \boldsymbol{\sigma} \\ -\boldsymbol{\sigma} & 0 \end{pmatrix};$$

$$\gamma_5 = \gamma^5 = i\gamma_0\gamma_1\gamma_2\gamma_3 = -i\gamma^0\gamma^1\gamma^2\gamma^3 = -\begin{pmatrix} 0 & 1 \\ 1 & 0 \end{pmatrix}.$$

(The only difference with the notation of the well-known book by Bjorken and Drell is the sign in the definition of γ_5.)

$$\gamma^\mu\gamma^5 = -\gamma^5\gamma^\mu, \left(\gamma^5\right)^2 = 1.$$

The "scalar product" of γ^μ matrices by a 4 -vector A^μ :

$$\hat{A} \equiv A^\mu\gamma_\mu \equiv A_\mu\gamma^\mu \equiv A^0\gamma^0 - \boldsymbol{A}\cdot\boldsymbol{\gamma}.$$

By multiplying $\gamma^\mu\gamma^\nu + \gamma^\nu\gamma^\mu = 2g^{\mu\nu}$ by $g_{\mu\nu}, A_\mu B_\nu$, and finally by A_ν, we obtain, respectively:

$$\gamma^\mu\gamma_\mu = 4,$$
$$\hat{A}\hat{B} + \hat{B}\hat{A} = 2AB,$$
$$\gamma^\mu\hat{A} + \hat{A}\gamma^\mu = 2A^\mu.$$

If this last equality is multiplied from the right by $R\gamma_\mu$, where R is an arbitrary matrix expression, we obtain

$$\gamma^\mu\hat{A}R\gamma_\mu + \hat{A}\gamma^\mu R\gamma_\mu = 2R\hat{A},$$

whence

$$\begin{aligned} &\text{for } R = 1: && \gamma^\mu\hat{A}\gamma_\mu = -2\hat{A} \\ &\text{for } R = \hat{B}: && \gamma^\mu\hat{A}\hat{B}\gamma_\mu = 2\hat{A}\hat{B} + 2\hat{B}\hat{A} = 4AB \\ &\text{for } R = \hat{B}\hat{C}: && \gamma^\mu\hat{A}\hat{B}\hat{C}\gamma_\mu = -2\hat{C}\hat{B}\hat{A}. \end{aligned}$$

29.3.2 Trace of γ-matrices

The trace, Tr , is the sum of diagonal elements of a matrix.

$$\operatorname{Tr}\gamma^\mu = 0, \quad \operatorname{Tr}\gamma^5 = 0, \quad \operatorname{Tr} I = 4.$$

By definition,

$$\operatorname{Tr}\gamma^{\alpha_1}\gamma^{\alpha_2}\cdots\gamma^{\alpha_{n-1}}\gamma^{\alpha_n} = \operatorname{Tr}\gamma^{\alpha_2}\cdots\gamma^{\alpha_{n-1}}\gamma^{\alpha_n}\gamma^{\alpha_1},$$

whence, using that $(\gamma^5)^2 = 1$ and $\gamma^5\gamma^\mu = -\gamma^\mu\gamma^5$, it is not difficult to derive that the trace of a product of an odd number of matrices is zero:

$$\begin{aligned}\operatorname{Tr}\gamma^{\alpha_1}\gamma^{\alpha_2}\cdots\gamma^{\alpha_{n-1}}\gamma^{\alpha_n} &= \operatorname{Tr}\gamma^5\gamma^5\gamma^{\alpha_1}\gamma^{\alpha_2}\cdots\gamma^{\alpha_{n-1}}\gamma^{\alpha_n}\\ &= \operatorname{Tr}\gamma^5\gamma^{\alpha_1}\gamma^{\alpha_2}\cdots\gamma^{\alpha_{n-1}}\gamma^{\alpha_n}\gamma^5\\ &= -\operatorname{Tr}\gamma^{\alpha_1}\gamma^{\alpha_2}\cdots\gamma^{\alpha_{n-1}}\gamma^{\alpha_n} = 0.\end{aligned}$$

The following reduction formula for the case of even n can be obtained by using the relation $\gamma^\alpha\gamma^\beta + \gamma^\beta\gamma^\alpha = 2g^{\alpha\beta}$ and by a method similar to that used above:

$$\begin{aligned}\operatorname{Tr}\gamma^{\alpha_1}\gamma^{\alpha_2}\cdots\gamma^{\alpha_{n-1}}\gamma^{\alpha_n} =& g^{\alpha_1\alpha_2}\operatorname{Tr}\gamma^{\alpha_3}\gamma^{\alpha_4}\cdots\gamma^{\alpha_{n-1}}\gamma^{\alpha_n}\\ &- g^{\alpha_1\alpha_3}\operatorname{Tr}\gamma^{\alpha_2}\gamma^{\alpha_4}\cdots\gamma^{\alpha_{n-1}}\gamma^{\alpha_n} + \cdots\\ &+ (-1)^n g^{\alpha_1\alpha_n}\operatorname{Tr}\gamma^{\alpha_2}\gamma^{\alpha_3}\cdots\gamma^{\alpha_{n-1}}.\end{aligned}$$

In the case $n = 2$ and $n = 4$ we obtain

$$\begin{aligned}\operatorname{Tr}\gamma^\alpha\gamma^\beta &= 4g^{\alpha\beta}\\ \operatorname{Tr}\gamma^\alpha\gamma^\beta\gamma^\gamma\gamma^\delta &= 4\left(g^{\alpha\beta}g^{\gamma\delta} + g^{\alpha\delta}g^{\beta\gamma} - g^{\alpha\gamma}g^{\beta\delta}\right)\end{aligned}$$

As follows from the definition $\gamma^5 = -i\gamma^0\gamma^1\gamma^2\gamma^3$

$$\operatorname{Tr}\gamma^5\gamma^\alpha\gamma^\beta\gamma^\gamma\gamma^\delta = 4i\varepsilon^{\alpha\beta\gamma\delta},$$

where $\varepsilon^{\alpha\beta\gamma\delta}$ is a completely antisymmetric tensor of rank four ($\varepsilon^{0123} = 1$).

$$\varepsilon^{\alpha\beta\gamma\delta}\varepsilon_{\mu\nu\rho\sigma} = -\begin{Vmatrix}\delta^\alpha_\mu & \delta^\alpha_\nu & \delta^\alpha_\rho & \delta^\alpha_\sigma\\ \delta^\beta_\mu & \delta^\beta_\nu & \delta^\beta_\rho & \delta^\beta_\sigma\\ \delta^\gamma_\mu & \delta^\gamma_\nu & \delta^\gamma_\rho & \delta^\gamma_\sigma\\ \delta^\delta_\mu & \delta^\delta_\nu & \delta^\delta_\rho & \delta^\delta_\sigma\end{Vmatrix}.$$

Multiplication of this expression by δ^σ_δ yields

$$\varepsilon^{\alpha\beta\gamma\delta}\varepsilon_{\mu\nu\rho\delta} = -\begin{Vmatrix}\delta^\alpha_\mu & \delta^\alpha_\nu & \delta^\alpha_\rho\\ \delta^\beta_\mu & \delta^\beta_\nu & \delta^\beta_\rho\\ \delta^\gamma_\mu & \delta^\gamma_\nu & \delta^\gamma_\rho\end{Vmatrix}.$$

(We have made use of the relations

$$\delta^\alpha_\sigma\delta^\sigma_\delta = \delta^\alpha_\delta, \quad \delta^\delta_\sigma\delta^\sigma_\delta = 4.)$$

Likewise, we can derive

$$\begin{aligned}\varepsilon^{\alpha\beta\gamma\delta}\varepsilon_{\mu\nu\gamma\delta} &= -2\begin{Vmatrix}\delta^\alpha_\mu & \delta^\alpha_\nu\\ \delta^\beta_\mu & \delta^\beta_\nu\end{Vmatrix},\\ \varepsilon^{\alpha\beta\hat{\gamma}\delta}\varepsilon_{\mu\beta\gamma\delta} &= -6\delta^\alpha_\mu\\ \varepsilon^{\alpha\beta\gamma\delta}\varepsilon_{\alpha\beta\gamma\delta} &= -24.\end{aligned}$$

29.3.3. Dirac bispinor

The Dirac equation for a free particle with mass m and 4-momentum p has the form

$$(\hat{p} - m)u = 0$$

where u is a four-component spinor (bispinor)

$$u = \begin{pmatrix} u_1 \\ u_2 \\ u_3 \\ u_4 \end{pmatrix}.$$

Let us define the conjugate bispinor as

$$\bar{u} = u^+\gamma^0 = (u_1^*, u_2^*, -u_3^*, -u_4^*)\,.$$

It satisfies the equation

$$\bar{u}(\hat{p} - m) = 0.$$

29.3.4. Four-fermion invariants and Fierz identities for Dirac matrices

In all, 16 bilinear terms can be constructed using bispinors $\bar{a}$ and b which, in the general case, correspond to two different particles. The linear combinations of these terms form five different Lorentz-covariant quantities

Covariant quantity		Number of components
$\bar{a}b$	scalar	1
$\bar{a}\gamma^\alpha b$	vector	4
$\sqrt{\frac{1}{2}}\bar{a}\sigma^{\alpha\beta}b$	tensor	6
$\bar{a}\gamma^5\gamma^\alpha b$	axial vector	4
$\bar{a}\gamma^5 b$	pseudoscalar	1

Here $\sigma^{\alpha\beta} = \frac{1}{2}\left(\gamma^\alpha\gamma^\beta - \gamma^\beta\gamma^\alpha\right)$. The factor $\sqrt{\frac{1}{2}}$ is introduced into the definition of the tensor in order to normalize each of the six components of the tensor to unity (actually, to -1):

$$\begin{aligned}\sqrt{\frac{1}{2}}\boldsymbol{\sigma}_{\alpha\beta}\sqrt{\frac{1}{2}}\boldsymbol{\sigma}^{\alpha\beta} &= \frac{1}{4}\left(\gamma_\alpha\gamma_\beta - \gamma_\beta\gamma_\alpha\right)\gamma^\alpha\gamma^\beta \\ &= \frac{1}{4}\left(\gamma_\alpha\gamma_\beta\gamma^\alpha\gamma^\beta - \gamma_\beta\gamma_\alpha\gamma^\alpha\gamma^\beta\right) = -6.\end{aligned}$$

The remaining covariants are normalized in the same manner:

$$1 \cdot 1 = 1, \quad \gamma_\alpha\gamma^\alpha = 4, \quad \gamma_\alpha\gamma_5\gamma^\alpha\gamma^5 = -4, \quad \gamma_5\gamma^5 = 1.$$

It is possible, of course, to normalize all five variants to $+1$, by introducing i into the definitions of the tensor and the axial vector; traditionally, however, this is not done.

The Lorentz scalar can be constructed out of four bispinors $\bar{a}, b, \bar{c}, d$ in five different ways:

$$\begin{array}{cc} (\bar{a}b)(\bar{c}d) & \text{S-variant,} \\ (\bar{a}\gamma_\alpha b)\,(\bar{c}\gamma^\alpha d) & \text{V-variant,} \\ \frac{1}{2}\,(\bar{a}\sigma_{\alpha\beta}b)\left(\bar{c}\sigma^{\alpha\beta}d\right) & \text{T-variant,} \\ (\bar{a}\gamma_\alpha\gamma_5 b)\,(\bar{c}\gamma^\alpha\gamma^5 d) & \text{A-variant,} \\ (\bar{a}\gamma_5 b)\,(\bar{c}\gamma^5 d) & \text{P-variant.} \end{array}$$

Sixteen matrices ($1, \gamma_\alpha, \sigma_{\alpha\beta}, \gamma_5\gamma_\alpha, \gamma_5$) form a complete system so that any one of the above variants can be expressed as a linear superposition of variants with a changed sequence of spinors:

$$(\bar{a}O_i b)\left(\bar{c}O^i d\right) = \sum_k c_{ik}\left(\bar{a}O_k d\right)\left(\bar{c}O^k b\right),$$

where

$$O_S = 1, \quad O_V = \gamma_\alpha, \quad O_T = \sigma_{\alpha\beta}/\sqrt{2}, \quad O_A = \gamma_5\gamma_\alpha, \quad O_P = \gamma_5.$$

It can be shown (see the next section) that the coefficients c_{ik} have the values given in the table below (Fierz table):

	S	V	T	A	P
S	$\frac{1}{4}$	$\frac{1}{4}$	$-\frac{1}{4}$	$-\frac{1}{4}$	$\frac{1}{4}$
V	1	$-\frac{1}{2}$	0	$-\frac{1}{2}$	-1
T	$-\frac{3}{2}$	0	$-\frac{1}{2}$	0	$-\frac{3}{2}$
A	-1	$-\frac{1}{2}$	0	$-\frac{1}{2}$	1
P	$\frac{1}{4}$	$-\frac{1}{4}$	$-\frac{1}{4}$	$\frac{1}{4}$	$\frac{1}{4}$

Signs in the table correspond to the case of commuting spinors (c-numbers); in the case of q-numbers all coefficients change signs. Note that the table is symmetric with respect to inversion relative to the central element c_{TT} . Note also that the table must be read from left to right, but not downward. The reason is that our five invariant amplitudes are not orthogonal to one another: the Fierz matrix is not a matrix of orthogonal rotation. It is easy to verify, by looking at the Fierz matrix, that the permutation $b \leftrightarrow d$ transforms two combinations of variants into themselves with the plus sign, and three combinations with the minus sign (under the assumption of commuting bispinors):

$$\begin{array}{lll} 3(\mathrm{S}+\mathrm{P})-\mathrm{T}, & 2(\mathrm{S}-\mathrm{P})+\mathrm{V}-\mathrm{A} & \text{symmetrical,} \\ \mathrm{V}+\mathrm{A}, & \mathrm{S}+\mathrm{P}+\mathrm{T}, & 2(\mathrm{S}-\mathrm{P})-(\mathrm{V}-\mathrm{A}) \end{array} \qquad \text{antisymmetrical.}$$

In the non-relativistic limit, symmetric combinations transform into $3 + \boldsymbol{\sigma}\cdot\boldsymbol{\sigma}$, and anisymmetric ones into $1 - \boldsymbol{\sigma}\cdot\boldsymbol{\sigma}$ (indeed, in this limit $\mathrm{S} \to \mathrm{V} \to 1,\ \mathrm{A} \to\ \mathrm{T} \to -\boldsymbol{\sigma}\cdot\boldsymbol{\sigma}, \mathrm{P} \to 0$).
We recall that the expression $\frac{1}{4}(3 + \boldsymbol{\sigma}_1\cdot\boldsymbol{\sigma}_2)$ is a projection operator of a state with total spin $\boldsymbol{S}$ equal to unity, and the expression $\frac{1}{4}(1 - \boldsymbol{\sigma}_1\cdot\boldsymbol{\sigma}_2)$ is a projection operator of a state with $S = 0$. This is readily shown if we raise to the second power the equality

$$S = \frac{1}{2}\boldsymbol{\sigma}_1 + \frac{1}{2}\boldsymbol{\sigma}_2;$$
$$S(S+1) = \frac{1}{4}\boldsymbol{\sigma}_1^2 + \frac{1}{4}\boldsymbol{\sigma}_2^2 + \frac{1}{2}\boldsymbol{\sigma}_1\cdot\boldsymbol{\sigma}_2 = \frac{1}{2}(3 + \boldsymbol{\sigma}_1\cdot\boldsymbol{\sigma}_2).$$

We find, therefore, that the non-relativistic and relativistic symmetry properties are in complete agreement. Indeed, the state with $S = 0$ is antisymmetric under permutation of the spinors forming it, while that with $S = 1$ is symmetric.

So far we have been discussing five Lorentz scalars. The same Fierz matrix relates five Lorentz pseudoscalars. This is easily verified if we substitute, for instance, d by $\gamma_5 d$ in the above four-fermion expressions.

Two relations are encountered especially often in calculations of weak processes:

$$\bar{a}\gamma_\alpha(1+\gamma_5)b\cdot\bar{c}\gamma^\alpha(1+\gamma_5)d = -\bar{a}\gamma_\alpha(1+\gamma_5)d\cdot\bar{c}\gamma^\alpha(1+\gamma_5)b,$$
$$\bar{a}\gamma_\alpha(1+\gamma_5)b\cdot\bar{c}\gamma^\alpha(1-\gamma_5)d = +2\bar{a}(1-\gamma_5)d\cdot\bar{c}(1+\gamma_5)b.$$

These formulas are readily obtained from the Fierz coefficient of the V-variant. The first of them is obtained by means of the substitutions

$$\bar{a} \to \bar{a}\,(1-\gamma_5)\,, \quad b \to (1+\gamma_5)\,b,$$
$$\bar{c} \to \bar{c}\,(1-\gamma_5)\,, \quad d \to (1+\gamma_5)\,d.$$

The second one is obtained by means of the substitutions

$$\bar{a} \to \bar{a}\,(1-\gamma_5)\,, \quad b \to (1+\gamma_5)\,b,$$
$$\bar{c} \to \bar{c}\,(1+\gamma_5)\,, \quad d \to (1-\gamma_5)\,d.$$

29.3.5 Derivation of Fierz identities for Dirac matrices

In this section, we give an explicit derivation of the Fierz matrix discussed in sect. 29.3.4. First we consider some auxiliary relations.

An arbitrary $4 \times 4\gamma$-matrix can be presented as a linear combination of $16\gamma_A$ matrices:

$$\gamma = \frac{1}{4}\sum_A C_A\gamma_A, \quad A = 1,\ldots,16.$$
$$A = 1 \quad : 1 \text{ unit matrix, S-variant;}$$
$$A = 2,3,4,5 \quad : \gamma^0,\gamma^1,\gamma^2,\gamma^3, \text{ V-variant;}$$
$$A = 6,7,8,9,10,11 \quad : \sigma^{10},\sigma^{20},\sigma^{30},\sigma^{12},\sigma^{23},\sigma^{31}, \text{ T-variant;}$$
$$A = 12,13,14,15 \quad : \gamma^5\gamma^0,\gamma^5\gamma^1,\gamma^5\gamma^2,\gamma^5\gamma^3, \text{ A-variant;}$$
$$A = 16 \quad : \gamma^5, \text{ P-variant .}$$

Hence,

$$C_A = \Delta_A \operatorname{Tr}\gamma\gamma_A,$$

where

$$\Delta_A = \frac{1}{4}\operatorname{Tr}\gamma_A\gamma_A.$$

It is not difficult to demonstrate that

$$\Delta_A = +1 \quad \text{for } A = 1,2,6,7,8,13,14,15,16$$
$$\Delta_A = -1 \quad \text{for } A = 3,4,5,9,10,11,12$$

This gives:

$$\gamma = \frac{1}{4}\sum_A \Delta_A \operatorname{Tr}(\gamma\gamma_A)\,\gamma_A,$$

or, if the matrix indices are written explicitly,

$$\gamma^i_k = \frac{1}{4}\sum_A \Delta_A\left(\gamma^l_m\gamma^m_{Al}\right)\gamma^i_{Ak}$$

The last equality holds if

$$\frac{1}{4}\sum_A \Delta_A\gamma^m_{Al}\gamma^i_{Ak} = \delta^m_k\,\delta^i_l$$

Substituting $m \to m'$ and $l \to l'$ in the above expression, and multiplying by a tensor $F^m_{m'}G'_l$ in which F and G are matrix expressions, we arrive at the basic relation yielding the coefficients of the Fierz matrix:

$$F_k^m G_l^i = \frac{1}{4}\sum_A \Delta_A \left(F\gamma_A G\right)_l^m \left(\gamma_A\right)_k^i$$

We shall obtain exactly what we need if we multiply this expression by the spinors $\bar{a}^k, b_m, \bar{c}^l, d_i$; the spinors b_m and d_i change partners when we go from the left-hand side of the equation to the right-hand side.

Let us now derive the Fierz matrix row by row.

Scalar variant. In this case $F = G = 1$. Negative values of $\Delta_3, \Delta_4, \Delta_5$ give the correct sign in the scalar product $\gamma^\alpha\gamma_\alpha = \gamma_0\gamma_0 - \gamma\cdot\gamma$. The negative sign of c_{SA} appears because $\Delta_{12} = -1$. The negative sign of c_{ST} is easily confirmed if we take into account that the term $\sigma^{10}\sigma^{10}$ enters the sum $\sigma^{\alpha\beta}\sigma_{\alpha\beta}$ with a minus sign (due to the pseudo-euclidean metric).

Pseudoscalar variant. $F = G = \gamma_5$. Since γ^α commutes with $\gamma^5, c_{\mathrm{PV}} = -c_{\mathrm{SV}}, c_{\mathrm{PA}} = -c_{\mathrm{SA}}$.

Vector variant. $F = \gamma^\alpha, G = \gamma_\alpha$. The following relations determine the coefficients of the second row of the Fierz matrix:

$$\begin{array}{lll} \gamma^\alpha\gamma_A\gamma_\alpha & = 4\gamma_{\mathrm{A}} & \text{for} \\ & = -2\gamma_A & \text{for} \\ & = 0 & \text{for} \\ & = 2\gamma_A & = \gamma^\mu \\ & = -4\gamma_A & \text{for} \\ & \text{for} & \gamma_A = \gamma^{\mu\nu} \\ & \gamma_A = \gamma^5 & \end{array}$$

Axial variant. $F = \gamma^5\gamma^\alpha, G = \gamma_5\gamma_\alpha$. Calculations are similar to those of the preceding case.

Tensor variant. $F = \sqrt{\frac{1}{2}}\sigma^{\alpha\beta}, G = \sqrt{\frac{1}{2}}\sigma_{\alpha\beta}$. The following relations are used to calculate the Fierz coefficients:

$$\begin{array}{lll} \sigma^{\alpha\beta}\gamma_A\sigma_{\alpha\beta} & = -12\gamma_A & \text{for} \\ & = 0 & \text{for} \\ & = -4\gamma_A & \text{for} \\ & = 0 & \gamma_A = \gamma^\mu \\ & = -12\gamma_A & \text{for} \\ & \text{for} & \gamma_A = \gamma^5\gamma^\mu \\ & = \gamma^5. & \end{array}$$

The Fierz relations for longitudinal spinors are obtained by taking $F = \gamma^\alpha\left(1+\gamma_5\right), G = \gamma_\alpha\left(1+\gamma_5\right)$, or $F = \gamma^\alpha\left(1+\gamma_5\right), G = \gamma_\alpha\left(1-\gamma_5\right)$.

5.29.4 29.4. Rules for the calculation of probabilities

29.4.1. S - and T-matrices

Consider a set of physical states which are transformed into one another due to interactions. We shall characterize the transition from state i to state f by a quantity S_{fi}. The set of all values of S_{fi} forms the scattering matrix, also referred to as S-matrix. With all interactions switched off, the S-matrix turns into a unit matrix I : each state is transformed into itself. This means that physical processes occur if the T-matrix is non-zero, with T defined by the relation

$$S = I + iT.$$

Let us introduce the process amplitude M_{fi} as the quantity defined by the relation

$$T_{\text{fi}} = (2\pi)^4 \delta^4 (p_{\text{f}} - p_{\text{i}}) M_{\text{fi}}$$

where p_{i} and p_{f} are 4 -momenta of the initial and final states, and the δ-function expresses in an explicit form the energy-momentum conservation law:

$$\delta^4 (p_{\text{f}} - p_{\text{i}}) = \delta (p_{\text{f}}^x - p_{\text{i}}^x) \delta (p_{\text{f}}^y - p_{\text{i}}^y) \delta (p_{\text{f}}^z - p_{\text{i}}^z) \delta (E_{\text{f}} - E_{\text{i}}) .$$

For the sake of brevity the subscripts f and i in M_{fi} are hereafter dropped.

29.4.2. Probability and cross sections

The square of the absolute value of T_{fi} determines the transition probability from the initial state i to the final state f :

$$\overline{w_{\text{fi}}} = |T_{\text{fi}}|^2 = (2\pi)^4 \delta^4 (p_{\text{f}} - p_{\text{i}}) (2\pi)^4 \delta(0) |M|^2 .$$

In order to calculate $\overline{w_{\text{fi}}}$, introduce a four-dimensional normalization volume VT, which of course will be eliminated from the final result. As follows from the definition of δ^4, for $V \to \infty$ and $T \to \infty$

$$(2\pi)^4 \delta^4(0) = VT$$

In order to calculate the transition probability into a group of states instead of a single final state f , we must multiply $\overline{w_{\text{fi}}}$ by the element of the phase-space volume $\mathrm{d}\bar{\Phi}$ which is written as

$$\mathrm{d}\bar{\Phi} = \prod_{l=1}^{n} \frac{\mathrm{d}\boldsymbol{k}_l V}{(2\pi)^3},$$

where n is the number of particles in the final state, and $\boldsymbol{k}_l$ is the 3 -momentum of the l th particle.

Now we must take care of the correct normalization of the expression for the transition probability. Wave functions of particles will be normalized in such a manner that each unit volume contains $2E$ particles, where E is the energy of a particle. It is clear that this normalization corresponds, in the case of scalar particles, to the wave function $\varphi = \exp(-ikx)$. Indeed, in this case the particle density is

$$i \left(\varphi^* \frac{\partial \varphi}{\partial t} - \varphi \frac{\partial \varphi^*}{\partial t} \right) = 2E.$$

The normalized probability is obtained by dividing $\overline{w_{\text{fi}}}$ by N :

$$N = \prod_{l=1}^{n} (2E_l V) \prod_{i=1}^{k} (2E_i V) ,$$

where k is the number of particles in the initial state. A decay corresponds to $k = 1$, and a collision of two particles to $k = 2$.

As a result, the following expression is obtained for the normalized probability transition per unit time:

$$\mathrm{d}w_{\text{fi}} = \frac{\bar{w}_{\text{fi}}}{T} \frac{\mathrm{d}\bar{\Phi}}{N} = \frac{V|M|^2}{\prod_{i=1}^{k} (2E_i V)} \mathrm{d}\Phi,$$

where

$$\mathrm{d}\Phi = (2\pi)^4 \delta^4 \left(p_\mathrm{f} - p_\mathrm{i}\right) \prod_{l=1}^{n} \frac{\mathrm{d}\boldsymbol{k}_l}{(2\pi)^3 2E_l}$$

We obtain for particle decay rate ($k = 1$):

$$\mathrm{d}\Gamma = \frac{1}{2E_\mathrm{a}} |M|^2 \, \mathrm{d}\Phi$$

where E_a is the energy of the decaying particle. A collision of two particles ($k = 2$) is usually characterized by the cross section defined by

$$\mathrm{d}w_\mathrm{fi} = \mathrm{d}\sigma \cdot j,$$

where j is the flux density. The flux density in the laboratory reference frame where particle a is at rest and particle b impinges on it at a velocity v_b, is

$$j = \frac{v_\mathrm{b}}{V}.$$

As a result, the cross section is

$$\mathrm{d}\sigma = \frac{\mathrm{d}w_\mathrm{fi}}{j} = \frac{1}{2m_\mathrm{a} 2E_\mathrm{b} v_\mathrm{b}} |M|^2 \, \mathrm{d}\Phi$$

The quantity $I = m_\mathrm{a} E_\mathrm{b} v_\mathrm{b} = m_\mathrm{a} \left|\boldsymbol{p}_\mathrm{b}\right|$ can be written in an invariant form:

$$I = \sqrt{\left(p_\mathrm{a} p_\mathrm{b}\right)^2 - p_\mathrm{a}^2 p_\mathrm{b}^2}$$

and finally we obtain:

$$\mathrm{d}\sigma = \frac{1}{4\sqrt{\left(p_\mathrm{a} p_\mathrm{b}\right)^2 - m_\mathrm{a}^2 m_\mathrm{b}^2}} |M|^2 \, \mathrm{d}\Phi.$$

29.4.3. Particles with non-zero spin

So far we have been discussing the case of zero-spin particles. The formulas derived above are readily generalized to the case of particles with arbitrary
spin. The most typical situation is the calculation of Γ and σ when the polarization states of the initial particles are not fixed, and those of the final particles are not measured. In this case

$$\mathrm{d}\Gamma = \frac{1}{2J_\mathrm{a} + 1} \frac{1}{2E_\mathrm{a}} \overline{|M|^2} \, \mathrm{d}\Phi,$$

where J_a is the spin of the decaying particle, and

$$\mathrm{d}\sigma = \frac{1}{\left(2J_\mathrm{a} + 1\right)\left(2J_\mathrm{b} + 1\right)} \frac{1}{4\sqrt{\left(p_\mathrm{a} p_\mathrm{b}\right)^2 - m_\mathrm{a}^2 m_\mathrm{b}^2}} \overline{|M|^2} \, \mathrm{d}\Phi,$$

where J_a and J_b are spins of colliding particles. The bar over $|M|^2$ denotes summation over spin states of both the initial and final particles. The factors $1/\left(2J_\mathrm{a} + 1\right)$ and $1/\left(2J_\mathrm{a} + 1\right)\left(2J_\mathrm{b} + 1\right)$ take into account that we actually need to carry out averaging over polarization states of the initial particles and not the summation.

Summation over polarization states of particles with spin $\frac{1}{2}$ is easily realized by means of the relativistic-invariant density matrix:

$$\sum_s u_\imath(s)\bar{u}^k(s) = (\hat{p}+m)^k_i,$$

where p is the 4 -momentum of the particle, and m is its mass. If the spin state, s, of the particle is fixed, then

$$u(s)\bar{u}(s) = \frac{1}{2}(\hat{p}+m)\,(1-\gamma_5\hat{s})$$

(and $v(s)\bar{v}(s) = \frac{1}{2}(\hat{p}-m)\,(1-\gamma_5\hat{s})$ for an antiparticle with 4-momentum p), where

$$s^\mu = \begin{cases} s^0 = \boldsymbol{p}\cdot\boldsymbol{\xi}/m \\ \boldsymbol{s} = \boldsymbol{\xi} + (\boldsymbol{p}\cdot\boldsymbol{\xi})\boldsymbol{p}/m(m+E) \end{cases}$$

and $\boldsymbol{\xi}$ is a unit vector in the direction of polarization of the particle in its rest frame [A] It can easily be shown that

$$s^2 = -1, \quad sp = 0.$$

The relativistic-invariant density matrix, summed over spin states of a massive spin-1 particle, has the form:

$$\sum_s \varphi_\mu(s)\varphi^*_\nu(s) = -\left(g_{\mu\nu} - \frac{p_\mu p_\nu}{m^2}\right),$$

while for the photon

$$\sum_s e_\mu(s)e^*_\nu(s) = -g_{\mu\nu}.$$

5.30 30 Tables of experimental data*

CONTENTS 30.1. Physical and numerical constants and parameters 330
30.1.1. Physical and numerical constants 330
30.1.2. Electroweak interaction parameters 331
30.2. Tables of particle properties 332
30.2.1. Stable particle table 332
30.2.2. Addendum to Stable particle table 339
30.2.3. Notes to Stable particle table 341
30.2.4. Additional notes to Stable particle table 342
30.3. Weak decays and $\Delta I = \frac{1}{2}$ rule 343
30.3.1. Test of $\Delta I = \frac{1}{2}$ rule for K -decays 343
30.3.2. Tests of $\Delta I = \frac{1}{2}$ rule for hyperon decays 346
30.4. CP and CPT invariances 350
30.4.1. Violation of CP invariance in K^0 decays 350
30.4.2. Electric dipole moment of the neutron 350
30.4.3. Search for T-odd muon polarization in $\mathrm{K}^0_{\mu 3}$ decay 350
30.4.4. Test of CPT invariance 351
30.5. Conservation of leptonic numbers 352
30.5.1. Neutrino oscillations 352
30.5.2. $\mu \leftrightarrow$ e and $\tau \to \mu$(e) processes 353
30.6. Selection rules for the weak current 353
30.6.1. Absence of semileptonic decays with $\Delta S \neq \Delta Q$ 353
30.6.2. Suppression of hadronic decays with $\Delta S > 1$ or $\Delta C = -\Delta S$ 354

30.6.3. Absence of decays with $\Delta Q = 0$ for $\Delta S \neq 0$ 354
30.6.4. Absence of processes with $\Delta Q = 0$ for $\Delta S \neq 0$ or $\Delta C \neq 0$ 355
Sections 30.1.1, 30.2.1, 2, 3, and 30.3 are reproduced without modifications from the review [1] (referred to below as PDG); some important new results are added in section 30.2.4 (seealso section 30.6.3). Sections 30.4.1 and 30.4.4 are based on the Data Card Listings of PDGand the table of ref. [2], respectively. The upper bounds of the physical values listed in tables ofthis chapter are given at 90% confidence level. The data cited from PDG are given withoutreferences throughout the chapter.
References
[1] Particle Data Group, Rev. Mod. Phys. 52 (1980) No. 2, Part II
[2] H. Poth, Phys. Lett. 77B (1978) 321

5.30.1 30.1. Physical and numerical constants and parameters

30.1.1. Physical and numerical constants*

PHYSICAL CONSTANTS

[0]*This chapter was complied by I. S. Tsukerman. The author expresses his thanks to the Particle Data Group (N. Barash-Schmidt, C. Bricman, R. L. Crawford, C. Dionisi, C. P. Horne, R. L. Kelly, M. J. Losty, M. Mazzucato, L. Montanet, A. Rittenberg, M. Roos, T. Shimada, T. G. Trippe, C. G. Wohl, and G. P. Yost) and to Reviews of Modern Physics for kind permission to reprint from Review of Particle Properties the material contained in sections 30.1.1, 30.2.1, 30.2.2, 30.2.3, and 30.3 .

$N_A \ldots\ldots = 6.022045(31) \times 10^{23}$ mole^{-1}
$V_m \ldots\ldots = 22413.83(70)$cm^3 mole $^{-1}$ = molar volume of ideal gas at STP.
c ..... $= 2.99792458(1.2) \times 10^{10}$ cmsec^{-1}
e $\ldots\ldots\ldots = 4.803242(14) \times 10^{-10}$ esu $= 1.6021892(46) \times 10^{-19}$ coulomb
1MeV $\ldots = 1.6021892(46) \times 10^{-6}$erg
$\hbar = h/2\pi = 6.582173(17) \times 10^{-22}$MeVsec $= 1.0545887(57) \times 10^{-27}$ergsec
$\hbar c \ldots\ldots\ldots = 1.9732858(51) \times 10^{-11}$MeVcm $= 197.32858(51)$MeV fermi
$(\hbar c)^2 \ldots. = 0.3893857(20)$GeV^{2}mb
$\alpha \ldots\ldots\ldots = e^2/\hbar c = 1/137.03604(11)$
$k_{\text{Boltzmann}} = 1.380662(44) \times 10^{-16}$erg°K^{-1}
$= 8.61735(28) \times 10^{-11}$MeV°K$^{-1} = 1eV/11604.50(36)$°K
$\sigma_{\text{Stef. Boltz.}} = 5.67032(71) \times 10^{-5}$ergsec^{-1} cm^{-2}°K^{-4}
$= 3.53911(44) \times 10^{7}$eVsec^{-1} cm^{-2}°K^{-4}
$m_e \ldots\ldots\ldots = 0.5110034(14)$MeV $= 9.109534(47) \times 10^{-28}$ g
$m_p \ldots\ldots\ldots = 938.2796(27)$MeV $= 1836.15152(70) m_e = 6.722795(61) m_{\pi\pm} \ldots\ldots = 1.007276470(11)$amu
1amu $\ldots = 1/12 m_{C^{12}} = 931.5016(26)$MeV
$m_d \ldots\ldots\ldots = 1875.6280(53)$MeV
$r_e \ldots\ldots\ldots = e^2/m_e c^2 = 2.8179380(70)$ fermi (1 fermi $= 10^{-13}$ cm)
$\lambda_e \hbar/m_e c = r_e \alpha^{-1} = 3.8615905(64) \times 10^{-11}$ cm
$a_{\infty\ \text{Bohr}} \ldots = \hbar^2/m_e e^2 = r_e \alpha^{-2} = 0.52917706(44)$Å $\left(1$Å $= 10^{-8}$ cm$\right)$
$\sigma_{\text{Thomson ..}} = (8/3)\pi r_e^2 = 0.6652448(33)$ barn (1 barn $= 10^{-24}$ cm^2)
$\mu_{\text{Bohr}} \ldots. = e\hbar/2m_e c = 0.57883785(95) \times 10^{-14}$MeV gauss $^{-1}$
$\mu_N \ldots\ldots\ldots = e\hbar/2m_p c = 3.1524515(53) \times 10^{-18}$MeV gauss $^{-1}$
μ_p/μ_{Bohr} . $= 0.001521032\ 209(16)$
$\frac{1}{2}\omega^e_{\text{cyclotron}} = e/2m_e c = 8.794024(25) \times 10^{6}$radsec^{-1} gauss $^{-1}$
$\frac{1}{2}\omega^p_{\text{cyclotron}} = e/2m_p c = 4.789378(14) \times 10^{3}$radsec^{-1} gauss $^{-1}$
Hydrogen-like atom (nonrelativistic, μ = reduced mass):
$\left(\frac{v}{c}\right)_{\text{rms}} = \frac{z\alpha}{n}; E_n = \frac{\mu}{2}v^2 = \frac{\mu}{2}\left(\frac{cz\alpha}{n}\right)^2; a_n = \frac{n^2\hbar}{\mu z c \alpha}$
$R_\infty = m_e e^4/2\hbar^2 = m_e c^2 \alpha^2/2 = 13.605804(36)$eV (Rydberg)
$= m_e c\alpha^2/2h = 109737.3177(83)$cm^{-1}
$pc = 0.3$Hρ(MeV, kilogauss, cm)
1 year (sidereal) $\ldots\ldots\ldots = 365.256$ days $= 3.1558 \times 10^7$ sec $(\approx \pi \times 10^7$sec)
density of dry air ..... $= 1.204$mgcm^{-3} (at 20°C, 760 mm)
acceleration by gravity $\ldots = 980.62$ cmsec^{-2} (sea level, 45°)
gravitational constant .... $= 6.6720(41) \times 10^{-8}$ cm^3 g^{-1}sec^{-2}
1 atmosphere $\ldots\ldots\ldots\ldots = 1.01325$ bar (1bar $= 10^6$ dynes cm^{-2})
1 eV per particle..... $= 11604.50(36)$°K(from $E = kT$)

NUMERICAL CONSTANTS

$$\pi = 3.1415927$$
$$e = 2.7182818$$
$$\ln 2 = 0.6931472$$
$$\log_{10} 2 = 0.3010300$$
$$1\text{rad} = 57.2957795\text{deg}$$
$$1/e = 0.3678794$$
$$\ln 10 = 2.3025851$$
$$\log_{10} e = 0.4342945$$

$$\sqrt{\pi} = 1.77245385$$
$$\sqrt{2} = 1.4142136$$
$$\sqrt{3} = 1.7320508$$
$$\sqrt{10} = 3.1622777$$

Notes to Physical Constants

Revised April 1980 by Barry N. Taylor. Originally prepared by Stanley J. Brodsky, based mainly on the "1973 Least-Squares Adjustment of the Fundamental Constants," by E. R. Cohen and B. N. Taylor, J. Phys. Chem. Ref. Data 2, 663 (1973). The figures in parentheses correspond to the one-standard-deviation uncertainty in the last digits of the main number. The equivalent uncertainty in parts per million (ppm) is given in the last column. Note that the uncertainties of the output values of a least-squares adjustment are in general correlated, and the general law of error propagation must be used in calculating additional quantities.

The set of constants resulting from the 1973 adjustment of Cohen and Taylor has been recommended for international use by CODATA (Committee on Data for Science and Technology), and is the most up-to-date, generally accepted set currently available. However, since the publication of the 1973 adjustment, a number of new experiments have been completed, yielding improved values for some of the consants: $N_A = 6.0220978(63) \times 10^{23}$ mole $^{-1}(1.04\text{ppm}); \alpha^{-1} = 137.035963(15)(0.11\text{ppm})$ [obtained using the Josephson effect]; and $R_\infty = 109737.31476(32)\text{cm}^{-1}(0.003\text{ppm})$. But it must be realized that, since the output values of a least-squares adjustment are related in a complex way and a change in the measured value of one constant usually leads to corresponding changes in the adjusted values of others, one must be cautious in carrying out calculations using both the output values from the 1973 adjustment and the results of more recent experiments. A new adjustment is planned for completion by early 1982.

30.1.2. Electroweak interaction parameters

$$G = G_\mu = (1.16632 \pm 0.00004) \cdot 10^{-5}\text{GeV}^{-2}$$

(without higher order electroweak corrections (see review [1]));

$$|\sin\theta_\text{C}| = |\sin\theta_1 \cos\theta_3| = 0.219 \pm 0.011,$$
$$|\cos\theta_1| = 0.9737 \pm 0.0025;$$
$$\sin^2\theta_\text{W} = 0.230 \pm 0.009, \quad \rho = 1.010 \pm 0.098 [2],$$
$$\sin^2\theta_\text{W} = 0.238 \pm 0.011, \quad \rho = 1 \text{ (fixed) } [3].$$

Phenomenological neutral current couplings [2]:

g_L^u	g_L^d	g_R^u	g_R^d	g_V^e	g_A^e
0.351	-0.415	-0.179	-0.010	0.043	-0.545
$\pm$.037	$\pm$.055	$\pm$.032	$\pm$.046	$\pm$.066	$\pm$.045

References

[1] M. M. Nagels et al., Nucl. Phys. B147 (1979) 189
[2] K. Winter, Proc. Int. Symp. on Lepton and Photon Interactions at High Energies, Batavia, 1979, p. 258
[3] I. Liede, M. Roos, Nucl. Phys. B167 (1980) 397

5.30.2 30.2. Tables of particle properties

30.2.1. Stable Particle Table

Reprinted from PDG. For additional parameters, see section 30.2.2.
Quantities in italics have changed by more than one (old) standard deviation since April 1978.

		Mass	Mean life	Partial decay mode		
	$I^G\,(J^P)\,C_n$ [a]	(MeV)	(sec)	~~Mode~~	~~Fraction~~ [b]	
Particle		Mass ^{2}(GeV)^2	$c\tau$ (cm)			p or $p_{\max}$ [c] (MeV/c)
γ	$0,1\,(1^-)-$	0 ($< 6\times10^{-22}$)	-			stable
$\nu_{\rm e}$	$J=\frac{1}{2}$	0 (<0.00006)	stable ($> 3\times10^8$ $m_{\nu e}$(MeV))			stable
e	$J=\frac{1}{2}$	0.5110034 $\pm.0000014$	stable ($> 5\times10^{21}$y)			stable
ν_μ	$J=\frac{1}{2}$	$0(<0.57)$	stable ($> 2.6\times10^4$ m_ν(MeV))			stable
		105.65946	$\pm.000077$	$\mu^-\quad d$	$\left(\begin{smallmatrix}e\end{smallmatrix}\quad 1.4\pm0.4\right)$ %	53
	μ	$m^2 = 0.01116392$	$c\tau = 6.5868\times10^4$	$e^-\gamma\gamma$	$(<4)\times10^{-6}$	53
	$J=\frac{1}{2}$	$m_\mu - m_{\pi^*} = -33.9074$		$e^-e^+e^-$	$(<1.9)\times10^{-9}$	53
		$\pm.0012$		$e^-\gamma$	$(<1.9)\times10^{-10}$	53
				$e\ \nu_e\bar{\nu}_\mu$	($<$25	53
	$J=\frac{1}{2}$ [f]	1784	$<2.3\times10^{-12}$	$\tau^-\quad d$	(17.9 ± 1.5)%	889
		±4		$e^-\bar{\nu}\nu$	(17.0 ± 1.1)%	892
τ		$m^2 = 3.18$		hadron $^-$neutrals	(33 ± 10)%	
			$c\tau < 0.07$	† [$\pi^-\nu$	(8.2 ± 2.6)%]	887
				† [$\rho^-\nu$	(22 ± 4)%]	723
				† [$\mathbf{K}^-$ neutrals	(small)]	

				$e^-\gamma + \mu^-\gamma$ 3(hadron $^\pm$) neutrals
				† $[\pi^-\rho^0\nu$
				† $[\pi^-\pi^-\pi^+\nu($ incl. $\pi\rho\nu)$
				† $[\pi^-\pi^-\pi^+ (\geq 0\pi^0)\,\nu$ $(\geq 3$ chgd.) neutral
				† [e$^-$ chgd. parts. $+\mu^-$chgd. parts.
		139.5669	2.6030×10^{-8}	$\pi^+ \mathbf{7}_{\mu^+}{}^{\boldsymbol{d}}{}_{\boldsymbol{v}}$
	$1^-(0^-)$		$\pm.0023$	$e^+\nu$
	$1^-(0^-)$	$\pm.0012$	$c\tau = 780.4$	$\mu^+\nu\gamma$
		$m^2 = 0.0194789$	$(\tau^+ - \tau^-)/\bar{\tau} =$	$e^+\nu\pi^0$
			$(0.05 \pm 0.07)\%$	$e^+\nu\gamma$
			(test of CPT)	$e^+\nu e^+e^-$
		134.9626	0.828×10^{-16}	$\gamma\gamma$
		$\pm.0039$	$\pm.057$ S = 1.8*	γe^+e^-
	$1^-(0^-)+$	$m^2 = 0.0182149$	$c\tau = 2.5 \times 10^{-6}$	$\gamma\gamma\gamma$
		$m_{\pi^\pm} - m_{\pi^0} = 4.6043$		$e^+e^-e^+e^-$
		$\pm.0037$		$\gamma\gamma\gamma\gamma$
π^0				e^+e^-
		548.8	$\Gamma = (0.85 \pm 0.12)$keV	
		± 0.6	Neutral decays	
		S = 1.4*	$(71.0 \pm 0.7)\%$	$\gamma\gamma$ $\pi^0\gamma\gamma$ $3\pi^0$
		$m^2 = 0.3012$	S = 1.1*	$\pi^+\pi^-\pi^0$
				$\pi^+\pi^-\gamma$
	$0^+(0^-)+$			$e^+e^-\gamma$
				$e^+e^-\pi^0$
				$\pi^+\pi^-$
			Charged decays	$e^+e^-\pi^+\pi^-$
			$(29.0 \pm 0.7)\%$	$\pi^+\pi^-\pi^0\gamma$
			S = 1.1*	$\pi^+\pi^-\gamma\gamma$
				$\mu^+\mu^-$
η				$\mu^+\mu^-\gamma$
				$\mu^+\mu^-\pi^0$
				e^+e^-

		Mass	Mean life	Partial decay mode	
	$I^G\left(J^P\right)C_n{}^a$	(MeV)	(sec)		
Particle		Mass [2] $(\text{GeV})^2$	$c\tau$ (cm)	Mode	Fraction [b]
			K^+7^d		
		± 0.015	$\pm .0026$ S = 1.9*	$\pi^+\pi^0$	$(21.16 \pm 0.15)\%$
		$\mathrm{m}^2 = 0.24371$	$c\tau = 370.9$	$\pi^+\pi^+\pi^-$	$(5.59 \pm 0.03)\%$ S = 1
			$(\tau^+ - \tau^-)/\bar{\tau} =$	$\pi^+\pi^0\pi^0$	$(1.73 \pm 0.05)\%$ S = 1.3
			$(.11 \pm .09)\%$	$\mu^+\nu\pi^0$	$(3.20 \pm 0.09)\%$ S = 1
			(test of CPT)	$\mathrm{e}^+\nu\pi^0$	$(4.82 \pm 0.05)\%$ S = 1
			S = 1.2*	$\mu^+\nu\gamma$	$^e(5.8 \pm 3.5) \times 10^{-3}$
				$\mathrm{e}^+\nu\pi^0\pi^0$	$\left(1.8^{+2.4}_{-0.6}\right) \times 10^{-5}$
		$\mathrm{m_K} = -\mathrm{m_{K^0}} = -4.01$		$\mathrm{e}^+\nu\pi^+\pi^-$	$(3.90 \pm 0.15) \times 10^{-5}$
		± 0.13		$\mathrm{e}^-\bar{\nu}\pi^+\pi^+$	$(< 5) \times 10^{-7}$
		S = 1.1*		$\mu^+\nu\pi^+\pi^-$	$(0.9 \pm 0.4) \times 10^{-5}$
				$\boldsymbol{\mu^-\bar{\nu}\pi^+\pi^+}$	$(< 3.0) \times 10^{-6}$
				$\mathrm{e}^+\nu$	$(1.54 \pm 0.09) \times 10^{-5}$
				$\mathrm{e}^+\nu\gamma(\mathrm{SD}+)^l$	$(1.52 \pm 0.23) \times 10^{-5}$
				$\mathrm{e}^+\nu\gamma(\mathrm{SD}-)^t$	$(< 1.0) \times 10^{-4}$
				$\pi^+\pi^0\gamma$	$^{J,e}(2.75 \pm 0.16) \times 10$
				$\pi^+\pi^+\pi^-\gamma$	$^e(1.0 \pm 0.4) \times 10^{-4}$
				$\mu^+\nu\pi^0\gamma$	$^e(< 6) \times 10^{-5}$
				$\mathrm{e}^+\nu\pi^0\gamma$	$^e(3.7 \pm 1.4) \times 10^{-4}$
				$\mathrm{e}^+\mathrm{e}^-\pi^+$	$(2.6 \pm 0.5) \times 10^{-7}$
				$\mathrm{e}^+\mathrm{e}^+\pi^-$	$((< 1) \times 10^{-8}$
				$\mu^+\mu^-\pi^+$	$(< 2.4) \times 10^{-6}$
				$\pi^+\gamma\gamma$	$^e(< 3.5) \times 10^{-5}$
				$\pi^+\gamma\gamma\gamma$	$^e(< 3.0) \times 10^{-4}$
				$\pi^+\nu\bar{\nu}$	$(< 0.6) \times 10^{-6}$
				$\pi^+\gamma$	$(< 4$
				$\mathrm{e}^+\mu^\pm\pi^\mp$	$(< 7$
				$\mathrm{e}^-\mu^+\pi^+$	$(< 5$

K^0 / $\overline{K^0}$	$\frac{1}{2}(0^-)$	497.6750% K_{Short} , 50% K_{Long} ± 0.13 $S = 1.1^*$ $m^2 = 0.24768$			
		0.8923×10^{-10}	$\pi^+\pi^-$	$(68.61 \pm 0.24)^{\%}$	2
		$\pm .0022$	$\pi^0\pi^0$	$(31.39^{(1.24)\%\ S\ =\ 1.1*}$	2
	$\frac{1}{2}(0^-)$	$c\tau = 2.675$	$\mu^+\mu^-$	$(< 3.2) \times 10^{-7}$	2
			e^+e^-	$(< 3.4) \times 10^{-4}$	2
			$\pi^+\pi^-\gamma$	$^e(1.85 \pm 0.10) \times 10^{-3}$	2
K^0_S			$\gamma\gamma$	$(< 0.4) \times 10^{-3}$	2
		5.183×10^{-8}	$\boldsymbol{\pi^0\pi^0\pi^0}$	$(21.5 \pm 0.7)\%\ S = 1.3^*$	1
		± 0.40	$\pi^+\pi^-\pi^0$	$(12.39 \pm 0.18)\%\ S = 1.2^*$	1
		$c\tau = 1554$	$\pi^\pm\mu^\mp\nu$	$(27.0 \pm 0.5)\%\ S = 1.1^*$	2
			$\pi^\pm e^\mp\nu$(incl. $\pi e\nu\gamma$)	$(38.8 \pm 0.5)\%\ S = 1.1^*$	2
			$\pi e\nu\gamma$	$^e(1.3 \pm 0.8)\%$	2
			$\pi^+\pi^-$	$^k(0.203 \pm 0.005)\%$	2
			$\pi^0\pi^0$	$^k(0.094 \pm 0.018)\%\ S = 1.5^*$	2
			$\pi^+\pi^-\gamma$	$^e(6.0 \pm 2.0) \times 10^{-5}$	2
	$\frac{1}{2}(0^-)$		$\pi^0\gamma\gamma$	$(< 2.4\ \ ) \times 10^{-4}$	2
			$\gamma\gamma$	$(4.9 \pm 0.5) \times 10^{-4}$	2
		$m_{K_L} - m_{K_S} = 0.5349 \times 10^{10} \hbar sec^{-1}$	$e\mu$	$(< 2.0) \times 10^{-9}$	2
		± 0.0022	$\mu^+\mu^-$	$(9.1 \pm 1.9) \times 10^{-9}$	2
			$\mu^+\mu^-\gamma$	$(< 7.8) \times 10^{-6}$	2
			$\mu^+\mu^-\pi^0$	$(< 5.7) \times 10^{-5}$	1
			e^+e^-	$(< 2.0) \times 10^{-9}$	2
			$e^+e^-\gamma$	$(< 2.8) \times 10^{-5}$	2
			$\pi^+\pi^-e^+e^-$	$(< 8.8) \times 10^{-6}$	2
K^0_L			$\boldsymbol{\pi^0\pi^\pm e^\mp\nu}$	$(< 2.2) \times 10^{-3}$	2

Particle	$I^G\left(J^P\right) C_n{}^a$	Mass Mean life		
		Mass [2] (GeV) [2]	(sec)	Mode
				$D^+ \overbrace{K^-}^{d}$ anything
				$1868.3'$
				$\left(2.5^{+35}_{-1}\right) \times 10^{-13}$
				K^-
				$\left(\ 10\ \ \pm 7\ \right)\%$
$D^\pm$	$\frac{1}{2}\,(0^-)^f$	$m^2 = 3.491$	$c\tau = 0.007$	† $[\overline{K} * (892)^0 \boldsymbol{\pi}^+$
		$m_{D^+} - m_{D^0} = 5.0$		† $[K^- K^+ \pi^+$
		± 0.8		$\overline{K}{}^0$ anything
				† $\left[\overline{K}{}^0 \boldsymbol{\pi}^+\right.$
				$e^\pm$anything
				K^+anything
				$K^+ \pi^+ \pi$
	$\frac{1}{2}\,(0^-)^f$	1863.1^1	$\left(3.5^{+35}_{-17}\right) \times 10$	$D^{\,0d}$
		± 0.9		† $[K^- \pi^\dagger$
		$m^2 = 3.471$	$c\tau = 0.01$	† $[K^- \pi^+ \pi^0$
				† $[K^- \pi^+ \pi^+ \pi^-$
D^0				$\overline{K}{}^0$ anything $+K^0$
$\overline{D}{}^0$			$\frac{\Gamma\left(D^0 \to \overline{D}{}^0 \to\ K^+ \pi^{--}\right)}{\Gamma(D^0 \to\ K\tau)} < 0.16$	† $\left[\overline{K}{}^0 \boldsymbol{\pi}^0 + K^0 \boldsymbol{\pi}^0\right.$
				† $\left[\overline{K}{}^0 \boldsymbol{\pi}^+ \boldsymbol{\pi}^- + K^0 \boldsymbol{\pi}\right.$
				e^+anything
				$\pi^+ \pi$
				$K^+ K^-$
p	$2\left(\frac{1}{2}^+\right)$	$938.2796 \pm 0.0027 m^2 = 0.880369$	stable ($> 10^{30}$y)	stable

	$O\left(\frac{1}{2}^+\right)$	1115.60 ±0.05	2.632×10^{-10} ±.020 S = 1.6*	p π^- $n\pi^0$	$(64.2 \pm 0.5)\%$ ($35.8^{-0.5}$)% $(8.07 \pm 0.28) \times 10^{-4}$	
			$c\tau = 7.89$		$(1.57 \pm 0.35) \times 10^{-4}$	
Λ					[e] $(0.85 \pm 0.14) \times 10^{-3}$	
		S = 1.2* $m^2 = 1.2446$ $m_\Lambda - m_{\Sigma^0} = -76.86$ ±0.08		$pe^-\nu$ $p\mu^-\nu$ $p\pi^-\gamma$		
		1189.36		$p\pi^0$	$(51.64 \pm 0.30)\%$	1
		±0.06	0.800×10^{-10}	$n\pi^+$	(48.36)%	1
		S = 1.8*	±.004	$p\gamma$	$(1.24 \pm 0.18) \times 10^{-3}$ S = 1.4*	2
	($1\frac{1}{2}^+$)	$m^2 = 1.4146$	$c\tau = 2.40$	$n\pi^+\gamma$	[e] $(0.93 \pm 0.10) \times 10^{-3}$	1
				$\Lambda e^+\nu$	$(2.02 \pm 0.47) \times 10^{-5}$	7
			$\frac{\Gamma(\Sigma^+ \to l^+ n\nu)}{\Gamma(\Sigma^- \to l^- n\nu)} < .04$	$n^+\nu$	$(< 3.0) \times 10^{-5}$	2
Σ^+		$m_{\Sigma^+} - m_{\Sigma^-} = \begin{matrix} -7.98 \\ \pm .08 \end{matrix}$		$ne^+\nu$	$(< 0.5) \times 10^{-5}$	2
		S = 1.2*		pe^+e^-	$(< 7) \times 10^{-6}$	2
		1192.46	5.8×10^{-20}	$\Lambda\gamma$	100 %	7
	$1\left(\frac{1}{2}^+\right)^p$	±0.08	±1.3	Λe^+e^-	[g] $(5.45) \times 10^{-3}$	7
Σ^0		$m^2 = 1.4220$	$c\tau = 1.7 \times 10^{-9}$	$\Lambda\gamma\gamma$	(<3)%	7
		1197.34	1.482×10^{-10}	$n\pi^-$	100 %	1
		±0.05	±.011 S = 1.3*	$ne^-\nu$	$(1.08 \pm 0.04) \times 10^{-3}$	2
	$1\left(\frac{1}{2}^+\right)$	$m^2 = 1.4336$	$c\tau = 4.44$	$n\mu^-\nu$	$(0.45 \pm 0.04) \times 10^{-3}$	2
				$\Lambda e^-\nu$	$(0.61 \pm 0.05) \times 10^{-4}$	7
Σ^-		$m_{\Sigma^0} - m_{\Sigma^-} = -4.88$		$n\pi^-\gamma$	[e] $(4.6 \pm 0.6) \times 10^{-4}$	1

Particle	$I^G\left(J^P\right)C_n$ [a]	Mass Mass [2] $(\mathrm{GeV})^2$	Mean life (sec)	Partial decay mode Mode	Fraction [b]	p or p
		1314.9	2.90×10^{-10}	$\Lambda\pi^0$	100	135
		± 0.6	$\pm .10$	$\Lambda\gamma$	$(0.5 \pm 0.5)\%$	184
		$m^2 = 1.7290$	$c\tau = 8.69$	$\Sigma^0\gamma$	$(< 7)\%$	117
				$p\pi$	$(< 3.6) \times 10^{-5}$	299
	$\frac{1}{2}\left(\frac{1}{2}^+\right)^q$			$pe^-\nu$	$\left(< 1.3 \right) \times 10^{-3}$	323
				$\Sigma^+e^-\nu$	$(< 1.1) \times 10^{-3}$	120
				$\Sigma^-e^+\nu$	$(< 0.9) \times 10^{-3}$	112
		$m_{\Xi^0} - m_{\Xi^-} = -6.4$		$\Sigma^+\mu^-\nu$	$(< 1.1) \times 10^{-3}$	64
		$\pm .6$		$\Sigma^-\mu^+\nu$	$(< 0.9) \times 10^{-3}$	49
Ξ^0				$p\mu^-\nu$	$(< 1.3) \times 10^{-3}$	309
		1321.32	1.641×10^{-10}	$\Lambda\pi^-$	100	139
		± 0.13	$\pm .016$	$\Lambda e^-\nu$	$(2.8 \pm 1.2) \times 10^{-4}$	190
		$m^2 = 1.7459$	$c\tau = 4.92$	$\Sigma^0e^-\nu$	$\left(< 5 \right) \times 10^{-4}$	123
				$\Lambda\mu^-\nu$	$(3.1 \pm 1.2) \times 10^{-4}$	163
				$\Sigma\mu^-\nu$	$\left(< 8 \right) \times 10^{-4}$	70
				$n\pi^-$	$(< 1.1) \times 10^{-3}$	303
	$\frac{1}{2}\left(\frac{1}{2}^+\right)^q$			$ne^{-\nu}$	$(< 3.2) \times 10^{-3}$	327
				$n\mu^-\nu$	$(< 1.5))\%$	313
				$\Sigma^-\gamma$	$(< 1.2) \times 10^{-3}$	118
				$p\pi^-\pi^-$	$\left(< 4 \right) \times 10^{-4}$	223
				$p\pi^-e^-\nu$	$\left(< 4 \right) \times 10^{-4}$	304
				$p\pi^-\mu^-\nu$	$(< 4) \times 10^{-4}$	250
Ξ^-				$\Xi^0e^-\nu$	$(< 2.3) \times 10^{-3}$	6
		1672.22	0.82×10^{-10}	ΛK^-	$(68.6 \pm 1.3)\%$	211
		$\pm .31$	$\pm .03$	$\Xi^0\pi^-$	$(23.4 \pm 1.3)\%$	293
		$m^2 = 2.7963$	$c\tau = 2.5$	$\Xi^-\pi^0$	$(8.0 \pm 0.8)\%$	290
	$0\left(\frac{3}{2}^+\right)^q$			$\Xi^0e^-\nu$	$(\tilde{}1)\%$	319
				$\Xi(1530)^0\pi^-$	$(\sim 2) \times 10^{-3}$	15
				$\Lambda\pi^-$	$(< 1.3) \times 10^{-3}$	449
Ω^-				$\Xi^-\gamma$	$(< 3.1) \times 10^{-3}$	314

Magnetic Moment e $1.00115965241\frac{e\hbar}{2\ m_e c}$ $\pm.00000000020$				
μ	$1.001165924\frac{e\hbar}{2\ m_\mu c}$ $\pm.000000009$			
				$\rho = 0.752 \pm 0.003$ $\xi = 0.972 \pm 0.013$ $\mid g_A/g_v \mid = 0.86^{+0.33}_{-0.11}$
η	Mode $\pi^+\pi^-\pi^0$ $\pi^+\pi^-\gamma$			Left-right asymmetry $(0.12 \pm .17)\%$ $(0.88 \pm .40)\%$
$K^\pm$ $K^\pm$	Mode $\mu\nu$		Partial rate ($\mathbf{sec}^{-1}$) $(51.33 \pm 0.17) \times 10^6$ S = 1.2* $(17.10 \pm 0.13) \times 10^6$ S = 1.1* $(4.52 \pm 0.02) \times 10^6$ S = 1.1* $(1.40 \pm 0.04) \times 10^6$ S = 1.3* $(2.58 \pm 0.07) \times 10^6$ S = 1.7* $(3.90 \pm 0.04) \times 10^6$ S = 1.1*	Slope parameters for $K \rightarrow \mathbf{3\pi^t}$ K^+ – K^- – $K^\pm$ – K^0_L –
K^0_S $\pi^+\pi^-$ $^k(0.7689 \pm .0033) \times 10^{10}$ $\pi^0\pi^0$ $^k(0.3517 \pm .0029) \times 10^{10}$ **S** = 1.1*				K^+_{l3} { $\lambda^e_+ = 0.029 \pm .004$ $\lambda^\mu_+ = 0.026 \pm .008$ $\lambda^\mu_0 = -0.003 \pm .007$ See Data Card Listings for ξ, f_s, and

*Reprinted from PDG

	Decay parameters [v]				
Magnetic					
			ϕ (degree)	$\gamma \quad \Delta$ (degree)	g_A/g_V
			ϕ (degree)	$\gamma \quad \Delta$ (degree)	g_v/g_A
p $\pm .0000011$					
n^w -1.91304184 $\pm .00000088$	pe $^-\nu$ pe$^-\nu$				-1.254 ± 0.0
$\Lambda^w \quad -0.614 \pm .005$	p π^- nπ^0	0.642 ± 0.013	$(-6.5 \pm 3.5)^\circ$	$0.76\ (7.7^{+4.0}_{-4.1})^\circ$	-0.62 ± 0.05
Σ^+ $2.33 \pm .13$	p π^0	-0.979 ± 0.016	$(36 \pm 34)^\circ$	0.17	
	nπ^+	$+0.068 \pm 0.013$	$(167 \pm 20)^\circ$	-0.97	
	pr	$-1.03^{+0.52}_{-0.42}$	S = 1.1*		
	nπ^-	-0.068 ± 0.008	$(10 \pm 15)^\circ$		$\pm(0.385 \pm 0.$
-1.41 $\pm .25$	ne$^-\nu$			$(82^{+12}_{-13})^\circ$	$\pm(0.384 \pm 0.070)$S = 2.3*
	Λe$^-\nu$				
Ξ^0 -1.20 $\pm .06$	$\Lambda\pi^0$	-0.47 ± 0.05S = 1.3*	$(21 \pm 12)^\circ$	$0.84 \quad (216^{+13}_{-19})^\circ$	
$\Xi^- -1.85 \pm .75$	$\Lambda\pi^-$	-0.403 ± 0.017	$(2 \pm 6)^\circ$ $S = 1.1^*$	$0.92(185 \pm 13)^\circ$	
Ω^-	ΛK$^-$			-0.26 ± 0.33	

30.2.3. Notes to Stable Particle Table*

→ Indicates an entry in the Stable Particle Data Card Listings not entered in the Stable Particle Table. This is the case for ν_τ, for the charmed-strange meson $F^=$, and for listings of searches for heavy leptons other than $\tau^\pm$, intermediate boson searches, quark searches, magnetic monopole searches, charm searches, and other particle searches.

- S = Scale factor = $\sqrt{\chi^2/(N-1)}$, where N ≈ number of experiments. S should be ≈ 1. If S > 1, we have enlarged the error of the mean, $\delta\bar{x}$; i.e., $\delta\bar{x} \rightarrow$ S$\delta\bar{x}$. This convention is still inadequate, since if $S \gg 1$ the experiments are probably inconsistent, and therefore the real uncertainty is probably even greater than $\mathbf{S\delta x}$. See text, and ideograms in Stable Particle Data Card Listings.
  † Square brackets indicate a subreaction of the previous (unbracketed) decay mode.
  a. The baryon number B , strangeness S , and charm C of the hadrons which appear in the tables are as follows:

Mesons (B = 0)	S	C	Baryons (B = 1)	S	C
π, η	0	0	p, n	0	0
K^+, K^0	+1	0	Λ, Σ	-1	0
$K^-, \overline{K}^0$	-1	0	Ξ	-2	0
D^+, D^0	0	+1	Ω^-	-3	0
$D^-, \overline{D}^0$	0	-1	Λ_c^+	0	+1

b. Quoted upper limits correspond to a 90% confidence level.
c. In decays with more than two bodies, p_{max} is the maximum momentum that any particle can have.
d. For simplicity, decay mode charge states are written for the particle shown. For antiparticle modes all particles must be charge conjugated.
e. See Stable Particle Data Card Listings for energy limits used in this measurement.
f. . Quantum numbers shown are favored but not yet established. See Data Card Listings.
g. Theoretical value; see also Stable Particle Data Card Listings.
h. See note in Stable Particle Data Card Listings.
i. Structure-dependent part with positive (SD +) and negative (SD -) photon helicity.
j. The direct emission branching fraction is $(1.56 \pm .35) \times 10^{-5}$.
k. The $K_S^0 \rightarrow \pi\pi$ and $K_L^0 \rightarrow \pi\pi$ rates (and branching fractions) are from independent fits and do not include results of $K_L^0 - K_S^0$ interference experiments. The $|\eta_{+-}|$and $|\eta_{00}|$ values given in the addendum are these rates combined with the $|\eta_{+-}|$and $|\eta_{00}|$ results from interference experiments.
l. Error does not include 0.13% uncertainty in the absolute SPEAR energy calibration. Assumes $m_\psi = 3095$MeV.
m. This is a weighted average of $D^\pm(44\%)$ and $D^0(56\%)$ branching fractions.
n. Limit from neutrality-of-matter experiments. Assumes $|q_n| = |q_p| - |q_e|$.
p. J^P not measured for Σ^0. Assumed same as $\Sigma^\pm$to allow isotriplet association.
q. P for Ξ and J^P for Ω^-not yet measured. Values shown are SU(3) predictions.
r. J^P for Λ_c^+not yet measured. Values shown are SU(4) predictions.
s. $|g_A/g_V|$ defined by $g_A^2 = |C_A|^2 + |C'_A|^2$, $g_V^2 = |C_V|^2 + |C'_V|^2$, and $\Sigma\langle\bar{e}|\Gamma_t|\mu\rangle\langle\bar{\nu}|\Gamma_i\,(C_i + C'_i\gamma_5)\,|\nu\rangle$; ϕ defined by $\cos\phi = -\,\mathrm{Re}\,(C_A^* C'_V + C'_A C^*_V)\,/g_A g_V$ [for more details, see text Section VI A].

t. The definition of the slope parameter of the Dalitz plot is as follows [see also text Section VI B.1]:

$$|M|^2 = 1 + g\left(\frac{s_3 - s_0}{m_{\pi^+}^2}\right)$$

[0]*Reprinted from PDG

u. The definition for the CP violation parameters is as follows [see also text Section VI B.3]:

$$\eta_{+-} = |\eta_{+-}|\, e^{i\phi_{+-}} = \frac{\mathrm{A}\left(\mathrm{K_L^0} \to \pi^+\pi^-\right)}{\mathrm{A}\left(\mathrm{K_S^0} \to \pi^+\pi^-\right)}, \quad \eta_{00} = |\eta_{00}|\, e^{i\phi_{00}} = \frac{\mathrm{A}\left(\mathrm{K_L^0} \to \pi^0\pi^0\right)}{\mathrm{A}\left(\mathrm{K_S^0} \to \pi^0\pi^0\right)}$$

$$\delta = \frac{\Gamma\left(\mathrm{K_L^0} \to l^+\right) - \Gamma\left(\mathrm{K_L^0} \to l^-\right)}{\Gamma\left(\mathrm{K_L^0} \to l^+\right) + \Gamma\left(\mathrm{K_L^0} \to l^-\right)}, \quad |\eta_{+-0}|^2 = \frac{\Gamma\left(\mathrm{K_S^0} \to \pi^+\pi^-\pi^0\right)^{\text{CP viol.}}}{\Gamma\left(\mathrm{K_L^0} \to \pi^+\pi^-\pi^0\right)}$$

$$|\eta_{000}|^2 = \frac{\Gamma\left(\mathrm{K_S^0} \to \pi^0\pi^0\pi^0\right)^{\text{CP viol.}}}{\Gamma\left(\mathrm{K_L^0} \to \pi^0\pi^0\pi^0\right)}.$$

v. The definition of these quantities is as follows [for more details on sign convention, see text Section VI B]:

$$\boldsymbol{\alpha} = \frac{2|\ s\|p|\cos\Delta}{|s|^2+|p|^2} \quad \boldsymbol{\beta} = \frac{-2|\ s\|p|\sin\Delta}{|s|^2+|p|^2} \quad \left| \quad \boldsymbol{\beta} = \sqrt{1-\boldsymbol{\alpha}^2}\sin\phi \quad \gamma = \sqrt{1-\boldsymbol{\alpha}^2}\cos\phi \right. \quad \left| \quad \mathrm{g_A/g_V} \text{ defined by } \langle \mathbf{B_f}|\, \gamma_\lambda\left(\mathrm{g_V} - \mathrm{g_A}\gamma_5\right)|\mathbf{B_i}\rangle \right. \quad \delta \text{ defined by } \mathrm{g_A/g_V} = |\mathrm{g_A/g_V}|\, \mathrm{e}^{\mathrm{i}\delta}$$

w. For limits on electric dipole moment of n and Λ, see Data Card Listings.

30.2.4. Additional notes to Stable Particle Table

Some important results of the recent mass and lifetime measurements are given below:

ν_{e}	$m_{\nu_{\mathrm{e}}} < 35\mathrm{eV}$ [1]; $14\mathrm{eV} \le m_{\nu_{\mathrm{e}}} \le 46\mathrm{eV}$ (99% c.l.) [2]
$\tau^{\pm}$	$\tau_\tau \pm < 1.4 \cdot 10^{-12}\,\mathrm{sec}$(95% c.l.) [3]
$\mathrm{D}^{\pm}$	$\tau_{\mathrm{D}^{\pm}} = 11.2 \pm 5.1[4], 2.5^{+2.2}_{-1.1}[5], 10.4^{+3.9}_{-2.9}[6], 10.3^{+10.5}_{-4.1}[7]\ (\times 10^{-13}\mathrm{sec})$
$\mathrm{D}^{\ 0}$	$\tau_{\mathrm{D}^0} = 3.7 \pm 2.8[4], 0.53^{+.57}_{-.25}[5], < 2.1(95\%\ \text{c.l. })[6], 1.00^{+.52}_{-.31}[7]\ (\times 10^{-13}\mathrm{sec})$
n	$\tau_{\mathrm{n}} = 877 \pm 8[8], 937 \pm 18[9](\mathrm{sec})$
Λ_{c}^+	$^4\ \mathrm{m}_{\Lambda_{\mathrm{c}}^+} = 2.285 \pm 0.003\mathrm{GeV}[10], \tau_{\Lambda_{\mathrm{c}}^+} = \left(1.14^{+.90}_{-.44}\right) \cdot 10^{-13}\,\mathrm{sec}[7]$

References

[1] V. A. Lubimov, Proc. 18th Int. Conf. High Energy Phys., Tbilisi (1976), Vol. 2, p. B118
[2] V. A. Lubimov et al., Phys. Lett. 94B (1980) 266
[3] R. Brandelick et al., Phys. Lett. 92B (1980) 199
[4] R. H. Schindler, SLAC Report No. 219 (1979)
[5] D. Allasia et al., Nucl. Phys. B176 (1980) 13
[6] W. Bacino et al., Phys. Rev. Lett. 45 (1980) 329
[7] N. Ushida et al., Phys. Rev. Lett. 45 (1980) 1049 and 1053
[8] L. N. Bondarenko et al., Pis'ma ZhETF 28 (1978) 329 [JETP Lett. 28 (1978) 303]
[9] J. Byrne et al., Phys. Lett. 92B (1980) 274
[10] P. Musset, Proc. Neutrino '80 Conf., Erice (1980)

5.30.3 30.3. Weak decays and $\Delta I = \frac{1}{2}$ rule*

30.3.1. Test of $\Delta I = \frac{1}{2}$ rule for K-decays

The quantities of interest for making tests of theoretical predictions regarding the $\Delta I = \frac{1}{2}$ rule for K decay are usually partial decay rates for single channels or special sums of.channels. It is not possible to compute the errors on sums, differences, and ratios of partial decay rates from the information given in the Table of Stable Particles because of the presence of off-diagonal terms in the error matrix. For this reason we give some of these quantities in table 1. Throughout this appendix, numbers in italics are used to indicate that a quantity has changed

by more than one (old) standard deviation since our previous edition, and S gives the scale factor included in the quoted error because of inconsistencies in the data (see footnote at end of Stable Particle Table for definition of S).

Table 1
(000) and $(+-0)$ refer to the sign of the pions into which the $K_{L

$ decays.}

$\Gamma_{K^+_{13}} = \Gamma_{K^+_{e3}} + \Gamma_{K^+_{\mu 3}}$	$= (6.484 \pm 0.089) 10^6 \text{sec}^{-1}$	
$\Gamma_{K^+_{\mu 3}}/\Gamma_{K^+_{e3}}$	$= 0.663 \pm 0.018$	S = 1.7*
$\Gamma_{K^+_{\tau}}/\Gamma_{K^+_{\tau}}$	$= 3.226 \pm 0.082$	
$\Gamma_{K^0_{13}} = \Gamma_{K^0_{e3}} + \Gamma_{K^0_{\mu 3}}$	$= (12.70 \pm 0.15) 10^6 \text{sec}^{-1}$	S = 1.1*
$\Gamma_{K^0_{\mu 3}}/\Gamma_{K^0_{e3}}$	$= 0.695 \pm 0.017$	
$\Gamma_{K^0(000)}/\Gamma_{K^0(+-0)}$	$= 1.733 \pm 0.076$	S = 1.3*

1. Leptonic decay rates

The $\Gamma_{K_{/3}}$ rates are useful in testing the leptonic $\Delta I = \frac{1}{2}$ rule in the way suggested by Trilling [1]. The predictions are

$$\Gamma_{K^0_{13}}/2\Gamma_{K^+_{13}} = 1.012, \text{ a phase-space factor [2]},$$

and

$$\Gamma^0_{K^0_{\mu 3}}/\Gamma_{K^0_{e3}} = \Gamma_{K^+_{\mu 3}}/\Gamma_{K^+_{e3}}.$$

From Table 1,

$$\Gamma_{K^0_{13}}/2\Gamma_{K^+_{13}} = 0.979 \pm 0.018$$

and

$$\left[\frac{\Gamma_{K^0_{e3}}}{\Gamma_{K^0_{\mu 3}}}\right]^{\Gamma_{K^+_{\mu 3}}}_{\Gamma_{K^+_{e3}}} = 1.048 \pm 0.038.$$

These results seem to show a less than 2σ disagreement with the predictions, but the errors should be regarded with caution in view of the internal disagreements in the data. (Note the ideograms in the Data Listings for the charged K meson.)

2. Three-pion decays

We follow here the tests done by Mast et al. [3], based on the general analysis of K decays suggested by Zemach [4]. Both decay rates (Γ) and slopes (g , the energy dependence of the Dalitz plot distributions) are used. The $\Delta I = 1/2$ rule predicts that the following test quantities are all equal to zero:

[0]*Reprinted from PDG

$$\text{Test 1} = \frac{2}{3}\frac{\Gamma_{\mathrm{K}^0(000)}}{\phi_1}\left[\frac{\Gamma_{\mathrm{K}^0(+-0)}}{\phi_2}\right]^{-1} - 1,$$

$$\text{Test 2} = \frac{1}{4}\frac{\Gamma_{\mathrm{K}^+_\tau}}{\phi_3}\left[\frac{\Gamma_{\mathrm{K}^+_{\tau+}}}{\phi_4}\right]^{-1} - 1,$$

$$\text{Test 3} = \frac{1}{2}\frac{\Gamma_{\mathrm{K}^+_\tau}}{\phi_3}\left[\frac{\Gamma_{\mathrm{K}^0(+-0)}}{\phi_2}\right]^{-1} - 1,$$

$$\text{Test 4} = \frac{1}{2}\,\mathrm{g}_{\mathrm{K}^+_{\tau+}} + \mathrm{g}_{\mathrm{K}^+_\tau},$$

$$\text{Test 5} = \mathrm{g}_{\mathrm{K}^0(+-0)} + \mathrm{g}_{\mathrm{K}^+_\tau} - \frac{1}{2}\,\mathrm{g}_{\mathrm{K}_{\tau+}}.$$

The ϕ_l are phase-space factors which have been calculated as described in Mast et al. [3] by use of a relativistic formulation and the masses and slopes from this edition. The factors labeled UDP are the relative areas of the Dalitz plot's, assuming a uniform distribution. The NUDP include the observed slopes (see below). The CNUDP have been calculated by including the final-state Coulomb interaction. The values are:

	Method		
$\phi_1(000) =$	UDP	NUDP	CNUDP
$\phi_2(+-0) =$	1.490	1.490	1.444
$\phi_3(++-) =$	1.221	1.303	1.287
$\phi_4(+00) =$	1.000	1.000	1.000
	1.247	1.173	1.137

For convenience, we repeat the slope parameters tabulated in the Stable Particle Table. They are as follows:

$g_{\mathrm{K}^+_\tau}$	$= -0.215 \pm 0.004$	S = 1.4*
$g_{\mathrm{K}^-_\tau}$	$= -0.217 \pm 0.007$	S = 2.5*
$\bar{g}_{\mathrm{K}^+_\tau}$	$= -0.215 \pm 0.003$	
$g_{\mathrm{K}^+_\tau}$	$= 0.607 \pm 0.030$	$S = 1.7^*$
$g_{\mathrm{K}^0(+-0)}$	$= 0.670 \pm 0.014$	S = 1.6*

A difference in the $\tau^+$and τ^-slopes would be an indication of CP violation in this decay. Since no difference is observed at this time, we average the two and use this value in Test 4 and Test 5.

We use the CNUDP factors and the rates and slopes reported in this edition to compute the five test quantities which the $\Delta I = \frac{1}{2}$ rule predicts to be zero. The results are:

$$\text{Test 1} = 0.030 \pm 0.045$$
$$\text{Test 2} = -0.083 \pm 0.023$$
$$\text{Test 3} = 0.216 \pm 0.020$$
$$\text{Test 4} = 0.088 \pm 0.016$$
$$\text{Test 5} = 0.152 \pm 0.021$$

The three-pion final state can be in isospin states $I = 1, 2, 3$. Tests 1 and 2 test the existence of isospin $I = 3$ in the final state. Since the rate tests (Tests 1, 2, and 3) could differ from zero by as much as 0.1 owing to the mass differences and the occurrence of big slopes [5], no evidence for $I = 3$ is found. Test 4 is related to the $I = 2$ amplitude in the final state and indicates the presence of $I = 2$. Tests 3 and 5 give information on the $\Delta I = \frac{3}{2}$ part of the $I = 1$ amplitude relative to the $\Delta I = \frac{1}{2}$ part. Both tests indicate the presence of $\Delta I = \frac{3}{2}$.

References

[1] G. Trilling, K-Meson Decays, UCRL-16473 (updated from Argonne Conference Proceedings, 1965, p. 115)
[2] N. Brene (CERN), private communication. In our Jan. 1968 edition we had erroneously used 1.04
[3] T. S. Mast, L. K. Gershwin, M. Alston-Garnjost, R. O. Bangerter, A. Barbaro-Galtieri, J. J. Murray, F. T. Solmitz, and R. D. Tripp, Phys. Rev. 183, 1200 (1969)
[4] C. Zemach, Phys. Rev. 133, B1201 (1964)
[5] C. Bouchiat and M. Veltman, Topical Conference on weak interactions, CERN 69-7 (1969) p. 225

30.3.2. Test of $\Delta I = \frac{1}{2}$ rule for hyperon decays

1. Non-leptonic decay amplitudes

In this edition we again use the new convention for the amplitudes A and B adopted in 1973. Some theorists have suggested that dimensionless amplitudes are more useful to them than the ones appearing in the literature. Berge [1] used a convention with A and B in units of $\sec^{-1/2}$. Samios [2] used a convention which gave A and B in units of $(\ \mathrm{MeV} \cdot \sec)^{-1/2}$. Following is the convention suggested by Jackson [3], which gives dimensionless A and B.

The effective Lagrangian density for non-leptonic hyperon decays ($\mathrm{B}_1 \rightarrow\ \mathrm{B}_2 + \pi$) can be written

$$\mathcal{L}_{\text{eff}} = G\mu_c^2 \left[\bar{\psi}_2 \left(A + B\gamma_5\right) \psi_1\right] \phi_\pi,$$

where $G = 10^{-5} m_p^{-2}$ is a coupling constant characteristic of first-order weak decays, μ_c is the charged pion mass, and A and B are dimensionless complex numbers giving the relative amplitudes of the parity-violating and parityconserving decays, respectively. The matrix γ_5 is to be taken in the Pauli form, $\gamma_5 = \begin{pmatrix} 0 & -I \\ -I & 0 \end{pmatrix}$. The invariant amplitude for the decay is

$$\mathscr{N} = G\mu_c^2 \left[\bar{u}(p) \left(A + B\gamma_5\right) u(P)\right],$$

where P is the 4 -momentum of the decaying hyperon of mass M, and p is the 4 -momentum of the baryon decay product of mass m. With the normalization convention, $\bar{u}_i u_i = 2m_i$, the Pauli form of the matrix element in the rest frame of the decaying hyperon is

$$\mathscr{N} = G\mu_c^2 \left\langle \chi_2 \right| \sqrt{2M(E+m)} A + \sqrt{2M(E-m)} B \boldsymbol{\sigma} \cdot \boldsymbol{q} \left| \chi_1 \right\rangle,$$

where E is the total energy of the final baryon and $\hat{\boldsymbol{q}}$ is a unit vector in the direction of motion of the final baryon. Comparison with Sec. VI D of the text shows that the amplitudes s and p defined there are proportional to A and B :

$$\frac{p}{s} = \left(\frac{E-m}{E+m}\right)^{1/2} \frac{B}{A} = \left[\frac{(M-m)^2 - \mu^2}{(M+m)^2 - \mu^2}\right]^{1/2} \frac{B}{A}.$$

Here μ is the mass of the pion entering the decay. The parameters α, β, and γ can therefore be expressed in terms of A and B, rather than s and p, if desired.

The decay rate for $\mathbf{B}_1 \rightarrow \mathbf{B}_2 + \pi$ is

$$\Gamma = \frac{G^2 \mu_c^4}{8\pi} q \left\{ \left[\frac{(M+m)^2 - \mu^2}{M^2}\right] |A|^2 + \left[\frac{(M-m)^2 - \mu^2}{M^2}\right] |B|^2 \right\},$$

where q is the c.m. momentum of the decay products. For reference, the dimensionless constant in this expression has the value $G^2 \mu_\mathrm{c}^4 / 8\pi = 1.9488 \times 10^{-15}$.

Table 1 summarizes the amplitudes A and B for the nonleptonic decays of the Λ, Σ, and Ξ hyperons. These amplitudes have been calculated by using the experimental data for mean lives, branching ratios, and the decay asymmetry α given in the Stable Particle Table of this review. Time-reversal invariance is assumed and final-state interactions are neglected, so A and B are taken to be relatively real. The subscript on the hyperon refers to the sign of the decaying pion. The statistical correlation coefficient

$$C_{AB} = \frac{\langle \Delta A \Delta B \rangle}{\sqrt{\langle \Delta A^2 \rangle \langle \Delta B^2 \rangle}}$$

is also given. The absolute signs of A and B have been assigned, using the following convention. Taking $A\left(\Lambda_-^0\right)$ as positive, the other S -wave decay amplitudes are chosen to give an approximate fit to the triangular relationships

$$\sqrt{2}A\left(\Sigma_0^+\right) + A\left(\Sigma_+^+\right) = A\left(\Sigma_-^-\right)$$

and

$$\sqrt{3}A\left(\Sigma_0^+\right) + A\left(\Lambda_-^0\right) = 2A\left(\Xi_-^-\right).$$

The signs of the B amplitudes relative to those of the corresponding A amplitudes are determined by the sign of the appropriate α decay parameter.

Table 1

$M \to m + \mu$	A	B	C_{AB}
$\Lambda_-^0 \to p + \pi^-$	1.47 ± 0.01	9.98 ± 0.24	-0.289
$\Lambda_0^0 \to n + \pi^0$	-1.07 ± 0.02	-7.14 ± 0.56	-0.741
$\Sigma_+^+ \to n + \pi^+$	0.06 ± 0.01	19.07 ± 0.07	-0.038
$\Sigma_0^+ \to p + \pi^0$	1.48 ± 0.05	-12.04 ± 0.58	0.982
$\Sigma_-^- \to n + \pi^-$	1.93 ± 0.01	-0.65 ± 0.07	0.003
$\Xi_0^0 \to \Lambda + \pi^0$	1.54 ± 0.03	-6.43 ± 0.66	0.188
$\Xi_-^- \to \Lambda + \pi^-$	2.04 ± 0.01	-6.93 ± 0.31	0.268

2. Tests of the $\Delta I = \frac{1}{2}$ rule

(a) Λ Decay

For Λ decay the $\Delta I = \frac{1}{2}$ rule predicts that $\Gamma_0/\Gamma_- = 0.50$ and $\alpha_0 = \alpha_-$. In order to determine the magnitude of possible $\Delta I = \frac{3}{2}$ amplitudes present we write the linear expressions [4] for the $\Delta I = \frac{3}{2} A$ - and B-wave amplitudes in terms of $\Delta\alpha$, where $\Delta\alpha$ is the measured value of α_0/α_-minus the predicted value, and in terms of $\Delta\Gamma$ similarly defined. Evaluating these we find

$$\Delta\alpha = -1.54 A_3/A_1 + 1.61 B_3/B_1,$$
$$\Delta\Gamma = 1.84 A_3/A_1 + 0.25 B_3/B_1.$$

Here the $\Delta I = \frac{3}{2}$ amplitudes are expressed relative to the $\Delta I = 1/2$ amplitudes. The numerical values of the coefficients depend on the ratio B/A. The uncertainties in the coefficients are small compared to the uncertainties in $\Delta\alpha$ and $\Delta\Gamma$. Final-state πN interactions have been included in these relations but have a very small effect. From the Stable Particle Table,

$$\Delta\alpha = 0.006 \pm 0.066, \quad \Delta\Gamma = 0.058 \pm 0.012,$$

and hence

$$A_3/A_1 = 0.027 \pm 0.008,$$
$$B_3/B_1 = 0.030 \pm 0.037.$$

The possible $3\% \Delta I = \frac{3}{2} A$-wave amplitude is due to the disagreement of decay rates with prediction. At this level the results are sensitive to electromagnetic corrections. However, in Λ decay the phase space correction and the other radiative corrections appear to be about equal in magnitude and have opposite signs [5, 6], and hence cancel each other in the correction to the decay rates.

(b) Ξ Decay

The analysis for Ξ decay is very similar to that for Λ decay. If the $\Delta I = \frac{1}{2}$ rule is valid, $\Gamma_0 (\Xi^0) / \Gamma_- (\Xi^-) = 0.50$ and $\alpha_0 = \alpha_-$. For this case the expressions linear in $\Delta I = \frac{3}{2} A$ - and B-wave amplitudes are [4]

$$\Delta\alpha = 1.37 A_3/A_1 - 1.37 B_3/B_1,$$
$$\Delta\Gamma = -1.44 A_3/A_1 - 0.06 B_3/B_1.$$

From the Stable Particle Table,

$$\Delta\alpha = 0.18 \pm 0.12, \quad \Delta\Gamma = 0.066 \pm 0.020$$

and we find

$$A_3/A_1 = -0.038 \pm 0.014$$
$$B_3/B_1 = -0.17 \pm 0.09$$

(c) $\sum$ Decay

The traditional test of the $\Delta I = 1/2$ rule in Σ decay is that the amplitudes satisfy the relationship

$$\sqrt{2}\Sigma_0^+ + \Sigma_+^+ - \Sigma_-^- = 0.$$

Graphically this is equivalent to closing the Σ triangle when the amplitudes are plotted on A, B axes. Including $\Delta I \geq \frac{3}{2}$ amplitudes in Σ decay analysis, the " Σ triangle" relationship becomes

$$\sqrt{2}A_0 + A_+ - A_- = -3\sqrt{\frac{2}{5}} A_3 + \frac{2}{\sqrt{15}} A_5,$$

where A_3 and A_5 are $\Delta I = 3/2$ and $\Delta I = 5/2$ amplitudes, respectively. There is a similar equation for the B amplitudes. From table 1 ,

$$\sqrt{2}A_0 + A_+ - A_- = 0.22 \pm 0.09, \sqrt{2}B_0 + B_+ - B_- = 2.7 \pm 1.0.$$

If we neglect the $\Delta I = \frac{5}{2}$ amplitudes and assume all amplitudes to be real we can solve for possible $\Delta I = \frac{3}{2}$ amplitudes. The result is

$$\frac{A_3}{A_-} = -0.061 \pm 0.024, \frac{B_3}{B_+} = -0.074 \pm 0.027.$$

Thus for hyperon decay, present experimental data limit $\Delta I = 3/2$ amplitudes to less than about 5%.

3. The Lee-Sugawara relation

From table 1 the Lee-Sugawara relation [7, 8], $\sqrt{3}\Sigma_0^+ + \Lambda_-^0 - 2\Xi_-^- = 0$, is satisfied to -0.07 ± 0.11 for the A amplitudes, and to 3.0 ± 1.9 for the B amplitudes.

References

[1] J. P. Berge, in Proc. of the 13th Int. Conf. on high-energy physics, Berkeley, (1966) (University of California Press, Berkeley, 1967), p. 46
[2] N. P. Samios, International Conference on weak interactions, Argonne, (1965), p. 189
[3] J. D. Jackson, private communication (1973).
[4] See O. E. Overseth and S. Pakvasa, Phys. Rev. 184 (1969) 1663. The expression for Γ_0/Γ_- for Λ decay should read

$$\frac{\Gamma_0}{\Gamma_-} \approx \frac{1}{2}\left\{1 + 3\sqrt{2} \times \left[\frac{S_{11}S_{33}\cos(\delta_1 - \delta_3) + P_{11}P_{33}\cos(\delta_{11} - \delta_{31})}{S_{11}^2 + P_{11}^2}\right]\right\}.$$

[5] See A. A. Belavin and I. M. Narodetsky, Yad. Fiz. 8 (1968) 978 [Soviet J. Nucl. Phys. 8 (1969) 568]
[6] G. W. Intemann, private communication (19'73)
[7] See B. W. Lee, Phys. Rev. Lett. 12 (1964) 83
[8] See H. Sugawara, Prog. Theor. Phys. 31 (1964) 213

5.30.4 30.4. CP and CPT invariances*

30.4.1. Violation of CP invariance in K^0 decays

Experimental data on η_{+-}, η_{00}, and δ characterizing CP violation in $\mathrm{K_L^0}$ decays see in section 30.2.2.

The model of superweak interaction [1] corresponds to the following values of the parameters:

$$\phi_{+-} = \phi_{00} = \arctan\left[2\Delta m\tau\left(K_S^0\right)/\hbar\right] = (43.67 \pm 0.14)^\circ,$$
$$\mathrm{Re}\,\varepsilon = |\eta_{+-}|\left[1 + 2\Delta m\tau\left(K_S^0\right)/\hbar\right] = (1.645 \pm 0.016)\cdot 10^{-3}.$$

The experimental value of the last quantity,

$$\mathrm{Re}\,\varepsilon = (1.621 \pm 0.088)\cdot 10^{-3},$$

is found from the relation

$$\mathrm{Re}\,\varepsilon = \delta|1 - x|^2/2\left(1 - |x|^2\right)$$

where x is the ratio of amplitudes corresponding to transitions with $\Delta Q = -\Delta S$ and $\Delta Q = +\Delta S$, that is

$$x = A\left(\mathrm{K^0} \to \pi^+\ell^-\bar{\nu}\right)/A\left(\mathrm{K^0} \to \pi^-\ell^+\nu\right);$$

the value of x will be given below (see the text following table in section 30.6.1).

Reference

[1] L. Wolfenstein, Phys. Lett. 13 (1964) 562

30.4.2. Electric dipole moment of the neutron

$$d_\mathrm{n} = \begin{cases} (5 \pm 15)\cdot 10^{-25} e\cdot\ \mathrm{cm} \\ (4 \pm 7.5)\cdot 10^{-25} e\cdot\ \mathrm{cm}[1]. \end{cases}$$

Reference

[1] I. S. Altaryov et al., Pis'ma ZhETF 29 (1979) 794 [JETP Lett. 29 (1979) 730]

30.4.3. Search for T-odd muon polarization in $K^0_{\mu 3}$ decay

Measurements of the muon polarization, P_{μ^+}, normal to the plane of $\mathrm{K}^0_{\mathrm{L}} \to \pi^- \mu^+ \nu$ decay, give the result [1]: $P_{\mu^+} = 0.0021 \pm 0.0048$.

Non-conservation of CP parity corresponds to non-zero relative phase of the form factors $f_+$and $f_-$of $\mathrm{K}_{\mu 3}$ decay, that is to $\mathrm{Im}\,\xi \neq 0$ where $\xi = f_-/f_+$. The electromagnetic interactions of $\pi^-$and μ^+in the final state gives rise to the same effect [2,3].

The experimental value of P_μ given above determines $\mathrm{Im}\,\xi|_{\mathrm{exp}}$, which must be compared with the value of $\mathrm{Im}\,\xi|_{\mathrm{e.m.}}$ which is due to the interaction in the final state. These quantities are [1]:

$$\mathrm{Im}\,\xi|_{\mathrm{exp}} = 0.012 \pm 0.026, \quad \mathrm{Im}\,\xi|_{..\mathrm{m.}} = 0.008.$$

References

[1] M. P. Schmidt et al., Phys. Rev. Lett. 43 (1979) 556
[2] N. Byers, S. W. MacDowell, C. N. Yang, High energy physics and elementary particles (IAEA, Vienna, 1965) p. 953
[3] L. B. Okun, I. B. Khriplovich, Yad. Fiz., 6 (1967) 821 [Sov. J. Nucl. Phys. 6 (1968) 598] (Here the coefficient in front of $\mathrm{Im}\,\xi|_{\mathrm{e.m.}}$, derived in [2], is corrected.)

30.4.4. Test of CPT invariance [1]

	$(m_+ - m_-)/m$	$(\tau_+ - \tau_-)/\tau$	$(g_+ - g_-)/g$
$\mathrm{e}^-/\mathrm{e}^+$			$< 1.2 \cdot 10^{-8}$
μ^-/μ^+	$-(2 \pm 5) \cdot 10^{-6}$	$(7.9 \pm 10) \cdot 10^{-4}$ $-(4 \pm 9) \cdot 10^{-4}$	$(2.6 \pm 1.7) \cdot 10^{-8}$
$\mathrm{p}/\overline{\mathrm{p}}$	$(7.6 \pm 3.9) \cdot 10^{-5}$	a	$-(0.4 \pm 7.2) \cdot 10^{-3}$ [b]
π^+/π^-	$-(2.4 \pm 4.7) \cdot 10^{-5}$	$(5.3 \pm 6.8) \cdot 10^{-4}$[c]	
$\mathrm{K}^+/\mathrm{K}^-$	$-(1.3 \pm 1.1) \cdot 10^{-4}$	$(1.1 \pm 0.9) \cdot 10^{-3}$	

Notations: m, τ, g denote mass, lifetime, and g-factor; indices $\pm$ indicate the sign of the particle charge.

[a] The experimental result for the antiproton lifetime for the decay $\overline{\mathrm{p}} \to \mathrm{e}^+\pi^0$ is [2]:

$$\tau\left(\overline{\mathrm{p}} \to \mathrm{e}^+\pi^0\right) > 1700 \text{ hours}.$$

[b] Actually this result was obtained for the relative difference between magnetic moments of the proton and antiproton, $(\mu_+ - \mu_-)/\mu$.

[c] See PDG.

References

[1] H. Poth, Phys. Lett. 77B (1978) 321
[2] M. Bell et al., Phys. Lett. 86B (1979) 215

[0]*Absence of reference means PDG as the source of the corresponding experimental data.

5.30.5 30.5. Conservation of leptonic numbers

30.5.1. Neutrino oscillations

$\nu_\mu \leftrightarrow \nu_\mathrm{e}, \bar{\nu}_\mu \leftrightarrow \bar{\nu}_\mathrm{e}$, GGM, CERN PS [1]:	$\nu_\mathrm{e} \leftrightarrow \nu_l, i \neq \mathrm{e}$, BNL solar ν_e detector:
$P(\nu_\mu \to \nu_\mathrm{e}) / P(\nu_\mu \to \nu_\mu) = -0.03(10) \cdot 10^{-2}$,	$P(\nu_\mathrm{e} \to \nu_\mathrm{e}) = 1.6(4)/(\sim 4.7)$[2],
$P(\bar{\nu}_\mu \to \bar{\nu}_\mathrm{e}) / P(\bar{\nu}_\mu \to \bar{\nu}_\mu) = 0.02(7) \cdot 10^{-2}$,	$0.5 \leq \sin^2 2\alpha \leq 0.8$ and $0.7 \leq \Delta m^2 \left(\mathrm{eV}^2\right) \leq 1.0$ (68%
$\bar{\nu}_\mu \leftrightarrow \bar{\nu}_\mathrm{e}$, LAMPF: $P(\bar{\nu}_\mu \to \bar{\nu}_\mathrm{e}) < 0.098$ [5]	$\bar{\nu}_\mathrm{e} \leftrightarrow \bar{\nu}_t, i \neq \mathrm{e}$, Fission reactor, ILL [7]:
$\Delta m^2 \leqslant 0.9 - 1.8\mathrm{eV}^2$ for $\sin^2 2\alpha = 1.0 - 0.3$ [6]	$\bar{\nu}_\mathrm{e}\mathrm{p} \to \mathrm{e}^+\mathrm{n}, \Delta m^2 \lesssim 0.2 - 0.14$ for $\sin^2 2\alpha = 0.5 - 1.0$
$\nu_\mu \leftrightarrow \nu_\tau$, HES, FNAL: $P(\nu_\mu \to \nu_\tau) < 0.63 \cdot 10^{-2}$;	$\nu_\mathrm{e} \leftrightarrow \nu_1, i \neq \mathrm{e}$, LAMPF: $P(\nu_\mathrm{e} \to \nu_\mathrm{e}) = 1.09\binom{37}{41}$;
$\Delta m^2 \leqslant 3 - 25\mathrm{eV}^2$ for $\sin^2 2\alpha = 1.0 - 0.02$ [8]	$\Delta m^2 \leqslant 2.5 - 4.0\mathrm{eV}^2$ for $\sin^2 2\alpha = 1.0 - 0.6$ [6]
$\nu_\mathrm{e} \leftrightarrow \nu_\tau$, BEBC, CERN SPS:	$\nu_\mathrm{e} \leftrightarrow \nu_t, i \neq \mathrm{e}$, BEBC: $P(\nu_\mathrm{e} \to \nu_\mathrm{e}) = 1.04(15)$;
$P(\nu_\mathrm{e} \to \nu_\tau) < 0.35$[9]	$\Delta m^2 \leqslant 60 - 150\mathrm{eV}^2$ for $\sin 2\alpha = 1.0 - 0.5$ [10]

Notations: (i) GGM: Gargamelle bubble chamber; LAMPF: Los Alamos Meson Physics Facility; ILL Institut Laue-Langevin; HES: hybrid emulsion spectrometer; BEBC: Big European Bubble Chamber; (ii) P, α, and Δm^2 denote the transition probability averaged, the mixing angle, and the difference of squares masses of neutrinos, respectively; for instance, in the case of $\nu_\mu \leftrightarrow \nu_\mathrm{e}$ mixing:

$$\begin{aligned} \nu_\mathrm{e} &= \nu_1 \cos\alpha + \nu_2 \sin\alpha, \\ \nu_\mu &= -\nu_1 \sin\alpha + \nu_2 \cos\alpha, \end{aligned} \qquad \Delta m^2 = \left| m^2(\nu_1) - m^2(\nu_2) \right|;$$

(iii) The figures in parentheses correspond to the one-standard-deviation uncertainty in the last digits main number.

Note: Limits on "exotic" oscillations $\nu_\mu, \nu_\mathrm{e} \leftrightarrow \bar{\nu}_{\mu\mathrm{L}}$ may be inferred from ref. [11] if one additionally assumes that $\bar{\nu}_{\mu\mathrm{L}}$ could produce $\mu^+$when interacting with nucleons.

References

[1] E. Bellotti, et al., Lett. Nuovo Cim. 17 (1976) 553;
J. Blietschatu et al., Nucl. Phys. B133 (1978) 205
[2] J. K. Rowley, B. T. Cleveland, R. Davis, Jr., and C. Evans, Proc. Neutrino '77 Conf., vol. 1, p. 15
[3] R. Ehrlich, Phys. Rev. D18 (1978) 2323
[4] E. Pasierb et al., Phys. Rev. Lett. 43 (1979) 96;
F. Reines et al., Phys. Rev. Lett. 45 (1980) 1307
[5] S. E. Willis et al., Phys. Rev. Lett. 44 (1980) 522; 45 (1980) 1370E
[6] P. Nmethy et al., Phys. Rev. D23 (1981) 262
[7] F. Boehm et al., Phys. Lett. 97B (1980) 310
[8] N. Ushida et al., Phys. Rev. Lett. 47 (1981) 1694.
[9] P. Fritze et al., Phys. Lett. 96B (1980) 427
[10] H. Deden et al., Phys. Lett. 98B (1980) 310
[11] M. Holder et al., Phys. Lett. 74B (1978) 277

30.5.2. $\mu \leftrightarrow e$ and $\tau \to \mu(e)$ processes

$\mu^+ \to e^+\gamma$, LAMPF: $B < 1.9 \cdot 10^{-10}$[1]	$\mu^+ \to e^+\gamma\gamma$, LAMPF: $B < 5 \cdot 10^{-8}$[2]	$\mu^+ \to e^+e$
$\mu^{-32}\,\mathrm{S} \to e^{-32}\,\mathrm{S}^*, \mathrm{SIN}: R < 1.5 \cdot 10^{-10}$(99% c.l.)[4]		$\mu^{-127}\mathrm{I} \to e$ $R < 3$
$e^-e^- \to \mu^-\mu^-$[b,c], SLAC: $\sigma < 0.67 \cdot 10^{-32}\ \mathrm{cm}^2$[7]	$\mu^+ \to e^+\bar{\nu}_e\nu_\mu$[c], LAMPF: $B < 0.098$[8]	$\bar{\nu}_\mu e^- \to \mu^-$ R
$\tau \to e\gamma$, SLAC: $B < 0.026$ [10]	$\tau \to ee^+e^-$, SLAC: $B < 0.006$ [11]	$\tau \to \mu\gamma$, S

Notations: B, R, and σ denote relative decay rate, ratio of the cross sections of the forbidden process to that of corresponding allowed one, and total cross section, respectively.
[a] For the "elastic" process, without the final nucleus breaking.
[b] If the process under consideration is described by four-fermion interaction with the hamiltonian $H = \left(G'/\sqrt{2}\right)(\bar{\mu}O_\alpha e)(\bar{\mu}O_\alpha e) + \mathrm{h.c.}$, where $O_\alpha = \gamma_\alpha(1+\gamma_5)$, then the upper bound of σ given above corresponds to the following upper bound on the coupling constant:

$$G' < 6.1 \cdot 10^{-3} m_p^{-2} \quad (m_p \text{ is the proton mass }).$$

[c] The process is allowed by multiplicative but not additive leptonic number conservation.

References

[1] J. D. Bowman et al., Phys. Rev. Lett. 42 (1979) 556
[2] J. D. Bowman et al. Phys. Rev. Lett. 41 (1978) 442
[3] S. M. Korenchenko et al., ZhETF 70 (1976) 3 [JETP 43 (1976) 1]
[4] A. Badertscher et al., Proc. 19th Int. Conf. High Energy Phys., Tokyo, 1978, p. 1019 (contributed paper 950); quoted from the report by G. Altarelli, ibid., p. 441
[5] A. Badertscher et al., Phys. Lett. 79B (1978) 371
[6] R. Abela et al., Phys. Lett. 95B (1980) 318
[7] W. C. Barber et al., Phys. Rev. Lett. 22 (1969) 902
[8] E. Willis et al., Phys. Rev. Lett. 44 (1980) 522; 45 (1980) 1370E
[9] M. Jonker et al., Phys. Lett. 93B (1980) 203
[10] M. L. Perl, Proc. Int. Symp. on lepton and photon interactions at high energies, Hamburg, 1977, p. 145
[11] G. J. Feldman, Proc. 19th Int. Conf. high energy phys., Tokyo, 1978, p. 777

5.30.6 30.6. Selection rules for the weak current*

30.6.1. Absence of semileptonic decays with $\Delta S \neq \Delta Q$

$K^+ \to \pi^+\pi^+e^-\bar{\nu}_e$	$< 5 \cdot 10^{-7}$	$\Xi^0 \to \Sigma^-e^+(\mu^+)\nu$	$< 9 \cdot 10^{-4}$
$K^+ \to \pi^+\pi^+\mu^-\bar{\nu}_\mu$	$< 3 \cdot 10^{-6}$	$\Xi^0 \to pe^-(\mu^-)\bar{\nu}$	$< 1.3 \cdot 10^{-3}$
$\Sigma^+ \to ne^+\nu_e$	$< 5 \cdot 10^{-6}$	$\Xi^- \to ne^-\bar{\nu}_e$	$< 3.2 \cdot 10^{-3}$
$\Sigma^+ \to n\mu^+\nu_\mu$	$< 3 \cdot 10^{-5}$	$\Xi^- \to n\mu^-\bar{\nu}_\mu$	$< 1.5 \cdot 10^{-2}$

Mean values of x, the ratio of the amplitude of $K^0 \to \pi^+\ell^-\bar{\nu}\left(\overline{K}^0 \to \pi^-\ell^+\nu\right)$ decays, corresponding to $\Delta Q = -\Delta S$, to that of $K^0 \to \pi^-\ell^+\nu\left(\overline{K}^0 \to \pi^+\ell^-\bar{\nu}\right)$ decays, corresponding to $\Delta Q = \Delta S$, are equal to (see section 30.2.2):

[0]*This section gives upper limits of the branching ratios. Absence of reference means PDG as the source of the corresponding experimental data.

$$\langle \mathrm{Re}\, x \rangle \equiv \left\langle \mathrm{Re}\, \frac{A(\Delta Q = -\Delta S)}{A(\Delta Q = \Delta S)} \right\rangle = 0.009 \pm 0.020$$
$$\langle \mathrm{Im}\, x \rangle \equiv \left\langle \mathrm{Im}\, \frac{A(\Delta Q = -\Delta S)}{A(\Delta Q = \Delta S)} \right\rangle = -0.004 \pm 0.026$$

30.6.2. Suppression of hadronic decays with $\Delta S > 1$ or $\Delta C = -\Delta S$

$\Delta S > 1$	$\Xi^0 \to \mathrm{p}\pi^-$	$< 3.6 \cdot 10^{-5}$	$\Xi^- \to \mathrm{p}\pi^-\pi^-$	$< 4 \cdot 10^{-4}$
	$\Xi^- \to \mathrm{n}\pi^-$	$< 1.1 \cdot 10^{-3}$	$\Omega^- \to \Lambda\pi^-$	$< 1.3 \cdot 10^{-3}$
$\Delta C = -\Delta S$	$\mathrm{D}^0 \to \mathrm{K}^+\pi^-$	$< 5 \cdot 10^{-3}$	$\mathrm{D}^+ \to \mathrm{K}^+\pi^+\pi^-$	$< 2 \cdot 10^{-3}$

30.6.3. Absence of decays with $\Delta Q = 0$ for $\Delta S \neq 0$[a]

$\mathrm{K}^+ \to \pi^+\nu\bar{\nu}$	$< 5.6 \cdot 10^{-7}$	$\mathrm{K}^0_\mathrm{L} \to \mu^+\mu^-$	$(9.1 \pm 1.9) \cdot 10^{-9}$
$\mathrm{K}^+ \to \pi^+\mathrm{e}^+\mathrm{e}^-$	$(2.6 \pm 0.5) \cdot 10^{-7}$	$\mathrm{K}^0_\mathrm{L} \to \pi^0\mathrm{e}^+\mathrm{e}^-$	$< 2.3 \cdot 10^{-6}$[2]
$\mathrm{K}^+ \to \pi^+\mu^+\mu^-$	$< 2.4 \cdot 10^{-6}$	$\mathrm{K}^0_\mathrm{L} \to \pi^0\mu^+\mu^-$	$< 1.2 \cdot 10^{-6}$[2]
$\mathrm{K}^+ \to \pi^\pm\mathrm{e}^+\mu^\mp$	$< 7 \cdot 10^{-9}$	$\mathrm{K}^0_\mathrm{L} \to \pi^+\pi^-\mathrm{e}^+\mathrm{e}^-$	$< 5 \cdot 10^{-6}$[3]
$\mathrm{K}^+ \to \pi^+\mathrm{e}^-\mu^+$	$< 5 \cdot 10^{-9}$	$\mathrm{K}^0_\mathrm{L} \to \mathrm{e}^+\mathrm{e}^-\gamma$	$(1.7 \pm 0.9) \cdot 10^{-5}$[2]
$\mathrm{K}^0_\mathrm{S} \to \mathrm{e}^+\mathrm{e}^-$	$< 3.4 \cdot 10^{-4}$	$\mathrm{K}^0_\mathrm{L} \to \mu^+\mu^-\gamma$	$(2.8 \pm 2.8) \cdot 10^{-7}$[2]
$\mathrm{K}^0_\mathrm{S} \to \mu^+\mu^-$	$< 3.2 \cdot 10^{-7}$	$\mathrm{K}^0_\mathrm{L} \to \mathrm{e}^+\mathrm{e}^-\mathrm{e}^+\mathrm{e}^-$	$< 5.8 \cdot 10^{-5}$[3]
$\mathrm{K}^0_\mathrm{L} \to \mathrm{e}^+\mathrm{e}^-$ ($\mathrm{e}^\pm\mu^\mp$)	$< 2 \cdot 10^{-9}$[1][b]	$\mathrm{K}^0_\mathrm{L} \to \mathrm{e}^+\mathrm{e}^-\mu^+\mu^-$	$< 1.1 \cdot 10^{-5}$[3]

[a] The data are given on decays which would be induced by strangeness-nonconserving neutral currents. Some of the decays can be caused by non-leptonic charged currents together with the electromagnetic interaction.
[b] The value of $B\left(\mathrm{K}^0_\mathrm{L} \to \mu^+\mu^-\right) < 3{\cdot}10^{-9}$ obtained in the same experiment [1] is in contradiction with the results of other experiments.

References

[1] A. R. Clark et al., Phys. Rev. Lett. 26 (1971) 1667
[2] A. S. Carrol et al., Phys. Rev. Lett. 44 (1980) 525
[3] V. M. Berezin et al., Preprint ITEP-47 (1980) (In Russian)

30.6.4. Absence of processes with $\Delta Q = 0$ for $\Delta S \neq 0$ or $\Delta C \neq 0$

$\sigma\left(\nu_\mu\mathrm{N} \to \nu_\mu\Lambda\left(\Sigma^0\right)\mathrm{X}\right)/\sigma\left(\nu_\mu\mathrm{N} \to \nu_\mu\mathrm{X}\right) < 5.4 \cdot 10^{-3}$	[1]
$\frac{\sigma(\nu_\mu\mathrm{N}\to\nu_\mu\mathrm{CX})}{\sigma(\nu_\mu\mathrm{N}\to\nu_\mu\mathrm{X})}\Big\vert_{E_\mathrm{X}>1\mathrm{GeV}} B\left(\mathrm{C} \to e^+ + \cdots\right)\Big\vert_{E_\mathrm{e}+>02\mathrm{GeV}} < 1.3 \cdot 10^{-3}$	[2]
$\frac{\sigma(\nu_\mu\mathrm{N}\to\nu_\mu\mathrm{CX})}{\sigma(\nu_\mu\mathrm{N}\to\nu_\mu\mathrm{X})}\Big\vert_{E_\mathrm{X}>100\mathrm{GeV}} B\left(\mathrm{C} \to \mu^+ + \cdots\right) < 3.9 \cdot 10^{-3}$	[3]
$\frac{\sigma(\bar{\nu}_\mu\mathrm{N}\to\bar{\nu}_\mu\mathrm{CX})}{\sigma(\bar{\nu}_\mu\mathrm{N}\to\bar{\nu}_\mu\mathrm{X})} B\left(\mathrm{C} \to \mathrm{e}^+ + \cdots\right) < 1.4 \cdot 10^{-3}$	[4]
$\sigma\left(\nu_\mu\mathrm{N} \to \nu_\mu\mathrm{CX}\right)/\sigma\left(\nu_\mu\mathrm{N} \to \mu^-\mathrm{CX}\right) \leq 0.08$	[5]

Notations: σ and B denote the cross section and the relative decay rates, respectively; C denotes a charmed particle, and X all other hadrons.

References

[1] J. Blietschau et al., Phys. Lett. 71B (1977) 231
[2] H. Deden et al., Phys. Lett. 67B (1977) 474
[3] M. Holder et al., Phys. Lett. 74B (1978) 277
[4] V. Efremenko et al., Phys. Lett. 88B (1979) 181
[5] C. Baltay, Proc. Neutrino '78 Conf., p. 533

6 Standard Model by Zhou

6.1 Introduction

6.1.1 Particle and Interactions

First, we summarize some ancient history.

• In the early 1960s, the Eightfold Way was introduced, followed by the quark model. Quark confinement was postulated to explain why free quarks had not been seen, while quark color was added for consistency with the Pauli exclusion principle.

• By the late 1960s and early 1970s, deep inelastic scattering experiments at SLAC and CERN found evidence for substructure in the proton, pointlike particles called partons, analogous to how Rutherford had found substructure in the atom. However, there was still widespread skepticism over the quark model, so partons were not identified with quarks.

• In 1974, groups led by Ting at Brookhaven and Richter at SLAC simultaneously found a new particle, called the J/ψ, a meson which was both extremely heavy and relatively long-lived. This set off a flurry of theoretical activity called the November revolution.

• The quark model explained the new particle as a bound state of a charm and anti-charm quark; it has excited states in analogy with positronium, which are collectively called "charmonium". It also predicted many new mesons and baryons containing charm quarks, organized into multiplets by group theory, which were quickly found.

• At this point, the elementary particles could be organized into families containing two quarks and one lepton each, but measurements of CP violation motivated a third generation. In 1975, the tau lepton was found. Then, a few years later, the upsilon meson was found and postulated to be a bottom and anti-bottom quark. Throughout the 1980s, more B mesons were discovered, and today LHCb and Belle II are devoted to studying them.

• The top quark would complete the third generation, and measurements of $B^0/\bar{B}^0$ oscillations indicated it had a huge mass. It was thus too heavy to be produced until 1995, at Fermilab's Tevatron, leading to the table of masses below.

particle	mass	mass determined by
up	2.2MeV	lattice computations of light meson/baryon masses
down	4.7MeV	lattice computations of light meson/baryon masses
strange	95MeV	lattice computations of light meson/baryon masses
charm	1.3GeV	charmonium and D meson masses
bottom	4.2GeV	bottomonium and B meson masses
top	170GeV	production at LHC
e^-	0.5MeV	hydrogen spectroscopy
μ^-	106MeV	muonium hyperfine splitting
τ^-	1.78GeV	production at BES III
$W^\pm$	80GeV	production at LEP
Z	91GeV	production at LEP
H^0	125GeV	production at LHC

Note that quarks don't exist as free particles, so the definition of their mass is somewhat ambiguous. For instance, the up mass may be as high as 5MeV under some definitions.

• Finally, the weak interaction (as understood by Fermi's effective four-fermion interaction) was suspected to be mediated by an intermediate vector boson. By 1960, Glashow had formulated a unified electroweak theory, though there was no mechanism to break the symmetry. In 1964, the Higgs mechanism was discovered, and in 1967, Weinberg and Salam showed how it could break electroweak symmetry, predicting the $W^\pm$and Z bosons.

• In 1983, the intermediate vector bosons were discovered at CERN's super proton synchrotron. In the 1990s, LEP was constructed to perform precision tests of the electroweak theory.

Next, we summarize the Standard Model (SM) interactions.

• The basic QED and QCD vertices are simple: charged particles emit photons and colored particles emit gluons. There are also ggg and $gggg$ vertices.

• The fundamental neural weak vertex is $Zf\bar{f}$ for any fermion f. For example, a Z could mediate neutrino-electron scattering. The Z behaves a lot like the photon, except that it also couples to neutrinos.

• The fundamental leptonic charged weak vertex is $W\ell\nu$, i.e. a W boson can decay into a lepton and its corresponding antineutrino. This vertex mediates the decay of the muon.

• Finally, the quark charged weak vertex converts an up-type quark to a down-type quark, e.g. Wud'. However, the quarks are defined in the mass basis, while this interaction is diagonalized in a different basis. Then W emission can convert an up quark to a down quark, but also to a strange or bottom quark.

• The two bases are related by the CKM matrix; the magnitudes of the matrix elements are

$$\begin{pmatrix} d' \\ s' \\ b' \end{pmatrix} = \begin{pmatrix} 0.974 & 0.227 & 0.004 \\ 0.227 & 0.973 & 0.042 \\ 0.008 & 0.042 & 0.999 \end{pmatrix} \begin{pmatrix} d \\ s \\ b \end{pmatrix}$$

Then most weak decays stay in the same generation. Crossing between adjacent generations is rare but possible, while crossing between the first and third generation is rarer still.

• For example, a charged weak interaction mediates beta decay. A baryon can decay into another baryon while emitting a photon by emitting and reabsorbing a W, which emits a photon. (This photon is necessary by energy-momentum conservation.)

• It is now known that neutrinos have mass. Neutrinos are defined in the flavor basis, so the weak vertex is unchanged. Instead, the flavor eigenstates oscillate into each other due to their mismatch with the mass eigenstates. The analogue of the CKM matrix is the PMNS matrix.

• The force carriers have interactions $WWZ, WWZZ, WWWW, WW\gamma, WW\gamma Z$, and $WW\gamma\gamma$.

• In the SM, the Higgs interacts with all fermions by Yukawa couplings. It also interacts with the weak mediators with vertices $WWH, ZZH, WWHH$, and $ZZHH$, and with itself as HHH and $HHHH$. One-loop diagrams also provide effective vertices $ggH, \gamma\gamma H$, and γZH.

• At LEP, the Higgs was searched for by Z Bremsstrahlung,

$$e^+ + e^- \to Z^* \to Z + H$$

This ruled out Higgs masses below 114GeV, while perturbative unitarity arguments disfavored masses above 200GeV.

• At hadron colliders, the main production mechanism is actually a one-loop "gluon fusion" process $gg \to H$, which dominantly goes through a t loop, because the heavy t quark has the largest coupling with the Higgs. (This is an example of "non-decoupling". We usually expect heavy particles to be irrelevant, but they remain relevant because they must couple more strongly to the Higgs to get mass. Thus, Higgs measurements already rule out a heavy 4 th generation that gets mass the same way as the other 3.)

• There are other important production mechanisms which occur at tree level, including:

$-gg \to g^* \to t\bar{t}H$ (radiation off a top quark, measuring the top Yukawa)

• $q\bar{q} \to q\bar{q}H$ (each quark radiates a W or Z, and the two fuse)

$-q\bar{q} \to V^* \to VH$ (W or Z Bremsstrahlung)

These processes have all been observed and match Standard Model expectations to around the 20% level. Note that direct quark fusion, $q\bar{q} \to H$, is unlikely because all Yukawa couplings besides the top are small.

• The reason gluon fusion is dominant, despite being loop-induced, is because (1) it doesn't involve any weak couplings, and (2) at proton-proton colliders, the constituents ("partons") are dominantly gluons and quarks, with a smaller contribution from antiquarks. (There are some antiquarks, because of QCD effects, and the specific amounts of each particle are characterized by parton distribution functions.)

• The most likely Higgs decays are to pairs of heavy particles, such as τ, b, W, Z, or t. All of these are possible (though suppressed) since the W, Z, and t may be produced as virtual particles which then decay, though the Higgs is light enough for $H \to t\bar{t}$ to be very rare.

• The discovery of the Higgs was made by the clean decay channels of $H \to \gamma\gamma$, which occurs through a loop diagram, and $H \to ZZ \to 4$ leptons, though couplings to the other particles were later measured as well.

• One way that experimentalists characterize their knowledge of the Higgs couplings is the " κ framework", which is an ad hoc scaling of each Higgs coupling by a factor κ_i. This violates gauge invariance and doesn't yield a consistent quantum field theory, so one can't compute higher order corrections, or get accurate kinematics. But measurements indicate $\kappa_i \approx 1$ to about 10% accuracy for the weak bosons and the heaviest fermions.

• At the same time, over the past few decades, more accurate calculations have reduced the theory uncertainty, with the standard now "next to next to next to leading order" ($\mathrm{N^3LO}$), which is good to within a few percent. However, more accurate calculations will be needed for the "high luminosity" (HL) phase of the LHC, which will further shrink experimental uncertainties.

• We can also try to measure the Higgs trilinear coupling, which would help confirm the nature of its potential. Varying the trilinear coupling affects the rate of two Higgs production, though the uncertainties at the HL-LHC will remain of order 100%.

• Proposed future "Higgs factory" e^+e^-colliders, such as the ILC, could substantially improve the precision. For instance, they can operate at around 230GeV to produce Higgs from Z Bremsstrahlung (slightly above $m_H + m_Z$, to remove phase space suppression), around 250GeV to produce Higgs pairs, and at 350GeV to produce top pairs and measure the top mass. It will also be possible to directly measure the Higgs width, since the kinematics is much cleaner.

• On all these fronts, we could do much better with a $\mu^+\mu^-$collider, since muons couple much more strongly to the Higgs, but the technology to build one doesn't yet exist. It's not hard to get the muons (e.g. electron-positron colliders make the positrons by just directing a beam into a wall), but it seems challenging to form the muons into a beam before they decay.

Note. Before going on, it's nice to step back and appreciate the massive engineering effort that goes into particle colliders. The Large Hadron Collider (LHC) sits inside a 27 km circular tunnel, buried 100 m underground due to a combination of radiation shielding and political reasons. Inside the tunnel, beams of protons circulate in two separate tubes in opposite directions. There are thousands of superconducting NbTi magnets distributed throughout, to keep the beam going in a circle. This acceleration causes energy loss due to Bremsstrahlung, so the protons are pushed along by thousands of superconducting radiofrequency (SRF) cavities, whose oscillating fields are timed to accelerate the protons as they pass by. The whole system must be cooled with liquid helium to cryogenic temperatures, to maintain superconductivity. An unplanned rise in temperature can cause an explosive "magnet quench", which knocked the LHC out of commission in 2008.

The proton beams are organized into thousands of "bunches" of about 10^{11} protons each, spaced only 25 ns apart. They are focused to a transverse size of 16 microns (smaller for the upcoming "High Luminosity" LHC) to increase the chance of an interesting event when the bunches collide at the centers of the detectors. Maintaining this high beam quality is an entire field of study, involving hundreds of physicists and a number of dedicated journals. The beam is carefully focused using about a thousand specialized magnets, such as quadrupoles, sextupoles,

octupoles, and decapoles. And of course, the entire beamline needs to be a vacuum as empty as outer space, to avoid scattering the beam protons.

The proton beam for the LHC needs to already be at a relatively high energy before entering, so the energy is built up through a series of smaller accelerators. Protons are injected into the LHC from the Super Proton Synchrotron (SPS), which discovered the W and Z bosons. The SPS in turn receives them from the Proton Synchrotron, which gets them from the Proton Synchrotron Booster, which gets them from Linac4, which gets them from ionizing hydrogen, which comes from a single little bottle of hydrogen gas. The beam itself degrades as more collisions happen, so it needs to be safely "dumped" and reformed every few hours, repeating this entire process.

The LHC supports many experiments. People often think of ATLAS and CMS, the general purpose experiments which analyze high-energy proton-proton collisions. But there's also ALICE (measuring collisions of lead nuclei, to study quark gluon plasma), LHCb (with a specialized detector to see hadrons containing b quarks, to study CP violation and flavor anomalies), LHCF and TOTEM (downstream of the ATLAS and CMS collision points, to study forward produced particles for cosmic ray physics), MoEDAL-MAPP (near LHCb, to search for produced magnetic monopoles), and soon FASER (far downstream of the ATLAS collision point, to study new light particles). There are also some proposed small experiments, such as MATHUSLA (an above-ground detector, to see long-lived particles), MilliQan (millicharged particles), and CODEX-b (like MATHUSLA, but near LHCb).

The enormous detectors in these experiments use a variety of techniques to infer what happened

in the collision. Powerful magnets bend the trajectories of charged particles, measuring their momentum. Calorimeters are solid components which absorb energy from the particles through the ionization or excitation of particles, which measures their energy. There are also "trackers", often filled with sparse gas, which allow the particles to pass through with lower energy loss. Particles going through the trackers leave a trail of ionized gas, which can be pushed towards a detector with an electric field. Modern trackers have exquisite sensitivity, allowing the paths of particles to be known to finer than millimeter precision. The rate at which the particles lose energy is also measured and can be described by the Bethe-Bloch formula. All of these pieces of information are used together to identify the particle and figure out what happened in the collision.

6.1.2 Symmetries and Conservation Laws

Next, we summarize considerations for computing decay rates and cross sections.

• The SM has three conserved quantities: charge, baryon number (or equivalently quark number) and lepton number. If we ignore neutrino oscillations, the individual lepton flavors are conserved. If we ignore charged weak interactions, the individual quark numbers are conserved. If we ignore all weak interactions, parity is conserved.

• Energy conservation forbids decays of particles into heavier particles. It places no restriction on scattering, since the incoming energy can be arbitrary.

• A decay is more likely if the products are much lighter than the decaying particle, because there is more available phase space volume; this is the reason neutron decay is so slow.

• Generally, a strong decay takes about 10^{-23} seconds, an electromagnetic decay takes 10^{-16}, and a weak decay takes at least 10^{-13}, higher if generation mixing occurs.

• Finally, the OZI/Zweig rule states that any diagram which can be cut in half by only cutting gluon lines is suppressed. This is because the reaction requires hard gluons, and QCD is weak at high energies.

Next, we give a qualitative overview of the discrete symmetries of the SM.

• In 1956, Sachs and Wu found that nature did not respect parity symmetry. In the beta decay of cobalt 60, it was found that the emitted electron came out opposite to the nuclear spin, which may be aligned with a magnetic field. This violates parity since spin and magnetic fields are axial vectors while the emission velocity is a true vector.

• Parity violation can also be seen from the helicity of the neutrino, which is Lorentz invariant assuming the neutrino is massless. Defining right-handed helicity to mean spin pointing along the direction of motion, we would expect neutrinos to be left-handed and right-handed with equal frequency by parity invariance. Instead, experiments find that all neutrinos are left-handed and all antineutrinos are right-handed, where the helicity of the neutrino is not directly measured but inferred from the helicities of the other products of a decay.

• In the absence of the weak force, parity places constraints on allowed particle decays.

• Vector particles such as the photon have parity -1 and axial vectors have parity +1. Conversely, scalars have parity +1 and pseudoscalars have parity -1.

• The individual quark numbers and lepton numbers are conserved, so we are free to assign any parity to them. By convention, we assign parity +1 to leptons and quarks (and thereby also to the proton and neutron). We will show below that this implies parity -1 for antiquarks and antileptons. In particular, this means that a bound state consisting of a fermion and its antiparticle has a factor of -1 in its intrinsic parity.

• Note that parity cannot be defined for neutrinos in the Standard Model, as it would map a left-helicity neutrino to a right-helicity neutrino, which doesn't exist.

• In a two-body decay with angular momentum ℓ, there is an extra factor of $(-1)^\ell$.

• For example, with $\ell = 0$, we expect to have pseudoscalar and vector mesons, corresponding to spin 0 and 1 respectively. These are indeed the lowest-energy meson octets; there are also higher-energy positive parity meson octets corresponding to excited states with $\ell = 1$.

• One early hint of parity violation was the 'theta-tau' puzzle in the 1950s. Two mesons, called the θ and the τ, decayed as

$$\theta^+ \to \pi^+ + \pi^0, \quad \tau^+ \to \pi^+ + \pi^0 + \pi^0$$

Every particle involved has spin 0, so there can be no orbital angular momentum. Then the θ and τ must have parity 1 and -1, but they had nearly the same mass. The resolution is that they are indeed the same particle, the K^+, and the first decay violates parity.

• Next, we turn to charge conjugation, which replaces particles with antiparticles by flipping the sign of all internal quantum numbers. Only particles that are their own antiparticles can be eigenstates of C, severely restricting its use.

• The photon has $C = -1$, since it is sourced classically by a current which flips under C.

• Consider a spin 1/2 particle and its antiparticle with total orbital angular momentum ℓ and total spin s. We get a factor of $(-1)^\ell$ from the orbital part, a factor of -1 from identical particle exchange, and a factor of $(-1)^{s+1}$ from the antisymmetry/symmetry of the singlet/triplet. Then $C = (-1)^{\ell+s}$.

• For example, the neutron pion π^0 has $C = +1$, so it can't decay into an odd number of photons.

• For the strong interactions, where isospin is conserved, we may define the G-parity

$$G = Ce^{i\pi I_2}.$$

This is more useful because charged mesons can have definite G-parity. For example, the charged pion $\pi^+$is mapped to $\pi^-$and then back to $\pi^+$by C, so it has definite G-parity.

Next, we turn to the subtler case of CP symmetry.

• As we've seen, the leptonic weak decays violate parity. For example, in the decay

$$\pi^+ \to \mu^+ + \nu_\mu$$

the antimuon is always left-handed, while it would be right-handed in the parity-flipped version. Similarly, in the decay

$$\pi^- \to \mu^- + \bar{\nu}_\mu$$

the muon is always right-handed. Thus C symmetry is also violated, since the charge conjugate would have a right-handed antimuon, but CP symmetry is not.

• One useful system for testing CP symmetry is the decay of the neutral kaon K^0 and $\bar{K}^0$. The K^0 and $\bar{K}^0$ mix by a $W^\pm$loop, so neutral kaons found in the lab are mixtures of the two. Both K^0 and $\bar{K}^0$ have $P = -1$ and $C = +1$, and the states

$$|K_1\rangle = \left|K^0\right\rangle - \left|\bar{K}^0\right\rangle, \quad |K_2\rangle = \left|K^0\right\rangle + \left|\bar{K}^0\right\rangle$$

have $CP = +1$ and $CP = -1$ respectively.

• Assuming CP is conserved in the weak interactions, $|K_1\rangle$ and $|K_2\rangle$ decay in different ways. Since a pion has $CP = -1$, the most common decays are

$$K_1 \to 2\pi, \quad K_2 \to 3\pi$$

The first decay is much faster because there is more phase space available. Therefore, a neutral kaon should quickly turn into an eigenstate $|K_2\rangle$ of CP. Concretely, this means that a beam of kaons should initially have many 2π decays, and later have only 3π decays.

• The neutral kaons provide another example where two bases mismatch, and the one we use is dictated by convenience. If we are studying strong interactions, we want the K^0 and $\bar{K}^0$, but if we are studying weak decays, we want the K_1 and K_2.

• In 1964, the Cronin-Fitch experiment established that the weak interaction does not conserve CP. This was done by taking a beam of neutral kaons, waiting for a time much greater than the lifetime of the K_1, and detecting residual 2π decays (about 0.2% of the total); this is only possible if the K_2 decay violates CP.

• In general, two particles can mix if they have approximately the same mass and the same relevant conserved quantities. For example, the particles always must have the same baryon number, but they don't have to have the same isospin if the mixing is by a weak process. In the case of neutrinos, lepton number is violated, but this is acceptable as the neutrino mass terms explicitly break lepton number conservation.

• Similarly, the B^0 and $\bar{B}^0$ mesons can mix. Oscillations between the B^0 and $\bar{B}^0$ were observed at Fermilab in 2006, and the decays of the B mesons have been observed to violate CP. Most measurements of CP violation are with neutral B-mesons or neutral kaons; many of the few other candidates are long-lived enough.

Next, we turn to T and CPT symmetry.

• T symmetry does not forbid decays, since no particle is in an eigenstate of T. It imposes detailed balance for reactions, but it is often difficult to set up a backwards reaction. For example, the reverse of the weak decay $\Lambda \to p^+ + \pi^-$is difficult to observe because the proton and pion interact by the strong force. To remove contamination from other forces, we might turn to neutrinos, but it is hard to control them.

• As such, the most sensitive searches for T violation come from measurements of the electric dipole moment of elementary particles; such a dipole moment would violate both P and T. So far, all experiments have found the dipole moment to be zero within error.

• However, we do expect T violation to occur, since CPT must be a symmetry and CP is violated. T violation has been directly observed at BaBar at SLAC in 2012.

• One prediction of CPT symmetry is that every particle must have the same mass and lifetime as its antiparticle. (This is also true of C symmetry, but we know that to be broken.) This has been verified to great accuracy for many particles. Another result is that helicities must

be symmetric about zero: if there exists a helicity λ state, there must also be a corresponding helicity $-\lambda$ state.

• One should always keep in mind that just about all of these exact symmetries, such as Lorentz symmetry, CPT symmetry, etc. are all strongly spontaneously broken in our universe. For example, the presence of the CMB breaks Lorentz symmetry. When we talk about verifying these symmetries, we always imagine experiments that are insensitive to the symmetry-breaking background.

Finally, we turn to the sources and consequences of CP and T violation.

• CP violation can be caused by complex phases in the CKM or PMNS matrices; the former is what accounts for CP violation in kaon and B-meson decay. For $n < 3$ generations such phases can always be removed by redefining the quark fields, so the observation of CP violation led to the prediction of a third generation, where there is one residual phase.

• CP violation can also come from $F\widetilde{F} = F \wedge F$ terms for the electromagnetic, weak, and strong forces; specifically, such a term breaks both P and CP. However, this term is more subtle since it is a total derivative, and hence a boundary term.

• In electromagnetism, the term always integrates to zero for finite-energy configurations; there are no $U(1)$ instantons.

• The chiral anomaly allows the weak theta term to be removed by a rotation of all quark fields, which is just the symmetry $U(1)_B$, as only left-chiral quarks couple to the weak force.

• For the strong force, the term has a nontrivial effect, and induces a neutron electric dipole moment. Experiments indicate that this term is very small; the strong CP problem asks for a natural explanation.

• CP violation is said to "distinguish matter from antimatter". This comes from its presence in the Sakharov conditions for baryogenesis, the origin of a net matter-antimatter asymmetry in the universe. They are:

• Violation of baryon number conservation, i.e. the existence of reactions $i \to f$ where i and f have different baryon number. This can be supplied by grand unified theories; it also occurs extremely rarely in the SM through sphalerons, as discussed in the notes on Quantum Field Theory.

• C violation. This is necessary since otherwise the net baryon number produced by $i \to f$ will be balanced by $i^* \to f^*$. The SM has very strong C violation.

• CP violation. This is necessary since otherwise $i \to f$ will be balanced by $i_P^* \to f_P^*$. The CP violation in the SM is quite small, and probably not enough to account for baryogenesis.

• Departure from thermal equilibrium. Otherwise, $i \to f$ will be balanced by $f \to i$, by detailed balance. Equivalently, we can't go from $\mu_B = 0$ to $\mu_B \neq 0$. We could exit equilibrium, e.g. after a first-order phase transition. However, the electroweak and QCD phase transitions appears be smooth crossovers in the SM, which cannot do the job.

As discussed in detail below, it can be ambiguous to define C or CP, or in some extreme cases impossible to define them at all. "C and CP violation" really stands for the absence of any symmetry which would relate processes, causing the net baryon number produced to cancel.

• One alternative possibility is "leptogenesis". In the SM, B and L are violated by nonperturbative effects while $B - L$ remains conserved; then leptons can be created, and turn into baryons. Note that the lepton number of the universe might or might not be zero, since we can't measure the neutrinos well.

Note. How complex phases in the CKM matrix cause observable CP violation. Consider a process and its CP-reverse. Under the standard electroweak theory, the matrix elements are

$$\mathcal{M} \sim |\mathcal{M}|e^{i\phi}e^{i\theta}, \quad \widetilde{\mathcal{M}} \sim |\mathcal{M}|e^{i\phi}e^{-i\theta}$$

where the CKM phase $e^{i\phi}$ is not conjugated. However, the magnitudes of the amplitudes are the same, so this has no observable effect. However, if the process can occur in multiple

ways,

$$\mathcal{M} \sim |\mathcal{M}_1|\, e^{i\phi_1} e^{i\theta_1} + |\mathcal{M}_2|\, e^{i\phi_2} e^{i\theta_2}$$

then $|\mathcal{M}|$ and $|\widetilde{\mathcal{M}}|$ can differ because the terms can interfere differently. In the case of B-meson decay, there is a tree level process, and the next most significant contribution is from a "penguin diagram" involving a W loop. In fact, this is generic: one can show that the leading CP violation must involve loop-level processes; interference between just tree-level processes isn't enough. As a result, CP violation is in some sense always small, no matter how large the phases are, since it's always loop suppressed.

6.1.3 Bound States

Next, we briefly discuss nonrelativistic bound states.

• First, note that the potential energy and kinetic energy should be of the same order by the virial theorem. Thus a system is nonrelativistic if its binding energy is small compared with its mass energy.

• For example, light quark bound states are always relativistic, but charmonium $c\bar{c}$ and bottomonium $b\bar{b}$ are not. We don't count toponium $t\bar{t}$ since its lifetime is too short to be observed.

• The archetypical example of such a system is the hydrogen atom, where the energy levels are $\alpha^2 mc^2$ where m is the mass of the electron.

• Fine structure comes from the lowest-order relativistic correction and the spin-orbit coupling of the electron. It can be calculated with the Dirac equation and contributes $\alpha^4 mc^2$.

• The Lamb shift comes from QED effects and contributes $\alpha^5 mc^2$.

• The hyperfine structure comes from the spin of the proton. The proton's magnetic moment is much smaller than that of the electron since it is much heavier. It has a spin-spin interaction as well as a spin-orbit coupling with the electron and contributes $(m/m_p)\,\alpha^4 mc^2$.

• Positronium behaves very similarly to hydrogen; using the reduced mass, its energy levels are like those of hydrogen with an electron half as massive.

• One major difference is that the hyperfine structure is now of the same order as the fine structure.

• Since both the particles move quickly, there is another $\alpha^4 mc^2$ correction due to the propagation time for the electromagnetic field.

• The electron and positron can also temporarily annihilate into a virtual photon. Since the probability for this process is proportional to $|\psi(0)|^2$, at lowest order it only occurs for $\ell = 0$. Since the photon has spin one, it only occurs in the triplet configuration $s = 1$.

• Finally, the electron and positron can annihilate. Positronium has C eigenvalue $(-1)^{\ell+s}$ while a state with n photons has $(-1)^n$, restricting the number of photons produced. By the same logic as above, annihilation only occurs at lowest order for $\ell = 0$, usually producing 2 photons for the spin singlet and 3 for the spin triplet. The decay of the triplet state (called ortho-positronium) is hence slower, by roughly a factor of α.

• Finally, we turn to 'quarkonium', a system of a quark and its antiquark. In this case, the energy levels are far enough apart that we regard excited states as entirely different particles.

• The energy levels can be found numerically using the ansatz

$$V(r) = -\frac{4}{3}\frac{\alpha_s}{r} + F_0 r$$

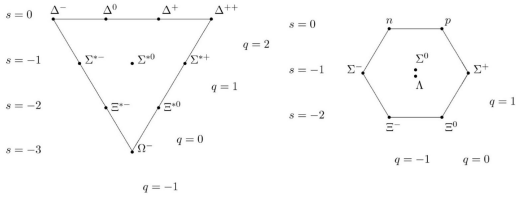
where the factor of $4/3$ is a color factor. The second factor is purely an empirical guess; the numerics also work well if we use $\log r$ or r^2.

• When the J/ψ was discovered, in the "November revolution" of 1974, it was quickly identified as the 1^3S_1 state of charmonium, where this notation should be read as $n = 1$, $2s + 1 = 3, \ell = 0$, and $j = 1$, where j is the total angular momentum; it was known that $s = 1$ because it was produced through a virtual photon.

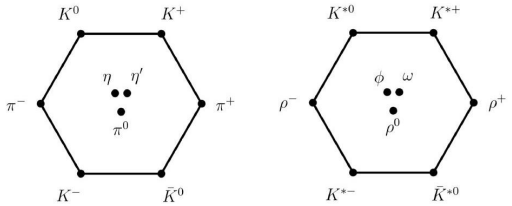
• Shortly afterward, the 1^1S_0 and 2^3S_1 states were found, and eventually all of the $n = 1$ and $n = 2$ states. For $n \leq 2$, charmonium decays slowly by an OZI-suppressed process where the c and $\bar{c}$ annihilate to gluons, making it an exceptionally narrow resonance, but for $n > 2$ charmonium decays quickly via $\psi \to D^+D^-$.

• In 1977, the upsilon meson Υ was quickly identified as the 1^3S_1 state of bottomonium, and states of bottomonium have been found up to $n = 6$.

Note. Before tackling the light mesons and baryons, we show the lowest energy meson nonets and the lowest energy baryon octet and decouplet. The baryons are shown below.



The pseudoscalar and vector mesons are shown below, with the pseudoscalars at left.



Next, we consider the light quark mesons. In this case, we can't say anything quantitative about the bound state masses, so we focus on the wavefunctions.

• For simplicity, we consider the ground state $n = 1$ and $\ell = 0$, so we only have to think about the quark flavor and spin. Since isospin and spin commute, the mesons can be organized into groups of definite flavor $\mathfrak{su}(3)$ representation and spin, e.g. the meson octets and singlets we've already seen. Excited states will give further meson multiplets.

• In our case, we expect $3 \times 3 \times 2 \times 2 = 36$ states in total. They are organized into:

• A pseudoscalar octet with spin $J = 0$, containing 8 states.

• A pseudoscalar singlet η' with spin $J = 0$, containing 1 state.

• A vector octet with spin $J = 1$, containing 24 states.

• A vector singlet with spin $J = 1$, containing 3 states.

The octet and singlet can be superposed to form a nonet.

• Now, we can write down the wavefunctions of these states. Since we've restricted to $n = 1$ and $\ell = 0$, the position space wavefunction is rather trivial; the color wavefunction must simply be the color singlet, and the spin wavefunction is totally independent of the flavor wavefunction. So the only nontrivial part we need is the flavor wavefunction.

• We focus on the states with $I_3 = 0$, which occupy the center of the pseudoscalar nonet. The pions in this row form an isospin triplet, so the π^0 is the $I_3 = 0$ state of the triplet, $u\bar{u} - d\bar{d}$.

(Naively we would think there should be a plus sign here, because a minus sign indicates a spin singlet state, but the minus sign is correct, as explained below.)

• The remaining states with $I_3 = 0$ are

$$\eta = u\bar{u} + d\bar{d} - 2s\bar{s}, \quad \eta' = u\bar{u} + d\bar{d} + s\bar{s}$$

where the η' is just the $\mathfrak{su}(3)$ singlet.

• The situation is slightly different for the vector mesons; here the equivalents of the η and η' mix, to form the physical states

$$\omega = u\bar{u} + d\bar{d}, \quad \phi = s\bar{s}$$

This occurs because $\mathfrak{su}(3)$ is broken by quark masses, and the strange quark is quite heavy. The reason this mixing doesn't happen for η and η' is that the singlet η' has a large contribution to its mass due to instanton effects.

• The ϕ is the strange quark analogue of the J/ψ. It decays slowly because it's too light to decay into two mesons with one s or $\bar{s}$ each, and an $s\bar{s} \to g^* \to \ldots$ decay is OZI suppressed; in fact, this was how the OZI rule was discovered.

• The mesons in the pseudoscalar nonet and vector nonet differ in mass, so part of the strong force must be spin-dependent. A good empirical model for the meson masses is

$$M = m_1 + m_2 + A\frac{\mathbf{S}_1 \cdot \mathbf{S}_2}{m_1 m_2}$$

where we divide the spins by the masses to get magnetic moments, and the constant A and the effective quark masses m_i are fit numerically.

• Heuristically, the effective quark masses account for the bare quark masses and the QCD field energy each quark carries around. The other term accounts for spin-spin coupling through color magnetic moments, which are inversely proportional to the masses. We've already accounted for the "color electric" force; it just binds the quarks together independent of their flavor and is counted in the effective masses.

Note. Why are the vector mesons heavier? Consider an analogy with positronium. The energy is lowest when the magnetic moments are aligned, but since the charges are opposite, this corresponds to the spins anti-aligned, giving a total of spin 0. The same reasoning holds for mesons, though it's color charge rather than electric charge that's opposite. For baryons, the situation is more complicated because the color charges differ by more than just a sign, but the same idea holds.

We can get plenty of insight from our simple model above. For example, the splitting between K and K^* is smaller than the splitting between π and ρ because it involves the strange quark, which has a larger mass. Another example is the $\Sigma - \Lambda$ splitting. The Σ^0 and Λ have exactly the same quark content uds, but the latter has isospin zero, so the u and d quarks are antisymmetric in flavor and hence antisymmetric in spin. Since the u - d spin-spin interaction is the most important, the Λ is slightly lighter.

Note. Extra sign flips arise because there are two competing and incompatible sign conventions. We would like to define the antiparticles by charge conjugation, e.g. $|\bar{u}\rangle = C|u\rangle$, i.e. so the matrix elements of C are all positive. On the the other hand, we want to work with eigenstates of I_3 and I^2 under the Cordan-Shortley phase convention, under which the $I_\pm$have real positive entries.

By definition, charge conjugation flips the isospin,

$$CI_3C^{-1} = -I_3.$$

As a result, it must exchange raising and lowering operators, so

$$CI_\pm C^{-1} = \alpha I_\mp$$

where $\alpha = \pm 1$, because the transformed $I_\pm$operators must be Hermitian conjugates. We choose $\alpha = -1$, which implies

$$CI_1C^{-1} = -I_1, \quad CI_2C^{-1} = I_2.$$

Now consider the isospin doublet $\{|u\rangle, |d\rangle\}$ and their images under $C, |\bar{u}\rangle, |\bar{d}\rangle$. If we didn't care about sign conventions, we would have a new isospin doublet $\{|\bar{d}\rangle, |\bar{u}\rangle\}$, but

$$I_+|\bar{u}\rangle = I_+ C|u\rangle = -CI_-|u\rangle = -C|d\rangle = -|\bar{d}\rangle.$$

Then for the Cordan-Shortley phase convention to apply we must introduce a relative sign, though a global sign is still arbitrary; we thus choose the isospin doublet $\{-|\bar{d}\rangle, |\bar{u}\rangle\}$. We can then use standard tables of Clebsch-Gordan coefficients to add isospin.

Note. The role of antisymmetrization of the wavefunction. At the level of quantum field theory, the wavefunction for any system of fermions must always be antisymmetrized, whether the fermions are the same 'type' or not, because all fermion creation operators anticommute,

$$\langle 0 \left| a_x b_y b_y^\dagger a_x^\dagger \right| 0 \rangle = - \langle 0 \left| b_y a_x b_y^\dagger a_x^\dagger \right| 0 \rangle$$

In wavefunction notation, the state of n fermions lives in the totally antisymmetric subspace of $\mathcal{H}^{\otimes n}$, where the single-particle space $\mathcal{H}$ includes fermions of all positions, spins, flavors, and colors. The exchange operation swaps all of these properties, not just the positions.

However, if some particle has a property that none of the other particles share, it can be excluded from the antisymmetrization without any effect. For example, if an electron is far away from all the others, we can turn off the antisymmetrization because the only effect is to remove the exchange force, which that electron doesn't feel; the electron is 'distinguishable by its position'. Similarly, if only one electron in an atom has spin up, we can treat it naively because it won't violate the exclusion principle.

In the case of mesons, the constituents can always be treated as distinguishable because only one of them will be an antiquark. But most baryons contain quarks with the same flavors, in which case the antisymmetrization matters.

Finally, we turn to the light baryons, carefully accounting for the antisymmetrization. The wavefunction has four parts: position, color, flavor, and spin.

• The position wavefunction is more complicated; the orbital angular momentum must be described by two parameters (e.g. the angular momentum $\mathbf{L}$ of the first two particle about their center of mass, and the angular momentum $\mathbf{L}'$ of their center of mass and the third particle about the combined center of mass). We ignore these problems by restricting to $n = 1$ and $\ell = \ell' = 0$, so the position wavefunction is symmetric.

• The color wavefunction must always be the color singlet, i.e. the 1 in

$$3 \times 3 \times 3 = 1 + 8 + 8 + 10.$$

This is antisymmetric and always the same, so we don't write it.

• Now the combined spin and flavor wavefunctions must be symmetric. In the case of spin,

$$2 \times 2 \times 2 = 2_{ma} + 2_{ma} + 4_s$$

where the 4 is spin 3/2 and contains totally symmetric wavefunctions, and the 'ma' stands for 'mixed antisymmetry'. The decomposition of the remainder into $2 + 2$ is not unique; for example, we have

$$\left|\frac{1}{2}\frac{1}{2}\right\rangle_{12} = |10 - 01\rangle|1\rangle, \quad \left|\frac{1}{2} - \frac{1}{2}\right\rangle_{12} = |10 - 01\rangle|0\rangle$$

which is antisymmetric in slots 1 and 2, but also a 2 antisymmetric in 2 and 3, and a 2 antisymmetric in 1 and 3.

• Finally, we turn to the flavor wavefunction, where

$$3 \times 3 \times 3 = 1_a + 8_{ma} + 8_{ma} + 10_s.$$

We can build an allowed baryon multiplet with $10_s \times 4_s$, giving the spin 3/2 baryon decuplet.

• Many of the remaining states are forbidden, since we can't build symmetric combinations from them. However, we can build a baryon octet out of the mixed antisymmetric representations,

$$\psi \sim \psi_{12}(\text{ spin })\psi_{12}(\text{ flavor }) + \psi_{23}(\text{ spin })\psi_{23}(\text{ flavor }) + \psi_{13}(\text{spin})\psi_{13}(\text{ flavor })$$

This accounts for all of the low-energy baryons.

• Similarly, we can construct a totally antisymmetric combination

$$\psi \sim \psi_{12}(\text{ spin })\left(\psi_{31}(\text{ flavor }) + \psi_{32}(\text{ flavor })\right) + \text{ cyclic}$$

This would be the baryon octet if quark color didn't exist; it appears for excited states with nonzero angular momentum.

• As an application, we can compute the magnetic moments of the baryons by

$$\boldsymbol{\mu} = \boldsymbol{\mu}_1 + \boldsymbol{\mu}_2 + \boldsymbol{\mu}_3, \quad \boldsymbol{\mu}_i = \frac{q}{m_i}\mathbf{S}_i$$

where m_i is the effective quark mass. Specifically, we usually calculate the z-component of $\boldsymbol{\mu}$ in the spin up configuration, so we need the expectation value of $\sum_i \mu_i^z$.

• As an explicit example, consider the proton. The wavefunction is

$$\left|p, +\frac{1}{2}\right\rangle = (|101\rangle - |011\rangle)(|udu\rangle - |duu\rangle) + (|110\rangle - |101\rangle)(|uud\rangle - |udu\rangle) + (|110\rangle - |011\rangle)(|uud\rangle - |duu\rangle)$$

and we can expand out the 12 terms and evaluate the magnetic moment to be $(4\mu_u - \mu_d)/3$, within 1% of the experimental result.

• As with the mesons, we can compute the masses using the empirical formula

$$M = m_1 + m_2 + m_3 + A\left[\frac{\mathbf{S}_1 \cdot \mathbf{S}_2}{m_1 m_2} + \frac{\mathbf{S}_1 \cdot \mathbf{S}_3}{m_1 m_3} + \frac{\mathbf{S}_2 \cdot \mathbf{S}_3}{m_2 m_3}\right]$$

For example, for the baryon decouplet, all pairs of spins are 'parallel', so
which implies that

$$(\mathbf{S}_1 + \mathbf{S}_2)^2 = S_1^2 + S_2^2 + 2\mathbf{S}_1 \cdot \mathbf{S}_2, \quad \mathbf{S}_1 \cdot \mathbf{S}_2 = \frac{\hbar^2}{4}$$

$$M_{\Sigma^*} = 2m_u + m_s + \frac{\hbar^2 A'}{4}\left(\frac{1}{m_u^2} + \frac{2}{m_u m_s}\right)$$

These predictions are also within 1% of the experimental results, though we need to fit the quark masses differently.

Note. We can also arrive at the above result with more powerful machinery. We combine flavor and spin into an $\mathfrak{su}(6)$ symmetry and use the fact

$$6 \times 6 \times 6 = 56_s + 70_{ms} + 70_{ma} + 20_a.$$

Then the 56_s is exactly the set with the right symmetry. Restricting to $\mathfrak{su}(3) \oplus \mathfrak{su}(2)$ gives

$$56_s \to (10, 4) + (8, 2)$$

which are exactly the baryon decuplet and octet. The other possibly useful representation is the antisymmetric one, which breaks up as

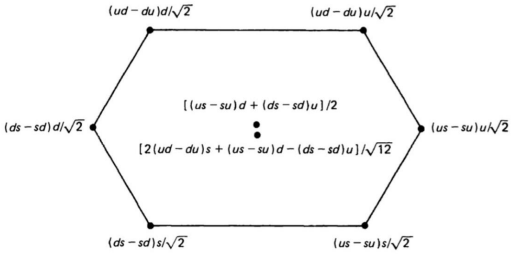
$$20_a \to (8,2) + (1,4).$$

For the mesons, we have

$$6 \times \overline{6} = 35 + 1 \to (8,1) + (8,3) + (1,3) + (1,1)$$

which reproduces the two octets and singlets seen before. One might worry that combining a spacetime and internal symmetry in this way is forbidden by the Coleman-Mandula theorem, but there's no problem because we're working nonrelativistically. We can also handle magnetic moments; since the magnetic moment operator is in the adjoint 35, and 35×56 only contains 56 once, all of the moments can be expressed in terms of a single one, up to $\mathfrak{su}(6)$ breaking.

Example. We construct the spin wavefunctions using the usual $\mathfrak{su}(2)$ procedure. We can handle flavor with an ad hoc method. The 10_s is easy because the wavefunctions are totally symmetric and the quark content is fixed by the strangeness and isospin; for example, the Δ^0 is $|ddu\rangle + |dud\rangle + |udd\rangle$. The 1_a is simply the totally antisymmetric combination.



Now consider the 8_{ma} antisymmetric in the first two particles. The outer six states are found by taking the known quark content and simply antisymmetrizing the first two particles. One of the center states is part of an isospin triplet and can be found by isospin raising $(|ds\rangle - |sd\rangle)|d\rangle$. The other center state is found by orthogonality with this state and the 1_a.

6.1.4 Quantum Chromodynamics

Next, we perform some elementary computations in quantum chromodynamics. We begin with the cross-section for $e^+e^- \to$ hadrons.

• Quarks can be pair produced by $e^+e^- \to \gamma^* \to q\bar{q}$. As the high-energy quarks separate, they emit gluons which emit quark-antiquark pairs. Eventually, each group of particles turns into a "jet" of hadrons, whose direction is correlated with that of the original hard quark.

• Note that to make the jets colorless, a quark or antiquark needs to be transferred between them. This doesn't make much of a difference, since it will be much lower-energy than the original hard quarks.

• The quarks can also emit a hard gluon, $\gamma^* \to q\bar{q}g$. In this case, we get a three-jet event; such events were key in establishing that gluons existed.

• Neglecting the masses of all particles, the cross-section for this process is

$$\sigma = \frac{\pi}{3}\frac{Q^2\alpha^2}{E^2}$$

where Q is the charge of the quark. Therefore,

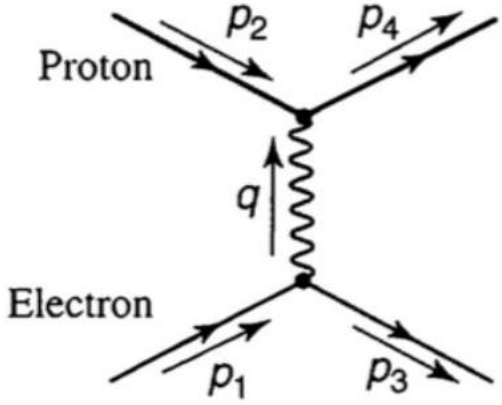
$$R = \frac{\sigma\left(e^+e^- \to \text{ hadrons }\right)}{\sigma\left(e^+e^- \to \mu^+\mu^-\right)} = 3\sum_i Q_i^2$$

where the 3 is for the three colors of quarks, and the sum is over quarks with masses much less than E. We expect Q to look like a step function, jumping up for every flavor of quark.

• There are a few complications. Each step should be smoothed out by the masses. We have neglected the interaction of the two final-state quarks, but this is very important near a resonance, where the cross-section has a peak. Above about 50GeV, R quickly increases because of the Z^0 peak. But overall, the data fits reasonably well, and unambiguously establishes three quark colors.

Next, we turn to elastic electron-proton scattering, mediated by a photon.

• At the most naive level, suppose the proton is a Dirac point charge.



If the momentum transfer is q, the spin-averaged amplitude is

$$|\mathcal{M}|^2 = \frac{e^4}{q^4} L_e^{\mu\nu} L^p_{\mu\nu}, \quad L_e^{\mu\nu} = 2\left(p_1^\mu p_3^\nu + p_1^\nu p_3^\mu + \eta^{\mu\nu}\left(m^2 - p_1 \cdot p_3\right)\right)$$

where the L factors come from the traces.

• In reality, the proton is much more complicated, and we can parametrize our ignorance with form factors. Letting p be the initial proton momentum, we may write the proton factor as

$$K^{\mu\nu} = -K_1 \eta^{\mu\nu} + \frac{K_2}{M^2} p^\mu p^\nu + \frac{K_4}{M^2} q^\mu q^\nu + \frac{K_5}{M^2}\left(p^\mu q^\nu + p^\nu q^\mu\right)$$

We haven't written the antisymmetric combination, which would have coefficient K_3, since $L^{\mu\nu}$ is symmetric.

• Next, we can check that $q_\mu L^{\mu\nu} = 0$, which means that we can choose $K^{\mu\nu}$ so that $q_\mu K^{\mu\nu} = 0$ without affecting the result. This allows us to eliminate K_4 and K_5, giving

$$K^{\mu\nu} = K_1\left(q^2\right)\left(-\eta^{\mu\nu} + \frac{q^\mu q^\nu}{q^2}\right) + \frac{K_2\left(q^2\right)}{M^2}\left(p^\mu + q^\mu/2\right)\left(p^\nu + q^\nu/2\right)$$

where $K_1\left(q^2\right)$ and $K_2\left(q^2\right)$ have absorbed the effects of K_4 and K_5, and depend on q. For example, for the original point charge model, $K_1 = -q^2$ and $K_2 = 4M^2$.

• The cross section is given by the Rosenbluth formula

$$\frac{d\sigma}{d\Omega} = \left(\frac{\alpha}{4ME\sin^2(\theta/2)}\right)^2 \frac{E'}{E}\left(2K_1 \sin^2(\theta/2) + K_2 \cos^2(\theta/2)\right)$$

where E and E' are the initial and final electron energies, and we have assumed $E \gg m$. As a check, when $E \ll M$, the point charge form factors work. Then our result reduces to the Mott formula, which describes electron scattering off a heavy pointlike target.

• The form factors $K_1\left(q^2\right)$ and $K_2\left(q^2\right)$ are measured by experiment and indicate the proton is not pointlike, as expected from QCD.

Next, we turn to the Feynman rules for QCD itself. The coupling is g_s, and we define $\alpha_s = g_s^2/4\pi$.

• Quarks are specified by both a spinor polarization and a color. We label the colors with mid-Latin letters and call them red, blue, and green.

• There is a gluon and two quark vertex, so the gluon colors must live in $3 \times \overline{3} = 8 + 1$. The elements of $3 \times \overline{3}$ have colors like $r\bar{r}$ ('red anti-red') and $b\bar{g}$ ('blue anti-green'). The color singlet $r\bar{r} + b\bar{b} + g\bar{g}$ is analogous to the meson singlet.

• One might wonder whether there is a ninth gluon. Theoretically, this is equivalent to the choice of gauge group $\mathfrak{su}(3)$ or $\mathfrak{u}(3)$. Since the ninth gluon would be a color singlet, it would not be confined, and would instead mediate a long-range force between color singlets; it would have an independent coupling since $\mathfrak{u}(3)$ is not semisimple. Such a force would appear as an anomalous contribution to gravity, and there was a brief excitement over this in 1986.

• The eight gluons can be put in correspondence with the eight Gell-Mann matrices λ^α, where

$$\lambda^1 = \begin{pmatrix} 1 & 1 \\ & \end{pmatrix}, \quad \lambda^2 = \begin{pmatrix} i & -i \\ & \end{pmatrix}, \quad \lambda^3 = \begin{pmatrix} 1 & \\ & -1 \end{pmatrix}, \quad \lambda^4 = \begin{pmatrix} & 1 \\ & \end{pmatrix}$$

$$\lambda^5 = \begin{pmatrix} & -i \\ i & \end{pmatrix}, \quad \lambda^6 = \begin{pmatrix} & 1 \\ 1 & \end{pmatrix}, \quad \lambda^7 = \begin{pmatrix} & -i \\ i & \end{pmatrix}, \quad \lambda^8 = \frac{1}{\sqrt{3}} \begin{pmatrix} 1 & & \\ & 1 & \\ & & -2 \end{pmatrix}$$

which are normalized to match the Pauli matrices, with $\text{tr}\left(\lambda^\alpha \lambda^\beta\right) = 2\delta^{\alpha\beta}$. The colors can be read off the columns and the anticolors off the rows, so that λ^1 essentially means 'red anti-blue plus blue anti-red'.

• We define $T^\alpha = \lambda^\alpha/2$, so the structure constants are

$$\left[T^\alpha, T^\beta\right] = i f^{\alpha\beta\gamma} T^\gamma$$

By direct calculation, we have

$$f^{123} = 1, \quad f^{147} = f^{246} = f^{257} = f^{345} = f^{516} = f^{637} = \frac{1}{2}, \quad f^{458} = f^{678} = \frac{\sqrt{3}}{2}$$

with all other nonzero structure constants related by total antisymmetry.

• The Feynman rules for QCD are as follows.

• Incoming quarks have a color and spin polarization $u^s(p)c$. Similarly, outgoing quarks have $c^\dagger$, incoming antiquarks have $c^\dagger$, and outgoing antiquarks have c.

• Incoming gluons have a color and polarization $\epsilon_\mu(p)a^\alpha$, and outgoing gluons have $\epsilon_\mu^*(p)a^{\alpha *}$.

• The propagators are the same as usual, with delta functions in color space.

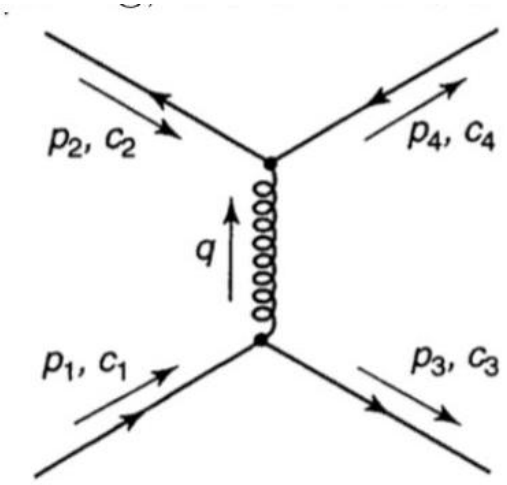
• The qqg vertex gives a factor of $-ig_s\lambda^a\gamma^\mu/2$.

• The ggg vertex with colors α, β, and γ has a factor of $f^{\alpha\beta\gamma}$ along with other terms. The gggg vertex is similar, with two structure constants.

• Many simple processes will have amplitudes that look just like the QED amplitudes, but with an additional 'color factor'. A useful rule for finding these factors is

$$\lambda^\alpha_{ij}\lambda^\alpha_{k\ell} = 2\delta_{i\ell}\delta_{jk} - \frac{2}{3}\delta_{ij}\delta_{k\ell}$$

Example. Quark and antiquark scattering, $u + \bar{d} \to u + \bar{d}$. At lowest order, there is one diagram.



The amplitude is the same as in QED except for a color factor, so the potential is

$$V(r) = -f\frac{\alpha_s}{r}, \quad f = \frac{1}{4}\left(c_3^\dagger \lambda^\alpha c_1\right)\left(c_2^\dagger \lambda^\alpha c_4\right)$$

First, suppose the quark and antiquark are part of a color octet. For concreteness, let the incoming quark and antiquark be red and anti-blue, respectively. By color conservation, the outgoing quark and antiquark must also be red and anti-blue, respectively. Then

$$f = \frac{1}{4}\lambda_{11}^\alpha \lambda_{22}^\alpha = -\frac{1}{6}$$

The color singlet state is $(r\bar{r} + b\bar{b} + g\bar{g})/\sqrt{3}$, so there are nine terms in all; for example, the part where the quarks come in $r\bar{r}$ and leave $b\bar{b}$ is $(1/4)(1/3)\lambda_{21}^\alpha \lambda_{12}^\alpha$. They can be compactly written as

$$f = \frac{1}{4}\frac{1}{3}\lambda_{ij}^\alpha \lambda_{ji}^\alpha = \frac{1}{12}\,\mathrm{tr}\,(\lambda^\alpha \lambda^\alpha) = \frac{4}{3}$$

Then the force between a quark and antiquark is only attractive if they form a color singlet! This is nice, but only suggestive; after all, we worked to lowest order, which required asymptotic freedom, but confinement does not occur in this regime.

Note. In the case $u + \bar{u} \to u + \bar{u}$, we would also have the s-channel diagram. In the case where the incoming quarks form a color singlet, this is automatically zero since a singlet cannot couple to an octet.

Example. Quark and quark scattering, $u + d \to u + d$. The color factor is very similar,

$$f = \frac{1}{4}\left(c_3^\dagger \lambda^\alpha c_1\right)\left(c_4^\dagger \lambda^\alpha c_2\right)$$

where the labels on the c_i are as above. Now, $3 \times 3 = 6 + \overline{3}$, so we must consider the sextet and triplet configurations. They contain the symmetric and antisymmetric parts, respectively:

$$\left\{rr, bb, gg, \frac{rb+br}{\sqrt{2}}, \frac{bg+gb}{\sqrt{2}}, \frac{gr+rg}{\sqrt{2}}\right\}, \quad \left\{\frac{rb-br}{\sqrt{2}}, \frac{bg-gb}{\sqrt{2}}, \frac{gr-rg}{\sqrt{2}}\right\}.$$

For the sextet, we take rr, which gives

$$f = \frac{1}{4}\lambda_{11}^\alpha \lambda_{11}^\alpha = \frac{1}{3}$$

For the triplet, we take $(rb - br)/\sqrt{2}$, which gives four terms,

$$f = \frac{1}{4}\frac{1}{2}\left(\lambda_{11}^{\alpha}\lambda_{22}^{\alpha} - \lambda_{21}^{\alpha}\lambda_{12}^{\alpha} - \lambda_{12}^{\alpha}\lambda_{21}^{\alpha} + \lambda_{22}^{\alpha}\lambda_{11}^{\alpha}\right) = -\frac{2}{3}$$

Then the triplet is attractive and the sextet is not. There aren't triplets observed in nature, but note that the color singlet for three quarks is totally antisymmetric, so any two of the quarks form a color triplet. Then every quark in a color singlet baryon attracts every other quark, as expected.

Example. Pair annihilation. Consider the decay of charmonium. There are two tree-level QED diagrams, $c + \bar{c} \to \gamma + \gamma$, and three tree-level QCD diagrams, $c + \bar{c} \to g + g$. By angular momentum addition, the amplitude is only nonzero if the charmonium is in the spin singlet state. One can show that the two amplitudes differ only by the color factor

$$f = \frac{1}{8}a_3^{\alpha}a_4^{\beta}\left(c_2^{\dagger}\left\{\lambda^{\alpha},\lambda^{\beta}\right\}c_1\right) = \frac{1}{8\sqrt{3}}a_3^{\alpha}a_4^{\beta}\,\mathrm{tr}\left\{\lambda^{\alpha},\lambda^{\beta}\right\} = \frac{1}{2\sqrt{3}}a_3^{\alpha}a_4^{\alpha}$$

where we used the fact that charmonium is in the color singlet state. Now we need to construct the singlet state for two gluons, i.e. the 1 in

$$8 \times 8 = 27 + 10 + \overline{10} + 8 + 8 + 1$$

One can show that this state has the form $\sum_{i=1}^{8}|i\rangle|i\rangle/\sqrt{8}$ where $|i\rangle$ is the gluon state corresponding to the Gell-Mann matrix λ_i, so

$$f = \frac{1}{2\sqrt{3}}\frac{8}{\sqrt{8}} = \sqrt{2/3}$$

The rate of the decay can be computed if $|\psi(0)|^2$ is known, since this gives the incident flux. Though we can't calculate this, we can calculate the ratio of the decay rate to gg to the decay rate to $\gamma\gamma$, calculated in QED.

Note. Consider two objects in color representations A and B. Their interaction is proportional to

$$T_a^A T_b^B = \frac{1}{2}\left(T_a^2 - T_a^{A^2} - \left(T_a^B\right)^2\right)$$

where $T_a = T_a^A + T_a^B$ is a generator for total color. Then the attraction is strongest when the total state has the least color. The same reasoning goes for ordinary electromagnetic interactions or spin-spin interactions; the net effect will usually be to minimize or maximize the 'charge' of the composite state. This attraction is what leads to color confinement.

6.2 Symmetries

6.2.1 Chiral and Gauge Symmetries

We begin by reviewing some conventions for Dirac spinors.

• Let $\psi(x)$ be a Dirac spinor field. The Dirac equation is

$$(i\not{\partial} - m)\psi = 0$$

and the adjoint field $\bar{\psi} = \psi^{\dagger}\gamma^0$ satisfies

$$\bar{\psi}(-i\overleftarrow{\partial} - m) = 0$$

where the left arrow indicates the derivative acts to the left.

• The gamma matrices satisfy the anticommutation relations

$$\{\gamma^\mu, \gamma^\nu\} = 2\eta^{\mu\nu}, \quad \eta = \text{diag}(1, -1, -1, -1)$$

where there is an implicit identity matrix on the right-hand side. In the chiral representation,

$$\gamma^0 = \begin{pmatrix} 0 & 1 \\ 1 & 0 \end{pmatrix}, \quad \gamma^i = \begin{pmatrix} 0 & \sigma^i \\ -\sigma^i & 0 \end{pmatrix}$$

• Dirac masses are not fundamental; in this course we will be more concerned with massless fermions. Then the chirality projection operators become more important. We define

$$\gamma^5 = i\gamma^0\gamma^1\gamma^2\gamma^3 = \begin{pmatrix} -1 & 0 \\ 0 & 1 \end{pmatrix}, \quad \left(\gamma^5\right)^2 = 1, \quad \left\{\gamma^5, \gamma^\mu\right\} = 0$$

where the sign of γ^5 differs between references. Then if ψ solves the massless Dirac equation $\not{\partial}\psi = 0$, then $\gamma^5\psi$ does as well, $\not{\partial}\left(\gamma^5\psi\right) = 0$.

• We define the projection operators

$$P_L = \frac{1-\gamma^5}{2}, \quad P_R = \frac{1+\gamma^5}{2}, \quad \psi_L = P_L\psi, \quad \psi_R = P_R\psi$$

where it is straightforward to show the P_L and P_R project onto orthogonal subspaces,

$$\left(P_{L,R}\right)^2 = P_{L,R}, \quad P_L P_R = P_R P_L = 0, \quad P_L + P_R = 1$$

In the chiral representation, ψ_L/ψ_R has only the upper/lower two components nonzero.

• It's important to note that a lot of the facts above are conventional. For example, $(\psi_L)^*$ is clearly right-chiral in terms of its Lorentz transformation properties, because the left-chiral and right-chiral representations are conjugate, but it is annihilated by P_R because its bottom two components remain zero. When we consider the charge conjugation of fields, we will include a "charge conjugation matrix" whose purpose is to rearrange the components of the naive complex conjugate so that the familiar properties still hold.

• Note that the adjoints of the left-chiral and right-chiral fields satisfy

$$\bar{\psi}_L(x) = \bar{\psi}(x)P_R, \quad \bar{\psi}_R(x) = \bar{\psi}(x)P_L$$

Thus if we stick to only ψ and $\bar{\psi}$, then P_R projects right-chirality from both directions.

• A massless Dirac fermion has a $U(1)_L \times U(1)_R$ chiral symmetry. The Dirac Lagrangian is

$$\mathcal{L} = \bar{\psi}_L i\not{\partial}\psi_L + \bar{\psi}_R i\not{\partial}\psi_R - m\left(\bar{\psi}_R\psi_L + \bar{\psi}_L\psi_R\right)$$

where we get a chirality flip from anticommuting past $\not{\partial}$. Then when $m = 0$, we can rotate the phases of ψ_L and ψ_R independently. Adding the mass term requires the phases to be rotated the same way, breaking the symmetry to a $U(1)_V$ "vector" symmetry. Rotating the phases oppositely gives a $U(1)_A$ "axial" transformation.

Next, we review the process of gauging a symmetry.

• We would like to gauge the $U(1)_V$ symmetry, $\psi \to e^{i\alpha(x)}\psi$, but then

$$\bar{\psi}i\not{\partial}\psi \to \bar{\psi}i\not{\partial}\psi - \left(\bar{\psi}\gamma^\mu\psi\right)\partial_\mu\alpha.$$

To do this, we introduce the covariant derivative,

$$D_\mu\psi = \left(\partial_\mu + igA_\mu\right)\psi, \quad A_\mu(x) \to A_\mu(x) - \frac{1}{g}\partial_\mu\alpha(x), \quad D_\mu\psi(x) \to e^{i\alpha(x)}D_\mu\psi(x)$$

We cannot gauge the axial symmetry, even in the massless case, because of the chiral anomaly. Note that sources may differ on the sign of g, or pull a factor of g out from $\alpha(x)$.

• The kinetic term of the gauge field is

$$\mathcal{L} = -\frac{1}{4}F_{\mu\nu}F^{\mu\nu}, \quad [D_\mu, D_\nu] = igF_{\mu\nu}, \quad F_{\mu\nu} = \partial_\mu A_\nu - \partial_\nu A_\mu$$

where $F_{\mu\nu}$ is gauge invariant.

• The procedure for non-abelian gauge symmetry is similar. The matter field now transforms in a unitary representation r of the gauge group G, with transformation

$$\psi_i(x) \to \exp\left(it^a\alpha^a(x)\right)_{ij}\psi_j(x) = U_{ij}\psi_j(x), \quad \bar{\psi}_i(x) \to \bar{\psi}_j(x)\exp\left(-it^a\alpha^a(x)\right)_{ji} = \bar{\psi}_j(x)\left(U^\dagger\right)_{ji}$$

where the t^a are the Hermitian generators in this representation, and satisfy

$$\left[t^a, t^b\right] = if^{abc}t^c, \quad \operatorname{tr} t^a t^b = T(r)\delta^{ab}$$

where $T(r)$ is the Dynkin index, which is $1/2$ for the fundamental representation.

• The covariant derivative is

$$\left(D_\mu\right)_{ij} = \partial_\mu\delta_{ij} + ig\left(t^a A^a_\mu\right)_{ij}, \quad \left(D_\mu\psi(x)\right)_i \to \left(U(x)D_\mu\psi(x)\right)_i$$

where we have introduced a Lie algebra valued field A_μ that transforms as

$$A_\mu \to UA_\mu U^{-1} + \frac{i}{g}\left(\partial_\mu U\right)U^{-1}$$

where we now drop the matrix indices i and j.

• More generally, we define the covariant derivative of any object X similarly, but with A_μ in the appropriate representation; then the covariant derivative DX transforms just like X. For example, the infinitesimal transformation of A_μ itself is

$$A_\mu \to A_\mu - \frac{1}{g}\left(\partial_\mu\alpha + ig\left[A_\mu, \alpha\right]\right) = A_\mu - \frac{1}{g}D_\mu\alpha$$

where the D_μ acts as if α is in the adjoint representation. Note that A_μ doesn't transform in any definite representation, much like how the connection in GR is not a tensor.

• Dropping the i and j indices, the field strength is

$$[D_\mu, D_\nu] = igt^a F^a_{\mu\nu}, \quad F^a_{\mu\nu} = \partial_\mu A^a_\nu - \partial_\nu A^a_\mu - gf^{abc}A^b_\mu A^c_\nu$$

That is, as in general relativity, the commutator of two covariant derivatives is a tensor, not a differential operator. Then the field transforms in the adjoint representation, as

$$\left[D_\mu, D_\nu\right]\psi \to U\left[D_\mu, D_\nu\right]\psi = U\left[D_\mu, D_\nu\right]U^\dagger U\psi, \quad F_{\mu\nu} \to UF_{\mu\nu}U^\dagger$$

Then a gauge invariant kinetic term is

$$\mathcal{L} = -\frac{1}{4}F^a_{\mu\nu}F^{a\mu\nu} = -\frac{1}{2}\operatorname{tr} F_{\mu\nu}F^{\mu\nu}$$

In combination with the fermion kinetic term $\bar{\psi}(i\not{D} - m)\psi$, this is the most general renormalizable gauge invariant Lagrangian in dimension 4 with P and T symmetry.

• More generally, we can think of the field as an infinitesimal Wilson loop. In a sense, the most general gauge invariant observable is the trace of a Wilson loop.

• In some sources, for e.g. gauge group $SU(n)$, the gauge field A_μ is thought of as an $n \times n$ matrix rather than an abstract element of $\mathfrak{su}(n)$, leading to equations like

$$D_\mu F_{\nu\rho} = \partial_\mu F_{\nu\rho} + ig\,[A_\mu, F_{\nu\rho}]$$

Another example is a matter field which transforms in the adjoint representation, with

$$\mathcal{L} = \operatorname{tr} \bar{\psi}(i\not{D} - m)\psi, \quad \psi \to U\psi U^{-1}$$

where U is the same gauge transformation we would have in the fundamental representation, ψ is now a matrix, and A_μ again acts by commutator in the covariant derivative. Expressions like these are less mathematically general but can be easy to compute with.

Note. Symmetries will manifest in several ways below.

• The symmetry can be intact, e.g. the gauge symmetries $U(1)_{EM}$ and $SU(3)_C$.

• The symmetry can be anomalous, holding in the classical theory but not the quantum theory, e.g. the global axial symmetry $U(1)_A$.

• The symmetry can be explicitly broken in the Lagrangian, e.g. isospin $SU(2)$ or generally flavor $SU(6)$. This is useful as long as the symmetry is approximate.

• The symmetry can be spontaneously broken, i.e. the vacuum does not respect the symmetry though the Lagrangian does, e.g. $SU(2)_L \times U(1)_Y$ is spontaneously broken to $U(1)_{EM}$.

6.2.2 Discrete Symmetries

Before beginning with parity, we review discrete spacetime symmetries naively.

• Let W be an operator on a Hilbert space with inner product $(\cdot, \cdot)$. If W is unitary and linear,

$$(W\Phi, W\Psi) = (\Phi, \Psi), \quad W(\alpha\Phi + \beta\Psi) = \alpha W\Phi + \beta W\Psi$$

If W is anti-unitary and hence anti-linear,

$$(W\Phi, W\Psi) = (\Phi, \Psi)^*, \quad W(\alpha\Phi + \beta\Psi) = \alpha^* W\Phi + \beta^* W\Psi$$

Wigner's theorem states that groups of operators that preserve norms (and hence observable probabilities) must be unitary or anti-unitary.

• Let $W(\Lambda, a)$ be the operator on the state space that corresponds to a Poincare transformation consisting of a Lorentz transformation Λ followed by a translation a. Then

$$W\left(\Lambda_2, a_2\right) W\left(\Lambda_1, a_1\right) = W\left(\Lambda_2, \Lambda_1, \Lambda_2 a_1 + a_2\right)$$

We also consider the improper Poincare transformations of parity and time reversal, defining

$$\widehat{P} = W(\mathcal{P}, 0), \quad \widehat{T} = W(\mathcal{T}, 0)$$

• We now consider an infinitesimal proper Poincare transformation,

$$\Lambda^\mu_\nu = \delta^\mu_\nu + \omega^\mu_\nu, \quad a^\mu = \epsilon^\mu.$$

The corresponding quantum operator is expanded as

$$W(1 + \omega, \epsilon) = 1 + \frac{i}{2}\omega_{\mu\nu} J^{\mu\nu} - i\epsilon_\mu P^\mu$$

where the operators $J^{\mu\nu}$ and P^μ are Hermitian and are physically

$$\text{energy } H = P^0, \quad \text{momentum } \mathbf{P} = \left(P^1, P^2, P^3\right)$$

and

$$\text{angular momentum } \mathbf{J} = \left(J^{23}, J^{31}, J^{12}\right), \quad \text{Lorentz boosts } \mathbf{K} = \left(J^{01}, J^{02}, J^{03}\right)$$

• Considering $\widehat{P}W(\Lambda, a)\widehat{P}^{-1}$ and $\widehat{T}W(\Lambda a)\widehat{T}^{-1}$ for an infinitesimal translation,

$$\widehat{P}iP^\mu\widehat{P}^{-1} = i\mathcal{P}^\mu_\nu P^\nu, \quad \widehat{T}iP^\mu\widehat{T}^{-1} = i\mathcal{T}^\mu_\nu P^\nu$$

In particular, focusing on the time component, we have

$$\widehat{P}iH\widehat{P}^{-1} = iH, \quad \widehat{T}iH\widehat{T}^{-1} = -iH$$

If $\widehat{P}$ were antilinear, then it would flip H in conjugation, implying a negative energy state for every positive energy state. This is unacceptable, as it would forbid the existence of a ground state, so $\widehat{P}$ is linear and hence unitary. Similarly, $\widehat{T}$ is anti-unitary.

• With the linearity and antilinearity established, we can now conjugate our other operators by $\widehat{P}$ and $\widehat{T}$ to see how they transform. We find

$$\widehat{P}\mathbf{P}\widehat{P}^{-1} = -\mathbf{P}, \quad \widehat{P}\mathbf{J}\widehat{P}^{-1} = \mathbf{J}, \quad \widehat{P}\mathbf{K}\widehat{P}^{-1} = -\mathbf{K}$$

and

$$\widehat{T}\mathbf{P}\widehat{T}^{-1} = -\mathbf{P}, \quad \widehat{T}\mathbf{J}\widehat{T}^{-1} = -\mathbf{J}, \quad \widehat{T}\mathbf{K}\widehat{T}^{-1} = \mathbf{K}$$

Moreover, upon applying the relations above, we find that parity acts on one-particle states by changing their momenta and angular momenta as implied above, along with a phase factor η_P which depends only on the particle species, called the intrinsic parity.

• Under the naive assumptions we have made above, $\widehat{P}$ and $\widehat{T}$ automatically commute with H. That is, our initial assumptions are equivalent to assuming that $\widehat{P}$ and $\widehat{T}$ violation don't occur! To allow it, we need to think more carefully.

First, we review the basics of representation theory, as covered in the notes on Group Theory.

• The representations of $SO(3)$ are indexed by a nonnegative integer s called the spin. The double/universal cover of $SU(2)$ are indexed by a half-integer, and representations of $SU(2)$ correspond to projective representations of $SO(3)$.

• If we include Lorentz boosts, we arrive at the connected Lorentz group $SO(3,1)_0$, whose double/universal cover is $SL(2,\mathbb{C})$. In general, such a double cover is called a spin group. The finite-dimensional representations are indexed by two half-integers (s_1, s_2), where $s_1 + s_2$ is called the spin. When s is half-integer, the representation is projective.

• Note that restricting to rotations does not produce the spin $s_1 + s_2$ representation of $SU(2)$. Instead, every spin from $|s_1 - s_2|$ to $s_1 + s_2$ in integer steps is represented.

• If $s_2 = 0$, the representation is said to be left-chiral or left-handed, and if $s_1 = 0$, the representation is said to be right-chiral or right-handed. Otherwise, chirality is not defined.

• Fields transform in finite-dimensional non-unitary representations of the Lorentz group, while particles transform in infinite-dimensional unitary representations of the Poincare group, which we take to be $SO(3,1)_0 \rtimes \mathbb{R}^4$. These representations and the vectors in them are labeled by several quantum numbers.

• The mass M labels the physical mass of the particle.

• When $M > 0$, the irreps are labeled by an integer spin s, so that for each momentum, there are $2s + 1$ spin states. These states can be indexed by the helicity h, i.e. the projection of spin along the direction of momentum; Lorentz transformations change h.

• When $M = 0$, the irreps have one state for each momentum, indexed by the integer helicity h. Then the helicity is Lorentz invariant. A helicity h particle is also loosely called a massless spin $s = h$ particle.

• To switch to quantum fields, a massive particle of spin s is embedded in a field of spin s, and a relativistic wave equation is used to eliminate the extra degrees of freedom.

• Using the double cover $SL(2, \mathbb{C}) \rtimes \mathbb{R}^4$, the spin s and helicity h may be half-integer.

• Sometimes one hears that "for massless particles, chirality is the same thing as helicity". This is an oversimplification that can lead to confusion. Helicity is defined for particles, chirality is defined for fields, and the two can behave rather differently.

Next, we confront the issue of discrete symmetries, and their possible violation.

• We introduce parity and time reversal by going to the group $O(3, 1)$. Ignoring the issue of projective representations, the assertion that the Hilbert space carries a representation of $O(3, 1) \rtimes \mathbb{R}^{3,1}$ carries dynamical content, because it automatically implies $\widehat{P}$ and $\widehat{T}$ are conserved. That is, postulating a representation of a set of physical operations exists is a nontrivial statement about the dynamics, when one of the operations is time translation.

• For spinless particles, if we have a representation of $O(3, 1) \rtimes \mathbb{R}^{3,1}$, then $\widehat{P}^2 = 1$ and particles have parity \pm 1. Now consider a spinless theory that violates parity. In this case, we can still talk about parity for asymptotic states, because they are free; we define parity just as in the free theory. This is why we can speak about the change of parity in a scattering process.

• More generally, we must allow projective representations. For the Poincare group, it suffices to promote $SO(3, 1)_0$ to $SL(2, \mathbb{C})$. There is a two-to-one map $\pi : SL(2, \mathbb{C}) \to SO(3, 1)_0$, which can be extended to include the parity operation.

• However, there are two ways to incorporate parity; if $\mathcal{P} \in O(3, 1)$ is parity, then $\pi^{-1}(\mathcal{P})$ contains two elements. Letting $\pi(P) = \mathcal{P}$, we have

$$\pi\left(P^2\right) = \mathcal{P}^2 = 1$$

which implies that $P^2 = \pm 1$. This is a genuine physical ambiguity, and it isn't presently known which is the right option in reality.

• In the case $M > 0$, if $P^2 = 1$ then $\widehat{P}^2 = 1$, and for each s we have two representations, of intrinsic parities \pm 1. If $P^2 = -1$, we instead have $\widehat{P}^2 = (-1)^F$ where F is the fermion number. Specifically, for integer s the intrinsic parities are \pm 1 and for half-integer s the intrinsic parities are $\pm i$. This doesn't contradict the fact that $P^2 = -1$ because for integer $s, -1$ is represented as $+1$.

• However, Dirac fermions carry other conserved quantum numbers, and we may replace $\widehat{P}$ with $\widehat{P}e^{i\alpha Q}$ for any conserved charge Q to find the same experimental consequences; in the SM the conservation of electric charge, lepton number, and baryon number are sufficient to redefine parity so that $\widehat{P}^2 = 1$ in all cases. Stated another way, other conservation laws always rule out possible experimental tests between the situations above.

• On the other hand, if a Majorana fermion were discovered, it would carry no conserved charges, so it could distinguish between the possibilities. Specifically, if $\widehat{P}^2 = (-1)^F$, then no process which conserves parity can turn this particle into three copies of itself, since $(\pm i) \neq (\pm i)^3$.

• In the case $M = 0$, parity implies that irreps must contain helicities of $\pm\lambda$ in pairs; this is also a consequence of CP or CPT. However, if we also demand that parity does not change the values of internal quantum numbers, then there's no reasonable way to define parity for a theory with a single Weyl spinor. The helicities still come in pairs, but the pairing requires flipping internal quantum numbers; we instead call this symmetry CPT.

• In the real world, parity is not conserved, but with the exception of chiral theories (e.g. with a single Weyl spinor) where parity cannot even be reasonably defined, the free Hamiltonian

always commutes with parity. Thus parity can be defined in terms of the free theory, allowing the parities of asymptotic particles to be defined.

• In the above discussion, we have neglected time reversal. When we account for both parity and time reversal and allow for projective representations, we find eight possibilities in total, though the so-called Pin groups are the mathematically nicest.

6.2.3 Parity

Now we investigate parity more precisely, beginning with the scalar field. As we motivated above, we focus on defining parity on free fields.

• A scalar field has plane wave expansion

$$\phi(x) = \sum_p a(p)e^{-ipx} + c^\dagger(p)e^{ipx}, \quad \sum_p = \int \frac{d\mathbf{p}}{2E_\mathbf{p}}$$

where $a^\dagger(p)/c^\dagger(p)$ create particles/antiparticles with momentum p. We use the relativistic normalization convention, so the created states have squared norm $2E_\mathbf{p}$.

• Now, parity should preserve the number of particles and flip the momentum, so

$$\widehat{P}a^\dagger(p)|0\rangle = \eta^{a*}a^\dagger\left(p_P\right)|0\rangle$$

where p_P is the parity-flipped four-momentum and η^{a*} is a phase, by unitarity.

• Inserting $\widehat{P}^{-1}\widehat{P} = 1$ above and assuming the vacuum is parity invariant, $\widehat{P}|0\rangle = |0\rangle$, we find

$$\widehat{P}a^\dagger(p)\widehat{P}^{-1} = \eta^{a*}a^\dagger\left(p_P\right), \quad \widehat{P}c^\dagger(p)\widehat{P}^{-1} = \eta^{c*}c^\dagger\left(p_P\right)$$

Taking the adjoint, we find

$$\widehat{P}a(p)\widehat{P}^{-1} = \eta^{a}a\left(p_P\right), \quad \widehat{P}c(p)\widehat{P}^{-1} = \eta^{c}c\left(p_P\right).$$

• Now, the parity conjugate of the scalar field is defined as

$$\phi^P(x) \equiv \widehat{P}\phi(x)\widehat{P}^{-1} = \sum_p \eta^a a\left(p_P\right)e^{-ipx} + \eta^{c*}c^\dagger\left(p_P\right)e^{ipx} = \sum_p \eta^a a(p)e^{-ip_Px} + \eta^{c*}c^\dagger(p)e^{ip_Px}$$

where we reindexed the sum. This looks rather different from our previous expression; moreover, $\left[\phi(x), \phi^\dagger(y)\right]$ does not necessarily vanish for spacelike x and y.

• These problems are solved if $\eta^a = \eta^{c*} \equiv \eta_P$, so

$$\phi^P(x) = \eta_P\phi\left(x_P\right).$$

The phase η_P is called the intrinsic parity of ϕ.

• If ϕ is a real field, then $c(p) = a(p)$, so $\eta^c = \eta^a$, which implies that η_P is real, and hence it is \pm 1. The case +1 is a scalar, and the case -1 is a pseudoscalar.

• On the other hand, for a complex field η_P can be an arbitrary phase, but there is a $U(1)$ internal symmetry which may yield a conserved charge Q. In this case, we can always replace $\widehat{P}$ with $\widehat{P}e^{-i\alpha Q}$, where α may be chosen so that $\widehat{P}^2 = 1$, so that $\eta_P = \pm 1$.

• Another way of saying this is that the complex scalar isn't really a different case than a real scalar. Everything that can be expressed in terms of complex scalars can be expressed in terms of pairs of real scalars with appropriate $U(1)$ symmetries. Choosing a description in terms of complex scalars is purely a matter of convention and convenience, which pays off when the $U(1)$ symmetries at least approximately hold in the interacting theory.

• In the case of vector fields, we have

$$V^\mu(x) = \sum_{p,\lambda} \epsilon^{\lambda\mu}(p) a^\lambda(p) e^{-ipx} + \epsilon^{\lambda\mu^*}(p) c^{\lambda^*}(p) e^{ipx}$$

where the $\epsilon^{\lambda\mu}$ are polarization vectors. It can be shown, using the desired properties of parity defined in the previous section, that they transform as

$$\epsilon^{\lambda\mu}\left(p_P\right) = -\mathcal{P}^\mu_\nu \epsilon^{\lambda\nu}(p)$$

• The rest of the argument goes as before, so for a real vector field

$$\widehat{P} V^\mu(x) \widehat{P}^{-1} = -\eta_P \mathcal{P}^\mu_\nu V^\nu\left(x_P\right)$$

where $\eta_P = -1$ for a polar vector and $\eta_P = 1$ for an axial vector.
We now review conventions for the Dirac field, which is more subtle.
• A solution to the free Dirac equation can be expanded as

$$\psi(x) = \sum_{p,s} b^s(p) u^s(p) e^{-ipx} + d^{s\dagger}(p) v^s(p) e^{ipx}$$

where $b^\dagger$ and $d^\dagger$ create particles and antiparticles of momentum p, and the spinors satisfy

$$(\not{p} - m) u(p) = 0, \quad (\not{p} + m) v(p) = 0$$

for components $s = \pm 1/2$. In the chiral representation their components are

$$u^s(p) = \begin{pmatrix} \sqrt{p\cdot\sigma}\xi^s \\ \sqrt{p\cdot\bar{\sigma}}\xi^s \end{pmatrix}, \quad v^s(p) = \begin{pmatrix} \sqrt{p\cdot\sigma}\zeta^s \\ -\sqrt{p\cdot\bar{\sigma}}\zeta^s \end{pmatrix}, \quad \sigma = (1, \boldsymbol{\sigma}), \quad \bar{\sigma} = (1, -\boldsymbol{\sigma})$$

and a useful basis of two-component spinors is $\xi^{1/2} = (1,0)^T$ and $\xi^{-1/2} = (0,1)^T$, which have spin up and spin down along $\hat{z}$ for both the positive and negative frequency solutions. We'll use a different basis for the negative frequency solutions for convenience, as explained below.
• The spin angular momentum operator can be found by taking the conserved quantity due to rotations and subtracting off the orbital contribution, giving

$$S_i = \frac{i}{4}\epsilon_{ijk}\gamma^j\gamma^k = \frac{1}{2}\begin{pmatrix} \sigma^i & 0 \\ 0 & \sigma^i \end{pmatrix}, \quad \gamma^5 S^i = S^i\gamma^5 = \frac{1}{2}\gamma^0\gamma^i$$

Multiplying the massless Dirac equation $\not{p}u = \not{p}v = 0$ by γ^0/p^0 then gives

$$\left(1 - 2\mathbf{S}\cdot\hat{\mathbf{p}}\gamma^5\right) u^s(p) = \left(1 - 2\mathbf{S}\cdot\hat{\mathbf{p}}\gamma^5\right) v^s(p) = 0$$

• For a classical solution to the Dirac equation, define $h = \mathbf{S}\cdot\hat{\mathbf{p}}$. Inserting a factor of $P_L + P_R$,

$$h u^s_{L,R} = \mp\frac{1}{2} u^s_{L,R}, \quad h v^s_{L,R} = \mp\frac{1}{2} v^s_{L,R}$$

where the L/R subscripts indicate left-chiral or right-chiral Weyl fields.
• The physical interpretation is a bit tricky. For positive frequency solutions, h is equal to the helicity λ of the corresponding particle. For negative frequency solutions, the parameter p is the opposite of the physical momentum, as they are proportional to e^{ipx} rather than e^{-ipx}.
• Upon quantization negative frequency solutions become holes, which flips $p, \mathbf{S}$, and all other quantum numbers. The fact that p is already flipped once in the definition of $v^s(p)$ means that the particle corresponding to $v^s(p)$ indeed has momentum p, with no sign. But

since the spin is flipped, we have $h = -\lambda$ for negative frequency solutions. Since the charge is flipped, these particles are called antiparticles.

• Thus, a left-chiral Weyl field annihilates a left-helicity (negative helicity) particle and creates a right-helicity (positive helicity) antiparticle. Similarly, a right-chiral Weyl field annihilates a right-helicity particle and creates a left-helicity antiparticle. We see that each of these Lorentz irrep fields gives rise to two Poincare particle irreps.

• For example, a "left-chiral antiquark field" is one which annihilates a left-helicity antiquark. It would be the charge conjugate of a left-chiral quark field, and the parity conjugate of a right-chiral antiquark field, assuming these fields exist at all in the theory; if they are not, parity and charge conjugation aren't defined.

• For reference, for a massless particle moving in the $+\hat{\mathbf{z}}$ direction, we have

$$\text{spin up: } u(p) = \begin{pmatrix} 0 \\ 0 \\ 1 \\ 0 \end{pmatrix}, v(p) = \begin{pmatrix} 1 \\ 0 \\ 0 \\ 0 \end{pmatrix}, \quad \text{spin down: } u(p) = \begin{pmatrix} 0 \\ 1 \\ 0 \\ 0 \end{pmatrix}, v(p) = \begin{pmatrix} 0 \\ 0 \\ 0 \\ 1 \end{pmatrix}$$

where spin up indicates positive helicity λ.

Next, we turn to the parity transformation of the Dirac field.

• By the same reasoning as for the scalar field, we should have

$$\widehat{P} b^s(p) \widehat{P}^{-1} = \eta^b b^s\left(p_P\right), \quad \widehat{P} d^{s\dagger} \widehat{P}^{-1} = \eta^{d*} d^{s\dagger}\left(p_P\right)$$

Therefore, the transformation of the Dirac field is

$$\psi^P(x) \equiv \widehat{P}\psi(x)\widehat{P}^{-1} = \sum_{p,s} \eta^b b^s(p) u^s\left(p_P\right) e^{-ipx_P} + \eta^{d*} d^{s\dagger}(p) v^s\left(p_P\right) e^{ipx_P}$$

where we reindexed the sum as for the scalar field.

• One can show that the spinors transform as

$$u^s\left(p_P\right) = \gamma^0 u^s(p), \quad v^s\left(p_P\right) = -\gamma^0 v^s(p)$$

as can be verified in the chiral basis using $p \cdot \sigma = p_P \cdot \bar{\sigma}$. Requiring the transformed field to take the same form as the original field, we must have

$$\psi^P(x) = \eta_P \gamma^0 \psi\left(x_P\right), \quad \eta_P = \eta^b = -\eta^{d*}$$

Similarly, for the adjoint field we have

$$\bar{\psi}^P(x) = \eta_P^* \bar{\psi}\left(x_P\right) \gamma^0$$

• By applying projectors, we find that parity flips the chirality,

$$\widehat{P}\psi_L(x)\widehat{P}^{-1} = \eta_P \gamma^0 \psi_R\left(x_P\right), \quad \widehat{P}\bar{\psi}_L\widehat{P}^{-1} = \eta_P^* \bar{\psi}_R\left(x_P\right)\gamma^0$$

This is a special case of the fact that parity maps the (s_1, s_2) Lorentz irrep to (s_2, s_1). We can then straightforwardly check that ψ^P satisfies the Dirac equation, that $\bar{\psi}\psi$ is a scalar and $\bar{\psi}\gamma^5\psi$ is a pseudoscalar, and so on.

• We have freedom in choosing the phase η_P as described above, using global $U(1)$ symmetries, and in the SM this freedom is used to set the intrinsic parities of the proton, neutron, and charged leptons to $+1$. Note that this point is unrelated to the transformations of Dirac bilinears, where η_P cancels out.

• We also note that, regardless of phase adjustments, we have $\eta^b \eta^d = -1$, which means that a two-particle state containing a fermion and its antiparticle has an extra factor of -1 in its intrinsic parity, as we previously noted in our qualitative overview. This logic holds unchanged for Majorana fermions, where the fermion and its antiparticle coincide. The same result holds for the charge conjugate of a fermion and its antiparticle.

6.2.4 Charge Conjugation

Charge conjugation is different from the other discrete symmetries, since it does not arise from the structure of $O(3,1)$. Instead, it arises from the generic prediction of antiparticles in quantum field theory. It is especially confusing because there are two related notions of it.

• Consider a set of classical fields ψ_i that transform under some representation R. Then the complex conjugate fields ψ_i^* transform under the conjugate representation R^*, though they generally won't be in the "standard" basis. We return to the standard basis using a "charge conjugation matrix" C, and call the operation $\psi \to \psi^{(c)} = C\psi^*$ charge conjugation.

• Since the $(1/2, 0)$ and $(0, 1/2)$ Lorentz representations are conjugate, this notion of charge conjugation flips the chirality. This is the notion of charge conjugation we used when studying group theory. It comes from the classical theory, and useful mainly for constructing real, singlet Lagrangians. It is not the same as the $\widehat{C}$ we study below, which instead corresponds to the intuitive idea of "exchanging matter and antimatter".

• To translate this idea to particles, let ψ transform under a representation R of an internal symmetry group. Then ψ annihilates particles which transform under R and creates particles which transform under R^*, and are hence called antiparticles.

• The field $\psi^{(c)}$ simply does the reverse: it annihilates what ψ creates, and vice versa. In particular, classical charge conjugation doesn't modify the particle content at all; a Lagrangian written in terms of only ψ is equivalent to one written in terms of only $\psi^{(c)}$.

• Note that if R is complex, the particles definitely cannot be identified with their antiparticles, while if R is real they might or might not be.

• The situation is more complicated when we are talking about spacetime symmetries, since fields have Lorentz symmetry and particles have Poincare symmetry; we've seen how chirality for fields corresponds to helicity for particles above.

• A rough heuristic is that classical charge conjugation conjugates both internal and spacetime representations, while, in a $\widehat{C}$-symmetric theory, $\widehat{C}$ conjugates exactly the internal representations (when acting on the free "in/out" states), and in a $\widehat{C}$-asymmetric theory, $\widehat{C}$ might not even defined on those states at all. In terms of representations, the two notion of charge conjugation differ essentially by a parity transformation, leading to confusion when people use different versions of it.

Now we define $\widehat{C}$, starting with the scalar field.

• We begin by demanding that the particle and antiparticle operators should be exchanged,

$$\widehat{C}a(p)\widehat{C}^{-1} = \eta_C c(p), \quad \widehat{C}c(p)\widehat{C}^{-1} = \eta_C^* a(p)$$

where we used Lorentz invariance as before to constrain the phases. Then we have, for instance

$$\widehat{C}|p,\ \text{particle}\ \rangle = \widehat{C}a^\dagger(p)|0\rangle = \eta_C^* c^\dagger(p)|0\rangle = \eta_C^*|p,\ \text{antiparticle}\ \Big\rangle$$

• In terms of the fields, we have

$$\widehat{C}\phi(x)\widehat{C}^{-1} = \eta_C \phi^\dagger(x), \quad \widehat{C}\phi^\dagger(x)\widehat{C}^{-1} = \eta_C^* \phi(x).$$

For a real scalar field, this implies $\eta_C = \pm 1$, while for a complex scalar field we can perform a rotation so that $\eta_C = 1$. In the former case, this means that particles are eigenstates of $\widehat{C}$, so the symmetry can provide selection rules.

• The photon field must obey

$$\widehat{C} A_\mu(x) \widehat{C}^{-1} = -A_\mu(x)$$

for $\widehat{C}$ to be a symmetry of QED. That is, photons have intrinsic charge eigenvalue $\widehat{C} = -1$. Physically, this is because the coupling to matter is in the form $A^\mu J_\mu$, where the current J_μ certainly flips sign under charge conjugation.

Next, we proceed to the Dirac field.

• We define the positive frequency and negative frequency basis spinors to be related by

$$\zeta^s = i\sigma^2 \xi^{s*}$$

This gives an extra sign flip at the classical level, which ensures that the particles created by $b^{s\dagger}(p)$ and $d^{s\dagger}(p)$ have the same physical spin, just as they have the same physical momentum.

• Next, we define a charge conjugation matrix C that acts on spinors by

$$\gamma^{\mu T} = -C^{-1} \gamma^\mu C$$

One can show that C is real, anti-symmetric, and unitary, $\gamma^{5^T} = C^{-1}\gamma^5 C$, and the $\gamma^\mu C$ are symmetric, using only the properties of the Clifford algebra. For the chiral representation,

$$C = -i\gamma^0\gamma^2 = \begin{pmatrix} i\sigma_2 & 0 \\ 0 & -i\sigma_2 \end{pmatrix}$$

• Under these definitions, we have the simple relationships

$$v^s(p) = C\bar{u}^{sT}(p), \quad u^s(p) = C\bar{v}^{sT}(p)$$

• Now, for the Dirac field, we have

$$\widehat{C} b^s(p) \widehat{C}^{-1} = \eta_C d^s(p), \quad \widehat{C} d^{s\dagger}(p) \widehat{C}^{-1} = \eta_C b^{s\dagger}(p)$$

where the phases are equated as usual, and we used the fact that $\widehat{C}$ doesn't change spacetime quantum numbers such as momentum and spin. Thus $\widehat{C}$ preserves helicity.

• Since a right-chiral field is defined by annihilating positive helicity, $\widehat{C}$ preserves chirality for quantum fields. Note this is the opposite of the result for classical charge conjugation.

• The charge conjugated field ψ^c, not to be confused with $\psi^{(c)}$, is

$$\psi^c(x) \equiv \widehat{C}\psi(x)\widehat{C}^{-1} = \eta_C \sum_{p,s} d^s(p) u^s(p) e^{-ipx} + b^{s\dagger}(p) v^s(p) e^{ipx}$$

On the other hand, the adjoint field transposed to a column vector is

$$\bar{\psi}^T(x) = \sum_{p,s} b^{s\dagger}(p) \bar{u}^{sT}(p) e^{ipx} + d^s(P) \bar{v}^{sT}(p) e^{-ipx}$$

Therefore, by our spinor identities we have

$$\psi^c(x) = \eta_C C \bar{\psi}^T(x), \quad \bar{\psi}^c(x) = -\eta_C^* \psi^T(x) C^{-1}$$

These equations can also be used (sometimes unwittingly) to define $\widehat{C}$ on classical fields, with the caveat that this differs from classical charge conjugation by a parity transformation.

Note. In practice, the simple definition of $\widehat{C}$ above might not work, while a slightly different definition which lacks some of the usual properties of $\widehat{C}$ (such as flipping all internal quantum numbers) may be more useful. For example, in the Standard Model with a sterile neutrino, charge conjugation must exchange the active and sterile neutrinos, if it is to keep the spacetime quantum numbers the same. But the active and sterile neutrinos don't have opposite internal quantum numbers, e.g. the active neutrinos have hypercharge and the sterile neutrinos don't. A strict interpretation would lead to the conclusion that $\widehat{C}$ can't be defined in such a theory. However, it is more common to loosen the criteria and allow $\widehat{C}$ to be defined this way anyway. This is useful because it leads to an approximate symmetry, which is only broken by weak interactions.

This illustrates an important point when discussing discrete symmetries. The point of symmetries is precisely to be able to use them to understand the dynamics. It doesn't make sense to worry about whether some operator is "the true $\widehat{C}$ " in some metaphysical sense. Nature doesn't care: the theory described above will still have a $\widehat{C}$-like symmetry constraining it, whether we call it that or not. As another example, in some "left-right symmetric theories", it is conventional to allow parity to switch the internal representations of $SU(2)_L$ and $SU(2)_R$, which is again useful precisely because it leads to an approximate symmetry. (However, to give credit to the mathematicians, the definition of $\widehat{C}\widehat{P}\widehat{T}$ is more "canonical", because it is the conserved quantity guaranteed to us by the CPT theorem. This operator always flips all internal quantum numbers and the helicity.)

Finally, we can check on a few applications of charge conjugation.

• The charge conjugate spinor ψ^c satisfies the Dirac equation. To see this, take the transpose of the Dirac equation for $\bar{\psi}$ for

$$\left(-i\gamma^{\mu T}\partial_\mu - m\right)\bar{\psi}^T(x) = 0$$

Inserting factors of $C^{-1}C$ and using $\gamma^{\mu T} = -C^{-1}\gamma^\mu C$ gives the result.

• A Majorana fermion has $b^s(p) = d^s(p)$. That is, they are Dirac fermions that are their own antiparticles, $\psi^c = \psi$. They arise from quantizing solutions to the Dirac equation obeying a reality condition. Then a spin up Majorana fermion can be described by either the spinor $\zeta^{1/2}$ or $\xi^{1/2}$, where the spinors are related by $\zeta^s = i\sigma^2\xi^{s*}$. Note that a Majorana field doesn't have a definite chirality, just like a Dirac field.

• The vector current is odd under $\widehat{C}$. To see this cleanly, write

$$j^\mu(x) = \frac{1}{2}\left(\bar{\psi}\gamma^\mu\psi - \psi^T\gamma^{\mu T}\bar{\psi}^T\right) = \frac{1}{2}\left(\gamma^\mu\right)_{ij}\left[\bar{\psi}_i(x), \psi_j(x)\right]$$

where the sign flip from the transpose is explained in the notes on Quantum Field Theory. Applying charge conjugation, we have

$\widehat{C}j^\mu\widehat{C}^{-1} = \frac{1}{2}\left(\gamma^\mu\right)_{ij}\left[\widehat{C}\bar{\psi}_i\widehat{C}^{-1}, \widehat{C}\psi_j\widehat{C}^{-1}\right] = -\frac{1}{2}\left(\gamma^\mu\right)_{ij}\left[\left(\psi^T C^{-1}\right)_i, \left(C\bar{\psi}^T\right)_j\right] = \frac{1}{2}\left(\gamma^\mu\right)_{\ell k}\left[\psi_k, \bar{\psi}_\ell\right] = -j^\mu$.

On the other hand, we know that the electromagnetic field is coupled as $A^\mu j_\mu$, so for QED to be charge conjugation invariant, we must define $\widehat{C}A_\mu\widehat{C}^{-1} = -A_\mu$.

• Similarly, one can show that the axial current is even under $\widehat{C}$. This implies that it is impossible to couple a linear combination of the vector and axial currents to a single field without violating $\widehat{C}$, and this is exactly what happens in the weak interactions.

Majorana spinors can be a bit confusing, because people use the term in many distinct ways, so we treat them carefully.

• To avoid confusion, we start with two-component Weyl fields, since Dirac and Majorana fields are built out of them. Suppose we have a left-chiral Weyl spinor field ψ which transforms under a representation R of an internal symmetry group. It annihilates a particle with negative

helicity in the representation R, and creates a particle with positive helicity in the representation $\bar{R}$.

• In general, complex conjugating a quantum field just reverses which particles it creates and annihilates. The conjugate field $\psi^\dagger$ is a right-chiral Weyl spinor with internal symmetry representation $\bar{R}$. It annihilates a particle with positive helicity in the representation $\bar{R}$, and creates a particle with negative helicity in the representation R.

• Therefore, to describe a set of particles with $|h| = 1/2$, we can use only left-chiral Weyl fields, or only right-chiral Weyl fields, or a mixture of both. The field content of a theory is somewhat arbitrary. Note that the framework of fields can only describe particles which come in matterantimatter pairs: for every particle species transforming in a given internal representation, there must be another particle species with opposite helicity and the same mass, transforming in the conjugate internal representation. This is a consequence of CPT symmetry.

• With a single left-chiral Weyl field ψ, there are only two ways to produce quadratic Lorentzinvariant terms in the Lagrangian. We know ψ transforms in $(1/2, 0)$, and its conjugate transforms in $(0, 1/2)$. Since $(1/2, 0) \times (1/2, 0) = (1, 0) + (0, 0)$, contracting the field with itself can yield a scalar. Since $(1/2, 0) \times (0, 1/2) = (1/2, 1/2)$, contracting the field with its conjugate yields a four-vector, which can yield a scalar upon contraction with ∂^μ.

• Therefore the two possible Lagrangian terms are

$$\mathcal{L} \supset i\psi^\dagger \bar{\sigma}^\mu \partial_\mu \psi + m\psi\psi$$

where the second term is a two-component spinor contraction, defined in the notes on Supersymmetry, and the $\bar{\sigma}^\mu$ are just coefficients that isolate the appropriate scalar contraction.

• Now suppose ψ transforms in a representation R of an internal symmetry group. The first term is automatically invariant, but the second term transforms as $R \times R$, so it can only be invariant if R is a real representation. The logic is precisely the same if the symmetry group is a gauge group, except that ∂_μ must be replaced with an appropriate covariant derivative D_μ.

• For a right-chiral Weyl field χ, the logic is the same, but the terms are written as

$$\mathcal{L} \supset i\chi^\dagger \sigma^\mu \partial_\mu \chi + m\chi\chi$$

Again, with a gauge field, ∂_μ is replaced with a covariant derivative.

• Now, we can always stack a Weyl field and its conjugate into a four-component spinor field,

$$\Psi = \begin{pmatrix} \psi \\ \psi^{(c)} \end{pmatrix}$$

This is just a change of notation. There are still two possible terms in the Lagrangian,

$$\mathcal{L} \supset \frac{1}{2}\bar{\Psi}(i\not{\partial} - m)\Psi$$

which are just the same as the original ones, up to conventions for factors of 2, once one expands out the products. As before, the mass term is only allowed if R is real.

• Here's the tricky part: if there's a gauge field, the kinetic term should become

$$\mathcal{L} \supset \frac{1}{2}\bar{\Psi}\left(i\left(\not{\partial} + ie\gamma^5 A\right) - m\right)\Psi$$

That is, we do not use the minimal coupling prescription. Minimal coupling is a procedure for generating a scalar Lagrangian given fields which transform in known representations. But in general, Ψ does not transform in a well-defined representation of the internal symmetry group, because the top half transforms in R and the bottom half transforms in $\bar{R}$. Again, we

can confirm the γ^5 has to be there by expanding everything in components. (A more common way to do this would be to add a chiral projector P_L. It leads to the same result when expanded in components, but our way treats the two halves of Ψ symmetrically.)

• Calculations with Standard Model fermions can be done with either two-component or fourcomponent spinor fields. In both cases, explicit mass terms are forbidden, but masses are permitted by the Higgs mechanism. The advantage of four-component notation is that one can use familiar techniques for the traces of gamma matrices; the disadvantage is that γ^5 appears.

• Now we're ready to answer the key question: what is a Dirac spinor? Often, particles transforming in a representation R can be paired with other particles, of the same mass and same helicity, transforming in the representation $\bar{R}$. For instance, this can be done for all particles if the theory is symmetric under charge conjugation. We can describe a pair of such particle species using a pair of left-chiral and right-chiral Weyl spinor fields, ψ and χ, which transform in the same representation R.

• This allows a new term in the Lagrangian: we can contract one with the conjugate of the other to get a scalar, no matter what R is. This is called a Dirac mass term, and it is most easily written in four-component notation. Stacking these fields into a four-component spinor,

$$\Psi = \begin{pmatrix} \psi \\ \chi \end{pmatrix}$$

the Lagrangian is

$$\mathcal{L} \supset \bar{\Psi}(i(\not{\partial} + ie\not{A}) - m)\Psi$$

where there's no factor of 1/2, since the two halves of Ψ are distinct particles, and we simply have a covariant derivative with no need for γ^5, since both halves of Ψ transform in R. At the level of two-component spinors the Dirac mass term looks like $\psi\chi + \bar{\psi}\bar{\chi}$.

• There are at least two distinct ways to define Majorana spinors.

• Starting with a Dirac spinor transforming in a representation R, one can define a Majorana spinor by additionally imposing a reality condition $\Psi^{(c)} = \Psi$. In our language, this is equivalent to setting $\psi = \chi$, and demanding invariance of the kinetic term implies R must be real. This is the source of the claim that Majorana spinors can't be charged.

• Starting with a Weyl spinor transforming in a representation R, one can define a Majorana spinor by stacking it on its conjugate. Demanding invariance of the explicit mass term implies R must be real, but if there is no such term, R can be arbitrary. This is not contradictory with the previous point, because in this case Ψ does not transform in a well-defined representation of the internal symmetry group.

Note. Imposing a reality condition might seem a bit artificial; alternatively, it's simple to produce Majorana spinors starting from only Dirac spinors. For example, suppose there is a global $U(1)$ symmetry, a Dirac field with charge 1, and a scalar field H with charge -2. We can then write down terms like $\psi\psi H$, which turns into a Majorana mass for ψ when H gets a vev. This doesn't contradict the statement that massive Majorana spinors can't be charged, because the $U(1)$ is spontaneously broken by H.

This simple mechanism won't show up in typical textbooks, because they often only consider the $U(1)$ of electromagnetism, which we know holds to extreme precision. However, it's a common tool in model building for dark matter, where we might have a "dark" $U(1)$ separate from the Standard Model gauge groups. When the Majorana mass terms are much larger than the Dirac mass term, we get two distinct Majorana spinors, while if they're smaller, then we have the "pseudo-Dirac" case where the Majoranas ψ and χ have only a small splitting. The same idea can be applied to separate the components of a complex scalar, giving the "inelastic scalar" case. The latter two are concrete examples of "inelastic dark matter", where collisions

can excite or de-excite the dark matter by interconverting the two particle species, leading to distinctive experimental signatures.

Note. Chiral gauge theories. Consider the fermions in a gauge theory. If, for every positive helicity particle in a representation R of the gauge group G, there is a negative helicity particle in the same representation R, the theory is not chiral; it doesn't distinguish between the two helicities.

Suppose we write all spinor fields in a theory as left-chiral Weyl spinors. They are collectively in a large representation S, and if S is not complex, the theory is not chiral. This remains true if spontaneous symmetry breaking reduces G to $H \subseteq G$, because S will still remain real; it will split into real representations plus pairs of conjugate representations of H.

This places a strong constraint on GUTs, because the SM is a chiral gauge theory. If S were not complex in a GUT, then it would yield unwanted extra "mirror matter" transforming in the conjugates of the SM particle representations. The mirror matter would have to be made very heavy while keeping ordinary matter light, and it is unclear how to achieve this naturally.

6.2.5 Time Reversal

We conclude with time reversal symmetry.

- We recall that time reversal symmetry takes $x \to x_T, p \to p_T$ where

$$x_T^\mu = \left(-x^0, \mathbf{x}\right), \quad p_T^\mu = \left(p^0, -\mathbf{p}\right).$$

In addition, time reversal flips the sign of the angular momentum. Note that $p_T x = -p x_T$.

- For the scalar field, we have

$$\widehat{T} a(p) \widehat{T}^{-1} = \eta_T a\left(p_T\right), \quad \widehat{T} c^\dagger(p) \widehat{T}^{-1} = \eta_T c^\dagger\left(p_T\right)$$

where the phases are equal as usual. Then

$$\widehat{T}\phi(x)\widehat{T}^{-1} = \sum_p \widehat{T}a(p)\widehat{T}^{-1}e^{ipx} + \widehat{T}c^\dagger(p)\widehat{T}^{-1}e^{-ipx} = \eta_T \sum_p a(p)e^{-ipx_T} + c^\dagger(p)e^{ipx_T} = \eta_T \phi\left(x_T\right)$$

where we used the antilinearity of $\widehat{T}$ in the first step, then reindexed the sum.

- For the Dirac field, we define

$$\widehat{T} b^s(p) \widehat{T}^{-1} = \eta_T (-1)^{1/2-s} b^{-s}\left(p_T\right), \quad \widehat{T} d^{s\dagger} \widehat{T}^{-1} = \eta_T (-1)^{1/2-s} d^{-s^\dagger}\left(p_T\right), \quad s = \pm 1/2$$

where b maps to b because both the momentum and spin are flipped, keeping the helicity the same, and the extra phase factors are again constrained by Lorentz invariance.

- Given this definition, one can show the spinors satisfy

$$(-1)^{1/2-s} u^{-s^*}\left(p_T\right) = -C^{-1}\gamma^5 u^s(p), \quad (-1)^{1/2-s} v^{-s^*}\left(p_T\right) = -C^{-1}\gamma^5 v^s(p)$$

and we define

$$B = C^{-1}\gamma^5 = -\gamma^5 C = \gamma^1\gamma^3 = \begin{pmatrix} i\sigma^2 & 0 \\ 0 & i\sigma^2 \end{pmatrix}$$

- It is then straightforward to show that the Dirac field transforms as

$$\widehat{T}\psi(x)\widehat{T}^{-1} = \eta_T B \psi\left(x_T\right), \quad \widehat{T}\bar{\psi}(x)\widehat{T}^{-1} = \eta_T^* \bar{\psi}\left(x_T\right) B^{-1}$$

Then $\bar{\psi}(x)\psi(x) \to \bar{\psi}(x_T)\psi(x_T)$, which makes sense since charge density is T-even classically.

• To check the transformation properties of other bilinears, we use

$$B^{-1}\gamma^{5^*}B = \gamma^5, \quad B^{-1}\gamma^{0^*}B = \gamma^0, \quad B^{-1}\gamma^{i*}B = -\gamma^i$$

Then we have

$$\widehat{T}\bar{\psi}(x)\gamma^\mu\psi(x)\widehat{T}^{-1} = \bar{\psi}(x_T)B^{-1}\gamma^{\mu*}B\psi(x_T)$$

so that $\bar{\psi}\gamma^\mu\psi$ has its spatial parts flipped. The axial current $\bar{\psi}\gamma^5\gamma^\mu\psi$ transforms the same way, essentially because $\widehat{T}$ is blind to chirality, and the currents only differ by chirality.

• We may also explicitly check that chirality is preserved, as

$$\widehat{T}\psi_L\widehat{T}^{-1} = \eta_T B\psi_L(x_T), \quad \widehat{T}\bar{\psi}_L\widehat{T}^{-1} = \eta_T^*\bar{\psi}_L(x_T)B^{-1}$$

We now apply time reversal symmetry to S-matrix elements.

• The definition of the S-matrix in the interaction picture is

$$S = T\exp\left(-i\int dtV(t)\right), \quad V(t) = -\int d\mathbf{x}\mathcal{L}_I(x)$$

For example, in QED, the interaction term is $\mathcal{L}_I = -e\bar{\psi}\gamma^\mu A_\mu\psi$.

• In a theory with C, P, and T symmetry, the Lagrangian is C, P, and T-even. The first two imply that the S-matrix satisfies

$$\widehat{P}S\widehat{P}^{-1} = S, \quad \widehat{C}S\widehat{C}^{-1} = S$$

Then the amplitude for $|i\rangle \to |f\rangle$ is the same as the amplitude for $\widehat{P}|i\rangle \to \widehat{P}|f\rangle$ or $\widehat{C}|i\rangle \to \widehat{C}|f\rangle$.

• Time reversal is more complicated. Note that $V(t)$ is real, and the time ordering puts later times to the left. Under conjugation by $\widehat{T}$, the factors of $-i$ are conjugated, and the time ordering is now in reverse. This is equivalent to an overall complex conjugation, so

$$\widehat{T}S\widehat{T}^{-1} = S^\dagger$$

Now we have

$$\langle i_T|S|f_T\rangle = \left\langle i\left|\widehat{T}^\dagger\right|S\widehat{T}|f\right\rangle = \left\langle i\left|\widehat{T}^\dagger S\widehat{T}\right|f\right\rangle^* = \langle f|S|i\rangle$$

where the bar indicates the direction the antilinear operators act; swapping the direction picks up a complex conjugation. Then the amplitude for $|i\rangle \to |f\rangle$ equals that for $\widehat{T}|f\rangle \to \widehat{T}|i\rangle$.

Note. A summary table for gamma matrices. The fourth column is representation-independent, the first three are highly representation-dependent, and the last two are by definition.

	γ^*	γ^T	$\gamma^\dagger$	γ^{-1}	$C^{-1}\gamma C$	$B^{-1}\gamma B$
0	+	+	+	+	$(-)^T$	$(+)^*$
1	+	-	-	-	$(-)^T$	$(-)^*$
2	-	+	-	-	$(-)^T$	$(-)^*$
3	+	-	-	-	$(-)^T$	$(-)^*$
5	+	+	+	+	$(+)^T$	$(+)^*$

Note. A summary table for discrete symmetries, for a real scalar ϕ, a real vector V^μ, the special case A^μ, and Dirac bilinears. For objects with vector indices, we define $\mathcal{P} = \text{diag}(1,-1,-1,-1)$ and $\mathcal{T} = -\mathcal{P} = \text{diag}(-1,1,1,1)$.

	ϕ	V^μ	A^μ	$\bar{\psi}\psi$	$i\bar{\psi}\gamma^5\psi$	$\bar{\psi}\gamma^\mu\psi$	$\bar{\psi}\gamma^\mu\gamma^5\psi$	$\bar{\psi}\sigma^{\mu\nu}\psi$	∂_μ
$\widehat{C}$	$\eta_c = \pm 1$	η_c	-1	1	1	-1	1	-1	1
$\widehat{P}$	$\eta_p = \pm 1$	$\eta_p \mathcal{P}$	$\mathcal{P}$	1	-1	$\mathcal{P}$	$-\mathcal{P}$	$\mathcal{P}^\mu \mathcal{P}^\nu$	$\mathcal{P}$
$\widehat{T}$	$\eta_t = \pm 1$	$\eta_t \mathcal{T}$	$-\mathcal{T}$	1	-1	$-\mathcal{T}$	$-\mathcal{T}$	$-\mathcal{T}^\mu \mathcal{T}^\nu$	$\mathcal{T}$
$\widehat{C}\widehat{P}\widehat{T}$	1	-1	-1	1	1	-1	-1	1	-1

where the last line requires choosing $\eta_c \eta_p \eta_t = 1$, which can always be arranged. Note that CPT just gives a factor of -1 for each Lorentz index, so any Lorentz invariant Lagrangian is automatically CPT invariant. In addition, in non-abelian gauge theories, the potential, field strength, and current transform under C and P with extra matrix transposes.

6.3 Spontaneous Symmetry Breaking

6.3.1 Classical Fields

We know that statistical fields can experience spontaneous symmetry breaking, so similarly quantum fields can as well. We begin with the case of classical field theory. Note that despite the formal similarity, nothing we say will have anything to do with phase transitions; all of our quantum field theory is at zero temperature.

Example. The linear sigma model. Consider N real scalar fields with Lagrangian

$$\mathcal{L}(\phi, \partial_\mu \phi) = \frac{1}{2}(\partial_\mu \phi)^2 + \frac{1}{2}\mu^2 \phi^2 - \frac{\lambda}{4}\phi^4$$

where ϕ has N components, and we've suppressed dot products. Then the Lagrangian has an $O(N)$ symmetry. The dispersion relation about $\phi = 0$ contains excitations with negative mass squared, indicating a potential maximum rather than a minimum. The lowest-energy classical field configuration is a constant field ϕ_0. The potential is minimized for

$$\phi_0^2 = \frac{\mu^2}{\lambda}$$

Since ϕ_0 can only take a single value, choosing it breaks the $O(N)$ symmetry down to $O(N-1)$, since we are still free to rotate in the directions orthogonal to ϕ_0. Suppose we pick

$$\phi_0 = (0, 0, \ldots, 0, v), \quad v = \frac{\mu}{\sqrt{\lambda}}$$

We can expand the Lagrangian about the minimum by defining

$$\phi(x) = \left(\pi^1(x), \ldots, \pi^{N-1}(x), v + \sigma(x)\right)$$

Then we have

$$\mathcal{L} = \frac{1}{2}\left(\partial_\mu \pi^k\right)^2 + \frac{1}{2}(\partial_\mu \sigma)^2 - \frac{1}{2}\left(2\mu^2\right)\sigma^2 + \text{ cubic and quartic interactions.}$$

That is, we find one massive field and $N-1$ massless fields. In the case $N = 2$, this reduces to the usual picture of a "Mexican hat potential".

Note. The crucial step that breaks the symmetry is selecting a specific vacuum state, not rewriting the Lagrangian. The new Lagrangian still has an $O(N)$ symmetry, though it's harder to see as it's nonlinearly realized; we couldn't have broken any symmetry because we merely redefined variables.

Note. Consider $N = 1$, where the broken symmetry is a discrete symmetry, $\mathbb{Z}_2$. In this case the experimental signature is not a Goldstone boson, but a domain wall. Without symmetry breaking, the $\mathbb{Z}_2$ symmetry means that the parity of the number of particles is conserved. With

spontaneous symmetry breaking, we see cubic interaction terms, but the symmetry is still there, in a sense, because we can think of the fourth particle as coming from our vacuum, which acts as a source.

Example. We don't need to begin with negative squared masses. In the case of a potential $V(\phi) \sim -|\phi|^4 + |\phi|^6$ for a complex scalar ϕ, we start with two massless particles and end up with one massive particle and one massless Goldstone boson after symmetry breaking.

Note. To prove Goldstone's theorem classically, consider a Lagrangian of the form

$$\mathcal{L} = \text{ kinetic } - V(\phi)$$

and let ϕ_0 be a constant field that minimizes V. Then we have

$$\frac{\partial V}{\partial \phi^a} = 0, \quad \frac{\partial^2 V}{\partial \phi^a \partial \phi^b} \equiv m_{ab}^2$$

where the derivatives are evaluated at ϕ_0. The number of Goldstone bosons is equal to the number of zero eigenvalues of the symmetric mass matrix m_{ab}^2. Now, a general continuous symmetry transformation has the form

$$\phi \to \phi + \alpha \Delta(\phi)$$

where α is infinitesimal. The condition for this to leave the Lagrangian invariant is

$$\Delta^a(\phi) \frac{\partial}{\partial \phi^a} V(\phi) = 0$$

Differentiating with respect to ϕ^b and evaluating at $\phi = \phi_0$ gives

$$\Delta^a(\phi_0) \left(\frac{\partial^2 V}{\partial \phi^a \partial \phi^b} \right) = 0$$

Now, the symmetry is spontaneously broken if $\Delta(\phi_0) \neq 0$, since it changes the vacuum. Then $\Delta(\phi_0)$ is an eigenvector of the mass matrix with zero eigenvalue, and hence a Goldstone boson.

Note. To count the Goldstone bosons, let G act on the fields leaving the Lagrangian invariant and let $H \subset G$ leave the vacuum ϕ_0 invariant. Let M be the set of vacua. If the vacuum degeneracy is entirely due to the group G, then the action of G on M must be transitive; that is, if it were not, we should really be working with a larger initial symmetry group. Then by the orbit-stabilizer theorem, $M \cong G/H$. The number of Goldstone bosons is simply the number of independent directions we can travel along M,

$$\dim M = \dim G - \dim H$$

so there are $\dim G - \dim H$ Goldstone bosons as desired. For example, in our model above, the initial symmetry group had dimension $N(N-1)/2$ and the new symmetry group had dimension $(N-1)(N-2)/2$, a decrease of $N-1$, and there were indeed $N-1$ Goldstone bosons. In words, the vacua live in the coset space, while the Goldstone bosons live in the tangent space to this space.

Note. The Goldstone boson counting doesn't depend on how we describe the symmetries. Consider the linear sigma model with N complex scalar fields; then a similar analysis to the above shows that the $U(N)$ symmetry is broken to $U(N-1)$, giving $2N-1$ Goldstone bosons. But the system actually has the larger symmetry group $O(2N)$ when written in terms of $2N$ real scalar fields, which is broken to $O(2N-1)$. This also gives $2N-1$ Goldstone bosons. These results match, even though $O(2N)$ is larger than $U(N)$, because the action of $U(N)$ alone on the vacua is still transitive.

Note. Here's another way of thinking about Goldstone bosons. When there's spontaneous continuous symmetry breaking, we can define our fields about the symmetry broken vacuum, around which there will be a symmetry which locally looks like a shift. That implies a Noether current of the form $J^\mu \sim \partial^\mu \phi +$ (nonlinear terms). Conservation of that current gives $\partial^2 \phi =$ (nonlinear terms), implying that ϕ is massless. Furthermore, the existence of the shift symmetry means couplings of ϕ, at least at leading order, should only involve derivative terms like $\partial^\mu \phi$.

6.3.2 Quantum Fields

In the quantum case, proving Goldstone's theorem is significantly trickier.

Note. The first puzzle is why spontaneous symmetry breaking should even be possible. For a $\mathbb{Z}_2$ symmetry, there are two candidate vacua $|\pm\rangle$. This is analogous to the case of a double well potential in quantum mechanics. In that case, quantum tunneling between them splits the degeneracy, and the true ground state is the symmetric combination; both energy eigenstates have zero vev.

This reasoning does not apply to quantum field theory because there are many more degrees of freedom. Then the amplitude for tunneling between the $|\pm\rangle$ vacua is exponentially suppressed; it is analogous to the amplitude for an infinite set of double well oscillators to all tunnel at once. Hence the symmetry may be broken by any effect that does not treat the $|\pm\rangle$ states symmetrically, such as a tiny external field. This is the same reason that all macroscopic objects have a definite orientation, even though their quantum ground state is spherically symmetric.

Note. Spontaneous symmetry breaking can be justified without needing any external field. Suppose we have a set of orthogonal degenerate vacuum states $|n\rangle$, where a vacuum state is defined as a state with zero momentum not part of a continuum of states, with no amplitude for tunneling between them by the arguments above. Consider local operators $A(x)$ and $B(y)$. Inserting the identity,

$$\langle n|A(x)B(y)|n'\rangle = \sum_m \langle n|A(x)|m\rangle \langle m|B(y)|n'\rangle + \sum_N \int d\mathbf{p} \langle n|A(x)|N_\mathbf{p}\rangle \langle N_\mathbf{p}|B(y)|n'\rangle$$

where N indexes over non-vacuum states. By the translational invariance of the vacuum, we have

$$\langle n|A(x)B(y)|n'\rangle = \sum_m \langle n|A(0)|m\rangle \langle m|B(0)|n'\rangle + \sum_N \int d\mathbf{p} e^{-i\mathbf{p}\cdot(\mathbf{x}-\mathbf{y})} \langle n|A(0)|N_\mathbf{p}\rangle \langle N_\mathbf{p}|B(0)|n'\rangle$$

Then in the limit $|\mathbf{x}-\mathbf{y}| \to \infty$, the integral term goes to zero. Moreover, at spacelike separation $A(x)$ and $B(y)$ commute, so the matrices $\langle n|A(x)|m\rangle$ and $\langle m|B(y)|n'\rangle$ commute and can be simultaneously diagonalized.

Now, in a theory with one vacuum $|0\rangle$, we take as an axiom the cluster decomposition principle, which states that in the limit of large separation,

$$\langle 0|A(x)B(y)|0\rangle \to \langle 0|A(x)|0\rangle\langle 0|B(y)|0\rangle.$$

In this case, cluster decomposition only holds if we work in a basis of vacua where A and B are diagonal. In our examples above, the quantum field ϕ itself is a local operator, picking out the $|\pm\rangle$ states as valid vacua.

Note. Spontaneous symmetry breaking appears in the path integral through the choice of boundary condition. In the case of quantum mechanics, these boundary conditions don't matter for long times because of quantum tunneling, but for quantum field theory they do.

Note. We can easily prove Goldstone's theorem with the effective action. Considering a scalar field theory for simplicity, we have an effective potential $V_{\text{eff}}(\phi)$ whose minima give the allowed vevs. Assuming the symmetry is linearly realized on the fields, $V_{\text{eff}}(\phi)$ shares the same symmetries, as shown in the notes on Quantum Field Theory. Then our classical argument goes through, showing that broken symmetries give zero eigenvalues of the matrix of second derivatives of $V_{\text{eff}}(\phi)$. On the other hand, this matrix is related to the reciprocal of the momentum-space propagator by

$$\frac{\partial^2 V_{\text{eff}}(\phi)}{\partial\phi_n \partial\phi_m} = \Delta^{-1}_{nm}(p=0)$$

Then a zero eigenvalue of V_{eff} corresponds to a zero eigenvalue of the exact mass matrix, and hence a massless particle.

We now show Goldstone's theorem without using the effective action, in scalar field theory.

• Let ϕ be a vector of scalar fields and consider a continuous symmetry group G with generators indexed by a, with corresponding conserved currents $j^{\mu a}(x)$ and conserved charges Q^a. For the infinitesimal symmetry $\phi \to \phi + \epsilon t^a \phi$, Noether's theorem gives

$$Q^a = \int d\mathbf{x} J^a_0(\mathbf{x}) = \int d\mathbf{x} \pi_i(\mathbf{x}) t^a \phi^i$$

where we work in Schrodinger picture, and $[H, Q^a] = 0$.

• The charge Q^a generates the symmetry transformation just as it does classically: using the equal-time commutation relations, we have

$$[Q^a, \phi(0)] = -it^a\phi(0)$$

Then intuitively, the current $J^a_0(\mathbf{x})$ generates the symmetry "localized" near $\mathbf{x}$. For example, if the symmetry rotates ϕ_1 into ϕ_2, then $J_0(\mathbf{x})$ creates a "pion" $\phi_1\bar{\phi}_2$ localized at $\mathbf{x}$.

• By definition, spontaneous symmetry breaking exists if the vacuum $|0\rangle$ is charged, $Q^a|0\rangle \neq 0$. Since H and Q^a commute, $Q^a|0\rangle$ is degenerate with $|0\rangle$.

• Next, we construct the states

$$|\pi^a(\mathbf{p})\rangle \sim \int d\mathbf{x} e^{i\mathbf{p}\cdot\mathbf{x}} J^a_0(\mathbf{x})|0\rangle$$

If E_0 is the vacuum energy, then these states have energy $E_0 + E(\mathbf{p})$. But when $\mathbf{p}$ is zero, the state is proportional to $Q|0\rangle$ and hence has energy E_0, so $E(0) = 0$. Then the states must satisfy a massless dispersion relation; they are the desired Goldstone bosons.

• Note that ϕ need not be a fundamental field. For example, in a theory with Dirac spinors, we could take $\phi = \bar{\psi}\psi$.

We can also show this result more formally.

• By inserting copies of the identity $\sum_n |n\rangle\langle n| = 1$ and using the translational invariance of the vacuum, we find

$$\langle 0\,|[j^{a\mu}(x), \phi(0)]|\,0\rangle = i\int d^4k \rho^{a\mu}(x)e^{-ikx} - \tilde{\rho}^{a\mu}(x)e^{ikx}$$

where we define the spectral densities

$$i\rho^{a\mu}(k) = \sum_n \delta(k - p_n)\langle 0\,|j^{a\mu}(0)|\,n\rangle\langle n|\phi(0)|0\rangle, \quad i\tilde{\rho}^{a\mu}(k) = \sum_n \delta(k-p_n)\langle 0|\phi(0)|n\rangle\langle n\,|j^{a\mu}(0)|\,0\rangle\,.$$

These are analogous to the spectral densities we found for the exact propagator, except that instead of $\phi \to \phi$ we are describing the amplitude for $\phi \to B$ where B is the particle created by the current. We will see that B can be interpreted as a Goldstone boson.

• Since ρ and $\tilde{\rho}$ are Lorentz vectors that only depend on k, they must be proportional to k^μ. They must also be zero for negative energy since the states all have positive energy. Then

$$\rho^{a\mu}(k) = k^\mu \theta\left(k^0\right) \rho^a\left(k^2\right), \quad \tilde{\rho}^{a\mu}(k) = k^\mu \theta\left(k^0\right) \tilde{\rho}^a\left(k^2\right)$$

Substituting this in, we have

$$\langle 0 \left| [j^{a\mu}(x), \phi(0)] \right| 0 \rangle = -\partial^\mu \int d^4k \theta\left(k^0\right) \left(\rho^a\left(k^2\right) e^{-ikx} + \tilde{\rho}^a\left(k^2\right) e^{ikx}\right).$$

• At this point, the result looks similar to the free propagator,

$$\langle 0|\phi(z)\phi(y)|0\rangle = \int \frac{d^4p}{(2\pi)^3} \theta\left(p^0\right) \delta\left(p^2 - \sigma\right) e^{-ip(z-y)} = D(z-y,\sigma)$$

where σ is the mass squared, but with weighting factors ρ^a and $\tilde{\rho}^a$. We write

$$\rho\left(k^2\right) = \int d\sigma \rho(\sigma) \delta\left(k^2 - \sigma\right)$$

and plug this in to find

$$\langle 0 \left| [j^{a\mu}(x), \phi(0)] \right| 0 \rangle = -(2\pi)^3 \partial^\mu \int d\sigma \rho^a(\sigma) D(x,\sigma) + \tilde{\rho}^a(\sigma) D(-x,\sigma)$$

• Now, the left-hand side must vanish at spacelike separation by causality. We know that for spacelike x, $D(x,\sigma) = D(-x,\sigma)$, so $\rho^a(\sigma) = -\tilde{\rho}^a(\sigma)$. Then we have

$$\langle 0 \left| [j^{a\mu}(x), \phi(0)] \right| 0 \rangle = -\partial^\mu \int d\sigma \rho^a(\sigma) i\Delta(x,\sigma)$$

where

$$i\Delta(x,\sigma) = (2\pi)^3 (D(x,\sigma) - D(-x,\sigma)) = \int d^4k \delta\left(k^2 - \sigma\right) \operatorname{sign}\left(k^0\right) e^{-ikx}$$

• Next, apply ∂_μ to both sides. By current conservation, the left-hand side vanishes, and we can simplify the right-hand side with the Klein-Gordan equation, for

$$0 = \int d\sigma \sigma \rho^a(\sigma) i\Delta(x,\sigma)$$

For this to hold for all x, we require $\sigma\rho^a(\sigma) = 0$, since σ and ρ are positive.

• In the case where $\rho^a(\sigma) = 0$, we have $\langle 0 \left| [Q^a, \phi(0)] \right| 0 \rangle \propto \langle 0 \left| t^a \phi(0) \right| 0 \rangle = t^a \phi_0 = 0$, so the symmetry is unbroken. Otherwise, we have $\rho^a(\sigma) = N^a \delta(\sigma)$ and we can explicitly calculate

$$t^a \phi_0 = i \langle 0 \left| [Q^a, \phi(0)] \right| 0 \rangle = N^a \int d\mathbf{x} \partial^0 \Delta(x,0) = -(2\pi)^3 N^a \neq 0$$

so the symmetry is indeed broken. Returning to the definition of the spectral density, there must be families of massless states $|B(p)\rangle$ where

$$\langle 0 \left| j^{\mu a}(0) \right| B(p) \rangle = i F_B^a p^\mu, \quad \langle B(p)|\phi(0)|0\rangle = Z^B$$

by dimensional analysis and Lorentz invariance. The states $|B(p)\rangle$ are spinless since $\phi(0)|0\rangle$ is rotationally invariant and carry the same quantum numbers as j^0. They are the desired Goldstone bosons.

Note. There is another simple proof that Goldstone bosons remain massless, though it is only valid perturbatively. If the exact propagator $\Delta(k^2)$ of a Goldstone bosons is to retain a pole at $k^2 = 0$, then the self-energy should satisfy $\Pi(k^2 = 0) = 0$. However, Goldstone bosons are derivatively coupled, so all diagrams one can draw come with powers of the external momentum k. Since $\Pi(k^2 = 0)$ can be evaluated at $k = 0$, these diagrams vanish.

Note. There are several exceptions to Goldstone's theorem. In $d \leq 2$, the Mermin-Wagner theorem ensures that spontaneous continuous symmetry breaking can never occur in the first place; concretely, the effective potential will never develop an instability at $\phi = 0$.

Gauge symmetry also complicates the picture. If a global symmetry is gauged then its current cannot create Goldstone bosons, because it merely takes a state to the very same physical state. If we try to work only with physical states, we either lose manifest Lorentz invariance, which invalidates the formal proof above, or we have states with negative norm (e.g. in Lorenz gauge). This also invalidates the proof above since ρ may be negative. Instead, we would see that the would-be Goldstone bosons are "eaten" to produce massive gauge bosons.

6.3.3 Gauge Theories

We now consider the case where spontaneous symmetry breaking occurs to a global symmetry, whose corresponding local symmetry is gauged.

Note. This situation is also called "spontaneous breaking of a gauge symmetry", but this is a misnomer. The local gauge symmetry remains a gauge symmetry; the choice of vacuum doesn't affect the fact that states related by a gauge transformation are physically the same. Actually breaking gauge symmetry would be disastrous; it occurs in the case of a gauge anomaly and destroys the Ward identities, making the theory inconsistent. Breaking the global symmetry does not violate gauge symmetry since we require gauge transformations to vanish at infinity.

Incidentally, it is also possible to have local symmetries that are not gauge symmetries, e.g. in lattice spin systems considered in the notes on Statistical Field Theory. However, Elitzur's theorem states that such a local symmetry can never be broken. There are two ways to argue this. We can imagine introducing a symmetry breaking field h and taking the limits $N \to \infty$ followed by $h \to 0$, in which case a global symmetry is broken because the energy cost Nh goes to infinity, while a local symmetry isn't because the energy cost is $O(h)$ which goes to zero.

Alternatively, suppose there is no external field; then we care about tunneling between ground states related by the symmetry by local thermal fluctuations. Suppose the symmetry is discrete. In the case of a global symmetry, there is an extensive energy cost since we must form a domain wall, and hence cannot happen for $d > 1$. But in the case of a local symmetry, we can always relate two such ground states by a series of local transformations which each cost no energy.

Thus, a local gauge symmetry can't be broken in a consistent theory, while a local non-gauge symmetry can't be broken at all.

Example. The abelian Higgs model. Consider the theory of scalar QED with a potential,

$$\mathcal{L} = -\frac{1}{4}(F_{\mu\nu})^2 + |D_\mu \phi|^2 - V(\phi), \quad V(\phi) = -\mu^2 \phi^* \phi + \frac{\lambda}{2}(\phi^* \phi)^2, \quad \lambda > 0$$

with $D_\mu = \partial_\mu + ieA_\mu$. This Lagrangian has the $U(1)$ gauge symmetry

$$\phi(x) \to e^{i\alpha(x)}\phi(x), \quad A_\mu(x) \to A_\mu(x) - \frac{1}{e}\partial_\mu \alpha(x)$$

As usual, the field ϕ acquires a vev

$$\langle \phi \rangle = \phi_0 = \left(\frac{\mu^2}{\lambda}\right)^{1/2}$$

which we have chosen to be real, breaking the global $U(1)$ symmetry. Expanding about the vev,

$$\phi(x) = \phi_0 + \frac{1}{\sqrt{2}}\left(\phi_1(x) + i\phi_2(x)\right)$$

for real scalar fields ϕ_1 and ϕ_2, where we've chosen the constant so that the ϕ_i have canonical kinetic terms. Now the potential becomes

$$V(\phi) = -\frac{1}{2\lambda}\mu^4 + \mu^2\phi_1^2 + \text{ interactions}$$

so ϕ_1 has a mass $m = \sqrt{2}\mu$ and it appears that ϕ_2 is a massless Goldstone boson. However, there are new terms in the kinetic term of ϕ,

$$|D_\mu\phi|^2 = \frac{1}{2}\left(\partial_\mu\phi_1\right)^2 + \frac{1}{2}\left(\partial_\mu\phi_2\right)^2 + \sqrt{2}e\phi_0 A_\mu\partial^\mu\phi_2 + e^2\phi_0^2 A_\mu A^\mu + \text{ interactions.}$$

The first new term allows the photon and ϕ_2 to mix, while the second term is a photon mass term. In particular, it turns out that the ϕ_2 becomes the third, longitudinal mode of the now massive photon. The easiest way to see this is to go to unitary gauge, where ϕ is real. Then

$$|D_\mu\phi|^2 = \left(\partial_\mu\phi\right)^2 + e^2\phi^2 A_\mu A^\mu$$

which provides a photon mass term, $m_A = \sqrt{2}e\phi_0$, with no massless Goldstone bosons. We say the Goldstone boson ϕ_2 has been "eaten" by the gauge boson to gain mass, keeping the total number of degrees of freedom the same.

Note. To see how the Goldstone boson is eaten diagrammatically, note that the Goldstone-photon vertex has a factor of $m_A k^\mu$. Resumming the propagator using the photon mass vertices gives a pole in the appropriate place, and including the Goldstone-photon vertex provides the right numerator. This can be seen at lowest order, where the correction is

$$im_A^2\left(\eta^{\mu\nu} - \frac{k^\mu k^\nu}{k^2}\right)$$

which is exactly the right numerator polarization structure for a massive particle.

Note. One has to be careful with unitary gauge. Consider scalar QED without symmetry breaking. If we switch to unitary gauge, we apparently find a real scalar and a massless vector, without gauge symmetry; the number of degrees of freedom appears to have dropped. The problem is that now the vector has a third, massive, spin zero degree of freedom.

Next, we consider a generic non-abelian example.

• Consider a theory of scalar fields ϕ_i invariant under a compact group G, represented by

$$\phi_i \to \left(1 + i\alpha^a t^a\right)_{ij}\phi_j = \left(1 - \alpha^a T^a\right)_{ij}\phi_j$$

Without loss of generality we can work with only real fields. Since the representation is finitedimensional, it is unitary, so the t^a are imaginary and Hermitian, and the T^a are real and antisymmetric.

• Promoting the symmetry to a local gauge symmetry, the covariant derivative is

$$D_\mu\phi = \left(\partial_\mu + igA_\mu^a t^a\right)\phi = \left(\partial_\mu - gA_\mu^a T^a\right)\phi$$

Then the kinetic energy term for the ϕ_i is

$$\frac{1}{2}\left(D_\mu\phi_i\right)^2 = \frac{1}{2}\left(\partial_\mu\phi_i\right)^2 - gA_\mu^a\left(\partial_\mu\phi_i T_{ij}^a\phi_j\right) + \frac{1}{2}g^2 A_\mu^a A^{b\mu}\left(T^a\phi\right)_i\left(T^b\phi\right)_i.$$

• Now let the field acquire a vev, $\langle\phi_i\rangle = \phi_{0i}$. The last term yields a gauge boson mass term,

$$\Delta\mathcal{L} = \frac{1}{2}m_{ab}^2 A_\mu^a A^{b\mu}, \quad m_{ab}^2 = g^2 \left(T^a\phi_0\right)_i \left(T^b\phi_0\right)_i$$

The mass matrix is positive semidefinite, so the gauge bosons receive nonnegative masses.

• Suppose a generator T^a leaves the vacuum invariant, $T^a\phi_0 = 0$. Then the corresponding gauge boson is massless, as expected.

• The interaction between the Goldstone bosons and the gauge bosons is

$$\Delta\mathcal{L} = -gA_\mu^a \partial_\mu\phi_i \left(T^a\phi_0\right)_i$$

As expected, the only components of ϕ that mix are those parallel to $T^a\phi_0$ for some transformation T^a, which is precisely the set of Goldstone bosons. In other words, each massive gauge boson eats the Goldstone corresponding to the broken symmetry it generates. Just as in the abelian case, this provides the desired third polarization in the gauge boson propagator.

• The mass eigenstates in a gauge theory with gauge group G are multiplets of G. For example, quarks are color triplets and gluons form a color octet. In the case of symmetry breaking, one can show that mass eigenstates are instead multiplets of the unbroken gauge group H, by checking that the mass matrices all commute with the generators of H in the appropriate representation. For example, the particles in the SM have definite electric charge.

We now consider a series of non-abelian examples.

Example. Consider an $SU(2)$ gauge theory where ϕ transforms in the spinor representation. Then

$$D_\mu\phi = \left(\partial_\mu + igA_\mu^a\tau^a\right)\phi, \quad \tau^a = \frac{\sigma^a}{2}$$

If ϕ acquires a vev, then by the $SU(2)$ symmetry we can let it be

$$\langle\phi\rangle = \frac{1}{\sqrt{2}}\begin{pmatrix} 0 \\ v \end{pmatrix}$$

The mass term for the gauge bosons has the form

$$\Delta\mathcal{L} = \frac{1}{2}g^2 \begin{pmatrix} 0 & v \end{pmatrix} \tau^a\tau^b \begin{pmatrix} 0 \\ v \end{pmatrix} A_\mu^a A^{b\mu} = \frac{1}{4}g^2 \begin{pmatrix} 0 & v \end{pmatrix} \left\{\tau^a, \tau^b\right\} \begin{pmatrix} 0 \\ v \end{pmatrix} A_\mu^a A^{b\mu} = \frac{g^2v^2}{8} A_\mu^a A^{a\mu}$$

where we used $\left\{\tau^a, \tau^b\right\} = \delta^{ab}/2$. Therefore all three gauge bosons receive the mass $m_A = gv/2$.

Example. Consider the same example, but let ϕ transform in the vector representation. The covariant derivative is, in components,

$$\left(D_\mu\phi\right)_a = \partial_\mu\phi_a - g\epsilon_{abc}A_\mu^b\phi_c$$

and we choose the vev to be $\langle\phi_a\rangle = v\delta_{a3}$. Then the mass term is

$$\Delta\mathcal{L} = \frac{g^2v^2}{2}\left(\epsilon_{abc}A_\mu^b\delta_{c3}\right)^2 = \frac{g^2v^2}{2}\left(\left(A_\mu^1\right)^2 + \left(A_\mu^2\right)^2\right)$$

so we only get two massive gauge bosons. This makes sense, since the symmetry of rotations about the ϕ_3 axis is preserved. Since the model contains both massive and massless gauge bosons, it was once proposed as a candidate theory of the weak interaction, but it's not quite right: we require two massive bosons that only couple to left-handed fields (the $W^\pm$bosons), and one massive boson that couples to both handednesses (the Z). This can't be achieved by breaking $SU(2)$ in any way.

Example. Consider an $SU(3)$ gauge theory where ϕ transforms in the adjoint representation. Then

$$(D_\mu\phi)_a = \partial_\mu\phi_a - g f_{abc} A^b_\mu \phi_c, \quad \Delta\mathcal{L} = \frac{1}{2}(D_\mu\phi)_a (D^\mu\phi)_a \supset \frac{g^2}{2}\left(f_{abc}A^b_\mu\phi_c\right)^2$$

In this case, it's more convenient to work without components. We let $\Phi = \phi_a t^a$, so

$$D_\mu\Phi = \partial_\mu\Phi + ig[A_\mu, \Phi], \quad \Delta\mathcal{L} = \operatorname{tr}(D_\mu\Phi D^\mu\Phi) \supset -g^2 \operatorname{tr}\left(\left[t^a,\Phi\right]\left[t^b,\Phi\right]\right) A^a_\mu A^{b\mu}$$

where the normalization is fixed by using the Gell-Mann matrices. Now, we can always rotate Φ so that it is diagonal, but there are still several distinct possibilities. If $\Phi_0 = |\phi|\operatorname{diag}(1,1,-2)$, then the masses of the A^a_μ are

$$a \in \{1,2,3,8\} : 0, \quad a \in \{4,5,6,7\} : 3g|\phi|$$

so the symmetry is broken to $SU(2)\times U(1)$. If $\Phi_0 = |\phi|\operatorname{diag}(1,-1,0)$, then the masses are

$$a \in \{3,8\} : 0, \quad a \in \{1,2\} : 2g|\phi|, \quad a \in \{4,5,6,7\} : g|\phi|$$

and the symmetry is broken to $U(1)\times U(1)$. We see that matter fields in the adjoint can't break the symmetry corresponding to the Cartan subalgebra. To break these symmetries, we would have to add another matter field transforming in a different representation.

Now we give a more formal analysis of the Higgs mechanism.

• So far we have considered symmetry breaking by scalar fields picking up vevs, but other mechanisms could be possible; we will see such a mechanism for chiral symmetry in QCD. Hence we would like an analysis that is independent of how the symmetry is broken.

• Consider a theory with a global symmetry G and let α parametrize the global symmetry. By the usual Noether trick, if we promote α to $\alpha(x)$, then

$$\delta\mathcal{L} = -(\partial_\mu\alpha^a) J^{\mu a}, \quad \partial_\mu J^{\mu a} = 0$$

• We may couple this globally symmetric theory to a non-abelian gauge field by

$$\mathcal{L}' = \mathcal{L} + g A^a_\mu J^{\mu a} + O\left(A^2\right)$$

which has the effect of gauging the symmetry. By directly plugging in $\delta\mathcal{L}$, we see that $\mathcal{L}'$ is indeed gauge invariant, up to unspecified $O(A^2)$ terms. However, we will only need the linear term to compute matrix elements involving only one insertion of the gauge field.

• As mentioned above, if the global symmetry G is spontaneously broken, the currents $J^{\mu a}$ generate the Goldstone bosons,

$$\langle 0|J^{\mu a}(x)|\pi_k(p)\rangle = -ip^\mu F^a_k e^{-ipx}$$

Here, the F^a_k are only nonzero if the symmetry a is broken.

• As an example, in the cases we studied earlier, we have

$$J^{\mu a} = \partial_\mu\phi_i T^a_{ij}\phi_j$$

The Goldstone bosons are the ϕ_i which are shifted by the global transformation, and indeed,

$$\langle 0|J^{\mu a}(x)|\phi_i(p)\rangle = (T^a\phi_0)_i \langle 0|\partial^\mu\phi_i|\phi_i(p)\rangle = -ip^\mu (T^a\phi_0)_i e^{-ipx}$$

This is just of the form above, with the identification

$$F^a_i = T^a_{ij}\phi_{0j}$$

• Now, the vacuum polarization amplitude for the gauge bosons is

$$\Pi_{ab}^{\mu\nu}\left(k^2\right) = i\left(\eta^{\mu\nu} - \frac{k^\mu k^\nu}{k^2}\right)\left(m_{ab}^2 + O\left(k^2\right)\right)$$

where m_{ab} is the gauge boson mass matrix. To compute this, note that the pole at $k^2 = 0$ comes from the diagram with an intermediate Goldstone boson. Using our two equations involving $J^{\mu a}$ above, the $A_\mu^a \phi_j$ vertex factor is $-gk^\mu F_j^a$, giving

$$\Pi_{ab}^{\mu\nu}\left(k^2\right) \supset \left(gk^\mu F_j^a\right)\frac{i}{k^2}\left(-gk^\nu F_j^b\right)$$

so the gauge boson mass matrix is

$$m_{ab}^2 = g^2 F_j^a F_j^b$$

The mass matrix is again manifestly positive semidefinite.

Note. If we wanted to analyze how electroweak symmetry breaking occurred earlier in our universe, we would have to understand how thermal effects change the Higgs potential. This can be done using standard techniques from thermal field theory, which are sketched in my dissertation.

One should also account for quantum corrections to the potential, which can be quite important. For instance, in massless ϕ^4 theory coupled to a $U(1)$ gauge field, quantum effects cause spontaneous symmetry breaking even though it doesn't happen classically; the effective potential in this case is called the Coleman-Weinberg potential. We managed to ignore this above by either implicitly assuming weak coupling or working with the effective potential.

6.3.4 Quantization

In this section we consider the quantization of theories with spontaneous symmetry breaking of a gauged global symmetry.

• First, we focus on the abelian case. To establish conventions, we define

$$\mathcal{L} = -\frac{1}{4}F_{\mu\nu}F^{\mu\nu} + \left(D_\mu\phi\right)^*\left(D^\mu\phi\right) - \frac{g}{2}\left(\phi^*\phi - \frac{1}{2}v^2\right)^2, \quad D_\mu\phi = \partial_\mu\phi - ieA_\mu\phi$$

where the gauge transformations are

$$\phi \to e^{ie\alpha}\phi, \quad A_\mu \to A_\mu - \partial_\mu\alpha$$

The potential ensures $|\phi| = v/\sqrt{2}$. In unitary gauge, we can see that the gauge field gains a mass $M_A^2 = e^2v^2$. There is also a remaining massive scalar field corresponding to the radial part of ϕ. with mass $m^2 = gv^2$.

• As shown in the notes on Quantum Field Theory, the propagator for a massive vector boson is

$$D_{\mu\nu}\left(k^2\right) = -\frac{i}{k^2 - M_A^2 + i\epsilon}\left(\eta_{\mu\nu} - \frac{k_\mu k_\nu}{M_A^2}\right)$$

However, this makes renormalizability unclear, because the propagator does not fall off at high k. Since we are dealing with a gauge theory, we should also be more careful to account for Faddeev-Popov ghosts.

• To be more explicit, we show what happens before gauge fixing. We parametrize

$$\phi(x) = \frac{1}{\sqrt{2}}(v + f(x) + i\varphi(x))$$

where we use a global symmetry to set v real. Then the full kinetic term is

$$D_\mu\phi^* D^\mu\phi = \frac{1}{2}\partial_\mu f\partial^\mu f + \frac{1}{2}\partial_\mu\varphi\partial^\mu\varphi + \frac{1}{2}e^2v^2A_\mu A^\mu + evA^\mu\partial_\mu\varphi \\ - eA^\mu\left(\varphi\partial_\mu f - f\partial_\mu\varphi\right) + e^2vfA^\mu A_\mu + \frac{1}{2}A^\mu A_\mu\left(f^2+\varphi^2\right)$$

This is quite complicated, but the terms are mostly interaction terms; the most problematic term is the mixing term,

$$\mathcal{L} \supset evA^\mu\partial_\mu\varphi = -M_A\left(\partial_\mu A^\mu\right)\varphi$$

which, as we've seen, makes it difficult to interpret A^μ or φ alone.

• As such, any convenient gauge fixing must suppress this term. In path integral quantization, we may choose the gauge fixing function

$$F(A,\varphi) = \partial_\mu A^\mu - \xi M_A\varphi$$

Furthermore, we integrate over gauge fixings with a Gaussian weight of width ξ. As shown in the notes on Quantum Field Theory, the Lagrangian picks up the terms

$$\mathcal{L} \supset -\frac{1}{2\xi}F(A)^2 + \bar{c}\Delta_{\text{FP}}c$$

This is a generalization of R_ξ gauge.

• Unlike previous examples, the gauge fixing function F now depends on matter fields as well as the gauge field. To evaluate the Faddeev-Popov determinant, we go back to the definition,

$$\Delta_{\text{FP}} = \frac{\partial F}{\partial\alpha} = -\frac{\partial F}{\partial A_\mu}D_\mu + \frac{\partial F}{\partial\varphi}e(v+f) = -\partial^2 - \xi eM_A(v+f)$$

Since this is an abelian gauge theory, the ghosts do not couple to the gauge field directly, but have indirect effects by their coupling to f.

• Expanding the extra $F^2/2\xi$ terms, the mixing term is cancelled, leaving quadratic terms

$$\mathcal{L}_{\text{quad}} = \frac{1}{2}\left(\partial_\mu f\right)\left(\partial^\mu f\right) - \frac{1}{2}m^2f^2 + \frac{1}{2}\partial_\mu\varphi\partial^\mu\varphi - \frac{\xi}{2}M_A^2\varphi^2 \\ - \frac{1}{2}A_\mu\left(-\eta^{\mu\nu}\partial^2 + \left(1-\frac{1}{\xi}\right)\partial^\mu\partial^\nu - M_A^2\eta^{\mu\nu}\right)A_\nu - \bar{c}\partial^2c - \xi M_A^2v\bar{c}c$$

where the f mass term is from the potential for ϕ. The propagators are now

$$D_{\mu\nu}\left(k^2\right) = -\frac{i}{k^2 - M_A^2 + i\epsilon}\left(\eta_{\mu\nu} - (1-\xi)\frac{k_\mu k_\nu}{k^2-\xi M_A^2}\right), \quad D_\varphi\left(k^2\right) = \frac{i}{k^2-\xi M_A^2+i\epsilon}$$

and

$$D_c\left(k^2\right) = \frac{i}{k^2-\xi M_A^2}, \quad D_f\left(k^2\right) = \frac{i}{k^2-m_f^2}$$

Renormalizability is now easier to show, as all propagators fall off as $1/k^2$, but not all the fields are physical, as signaled by the ξ-dependent masses of φ and the ghost field. The f field is physical, and in the Standard Model will correspond to the Higgs boson.

• The physical results should not depend on ξ, which can be a useful cross-check in computations, just as it was in QED. The ξ-independence may be proven generally using the BRST symmetry of the gauge-fixed Lagrangian.

• One useful special case is $\xi = 0$, where the Goldstone boson φ is massless and the gauge field is fully transverse,

$$D_{\mu\nu}\left(k^2\right) = -\frac{i}{k^2 - M_A^2 + i\epsilon}\left(\eta_{\mu\nu} - \frac{k_\mu k_\nu}{k^2}\right), \quad D_\varphi\left(k^2\right) = \frac{i}{k^2 + i\epsilon}$$

Both propagators have poles at $k^2 = 0$, but they don't correspond to physical particles.

• Another useful special case is $\xi = 1$, where

$$D_{\mu\nu}\left(k^2\right) = -\frac{i\eta_{\mu\nu}}{k^2 - M_A^2 + i\epsilon}, \quad D_\varphi\left(k^2\right) = \frac{i}{k^2 - M_A^2 + i\epsilon}.$$

This gauge, called the Feynman-'t Hooft gauge, is the most convenient for general higher-order computations.

• We recover unitary gauge in the limit $\xi \to \infty$, where the unphysical fields decouple; the unphysical poles in k^2 go to infinity. This is called unitary gauge because every pole found by evaluating Feynman diagrams corresponds to the propagation of physical intermediate states, consistent with the Cutkosky rules, so unitarity is manifest.

• In 1972, 't Hooft and Veltman used R_ξ gauge to prove the renormalizability of the Standard Model at all orders in perturbation theory. For any finite ξ, it is easy to show that the divergences can be cancelled by a finite number of counterterms, since the usual power counting arguments will work. 't Hooft and Veltman additionally showed that the counterterms preserved local gauge invariance, and the ξ-independence of S-matrix elements.

Though we have now set up the trickiest Feynman rules, loop computations in the Standard Model are quite complicated, and we will not perform any in these notes.

6.4 Electroweak Theory

6.4.1 Gauge Theory

We now describe the Weinberg-Salam theory of the electroweak interaction.

• We postulate a gauge group $SU(2)_L \times U(1)_Y$, where the factors are called weak isospin and hypercharge, and a complex scalar field ϕ, called the Higgs field. The Higgs transforms as a weak isospin doublet with a $U(1)$ hypercharge $Y = 1/2$,

$$\phi(x) \to e^{i\alpha^a(x)\tau^a} e^{i\beta(x)/2}\phi(x), \quad \tau^a = \frac{\sigma^a}{2}.$$

• We suppose the Higgs acquires a vev, through the same potential as in the abelian Higgs model. Using the $SU(2)_L \times U(1)_Y$ global symmetry, without loss of generality we can pick

$$\phi_0 = \frac{1}{\sqrt{2}}\begin{pmatrix} 0 \\ v \end{pmatrix}$$

This breaks the symmetry to $U(1)_{\text{EM}}$, generated by gauge transformations with $\alpha^3(x) = \beta(x)$.

• The covariant derivative for the Higgs is

$$D_\mu\phi = \left(\partial_\mu + igA_\mu^a\tau^a + \frac{i}{2}g'B_\mu\right)\phi$$

and the Lagrangian is

$$\mathcal{L} = -\frac{1}{2}\,\mathrm{tr}\, F^A_{\mu\nu}F_{A\mu\nu} - \frac{1}{4}F^B_{\mu\nu}F^{B\mu\nu} + (D_\mu\phi)^\dagger (D^\mu\phi) - \mu^2|\phi|^2 - \lambda|\phi|^4.$$

Here, the field strengths are

$$F^{Aa}_{\mu\nu} = \partial_\mu A^a_\nu - \partial_\nu A^a_\mu - g\epsilon^{abc}A^b_\mu A^c_\nu, \quad F^B_{\mu\nu} = \partial_\mu B_\nu - \partial_\nu B_\mu$$

• Expanding out the gauge boson mass term, we have

$$\begin{aligned}\mathcal{L} &\supset \frac{1}{2}\begin{pmatrix} 0 & v \end{pmatrix}\left(gA^a_\mu\tau^a + \frac{1}{2}g'B_\mu\right)\left(gA^{b\mu}\tau^b + \frac{1}{2}g'B^\mu\right)\begin{pmatrix} 0 \\ v \end{pmatrix} \\ &= \frac{1}{2}\frac{v^2}{4}\left(g^2\left(A^1_\mu\right)^2 + g^2\left(A^2_\mu\right)^2 + \left(-gA^3_\mu + g'B_\mu\right)^2\right).\end{aligned}$$

Therefore, we find three massive vector bosons, which we write as

$$W^\pm_\mu = \frac{1}{\sqrt{2}}\left(A^1_\mu \mp iA^2_\mu\right), \quad Z^0_\mu = \frac{1}{\sqrt{g^2+g'^2}}\left(gA^3_\mu - g'B_\mu\right), \quad m_W = g\frac{v}{2}, \quad m_Z = \sqrt{g^2+g'^2}\frac{v}{2}$$

The fourth vector field, which is orthogonal to Z^0_μ, remains massless,

$$A_\mu = \frac{1}{\sqrt{g^2+g'^2}}\left(g'A^3_\mu + gB_\mu\right)$$

This field is identified with the QED vector potential.

• The general covariant derivative may be rewritten in terms of the mass eigenstates as

$$\begin{aligned}D_\mu &= \partial_\mu + igA^a_\mu T^a + iYg'B_\mu \\ &= \partial_\mu + \frac{ig}{\sqrt{2}}\left(W^+_\mu T^+ + W^-_\mu T^-\right) + \frac{i}{\sqrt{g^2+g'^2}}Z_\mu\left(g^2T^3 - g'^2Y\right) + i\frac{gg'}{\sqrt{g^2+g'^2}}A_\mu\left(T^3+Y\right)\end{aligned}$$

where the T^a are $SU(2)$ generators in the appropriate representation and $T^\pm = T^1 \pm iT^2$. To simplify this result, we define the electron charge e and electric charge Q as

$$e = \frac{gg'}{\sqrt{g^2+g'^2}}, \quad Q = T^3 + Y$$

Note that Y is sometimes defined with an extra factor of 2.

• Note that the Z also couples directly to anything with hypercharge, so it can couple to particles that are $SU(2)_L$ singlets. This isn't a phenomenological problem, because the photon can couple to anything the Z can. That is, the Z boson doesn't produce any new decays; at low energies its effect is totally washed out by that of the photon.

• Next, we define the weak mixing angle or Weinberg angle θ_w so that

$$\begin{pmatrix} Z^0 \\ A \end{pmatrix} = \begin{pmatrix} \cos\theta_w & -\sin\theta_w \\ \sin\theta_w & \cos\theta_w \end{pmatrix}\begin{pmatrix} A^3 \\ B \end{pmatrix}, \quad \cos\theta_w = \frac{g}{\sqrt{g^2+g'^2}}$$

Then the covariant derivative simplifies to

$$D_\mu = \partial_\mu + \frac{ig}{\sqrt{2}}\left(W^+_\mu T^+ + W^-_\mu T^-\right) + \frac{ig}{\cos\theta_w}Z_\mu\left(T^3 - \sin^2\theta_w Q\right) + ieA_\mu Q$$

and we have

$$e = g \sin\theta_w, \quad m_W = m_Z \cos\theta_w$$

• The theory is predictive: with just four parameters (g, g', μ^2, and λ), all of the masses and (self-)interactions of the electroweak bosons and the Higgs are fixed. For example, the Higgs trilinear and quartic couplings are predicted but currently not measured to any precision; they will be targeted by future colliders.

Note. In the Standard Model, the mechanism of spontaneous symmetry breaking is much less constrained than the other parts of it. It is therefore interesting to consider which of the above predictions follow solely from the spontaneous symmetry breaking pattern $SU(2)_L \times U(1)_Y \to U(1)_{\text{EM}}$, and which additionally rely on there being a single, $SU(2)_L$ doublet Higgs field.

We focus on the mass matrix of the four gauge bosons. First, note that $U(1)_{\text{EM}}$ transformations don't commute with two of the $SU(2)_L$ transformations; this implies that a pair of $SU(2)_L$ bosons pick up opposite electric charges. Thus, the mass matrix must take the form

$$\begin{pmatrix} m_1^2 & & & \\ & m_2^2 & & \\ & & m_3^2 & m^2 \\ & & m^2 & m_0^2 \end{pmatrix}$$

where additional off-diagonal terms are forbidden by $U(1)_{\text{EM}}$ symmetry, which additionally forces $m_1 = m_2 \equiv m_W$. Because $U(1)_{\text{EM}}$ is unbroken, there must be a massless gauge boson A_μ, which implies $m^2 = \pm|m_0 m_3|$. Requiring that A_μ take the same form as found above implies $\tan\theta_W = |m_0/m_3|$. Therefore, the only thing not determined is the mass of the Z-boson,

$$m_Z^2 = m_0^2 + m_3^2 = m_3^2/\cos^2\theta_W$$

This matches the Standard Model prediction precisely when $m_3 = m_W$. We can thus search for deviations from the Standard Model by measuring $\rho = m_W^2/(m_Z^2\cos^2\theta_W)$, which at tree level is $\rho_0 = 1$. Loop corrections contribute $\Delta\rho \approx 0.008$.

6.4.2 Coupling to Matter

Next, we couple fermions to the gauge bosons and Higgs. We begin with leptons.

• It suffices to find the $SU(2)_L$ and $U(1)_Y$ representations the fermions transform in; we can then read the interaction terms off the covariant derivative. We are guided by the experimental fact that the weak interactions only affect left-helicity particles and right-helicity antiparticles.

• We postulate the left-handed electron and electron neutrino fit in an isospin doublet,

$$L(x) = \begin{pmatrix} \nu_e(x) \\ e_L(x) \end{pmatrix}, \quad e_L(x) = \frac{1}{2}\left(1 - \gamma^5\right) e(x)$$

We define $R(x) = e_R(x)$. To get the observed electric charges, we need

$$Y = -\frac{1}{2} \text{ for } L(x), \quad Y = -1 \text{ for } R(x)$$

The lepton-gauge boson part of the electroweak Lagrangian is thus

$$\mathcal{L} \supset \bar{L} i \not{D} L + \bar{R} i \not{D} R$$

which is just the Weyl Lagrangian with covariant derivatives.

• Expanding out the covariant derivatives, we can show the interaction terms are

$$\mathcal{L} \supset -\frac{g}{2\sqrt{2}}\left(J^\mu W_\mu^+ + J^{\mu\dagger} W_\mu^-\right) - e J_{\mathrm{EM}}^\mu A_\mu - \frac{g}{2\cos\theta_W} J_n^\mu Z_\mu$$

where we have defined the leptonic charged weak, neutral weak, and electromagnetic currents

$$J^\mu = \bar{\nu}_e \gamma^\mu \left(1-\gamma^5\right) e, \quad J_n^\mu = \frac{1}{2}\left(\bar{\nu}_e \gamma^\mu \left(1-\gamma^5\right)\nu_e - \bar{e}\gamma^\mu\left(1-\gamma^5-4\sin^2\theta_w\right)e\right), \quad J_{\mathrm{EM}}^\mu = -\bar{e}\gamma^\mu e$$

Note that right-handed electrons can couple to the Z, as mentioned earlier. Also note that because $\sin^2\theta_w$ is close to $1/4$, the coupling of the charged leptons to the Z boson is almost purely axial, i.e. proportional to γ^5.

Note. One might wonder if the weak force can form bound states; for instance, the Z boson mediates an attractive interaction between neutrinos. However, while all potential wells in 1D and 2D have bound states, sufficiently weak potential wells in 3D don't, and indeed there are no weak bound states in the SM. However, certain models of WIMP dark matter could have them.

Next, we consider lepton couplings to the Higgs.

• Next, we wish to write down a mass term for the electron, but the Dirac mass term $m_e\left(\bar{e}_L e_R + \bar{e}_R e_L\right)$ is not gauge invariant. Instead, all mass terms in the SM come from Yukawa couplings to the Higgs. We work in unitary gauge where

$$\phi(x) = \frac{1}{\sqrt{2}}\begin{pmatrix} 0 \\ v + h(x) \end{pmatrix}$$

and choose $Y = 1/2$ for the Higgs doublet so that the Higgs boson h is electrically neutral. Note that the components of ϕ with charge are exactly the ones 'eaten' by the charged $W_\mu^\pm$.

• Then the coupling to the Higgs is

$$\mathcal{L} \supset -\sqrt{2}\lambda_e\left(\bar{L}\phi R + \bar{R}\phi^\dagger L\right) = -\lambda_e(v+h)\left(\bar{e}_L e_R + \bar{e}_R e_L\right) = -m_e\bar{e}e - \lambda_e h\bar{e}e$$

giving a mass $m_e = \lambda_e v$ and a Yukawa coupling λ_e to the Higgs, proportional to m_e. For now, we'll take the neutrino to be massless.

• In reality, there are three generations of leptons, so we write

$$L^1 = \begin{pmatrix} \nu_e \\ e_L \end{pmatrix}, \quad L^2 = \begin{pmatrix} \nu_\mu \\ \mu_L \end{pmatrix}, \quad L^3 = \begin{pmatrix} \nu_\tau \\ \tau_L \end{pmatrix}, \quad R^1 = e_R, \quad R^2 = \mu_R, \quad R^3 = \tau_R$$

Then the Higgs-lepton coupling has the generic form

$$\mathcal{L} \supset -\sqrt{2}\left(\lambda^{ij}\bar{L}^i\phi R^j + \lambda^{\dagger ij}\bar{R}^i\phi^\dagger L^j\right).$$

Here the generation indices are kept explicit, the spinor indices are contracted between $\bar{L}$ and R, and the weak isospin indices are contracted between L and ϕ. Note that the adjoint/dagger acts on all spaces, so $\bar{L}$ is a row vector in weak isospin space with $Y = 1/2$. Similarly, $\phi^\dagger$ is a row vector in weak isospin space with $Y = -1/2$.

• In general, the weak interactions and the Higgs interactions will pick out two different bases, the flavor basis and the mass basis. In the SM, neutrinos have no mass, so this problem doesn't arise. It also doesn't occur for the charged leptons, as we now show.

• Now λ is an arbitrary complex matrix, so it can't be diagonalized in the usual way. But since $\lambda\lambda^\dagger$ is Hermitian and positive, we have

$$\lambda\lambda^\dagger = U\Lambda^2 U^\dagger$$

where Λ^2 is diagonal and positive, and U is unitary. Taking Λ to also be diagonal and positive, we define $S = \lambda^\dagger U \Lambda^{-1}$, so S is unitary as well, and

$$\lambda^\dagger \lambda = S\Lambda^2 S^\dagger, \quad \lambda = U\Lambda S^{-1}$$

Hence we may diagonalize λ if we use different unitaries on both ends.

• We now redefine the lepton fields by

$$L^i \to U^{ij} L^j, \quad R^i \to S^{ij} R^j, \quad \bar{L}^i \to U^{ij^*} \bar{L}^j = \bar{L}^j \left(U^\dagger\right)^{ji}, \quad \bar{R}^i \to \bar{R}^j \left(S^\dagger\right)^{ji}$$

Here, the transformations for the barred quantities follow because taking the Dirac adjoint performs a complex conjugation. The covariant derivative terms aren't affected, while the mass matrix λ is diagonalized to Λ, as desired.

Note. More about weak isospin. Given two objects A^α and B^α in the fundamental representation of $SU(2)_L$, their inner product $A^{\alpha *} B^\alpha$ is invariant. To unpack this, we note that $A^{\alpha *} \equiv A_\alpha$ transforms in the antifundamental representation. The contraction $A_\alpha B^\alpha$ is then invariant; forming invariants is just a matter of matching up the indices, as for the Lorentz group. In the examples above, everything starts with an upper index, and taking the adjoint lowers the index. Note that the fundamental representation of $SU(2)$ is pseudoreal and hence similar to the antifundamental, i.e. we may raise and lower indices with $\epsilon^{\alpha\beta}$.

Next, we perform the same procedure for the quark fields.

• The left-handed quarks fit into $SU(2)_L$ doublets,

$$Q_L^i = \begin{pmatrix} u^i \\ d^i \end{pmatrix}_L = \left(\begin{pmatrix} u \\ d \end{pmatrix}_L \begin{pmatrix} c \\ s \end{pmatrix}_L \begin{pmatrix} t \\ b \end{pmatrix}_L \right)$$

To get the right electric charges, we take $Y = 1/6$.

• The right-handed quarks fit into $SU(2)_L$ singlets, which we write as

$$u_R^i = (u_R, c_R, t_R), \quad d_R^i = (d_R, s_R, b_R)$$

with hypercharge $Y = 2/3$ and $Y = -1/3$ respectively.

• The quarks couple to the gauge bosons by

$$\mathcal{L} \supset \bar{Q}_L i \not{D} Q_L + \bar{u}_R i \not{D} u_R + \bar{d}_R i \not{D} d_r$$

as usual. These terms violate C and P, but obey CP and T symmetry; note that here we are referring to the quantum $\widehat{C}$, so the CP symmetry acts on fields like classical C symmetry, conjugating them.

• The most general renormalizable gauge invariant quark-Higgs couplings are

$$\mathcal{L} \supset -\sqrt{2} \left(\lambda_d^{ij} \bar{Q}_L^i \phi d_R^j + \lambda_u^{ij} \bar{Q}_L^i \phi^c u_R^j + \text{ h.c. } \right), \quad \phi^{c\alpha} \equiv \epsilon^{\alpha\beta} \phi_\beta^\dagger.$$

In the second term, we need to use $\phi^\dagger$ to get hypercharge invariance, and a Levi-Civita to get a weak isospin invariant contracting with $\bar{Q}_\alpha$. Also, by hypercharge, there's no term involving u_R and d_R. Since CP conjugates the fields, the coupling is CP invariant if and only if λ_d^{ij} and λ_u^{ij} are real. Roughly speaking, complex physical parameters indicate CP violation.

• Next, we switch to the mass basis, as we did for the leptons. As before, we let

$$\lambda_u = K_u \Lambda_u S_u^\dagger, \quad \lambda_d = K_d \Lambda_d S_d^\dagger$$

and redefine the quark fields by

$$u_L \to K_u u_L, \quad d_L \to K_d d_L, \quad u_R \to S_u u_R, \quad d_R \to S_d d_R$$

Then we have, for example, in unitary gauge

$$\sqrt{2}\lambda_d^{ij}\bar{Q}_L^i\phi d_R^j \supset v\bar{d}_L^i\lambda_d^{ij}d_R^j \to v\bar{d}_L K_d^\dagger K_d\Lambda_d S_d^\dagger S_d d_R = v\bar{d}_L\Lambda_d d_R$$

and the quark mass term becomes

$$\mathcal{L} \supset -v\left(\Lambda_d^{ij}\bar{d}_L^i d_R^j + \Lambda_u^{ij}\bar{u}_L^i u_R^j + \text{ h.c. }\right) = -v\sum_i m_d^i\bar{d}_L^i d_R^i + m_u^i\bar{u}_L^i u_R^i + \text{ h.c.}$$

• Now, this redefinition affects the gauge couplings. The terms $\bar{u}_R i\not{D}u_R + \bar{d}_R i\not{D}d_r$ are not affected, but $\bar{Q}_L i\not{D}Q_L$ is because the covariant derivative mixes u_L and d_L. In particular, the charged weak current transforms as

$$J^\mu = \bar{u}^i\gamma^\mu\left(1-\gamma^5\right)d^i = 2\bar{u}_L^i\gamma^\mu d_L^i \to 2\bar{u}_L^i\gamma^\mu\left(K_u^\dagger K_d\right)^{ij}d_L^j$$

However, the neutral current remains diagonal, because it does not convert up-type quarks to down-type quarks. Thus the SM, at tree level, has no flavor-changing neutral currents.

• We define the CKM matrix by

$$K_u^\dagger K_d = V_{\text{CKM}} = \begin{pmatrix} V_{ud} & V_{us} & V_{ub} \\ V_{cd} & V_{cs} & V_{cb} \\ V_{td} & V_{ts} & V_{tb} \end{pmatrix}$$

The off-diagonal elements quantify the mismatch between the mass basis and the flavor basis. When we talk about an "up quark", we conventionally mean the mass basis.

Note. We began this discussion in the flavor basis, where we noted that gauge boson couplings are CP invariant, but introducing the mass terms broke CP symmetry. But usually we work in the mass basis, where we say that the mass terms have CP symmetry, while the gauge boson couplings break CP, as discussed below. So which term "really" breaks CP? Neither. The point is that there is no single "objective" definition of CP, because discrete symmetries are only defined up to an arbitrary linear transformation on the fields. This extra transformation can be chosen to leave the gauge boson couplings invariant, or the mass terms invariant, but not both at once.

Next, we'll introduce a useful way to count degrees of freedom, and apply it to the CKM matrix.

• Consider an atom in an external electric or magnetic field. Naively, the field has three degrees of freedom, but we can always take it to be along the z-axis, giving only one degree of freedom. The reason is that the atom and field still have $SO(3)$ symmetry provided we rotate them together, so we can align the field with the z-axis without loss of generality. To count the number of degrees of freedom of the perturbation, we note that the atom alone has only $SO(2)$ symmetry, by rotations orthogonal to the field direction. We have lost $3-1=2$ symmetry generators, which were the ones used to align the field with the z-axis, so the field is described by only $3-2=1$ parameter.

• In a more general situation, suppose that some couplings break a symmetry. We can formally think of the couplings as spurions (i.e. effectively as external fields) which transform under that symmetry, reducing the reasoning to the previous case. The number of parameters needed to break the couplings is the naive number, minus the number of broken symmetry generators.

• Now consider a general $n\times n$ complex matrix. Each entry is a complex number with a magnitude and phase, so there are n^2 real parameters and n^2 phase parameters.

• An $n\times n$ orthogonal matrix has $n(n-1)/2$ real parameters. However, an orthogonal matrix can just be thought of as a unitary matrix with the phases removed, and a unitary

matrix has n^2 parameters, so a unitary matrix has $n(n-1)/2$ real parameters and $n(n+1)/2$ phases.

• This reasoning can also be understood by realizing that unitary matrices correspond with ordered bases of $\mathbb{C}^n$. The first basis vector is described by $n-1$ real parameters, for the magnitudes of the components, and n phases, for the phases of the components. Restricting to the orthogonal subspace, the second basis vector is described by $n-2$ real parameters and $n-1$ phases, and so on.

• Now we apply these results to the CKM matrix. Without the Yukawa couplings, the quark sector has a $U(3)^3$ symmetry, by unitary transformations of u_R, d_R, and Q_L individually; this corresponds to 9 real parameters and 18 phases. Adding the Yukawa couplings breaks this to a $U(1)_B$ symmetry, which is 1 phase.

• The Yukawa couplings take the form of two 3×3 complex matrices, with 18 real parameters and 18 phases. Hence the quark sector has 9 real parameters (6 quark masses and 3 CKM angles) and 1 phase.

• One might worry that anomalies upset this parameter counting, once we account for quantum effects. Indeed, the $U(3)^3$ symmetry includes the axial $U(1)_A$ symmetry, which is anomalous. The corresponding new term is the QCD θ-term, which has no effect classically.

• In the above derivation, we derived the CKM matrix rather differently, as we used a $U(3)^4$ quark field redefinition, which is not a symmetry of the Lagrangian even for $\lambda_u = \lambda_d = 0$. This is precisely why the form of the rest of the Lagrangian changed, i.e. why we picked up the CKM matrix in the first place. We will find the physical parameters of the CKM matrix below explicitly, but this heuristic analysis using $U(3)^3$ symmetry tells us what to expect.

Example. Spurions are ubiquitous. Consider a theory of a complex scalar field and a Weyl fermion,

$$\mathcal{L} = (\partial_\mu \phi)^2 + i\psi^\dagger \not{\partial} \psi - m_\phi^2 |\phi|^2 - \frac{1}{2} m_\psi \psi^2 + \mathcal{L}_{\text{int}}$$

In the limit $m_\phi \to 0$, we recover a shift symmetry for the scalar, so m_ϕ is a spurion for this symmetry. Assuming the interaction obeys this theory, the mass of the scalar can't become much larger than m_ϕ, at least perturbatively. Similarly, m_ψ is a spurion for chiral symmetry. Scale invariance is restored when both mass terms go to zero, and supersymmetry is restored when the mass terms become equal. Supersymmetry effectively transfers the chiral symmetry of the spinor to the scalar. Next, we investigate the degrees of freedom in the CKM matrix.

• In the case of two generations, unitarity implies that V_{CKM} has four parameters, which can be expressed as an angle and three phases,

$$V_{\text{CKM}} = \begin{pmatrix} \cos\theta_c e^{i\alpha} & \sin\theta_c e^{i\beta} \\ -\sin\theta_c e^{i(\alpha+\gamma)} & \cos\theta_c e^{i(\beta+\gamma)} \end{pmatrix}$$

However, in the absence of the CKM matrix, the Lagrangian would be invariant under a global phase rotation of any quark field,

$$q_L^i \to e^{i\alpha^i} q_L^i, \quad q^i \in \{u, d, s, c\}$$

On the other hand, a rotation of all four quark simultaneously doesn't change the CKM matrix, because it is the $U(1)_B$ symmetry. Since the CKM matrix breaks three $U(1)$ symmetries, we can use them to remove all phases in the CKM matrix; then there is no CP violation. The remaining angle is called the Cabibbo angle.

• In this case, the charged weak current is

$$\frac{1}{2} J^\mu = \cos\theta_c \bar{u}_L \gamma^\mu d_L + \sin\theta_c \bar{u}_L \gamma^\mu s_L - \sin\theta_c \bar{c}_L \gamma^\mu d_L + \cos\theta_c \bar{c}_L \gamma^\mu s_L$$

• Kobayashi and Maskawa proposed a third generation of quarks, which would allow for CP violation. In this case, there are 3 angles and 6 phases, but only 5 quark phases available. Thus the CKM matrix can be parametrized in terms of three angles and one phase.

• The CKM matrix is conventionally written in terms of the Wolfenstein parameters,

$$V_{\text{CKM}} = \begin{pmatrix} 1-\lambda^2/2 & \lambda & A\lambda^3(\rho - i\eta) \\ -\lambda & 1-\lambda^2 & A\lambda^2 \\ A\lambda^3(1-\rho-i\eta) & -A\lambda^2 & 1 \end{pmatrix} + O\left(\lambda^4\right)$$

where $\lambda \approx 0.22, A \approx 0.81, \rho \approx 0.12$, and $\eta \approx 0.36$. This is useful because it parametrizes generation-mixing effects as powers of λ. For example, crossing from the first to the third generation is penalized by a factor λ^3. The CP violating phase is parametrized by η. Note that the top-left block is simply the 2×2 CKM matrix with Cabibbo angle λ.

• The unitarity of the CKM matrix is often tested by plotting unitarity triangles. We know that the inner product of any two distinct columns, or any two distinct rows, must vanish, and each inner product is the sum of three complex numbers, so there are six 'unitarity triangles' in the complex plane that must close. In most cases, the triangle is very flat because some terms are much bigger than others, so we usually plot

$$\sum_i V_{id} V_{ib}^* = 0$$

because every term is $O\left(\lambda^3\right)$.

Note. Summarizing the matter content, we have the isospin doublets

$$\phi = \frac{1}{\sqrt{2}} \begin{pmatrix} 0 \\ v+h \end{pmatrix}, Y = 1/2, \quad L = \begin{pmatrix} \nu_e \\ e_L \end{pmatrix}, Y = -1/2, \quad Q_L = \begin{pmatrix} u_L \\ d_L \end{pmatrix}, Y = 1/6$$

and the isospin singlets

$$R = e_R, Y = -1, \quad u_R, Y = 2/3, \quad d_R, Y = -1/3$$

Note that the hypercharge is always the average electric charge of a weak isospin multiplet.

Note. It's important to avoid thinking of the Higgs sector of the SM as obvious. Over the 50 years between its proposal and discovery, many influential physicists expressed skepticism, as described in the historical review The Theoretical Physics Ecosystem Behind the Discovery of the Higgs Boson.

At the time of its proposal, it was not clear that the Higgs mechanism (i.e. the pattern of electroweak symmetry breaking which gives mass to the W and Z bosons) was even necessary. Glashow had proposed a model in 1961 where these masses were simply put in by hand, as an explicit symmetry breaking, and viewed it as no less legitimate than breaking flavor symmetry by hand. The Higgs mechanism, proposed in 1964 and used to by Weinberg and Salam to complete the SM in 1967 and 1968, gained greater acceptance in 1971 when 't Hooft showed it to be renormalizable, in contrast to Glashow's setup. (But in the 1970s we also learned that renormalizability was less important of a criterion than had been thought, due to the rise of Wilsonian ideas.)

Even when the Higgs mechanism became more accepted, the Higgs boson was not. The Higgs field was simply the analogue of the Ginzburg-Landau order parameter field in superconductivity. In that case, the field was meant to measure some aspect of the collective behavior of the electrons, so the natural analogue would have been to view the Higgs field as representing a condensate of other particles. (Examples of such theories included top quark condensates, where top quarks play the role of electrons, and technicolor, which breaks electroweak symmetry by

strong gauge interactions, and has no discernible Higgs excitation at all.) Many physicists, especially condensed matter physicists, thought that postulating an elementary Higgs was naive, the result of taking an order parameter field too literally. A further issue, realized throughout the 1970s, is that an elementary Higgs boson requires fine tuning. As a result, thousands of papers have been written on alternatives to an elementary Higgs.

The current experimental results have mostly wiped out Higgsless theories, because we now know there is a new scalar with a mass of about 125GeV. Currently, it is known that this scalar has the same quantum numbers as the Higgs, and its direct Yukawa couplings to bottom and top quarks have been measured, assuming the Higgs vev is as expected. However, we have measured none of the other Yukawa couplings, or any features of the Higgs potential. For example, it is possible that there is "induced electroweak symmetry breaking",

$$V \supset \mu^2 H^\dagger \tilde{H} + m^2 |H|^2 + V(\tilde{H})$$

where a second Higgs doublet $\tilde{H}$ acquires a vev, creating a linear term in the Higgs potential and leading to the observed Higgs mass and vev. In this case, there could be no Higgs quartic term. In addition, some models with composite Higgs bosons remain viable. Distinguishing between these options would be a task for a post-LHC collider. Of course, if the Higgs continues to appear fundamental, and nothing else shows up, the fine-tuning problems pointed out 50 years ago would become even more severe.

6.4.3 Symmetries of the Standard Model

Now we step back and examine the symmetries of the SM, neglecting neutrino masses.

• All quarks couple to gluons with the same strength, because they all transform in the fundamental of $SU(3)_C$. In addition, all leptons couple to W bosons with equal strength, because all the L^i transform in the fundamental of $SU(2)_L$. This result is known as lepton universality.

• Lepton universality doesn't apply to quarks, because of the CKM matrix, but one can still get nice results upon summing over quarks. For example, for W^+decay at tree level, we have

$$\Gamma = \Gamma\left(W^+ \to e^+ \nu_e\right)\left(3 + 3\sum_{n=1}^{2}\sum_{m=1}^{3}|V_{nm}|^2\right)$$

where the first factor of 3 comes from the three generations of leptons, and the next factor of 3 comes from the three quark colors. Since the CKM matrix unitary, the sum is equal to 2, giving the simple result that the W^+decays to hadrons 2/3 of the time.

• All CP violation is due to the complex phase in the CKM matrix. Thus, any CP violating process must involve all three generations, giving a suppression of $\lambda^6 \sim 10^{-3}$. Measurements of CP violation are therefore sensitive probes of new physics.

• The only particles in the SM that connects fermions with different flavors are the W bosons, through the off-diagonal elements of the CKM matrix.

Next, we consider flavor changing neutral currents (FCNC).

• In QED, matter is coupled to photons through the interaction $A_\mu J^\mu_{\text{EM}}$. Therefore, if we integrate the photon out, we get an effective interaction $J^\mu_{\text{EM}} J_{\mu,\text{EM}}$. A similar structure appears when we integrate out all the other SM bosons, yielding a "charged current" interaction $J^\mu J_\mu$ and a "neutral current" interaction $J^\mu_n J_{\mu,n}$, distinguished by the electric charges of J^μ and J^μ_n.

• At tree level, charged current interactions are mediated by W bosons, while neutral current interactions (if we define the term rather inclusively) are mediated by the Z boson,

gluons, photons, and the Higgs. However, a loop of W bosons could also contribute to the neutral current interaction.

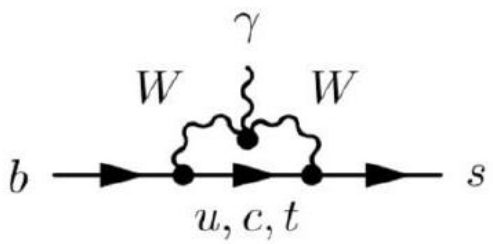
• The Standard Model turns out to have no tree-level FCNC, as we have already seen above. This is obvious for gluons and photons, whose interactions are flavor diagonal. For the Higgs, it occurs because the Yukawa couplings to the Higgs are proportional to the masses, but it wouldn't be true for a more complicated Higgs sector, such as a two Higgs doublet model.

• Tracing back, we might wonder why there was no CKM matrix for Z bosons, which would have led to tree-level FCNC. This occurred because all the up-type quarks (and down-type quarks) coupled to the Z boson identically. Thus, the matrix of couplings was proportional to the identity, and the matrices from changing to mass basis cancelled out, $K_\mu^\dagger K_\mu = K_d^\dagger K_d = I$.

• Now consider a general matter sector. The mass terms can connect fields with the same $SU(3)_C \times U(1)_{\text{EM}}$ irrep, so each type of irrep corresponds to a mass matrix. Meanwhile, fields in the same $SU(3)_C \times SU(2)_L \times U(1)_Y$ irrep couple the same way to the Z. Therefore, the logic above goes through as long as all fields with the same $SU(3)_C \times U(1)_{\text{EM}}$ irrep automatically have the same $SU(3)_C \times SU(2)_L \times U(1)_Y$ irrep.

• This holds in the SM, but before the discovery of the charm quark, the strange quark was proposed to be in an $SU(2)_L$ singlet, which would have led to tree-level FCNC with the down quark. This would have produced a sizable rate for the neutral kaon decay $K^0 \to \mu^+\mu^-$, but it was measured to be very rare, with a branching fraction of about 10^{-9}. That result led to the prediction of the charm quark.

• The GIM mechanism further suppresses FCNC, through a cancellation at loop level. Consider the process $b \to s\gamma$ by a W loop which emits a photon, as shown below.



Concretely, this might be part of a B meson decay process. The amplitude is proportional to

$$\sum_{i \in \{u,c,t\}} V_{ib} V_{is}^* f\left(m_i^2/m_W^2\right)$$

Now consider Taylor expanding the function f. At zeroth order, the result vanishes by unitarity of the CKM matrix. Beyond zeroth order, we can't have a bare factor of $\log\left(m_i^2/m_W^2\right)$, since this would blow up as $m_i \to 0$, which means the leading correction is at least suppressed by m_i^2/m_W^2 (possibly multiplied by a logarithm). This is small for everything but the very massive top quark, which is the reason flavor physics can be used to "measure" the top quark mass. However, the top quark amplitude is suppressed by several powers of the Wolfenstein parameter λ. Thus, either the top or charm quark loops could be dominant, depending on the circumstances.

• To estimate the contribution from the charm quark loop, note that

$$\int dp f\left(p^2\right) = \frac{1}{(4\pi)^2} \int dx x f(x)$$

so in general a loop gives a numerical factor of roughly $1/(4\pi)^2$. Then the amplitude scales as

$$\frac{1}{(4\pi)^2}\frac{m_c^2}{m_W^2}\frac{1}{m_W^2}$$

compared with a generic $1/\Lambda^2$ for new physics. Thus, in general, loop suppression of a process in the SM allows us to probe new physics at scales up to $\Lambda \sim 10 m_W \sim$ TeV, while the GIM mechanism gives an additional factor of m_W/m_c, reaching an incredible ~ 100TeV.

• However, new physics can still exist below this scale. For instance, a new particle's couplings could have a trivial flavor structure, coupling identically to each up-type and down-type quark, in which case FCNC is not modified at tree level. (One example is the minimal dark photon.)

• Alternatively, the new couplings could be proportional to (powers of) the existing Yukawa couplings. This is the paradigm of "minimal flavor violation", which makes the SM Yukawa couplings the only source of flavor violation. It also suppresses new FCNC, and is commonly used in SUSY model building. A final possibility is "flavor alignment", where the new couplings and the Yukawa couplings can be simultaneously diagonalized. So flavor constraints don't totally rule out new physics, but rather place strong constraints on how it can look.

Note. The general rule of thumb for loops given above is useful in many contexts. For example, corrections due to a gluon loop are of order $g_3^2/(4\pi)^2 \sim 10^{-2}$, corrections due to a photon loop are of order $e^2/(4\pi)^2 \sim 10^{-3}$, and weak loops are intermediate. On the other hand, depending on the process, loop corrections may also come with logarithmic factors, which could be as large as $\log\left(m_W^2/\Lambda_{\rm QCD}^2\right) \sim 10$ for gluon loops and $\log\left(m_W^2/m_e^2\right) \sim 20$ for photon loops.

Processes involving charged particles can also proceed with an extra photon in the final state. The rule of thumb is that the rate comes with a factor of $e^2(2\pi)/(2\pi)^3 = \alpha/\pi \sim 2\times 10^{-3}$, where the numerator comes from the angular integration and the denominator comes from the momentum integration measure. (The rest of the phase space integral is not substantially affected, as long as the photon is soft.) As a concrete example,

$$\frac{\mathrm{Br}\left(\mu^- \to e^- \bar{\nu}\nu\gamma\right)}{\mathrm{Br}\left(\mu^- \to e^- \bar{\nu}\nu\right)} = (1.4 \pm 0.4)\%$$

where the enhancement is due to a large logarithm $\log\left(m_\mu^2/m_e^2\right)$.

The SM also has a number of accidental global symmetries.

• An accidental symmetry is a symmetry that arises from the field content, renormalizability, and other symmetries, but is not put in by hand. For example, in QED, the most general renormalizable Lagrangian is

$$\mathcal{L} = -\frac{1}{4}F_{\mu\nu}F^{\mu\nu} + iaF_{\mu\nu}\widetilde{F}^{\mu\nu} + i\bar{\psi}\not{D}\psi + \bar{\psi}\left(m + i\gamma^5 m_5\right)\psi$$

However, the second term is a total derivative and the final term may be removed by a chiral rotation $\psi \to e^{i\alpha\gamma^5}\psi$. Then we have accidental C, P, and T symmetry.

• The SM also contains all possible renormalizable terms, and has several accidental symmetries: the baryon number $U(1)_B$ and the individual lepton numbers $U(1)_{L_e}, U(1)_{L_\mu}$, and $U(1)_{L_\tau}$. The dimension 5 neutrino mass violates both individual and total lepton number, while dimension 6 operators can violate baryon number.

• Note that either $U(1)_B$ or $U(1)_L$ alone is sufficient to prevent the proton from decaying. Also, if the proton decays, it must decay into an odd number of fermions by Lorentz invariance, which requires the parity of the fermion number to be conserved. The only fermions lighter than the proton are leptons, so lepton number must be violated in the decay.

• Proton decay has been tested stringently, placing a high bound on Λ. For a rough estimate, we have $\tau > 10^{33}$ years while the decay rate should be m_p^5/Λ^4 by dimensional analysis, where

the numerator accounts for the phase space; then $\Lambda > 10^{15}$GeV, a result similar to the bound from neutrino masses. Thus new physics is either very far away, or respects baryon number.

• Violations of the individual $U(1)_{L_i}$ have also been searched for, most stringently through the unobserved decay $\mu \to e\gamma$, which will be probed further by the upcoming MEG II experiment. There is also the upcoming Mu2e experiment, which will search for $\mu \to e$ conversion in nuclei.

• It turns out that anomalies violate B and L conservation, as discussed further in the notes on Quantum Field Theory, but $L_i - L_j$ remains exactly conserved, as does $B - L$ if there is a sterile neutrino. Neutrino masses break $L_i - L_j$, while Majorana neutrino masses also break L.

Note. In the Standard Model, the result $\rho_0 = 1$ follows from an approximate accidental symmetry. Since the Higgs is a complex doublet, thereby containing 4 real fields, its most general possible global symmetry is $O(4)$. This symmetry is preserved by the Higgs potential, as it only depends on the combination $\phi^\dagger\phi$. When the Higgs field develops a vev, it is broken to $O(3)$, and since $\mathfrak{o}(3) \cong \mathfrak{su}(2)$, this residual symmetry is called custodial $SU(2)$.

Writing it in terms of real fields is clunky, but we can work with complex fields by defining the Higgs matrix $\Phi = (\phi, \epsilon\phi^*)$. The Higgs potential is a function of $\mathrm{tr}\left(\Phi^\dagger\Phi\right)$, which preserves the $SU(2)_L \times SU(2)_R$ symmetry

$$\Phi \to L\Phi R^\dagger$$

where $L, R \in SU(2)$. The $SU(2)_L$ factor acts just like electroweak $SU(2)_L$, while $U(1)_Y \subseteq SU(2)_R$. When Φ acquires a vev, which we can take to be proportional to the identity, the diagonal subgroup corresponding to $L = R$ is preserved, and this is the custodial $SU(2)$.

The coupling to gauge fields can be written as

$$\mathcal{L} \supset \mathrm{tr}\,(D_\mu\Phi)^\dagger D^\mu\Phi, \quad D_\mu\Phi = \partial_\mu\Phi + igA_\mu^a\tau^a\Phi + \frac{i}{2}g'B_\mu\Phi\sigma_3$$

where the σ_3 is on the right, because ϕ and $\epsilon\phi^*$ have opposite hypercharge. The coupling to the $SU(2)_L$ gauge bosons is invariant under $SU(2)_L$ by construction, and under $SU(2)_R$ by the cyclic property of the trace. Therefore, if we set $g' = 0$, the custodial $SU(2)$ survives, and implies the three massive gauge bosons must be degenerate. For $g' \neq 0$, the same logic implies that a 3×3 block of the mass matrix must be proportional to the identity, which implies $\rho_0 = 1$.

This logic would not have applied if, e.g. the Higgs field had been an $SU(2)_L$ triplet, so measurements of ρ provide information about the mechanism of electroweak symmetry breaking. On the other hand, it is not necessary to have one $SU(2)_L$ doublet. There can be multiple doublets, or more radically, if electroweak symmetry had been broken solely by the QCD condensate, there would be the custodial symmetry $SU(2)_V$, which implies the same result.

The coupling to $U(1)_Y$ breaks custodial $SU(2)$, which leads to the radiative correction

$$\rho - 1 \supset -\frac{11G_F m_Z^2 \sin^2\theta_W}{24\sqrt{2}\pi^2}\log\frac{m_h^2}{m_Z^2}$$

in the $\overline{\mathrm{MS}}$ scheme. In addition, the Yukawa couplings generally break custodial symmetry. Within each generation of quarks, we have custodial symmetry if the up-type and down-type quarks have the same mass, i.e. if there is isospin symmetry. Therefore, the high mass of the top quark produces a significant loop correction to ρ,

$$\rho - 1 \supset \frac{3G_F}{8\sqrt{2}\pi^2}\left(m_t^2 + m_b^2 - 2\frac{m_t^2 m_b^2}{m_t^2 - m_b^2}\log\frac{m_t^2}{m_b^2}\right)$$

Measurements of ρ therefore allowed the huge top quark mass to be predicted before it was discovered. More generally, new physics corrections to the WW, ZZ, and $\gamma\gamma$, and γZ two-point functions (called "oblique" corrections, in contrast to direct modifications of the fermion-boson

couplings) are commonly parametrized by the so-called Peskin-Takeuchi parameters S, T, and U.

Note. Suppose that $B - L$ was gauged, and that the corresponding gauge boson was massless. The result is a long-range force which makes baryons repel, leptons repel, and baryons and leptons attract each other. It turns out that the constraints on the gauge coupling g are extremely strong. First, the energy levels of the deuteron would be shifted relative to hydrogen's by order g^2/e^2, placing a constraint $g^2 \lesssim 10^{-7}$ from spectroscopy. Next, for $g^2 \ll e^2$ there is a strong constraint from stellar physics, as otherwise $B - L$ gauge boson emission would dramatically accelerate stellar evolution since such particles could escape more readily than photons. This rules out couplings stronger than $g^2 \lesssim 10^{-20}$.

Even strong constraints come from terrestrial physics. Since the Earth is charge neutral, its $B - L$ charge is roughly its neutron number. This leads to a repulsion which would have destroyed the Earth unless the $B - L$ force is weaker than gravitational, $g^2 \lesssim G_N m_n^2 \sim (m_n/M_{\text{pl}})^2 \sim 10^{-36}$. (We can try to avoid this constraint by supposing the Earth has trapped a compensating number of neutrinos, but it doesn't work; if the residual charge is strong enough to keep neutrinos trapped, it is also strong enough to destroy the Earth.) But even if the Earth is stable, the presence of a $B - L$ force would cause different materials to feel different effective values of $\mathbf{g}$. Precision tests of the equivalence principle therefore bound $g^2 \lesssim 10^{-48}$. On the other hand, the constraints are significantly weaker if the $B - L$ gauge boson has a mass, and hence a finite range.

Note. In the limit of massless neutrinos, the SM has another long-range force: leptons can interact with each other through a loop of neutrinos. In fact, Feynman briefly speculated that this could explain the gravitational force! However, there is a major immediate obstacle. When a massless gauge boson is exchanged with momentum k, the matrix element is $\mathcal{M} \sim 1/k^2$, which implies $V(r) \sim 1/r$ in the Born approximation. For a neutrino loop, the matrix element is proportional to G_F^2, which implies $\mathcal{M} \sim k^2 G_F^2$ by dimensional analysis; Fourier transforming this gives $V(r) \sim 1/r^5$, which is dramatically different but still technically long-ranged. A more precise calculation gives

$$V(r) = \frac{G_F^2}{4\pi^3 r^5}$$

though at higher orders there is also nontrivial velocity dependence. Unfortunately, the force is so weak that it has never been observed.

Note. All dimension 6 operators, which number over 2,000, are considered in "Standard Model EFT" (SMEFT) analyses. These terms have various signatures, such as CP violation, baryon number violation, and changing the overall rates and high momentum tails of various processes. Choosing to express experimental results as constraints on SMEFT coefficients has some advantages: it is quite general and unambiguous, and can easily be combined between different searches. But it's hard to interpret the results, in terms of specific models of UV physics.

The SMEFT takes the Higgs doublet as a field, while the less popular HEFT uses the physical Higgs, i.e. the SMEFT expands about the electroweak symmetry preserving vacuum, while the HEFT expands about the physical vacuum. The SMEFT is more "straightforward" to work with, but the HEFT is more general, e.g. it can accommodate other Higgs sectors.

Finally, we take a look at some of the unsolved problems of the SM.

• The first problem is that the SM does not account for neutrino masses and mixings, which we've covered above. On astronomical and cosmological scales, the SM does not account for dark matter, which is neutral, colorless, cold, non-baryonic, and massive. It also does not contain enough CP violation to account for the matter/anti-matter asymmetry in our universe.

• The SM has three naturalness problems: the Higgs hierarchy problem, the cosmological

constant problem, and the strong CP problem. The first two are more urgent, in the sense that they are also fine-tuning problems; on the other hand, the strong CP problem can't be solved by anthropics, making it arguably more robust.

• There are also a number of problems which might or might not have an explanation.

• Why is the amount of matter, radiation, and vacuum energy in the universe roughly equal today? These quantities varied by many orders of magnitude in the universe's history.

• Why are there three fermion families, and why do they display a hierarchical structure in their masses and mixings? There are many candidate theories, but none are compelling enough to earn widespread acceptance.

• Why are the three gauge couplings all relatively close in size?

• Why are there four spacetime dimensions, and one time dimension?

• Why is electric charge quantized? This is not explained by $U(1)_Y$, because we must allow for projective representations, and the universal cover of $U(1)$ is $\mathbb{R}$. It could be explained by a grand unified theory where $U(1)_Y$ is embedded in a larger group.

6.4.4 Electroweak Decays

Next, we look at some concrete electroweak decay processes. First, we set up the effective field theory for the weak interaction.

• We recall the weak part of the Lagrangian has the form

$$\mathcal{L}_W = -\frac{g}{2\sqrt{2}}\left(J^\mu W_\mu^+ + J^{\mu\dagger} W_\mu^-\right) - \frac{g}{2\cos\theta_W} J_n^\mu Z_\mu$$

Therefore, expanding the S matrix, we have

$$\begin{aligned} S &= T\exp\left(i\int dx \mathcal{L}_W(x)\right) \\ &= 1 - \frac{g^2}{8}\int dx dx' J^{\mu\dagger}(x) D_{\mu\nu}^W(x-x') J^\nu(x') + \frac{1}{\cos^2\theta_W} J_n^{\mu\dagger}(x) D_{\mu\nu}^Z(x-x') J_n^\nu(x') + O\left(g^4\right). \end{aligned}$$

where $D_{\mu\nu}^W$ and $D_{\mu\nu}^Z$ are massive vector propagators.

• For the Z boson, the Euler-Lagrange equation is

$$\partial^2 Z_\mu - \partial_\mu \partial_\nu Z^\nu + m_Z^2 Z_\mu = -j_\mu$$

and taking the divergence of each side gives $m_Z^2 \partial_\mu Z^\mu = -\partial_\mu j^\mu$. Substituting this back into the equation of motion gives

$$\left(\partial^2 + m_Z^2\right) Z_\mu = -\left(\eta_{\mu\nu} - \frac{\partial_\mu \partial_\nu}{m_Z^2}\right) j^\nu$$

• The Green's function/propagator satisfies

$$Z_\mu(x) = i\int dy D_{\mu\nu}^Z(x-y) j^\nu(y)$$

and taking a Fourier transform yields the familiar massive vector boson propagator,

$$D_{\mu\nu}^Z(x-y) = \int dp e^{-ip(x-y)} \widetilde{D}_{\mu\nu}^Z(p), \quad \widetilde{D}_{\mu\nu}^Z(p) = \frac{i}{p^2 - m_z^2 + i\epsilon}\left(-\eta_{\mu\nu} + \frac{p_\mu p_\nu}{m_Z^2}\right)$$

The Green's function for the W boson is similar. At low energies, we can approximate

$$\widetilde{D}^{W/Z}_{\mu\nu}(p) \approx \frac{i\eta_{\mu\nu}}{m^2_{W/Z}}, \quad D^{W/Z}_{\mu\nu}(x-y) \approx \frac{i\eta_{\mu\nu}}{m^2_{W/Z}}\delta(x-y)$$

so that the weak interactions can be described by a four-fermion contact interactions.

• Therefore we get the same S-matrix using the effective weak Lagrangian

$$\mathcal{L}^{\text{eff}}_W(x) = -\frac{G_F}{2}\left(J^{\mu\dagger}(x)J_\mu(x) + \rho J^{\mu\dagger}_n(x)J_{n\mu}(x)\right), \quad \frac{G_F}{\sqrt{2}} = \frac{g^2}{8m^2_W}.$$

This is indeed an effective theory since the four-fermion operator has dimension 6. Higher-order diagrams would give further contributions, but they are suppressed by more powers of large masses; this is the reason we don't have to include the top quark, as it only appears internally in diagrams where there is already a W boson.

• Why do we include the effects of the W and Z boson, but not that of the Higgs boson? Integrating out the Higgs yields interactions of the form $\bar{f}f\bar{f}'f'$, but they are further suppressed by small Yukawa couplings $m_f m'_f/v^2$. In addition, these terms don't break symmetries the same way the W and Z-mediated interactions do, so when they do contribute to processes, they tend to be swamped by the larger strong or electromagnetic interactions.

Example. The muon's "Michel" decay, $\mu \to e\bar{\nu}_e\nu_\mu$. It occurs via the leptonic charged weak current,

$$J^\rho = \bar{\nu}_e\gamma^\rho\left(1-\gamma^5\right)e + \bar{\nu}_\mu\gamma^\rho\left(1-\gamma^5\right)\mu + \bar{\nu}_\tau\gamma^\rho\left(1-\gamma^5\right)\tau$$

Since the muon mass $m_\mu = 105\text{MeV}$ is much less than $m_W = 80\text{GeV}$, we can use the effective theory above, where

$$S - 1 = \int dx \mathcal{L}^{\text{eff}}_W(x)$$

Here, the position integration enforces momentum conservation. We will compute the amplitudes $\mathcal{M}$ which have $i\phi\left(\sum_i p_i\right)$ factored out of the matrix element. Factoring out the delta function is equivalent to dropping the position integration, so

$$\begin{aligned}
\mathcal{M} &= \left\langle e^-(k)\bar{\nu}_e(q)\nu_\mu(q')\left|\mathcal{L}^{\text{eff}}_W(0)\right|\mu^-(p)\right\rangle \\
&= -\frac{G_F}{\sqrt{2}}\left\langle e^-(k)\bar{\nu}_e(q)\left|\bar{e}\gamma^\rho\left(1-\gamma^5\right)\nu_e\right|0\right\rangle\left\langle\nu_\mu(q')\left|\bar{\nu}_\mu\gamma_\rho\left(1-\gamma^5\right)\mu\right|\mu^-(p)\right\rangle \\
&= -\frac{G_F}{\sqrt{2}}\bar{u}_e(k)\gamma^\rho\left(1-\gamma^5\right)v_{\nu_e}(q)\bar{u}_{\nu_\mu}(q')\gamma_\rho\left(1-\gamma^5\right)u_\mu(p)
\end{aligned}$$

where we picked up on-shell spinors, with no sign flips, and all phases canceled. We then sum over final spins and average over the initial spin, using $\gamma^{5\dagger} = \gamma^5$, for

$$\frac{1}{2}\sum_{\text{spins}}|\mathcal{M}|^2 = \frac{G_F^2}{4}S_1^{\rho\sigma}S_{2\rho\sigma}$$

where since the neutrinos are massless, the spinor traces are

$$S_1^{\rho\sigma} = \text{tr}\left[\left(\not{k}+m_e\right)\gamma^\rho\left(1-\gamma^5\right)\not{q}\gamma^\sigma\left(1-\gamma^5\right)\right], \quad S_{2\rho\sigma} = \text{tr}\left[\not{d}'\gamma_\rho\left(1-\gamma^5\right)\left(\not{p}+m_\mu\right)\gamma_\sigma\left(1-\gamma^5\right)\right]$$

We simplify the spinor traces using the usual identities, noting that $\left(1-\gamma^5\right)^2 = 2\left(1-\gamma^5\right)$, for

$$S_1^{\rho\sigma} = 8\left(k^\rho q^\sigma + k^\sigma q^\rho - (k\cdot q)\eta^{\rho\sigma} - i\epsilon^{\rho\sigma\mu\nu}k_\mu q_\nu\right), \quad S_{2\rho\sigma} = 8\left(p_\rho q'_\sigma + p_\sigma q'_\rho - (p\cdot q')\,\eta_{\rho\sigma} - i\epsilon_{\rho\sigma\mu\nu}q'^\mu p^\nu\right)$$

and contracting the Levi-Civitas with the identity

$$\epsilon^{\mu\nu\rho\sigma}\epsilon_{\mu\nu\lambda\tau} = -2\left(\delta^\rho_\lambda\delta^\sigma_\tau - \delta^\rho_\tau\delta^\sigma_\lambda\right)$$

where the minus sign comes from the determinant of the metric, we find

$$\frac{1}{2}\sum_{\text{spins}}|\mathcal{M}|^2 = 64G_F^2(p\cdot q)\,(k\cdot q')$$

Finally, we must perform the integral over final state momenta. We have

$$\Gamma = \frac{1}{2m_\mu}\int\frac{d\mathbf{k}d\mathbf{q}d\mathbf{q}'}{8k^0q^0q'^0}\phi\left(p-k-q-q'\right)\frac{1}{2}\sum_{\text{spins}}|\mathcal{M}|^2 = \frac{G_F^2}{8\pi^5 m_\mu}\int\frac{d\mathbf{k}d\mathbf{q}d\mathbf{q}'}{k^0q^0q'^0}\delta\left(p-k-q-q'\right)(p\cdot q)\,(k\cdot q')$$

To perform this tricky three-body integral it's best to separate out the massless neutrinos,

$$I_{\mu\nu}(Q) = \int\frac{d\mathbf{q}d\mathbf{q}'}{|\mathbf{q}|\,|\mathbf{q}'|}\delta\left(Q-q-q'\right)q_\mu q'_\nu, \quad Q = p-k$$

Then by Lorentz invariance we must have $I_{\mu\nu}(Q) = aQ_\mu Q_\nu + b\eta_{\mu\nu}Q^2$. Contracting with $\eta^{\mu\nu}$ and $Q^\mu Q^\nu$ and using the delta function to simplify, we find

$$a+4b = \frac{I}{2}, \quad a+b = \frac{I}{4}, \quad I = \int\frac{d\mathbf{q}d\mathbf{q}'}{|\mathbf{q}|\,|\mathbf{q}'|}\delta\left(Q-q-q'\right)$$

The integral I is Lorentz invariant, so we work in the center-of-mass frame $Q = (\sigma, \mathbf{0})$,

$$I = \int\frac{d\mathbf{q}}{|\mathbf{q}|^2}\delta(\sigma - 2|\mathbf{q}|) = 4\pi\int_0^\infty d|\mathbf{q}|\delta(\sigma-2|\mathbf{q}|) = 2\pi$$

from which we conclude $a = \pi/3$ and $b = \pi/6$. Then we find

$$\Gamma = \frac{G_F^2}{3m_\mu(2\pi)^4}\int\frac{d\mathbf{k}}{k^0}\left(2p\cdot(p-k)k\cdot(p-k) + (p\cdot k)(p-k)^2\right)$$

We work in the frame of the muon and approximate the electron as massless with energy E,

$$p = (m_\mu, 0, 0, 0), \quad k = (E, E, 0, 0)$$

which yields the final expression

$$\Gamma = \frac{2G_F^2 m_\mu}{3(2\pi)^3}\int_0^{m_\mu/2} dE E^2\left(3m_\mu - 4E\right) = \frac{G_F^2 m_\mu^5}{192\pi^3}$$

where the upper bound is attained when the neutrinos exit in the same direction. The size of this result is substantially smaller than one would get by counting 2π factors, mostly because the final phase space integral happens to give a numeric factor of $1/16$. However, a similar suppression often occurs whenever there is a three-body decay to light particles. Also

note that the energy distribution for the electron is monotonic: it is most likely to emerge with the maximum possible energy $m_\mu/2$, while the probability for lower energy is suppressed as E^2.

Note. Helicity suppression. Consider the case where the electron and muon neutrino exit in the z-direction and the electron antineutrino exits in the $-z$-direction. Then

$$|\mathcal{M}|^2 \propto k \cdot q' = \sqrt{m_e^2 + k_z^2} q_z' - k_z q_z'$$

which vanishes in the limit $m_e \to 0$. This is because in this limit, chirality coincides with helicity. Since the electron and muon neutrino are left-handed and the electron antineutrino is right-handed, the z components of the spin would sum to $-3/2$, so the decay is forbidden.

There are two ways to think about the effect of an electron mass. We can think of the electron as a Dirac spinor, in which case a left-handed electron does not have definite helicity, so the process is allowed. Alternatively, we can think of the electron as made of two massless Weyl spinors, where chirality and helicity match, and treat the mass as an interaction term that flips the chirality.

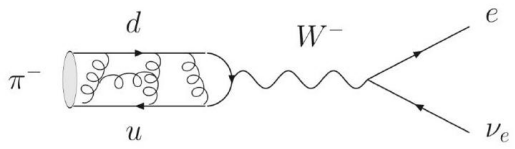
Note. The above decay channel is the only one allowed for the muon, so it provides a precise way to measure the Fermi constant,

$$\tau = \frac{1}{\Gamma} = 2.1970 \times 10^{-6} \text{ s}, \quad G_F = 1.164 \times 10^{-5} \text{GeV}^2$$

One-loop corrections only affect G_F at the per-million level. A similar calculation can be performed for the τ, which has the two leptonic decay channels $\tau \to e\bar{\nu}_e\nu_\tau$ and $\tau \to \mu\bar{\nu}_\mu\nu_\tau$, as well as decays into hadrons. We can estimate the decay rate in each leptonic channel by simply replacing m_μ by m_τ. Thus, one can measure G_F from these decays, and the results match that found for muons due to lepton universality.

Note. In the 1950s, it was thought that there was only one neutrino, a conclusion supported by lepton universality. However, this would imply the decay $\mu \to e\gamma$ was possible through a loop of a W boson and neutrino, with a branching ratio of order α. The nonobservation of this decay led to the conclusion that there was a separate neutrino for each generation.

Example. Pion decay, $\pi^- \to e\bar{\nu}_e$, has the Feynman diagram shown below.



The d and $\bar{u}$ quarks do not propagate freely, but rather are bound together by nonperturbative dynamics; thus we'll have to parametrize our ignorance using form factors. The decay is again solely through the charged weak current, where the hadronic weak current is

$$J^\mu = V^\mu - A^\mu, \quad V^\mu = \bar{u}\gamma^\mu \left(V_{ud}d + V_{us}s + V_{ub}b\right) + \ldots, \quad A^\mu = \bar{u}\gamma^\mu\gamma^5 \left(V_{ud}d + V_{us}s + V_{ub}b\right) + \ldots$$

where we've defined vector and axial components with definite parity, and the overall "vector minus axial" form is because the charged current only couples to left-handed quark fields. Then

$$\mathcal{M} = \left\langle e^-(k)\bar{\nu}_e(q) \left| \mathcal{L}_W^{\text{eff}}(0) \right| \pi^-(p) \right\rangle = -\frac{G_F}{\sqrt{2}} \bar{u}_e(k)\gamma_\mu \left(1 - \gamma^5\right) v_{\nu_e}(q) \left\langle 0 \left| J_{\text{had}}^\mu \right| \pi^-(p) \right\rangle$$

The QCD vacuum is parity even and the pion is parity odd. Then $\langle 0 | V_{\text{had}}^\mu | \pi^-(p) \rangle$ must be an axial vector, but there are no axial vectors it could be equal to, so it must simply be zero. On the other hand, $\langle 0 | A_{\text{had}}^\mu | \pi^-(p) \rangle$ must be a vector, so it has to be proportional to p^μ. We

cannot compute the matrix element perturbatively, so we absorb it into a single dimensionful parameter called the pion decay constant F_π, so that

$$\left\langle 0 \left| \bar{u}\gamma^\mu\gamma^5 d \right| \pi^-(p) \right\rangle = i\sqrt{2}F_\pi p^\mu$$

By momentum conservation we have $p = k + q$ and the on-shell spinor identities

$$\bar{u}_e(k)\not{k} = \bar{u}_e(k)m_e, \quad \not{q}v_{\nu_e}(q) = 0$$

so the amplitude simplifies to

$$\mathcal{M} = iG_F F_\pi m_e V_{ud} \bar{u}_e(k)\left(1-\gamma^5\right) v_{\nu_e}(q)$$

We expect helicity suppression, since the pion has spin zero and, in the pion's rest frame, the two particles come out back-to-back, giving a total of spin one in the massless limit. This is reflected in the fact that $\mathcal{M} \propto m_e$.

Next, summing over the final spins we have

$$\sum_{\text{spins}} |\mathcal{M}|^2 = 2\left|G_F F_\pi m_e V_{ud}\right|^2 \operatorname{tr}\left((\not{k}+m_e)\left(1-\gamma^5\right)\right) = 8\left|G_F F_\pi m_e V_{ud}\right|^2 (k\cdot q)$$

Abbreviating the squared quantity as C, the decay rate in the pion rest frame is

$$\Gamma = \frac{1}{m_\pi}\int \frac{d\mathbf{k}d\mathbf{q}}{4k^0q^0}\phi(p-k-q)\sum_{\text{spins}}|\mathcal{M}|^2 = \frac{C}{4\pi^2 m_\pi}\int \frac{d\mathbf{k}}{E|\mathbf{k}|}\delta\left(m_\pi - E - |\mathbf{k}|\right)(E+|\mathbf{k}|)|\mathbf{k}|$$

where we defined $E = k^0$ and integrated over $\mathbf{q}$ so that $q = (|\mathbf{k}|, -\mathbf{k})$. The angular integral is 4π, and integrating the delta function yields

$$\Gamma = \frac{C}{4\pi} m_\pi \left(1 - \frac{m_e^2}{m_\pi^2}\right)^2$$

We still don't know what F_π is, but we can compute branching ratios, such as

$$\frac{\Gamma\left(\pi \to e\bar{\nu}_e\right)}{\Gamma\left(\pi \to \mu\bar{\nu}_\mu\right)} = \frac{m_e^2}{m_\mu^2}\left(\frac{m_\pi^2 - m_e^2}{m_\pi^2 - m_\mu^2}\right)^2 = 1.28\times 10^{-4}$$

The experimental result is 1.230×10^{-4}, with the difference accounted for by loop diagrams.

Note. Above, we saw another example of helicity suppression, which is a rather common effect in the ultrarelativistic limit. Yet another example occurs in the scattering of spin-polarized electrons and positrons. If we neglect their masses, scattering via a photon is forbidden if the particles have the same helicities (and hence opposite angular momenta), because the resulting product of Poincare irreps has helicity zero, while photons have helicity \pm 1. This is an example of how the chiral components decouple in massless QED.

For this argument to work, it's essential that we think in terms of massless Poincare irreps with helicity, rather than massive Poincare irreps with spin, since the combination of two antiparallel spin 1/2 particles does have a spin 1 component (with $L_z = 0$). For this reason, when we account for a nonzero mass, the scattering can happen, but it's helicity suppressed.

An objection one could make for the muon and pion decays is: why can't the decay products come out with orbital angular momentum? Up to a basis change, orbital angular momentum just corresponds to a particular pattern of superposition of directions of the outgoing particles, with a state that looks like $\int d\Omega f(\hat{\mathbf{n}})|k\hat{\mathbf{n}}, -k\hat{\mathbf{n}}\rangle$. (Instead of an integral over angles, one could also express this state as a sum over l and m involving spherical harmonics, giving a partial wave

expansion. This is more useful for low-energy scattering, where the s-wave typically dominates, and in this case orbital angular momentum expresses itself as a non- s-wave component. But the point is that one doesn't need to do, and indeed can't do, both expansions at once; both bases here are complete.)

Now consider a symmetry argument involving only rotations about the z-axis. Such rotations don't rotate the $|k\hat{\mathbf{z}}, -k\hat{\mathbf{z}}\rangle$ with others, so the argument can be used to show that $f(\hat{\mathbf{z}}) = 0$ without caring about what the other values of $f(\hat{\mathbf{n}})$ are. And then, since $\hat{\mathbf{z}}$ was arbitrary, this shows that $f(\hat{\mathbf{n}}) = 0$ in general. This is the proper way to phrase the arguments we made above. (A slick, but somewhat mysterious way of summarizing this is that "the orbital angular momentum is perpendicular to the linear momentum, so it doesn't affect helicity".)

6.4.5 CP Violation

Finally, we investigate neutral kaon mixing, which demonstrates CP violation.

• Kaons are pseudoscalar mesons containing either a strange quark or a strange antiquark. The neutral kaons K^0 and $\bar{K}^0$ have quark content $\bar{s}d$ and $\bar{d}s$ respectively.

• Under $\widehat{C}$, the neutral kaons are mapped to each other. As discussed earlier, $\widehat{C}$ and $\widehat{P}$ have some freedom in phase redefinition, and we may choose these phases so that

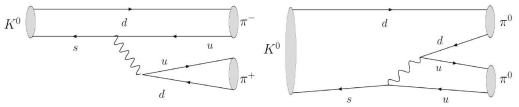
$$\widehat{C}\widehat{P}\left|K^0\right\rangle = -\left|\bar{K}^0\right\rangle, \quad \widehat{C}\widehat{P}\left|\bar{K}^0\right\rangle = -\left|K^0\right\rangle$$

We thus have the CP eigenstates

$$\left|K^0_{\pm}\right\rangle = \frac{\left|K^0\right\rangle \mp \left|\bar{K}^0\right\rangle}{\sqrt{2}}$$

so that K^0_+ is CP even and K^0_- is CP odd.

• We consider the decays of neutral kaons to two pions, either $\pi^+\pi^-$or $\pi^0\pi^0$. Since this is a flavor-changing interaction, it is mediated by a weak current, as shown below.



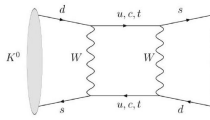
The pions are all pseudoscalars, and their total angular momentum must be zero since the kaon has spin zero, so parity simply exchanges the pions without any signs, and charge conjugation simply flips the charges. Thus both possible final states $|\pi^+\pi^-\rangle$and $|\pi^0\pi^0\rangle$ are CP even, and only $\left|K^0_+\right\rangle$ can decay to two pions if CP is conserved. The $\left|K^0_-\right\rangle$ should have a longer lifetime, being only able to decay to three pions or other final states.

• Experimentally, it is indeed observed that there are two neutral kaons, K^0_S and K^0_L, with a short and long lifetime respectively. We can create a pure sample of K^0_L by waiting for a time much longer than the lifetime of the K^0_S. However, we occasionally observe the K^0_L decay into two pions. Specifically, we have

$$\frac{\langle\pi^+\pi^-\left|H_W\right|K^0_L\rangle}{\langle\pi^+\pi^-\left|H_W\right|K^0_S\rangle} \approx \frac{\langle\pi^0\pi^0\left|H_W\right|K^0_L\rangle}{\langle\pi^0\pi^0\left|H_W\right|K^0_S\rangle} \approx 2.2\times10^{-3} \neq 0$$

indicating that CP is violated.

• To understand this physically, we consider how the K^0 and $\bar{K}^0$ mix. Since the strangeness changes by 2, the mixing must involve two W bosons and hence involves a loop. The most important contributions are from the six box diagrams shown below.



If CP symmetry holds, the amplitude for K^0 to transition to $\bar{K}^0$ is the same as the amplitude to go the other way, and the eigenstates $K^0_{S/L}$ coincide with the CP eigenstates.

• On the other hand, if we have a CP violating phase in the CKM matrix, the amplitude for $K^0 \to \bar{K}^0$ is not the same as that for $\bar{K}^0 \to K^0$. Thus the 'mass basis' is not the same as the 'CP basis', so the K^0_L can decay to two pions. Another way of phrasing this is that CP violating effects produce oscillations between the CP states $\left|K^0_\pm\right\rangle$.

Next, we investigate the oscillation quantitatively with a simple phenomenological model.

• We write the mass eigenstates as combinations of the CP eigenstates,

$$\left|K^0_S\right\rangle = \frac{\left|K^0_+\right\rangle + \epsilon_1 \left|K^0_-\right\rangle}{\sqrt{1+|\epsilon_1|^2}}, \quad \left|K^0_L\right\rangle = \frac{\left|K^0_-\right\rangle + \epsilon_2 \left|K^0_+\right\rangle}{\sqrt{1+|\epsilon_2|^2}}$$

Since the kaons decay, the mass eigenstates have complex energies. Here, we're making the 'Wigner-Weisskopf' assumption, i.e. we aren't keeping track of the 'environment' state at all, so we guarantee an exponential decay.

• The Hamiltonian is the weak Hamiltonian at next-to-leading order in perturbation theory,

$$H = H_W - \sum_n \frac{H_W|n\rangle\langle n|H_W}{E_n - m_0 - i\epsilon}$$

and we write its matrix elements as

$$\begin{pmatrix} \langle K^0|H|K^0\rangle & \langle K^0|H|\bar{K}^0\rangle \\ \langle \bar{K}^0|H|K^0\rangle & \langle \bar{K}^0|H|\bar{K}^0\rangle \end{pmatrix} = \begin{pmatrix} R_{11} & R_{12} \\ R_{21} & R_{22} \end{pmatrix}$$

• Now, we write the CPT operator as $\widehat{\Theta}$. We may choose the phases so that

$$\widehat{T}\left|K^0\right\rangle = \left|K^0\right\rangle, \quad \widehat{T}\left|\bar{K}^0\right\rangle = \left|\bar{K}^0\right\rangle$$

which implies that

$$\widehat{\Theta}\left|K^0\right\rangle = -\left|\bar{K}^0\right\rangle, \quad \widehat{\Theta}\left|\bar{K}^0\right\rangle = -\left|K^0\right\rangle.$$

Next, we note that under a CPT transformation,

$$\widehat{\Theta} H \widehat{\Theta}^{-1} = H^\dagger$$

• The only nontrivial constraint this yields is

$$R_{11} = \left\langle K^0 \left| \left(\widehat{\Theta}^{-1}\widehat{\Theta}\right)\right| H \left(\widehat{\Theta}^{-1}\widehat{\Theta}\right)|K^0\right\rangle = \left\langle \bar{K}^0 \left|H^\dagger\right| \bar{K}^0\right\rangle^* = R_{22}$$

where we picked up a complex conjugation by flipping the direction of action of $\widehat{\Theta}$.

• If we further had T invariance, which would imply CP invariance, then $\widehat{T}H\widehat{T}^{-1} = H^\dagger$, so

$$R_{12} = \left\langle K^0 \left|\widehat{T}^{-1}\widehat{T}\right| H\widehat{T}^{-1}\widehat{T}|\bar{K}^0\right\rangle = \left\langle \bar{K}^0|H|K^0\right\rangle = R_{21}$$

so a difference of R_{12} and R_{21} implies CP violation.

• Finally, assuming for simplicity that $\epsilon_1 = \epsilon_2 = \epsilon$, which turns out to be correct, one can straightforwardly calculate

$$\epsilon = \frac{\sqrt{R_{12}} - \sqrt{R_{21}}}{\sqrt{R_{12}} + \sqrt{R_{21}}}$$

The R_{ij} can be computed in perturbation theory, and then ϵ can be related to the branching ratios for $K^0_{S/L}$ decay, giving a quantitative calculation of a CP violating effect.

6.5 Neutrinos

6.5.1 Historical Review

Next, we turn to neutrino masses, the leading correction of the SM. We begin with a history of neutrino physics.

• 1914: Chadwick demonstrates the energy of the outgoing electron in β decay has a continuous spectrum, which seems to contradict energy-momentum conservation. (This took almost two decades from the discovery of β radiation, since such measurements were difficult.)

• A gap in progress occurs because of World War I.

• 1920s: there was much confusion around this time. Nuclei were thought to be made of protons and electrons, but this gave the wrong statistics and a much too large magnetic moment. Ignoring these issues, the continuous spectrum could then be explained by assuming violation of energy-momentum conservation, which was justified in a 1931 textbook by Gamow by saying that we already knew such electrons had to behave strangely because of all the other problems.

• 1930: Pauli postulates an additional, nearly undetectable light neutral fermion contained in the nucleus, called the neutron ν, that solves all the problems above. This is first presented in absentia by his "dear radioactive ladies and gentlemen" letter.

• 1932: Chadwick discovers the neutron. This is too heavy to be Pauli's postulated particle, so Fermi renames it to the neutrino, because that means "little neutron" in Italian. (The -ino ending was then hijacked for the rest of particle physics to mean a generic fermion, even if they aren't "little".)

• 1934: Fermi introduces a four-fermion theory of weak interactions, allowing calculations. This accounts for beta decay as the process $n \to p + e^- + \nu$. This is actually quite a theoretical advance, because it is the first example of fermion production not in particle-antiparticle pairs.

• 1935: the nucleus is understood as being composed of protons and neutrons, with the neutrinos and electrons being newly created upon decay. Yukawa postulates a nuclear strong force mediated by a "meson" (i.e. pion) to hold the nucleus together, with a Yukawa potential.

• 1937: the meson is "discovered" in cosmic rays, which has the right mass but seems to interact far too weakly with nuclei. A long confusion ensues, until people eventually realize it is a new particle, the muon, which is like a heavy electron. It is initially thought to be an excited state of the electron, but the expected decay $\mu^- \to e^-\gamma$ is not observed through many experiments.

• It turns out that cosmic rays are actually high-energy protons, which produce pions upon impact with atoms in the atmosphere. These pions decay into the muons that we call cosmic rays above; this is the most common decay because of helicity suppression.

• A gap in progress occurs because of World War II.

• 1947: Marshak and Bethe propose the "two-meson hypothesis", where π is produced in cosmic rays but quickly decays to μ. This ridiculous ad-hoc idea is confirmed to be correct; pions are observed in cosmic rays high in the atmosphere.

• 1956: Reines and Cowan observe the neutrino-induced reaction $\bar{\nu} + p \to n + e^+$in "project poltergeist", with a nuclear reactor as a neutrino source, directly benefiting from World War II technology. (Note that this gap between theory and experiment is already several decades!) Specifically, they observe the gamma rays due to the annihilation of the $e^+$and the absorption of the n, and require these two to be roughly coincident to reduce backgrounds.

• 1958: shortly after the Wu experiment (1956), neutrinos are observed by Goldhaber et al. to always have left-handed helicity, which would make sense if they were massless.

• 1962: at this point, the muon neutrino has been theorized, and electron/muon number conservation has been postulated to explain the absence of the decay $\mu^- \to e^-\gamma$. (Actually, this decay can occur due to neutrino masses, but is exceptionally rare in the SM because of the GIM

mechanism.) This means that pion decay is actually $\pi^- \to \mu^- \bar{\nu}_\mu$. A beam of muon neutrinos fired at nuclei is then expected to produce muons and not electrons, which is confirmed at Brookhaven in this year.

• 1968: the Homestake experiment detects solar electron neutrinos by the reaction

$$\nu_e + {}^{37}\mathrm{Cl} \to e^- + {}^{37}\mathrm{Ar}$$

and then filtering out the argon and measuring its decay. It finds 1/3 as much compared to detailed astrophysical calculations based on the proton-proton chain. The discrepancy is called the solar neutrino problem, and touched off decades of confusion and finger pointing. Many people thought that solar modeling or the neutrino experiments or both were mistaken, and both the theoretical and experimental values changed dramatically over time

• Note that nearly all of the neutrinos produced in the Sun are expected to be electron neutrinos. This is because the Sun is "low-energy" by the standards of particle physics. Neutrinos are hence only produced by charged current interactions, and there is not enough energy to form muons or taus. We also do not expect electron antineutrinos. The electron neutrinos produced have MeV scale energies. By comparison, atmospheric neutrinos from cosmic rays go into the GeV scale.

• The Homestake and related experiments are not sensitive to muon or tau neutrinos, because absorption by a nucleus would have to produce a muon or tau, and there is not enough energy to do so.

• 1957: Pontecorvo and Gribov formulate the theory of neutrino flavor oscillations, which violate electron/muon/tau number. The oscillations require neutrino masses, since massless particles "do not experience time" and hence can't oscillate. Later, Mikheyev, Smirnov, and Wolfenstein refine this into a solution for the solar neutrino problem, which we cover below.

• 1975: the tau is discovered at SLAC, leading to the prediction of the tau neutrino.

• 1970s to 1990s: followups on the Homestake experiment are done. SAGE and GALLEX/GNO use gallium (lower threshold energy) while SNO, Kamioka, and SuperK use oxygen nuclei in water (higher threshold energy, but cheaper), confirming the puzzling result. Some of these are repurposed proton decay experiments motivated by GUTs. Throughout this time, many aren't convinced the solar neutrino problem is a real one, since the experiments are difficult and the nuclear physics of the Sun is complicated.

• 1987: neutrinos from a supernova, SN1987A, are detected. The neutrinos arrive at about the same time as light (actually earlier, since the light is delayed during core collapse), providing a strong upper bound on the neutrino mass.

• 1998: Super-Kamiokande provides definitive evidence for atmospheric neutrino oscillations. These neutrinos are created from cosmic rays by reactions like

$$\pi^+ \to \mu^+ + \nu_\mu \to e^+ + \nu_e + \bar{\nu}_\mu + \nu_\mu$$

For a detector on the ground, one expects an equal rate of muon neutrinos coming down and up from the other side of the Earth, by a shell-theorem like argument, assuming the isotropy of high-energy cosmic rays. But Super-Kamiokande found almost exactly half as much going up, which is explained by their oscillation into tau neutrinos.

• 2000: the ν_τ is directly observed by the DONUT experiment at Fermilab with the same strategy as for muon neutrinos, using a tau neutrino beam. This is a very difficult experiment. The discovery paper itself had only 4 events, and to date only about 10 tau events have been directly seen by all experiments combined! However, note that the ν_τ had earlier been observed indirectly from the Z decay width at LEP.

• 2001: the SNO experiment becomes sensitive to all three flavors of solar neutrinos. The experiment uses heavy water, containing deuterons (loosely bound pn bound states). Neutrinos

can scatter off the deuteron by a neutral current interaction (same for all three flavors), breaking it apart, and one then measures the produced neutron. SNO finds a total flux in accordance with expectation, decisively confirming that solar neutrinos oscillate.

• 2005: KamLAND uses reactor neutrinos to directly observe neutrino oscillations for anti-electron neutrinos. Varying the distance can be achieved because Japan has over 50 existing nuclear reactors at varying distances from the (stationary) detector. Sociologically, this is because Japan is an island and hence has plentiful water for reactor cooling.

• 2010s: Double Chooz (France), Daya Bay (China), and RENO (South Korea) all find that the parameter θ_{13} in the PMNS matrix is nonzero, using reactor neutrinos. NO ν a (Fermilab) and T2K (Japan) do the same with accelerator neutrinos. These experiments do not have the luxury of KamLAND's multiple sources; instead they generally use two detectors, a "near" one and a "far" one, to see how much the neutrino flux decreases.

• Reactor neutrino experiments find an unexpectedly large number of neutrinos at around 5MeV, which has not been resolved. There is also an outstanding accelerator neutrino anomaly from LSND, which was checked by MiniBooNE. MiniBooNE in turn found yet another anomaly, which has been checked by MicroBooNE, but the interpretation of all three experiments remains unclear. (Historically, neutrino physics has generated a very large number of anomalies.)

6.5.2 Neutrino Oscillations

Next, we take a closer look at neutrino oscillations.

• For the moment, we assume the neutrinos have Majorana masses and ignore issues of gauge invariance. We write the mass terms as

$$\mathcal{L} \supset -\frac{1}{2}\left(m_{ab}\bar{\nu}_a P_L \nu_b + \text{ h.c. }\right)$$

where the ν_a are the neutrino fields. We define the PMNS matrix V to map from the mass basis to the flavor basis. (Note that when one refers to just "the neutrinos", one means the flavor basis. This is in contrast to quarks, where one means the mass basis.)

• Now we count the degrees of freedom, for Majorana masses.

• The lepton sector has a $U(3)^2$ symmetry, with 6 real parameters and 12 phases.

• The lepton Yukawa coupling is a complex matrix with 9 real parameters and 9 phases.

• This leads a theory with 3 real parameters (the charged lepton masses) and the three $U(1)$ lepton number symmetries.

• When we introduce Majorana masses, these symmetries are broken completely.

• The matrix m above is complex symmetric, and has 6 real parameters and 6 phases.

• Hence the masses can be described in terms of 6 real parameters and 3 phases.

Of these parameters, 3 of the real parameters are just the neutrino masses.

• The rest are in the PMNS matrix, which can be written as

$$V = UK$$

where U has the same parametrization as the CKM matrix, and K can be chosen to be, e.g., $\text{diag}\,(e^{i\alpha_1}, e^{i\alpha_2}, 1)$. The matrix K can't be measured by neutrino oscillation experiments.

• Now consider the case where neutrinos have Dirac masses.

• This requires introducing a set of right-handed neutrino fields, which gives another $U(3)$ symmetry to use.

• The $U(1)^3 \times U(3)$ symmetry is broken to $U(1)_L$, allowing us to absorb 3 real parameters and 8 phases.

• The Yukawa coupling between the left-handed and right-handed neutrino fields is again a complex matrix with 9 real parameters and 9 phases.

• Hence the masses can be described in terms of 6 real parameters and 1 phase.

Again, 3 of the real parameters are neutrino masses, while the rest are in the PMNS matrix, which in this case can be written in the same form as the CKM matrix.

• While this parameter counting is comprehensive and reliable, it can be simplified if we only care about the PMNS matrix.

• This is naively a general unitary matrix with 3 real parameters and 6 phases.

• In the Majorana case, phases can only be removed by rephasing the charged lepton fields (since this rephases the flavor basis), giving 3 remaining phases.

• In the Dirac case, both the charged lepton and neutrino fields can be rephased, but a uniform phase shift does nothing to the PMNS matrix because of the $U(1)_L$ symmetry. This leaves $6-(6-1)=1$ phase.

• The matrix U is parametrized by three mixing angles θ_{12}, θ_{23}, and θ_{13}, and a CP-violating phase δ. Currently, all of the mixing angles have been found to be nonzero, though $\theta_{13} \approx 8^\circ$ is smaller than the rest and took much longer to measure, while δ is only nonzero at 2σ.

Next, we turn to neutrino oscillations.

• Neutrinos are typically produced and absorbed in charged-current weak interactions, i.e. in flavor eigenstates $|\nu_a\rangle$. We consider the amplitude

$$\langle \nu_b(\mathbf{x},t)|\nu_a(0,0)\rangle = \left\langle \nu_b \left| e^{-iHt+i\mathbf{P}\cdot\mathbf{x}} \right| \nu_a \right\rangle$$

and insert a complete basis of mass eigenstates $|\nu_i\rangle$, for

$$\langle \nu_b(\mathbf{x},t)|\nu_a(0,0)\rangle = \sum_{i,\sigma} \int d\mathbf{k} e^{-iE_i(k)t+i\mathbf{k}\cdot\mathbf{x}} \langle \nu_b|\nu_i(\mathbf{k},\sigma)\rangle \langle \nu_i(\mathbf{k},\sigma)|\nu_a\rangle$$

The spin part is flavor-independent; for simplicity we take the initial and final states to have spin up. But we also find flavor-dependent phases since the dispersion relations $E_i(k)$ differ.

• We apply the ultrarelativistic approximation,

$$|\mathbf{x}| \approx t, \quad |\mathbf{k}| \approx E - m_i^2/E$$

which yields the simplification

$$\langle \nu_b(\mathbf{x},t)|\nu_a(0,0)\rangle = e^{i\xi} \sum_i e^{im_i^2 L/2E} \langle \nu_b|\nu_i\rangle \langle \nu_i|\nu_a\rangle = e^{i\xi} \sum_i e^{-im_i^2 L/2E} V_{bi} V_{ai}^*$$

where ξ is an unimportant global phase.

• Squaring, we find the probability is

$$P_{\nu_a\to\nu_b}(E,L) = \sum_{ij} e^{-i\left(m_i^2-m_j^2\right)L/2E} V_{bi} V_{bj}^* V_{aj} V_{ai}^*$$

where the overall phases in K have canceled out; neutrino oscillations cannot measure them.

• For concreteness, we can focus on the case of two neutrinos, where

$$P_{\nu_a\to\nu_b}(E,L) \approx \sin^2(2\theta) \sin^2\left(\frac{\Delta m^2 L}{4E}\right)$$

The length scale of oscillations is

$$\lambda = \frac{2E}{\Delta m^2} = 500 \text{ m} \left(\frac{E}{1\text{GeV}}\right)\left(\frac{1\text{eV}^2}{\Delta m^2}\right), \quad \Delta m^2 \lesssim 3\times 10^{-3}\text{eV}^2$$

Here, typical atmospheric and accelerator neutrinos have an energy of 1GeV, so λ is much greater than the thickness of the atmosphere, but much less than the size of the Earth. Reactor neutrinos have lower energies, and can be used to probe smaller mass splittings.

• In the limit of small L, we of course have

$$P_{\nu_a \to \nu_b}(E, L) \approx \sin^2(2\theta) \left(\frac{\Delta m^2 L}{4E} \right)^2$$

Accelerator neutrino experiments are in this regime, and there is a tradeoff between having large L and higher probability of oscillation, and smaller L with higher flux. The distances are of order 100 km.

• In the limit of large L, we note that E typically has some range, so the rapidly oscillating random phase averages the second factor to $1/2$, giving

$$P_{\nu_a \to \nu_b}(E, L) \approx \frac{1}{2} \sin^2(2\theta)$$

Atmospheric neutrino experiments are in this regime for up-going neutrinos. In between, the probability can oscillate.

Next, we consider some further subtleties of neutrino mixing.

Note. Just like the CKM matrix, the PMNS matrix breaks CP and hence T. Indeed, we have

$$P(\nu_a \to \nu_b) \neq P(\nu_b \to \nu_a)$$

and

$$P(\nu_a \to \nu_b) \neq P(\bar{\nu}_a \to \bar{\nu}_b)$$

where antineutrinos have mixing matrix V^*. (Also note that V^* is the matrix that appears in the Lagrangian, because neutrino fields create antineutrinos.) The differences of these probabilities is proportional to the Jarlskog invariant for the PMNS matrix. (cover in more detail) However, CPT implies that antineutrinos have the same masses as the corresponding neutrinos, which gives

$$P(\nu_a \to \nu_b) = P(\bar{\nu}_b \to \bar{\nu}_a)$$

in general.

Note. To define the PMNS matrix, we must fix a convention for the mass eigenstates. We let $m_1^2 < m_2^2$ and let m_3^2 be the one far from the other two. However, we don't know if m_3^2 is larger ("normal" hierarchy) or smaller ("inverted" hierarchy). Under this convention, the elements of the PMNS matrix are

$$V = \begin{pmatrix} V_{e1} & V_{e2} & V_{e3} \\ V_{\mu 1} & V_{\mu 2} & V_{\mu 3} \\ V_{\tau 1} & V_{\tau 2} & V_{\tau 3} \end{pmatrix} \sim \begin{pmatrix} 0.8 & 0.4 & 0.1 \\ 0.4 & 0.5 & 0.7 \\ 0.4 & 0.6 & 0.7 \end{pmatrix}$$

where the numbers above are extremely approximate. Assuming the neutrino mass is Dirac, the PMNS matrix has three physical angles and one physical phase, which we defined to as

$$\tan^2 \theta_{12} = \frac{|V_{e2}|^2}{|V_{e1}|^2}, \quad \tan^2 \theta_{23} = \frac{|V_{\mu 3}|^2}{|V_{\tau 3}|^2}, \quad V_{e3} = \sin \theta_{13} e^{-i\delta}$$

Current measurements of δ are still consistent with zero within a few sigma. Our knowledge of θ_{12} comes from solar neutrinos, θ_{23} from atmospheric neutrinos, and θ_{13} from reactor neutrinos.

From this matrix, we see that in the large L limit, we lose roughly half of both initial electron neutrinos and initial muon neutrinos, while "2" neutrinos are composed of each flavor equally. A nice way to remember this is to use the "tribimaximal" form,

$$|V_{ai}|^2 = \begin{pmatrix} 2/3 & 1/3 & 0 \\ 1/6 & 1/3 & 1/2 \\ 1/6 & 1/3 & 1/2 \end{pmatrix}$$

which was used in many earlier models, but is now ruled out, e.g. since θ_{13} is nonzero. This is important, as if it were zero, there would be no CP violation at all.

Note. Why are we allowed to restrict to two neutrino flavors sometimes? First, one oscillation frequency is several times smaller than the others, so for experiments with small lengths (e.g. reactor neutrinos) we can ignore the slow frequency. Second, for other ones (e.g. solar neutrinos) we often only measure electron neutrinos, and here $|V_{e3}|^2$ is quite small.

Note. Neutrino oscillations are a bit puzzling, because if the mass-basis neutrinos have different dispersion relations, then it is impossible for a flavor-basis neutrino to have a definite four-momentum. But the electroweak Feynman diagrams that produce flavor-basis neutrinos impose momentum conservation at every vertex, so the final state in the reaction $e^- + X \to X' + \nu_e$ looks like

$$|\text{ definite flavor } X', \nu_e\rangle = \sum_i |\text{ definite momentum } X', \nu_i\rangle$$

where each of the states on the right has a different momentum for X'. Tracing out the X', it would appear that we cannot have interference between the neutrino states. But this is no problem, for the same reason that a Stern-Gerlach apparatus doesn't destroy superpositions: the momenta of the X was not well-defined to begin with! In the case of solar neutrinos, even demanding that the X lie in the Sun requires a large enough spread in momentum that the X' states of different momentum almost completely overlap.

However, this raises the possibility that neutrino oscillations can decohere. For instance, this occurs if the distance traveled is great enough that the different components of the neutrino wavepacket stop overlapping. An exhaustive review of the subtleties of neutrino oscillations is given in Paradoxes of neutrino oscillations.

Note. If we used the formulas above, we would expect that the Homestake experiment saw 1/2 as many neutrinos as expected, rather than the actual 1/3. (Sometimes the 1/3 is naively explained by saying that there are 3 neutrino flavors, but this is a drastic oversimplification.) The 1/3 results from the MSW effect: while electron neutrinos are created at the center of the Sun, they will be affected by the electrons in the Sun, so that the neutrinos exiting the Sun are not electron neutrinos.

The mass eigenstates satisfy a Schrodinger equation in space,

$$i\frac{d}{dL}|\nu_i\rangle = \frac{m_i^2}{2E}|\nu_i\rangle$$

In terms of flavor eigenstates, we have

$$i\frac{d}{dL}|\nu_\beta\rangle = V_{\beta i}\frac{m_i^2}{2E}V_{i\alpha}^\dagger|\nu_\alpha\rangle$$

Tau neutrinos are not important here, so we restrict to two flavors,

$$i\frac{d}{dL}\begin{pmatrix} |\nu_e\rangle \\ |\nu_\mu\rangle \end{pmatrix} = \frac{\Delta m^2}{2E}\begin{pmatrix} \sin^2\theta & \cos\theta\sin\theta \\ \cos\theta\sin\theta & \cos^2\theta \end{pmatrix}\begin{pmatrix} |\nu_e\rangle \\ |\nu_\mu\rangle \end{pmatrix}$$

Now consider the interaction of electrons with electron-neutrinos, which is the leading (i.e. tree-level) interaction in this context. The effective four-fermion interaction is

$$\mathcal{L} \supset 2\sqrt{2}G_F\left(\bar{\nu}_{eL}\gamma_\mu e_L\right)\left(\bar{e}_L\gamma^\mu\nu_{eL}\right) = -2\sqrt{2}G_F\left(\bar{\nu}_{eL}\gamma_\mu\nu_{eL}\right)\left(\bar{e}_L\gamma^\mu e_L\right)$$

where we used a Fierz identity. In a matter background with electron number density N_e, in the matter rest frame, we may set

$$\langle \bar{e}_L \gamma_\mu e_L \rangle = \delta_{\mu 0} \frac{N_e}{2}$$

where the 1/2 is from the two possible helicities. The effective Lagrangian for electron neutrinos is

$$\mathcal{L} \supset \bar{\nu}_{eL} \not{\partial} \nu_{eL} - iA \left(\bar{\nu}_{eL} \gamma_0 \nu_{eL} \right), \quad A = \sqrt{2} G_F N_e.$$

The matter term produces an effective potential. To see this, consider the equation of motion

$$\left(\not{\partial} - iA\gamma_0 \right) |\nu_e\rangle = 0.$$

Multiplying by $\not{\partial} - iA\gamma_0$, we have

$$0 = \left(\partial^2 - 2iA\partial_0 + A^2 \right) |\nu_e\rangle = \left(E^2 - |\vec{p}|^2 \mp 2AE + A^2 \right) |\nu_e\rangle$$

where the other sign arises for antineutrinos. This gives the dispersion relation

$$E = |\vec{p}| \pm A$$

which shows the matter-induced potential. Hence the Schrodinger equation becomes

$$i \frac{d}{dL} \begin{pmatrix} |\nu_e\rangle \\ |\nu_\mu\rangle \end{pmatrix} = \left[\frac{\Delta m^2}{2E} \begin{pmatrix} \sin^2\theta & \cos\theta \sin\theta \\ \cos\theta \sin\theta & \cos^2\theta \end{pmatrix} + \begin{pmatrix} A & 0 \\ 0 & 0 \end{pmatrix} \right] \begin{pmatrix} |\nu_e\rangle \\ |\nu_\mu\rangle \end{pmatrix}$$

One way to parametrize this matrix is to subtract off a multiple of the identity, giving

$$\begin{pmatrix} A & (\Delta/2)\sin 2\theta \\ (\Delta/2)\sin 2\theta & \Delta \cos 2\theta \end{pmatrix}, \quad \Delta = \frac{\Delta m^2}{2E}$$

which can be written in the original form with a different Δ and θ,
$P(e \to \mu) = \sin^2(2\theta_M) \sin^2 \frac{\Delta_M L}{2}$, $\Delta_M = \sqrt{(A - \Delta\cos 2\theta)^2 + \Delta^2 \sin^2 2\theta}$, $\Delta_M \sin 2\theta_M = \Delta \sin 2\theta$.

Note that neutrinos and antineutrinos oscillate differently; this is compatible with CPT because the matter background spontaneously breaks it. Also note that the MSW effect depends on the sign of Δ, and hence can in principle tell between the normal and inverted mass hierarchy.

In the case of the Sun, A is high in the core, so that a produced $|\nu_e\rangle$ is approximately a mass eigenstate. As the neutrino exits, A adiabatically transitions to zero, so the neutrino exits in a mass eigenstate, namely the heavier one $|\nu_2\rangle$ because of avoided level crossing, and afterward do not oscillate. The fraction of electron-neutrinos we see is

$$P_{ee} = |\langle \nu_e | \nu_2 \rangle|^2 = \sin^2\theta \approx \frac{1}{3}$$

which is the correct result. So ironically, the first evidence for neutrino oscillations doesn't even involve neutrino oscillations. (Though strictly speaking, the Sun produces neutrinos with a wide range of energies, and this argument only applies to the high-energy ones. For lower-energy neutrinos, measured in experiments after Homestake, this effect is less important.) The MSW effect also causes a "day-night" effect for solar neutrinos, which have to pass through the Earth at night.

Note. Various signs get flipped for antineutrinos, which raises the question: does these results change if neutrinos are Majorana? The answer is actually no, because if so, then what we call "neutrino" and "antineutrino" just stands for left-helicity neutrino and right-helicity

neutrino in the lab frame, since that determines how we can detect them. (Strictly speaking, the weak force couples to definite chirality; the mismatch between chirality and helicity gives errors, but they are suppressed by powers of m_ν/E, which is tiny for all neutrinos ever detected.)

6.5.3 Neutrino Masses

Next, we consider the possibility of sterile neutrinos, first ignoring any gauge structure.

• In general, any fermion that mixes with ordinary neutrinos but does not couple to anything else in the SM is called a sterile neutrino. By definition, sterile neutrinos must have no charge under any gauge group.

• Concretely, suppose we introduce N sterile Majorana neutrino fields. (As mentioned above, this does not lose any generality. Only Lagrangian terms break symmetries, not how we package the fields in them.) The most general Majorana mass terms include mixing terms between the sterile and ordinary neutrinos, with mass matrix

$$\begin{pmatrix} m & \mu \\ \mu^T & M \end{pmatrix}$$

where m is the mass matrix introduced earlier.

• First, consider the case $\mu \ll m, M$. Then there is negligible mixing between sterile and ordinary neutrinos, and the sterile neutrinos don't do anything at all, though there may be constraints on them from cosmology.

• Next, consider the case of Dirac neutrinos, $m = M = 0$. In this case, we can write the fields as $N - 3$ massless decoupled sterile neutrinos and 3 massive Dirac neutrinos. The result is exactly analogous to the quark fields. Lepton number is conserved, and the phases α_i are all zero.

• It seems that it would be easy to rule out Dirac neutrinos, because ordinary neutrinos would quickly oscillate into sterile neutrinos, which have the opposite chirality, leading to an easily measurable missing probability. Chirality oscillations indeed occur for other fermions, but the the mixing angle between the chirality and mass basis in the Dirac equation goes to zero as the neutrino becomes ultrarelativistic. Since all neutrinos available are ultrarelativistic, the oscillation amplitude is extremely small. This effect is known as helicity suppression.

• On the other hand, if we have light sterile neutrinos, $m \sim \mu \sim M$, the previous argument doesn't apply. These models are indeed tightly constrained by "missing probability".

• Finally, seesaw neutrinos are the case $m \ll \mu \ll M$. The eigenvectors are almost purely sterile and normal, with masses on the order of M and $m + \mu^2/M$. These models are experimentally acceptable, since the sterile neutrinos are too heavy to be produced, and give the right neutrino mass naturally, as we'll see below.

• When it is asked whether neutrinos are Dirac or Majorana, a Dirac neutrino would simply correspond to $m = M = 0$. If there are Majorana mass terms, $U(1)_L$ is violated and neutrinos can annihilate themselves. This isn't forbidden, since $U(1)_L$ is merely an accidental global symmetry of the SM anyway, and is even anomalous.

• However, note that $U(1)_{B-L}$ is also an accidental global symmetry of the SM, which isn't anomalous. In extensions of the SM where $U(1)_{B-L}$ is gauged and not spontaneously broken, we must have $m = M = 0$. Alternatively, we could rule out these terms by just postulating that $U(1)_L$ or $U(1)_{B-L}$ are exact global symmetries.

• It would also be easy to tell the difference between Majorana or Dirac neutrinos if we could detect nonrelativistic neutrinos, which appear in the cosmic neutrino background. This is extremely challenging, since cross sections scale with the neutrino energy; we have never seen any nonrelativistic neutrinos.

Next, we embed the neutrino models above in a gauge invariant formalism.

• The simplest possible sterile neutrinos are a set of three right-handed neutrinos

$$N^i = \nu_R^i = (\nu_{eR}, \nu_{\mu R}, \nu_{\tau R})$$

which are gauge singlets. Then we can include a Yukawa mass term,

$$\mathcal{L} \supset -\sqrt{2}\left(\lambda_\nu^{ij} \bar{L}^i \phi^c N^j + \text{ h.c. }\right)$$

where we use ϕ^c to make the hypercharge work out. Integrating out the Higgs, this corresponds to the case of Dirac neutrinos. Such a term is not $SU(2)_L \times U(1)_Y$ invariant, but this is acceptable since the only residual symmetry below the Higgs scale is $U(1)_A$.

• We can also write down a gauge invariant Majorana mass term for the sterile neutrinos. The natural scales for the mass matrices are then

$$m \sim 0 \text{ (gauge invariance)}, \quad \mu \sim M_{\text{EW}}, \quad M \sim \Lambda$$

where Λ is the SM cutoff. We hence get a seesaw mechanism with neutrino masses Λ and M_{EW}^2/Λ, and the latter is the right mass if Λ is about the GUT scale, a compelling coincidence.

• To have Dirac neutrinos, we need to force M to be small somehow. For example, we could use an exact $B - L$ symmetry. However, μ must also be much smaller than M_{EW}. This is technically natural in the same way that the lightness of the up and down quarks relative to M_{EW} is, but it's a bit unsatisfying because it adds more unexplained flavor structure.

• If we assume that whatever physics produces the neutrino masses is heavy, then we can simply use effective field theory. Here, neutrinos receive mass by the dimension 5 "Weinberg operator",

$$\mathcal{L} \supset -\frac{Y^{ij}}{\Lambda}\left(L^{iT}\phi^c\right) C \left(\phi^{cT} L^j\right) + \text{ h.c.}$$

where the conjugates ensure gauge invariance. The mass is therefore about M_{EW}^2/Λ, giving a simple reason that the seesaw mechanism, and related mechanisms, work.

• From the effective field theory point of view, neutrino masses are the leading correction to the SM, because they are the only dimension 5 operator we can write down. If we take Λ to be near the GUT scale as inferred from the neutrino masses, then dimension 6 operators are very hard to measure.

• There are many more ways to UV complete the Weinberg operator. Above, we have only considered the "type I seesaw", which introduces a right-handed fermionic singlet. But one can also introduce a scalar weak triplet (type II seesaw) or a fermionic weak triplet (type III seesaw), as any of these can play the role of the intermediate heavy particle.

• There are also "radiative" mass generation models where the neutrino mass is only generated at loop level, such as the Zee model and the Ma model. The Ma model is called "scotogenic" ("from darkness") since the mass comes from neutrino interactions with a dark matter candidate.

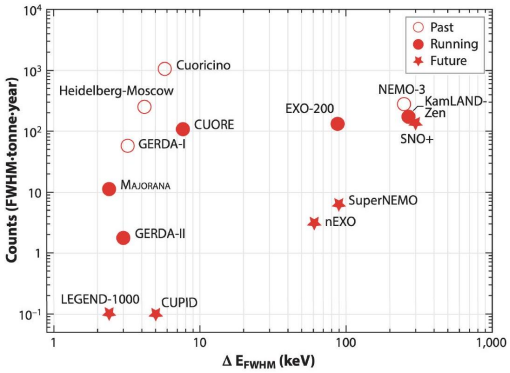
Note. Why did we discuss neutrino masses in a set of notes on the Standard Model? After all, doesn't the Standard Model require neutrino masses to be zero? This is debatable, because if one reads the term literally, as the standard model one uses to describe nature, then it has changed significantly since the advent of "the" Standard Model, and now includes neutrino masses. For some historical discussion, see The Once and Present Standard Model of Elementary Particle Physics.

Note. The clearest experimental signature for a Majorana mass term would be neutrinoless double beta decay. Some nuclei cannot decay by beta decay, because the resulting product is heavier, but can decay if two beta decays occur at once, a rare process. In neutrinoless

double beta decay, the two neutrinos produced annihilate, which is even rarer due to helicity suppression,

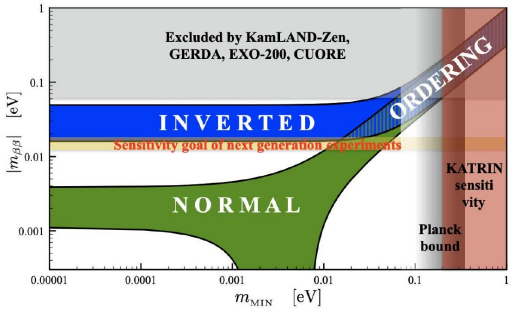
$$\Gamma \sim G_F^4 \frac{m_\nu^2}{E^2} E^9 \sim 10^{-31} \text{ years}^{-1}$$

assuming $m_\nu \sim 0.01\text{eV}, E \sim 1\text{MeV}$. The process can be identified by an incredibly sharp peak in the energy spectrum of the resulting electrons, which requires very sensitive energy measurements. Relevant experiments are reviewed here and here. Some experiments, with background count rate plotted against energy resolution, are shown below.



There is a tradeoff between large size, at the right of the plot, and good energy resolution, at the bottom. For example, CUORE uses precise bolometers (i.e. calorimeters) in a dilution fridge; it will upgrade to CUPID by adding a light detector to veto most of the background, in the form of degraded alpha particles. On the other extreme, KamLAND-Zen uses about 800 kg of liquid ^{136}Xe dissolved in liquid scintillator, and operates much like direct dark matter detection experiments, though its threshold is at MeV, while WIMP recoils are keV and lower.

Current experiments probe down to $\Gamma \sim 10^{-28}$ years $^{-1}$, while future experiments have the concrete goal of probing the inverted neutrino hierarchy.



Past experiments had the potential to probe heavier, quasi-degenerate neutrinos, but these are in tension with cosmology, so one needs to add epicycles to fix this. Thus, as experiments get more precise, we actually move towards testing the simplest models. Unfortunately, the possibility remains that a cancellation occurs for the normal hierarchy, making the rate very small.

6.6 Quantum Chromodynamics

6.6.1 Hadron Production

Before beginning, we consider the running coupling.

- We take the QCD Lagrangian to be

$$\mathcal{L} = -\frac{1}{4}F^{a\mu\nu}F_{a\mu\nu} + \sum_f \bar{q}_f \left(i\not{D} - m_f\right) q_f, \quad D_\mu = \partial_\mu + igA^a_\mu T^a$$

where $T^a = \lambda^a/2$ as usual, and the field is

$$F^a_{\mu\nu} = \partial_\mu A^a_\nu - \partial_\nu A^a_\mu - g f^{abc} A^b_\mu A^c_\nu$$

• In general, the one-loop beta function for the coupling is

$$\beta(g) = -\beta_0 \frac{g^3}{16\pi^2}, \quad \beta_0 = \frac{11}{3}C_A - \frac{4}{3}\sum_f T_f$$

where C_A is the quadratic Casimir of the adjoint representation, and T_f is the Dynkin index of the representation for quark flavor f. We see that fermions provide screening, while nontrivial gluon-gluon interactions provide 'antiscreening', which favor asymptotic freedom.

• In the case of QCD, we have the group $SU(3)$, so $C_A = 3$, and all the quarks transform in the fundamental representation where $T_F = 1/2$, so

$$\beta(g) = -\beta_0 \frac{g^3}{16\pi^2}, \quad \beta_0 = 11 - \frac{2}{3}N_f$$

where N_f is the number of flavors. Then the beta function is negative if $N_f < 33/2$. This also holds for QED, where $C_A = 0$ and the beta function is positive for any nonzero N_f.

• For high energies, we have $N_f = 6$, so the beta function is negative. Defining $\alpha_s = g^2/4\pi$,

$$\frac{d\alpha_s}{d\log\mu} = -\frac{\beta_0}{2\pi}\alpha_s^2$$

Integrating, we have

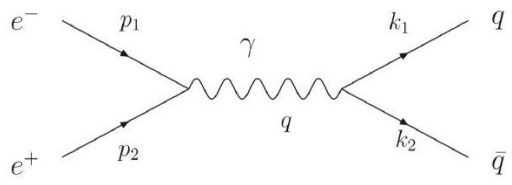
$$\alpha_s(\mu) = \frac{2\pi}{\beta_0} \frac{1}{\log\left(\mu/\mu_0\right) + 2\pi/\beta_0\alpha_s\left(\mu_0\right)} = \frac{2\pi}{\beta_0 \log\left(\mu/\Lambda_{\text{QCD}}\right)}$$

where we defined Λ_{QCD} as the scale where the coupling diverges.

• We're implicitly using a mass-independent scheme, so each quark continues to contribute even when μ is much less than its mass. In practice, when we drop below the top quark mass we 'manually' stop its running, matching the coupling and then setting $N_f = 5$, and so on. Doing this yields $\Lambda_{\text{QCD}} \approx 200 - 500\text{MeV}$, though the answer depends on the subtraction scheme.

Next, we consider the cross section for $e^+e^- \to$ hadrons.

• First, we consider the process $e^+e^- \to q\bar{q}$, which we treat perturbatively by asymptotic freedom. By simplicity we consider only the tree-level process where the intermediate particle is a virtual photon, as shown below.



• If the quarks have electric charge eQ, the matrix element is

$$\mathcal{M} = (-ie)^2 Q \bar{u}_q\left(k_1\right)\gamma^\mu v_q\left(k_2\right)\frac{-i\eta_{\mu\nu}}{q^2}\bar{v}_e\left(p_2\right)\gamma^\nu u_e\left(p_1\right)$$

Neglecting the quark and electron masses and summing/averaging over spins,

$$\frac{1}{4}\sum_{\text{spins}}|\mathcal{M}|^2 = \frac{e^4Q^2}{4q^4}\operatorname{tr}\left(\not{k}_1\gamma^\mu\not{k}_2\gamma^\nu\right)\operatorname{tr}\left(\not{p}_1\gamma_\mu\not{p}_2\gamma_\nu\right) = \frac{8e^4Q^2}{q^4}\left[\left(p_1\cdot k_1\right)\left(p_2\cdot k_2\right)+\left(p_2\cdot k_1\right)\left(p_1\cdot k_2\right)\right]$$

• Next, we work in the center of mass frame,

$$p_1 = (|\mathbf{p}|,\mathbf{p}), \quad k_1 = (|\mathbf{k}|,\mathbf{k}), \quad \mathbf{p}\cdot\mathbf{q} = |\mathbf{p}||\mathbf{q}|\cos\theta, \quad q = (2|\mathbf{p}|,0)$$

where we have

$$\frac{1}{4}\sum_{\text{spins}}|\mathcal{M}|^2 = e^4Q^2\left(1+\cos^2\theta\right)$$

• Next, the basic formula for the differential cross section is

$$d\sigma = \frac{1}{|\mathbf{v}_1-\mathbf{v}_2|}\frac{1}{4p_1^0p_2^0}\frac{d\mathbf{k}_1}{2k_1^0}\frac{d\mathbf{k}_2}{2k_2^0}\phi\left(q-k_1-k_2\right)\frac{1}{4}\sum_{\text{spins}}|\mathcal{M}|^2$$

Since the particles are massless, $|\mathbf{v}_1-\mathbf{v}_2| = 2$, giving

$$d\sigma = \frac{e^4Q^2}{8\pi^2q^2}\frac{d\mathbf{k}_1}{4\left|\mathbf{k}_1\right|^2}\delta\left(\sqrt{q^2}-2\left|\mathbf{k}_1\right|\right)\left(1+\cos^2\theta\right)$$

• Writing $d\mathbf{k}_1 = \left|\mathbf{k}_1\right|^2 d\left|\mathbf{k}_1\right| d\Omega$ and performing the delta function gives

$$\frac{d\sigma}{d\Omega} = \frac{\alpha^2Q^2}{4q^2}\left(1+\cos^2\theta\right)$$

using $\alpha = e^2/4\pi$, and performing the angular integration gives

$$\sigma = \frac{4\pi\alpha^2}{3q^2}Q^2$$

This matches the result from our more specific formulas for the cross section.

• Note that the cross section only depends on the identity of the final particles through Q. Then to reduce experimental and theoretical uncertainties, we can test this result by comparing it to the cross section for $e^+e^-\to\mu^+\mu^-$.

Next, we account for the hadronic final states.

• Let $|X\rangle$ denote a generic hadronic final state and let $|0\rangle$ denote the QCD vacuum. Then the amplitude to produce $|X\rangle$ is approximately

$$\mathcal{M}_X = \frac{e^2}{q^2}\left\langle X\left|J_h^\mu\right|0\right\rangle\bar{v}_e\left(p_2\right)\gamma_\mu u_e\left(p_1\right), \quad J_h^\mu = \sum_f Q_f\bar{q}_f\gamma^\mu q_f$$

where J_h^μ is the hadronic electric current, and we are essentially assuming that the process goes as $e^+e^-\to\gamma^*\to q\bar{q}\to$ hadrons with a clean separation between the steps. Summing over all final states gives

$$\sigma = \frac{1}{8p_1^0p_2^0}\sum_X\frac{1}{4}\sum_{\text{spins, }p_X}\phi\left(q-p_X\right)\left|\mathcal{M}_X\right|^2$$

where the sum over p_X includes the appropriate Lorentz invariant phase space factors.

• To simplify this, we introduce the hadronic spectral density as we did for a scalar field,

$$\rho_h^{\mu\nu}(q) = (2\pi)^3 \sum_{X,p_X} \delta\left(q - p_X\right) \langle 0 \left| J_h^\mu \right| X \rangle \langle X \left| J_h^\nu \right| 0 \rangle$$

By Lorentz invariance, it is proportional to a linear combination of $g^{\mu\nu}$ and $q^\mu q^\nu$. The Ward identity gives $q_\mu \rho^{\mu\nu} = q_\nu \rho^{\mu\nu} = 0$, so

$$\rho_h^{\mu\nu}(q) = \left(-\eta^{\mu\nu} q^2 + q^\mu q^\nu\right) \theta\left(q^0\right) \rho_h\left(q^2\right)$$

where the theta function exists because the $|X\rangle$ states have positive energy.

• The cross section in the center of mass frame thus simplifies to

$$\sigma = \frac{16\pi^3 \alpha^2}{q^2} \rho_h\left(q^2\right)$$

In general, $\rho_h\left(q^2\right)$ is a complicated nonperturbative function.

• In order to make progress, we essentially neglect hadronization entirely, writing

$$\sum_{X \in \text{ hadrons}} |X\rangle \left\langle X \right| = \sum_{Y \in q,\bar{q},g \text{ states}} \left| Y \right\rangle \langle Y|$$

Switching from a hadron-level to quark-level description of the process is called quark-hadron duality. Using this assumption, the computation is essentially identical to our earlier computation for $q\bar{q}$ final states.

• Concretely, the spectral density is now

$$\rho_h^{\mu\nu}\left(q^2\right) = N_c \sum_f Q_f^2 \int \frac{d\mathbf{k}_1 d\mathbf{k}_2}{4k_1^0 k_2^0} (2\pi)^3 \delta\left(q - k_1 - k_2\right) \operatorname{tr}\left(\left(\not{k}_1 + m_f\right) \gamma^\mu \left(\not{k}_2 - m_f\right) \gamma^\nu\right)$$

where the final state are on-shell, $k_1^2 = k_2^2 = m_f^2$. Unlike our previous computation, we maintain the masses of the quarks. We know the integral must take the form

$$I^{\mu\nu} = A q^\mu q^\nu + B \eta^{\mu\nu}$$

where A and B are found by contracting both sides with $\eta_{\mu\nu}$ and $q_\mu q_\nu$. We thus find

$$\rho_h\left(q^2\right) = \frac{N_c}{12\pi^2} \sum_f Q_f^2 \theta\left(q^2 - 4m_f^2\right) \left(1 - \frac{4m_f^2}{q^2}\right)^{1/2} \frac{q^2 + 2m_f^2}{q^2}$$

• Neglecting the specific dependence on the quark masses, we have

$$\sigma = N_c \frac{4\pi\alpha^2}{3q^2} \sum_f Q_f^2$$

where the sum is over all quarks light enough to be produced; we thus expect a series of plateaus between jumps. Experimental results confirm that $N_c = 3$ and display the same plateaus, with extra resonances throughout. There is a resonance between each plateau, corresponding to the lightest meson containing the new quark that can be produced, e.g. the J/ψ for the charm quark. The result is good for $\sqrt{s} \in [2, 20]\text{GeV}$. At high energies, we run into the broad Z pole, while at low energies, α_s is large.

Next, we discuss jets and higher-order corrections.

• At next-to-leading order, we must account for a gluon loop on the $q\bar{q}\gamma$ vertex. The loop is UV finite after renormalization but IR divergent, giving a divergent negative contribution

to the cross section. This cancels with the IR divergences in the tree-level cross section for $e^+e^- \to q\bar{q}g$. Thus the total cross section for

$$e^+e^- \to q\bar{q} + \text{ possible soft gluons}$$

is finite, and the result is that the total cross-section is multiplied by $1 + \alpha/\pi$. Physically, the q and $\bar{q}$ are seen as jets, so we've computed the differential cross-section for jet production.

• Intuitively, the intermediate photon is very far off-shell, decaying in time $1/\sqrt{q^2}$ by the energytime uncertainty principle. The emission of soft gluons takes place over a much longer timescale, so it can't retroactively change how the photon decayed. Thus the IR divergences simply account for how the hard quarks are "dressed" after their production and cannot affect the total rate, so they must cancel. Indeed, the corrections in the next-to-leading order cross section come from kinematic regions where the virtual gluon is hard.

• The formal proof that IR divergences cancel is rather difficult. For QED, the result is the Bloch-Nordsieck theorem, while for the general non-abelian case it is the KLN theorem.

• Similarly, consider the tree-level differential cross-section for $e^+e^- \to q\bar{q}g$. By the above considerations, when the gluon is soft, we see two jets, not three. If we restrict to regions where gluon is sufficiently hard, we can trust the result, giving a QCD prediction for the distribution of three-jet events.

• A related question is what scale to choose for the running coupling α_s. Intuitively, it should be set at the scale of the momenta in the question, i.e. $\sqrt{s}$ for the dijets. However, for more complicated processes there will be multiple invariant momenta; for the three-jet event, one might choose the transverse momentum of the gluon.

• Since the running coupling takes the form

$$\alpha_s(\mu) \sim \frac{1}{\log(\mu/\Lambda)}$$

modifying the scale μ by a factor of 2 changes α_s by $O\left(\alpha_s^2\right)$. Thus ambiguities in the scale can be resolved by computing to the next order.

Finally, we take a closer look at the spectral density.

• We define the two-point function

$$\Pi_h^{\mu\nu}(x,y) = i\left\langle 0\left|TJ^\mu(x)J^\mu(y)\right|0\right\rangle.$$

Since J^μ is the hadronic electric current, we have the QED Ward identity is $q_\mu\Pi_h^{\mu\nu} = 0$, so

$$\Pi_h^{\mu\nu}(q) = \left(-\eta^{\mu\nu}q^2 + q^\mu q^\nu\right)\Pi_h\left(q^2\right)$$

Intuitively, since the hadronic current couples as $J^\mu A_\mu$, the two-point function is essentially the set of hadronic loop corrections to the amputated photon propagator.

• The analogue of the Kallen-Lehmann spectral representation for vectors gives

$$\Pi_h\left(q^2\right) = \int_0^\infty ds \frac{\rho_h(s)}{s - q^2 - i\epsilon}$$

Then $\Pi_h\left(q^2\right)$, as a function of complex q^2, gets a branch cut starting at the masses of the lightest hadrons.

• Note that we can compute $\Pi_h\left(q^2\right)$ at large spacelike momenta, $-q^2 \gg 1$, where perturbation theory holds and we are far from the nonanalyticities. We can then analytically continue to large timelike momenta, which are relevant for hard scatterings.

• We can then use this information to compute $\rho_h\left(q^2\right)$ and thereby make experimental predictions. Note that we may invert the formula above for

$$\rho_h\left(q^2\right)=\lim_{\delta\to 0}\frac{\Pi_h\left(q^2+i\delta\right)-\Pi_h\left(q^2-i\delta\right)}{2\pi i}.$$

This can be computed by integrating the derivative of $\Pi_h(z)$ along any contour connecting the two points. In particular, we can take a large circle of radius q^2. We won't go into much more detail here, but the idea of performing QCD computations by taking advantage of analyticity is related to S-matrix theory and dispersion relations, and leads to "sum rules".

6.6.2 Deep Inelastic Scattering

First, we review the basics of the deep inelastic scattering process.

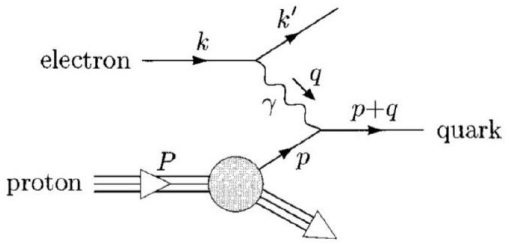
• Historically, the first hint that the strong interaction was asymptotically free came from hadronhadron scattering experiments. In these experiments, the hadrons were shattered into many constituents, but most of them had low transverse momentum, indicating that the components of the hadrons were loosely bound and could not absorb a large momentum.

• We need to talk about transverse momentum because, while the lab frame coincides with the CM frame of the two protons, it generally doesn't coincide with the CM frame of two proton constituents colliding, which may have a longitudinal boost. Another way to quantify the momentum transfer q is via its square q^2, as if q^2 is large and spacelike, the components of $\mathbf{q}$ must be large in any frame.

• In the 1960 s, deep inelastic scattering experiments involving electrons and protons indicated that the proton was made of a small number of pointlike constituents, called partons. The physical picture is that the hard scattering involved a photon exchange between one electron and one parton, while subsequent small- q^2 exchanges between the struck parton and the others produced jets, as we've seen above.

• Just as in Newtonian mechanics, elastic scattering refers to a scattering event where kinetic energy is conserved. In deep inelastic scattering, the proton instead absorbs energy, shattering into many pieces.

• Specifically, consider the following process.



From our earlier work, we know that

$$\sum_{\text{spins}}|\mathcal{M}|^2\sim e^4Q_i^2\frac{s^2+u^2}{t^2}$$

where s,t, and u are the Mandelstam variables for the electron-quark collision.

• Approximating the electron and quark as massless, we find

$$\frac{d\sigma}{dt}\sim\frac{\alpha^2Q_i^2}{s^2}\frac{s^2+(s+t)^2}{t^2}$$

Note that $t=q^2$. Since the momentum transfer is spacelike, we define $Q^2=-q^2$ for convenience.

• Suppose the parton carries a fraction ξ of the proton's momentum, $p=\xi P$. Then

$$s = (p+k)^2 = 2p\cdot k = 2\xi P\cdot k = \xi s'$$

where s' is a Mandelstam variable for the electron-proton collision. Since the electron-parton scattering is elastic,

$$0 \approx (p+q)^2 = 2p\cdot q + q^2 = 2\xi P\cdot q - Q^2$$

so we may measure ξ from observations of the electron alone,

$$\xi = x \equiv \frac{Q^2}{2P\cdot q}$$

• We let $f_i(x)$ be a parton distribution function, denoting the probability that the constituent i carries longitudinal momentum fraction x. Combining our results,

$$\frac{d^2\sigma}{dxdQ^2} \sim \sum_i f_i(x) Q_i^2 \frac{\alpha^2}{Q^4}\left(1+\left(1-\frac{Q^2}{xs'}\right)^2\right)$$

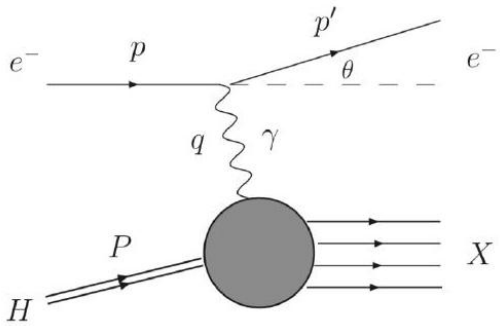
The only part of this cross section that depends on the strong interaction is $f_i(x)$, while everything else is just from the QED amplitude and the phase space kinematics. Dividing the cross section by these extra factors gives a cross section independent of Q^2, a prediction known as Bjorken scaling, validated to 10% accuracy for $Q \gtrsim 1\text{GeV}$.

• Physically, Bjorken scaling means that the proton appears the same to an electromagnetic probe, no matter how hard the proton is struck. This is sensible, because for high Q, the scattering process is much faster than the internal dynamics of the proton.

• On the other hand, Bjorken scaling should be corrected by emission of high-momentum partons; this remains possible at arbitrarily high energies as the strong coupling only decays to zero logarithmically. Thus the parton distribution functions depend logarithmically on Q^2 and their RG evolution equations are called the Altarelli-Parisi or DGLAP equations.

Next, we turn to a quantitative analysis of the cross section for deep inelastic scattering.

• We consider a scattering process $H + e^- \to X + e^-$, where X stands for a hadronic final state.



Applying ordinary QED to the interaction, we have

$$\mathcal{M} = (-ie)^2 \bar{u}_e(p')\gamma^\mu u_e(p)\frac{-i\eta_{\mu\nu}}{q^2}\langle X|J_h^\nu|H(P)\rangle$$

• Working in the hadron rest frame, we have

$$d\sigma = \frac{1}{4EM}\frac{d\mathbf{p}'}{2p'^0}\sum_{X,p_X}\phi(q+P-p_X)\frac{1}{2}\sum_{\text{spins}}|\mathcal{M}|^2$$

where the sum over p_X includes the Lorentz invariant phase space factors for a variable number of final state particles, we average over the initial spin of the electron, assuming the hadron H is spinless, and M is the mass of H.

• The squared matrix element takes the form

$$\frac{1}{2}\sum_{\text{spins}}|\mathcal{M}|^2 = \frac{e^4}{2q^4}L_{\mu\nu}\left\langle H(P)\left|J_h^\mu\right|X\right\rangle\left\langle X\left|J_h^\nu\right|H(P)\right\rangle$$

Treating the electron as massless, we have

$$L_{\mu\nu} = \sum_{\text{spins}}\bar{u}(p)\gamma_\mu u\left(p'\right)\bar{u}\left(p'\right)\gamma_\nu u(p) = \text{tr}\left(\not{p}\gamma_\mu\not{p}'\gamma_\nu\right) = 4\left(p_\mu p'_\nu + p'_\mu p_\nu - \eta_{\mu\nu}p\cdot p'\right)$$

• Next, we define

$$W_H^{\mu\nu}(q,P) = \frac{1}{4\pi}\sum_X \phi\left(q+P-p_X\right)\left\langle H(P)\left|J_h^\mu\right|X\right\rangle\left\langle X\left|J_h^\nu\right|H(P)\right\rangle$$

so the differential cross section is

$$E'\frac{d\sigma}{d\mathbf{p}'} = \frac{1}{32\pi^2 EM}\frac{e^4}{q^4}L_{\mu\nu}W_H^{\mu\nu}$$

• Since $W_H^{\mu\nu}$ is contracted with $L_{\mu\nu}$, we can take it to be symmetric. By current conservation, $q^\mu L_{\mu\nu} = 0$, which means we can choose $q_\mu W_H^{\mu\nu} = 0$. Then we have two form factors,

$$W_H^{\mu\nu} = \left(-\eta^{\mu\nu} + \frac{q^\mu q^\nu}{q^2}\right)W_1 + \left(P^\mu - \frac{P\cdot q}{q^2}q^\mu\right)\left(P^\nu - \frac{P\cdot q}{q^2}q^\nu\right)W_2$$

where W_1 and W_2 are Lorentz scalars that only depend on

$$Q^2 \equiv -q^2 = 2p\cdot p', \quad \nu = P\cdot q$$

Using $q^\mu L_{\mu\nu} = 0$ we find

$$L_{\mu\nu}W_H^{\mu\nu} = 8p\cdot p'W_1 + 4\left(2(p\cdot P)\left(p'\cdot P\right) - M^2 p\cdot p'\right)W_2 = 4Q^2W_1 + 2M^2\left(4EE' - Q^2\right)W_2$$

where E and E' are the initial and final electron energies.

• Introducing the dimensionless variables

$$x = \frac{Q^2}{2\nu}, \quad y = \frac{P\cdot q}{P\cdot p} = \frac{\nu}{ME}$$

where $x, y \in [0,1]$ and taking the high-energy limit,

$$L_{\mu\nu}W_H^{\mu\nu} \approx 8EM\left(xyW_1 + \frac{1-y}{y}\nu W_2\right)$$

where we neglected the Q^2W_2 term since it is a factor of M/E smaller.

• Next, the momentum differential may be rewritten as

$$d\mathbf{p}' = 2\pi E'^2 d(\cos\theta)dE' = \pi E' dQ^2 dy = 2\pi E' dx dy$$

Therefore, the differential cross section is

$$\frac{d\sigma}{dxdy} = \frac{4\pi\alpha^2}{Q^4} 2ME\left(xy^2 F_1\left(x,Q^2\right) + (1-y)F_2\left(x,Q^2\right)\right)$$

where we have defined the dimensionless structure functions $F_1 = W_1$ and $F_2 = \nu W_2$.

We can further parametrize the structure functions using light-cone variables.

• Given an arbitrary four-vector V^μ we define

$$V^\pm = V^0 \pm V^3, \quad \mathbf{V}_\perp = \left(V^1, V^2\right)$$

so the inner product is

$$V \cdot U = \frac{1}{2}\left(V^+U^- + V^-U^+\right) - \mathbf{V}_\perp \cdot \mathbf{U}_\perp$$

• Again working in the rest frame of the hadron, we choose the photon momentum to be along $\hat{e}_3$, so $\mathbf{P}_\perp = \mathbf{q}_\perp = 0$. Then

$$Q^2 = -q^+q^-, \quad \nu = \frac{1}{2}\left(q^+P^- + q^-P^+\right)$$

In the deep inelastic limit, we take $q^- \to \infty$ with $q^+ \sim P^+$, giving

$$x \sim -\frac{q^+}{P^+}, \quad \nu \sim \frac{q^-P^+}{2}$$

• Also, in this frame we have

$$W_H^{+-}(q,P) = -W_1 + \left(P - \frac{P\cdot q}{q^2}q\right)^2 W_2 = -W_1 + \left(M^2 + \frac{\nu^2}{Q^2}\right)W_2 \equiv F_L\left(x,Q^2\right)$$

In the deep inelastic limit,

$$F_L\left(x,Q^2\right) \approx -F_1\left(x,Q^2\right) + \frac{1}{2x}F_2\left(x,Q^2\right)$$

We also have the identities

$$W_H^{++}(q,P) = \frac{\left(q^+\right)^2}{Q^2}F_L\left(x,Q^2\right), \quad W_H^{--}(q,P) = \frac{\left(q^-\right)^2}{Q^2}F_L\left(x,Q^2\right)$$

Thus everything can be parametrized in terms of the longitudinal structure function F_L.

We can further simplify by applying the parton model, writing the structure functions in terms of parton distribution functions, but we won't go into the details here.

6.6.3 Chiral Symmetry

We now introduce the chiral symmetry of QCD, leading up to chiral perturbation theory.

• We consider QCD with N flavors of quarks,

$$\mathcal{L} = -\frac{1}{4}G_a^{\mu\nu}G_{a\mu\nu} + \sum_i \bar{q}_i\left(i\not{D} - m_f\right)q_i$$

We suppress color indices for the quarks throughout, contracting them implicitly.

• For massless quarks, we have the symmetry group

$$G = U(1)_L \times U(1)_R \times SU(N)_L \times SU(N)_R$$

from unitary rotations of the left-chiral and right-chiral quarks. This group may be generated by a combination of vector symmetries, which rotate them the same way, and axial symmetries, which rotate them oppositely.

• The $U(1)_V$ and $U(1)_A$ symmetries are

$$q \to \exp(-i\theta)q, \quad q \to \exp\left(-i\theta\gamma_5\right) q$$

where q is a vector of the quark fields, with conserved currents

$$V_\mu = \bar{q}\gamma_\mu q, \quad A_\mu = \bar{q}\gamma_\mu\gamma_5 Q$$

The $U(1)_V$ symmetry corresponds to baryon number, while the $U(1)_A$ symmetry is anomalous. Since $U(1)$ is abelian, these symmetries do not yield any degeneracies.

• The vector and axial $SU(N)$ symmetries are

$$q \to \exp\left(-i\alpha^a T^a\right) q, \quad q \to \exp\left(-i\alpha^a T^a\gamma_5\right) q$$

respectively. The corresponding conserved currents are

$$V_\mu^a = \bar{q}\gamma_\mu T^a q, \quad A_\mu^a = \bar{q}\gamma_\mu\gamma_5 T^a q$$

The total axial charge is parity-odd, since γ_0 and γ_5 anticommute, and thus it should yield degeneracies between hadrons with opposite parities. But no such degeneracies are observed.

• Sometimes we will be sloppy and write $SU(N)_L \times SU(N)_R \cong SU(N)_V \times SU(N)_A$. This isn't correct, because composing axial transformations instead yields all of $SU(N)_L \times SU(N)_R$. We can define $SU(N)_A$ as the coset space $SU(N)_L \times SU(N)_R / SU(N)_V$, which is a manifold that is topologically $SU(N)$, but it does not have a group structure. Similarly, the set of axial generators $\mathfrak{su}(N)_A$ is well-defined, but it is not an algebra, because the bracket isn't closed. (However, this doesn't change the fact that the generators correspond to conserved currents, as long as each individual one indeed generates a symmetry.)

• Also note that a set of N uncharged quarks has a much larger symmetry group, since we can separate the two chiral components of each Dirac field,

$$\mathcal{L} = i\overline{q_L}\not{\partial} q_L + i\overline{q_R}\not{\partial} q_R.$$

Using charge conjugation, we can rewrite this in terms of $2N$ Weyl fields,

$$\mathcal{L} = i\bar{\Psi}\not{\partial}\Psi, \quad \Psi = \begin{pmatrix} \psi_L \\ (\psi_c)_L \end{pmatrix}, \quad \psi_c = C\psi^*$$

which has an $SU(2N) \times U(1)$ symmetry. This is a perfectly legitimate symmetry, but it is hidden when working with Dirac fields because in that case it would be partly antilinear. It is not useful in QCD, because the extra symmetries are broken by the coupling to the gauge field.

• Now we consider quark masses, which break further symmetries. Mass terms have the form

$$\mathcal{L} \supset \overline{q_L} M q_R + \text{ h.c.}$$

so that under a chiral transformation,

$$M \to L^\dagger M R$$

Hence a chiral field redefinition can be used to make M real and diagonal.

• Mass terms always break axial symmetry. If all the masses are different, the symmetry is broken down to $U(1)^N$, the individual quark numbers. If the masses are the same, the full

vector symmetry is preserved. (The different quark electric charges also break symmetries, but we ignore these because electromagnetism is weak.)

• In QCD, only the up, down, and strange quarks are reasonably light. If we consider only the up and down, the small mass difference means $SU(2)_V$ is a very good symmetry; it is isospin. Since their absolute masses are small compared to Λ_{QCD}, $SU(2)_A$ should be almost as good, but this is not observed.

To fix this problem, we introduce the quark condensate, starting with two quark flavors.

• We postulate the QCD vacuum has a "quark condensate" analogous with the condensate of Cooper pairs in a superconductor,

$$\langle \Omega \left| \bar{q}_{Ri} q_{Lj} \right| \Omega \rangle = -v^3 \delta_{ij}, \quad v \approx 250\text{GeV}$$

where the minus sign ensures the vacuum energy is lowered. It isn't known exactly how to show the right-hand side is proportional to δ_{ij}, but we know this must be the case, or else $SU(2)_V$ would be badly broken.

• The vacuum is only invariant under $U(1)_V$ and $SU(2)_V$, so we expect pseudo-Nambu-Goldstone bosons (PNGBs) from the broken symmetries, $U(1)_A$ and " $SU(2)_A$ ". This hypothesis was once called "partially conserved axial current" (PCAC).

• The formation of the quark condensate occurs in a phase transition, which occurs approximately concurrently with the confinement transition for QCD, since Λ_{QCD} is the only relevant mass scale in the theory. However, in supersymmetric gauge theories only confinement occurs.

• The PNGBs corresponding to $SU(2)_A$ are the pions, which are indeed far lighter than any other hadron. They are generated by the axial current,

$$\left\langle \Omega \left| A^a_\mu(x) \right| \pi^b(q) \right\rangle = i f_\pi q_\mu \delta^{ab} e^{-iqx}, \quad f_\pi \approx 92\text{MeV}$$

However, there is no PNGB observed for $U(1)_A$, and this was called the $U(1)_A$ problem.

• Because of the axial anomaly, the $U(1)_A$ current obeys

$$\partial_\mu J^\mu_5 = \frac{\alpha_s}{4\pi} G^{\mu\nu}_a \tilde{G}_{a\mu\nu}, \quad J^\mu_5 = \frac{1}{2} \bar{Q} \gamma^\mu \gamma_5 Q$$

However, this doesn't solve the $U(1)_A$ problem alone because $G\tilde{G}$ is a total derivative, so one can define a modified (approximately) conserved axial current, which again requires a PNGB. The real resolution requires accounting for QCD instantons, as covered in the notes on Quantum Field Theory.

• More generally, we may extend to three flavors, where the PNGBs corresponding to $SU(3)_A$ are the three pions, the four kaons, and the η. The particle that should be the PNGB for $U(1)_A$ is the η', which is much heavier; this is the $U(1)_A$ problem again. Explicitly, the masses are

$$\pi^\pm, \pi^0 : 140\text{MeV}, \quad K^\pm, K^0, \bar{K}^0 : 500\text{MeV}, \quad \eta : 550\text{MeV}, \quad \eta' : 950\text{MeV}$$

These mesons are pseudoscalars because they are the Goldstone bosons related to the breaking of axial symmetry, and axial symmetries pick up an extra sign under parity.

• Note that for two quark flavors, the $SU(2)_L$ symmetry is simply weak isospin, which uncoincidentally is also called $SU(2)_L$. Hence the quark condensate would break electroweak symmetry if the electroweak phase transition hadn't done it already.

Example. Alternative scenarios of symmetry breaking. First suppose the color group was $SO(3)$ and the quarks transformed in the 3. Since this representation is real, we may write the theory in terms of $2N$ Weyl spinors $\chi_{\alpha i}$ transforming in the 3. The symmetry group is $SU(2N)$, and the $U(1)$ factor is anomalous as before. The condensate that preserves the most symmetry is

$$\langle \Omega \left| \chi_{\alpha i} \chi_{\alpha j} \right| \Omega \rangle = -v^3 \delta_{ij}$$

and the remaining symmetry group is $SO(2N)$, by redefinitions of the form

$$\chi_{\alpha i} \to O_{ij} \chi_{\alpha j}$$

Next, suppose that the color group was $SU(2)$ and the quarks transformed in the 2. By the same reasoning, the symmetry group is $SU(2N)$. The general form of the condensate is

$$\left\langle \Omega \left| \epsilon^{\alpha\beta} \chi_{\alpha i} \chi_{\alpha j} \right| \Omega \right\rangle = -v^3 \eta_{ij}$$

where the $\epsilon^{\alpha\beta}$ factor is necessary to get a color singlet, which forces η_{ij} to be antisymmetric. Then the most symmetric condensate is one where $\eta^2 = -I$, preserving the symmetry $Sp(2N)$.

Example. Consider N real scalar fields that transform in a representation R. If R is real, the flavor symmetry is clearly $SO(N)$. If R were complex, there would have to be another N real scalar fields transforming in $\bar{R}$, because the overall representation must be real; they are collectively equivalent to N complex scalar fields transforming in R with flavor symmetry $SU(N)$. If R is pseudoreal, it turns out the flavor symmetry is not $SO(N)$, but $Sp(2N)$.

6.6.4 Chiral Perturbation Theory

Putting aside the $U(1)_A$ problem, we can be more quantitative using chiral perturbation theory, historically one of the most sophisticated examples of effective field theory, which describes the low-energy dynamics of QCD. We begin by ignoring quark masses.

• In chiral perturbation theory, we allow the quark condensate to vary,

$$\delta_{ij} \to U_{ij}(x), \quad U(x) = \exp\left(\frac{2i\pi^a(x) T^a}{f_\pi}\right)$$

so the fields $\pi^a(x)$ correspond to the pions and other light mesons. Since we are ignoring $U(1)_A$, we have $U(x) \in SU(3)$, and the T^a are the Gell-Mann matrices. If we only consider the up and down quarks, then $U(x) \in SU(2)$ and the T^a are the Pauli matrices.

• The field $U(x)$ transforms in the bifundamental of $SU(3)_L \times SU(3)_R$,

$$U(x) \to L U(x) R^\dagger$$

The pion fields $\pi^a(x)$ parametrize the vacuum manifold. For a vector transformation we have

$$U(x) \to L U(x) L^\dagger, \quad \pi(x) \to L \pi(x) L^\dagger$$

while for an axial transformation,

$$U(x) \to L U(x) L, \quad \pi(x) \to \pi^a(x) + f_\pi \alpha^a + \ldots, \quad L = e^{i\alpha^a T^a}$$

• We see the unbroken symmetries act on the $\pi^a(x)$ linearly, while the broken symmetries act infinitesimally by shifts, ensuring the Goldstone bosons are massless. The general procedure for writing broken and unbroken symmetries in this form is called the CCWZ construction. At the quantum level, we build our Hilbert space on the physical vacuum. The unbroken symmetries act on this Hilbert space, while the broken symmetries relate these states to excitations about other vacuums, and hence do not yield degeneracies.

• Next, we write down every term consistent with the symmetries. The Lagrangian must be invariant under $SU(3)_L \times SU(3)_R$, which means that a U must always be next to a $U^\dagger$. But we always need derivatives, because $U^\dagger U = 1$. Hence we have

$$\mathcal{L} = \frac{f_\pi^2}{4} \operatorname{tr}\left(\partial_\mu U^\dagger \partial^\mu U\right) + \dots$$

Since U is a nonlinear function of the pion fields, the quadratic term alone is enough to do nontrivial computations. Expanding and neglecting $O(1)$ factors and $SU(3)$ indices,

$$\mathcal{L} = \frac{1}{2}\partial_\mu \pi \partial^\mu \pi + \frac{1}{f_\pi^2}\pi^2 \partial_\mu \pi \partial^\mu \pi + \dots$$

In particular, the symmetry ensures that there are no relevant interaction terms at all!

• There are relations between the infinitely many coefficients in the Lagrangian in terms of π. These relations were originally understood by current algebra, but in chiral perturbation theory, we get them easily because we know that U transforms linearly.

• The second term above is the leading contribution to $\pi\pi \to \pi\pi$ scattering. The cross section can be estimated as follows.

• If the pions are relativistic, we may ignore their masses, so the only mass scales are f_π and the Mandelstam variables.

• The f_π can only enter through the matrix element, $\mathcal{M} \propto 1/f_\pi^2$, so $\sigma \propto 1/f_\pi^4$.

• By dimensional analysis, σ has degree 1 in the Mandelstam variables. There is no way to get a Mandelstam variable in the denominator, because we aren't doing any kind of particle exchange (compare the $1/t$ in $e^+e^- \to e^+e^-$scattering).

• In general, for two particles in the final state, the phase space integrals will contribute a factor like $1/8\pi$, while for three particles we get $1/64\pi^3$.

Therefore, we conclude $\sigma \sim (s+t)/8\pi f_\pi^4$.

• Contributions also come from higher order terms, such as

$$\mathcal{L} \supset \operatorname{tr}\left(\partial_\mu U^\dagger \partial^\mu U\right)^2 \supset \frac{1}{f_\pi^4}\left(\partial_\mu \pi \partial^\mu \pi\right)^2$$

The matrix element here is smaller by a factor of p^2/f_π^2. Hence the cross section, which is the square of the sum of the matrix elements, is modified by $O\left(p^2/f_\pi^2\right)$. Hence chiral perturbation theory is a perturbation series in p^2/f_π^2.

• For pion-pion scattering at tree level, only the terms quadratic and quartic in U can contribute, since all others have too many powers of π. Hence tree level results are fully parametrized by only a few parameters, and the real test is controlling the loop corrections. The logarithms in cross sections due to loops are called chiral logs and are a signature of quantum effects.

• Loop corrections are suppressed by a factor of $1/(4\pi)^2$, so the real expansion parameter is $p/4\pi f_\pi$. Hence we were justified in treating the pions relativistically, because

$$4\pi f_\pi \approx 1\text{GeV} \gg m_\pi$$

Moreover, we may estimate error of any calculation to n loops as $(p/4\pi f_\pi)^{n+1}$.

Note. Chiral perturbation theory is closely related to sigma models. In the original linear sigma model, one takes a set of two complex scalar fields and performs spontaneous symmetry breaking, yielding a massive field σ and massless Goldstone bosons associated with the pions. At low energies, the σ decouples, yielding a "nonlinear sigma model", which now is a generic term for any field theory whose fields take values on a manifold. Chiral perturbation theory is simply a nonlinear sigma model where the σ would have corresponded to a variation of v.

Next, we account for the quark masses and other couplings.

• We are justified in treating the strange quark mass perturbatively because $m_s \ll 4\pi f_\pi$. In general, a mass will contribute to the Lagrangian as

$$\mathcal{L} \supset -\bar{q}_L M q_R + \text{ h.c.}$$

where M is a complex matrix. If we simply replace $\overline{q_L} q_R$ with its vev, we get the leading term,

$$\mathcal{L} = v^3 \operatorname{tr}\left(MU + M^\dagger U^\dagger\right).$$

We can find higher-order terms by treating M as a spurion field that transforms as $M \to LMR^\dagger$.

• Expanding this leading term, we have

$$\mathcal{L} \supset -\frac{4v^3}{f_\pi^2} \operatorname{tr}\left(MT^a T^b\right) \pi^a \pi^b = -\frac{2v^3}{4_\pi^2} \operatorname{tr}\left(M\left\{T^a, T^b\right\}\right) \pi^a \pi^b$$

In the case of two quark flavors, this may be simplified using $\left\{T^a, T^b\right\} = \delta^{ab}/2$ for $SU(2)$ generators. We find that all three pions satisfy the Gell-Mann-Oakes-Renner equation

$$m_\pi^2 = 2\left(m_u + m_d\right) v^3 / f_\pi^2$$

In reality, the pions are split due to electromagnetic effects.

• For three quark flavors, a longer version of the same computation relates the pion, kaon, and η masses, giving the Gell-Mann-Okubo formula.

• To establish the parameter f_π is really the pion decay constant, we can couple the pion fields to leptons using the four-Fermi interaction and calculate the decay rate.

• To compute nucleon-pion scattering, for two quark flavors, we have a Dirac nucleon field

$$N = \begin{pmatrix} p \\ n \end{pmatrix}$$

that transforms as

$$P_L N \to L P_L N, \quad P_R N \to R P_R N$$

The only possible mass term for the nucleons is

$$\mathcal{L} \supset -m_N \bar{N}\left(U^\dagger P_L + U P_R\right) N$$

which yields a pion-nucleon-nucleon coupling.

• Alternatively, we may couple the pion fields to quark fields, which transform similarly. This is valid for energies above Λ_{QCD} and below $4\pi f_\pi$. In both cases we write down all terms consistent with chiral symmetry.

• To account for the different electric charges of the quarks, pions, or nuclei, we simply promote derivatives in the chiral Lagrangian to covariant derivatives.

Further refinements, including a solution to the $U(1)_A$ problem, require an understanding of anomalies, which are covered in the notes on Quantum Field Theory.

6.6.5 The Strong CP Problem

First, we introduce the strong CP problem.

• The θ parameter is modified by chiral rotations of the quark fields by the chiral anomaly. Specifically, after electroweak symmetry breaking the quark mass matrices are neither Hermitian nor diagonal; integrating out the Higgs we have

$$\mathcal{L} \supset \bar{q}_{R_i} M_{ij} q_{L_j} + \text{ h.c.}$$

and the matrix may be diagonalized by $SU(N_f)_A \times SU(N_f)_V$ transformations on the quark fields. To remove the overall phase, we require $U(1)_A$ transformations,

$$q_R \to e^{i\alpha/2} q_R, \quad q_L \to e^{-i\alpha/2} q_L$$

which shift the vacuum angle by an amount proportional to α, as can be understood by considering the $SU(3)^2 U(1)_A$ anomaly. The invariant quantity is

$$\bar{\theta} = \theta - \arg\det M$$

where M is the quark mass matrix.

• The value of $\bar{\theta}$ may be measured from the neutron electric dipole moment, yielding

$$\bar{\theta} \lesssim 10^{-10}$$

The strong CP problem asks why this holds. It is especially puzzling because the two contributions to $\bar{\theta}$ appear to be completely unrelated.

• The chiral anomaly explains why all the θ-vacua are equivalent if any quark, such as the up quark, is exactly massless. In that case we can perform arbitrary chiral rotations on that quark field without physical effect, rotating θ to zero. This was once proposed as a solution to the strong CP problem, though it is disfavored by lattice computations.

• For the purposes of calculation, it's most useful to rotate so that $\theta = 0$, and work with the complex masses in chiral perturbation theory. The presence of the masses yields a $\bar{\theta}$-dependent QCD vacuum energy, which will provide the axion potential. This setup is also used to compute the neutron electric dipole moment.

We now compute the QCD vacuum energy.

• By rotating $\bar{\theta}$ into the quark mass matrix, we can take without loss of generality,

$$\theta = 0, \quad M = \begin{pmatrix} m_u & & \\ & m_d & \\ & & m_s e^{-i\bar{\theta}} \end{pmatrix}$$

where the m_i are all real. As a result, to minimize the vacuum energy, the pion fields pick up vevs. We can neglect all non-diagonal fields, because if they picked up a vev, they would break $U(1)_A$ symmetry. The general intuition here is that a minimum is often a point of enhanced symmetry (the exception being spontaneous symmetry breaking), which is essentially the reason that the vacuum energy is minimized at the CP preserving point $\theta = 0$.

• Plugging this expression in, we find

$$\mathcal{L} \supset 2v^3 \left(m_u \cos\varphi_u + m_d \cos\varphi_d + m_s \cos\left(\varphi_s + \bar{\theta}\right) \right)$$

where the pion fields are

$$U = \operatorname{diag}\left(e^{i\varphi_u}, e^{i\varphi_d}, e^{i\varphi_s}\right), \quad \varphi_u + \varphi_d + \varphi_s = 0$$

We wish to maximize this expression to minimize the potential energy.

• Since $m_s \gg m_u, m_d$, we will have $\varphi_u + \varphi_d \approx \bar{\theta}$. Deviations from this equality can lower the potential energy by terms higher order in m_u/m_s, which we neglect. Differentiating, we have

$$m_u \sin\varphi_u = m_d \sin\varphi_d$$

By applying the law of sines and law of cosines to an appropriately chosen triangle,

$$\frac{\sin\varphi_u}{m_d} = \frac{\sin\varphi_d}{m_u} = \frac{\sin\bar{\theta}}{\sqrt{m_u^2 + m_d^2 + 2m_u m_d \cos\bar{\theta}}}$$

Plugging this in and using the Gell-Mann-Oakes-Renner equation, we find the vacuum energy

$$V(\bar{\theta}) = -m_\pi^2 f_\pi^2 \sqrt{1 - \frac{4m_u m_d}{(m_u + m_d)^2} \sin^2\left(\frac{\bar{\theta}}{2}\right)} \approx \frac{1}{2} m_\pi^2 f_\pi^2 \frac{m_u m_d}{(m_u + m_d)^2} \bar{\theta}^2$$

Part III
Reactions and Decays of Particles

7 Other reactions

Let's discuss other reactions and decays with particles.

7.1 Rare Weak Decays of the Omega Baryon by Mommers

7.1.1 Introduction

QCD and the spirit of effective field theories

Our current understanding of elementary particles is realized in the Standard Model of particle physics. The model describes the strong and electroweak interactions, with gravity remaining absent. Via the Higgs mechanism the electroweak interaction breaks down into the electromagnetic and weak interactions [1. The spontaneous breaking of electroweak symmetry gives rise to the massless gauge boson of quantum electrodynamics (the photon) and to the three massive gauge bosons that generate the weak force ($W^{\pm}$and Z^0). The gauge bosons of the strong interaction are the gluons and the strong force due to exchange of gluons is described by quantum chromodynamics (QCD). QCD is a non-Abelian gauge theory based on SU(3) gauge symmetry, whose conserved charges are called colors.

A salient feature of QCD is that it is strongly coupled at low energies [2], [3]. Its microscopic degrees of freedom, quarks and gluons, are confined to observable, colorless hadrons. Consequently, a perturbative expansion in the coupling constant is no longer valid. Low-energy QCD is an area of ongoing research, and there are many approaches for solving it [4]. One approach, and the mainstay of this thesis, is the use of effective field theories (EFTs).

Effective theories are nothing new in physics. As their name suggests, effective theories model a certain effect, but not necessarily its cause. Calculations are done by expanding to order n in a small, power-counting parameter δ[5]. One can then compute experimentally-measurable quantities up to some finite error of order δ^{n+1}. What is important here is that this expansion in δ is systematic. With enough time and patience it should in principle be possible to expand up to arbitrary order in δ and make the theoretical error as small as desired.

EFTs are powerful, not only because they provide a systematic way to cull errors but also because they can be used in a traditionally non-perturbative regime. An EFT of a more microscopic QFT (say QCD) is constructed by "writing down the most general possible Lagrangian, including all terms consistent with assumed symmetry principles" [6]. In principle, such a Lagrangian has an infinite amount of terms. In practice, although all terms are equal, some are more equal than others. The power-counting scheme ranks interactions based on the order of δ where they become relevant, giving an indication what terms are safe to drop. If done properly, the ordinarily non-renormalizable EFT can be renormalized up to the given power-counting order [7]. The unique EFT of QCD at low energies is chiral perturbation theory (χPT).

Chiral perturbation theory is based on the eponymous (broken) chiral symmetry of QCD (although it should be noted that much of χPT was developed before QCD[8]). When the relevant momentum scale p is much smaller than the chiral-symmetry-breaking scale $\Lambda_\chi \sim$ 1GeV, a good expansion parameter is $\delta = p/\Lambda_\chi$. Historically, χPT described pion fields. Later, it was extended to light meson fields [6], 9] (such as the kaon), octet baryons (such as the proton) and decuplet baryons (such as the Omega baryon) [7, 10, [1].

Hyperon decays and the particle zoo

Ne'eman and Gell-Mann famously brought order to the particle zoo by introducing the organizational principles of the eightfold way [12], [13]. It suggests low-lying spin-0 mesons be collected into an octet and a singlet. The octet contains the kaons ($K^0, K^{\pm}$and $\bar{K}^0$), pions ($\pi^{\pm}$and π^0) and the eta meson (η). The singlet contains the eta prime meson (η'). In a similar fashion, low-lying spin- 1/2 baryons are also part of an octet containing the neutron (n), the proton (p), the Sigma baryons Table 1.1: An overview of important particles appearing in this thesis. Data from [14.

Particle $^{\text{charge}}$	Quark content	Mass [MeV]	Spin $^{\text{parity}}$	Mean lifetime [s]
π^+	$u\bar{d}$	139.57039 ± 0.00018	0^-	$(2.6033 \pm 0.0005) \times 10^{-8}$
π^-	$d\bar{u}$	139.57039 ± 0.00018	0^-	$(2.6033 \pm 0.0005) \times 10^{-8}$
π^0	$\frac{1}{\sqrt{2}}(u\bar{u} - d\bar{d})$	134.9768 ± 0.0005	0^-	$(8.43 \pm 0.13) \times 10^{-17}$
Ξ^-	dss	1321.71 ± 0.07	$\frac{1}{2}^+$	$(1.639 \pm 0.015) \times 10^{-10}$
Ξ^0	uss	1314.86 ± 0.20	$\frac{1}{2}^+$	$(2.90 \pm 0.09) \times 10^{-10}$
Ξ^{*-}	dss	1535.0 ± 0.6	$\frac{3}{2}^+$	$(6.7 \pm 1.3) \times 10^{-23}$
Ξ^{*0}	uss	1531.80 ± 0.32	$\frac{3}{2}^+$	$(7.2 \pm 0.4) \times 10^{-23}$
Ω^-	sss	1672.45 ± 0.29	$\frac{3}{2}^+$	$(0.821 \pm 0.011) \times 10^{-10}$

($\Sigma^{\pm}$and Σ^0), the cascades ($\Xi^-$and Ξ^0) and the strange Lambda baryon (Λ). Low-lying spin-3/2 baryons form a decuplet with the Delta baryons ($\Delta^{++}, \Delta^{\pm}, \Delta^0$), more Sigma baryons ($\Sigma^{*\pm}$ and Σ^{*0}), more cascades (Ξ^{*-} and Ξ^{*0}) and the Omega baryon (Ω^-).

Let us take a closer look at the Omega baryon, the pions and some of the cascades that form the bedrock of this thesis. Table 1.1 summarizes important properties. The pions, being Goldstone bosons, are rather light, and the octet and decuplet baryons are comparatively heavy. Notice that particles in the same multiplet have similar masses.

Baryons that contain one or more strange quarks and no charm, bottom or top quarks are called hyperons. So, the Omega baryon and the cascades are all hyperons. It is also helpful to spell out some more decay-related jargon. The decay mode of a baryon into a lighter baryon and X is called

- semileptonic if X contains a dilepton,
- radiative if X is a photon, and
- nonleptonic if X only contains hadrons.

Chiral perturbation theory is a valuable tool in the study of hyperon decays, be they in any of the above types. Historically, to make calculations analytically tractable, one often worked in the heavy-baryon approximation. In the heavy-baryon approximation relativistic effects are integrated out [10], which works well for systems where those effects are not important. For example, consider the decay $A \to BC$. If $m_A \gg m_B, m_C$, the system is relativistic. If $m_A - m_B \ll m_A, m_B$, relativistic effects are important for the dynamics of C, but not for A and B. If $m_A \approx m_B + m_C$ the system is non-relativistic and the heavy-baryon approximation works best.

The decay $\Omega^- \to \Xi^-\pi^+\pi^-$is of particular experimental and theoretical interest. Heavy-baryon calculations suggest that this decay is dominated by a $\Xi^{*0}(1530)$ resonance $[15 - 17$. Measurements, however, suggest otherwise [18]. This leaves us with several questions: Are relativistic effects important after all? Does χPT break down for this decay? Are the experimental

data correct? The aim of this thesis is to resolve (at least theoretically) these questions via leading-order (LO), tree-level calculations.

The secondary aim of this thesis is to extend some results regarding semileptonic Omega decays. The decay $\Omega^- \to \Xi^0 \mu^- \bar{\nu}_\mu$ goes with low-energy constants (LECs) that also appear in axial-vector transition form factors of a nucleon to a Delta [19]. Empirical data is scanty, or even nonexistent. To that end, we point out what observables are sensible to measure in order to pin down the LECs. This is done at next-to-leading order (NLO), which is still tree level.

There are two remaining points that need to be addressed. First, why should we revisit Omega decays? After all, the tension between experiment and theory has been a well-established fact for over two decades. It is worthwhile to investigate Omega decays expressly now, as Omega baryons are and will be produced in several running and upcoming experiments. These include BESIII, LHCb, Belle-II and PANDA 20]-25]. The intention of this work is to remind experimental groups of a gap in the data and spur them into patching it. Second, we should justify why we will do our calculations at tree-level and either LO or NLO. In short, we are largely constrained by the absence of experimental data. For example, higher-order calculations of nonleptonic decays would introduce new LECs. These LECs would have a large uncertainty due to a lack of data, rendering the higher-order calculations phenomenologically useless. For the semileptonic decay a similar reasoning holds. There, we are fortunate enough to be able to reach NLO. Because we only consider dominant contributions we cannot expect miracles. Our calculations will definitely give results that have the right order of magnitude, and they should be within $20 - 30\%$ of the 'true' value.

Organization of the thesis

This thesis is organized as follows:

- In chapter 2 we compile various textbook knowledge needed for χPT, ranging from decay kinematics, irreducible SU(3) tensor methods and the Rarita-Schwinger formalism.
- In chapter 3 we introduce the leading-order chiral Lagrangian, its diagrammatics and the $\Delta I = 1/2$ rule.
- In chapter 4 we systematically review different chiral conventions that are in use in the literature. We also review heavy-baryon chiral perturbation theory.
- In chapter 5 we calculate and analyze the differential decay distribution for $\Omega^- \to \Xi\pi\pi$ decays and make parameter-free predictions for the lower bound of the branching fraction.
- In chapter 6 we calculate the decay width for the semileptonic Omega decay $\Omega^- \to \Xi^0 \mu^- \bar{\nu}_\mu$. In addition, we discuss the radiative Omega decay $\Omega^- \to \Xi^- \gamma$.
- In chapter 7 we summarize our findings and offer suggestions for further research.

Original work in thesis

The following is a (nonexhaustive) list of novel calculations in this thesis:

- a completely relativistic calculation of the decay width of $\Omega^- \to \Xi^- \pi^+ \pi^-$(previous calculations were non-relativistic),
- a completely relativistic calculation of the decay widths of $\Omega^- \to \Xi^0 \pi^- \pi^0$ and $\Omega^- \to \Xi^- \pi^0 \pi^0$ (no prior calculations exist),
- fully differential Dalitz plots for the three aforementioned decays,

- an explicit $\Delta I = 1/2$-focused treatment of two- and three-body Omega decays,
- a completely relativistic calculation of the decay $\Omega^- \to \Xi^0 \mu^- \bar{\nu}_\mu$.

7.1.2 Theoretical preliminaries

In this chapter we briefly review some theoretical preliminaries for chiral perturbation theory. Most, if not all, of the theory should be familiar, and to that end we will be somewhat terse in our exposition.

Kinematics

As this work is concerned with particle decays, it is important that we review basic kinematic theory. In our review we follow ref. 14. The main quantity of interest is the decay rate (or width) Γ, which is the inverse of a particle's lifetime. It is defined in the decaying particle's rest frame. If a particle has multiple decay channels, the total decay rate will be the sum of the partial decay rates. The branching ratio (or fraction) $\mathcal{B}$, of a particular channel is the ratio of the channel's partial decay rate over the total decay rate.

Let the decaying particle have momentum P and mass M, and the n particles into which it decays have momentum p_i and mass m_i, with energies $E_i = \sqrt{\boldsymbol{p}_i^2 + m_i^2}$ in the rest frame of the decaying particle. Then, the differential decay rate is given by

$$\mathrm{d}\Gamma(1 \to n) = \frac{(2\pi)^4}{2M} |\mathcal{M}(1 \to n)|^2 \delta^{(4)} \left(P - \sum_{i=1}^{n} p_i \right) \prod_{i=1}^{n} \frac{\mathrm{d}p_i}{(2\pi)^3 2E_i},$$

where $\mathcal{M}(1 \to n)$ is the Lorentz-invariant matrix element (also known as the Feynman matrix element) [26]. We can integrate the differential decay rate to get the total decay rate

$$\Gamma(1 \to n) = \frac{1}{\prod_i (N_i!)} \int \mathrm{d}\Gamma(1 \to n),$$

where N_i is the number of indistinguishable final particles of type i. Often, we do not care about the spin and polarization of our particles. When this is the case, we will work with the spin-averaged Feynman matrix element,

$$|\mathcal{M}(1 \to n)|^2 \mapsto \left\langle |\mathcal{M}(1 \to n)|^2 \right\rangle = \frac{1}{\sum_i} \sum_{i,f} |\mathcal{M}(1 \to n)|^2,$$

which simplifies our calculations. Here, i and f denote the initial and final spins and polarizations. In general, $\langle |\mathcal{M}(1 \to n)|^2 \rangle$ depends on at most $3n - 7$ independent variables and is a constant if $n \leq 2$ 27.

Two-body decay

The simplest decay process is a two-body decay ($n = 2$). In this case the spin-averaged matrix element is constant and the decay rate is given by

$$\Gamma(1 \to 2) = \frac{|\boldsymbol{p}_1|}{8\pi M^2} \left\langle |\mathcal{M}(1 \to 2)|^2 \right\rangle \Theta\left(M - m_1 - m_2\right).$$

The modulus of the center-of-mass momentum is

$$|\boldsymbol{p}_1| = \frac{\lambda^{1/2}\left(M^2, m_1^2, m_2^2\right)}{2M},$$

where $\lambda(a, b, c)$ is the Källén function and $\Theta(x)$ is the Heaviside step function.

Three-body decay

For a three-body decay, the spin-averaged matrix element can depend on at most two independent variables. We will use

$$m_{12}^2 = (p_1 + p_2)^2\,, \quad m_{23}^2 = (p_2 + p_3)^2\,.$$

Alternatively, we will use the notation where $m_{12}^2 = m^2(AB)$, where A and B are the particles corresponding to momentum one and two. A third, dependent variable is

$$m_{13}^2 = (p_1 + p_3)^2\,,$$

related to the other two by

$$m_{12}^2 + m_{23}^2 + m_{13}^2 = M^2 + m_1^2 + m_2^2 + m_3^2.$$

We can express the inner product of all combinations of the momenta in terms of the particle masses and the two independent variables,

$$\begin{aligned}
p_1 \cdot p_2 &= \tfrac{1}{2}\left(m_{12}^2 - m_1^2 - m_2^2\right), & p \cdot p_1 &= \tfrac{1}{2}\left(-m_{23}^2 + M^2 + m_1^2\right),\\
p_1 \cdot p_3 &= \tfrac{1}{2}\left(-m_{12}^2 - m_{23}^2 + M^2 + m_2^2\right), & p \cdot p_2 &= \tfrac{1}{2}\left(m_{12}^2 + m_{23}^2 - m_1^2 - m_3^2\right),\\
p_2 \cdot p_3 &= \tfrac{1}{2}\left(m_{23}^2 - m_2^2 - m_3^2\right), & p \cdot p_3 &= \tfrac{1}{2}\left(-m_{12}^2 + m^2 + m_3^2\right).
\end{aligned}$$

The kinematic boundaries are given by

$$\begin{aligned}
(m_1 + m_2)^2 \leq m_{12}^2 \leq (M - m_3)^2\\
\left(m_{23}^2\right)_{\min} \leq m_{23}^2 \leq \left(m_{23}^2\right)_{\max}
\end{aligned}$$

with

$$\begin{aligned}
\left(m_{23}^2\right)_{\max} &= (E_2^* + E_3^*)^2 - \left(\sqrt{E_2^{*2} - m_2^2} - \sqrt{E_3^{*2} - m_3^2}\right)^2\\
\left(m_{23}^2\right)_{\min} &= (E_2^* + E_3^*)^2 - \left(\sqrt{E_2^{*2} - m_2^2} + \sqrt{E_3^{*2} - m_3^2}\right)^2
\end{aligned}$$

where

$$E_2^* = \frac{m_{12}^2 - m_1^2 + m_2^2}{2\sqrt{m_{12}^2}}, \quad E_3^* = \frac{-m_{12}^2 + M^2 - m_3^2}{2\sqrt{m_{12}^2}},$$

are the energy of particles two and three in the frame where $\boldsymbol{p}_1 + \boldsymbol{p}_2 = \boldsymbol{0}$. In these variables, the double-differential decay rate is given by

$$\frac{\mathrm{d}^2\Gamma(1 \to 3)}{\mathrm{d}m_{12}^2\,\mathrm{d}m_{23}^2} = \frac{1}{32(2\pi)^3 M^3}\left\langle|\mathcal{M}(1 \to 3)|^2\right\rangle$$

It is often convenient to change variables from m_{23}^2 to $\cos\theta$, where θ is the angle between the three-momenta $\boldsymbol{p}_2$ and $\boldsymbol{p}_3$ in the frame where $\boldsymbol{p}_1 + \boldsymbol{p}_2 = \boldsymbol{0}$. We can do so using

$$\begin{aligned}
m_{23}^2 &= (p_2 + p_3)^2 = (E_2^* + E_3^*)^2 - \boldsymbol{p}_2^2 - \boldsymbol{p}_3^2 - 2\,|\boldsymbol{p}_2|\,|\boldsymbol{p}_3|\cos\theta,\\
\mathrm{d}m_{23}^2 &= -2\,|\boldsymbol{p}_2|\,|\boldsymbol{p}_3|\,\mathrm{d}\cos\theta,
\end{aligned}$$

where

$$|\boldsymbol{p}_2| = \frac{\lambda^{1/2}\left(m_{12}^2, m_1^2, m_2^2\right)}{2\sqrt{m_{12}^2}}, \quad |\boldsymbol{p}_3| = \frac{\lambda^{1/2}\left(m_{12}^2, M^2, m_3^2\right)}{2\sqrt{m_{12}^2}}.$$

The kinematic limits of $\cos\theta$ are $(m_{23}^2)_{\max} \mapsto -1$ and $(m_{23}^2)_{\min} \mapsto 1$. The two differential decay rates are related via

$$\frac{\mathrm{d}^2\Gamma(1\to 3)}{\mathrm{d}m_{12}^2\,\mathrm{d}\cos\theta} = -2\,|\boldsymbol{p}_2|\,|\boldsymbol{p}_3|\,\frac{\mathrm{d}^2\Gamma(1\to 3)}{\mathrm{d}m_{12}^2\,\mathrm{d}m_{23}^2}.$$

SU(3) symmetry

In SU(3) chiral perturbation theory the degrees of freedom are the hadrons that we can construct from the u, d and s quarks. We may organize these hadrons into multiplets. In order to understand how these multiplets are used in the chiral Lagrangian, let us briefly review some SU(3) representation-theory. We will begin by encoding multiplets in SU(3) tensors. Then, we will learn how to appropriately combine multiplets. Finally, we will see how these multiplets form the building blocks for the flavor structure of the chiral Lagrangian. By and large this section will follow refs. 28] 30.

Tensor methods

An element of SU(3) is a 3×3 unitary matrix with unit determinant. The group SU(3) has two Casimir operators. Therefore, we can label its irreducible representations (irreps) with two numbers: (n, m). These are the Dynkin coefficients. The dimension of an irrep is given by

$$D(n,m) = \frac{1}{2}(n+1)(m+1)(n+m+2).$$

We can also label irreps by their dimension,

$$\begin{aligned}
&(1,0) = \mathbf{3}, \quad (0,1) = \overline{\mathbf{3}},\\
&(2,0) = \mathbf{6}, \quad (0,2) = \overline{\mathbf{6}},\\
&(1,1) = \mathbf{8},\\
&(3,0) = \mathbf{10}, \quad (0,3) = \overline{\mathbf{10}},\\
&(2,2) = \mathbf{27},\\
&(4,1) = \mathbf{35}, \quad (1,4) = \overline{\mathbf{35}}.
\end{aligned}$$

To be clear, in this notation the dimension of the irrep $(1,0)$, or equivalently $\mathbf{3}$, is $D(1,0) = 3$. Let U be an element of the three-dimensional irrep, i.e., $U \in (1,0)$. Correspondingly, $U^* \in (0,1)$. A complex vector $T \in \mathbb{C}^3$ transforms under U as

$$T_i \mapsto T_i' = U_{ij}T_j,$$

where $T' \in \mathbb{C}^3$. The conjugate vector transforms as

$$T_i^* \mapsto T_i^* = U_{ij}^* T_j^* = T_j^* U_{ji}^\dagger$$

In lieu of tensor analysis, let us introduce upper and lower indices,

$$T_i \mapsto T^i, \quad T_i^* \mapsto T_i, \quad U_{ij} \mapsto U_j^i, \quad U_{ij}^* \mapsto U_i^{\,j}.$$

The scalar product

$$A^i B_i$$

the Kronecker symbol

$$\delta^i_j = \begin{cases} 1 & \text{if } i = j, \\ 0 & \text{if } i \neq j, \end{cases}$$

and the totally antisymmetric Levi-Civita symbol

$$\epsilon^{i_1 i_2 i_3} = \epsilon_{i_1 i_2 i_3} = \begin{cases} 1 & \text{if } (i_1, i_2, i_3) \text{ is an even permutation of } (1,2,3), \\ -1 & \text{if } (i_1, i_2, i_3) \text{ is an odd permutation of } (1,2,3), \\ 0 & \text{otherwise,} \end{cases}$$

are all invariant under action of SU(3). The Kronecker symbol and the totally antisymmetric Levi Civita symbol transform as tensors. A rank (n, m) tensor transforms as

$$T^{i_1 \ldots i_n}_{j_1 \ldots j_m} = U^{i_1}_{k_1} \ldots U^{i_n}_{k_n} U^{l_1}_{j_1} \ldots U_{j_m}{}^{l_m} T^{k_1 \ldots k_n}_{l_1 \ldots l_m}$$

In general, such a tensor is reducible into irreducible parts. A tensor of rank (n, m) is reducible if through contraction a new nonzero tensor of rank (n', m') can be formed, with $n' + m' < n + m$. As a consequence, an irreducible (n, m) tensor must satisfy

$$T^{i_1 \ldots i_n}_{j_1 \ldots j_m} \delta^{j_1}_{i_1} = 0$$

and must be completely symmetric in its upper and lower indices separately.

The first statement should be obvious. The second one less so. To see why it is true, let us start with a rank $(2, 0)$ tensor. It can be decomposed into a symmetric and an antisymmetric part,

$$T^{(ij)} = \frac{1}{2}\left(T^{ij} + T^{ji}\right), \quad T^{[ij]} = \frac{1}{2}\left(T^{ij} - T^{ji}\right).$$

A similar decomposition holds for a rank $(0, 2)$ tensor. The symmetric part is irreducible. The antisymmetric part can be expressed as a lower-rank tensor,

$$T^{[ij]} = \epsilon^{ijk} T_k$$

and so is reducible. For an $(n, 0)$ tensor,

$$T^{i_1 i_2 i_3 \ldots i_n} = T^{(i_1 i_2) i_3 \ldots i_n} + T^{[i_1 i_2] i_3 \ldots i_n} = S^{i_1 \ldots i_n} + A^{i_1 \ldots i_n}.$$

The tensors S and A are symmetric and antisymmetric in their first two indices, respectively. Using the Levi-Civita symbol we can reduce the antisymmetric tensor. For the symmetric part,

$$S^{i_1 \ldots i_n} = S^{i_1 (i_2 i_3) i_4 \ldots i_n} + S^{i_1 [i_2 i_3] i_4 \ldots i_n}.$$

Again, we can reduce the antisymmetric part. What remains is a tensor that is symmetric between i_1 and i_2 as well as between i_2 and i_3. Clearly, we can continue to peel off the reducible parts of T by symmetrizing different indices. In the end, we are left with an irreducible rank $(n', 0)$ tensor, with $n' \leq n$, that is totally symmetric in its indices. Hence, any irrep must be totally symmetric in its upper and lower indices separately.

Irreducible SU(3)-tensors

Next, let us see how to combine and reduce different representations. It is convenient to use notation where we write the direct product of two irreps $A^{i_1 \ldots i_n}_{j_1 \ldots j_m} B^{i_{n+1} \ldots i_{n'}}_{j_{m+1} \ldots j_{m'}} = T^{i_1 \ldots i_n i_{n+1} \ldots i_{n'}}_{j_1 \ldots j_m j_{m+1} \ldots j_{m'}}$ as $(n, n'; m, m')$. We will also need a generalization of eq. 2.29) to (i_n and i_{n+1} are chosen arbitrarily),

$$T^{i_1\ldots[i_n i_{n+1}]i_{n+2}\ldots i_{n'}}_{j_1\ldots j_{m'}} = \epsilon^{k i_n i_{n+1}} T^{i_1\ldots i_{n-1} i_{n+1}\ldots i_{n'}}_{k j_1\ldots j_{m'}}.$$

Remarkably, T' is completely symmetric in its lower indices. This may be proven by contracting any pair of its lower indices with an invariant symbol and showing that the result vanishes.

In order to reduce T into irreps we must do the following:

1. Contract in all possible ways indices from n with m' and indices from m with n', splitting T into several tensors.
2. For each of these tensors pick two indices that are both up or both down and split the tensor into a part that is antisymmetric in these indices and a part that is symmetric in these indices.
3. Trade in the two upper or lower antisymmetric indices for one lower or upper index, respectively.
4. Repeat steps $2-3$ until T is split into totally symmetric traceless tensors.

The first part may be written as

$$\begin{aligned}(n,m)\otimes(n',m') &= (n,n';m,m')\oplus(n-1,n';m,m'-1)\oplus(n,n'-1;m-1,n')\oplus\ldots \\ &= \bigoplus_{i=0}^{\min(n,m')}\bigoplus_{j=0}^{\min(m,n')}(n-i,n'-j;m-j,m'-i)\,.\end{aligned}$$

Then, for each of the terms in the direct sum parts two and three state (sums where min $(k,k')<1$ should not be carried out),

$$\begin{aligned}(n,n';m,m') &= (n+n',m+m') \\ &\times\bigoplus_{i=1}^{\min(n,n')}(n+n'-2i,m+m'+i)\bigoplus_{j=1}^{\min(m,m')}(n+n'+j,m+m'-2j)\,.\end{aligned}$$

For example,

$$\begin{aligned}(1,0)\otimes(0,1) &= (1,0;0,1)\oplus(0,0;0,0),\\ (1,0;0,1) &= (1,1),\\ (0,0;0,0) &= (0,0).\end{aligned}$$

Less trivial is

$$\begin{aligned}(1,1)\otimes(1,1) &= (1,1;1,1)\oplus(1,0;0,1)\oplus(0,1;1,0)\oplus(0,0;0,0),\\ (1,1;1,1) &= (2,2)\oplus(0,3)\oplus(3,0),\\ (0,1;1,0) &= (1,1),\end{aligned}$$

and

$$\begin{aligned}(1,1)\otimes(3,0) &= (1,3;1,0)\oplus(1,2;0,0),\\ (1,3;1,0) &= (4,1)\oplus(2,2),\\ (1,2;0,0) &= (3,0)\oplus(1,1).\end{aligned}$$

What we have proven is that

$$\begin{aligned}\mathbf{3}\otimes\overline{\mathbf{3}}&=\mathbf{1}\oplus\mathbf{8},\\ \mathbf{8}\otimes\mathbf{8}&=\mathbf{1}\oplus\mathbf{8}\oplus\mathbf{8}\oplus\mathbf{10}\oplus\overline{\mathbf{10}}\oplus\mathbf{27},\\ \mathbf{8}\otimes\mathbf{10}&=\mathbf{8}\oplus\mathbf{10}\oplus\mathbf{27}\oplus\mathbf{35}.\end{aligned}$$

Additionally, it is possible to show that

$$\mathbf{3}\otimes\mathbf{3}\otimes\mathbf{3}=\mathbf{1}\oplus\mathbf{8}\oplus\mathbf{8}\oplus\mathbf{10}.$$

We would like to have an explicit form of the decompositions in terms of tensors. This amounts to symmetrizing indices and removing traces. Starting with eq. 2.38, we reduce a rank $(1,1)$ tensor by subtracting the trace,

$$A^iB_j=T^i_j=\frac{1}{3}\delta^i_jT^k_k+\left(T^i_j-\frac{1}{3}\delta^i_jT^k_k\right).$$

In other words, the irreducible tensors that we can build are

$$\begin{aligned}\mathbf{1}\ni\mathcal{S}&=A^iB_i,\\ \mathbf{8}\ni\mathcal{O}^i_j&=A^iB_j-\frac{1}{3}\delta^i_jA^kB_k.\end{aligned}$$

For eq. 2.39 we want to decompose

$$A^{i_1}_{j_1}B^{i_2}_{j_2}.$$

Remember that A and B are each traceless. We have

$$\begin{aligned}\mathbf{1}\ni\mathcal{S}&=A^i_jB^j_i,\\ \mathbf{8}\ni\mathcal{F}^i_j&=A^i_kB^k_j-A^k_jB^i_k,\\ \mathbf{8}\ni\mathcal{D}^i_j&=A^i_kB^k_j+A^k_jB^i_k-\frac{2}{3}\delta^i_j\mathcal{S},\\ \mathbf{10}\ni\mathcal{T}^{i_1i_2i_3}&=A^{i_1}_{j_1}B^{i_2}_{j_2}\epsilon^{j_1j_2i_3}+\text{ all permutations of }(i_1,i_2,i_3),\\ \overline{\mathbf{10}}\ni\overline{\mathcal{T}}_{j_1j_2j_3}&=A^{i_1}_{j_1}B^{i_2}_{j_2}\epsilon_{i_1i_2j_3}+\text{ all permutations of }(j_1,j_2,j_3),\\ \mathbf{27}\ni\mathcal{I}^{i_1i_2}_{j_1j_2}&=\mathcal{R}^{i_1i_2}_{j_1j_2}-\frac{1}{5}\left(\delta^{i_1}_{j_1}\mathcal{D}^{i_2}_{j_2}+\delta^{i_2}_{j_1}\mathcal{D}^{i_1}_{j_2}+\delta^{i_1}_{j_2}\mathcal{D}^{i_2}_{j_1}+\delta^{i_2}_{j_2}\mathcal{D}^{i_1}_{j_1}\right)-\frac{1}{6}\left(\delta^{i_1}_{j_1}\delta^{i_2}_{j_2}+\delta^{i_2}_{j_1}\delta^{i_1}_{j_2}\right)\mathcal{S},\end{aligned}$$

where

$$\mathcal{R}^{i_1i_2}_{j_1j_2}=A^{i_1}_{j_1}B^{i_2}_{j_2}+A^{i_2}_{j_1}B^{i_1}_{j_2}+A^{i_1}_{j_2}B^{i_2}_{j_1}+A^{i_2}_{j_2}B^{i_1}_{j_1},$$

which satisfies

$$\mathcal{R}^{ik}_{jk}=\mathcal{D}^i_j+\frac{2}{3}\delta^i_j\mathcal{S}.$$

The process for eq. 2.40 is similar. We want to decompose

$$A^{i_1}_jB^{i_2i_3i_4}$$

We have

$$
\begin{aligned}
8 \ni \mathcal{O}_j^i \quad &= \epsilon_{jkm} A_n^k B^{imn}, \\
10 \ni \mathcal{T}^{i_1 i_2 i_3} &= A_k^{i_1} B^{i_2 i_3 k} + A_k^{i_2} B^{i_3 i_1 k} + A_k^{i_3} B^{i_1 i_2 k}, \\
\mathbf{27} \ni \mathcal{I}_{j_1 j_2}^{i_1 i_2} &= \left(\epsilon_{j_1 mk} A_{j_2}^m + \epsilon_{j_2 mk} A_{j_1}^m\right) B^{i_1 i_2 k} \\
&- \frac{1}{5} A_n^m \left(\epsilon_{j_1 mk} \delta_{j_2}^{i_1} B^{n i_2 k} + \epsilon_{j_1 mk} \delta_{j_2}^{i_2} B^{n i_1 k} + \epsilon_{j_2 mk} \delta_{j_1}^{i_1} B^{n i_2 k} + \epsilon_{j_2 mk} \delta_{j_1}^{i_2} B^{n i_1 k}\right), \\
35 \ni \mathcal{Q}_j^{i_1 i_2 i_3 i_4} &= A_j^{i_1} B^{i_2 i_3 i_4} + A_j^{i_2} B^{i_3 i_4 i_1} + A_j^{i_3} B^{i_4 i_1 i_2} + A_j^{i_4} B^{i_1 i_2 i_3}, \\
&- \frac{1}{5} \delta_j^{i_1} \left(A_k^{i_2} B^{k i_3 i_4} + A_k^{i_3} B^{k i_4 i_2} + A_k^{i_4} B^{k i_2 i_3}\right) \\
&- \frac{1}{5} \delta_j^{i_2} \left(A_k^{i_1} B^{k i_3 i_4} + A_k^{i_3} B^{k i_4 i_1} + A_k^{i_4} B^{k i_1 i_3}\right) \\
&- \frac{1}{5} \delta_j^{i_3} \left(A_k^{i_1} B^{k i_2 i_4} + A_k^{i_2} B^{k i_4 i_1} + A_k^{i_4} B^{k i_1 i_2}\right) \\
&- \frac{1}{5} \delta_j^{i_4} \left(A_k^{i_1} B^{k i_2 i_3} + A_k^{i_2} B^{k i_3 i_1} + A_k^{i_3} B^{k i_1 i_2}\right).
\end{aligned}
$$

For eq. 2.41 we want to reduce

$$A^{i_1} B^{i_2} C^{i_3}$$

We find

$$
\begin{aligned}
\mathbf{1} \ni \mathcal{S} &= \epsilon_{i_1 i_2 i_3} A^{i_1} B^{i_2} C^{i_3} \\
\mathbf{8} \ni \mathcal{F}_j^i &= \epsilon_{jkm} A^k B^m C^i - \frac{1}{3} \delta_j^i \epsilon_{kmn} A^k B^m C^n \\
\mathbf{8} \ni \mathcal{D}_j^i &= \epsilon_{jkm} \mathcal{R}^{ik} C^m \\
\mathbf{10} \ni \mathcal{T}^{i_1 i_2 i_3} &= \mathcal{R}^{i_1 i_2} C^{i_3} + \mathcal{R}^{i_2 i_3} C^{i_1} + \mathcal{R}^{i_3 i_1} C^{i_2}
\end{aligned}
$$

where

$$\mathcal{R}^{i_1 i_2} = A^{i_1} B^{i_2} + B^{i_1} A^{i_2}$$

Building hadrons

Let us apply these tensor methods to build hadrons from quarks. The light quarks and antiquarks are in $\mathbf{3}$ and $\overline{\mathbf{3}}$, respectively,

$$\left(q^i\right) = (u, d, s), \quad (q_j) = (\bar{u}, \bar{d}, \bar{s})^\top.$$

Recall the minimum quark content of several light mesons,

$$
\begin{aligned}
&\pi^+ \sim u\bar{d}, \quad \pi^- \sim d\bar{u}, \quad \pi^0 \sim \frac{1}{\sqrt{2}}(u\bar{u} - d\bar{d}), \\
&K^+ \sim u\bar{s}, \quad K^- \sim s\bar{u}, \quad K^0 \sim d\bar{s}, \quad \bar{K}^0 \sim s\bar{d}, \quad \eta \sim \frac{1}{\sqrt{6}}(u\bar{u} + d\bar{d} - 2s\bar{s}).
\end{aligned}
$$

We can build mesons from quarks using eq. 2.43,

$$\Phi_j^i \sim \left(q^i q_j - \frac{1}{3} \delta_j^i q^k q_k\right).$$

If we interpret the top index as labeling the row and the bottom index as labeling the column we can write

$$\Phi \sim \begin{pmatrix} \frac{1}{3}(2u\bar{u} - d\bar{d} - s\bar{s}) & u\bar{d} & u\bar{s} \\ d\bar{u} & \frac{1}{3}(-u\bar{u} + 2d\bar{d} - s\bar{s}) & d\bar{s} \\ s\bar{u} & s\bar{d} & \frac{1}{3}(-u\bar{u} - d\bar{d} + 2s\bar{s}) \end{pmatrix}$$

By identifying the quarks we define

$$\Phi = \begin{pmatrix} \pi^0 + \frac{1}{\sqrt{3}}\eta & \sqrt{2}\pi^+ & \sqrt{2}K^+ \\ \sqrt{2}\pi^- & -\pi^0 + \frac{1}{\sqrt{3}}\eta & \sqrt{2}K^0 \\ \sqrt{2}K^- & \sqrt{2}\bar{K}^0 & -\frac{2}{\sqrt{3}}\eta \end{pmatrix}.$$

The multiplicative factor $\sqrt{2}$ is convention.

Octet baryons live in combinations of the two octets from eq. (2.48), and the symmetry of their state is much more involved than the mesons. Nevertheless, the flavors that appear in $\mathcal{F}^i_j$ and $\mathcal{D}^i_j$ are the same. Neglecting quark ordering gives the following flavor assignment:

$$\begin{array}{lll} n \sim udd, & p \sim uud, & \Lambda \sim uds, \\ \Sigma^- \sim sdd, & \Sigma^0 \sim uds, & \Sigma^+ \sim uus, \\ \Xi^- \sim dss, & \Xi^0 \sim uss, & \end{array}$$

and from our tensor operators we find the following structure

$$B \sim \begin{pmatrix} uds & usu & udu \\ dds & dsu & dud \\ sds & ssu & \text{sud} \end{pmatrix}$$

The B here is not the same as the B in section 2.2.1 which is a placeholder for a generic tensor. To fix the normalization of the diagonal we require that $\text{tr}\left(B^\dagger B\right) = \sum_{i=1}^{8} \psi_i^* \psi_i$, where ψ_i stands for the different octet baryons. We then use that isospin, SU(2), acts on the upper left 2×2 block only, so that B^3_3 must have isospin zero. This gives

$$B = \begin{pmatrix} \frac{1}{\sqrt{2}}\Sigma^0 + \frac{1}{\sqrt{6}}\Lambda & \Sigma^+ & p \\ \Sigma^- & -\frac{1}{\sqrt{2}}\Sigma^0 + \frac{1}{\sqrt{6}}\Lambda & n \\ \Xi^- & \Xi^0 & -\frac{2}{\sqrt{6}}\Lambda \end{pmatrix}.$$

The decuplet baryons are constructed using the totally symmetric tensor in eq. 2.48 and are normalized so that $\left(T^{abc}\right)^* T^{abc} = \sum_{i=1}^{10} \phi_i^* \phi_i$, where ϕ_i stands for the decuplet baryons. From the flavor assignments

$$\begin{array}{llll} uu \sim\sim \Delta^{++}, & uud \sim \Delta^+, & udd \sim \Delta^0, & ddd \sim \Delta^-, \\ \text{uus} \sim \Sigma^{*+}, & \text{uds} \sim \Sigma^{*0}, & dds \sim \Sigma^{*-}, & \\ \text{uss} \sim \Xi^{*0}, & dss \sim \Xi^{*-}, & & \\ sss \sim \Omega^-, & & & \end{array}$$

we find

$$\begin{array}{llllll} T^{111} & = \Delta^{++}, & T^{12} = \frac{1}{\sqrt{3}}\Delta^+, & T^{122} = \frac{1}{\sqrt{3}}\Delta^0, & T^{222} = \Delta^-, \\ T^{113} & = \frac{1}{\sqrt{3}}\Sigma^{*+}, & T^{123} = \frac{1}{\sqrt{6}}\Sigma^{*0}, & T^{223} = \frac{1}{\sqrt{3}}\Sigma^{*-}, & \\ T^{133} & = \frac{1}{\sqrt{3}}\Xi^{*0}, & T^{233} = \frac{1}{\sqrt{3}}\Xi^{*-}, & & \\ T^{333} & = \Omega^-. & & & \end{array}$$

SU(3)-invariant interactions

We have seen how to encode hadron fields into tensors. Next, we would like to build SU(3)-invariant interactions. This section is merely illustrative. We do not endeavor to make an exhaustive list of all possible interactions. That, in general, can be somewhat tricky (see, for instance, ref. [43]) and lies outside of the scope of this thesis. Since the Lagrangian is a singlet, we content ourselves by constructing

$$\begin{aligned}\mathbf{8}\otimes\mathbf{8}\otimes\overline{\mathbf{8}} &= \mathbf{1}\oplus\dots,\\ \overline{\mathbf{10}}\otimes\mathbf{8}\otimes\mathbf{8} &= \mathbf{1}\oplus\dots\end{aligned}$$

Explicitly, singlets are constructed by contracting all indices. We have seen that $\mathbf{8}\otimes\mathbf{8}$ contains two octets irreps. One is of mixed symmetric type and the other is of mixed antisymmetric type. Hence, we expect $\mathbf{8}\otimes\mathbf{8}\otimes\overline{\mathbf{8}}$ to have two different couplings. Indeed, we may write

$$\begin{aligned}c_1\,\mathrm{tr}(\bar{B}\Phi B)+c_2\,\mathrm{tr}(\bar{B}B\Phi) =& \frac{(c_1+c_2)}{2}[\mathrm{tr}(\bar{B}\Phi B)+\mathrm{tr}(\bar{B}B\Phi)]\\ &+\frac{(c_1-c_2)}{2}[\mathrm{tr}(\bar{B}\Phi B)-\mathrm{tr}(\bar{B}B\Phi)],\end{aligned}$$

where we construct an interaction that is symmetric under exchange of B and Φ and an interaction that is antisymmetric. We denote the coupling constants as c_1 and c_2.

We can also create a decuplet from $\mathbf{8}\otimes\mathbf{8}$, so that the interaction $\overline{\mathbf{10}}\otimes\mathbf{8}\otimes\mathbf{8}$ looks like

$$\epsilon^{ade}\bar{T}_{abc}\Phi^b_d B^c_e$$

Because all couplings are SU(3) invariant, it is tempting to derive vertices not from the Lagrangian but directly from SU(3) Clebsch-Gordan coefficients. If we use eqs. 2.54, 2.57) and 2.58) this would give some wrong signs. The reason is that Clebsch-Gordan coefficients (usually) follow the Condon-Shortley convention and we do not. We want that the physical fields annihilate their respective states. So, the Ξ^-field operator should annihilate $|\Xi^-\rangle$. Following the Condon-Shortley convention would imply that the Ξ^-field operator annihilates the physical state $-|\Xi^-\rangle$.

Sometimes in the literature the fields inside the multiplets or the flavor contractions are not stated explicitly. This can make it very tedious to reconstruct what the authors have done. We will come back to this in section 4.1

Spin-3/2 fields

Since we are treating decuplet baryons as fundamental degrees of freedom, we will need to develop some formalism for spin-3/2 particles. Deriving equations of motion of a free spin- s field is quite involved. This is doubly so when one introduces interactions. To not stray too far outside the scope of this thesis we state only the main results. In any case, a complete treatment may be found in ref. 31]. Our point of departure will be a discussion on (representations of) the Lorentz group. Our exposition follows that of ref. 26] and proofs of much of the following may be found therein.

The Lorentz group

Let x be coordinates of an inertial frame (in four spacetime dimensions). A Lorentz transformation is a linear, homogeneous change of coordinates

$$x^\mu \mapsto x'^\mu = \Lambda^\mu_\nu x^\nu$$

which preserves x^2. This implies

$$g_{\mu\nu}\Lambda^\mu_\rho\Lambda^\nu_\sigma = g_{\rho\sigma}.$$

Clearly, $\Lambda^\mu_\nu = \delta^\mu_\nu$ is a valid Lorentz transformation. There also exists an inverse transformation,

$$\left(\Lambda^{-1}\right)^\rho_\nu = \Lambda^\rho_\nu$$

The set of all Lorentz transformations forms a group.

The Lorentz group, or $\mathrm{O}(1,3)$, is not connected, but splits into four subgroups that are each connected. We can classify these subgroups by whether $\det\Lambda = \pm 1$ (proper or improper, respectively) and whether $\Lambda^0_0 \geq 1$ (orthochronous) or ${\Lambda^0}_0 \leq -1$ (antichronous). We are interested in the proper, orthochronous Lorentz transformations, or $\mathrm{SO}^+(1,3)$. Henceforth, all Lorentz transformations are assumed to be of this type. The other three branches are related to the proper orthochronous Lorentz transformation,

- $\mathrm{SO}^+(1,3)\times$ spatial reflection = improper, orthochronous.
- $\mathrm{SO}^+(1,3)\times$ time reversal = proper, antichronous.
- $\mathrm{SO}^+(1,3)\times$ spacetime reflection = improper, antichronous.

An infinitesimal Lorentz transformation may be written as

$$\Lambda^\mu_\nu = \delta^\mu_\nu + \delta\omega^\mu{}_\nu$$

where $\delta\omega_{\mu\nu} = -\delta\omega_{\nu\mu}$. It follows that there are six independent infinitesimal Lorentz transformations: three rotations by an angle $\delta\theta$ around a unit vector $\hat{n}$ and three boosts in the direction of $\hat{n}$ with a rapidity $\delta\eta$

$$\delta\omega_{ij} = -\epsilon_{ijk}\hat{n}_k\delta\theta, \quad \delta\omega_{i0} = \hat{n}_i\delta\eta$$

respectively. We associate a unitary operator $U(\Lambda)$ to each Lorentz transformation, satisfying

$$U\left(\Lambda'\Lambda\right) = U\left(\Lambda'\right)U(\Lambda).$$

For infinitesimal transformations this amounts to

$$U(1+\delta\omega) = 1 + \frac{i}{2}\delta\omega_{\mu\nu}M^{\mu\nu},$$

where $M^{\mu\nu}$ are the generators of the group (a set of Hermitian operators), satisfying

$$M^{\mu\nu} = -M^{\nu\mu}, \quad U(\Lambda)^{-1}M^{\mu\nu}U(\Lambda) = \Lambda^\mu_\rho\Lambda^\nu_\sigma M^{\rho\sigma}.$$

The commutator of the generators specifies the Lie algebra of the Lorentz group,

$$[M^{\mu\nu}, M^{\rho\sigma}] = i\left(g^{\mu\rho}M^{\nu\sigma} - g^{\nu\rho}M^{\mu\sigma}\right) - (\rho \leftrightarrow \sigma),$$

which subsumes the Lie algebras of the angular momentum operator $\boldsymbol{J}$ and of the boost operator $\boldsymbol{K}$. By identifying $J_i = \frac{1}{2}\epsilon_{ijk}M^{jk}$ and $K_i = M^{i0}$ we find

$$[J_i, J_j] = i\epsilon_{ijk}J_k, \quad [J_i, K_j] = i\epsilon_{ijk}K_k, \quad [K_i, K_j] = -i\epsilon_{ijk}J_k.$$

Representations of the Lorentz group

Under a Lorentz transformation a field $\phi_A(x)$ with a generic Lorentz index $A = \mu_1\mu_2\ldots\mu_n$ transforms as

$$U(\Lambda)^{-1}\phi_A(x)U(\Lambda) = L_A^B(\Lambda)\phi_B\left(\Lambda^{-1}x\right)$$

where $L_A^B(\Lambda)$ is a (matrix) representation of the Lorentz group obeying the group composition rule,

$$L_A^B\left(\Lambda'\right)L_B^C(\Lambda) = L_A^C\left(\Lambda'\Lambda\right).$$

Note that other capital indices, like B or C, stand for other generic Lorentz indices. For an infinitesimal transformation,

$$L_A^B(1+\delta\omega) = \delta_A^B + \frac{i}{2}\delta\omega_{\mu\nu}\left(S^{\mu\nu}\right)_A^B.$$

Note that unlike the operators $M^{\mu\nu}$, the matrices $S^{\mu\nu}$ are not necessarily Hermitian. By defining

$$N_i = \frac{1}{2}\left(J_i - iK_i\right), \quad N_i^\dagger = \frac{1}{2}\left(J_i + iK_i\right),$$

one can rewrite eq. 2.68 into

$$[N_i, N_j] = i\epsilon_{ijk}N_k, \quad \left[N_i^\dagger, N_j^\dagger\right] = i\epsilon_{ijk}N_k^\dagger, \quad \left[N_i, N_j^\dagger\right] = 0.$$

The Lie algebra of the Lorentz group splits into two SU(2) Lie algebras. This means that representations of the Lie algebra of the Lorentz group are specified by two integers or half-integers, n and m. These are related to the eigenvalues of the Casimir operators $\boldsymbol{N}^2$ and $\left(\boldsymbol{N}^\dagger\right)^2, n(n+1)$ and $m(m+1)$, respectively. We label the representations as $(2n+1, 2m+1)$. The dimension of a representation is given by

$$D(2n+1, 2m+1) = (2n+1)(2m+1).$$

Common nomenclature includes 26, 32.

$$\begin{aligned}(1,1) &= \text{ scalar},\\ (2,1) &= \text{ left-handed spinor}\,, \quad (1,2) = \text{ right-handed spinor},\\ (2,2) &= \text{ vector}\end{aligned}$$

Handedness refers to the chirality of an object in that representation. A Dirac spinor is in the representation $(2,1)\oplus(1,2)$, and has left- and right-handed parts.

Finally, having discussed Lorentz transformations, let us briefly return to the decay width. Recall that $\mathrm{d}\Gamma \sim (1/m_\Omega)\,\langle|\mathcal{M}|^2\rangle\,\mathrm{dLIPS}$, where LIPS stands for Lorentz-invariant phase space. There is a subtlety here. The formula applies to Omega baryons at rest. Otherwise we need to add a time-dilation factor m_Ω/E_Ω. Nonetheless, we can still express the Lorentz-invariant m_{23}^2 in terms of an angle defined in a particular frame that is not the rest frame of the Omega. However, this does not mean we calculate Γ in that frame.

The Rarita-Schwinger formalism

One way of representing a spin-3/2 particle is by using the 8-dimensional representation $(4,1)\oplus(1,4)$. In practice, it turns out to be convenient to instead take the direct product of a spinor and a vector representation [26], 33],

$$(2,2)\otimes[(2,1)\oplus(1,2)] = (3,2)\oplus(1,2)\oplus(2,3)\oplus(2,1),$$

giving a vector-spinor ψ^μ (we have suppressed the spinor index). In the above decomposition we not only have the spin- 1/2 components in $(2,1)\oplus(1,2)$, which we should project away, but also additional unwanted spin- 1/2 components in $(2,3)\oplus(3,2)$ (the part that contains the spin-3/2 components). We can get rid of these spin- 1/2 contaminants by demanding that the vector spinor satisfies constraint equations,

$$\gamma_\mu\psi^\mu = 0, \quad \partial_\mu\psi^\mu = 0$$

The free Lagrangian for a massive spin-3/2 field is given by 34, 35.

$$\mathcal{L}_{\text{RS}} = \bar{\psi}^\mu \Upsilon_{\mu\nu}\psi^\nu$$

with

$$\begin{aligned}\Upsilon_{\mu\nu} = {} & (i\partial_\kappa\gamma^\kappa - m)\, g_{\mu\nu} + iA\,(\gamma_\mu\partial_\nu + \gamma_\nu\partial_\mu) + \frac{i}{2}\left(3A^2+2A+1\right)\gamma_\mu\partial^\kappa\gamma_\kappa\gamma_\nu \\ & + m\left(3A^2+3A+1\right)\gamma_\mu\gamma_\nu\end{aligned}$$

where A is an arbitrary parameter with the restriction $A \neq -\frac{1}{2}$. We fix $A=-1$, so that the Lagrangian simplifies to the known Rarita-Schwinger Lagrangian,

$$\mathcal{L}_{\text{RS}} = \bar{\psi}^\mu\left[(i\partial_\kappa\gamma^\kappa - m)\, g_{\mu\nu} - i\,(\gamma_\mu\partial_\nu + \gamma_\nu\partial_\mu) + i\gamma_\mu\partial^\kappa\gamma_\kappa\gamma_\nu + m\gamma_\mu\gamma_\nu\right]\psi^\nu$$

We can rewrite this in a more compact form using anti-symmetrized products of Gamma matrices 11

$$\gamma^{\mu\nu} = \frac{1}{2}[\gamma^\mu,\gamma^\nu] = -i\sigma^{\mu\nu}, \quad \gamma^{\mu\nu\alpha} = \frac{1}{2}\{\gamma^{\mu\nu},\gamma^\alpha\} = i\epsilon^{\mu\nu\alpha\beta}\gamma_\beta\gamma_5$$

giving

$$\mathcal{L}_{\text{RS}} = \bar{\psi}_\mu\left(i\gamma^{\mu\nu\alpha}\partial_\alpha - m\gamma^{\mu\nu}\right)\psi_\nu$$

The equations of motion (EoM) are

$$0 = \partial_\alpha\frac{\partial\mathcal{L}_{\text{RS}}}{\partial\left(\partial_\alpha\bar{\psi}_\beta\right)} - \frac{\partial\mathcal{L}_{\text{RS}}}{\partial\bar{\psi}_\beta} = \left(i\gamma^{\beta\nu\alpha}\partial_\alpha - m\gamma^{\beta\nu}\right)\psi_\nu$$

Note that eq. 2.81) automatically generates the constraint equations. To see this, we first take the derivative of the EoM,

$$\begin{aligned}\partial_\beta\left(i\gamma^{\beta\nu\alpha}\partial_\alpha\psi_\nu - m\gamma^{\beta\nu}\psi_\nu\right) &= i\gamma^{\beta\nu\alpha}\partial_\alpha\partial_\beta\psi_\nu - m\gamma^{\beta\nu}\partial_\beta\psi_\nu \\ &= -i\gamma^{\alpha\nu\beta}\partial_\alpha\partial_\beta\psi_\nu - m\gamma^{\beta\nu}\partial_\beta\psi_\nu \\ &= -m\partial_\alpha\gamma^{\alpha\nu}\psi_\nu - m\partial_\beta\gamma^{\beta\nu}\psi_\nu \\ &= 0\end{aligned}$$

Therefore,

$$\gamma^{\mu\nu}\partial_\mu\psi_\nu = 0$$

We can also contract the EoM with a gamma matrix allowing us to make the following simplifications,

$$\gamma_\beta\gamma^{\beta\nu} = \gamma_\beta\gamma^{[\beta}\gamma^{\nu]} = 3\gamma^\nu,$$
$$\gamma_\beta\gamma^{\beta\nu\alpha} = \gamma_\beta\gamma^{[\beta}\gamma^\nu\gamma^{\alpha]} = 2\gamma^{\nu\alpha},$$

giving us

$$0 = \gamma_\beta\left(i\gamma^{\beta\nu\alpha}\partial_\alpha\psi_\nu - m\gamma^{\beta\nu}\psi_\nu\right) = 2i\gamma^{\nu\alpha}\partial_\alpha\psi_\nu - 3m\gamma^\nu\psi_\nu$$

Using eq. 2.85, this implies

$$\gamma^\nu\psi_\nu = 0$$

We can put this back into eq. 2.85 to find

$$0 = \gamma^{\mu\nu}\partial_\mu\psi_\nu = -\frac{1}{2}\gamma^\nu\gamma^\mu\partial_\mu\psi_\nu = -\partial^\mu\psi_\mu$$

Inserting this result into the original EoM gives us

$$0 = \left(i\gamma^{\mu\nu\alpha}\partial_\alpha - m\gamma^{\mu\nu}\right)\psi_\nu = \frac{i}{3!}\left(6\gamma^\mu g^{\nu\alpha} - 6\gamma^\alpha g^{\nu\mu}\right)\partial_\alpha\psi_\nu + mg^{\mu\nu}\psi_\nu = -i\not{\partial}\psi^\mu + m\psi^\mu$$

In other words, the Lagrangian generates

$$(i\not{\partial} - m)\psi_\mu = 0,$$
$$\partial\cdot\psi = 0,$$
$$\gamma\cdot\psi = 0.$$

So, eq. 2.81 is uniquely equivalent to giving the Lagrangian

$$\mathcal{L}_{\mathrm{RS},2} = \bar{\psi}^\mu(i\not{\partial} - m)\psi_\mu$$

and supplying the constraints $\partial\cdot\psi = 0$ and $\gamma\cdot\psi = 0$ on the side.
The propagator $P^T_{\mu\nu}(p)$ may be found by converting eq. 2.78 to momentum space and solving

$$\Upsilon_\mu{}^\kappa(p)P^T_{\kappa\nu}(p) = g_{\mu\nu}.$$

We get 36

$$P^T_{\mu\nu}(p) = \frac{-i(\not{p} + m)}{p^2 - m^2}\left(g_{\mu\nu} - \frac{1}{3}\gamma_\mu\gamma_\nu - \frac{2p^\mu p^\nu}{3m^2} + \frac{p^\mu\gamma^\nu - p^\nu\gamma^\mu}{3m}\right)$$

On shell, this propagator only propagates spin-3/2 fields. The spin- 1/2 fields are 'frozen'. This can be made more apparent by defining spin projection operators, given by 37

$$
\begin{aligned}
P^{3/2}_{\mu\nu}(p) &= g_{\mu\nu} - \frac{1}{3}\gamma_\mu\gamma_\nu - \frac{1}{3p^2}\left(\not{p}\gamma_\mu p_\nu + p_\mu\gamma_\nu\not{p}\right), \\
\left(P^{1/2}_{11}\right)_{\mu\nu}(p) &= \frac{p_\mu p_\nu}{p^2}, \\
\left(P^{1/2}_{22}\right)_{\mu\nu}(p) &= \frac{1}{3}\gamma_\mu\gamma_\nu - \frac{p_\mu p_\nu}{p^2} + \frac{1}{3p^2}\left(\not{p}\gamma_\mu p_\nu + p_\mu\gamma_\nu\not{p}\right), \\
\left(P^{1/2}_{12}\right)_{\mu\nu}(p) &= \frac{1}{\sqrt{3}p^2}\left(\not{p}p^\mu\gamma^\nu - p^\mu p^\nu\right), \\
\left(P^{1/2}_{21}\right)_{\mu\nu}(p) &= \frac{1}{\sqrt{3}p^2}\left(p^\mu p^\nu - \not{p}\gamma\mu p^\nu\right),
\end{aligned}
$$

satisfying (no sum over J)

$$
P^{3/2} + P^{1/2}_{11} + P^{1/2}_{22} = 1, \quad \left(P^I_{ij}\right)_{\mu\nu}\left(P^J_{kl}\right)^{\nu\delta} = \delta^{IJ}\delta_{jk}\left(P^J_{il}\right)_\mu{}^\delta.
$$

These operators do not depend on m, the mass of the spin-3/2 particle. The propagator becomes,

$$
\begin{aligned}
P^T_{\mu\nu}(p) =& \frac{-i(\not{p}+m)}{p^2-m^2}P^{3/2}_{\mu\nu}(p) + \frac{2i}{3m^2}(\not{p}+m)\left(P^{1/2}_{22}\right)_{\mu\nu}(p) \\
&- \frac{i}{\sqrt{3}m}\left[\left(P^{1/2}_{12}\right)_{\mu\nu}(p) + \left(P^{1/2}_{21}\right)_{\mu\nu}(p)\right]
\end{aligned}
$$

Only the propagator of the spin-3/2 part has a pole for the onshell condition $p^2 = m^2$. The spin-1/2 parts do not have poles. One could artificially reintroduce poles and see that the spin-1/2 modes become infinitely heavy,

$$
\frac{1}{-m^2} = \frac{1}{\epsilon p^2 - m^2} = \frac{1}{\epsilon}\frac{1}{p^2 - m^2/\epsilon}, \qquad \text{for } \epsilon \to 0,
$$

which is what we mean by frozen. However, these frozen modes can resurface in interaction terms [38]. Frozen-mode contributions cannot be ignored. It has been shown, for instance, that 'inconsistent couplings' that do not take the Rarita-Schwinger constraint equations into account can lead to superluminal propagation [39]. There are several approaches to make interactions consistent, most of which make calculations more tedious [11], [40], [41]. Fortunately, at LO the simplest interaction terms suffice, as contact interactions can be pushed to NLO [42]. So, for the scope of this thesis we can restrict ourselves to the simplest interaction terms.

7.1.3 Chiral perturbation theory

Having covered the necessary theory, we turn to the chiral Lagrangian containing the strong and weak interactions. We will systematically derive interaction vertices and list relevant propagators and sources. The purpose of this chapter is to set the stage for the calculation of three-body Omega decays.

The leading-order chiral Lagrangian

We are interested in the Lagrangian [10], [15, 43]

$$
\mathcal{L} = \mathcal{L}_{\mathrm{S}} + \mathcal{L}_{\mathrm{EW}}
$$

where $\mathcal{L}_{\mathrm{S}}$ is the leading-order chiral Lagrangian containing the strong interactions and $\mathcal{L}_{\mathrm{EW}}$ is the Lagrangian containing the electroweak interactions. Explicitly,

$$
\begin{aligned}
\mathcal{L}_{\mathrm{S}} =& \operatorname{tr}\left[\bar{B}\left(i\not{D}-m_8\right)B\right]+\bar{T}^{\mu}_{abc}\left[i\gamma_{\mu\nu\alpha}\left(D^{\alpha}T^{\nu}\right)^{abc}-\gamma_{\mu\nu}m_{10}\left(T^{\nu}\right)^{abc}\right]\\
&+\frac{D}{2}\operatorname{tr}\left(\bar{B}\gamma^{\mu}\gamma_5\left\{u_{\mu},B\right\}\right)+\frac{F}{2}\operatorname{tr}\left(\bar{B}\gamma^{\mu}\gamma_5\left[u_{\mu},B\right]\right)\\
&+\frac{h_A}{2\sqrt{2}}\left(\epsilon^{ade}\bar{T}^{\mu}_{abc}\left(u_{\mu}\right)^{b}_{d}B^{c}_{e}+\epsilon_{ade}\bar{B}^{e}_{c}\left(u^{\mu}\right)^{d}_{b}T^{abc}_{\mu}\right)-\frac{H_A}{2}\bar{T}^{\mu}_{abc}\gamma_{\nu}\gamma_5\left(u^{\nu}\right)^{c}_{d}T^{abd}_{\mu}\\
&+\frac{F_{\pi}^2}{4}\operatorname{tr}\left(u_{\mu}u^{\mu}+\chi_{+}\right),\\
\mathcal{L}_{\mathrm{EW}} =& h_C\bar{T}^{\mu}_{abc}\left[u\left(h+h^{\dagger}\right)u^{\dagger}\right]^{c}_{d}T^{abd}_{\mu}+\frac{h_{\pi}F_{\pi}^2}{4}\operatorname{tr}\left[u\left(h+h^{\dagger}\right)u^{\dagger}u_{\mu}u^{\mu}\right].
\end{aligned}
$$

Here, Φ, B and T are the dynamical fields defined in section 2.2.3 (we suppress indices when they are clear from context). Additionally,

$$U=\exp\left(i\Phi/F_{\pi}\right)=u^2.$$

The chirally-covariant derivative is defined as

$$
\begin{aligned}
D^{\mu}B &= \partial^{\mu}B+\left[\Gamma^{\mu},B\right],\\
\left(D^{\mu}T\right)^{abc} &= \partial^{\mu}T^{abc}+\left(\Gamma^{\mu}\right)^{a}_{d}T^{dbc}+\left(\Gamma^{\mu}\right)^{b}_{d}T^{adc}+\left(\Gamma^{\mu}\right)^{c}_{d}T^{abd},\\
\left(D^{\mu}\bar{T}_{abc}\right. &= \partial^{\mu}\bar{T}_{abc}-\left(\Gamma^{\mu}\right)^{d}_{a}\bar{T}_{dbc}-\left(\Gamma^{\mu}\right)^{d}_{b}\bar{T}_{adc}-\left(\Gamma^{\mu}\right)^{d}_{c}\bar{T}_{abd},\\
\nabla_{\mu}U &= \partial_{\mu}U-i\left(v_{\mu}+a_{\mu}\right)U+iU\left(v_{\mu}-a_{\mu}\right),
\end{aligned}
$$

with

$$\Gamma_{\mu}=\frac{1}{2}\left(u^{\dagger}\left[\partial_{\mu}-i\left(v_{\mu}+a_{\mu}\right)\right]u+u\left[\partial_{\mu}-i\left(v_{\mu}-a_{\mu}\right)\right]u^{\dagger}\right).$$

External sources may be turned on to introduce interactions with external fields. The sources are h, v_{μ}, a_{μ}, s and p. We can rewrite the external vector sources v_{μ} and the axial-vector sources a_{μ} into right- and left-handed external vector sources, $r_{\mu}=v_{\mu}+a_{\mu}$ and $l_{\mu}=v_{\mu}-a_{\mu}$, respectively. Furthermore, the scalar source s and the pseudoscalar source p can be combined into

$$\chi=2B_0(s+ip),$$

from which we define

$$\chi_{\pm}=u^{\dagger}\chi u^{\dagger}\pm u\chi^{\dagger}u$$

The scalar source s contains the quark mass matrix diag (m_u, m_d, m_s), which provides the masses for the Goldstone bosons encoded in Φ. Nonleptonic decays are studied via the replacement $h_{ab}=\delta_{a2}\delta_{3b}$, which selects $s\to d$ transitions [44]. Note that $h+h^{\dagger}=\lambda_6$. Replacements for semileptonic and radiative decays are given together with elements of the NLO Lagrangian in section 6.1. Finally, we construct a source-like term from the meson fields,

$$u_{\mu}=iu^{\dagger}\left(\nabla_{\mu}U\right)u^{\dagger}=u^{\dagger}_{\mu}$$

What remains are several constants: m_8 and m_{10} are the baryon and octet masses in the chiral limit. The low-energy constants are $h_A, h_C, h_{\pi}, H_A, B_0, D$ and F. LECs parameterize different interactions, and their numerical values are obtained from fits to data. The pion-decay constant is $F_{\pi}=92.4\mathrm{MeV}$. In practice, we take the physical masses for all the states. Formally, this can be achieved by adding NLO mass-splitting terms [43] to the Lagrangian in

eq. 3.2. In our convention $g_A = D + F$ and h_A are positive. This leads to a positive D and F. We will discuss signs of coupling constants further in section 4.1.2

It is also a good idea to review how the fields transform under a chiral transformation. Let L, R and h_V be representations of $\mathrm{SU}(3)_L, \mathrm{SU}(3)_R$ and $\mathrm{SU}(3)_V$, where the subscripts L, R and V refer to left-handed, right-handed and vector-like transformations, respectively. One can show that 7

$$U \mapsto RUL^\dagger, \quad u \mapsto Ruh_V^\dagger = h_V u L^\dagger, \quad u_\mu \mapsto h_V u_\mu h_V^\dagger, \quad h \mapsto LhL^\dagger,$$
$$B \mapsto h_V B h_V^\dagger, \quad T_\mu^{abc} \mapsto (h_V)_d^a (h_V)_e^b (h_V)_f^c T_\mu^{def}, \quad \bar{T}^\mu_{abc} \mapsto \left(h_V^\dagger\right)_a^d \left(h_V^\dagger\right)_b^e \left(h_V^\dagger\right)_c^f \bar{T}^\mu_{def},$$

which implies that the combination $uhu^\dagger$ transforms like an octet baryon,

$$uhu^\dagger \mapsto h_V u L^\dagger L h L^\dagger L u^\dagger h_V^\dagger = h_V \left(uhu^\dagger\right) h_V^\dagger.$$

Up to this point we have been coy about the exact definition of leading order and next-to-leading order. It is time we become more precise, which we will do using some aspects of power counting. As discussed in the introduction, the power-counting parameter of χPT is p/Λ_χ, where the momentum p of a given process should be on the order of the mass of the light meson fields. The chiral Lagrangian may be expanded in p^n as 45

$$\mathcal{L}_\chi = \sum_n \mathcal{L}^{(n)}$$

The order of the Lagrangian $\mathcal{L}^{(n)}$ is n.

The LO Lagrangian for the meson sector is $\mathcal{L}^{(2)}$ and the NLO meson Lagrangian is $\mathcal{L}^{(4)}$. The order n is even because all building blocks of the chiral Lagrangian are of even order in the power counting. The exception are derivatives. However, they carry a Lorentz indices and thus also must come in pairs. There is no nontrivial contribution at $\mathcal{O}\left(p^0\right)$. One assumes that 7

$$U \in \mathcal{O}\left(p^0\right), \quad \nabla_\mu U \in \mathcal{O}\left(p^1\right), \quad \chi \in \mathcal{O}\left(p^2\right).$$

Unlike the power counting for the meson sector, the power counting for the baryon sector is not straightforward. We will touch on this later in chapter 4. The baryon components in $\mathcal{L}_\mathrm{S}$ form the complete Lagrangian of $\mathcal{O}(p)$. There are no nontrivial terms of $\mathcal{O}\left(p^0\right)$. We have 7], 43], 45, , 46],

$$B \in \mathcal{O}\left(p^0\right), \quad D_\mu B \in \mathcal{O}\left(p^0\right), \quad \left(i\not{D} - m_8\right) B \in \mathcal{O}\left(p^1\right),$$
$$T^\mu \in \mathcal{O}\left(p^0\right), \quad D_\mu T^\mu \in \mathcal{O}\left(p^1\right), \quad \left(i\not{D} - m_{10}\right) T^\mu \in \mathcal{O}\left(p^1\right),$$
$$1, \gamma_\mu, \gamma_\mu\gamma_5 \in \mathcal{O}\left(p^0\right), \quad \gamma_5 \in \mathcal{O}\left(p^1\right)$$

Each interaction term of order n produces vertices of the same order. Consider a Feynman amplitude $\mathcal{M}$ that only involves mesons. The chiral dimension of the corresponding diagram with V_n vertices at order n and L loops is given by 7

$$\dim(\mathcal{M}) = \sum_n (n-2)V_n + 2L + 2.$$

Notice that loops automatically push the diagram to a higher chiral dimension. Diagrams with a higher chiral dimensions are suppressed. To be clear, the order of the chiral Lagrangian need not be same as the chiral dimension of a diagram. The inclusion of baryons makes eq. 3.18 more complicated, and potentially problematic (its exact expression is not relevant for us). We will come back to this in section 4.2

The $\Delta I = 1/2$ rule

It is important to realize that the $s \to d$ transition part of the Lagrangian $\mathcal{L}_{\rm EW}$, contains an approximation. On a quark level, this part should be 47

$$\mathcal{L}_{\Delta S=1} \sim \bar{u}_L \gamma^\mu s_L \bar{d}_L \gamma_\mu u_L$$

where the subscript L denotes left-handed chirality. This is an element of the following tensor,

$$\overline{\mathbf{3}} \otimes \mathbf{3} \otimes \overline{\mathbf{3}} \otimes \mathbf{3} \sim T^{i_1 i_2}_{j_1 j_2} = \bar{q}_{L j_1} \gamma^\mu q_L^{i_1} \bar{q}_{L j_2} \gamma_\mu q_L^{i_2}$$

We can reduce this tensor in the usual way,

$$\begin{aligned} \mathbf{3} \otimes \overline{\mathbf{3}} \otimes \mathbf{3} \otimes \overline{\mathbf{3}} &= (\mathbf{1} \otimes \mathbf{8}) \oplus (\mathbf{1} \otimes \mathbf{8}) \\ &= \mathbf{1} \oplus 2 \cdot \mathbf{8} \oplus (\mathbf{8} \otimes \mathbf{8}) \\ &= 2 \cdot \mathbf{1} \oplus 4 \cdot \mathbf{8} \oplus \mathbf{10} \oplus \overline{\mathbf{10}} \oplus \mathbf{27} \end{aligned}$$

Explicitly,

$$\begin{aligned} 2 \cdot \mathbf{1} &\ni T^{kn}_{kn}, \quad T^{nk}_{kn}, \\ 4 \cdot \mathbf{8} &\ni T^{ki}_{kj} - \frac{1}{3}\delta^i_j T^{kn}_{kn}, \quad T^{ik}_{jk} - \frac{1}{3}\delta^i_j T^{kn}_{kn}, \quad T^{ki}_{jk} - \frac{1}{3}\delta^i_j T^{kn}_{nk}, \quad T^{ik}_{kj} - \frac{1}{3}\delta^i_j T^{kn}_{nk}, \\ \mathbf{10} &\ni \epsilon^{i_1 km} T^{i_2 i_3}_{km} + \text{ all permutations of } (i_1, i_2, j_3), \\ \overline{\mathbf{10}} &\ni \epsilon_{j_1 km} T^{km}_{j_2 j_3} + \text{ all permutations of } (i_1, i_2, j_3), \\ \mathbf{27} &\ni T^{i_1 i_2}_{j_1 j_2} + T^{i_2 i_1}_{j_1 j_2} + T^{i_1 i_2}_{j_2 j_1} + T^{i_2 i_1}_{j_2 j_1} - \text{ traces}, \end{aligned}$$

From eq. (3.19,,$T^{i_1 i_2}_{j_1 j_2} = T^{i_2 i_1}_{j_2 j_1}$. Therefore,

$$\begin{aligned} &\epsilon^{i_1 km} T^{i_2 i_3}_{km} + \text{ all permutations of } (i_1, i_2, j_3) \\ &= \epsilon^{i_1 km} T^{i_3 i_2}_{mk} + \text{ all permutations of } (i_1, i_2, j_3) \\ &= -\epsilon^{i_1 km} T^{i_3 i_2}_{km} + \text{ all permutations of } (i_1, i_2, j_3) \\ &= -\epsilon^{i_1 km} T^{i_2 i_3}_{km} + \text{ all permutations of } (i_1, i_2, j_3), \end{aligned}$$

which means that eq. 3.19 is not in **10** and $\overline{\mathbf{10}}$. Likewise,

$$T^{kn}_{kn}, \quad T^{nk}_{kn}, \quad T^{ki}_{kj}, \quad T^{ik}_{jk}, \quad T^{ki}_{jk}$$

all do not contain eq. (3.19). This leaves only one octet and the 27-plet from eq. (3.20). Hence, $s \to d$ transitions contain a part that transforms as $(\mathbf{8}, \mathbf{1})$ and as $(\mathbf{27}, \mathbf{1})$ under $\mathrm{SU}(3)_L \times \mathrm{SU}(3)_R$. The left-handed octet only contains $\Delta I = 1/2$ transitions while the left-handed 27-plet contains both $\Delta I = 1/2$ and $\Delta I = 3/2$ transitions [48], [49]. From phenomenology it is known that the octet term dominates the 27-plet term [50], [51]. Therefore, $\Delta I = 1/2$ transitions are enhanced as compared to $\Delta I = 3/2$ transitions. This is called the $\Delta I = 1/2$ rule.

To illustrate this point, let us work out several examples. To start, consider the decays $\Lambda \to N\pi$ (where N stands for a nucleon, p or n). If $\Delta I = 1/2$ processes are dominant then the ClebschGordans for the final state are

$$\begin{aligned} p\pi^- &: \left\langle I = \frac{1}{2}, I_3 = -\frac{1}{2} | I_\pi = 1, I_{\pi 3} = -1, I_p = \frac{1}{2}, I_{p3} = \frac{1}{2} \right\rangle = -\sqrt{\frac{2}{3}} \\ n\pi^0 &: \left\langle I = \frac{1}{2}, I_3 = -\frac{1}{2} | I_\pi = 1, I_{\pi 3} = 0, I_n = \frac{1}{2}, I_{n3} = -\frac{1}{2} \right\rangle = \frac{1}{\sqrt{3}} \end{aligned}$$

which implies

$$\frac{\Gamma\left(\Lambda \to p\pi^-\right)}{\Gamma\left(\Lambda \to n\pi^0\right)} \approx \left(\frac{-\sqrt{\frac{2}{3}}}{\sqrt{\frac{1}{3}}}\right)^2 = 2.$$

If instead $\Delta I = 3/2$ processes are dominant

$$p\pi^- : \left\langle I = \frac{3}{2}, I_3 = -\frac{1}{2} | I_\pi = 1, I_{\pi 3} = -1, I_p = \frac{1}{2}, I_{p3} = \frac{1}{2} \right\rangle = \frac{1}{\sqrt{3}}$$
$$n\pi^0 : \left\langle I = \frac{3}{2}, I_3 = -\frac{1}{2} | I_\pi = 1, I_{\pi 3} = 0, I_n = \frac{1}{2}, I_{n3} = -\frac{1}{2} \right\rangle = \sqrt{\frac{2}{3}}$$

which implies

$$\frac{\Gamma\left(\Lambda \to p\pi^-\right)}{\Gamma\left(\Lambda \to n\pi^0\right)} \approx \frac{1}{2}.$$

Experiments find the ratio to be approximately 1.78 [14], which is quite close to 2.

For the decays $\Xi \to \Lambda\pi$, we couple an initial state with $I_\Xi = \frac{1}{2}$ and the weak transition $I_W = \Delta I = \frac{1}{2}$ or $\frac{3}{2}$ to a final state with $I_{\Lambda\pi} = 1$. If $I_W = \frac{1}{2}$,

$$\Xi^0 : \left\langle I = 1, I_3 = 0 | I_\Xi = \frac{1}{2}, I_{\Xi 3} = \frac{1}{2}, I_W = \frac{1}{2}, I_{W3} = -\frac{1}{2} \right\rangle = \frac{1}{\sqrt{2}},$$
$$\Xi^- : \left\langle I = 1, I_3 = -1 | I_\Xi = \frac{1}{2}, I_{\Xi 3} = -\frac{1}{2}, I_W = \frac{1}{2}, I_{W3} = -\frac{1}{2} \right\rangle = 1,$$

which implies

$$\frac{\Gamma\left(\Xi^- \to \Lambda\pi^-\right)}{\Gamma\left(\Xi^0 \to \Lambda\pi^0\right)} \approx 2.$$

When $I_W = 3/2$

$$\Xi^0 : \left\langle I = 1, I_3 = 0 | I_\Xi = \frac{1}{2}, I_{\Xi 3} = \frac{1}{2}, I_W = \frac{3}{2}, I_{W3} = -\frac{1}{2} \right\rangle = -\frac{1}{\sqrt{2}},$$
$$\Xi^- : \left\langle I = 1, I_3 = -1 | I_\Xi = \frac{1}{2}, I_{\Xi 3} = -\frac{1}{2}, I_W = \frac{3}{2}, I_{W3} = -\frac{1}{2} \right\rangle = \frac{1}{2},$$

which implies

$$\frac{\Gamma\left(\Xi^- \to \Lambda\pi^-\right)}{\Gamma\left(\Xi^0 \to \Lambda\pi^0\right)} \approx \frac{1}{2}.$$

Measurements find the ratio to be approximately 1.77 [14]. Again, the $\Delta I = 1/2$ seems to hold.

Calculation-wise the decays $\Omega^- \to \Xi\pi$ are identical to the decays $\Lambda \to N\pi$, where we make the identifications $\Xi^0 \sim p$ and $\Xi^- \sim n$. If the isospin selection rule holds we should find a value close to

$$\frac{\Gamma\left(\Omega^- \to \Xi^0\pi^-\right)}{\Gamma\left(\Omega^- \to \Xi^-\pi^0\right)} \approx 2.$$

Measurements give approximately 2.74[14]. This is nowhere near the predicted value, and we must conclude that the $\Delta I = 1/2$ rule seems not to hold for this decay.

We would like to stress that in principle the ratio 3.33 can reach any value, and the isospin 1/2 or 3/2 dominated values are limiting cases. We can write the ratio as 44

$$\frac{\Gamma\left(\Omega^- \to \Xi^0\pi^-\right)}{\Gamma\left(\Omega^- \to \Xi^-\pi^0\right)} = \left|\frac{-\sqrt{\frac{2}{3}}\mathcal{A}_{1/2} + \frac{1}{\sqrt{3}}\mathcal{A}_{3/2}}{\frac{1}{\sqrt{3}}\mathcal{A}_{1/2} + \sqrt{\frac{2}{3}}\mathcal{A}_{3/2}}\right|^2 = \left|\frac{-\sqrt{2}\mathcal{A}_{1/2} + \mathcal{A}_{3/2}}{\mathcal{A}_{1/2} + \sqrt{2}\mathcal{A}_{3/2}}\right|^2 = \left|\frac{-\sqrt{2}+r}{1+\sqrt{2}r}\right|^2,$$

where $r = \mathcal{A}_{3/2}/\mathcal{A}_{1/2}$. Here, $\mathcal{A}_{1/2}$ contains the $\Delta I = 1/2$ parts of the decay amplitude and $\mathcal{A}_{3/2}$ contains the $\Delta I = 3/2$ parts of the decay amplitude. When $r \to 0$, the amplitude $\mathcal{A}_{1/2}$ is dominant, while when $r \to \pm\infty$, the amplitude $\mathcal{A}_{3/2}$ is dominant. Notice how when neither amplitude is dominant the ratio can take any positive value, or even zero. For example, when $\mathcal{A}_{1/2}$ and $\mathcal{A}_{3/2}$ are of a similar size but of opposite sign the ratio blows up.

It appears that the $\Delta I = 1/2$ rule is often satisfied, but not always (provided the data are correct). At this point, we can follow two lines of thought. Either we forgo the isospin selection rule, or we check what happens when we posit it to be true. There are not enough data for the former. Correspondingly, we concern ourselves with the latter line of reasoning. If nothing else, that line can sharpen the contrast between reality and assumption, and help guide experimental searches that scrutinize the $\Delta I = 1/2$ rule. Indeed, in section 5.2 we will see that differential data on three-body decays contain much more information than just a comparison of two numbers.

So, to be clear, in this thesis we assume the $\Delta I = 1/2$ rule to be true and explore the consequences. Hence, in our Lagrangian we only consider processes characterized by $(\mathbf{8},\mathbf{1})$ leading to $\Delta I = 1/2$. In practice this means including

$$h_C \bar{T}^{\mu}_{abc}\left[u\left(h+h^\dagger\right)u^\dagger\right]^c_d (T^\mu)^{abd} + \frac{h_\pi F_\pi^2}{4}\,\mathrm{tr}\left[u\left(h+h^\dagger\right)u^\dagger u_\mu u^\mu\right]$$

into our final Lagrangian. We reiterate that the transformation rule for h, given in eq. (3.13), is consistent with the transformation properties of the left-handed octet $(\mathbf{8},\mathbf{1})$ (as it should).

Propagators and sources

Let us summarize the propagators and sources. Proofs and derivations may be found in any good quantum field theory textbook. See, for instance, refs. [26], [27], [33], [52].

The propagators are given by

$$\xrightarrow{p} = P^\Phi(p,m) = \frac{i}{p^2 - m^2 + i\epsilon} \quad \text{(scalar boson)},$$

$$\xrightarrow{p} \sim \mu = P^g_{\mu\nu}(p) = \frac{-ig_{\mu\nu}}{p^2 + i\epsilon} \quad \text{(massless vector boson)},$$

$$\overset{p}{\underset{\sim}{\sim}} = P^W_{\mu\nu}(p,m) = \frac{-i}{p^2 - m^2 + i\epsilon}\left(g_{\mu\nu} - \frac{p_\mu p_\nu}{p^2}\right) + \frac{i}{m^2}\frac{p_\mu p_\nu}{p^2} \quad \text{(vector boson)},$$

$$\xrightarrow{p} = P^B(p,m) = \frac{i(\not{p}+m)}{p^2 - m^2 + i\epsilon} \quad \text{(spin-1/2 fermion)},$$

$$\nu \xrightarrow{p} \mu = P^T_{\mu\nu}(p,m) = -\frac{i(\not{p}+m)}{p^2 - m^2 + i\epsilon}P^{3/2}_{\mu\nu}(p)$$
$$+ \frac{2i}{3m^2}(\not{p}+m)\frac{p_\mu p_\nu}{p^2}$$
$$- \frac{i}{3m}\frac{p_\mu p^\alpha \gamma_{\alpha\nu} + \gamma_{\mu\alpha}p^\alpha p_\nu}{p^2} \quad \text{(spin-3/2 fermion)},$$

where m refers to the mass of the particle. When a momentum hits a pole in a propagator we can make the replacement $\epsilon \to m\Gamma$, where Γ is the particle's total decay width. Also useful are the adjoints of some of the propagators. When $\epsilon = 0$ we have

$$\bar{P}^{\Phi}(p,m) = -P^{\Phi}(p,m),$$
$$\bar{P}^{B}(p,m) = -P^{B}(p,m).$$

In general, also

$$\bar{P}^{T}_{\mu\nu} = \gamma_0 \left(P^{T}_{\mu\nu}\right)^{\dagger} \gamma_0 = \bar{P}^{3/2}_{\mu\nu} \frac{i(\not{p}+m)}{p^2-m^2-i\epsilon} - \frac{2i}{3m^2}(\not{p}+m)\frac{p_\mu p_\nu}{p^2} - \frac{i}{3m}\frac{p_\mu p^\alpha \gamma_{\alpha\nu} + \gamma_{\mu\alpha}p^\alpha p_\nu}{p^2},$$

with

$$\bar{P}^{3/2}_{\mu\nu} = g_{\mu\nu} - \frac{1}{3}\gamma_\nu\gamma_\mu - \frac{1}{3p^2}\left(\gamma_\mu p_\nu \not{p} + \not{p} p_\mu \gamma_\nu\right).$$

The sources are given by

$$\overset{p}{\longrightarrow} = 1(\text{ scalar boson })$$
$$\overset{p}{\longrightarrow} = \epsilon_\mu(\boldsymbol{p},\lambda), \quad \overset{p}{\longrightarrow} = \epsilon^*_\mu(\boldsymbol{p},\lambda) \quad \text{(initial/final vector boson)},$$
$$\overset{p}{\longrightarrow} = u(p,s), \quad \overset{p}{\longrightarrow} = \bar{u}(\boldsymbol{p},s) \quad \text{(initial/final spin-1/2 fermion)},$$
$$\overset{p}{\longleftarrow} = \bar{v}(\boldsymbol{p},s), \quad \overset{p}{\longleftarrow} = v(\boldsymbol{p},s) \quad \text{(initial/final spin-1/2 antifermion)},$$
$$\overset{p}{\longrightarrow} \mu = \mu_\mu(\boldsymbol{p},\sigma), \quad \overset{p}{\longrightarrow} \mu = \bar{\mu}_\mu(\boldsymbol{p},\sigma) \quad \text{(initial/final spin-3/2 fermion)},$$
$$\mu \overset{p}{\longleftarrow} = \bar{\nu}_\mu(\boldsymbol{p},\sigma), \quad \mu \overset{p}{\longleftarrow} = \nu_\mu(\boldsymbol{p},\sigma) \quad \text{(initial/final spin-3/2 antifermion)},$$

where $\epsilon_\mu(\boldsymbol{p},\lambda)$ is the polarization vector with polarization $\lambda(\pm 1$ for massless vectors and $0,\pm 1$ for massive vectors). The Dirac spinors are $u(\boldsymbol{p},s)$ and $v(\boldsymbol{p},s)$ and have spin orientation $s = \pm\frac{1}{2}$. The Rarita-Schwinger vector-spinors [34] are $\mu_\mu(\boldsymbol{p},\sigma)$ and $\nu_\mu(\boldsymbol{p},\sigma)$ with spin orientation $\sigma = \frac{3}{2}, \frac{1}{2}, -\frac{1}{2}, -\frac{3}{2}$.

The vector-spinors are built from a spin- 1/2 spinor and a spin- 1 polarization vector using the Clebsch-Gordan coefficients $(J, M|j_1, m_1; j_2, m_2)$,

$$\mu_\mu(\boldsymbol{p},\sigma) = \sum_{\lambda,s}\left(\frac{3}{2},\sigma|1,\lambda;\frac{1}{2},s\right) u(\boldsymbol{p},s)\epsilon_\mu(\boldsymbol{p},\lambda),$$
$$\bar{\mu}_\mu(\boldsymbol{p},\sigma) = \sum_{\lambda,s}\left(\frac{3}{2},\sigma|1,\lambda;\frac{1}{2},s\right) \bar{u}(\boldsymbol{p},s)\epsilon^*_\mu(\boldsymbol{p},\lambda),$$
$$\nu_\mu(\boldsymbol{p},\sigma) = \sum_{\lambda,s}\left(\frac{3}{2},\sigma|1,\lambda;\frac{1}{2},s\right) v(\boldsymbol{p},s)\epsilon_\mu(\boldsymbol{p},\lambda),$$
$$\bar{\nu}_\mu(\boldsymbol{p},\sigma) = \sum_{\lambda,s}\left(\frac{3}{2},\sigma|1,\lambda;\frac{1}{2},s\right) \bar{v}(\boldsymbol{p},s)\epsilon^*_\mu(\boldsymbol{p},\lambda).$$

Next, let us recall some useful identities. The polarization vectors satisfy

$$\begin{aligned} p^\mu\epsilon_\mu(\boldsymbol{p},\lambda) &= 0 \\ \sum_\lambda \epsilon^*_\mu(\boldsymbol{p},\lambda)\epsilon_\nu(\boldsymbol{p},\lambda) &= -g_{\mu\nu} + \tfrac{p_\mu p_\nu}{m^2} && \text{(massive vector boson)}, \\ \sum_\lambda \epsilon^*_\mu(\boldsymbol{p},\lambda)\epsilon_\nu(\boldsymbol{p},\lambda) &= -g_{\mu\nu} + \tfrac{p_\mu p_\nu}{(k\cdot n)^2} + \tfrac{k_\mu n_\nu + k_\nu n_\mu}{k\cdot n} && \text{(massless vector boson)}, \end{aligned}$$

where $(n^\mu) = (1, 0, 0, 0)$. In most practical cases, when we sum over the polarizations of massless vector bosons we can ignore the terms going with n, because they are not Lorentz covariant and, based on a Ward identity, will drop out when we compute observables. The Dirac spinors satisfy

$$\begin{aligned}(\not{p} - m)u(\boldsymbol{p}, s) &= 0\\ (\not{p} + m)v(\boldsymbol{p}, s) &= 0\\ \sum_s u_j(\boldsymbol{p}, s)\bar{u}_k(\boldsymbol{p}, s) &= (\not{p} + m)_{jk}\\ \sum_s v_j(\boldsymbol{p}, s)\bar{v}_k(\boldsymbol{p}, s) &= (\not{p} - m)_{jk}\end{aligned}$$

with $p^0 = \sqrt{\boldsymbol{p}^2 + m^2}$. Because we can decompose the vector-spinors into a Dirac spinor and a polarization vector, they satisfy similar relationships (with analogous ones for ν_μ) [53],

$$\begin{aligned}p^\mu \mu_\mu(\boldsymbol{p}, \sigma) &= 0,\\ \gamma^\mu \mu_\mu(\boldsymbol{p}, \sigma) &= 0,\\ (\not{p} - m)\mu_\mu(\boldsymbol{p}, \sigma) &= 0,\\ \sum_\sigma \mu_\mu(\boldsymbol{p}, \sigma)\bar{\mu}_\nu(\boldsymbol{p}, \sigma) &= -(\not{p} + m)P^{3/2}_{\mu\nu}(p).\end{aligned}$$

Vertices

To calculate decay widths at leading order we need to derive three- and four-point vertex factors. In doing so, we follow refs. [9], [54]. In principle one could expand the Lagrangian and read off all possible interactions. We will be more economical and write generic vertex factors involving any spin-1/2 baryon, spin-3/2 baryon or Goldstone boson.

The first step is to separate the field data and tensor data. We put the fields into different field tuples,

$$\begin{aligned}\left(B^i\right) &= \left(\Sigma^+, \Sigma^-, \Sigma^0, p, \Xi^-, n, \Xi^0, \Lambda\right)\\ \left(\Phi^j\right) &= \left(\pi^+, \pi^-, \pi^0, K^+, K^-, K^0, \bar{K}^0, \eta\right),\\ \left(T^n\right) &= \left(\Sigma^{*+}, \Sigma^{*-}, \Sigma^{*0}, \Delta^+, \Xi^{*-}, \Delta^0, \Xi^{*0}, \Delta^{++}, \Delta^-, \Omega^-\right).\end{aligned}$$

The ordering of the fields inside the tuples is such that they can be conveniently related to the same fields repackaged inside the matrix B with Gell-Mann matrices. When we refer to (say) a field B^i we mean any arbitrary field inside the tuple (B^i). The position of the $i, j = 1, \ldots, 8$, and $n = 1, \ldots, 10$ indices is irrelevant. Corresponding tuples for barred fields look the same but with a bar on each field. For the 3×3 traceless matrices we use the basis b_i, defined via the Gell-Mann matrices as

$$\begin{aligned}b_1 &= \tfrac{1}{\sqrt{2}}\left(\lambda_1 + i\lambda_2\right), & & & b_2 &= \tfrac{1}{\sqrt{2}}\left(\lambda_1 - i\lambda_2\right), \quad b_3 = \lambda_3,\\ b_4 &= \tfrac{1}{\sqrt{2}}\left(\lambda_4 + i\lambda_5\right), & b_5 &= \tfrac{1}{\sqrt{2}}\left(\lambda_4 - i\lambda_5\right),\\ b_6 &= \tfrac{1}{\sqrt{2}}\left(\lambda_6 + i\lambda_7\right), & b_7 &= \tfrac{1}{\sqrt{2}}\left(\lambda_6 - i\lambda_7\right), \quad b_8 = \lambda_8.\end{aligned}$$

One may verify that $b_1 = b_2^\top, b_4 = b_5^\top, b_6 = b_7^\top, b_3 = b_3^\top$ and $b_8 = b_8^\top$. The building blocks for a basis of totally symmetric $3 \times 3 \times 3$ tensors are the tensors e_{abc}, whose components are zero except for the abc-element, which is one (so e_{131} is a $3 \times 3 \times 3$ tensor, where only the 131-component $(e_{131})_{131} = 1$). The basis elements t_n are given by

$$
\begin{aligned}
t_1 &= \tfrac{1}{\sqrt{3}}\left(e_{113}+e_{131}+e_{311}\right), \quad t_2 = \tfrac{1}{\sqrt{3}}\left(e_{223}+e_{232}+e_{322}\right), \\
t_3 &= \tfrac{1}{\sqrt{6}}\left(e_{123}+e_{132}+e_{213}+e_{231}+e_{312}+e_{321}\right), \\
t_4 &= \tfrac{1}{\sqrt{3}}\left(e_{112}+e_{121}+e_{211}\right), & t_5 &= \tfrac{1}{\sqrt{3}}\left(e_{233}+e_{323}+e_{332}\right), \\
t_6 &= \tfrac{1}{\sqrt{3}}\left(e_{122}+e_{212}+e_{221}\right), & t_7 &= \tfrac{1}{\sqrt{3}}\left(e_{133}+e_{313}+e_{331}\right), \quad t_{10} = e_{333}. \\
t_8 &= e_{111}, & t_9 &= e_{222},
\end{aligned}
$$

The fields are split from their tensor structure as

$$
\Phi_b^a = \Phi^j \left(b_j\right)_b^a, \quad B_b^a = \frac{1}{\sqrt{2}} B^i \left(b_i\right)_b^a, \quad T_\mu^{abc} = T_\mu^n \left(t_n\right)^{abc}.
$$

Note that

$$
\bar{B}_b^a = \frac{1}{\sqrt{2}} \bar{B}^i \left(b_i^\top\right)_b^a
$$

Finally, we have to expand several structures in Φ. We find

$$
\begin{aligned}
u &= \exp\left(\frac{i\Phi}{2F_\pi}\right) \sim 1 + \frac{i\Phi}{2F_\pi} \\
\nabla^\mu U \sim \partial^\mu U &\sim \frac{i}{F_\pi}\partial^\mu\Phi - \frac{1}{2F_\pi^2}\left[\left(\partial^\mu\Phi\right)\Phi + \Phi\partial^\mu\Phi\right] \\
u^\mu &= i u^\dagger \left(\nabla^\mu U\right) u^\dagger \sim -\frac{1}{F_\pi}\partial^\mu\Phi.
\end{aligned}
$$

With this formalism, let us derive compact expressions for several vertices. We use circles to denote strong vertices and squares to denote weak vertices.

1 $T_\mu^n \to B^i\Phi^j$

For the vertex $T_\mu^n \to B^i\Phi^j$, the relevant part of the Lagrangian is

$$
\frac{h_A}{2\sqrt{2}}\epsilon_{ade}\bar{B}_c^e \left(u^\mu\right)_b^d T_\mu^{abc}
$$

which becomes

$$
-\frac{h_A}{2\sqrt{2}F_\pi}\epsilon_{ade}\bar{B}_c^e \left(\partial^\mu\Phi\right)_b^d T_\mu^{abc}.
$$

The vertex factor is

$$
T_\mu^n \longrightarrow \bigcup_{B^i}^{p_\Phi} \underbrace{\Phi^j}_{i} = V_\mu^{T\to\Phi B} = \frac{h_A}{2\sqrt{2}F_\pi} c_{nij}^{T\to\Phi B} p_\mu^\Phi,
$$

where we have defined a flavor factor,

$$
c_{nij}^{T\to\Phi B} = \frac{1}{\sqrt{2}}\epsilon_{ade}\left(b_i^\top\right)_c^e \left(b_j^\top\right)_b^d \left(t_n\right)^{abc}.
$$

There are several subtle points one has to keep track of when going from the Lagrangian to the vertex. First, we gain a factor of i (when deriving the vertex from iS, where S is the action) which is canceled by the $-i$ we get from the derivative of the Goldstone field, since we Fourier transform the fields as

$$\Phi^j(x) = \int \frac{\mathrm{d}^4 q}{(2\pi)^4} e^{-iq\cdot x} \Phi^j(q).$$

A consequence of this convention for the Fourier transform is that all momenta flow towards the vertex. This means that when we want an outgoing B^i and an outgoing Φ^j, we look for the part of the Lagrangian containing $\bar{B}^i$ and $\Phi^{\bar{j}}$, where $\Phi^{\bar{j}}$ is the Goldstone boson that is conjugate to Φ^j (so if $\Phi^{j=1} = \pi^+$, then $\Phi^{\bar{j}=2} = \pi^-$). We can use $b_j = b^T_{\bar{j}}$ and $p_{\Phi_j} = -p_{\Phi_{\bar{j}}}$ to skip the intermediate step of going from $\Phi^{\bar{j}}$ to Φ^j.

2 $T^{n_1} \to T^{n_2}$

For $T^{n_1} \to T^{n_2}$ the relevant part of the Lagrangian is

$$h_C \bar{T}^\mu_{abc} \left(uhu^\dagger\right)^c_d T^{abd}_\mu.$$

We find

$$T^{n_1} \xrightarrow{\longrightarrow} T^{n_2} = V^{T\to T} = i h_C c^{T\to T}_{n_1 n_2}$$

where

$$c^{T\to T}_{n_1 n_2} = (t_{n_2})_{abc}\, h^c_d\, (t_{n_1})^{abd}\,.$$

This conversion-type vertex might seem a bit odd at first sight. It encodes an $s \to d$ transition in the decuplet baryon sector, where microscopic dynamics are absorbed in the LEC h_C. There are other ways to implement the transition, for instance by invoking the W boson explicitly. In our case this vertex allows an $\Omega^- \to \Xi^{*-}$ transition. On the quark level there should be other particles involved as well. Loosely speaking, our two-point vertex collapses all the other particles to a point, and their effects are shuffled into h_C. At the end of the day, whether we use this unconventional vertex or another method is not relevant. The results will be the same and, practically, the way we implement the transition here is the most economical.

3.3.3 $T^{n_1} \to T^{n_2}\Phi^j$

For $T^{n_1} \to T^{n_2}\Phi^j$ the relevant parts of the Lagrangian are

$$-\frac{H_A}{2} \bar{T}^\mu_{abc} \gamma_\nu \gamma_5 \left(u^\nu\right)^c_d T^{abd}_\mu + h_C \bar{T}^\mu_{abc} \left[u\left(h + h^\dagger\right) u^\dagger\right]^c_d T^{abd}_\mu.$$

This gives two vertices. The first is

$$T^{n_1} \xrightarrow[T^{n_2}]{} \prod_i^{\Phi^j} = V_1^{T\to T\Phi} = -\frac{H_A}{2F_\pi} c^{T\to T\Phi}_{n_1 n_2 j} \not{p}_\Phi \gamma_5$$

where

$$c^{T\to T\Phi}_{1 n_1 n_2 j} = (t_{n_2})_{abc} \left(b^\top_j\right)^c_d (t_{n_1})^{abd}\,.$$

The second is

$$T^{n_1} \longrightarrow \prod_{T^{n_2}}^{p_\Phi} \Phi^{\Phi^j} = V_2^{T\to T\Phi} = -\frac{h_C}{2F_\pi} c^{T\to T\Phi}_{2 n_1 n_2 j},$$

where

$$c^{T\to T\Phi}_{2 n_1 n_2 j} = (t_{n_2})_{abc} \left[b^\top_j, h + h^\dagger\right]^c_d (t_{n_1})^{abd}\,.$$

3.3.4 $B^{i_1} \to B^{i_2}\Phi^j$

For $B^{i_1} \to B^{i_2}\Phi^j$ the relevant parts of the Lagrangian are

$$\frac{D}{2}\,\mathrm{tr}\left(\bar{B}\gamma^\mu\gamma_5\left\{u_\mu, B\right\}\right) + \frac{F}{2}\,\mathrm{tr}\left(\bar{B}\gamma^\mu\gamma_5\left[u_\mu, B\right]\right).$$

We find

$$B^{i_1} \longrightarrow \bigvee_{B^{i_2}}^{p_\Phi} \underbrace{\Phi^j}_{i} = V^{B\to B\Phi} = \frac{1}{2F_\pi}\left(Dc^{B\to}_{1i_1i_2j} + Fc^{B\to B}_{2i_1i_2j}\right)\not{p}_\Phi\gamma_5$$

where

$$c^{B\to B\Phi}_{1i_1i_2j} = \frac{1}{2}\,\mathrm{tr}\left(b^\top_{i_2}\left\{b^\top_j, b_{i_1}\right\}\right), \quad c^{B\to B\Phi}_{2i_1i_2j} = \frac{1}{2}\,\mathrm{tr}\left(b^\top_{i_2}\left[b^\top_j, b_{i_1}\right]\right).$$

5 $\Phi^{j_1} \to \Phi^{j_2}\Phi^{j_3}$

For $\Phi^{j_1} \to \Phi^{j_2}\Phi^{j_3}$ the relevant part of the Lagrangian is

$$\frac{h_\pi F_\pi^2}{4}\,\mathrm{tr}\left[\left(h + h^\dagger\right)\partial_\mu U^\dagger \partial^\mu U\right].$$

This gives

$$\Phi^{j_1} \xrightarrow[p_{\Phi_1}]{p_{\Phi_2}}$$

where

$$c^{\Phi\to\Phi}_{j_1j_2j_3} = \mathrm{tr}\left(\left[h + h^\dagger, b_{j_1}\right] b_{j_2} b_{j_3}\right).$$

Note that there is a sum over the repeated indices of the momenta and flavor factor.

7.1.4 The heavy-baryon formalism

All calculations in this work are relativistic. This is made possible by the availability of computeralgebra packages that simplify much of the tedious Dirac algebra. Historically, these packages were not available and the calculations had to be done by hand. To make them more tractable it was common to work within the heavy-baryon approximation. In it, one treats the system at hand as non-relativistic. Furthermore, the heavy-baryon formalism established the proper way of power counting, which was later extended to relativistic calculations 77. Because we want to compare our work to previous calculations, it is worthwhile to review the heavy-baryon formalism (also see, for instance, refs. 10], [15], 44] and references therein).

Conventions

The starting point in comparing our calculations to previous calculations is matching notation. In the literature there are two notations and sets of convention in use. We follow the notation and conventions used in ref. [43]. Although the authors of this paper did not come up with the nomenclature, we will nonetheless refer to the style they use as 'Holmberg' style. Another notation is found in refs. [10], [15. We refer to this style as 'Jenkins' style. Unfortunately, harmonizing the Holmberg style and the Jenkins style is much more messy than one would expect, because different symbols do not always share the naively expected correspondence. An overview of the developments of the following sections may be found in appendix A

A correction to field-transformation rules

First, we want to point out that the transformation properties of the Goldstone fields given in refs. 19], 43] are incorrect. The correct transformation rules are given in eq. (3.13) of this work. The correction is

$$\begin{aligned} U \mapsto LUR^\dagger \to \quad & U \mapsto RUL^\dagger \\ u \mapsto Luh_V^\dagger = h_V u R^\dagger \to \quad & u \mapsto Ruh_V^\dagger = h_V u L^\dagger \end{aligned}$$

Second, the baryon states in ref. 10 suffer from an ambiguity. In our notation upper flavor indices transform according to the fundamental representation while, lower flavor indices transform according to the anti-fundamental representation. In Jenkins' notation the position is reversed:

$$\begin{aligned} &\text{This work:} && T_\mu^{abc} \mapsto (h_V)_d^a \, (h_V)_e^b \, (h_V)_f^c \, T_\mu^{def}, \\ &\text{Jenkins' work:} && T_{abc}^\mu \mapsto (h_V)_a^d \, (h_V)_b^e \, (h_V)_c^f \, T_{def}^\mu. \end{aligned}$$

The only way to reconcile the notational conflict is to flip the position of the flavor indices when going from one notation to the other. In our work, we associate the upper index with the rows of h_V and the lower index with the columns of h_V. In Jenkins' notation the upper indices refer to columns and the lower indices the rows. Furthermore, we can show that insisting on our row-column convention and using Jenkins' notation leads to errors. For example, it would imply a coupling between $\Sigma^-$to $\bar{p}$ and $\bar{K}^0$, which violates strangeness conservation.

Untangling ambiguous notation and implicit structures

Next, we would like to point out a caveat that is present in Scherer and Schindler's highly-cited review of χPT. When one looks at eq. (4.20) on pg. 154 of ref. [7] it appears that our Lagrangian and Scherer's Lagrangian is the same, except that D_{Scherer} and F_{Scherer} should gain a sign with respect to our D and F. However, the quoted numerical values of D_{Scherer} and F_{Scherer} have a positive sign, like our D and F. Thus, the Lagrangian on pg. 154 of ref. [7] (suppressing Scherer subscripts),

$$\mathcal{L}_{\text{MB}}^{(1)} = \text{tr}\left[\bar{B}\left(i\not{D} - M_0\right)B\right] - \frac{D}{2}\,\text{tr}\left(\bar{B}\gamma^\mu\gamma_5\left\{u_\mu, B\right\}\right) - \frac{F}{2}\,\text{tr}\left(\bar{B}\gamma^\mu\gamma_5\left[u_\mu, B\right]\right)$$

is inconsistent with our conventions. Moreover, Scherer is internally inconsistent. The SU(2)-reduced Lagrangian, given in eq. (4.17) on pg. 152 of ref. [7,

$$\mathcal{L}_{\pi N}^{(1)} = \bar{\Psi}\left(i\not{D} - m + \frac{g_A}{2}\gamma^\mu\gamma_5 u_\mu\right)\Psi$$

where $\Psi = (p, n)^\top$ and g_A is a constant, is consistent with ours. To see this, note that $\mathcal{L}_{\text{MB}}^{(1)}$, which lives in $\text{SU}(3)_L \times \text{SU}(3)_R$, should reduce to $\mathcal{L}_{\pi N}^{(1)}$, which lives in $\text{SU}(2)_L \times \text{SU}(2)_R \times \text{U}(1)_V$. We can then relate D and F to g_A. The quoted value for g_A is positive [7. When we reduce eq. (4.1) to eq. 4.2 we find $g_A = -(D + F)$. So, demanding that D, F and g_A are positive is not possible. In principle there is nothing wrong with this, and conceptually everything is fine. It does, however, make comparing Scherer's work to our work tricky. So, since most of the notation in ref. [7] is identical to ours, save for some irksome minus signs, we will not consider Scherer's work when constructing our symbol compendium.

This begs a more general question, though. When is a sign choice a convention? The creation operator of a field creates a field up to a phase (for definiteness, let us pick +1 or -1). Therefore, if our theory has multiple coupling constants, we always have the freedom to pick the sign of one of them. We have one sign choice per field. For example, in eq. (3.55) the

pion field appears in odd powers. Thus, in eq. 4.2 we can pick g_A to be positive. After we have fixed the sign of a coupling constant, the signs of other coupling constants relative to it are not a convention. So, if we pick g_A positive, then the relative sign of D and F to g_A is not convention.

Finally, note that it is common in the literature to keep the SU(3) indices implicit [10], [15], [51]. This also means that SU(3) invariant symbols are not written down. Furthermore, in some works the Rarita-Schwinger equation is written like in eq. 2.95 instead of like in eq. 2.81, and the constraint equations must be enforced after the fact.

Matching notation

Let us compare what symbols are used to denote the same thing. We will denote symbols in our notation without any extra decoration. Symbols from refs. 10], [15], [44] will carry a 'Jenkins' subscript.

By comparing the transformation rules of the fields in refs. [10], [44] to the ones in ref. [43], we find

$$\begin{aligned} U &= \Sigma^\dagger_{\text{Jenkins}} , & u &= \xi^\dagger_{\text{Jenkins}} , \\ B &= B_{\text{Jenkins}} , & h_V &= U_{\text{Jenkins}} , \\ L/R &= L/R_{\text{Jenkins}} . \end{aligned}$$

As a consequence, the particle fields in ref. [10] gain a relative phase compared to our particle fields (i.e. $\eta = -\eta_{\text{Jenkins}}, \ldots$). To be clear, B_{Jenkins} contains 'Jenkins fields' and B contains 'our' fields.

Only then is B formally the same as B_{Jenkins}. Furthermore, there is some rescaling,

$$\Phi = -2\pi_{\text{Jenkins}}$$

where, again, Φ contains our fields and π contains Jenkins' fields. In ref. [10] sources are not included. If we set our sources, l_μ and r_μ, to zero we have

$$\begin{aligned} \Gamma^\mu|_{l_\nu, r_\nu = 0} &= V^\mu_{\text{Jenkins}} , \\ u^\mu|_{l_\nu, r_\nu = 0} &= 2A^\mu_{\text{Jenkins}} . \end{aligned}$$

The covariant derivative is written as

$$D^\mu = \mathcal{D}^\mu_{\text{Jenkins}}$$

For the constants,

$$\begin{aligned} F_\pi &= f_{\text{Jenkins}} , & & \\ m_8 &= (m_B)_{\text{Jenkins}} , & m_{10} &= (m_T)_{\text{Jenkins}} , \\ D &= D_{\text{Jenkins}} , & F &= F_{\text{Jenkins}} , \\ h_A &= \sqrt{2}\mathcal{C}_{\text{Jenkins}} , & H_A &= -\mathcal{H}_{\text{Jenkins}} . \end{aligned}$$

Heavy-baryon chiral perturbation theory

We now return to the problematic power counting of the baryon sector, mentioned in section 3.1. In general, one wants to describe a low-energy system by an effective field theory. Technically, one expansion parameter is the number of derivatives in an interaction term. In this way the number of possible interaction terms is limited. Derivatives translate to momenta, so the expansion makes sense if the momenta are small. Baryon masses are not constrained to vanish

in the chiral limit, so m_8 and m_{10} cannot be treated as small quantities. Instead, they are comparable to $4\pi F_\pi \approx \Lambda_\chi$, where chiral perturbation theory breaks down 7. Therefore, partial derivatives, and in extension momenta, acting on the baryons are bigger than expected. A consequence is that loop corrections are not necessarily suppressed, see ref. [45] and references therein.

A popular way to reconcile baryons with power counting is the heavy-baryon formalism. The basic idea is to approximate the baryon fields as (non-relativistic) heavy static fermions [10]. Let

$$p^\mu = m_B v^\mu + k^\mu$$

be the baryon momentum where

$$v^2 = 1, \quad v^0 \geq 1$$

with v^μ the baryon four-velocity and k^μ a small residual momentum arising from low-energy interactions (a lucid physical explanation may be found in refs. [55], [56]). Notice that when $m_B \to \infty, p^\mu/m_B = v^\mu_{\text{baryon}} = v^\mu$ and $[v^\mu, x^\nu] = ig^{\mu\nu}/m_B \to 0$. Hence, we can simplify our LO Lagrangian by throwing away all terms of $\mathcal{O}(1/m_B)$ and higher. Doing so with our Lagrangian will reproduce the heavy-baryon Lagrangian found in refs. [10], [44], [57].

We start by expressing our relativistic Lagrangian in Jenkins' notation, so we can directly compare the end result. This means we suppress some of the multiplet structure and remove the constraint equations from the LO Lagrangian. We get

$$\begin{aligned}\mathcal{L}_{\text{Jenkins}} =& i\,\mathrm{tr}(\bar{B}\not{D}B) - m_B\,\mathrm{tr}(\bar{B}B) + D\,\mathrm{tr}\left(\bar{B}\gamma^\mu\gamma_5\{A_\mu, B\}\right) + F\,\mathrm{tr}\left(\bar{B}\gamma^\mu\gamma_5[A_\mu, B]\right) \\ & - i\bar{T}^\mu\not{D}T_\mu + m_T\bar{T}^\mu T_\mu + \mathcal{C}\left(\bar{T}^\mu A_\mu B + \bar{B}A_\mu T^\mu\right) + \mathcal{H}\bar{T}^\mu\gamma_\nu\gamma_5 A^\nu T_\mu \\ & + \frac{f^2}{4}\,\mathrm{tr}\,\partial_\mu\Sigma\partial^\mu\Sigma^\dagger.\end{aligned}$$

The following non-relativistic reduction is in the same spirit as ref. [7]. In principle, it is also possible to use path integrals [58]. We decompose the fields into their heavy and light parts,

$$\begin{aligned} B_v^L &= e^{im_B v\cdot x}P_{v+}B, \quad B_v^H = e^{im_B v\cdot x}P_{v-}B, \\ T_v^{L\mu} &= e^{im_B v\cdot x}P_{v+}T^\mu, \quad T_v^{H\mu} = e^{im_B v\cdot x}P_{v-}T^\mu, \end{aligned}$$

where

$$B = e^{-im_B v\cdot x}\left(B_v^L + B_v^H\right), \quad T_\mu = e^{-im_B v\cdot x}\left(T_{v\mu}^L + T_{v\mu}^H\right),$$

with projection operators

$$P_{v\pm} = \frac{1}{2}(1 \pm \not{v})$$

Some useful relations are

$$\begin{aligned} P_{v\pm}^2 &= \frac{1}{2}(1\pm\not{v})\frac{1}{2}(1\pm\not{v}) = \frac{1}{4}(1 \pm 2\not{v} + \not{v}\not{v}) = \frac{1}{4}(2 \pm 2\not{v}) = P_{v\pm}, \\ P_{v\pm}P_{v\mp} &= \frac{1}{2}(1\pm\not{v})\frac{1}{2}(1\mp\not{v}) = \frac{1}{4}(1 - \not{v}\not{v}) = 0, \\ P_{v+} + P_{v-} &= \frac{1}{2}(1+\not{v}) + \frac{1}{2}(1-\not{v}) = 1, \\ \not{v}e^{imv\cdot x}P_{v\pm} &= e^{imv\cdot x}\not{v}\frac{1}{2}(1\pm\not{v}) = e^{imv\cdot x}\frac{1}{2}(\not{v}\pm 1) = \pm e^{imv\cdot x}P_{v\pm}. \end{aligned}$$

The basic idea is that a free field B (say) has a rapidly-oscillating part which we compensate by the phase factor $\exp(\mathrm{im}_B v\cdot x)$. Therefore, derivatives acting on B_v^L produce only small momenta. So, the light field qualifies as a building block for an EFT where all derivatives are counted as small quantities. What remains is integrating out B_v^H (see refs. [59], 60]).

Before doing just this, note that in quite some literature [10, [44], [57] a seemingly-different definition of the light fields is used (also for the decuplet fields). There, the light field is defined as

$$B_v = e^{im_B \not{v} v\cdot x} B$$

with the additional constraint

$$P_{v+} B_v = B_v$$

It is not immediately obvious that $B_v = B_v^L$. To see why, let us rewrite the exponential,

$$\begin{aligned}
e^{im_B \not{v} v\cdot x} &= \sum_{n=0}^{\infty} \frac{(-1)^n (m_B \not{v} v\cdot x)^{2n}}{(2n)!} + i \sum_{n=0}^{\infty} \frac{(-1)^n (m_B \not{v} v\cdot x)^{2n+1}}{(2n+1)!} \\
&= \sum_{n=0}^{\infty} \frac{(-1)^n (m_B v\cdot x)^{2n}}{(2n)!} + i\not{v} \sum_{n=0}^{\infty} \frac{(-1)^n (m_B v\cdot x)^{2n+1}}{(2n+1)!} \\
&= \frac{e^{im_B v\cdot x} + e^{-im_B v\cdot x}}{2} + \not{v} \left(\frac{e^{im_B v\cdot x} - e^{-im_B v\cdot x}}{2} \right) \\
&= \frac{1}{2}(1+\not{v}) e^{im_B v\cdot x} + \frac{1}{2}(1-\not{v}) e^{-im_B v\cdot x} \\
&= P_{v+} e^{im_B v\cdot x} + P_{v-} e^{-im_B v\cdot x}
\end{aligned}$$

Combining this with eq. 4.15,

$$\begin{aligned}
B_v = P_v B_v &= P_{v+} e^{im_B \not{v} v\cdot x} B \\
&= P_{v+} \left(P_{v+} e^{im_B v\cdot x} + P_{v-} e^{-im_B v\cdot x} \right) B = P_{v+} e^{im_B v\cdot x} B = e^{im_B v\cdot x} P_{v+} B \\
&= B_v^L .
\end{aligned}$$

So, the two definitions are equivalent.

We are now going to integrate out the heavy field which, as we will see, will be $\mathcal{O}(1/m_B)$. We start by using the equation of motion (EoM) of B,

$$\left(i\not{D} - m_B\right) B + D\gamma^\mu\gamma_5 \{A_\mu, B\} + F\gamma^\mu\gamma_5 [A_\mu, B] + \mathcal{C} A_\mu T^\mu = 0,$$

and rewriting it into equations of motion of the heavy and light parts. We insert eq. (4.13) into eq. (4.18), multiply by $e^{im_B v\cdot x}$ and find

$$\begin{aligned}
0 =& i\not{D} B_v^L + D\gamma^\mu\gamma_5 \left\{A_\mu, B_v^L\right\} + F\gamma^\mu\gamma_5 \left[A_\mu, B_v^L\right] + \mathcal{C} A_\mu T_v^{L\mu} \\
&+ \left(i\not{D} - 2m_B\right) B_v^H + D\gamma^\mu\gamma_5 \left\{A_\mu, B_v^H\right\} + F\gamma^\mu\gamma_5 \left[A_\mu, B_v^H\right] + \mathcal{C} A_\mu T_v^{H\mu}
\end{aligned}$$

since

$$\begin{aligned}
i\not{\partial} B &= i\not{\partial} \left[e^{-im_B v\cdot x} \left(B_v^L + B_v^H\right)\right] = m_B \not{v} e^{-im_B v\cdot x} \left(B_v^L + B_v^H\right) + i e^{-im_B v\cdot x} \not{\partial} \left(B_v^L + B_v^H\right) \\
&= e^{-im_B v\cdot x} \left(i\not{\partial} + m_B\right) B_v^L + e^{-im_B v\cdot x} \left(i\not{\partial} - m_B\right) B_v^H .
\end{aligned}$$

To get the EoMs of each component we multiply eq. 4.19 with the corresponding projector.

It is helpful to work out some algebra of the projection operators. Let a_μ be an arbitrary four-vector. Define the orthogonal component

$$a_\perp^\mu = a^\mu - v\cdot a v^\mu$$

so that

$$v\cdot a_\perp = 0$$

Also, recall that

$$\not{L} = \gamma^\mu\gamma^\nu v_\mu a_\nu = \left(2g^{\mu\nu} - \gamma^\nu\gamma^\mu\right) v_\mu a_\nu = 2v\cdot a - \not{v}\not{a}.$$

Then,

$$P_{v\pm}\not{K} = \frac{1}{2}(1\pm\not{v})\not{K} = \pm v\cdot a + \not{K}P_{v\mp},$$

and

$$P_{v\pm} = \frac{1}{2}(1\pm\not{v}) = \not{v}\frac{1}{2}(\not{v}\pm 1) = \pm\not{v}P_{v\pm}.$$

Thus,

$$\begin{aligned}
P_{v\pm}\not{A}P_{v\pm} &= \left(\pm v\cdot a + \not{K}P_{v\mp}\right) P_{v\pm} = \pm v\cdot a P_{v\pm}\\
P_{v\pm}\not{A}P_{v\mp} &= \left(\pm v\cdot a + \not{v}P_{v\mp}\right) P_{v\mp} = \left(\pm v\cdot a\not{v}\not{v} + \not{A}\right)P_{v\mp} = \left(-v\cdot a\not{v} + \not{A}\right)P_{v\mp} = \not{v}_\perp P_{v\mp}.
\end{aligned}$$

Finally,

$$\begin{aligned}
P_{v\pm}\gamma^\mu P_{v\pm} &= \frac{1}{2}\left(1\pm v_\nu\gamma^\nu\right)\gamma^\mu P_{v\pm} = \frac{1}{2}\left(\gamma^\mu \pm 2g^{\mu\nu}v_\nu \mp \gamma^\mu\gamma^\nu v_\nu\right) P_{v\pm} = \gamma^\mu P_{v\mp}P_{v\pm} \pm v^\mu P_{v\pm}\\
&= \pm v^\mu P_{v\pm}\\
P_{v\pm}\gamma^\mu P_{v\mp} &= \frac{1}{2}\left(1\pm v_\nu\gamma^\nu\right)\gamma^\mu P_{v\mp} = \frac{1}{2}\left(\gamma^\mu \pm 2g^{\mu\nu}v_\nu \mp \gamma^\mu\gamma^\nu v_\nu\right) P_{v\mp} = \left(\gamma^\mu \pm v^\mu\right) P_{v\mp}
\end{aligned}$$

Any term with γ_5 can be simplified using

$$\gamma_5 P_{v\pm} = \gamma_5\frac{1}{2}(1\pm\not{v}) = \frac{1}{2}(1\mp\not{v})\gamma_5 = P_{v\mp}\gamma_5,$$

and the relations above. To summarize,

$$\begin{aligned}
P_{v\pm}\not{P}P_{v\pm} &= \pm v\cdot a P_{v\pm}, & P_{v\pm}\not{v}P_{v\mp} &= \not{A}_\perp P_{v\mp} = P_{v\pm}\not{A},\\
P_{v\pm}\not{A}\gamma_5 P_{v\pm} &= \not{v}_\perp\gamma_5 P_{v\pm}, & P_{v\pm}\not{\gamma}\gamma_5 P_{v\mp} &= \pm v\cdot a\gamma_5 P_{v\mp} = \pm v\cdot a P_\pm\gamma_5,\\
P_{v\pm}\gamma^\mu P_{v\pm} &= \pm v^\mu P_{v\pm}, & P_{v\pm}\gamma^\mu P_{v\mp} &= \left(\gamma^\mu \pm v^\mu\right) P_{v\mp},\\
P_{v\pm}\gamma^\mu\gamma_5 P_{v\pm} &= \left(\gamma^\mu \pm v^\mu\right)\gamma_5 P_{v\pm}, & P_{v\pm}\gamma^\mu\gamma_5 P_{v\mp} &= \pm v^\mu\gamma_5 P_{v\mp}.
\end{aligned}$$

Before we can project out the EoMs, we need that (with a similar expression for the decuplet states)

$$B_V^L = P_{v+}B_V^L, \quad B_v^H = P_{v-}B_v^H.$$

Notice that we can convert all terms in $P_{v\pm}$ (EoM) into terms like $P_{v\pm}\ldots P_{v\pm}$ and $P_{v\pm}\ldots P_{v\mp}$. Let us simplify each of these 'sandwich terms' (recall that A_μ only contains Goldstone fields, and thus has a trivial spinor structure, meaning it commutes with the projectors). First, the derivatives,

$$
\begin{aligned}
&P_{v+} i\not{\mathcal{D}} B_v^L = P_{v+} i\not{\mathcal{D}} P_{v+} B_v^L = iv\cdot\mathcal{D} B_v^L,\\
&P_{v-} i\not{\mathcal{D}} B_v^L = P_{v-} i\not{\mathcal{D}} P_{v+} B_v^L = i\not{\mathcal{D}}_\perp B_{vL}\\
&P_{v+}\left(i\not{\mathcal{D}} - 2m_B\right) B_v^H = P_{v+}\left(i\not{\mathcal{D}} - 2m_B\right) P_{v-} B_v^H = i\mathcal{D}_\perp B_v^H,\\
&P_{v-}\left(i\not{\mathcal{D}} - 2m_B\right) B_v^H = P_{v-}\left(i\not{\mathcal{D}} - 2m_B\right) P_{v-} B_v^H = \left(-v\cdot\mathcal{D} - 2m_B\right) B_v^H.
\end{aligned}
$$

Second, the commutators,

$$
\begin{aligned}
&P_{v+}\gamma^\mu\gamma_5\left\{A_\mu, B_v^L\right\} = P_{v+}\gamma^\mu\gamma_5 P_{v+}\left\{A_\mu, B_v^L\right\} = \left(\gamma^\mu + v^\mu\right)\gamma_5\left\{A_\mu, B_v^L\right\},\\
&P_{v-}\gamma^\mu\gamma_5\left\{A_\mu, B_v^L\right\} = P_{v-}\gamma^\mu\gamma_5 P_{v+}\left\{A_\mu, B_v^L\right\} = -v^\mu\gamma_5\left\{A_\mu, B_v^L\right\},\\
&P_{v+}\gamma^\mu\gamma_5\left\{A_\mu, B_v^H\right\} = P_{v+}\gamma^\mu\gamma_5 P_{v-}\left\{A_\mu, B_v^H\right\} = v^\mu\gamma_5\left\{A_\mu, B_v^H\right\},\\
&P_{v-}\gamma^\mu\gamma_5\left\{A_\mu, B_v^H\right\} = P_{v-}\gamma^\mu\gamma_5 P_{v-}\left\{A_\mu, B_v^H\right\} = \left(\gamma^\mu - v^\mu\right)\gamma_5\left\{A_\mu, B_v^H\right\},\\
&P_{v+}\gamma^\mu\gamma_5\left[A_\mu, B_v^L\right] = P_{v+}\gamma^\mu\gamma_5 P_{v+}\left[A_\mu, B_v^L\right] = \left(\gamma^\mu + v^\mu\right)\gamma_5\left[A_\mu, B_v^L\right],\\
&P_{v-}\gamma^\mu\gamma_5\left[A_\mu, B_v^L\right] = P_{v-}\gamma^\mu\gamma_5 P_{v+}\left[A_\mu, B_v^L\right] = -v^\mu\gamma_5\left[A_\mu, B_v^L\right]\\
&P_{v+}\gamma^\mu\gamma_5\left[A_\mu, B_v^H\right] = P_{v+}\gamma^\mu\gamma_5 P_{v-}\left[A_\mu, B_v^H\right] = v^\mu\gamma_5\left[A_\mu, B_v^H\right],\\
&P_{v-}\gamma^\mu\gamma_5\left[A_\mu, B_v^H\right] = P_{v-}\gamma^\mu\gamma_5 P_{v-}\left[A_\mu, B_v^H\right] = \left(\gamma^\mu - v^\mu\right)\gamma_5\left[A_\mu, B_v^H\right].
\end{aligned}
$$

And finally,

$$
\begin{aligned}
&P_{v+} A_\mu T_v^{L\mu} = A_\mu T_v^{L\mu},\\
&P_{v-} A_\mu T_v^{L\mu} = 0\\
&P_{v+} A_\mu T_v^{H\mu} = 0\\
&P_{v-} A_\mu T_v^{H\mu} = A_\mu T_v^{H\mu}.
\end{aligned}
$$

This gives for our EoMs,

$$
\begin{aligned}
0 =& iv\cdot\mathcal{D} B_v^L + D\left(\gamma^\mu + v^\mu\right)\gamma_5\left\{A_\mu, B_v^L\right\} + F\left(\gamma^\mu + v^\mu\right)\gamma_5\left[A_\mu, B_v^L\right] + \mathcal{C} A_\mu T_v^{L\mu}\\
&+ i\mathcal{D}_\perp B_v^H + Dv^\mu\gamma_5\left\{A_\mu, B_v^H\right\} + Fv^\mu\gamma_5\left[A_\mu, B_v^H\right]
\end{aligned}
$$

and

$$
\begin{aligned}
0 =& i\mathcal{D}_\perp B_v^L - Dv^\mu\gamma_5\left\{A_\mu, B_v^L\right\} - Fv^\mu\gamma_5\left[A_\mu, B_v^L\right]\\
&- \left(v\cdot\mathcal{D} + 2m_B\right) B_v^H + D\left(\gamma^\mu - v^\mu\right)\gamma_5\left\{A_\mu, B_v^H\right\} + F\left(\gamma^\mu - v^\mu\right)\gamma_5\left[A_\mu, B_v^H\right] + \mathcal{C} A_\mu T_v^{H\mu}
\end{aligned}
$$

The derivative $\mathcal{D}_\mu B_v^L$ but also the derivative $\not{\mathcal{D}}_\perp B_v^H$ are small. The only large derivative is $v\cdot\mathcal{D} B^H$, and in particular the contribution $\left(v\cdot\mathcal{D} + 2m_B\right) B_v^H = \mathcal{O}\left(m_B\right) B_v^H$.

We can formally solve eq. 4.37) for B_v^H in terms of B_v^L for each of the individual baryon fields. It should be clear from eq. 4.37 that the general structure will be like

$$
\left(B_v^H\right)_b^a = \left[\left(\cdots + 2m_B\right)^{-1}\left(\ldots T_v^{H\mu} + \ldots B_v^L\right)\right]_b^a = \mathcal{O}\left(\frac{1}{m_B}\right).
$$

This, together with the smallness of $\mathcal{D}_\perp$, means that in eq. 4.36 we can ignore the heavy fields and find an EoM purely for the light fields,

$$
0 = iv\cdot\mathcal{D} B_v^L + D\left(\gamma^\mu + v^\mu\right)\gamma_5\left\{A_\mu, B_v^L\right\} + F\left(\gamma^\mu + v^\mu\right)\left[A_\mu, B_v^L\right] + \mathcal{C} A_\mu T_v^{L\mu}
$$

A Lagrangian that produces these dynamics is

$$
\begin{aligned}
\mathcal{L}_{B_v^L} =& i\,\mathrm{tr}\,\bar{B}_v^L (v\cdot\mathcal{D}) B_v^L + D\,\mathrm{tr}\,\bar{B}_v^L\left(\gamma^\mu + v^\mu\right)\gamma_5\left\{A_\mu, B_v^L\right\} + F\,\mathrm{tr}\,\bar{B}_v^L\left(\gamma^\mu + v^\mu\right)\left[A_\mu, B_v^L\right]\\
&+ \mathcal{C}\bar{B}_v^L A_\mu T_v^{L\mu}.
\end{aligned}
$$

We can play the same game for the decuplet fields. We first isolate the EoM from eq. (4.11),

$$0 = -i\not{D} T_\mu + m_T T_\mu + \mathcal{C} A_\mu B + \mathcal{H}\gamma_\nu\gamma_5 A^\nu T_\mu$$

and split the fields into their heavy and light components (multiplying with $e^{im_B v\cdot x}$),

$$0 = \Delta m T^L_{v\mu} + (m_T + m_B)\, T^H_{v\mu} - i\not{D}\left(T^L_{v\mu} + T^H_{v\mu}\right) + \mathcal{C} A_\mu \left(B^L_v + B^H_v\right) + \mathcal{H}\gamma_\nu\gamma_5 A^\nu \left(T^L_{v\mu} + T^H_{v\mu}\right).$$

Note that we pick up an extra term, with $\Delta m = m_T - m_B$, because the fields have been parameterized using m_B, not m_T. Therefore, the whole scheme requires that $m_T - m_B$ is counted as a small quantity. There are different suggestions in the literature on how to relate $m_T - m_B$ to the Goldstone boson masses [44, 58], 61. For instance, $m_T - m_B = \mathcal{O}\left(m_K^2\right), m_T - m_B = \mathcal{O}\left(m_\pi\right)$, or $m_T - m_B = \mathcal{O}\left(\sqrt{m_\pi}\right)$. These differences matter when going beyond LO.

Next, we project out the heavy and light EoM,

$$0 = \Delta m T^L_{v\mu} - iv\cdot\mathcal{D} T^L_{v\mu} + \mathcal{C} A_\mu B^L_v + \mathcal{H}\left(\gamma_\nu + v_\nu\right)\gamma_5 A^\nu T^L_{\nu\mu} - i\not{D}_\perp T^H_{v\mu} + \mathcal{H} v_\nu\gamma_5 A^\nu T^H_{v\mu},$$

and

$$0 = (m_T + m_B)\, T^H_{v\mu} + iv\cdot\mathcal{D} T^H_{v\mu} + \mathcal{C} A_\mu B^H_v + \mathcal{H}\left(\gamma_\nu - v_\nu\right) A^\nu T^H_{v\mu} - i\not{D}_\perp T^L_{v\mu} - \mathcal{H} v_\nu\gamma_5 A^\nu T^L_{v\mu}.$$

We isolate $T^H_{v\mu}$,

$$T^H_{v\mu} = \left[m_T + m_B + iv\cdot\mathcal{D} + \mathcal{H}\left(\gamma_\nu - v_\nu\right) A^\nu\right]^{-1}\left[\mathcal{C} A_\mu B^H_v - \left(i\not{D}_\perp + \mathcal{H} v_\nu\gamma_5 A^\nu\right) T^L_{v\mu}\right] = \mathcal{O}\left(\frac{1}{m_B}\right),$$

and find for the EoM of the light fields,

$$0 = \Delta m T^L_{v\mu} - iv\cdot\mathcal{D} T^L_{v\mu} + \mathcal{C} A_\mu B^L_v + \mathcal{H}\left(\gamma_\nu + v_\nu\right)\gamma_5 A^\nu T^L_{\nu\mu}.$$

A suitable Lagrangian is given by

$$\mathcal{L}_{T^L_{v\mu}} = \Delta m \bar{T}^{L\mu}_v T^L_{v\mu} - i\bar{T}^{L\mu}_v (v\cdot\mathcal{D}) T^L_{v\mu} + \mathcal{C}\bar{T}^{L\mu}_v A_\mu B^L_v + \mathcal{H}\bar{T}^{L\mu}_v\left(\gamma_\nu + v_\nu\right)\gamma_5 A^\nu T^L_{\nu\mu}.$$

To get the lowest-order heavy-baryon Lagrangian we combine $\mathcal{L}_{B^L_v}, \mathcal{L}_{T^L_{v\mu}}$ and the Lagrangian for the Goldstone bosons, giving

$$\begin{aligned}\mathcal{L}^0_v =& i\,\mathrm{tr}\left[\bar{B}^L_v (v\cdot\mathcal{D}) B^L_v\right] + D\,\mathrm{tr}\left[\bar{B}^L_v\left(\gamma^\mu + v^\mu\right)\gamma_5\left\{A_\mu, B^L_v\right\}\right] + F\,\mathrm{tr}\left[\bar{B}^L_v\left(\gamma^\mu + v^\mu\right)\gamma_5\left[A_\mu, B^L_v\right]\right] \\ &+ \mathcal{C}\bar{B}^L_v A_\mu T^{L\mu}_v + \Delta m \bar{T}^{L\mu}_v T^L_{v\mu} - i\bar{T}^{L\mu}_v (v\cdot\mathcal{D}) T^L_{v\mu} + \mathcal{C}\bar{T}^{L\mu}_v A_\mu B^L_v \\ &+ \mathcal{H}\bar{T}^{L\mu}_v\left(\gamma_\nu + v_\nu\right)\gamma_5 A^\nu T^L_{\nu\mu} + \frac{1}{4} f^2\,\mathrm{tr}\left(\partial_\mu\Sigma\partial^\mu\Sigma^\dagger\right).\end{aligned}$$

The remaining step is to clean up notation using the spin operators (some properties may be found in ref. [10], defined as

$$S^\mu_v = -\frac{1}{2}\gamma_5\left(\gamma^\mu\psi - v^\mu\right)$$

We have (with the same calculation for the decuplet states)

$$\left(\gamma^\mu + v^\mu\right)\gamma_5 B^L_v = -\gamma_5\gamma^\mu\psi B^L_v + \gamma_5 v^\mu B^L_v = -\gamma_5\left(\gamma^\mu\psi - v^\mu\right) B^L_v = 2S^\mu_v B^L_v.$$

Filling this into the Lagrangian and dropping the L superscript gives

$$\begin{aligned}\mathcal{L}_v^0 =& i\,\mathrm{tr}\left[\bar{B}_v(v\cdot\mathcal{D})B_v\right] + 2D\,\mathrm{tr}\left(\bar{B}_v S_v^\mu \{A_\mu, B_v\}\right) + 2F\,\mathrm{tr}\left(\bar{B}_v S_v^\mu [A_\mu, B_v]\right) - i\bar{T}_v^\mu (v\cdot\mathcal{D})T_{v\mu} \\ &+ \mathcal{C}\left(\bar{T}_v^\mu A_\mu B_v + \bar{B}_v A_\mu T_v^\mu\right) + 2\mathcal{H}\bar{T}_v^\mu S_{v\nu} A^\nu T_{v\mu} + \Delta m \bar{T}_v^\mu T_{v\mu} + \frac{1}{4}f^2\,\mathrm{tr}\left(\partial_\mu\Sigma\partial^\mu\Sigma^\dagger\right)\end{aligned}$$

which is precisely the heavy-baryon Lagrangian in refs. [10], [15], 44], [57]. Now, when power counting loop diagrams are once again suppressed. Note that in the past even tree-level calculations were done in the heavy-baryon formalism. It guarantees a systematic starting point for an expansion and is simpler than relativistic calculations, as in relativistic calculations loops produce powercounting breaking contributions. Currently though, it is known how to deal with the power-counting breaking terms in a systematic way [7. Therefore, we can safely start from and do leading-order relativistic calculations.

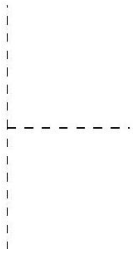
7.1.5 Nonleptonic three-body Omega decays

In this chapter we are going to analyze three decays: 1) $\Omega^- \to \Xi^-\pi^+\pi^-$, 2) $\Omega^- \to \Xi^0\pi^-\pi^0$ and 3) $\Omega^- \to \Xi^-\pi^0\pi^0$. For all three decays we will derive a parameter-free lower bound for the branching ratio. We will provide a detailed analysis of decay 1 as this is the only decay for which there are experimental data available. It turns out that there is significant disagreement between theory and experiment.

Deriving Feynman matrix elements

Allowed dominant diagram topologies

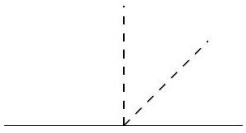
The first step is to derive the relevant dominant diagrams. This means that, per diagram, we will have several strong interactions and one weak interaction. Diagrams with more than one weak process are suppressed. Loops are also suppressed. We consider all tree-level diagrams generated by the Lagrangians (3.3) and (3.2). In general, we can distinguish three classes of diagrams, given in fig. 5.1. We have suppressed the particle labels.



(a) Type 1



(b) Type 2



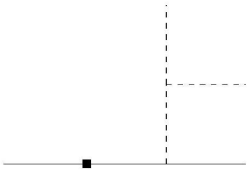
(c) Type 3

Figure 5.1: The three tree-level diagram topologies for the $\Omega \to \Xi\pi\pi$ decays. Solid lines indicate baryons while dashed lines indicate mesons.

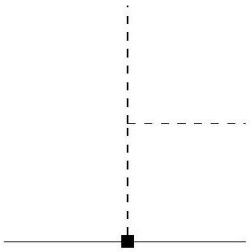
Next, we want to distribute the weak vertex which, like in the previous chapter, we denote with a black square. When relevant, strong interactions will be denoted with a black dot. Vertices without a dot are always strong vertices. Figure 5.2 shows the options for diagrams of type 1. Of the diagrams in fig. 5.2 the single valid one is 1e. The other diagrams would violate parity at a strong vertex. As an example, consider diagram 1a. The only energetically-allowed meson state which decays into two pions is the kaon, which has $J^P = 0^-$. Pions also have $J^P = 0^-$, which means that the relative orbital angular momentum of the pion-pion system must be 0. This implies that the parity of the decaying kaon is $(-1)(-1)(-1)^0 = +1$, a contradiction.

Figure 5.3 shows diagrams of type 2. Here, the only allowed diagrams are 2a and 2 b. In diagrams 2c − e and 2 g strangeness conservation demands that the first vertex from the left is of type $\Omega - \Omega - \pi$. However, this violates isospin conservation. Diagram 2f is in principle allowed, but is strongly suppressed by a factor of m_π^2 and not relevant at LO 15.

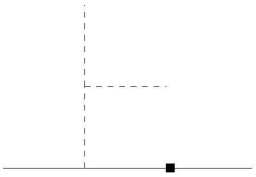
Finally, fig. 5.4 shows all possible diagrams of type 3. Four-point LO interactions are only generated if the initial and final baryon belong to the same multiplet. The direct weak transition, vertex (3.58), is only possible if initial and final baryon have the same spin, excluding all four diagrams.



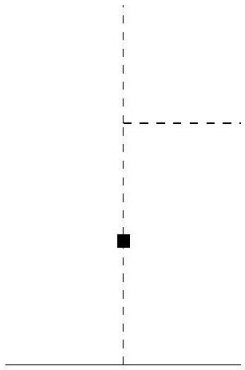
(a) Type 1a



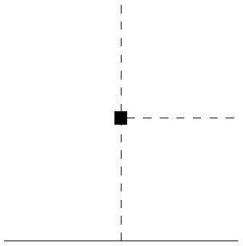
(b) Type 1*b*



(c) Type 1c



(d) Type 1 d



(e) Type 1e
(f) Type 1f
Figure 5.2: All possible diagrams of type 1 for the decay $\Omega^- \to \Xi\pi\pi$.



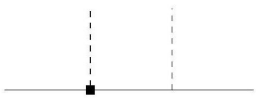
(a) Type 2a



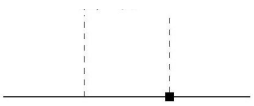
(c) Type 2c



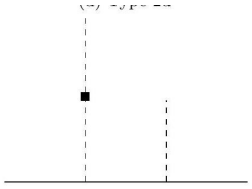
(e) Type 2e



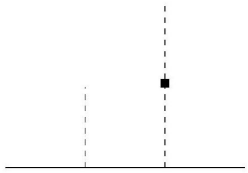
(b) Type 2*b*



(d) Type 2 d

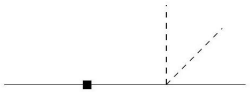


(f) Type 2f

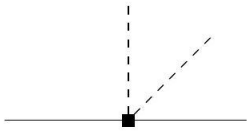


(g) Type 2 g

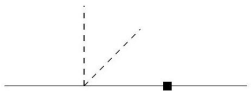
Figure 5.3: All possible diagrams of type 2 for the decay $\Omega^- \to \Xi\pi\pi$.



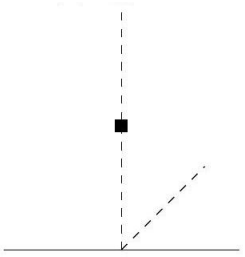
(a) Type 3a



(b) Type 3 b



(c) Type 3c



(d) Type 3d

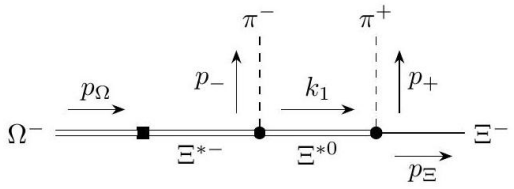
Figure 5.4: All possible diagrams of type 3 for the decay $\Omega^- \to \Xi\pi\pi$.

Diagrams per decay process

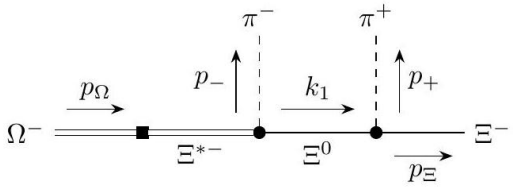
Having derived the general dominant tree-level diagram topologies, we can fill in the particles. The diagrams for the decays: 1) $\Omega^- \to \Xi^-\pi^+\pi^-$, 2) $\Omega^- \to \Xi^0\pi^-\pi^0$, and 3) $\Omega^- \to \Xi^-\pi^0\pi^0$ are shown in figs. 5.5, 5.6 and 5.7 respectively. The intermediate momenta are

$$k_1 = p_b + p_\Xi, \quad k_2 = p_a + p_\Xi, \quad \tilde{k} = p_a + p_b,$$

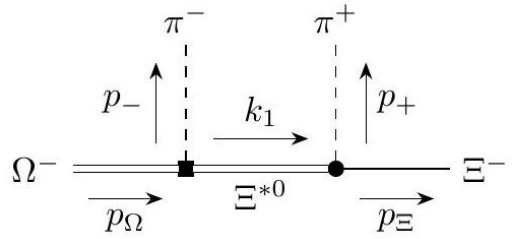
where $p_a = (p_-, p_-, p_{02})$ and $p_b = (p_+, p_0, p_{01})$. Appendix B gives an overview of the values of different vertices.



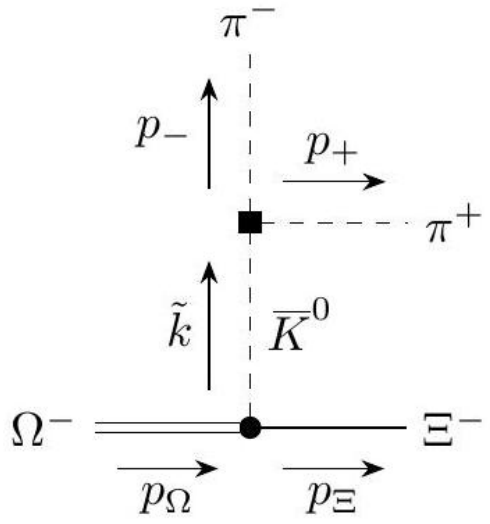
(a) Diagram 1



(b) Diagram 2

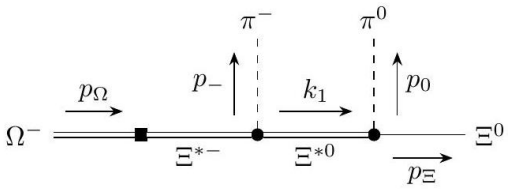


(c) Diagram 3

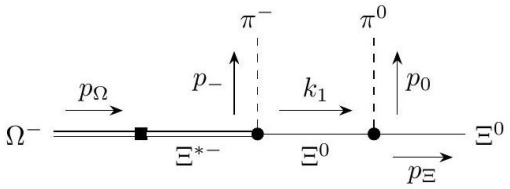


(d) Diagram 4

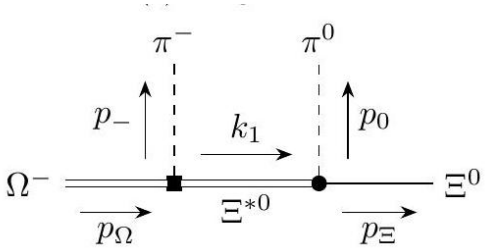
Figure 5.5: The dominant diagrams for the decay $\Omega^- \to \Xi^-\pi^+\pi^-$.



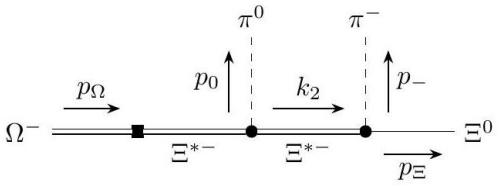
(a) Diagram 1a



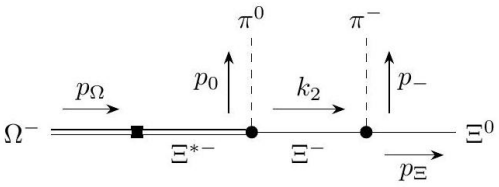
(c) Diagram 2a



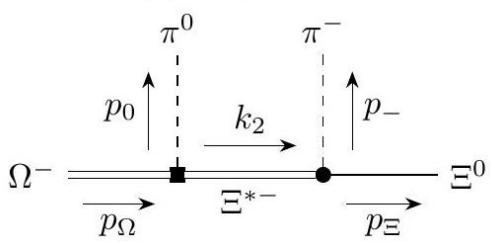
(e) Diagram 3a



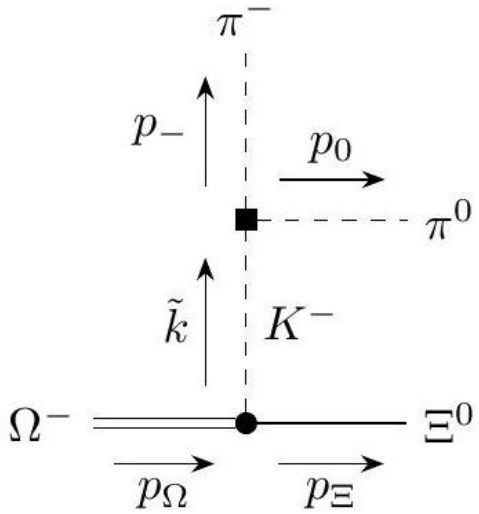
(b) Diagram 1b



(d) Diagram 2 b

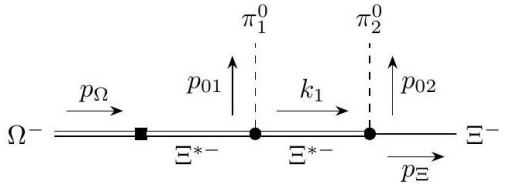


(f) Diagram 3b

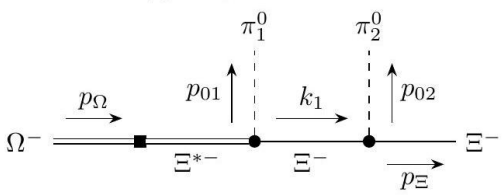


(g) Diagram 4a

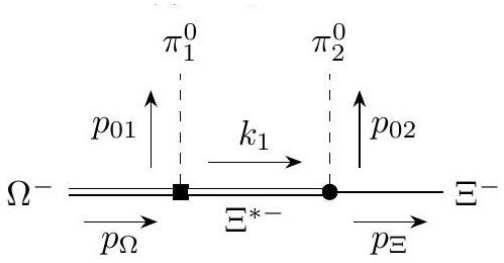
Figure 5.6: The dominant diagrams for the decay $\Omega^- \to \Xi^0\pi^-\pi^0$.



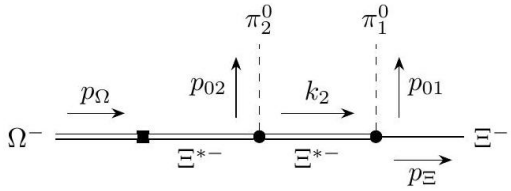
(a) Diagram 1a



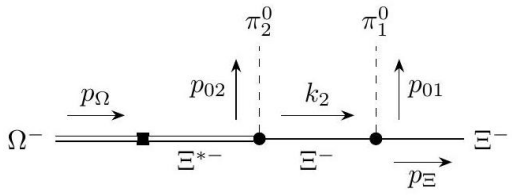
(c) Diagram 2a



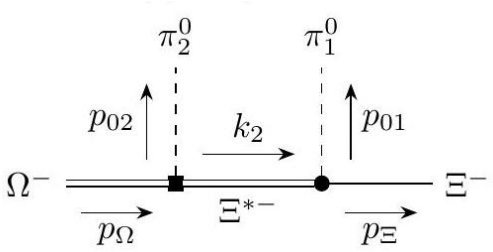
(e) Diagram 3a



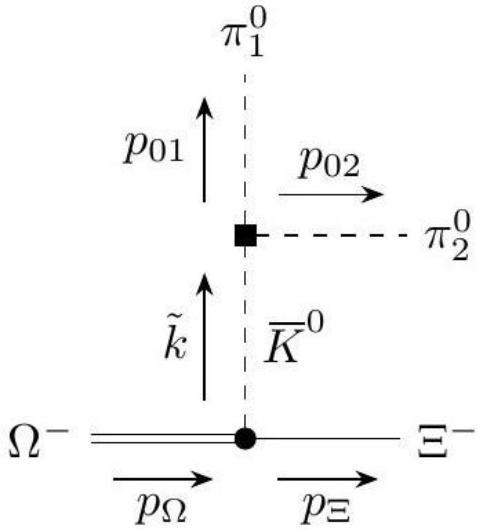
(b) Diagram 1b



(d) Diagram 2b



(f) Diagram 3b



(g) Diagram 4a

Figure 5.7: The dominant diagrams for the decay $\Omega^- \to \Xi^-\pi^0\pi^0$.

Analytic structure of the Feynman matrix elements

For decays 1-3 the generic structure of the Feynman matrix element is

$$\mathcal{M}_i\left(\Omega^- \to \Xi\pi\pi\right) = \bar{u}\left(p_\Xi\right)\beta_i^\sigma \mu_\sigma\left(p_\Omega\right),$$

where β_i^σ depends on what decay i we consider. For decay $1, \Omega^- \to \Xi^-\pi^+\pi^-$we find,

$$\begin{aligned}\beta_1^\sigma =& \frac{h_A H_A h_C}{18\sqrt{2}F_\pi^2} p_+^\mu P_{\mu\nu}^T\left(k_1, m_{\Xi^*}, \epsilon\right) \not{p}_- \gamma_5 P_T^{\nu\sigma}\left(p_\Omega, m_{\Xi^*}\right) \\ &+ \frac{h_A h_C (D-F)}{6\sqrt{2}F_\pi^2} p_-^\mu \not{p}_+ \gamma_5 P^B\left(k_1, m_\Xi\right) P_{\mu\nu}^T\left(p_\Omega, m_{\Xi^*}\right) g^{\nu\sigma} \\ &- \frac{i h_A h_C}{6\sqrt{2}F_\pi^2} p_+^\mu P_{\mu\nu}^T\left(k_1, m_{\Xi^*}, \epsilon\right) g^{\nu\sigma} - \frac{i h_A h_\pi}{4\sqrt{2}F_\pi^2} P^\Phi\left(\tilde{k}, m_K\right) \tilde{k}^\sigma\left(\tilde{k}\cdot p_+ + p_+ \cdot p_-\right).\end{aligned}$$

For decay $2, \Omega^- \to \Xi^0\pi^-\pi^0$, we find

$$\begin{aligned}
&\beta_2^\sigma = \\
&\frac{h_A H_A h_C}{36F_\pi^2}\left(p_0^\mu P_{\mu\nu}^T\left(k_1, m_{\Xi^*}, \epsilon\right)\not{p}_- \gamma_5 P_T^{\nu\sigma}\left(p_\Omega, m_{\Xi^*}\right) - p_-^\mu P_{\mu\nu}^T\left(k_2, m_{\Xi^*}, \epsilon\right)\not{p}_0\gamma_5 P_T^{\nu\sigma}\left(p_\Omega, m_{\Xi^*}\right)\right) \\
&+ \frac{h_A h_C(D-F)}{12F_\pi^2}\left(p_-^\mu \not{p}_0\gamma_5 P^B\left(k_1, m_\Xi\right) P_{\mu\nu}^T\left(p_\Omega, m_{\Xi^*}\right) - p_0^\mu \not{p}_-\gamma_5 P^B\left(k_2, m_{\Xi^*}\right) P_{\mu\nu}^T\left(p_\Omega, m_{\Xi^*}\right)\right) g^{\nu\sigma} \\
&- \frac{i h_A h_C}{12F_\pi^2}\left(p_0^\mu P_{\mu\nu}^T\left(k_1, m_{\Xi^*}, \epsilon\right) - p_-^\mu P_{\mu\nu}^T\left(k_2, m_{\Xi^*}, \epsilon\right)\right) g^{\nu\sigma} + \frac{i h_A h_\pi}{8F_\pi^2} P^\Phi\left(\tilde{k}, m_K\right)\tilde{k}^\sigma\left(\tilde{k}\cdot p_- - \tilde{k}\cdot p_0\right).
\end{aligned}$$

For decay $3, \Omega^- \to \Xi^-\pi^0\pi^0$, we find

$$\begin{aligned}
&\beta_3^\sigma = \\
&- \frac{h_A H_A h_C}{36\sqrt{2}F_\pi^2}\left(p_{20}^\mu P_{\mu\nu}^T\left(k_1, m_{\Xi^*}, \epsilon\right)\not{p}_{10}\gamma_5 P_T^{\nu\sigma}\left(p_\Omega, m_{\Xi^*}\right) + p_{10}^\mu P_{\mu\nu}^T\left(k_2, m_{\Xi^*}, \epsilon\right)\not{p}_{20}\gamma_5 P_T^{\nu\sigma}\left(p_\Omega, m_{\Xi^*}\right)\right) \\
&+ \frac{h_A h_C(D-F)}{12\sqrt{2}F_\pi^2}\left(p_{10}^\mu \not{p}_{20}\gamma_5 P^B\left(k_2, m_\Xi\right) P_{\mu\nu}^T\left(p_\Omega, m_{\Xi^*}\right) + p_{20}^\mu \not{p}_{10}\gamma_5 P^B\left(k_1, m_\Xi^*\right) P_{\mu\nu}^T\left(p_\Omega, m_{\Xi^*}\right)\right) g^{\nu\sigma} \\
&+ \frac{i h_A h_C}{12\sqrt{2}F_\pi^2}\left(p_{20}^\mu P_{\mu\nu}^T\left(k_2, m_{\Xi^*}, \epsilon\right) + p_{10}^\mu P_{\mu\nu}^T\left(k_1, m_{\Xi^*}, \epsilon\right)\right) g^{\nu\sigma} \\
&+ \frac{i h_A h_\pi}{8\sqrt{2}F_\pi^2} P^\Phi\left(\tilde{k}, m_K\right)\tilde{k}^\sigma\left(2p_{10}\cdot p_{20} + \tilde{k}\cdot\left[p_{10}+p_{20}\right]\right).
\end{aligned}$$

Propagators that do not explicitly contain an ϵ in their argument do not hit a pole. For decay 2, we approximate $m_{\Xi^{*-}} \approx m_{\Xi^{*0}} \approx \left(m_{\Xi^{*-}} + m_{\Xi^{*0}}\right)/2 = m_{\Xi^*}$. We do the same approximation for the masses of $\Xi^-$and Ξ^0.

We can check whether these expressions make sense via several consistency checks. As an example, consider the final term in decay $2 \sim \tilde{k}\cdot p_- - \tilde{k}\cdot p_0$. Up to differences in the neutral and charged pion mass this term is zero, which is expected. By angular-momentum conservation for the decay $K \to \pi\pi$ we have $L = J = 0$, where L is the orbital angular momentum of the 2π system and J is the total angular momentum of the transition. The isospin of the two pions is either $I_{2\pi} = 0, 2$, because of Bose-Einstein symmetry (which demands that $J + I$ is even). But, $\pi^-\pi^0$ cannot have $I_{2\pi} = 0$, so $I_{2\pi} = 2$. This is a $\Delta I = 3/2$ transition because $I_K = 1/2$. That transition is not supported by our Lagrangian, so the term should be zero.

For the spin-averaged matrix element we find

$$\left\langle\left|\mathcal{M}_i\left(\Omega^- \to \Xi\pi\pi\right)\right|^2\right\rangle = -\frac{1}{4}\,\mathrm{tr}\left[\left(\not{p}_\Xi + m_\Xi\right)\beta_i^\sigma\left(\not{\phi}_\Omega + m_\Omega\right)P_{\sigma\tau}^{3/2}\bar{\beta}_i^\tau\right]$$

where $\bar{\beta}_i^\tau = \gamma_0\left(\beta_i^\tau\right)^\dagger\gamma_0$ and there is no sum over i. We evaluate traces using FeynCalc 62 -64. Diagrams 1 (for decays 2 and 3 this means diagrams 1a and 1b) and 2 do not interfere with diagrams 3 and 4. To see this, note that terms in $\mathcal{M}$ from diagrams 1 and 2 go with a γ_5 while terms from diagrams 3 and 4 do not [the first two terms and last two terms in eqs. (5.3), (5.4) and(5.5)]. Under parity the former transform opposite to the latter, and we call them conserving type and violating type, respectively. Let us group terms in eq. (5.6) by whether or not there is a γ_5,

$$\left\langle|\mathcal{M}|^2\right\rangle \sim \mathrm{tr}\left\{\left[(\text{v type}) + (\text{ c type})\gamma_5\right]\left[(\text{ v type}) + (\text{ c type})\gamma_5\right]\right\}.$$

The interference term will go like tr [(v type) (c type) γ_5]. If (v type) (c type) contains an odd number of gamma matrices the trace will be zero. If there are an even number of gamma

matrices, the trace (including the γ_5) will give a Levi-Civita symbol. The only thing with which the symbol can contract are momenta. All momenta lie in the same plane, so this term must be zero. Hence, there can be no interference terms. We also see this numerically.

Dalitz distributions for the decays $\Omega^- \to \Xi\pi\pi$

To get a feeling for the three-body Omega decays, let us explore their Dalitz distributions. The following will be a qualitative discussion of the main features of the distributions. These are independent of the values of the LECs, if the LECs are varied within their physical limits. To be clear though, numerically we use

$$D = 0.80, \quad F = 0.46, \quad h_\pi = -3.12 \times 10^{-7}, \quad h_A = 2.0, \quad H_A = 2.0, \quad h_C = 5.1 \times 10^{-8}\text{GeV}.$$

Here, only h_C is dimensionfull. In section 5.2.1, we will become more quantitative and explain why we use the aforementioned LEC values.

Let us start with the decay $1, \Omega^- \to \Xi^-\pi^+\pi^-$. As explained in chapter 2, the Feynman matrix element depends on two different variables. We pick

$$m^2\left(\Xi^-\pi^+\right) = \left(p_\Xi + p_+\right)^2, \quad m^2\left(\Xi^-\pi^-\right) = \left(p_\Xi + p_-\right)^2.$$

Then, the double differential decay width is

$$\mathrm{d}\Gamma\left(\Omega^- \to \Xi^-\pi^+\pi^-\right) = \frac{1}{32\left(2\pi m_\Omega\right)^3}\left\langle\left|\mathcal{M}\left(\Omega^- \to \Xi^-\pi^+\pi^-\right)\right|^2\right\rangle \mathrm{d}m^2\left(\Xi^-\pi^+\right)\mathrm{d}m^2\left(\Xi^-\pi^-\right).$$

Alternatively, we may use $\cos\theta$ as a second variable instead of $m^2\left(\Xi^-\pi^-\right)$. Here, θ is the angle between $\boldsymbol{p}_\Xi$ and $\boldsymbol{p}_-$in the frame where $\boldsymbol{p}_+ + \boldsymbol{p}_\Xi = \boldsymbol{0}$. This is illustrated in fig. 5.8

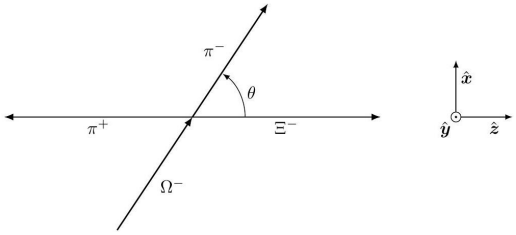
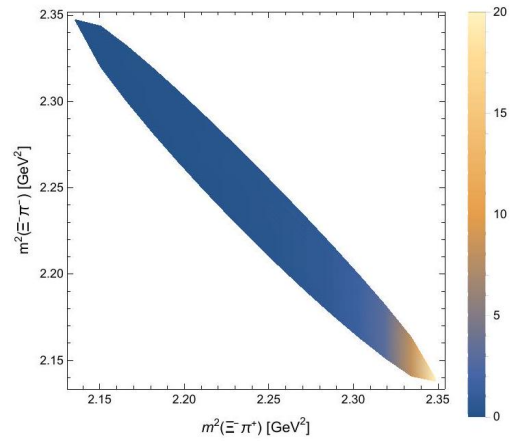
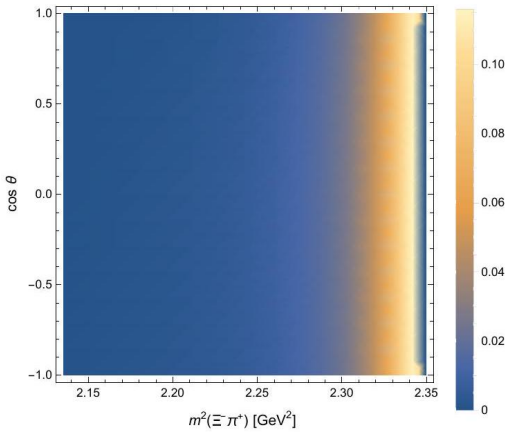


Figure 5.8: The kinematics for the decay $\Omega^- \to \Xi^-\pi^+\pi^-$in the frame where $\boldsymbol{p}_+ + \boldsymbol{p}_\Xi = \boldsymbol{0}$.

The result of eq. 5.9 is shown in fig. 5.9. The main feature of the Dalitz distribution is the peak of the $\Xi^{*0}(1530)$ resonance. All other features are washed away because the resonance is so prominent. It is caused by diagram 3 of fig. 5.7, which leads to the third term $\sim h_A h_C$ on the right-hand side of eq. (5.3). As we will see in the following, the other diagrams are numerically much less important if their parameters are kept in a reasonable (bound by experiments) range. The numerical dominance of one diagram over all others also implies that interference effects are small. We will frequently come back to this aspect.



(a) Two invariant masses as variables.



(b) An invariant mass and an angle as variables.

Figure 5.9: Dalitz plots for the decay $\Omega^- \to \Xi^-\pi^+\pi^-$, normalized by the total decay width. The resonance $\Xi^*(1530)$ is clearly visible.

We can be somewhat more precise about the relative numerical importance of each diagram. The main message of what we discuss here still holds if the LECs are varied within their respective uncertainties. Moreover, the ordering of the diagrams is similar for the other two Omega decays. Therefore, for definiteness, we restrict this part to the decay $\Omega^- \to \Xi^-\pi^+\pi^-$using the parameter values (5.8. We can factor the decay width as

$$\Gamma = \sum_{i,j} \Gamma_{ij}$$

where Γ_{ij} is the contribution to the decay width from diagrams i and j. The numerically dominant term is Γ_{33}. To get an indication of the relative sizes of the other diagrams we calculate $\sqrt{|\Gamma_{11}/\Gamma_{33}|}, \sqrt{|\Gamma_{12}/\Gamma_{33}|}, \ldots, \sqrt{|\Gamma_{44}/\Gamma_{33}|}$. We find

$$\begin{array}{c} \Gamma_1 \\ \Gamma_1 \\ \Gamma_2 \\ \Gamma_3 \\ \Gamma_4 \end{array} \begin{pmatrix} 0.19 & 0.00072 & 0 & 0 \\ 0.00072 & 0.018 & 0 & 0 \\ 0 & 0 & 1 & 0.22 \\ 0 & 0 & 0.22 & 0.09 \end{pmatrix},$$

where the entry in the i th row and j th column of the above matrix contains $\sqrt{|\Gamma_{ij}/\Gamma_{33}|}$. Note that also numerically v-type and c-type diagrams do not interfere. The other resonant

diagram, diagram 1, is subdominant to the third diagram. The nonresonant diagrams provide only small contributions to the total decay width. The interference terms between diagrams 1 and 2 are essentially negligible, while the interference terms between between diagram 3 and 4 are comparable in size to diagram 1. Previous (heavy baryon) work states that the terms coming from diagram 4 are larger than expected [15]. From the above matrix it is clear that the interference terms are the driving force behind the larger-than-expected contribution. So, if we were to order the diagrams by their numerical importance by only looking at the terms $\sim \Gamma_{ii}$, we would have

$$\text{diagram 3} > \text{ diagram 1} > \text{ diagram 4} > \text{ diagram 2}.$$

However, given the importance of some of the interference terms, a more sensible ordering may be

$$\text{diagram 3} > \text{ diagram 4} > \text{ diagram 1} > \text{ diagram 2}.$$

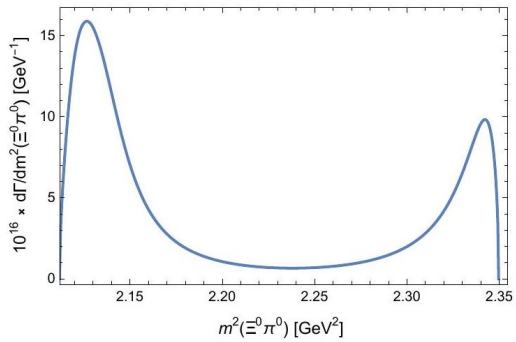
Moving on, for decays 2-3, $\Omega^- \to \Xi^0\pi^-\pi^0$ and $\Omega^- \to \Xi^-\pi^0\pi^0$, we will be more brief as there are no experimental data available. For decay 2 we pick the kinematic variables

$$m^2\left(\Xi^0\pi^0\right) = \left(p_\Xi + p_0\right)^2, \quad m^2\left(\Xi^0\pi^-\right) = \left(p_\Xi + p_-\right)^2.$$

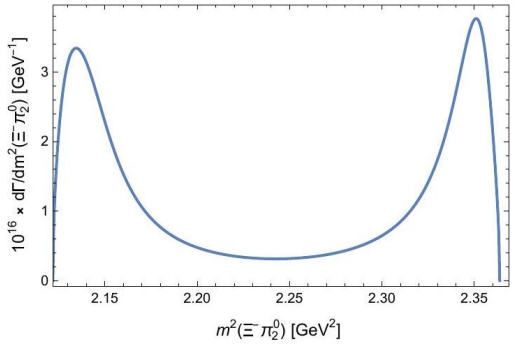
For decay 3, we pick

$$m^2\left(\Xi^-\pi_2^0\right) = \left(p_\Xi + p_{02}\right)^2, \quad m^2\left(\Xi^0\pi_1^0\right) = \left(p_\Xi + p_{01}\right)^2$$

The distributions for decay 2 and 3 are both double peaked, as can been seen from figs. 5.10a and 5.10 b The appearance of double-peaked distributions is not entirely surprising. The right peak



(a) $\Omega^- \to \Xi^0\pi^-\pi^0$



(b) $\Omega^- \to \Xi^- \pi^0 \pi^0$

Figure 5.10: The differential decay distribution for two different Omega decays. Both distributions are double-peaked.

is the familiar $\Xi^*(1530)$ resonance. The left peak arises due to symmetry reasons. Notice that as compared to decay 1, decays 2 and 3 have three extra diagrams. Between (say) diagram 3a and 3 b there is a symmetry under exchange of the pion momenta. This means that the Dalitz distribution in the two kinematic variables should be symmetric (because in the isospin-symmetric limit pion masses are the same). For example, fig. 5.11a shows said Dalitz distribution for decay 3. The dashed black line is the symmetry axis. The peak at $m\,(\Xi^-\pi_2^0) = 1.530\text{GeV}$ gets folded to the upper-left corner. There, it is no longer a vertical line but a horizontal one. The peak gets smeared out over $m\,(\Xi^-\pi_2^0)$ as compared to the original resonance. In fact, from eqs. 2.10) and 2.11) we can calculate the left peak's location, shown by the dashed red line.

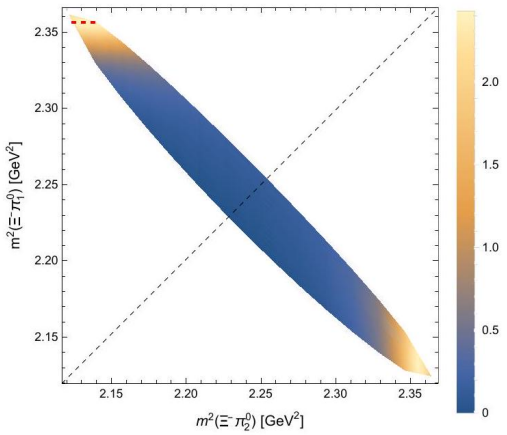
Next, we convert one of the kinematic variables to $\cos\theta$. The new Dalitz plot is shown in fig. 5.11 b The red dashed line in fig. 5.11a gets mapped to the red dashed line in fig. 5.11b. Clearly, this corresponds to the left peak. Since we are close to the edges of our phase space the angular dependence will be small. Therefore, the right peaks in fig. 5.10 are not smeared out very much. What about the relative magnitude of the two peaks? The left peak comes from the square of diagram 3a and the right peak from the square of diagram 3 b, the numerically dominant diagrams. Therefore, up to some small corrections, the relative peak size should be determined by the square of the Clebsch-Gordan coefficients for decays

$$\Xi^{*-} \to \Xi^- \pi^0, \Xi^0 \pi^-,$$
$$\Xi^{*0} \to \Xi^- \pi^+, \Xi^0 \pi^0.$$

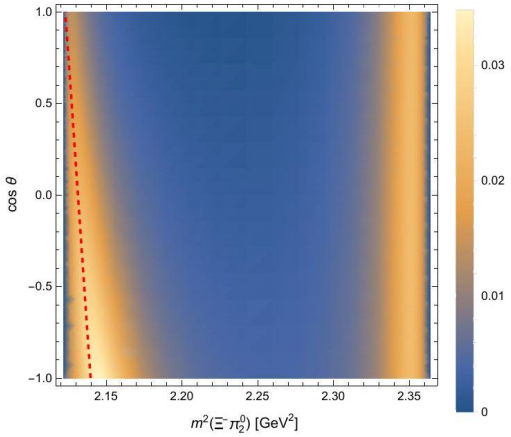
Coefficients can be extracted from the vertices. We find that the Ξ^{*0} channels should be suppressed by a factor of $\frac{1}{2}$ compared to Ξ^{*-} channels. This is (approximately) visible in the peak sizes in fig. 5.10a Meanwhile, fig. 5.10b should have approximately the same peak size but with a somewhat smeared-out left peak (lowering its height relative to the right peak), which is indeed what we observe.

Varying parameters

We have discussed the main, qualitative features of our decays. Now, we would like to calculate a number, the branching fraction. To do so we need to pin down several parameters: h_A, H_A, h_C, h_π and $(D-F)$. Known values of these parameters from tree-level fits still have quite some



(a) Two invariant masses as variables.



(b) An invariant mass and an angle as variables.

Figure 5.11: The double differential decay distribution for $\Omega^- \to \Xi^-\pi^0\pi^0$, normalized by the total decay width. The red line indicates where, due to symmetry reasons, a resonance like $\Xi^*(1530)$ must appear.

uncertainty [15], [4], [44. To that end, it is worth investigating what happens when we vary the parameters inside their error bars around their central values.

We will not vary h_π, D and F. The value of h_π is determined from kaon decays [65], 66] and falls outside of the scope of this thesis. The values of D and F are well determined and, in our case, terms proportional to $D - F$ are numerically insignificant. We use

$$D = 0.80, \quad F = 0.46, \quad h_\pi = -3.12 \times 10^{-7}.$$

This leaves h_A, H_A and h_C. We have two different options to determine the parameters. We can either consider our theory in the limit of a large number of colors N_c, or we can fit to data. For the former, $h_A = (3/\sqrt{2})g_A$ and $H_A = (9/5)g_A$ [11, where $g_A \approx 1.267$ is the well-known axial coupling of the nucleon 61]. In practice the number of colors is far from large. Therefore, such ideas need to be tested. So, fits are better, which will hopefully be similar to the large-N_c-limit values. However, because we only consider LO terms, fits for specific parameters will give somewhat different results depending on what decay we consider. Fits for h_A have been done in ref. [43], whose values we adopt. There is no simple observable to determine H_A, so as an upper limit we pick the large-color limit from ref. [1] and as a lower limit we pick minus that value. This gives

$$h_A = 2.4 \pm 0.5, \quad -2.27 \leq H_A \leq 2.27.$$

We determine h_C by fitting to the decay width $\Omega^- \to \Xi^0\pi^-$, taken from the Particle Data Group [14. The relevant diagram is shown in fig. 5.12.

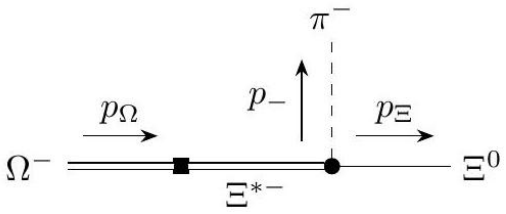


Figure 5.12: The LO Feynman diagram for the decay $\Omega^- \to \Xi^0\pi^-$.

The corresponding spin-averaged matrix element is given by

$$\left\langle \left| \mathcal{M}\left(\Omega^- \to \Xi^0\pi^-\right) \right|^2 \right\rangle = \frac{h_A^2 h_C^2}{432 F_\pi^2} \frac{\left(m_\Omega^2 - 2m_\Omega m_\Xi - m_\pi^2 + m_\Xi^2\right)\left(m_\Omega^2 + 2m_\Omega m_\Xi - m_\pi^2 + m_\Xi^2\right)^2}{m_\Omega^2 \left(m_\Omega - m_{\Xi*}\right)^2}.$$

Figure 5.13 shows the result of the fit. Neglecting the small uncertainties we see that $h_A \propto h_C^{-1}$ and

$$3.5 \times 10^{-8}\text{GeV} \leq |h_C| \leq 5.4 \times 10^{-8}\text{GeV}.$$

In principle, we could also fit to the decay $\Omega^- \to \Xi^-\pi^0$ or the decay $\Omega^- \to \Lambda K^-$. As we use the value of h_A from cascade decays, it makes more sense to not include kaon decays. Because we work with the LO Lagrangian, some of the higher-order contributions get absorbed into the fitted values for the LECs. This means that when we fit to different decays at LO, the LECs will have a spread in their values. If we use LEC values from kaon decays for cascade decays, we would be adding dynamics that are not there in cascade decays. We do not fit to the decay $\Omega^- \to \Xi^-\pi^0$ because χPT calculations differ from measured values (as it is unclear if the $\Delta I = 1/2$ rule holds) [44]. Therefore, fits to this decay could give a misleading value for h_C. We deem this situation more likely than both χPT and the measurement of $\Omega^- \to \Xi^0\pi^-$being wrong.

Note that this fit does not determine the sign of h_C, only its magnitude. We have checked that major features, like resonances, in (say) Dalitz plots do not change when we flip the sign of h_C. Any observables that we calculate will have their values shifted by at most 10% or so. Therefore, in the discussion above, where we explored the differential distribution of the three-body Omega decays, we stuck to a positive sign for h_C. When we make a prediction, like in section 5.3 we take both signs into account.

One might wonder why we are going through the trouble of fitting h_C ourselves. After all, have similar fits not been done in refs. [15], [44], 67]? The point is that the relative sign between h_C and h_π is unclear in these fits. This relative sign is not convention. In ref. [44] both h_C and h_π are given. However, h_π appears to have a different sign as compared to other literature [15], [66]. We do not know where this sign change comes from. A possible answer comes from the field redefinition, as explained in section 4.1.3 In ref. [67] the authors do a one-loop fit, but fail to mention the value of h_π that they use. Lastly, ref. [15] takes the sign of h_π from literature. Whether the relative sign is correct, then, is not guaranteed. Fortunately, in practice the relative sign between h_π and h_C is not that important, because diagram 4, which is $\sim h_\pi$, is subdominant relative to the resonant diagram 3. Therefore, it is sufficient to stick to our fits.

Next, we would like to know the effects of varying H_A and h_A. In the parameter space that we consider $\mathcal{B}(\Omega^- \to \Xi^-\pi^+\pi^-)$is monotonically increasing for increasing h_A. Hence, using the lowest value and highest values for h_A gives a lower and upper bound for the branching ratio. We have plotted this in fig. 5.14

We can see that for a given value of h_A varying H_A only changes the branching ratio by $\sim 5\%$. To

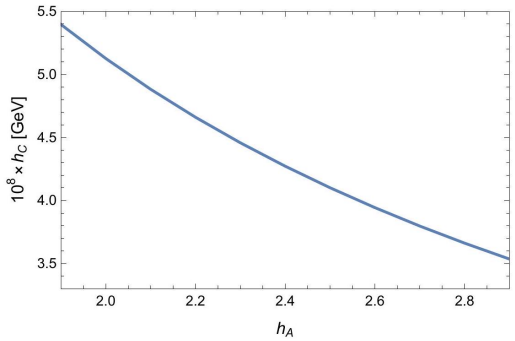


Figure 5.13: A fit for h_C (greater than zero) of the decay width for the decay $\Omega^- \to \Xi^0\pi^-$for different h_A.

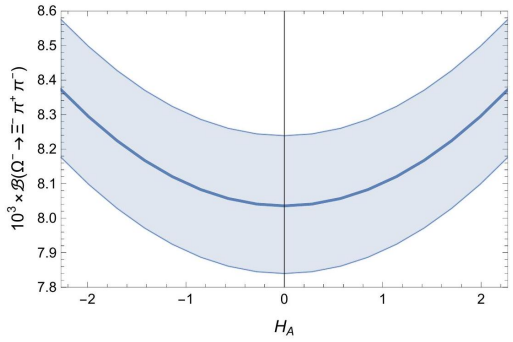


Figure 5.14: The branching ratio for the decay $\Omega^- \to \Xi^-\pi^+\pi^-$for varying h_A and H_A, with positive h_C. In the shaded region $1.9 \leq h_A \leq 2.9$, giving the lower and upper bound, respectively. The curve represents the central value where $h_A = 2.4$.

explain this, note that the system is largely non-relativistic and that its phase space is dominated by the Ξ^{*0} (1530) resonance. The numerically dominant diagram is 3, with other diagrams being subdominant. Only diagram 1 $\propto H_A$. Let p stand for a typical momentum scale, in this case p_-, which is the momentum of $\pi^-$when $\pi^+$and Ξ^-emerge from the Ξ^{*0} at its peak mass. In other words, in the Omega rest frame $\left|\boldsymbol{p}_-\right| = \lambda^{1/2}\left(m_\Omega^2, m_\pi^2, m_{\Xi^*}^2\right)/\left(2m_\Omega\right) \approx 17\text{MeV}$. The resonance emerges from a vertex in diagram 1, which is proportional to p^1, while in diagram 3 the resonance emerges from a vertex proportional to p^0. From quantum mechanics we know that this corresponds to a p wave and an s wave, respectively (since the momentum scaling must be $\sim p^\ell$) 68. So, the matrix element of diagram 1 is suppressed relative to diagram 3 by roughly the square of $\left|\boldsymbol{p}_-\right|/\left(m_\Omega - m_{\Xi^*}\right) \approx 17/140 \approx 0.12$. Indeed H_A only changes the branching ratio on the order of a couple percent (since $0.12^2 \approx 0.014$).

The small effect of H_A is also evident in the angular distribution. In fig. 5.15 the dashed orange line shows the 'normal' angular distribution where numerically we use $h_A = 2.0, h_C = 5.1 \times 10^{-8}\text{GeV}$ and $H_A = 2.0$. We normalize the decay distribution to its minimum value. Here, the s wave is dominant. This is clear in the distribution as there is only a negligible angular variation. Meanwhile, the solid blue line shows the normalized angular distribution when we artificially make the p wave dominant. We do this by setting $D = F = h_\pi = 0$ and $H_A = 2.0 \times 10^3$. In this way we make diagram 1 dominant over diagram 3. We see that the angular variation is much larger.

The angular dependence may be derived from general considerations. In fact, we need not use quantum field theory at all (making this alternative calculation a useful consistency check). Let $D^j_{m'm}(\alpha, \beta, \gamma)$ be the Wigner D-matrix 69. and $d^j_{m'm}(\beta) = D^j_{m'm}(0, \beta, 0)$ be the small Wigner d-matrix. We know that 68

$$\frac{\mathrm{d}\Gamma\left(\Omega^- \to \Xi^-\pi^+\pi^-\right)}{\mathrm{d}\cos\theta} \propto \sum_{m',m} w_{m'm}\left|d^{s_\Omega}_{m'm}\right|^2,$$

where s_Ω is the spin of the Omega baryon and m' and m the helicities (magnetic quantum numbers) of the cascade and the Omega baryons. We can extract the angular dependence and its corresponding weight $w_{m'm}$ from

$$\left\langle \Xi^-\pi^+\pi^-, m_\Xi, \theta | \Omega^-, m_\Omega \right\rangle$$

where m_i is the magnetic quantum number, not to be confused with the mass (we suppress $m_\pi = 0$). The angular dependence will come from a small Wigner d-matrix. Its weight comes from Clebsch-Gordan coefficients. If we assume that our decay is dominated by the $\Xi^{*0}(1530)$ resonance

$$\begin{aligned}\left\langle \Xi^-\pi^+\pi^-, m_\Xi, \theta | \Omega^-, m_\Omega \right\rangle &\propto \sum_{m_{\Xi^*}} \left\langle \Xi^-\pi^+, m_\Xi, \theta | \Xi^{*0}, m_{\Xi^*} \right\rangle \left\langle \pi^-\Xi^{*0}, m_{\Xi^*} | \Omega^-, m_\Omega \right\rangle, \\ &= \left\langle \Xi^-\pi^+, m_\Xi, \theta | \Xi^{*0}, m_\Omega \right\rangle \left\langle \pi^-\Xi^{*0}, m_\Omega | \Omega^-, m_\Omega \right\rangle.\end{aligned}$$

In the first line we have inserted a complete set of particle states. We are in the rest frame of Ξ^{*0}. We pick the spin-quantization axis parallel to $\boldsymbol{p}_\Omega = \boldsymbol{p}_-$. It follows that $m_{\Xi^*} = m_\Omega$. Next, we expand eq. (5.14) 70

$$\begin{aligned}&\left\langle \Xi^-\pi^+, m_\Xi, \theta | \Xi^{*0}, m_\Omega \right\rangle \left\langle \pi^-\Xi^{*0}, m_\Omega | \Omega^-, m_\Omega \right\rangle \\ &\propto d^{s_{m^*}=3/2}_{m_\Omega m_\Xi}(\theta) \left\langle \pi^-\Xi^{*0}, m_\Omega | \Omega^-, m_\Omega \right\rangle, \\ &\propto d^{s_{m^*}=3/2}_{m_\Omega m_\Xi}(\theta) \left\langle s_1 = \frac{3}{2}, m_1 = m_{\Xi^*}, s_2 = 0, m_2 = 0 | J_\Omega = \frac{3}{2}, m_\Omega \right\rangle, \\ &\propto d^{3/2}_{m_\Omega m_\Xi}(\theta) \sum_{L,S,J,M} T^{LSJM} \left\langle s_1 = \frac{3}{2}, m_1 = m_{\Xi^*}, s_2 = 0, m_2 = 0 | J, M; L, S \right\rangle \left\langle J, M; L, S | J_\Omega = \frac{3}{2}, m_\Omega \right\rangle \\ &= d^{3/2}_{m_\Omega m_\Xi}(\theta) \sum_{L,S} T^{LS} \left\langle s_1 = \frac{3}{2}, m_1 = m_{\Xi^*}, s_2 = 0, m_2 = 0 | J_\Omega, m_\Omega; L, S \right\rangle.\end{aligned}$$

In the fourth line we have inserted a complete set of states. We change from the helicity states to the LS basis of orbital angular momentum L and total spin S[70]. In the proportionality signs we absorb the reduced matrix elements we get from going from a particle basis to an angular-momentum basis. Here, T^{LSJM} are the reduced matrix elements which we keep explicit. We define $T^{LS} = T^{LSJ_\Omega m_\Omega}$. Again, we expand using Clebsch-Gordan coefficients $C\left(j_1, j_2, J; m_1, m_2\right) \delta_{m, m_1+m_2}$,

$$\begin{aligned}&d^{3/2}_{m_\Omega m_\Xi}(\theta) \sum_{L,S} T^{LS} \left\langle s_1 = \frac{3}{2}, m_1 = m_{\Xi^*}, s_2 = 0, m_2 = 0 | J_\Omega, m_\Omega; L, S \right\rangle \\ &\propto d^{3/2}_{m_\Omega m_\Xi}(\theta) \sum_{L} T^{L\frac{3}{2}} C\left(L, \frac{3}{2}, \frac{3}{2}; 0, m_\Omega\right) C\left(\frac{3}{2}, 0, \frac{3}{2}; m_\Omega, 0\right) \\ &= d^{3/2}_{m_\Omega m_\Xi}(\theta) \sum_{L} T^{L\frac{3}{2}} C\left(L, \frac{3}{2}, \frac{3}{2}; 0, m_\Omega\right) \\ &= d^{3/2}_{m_\Omega m_\Xi}(\theta) \left[T^{0\frac{3}{2}} C\left(0, \frac{3}{2}, \frac{3}{2}; 0, m_\Omega\right) + T^{1\frac{3}{2}} C\left(1, \frac{3}{2}, \frac{3}{2}; 0, m_\Omega\right) \right]\end{aligned}$$

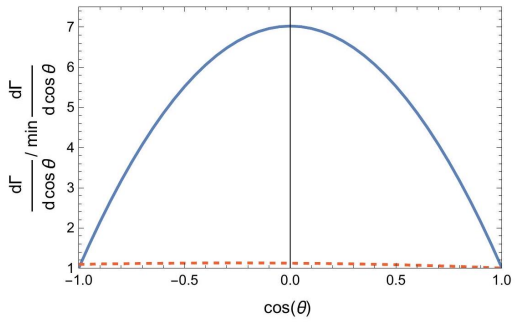


Figure 5.15: The angular distribution for the decay $\Omega^- \to \Xi^-\pi^+\pi^-$normalized by its minimum value. The dashed orange line shows the s-wave-dominated distribution and the solid blue line shows the artificially-enhanced p-wave-dominated distribution. In the final line, the first

component corresponds to the s wave and the second component corresponds to the p wave. We have the following Clebsch-Gordan coefficients 14

$$\begin{array}{ll} C\left(0,\frac{3}{2},\frac{3}{2};0,\frac{3}{2}\right)=1, & C\left(0,\frac{3}{2},\frac{3}{2};0,\frac{1}{2}\right)=1, \\ C\left(0,\frac{3}{2},\frac{3}{2};0,-\frac{1}{2}\right)=1, & C\left(0,\frac{3}{2},\frac{3}{2};0,-\frac{3}{2}\right)=1, \\ C\left(1,\frac{3}{2},\frac{3}{2};0,\frac{3}{2}\right)=\frac{3}{\sqrt{15}}, & C\left(1,\frac{3}{2},\frac{3}{2};0,\frac{1}{2}\right)=\frac{1}{\sqrt{15}} \\ C\left(1,\frac{3}{2},\frac{3}{2};0,-\frac{1}{2}\right)=-\frac{1}{\sqrt{15}}, & C\left(1,\frac{3}{2},\frac{3}{2};0,\frac{3}{2}\right)=-\frac{3}{\sqrt{15}}. \end{array}$$

If either the s wave or the p wave is dominant then only one term in eq. 5.16) is relevant. For the s wave

$$\frac{\mathrm{d}\Gamma\left(\Omega^{-}\to\Xi^{-}\pi^{+}\pi^{-}\right)}{\mathrm{d}\cos\theta}\propto\left|d^{3/2}_{\frac{3}{2}\frac{1}{2}}(\theta)\right|^{2}+\left|d^{3/2}_{\frac{1}{2}\frac{1}{2}}(\theta)\right|^{2}+\left|d^{3/2}_{-\frac{1}{2}\frac{1}{2}}(\theta)\right|^{2}+\left|d^{3/2}_{-\frac{3}{2}\frac{1}{2}}(\theta)\right|^{2}=1,$$

where we have used that $d^{j}_{m'm}(\theta)=d^{j}_{-m'-m}(\theta)$. So, indeed the s wave is isotropic. For the p wave,

$$\begin{aligned}\frac{\mathrm{d}\Gamma\left(\Omega^{-}\to\Xi^{-}\pi^{+}\pi^{-}\right)}{\mathrm{d}\cos\theta}\propto&9\left|d^{3/2}_{\frac{3}{2}\frac{1}{2}}(\theta)\right|^{2}+\left|d^{3/2}_{\frac{1}{2}\frac{1}{2}}(\theta)\right|^{2}+\left|d^{3/2}_{-\frac{1}{2}\frac{1}{2}}(\theta)\right|^{2}+9\left|d^{3/2}_{-\frac{3}{2}\frac{1}{2}}(\theta)\right|^{2}\\ =&9\times3\left(\frac{1+\cos\theta}{2}\right)^{2}\sin^{2}\frac{\theta}{2}+\left(\frac{3\cos\theta-1}{2}\right)^{2}\cos^{2}\frac{\theta}{2}\\ &+\left(\frac{3\cos\theta+1}{2}\right)^{2}\sin^{2}\frac{\theta}{2}+9\times3\left(\frac{1-\cos\theta}{2}\right)^{2}\cos^{2}\frac{\theta}{2}\\ =&7-6\cos^{2}\theta,\end{aligned}$$

which is exactly the distribution that we observe as the blue line in fig. 5.15

The size of the relativistic correction

We would like to check how big the relativistic correction is. In the rest frame of the Omega baryon the largest momentum is $|\boldsymbol{p}|=189\mathrm{MeV}$[14] while the mass is at least $m=m_{\Xi}\approx 1314\mathrm{MeV}$. Hence, $p^2/m^2\approx 0.02$. So, we expect the relativistic correction to be on the order of a couple of percent.

In the heavy baryon approximation the Feynman matrix element is [15, 17

$$\mathcal{M}\left(\Omega^{-}\to\Xi^{-}\pi^{+}\pi^{-}\right)=\bar{u}\left(p_{\Xi}\right)\left[\left(A_{+}+2B_{+}S_{v}\cdot p_{-}\right)p_{+}^{\mu}+\left(A_{-}+2B_{-}S_{v}\cdot p_{+}\right)p_{-}^{\mu}\right]\mu_{\mu}\left(p_{\Omega}\right).$$

The squared matrix element is given by 15

$$\begin{aligned}\left\langle\left|\mathcal{M}\left(\Omega^{-}\to\Xi^{-}\pi^{+}\pi^{-}\right)\right|^{2}\right\rangle=&\frac{4}{3}m_{\Omega}m_{\Xi}\left[\left|A_{+}\right|^{2}\boldsymbol{p}_{+}^{2}+\left|A_{-}\right|^{2}\boldsymbol{p}_{-}^{2}+2\,\mathrm{Re}\left(A_{+}^{*}A_{-}\right)\boldsymbol{p}_{+}\cdot\boldsymbol{p}_{-}\right.\\ &\left.+\left(\left|B_{+}\right|^{2}+\left|B_{-}\right|^{2}+\mathrm{Re}\left(B_{+}^{*}B_{-}\right)\right)\boldsymbol{p}_{+}^{2}\boldsymbol{p}_{-}^{2}+\mathrm{Re}\left(B_{+}^{*}B_{-}\right)\left(\boldsymbol{p}_{+}\cdot\boldsymbol{p}_{-}\right)^{2}\right],\end{aligned}$$

where

$$\begin{aligned}A_{+}&=\frac{h_{A}h_{C}}{6\sqrt{2}F_{\pi}^{2}\left(E_{\Xi}+E_{+}-m_{\Xi^{*}}+\frac{i}{2}\Gamma_{\Xi^{*}}\right)},\quad A_{-}=\frac{-h_{A}h_{\pi}}{4\sqrt{2}F_{\pi}^{2}}\frac{\left(m_{\pi}^{2}-m^{2}\left(\pi^{+}\pi^{-}\right)\right)}{\left(m_{K}^{2}-m^{2}\left(\pi^{+}\pi^{-}\right)\right)},\\ B_{+}&=\frac{h_{A}h_{C}H_{A}}{18\sqrt{2}F_{\pi}^{2}\left(m_{\Omega}-m_{\Xi^{*}}\right)\left(E_{\Xi}+E_{+}-m_{\Xi^{*}}+\frac{i}{2}\Gamma_{\Xi^{*}}\right)},\\ B_{-}&=-\frac{h_{A}(D-F)h_{C}}{6\sqrt{2}F_{\pi}^{2}\left(m_{\Omega}-m_{\Xi^{*}}\right)\left(E_{\Xi}+E_{+}-m_{\Xi}\right)}-\frac{h_{A}h_{C}H_{A}}{27\sqrt{2}F_{\pi}^{2}\left(m_{\Omega}-m_{\Xi^{*}}\right)\left(E_{\Xi}+E_{+}-m_{\Xi^{*}}+\frac{i}{2}\Gamma_{\Xi^{*}}\right)},\end{aligned}$$

with E_i the energy of particle i in the rest frame of the Omega baryon. Here, $m^2(\pi^+\pi^-) = (p_+ + p_-)^2$. Note that ref. 15 uses different values for the parameters H_A and h_C. We have just seen that the difference in H_A does not affect the result much. As for h_C, our chosen value reproduces the measured branching fraction of $\Omega^- \to \Xi^0\pi^-$, whereas the parameter values in ref. 15 give a value that is off by 45% for the branching fraction. Perhaps this is because the authors of ref. 15 have also fitted to the decay $\Omega^- \to \Xi^-\pi^0$, contrary to ref. [44]. From the discussion in section 3.1.1 we have seen this may give problematic results.

In any case, analytically the heavy-baryon expression shares the same features as our relativistic calculation. For instance, let us take a closer look at the angular distribution and the relative importance of the diagrams.

For the angular distribution, in eq. 5.22 the only relevant terms for a p-wave-dominated decay are $B_+$and the second part of B_-, satisfying $B_+/B_- \approx -3/2$. From eq. (5.21), in the frame where $\boldsymbol{p}_+ + \boldsymbol{p}_\Xi = \boldsymbol{0}$, the only term that can have an angular dependence is $\boldsymbol{p}_+ \cdot \boldsymbol{p}_- \sim \cos\theta$. Hence, we can read off the (normalized) angular dependence, which goes like $7 - 6\cos^2\theta$, and matches what we have seen earlier.

The relative importance of the diagrams in the heavy-baryon approximation is like that of the relativistic case. For the decay $\Omega^- \to \Xi^{*0}\pi^-$the typical momentum $|\boldsymbol{p}|$ is 17MeV. When we compare diagrams 3 and 1 (meaning $A_+$and B_+) we (again) see in eq. (5.21) a suppressing factor $\boldsymbol{p}_-^2/\left(m_\Omega - m_{\Xi^*}\right)^2$ of diagram 1 relative to diagram 3. This factor is also on the order of a few percent.

To estimate the size of the relativistic correction we use the same parameter values as before. We find

$$\mathcal{B}\left(\Omega^- \to \Xi^-\pi^+\pi^-\right) = 8.1 \times 10^{-3}, \quad \mathcal{B}_{\text{HB}}\left(\Omega^- \to \Xi^-\pi^+\pi^-\right) = 8.9 \times 10^{-3},$$

where HB denotes heavy baryon. The relativistic correction is on the order of ten percent, which is somewhat larger than expected. A possible explanation is the importance of terms that go with h_π, which appear to be less important in the relativistic case as compared to the heavy-baryon case. If we make h_π twice as big in the relativistic calculation, we recover roughly the same value as we have now for $\mathcal{B}_{\text{HB}}$.

Let us further investigate the correction. Figure 5.16 shows the distribution of the $\Xi^-\pi^+$invariant mass. Although the relativistic distribution is a little smaller in magnitude, its qualitative features closely match the heavy-baryon distribution.

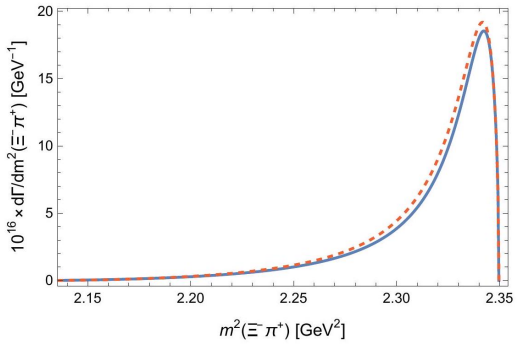


Figure 5.16: The distribution of the $\Xi^-\pi^+$invariant mass of $\Omega \to \Xi^-\pi^+\pi^-$. The solid blue line is our relativistic calculation and the dashed orange line is the heavy-baryon calculation.

Decay widths of decays into polarized cascades

Finally, we would like to investigate decay widths for different polarizations of $\Xi^-$for decay 1 (as this is the only decay that has been measured out of our selection). This polarization can

be measured from the further decay $\Xi^- \to \Lambda\pi^-$[45], [71] and the goal of this section is to check whether this is profitable. We still average over the spins of the Omega baryon. Doing so is experimentally justified as the decay $\Omega^- \to \Xi^-\pi^+\pi^-$is sufficiently rare that results where we also discriminate for different polarizations of Omega are difficult to test. Polarized spin- 1/2 spinors satisfy 26

$$u(\boldsymbol{p},s)\bar{u}(\boldsymbol{p},s) = \frac{1}{2}\left(1 + s\gamma_5 \not{K}\right)(\not{p} + m),$$

where $s = \pm$ specifies the spin orientation and n is a four-vector in the direction of the spinquantization axis, satisfying $n^2 = -1$ and $n \cdot p = 0$. In practice, we can use eq. 5.6 with the formal replacement

$$(\not{p}_\Xi + m_\Xi) \mapsto \frac{1}{2}\left(1 + s\gamma_5 \not{K}\right)(\not{p}_\Xi + m_\Xi).$$

We work with the same kinematic variables as for the unpolarized case, as shown in fig. 5.8 We have

$$\begin{aligned}
p_\Omega &= \left(E^*_\Omega, \left|\boldsymbol{p}_-\right|\sin\theta, 0, \left|\boldsymbol{p}_-\right|\cos\theta\right), \\
p_\Xi &= \left(E^*_\Xi, 0, 0, \left|\boldsymbol{p}_\Xi\right|\right), \\
p_+ &= \left(E^*_+, 0, 0, -\left|\boldsymbol{p}_\Xi\right|\right), \\
p_- &= \left(E^*_-, \left|\boldsymbol{p}_-\right|\sin\theta, 0, \left|\boldsymbol{p}_-\right|\cos\theta\right),
\end{aligned}$$

with

$$\left|\boldsymbol{p}_-\right| = \sqrt{\frac{\lambda\left(m^2\left(\Xi^-\pi^+\right), m_\Omega^2, m_\pi^2\right)}{4m^2\left(\Xi^-\pi^+\right)}}, \quad \left|\boldsymbol{p}_\Xi\right| = \sqrt{\frac{\lambda\left(m^2\left(\Xi^-\pi^+\right), m_\pi^2, m_\Xi^2\right)}{4m^2\left(\Xi^-\pi^+\right)}}.$$

We will explore the cases where the quantization axis is along $\hat{\boldsymbol{z}}(\|)$ or along $\hat{\boldsymbol{y}}(\perp)$,

$$n^\| = \frac{1}{m_\Xi}\left(\left|\boldsymbol{p}_\Xi\right|, 0, 0, E^*_\Xi\right), \quad n^\perp = (0,0,1,0).$$

We find

$$\begin{aligned}
\mathcal{B}^\|_+\left(\Omega^- \to \Xi^-\pi^+\pi^-\right) &= 4.1 \times 10^{-3}, \quad \mathcal{B}^\|_-\left(\Omega^- \to \Xi^-\pi^+\pi^-\right) = 4.1 \times 10^{-3}, \\
\mathcal{B}^\perp_+\left(\Omega^- \to \Xi^-\pi^+\pi^-\right) &= 4.0 \times 10^{-3}, \quad \mathcal{B}^\perp_-\left(\Omega^- \to \Xi^-\pi^+\pi^-\right) = 4.1 \times 10^{-3},
\end{aligned}$$

where \pm refers to the polarization in or against the direction of n. Clearly, the difference in the branching fractions is small. Note that also $\Delta\mathcal{B}^\| = \left|\mathcal{B}^\|_+ - \mathcal{B}^\|_-\right| \neq 0$. Thus, the overall polarization of the cascade emerging from the decay $\Omega^- \to \Xi\pi\pi$ is very small and out-of-plane, but not entirely perpendicular to the decay plane.

Let us explain why $\Delta\mathcal{B} \ll \mathcal{B}$ and why $\Delta\mathcal{B} \neq 0$. Following the discussion around eq. 5.77, we rewrite the squared matrix element into

$$\begin{aligned}
|\mathcal{M}|^2 \sim & \operatorname{tr}\left\{\left[(\text{v type}) + (\text{c type})\gamma_5\right]\left(1 + s\gamma_5 \not{K}\right)\left[(\text{v type}) + (\text{c type})\gamma_5\right]\right\} \\
= & (\text{v type})^2 + (\text{v type})^2 is\epsilon^{\mu\nu\alpha\beta} n_\mu (\text{ momenta})_{\nu\alpha\beta} \\
& + (\text{c type})^2 + (\text{c type})^2 is\epsilon^{\mu\nu\alpha\beta} n_\mu (\text{ momenta})_{\nu\alpha\beta} \\
& + (\text{v type})(\text{c type}) sn^\mu (\text{ momenta})_\mu.
\end{aligned}$$

In taking the trace we exchange the single γ_5 matrices and γ^μ matrices for a Levi-Civita symbol. No terms that go like $\epsilon^{\mu\nu\alpha\beta}$ (momenta) $_{\mu\nu\alpha\beta}$ survive since the momenta lie in a plane. When $n = n^\|$,

$$\left|\mathcal{M}^{\parallel}\right|^2 \sim (\text{ v type })^2 + (\text{ c type })^2 + (\text{ v type })(\text{ c type }) s n^{\mu} (\text{ momenta })_{\mu},$$

and when $n = n^{\perp}$,

$$\left|\mathcal{M}^{\perp}\right|^2 \sim (\text{ v type })^2 + (\text{ c type })^2 + \left[(\text{ v type })^2 + (\text{ c type })^2\right] i s \epsilon^{\mu\nu\alpha\beta} n_{\mu} (\text{ momenta })_{\nu\alpha\beta}.$$

In both cases, terms that go with s are suppressed with respect to polarization-independent terms. In eq. (5.27) the only polarization-dependent term is an interference term. When either v or c type objects dominate, the squared terms overwhelm the interference terms. In eq. (5.28) the polarization-dependent term goes with an i. Since $|\mathcal{M}|$ must be real the only surviving terms are cross terms. By the same reasoning as before, because they are interference terms cross terms are suppressed. We can verify this reasoning by, for instance, setting $D = F = H_A = 0$. This removes all c-type structures. Indeed, we find that the in-plane polarized amplitudes show no difference while the out-of-plane polarized amplitudes still differ.

We can also understand why the polarization-dependent terms in eq. 5.27) only contain interference terms between v- and c-type structures. All diagrams conserve parity individually. That is to say, if one were to construct a Lagrangian that would produce only diagram 1 or only diagram 2 (say), then this Lagrangian would be parity symmetric. The problem is, however, that diagrams 1 and 2 require a different parity assignment of the Omega baryon as compared to diagrams 3 and 4. Hence, the total process does not conserve parity. If we make either c type or v type contributions dominant, the process is essentially parity symmetric. Now, suppose that our Lagrangian is parity symmetric. We know our process is also rotation invariant. Therefore, using a parity transformation and a 180° rotation along the $\hat{\boldsymbol{y}}$ axis we can equate the two in-plane polarizations. Thus, any polarization-dependent term in $\left|\mathcal{M}^{\parallel}\right|^2$ must be an interference term.

In conclusion, it is not worth it to look at the polarization of the cascade in three-body Omega decays, as any polarization-dependent effects are small.

Parameter-free predictions

Let us integrate the Dalitz distributions to find the branching ratios. We get

$\mathcal{B}\left(\Omega^- \to \Xi^- \pi^+ \pi^-\right) = 8.1 \times 10^{-3}, \mathcal{B}\left(\Omega^- \to \Xi^0 \pi^0 \pi^-\right) = 12 \times 10^{-3}, \mathcal{B}\left(\Omega^- \to \Xi^- \pi^0 \pi^0\right) = 3.7 \times 10^{-3}$

The branching ratio for decay 2 is similar in magnitude to decay 1, while the branching ratio for decay 3 is smaller. Once again, we can understand this by looking at the resonance and extracting the Clebsch-Gordan coefficients from the vertices. We have

$$\begin{aligned}
\mathcal{B}\left(\Omega^- \to \Xi^- \pi^+ \pi^-\right) &\propto \left(\frac{1}{\sqrt{6}} \frac{1}{2\sqrt{3}}\right)^2 = \frac{1}{8 \times 9}, \\
\mathcal{B}\left(\Omega^- \to \Xi^0 \pi^- \pi^0\right) &\propto \left(\frac{1}{\sqrt{6}} \frac{1}{2\sqrt{6}}\right)^2 + \left(\frac{1}{2\sqrt{3}} \frac{1}{2\sqrt{3}}\right)^2 = \frac{1}{8 \times 9}, \\
\mathcal{B}\left(\Omega^- \to \Xi^- \pi^0 \pi^0\right) &\propto \frac{1}{2}\left[\left(\frac{1}{2\sqrt{3}} \frac{1}{2\sqrt{6}}\right)^2 + \left(\frac{1}{2\sqrt{3}} \frac{1}{2\sqrt{6}}\right)^2\right] = \frac{1}{4} \frac{1}{8 \times 9}.
\end{aligned}$$

The branching ratio for decay 1 and 2 should be the same while the branching fraction for decay 3 should be suppressed by a factor of four. Reassuringly, these relations are approximately satisfied. We cannot expect them to hold exactly, as in deriving the relations we throw away subdominant corrections.

In passing, we would like to touch on the frozen spin- 1/2 modes. When doing our numerical calculations, we included a factor a in the spin-3/2 propagator. Very schematically,

$$P^T \sim \frac{1}{p^2 - m^2} P^{3/2} + \frac{a}{-m^2} P^{1/2}$$

For normal calculation, $a = 1$. By subtracting the branching fraction with $a = 0$ from the total (theoretical) branching fraction we can estimate how large the contribution involving the frozen modes is. We call this contribution $\mathcal{B}_{\rm FM}$. We find

$$\begin{aligned}
\frac{\mathcal{B}_{\rm FM}\left(\Omega^- \to \Xi^-\pi^+\pi^-\right)}{\mathcal{B}\left(\Omega^- \to \Xi^-\pi^+\pi^-\right)} &= 1.76 \times 10^{-4}, \\
\frac{\mathcal{B}_{\rm FM}\left(\Omega^- \to \Xi^0\pi^-\pi^0\right)}{\mathcal{B}\left(\Omega^- \to \Xi^0\pi^-\pi^0\right)} &= 17 \times 10^{-4}, \\
\frac{\mathcal{B}_{\rm FM}\left(\Omega^- \to \Xi^-\pi^0\pi^0\right)}{\mathcal{B}\left(\Omega^- \to \Xi^-\pi^0\pi^0\right)} &= 17 \times 10^{-4}.
\end{aligned}$$

It is clear that the frozen modes are numerically not relevant. Parametrically, they are not of LO in the power counting.

So far, all predictions that we have made have some uncertainty because parameters like h_A and h_C are not well fixed. We can do better and construct lower bounds for

$$\frac{\mathcal{B}\left(\Omega^- \to \Xi\pi\pi\right)}{\mathcal{B}\left(\Omega^- \to \Xi^0\pi^-\right)}$$

which are (almost) parameter free. To start, recall that diagrams 1 and 2 do not interfere with diagrams 3 and 4. Therefore, the decay width will have a general form

$$\Gamma\left(\Omega^- \to \Xi\pi\pi\right) = \left|\Gamma_v\right|^2 + \left|\Gamma_c\right|^2 > \left|\Gamma_v\right|^2.$$

Compared to $\left|\Gamma_v\right|^2, \left|\Gamma_c\right|^2$ is numerically small (on the order of a couple of percent). Thus, the lower bound will not be much lower than the width itself. We can expand $\left|\Gamma_v\right|^2$ as

$$\left|\Gamma_v\right|^2 = a'\left(h_A h_C\right)^2 + b'\left(h_A h_\pi\right)^2 + c' h_A^2 h_C h_\pi,$$

where a', b' and c' are numbers that only depend on the kinematic factors and not on coupling constants. Hence, for eq. (5.32) [using eq. (5.12)]

$$\frac{\mathcal{B}\left(\Omega^- \to \Xi\pi\pi\right)}{\mathcal{B}\left(\Omega^- \to \Xi^0\pi^-\right)} > a + b\frac{h_\pi^2}{h_C^2} + c\frac{h_\pi}{h_C}.$$

Again, a, b and c are numbers that only depend on the kinematic factors. The final two terms in this expression are numerically subdominant to a. Therefore, eq. (5.35) is a robust lower bound. Of course, this statement depends on the values of h_π and h_A, because we use h_A to determine h_C. But, these values are not completely unknown and by building the ratio 5.32 we have eliminated the largest uncertainties.

In this calculation the sign of h_C matters. Since we are after a lower limit, we must pick whatever sign of h_C gives the lowest ratio. This automatically covers the other option. We can roughly estimate the parametric uncertainties in the calculation by varying h_A between its maximum and minimum value, 2.9 and 1.9, respectively, as well as by determining h_C not from fits to $\Omega^- \to \Xi^0\pi^-$ but from $\Omega^- \to \Xi^-\pi^0$ (we do not change what decay we use in the ratio because this decay is experimentally better determined than the other two-body Omega decay).

Before we present our results, we would like to stress the robustness of the lower bounds via another viewpoint. The spontaneous breaking of chiral symmetry relates in a model-independent way the transition amplitudes of a process $A \to B$ to processes with n additional

soft pions, $A \to B + n\pi_{\rm soft}$ [6] 72, 73. In other words, given the amplitude $A \to B$, we can predict the strength for the amplitude $A \to B + n\pi$ up to chiral corrections. For strong-interaction processes the number of pions must be even to conserve parity. But, for weak processes a parity-breaking amplitude $A \to B\pi$ follows from a parity-conserving amplitude $A \to B$, and a parity-conserving amplitude $A \to B\pi$ follows from a parity-breaking amplitude $A \to B$.

Physically, for $\Omega^- \to \Xi\pi$, the isospin selection rule implies the existence of an intermediate state with spin 3/2, strangeness -2 and isospin 1/2. There is a resonance with these quantum numbers, $\Xi^*(1530)$, which lies in the same flavor SU(3) multiplet as the Omega 14. If the process $\Omega^- \to \Xi\pi$ is dominated by such an intermediate state, then the decay is largely parity conserving, meaning the parity violating amplitude is phase-space suppressed. If the $\Delta I = 3/2$ amplitude mattered a lot, then the process would not be resonance dominated, as there is no resonance state in the energy range of the Omega baryon that has strangeness -2 and isospin 3/2. What is outlined here is the essence of the diagram in fig. 5.12

Taking the previous considerations together, the $\Delta I = 1/2$ selection rule and chiral symmetry relate the strength of the parity-conserving amplitude of $\Omega^- \to \Xi\pi$ to the parity violating amplitude of $\Omega^- \to \Xi\pi\pi$. Diagrams 3 in figs. 5.5.5.7 emerge by adding a soft (s wave) pion to the weak vertex of the diagram 5.12 It is this connection that we exploit to provide an estimate for the lower limit of the ratio of decay widths for the processes $\Omega^- \to \Xi\pi\pi$ and $\Omega^- \to \Xi\pi$. On a formal level, what we have described here is the appearance of u and $u^\dagger$ in eq. (3.3.

We find,

$$\begin{aligned}
\frac{\mathcal{B}\left(\Omega^- \to \Xi^-\pi^+\pi^-\right)}{\mathcal{B}\left(\Omega^- \to \Xi^0\pi^-\right)} &\gtrsim 2.9 \times 10^{-2},\\
\frac{\mathcal{B}\left(\Omega^- \to \Xi^0\pi^-\pi^0\right)}{\mathcal{B}\left(\Omega^- \to \Xi^0\pi^-\right)} &\gtrsim 5.1 \times 10^{-2},\\
\frac{\mathcal{B}\left(\Omega^- \to \Xi^-\pi^0\pi^0\right)}{\mathcal{B}\left(\Omega^- \to \Xi^0\pi^-\right)} &\gtrsim 1.2 \times 10^{-2}.
\end{aligned}$$

If we fill in the measured data [18] we find

$$\frac{\mathcal{B}\left(\Omega^- \to \Xi^-\pi^+\pi^-\right)}{\mathcal{B}\left(\Omega^- \to \Xi^0\pi^-\right)} = (0.16 \pm 0.03) \times 10^{-2}.$$

There is a disturbing discrepancy of an order of magnitude between theory and experiment. In the context of χPT this tension was first noted in ref. [15], though it was known earlier. We have shown that this tension remains in an essentially model-independent fashion. This aspect has not been noticed before.

For decays 1 and 3 we use $h_C < 0$, while for decay $2h_C > 0$ gives the smallest ratio. A fit using the decay $\Omega^- \to \Xi^-\pi^0$ always gives a ratio with a higher value than from a fit to the decay $\Omega^- \to \Xi^0\pi^-$. So, we do not need to consider it. How big is the effect of the terms that go with b and c in eq. (5.35)? Varying h_A changes the lower limits (LL). The change in the lower limits is small and is monotonic with h_A. This means that $h_A = 1.9$ gives the lowest possible value for the lower limit and $h_A = 2.9$ gives the highest possible value for the lower limit. We find

$$\begin{aligned}
2.9 &\geq \mathrm{LL}\left(\Omega^- \to \Xi^-\pi^+\pi^-\right) \times 10^2 \geq 2.8,\\
5.1 &\geq \mathrm{LL}\left(\Omega^- \to \Xi^0\pi^-\pi^0\right) \times 10^2 \geq 5.1\\
1.2 &\geq \mathrm{LL}\left(\Omega^- \to \Xi^-\pi^0\pi^0\right) \times 10^2 \geq 1.1.
\end{aligned}$$

For decays 1 and 3 the spread is on the order of 7-9% of the displayed lower bound. For decay 2 there is essentially no spread, as the only term that can cause the spread is almost zero

(as explained in section 5.1.3 with respect to h_π). The lower limit is still in disagreement with experiment, even when we take a possible spread in the lower limit due to LECs into account.

On the theory side the most straightforward explanation for the discrepancy between theory and experiment seems to be that SU(3)χPT breaks down. This is known to happen in, for example, nonleptonic decays of octet baryons [4]. Those decays have s- and p-wave contributions that each have SU(3)-symmetric and SU(3)-violating contributions. For the s wave SU(3)-violating contributions are small and χPT matches well to experiments. The SU(3)-violating portion of the p wave is not small, and correspondingly χPT results fit poorly to the data. But, even if χPT does not work properly, it is unlikely to be off by an entire order of magnitude.

Another possible explanation is that the $\Delta I = 1/2$ rule, introduced in section 3.1.1 is grossly violated. It behooves us to remember that the rule is phenomenological. Yet, in our Lagrangian we assume that it always holds. In section 3.1.1 we saw that the decays $\Omega^- \to \Xi\pi$ did not respect the selection rule. By chiral symmetry it is exactly these decays whose amplitude relates to the decay $\Omega^- \to \Xi^-\pi^+\pi^-$. So, seeing this, we should not be surprised to find that our prediction might be deficient. In turn, this means that $\Omega^- \to \Xi\pi\pi$ offers the opportunity to scrutinize the $\Delta I = 1/2$ rule.

On the experimental side one can wonder if the scanty data are sufficient. At present, the best measurement of the decay $\Omega^- \to \Xi^-\pi^+\pi^-$has just 100 events [18. Measurements of the chirallyconnected two-body decay have been called into question [51]. Moreover, previous measurements of the three-body decay claim to find data consistent with the resonance [74], [75] (albeit with almost no samples, so one can wonder how serious this claim really is), which is in conflict with more recent measurements that do not 18.

Of course, it may well be that both experiment and theory are lacking in some way. Regardless, the way forward is clear. The decay distributions of the decays $\Omega^- \to \Xi\pi\pi$ should be remeasured. This is important because clarity on the status of the $\Delta I = 1/2$ rule is necessary in guiding theoretical developments. Differential distributions contain much more information than just observing the deviation of one number, like the experimental ratio of 2.74 from the prediction in eq. (3.33). The $\Delta I = 1/2$ rule enters into predictions for CP violation of hyperon decays [76. Because this effect is so small, one cannot afford to let limited knowledge of the $\Delta I = 1/2$ rule obscure the interpretation of data.

7.1.6 Semileptonic and radiative Omega decays

We have thoroughly studied nonleptonic Omega decays. Now, we turn to semileptonic and radiative Omega decays. In particular, we will investigate the decays $\Omega^- \to \Xi^0\mu^-\bar{\nu}_\mu$ and $\Omega^- \to \Xi^-\gamma$. For both decays we calculate tree-level next-to-leading-order (NLO) contributions. We study NLO contributions of these decays as they provide a way to pin down the sign and possibly size of several low-energy constants (LECs) introduced in the NLO Lagrangian. The values of these LECs are required for state-of-the-art calculations of the axial-vector transition form factors of a nucleon to a Delta. This chapter is largely an extension of the work presented in ref. 19.

Note that in this chapter we address the NLO terms of the strong chiral Lagrangian coupled to external sources. For the electroweak chiral Lagrangian that governs the nonleptonic baryon decays there are too many NLO structures to be pinned down by data from two-body decays [44. Therefore, in the electroweak sector we restrict ourselves to the LO Lagrangian that we used in previous calculations.

Elements of the next-to-leading-order Lagrangian

The NLO Lagrangian has been worked out in ref. 43]. It is a sizable expression, so we only present relevant parts here. Namely,

$$\mathcal{L}_{\rm NLO} = ic_M\epsilon_{ade}\bar{B}_c^e\gamma_\mu\gamma_5\left(f_+^{\mu\nu}\right)_b^d T_\nu^{abc} + ic_E\epsilon_{ade}\bar{B}_c^e\gamma_\mu\left(f_-^{\mu\nu}\right)_b^d T_\nu^{abc} + \text{ H.c. },$$

where H.c. stands for Hermitian conjugate, c_M and c_E are low-energy constants and $f_\pm^{\mu\nu}$ are field strengths,

$$f_\pm^{\mu\nu} = uF_L^{\mu\nu}u^\dagger \pm u^\dagger F_R^{\mu\nu}u$$

where

$$F_{R/L}^{\mu\nu} = \partial^\mu\left(v^\nu \pm a^\nu\right) - \partial^\nu\left(v^\mu \pm a^\mu\right) - i\left[v^\mu \pm a^\mu, v^\nu \pm a^\nu\right].$$

Interactions with the W^-boson are introduced by the formal replacement

$$l_\mu = v_\mu - a_\mu \mapsto -\frac{g_w}{\sqrt{2}}W_\mu^+\begin{pmatrix}0 & V_{ud} & V_{us}\\ 0 & 0 & 0\\ 0 & 0 & 0\end{pmatrix} + \text{ H.c. } = -\frac{g_w}{\sqrt{2}}\left(W_\mu^+T_+ + W_\mu^-T_-\right),$$

with V_{ud} and V_{us} Cabibbo-Kobayashi-Maskawa matrix elements 77 and g_w the weak gauge-coupling constant. The weak-gauge coupling constant and the mass of the W-boson are related via the Fermi constant G_F, as $G_F/\sqrt{2} = g_w^2/\left(8m_W^2\right)$ 27. The right-handed sources are set to zero. The couplings to leptons come from the charged-current part of the electroweak Lagrangian

$$\mathcal{L}_{\rm CC} = \frac{g_w}{\sqrt{2}}\ell^+\gamma^\mu P_L\nu_\ell W_\mu^-,$$

where $P_{R/L} = \frac{1}{2}\left(1 \pm \gamma_5\right)$ and ℓ^+stands for a positively-charged lepton.
For radiative decays we introduce electromagnetic couplings via the formal replacement

$$v_\mu \to eA_\mu Q$$

where e is the proton charge, A_μ is the photon field and

$$Q = \begin{pmatrix}\frac{2}{3} & 0 & 0\\ 0 & -\frac{1}{3} & 0\\ 0 & 0 & -\frac{1}{3}\end{pmatrix}$$

is the quark-charge matrix.

$\Omega^- \to \Xi^0\mu^-\bar{\nu}_\mu$

The decay $\Omega^- \to \Xi^0 e^-\bar{\nu}_e$ has been studied in ref. [19]. We will repeat that calculation here. By flavor universality we can replace the electron mass with the muon mass to get the branching fraction for the decay $\Omega^- \to \Xi^0\mu^-\bar{\nu}_\mu$ for free. As kinematic variables we pick

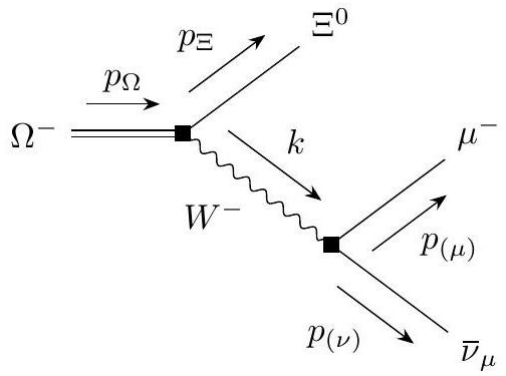
$$m^2\left(\mu^-\bar{\nu}_\mu\right) = \left(p_{(\mu)} + p_{(\nu)}\right)^2, \quad m^2\left(\Xi^0\bar{\nu}_\mu\right) = \left(p_\Xi + p_{(\nu)}\right)^2.$$

Instead of $m^2\left(\Xi^0\bar{\nu}_\mu\right)$ we also use $\cos\theta$, where θ is the angle between $\boldsymbol{p}_{(\nu)}$ and $\boldsymbol{p}_\Xi$ in the frame where $\boldsymbol{p}_{(\mu)} + \boldsymbol{p}_{(\nu)} = \boldsymbol{0}$. Numerically,

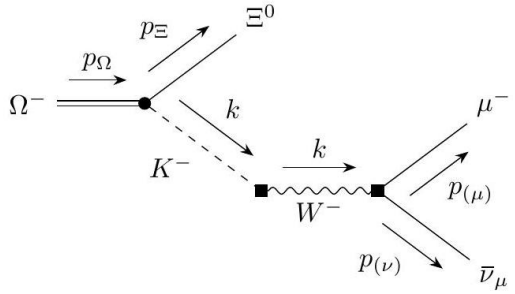
$$h_A = 2.0, \quad |V_{us}| = 0.2245, \quad G_F = 1.1663787 \times 10^{-5}\text{GeV}^{-2}.$$

Diagrams and vertices

The relevant diagrams are given in fig. 6.1



(a) Diagram 1



(b) Diagram 2

Figure 6.1: The two diagrams contributing to the decay $\Omega^- \to \Xi^0 \mu^- \bar{\nu}_\mu$ at NLO. In both, $k = p_{(\mu)} + p_{(\nu)}$.

An expansion of the Lagrangian in first order in Φ or W^-requires

$$u_\mu = iu^\dagger \left(\nabla_\mu U\right) u^\dagger \sim i\left(\partial_\mu U + iUl^\mu\right) \sim -\frac{1}{F_\pi}\partial_\mu \Phi - \frac{g_W}{\sqrt{2}}\left(W_\mu^+ T_+ + W_\mu^- T_-\right),$$
$$F_{R/L}^{\mu\nu} \sim \frac{1}{2}(1 \mp 1)\left(\partial^\mu l^\nu - \partial^\nu l^\mu - i\left[l^\mu, l^\nu\right]\right),$$
$$f_\pm^{\mu\nu} = uF_L^{\mu\nu}u^\dagger \pm u^\dagger F_R^{\mu\nu} u \sim F_L^{\mu\nu}.$$

For $T_\mu^n \to B^i W_\nu^-$the relevant part of the Lagrangian is

$$\frac{h_A}{2\sqrt{2}}\epsilon_{ade}\bar{B}_c^e \left(u^\mu\right)_b^d T_\mu^{abc} + ic_M \epsilon_{ade}\bar{B}_c^e \gamma_\mu\gamma_5 \left(f_+^{\mu\nu}\right)_b^d T_\nu^{abc} + ic_E\epsilon_{ade}\bar{B}_c^e\gamma_\mu \left(f_-^{\mu\nu}\right)_b^d T_\nu^{abc}$$

This gives

$$\frac{h_A g_w}{4}\epsilon_{ade}\bar{B}_c^e W^{+\mu}\left(T_+\right)_b^d T_\mu^{abc} - \frac{ig_W}{\sqrt{2}}\epsilon_{ade}\bar{B}_c^e\gamma_\mu\left(c_M\gamma_5 + c_E\right)\left(\partial^\mu W^{+\nu} - \partial^\nu W^{+\mu}\right)\left(T_+\right)_b^d T_\nu^{abc},$$

with a vertex

$$T_\nu^n \longrightarrow \bigvee_{B^i}^{W_\mu^-} = V_{\mu\nu}^{T\to BW^-} = \frac{ig_W}{\sqrt{2}} c_{ni}^{T\to BW^-}\left[\frac{h_A}{2\sqrt{2}}g_{\mu\nu} + \left(c_E - c_M\gamma_5\right)\left(kg_{\mu\nu} - \gamma_\mu k_\nu\right)\right],$$

where

$$c_{ni}^{T\to BW^-} = \frac{1}{\sqrt{2}}\epsilon_{ade}\left(b_i^\top\right)_c^e\left(T_+\right)_b^d\left(t_n\right)^{abc}.$$

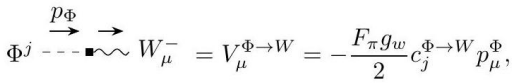
For $\Phi^i \to W_\mu^-$the relevant part of the Lagrangian is

$$\frac{F_\pi^2}{4}\operatorname{tr}\left(u_\mu u^\mu\right)$$

This gives

$$-\frac{F_\pi g_w}{2\sqrt{2}}\operatorname{tr}\left(W_\mu^+ T_+ \partial^\mu \Phi\right)$$

with a vertex

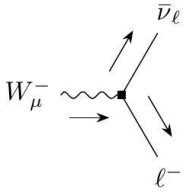


$$= V_\mu^{\Phi\to W} = -\frac{F_\pi g_w}{2}c_j^{\Phi\to W}p_\mu^\Phi,$$

where

$$c_j^{\Phi\to W^-} = \frac{1}{\sqrt{2}}\operatorname{tr}\left(T_+ b_j\right).$$

The interaction $W_\mu^- \to \ell^-\bar{\nu}_\ell$ is contained in the charged-current part of the electroweak Lagrangian from which we derive the vertex



$$= V_\mu^{W^-\to\ell^-\bar{\nu}_\ell} = \frac{ig_w}{\sqrt{2}}\gamma_\mu P_L.$$

Having derived all the relevant vertices, we can calculate the Feynman matrix element. We find

$$\mathcal{M}\left(\Omega^- \to \Xi^0\mu^-\bar{\nu}_\mu\right) = \bar{u}\left(p_{(\mu)}\right)\beta_\kappa v\left(p_{(\nu)}\right)\bar{u}\left(p_\Xi\right)\beta'^{\kappa\sigma}\mu_\sigma\left(p_\Omega\right),$$

where

$$\begin{aligned}\beta_\kappa &= -2\sqrt{2}G_F V_{us}\gamma_\kappa P_L\\ \beta'^{\kappa\sigma} &= \frac{h_A}{2\sqrt{2}}g^{\kappa\sigma} + \left(c_E - c_M\gamma_5\right)\left(\not{k}g^{\kappa\sigma} - \gamma^\kappa k^\sigma\right) - \frac{h_A k^\kappa k^\sigma}{2\sqrt{2}\left(k^2 - m_K^2\right)}.\end{aligned}$$

For vanishing quark masses the axial-vector current is conserved. This leads to $k_\kappa\beta'^{\kappa\sigma} = 0$, which is indeed the case when $m_K^2 \to 0$. Since the momentum of $W^-$is small, we can use the simplified propagator

$$P_{\mu\nu}^W = \frac{-i}{k^2 - m_W^2 + i\epsilon}\left(g_{\mu\nu} - \frac{k_\mu k_\nu}{k^2}\right) + \frac{i}{m_W^2}\frac{k_\mu k_\nu}{k^2} \approx \frac{ig_{\mu\nu}}{m_W^2}$$

In practice, this approximation is valid when $k \ll m_W$. For us, $k \sim m_\Omega = 1.67245\text{GeV}$ and $m_W = 80.379\text{GeV}$. So, the approximation is acceptable. The spin-averaged matrix element is

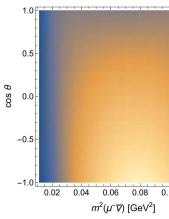
$$\begin{aligned}\left\langle\left|\mathcal{M}\left(\Omega^- \to \Xi^0\mu^-\bar{\nu}_\mu\right)\right|^2\right\rangle = &-\frac{1}{4}\operatorname{tr}\left[\left(\not{p}_\Xi + m_\Xi\right)\beta'^{\kappa\sigma}\left(\not{p}_\Omega + m_\Omega\right)P_{\sigma\tau}^{3/2}\left(p_\Omega\right)\bar{\beta}'^{\rho\tau}\right]\\ &\times\operatorname{tr}\left[\left(\not{p}_{(\mu)} + m_{(\mu)}\right)\beta_\kappa\left(\not{p}_{(\nu)} - m_{(\nu)}\right)\bar{\beta}_\rho\right].\end{aligned}$$

Note that we pick $m_{(\nu)} = 0\text{GeV}$.

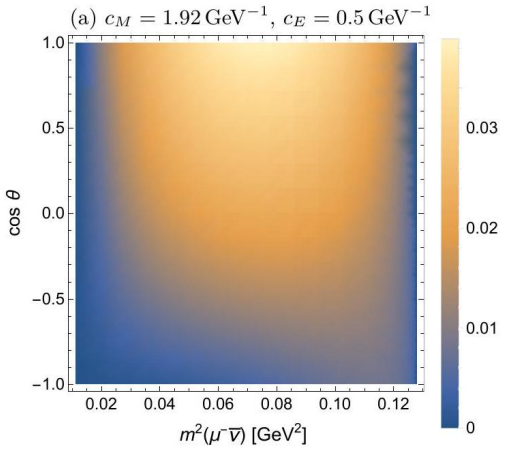
Dalitz distributions

At NLO the decay width depends on two new LECs, c_E and c_M. The magnitude of each of these constants has been narrowed down to one of two possible values [19], [43,

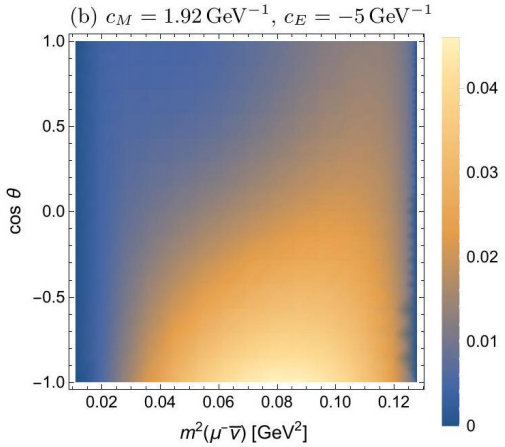
$$c_E = 0.5\text{GeV}^{-1} \quad \text{or} \quad c_E = -5\text{GeV}^{-1}, \quad c_M = \pm 1.92\text{GeV}^{-1}.$$



It is possible to distinguish four cases, as can be seen in fig. 6.2



(c) $c_M = -1.92\text{GeV}^{-1}, c_E = 0.5\text{GeV}^{-1}$



(d) $c_M = -1.92\text{GeV}^{-1}, c_E = -5\text{GeV}^{-1}$

Figure 6.2: Dalitz plots for the branching ratio of the decay $\Omega^- \to \Xi^0 \mu^- \bar{\nu}_\mu$ at NLO for different values of the LECs c_E and c_M. From the Dalitz plots it is possible to distinguish the four different cases.

At first glance, it appears that changing the sign of c_M is equivalent to replacing the angle θ by $\pi - \theta$. This is only true when the lepton masses go to zero, which is known as forward-backward asymmetry [1]. Because the mass of the muon is greater than the mass of the electron, it is easier to differentiate the four cases as compared to the decay $\Omega^- \to \Xi^0 e^- \bar{\nu}_e$. When we integrate over $\cos\theta$ it is still possible to distinguish between case a and case b, or case c and case d, but not between a and c or b and d. If we integrate over the invariant mass we can still

see a difference between all four cases in the angular distribution. This is shown in fig. 6.3. In any case, differential measurements of $\Omega^- \to \Xi^0 \mu^- \bar{\nu}_\mu$ would allow us to pin down the signs of the LECs.

In passing we remark that the Dalitz plots in ref. [19] appear to be flipped with respect to ours. The flip comes about because the authors use the angle between the cascade and the electron, while we use the angle between the cascade and the neutrino.

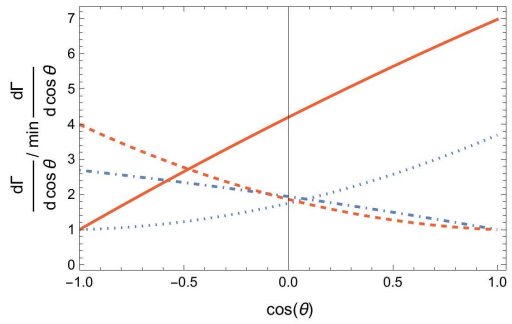


Figure 6.3: The normalized angular distribution for the decay $\Omega^- \to \Xi^0 \mu^- \bar{\nu}_\mu$ at NLO. The solid orange line corresponds to the parameter values in fig. 6.2a the dashed orange line corresponds to fig. 6.2 b, the dot-dashed blue line corresponds to fig. 6.2c and the dotted blue line corresponds to fig. 6.2 d

We conclude this section by calculating the branching ratio. The results are shown in fig. 6.4 The dashed orange line represents the LO branching ratio and the solid blue line represents the NLO branching ratio, using $c_M = 1.92\text{GeV}^{-1}$. No experimental data are available. As a consequence of flavor universality the branching fraction of the electronic decay should behave in the same way as the muonic case, where the only difference is the lepton mass. This is also what we see when comparing fig. 6.4 to the figure in ref. [19]. The predicted branching ratio for the muonic case is smaller than the electronic case by $\sim 30\%$.

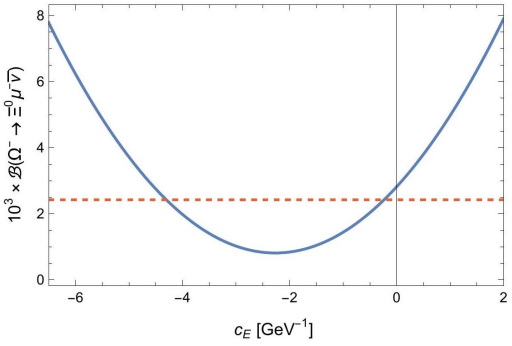


Figure 6.4: The LO (dashed, orange) and NLO (solid, blue) branching ratio for the decay $\Omega^- \to \Xi^0 \mu^- \bar{\nu}_\mu$. We let c_E vary and fix $c_M = 1.92\text{GeV}^{-1}$.

$\Omega^- \to \Xi^- \gamma$

The final decay that we will look at is $\Omega^- \to \Xi^- \gamma$. Originally, we were surprised that we could find no prior χPT calculation of its branching ratio in the literature (in contrast, there has been an investigation into decays of type $B \to B\gamma$[78), as radiative decuplet baryon decays may be used to pin down c_M. It turns out that many of these radiative decays, like this one, are forbidden at NLO. Therefore, the branching fraction from a chiral NLO calculation is zero. Despite the somewhat trivial result, we still include the calculation here, as it allows us to briefly discuss U spin.

Diagram and vertex

There are no low-lying spin-1/2 states with three strange quarks. Therefore, no weak process can occur after emission of a photon and we can conclude a priori that this decay is NLO. The only relevant diagram is fig. 6.5. The cascade resonance propagator enhances this diagram meaning it dominates over any diagram where a photon is produced at a weak vertex. The enhancement comes about because the denominator contains the difference of the Omega baryon and cascade resonance mass, which is small. Therefore, its reciprocal, the propagator, is big.

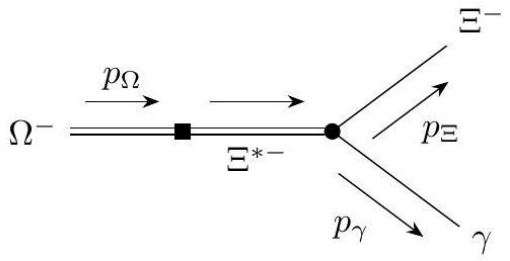


Figure 6.5: The NLO diagram that would dominate in the decay $\Omega^- \to \Xi^-\gamma$.

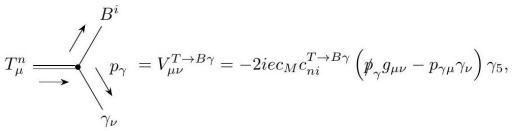
For the NLO vertices we start by expanding the Lagrangian to zeroth order in Φ, where this time we include a coupling to the photon field. We find

$$u_\mu = iu^\dagger\left(\nabla_\mu U\right)u^\dagger \sim i\left(\partial_\mu U + i\left[U, v_\mu\right]\right) \sim -\frac{1}{F_\pi}\left(\partial_\mu\Phi + ieA_\mu[\Phi, Q]\right)$$
$$F_{R/L}^{\mu\nu} \sim \partial^\mu v^\nu - \partial^\nu v^\mu = e\left(\partial^\mu A^\nu - \partial\nu A^\mu\right)Q = eF^{\mu\nu}Q$$
$$f_\pm^{\mu\nu} = uF_L^{\mu\nu}u^\dagger \pm u^\dagger F_R^{\mu\nu}u \sim e\left(1+\frac{i\Phi}{2F_\pi}\right)F^{\mu\nu}Q\left(1-\frac{i\Phi}{2F_\pi}\right) \pm e\left(1-\frac{i\Phi}{2F_\pi}\right)F^{\mu\nu}Q\left(1+\frac{i\Phi}{2F_\pi}\right)$$
$$\sim eF^{\mu\nu}Q(1\pm 1).$$

The relevant part of the Lagrangian is

$$ic_M\epsilon_{ade}\bar{B}_c^e\gamma_\mu\gamma_5\left(f_+^{\mu\nu}\right)_b^d T_\nu^{abc}$$

giving a vertex



with

$$c_{ni}^{T\to B\gamma} = \frac{1}{\sqrt{2}}\epsilon_{ade}\left(b_i^\top\right)_c^e Q_b^d\left(t_n\right)^{abc}.$$

Unfortunately, if we evaluate $c_{55}^{T\to B\gamma}$, we find that it is equal to zero. By extension, the decay width is zero.

Vanishing decay width

We could have anticipated the vanishing decay width by appealing to U-spin conservation. In the chiral Lagrangian U-spin conservation holds because we do not break flavor symmetry in the interactions (breaking of flavor symmetry for radiative decays happens at NNLO [43]). Like how isospin relates to the interchange of u and d quarks, U spin relates to the interchange of d and s quarks. Ξ^-belongs to the U-spin- $1/2$ doublet, while Ξ^{*-} belongs to the U-spin-$3/2$ quartet. So, if the radiative decay were to happen, the photon has to carry a U spin of 1.

The quark-antiquark currents with spin 1 are

$$\begin{aligned} \bar{d}\gamma_\mu s\,(U=1,U_3=-1)\,, \\ \frac{1}{\sqrt{2}}\left(\bar{d}\gamma_\mu d-\bar{s}\gamma_\mu s\right)(U=1,U_3=0) \\ \bar{s}\gamma_\mu d\,(U=1,U_3=1) \\ \frac{1}{\sqrt{2}}\left(\bar{d}\gamma_\mu d+\bar{s}\gamma_\mu s\right)(U=0,U_3=0) \end{aligned}$$

The photon couples to

$$-\frac{2}{3}\bar{u}\gamma_\mu u-\frac{1}{3}\left(\bar{d}\gamma_\mu d+\bar{s}\gamma_\mu s\right)$$

Both terms are U-spin 0 transitions. Thus, the photon has a U spin of 0 and not an admixture of U-spin 1. Therefore, a radiative decay is forbidden.

In the literature, previous theory estimates use the quark model (in the context of $s\to d\gamma$ transitions) [79], though there is no consensus on the exact value of the branching fraction [80]. The measured upper limit is 4.6×10^{-4}81.

Part IV
Problems

8 Typical Problems (???)

(так я мало что и прорешал еще...)

Part V
Special Particle Physics in a Nutshell

9 Other Statements

9.1 Other Phenomena

(напишу их тоже, скорее всего заготовок много может быть)

9.2 Particles in Cosmology

(тут очень важная связка, пропишу ее потом.)

9.3 Hypothetical Properties of Particles and Theories in a Nutshell

(много возможных теорий, на каждую имеющую смысл создам раздел.)

Part VI
Experimental particle physics

в плоть до того, как устроены сами коллайдеры разберусь
(также в проге раздел про анализ данных, там для фэч раздел с методами.)

10 Phenomena that are Used for Measurements

(??? ask someone who knows this)

10.0.1 Motion in Collider

типа посмотрим просто подробно, как это описывать?
простые задачи посчитаем.
начнем с понятий, которые у нас будут использоваться
светимость

11 Registration of Particles

(??? ask someone who knows this)

12 Some Experimental Setups

12.0.1 COMPASS

(???????????)

Part VII
Other Topics

Обсудим различные теории о частицах, которые иногда могут встретиться.

(то, о чем я слышал, но чем не занимаюсь.)

13 Lists and Tables of Properties of Particles

Обсудим типичные частицы и объекты.

(пока только частицы. такая не совсем про задачи, а про свойства, мб в другую часть перенесу их, пока так.)

13.0.1 Electron

обзор свойств электрона.

раскидаю максимально!!!! много параграфов из этого создастся.

(околообщефиз в этом параграфе)

Спин электрона.

Сложение моментов

В магнитном поле с градиентом $dB/dy = 300$ Тс/м отклонение должно составлять порядка 2 см.

Пучок атомов из источника и формируется двумя горизонтальными Щелями, проходит через отклоняющее магнитное поле и падает на фотопластинку.

Магнитное поле создается элеКтромагнитом, один полюс которого плоский, а другой сделан в виДе ножа.

Вблизи ножа поле имеет практически только z -Компоненту, величина которой B_z очень сильно зависит от z -Координаты.

Сила, действующая на магнитный момент в таком поле, равна

$$F_z = \mu_y \frac{\partial B_z}{\partial z}$$

Полученные Штерном и Герлахом результаты обладают двумя особенностями, полностью противоречащими классическим воззрениям:

1. Нет непрерывного распределения атомов по вертикали, а наблюдается дискретности, m.e. возможсны лиии некоторие из состояний.

2. Компонент всего две.

Что можно было бы ожидать, например, в случае водорода? Если атомы водорода находятся только в s -состоянии ($l = 0$), то ИХ магнитный момент в этом состоянии равен нулю.

Если же атомы водорода находятся в p -состоянии ($l = 1$), то следовало ожидать расщепления на три компоненты, соответствующие трем Возможным проекциям магнитного момента на ось z, т. е. состояниям со значениями магнитного квантового числа $m_l = 0, \pm 1$. В то же время, эксперимент показал, что пучок расщепляется лишь на две компоненты.

А это свидетельствует о наличии у атомов водорода еше какого-то момента импульса, назовем его s, равного $1/2$.

В 1925 г. американские физики-теоретики Дж. Уленбек и С. Гаудсмит (1902 – 1979), анализируя строение оптических спектров

(мы уже говорили о трудностях интерпретации дуплетов в спектрах щелочных металлов (??)),

пришли к выводу о наличии у электрона собственного механического момента, равного $\hbar/2$ (соответственно магнитное квантовое число $m_s = \pm 1/2$), и назвали его спином.

Уленбек и Гаудсмит исходили из грубой классической модели электрона в виде вращающегося заряженного шарика. Конечно, в квантовой механике, как мы это неоднократно подчеркивали, нельзя говорить ни о каком вращении электрона.

Наличие у него собственного механического момента импульса (спина) есть чисто квантовое явление.

Собственным моментом импульса обладают так же и другие элементарные частицы, в частности нейтрон, протон и т.д.

Еще одной неожиданностью результатов опытов Штерна и Герлаха явилось значение магнитного момента электрона, которое легко вычислить из величины расщепления.

Оказалось, что проекция магнитного момента электрона на выделенную ось, если ее записать аналогично орбитальному движению (6.24), равна

$$\mu_{s_z} = -2\frac{e}{2m}s_z = -2m_s\mu_{\text{Б}} = \pm\mu_{\text{Б}}$$

Таким образом, проекция спинового магнитного момента электрона равна одному магнетону Бора.

Для спина оказалось иным (вдвое большим!) гиромагнитное отношение, или другими словами, g -фактор электрона равен 2. Однако, точные измерения

последнего показали, что на самом деле это равенство — приблизительное.

Современная величина g-фактора равна

$$\frac{1}{2}g\left(e^{-}\right) = 1,0011596521884(43)$$

Следует отметить, что опыт Штерна-Герлаха на электронах невозможен, поскольку на движущиеся электроны, в силу их малой массы, действует не только градиент магнитного поля, но и само поле (сила Лоренца), и при этом оказывается, что смещение электронного пучка в результате действия силы Лоренца сравнимо со спиновым расщеплением.

К изучаемому нами классу явлений относятся также опыты Эйнштейна и де Гааза $(1878-1960)$ в 1915 г., которые мы и рассмотрим

В этих экспериментах образцы парамагнитных или ферромагнитных веществ в форме цилиндриков подвешивались на тонкой нити внутри соленоида.

Пропускание тока сопровождалось вращением цилиндра.

Таким образом, определялась связь между механическим и магнитным моментом вещества.

Вращение цилиндра при включении магнитного поля обусловлено тем,что магнитные моменты атомов μ ориентируются вдоль поля.

Это ведет к изменению суммы их механических моментов L, и по закону сохранения момента импульса цилиндр закручивается.

Как было показано в более поздних работах С.Барнетта, Дж. Стюарта и других, для образцов из Fe, Ni, Co

$$\frac{\mu}{L} = -\frac{e}{m}$$

т.е. вдвое больше, чем должно было быть для магнитного и механического моментов, связанных с орбитальным движением электронов (6.24).

Следовательно, магнетизм у этих веществ (ферромагнетиков) имеет спиновое происхождение, т.е. имеет чисто квантовомеханическую природу.

Электрон в атоме кроме спинового может обладать также орбитальным моментом, поэтому естественно возникает вопрос о том, по какому правилу складываются моменты в квантовой механике.

Угловые моменты - векторные величины, и складываться они должны по правилам сложения векторов.

Рассмотрим для простоты систему, состоящую только из двух частиц, имеющих орбитальные моменты l_1 и l_2. Пусть их суммарный момент равен $\mathbf{L}$ (рис. 6.10).

Отметим, что если система состоит из многих частиц, то результирующий момент находится путем последовательного сложения двух векторов.

Квантовый характер угловых моментов проявляется в квантовании как самой их абсолютной величины, так и их проекций.

Для суммарного момента это означает следующее:

$$|\mathbf{L}|^2 = \hbar^2 L(L+1)$$
$$L_z = \hbar m_L, \quad L = 0, 1, 2, 3, \ldots,$$
$$m_L = 0, \pm 1, \pm 2, \ldots, \pm L$$

Надо помнить, что у вектора $\mathbf{L}$ можно одновременно определить только его квадрат и проекцию момента на одну из координатных осей (мы выбираем ось z).

Наша задача - найти связь между квантовыми числами L и m_L и квантовыми числами складывающихся векторов l_1 и m_{l1}, l_2 и m_{l2}. Для этого рассмотрим проекции моментов на ось z(рис. 6.10)

Наибольшее возможное значение орбитального квантового числа L равно наибольшему значению m_L, т.е.

$$L_{\max} = m_{L_{\max}} = m_{l1_{\max}} + m_{l2_{\max}} = l_1 + l_2$$

Значение L минимально, когда проекции m_{l1} и m_{l2} максимальны, но имеют разные знаки.

Из рис. 6.10 ясно, что

$$L_{\min} = l_1 - l_2$$

Но поскольку отрицательные значения L бессмысленны, то вместо (6.35) выражение для $L_{\min}$ следует писать в виде

$$L_{\min} = |l_1 - l_2|$$

Это совсем не значит, что $L_{\min}$ соответствует антипараллельной ориентации векторов l_1 и l_2, а $L_{\max}$ -их параллельной ориентации, поскольку ни один из этих векторов не может быть направлен строго по какой-либо оси в силу соотношения неопределенностей.

Итак, возможные значения квантового числа суммарного момента лежат в диапазоне

$$|l_1 - l_2| \leqslant L \leqslant l_1 + l_2,$$

следовательно, L может принимать $2l_2 + 1$ значений, если $l_1 > l_2$, и $2l_1 + 1$ значений, если $\tilde{l}_2 > l_1$.

Но этим не ограничивается полное число возможных состояний системы двух частиц с моментами l_1 и l_2. Дело в том, что для каждого L (но разных m_l) имеется $2L + 1$ различных проекций (различных ориентаций в пространстве), поэтому полное число возможных состояний системы равно $\sum_{l_1-l_2}^{l_1+l_2}(2L+1)$. Это арифметическая прогрессия с разностью, равной 2, и общим числом членов

$$(2l_2+1) = \frac{[2(l_1+l_2)+1] + [2(l_1-l_2)+1]}{2}(2l_2+1) = (2l_1+1)(2l_2+1)$$

Это соотношение можно получить и иначе: число возможных состояний для первой частицы равно $(2l_1+1)$, для второй -$(2l_2+1)$, а для системы двух независимых частиц число состояний просто равно произведению возможных состояний каждой частицы, т.

е.

$(2l_1+1)(2l_2+1)$. Итак, квантовомеханические векторы можно складывать также, как обычные, но модуль любого из них равен $\hbar\sqrt{l(l+1)}$.

Полученный результат называется квантовым правилом сложения угловых моментов.

По этому же правилу находится суммарный момент частицы, если она участвует одновременно в двух вращениях.

Теперь можно перейти к вопросу о полных механическом и магнитном моментах электрона.

В силу наличия у электрона как

спинового, так и орбитального моментов, полный механический момент равен их сумме

$$\mathrm{j} = 1 + \mathrm{s}$$

Квантовое число j полного момента

$$j = |l \pm s| = \left| l \pm \frac{1}{2} \right|$$

Естественно, как подчеркивалось выше, длина вектора j

$$|\mathbf{j}| = \hbar\sqrt{j(j+1)}, \quad j_z = \hbar m_j$$

причем m_j принимает $2j+1$ значений.

Для суммарного магнитного момента ситуация резко осложняется из-за разных гиромагнитных отношений для спинового

и орбитального моментов, и в результате суммарный магнитный момент окаЗывается непараллельным суммарному механическому моменту (на рис.

6.11 изображена диаграмма сложения орбитального 1 и спИнового s моментов электрона и соответствующиХ магнитных моментов $\boldsymbol{\mu}_l$ и $\boldsymbol{\mu}_s$, причем механические моменты измеряются в единИЦах $\hbar$, а магнитные - в магнетонах Бора).

Следует обратить внимание на то, что величина вектора μ_l равна величине вектора 1, а длина вектора $\boldsymbol{\mu}_s$ вдвое больше длины s.

Поэтому вводится специальный коэффициент - так называемый фактор Ланде, который есть не что иное, как коэффициент пропорциональности между j и $\boldsymbol{\mu}_j$

$$\boldsymbol{\mu}_j = -g_{\text{л}}\,\mu\mathbf{j}$$

Это - то же гиромагнитное отношение, но не для частиц, а для атомных электронов.

Заметим, что (6.42) - соотношение между проекцией суммарного магнитного момента $\boldsymbol{\mu}_{\text{сум}}$ на $\mathbf{j}$ и величиной вектора j, а не соотношение между этими векторами.

Конкретное выражение для фактора Ланде через значения j, l и s легко получить.

В самом деле, с учетом того, что спиновый g -фактор равен 2, из (6.39) следует:

$$-\mu_j = \mu_{\text{B}}\mathrm{l} + 2\mu_e\mathrm{s}$$

Соответственно, проекция суммарного магнитного момента $\boldsymbol{\mu}_j$ на вектор j равна

$$-\mu_j = -\frac{\mu_j \mathrm{j}}{|\mathrm{j}|} = \mu\frac{\mathrm{lj} + 2\mathrm{sj}}{|\mathrm{j}|}$$

Значит

$$-\mu_j\frac{\mathrm{j}}{|\mathrm{j}|} = \mu\frac{\mathrm{lj} + 2\mathrm{sj}}{|\mathrm{j}|^2}\mathrm{j} = g_{\text{л}}\,\mu_{\text{Б}}\,\mathbf{j}$$

Мы получили соотношение между проекцией магнитного момента μ_j и вектором j.

Отсюда можно получить выражение для фактора Ланде:

$$g_{\text{л}} = \frac{1}{|\mathbf{j}|^2}(\mathbf{lj} + 2\mathbf{sj}) = \frac{1}{|\mathbf{j}|^2}[\mathbf{l}(\mathbf{l}+\mathbf{s}) + 2\mathbf{s}(\mathbf{l}+\mathbf{s})] = \frac{|\mathbf{l}|^2 + 2|\mathbf{s}|^2 + 3\mathbf{sl}}{|\mathbf{j}|^2}$$

или

$$g_{\text{л}}\,|\mathbf{j}|^2 = |1|^2 + 2|\mathbf{s}|^2 + 3\mathbf{sl}$$

Это - просто векторное соотношение.

В операторном виде оно имеет вид

$$g_{\text{л}}\,\widehat{j^2} = \widehat{l^2} + 2\widehat{s^2} + 3(\widehat{sl})$$

Операторное равенство означает и равенство средних значений, т.

е.

$$g_{\text{л}}\,\left\langle j^2\right\rangle = \left\langle l^2\right\rangle + 2\left\langle s^2\right\rangle + 3\langle sl\rangle$$

Первые два члена в правой части равенства (6.49) легко находятся по общему квантовомеханическому правилу для квадрата вектора (для любого вектора $\mathbf{M}$ имеем $M^2 = M(M+1)$), а среднее значение третьего члена вычислим, исходя из следующих соотношений:

$$\mathrm{j} = 1 + \mathrm{s} \to \mathrm{j}^2 = \mathrm{s}^2 + \mathrm{l}^2 + 2\ \mathrm{sl} \to \mathrm{sl} = \frac{1}{2}\left(|\mathrm{j}|^2 - |\mathrm{s}|^2 - |\mathrm{l}|^2\right)$$

Значит

$$\langle sl\rangle = \frac{1}{2}[j(j+1) - s(s+1) - l(l+1)]$$

и окончательно имеем

$$g_{\text{л}} = \tfrac{1}{j^2}\left[\langle l^2\rangle + \langle 2s^2\rangle + \tfrac{3}{2}\left(\langle j^2\rangle - \langle s^2\rangle - \langle l^2\rangle\right)\right] = \\ = \tfrac{1}{\langle j^2\rangle}\left[-\tfrac{\langle l^2\rangle}{2} + \tfrac{\langle s^2\rangle}{2} + \tfrac{3\langle l^2\rangle}{2}\right]$$

или

$$g_{\text{л}} = 1 + \frac{j(j+1) + s(s+1) - l(l+1)}{2j(j+1)}$$

Как получить электрон

я хз, что нужно взять и как выбивать их??

мб фотоэффект?

13.0.2 Positron

конструкция позитрона

у Дирака спишу просто и всё.

обоснование его существования

почему он существует?

Об антипротоне (?)

говорят общефизники, что да. теорфизники - хз

Сколько кварков в протоне?

(хз, там морские кварки, а верт дидер говорит, что любое нечетное число. разберусь потом.)

13.0.3 Photon

Фотон - самая простая и очень загадочная частица, про которую чаще всего возникают вопросы. Соберем теорию, чтобы четко понимать, что есть фотон с квантовой точки зрения.

(тут из Овча тоже свойства переношу)

(ландау т4 КЭД начало, применю свои знания квантовой механики для общих характеристик фотона)

(в дургое место перенесу)

Основные свойства фотона

О гамма кванте - фотоне большой частоты

запоминаю название

фотон это частица или волна

наиболее часто именно этот вопрос возникает.

Связь спина с поляризацией (?)

(как с поляризацией связан он? с направленностью? пропишу это, мб разве что в другом месте)

Мотивация изучать спин фотона (!?!?)

(? зачем его изучать?)

Обсудим теперь более подробно вопрос об излучении, возникающем при переходах атома из возбужденного состояния в основное либо в одно из нижележащих возбужденных состояний.

Для этого необходимо прежде всего разобрать вопрос о собственном моменте импульса фотона, т. е. его спине.

спин фотона

(тот же общефиз выгрузка пока. очень актуально разобраться.)

Из оптики известно, что световые волны являются поперечными и могут иметь различную поляризацию.

В качестве основных поляризационных состояний обычно рассматривают две взаимно перпендикулярные линейные поляризации.

В квантовой механике за исходные поляризации удобнее выбирать не линейные, а циркулярные, т.е. соответствующие вращению векторов электрического и магнитного полей световой волны по или против часовой стрелки.

Вектор момента импульса электромагнитного излучения направлен при этом по направлению (у правовращающегося) или против направления (у левовращающегося) движения фотона.

Переходя на язык квантовой механики, мы должны сказать, что у фотона есть спин, причем проекция спина на направление движения может принимать два значения - плюс или минус единицу.

Существование только двух возможных проекций спина, казалось бы, означает, что он равен $1/2$, поскольку такое значение спина обеспечивает, согласно правилам квантования, необходимое число проекций на заданную ось $2s + 1 = 2$. Однако подобное заключение полностью противоречит опыту, ибо в таком случае фотоны были бы фермионами.

Тогда, в частности, при испускании фотона атомом полный угловой момент последнего мог бы меняться на $1/2$, чего никогда не наблюдается.

Кроме того, при этом фотон подчинялся

быть не могло - в таком случае максимальная передаваемая передатчиком энергия была бы равна $\hbar\omega$.

следовательно, спин указанные необычные свойства фотона обусловлены равенством нулю его массы.

Отличие безмассовой частицы от массовой заключается в том, что для первой невозможно найти такую систему отсчета, в которой она покоится, поскольку она движется со скоростью света, т. е. нельзя определить спин как момент импульса частицы в системе отсчета, где она покоится. Поэтому у безмассовой частицы всегда есть только выделенное направление - направление ее скорости (волнового вектора).

Подчеркнем, что различие между системой отсчета и системой координат состоит в следующем: система отсчета всегда связана с материальными телами, тогда как система координат представляет собой математический образ, не связаный с какими-либо материальными телами.

Таким образом, для безмассовой частицы можно говорить лишь об аксиальной симметрии относительно этого выделенного направления; иными словами, для фотона пространство обладает аксиальной симметрией.

Выражение такой симметрии сохранение проекции момента на направление импульса, которая может быть равна только ± 1. Такие значения проекции момента импульса фотона на направление импульса соответствуют правовращательной и левовращательной круговой поляризации.

Значение «0» исключается поперечностью электромагнитных волн, так как нулевое значение проекции момента импульса фотона на направление его движения соответствовало бы продольной поляризации световой волны.

Отсюда следует достаточно сильное утверждение: понятие о спине фотона условно (для фотона нельзя последовательно различать спин и орбитальный момент как составные части его полного момента), и смысл имеет лишь полный момент импульса $j = 1, 2, 3, \ldots$ (нуль невозможен)

Прежде, чем перейти к описанию различных состояний фотона, кратко остановимся на вопросе о четности состояния.

Понятие «четность состояния» связано с операцией изменения направления осей координат на обратное (так называемая пространственная инверсия).

Обозначим соответствующий оператор через $\widehat{P}$. Его действие на волновую функцию состоит в замене $x \to -x, y \to -y, z \to -z$. Чтобы выяснить, каким может быть результат действия оператора $\widehat{P}$ на некоторую волновую функцию ψ, подействуем им на ψ дважды.

Тогда, по определению операции инверсии, мы должны получить ту же самую функцию (двукратное отражение осей координат ничего не меняет), т.е. $\widehat{P}^2\psi = \psi$. Отсюда следует, что собственными значениями оператора $\widehat{P}$ являются 1 : $\widehat{P}\psi = \pm\psi$. В соответствии с этим в квантовой механике различают четные и нечетные состояния (или состояния положительной и отрицательной четности).

Так например, четность состояния атома водорода равна $(-1)^l$, т.е. s - и d -состояния являются четными, а нечетными.

Процесс испускания или поглощения фотонов атомами должен происходить с соблюдением законов сохранения энергии, импульса и четности системы.

Теперь вернемся к состояниям фотона.

Для обозначения различных состояний с определенными моментами и четностями принята следующая терминология: фотон с моментом j и четностью, равной $(-1)^j$, называют 2^j -польным электрическим фотоном (или E -фотоном); если же у фотона с моментом j четность равна $(-1)^{j+1}$, то его называют 2^j -польным магнитным фотоном (или M -фотоном).

Иначе говоря, если обозначать состояние фотона с моментом j и четностью π как j^π, то: фотоны электрического типа -это фотоны типа $1^-, 2^+, 3^-, 4^+, \ldots$; магнитного типа -это фотоны типа $1^+, 2^-, 3^+, 4^-, \ldots$ Названия «электрического» и «магнитного» типа произошли оттого, что вектор тока является нечетной пространственной

функцией (он при отражении в зеркале меняет свое направление), а круговой ток (магнитный диполь) направление своего вращения при отражении в зеркале не меняет (рис.8.1)

Возможна иная интерпретация квантового числа j: число j указывает тиП симметрии, которым данное состояние обладает относительно вращения, т.е., образно говоря, дает изображение атома с разных сторон: $j = 0$ -сферическая симметрия, $j = 1$ -свойство симметрии вектора (диполя), $j = 2$ -пространственная симметрия квадруполя, $j = 3$ -пространственная симметрия октуполя и т.д.

Поэтому к слову «фотон» обычно добавляют «дипольный», «Квадрупольный», «октупольный» и т.д.

Поскольку структуру E0-мультиполя (сферическая симметрия имеет кулоновское поле точечного заряда, действие кулоновского поля иногда трактуют как результат обмена промежуточным виртуальным E0-фотоном.

Таким образом на самом деле спин фотона (вернее, его момент импульса) может быть любым, а не только равным 1. Если размер излучающей системы равен a, а ω - частота излучения, то электрическое поле квадруполя меньше поля диполя в $a\omega/c$ раз (c -скорость света).

Этот множитель можно представить в виде:

$$\frac{a\omega}{c} = \frac{2\pi\nu}{c}a = \frac{2\pi a}{\lambda}$$

Поскольку мы рассматриваем излучение атомов, то в данном случае a -размер атома, λ - длина волны излучения.

Мощность следовательно, «скорость» потери энергии возбужденным атомом при дипольном излучении в $(2\pi a/\lambda)^2$ раз больше, чем при квадрупольном, и соответственно, относительная продолжительность излучения, называемая временем жизни атома в возбужденном состоянии, будет обратно пропорциональна этой величине.

При излучении в видимом оптическом диапазоне длин ВОЛН справедлива следующая оценка:

$$\left(\frac{2\pi a}{\lambda}\right)^2 \approx \left(\frac{6,3\cdot 10^{-8}}{5\cdot 10^3\cdot 10^{-8}}\right)^2 \sim 10^{-6}$$

Если обозначить время жизни атома в возбужденном состоянии через τ, а обратную ему величину - вероятность перехода атома ИЗ возбужденного состояния - через w, то мы в результате получим

$$\frac{w_{E1}}{w_{E2}} = \frac{\tau_{E2}}{\tau_{E1}} = \left(\frac{\lambda}{2\pi a}\right)^2 \sim 10^6$$

Аналогичное соотношение имеет место между магнитным и электрическим переходами одинаковой мультипольности

$$\frac{\tau_{M1}}{\tau_{E1}} \approx \left(\frac{\lambda}{2\pi a}\right)^2$$

13.1 Hypothetical Particles from Cosmology

посмотрим, что там во вселенной происходит с точки зрения элементарных частиц.

связь с космологией вся в этой главе

14 Exotic Particles

14.1 Particles in Riemannian Surface

(???? see Redkov, a very exotic theory)

14.1.1 General Questions about Particles in Riemannian Surface

вопрос о количестве частиц

потом подумаю.

15 Other Phenomena

15.1 Passing Through Matter

(see book by Landau or note on ED, maybe I'll write it to the section about experiments later)

15.2 Air shower (???)

(??? see wiki)

16 Grand Unified Theories

16.1 GUE

(????)

17 Theories about Which It is Hard to Think Seriously

17.0.1 Phoenix theory (???)

Описание пхоеникса - пишу, что думаю, и забиваю. https://steemit.com/physics/@alienscientist/a-theory-of-everything-phoenix

стремная теория, на которую я не хочу тратить время, ибо я и знаю мало, и информации мало, и выглядит она стремной.

Может, когда-то пропишу, почему она стремная, это было бы полезно.

пока не могу сформалировать.

17.1 Ancient Theories (???)

польза этого знания разве что в идейных описаниях

по сути это все откинуто куда подальше, просто как и польза философии, общее создание нужных представлений тут происходит, так что тоже важно оставновиться.

Part VIII
Appendix

A Introduction

Приведем сполна раскрывающее подход к физике частиц предисловие.

A.1 Extra Motivation

(напишу что современная тема, много исследований про это, много открытий часто делается, на ютубе часто про это можно видео найти)

Физика частиц - один из главных разделов физики

потому что ты спросишь, а что вообще в природе есть и из чего мы состоим?

вот сразу сюда и попадаем мы.

очень много красивых экспериментальных графиков, которые интересно изучать

так что мои записи будут полны ими, потому что мне они нравятся.

классно, можно изучать, разве что подготовиться нужно к этому.

а можно кстати и не заметить это, заниматься какими-то задачами и не думать про эксперименты.

но в этом много красоты, много графиков показывается на конференциях, и очень круто их тоже смотреть.

разве что подготовиться нужно, так сразу непонятно, что там от чего отложено?

так что у меня отдельная глава про графики.

удивительно просто, сколько же много графиков!

квантовая механика в различных местах очень сильно используется.

сколько же квантовой механики нужно!

не всех глав, но многих.

так что занимаясь частицами, постоянно будут возвраты к квантовой механике, потому что в точности ее методы и нужны тут.

так что если квантовая механика слабая, имеет место неделю посидеть в ней, потом уже заниматься частицами.

чтобы познать микромир, нужно отдельно заниматься этими вопросами

как бы ни была развита теория поля, квантовая механика, все равно про эти вещи отдельно нужно думать.

это отдельный предмет, в общем.

и это важно понимать.

часто следует обращаться к оригинальным учебникам

а не смотреть ужасные пересказы их.

вот честно, тут полно ужаснейшей литературы!

Полезно мышление олимпиадника: создавать многие параграфы с решениями интересных задач, в этом сила структуры, что она держит наготове задачи

Поэтому в записи акцентирован подход, что вот задача, давайте ее решим И именно такие самые крутые книги, например, книга Левитова и Шитова про функцию Грина, например, Барбашовой по теоретической механике. Именно этот стиль очень важен для этого предмета. Также мы подходим ко всему как к выученному и пройденному, тренируемся просто и все.

очень много информации про установки и эксперименты

потому что полно научных станций.

так что это большие главы этой записи, про эксперименты.

там и методы и установки.

и это достаточно круто, там много огромных приборов и вообще, многие передовые исследования проводятся на эти темы.

очень много именных формул, о которых мы впервые слышим

информации очень много, при этом много ужасно написанного материала

куча презентаций, докладов, статей, книг.

очень сложно в этом плане, потому что нужно с информацией правильно работать, а также

и потеряться в этом очень легко, так что почти необходимо собрать какие-то простые базовые структуры по физике, потому что без опыта обработки информации можно тупо засесть вечно в тупик.

ибо сложность темы на самом деле не малая.

и казалось бы, почему столько фигово написанного материала?

а вот потому что раздел такой!

полно просто мусорных записей! так что их удаляем, без этого не деться никуда, по факту полно мусора. К сожалению. А хотелось бы изучить, да вот, нет, мусор всегда тут есть, ужасные принципиально непонятные изложения.

в таком я не роюсь.

так что лучше качать оригинальную литературу и их читать, чем переработанные пробовать понять.

если не создавать единую структуру, то каша в знаниях гарантирована

поэтому многие и не трогают физику частиц, потому что понятно, что у них не развит структурное мышление, поэтому и мотивации нет этим заниматься.

только со структурами темы эти начинают нормально заходить, без структур почти бесполезно про это думать.

преподавание обзоров физики элементарных частиц особенно ужасное

мб в каких-то лучших вузах на планете это и не так, но все, что я видел - там ФЭЧ отдельно отличается убогостью донесения материала.

так что сам беру и делаю, тут преподавания никакого и не происходит.

если не знаешь, как обрабатывать эту информацию, другие физические предметы в помощь, тут обучать никто не умеет.

разве что теоретические модели типа теории поля, стандартной модели, их неплохо дают, но это далеко не вся физика частиц.

A.2 Approach to Particle Physics

Осудим, какое мышление наиболее эффективное для усвоение предмета.

ФЭЧ, мышление: Пар: не нужно относиться к свойствам частиц как к экспериментальным фактам, ибо в них много связок тоже. Как Володя не нужно думать, пропишу это подробнее, это важно.

отдельно важно не скапливать материалы по ФЭЧ и или вписывать сразу или ждать, когда это понадобится в жизни

по ФЭЧ литературы целая тонна, причем большинство источников - какие-то недоделанные лекции, так что вписывать её бесполезно, нужно просто сесть и пройти. и сделается это только тогда, когда это на самом деле будет актуально.

до этого рыться - огромнейшая трата времени.

потому что на самом деле тонна лекций и методичек и качество их чаще всего далеко не лучшее, так что тут или вписываешь сразу в структуру, или удаляешь, никаких доработок не будет никогда

актуальность различных реакций

обсудим, какие реакции насколько нужны?

A.3 Literature on Particle Physics

A.3.1 Main Literature

Основная обучающая

[1] David Tong Particle Physics, CERN Lectures

Книга номер 1 для начала изучения.

[2] Окунь Л Б Лептоны и кварки

классна книга со многими выводами, но ее отдельно нужно изучать, тут пары недель не хватит.

[3] Prof. M.A. Thomson Michaelmas, лекции в Кембридже

очень классные лекции, которые я вижу в основе записи, потому что обзор очень много в них дан.

[4] Бюклинг Е., Каянти К. Кинематика элементарных частиц

Очень крутая кинематика. Сперва механику нормально проработаю, потом в ней главу с кинематикой, потом уже сполна в эти методы буду погружаться. Очень профессиональные методы.

Particle Data Group Particle physics booklet

помню, крутая книга, с которой и стартовать нужно, потому что самая компактная и крутая. как начну заниматься - в первую очередь по ней все главы и буду создавать. прямо очень крутая, пока что просто не до частиц.

Окунь Лептоны и кварки

помню

Перкинс Введение в физику высоких энергий

более 400 страниц теории, которую я уже итак знаю в общих чертах, так что мб выгружать буду из него многое. для базовой структуры, думаю, хорошая книга.

httpnuclphys.sinp.msu.ruseminarsem13.htm

хз хорошие ссылки

https://www.hep.phy.cam.ac.uk/~thomson/partIIIparticles/handouts/Handout_5_2011.pdf

хз хорошие ссылки

[5] М Е Пескин, Д В Шредер Введение в квантовую теорию поля

КТП и самые разные детали по ней брал, очень важная книга.

Профессиональная по физике частиц и КТП в контексте физики частиц

[6] Челлен, Г Физика элементарных частиц: Пер. с англ

интересные детали раскртыы мб нормально, так что посмотрю, вроде интересно почитать будет.

[7] Particle Data Group Particle Physics Booklet

Очень полезный саммари основных явлений с частицами, а также много таблиц со свойствами частиц.

популяраня литература

[8] Хорган, Джон Конец науки

классная книга, некоторые разделы в которой позволяют погрузиться в мир физики частиц. что же будет дальше в этой области? для прикладного уровня это супер важно!

Александр Гамов на ютубе канал - про частицы лекций много

эээ не смотрел, потом как-нибудь дойду, итак теории полно

A.3.2 Special Theoretical Literature

Лтература про гипотетические модели

[9] Volkov D.V., Akulov, V.P. Is the neutrino a goldstone particle?

Две страницы соображений про это, известная статья. Интересно, что же тогда?

Физическая лтература в помощь

[10] Белоусов, Бурмистров, Тернов задачи по теоретической физике

интересные задачи по кинематики, в рамках которых уже можно многое понять про частицы и их рассеяния.

[11] Ландау Л. Д. Теория поля

Описано введение в кинематику, которая в ФЭЧ используется и вообще, неплохая книга.

[12] Райдер, Льюис Квантовая теория поля

пара хороших моделей, схожих со Стандартной моделью описывается. мб и нормальная книга, просто мб это же и в других дается, тут не знаю...

[13] Ландау ЛД, Лифшиц ЕМ Теоретическая физика. Том 8. Электродинамика сплошных сред

Описано прохождение частиц через вещество и многое другое, но в рамках ФЭЧ вообще мало что там есть.

список книг для понимания строковского

мб до них дойду, не знаю просто. Вообще, выглядят стремными

[1] Г. Челлен, «Физика элементарных частиц», пер. с англ. Г.В. Ефимова, под ред. Р.М. Рындина, «Наука», Главн. ред. физико-математической литературы, М. 1966

[2] Р. Блин-Стойл, «Фундаментальные взаимодействия и атомное ядро», пер. с англ. под ред. И.С. Шапиро, «Мир», М., 1976.

[3] Юо.Комминз, Ф.Буксбаум, "Слабые взаимодействия лептонов и кварков", пер. с англ. А.В.Беркова, "Энергоатомиздат", М. 1987

[4] Дж.Д. Бьеркен, С.Д. Дрелл, «Релятивистская квантовая теория», том 1 «Релятивистская квантовая механика», пер. с англ. Б.О. Кербикова под ред. В.Б. Берестецкого, «Наука», Гл. ред. физико-математической литературы, М. 1978.

[5] Л.Б.Окунь, "Лептоны и кварки", М., Наука, 1981.

[6] И.М. Тернов, "Введение в физику спина релятивистских частиц", гл. 2, М., изд-во МГУ, 1997.

[7] И.М.Тернов и др., ЭЧАЯ 20(1989)51.

[8] С.М. Биленький, «.Лекции по физике нейтринных и лептон-нуклонных процессов», «Энергоатомиздат», М., 1981.

[9] S.M. Bilenky, ЭЧАЯ 44(2013)3.

[10] С. Газиорович, «Физика элементарных частиц», пер. с англ. под ред. А.Д. Суханова, «Наука», Главн. ред. физико-математической литературы, М. 1969.

[11] H. Paul, Nucl. Phys. A 154(1970) 160.

[12] Дж. Бернстейн, «Элементарные частицы и их токи», пер. с англ. Г.И. Кузнецова по ред. Я.А. Смородинского, «Мир», М., 1970.

Г. БЕТЕ, Ф. ГОФМАН МЕЗОНЫ И ПОЛЯ Том II МЕЗОНЫ

500 страниц про мезоны и разные с ними явления. 1 том мб тоже на 500 страниц, даже не открывал. Так что полно всего в физике частиц, можно когда-то месяц поизучать мезоны, если будет желание. По КТП нужна нормальная для этого подготовка.

A.3.3 Special Experimental Literature

[14] Mommers, C. J. G. Rare Weak Decays of the Omega Baryon (Dissertation). Supervisor Prof. Dr. Stefan Leupold http://uu.diva-portal.org/smash/get/diva2:1677385/FULLTEXT01.pdf

Хорошая подробная магистерская работа, в которой многому можно научиться про физику частиц, ну и в частности, про распад Омега-барионов.

Статьи про известные эксперименты

(???)

про моделирование ФЭЧ

тут же и по руту и его применениям мб будет что-то

A.3.4 Other Literature

Дополнительная обучающая, объясняющая

[15] Larkoski, Andrew J. Elementary Particle Physics: An Intuitive Introduction

Fermion physics recommends, I believe that it is a great book. Found it at the end of 2024 for free here https://www.zlibrary.to/filedownload/elementary-particle-physics-an-intuitive-in
Also, solutions are available here: https://pdfcoffee.com/elementary-particle-physics-by-larkosk
html

A.4 History in a Nutshell

начало исследований слабых взаимодействий с 1896г

Исследования слабых взаимодействий элементарных частиц идут с 1896 года.

Все началось с обнаружения явления испускания проникающего излучения солями урана.

Открыл это явление Беккерель, используя фотоэмульсию в качестве детектора.

С этого года можно отсчитывать историю исследования ядерных превращений в обшем смысле.

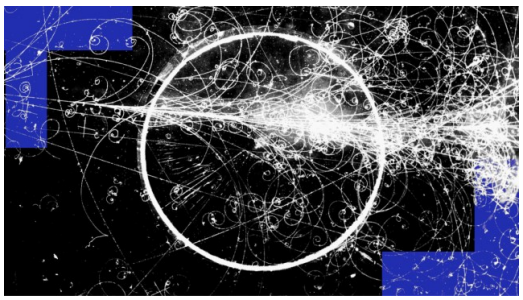
В 1927 году Паули предложил существование нейтрино

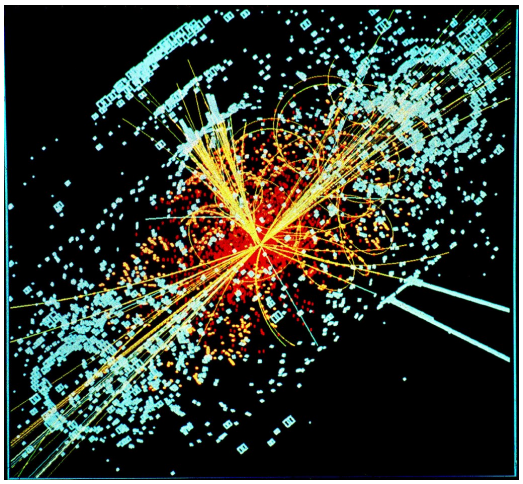
До 1956 года исследования слабых взаимодействий были направлены на установление вида эффективного гамильтониана, ответственного за эти взаимодействия.

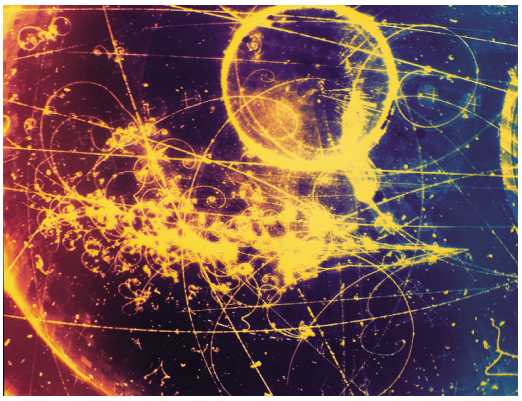
4-фермионный гамильтониан - был предложен Э.Ферми в 1934 году

С тех пор изменилось многое. На сегодняшний день мы знаем, что слабое и электромагнитное взаимодействия есть две стороны одного и того же взаимодействия, названного электрослабым. Это объединение провели Стивен Вайнберг и Абдус Салам. Тем не менее, многие факты и явления, связанные со слабым взаимодействием, по-прежнему заслуживают внимания и отдельного обсуждения.

A.5 Popular Introduction







A.6 Definitions

В данной записи текста будет много и будет много описаний. Если в других статьях часто наоборот, куча моделей и тренировок, то тут первая половина статьи - это точно просто описание происходящего, мб какие-то количественные подтверждения и совсем не много формул.

а вот вторую часть через стандартную модель и лагранжианы в планах сделать максимально количественной, научиться на самом деле это решать.

Список определений

(глоссарий потом добавлю, пока не актуально)

думаю, чтобы не запутаться - лучше составить список определений

мезоны

барионы

адроны

т.п.

Система единиц

про натуральные единицы и заготовки формул перехода написать.

$E = \gamma m$ $p = \gamma m v$ $E^2 - p^2 = m^2$

$[\text{ Mass }] = [\text{ Energy }] = [\text{ Momentum }] = [\text{Time }]^{-1} = [\text{Distance }]^{-1}$

$\hbar c \approx 197 \text{MeVfm}$

A.7 Puzzles for Different Cases

Обсудим в последовательности интересности задачки о элементарных частицах. В них важно уметь их красиво задавать, подчеркивая загадочность и нестандартность этого раздела физики, что я пытался написать в виде текста.

A.7.1 Typical Fundamental Questions

Из чего весь мир состоит и почему?

тут и порассуждаю в обзорном стиле

Какая частица самая элементарная?

считался атом

потом электрон и протон

потом кварки
и так все знают со школы.
но вот проблема, что это неправда.
На самом деле природа создана из полей, а частицы это лишь их проявления.
(интересно кстати это явно показать формулами, но я тупой слишком для этого еще)

Какие самые фундаментальные взаимодействия в природе?

Вопрос о фундаментальных взаимодействиях - самый типичный вопрос стандартной модели. Ниже он подробно (будет) отвечен, здесь приведем эту суть.

А кстати фундаментальыне взаимодействия с точки зрения теории струн, это что?

Какие есть фундаментальные симметрии в природе?

Если фундаментальные поля, зачем изучаем частицы?

почему тогда используем ктп?

Каков размер электрона?

Точечная частица.

Если бы у частицы были размеры, то с релятивистской инвариантностью возникнут пролебмы.

(володя сказал, что у ландау можно почитать)

Как теоретически определить, что такое частица в плоском пространстве?

Как определить, что такое частица в искривленном пространстве?

есть ли одно и то же скалярное поле для лептонов и кварков или нет?

Да и сам бозон Хиггса порождает массу новых вопросов... Например,

почему бозон Хиггса такой тяжелый?

Почти как t кварк... Другая серия вопросов:

почему у самых легких кварков «нижний» тяжелее

верхнего, а у остальных поколений все наоборот?

Почему такая большая разница между массами кварков разных поколений?

Как появляется масса у адронов?

Наконец,

есть ли экзотические адроны

(составленные из 4-х или 5-ти кварков, или вообще составленные только из глюонов, т. е. «глюболы») или они почему-то (почему?

) не существуют вообще?

Возвращаясь к: он

единственный бозону Хиггса или нет?

Как быть с кварк-лептонной аналогией, если известные нам нейтрино все же имеют конечную ненулевую массу за счет механизма «качелей», а значит, имеют (очень) массивных партнеров, которых должно быть не менее трех?

A.7.2 Fun General Questions

тут не такие умные вопросы, но тем не менее, кто совсем не знает физику, может ими интересоваться

что если засунуть руку на пучок частиц в коллайдере?

тем не менее, интересно.

A.7.3 Fun Hypothetical Questions

О элементарных частицах чего только не думали, так что загадок полно.

А если частицы это квантовые мини Вселенные?

(???? why this can't be?? it is a good question)

Один из вариантов:

Такое может быть.

Мини вселенная это квант нашей Вселенной.

Тогда может быть, то, что для нас размыто там - это на самом деле точный мир, просто мы принципиально не способны это увидеть.

А для микро вселенной наш мир - огромнейший и размытый.

В общем, мб разовью эту идею, но вообще, звучит как просто бред, так что правильнее и забить.

A.7.4 Very Hard, Unanswered General Questions

а жизнь и нематериальнаые духовные сущности никаких материальных объектов не принимают

зная физику частиц, можно ли понять, что будет после смерти?

B Special Mathematics and Physics

B.1 Algebra for Particle Physics

(тут много всего будет, см. курс Киселева например)

B.2 Physics for Particle Physics

(уже с этим многие задачи решаться будут)

B.2.1 Symmetries

типичные симметрии квантовой механики

Пусть у нас есть какая-то симметрия:

$$\Psi \to \Psi' = \hat{U}\Psi$$

Чтобы сохранялась нормировка вероятности, необходимо чтобы:

$$\langle\Psi|\Psi\rangle = \langle\Psi\prime|\Psi\prime\rangle = \langle\hat{U}\Psi|\hat{U}\Psi\rangle = \langle\Psi|\hat{U}^\dagger\hat{U}\Psi\rangle$$

Поэтому $[\hat{U}^\dagger\hat{U}] = 1$ т.е. $\hat{U}$ должен быть унитарным

Чтобы предсказания квантовой механики не менялись, нужно, чтобы матричные элементы оставались неизменными:

$$\langle\psi|\hat{H}|\psi\rangle = \left\langle\psi'|\hat{H}|\psi'\right\rangle = \left\langle\psi\left|\hat{U}^\dagger\hat{H}\hat{U}\right|\psi\right\rangle$$

т.е. нужно$\hat{U}^\dagger\hat{H}\hat{U} = \hat{H}$

Перепишем это, домножая на $\times\hat{U}$:

$$\hat{U}\hat{U}'\hat{H}\hat{U} = \hat{U}\hat{H} \Rightarrow \hat{H}\hat{U} = \hat{U}\hat{H}$$

Поэтому:

$$[\hat{H}, \hat{U}] = 0$$

Перейдем теперь к инфинитезимальным преобразованиям, то есть перепишем $\hat{U}$через $\hat{G}$ - генератор - и маленький параметр ε:

$$\hat{U} = 1 + i\varepsilon\hat{G}$$

Найдем свойства генераторов. Из свойства унитарности $\hat{U}$ следует, что:

$$\hat{U}\hat{U}^\dagger = (1 + i\varepsilon\hat{G})\left(1 - i\varepsilon\hat{G}^\dagger\right) = 1 + i\varepsilon\left(\hat{G} - \hat{G}^\dagger\right) + O\left(\varepsilon^2\right)$$

пренебрегая членами по порядку ε^2, получаем условие:
$\hat{G} = \hat{G}^\dagger$
т.е. $\hat{G}$ Эрмитов, поэтому соответствует наблюдаемой G !
Но даже больше, так как $[\hat{H}, \hat{U}] = 0 \Rightarrow [\hat{H}, 1 + i\varepsilon\hat{G}] = 0 \Rightarrow [\hat{H}, \hat{G}] = 0$
Но так как она соответствует наблюдаемой,

$$\frac{\mathrm{d}}{\mathrm{d}t}\langle\hat{G}\rangle = i\langle[\hat{H}, \hat{G}]\rangle = 0$$

B.2.2 Spinors

Спиноры очень хорошо описывают многие частицы, так что обсудим, как их конструировать.

C Bibliography

References

[1] Tong, D.: *Particle Physics, CERN Lectures*. https://www.damtp.cam.ac.uk/user/tong/particle.html.

[2] Окунь, Л. Б.: *Лептоны и кварки*. УРСС, 2005.

[3] Thomson, M.A.: *Michaelmas, лекции в Кембридже*. 2011.

[4] Бюклинг Е., Каянти К.: *Кинематика элементарных частиц*.

[5] Пескин, М and Шредер, Д: *Введение в квантовую теорию поля*. 2001.

[6] Челлен, Г: *Физика элементарных частиц: Пер. с англ.* Наука. Гл. ред. физ.-мат. лит., 1966.

[7] Particle Data Group, Zyla, P. A., Barnett, R. M., et. al.: *Review of Particle Physics*. Progress of Theoretical and Experimental Physics, 2020(8):083C01, August 2020, ISSN 2050-3911. https://doi.org/10.1093/ptep/ptaa104.

[8] Хорган, Джон: *Конец науки*. Взгляд на ограниченность знания на закате Века Науки. СПб, 1, 2001.

[9] Volkov D.V., Akulov, V.P.: *Is the neutrino a goldstone particle?* Physics Letters B, 46(1):109–110, 1973, ISSN 0370-2693. https://www.sciencedirect.com/science/article/pii/0370269373904905.

[10] Белоусов, Бурмистров, Тернов.: *задачи по теоретической физике*. Интеллект, 2013.

[11] Лифшиц Е. М., Ландау Л. Д.: *Теория поля*, volume 2. Наука, 2004.

[12] Райдер, Льюис: *Квантовая теория поля*. ПЛАТОН, 1998.

[13] Ландау, ЛД and Лифшиц, ЕМ: *Теоретическая физика. Том 8. Электродинамика сплошных сред*. книга, 1982.

[14] Mommers, C. J. G.: *Rare Weak Decays of the Omega Baryon (Dissertation)*. 2022. https://urn.kb.se/resolve?urn=urn:nbn:se:uu:diva-479009.

[15] Larkoski, Andrew J.: *Elementary Particle Physics: An Intuitive Introduction*. Cambridge University Press, 2019.

[16] Aoyama, T., Asmussen, N., Benayoun, M., Bijnens, J., Blum, T., Bruno, M., Caprini, I., Carloni Calame, C.M., and al et.: *The anomalous magnetic moment of the muon in the standard model*. Physics Reports, 887:1–166, December 2020, ISSN 0370-1573. http://dx.doi.org/10.1016/j.physrep.2020.07.006.